# Catalytic Enantioselective Formations of C–B, C–C and C–Si Bonds by Organic Molecules or Transition-Metal Complexes

Author: Hao Wu

Boston College

The Graduate School of Arts and Sciences

Department of Chemistry

# CATALYTIC ENANTIOSELECTIVE FORMATIONS OF C–B, C–C AND C–SI BONDS BY ORGANIC MOLECULES OR TRANSITION-METAL COMPLEXES

a dissertation

by

HAO WU

submitted in partial fulfillment of the requirements

for the degree of

Doctor of Philosophy

December 2015

# Catalytic Enantioselective Formations of C–B, C–C and C–Si Bonds by Organic Molecules or Transition-Metal Complexes

Hao Wu

Dissertation advisor: Prof. Amir H. Hoveyda

Catalytic enantioselective reactions are of great importance in synthetic organic chemistry. Thus, development of efficient, selective and easily accessible catalyst for various bond formations is the main task in our laboratories.

First, we have developed the first broadly applicable enantioselective boryl conjugate addition reactions to a variety of α,β-unsaturated carbonyls, promoted by a chiral Lewis basic *N*-heterocyclic carbene. The valuable β-boryl carbonyls were further used in complex molecule syntheses. The mechanism of these C–B bond formations was studied in details.

We have also developed a practical method for enantioselective addition of an allene unit to aryl-, heteroaryl- and alkyl-substituted Boc-aldimines. These efficient C–C bond formations, catalyzed by an aminophenol-derived boron-based catalyst, were further utilized in succinct syntheses of anisomycin and *epi*-cytoxazone.

Finally, chiral NHC–Cu complexes were employed for site-, diastereo- and enantioselective silyl conjugate additions to acyclic and cyclic dienones and dienoates. The precious enantiomerically enriched allylsilane obtained can be converted into a ketone-aldol type product, which is difficult to access through alternative methods.

# Table of Contents

# Chapter 1

## *N*-Heterocyclic Carbenes Catalyzed Enantioselective Boryl Conjugate Additions to α,β-Unsaturated Ketones, Esters, Weinreb Amides and Aldehydes

### *1.1. Introduction*

The chemistry of boron, especially in the region of organic chemistry, has advanced dramatically in the last century.[1] A tremendous amount of efforts have been made on development of organoboron reagents, transformations that construct C–B bonds, as well as functionalizations of those bonds. Most notable was the work by H. C. Brown and co-workers on hydroborations, honored as the Nobel Prize in 1979.[2] Their discoveries opened an entirely new avenue in both academic and industrial chemistry, since organoborons can be readily converted to other important compounds that have great values in biology and medication (the antidepressant Prozac®[3] and the cholesterol-lowering drug Lipitor®[4] as representatives). Another significant work by A. Suzuki and co-workers on cross-coupling reactions using organoboron compounds has further

(1) For representative reviews on organoboron chemistry, see: (a) Lappert, M. F. *Chem. Rev.* **1956**, *56*, 959–1064. (b) Thomas, S. E. *Organic Synthesis: The Roles of Boron and Silicon* (*Oxford Chemistry Primers)*; Oxford Science Publications: Oxford, 1992. (c) Miyaura, N. *Organoboron Compounds (Topics in Current Chemistry)*, **2002**, *219*, 11–59.

(2)(a) Brown, H. C.; Krishnamurthy, S. *Tetrahedron* **1979**, *35*, 567–607. (b) "The Nobel Prize in Chemistry 1979" The Nobel Foundation.

(3) Robertson D. W.; Krushinski J. H.; Fuller R. W.; Leander J. D. *J. Med. Chem.* **1988**, *31*, 1412–1417.

(4) Roth, B. D. *Progress in Medicinal Chemistry* **2002**, *40*, 1–22.

pushed the frontier of the utility of C–B bonds to construct biologically important molecules.[5]

Accordingly, development of methods to synthesize compounds that bear C–B bonds catalytically and enantioselectively is one of the central but still challenging goals in organic chemistry. One direct protocol is catalytic enantioselective boryl conjugate additions (BCAs) to α,β-unsaturated carbonyls. The product of such protocol contains a boron-substituted secondary carbon stereogenic center, which is highly valuable since the corresponding C–B bond can be readily converted into C–O (aldol product)[6], C–N[7], C–C[8], and more recently C–F bond[9]. It is worth to mention that catalytic enantioselective BCAs belonged to the transition-metal catalyzed region exclusively until our report in 2009, which involved an efficient boryl conjugate addition catalyzed by a small N-heterocyclic carbene (NHC) serving as Lewis base.[10] This method not only offers complementary reactivities and selectivities to the well-established metal-catalyzed alternatives, more importantly proceeds through a different pathway, one that sheds light on discoveries of other Lewis base catalyzed transformations.

In this chapter, I will first introduce the history on development of catalytic boryl conjugate additions, and then focus on our disclosures of enantioselective BCAs

(5) (a) Miyaura, N.; Suzuki, A. *Chem. Rev.* **1995**, *95*, 2457–2483. (b) "The Nobel Prize in Chemistry 2010" The Nobel Foundation.

(6) Carboni, B.; Ollivault, M.; Bouguenec, F. L.; Carrié, R.; Jazouli, M. *Tetrahedron Lett.* **1997**, *38*, 6665–6668.

(7) (a) Moran, W. J.; Morken, J. P. *Org. Lett.* **2006**, *8*, 2413–2415. (b) Mlynarski, S. N.; Karns, A. S.; Morken, J. P. *J. Am. Chem. Soc.* **2012**, *134*, 16449–16451.

(8) (a) Imao, D.; Glasspoole, B. W.; Laberge, V. S.; Crudden, C. M. *J. Am. Chem. Soc.* **2009**, *131*, 5024–5025. (b) Ohmura, T.; Awano, T.; Suginome, M. *J. Am. Chem. Soc.* **2010**, *132*, 13191–13193. (c) Sandrock, D.; Jean-Gérard, L.; Chen, C. Y.; Dreher, S. D.; Molander, G. A. *J. Am. Chem. Soc.* **2010**, *132*, 17108–17110.

(9) Li, Z.; Wang, Z.; Zhu, L.; Tan, X.; Li, C. *J. Am. Chem. Soc.* **2014**, *136*, 16439–16443.

(10) (a) Lee, K.-S.; Zhugralin, A. R.; Hoveyda, A. H. *J. Am. Chem. Soc.* **2009**, *131*, 7253–7255. (b) Lee, K.-S.; Zhugralin, A. R.; Hoveyda, A. H. *J. Am. Chem. Soc.* **2010**, *132*, 12766.

catalyzed by a chiral NHC. Related studies on its mechanism will be demonstrated in the next chapter.

### *1.1.1. Early Discoveries of Transition Metal-Catalyzed Boryl Conjugate Additions*

The first examples of catalytic boryl conjugate additions to α,β-unsaturated carbonyls are reported by Marder, Norman and co-workers.[11] Based on previous disclosures on metal-catalyzed diboration of simple alkenes[12], they expanded the substrate scope to α,β-unsaturated carbonyls, using $B_2(pin)_2$ and $B_2(cat)_2$ as diboron reagents (pin = pinacolato, cat = catecholato). As shown in Scheme 1.1.1, diborations occur with exclusive regioselectivity, affording 1,4-addition products **1.2**. Due to their instability towards moisture, the products were converted into β-boryl carbonyls **1.3** efficiently after aqueous workup. After simple oxidations, β-hydroxyl carbonyl **1.4a** was obtained in 80% yield, rendering the current method an alternative way to synthesize aldol product. In 2002, Kabalka and co-workers reported a similar BCA transformation catalyzed by Wilkinson's catalyst (not shown here).[13] Although α,β-unsaturated ketones, esters and nitriles are suitable substrates, the use of 10 mol % Rh(I) complex in the reactions limits the applicability of this method.

**Scheme 1.1.1. Pt-catalyzed Boryl Conjugate Additions**

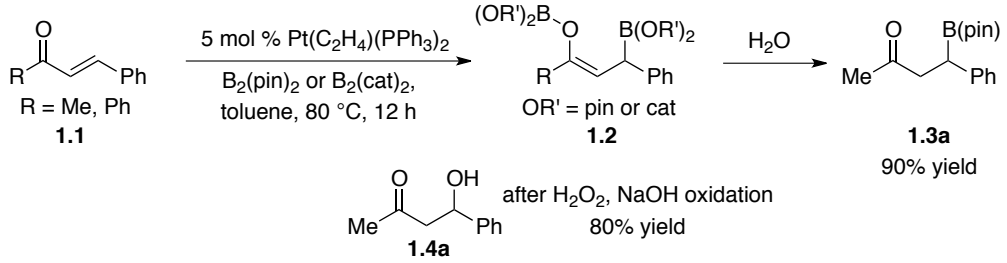


(11) Lawson, Y. G.; Lesley, M. J. G.; Norman, N. C.; Rice, C. R. Marder, T. B. *Chem. Commun.* **1997**, 2051–2052 .

(12) Baker, R. T.; Nguyen, P.; Marder, T. B.; Westcott, S. A. *Angew. Chem., Int. Ed.* **1995**, *34*, 1336–1338.

(13) Das, B. C.; Das, S.; Kabalka, G. W. *Tetrahedron Lett.* **2002**, *43*, 2323–2325.

In 2000, Hisomi and co-workers reported the first Cu-catalyzed BCAs (Scheme 1.1.2).[14] Notably, this early transition metal-catalyzed BCAs require a lower reaction temperature (22 ºC) and a shorter reaction time (10 h) than the more expensive Pt catalysis (80 ºC and 12 h, respectively). Both acyclic and cyclic enones are suitable substrates, except those bearing a β-substituted alkene (substrate for **1.3c**). The authors also demonstrated the importance of the phosphine ligand, as there is no reaction without $Bu_3P$. Interestingly, the reaction will proceed slowly (7% yield, 24 h) if only $Bu_3P$ is used (no CuOTf), suggesting it as an alternative and potentially effective catalyst.

**Scheme 1.1.2. Cu-catalyzed Boryl Conjugate Additions by Hosomi and co-workers**

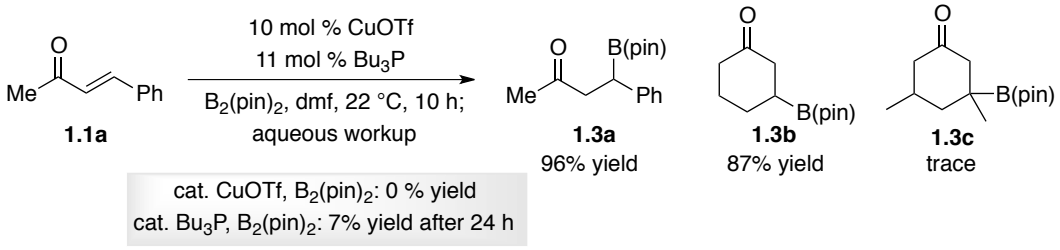


In the same year, Miyaura and co-workers published their progresses on Cu-catalyzed boryl conjugate additions.[15] While similar results were observed using catalytic amount of CuCl and AcOK (Scheme 1.1.3), the authors proposed the catalytic active species: Cu–B(pin), as allylB(pin) was obtained if allylchloride was treated in the same reaction condition. Interestingly, they also found a B(pin) allylic substitution reaction without any transition metal (the second equation of Scheme 1.1.3), where intermediate **1.5** was considered as the "nucleophilic boron species". Those disclosures are of great

(14) Hosomi, A.; Ito, H.; Tateiwa, J.-i.; Yamanaka, H. *Tetrahedron Lett.* **2000**, *41*, 6821–6825.

(15) (a) Ishiyama, T.; Miyaura, N.; Takahashi, K. *Chem. Lett.* **2000**, 982–983. (b) Ishiyama, T.; Miyaura, N.; Takahashi, K. *J. Organomet. Chem.* **2001**, *625*, 47–53.

significance in the development of transition metal free catalytic boryl conjugate additions.

**Scheme 1.1.3. Cu-catalyzed Boryl Conjugate Additions by Miyaura and co-workers**

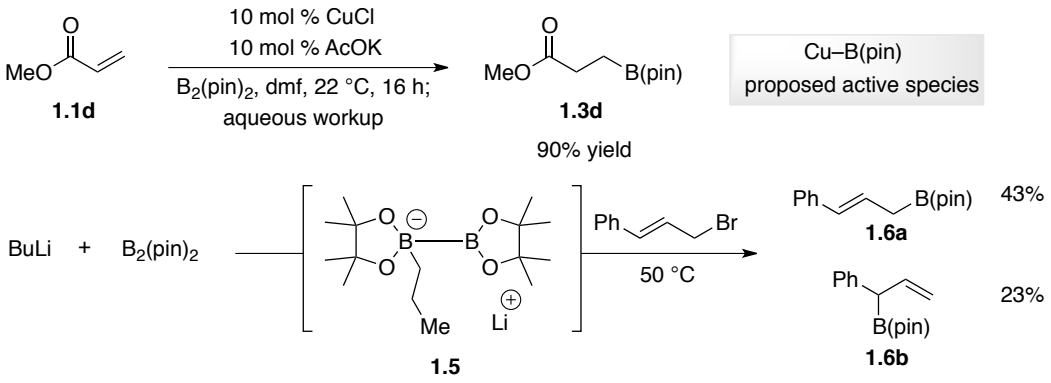


The work of Hosomi, Miyaura and their co-workers were very influential, but high catalyst loadings, poor substrate scopes and difficulties in developing the corresponding enantioselective reactions limited their applications. In 2006, Yun J. and co-workers changed the fate of Cu-catalyzed BCAs by involving an alcohol additive into the catalytic system (Scheme 1.1.4).[16] A catalytic amount of CuCl, base and a phosphine ligand (DPEphos) was applied in the reactions, similarly as previous disclosures. However, if 2 equiv of MeOH was used, the reactivity of BCA reactions was enhanced significantly (for **1.3e**, >98% conv vs 48% conv without MeOH). Clearly, MeOH plays a very important role. In the proposed mechanism, CuCl is converted into CuO*t*-Bu by treatment of NaO*t*-Bu, which is further transformed into LCu–B(pin), a key nucleophilic B(pin) intermediate in the catalysis (the details of this process will be discussed later). Upon substrate coordination and B(pin) addition, organocopper species **1.7** (in equilibrium with **1.8**) is formed, which was then protonated by MeOH to release the

(16) Mun, S.; Lee, J.-E.; Yun, J. *Org. Lett.* **2006**, *8*, 4887-4889.

product **1.3** and re-generate LCu–OMe. The catalytic cycle is closed by its reaction with $B_2(pin)_2$, forming LCu–B(pin). Not surprisingly, the process of releasing the product **1.3** from organocopper **1.7** or **1.8** will be greatly hampered if MeOH is not involved, since it involves a sterically hindered, yet non-nucleophilic organocopper (**1.7** or **1.8**) reacting with large $B_2(pin)_2$.

The aforementioned phosphine–Cu-catalyzed BCAs are not only very efficient, but can also be applied in a variety of substrates, including acyclic or cyclic ketones (**1.3f**, **1.3j**), esters (**1.3e, 1.3g** and **1.3h**) and nitriles (**1.3i**). The reliability and environmentally friendly catalyst of this method render it as a broadly applicable approach to synthesize β-boryl carbonyl compounds efficiently.

**Scheme 1.1.4. Highly efficient Cu-catalyzed BCAs by Yun *et al.***

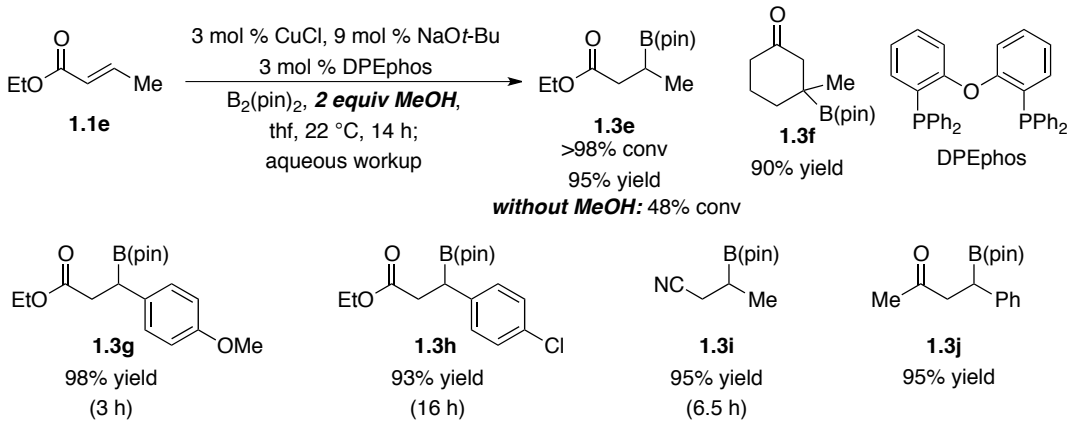

***Proposed mechanism:***

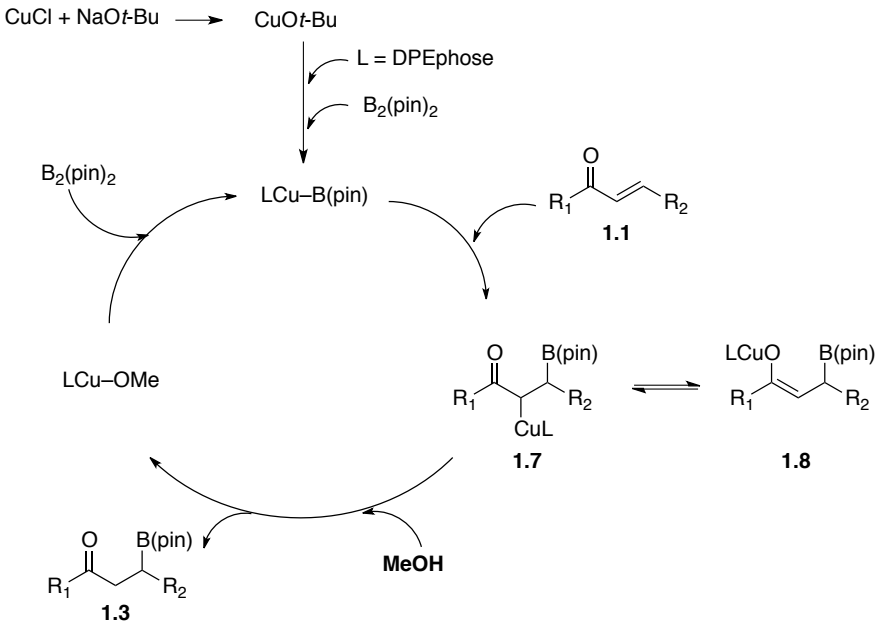


In 2005, Sadighi and co-workers obtained the first substantial evidence of LCu–B(pin) during their study on Cu-catalyzed diboration of $CO_2$.[17] In Scheme 1.1.5, an (NHC)Cu–B(pin) **1.10** was isolated as a crystal from the reaction between (NHC)Cu–O*t*-Bu **1.9** and $B_2(pin)_2$. In its X-ray structure, the Cu–B bond length is 2.002(3) Å and the C(1)–Cu(1)–B(1) angle is 168.1º. The authors also found out this (NHC)Cu–B(pin) reacts readily with $CO_2$, forming (NHC)Cu–OB(pin) **1.11** and CO, rendering it as a nucleophilic B(pin) species as well as a good catalyst to reduce $CO_2$ into CO.

(17) Laitar, D. S.; Müller, P.; Sadighi, J. P. *J. Am. Chem. Soc.* **2005**, *127*, 17196–17197.

**Scheme 1.1.5. Isolation of an (NHC)Cu–B(pin) complex by Sadighi *et al.***

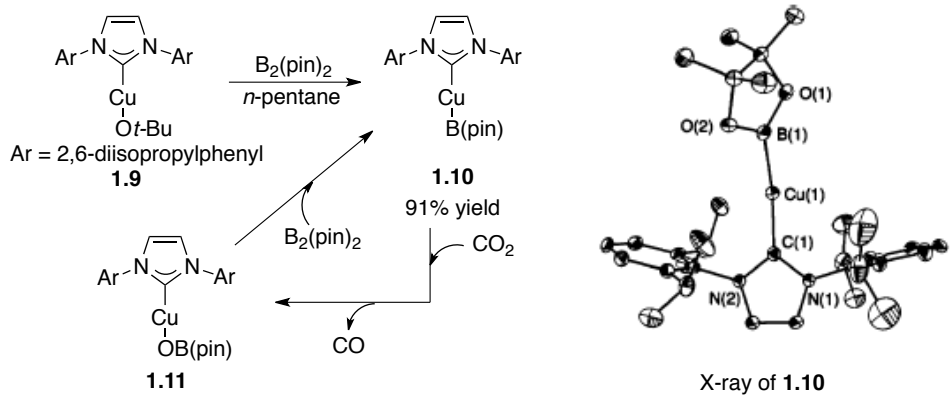


X-ray of **1.10**

Other transition metal-catalyzed non-enantioselective protocols, including those involving a Pd[18], Pt[19], Fe[20], Cu[21] and Ni[22] catalyzed ones, were also reported, some of which have comparable efficiencies with the aforementioned Yun's strategy. α,β-Unsaturated imines[23], sulfones[24] as well as ynones[25] are suitable substrates for BCA reactions. Those disclosures enriched possible catalyst systems for the development of enantioselective BCA reactions.

### *1.1.2. Transition Metal-Catalyzed Enantioselective Boryl Conjugate Additions*

(18) Bonet, A.; Gulyás, H.; Koshevoy, I. P.; Estevan, F.; Sanaú, M.; Ubeda, M. A.; Fernández, E. *Chem. Eur. J.* **2010**, *16*, 6382–6390.

(19) (a) Ali, H. A.; Goldberg, I.; Srebnik, M. *Organometallics* **2001**, *20*, 3962–3965. (b) Bell, N. J.; Cox, A. J.; Cameron, N. R.; Evans, J. S. O.; Marder, T. B.; Duin, M. A.; Elsevier, C. J.; Baucherel, X.; Tulloch, A. A. D.; Tooze, R. P. *Chem. Commun.* **2004**, 1854–1855.

(20) Bonet, A.; Sole, C.; Gulyás, H.; Fernández, E. *Chem. Asian. J.* **2011**, *6*, 1011–1014.

(21) (a) Bonet, A.; Lillo, V.; Ramírez, J.; Díaz-Requejo, M. M.; Fernández, E. *Org. Biomol. Chem.* **2009**, *7*, 1533–1535. (b) Gao, M.; Thorpe, S. B.; Santos, W. L. *Org. Lett.* **2009**, *11*, 3478–3481. (c) Cano, R.; Ramón, D. J.; Yus, M. *J. Org. Chem.* **2010**, *75*, 3458–3460. (d) Chea, H.; Sim, H.-S.; Yun, J. *Bull. Korean Chem. Soc.* **2010**, *31*, 551–552. (e) Gao, M.; Thorpe, S. B.; Kleeberg, C.; Slebodnick, C.; Marder, T. B.; Santos, W. L. *J. Org. Chem.* **2011**, *76*, 3997–4007. (f) Thorpe, S. B.; Calderone, J. A.; Santos, W. L. *Org. Lett.* **2012**, *14*, 1918–1921.

(22) Hirano, K.; Yorimitsu, H.; Oshima, K. *Org. Lett.* **2007**, *9*, 5031–5033.

(23) Sole, C.; Fernández, E. *Chem. Asian. J.* **2009**, *4*, 1790–1793.

(24) Moure, A. L.; Arrayás, R. G.; Carretero, J. C. *Chem. Commun.* **2011**, *47*, 6701–6703.

(25) (a) Lee, J.-E.; Kwon, J.; Yun, J. *Chem. Commun.* **2008**, 733–734. (b) Jung, H.-Y.; Feng, X.; Kim, H.; Yun, J. *Tetrahedron*, **2012**, *68*, 3444–3449. (c) Nagao, K.; Ohmiya, H.; Sawamura, M. *Org. Lett.* **2015**, *17*, 1304–1307.

In the previously mentioned report on Pt-catalyzed BCA reactions developed by Marder, Norman and their co-workers in 1997, the authors suggested their reactions could be potentially enantioselective if a chiral diboron reagent was used. While little success has been made since then, Yun and co-workers considered a different approach: utilizing a chiral ligand. In 2008, they reported the first Cu-catalyzed ***enantioselective*** boryl conjugate additions to α,β-unsaturated esters and nitriles (Scheme 1.1.6).[26] Among a variety of phosphine ligands, Josiphos turned out to be the most selective one. With only 2-3 mol % Phsophine–Cu catalyst at ambient temperature, β-boryl esters or nitriles that bear an alkyl, aryl or hetero-aryl substituent can be obtained efficiently (~90% yield) and enantioselectively (≥91:9 er). Again, alcohol (2 equiv) proves to be critical for efficient transformations.

In a later study, α,β-unsaturated acyclic ketones were found to be similarly effective in the BCA reaction condition (for example, **1.3n**, 79% yield, 94.5:5.5 er), except in some cases (sterically more hindered substrates, not shown here), lower enantioselectivity (such as 90.5:9.5 er) was observed.[27] The authors consider the decrease in enantioselectivity may come from background reactions catalyzed by CuOMe. The same group also showed two examples where α,β-unsaturated amides served as substrates in the Cu-catalyzed enantioselective BCA reactions.[28] In both cases, high enantioselectivity was observed (for example, **1.3o**, 98:2 er). Unfortunately, no isolation yield was reported. Enantioselective BCA reactions to synthetically more useful Weinreb amides were not reported either.

---

(26) Lee, J.-E.; Yun, J. *Angew. Chem. Int. Ed.* **2008**, *47*, 145–147.
(27) Sim, H.-S.; Feng, X.; Yun, J. *Chem. Eur. J.* **2009**, *15*, 1939–1943.
(28) Chea, H.; Sim, H.-S.; Yun, J. *Adv. Synth. Catal.* **2009**, *351*, 855–858.

In the more challenging reactions with β-substituted α,β-unsaturated esters, the authors disclosure MeDuphos as the optimized ligand. Thus, **1.3p** was isolated in 91% yield with 97:3 er. However, the same reaction to β-substituted α,β-unsaturated ketones is much less selective (no more than 82.5:17.5 er, not shown here), likely due to the competitive CuOMe catalyzed background reaction.

Phosphine–Cu-catalyzed enantioselective BCA reactions to cyclic enones and lactones are also efficient and selective.[29] However, the reaction seems to be sensitive to ring sizes and substituents of the substrates. For example, **1.3q** with a five-member ring is significantly less efficient (76% yield) and enantioselective (87:13 er) compared to its six-membered (**1.3b**, 92% yield, 99:1 er) or seven-membered variant (**1.3r**, 95% yield, 95:5 er). More strikingly, there is no reaction for **1.3s**. Clearly, the neighboring gem-dimethyl group dramatically inhibits the substrate coordination and/or B(pin) transfer. Unfortunately, the reaction with β-substituted cyclic ketones, although in good efficiency, results in a much poorer enantioselectivity (82:18 er for **1.3f**).

Notably, most phosphine ligands used in Yun's method are commercially available, although with a high price ((***R***,***S***)-Josiphos: ~$350/mmol, Sigma Aldrich®). In addition, high reliability as well as a broad substrate scope render the current method a broadly used one. For BCA reactions with unsubstituted α,β-unsaturated carbonyls and nitriles, it is still the state-of-art protocol. However, there are still limitations for the current method, such as the high $O_2$ and $H_2O$ sensitivity of copper(I) salt and phosphine ligands, competitive Cu–B(pin) additions to an alkyne, allene and aldehyde group in a multifunctional substrate, as well as low enantioselectivity for β-substituted cyclic and

(29) Feng, X.; Yun, J. *Chem. Commun.* **2009**, 6577–6579.

acyclic ketones. In the following discussion, methods that overcome one or more shortcomings will be provided.

**Scheme 1.1.6. Phosphine–Cu-catalyzed enantioselective BCAs by Yun *et al.***

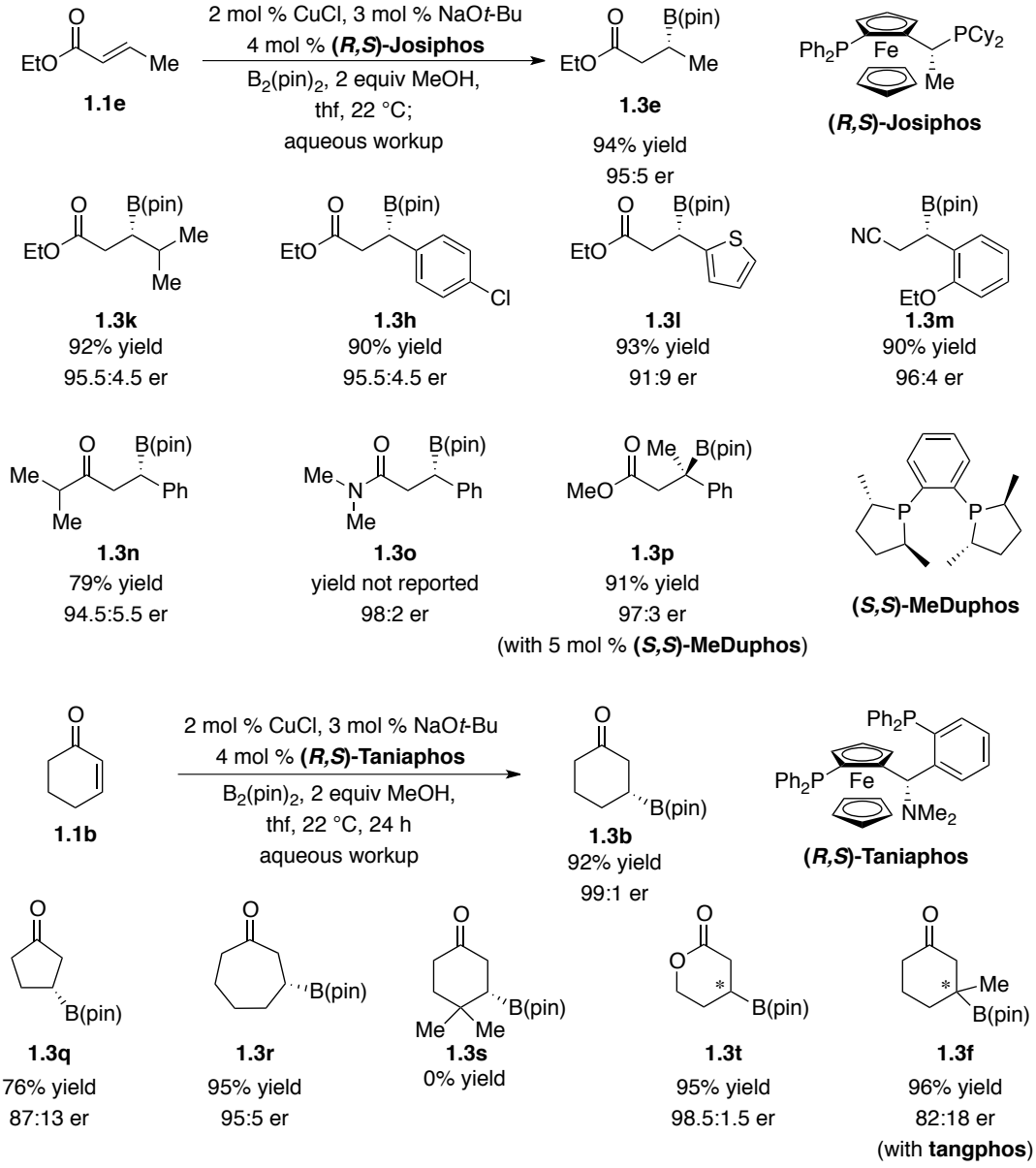


In addition, Arrayás, Carretero and co-workers found Yun's phosphine–Cu-catalyzed enantioselective reactions are also effective to α,β-unsaturated sulfonates.[24] The same is true with α,β-unsaturated imines, which proved to be also effective in the

same BCA reactions by Fernández and co-workers.[30] In 2014, Lam's group succeeded to promote selective 1,6-additions to α,β,γ,δ-unsaturated carbonyls with high efficiencies and enantioselectivities, using a similar catalytic system as Yun's method.[31] Additionally, Hall and co-workers utilized the phosphine–Cu-catalyzed BCA reactions to enantioselectively synthesize 1,1-diboryl carbonyls (containing a B(pin) and B(dan) moiety, dan = 1,8-diaminonaphthalenyl), which was further used in chemoselective cross coupling reactions.[32]

In 2010, A. H. our laboratories reported the first general catalytic enantioselective BCA reactions to β-substituted acyclic α,β-unsaturated carbonyls.[33] The catalytic active NHC–Cu-O*t*-Bu complex was generated *in situ* by treatment of the corresponding imidazolinium salt with CuCl and NaO*t*-Bu. A ligand screening resulted in the $C_1$ symmetric monodentate **1.12** as the optimized one (Scheme 1.1.7). The BCA reaction condition is similar as the previously mentioned Yun's method, except a lower reaction temperature is required for high enantioselectivity. β-Substituted acyclic α,β-unsaturated esters, ketones and thioesters are generally suitable substrates, although lower selectivities were observed for the two ketone cases reported. It is worth of mentioning that the β-boryl thioester (such as **1.3y**, 99:1 er) can be converted into the corresponding ketone or ester through a cross-coupling reaction or ester exchange, respectively, furnishing products that are of higher enantioselectivity than the ones from direct BCA

(30) (a) Solé, C.; Whiting, A.; Gulyás, H.; Fernández, E. *Adv. Synth. Catal.* **2011**, *353*, 376–384. (b) Solé, C.; Tatla, A.; Mata, J. A.; Whiting, A.; Gulyás, H.; Fernández, E. *Chem. Eur. J.* **2011**, *17*, 14248–14257. (c) Calow, A. D. J.; Batsanov, A. S.; Pujol, A.; Solé, C.; Fernández, E.; Whiting, A. *Org. Lett.* **2013**, *15*, 4810–4813.

(31) Luo, Y.; Roy, I. D.; Madec, A. G. E.; Lam, H. W. *Angew. Chem. Int. Ed.* **2014**, *53*, 4186–4190.

(32) Lee, J. C. H.; McDonald, R.; Hall, D. G. *Nature. Chem.* **2011**, *3*, 894–899.

(33) O'Brien, J. M.; Lee, K.-s.; Hoveyda, A. H. *J. Am. Chem. Soc.* **2010**, *132*, 10630–10633.

reactions to the corresponding unsaturated esters or ketones. In addition, the C–B bond oxidation of these β-boryl carbonyls leads to products that cannot be obtained easily from enantioselective Aldol reactions. In the end, models were proposed to explain the observed stereochemistry.

**Scheme 1.1.7. NHC–Cu-catalyzed enantioselective BCAs by Hoveyda *et al.***

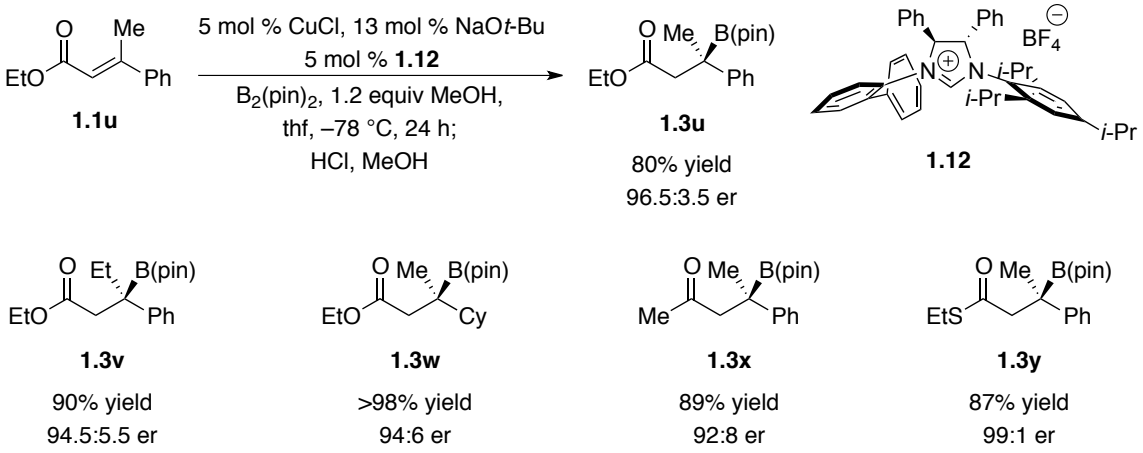


In terms of low enantioselectivity for β-substituted acyclic and cyclic ketones by Yun's method, Shibasaki and co-workers reported their protocols to address these issues. If β-substituted acyclic enones serve as substrate, they discovered diamine **1.13** as the optimal ligand for Cu-catalyzed BCA reactions (Scheme 1.1.8).[34] The substituents on the substrate (various alkyl or aryl ones) minimally affect the efficiency and enantioselectivity. Mechanistic investigations suggest that diamine–Cu(I) complex reacts with $B_2(pin)_2$ to generate an N-boryl diamine–CuB(pin), which behaves as the catalytic active species.

(34) Chen, I.-H.; Kanai, M.; Shibasaki, M. *Org. Lett.* **2010**, *12*, 4098–4101.

Interestingly, the optimal ligand for Cu-catalyzed BCA reactions to β-substituted cyclic ketones goes back to a bisphosphine ligand, **1.14** (QuinoxP*) in this case.[35] A variety of cyclic enones were tested in the catalytic reactions, most of which result in desired products with a high yield and enantiomeric ratio. The high values of these β-boryl carbonyls were demonstrated again in this report, where C–B bond oxidation, B(pin) hydrolysis into $B(OH)_2$ and BCA + Aldol reaction sequence were performed, leading to products which are difficult to obtain through other protocols.

**Scheme 1.1.8. Cu-catalyzed enantioselective BCAs by Shibasaki *et al.***

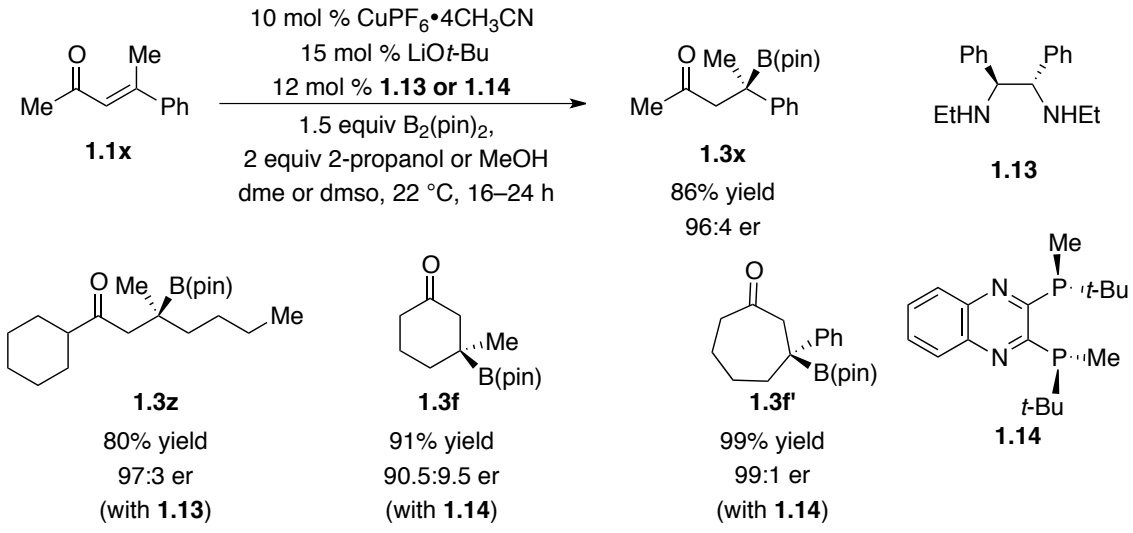


Notably, Kobayashi and co-workers reported a diamine–Cu(II)-catalyzed enantioselective boryl conjugate additions to di- or tri-substituted carbonyls.[36] $Cu(OH)_2$ was utilized as the Cu(II) source, and because of its stability, the reactions were performed in $H_2O$. The authors later developed three catalyst systems by alternating the Cu(II) salt, ligand and additives (AcOH), in order to tolerate a variety of α,β-unsaturated

(35) Chen, I.-H.; Yin, L.; Itano, W.; Kanai, M.; Shibasaki, M. *J. Am. Chem. Soc.* **2009**, *131*, 11664–11665.
(36) Kobayashi, S.; Xu, P.; Endo, T.; Ueno, M.; Kitanosono, T. *Angew. Chem. Int. Ed.* **2012**, *51*, 12763–12766.

carbonyls.[37] In addition to this study, Santos and co-workers also established their Cu(II)-catalyzed BCA reactions in 2012.[21f]

Besides the work mentioned above, other groups have also made significant contributions in this area, representatives of which are shown in Scheme 1.1.9. The Ni-catalyzed enantioselective BCA reactions by Fernández and co-workers resemble Yun's catalyst system, where a bisphosphine ligand gives the best enantioselectivity.[38] In the same year, Nishima and co-workers reported a bisoxazolinylphenyl–Rh(I) catalyzed BCA reactions.[39] Only 1 mol % Rh(I) catalyst is enough to promote the transformation with a high efficiency and comparable enantioselectivity. Their report also first included α,β-unsaturated amides, a class of important but challenging substrate due to its poorer electrophilicity than other carbonyl derivatives. Hong and co-workers also published an NHC–Cu-catalyzed enantioselective BCA reaction to a variety of α,β-unsaturated amides.[40] As shown in Scheme 1.1.9, synthetically useful Weinreb amides are good substrates, although the enantioselectivity is moderate (89:11 er). Other NHC–Cu-catalyzed enantioselective BCA strategies include the work by McQuade[41], Song[42] and more recently Scheit[43] and their co-workers.

(37) Kitanosono, T.; Xu, P.; Kobayashi, S. *Chem. Asian. J.* **2014**, *9*, 179–188.
(38) Lillo, V.; Geier, M. J.; Westcott, S. A.; Fernández, E. *Org. Biomol. Chem.* **2009**, *7*, 4674–4676.
(39) Shiomi, T.; Adachi, T.; Toribatake, K.; Zhou, L.; Nishiyama, H. *Chem. Commun.* **2009**, 5987–5989.
(40) Hirsch-Weil, D.; Abboud, K. A.; Hong, S. *Chem. Commun.* **2010**, *46*, 7525–7527.
(41) Park, J. K.; Lackey, H. H.; Rexford, M. D.; Kovnir, K.; Shatruk, M.; McQuade, D. T. *Org. Lett.* **2010**, *12*, 5008–5011.
(42) Zhao, L.; Ma, Y.; He, F.; Duan, W.; Chen, J.; Song, C. *J. Org. Chem.* **2013**, *78*, 1677–1681.
(43) Check, C. T.; Jang, K. P.; Schwamb, C. B.; Wong, A. S.; Wang, M. H.; Scheidt, K. A. *Angew. Chem. Int. Ed.* **2015**, *54*, 4264–4268.

**Scheme 1.1.9. Other representative work on transition metal-catalyzed BCAs**

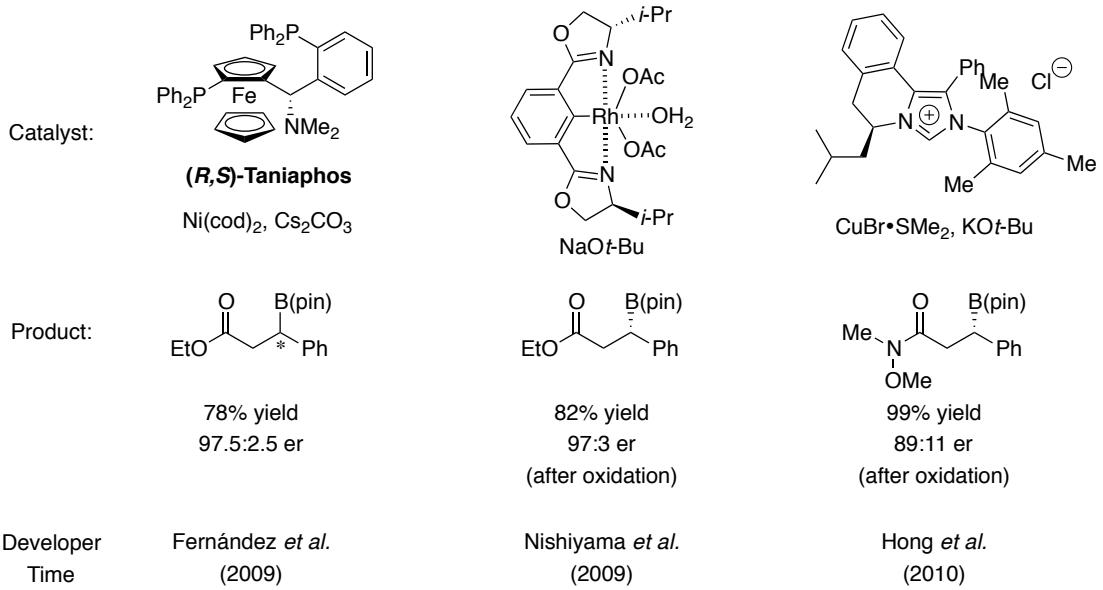


In addition, Ibrahem and Córdova in 2011 reported a proline derivative promoted Cu-catalzed enantioselective BCA reactions to α,β-unsaturated aldehydes, the products of which were transformed thorough Wittig olefinations without isolation.[44]

### *1.1.3. Boryl Conjugate Additions Catalyzed by a Transition Metal-Free Catalyst*

Catalytic enantioselective boryl conjugate additions provide an attractive platform to synthesize chiral molecules that contain a C–B bond. However, this type of transformations exclusively resided in the region of transition metal catalysis before the end of 2009. The aforementioned Cu (and other metals) catalyzed BCA reactions prove to be highly efficient and enantioselective towards α,β-unsaturated ketones, esters, nitriles and amides. Nevertheless, some common shortcomings of transition metal-catalyzed methods need to be pointed out:

(44) Ibrahem, I.; Breistein, P.; Córdova, A. *Angew. Chem. Int. Ed.* **2011**, *50*, 12036–12041.

(1) Most of the transition metal catalysts are sensitive to $O_2$ and/or $H_2O$. Thus, a rigorous removal of air and moisture is usually required in the reaction set-up (such as in a $N_2$ or Ar filled glove box).

(2) The substrate scope for each type of ligand is limited. There is no ligand that is suitable for all classes of substrates. For example, the most commonly used Josiphos ligand cannot promote reactions with cyclic substrates or β-substituted substrates with high enantioselectivity.

(3) The functional group compatibility of transition metal-catalyzed protocols (especially Cu-catalyzed ones) is not satisfying. Reports have shown Phosphine/NHC–Cu complexes are effective catalysts for Cu–B additions to aldehydes[45], imines[46], allenes[47] and alkynes[48]. Development of strategies that furnish the same C–B bond efficiently without interacting those functional groups in a muti-functional complex molecule is especially challenging.

With these flaws in mind, we would like to introduce the catalytic boryl conjugate addition reactions without any transition metal, ones that are mechanistically distinct from the traditional metal catalyzed ones. The first report belongs to our group in 2009, where a small NHC was discovered as an efficient catalyst.

---

(45) ref 10a.

(46) Beenen, M.; An, C.; Ellman, J. A. *J. Am. Chem. Soc.* **2008**, *130*, 6910–6911.

(47) (a) Meng, F.; Jang, H.; Jung, B.; Hoveyda, A. H. *Angew. Chem. Int. Ed.* **2013**, *52*, 5046–5051. (b) Meng, F.; Jung, M.; Haeffner, F.; Hoveyda, A. H. *Org. Lett.* **2013**, *15*, 1414–1417. and the references within.

(48) (a) Takahashi, K.; Ishiyama, T.; Miayura, N. *J. Organomet. Chem.* **2001**, *625*, 47−52. (b) Lee, J.-E.; Kwon, J.; Yun, J. *Chem. Commun.* **2008**, *44*, 733−734. (c) Kim, H. R.; Jung, I. G.; Yoo, K.; Jang, K.; Lee, E. S.; Yun, J.; Son, S. U. *Chem. Commun.* **2010**, *46*, 758−760. (d) Kim, H. R.; Yun, J. *Chem. Commun.* **2011**, *47*, 2943−2945. (e) Jang, H.; Zhugralin, A. R.; Lee, Y.; Hoveyda, A. H. *J. Am. Chem. Soc.* **2011**, *133*, 7859−7871.

In the very beginning of our study, the first question that we asked ourselves was: Why is the LCu-OR catalyzed BCA reaction so effective (L = ligand)? As shown in Scheme 1.1.10, the oxygen of Cu-OR binds to one of the borons in $B_2(pin)_2$, polarizing the B–B bond and promoting the other B(pin) unit to transfer to the Cu(I) center. What is the role of ligand? The Lewis basic ligand (phosphine or NHC) donate its electron density through Cu(I) into the orbitals of the alkoxide oxygen. According to the principle of Lewis base activation of Lewis acid,[49] the Cu(I) center becomes more Lewis acidic and the alkoxide oxygen becomes more Lewis basic. It is this enhanced Lewis basicity that facilitates the oxygen-boron binding and promotes the generation of LCu-B(pin) species.

The next questions were: Will a small organic Lewis basic itself sufficiently coordinate to the boron of $B_2(pin)_2$, polarize the B–B bond and promote the same BCA reaction? If so, will it be catalytic?

(49) For discussions on Lewis base activations of Lewis acids, see: (a) Guttmann, V. *The Donor–Acceptor Approach to Molecular Interactions*; Plenum Press, New York, 1978. (b) Denmark, S. E.; Beutner, G. L. *Angew. Chem., Int. Ed.* **2008**, *47*, 1560–1638.

**Scheme 1.1.10. B–B activation by a transition metal-alkoxide serving as the Lewis base**

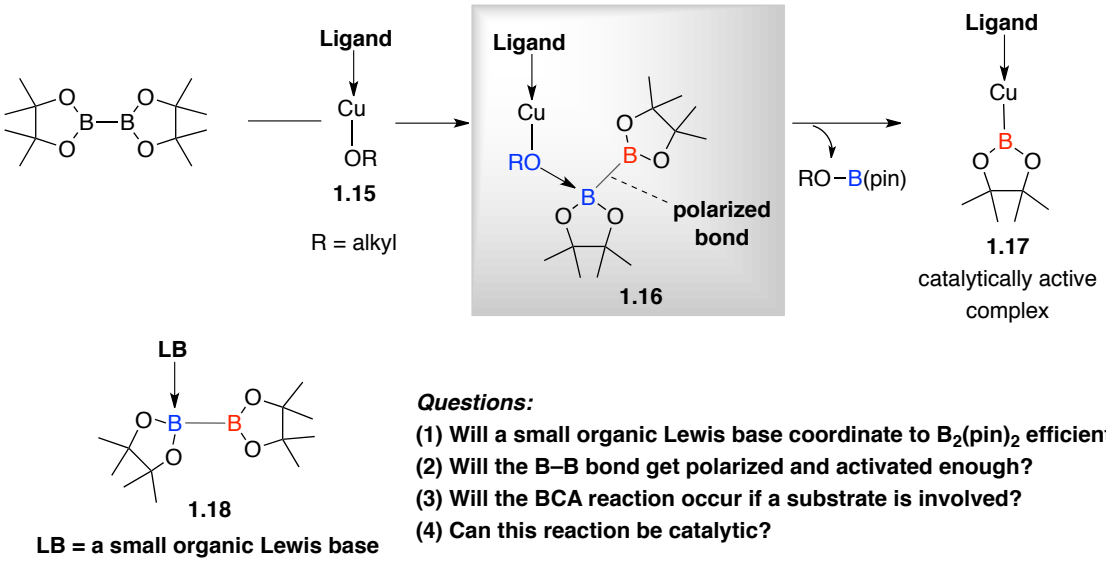


***Questions:***

**(1) Will a small organic Lewis base coordinate to $B_2(pin)_2$ efficiently?**
**(2) Will the B–B bond get polarized and activated enough?**
**(3) Will the BCA reaction occur if a substrate is involved?**
**(4) Can this reaction be catalytic?**

To answer these questions, a few small organic Lewis bases were chosen as candidates. Among them, we would like to study an N-heterocyclic carbene (NHC) first, due to its unique electronic nature: a strong σ donor and weak π acceptor (an introduction of NHC and its fruitful utility in organic synthesis will be detailed in the next chapter). When $B_2(pin)_2$ is treated with 1,3-biscyclohexylimidazolylidene **1.19** in thf-$d_8$ at –10 ºC, an NHC•diboron complex **1.20** is formed and characterized by $^{11}B$ NMR spectra (Scheme 1.1.11).[10] Specifically, the $^{11}B$ NMR signal of $B_2(pin)_2$ (30.1 ppm) disappears completely (>98% conv of $B_2(pin)_2$), and two signals (1.8 and 36.3 ppm) show up. The $sp^3$ hybridized boron (the blue one), which appears at 1.8 ppm, indicates the coordination of the NHC **1.19**. Interestingly, the $sp^2$ hybridized boron (the red one) appears as a more downfield signal (36.3 ppm) than $B_2(pin)_2$ (30.1 ppm). Clearly, the red boron becomes more ***electrophilic*** due to this NHC complexation. As the NHC coordinates to $B_2(pin)_2$, it polarizes the B–B bond towards the distal B(pin) unit. However, the extra electron density does not accumulate on the red boron atom of B(pin). Instead, it resides on the

two more electron negative oxygen atoms. Because of this Lewis base activation of Lewis acid scenario, the red boron turns more electrophilic, which means a downfield shift in $^{11}$B NMR spectra.

DFT calculations were also performed to simulate the B–B bond length of $B_2(pin)_2$ and NHC•diboron complex **1.20**. An increased bond length was observed from $B_2(pin)_2$ (1.703 Å) to NHC•diboron complex **1.20** (1.749 Å). This means the B–B bond gets weakened upon the NHC coordination. In 2012, Marder and co-workers reported the X-ray crystal structure of complex **1.20**. This critical work not only gives us the direct evidence of the existence of an NHC•diboron complex, but also suggesting its stability. The B–B length in this crystal structure is 1.743(2) Å, very similar as our calculated value 1.749 Å. It should be noted that NHC **1.19** is relatively a small one compared to the chiral NHCs we used for enantioselective reactions (see section **1.2**). The stability of NHC•diboron complex **1.19** must account for its lack of severe steric interaction between the NHC and the pinacol group of B(pin) units.

**Scheme 1.1.11. B–B bond activation by an NHC serving as the Lewis base**

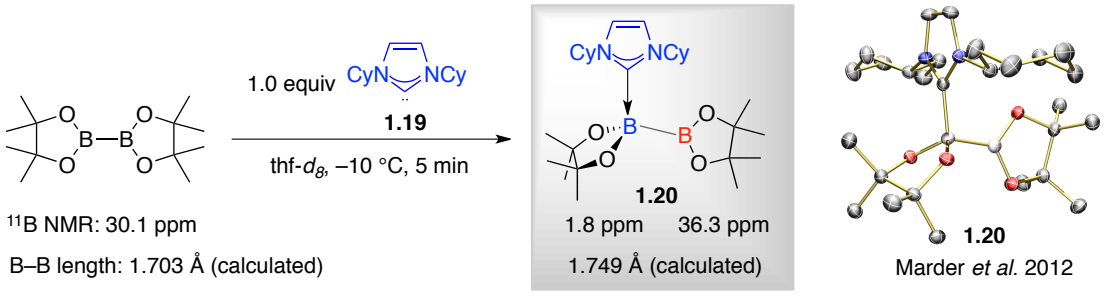


An NHC•diboron complex does not guarantee an efficient boryl conjugate addition. Thus, 2-cyclohexenone was treated with a mixture of 1.1 equiv $B_2(pin)_2$ and 10 mol % of an NHC (generated *in situ* from deprotonation of the corresponding imidazolium/imidazolinium salt)(Scheme 1.1.12).[10] It turned out that NHC derived from

imidazolium salt **1.21** was able to catalyze the BCA reaction very efficiently (>98% conv to **1.3b**). Increasing the size of the NHC N-aryl motifs (such as **1.22** and **1.23**) result in diminished reactivity (92% and 66% conv, **1.22** and **1.23**, respectively). The sterically most hindered NHC from **1.24** only gives the product with 45% conv. Those findings suggest that the NHC coordination of $B_2(pin)_2$ and/or subsequent B(pin) transfer are very sensitive to the substituent patterns of NHCs. In addition, the BCA reaction does not proceed without any NHC, or with less Lewis basic $PPh_3$ or $PCy_3$. This is not surprising since a similar reaction only proceed to 7% conv with $PBu_3$ (see Scheme 1.1.2). The result of $OPPh_3$ (50% conv) is very intriguing and unexpected, indicating it as an potential catalyst for Lewis base catalyzed transformations.

**Scheme 1.1.12. Catalyst screening of transition metal-free BCA reactions**[a]

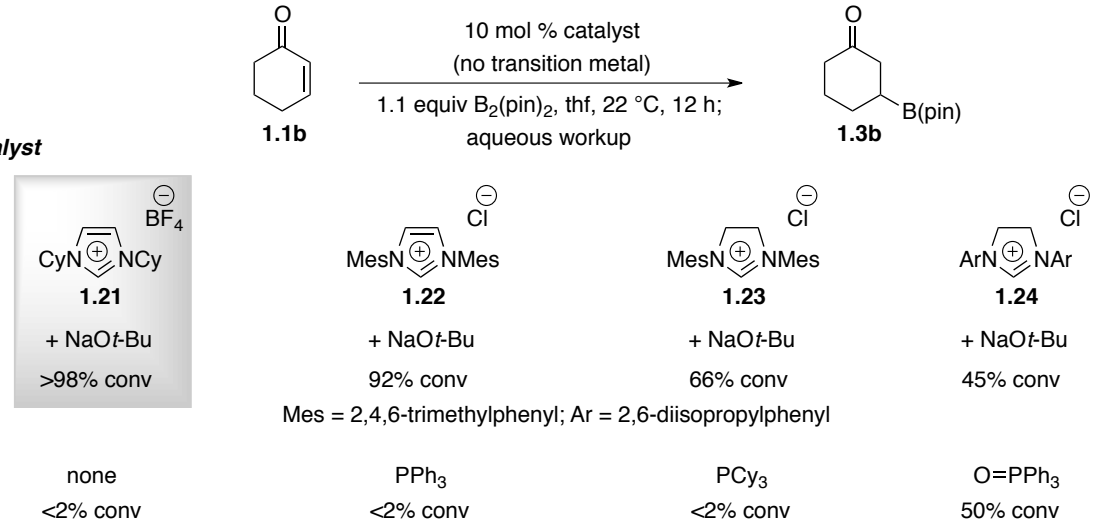


[a] Performed under a $N_2$ atm. Conversions to the desired product were determinied by analysis of 400 MHz $^1H$ NMR spectra of unpurifiled mixtures.

The NHC catalyzed boryl conjugate additions to α,β-unsaturated carbonyls proved to be very efficient and general. For example, cyclic enones with a different ring size (five to eight-membered ring) are equally effective substrates (**1.3b**, **1.3q** and **1.3r** for instance). Reactions with substrates that bear a sterically hindered neighboring

substituent are still amazingly efficient (**1.3s**, 98% yield with only 2.5 mol % cat in 1.0 h), especially compared to the same reaction with the previously mentioned phosphine–Cu catalyst (0% yield, see Scheme 1.1.6). Cyclic or acyclic esters (**1.3t** and **1.29**) are also suitable substrates, although a slightly higher catalyst loading (5 mol %) and longer reaction time (24 h) is required for a complete transformation. BCA reactions that generate boryl substituted quaternary carbon stereogenic centers (**1.25** and **1.30**), including the one bearing a bi-cyclic structure (**1.26**), are still quite efficient (91%, 92% and 78% yield, respectively).

Unlike most of the Cu-catalyzed BCA reactions, boryl enolate **1.31** can be isolated if aqueous workup is not used in the NHC catalyzed protocol (Scheme 1.1.14). More importantly, the reaction still proceeds with a high efficiency when 1-hexyne is added into the reaction solution, suggesting the alkyne group does not interfere the BCA process significantly (equation 1, Scheme 1.1.14). This is in contrast to its Cu-catalyzed alternatives, since involvement of 2.5 mol % CuO*t*-Bu completely shut down the reaction (<2% conv). In another example, benzaldehyde is applied instead of aqueous workup. The NHC catalyzed BCA reaction affords the β-boryl Aldol product **1.32** cleanly with a high diastereoselectivity (85% yield, >98:2 dr). The Cu-catalyzed one, however, gives only 31% of the desired product with 19% conv to benzaldehyde diboration.

**Scheme 1.1.13. Efficient BCA reactions catalyzed by a small NHC[a]**

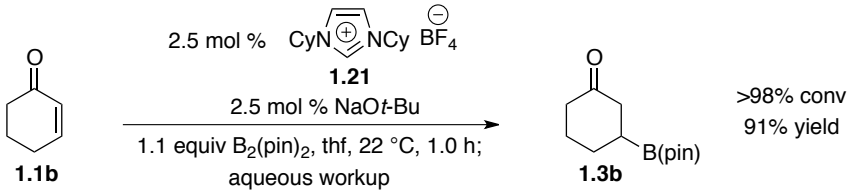


**1.1b** → **1.3b**: >98% conv, 91% yield

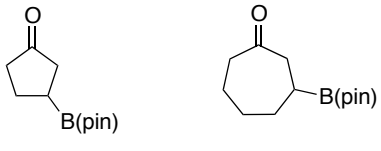

**1.3q**: >98% conv, 93% yield



**1.3r**: >98% conv, 93% yield

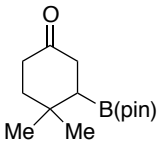

**1.3s**: >98% conv, 98% yield

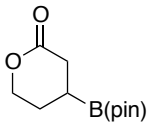

**1.3t**: >98% conv, 95% yield (5 mol % cat, 24 h)

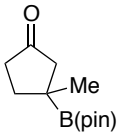

**1.25**: >98% conv, 91% yield (2.5 mol % cat, 12 h)

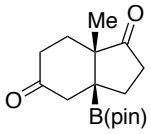

**1.26**: >98% conv, 78% yield, >98:2 dr (5 mol % cat, 6.0 h)

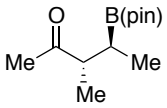

**1.27**: >98% conv, >98% yield, 2.5:1 dr

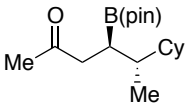

**1.28**: >98% conv, 70% yield, 7.2:1 dr (10 mol % cat, 2 h)

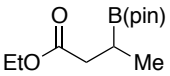

**1.29**: >98% conv, 93% yield (5 mol % cat, 24 h)

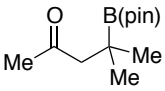

**1.30**: >98% conv, 92% yield (5 mol % cat, 6 h)

[a] Performed under a $N_2$ atm. Conversions to the desired product were determinied by analysis of 400 MHz $^1$H NMR spectra of unpurifiled mixtures. Yields of purified products are given.

**Scheme 1.1.14. Functional group compatibility of NHC catalyzed BCA reactions[a]**

(1)

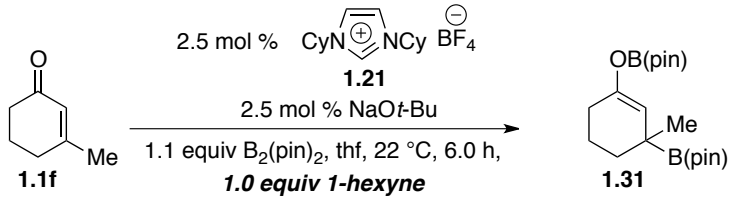


**1.1f** → **1.31**: **85% conv, 81% yield**

***with 2.5 mol % CuOt-Bu: <2% conv***

(2)

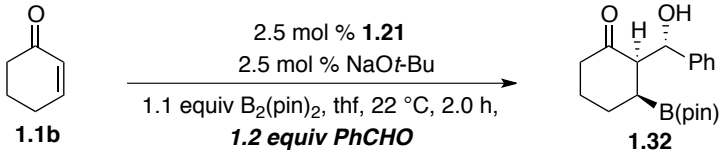


**1.1b** → **1.32**

***with 2.5 mol % CuOt-Bu: 31% yield, >98:2 dr***
***19% to benzaldehyde diboration***

**>98% conv**
**85% yield**
**>98:2 dr**

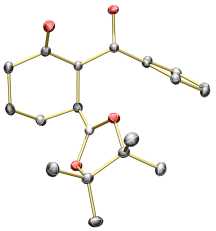

X-ray structure of **1.32**

[a] see Scheme 1.1.13.

The above examples clearly demonstrate a high functional group compatibility of the current transition metal-free method: without the use of metal salts, we avoid the possibility of metal-boryl addition to an alkyne and aldehyde group. In another word, it offers a complementary reactivity and selectivity pattern compared to the state of the art Cu-catalyzed transformations. In addition, the aforementioned experiments exclude the possibility of trace metal contaminations of our reactions, as addition of a metal leads to a different outcome.

The current strategy was utilized in Ibrahem and Córdova's work in 2012, where they report BCA/Wittig sequential reactions to afford homoallyl B(pin) compounds.[50] Higher temperature and excess MeOH were applied in those transformations, the reasons for which will be discussed in the next section.

Our initial proposed mechanism lies on the observation of NHC•diboron complex **1.20**. As mentioned before, the B–B bond of **1.20** is polarized and the electron density is pushed towards the uncoordinated B(pin) unit. This alternation in the electron distribution result in an enhancement of the nucleophilicity of the uncoordinated B(pin) unit. Thus, as an enone approaches the NHC•diboron complex, the B(pin) group transfers to the β-carbon of the enone, resulting in a negatively charged enolate which quickly combines with the positively charged NHC–B(pin) and forms intermediate **1.33**. This intermediate is in equilibrium with NHC bond boryl enolate **1.34**, which is further converted into the product **1.31** and releases the NHC. The C–B bond formation step was recently analyzed in our computational studies, the details of which will be illustrated in the next chapter.

(50) Ibrahem, I.; Breistein, P.; Córdova, A. *Chem. Eur. J.* **2012**, *18*, 5175–5179

The NHC-catalyzed boryl conjugate addition to a variety of α,β-unsaturated carbonyls unveils an entirely new avenue in the realm of catalysis. It is the first transition metal-free catalytic transformation to form C–B bonds. A number of Lewis base catalyzed protocols to construct C–B, C–Si and C–C bonds were discovered after this report. In the next section, I will focus on the development of an enantioselective version of this transformation and illustrate the knowledge we learned during our studies.

**Scheme 1.1.15. Proposed mechanism for NHC-catalyzed BCA reaction**

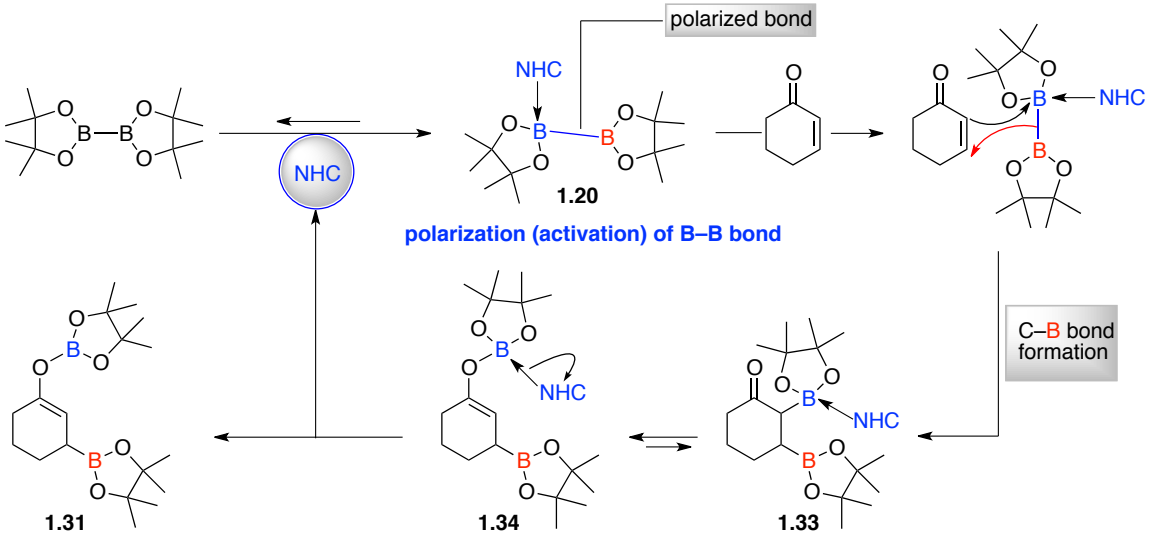


The strategy of using an NHC as the Lewis base catalyst can also be applied in the activation of B–Si bond and promote the silyl conjugate additions (SCAs).[51] Similarly as the BCA reactions, almost all the catalytic silyl conjugate addition reactions discovered require transition metal catalysts until our report in 2011.[52]

Unlike the related NHC-catalyzed BCA reaction, the SCA reaction does not proceed under the same reaction condition (equation 1, Scheme 1.1.16). This is not because the NHC coordination to $PhMe_2Si$–B(pin) is hampered, as the corresponding

(51) O'Brien, J. M.; Hoveyda, A. H. *J. Am. Chem. Soc.* **2011**, *133*, 7712–7715.

(52) For a recent review on metal-catalyzed enantioselective silyl conjugate additions, see: Hartmann, E.; Vyas, D. J.; Oestreich, M. *Chem. Commun.* **2011**, *47*, 7917–7932.

NHC•borylsilane complex **1.36** (>98% conv, within 5 min) was observed by $^{11}B$ NMR spectrum (the signal of $sp^3$ boron is 8.02 ppm). However, the efficiency of the SCA reaction is greatly enhanced if $H_2O$ is involved (95% conv, equation 2, Scheme 1.1.16). This is quite surprising since in the previously mentioned protocols (Cu- or NHC-catalyzed BCA reactions), exclusion of moisture is required to avoid catalyst decomposition. It is noteworthy that other proton additives (including MeOH) are not as good as $H_2O$ in this NHC-catalyzed SCA reaction. The role of $H_2O$ was not clear at that time, but one possible explanation could be that it hydrolyzes the $PhMe_2Si$-B(pin) into $PhMe_2Si$–$B(OH)_2$, a sterically less hindered species that facilitates the SCA process. In the next chapter, I have included our detailed mechanistic studies on this SCA transformation.

**Scheme 1.1.16. Initial discoveries of NHC-catalyzed SCA reactions**[a]

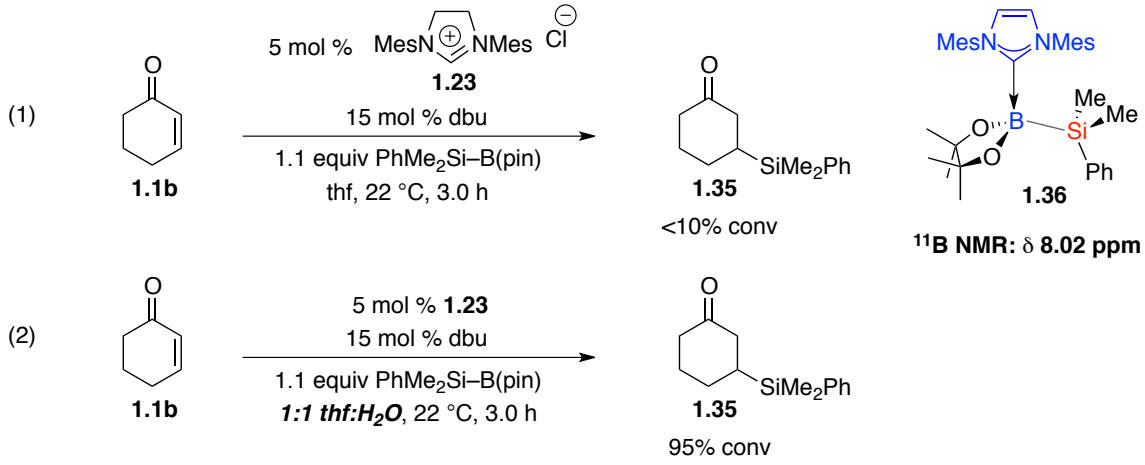


[a] See Scheme 1.1.12.

When a series of chiral NHC(s) were tested in the similar reaction condition, silyl conjugate additions were found to be ***enantioselective***! As shown in Scheme 1.1.17, the monodentate $C_2$-symmetric NHC derived from **1.37** was discovered as the optimal catalyst. Cyclic enones are generally effective substrates (such as **1.38** and **1.39**), of

which the enantiomeric ratios are from 90:10 to >98:2. SCA reactions with lactones (**1.40**) are efficient, but with diminished er (85:15 er). Acyclic α,β-unsaturated ketones (**1.41** and **1.43**, for instance), as well as esters (**1.44**) are slower substrates, with moderate to good enantioselectivity (87:13 to 95:5 er). Surprisingly, the one that bears a strong electron withdrawing substituent (**1.42**) completely shuts down the reaction, the reason for which will be discussed in the next chapter. Interestingly, α,β-unsaturated aldehydes (**1.45**) afford the desired products with good yields and ers. This is especially noteworthy since catalysts involving Cu are known to promote the Cu–B addition to an aldehyde group. In addition, NHC is able to react with an aldehyde group, forming Breslow intermediate, which can lead to a variety of transformations.[53] However, our NHC-catalyzed SCA reactions as well as the aforementioned BCA reactions seem not to be interfered by this well-established process.

The fact that the NHC-catalyzed SCA reactions are enantioselective tells us the chiral NHC is intimately involved in the C–Si bond transformation. Thus, enantioselective BCA reactions catalyzed by a chiral NHC are possible. It also teaches us a proton additive accelerates the NHC-catalyzed reactions, a strategy that is not obvious to us in the beginning.

(53) (a) Breslow, R. *J. Am. Chem. Soc.* **1958**, *80*, 3719–3726. (b) For a recent review on NHC-catalyzed reactions, see: Flanigan, D. M.; Romanov-Michailidis, F.; White, N. A.; Rovis, T. *Chem. Rev.* **2015**, DOI: 10.1021/acs.chemrev5b00060.

**Scheme 1.1.17. NHC-catalyzed enantioselective SCA reactions**[a]

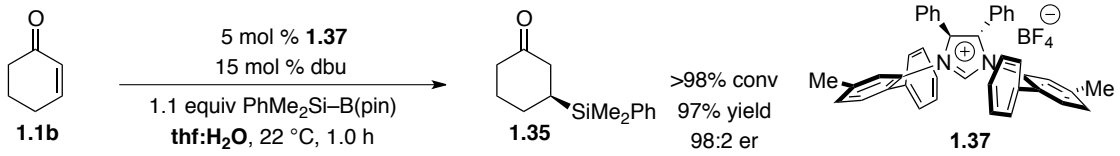


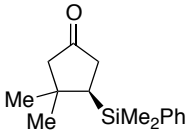

**1.38**
83% conv
73% yield, 94.5:5.5 er
(3.0 h)

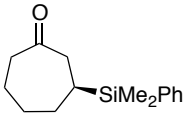

**1.39**
>98% conv
95% yield, 98:2 er
(3.0 h)

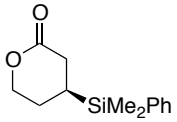

**1.40**
82% conv
71% yield, 85:15 er
(3.0 h)

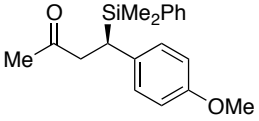

**1.41**
>98% conv
94% yield, 95:5 er
(7.5 mol % cat, 12 h)

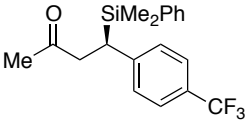

**1.42**
<2 % conv
(7.5 mol % cat, 12 h)

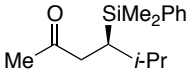

**1.43**
84% conv
81% yield, 87:13 er
(7.5 mol % cat, 12 h)

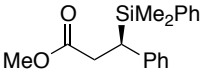

**1.44**
60% conv
54% yield, 95:5 er
(12.5 mol % cat, 12 h)

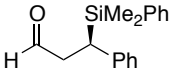

**1.45**
>98% conv
66% yield, 95:5 er
(12.5 mol % cat, 12 h)

[a] see Scheme 1.1.13.

Inspired by our NHC-catalyzed BCA reactions, Fernández and co-workers developed a series of phosphine-catalyzed boryl conjugate additions (Scheme 1.1.18).[54] The authors found out some mono-phosphines were good catalyst, including $PPh_3$ and $PCy_3$, while bis-phosphines are generally less effective. In additions, an excess amount of base ($Cs_2CO_3$) and alcohol (MeOH) are required for efficient reactions, likely because the coordination of phosphine to diboron is facilitated after converting $B_2(pin)_2$ into $(MeO)_2B–B(pin)$(the use of alcohol for NHC-catalyzed enantioselective reactions will be discussed in the next section). In addition, a higher temperature (70 ºC) is needed compared to the NHC-catalyzed protocol (see Scheme 1.1.13). This is not surprising

(54) (a) Bonet, A.; Gulyás, H.; Fernández, E. *Angew. Chem. Int. Ed.* **2010**, *49*, 5130–5134. (b) Pubill-Ulldemolins, C.; Bonet, A.; Gulyás, H.; Bo, C.; Fernández, E. *Org. Biomol. Chem.* **2012**, *10*, 9677–9682. (c) Pubill-Ulldemolins, C.; Bonet, A.; Bo, C.; Gulyás, H.; Fernández, E. *Chem. Eur. J.* **2012**, *18*, 1121–1126.

since $PPh_3$ is known to be less Lewis basic than the NHC derived from **1.21**, resulting in a weaker activation of the B–B bond of $B_2(pin)_2$. In this report, the substrate scope is quite limited (the differences between each substrate is small) and in many cases, isolation yields were not reported. Efficient BCA reactions to α,β-unsaturated ketones were observed if $PPh_3$ is used (**1.47**, **1.48** and **1.49**). However, when the "optimized" chiral phosphine (Josiphos) is subjected, lower conversions and unpredictable enantioselectivities significantly limit the applicability of the reactions (**1.47** to **1.50**). Esters as well as cyclic ketones give poor results (low conversion and poor enantioselectivity, respectively). Control experiments were performed to avoid the possibility of trace metal contamination.

The same group also studied the mechanism of the phosphine-catalyzed BCA reactions in details. Surprisingly, it is the complex **1.51**, not the phosphine•diboron complex, that was believed to be responsible for catalytic B(pin) transfer. **1.51** was characterized by $^{11}B$ NMR and $^{31}P$ NMR spectra, the former of which is similar as the NHC•diboron one previously discussed (see Scheme 1.1.11). Interestingly, the authors proposed a complicated transition state for the C–B bond formation, one that is hard to believe to account for the origin of the observed enantioselectivity.

Having noticed the reaction may be promoted by an alkoxide, Fernández and co-workers worked on developing this class of catalysts. In 2012, they reported the BCA reactions catalyzed by Verkade's base. This strong organic base (pKa = 26.2 in $H_2O$) deprotonates MeOH completely to generate methoxide anion, which activates the B-B bond and promote the B(pin) conjugate additions. It is noteworthy that 70 ºC and 24 h are

still required for complete reactions, suggesting that methoxide is still not as effective as the NHCs.

**Scheme 1.1.18. Phosphine/alkoxide-catalyzed BCA reactions by Fernández *et al.***

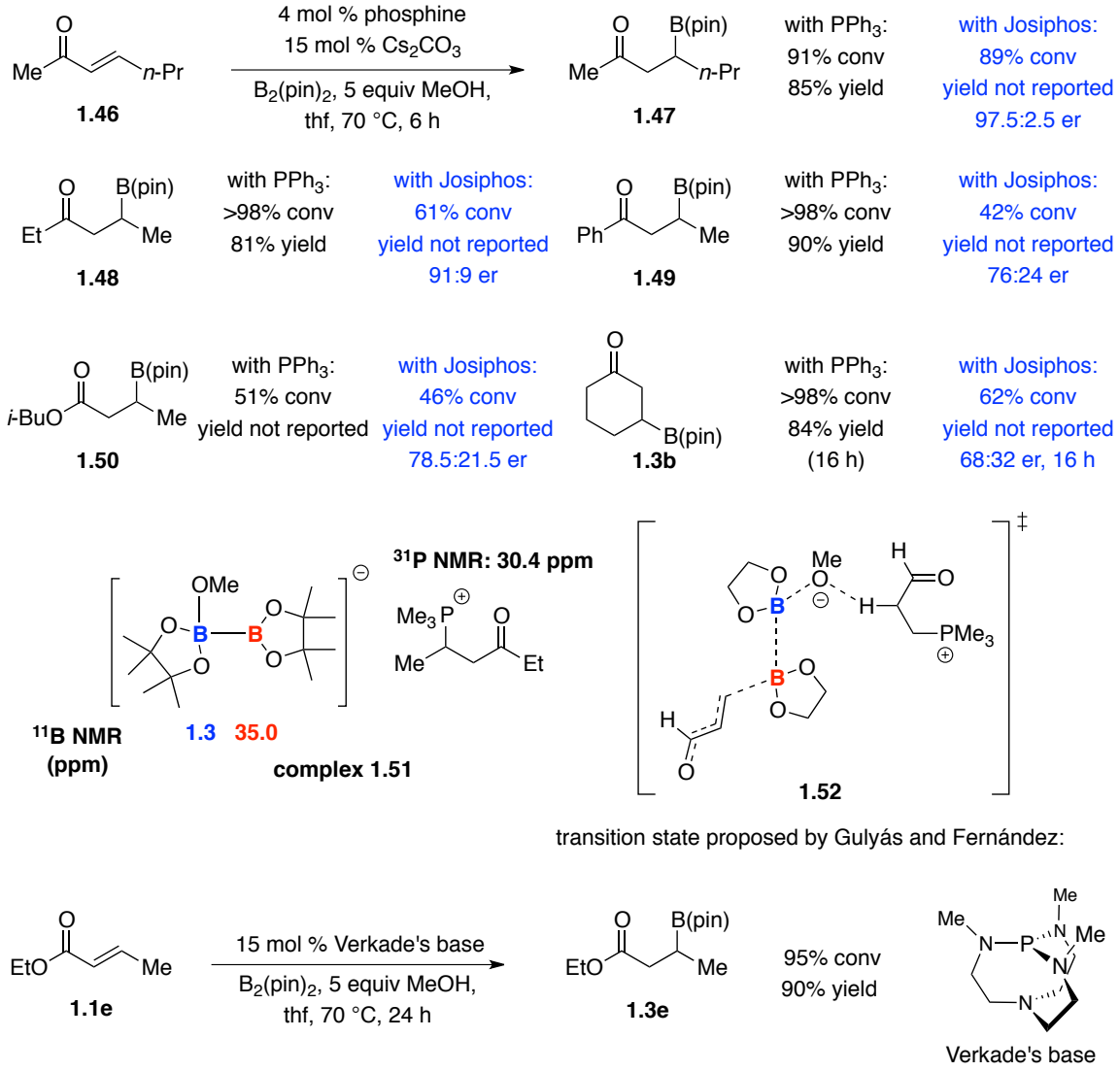


## *1.2. NHC-catalyzed Enantioselective Boryl Conjugate Additions to Generate Boron Substituted Tertiary Carbon Stereogenic Centers*

### *1.2.1. Initial Studies*

The enantioselective boryl conjugate addition reaction to α,β-unsaturated carbonyls by a chiral NHC is of great importance, since it not only offers a complementary reactivity and selectivity pattern compared to the well-established metal-catalyzed alternatives, but also provides a distinct mechanism to study. More specifically, mechanistic investigations of the Lewis base catalyzed reactions, especially the enantioselective ones, will help us to improve our enantioselective BCA reactions, as well as develop new types of transformations. It should be noted that there was no general strategy for transition metal-free enantioselective BCA reactions before this study, which was later reported in *J. Am. Chem. Soc.* in 2012.[55]

**Scheme 1.2.1. Inefficient BCA reactions catalyzed by a chiral NHC[a]**

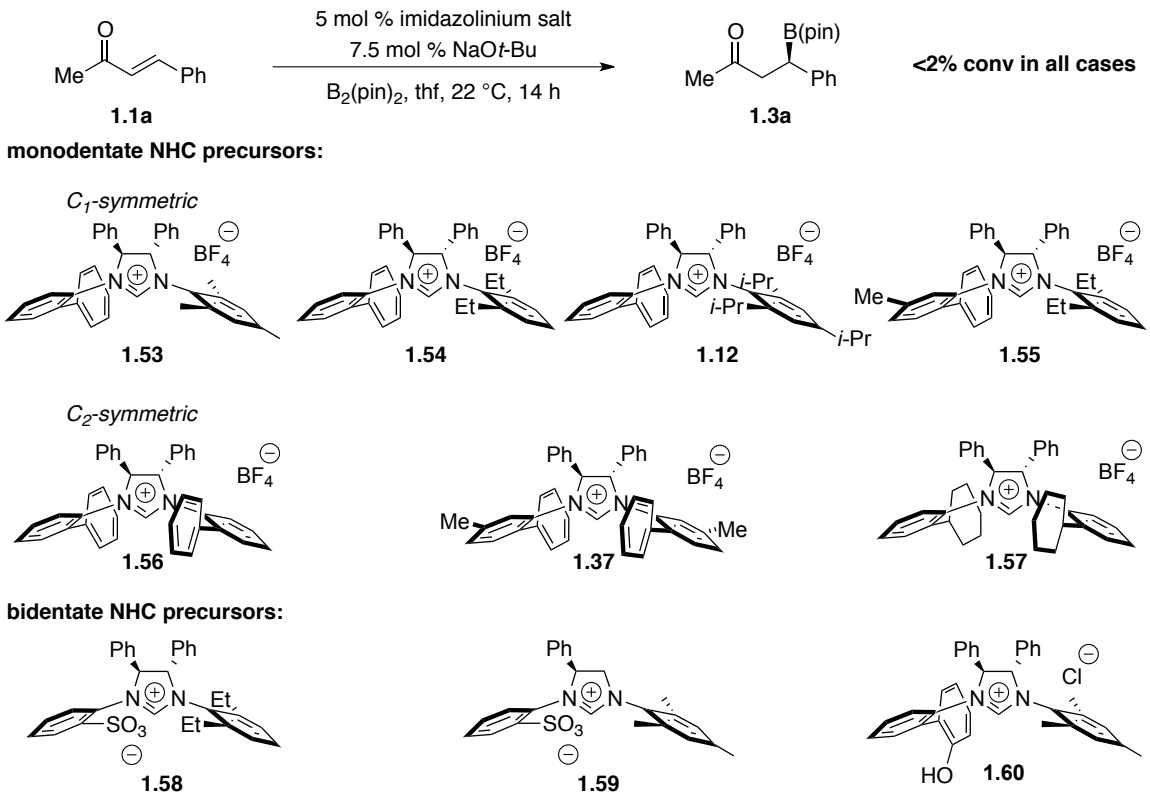


[a] see Scheme 1.1.13.

(55) Wu, H.; Radomkit, S.; O'Brien, J. M.; Hoveyda, A. H. *J. Am. Chem. Soc.* **2012**, *134*, 8277–8285.

In the very beginning of this project, a variety of chiral NHCs, ones that were developed in this group for different transformations,[56] were tested under the same reaction reported in 2009. As shown in Scheme 1.2.1, there is <2% conv for all the reactions, no matter what NHC is used. One hypothesis lies on the inefficient coordination of the chiral NHC to $B_2(pin)_2$, as the steric bulk of the N-aryl motifs of the NHC may have severe interactions with the pinacol group of $B_2(pin)_2$. This is later supported by the $^{11}B$ NMR study of the NHC•diboron complex **1.62** (Scheme 1.2.2). Although detected as two signals in the spectrum, the $sp^3$ hybridized boron appears at 12.2 ppm, a more downfield chemical shift than the ones of traditional $sp^3$ hybridized borons (typically between –30 to 10 ppm). This suggest a weak coordination of the NHC to $B_2(pin)_2$ occur in this case. It is possible that the B–B bond is not activated enough because of this weak coordination and/or the complex is sterically too encumbered to react with the substrate. Either will lead to inefficient BCA reactions. In addition, if NHC precursor **1.37** is used instead of **1.61** in the same reaction depicted in Scheme 1.2.2, there is no complex formation.

**Scheme 1.2.2. Inefficient BCA reactions catalyzed by a chiral NHC**

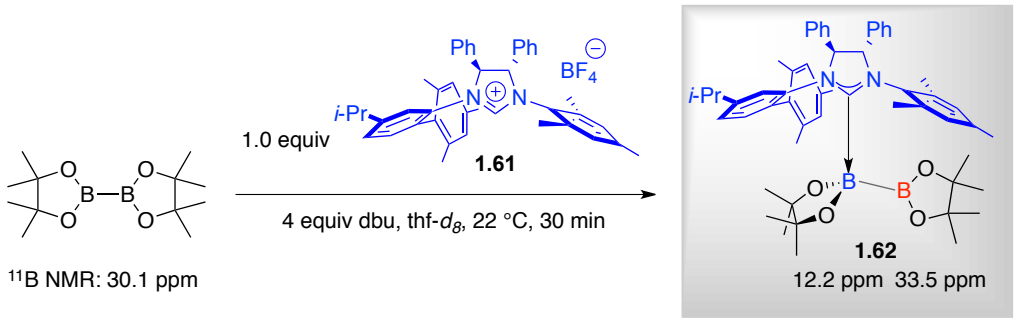


***No complex formation if 1.37 is used instead of 1.61.***

(56) (a) van Velduizen, J. J.; Campbell, J. E.; Giudici, R. E.; Hoveyda, A. H. *J. Am. Chem. Soc.* **2005**, *127*, 6877–6882. (b) Brown, M. K.; May, T. L.; Baxter, C. A.; Hoveyda, A. H. *Angew. Chem., Int. Ed.* **2007**, *46*, 1097-1100. (c) Lee, K.-s.; Hoveyda, A. H. *J. Org. Chem.* **2009**, *74*, 4455–4462.

Enlightened by the previous studies on NHC-catalyzed SCA reactions (Scheme 1.1.16), where $H_2O$ was used to facilitate the transformation, we attempted to add a proton additive in the chiral NHC-catalyzed BCA reactions. As shown in Table 1.2.1, addition of 20 equiv $H_2O$ results in a heterogeneous solution (entry 2). After 14 h, the reaction leads to a complex mixture and a complete decomposition of $B_2(pin)_2$ was observed. Fortunately, the use of MeOH instead of $H_2O$ gives the desired product **1.3a** in 68% conv and 81:19 er (entry 3). Although the enantioselectivity is moderate, this result is very important since it indicates the chiral NHC is intimately involved in the C–B bond formation step. To make sure there is no trace amount of transition metal involved in the reaction (trace amount of Zn, Cu *etc* were reported in some batches of NaO*t*-Bu), as well as maintain the high quality of the base (NaO*t*-Bu reacts with $H_2O$ and/or $CO_2$), we begin to test the applicability of an organic base, the high quality of which can usually be obtained by a simple distillation. While 20 mol % dbn (1,5-diazabicyclo[4.3.0]non-5-ene) gives the same conversion as 7.5 mol % NaO*t*-Bu, the use of dbu (1,8-diazabicyclo[5.4.0]undec-7-ene, pka = 13 in $H_2O$) enhances the reaction efficiency (85% conv, entry 5). BCA reactions will be hampered if less dbu (10 mol % dbu, 43% conv, entry 6) or less MeOH (1.2 equiv MeOH, 33% conv, entry 7) are applied. Interestingly, the reaction still proceeds to 21% conversion without the use of NHC (entry 8), which suggests a possible background process may corrode the enantioselectivity of the NHC-catalyzed reaction. The fact that methoxide is able to promote the reaction in a lower efficiency is consistent with the observation made by Fernández and co-workers (Scheme 1.1.18). Other alcohol additives (*i*-PrOH and *t*-BuOH) are not as effective as MeOH in the NHC-catalyzed BCA transformations.

**Table 1.2.1. Initial study of NHC-catalyzed Enantioselective BCA reactions**[a]

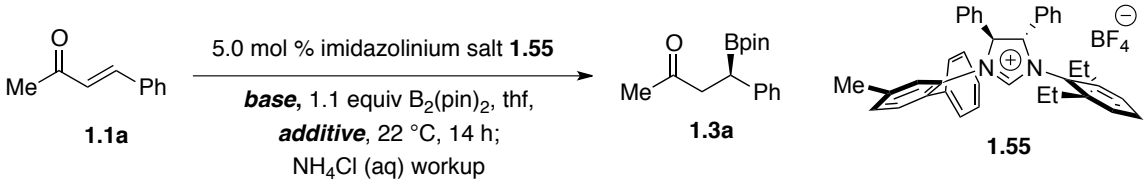


| entry | base | mol % (base) | additive | equiv (additive) | conv (%) | er |
|---|---|---|---|---|---|---|
| 1 | NaO*t*-Bu | 7.5 | - | 0 | <2 | - |
| 2 | NaO*t*-Bu | 7.5 | $H_2O$ | 20 | <5[b] | - |
| 3 | NaO*t*-Bu | 7.5 | MeOH | 20 | 68 | 81:19 |
| 4 | dbn[c] | 20 | MeOH | 20 | 68 | 84:16 |
| 5 | dbu | 20 | MeOH | 20 | 85 | 84:16 |
| 6 | dbu | 10 | MeOH | 20 | 43 | 85:15 |
| 7 | dbu | 20 | MeOH | 1.2 | 33 | 84:16 |
| 8[e] | dbu | 20 | MeOH | 20 | 21 | - |
| 9 | dbu | 20 | *i*-PrOH | 20 | 30 | - |
| 10 | dbu | 20 | *t*-BuOH | 20 | <5 | - |

[a] Performed under a $N_2$ atm. Conversions to the desired product were determinied by analysis of 400 MHz $^1$H NMR spectra of unpurifiled mixtures. Enantiomeric ratios (ers) were determined by HPLC analysis from the isolated products. [b] $B_2(pin)_2$ was completely decomposed. [c] dbn = 1,5-diazabicyclo[4.3.0]non-5-ene. [d] dbu = 1,8-diazabicyclo[5.4.0]undec-7-ene. [e] no imidazolinium salt is used.

Similar as previously mentioned SCA processes (Scheme 1.1.16), excess amount of base (20 mol % dbu) and MeOH used in the current reaction may account for a partial hydrolysis of $B_2(pin)_2$ into (MeO)(RO)B–B(pin) **1.63** (RO = MeO or pinacol). Indeed, we did observe a proton signal that appears at 1.23 ppm, the same as the methyl proton of free pinacol, in the $^1$H NMR spectra of the aforementioned reactions in Table 1.2.1. The resulting diboron **1.63** contains a boron that is less sterically hindered than the one with the pinacol, and thus can readily interact with a large chiral NHC to form complex **1.64** (Scheme 1.2.3). Because of the efficient coordination, the B–B bond gets activated and

promotes the B(pin) addition to unsaturated carbonyls. Further experiments aiming at elucidation of the features of complex **1.64** will be discussed in details in Chapter 2.

**Scheme 1.2.3. MeOH hydrolysis of $B_2(pin)_2$ facilitates the NHC coordination**

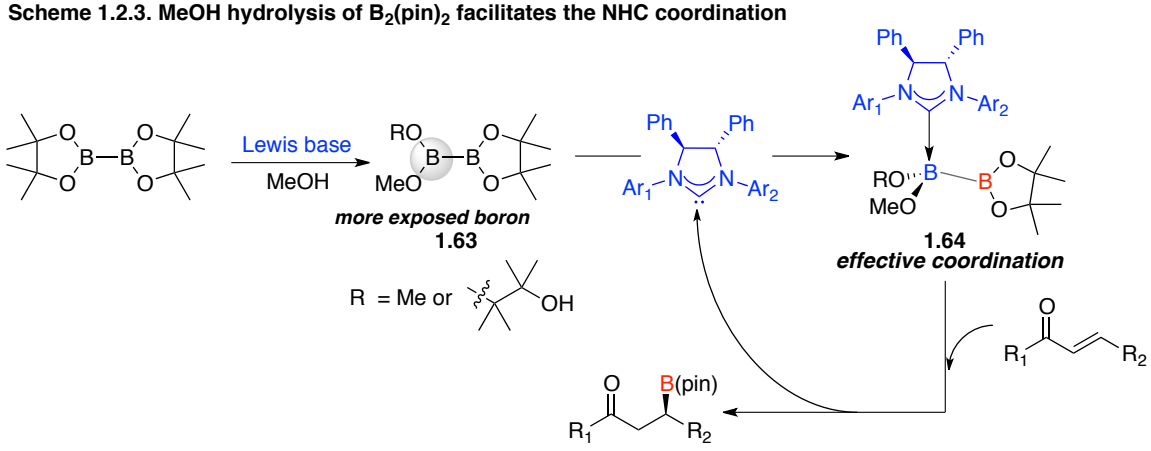


The enhanced reaction efficiency as an excess amount of base and MeOH are used is not limited to the reactions catalyzed by NHC derived from **1.55**. In Table 1.2.2, where a $C_2$-symmetric NHC (from deprotonation of **1.37**) serves as the catalyst, the same trend applies too. Interestingly, the conversions in Table 1.2.2 are generally lower than the ones in Table 1.2.1, but the enantioselectivities are slightly higher (entry 2–4, Table 1.2.2 vs entry 3, 6, 5, Table 1.2.1). Thus, a systematic catalyst screening is necessary for discovery of the optimal NHC for the current reaction.

**Table 1.2.2. The influence of base and MeOH in another NHC-catalyzed enantioselective BCA reactions[a]**

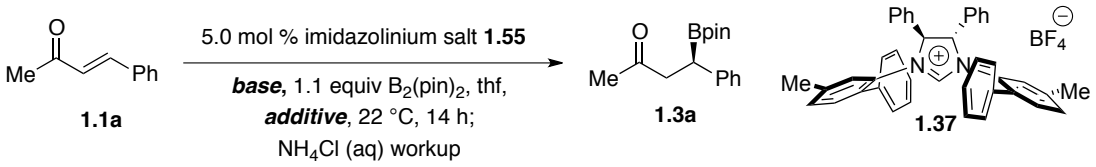


| entry | base | mol % (base) | additive | equiv (additive) | conv (%) | er |
|---|---|---|---|---|---|---|
| 1 | NaO*t*-Bu | 7.5 | - | 0 | <5 | - |
| 2 | NaO*t*-Bu | 7.5 | MeOH | 20 | 24 | 86.5:13.5 |
| 3 | dbu | 10 | MeOH | 20 | 31 | 90:10 |
| 4 | dbu | 20 | MeOH | 20 | 47 | 92:8 |

[a] See Table 1.2.1.

### *1.2.2. NHC Screening of the Catalytic Enantioselective BCA Reactions*

With the same reaction condition as entry 4, Table 1.2.2 (also as entry 5, Table 1.2.1), we have tried a variety of chiral imidazolinium salts, the results of which are summarized in Table 1.2.3. The sulfonate containing bidentate NHC (derived from **1.59**, entry 1) catalyzes the BCA reaction with moderate conversion (48%), but in low enantioselectivity (47:53 er). The same process with a monodentate NHC bearing a monophenyl backbone (derived from **1.64**, entry 2) is not efficient (30% conv). Thus, most of the catalyst investigations were performed on monodentate NHC(s) that contain a biphenyl backbone. Compared with the NHC from **1.53**, the more hindered one from **1.54** promotes the reaction with an enhanced enantioselectivity (81:19 er from **1.54** vs 56:44 er from **1.53**), although the conversions are both low. Further increasing the size of the symmetric N-aryl motif (**1.12**, entry 5) does not improve the results. A methyl substituent at the ortho position of the unsymmetric N-aryl motif (**1.65**, entry 6) diminishes both the reaction efficiency and selectivity. Fortunately, reactions with NHCs that bear a meta substituent of the unsymmetric N-aryl motif (**1.66** and **1.67**, entry 7 and 8) proceed with

enhanced conversions (82% and 78% conv., respectively). Further modifications of the NHCs result in the ortho mesityl substituted NHC, derived from **1.61** as the optimized one to promote the transformation with 81% conv. and 95:5 er. In addition, $C_2$-symmetric NHCs are also suitable catalysts, the one from **1.37** catalyze the reaction with a comparable efficiency and selectivity (87% conv., 92:8 er, entry 13). Interestingly, we found increasing the amount of MeOH used in the reaction improves its efficiency. Thus, when the NHC from **1.61** serve as the catalyst, the BCA reaction finishes in 14 h with a high enantioselectivity (>98% conv, 96:4 er, entry 15).

It should be noted that the synthesis of $C_2$-symmetic imidazolinium salt **1.37** is much easier than the $C_1$-symmetric **1.61**. Thus, we also investigated the NHC from **1.37** in our following reactions with different substrates.

**Table 1.2.3. Catalyst screening for NHC-catalyzed enantioselective BCA reactions**[a]

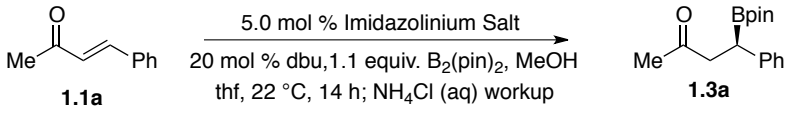


**1.1a** **1.3a**

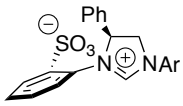

**1.59** Ar = 2,6-$(Et)_2C_6H_3$

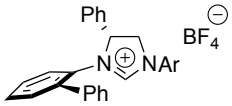

**1.64** Ar = 2,6-$(Et)_2C_6H_3$

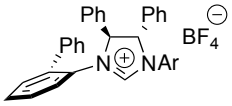

**1.53** Ar = Mes
**1.54** Ar = 2,6-$(Et)_2C_6H_3$
**1.12** Ar = 2,6-$(i\text{-}Pr)_2C_6H_3$

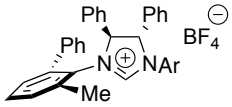

**1.65** Ar = 2,6-$(Et)_2C_6H_3$

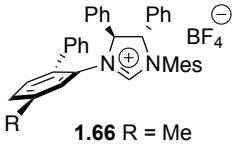

**1.66** R = Me
**1.67** R = *i*-Pr

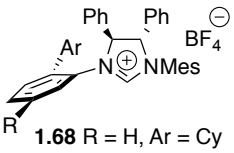

**1.68** R = H, Ar = Cy
**1.69** R = H, Ar = Mes
**1.61** R = *i*-Pr, Ar = Mes

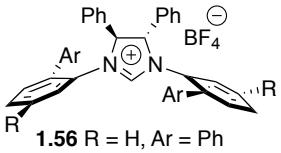

**1.56** R = H, Ar = Ph
**1.37** R = Me, Ar = Ph
**1.57** R = H, Ar = Cy

| entry | Imida. Salt | conv (%) | er |
|---|---|---|---|
| 1 | **1.59** | 48 | 47:53 |
| 2 | **1.64** | 30 | 31:69 |
| 3 | **1.53** | 10 | 56:44 |
| 4 | **1.54** | 37 | 81:19 |
| 5 | **1.12** | 24 | 80:20 |
| 6 | **1.65** | 25 | 72:28 |
| 7 | **1.66** | 82 | 80.5:19.5 |
| 8 | **1.67** | 78 | 76:24 |
| 9 | **1.68** | 37 | 72:28 |
| 10 | **1.69** | 30 | 94:6 |
| 11 | **1.70** | 81 | 95:5 |
| 12 | **1.56** | 35 | 82:18 |
| 13 | **1.37** | 87 | 92:8 |
| 14 | **1.57** | 14 | 35:65 |
| 15[b] | **1.61** | >98% | 96:4 |

[a] See Table 1.2.1. [b] with 60 equiv of MeOH.

The synthetic route of imidazolinium salt **1.37** is summarized in Scheme 1.2.4. 2-Bromo-4-methyl aniline **1.70** is subjected into a modified Sandmeyer reaction.[57] The resulting **1.71** is coupled with the chiral diamine twice, forming the diamine **1.72** in 71% yield, which is cyclized with triethyl orthoformate and $NH_4BF_4$ to afford the desired imidazolinium salt **1.37**. Although only three steps and 23% overall yield are obtained in this synthesis, the low efficiency of the Sandmeyer reaction and the use of a high loading precious transition metal (10 mol % $Pd(OAc)_2$) in the cross-coupling reaction still remain to be improved.

**Scheme 1.2.4. Synthesis of imidazolinium salt 1.37**

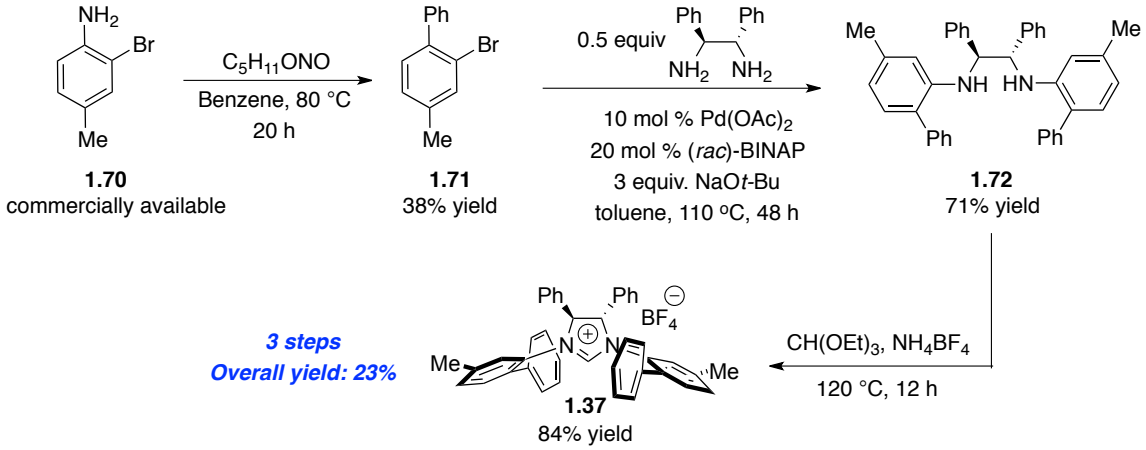


As a comparison, the synthesis of imidazolinium salt **1.61** begins with a similar Sandmeyer reaction but affording the corresponding iodide **1.74** efficiently. The Suzuki cross-coupling reaction with mesityl B(pin) results in the key bromide **1.75** in 83% yield and complete regioselectivity (<2% cross coupling with Br). Next, two Buchwald-Hartwig C–N cross-coupling reactions give the diamine **1.77** with good yields (75% and 72% yield, respectively). The synthesis finishes with the cyclization reaction to furnish

(57) For a review on Sandmeyer reaction, see: Hodgson, H. H. *Chem. Rev.* **1947**, *40*, 251–277.

imidazolinium salt **1.61** in five steps with a 31% overall yield. Again, the use of 20 mol % $Pd(OAc)_2$ and 40 mol % BINAP, although necessary, renders the synthesis costly.

**Scheme 1.2.5. Synthesis of imidazolinium salt 1.61**

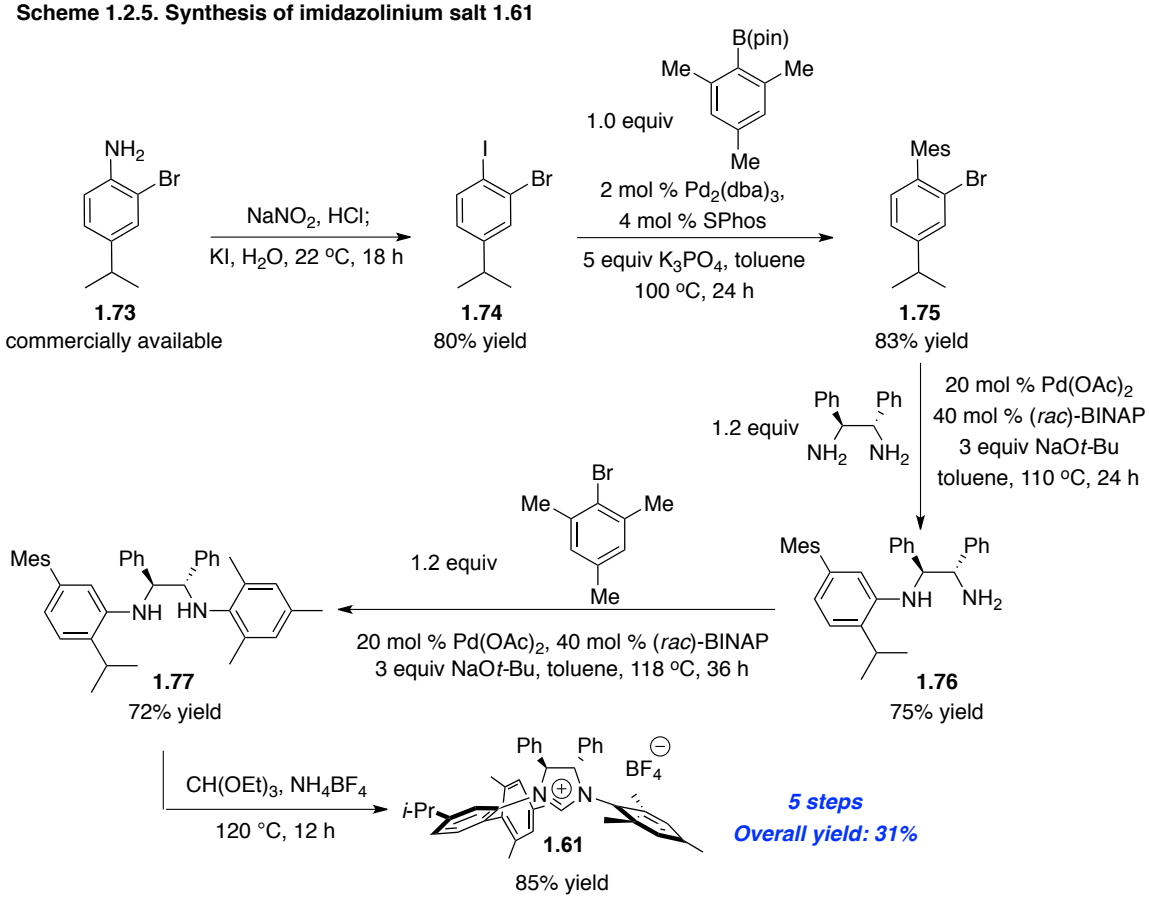


### *1.2.3. Catalytic Enantioselective BCA Reactions to α,β-Unsaturated Acyclic Ketones*

With the optimized BCA reaction condition in hand, a series of acyclic α,β-unsaturated ketones are investigated (Table 1.2.4). With 5 mol % imidazolinium salt **1.37**, enone **1.1a** proceed to 87% conv. (82% yield) and 92:8 er, while with **1.61** under otherwise the same reaction condition, an improved yield (92%) and enantioselectivity (96:4 er) were obtained. The BCA reaction with an ortho-methyl phenyl substituted enone (**1.78a**, entry 3) requires a higher temperature (50 ºC) to proceed to 95% conv. (~15% conv. at 22 ºC), but the enantioselectivity is diminished (85.5:14.5 er).

Surprisingly, the eletron-rich enone (**1.78b**, entry 4) accelerates the reaction (90% conv., 2.5 mol % catalyst used), while the electron-poor ones (**1.78c-e**, entries 5-7) slow the process (41%, 60% and 69% conv., respectively). Interestingly, proto-deborations (saturated ketones) were observed as the byproduct in those reactions (for **1.78e**, the saturated ketone is the only product), which will be further explained later. The NHC-catalyzed enantioselective BCA reaction accommodates enones with a hetero-aryl (**1.78f**, entry 8) and alkyl substituents (**1.78g-j**, entries 9–12), with good efficiencies (73–94% yield) and enantioselectivities (90:10 to 94.5:5.5 er). The reaction with *trans*-chalcone is slightly slower (82% conv in 18 h) but with a similar er (93.5:6.5 er).

**Table 1.2.4. NHC-catalyzed enantioselective BCA reactions to acyclic enones**[a]

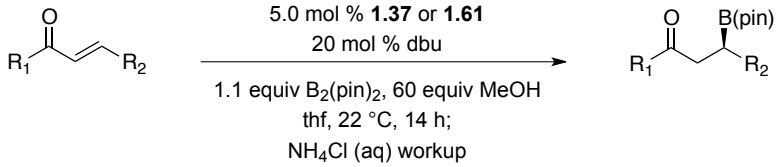


| entry | substrate ($R_1$; $R_2$) | imidazolinium salt | conv (%) | yield (%) | er |
|---|---|---|---|---|---|
| 1 | **1.1a** (Me; Ph) | **1.37** | 87 | 82 | 92:8 |
| 2 | **1.1a** (Me; Ph) | **1.61** | >98 | 92 | 96:4 |
| 3[b] | **1.78a** (Me; 2-Me$C_6H_4$) | **1.61** | 95 | 90 | 85.5:14.5 |
| 4[c] | **1.78b** (Me; 4-MeO$C_6H_4$) | **1.61** | 90 | 80 | 94:6 |
| 5[d] | **1.78c** (Me; 3-Br$C_6H_4$) | **1.61** | 41 | - | 90.5:9.5 |
| 6[e] | **1.78d** (Me; 4-Br$C_6H_4$) | **1.61** | 60 | 43 | 92:8 |
| 7[f] | **1.78e** (Me; 4-$CF_3C_6H_4$) | **1.61** | 69 | - | - |
| 8 | **1.78f** (Me; 2-furyl) | **1.61** | 75 | 73 | 92:8 |
| 9 | **1.78g** (Me; *n*-pentyl) | **1.61** | >98 | 94 | 94.5:5.5 |
| 10 | **1.78h** (Me; *i*-Pr) | **1.61** | >98 | 93 | 94:6 |
| 11 | **1.78i** (*n*-Bu; Ph) | **1.61** | 81 | 76 | 91:9 |
| 12[g] | **1.78j** (*i*-Pr; Ph) | **1.61** | 94 | 90 | 90:10 |
| 13[h] | **1.78k** (Ph; Ph) | **1.61** | 82 | 72 | 93.5:6.5 |

[a] See Scheme 1.1.13. [b] Reaction performed at 50 °C. [c] Reaction performed with 2.5 mol % **1.61** and 10 mol% dbu. [d] 12% Proto-deboration product was observed by analysis of 400 MHz $^1$H NMR spectra of the unpurified mixture. [e] 10% Proto-deboration product was observed by analysis of 400 MHz $^1$H NMR spectra of the unpurified mixture. [f] Only proto-deboration product was observed. [g] Reaction performed with 7.5 mol % **1.61** nd 30 mol % dbu. [h] Reaction time = 18 h.

Since deprotonation of the imidazolinium salt as well as MeOH hydrolysis of $B_2(pin)_2$ require an excess amount of base, we hypothesize that increasing the amount of dbu should facilitate those processes, and thus lead to a faster reaction. Indeed, the reactions with 100 mol % dbu (vs 20 mol % dbu) proceed with higher conversions, as depicted in Scheme 1.2.6. The enhancement in selectivity tells that, at a lower concentration of dbu, the incomplete formation of NHC as well as a lower concentration of (RO)(MeO)B–B(pin) **1.63** result in a background process catalyzed by an achiral

Lewis base (most likely the methoxide anion). It should be pointed out that the strategy of using 100 mol % dbu (vs 20 mol %) does not apply for all the cases, where a larger degree of proto-deborations and methoxide conjugate additions were observed.

**Scheme 1.2.6. Influence of dbu on NHC-catalyzed enantioselective BCA reactions[a]**

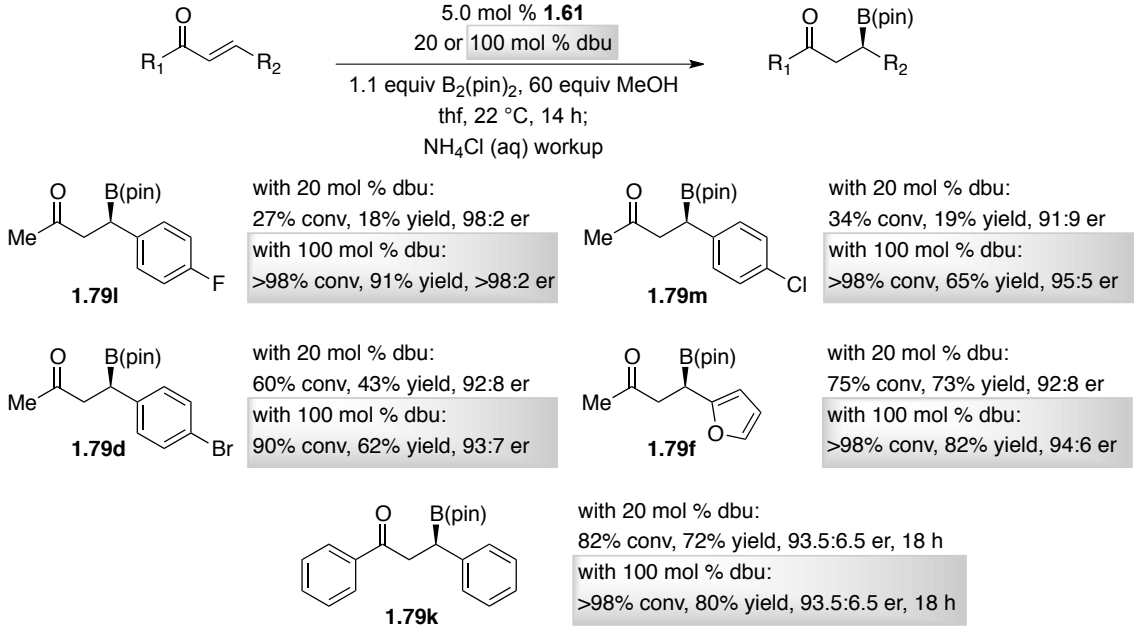


[a] See Scheme 1.1.13.

To support the hypothesis that saturated ketones observed in some cases come from the proto-deboration, not hydride reduction of the enone, the following experiments were conducted (Scheme 1.2.7). When **1.79c** was subjected into the BCA reaction condition (without the use of $B_2(pin)_2$), the saturated ketone **1.80c** formed completely (98% conv, 90% yield, equation 1). This suggests the saturated carbonyl may result from protonation of the C–B bond by MeOH. It is possible that the neighbored carbonyl oxygen coordinates to the boron of B(pin) in **1.79c**, activates the C–B bond, so that the protonation of such a bond by MeOH is more easily. We also tried to use HB(pin) instead of $B_2(pin)_2$ in the BCA reaction condition, assuming that the saturated ketone may come from the hydride reduction of the enone olefin (equation 2). However, the reaction does

not give any saturated ketone **1.80g**. Instead, a 1,2-reduction product **1.81** forms with 6% conversion. As a result, we draw the conclusion that the saturated ketones are likely formed through the proto-deboration of the C–B bond of product.

**Scheme 1.2.7. Experiments support the saturated ketones come from proto-deboration**[a]

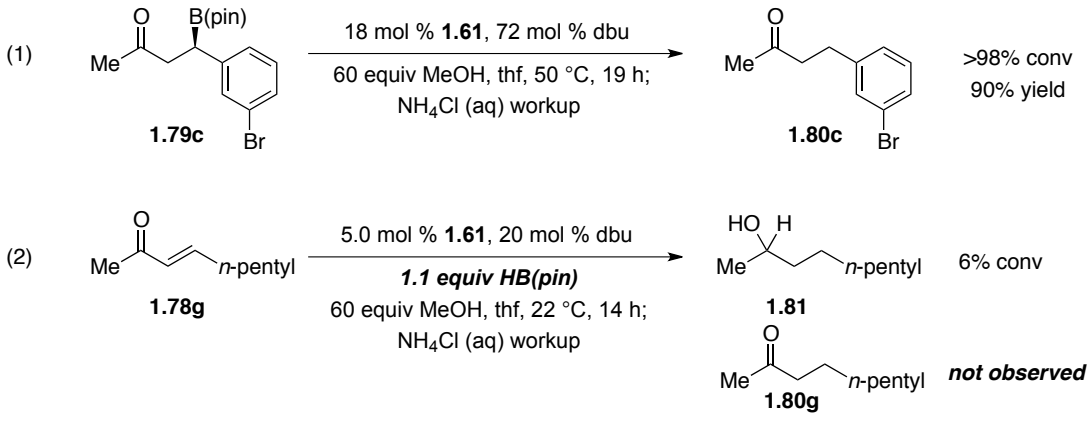


[a] See Scheme 1.1.13.

### *1.2.4. Catalytic Enantioselective BCA Reactions to α,β-Unsaturated Acyclic Esters*

The NHC-catalyzed enantioselective BCA reactions are also effective to α,β-unsaturated esters (enoates). As depicted in Scheme 1.2.8, methyl esters (**1.82a-c**) as well as a more sizable *tert*-butyl ester (**1.82d**) are suitable substrates. The reactions generate β-boryl esters in 62–87% yield and 94:6 to 98:2 er, although in some cases (**1.83b** and **1.83d**) a higher temperature is required for complete conversions. For **1.83b**, we use 7.5 mol % of the NHC precursor **1.61** and ten hours as the reaction time to minimize proto-deboration of the product. It is notable that the current processes are similar in terms of efficiency and enantioselectivity as the phosphine–Cu-catalyzed protocol described before (Scheme, 1.1.6).

**Scheme 1.2.8. NHC-catalyzed enantioselective BCA reactions to enoates[a]**

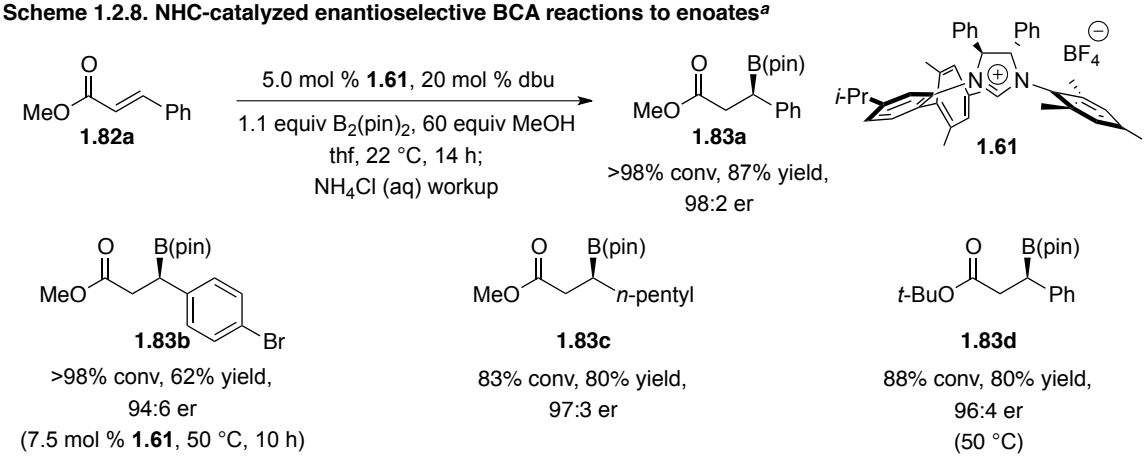


[a] See Scheme 1.1.13.

### *1.2.5. Catalytic Enantioselective BCA Reactions to α,β-Unsaturated Weinreb Amides*

Since developed by Steven M. Weinreb and Steven Nahm in 1981, N,O-dimethylhydroxyamide (Weinreb amide) has been widely used in the synthesis of ketones, aldehydes, amides and heterocycles.[58] Thus, we tested our BCA reactions to α,β-unsaturated Weinreb amides, in order to obtain those synthetically useful β-boryl amides. It is worth mentioning that the reactions with these Weinreb amides are generally slower. In all the cases, higher reaction temperatures and/or longer reaction times are required. In addition, besides the desired products, there are β-boryl methyl esters observed. The ratio of the two products depends on the reaction time, temperature as well as the equivalent of MeOH (the reactions with **1.84a** as an example, Scheme 1.2.9). Apparently, increasing the reaction temperature from 50 to 66 ºC results in more of the β-boryl methyl ester (entry 2 vs 1). Considering the methyl ester may come from a transesterification reaction, less amount of MeOH (30 vs 60 equiv.) was used (entry 3). The formation of the methyl ester was indeed slowed and the ratio of amide to ester is

(58) Nahm, S.; Weinreb, S. M. *Tetrahedron Lett.* **1981**, *22*, 3815–3818.

around 3:1. In this case, however, longer reaction time is needed for a reasonable conversion of the BCA reaction. The substrate scope of Weinreb amides in the NHC-catalyzed BCA reactions is shown below. While aryl- and alkyl-substituted unsaturated Weinreb amides are both effective substrates, less amount of MeOH is used in the former cases to minimize the transesterification reaction as well as proto-deboration (**1.85b**). The enantiomeric ratio of **1.85a** (86.5:13.5 er) is significantly lower than others, the reason for which is still unknown. Notably, there is only one example of Cu-catalyzed enantioselective BCA reaction to a Weinreb amide,[40] rendering the current process an attractive strategy to access such versatile compounds.

**Scheme 1.2.9. NHC-catalyzed enantioselective BCA reactions to unsaturated Weinreb amides**[a]

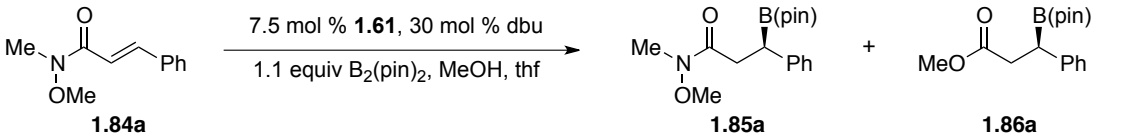


**1.84a** **1.85a** **1.86a**

**transesterification product**

| entry | time (h) | temp (°C) | equiv of MeOH | conv to **1.85a** (%) | conv to **1.86a** (%) |
|---|---|---|---|---|---|
| 1 | 14 | 50 | 60 | 24 | 16 |
| 2 | 24 | 66 | 60 | 27 | 47 |
| 3 | 36 | 50 | 30 | 65 | 21 |

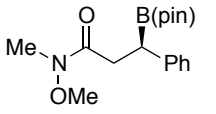


**1.85a**

86% conv, 61% yield
86.5:13.5 er
(7.5 mol % **1.61**, 30 equiv MeOH, 50 °C, 36 h)

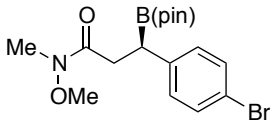


**1.85b**

>98% conv, 70% yield,
94:6 er
(7.5 mol % **1.61**, 30 equiv MeOH, 50 °C, 10 h)

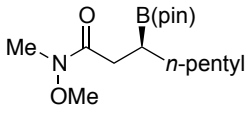


**1.85c**

77% conv, 74% yield,
95:5 er
(7.5 mol % **1.61**, 60 equiv MeOH, 50 °C, 14 h)

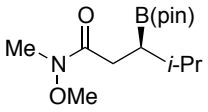


**1.85d**
67% conv, 60% yield,
95:5 er
(7.5 mol % **1.61**, 60 equiv MeOH,
50 °C, 24 h)

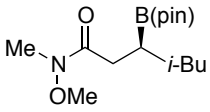


**1.85e**
78% conv, 73% yield,
95:5 er
(7.5 mol % **1.61**, 60 equiv MeOH,
66 °C, 24 h)

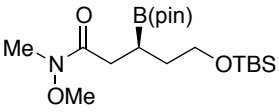


**1.85f**
96% conv, 92% yield,
93:7 er
(7.5 mol % **1.61**, 60 equiv MeOH,
66 °C, 24 h)

[a] See Scheme 1.1.13.

We also investigated how the transesterification process works to give the methyl ester product. In equation 1 of Scheme 1.2.10, unsaturated Weinreb amide does not undergo transesterification in the BCA reaction condition (without $B_2(pin)_2$). This is not surprising as the reaction solution is just mildly basic (30 mol % dbu in thf/MeOH). However, if β-boryl amide **1.85a** was subjected into the reaction condition, a complete formation of methyl ester **1.86a** was observed after 21 hours (eq. 2). It is possible that the carbonyl oxygen gets activated by coordination to the neighbored boron of the B(pin) unit. As a result, the electrophilicity of the carbonyl group is enhanced and the methoxide anion can readily interact with the carbonyl $\pi^*$ orbital to initiate the transesterification reaction.

**Scheme 1.2.10. Experiments that support the carbonyl activation in the transesterification process[a]**

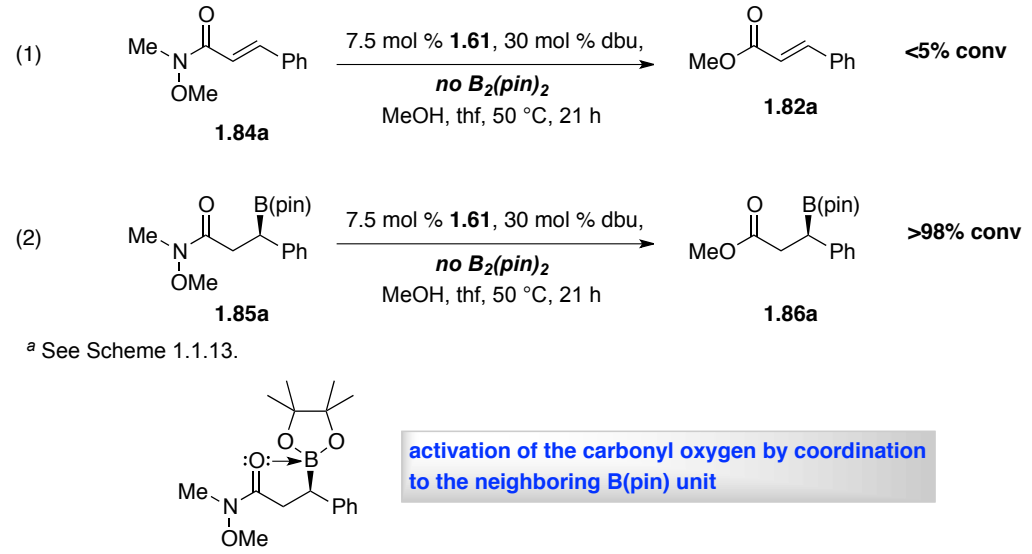


[a] See Scheme 1.1.13.




### *1.2.6. Catalytic Enantioselective BCA Reactions to α,β-Unsaturated Aldehydes*

As mentioned in the achiral NHC-catalyzed BCA reactions, one advantage of the current catalyst system (vs the transition metal catalysis) relies on the chemoselective boryl conjugate additions in the presence of an aldehyde group (vs Cu–B(pin) addition to the aldehyde carbonyl). Additionally, it has been reported that an enantioselective NHC–Cu-catalyzed BCA reaction to cinnamaldehyde affords the desired product in 70:30 er (86% conv., yield not reported).[59] Lastly, a recent report by Ibrahelm and co-workers established a Cu-catalyzed protocol to *in situ* generated unsaturated iminiums, an important strategy to access β-boryl aldehyde enantioselectively.[44] However, the use of an air- and moisture-sensitive $Cu(OTf)_2$ and a Brønsted acid ($o$-$FC_6H_4CO_2H$) is required. Thus, we were eager to investigate our NHC-catalyzed enantioselective BCA reactions to α,β-unsaturated aldehydes (enals).

(59) Lillo, V.; Prieto, A.; Bonet, A.; Díaz-Requejo, M. M.; Ramírez, J.; Pérez, P. J.; Fernández, E. *Organometallics,* **2009**, *28*, 659–662.

**Scheme 1.2.11. NHC-catalyzed enantioselective BCA reactions to enals**[a]

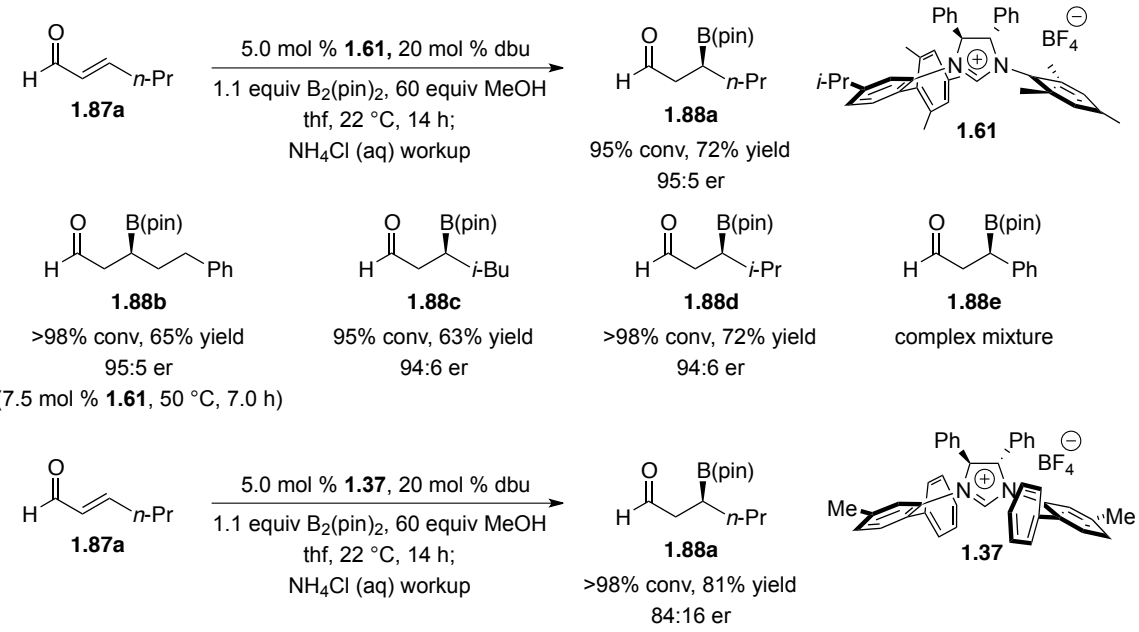


[a] See Scheme 1.1.13.

As shown in Scheme 1.2.11, the BCA reactions with alkyl-substituted enals are highly efficient (≥95% conv.) and enantioselective (~95:5 er). Neither the α or β-branched alkyl group affects the reaction. The reduced isolation yields (63–72% yield) are due to the instability of β-boryl aldehydes on silica gel. Efforts to promote BCA reactions to aryl-substituted unsaturated aldehydes (for example, cinnamaldehyde) failed. The resulting complex mixture may come from NHC additions to the carbonyl groups of substrate and/or the β-boryl aldehyde (forming Breslow intermediates), as well as methoxide conjugate additions to unsaturated aldehydes (a minor byproduct also observed in the BCA reactions to alkyl-substituted enals).

BCA reactions to enals with the more readily accessible **1.37** are equally efficient (>98% conv., 81% yield), but less enantioselective (84:16 er). It is likely that the NHC–diboron species derived from **1.37** is poorer at differentiating the enantiotopic faces of a small enal molecule, since it is sterically less hindered than the NHC–diboron from **1.61**.

### *1.2.7. Catalytic Enantioselective BCA Reactions to α,β-Unsaturated Cyclic Ketones*

Enantioselective BCA reactions to cyclic enones are still challenging, either catalyzed by transition metal complexes or transition metal-free Lewis bases. For the former class of catalysts, the reactions are less enantioselective with cyclopentenone, as well as dramatically inhibited with substrates that contain a sizable neighboring gem-dimethyl group (Scheme 1.1.6). For the latter class, only one example was reported in the phosphine-catalyzed enantioselective BCA reactions (cyclohexenone, 68:32 er, Scheme 1.1.18). Within this context, we started the NHC screening for reactions with cyclopentenone, which served as the model substrate.

**Table 1.2.5. NHC screening for enantioselective BCA reactions with cyclopentenone[a]**

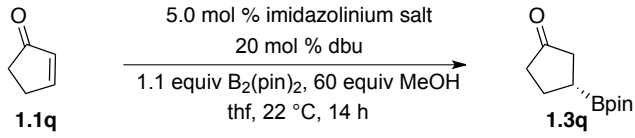


**1.1q** **1.3q**

**without NHC 25% conv**

[a] See Scheme 1.1.13.

| entry | Imidazolinium Salt | conv | yield | er |
|---|---|---|---|---|
| ***$C_1$-symmetric*** | | | | |
| 1 | 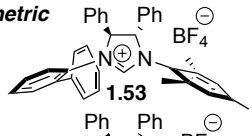 **1.53** | >98% | 99% | 69:31 |
| 2 | 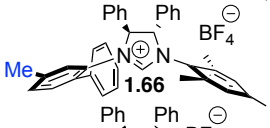 **1.66** | >98% | 97% | 68:32 |
| 3 | 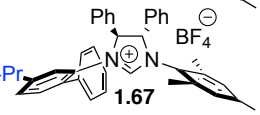 **1.67** | >98% | 97% | 65:35 |
| 4 | 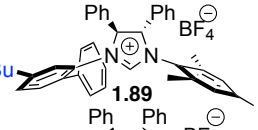 **1.89** | 73% | 66% | 61:39 |
| 5 | 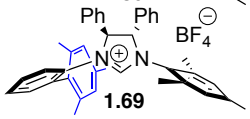 **1.69** | 93% | 90% | 85:15 |
| 6 | 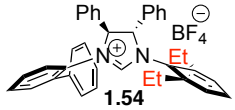 **1.54** | >98% | 97% | 73:27 |
| 7 | 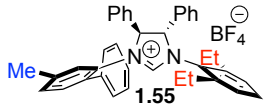 **1.55** | 87% | 57% | 70:30 |
| 8 | 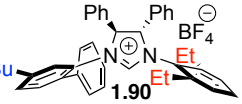 **1.90** | >98% | 86% | 64:36 |
| 9 | 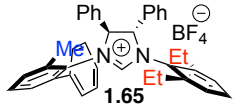 **1.65** | >98% | 84% | 71:29 |
| 10 | 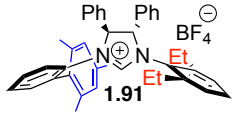 **1.91** | >98% | 95% | 87:13 |
| 11 | 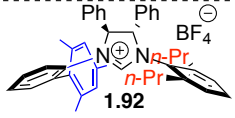 **1.92** | 60% | 45% | 84:16 |
| 12 | 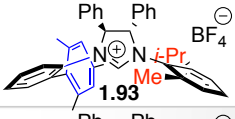 **1.93** | 87% | 81% | 90:10 |
| 13 | 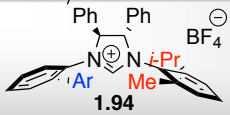 **1.94** | 90% | 80% | 92:8 Ar = 2,4,6-(*i*-Pr)$_3$C$_6$H$_2$ |
| 14 | 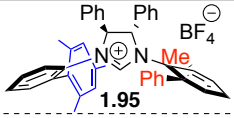 **1.95** | >98% | 97% | 80:20 |
| 15 | 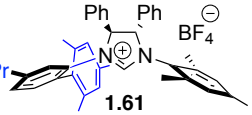 **1.61** | >98% | 95% | 65:35 |
| 16 | 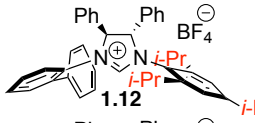 **1.12** | >98% | 95% | 70:30 |
| 17 | 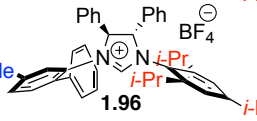 **1.96** | 74% | 69% | 68:32 |
| 18 | 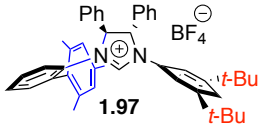 **1.97** | 90% | 80% | 55:45 |
| ***$C_2$-symmetric*** | | | | |
| 19 | 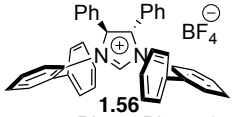 **1.56** | 60% | 51% | 56:44 |
| 20 | 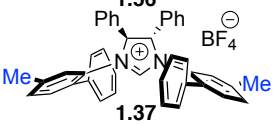 **1.37** | 93% | 69% | 67:33 |
| 21 | 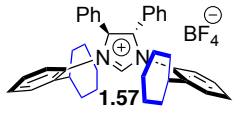 **1.57** | 73% | 72% | 53:47 |

As shown in Table 1.2.5, BCA reactions with cyclopentenone catalyzed by a $C_1$-symmetric NHC (entries 1–18) are generally efficient (60 to >98% conv.). However, the

enantioselectivities vary significantly. From entry 1 to entry 4, increasing the size of the *meta*-substituent of the unsymmetric N-aryl motif of NHC affects the selectivity slightly (61:39 to 68:32 er). Replacement of the *ortho*-phenyl group with a more sizable mesityl group significantly improve the er (**1.69**, 85:15 er, entry 5). Alternating the symmetric N-aryl motif of NHC from mesityl to 2,6-diethylphenyl and even 2,6-dipropylphenyl influence the selectivity little, comparing the results in entries 1–5 to entries 6–11. For instance, the enantiomeric ratio of reaction with **1.69** is 85:15, similar as the one with **1.91** (87:13 er) and the one with **1.92** (84:16 er). Fortunately, differentiating the two substituents of the symmetric N-aryl motif from Me, Me to Me, *i*-Pr results in an enhanced enantioselectivity (**1.93**, 90:10 er, entry 12). However, changing it to Me, Ph groups dramatically diminish the selectivity (**1.95**, 80:20 er, entry 14). Further improvement of the er (90:10, **1.93**) relates to an installation of a sterically hindered 2,4,6-triisopropylphenyl group (Trip) at the *ortho* position of the phenyl moiety (**1.94**, 92:8 er, entry 13). It is this NHC precursor that was chosen as the optimized one. Interestingly, the absolute stereochemistry of enantiomerically enriched product **1.3q** is opposite with acyclic β-boryl carbonyls. we will explain this by computational analysis in the next chapter. The NHC that is optimized for reactions with acyclic substrates (derived from **1.61**) catalyzes the BCA reaction to cyclopentenone with only 65:35 er. Further modifications of the imidazolinium salts, including installations of a trip group, result in low enantioselectivity (entries 16–18). $C_2$-symmetric NHC(s) are also effective for cyclopentenone, but non-enantioselective. The screening of NHC(s) implies the difficulty in controlling the stereochemistry in the C–B bond formation step for the small cyclic

enone. It is notable that the reaction proceeds to 25% conv. even if NHC is not involved, which suggests there is a background process likely catalyzed by the methoxide anion.

**Table 1.2.6. NHC screening for enantioselective BCA reactions with cyclohexenone[a]**

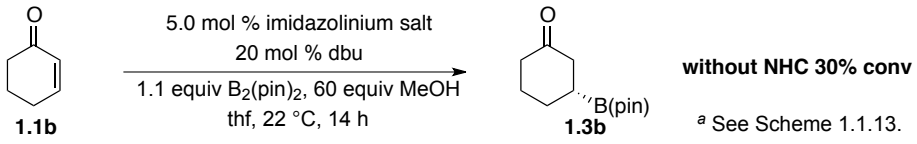


**1.1b** **1.3b**

**without NHC 30% conv**

[a] See Scheme 1.1.13.

| entry | Imidazolinium Salt | conv | yield | er | entry | Imidazolinium Salt | conv | yield | er |
|---|---|---|---|---|---|---|---|---|---|
| ***$C_1$-symmetric*** | | | | | | | | | |
| 1 | 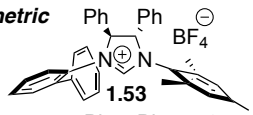 **1.53** | >98% | 90% | 56:44 | 12 | 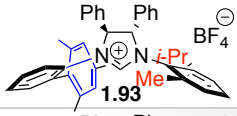 **1.93** | >98% | 94% | 78:22 |
| 2 | 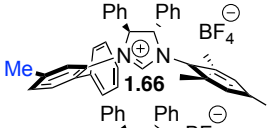 **1.66** | 92% | 86% | 56:44 | 13 | 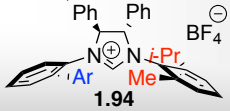 **1.94** | >98% | 94% | 83:17 |
| | | | | | | | Ar = 2,4,6-(*i*-Pr)$_3$C$_6$H$_2$ | | |
| 3 | 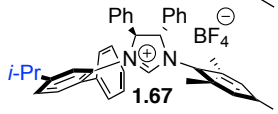 **1.67** | >98% | 91% | 46:54 | 14 | 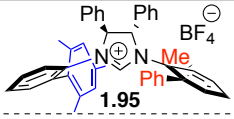 **1.95** | 71% | 59% | 61:39 |
| 4 | 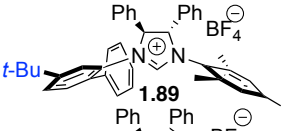 **1.89** | >98% | 97% | 37:63 | 15 | 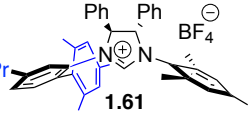 **1.61** | 64% | 57% | 57:48 |
| 5 | 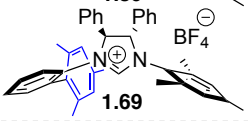 **1.69** | >98% | 94% | 68:32 | 16 | 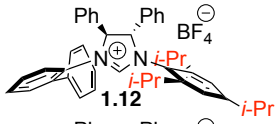 **1.12** | - | - | - |
| 6 | 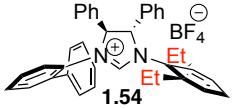 **1.54** | >98% | 97% | 65:35 | 17 | 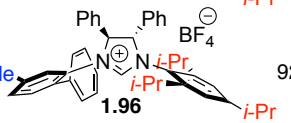 **1.96** | 92% | 89% | 60:40 |
| 7 | 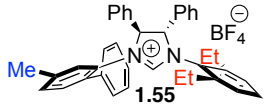 **1.55** | >98% | 92% | 60:40 | 18 | 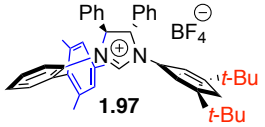 **1.97** | - | - | - |
| 8 | 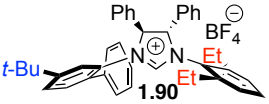 **1.90** | 82% | 70% | 48:52 | ***$C_2$-symmetric*** | | | | |
| 9 | 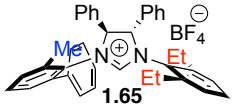 **1.65** | 67% | 62% | 59:41 | 19 | 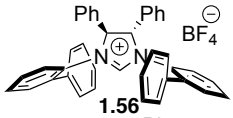 **1.56** | 77% | 68% | 57:43 |
| 10 | 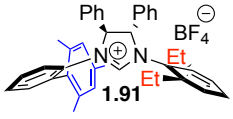 **1.91** | >98% | 97% | 78:22 | 20 | 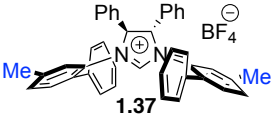 **1.37** | 98% | 93% | 56:44 |
| 11 | 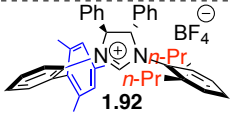 **1.92** | >98% | 94% | 77:23 | 21 | 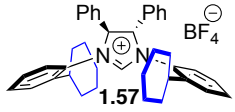 **1.57** | 98% | 90% | 52:48 |

The same NHC screening was also performed on cyclohexenone (Table 1.2.6). Although high reaction efficiencies were achieved in most of the cases again, the enantioselectivity is generally low (~60:40 er). From entry 1 to 5, alternation of the unsymmetric N-aryl motif of NHC does not improve the er(s). Nevertheless, the reverse enantioselectivities observed for reactions with NHC from **1.67** (entry 3) and **1.89** (entry 4), compared with entries 1–2, does indicate some influence of the size of *meta*-substituent on the N-aryl group. The same trend was also observed for examples from entry 6 to 10, among which the highest er was obtained for **1.91** (78:22 er, entry 10). Further modifications of the NHC(s) lead to the optimized one derived from **1.94 (**>98% conv., 93% yield, 83:17 er), the same one for the reaction with cyclopentenone. The $C_2$-symmetric NHC(s) does not catalyze the BCA reaction selectively (entries 19–21). Similarly as cyclopentenone, the background reaction with cyclohexenone (without NHC) proceeds to ~30% conv. after 14 hours, which is a potential reason why the NHC-catalyzed process is not very enantioselective.

Unfortunately, the NHC-catalyzed enantioselective BCA reactions with cycloheptenone are even lower in enantioselectivity. Three different NHC(s) were investigated in the processes (Scheme 1.2.12). Again, the NHC derived from **1.94** proves to be the best one, although the enantiomeric ratio is only 71:29 er.

**Scheme 1.2.12. NHC screening for enantioselective BCA reactions with cycloheptenone[a]**

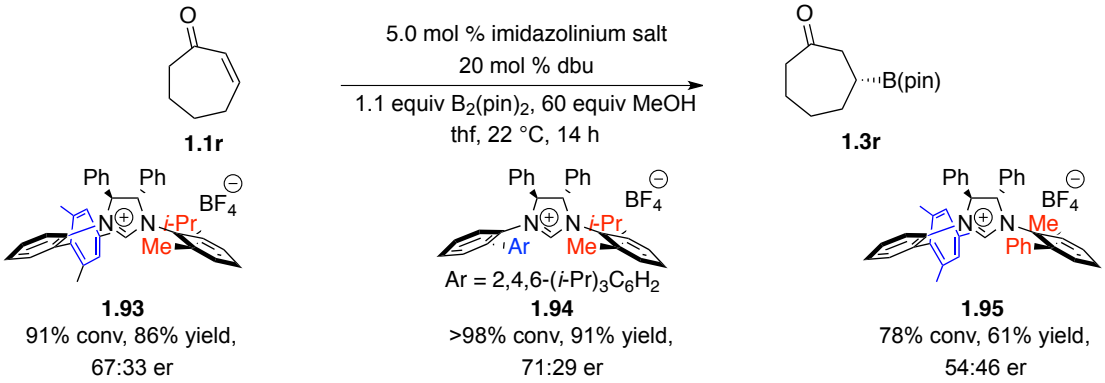


**1.1r** → **1.3r**

**1.93**
91% conv, 86% yield,
67:33 er

**1.94**
>98% conv, 91% yield,
71:29 er

**1.95**
78% conv, 61% yield,
54:46 er

[a] See Scheme 1.1.13.

It should be noted that the synthesis of **1.94** is difficult. Through a similar synthetic route as **1.37** and **1.61**, imidazolinium salt **1.94** was obtained only in ~5% overall yield. The challenge of the synthesis is the inefficient Pd-catalyzed C–N cross coupling reactions.

**Table 1.2.7. Solvent and temperature screening[a]**

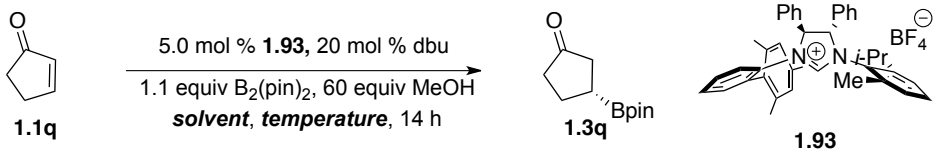


**1.1q** → **1.3q**

**1.93**

| entry | solvent | temperature | conv | yield | er |
|---|---|---|---|---|---|
| 1 | thf | 22 °C | 87% | 81% | 90:10 |
| 2 | dme | 22 °C | 80% | 63% | 90:10 |
| 3 | $CH_2Cl_2$ | 22 °C | >98% | 92% | 84:16 |
| 4 | toluene | 22 °C | 84% | 77% | 86:14 |
| 5 | thf | 4 °C | 80% | 73% | 89:11 |

[a] See Scheme 1.1.13.

To investigate how the solvent and reaction temperature affect the BCA transformations, we worked on a series of experiments (shown in Table 1.2.7). Dimethoxyethane (dme) behaves similarly as thf, except a slight diminish in the reaction

efficiency (entry 2). The use of dichloromethane significantly lowers the selectivity from 90:10 er to 84:16 er (entry 3). Non-polar solvent, such as toluene, does not improve the reaction either (entry 4). The reaction temperature does not seem to affect the enantioselectivity, while a drop in conversion (from 87% to 80%) was observed if the reaction was cooled from 22 ºC to 4 ºC (entry 5).

As stated above, there is a notable background process for reactions with cyclic enones (25–30% conv. without NHC), which likely arises from methoxide activation of $B_2(pin)_2$. One way to diminish such a process would be involvement of a biphasic solution in the BCA reaction (inspired by our NHC-catalyzed SCA reactions), where the effective concentration of $RO^-$ anion in the organic phase would be decreased. In entry 1 of Table 1.2.8, the β-boryl ketone **1.3r** was obtained in 60:40 er if a mixture of thf and MeOH (homogeneous solution) was used. Alternating the solvent into thf:$H_2O$ = 1:3 results in a biphasic reaction solution. However, the reaction efficiency is very low (20% conv.). The use of $Et_2O$ and $H_2O$ mixture does not improve the reaction conversion. To further diminish the hydroxide concentration in the organic layer, 2-methyl-tetrahydrofuran (2-Me-thf) was used instead of thf. It is well-known the solubility of 2-Me-thf in $H_2O$ is much smaller than thf (2-Me-thf: 13g/100g $H_2O$ at 25 ºC, thf: miscible in $H_2O$). However, in entry 4, the reaction still only proceeds in 18% conv. after 14

hours.

**Table 1.2.8. Investigation of biphasic systems in the catalytic BCA reactions**[a]

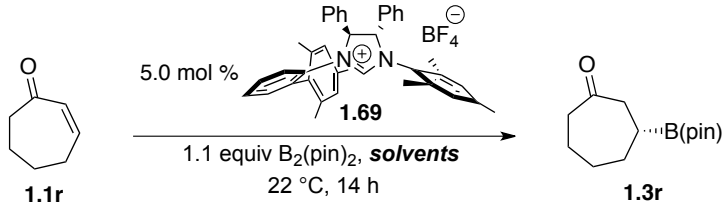


**1.1r** **1.3r**

| entry | solvent conditions | dbu (mol %) | conv(%) | er |
|---|---|---|---|---|
| 1 | thf/60 equiv MeOH (homogeneous) | 20 | >98 | 60:40 |
| 2 | thf:$H_2O$ = 1:3 (biphasic) | 20 | 20 | 52:48 |
| 3 | $Et_2O$:$H_2O$ = 1:3 (biphasic) | 20 | 10 | - |
| 4 | 2-Me-thf:$H_2O$ = 1:3 (biphasic) | 20 | 18 | 62:38 |
| 5 | 2-Me-thf:$H_2O$ = 1:1.5 (biphasic) | 20 | 59–98 | 60:40 |
| 6 | 2-Me-thf:$H_2O$ = 1:1.5 (biphasic) | 40 | >98 | 60:40 |

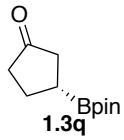


**1.3q**

**2-Me-thf:$H_2O$ = 1:1.5:**
>98% conv, 68% yield, 81:19 er
**thf/60 equiv MeOH:**
93% conv, 90% yield, 85:15 er

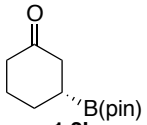


**1.3b**

**2-Me-thf:$H_2O$ = 1:1.5:**
93% conv, 75% yield, 64:36 er
**thf/60 equiv MeOH:**
>98% conv, 94% yield, 68:32 er

[a] See Scheme 1.1.13.

Having noticed that too much $H_2O$ may cause $B_2(pin)_2$ decomposition, a phenomenon observed before in the reactions with acyclic enones, we tried 2-Me-thf:$H_2O$ = 1:1.5 instead of 1:3. The result of entry 5 clearly supports our hypothesis and 59–98% (several trials) conversions were observed, although the enantioselectivity remains unchanged (60:40 er). Increasing the amount of dbu does not help to enhance the catalyst activity (entry 6). Cyclopentenone as well as cyclohexenone were also subjected into the 2-Me-thf:$H_2O$ = 1:1.5 condition, where lower yields and enantiomeric ratios were observed in both cases.

**Scheme 1.2.13. NHC-catalyzed enantioselective BCA reactions to cyclic unsaturated carbonyls**[a]

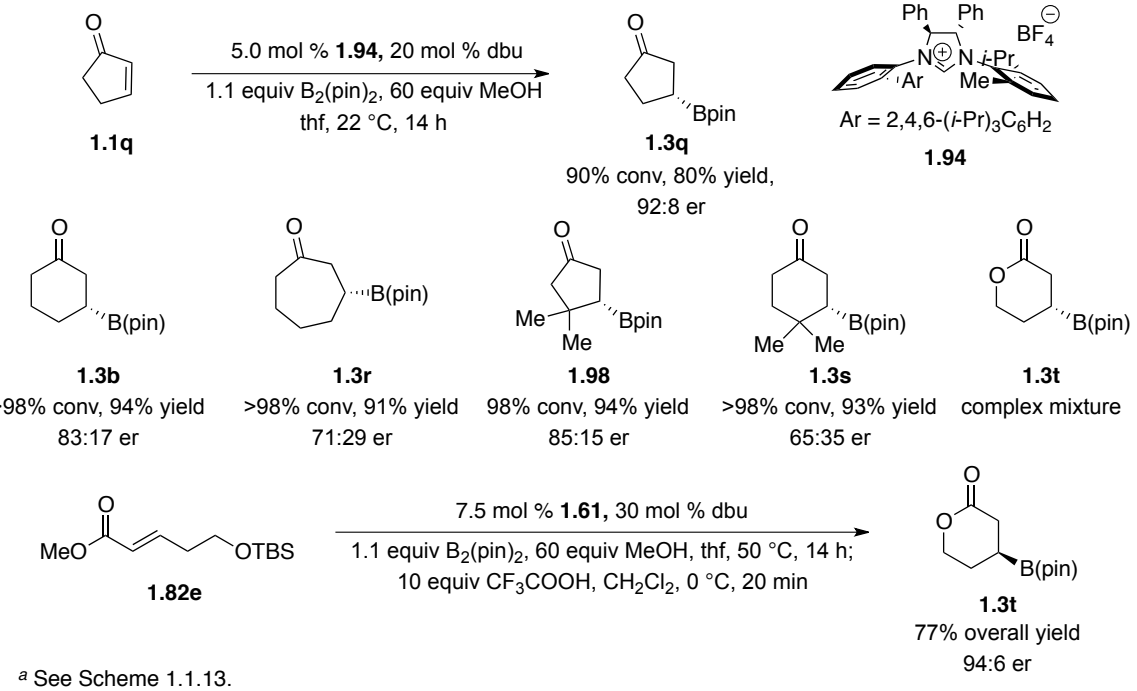


[a] See Scheme 1.1.13.

With the optimized reaction condition in hand, a few cyclic enones were subjected in the NHC-catalyzed enantioselective BCA reactions. As summarized in Scheme 1.2.13, expanding the ring size from five- to seven-membered rings greatly diminishes the selectivity (**1.3q**, **1.3b** and **1.3r**), while the yields are all high. The reactions with sterically congested gem-dimethyl substituted cyclic enones are noteworthy, since the phosphine–Cu-catalyzed strategy gives no conversion (see Scheme 1.1.6). In our transition metal-free system, **1.98** and **1.3s** can still be obtained in high yields (93% and 94% yield, respectively). BCA reactions with an unsaturated lactone afford a complex mixture, due to the MeOH promoted lactone ring rupture. However, the same product can be generated through a sequential process: an enantioselective BCA reaction to the acyclic ester **1.82e**, deprotection of TBS group (*tert*-butyldimethylsilyl) and lactone formation in a 77% overall yield and 94:6 er.

### *1.2.8. Other Important Observations*

During our study in the NHC-catalyzed enantioselective BCA reactions to acyclic and cyclic unsaturated carbonyls, a series of other substrates were investigated (Scheme 1.2.14). Beginning with the reaction with *cis*-enone **1.1a'**, we found the efficiency as well as enantioselectivity were dramatically dropped (32% conv., 28% yield and 54.5:46.5 er, equation 1). It is likely that the phenyl substituent of **1.1a'** interacts with the sizable NHC•diboron complex during the C–B bond formation step, resulting in an increased activation energy to reach the transition state. Thus the conversion of this reaction is significantly lower than the one with *trans*-enone **1.1a** (32% conv. vs >98% conv. in Table 1.2.4). No enantioselectivity (54.5:46.5 er) in this case further supports the hypothesis of the inhibited catalysis and implies a notably competitive background process.

α,β,γ,δ-Unsaturated carbonyls (**1.99**) are effective substrates for BCA reactions (equation 2). However, the resulting allyl B(pin) is unstable in the basic protic solution, leading to a mixture of proto-deboration products (**1.100** and **1.101**) completely.

Unfortunately, unsaturated thioesters (**1.1y**), nitriles (**1.103**) and nitro alkenes (**1.105**) are not suitable for our catalytic process. In equation 3, the transesterification as well as sulfur conjugate addition occur, while in equation 4, substrates are completely ineffective. The nitro alkene (**1.105**) leads to a complex mixture that is difficult to analyze.

**Scheme 1.2.14. Other observations in the study of NHC-catalyzed enantioselective BCA reactions[a]**

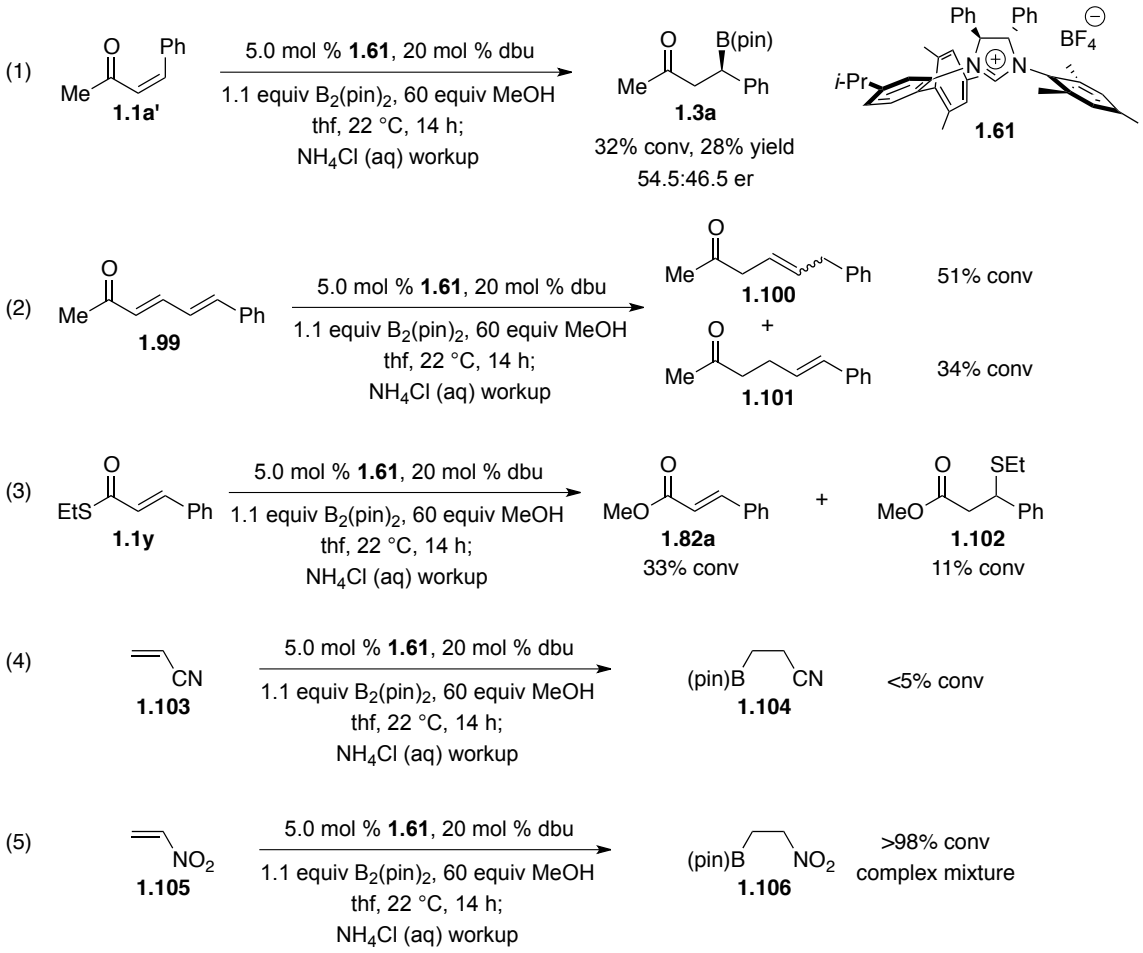


[a] See Scheme 1.1.13.

## *1.3. NHC-catalyzed Enantioselective Boryl Conjugate Additions to Generate Boron Substituted Quaternary Carbon Stereogenic Centers*

Lewis base (especially NHC) catalyzed enantioselective boryl conjugate additions provide effective alternatives to the Cu-catalyzed strategies. Soon after our successful development of reactions that generate boron substituted tertiary carbon stereogenic centers, my colleague Suttipol Radomkit (Benz) disclosed the first transition metal-free BCA reactions to trisubstituted unsaturated carbonyls.[60] The synthesis of quaternary

(60) Radomkit, S.; Hoveyda, A. H. *Angew. Chem. Int. Ed.* **2014**, *53*, 3387–3391.

carbon stereogenic centers, especially those that contain a C–B bond, still remains challenging. The products are of great interest, since simple oxidizing the C–B bonds of those compounds generate ketone aldol products that cannot easily be obtained through other protocols.

Similarly as the BCA reactions to disubstituted enones and enoates, an excess amount of dbu and MeOH is required for efficient transformations. The reactions are also not required for rigorous exclusion of air and moisture. The NHC screening result in **1.93** and **1.69** as the optimized catalyst precursors, the former of which gives the highest enantioselectivities to cyclic substrates while the latter is more suitable for acyclic ones (Scheme 1.3.1).

Reactions with cyclic substrates are very efficient (83% to >98% conv.) and highly enantioselective (≥95:5 er). Notably, for substrate **1.1f**, only 1 mol % **1.93** is sufficient (87% conv., 84% yield, 95:5 er). The reaction affording **1.111** is noteworthy, since the phosphine–Cu-catalyzed BCA protocol is not suitable in this case and a complex mixture was observed, which is likely resulted from Cu–B(pin) addition to the allene unit. It should also be mentioned that the reactions with trisubstituted cyclic enones are far more enantioselective than the ones with disubstituted ones (such as cyclohexenone, see Table 1.2.6). Detailed computational studies will be provided in the next chapter to help understand this difference. Moreover, the optimal imidazolinium salt **1.93** is much easier to access than the more sizable one (**1.94**) for reactions with disubstituted cyclic enones in Scheme 1.2.13 (23% overall yield vs ~5% overall yield).

**Scheme 1.3.1. NHC-catalyzed enantioselective BCAs to generate boron substituted quaternary centers[a]**

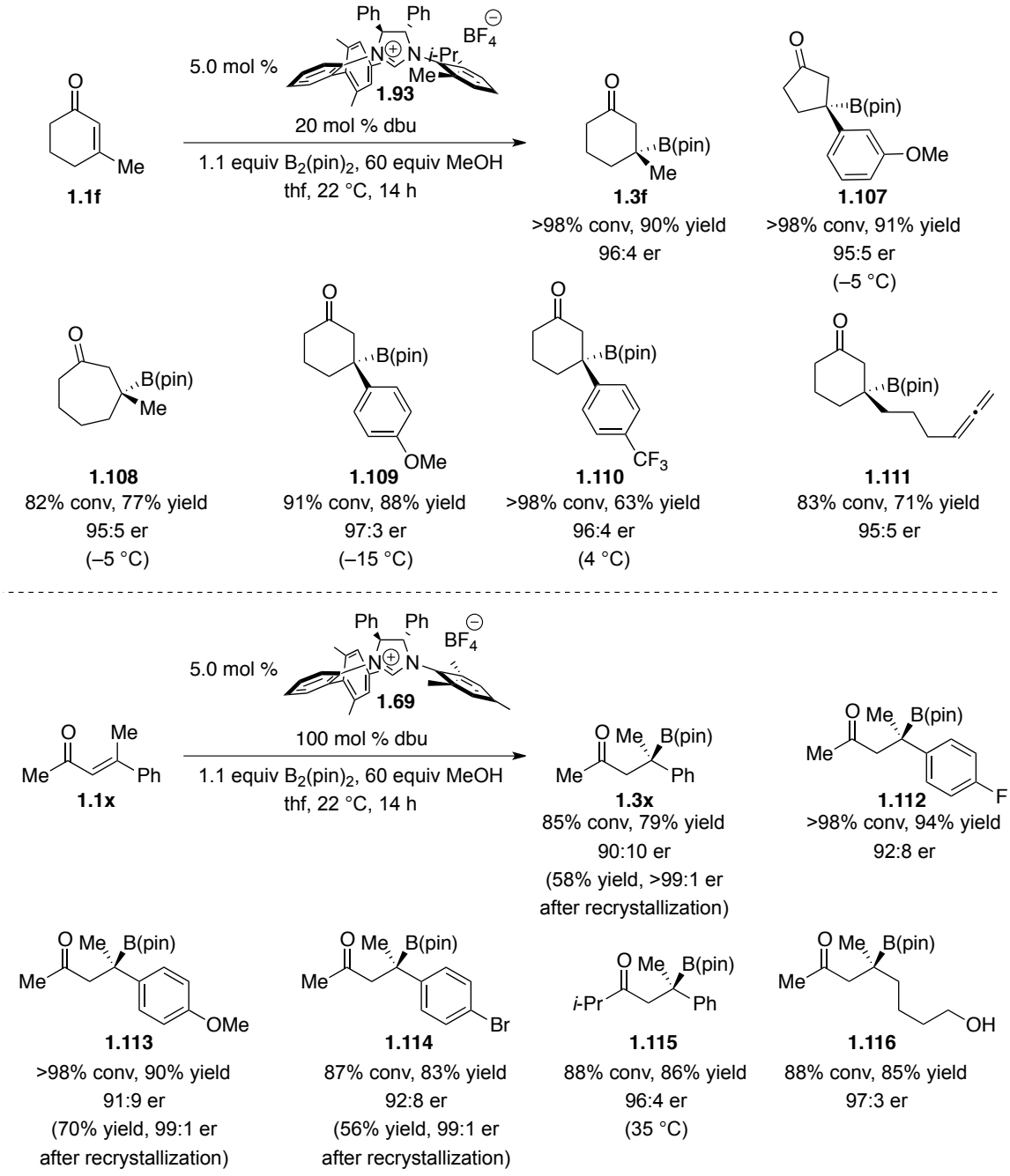


[a] See Scheme 1.1.13.

The BCA reactions with acyclic enones are less efficient than the cyclic ones, and thus require the use of 100 mol % dbu (for other cases, see Scheme 1.2.6), or increased reaction temperature (35 °C). The enantiomeric ratios for most of products are slightly

lower than those for cyclic ones (92:8 vs ~95:5 er). However, after recrystallization, some of the products (**1.3x**, **1.113** and **1.114**) can be delivered with exceptional enantiomeric purity (≥99:1 er). The current process compensates the NHC–Cu-catalyzed one, since the latter gives lower selectivities (≤92:8 er). However, unsaturated esters as well as Weinreb amides are inefficient in this NHC-catalyzed method.

The NHC-catalyzed enantioselective BCA reaction to trisubstituted enones is the first transition metal-free catalytic strategy for enantioselective synthesis of boron substituted quaternary centers, such a transformation that values a lot in the collection of C–B bond formation reactions.

## *1.4. Functional Group Compatibilities and Limitations of NHC-catalyzed Enantioselective Boryl Conjugate Addition Reactions*

One of the many motivations for our development of transition metal-free protocols in catalysis was the expectation that those processes offer complementary reactivity as well as selectivity patterns vs the well-established metal catalyzed ones. Such expectation was based on the distinct mechanisms of transformations promoted by organic molecule compared with the ones by transition metal complexes. As illustrated in Scheme 1.1.14, the achiral NHC-catalyzed BCA reactions are not hampered by the addition of an alkyne or aldehyde, critical observations that were also appreciated in our enantioselective BCA reactions.

In the Scheme 1.4.1, NHC-catalyzed enantioselective BCA reactions and known phosphine–Cu-catalyzed protocols are compared case by case, where one equivalent additive is involved (containing a different functional group). For the reaction with **1.1a**, both methods are very effective (>98% conv., 92–93% yield) without any additive,

although the enantioselectivity of the Cu-catalyzed one is slightly lower (85:15 er). It is likely that the optimal ligand is not Josiphos for this particular substrate. Addition of a weak acid (phenol) does not affect the transition metal-free protocol, probably because the excess amount of MeOH and dbu presented diminishes the effect of phenol. However the reaction catalyzed by the phosphine–Cu complex is significantly slowed, a phenomenon likely due to the lower reactivity of phosphine–Cu-OPh than phosphine-Cu-O*t*-Bu in the reaction with $B_2(pin)_2$.

**Scheme 1.4.1. NHC- or Cu-catalyzed enantioselective BCA reactions with a variety of additives**[a]

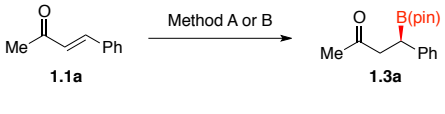


| additive (1.0 equiv): | Method A: 5 mol % 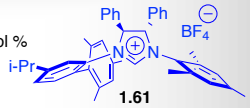 1.61; 1.1 equiv $B_2(pin)_2$, 20 mol % dbu, thf, MeOH, 22 °C, 14 h; | Method B: 3 mol % (*R*,*S*)-Josiphos, 3 mol % CuCl, 3 mol % NaO*t*-Bu, 1.1 equiv $B_2(pin)_2$, 1.0 equiv MeOH, thf, 22 °C, 24 h |
|---|---|---|
| no additive | >98% conv<br>92% yield<br>96:4 er | >98% conv<br>93% yield<br>85:15 er |
|  | >98% conv<br>88% yield<br>94:6 er | 64% conv<br>54% yield<br>85:15 er |
|  | 54% conv<br>48% yield<br>95:5 er<br>65% conv<br>56% yield<br>92:8 er<br>(7.5 mol %, 50 °C) | 16% conv<br>9% yield<br>63:37 er<br>32% conv<br>16% yield<br>84:16 er<br>(7.5 mol %, 50 °C) |
| 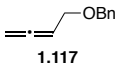 1.117 | 52% conv<br>44% yield<br>95:5 er<br>82% conv<br>74% yield<br>93:7 er<br>(7.5 mol %, 50 °C) | complex mixture |

[a] See Scheme 1.1.13.

Interestingly, the presence of benzaldehyde slows both catalyzed BCA reactions. As a result, the NHC-catalyzed one is much slowed (54% conv.), while the metal-catalyzed alternative is greatly hampered (only 16% conv.). As mentioned before, in the former case, the NHC may reversibly interact with benzaldehyde, forming a Breslow-type intermediate; But the Cu–B(pin) addition to the carbonyl moiety of the aldehyde in the latter one almost completely beats out the BCA reaction. After reaction optimizations,

65% conv., 56% yield and 92:8 er can be reached in the NHC-catalyzed reaction, a result much better than the corresponding Cu-catalyzed one.

Perhaps the most astonishing observation came with the reactions involving an equivalent of allene **1.117**. Although the reaction promoted by a chiral NHC was moderately affected (82% conv., 74% yield, 93:7 er with 5.0 mol % catalyst at 50 °C), the Cu-catalyzed reaction leads to a complex mixture, likely arised from the Cu–B(pin) addition to the allene and following transformations with enone **1.1a**.

**Scheme 1.4.1. NHC- or Cu-catalyzed enantioselective BCA reactions with enones containing an alkyne**[a]

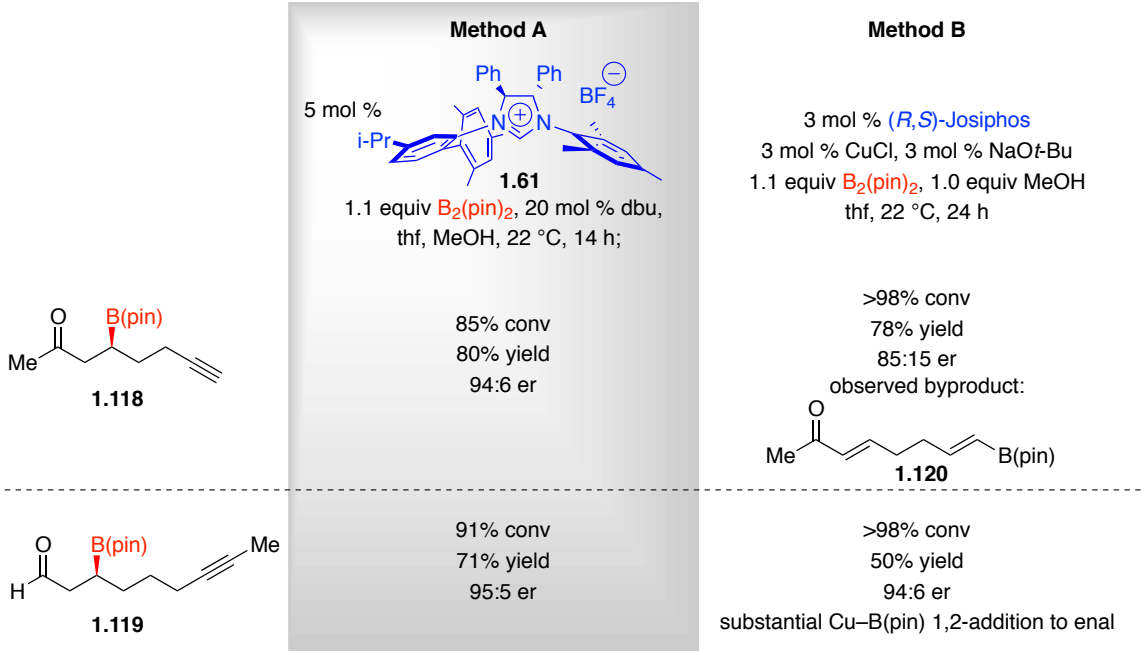


[a] See Scheme 1.1.13.

In another aspect for demonstration of the functional group compatibility, the NHC reaction with an enone with an alkyne group, is highly efficient and enantioselective (**1.118**, 80% yield, 94:6 er). The observation is in contrast with its phosphine–Cu-catalyzed alternative, where the Cu–B(pin) addition to the alkyne group was observed (**1.120**, Scheme 1.4.2). In another example, where the substrate bears both

of an alkyne and aldehyde group, a higher yield was obtained using the NHC-catalyzed protocol (71% yield), compared to the 50% yield with the metal-catalyzed one. The 1,2-copper boron addition of the enal is not surprisingly the major byproduct (**1.119**, Scheme 1.4.2).

Although advantages of NHC-catalyzed enantioselective BCA reactions are worth of mentioning, their limitations compared to the state of the art phosphine–Cu catalysis cannot be omitted either. Generally, reactions promoted by a chiral NHC requires 5–7.5 mol % catalyst loading, higher than 1–5 mol % in the phosphine–Cu-catalyzed system. In addition, some NHC(s) precursors, such as the optimized one (**1.94**) for cyclic substrates, are very difficult to synthesize (~5% overall yield) and not yet commercialized. However, most of phosphine ligands used in the Cu-catalyzed BCA reactions can be bought from reliable vendors. Some NHC-catalyzed BCA reactions accompany proto-deborations and/or transesterifications as side reactions, due to the use of excess amount of dbu and MeOH. These byproducts are less likely to be formed in the metal-catalyzed BCA reactions. Lastly, our NHC-catalyzed approach is limited in the region of di-substituted cyclic enones, since the enantiomeric purities of products obtained are low. The phosphine-Cu-catalyzed one, however, gives generally high enantioselectivities with cyclic substrates (except those with a gem-dimethyl group)(Scheme 1.1.6).

## *1.5. Applications of NHC-catalyzed Enantioselective Boryl Conjugate Addition Reactions in Total Synthesis*

The aforementioned NHC-catalyzed enantioselective BCA processes have been utilized in two cases of total synthesis. The first one, the synthesis of anti-proliferative

(+)-neopeltolide by my colleague Miao Yu, was depicted in Scheme 1.5.1.[61] Weinreb amide **1.121**, which was synthesized by one step from commercially available materials, serves as the substrate. The NHC-catalyzed enantioselective BCA reaction followed by $NaBO_3$ oxidation affords the corresponding β-hydroxy amide with 86% overall yield and 95:5 er. Importantly, 1.2 g of material was delivered using this strategy. The reaction also does not require a rigorous exclusion of air and moisture. The fact that our NHC-catalyzed BCA reactions are easy to operate and suitable for gram scale preparations ensures the material delivery in the muti-step synthesis of complex molecules. The NHC-catalyzed synthesis of β-hydroxy amide **1.122** in a high enantiomeric purity is a more efficient approach compared to an aldol reactios involving a chiral auxiliary and subsequent conversion into the desired amide. In addition, as far as we know, catalytic enantioselective acetate aldol reactions with Weinreb amides have not been reported. **1.122** was further converted into alcohol **1.123** in four steps, which was used to construct the macrocycle moiety of neopeltolide.

(61) Yu, M.; Schrock, R. R.; Hoveyda, A. H. *Angew. Chem. Int. Ed.* **2015**, *54*, 215–220.

**Scheme 1.5.1. Application in the total synthesis of neopeltolide**

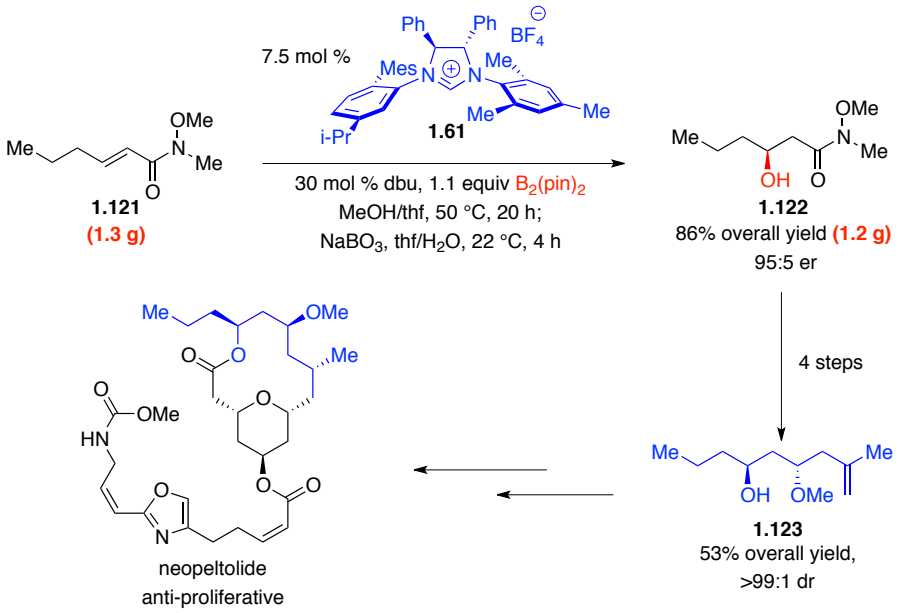


- Rigorous exclusion of $O_2$ and $H_2O$ not required
- Suitable for gram scale preparation of materials
- Selective acetate aldol processes with Weinreb amides not known

**Scheme 1.5.2. Application in the total synthesis of crassinervic acid**

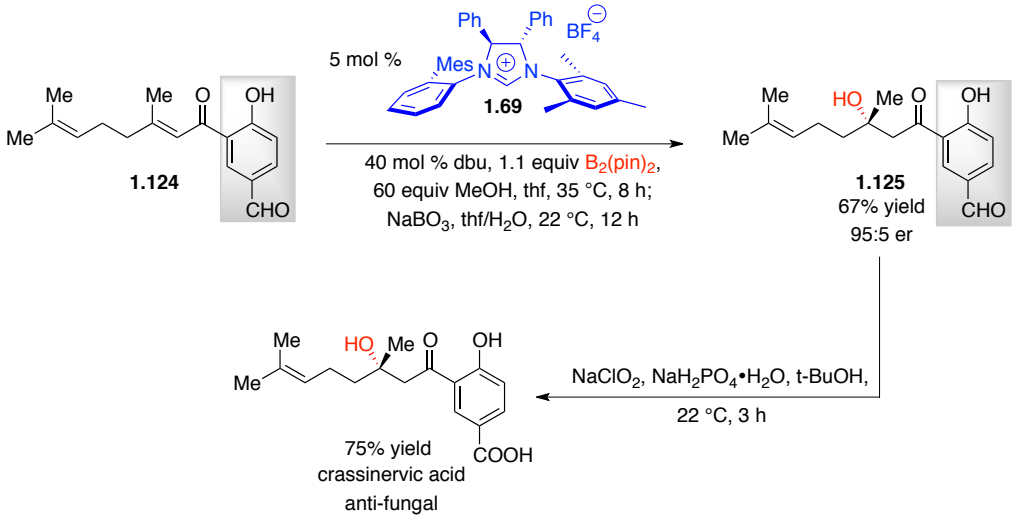


Less than 20% yield for the BCA/oxidation sequence if a Cu-catalyzed protocol is used.

In the synthesis of (–)-crassinervic acid, my colleague Suttipol Radomkit utilized the NHC-catalyzed enantioselective BCA reaction with a muti-functional substrate **1.124** (phenol/aldehyde), affording the desired β-hydroxy ketone in 67% yield and 95:5 er after

the C–B bond oxidation.[60] Notably, the same transformation was much less effective (<20% yield) if a Cu-catalyzed protocol is applied.

The above important disclosures imply that the current NHC-catalyzed processes are suitable for preparations of materials in a reasonable quantity in the beginning of a total synthesis, as well as for C–B bond formations at a fairly late stage of synthesis (muti-functional substrates). Thus, the current method serves as a good candidate in the industrial synthesis of biologically active compounds.

## *1.6. Other Discoveries of NHC-catalyzed Transformations*

In addition to enantioselective boryl conjugate additions, we also tried to develop new transformations using the NHC-catalyzed reaction conditions. In the equation 1 of Scheme 1.6.1, allyl bromide was utilized to afford allyl B(pin) through an allylic substitution process. The reaction proceeds to 62% conv., giving the $S_N2$ product **1.127**, if a chiral NHC and NaO*t*-Bu was used. Unfortunately, we did not detect any formation of the more valuable $S_N2$' product, no matter what NHC was used. The reaction also forms a trace amount of methoxide substitution product **1.128** (7%). In addition, if dbu was employed instead of NaO*t*-Bu, only a complex mixture (70%) was observed, the reason of which is still unknown. We also found the decomposition of **1.126** if MeOH was not used. Strangely, achiral NHC(s) (such as **1.19**) are not able to promote the boryl allylic substitution. Instead, ~30% conv. to methoxide allylic substitution product **1.128** was observed. This reactivity difference between achiral and chiral NHC(s) is worth of exploration. Lastly, other electrophiles, including allylic phosphates or carbonates, are not effective substrates (<5% conv.).

Besides the allylic substitution, we have also tried to use our NHC-catalyzed strategy to promote boryl aromatic substitutions. The representative substrate was **1.129**, a chloro-benzene that bears an electron withdrawing acetyl group and an electron donating methoxide group (shown in eq. 2). We wish this substitution pattern would polarize the aromatic ring, facilitating the boryl aromatic substitution. Unfortunately, all the trials failed. The substrate remained inactive (<5% conv.) no matter what NHC(s) were employed. Other chloro- or bromo-substituted arenes were not effective either. It is likely that the substrate is not able to interact with the polarized B–B bond of the NHC•diboron complex, which leads to failed C–B bond formation.

**Scheme 1.6.1. Other discoveries of NHC-catalyzed processes**

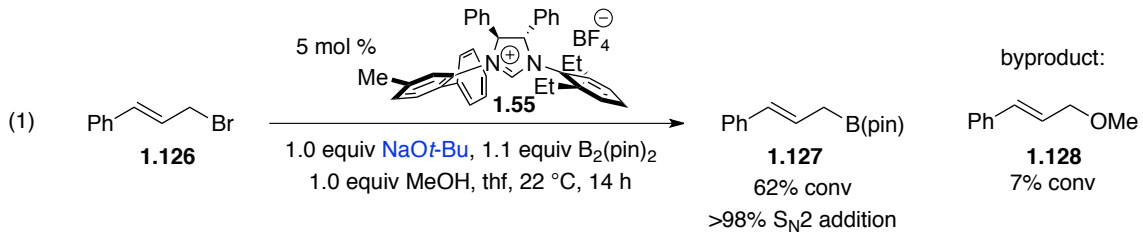


**Note:** 1. If dbu was used instead of NaO*t*-Bu, 70% conv to a complex mixture was observed.
2. If MeOH was not involved, we only observed decomposition of **1.126** (<5% **1.127**).
3. If achiral NHC(s) was used (such as **1.19**), ~30% conv to **1.128** was observed (<5% **1.127**).

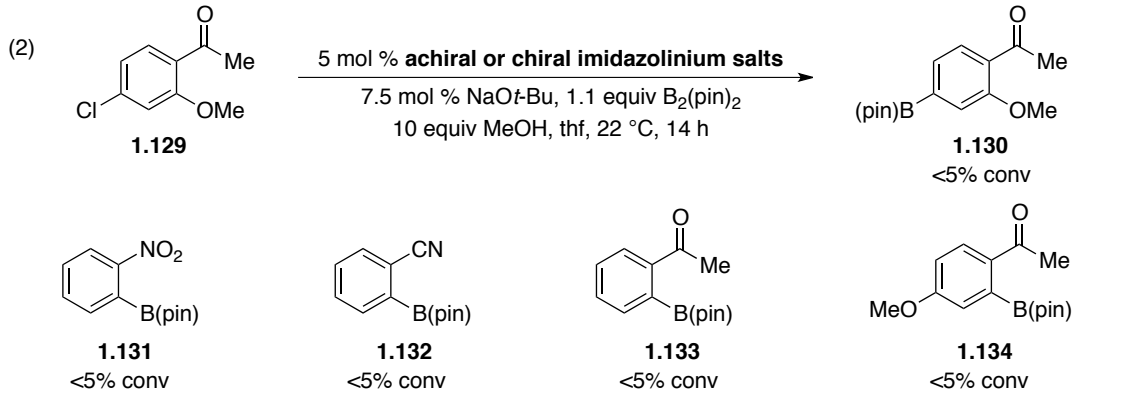

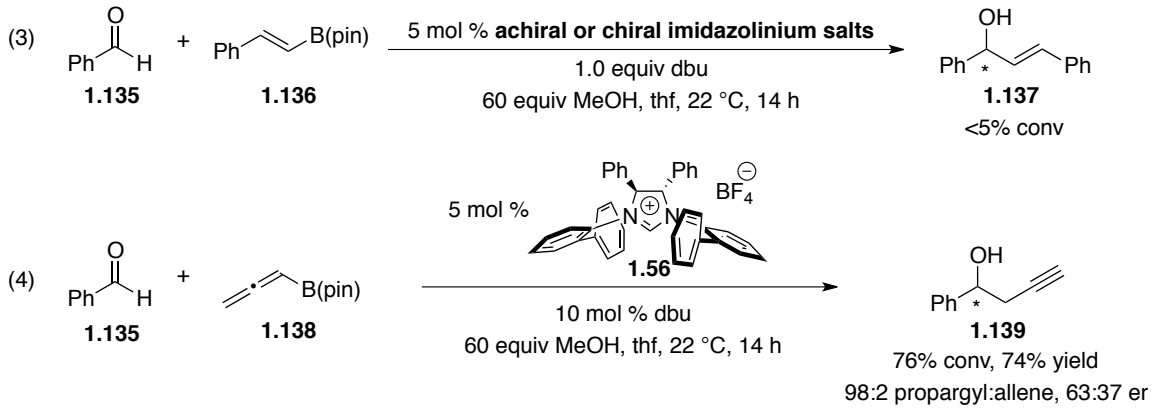


**Note:** 1. If NHC and base were not involved, 13% conv to **1.139** was observed.
2. If MeOH was not involved, 11% conv to **1.139** was observed.
3. If 4 °C was used instead of 22 °C, **1.139** was obtained in 40% conv, 28% yield, 51:49 er.

The attempt to promote alkenyl additions to aldehyde by an NHC was also unsuccessful (eq. 3). Accordingly, there was no reaction if benzaldehyde and alkenyl B(pin) were added into the solution of NHC (equation 3). It is possible that the NHC cannot activate the C–B bond of an alkenyl B(pin). In addition, the pinacol unit of this B(pin) is more resistant towards the MeOH hydrolysis than $B_2(pin)_2$ (no free pinacol was detected in the reaction solution).

However, if the alkenyl B(pin) is replaced with an allenyl B(pin) (**1.138**), the propargyl addition reaction occurs. In the equation 3, we detected 76% conv. (74% yield) to the homopropargyl alcohol **1.139** with a 98:2 propargyl:allenyl ratio. Without the use of an NHC and dbu, the reaction also gives **1.139** but with much more diminished efficiency (13% conv.). An excess amount of MeOH is also required for the effective transformation. Nevertheless, the propargyl addition reaction is not enantioselective. After a screening of NHC(s), the highest er we obtained is 63:37 with imidazolinium salt **1.56**. Lowing the reaction temperature does not help to improve the enantioselectivity. Instead, the reaction efficiency suffered when 4 °C was employed (40 % conv., 28%

yield). The low enantioselectivity observed for this NHC-catalyzed transformation may be because the NHC is too far away from the C–C bond formation (propargyl addition may go through an open transition state), and the substituents on the NHC cannot reach to interact with the aldehyde. Another type of catalyst (aminophenol derived boron catalyst) for a similar transformation (allenyl additions to aldehydes) will be discussed in the chapter 3.

## *1.7. Conclusions*

The NHC-catalyzed boryl conjugate addition reaction, especially the enantioselective protocol, is believed to be a useful tool to construct C–B bonds in the synthesis of biologically active molecules. Our strategy is suitable for a variety of α,β-unsaturated carbonyls, including cyclic and linear ketones, esters, Weinreb amides and even challenging aldehydes, delivering β-boryl carbonyls that bear a tertiary or a quaternary carbon center with high efficiencies and enantioselectivities. The current strategy not only, offers complementary reactivity and selectivity profiles vs the well-established Cu-catalyzed alternatives, rendering its potential utility in the synthetic organic chemistry; but also provides a distinct reaction pathway to study. An understanding of the key mechanistic factors will provide some insight that is crucial for development of other Lewis base-catalyzed transformations in the future.

## *1.8. Acknowledgment*

I thank Prof. Amir H. Hoveyda for giving me this great project to study. I am also grateful to Kang-sang Lee and Jeannette M. Garcia for their mentorship on this project. Suttipol Radomkit deserve my thanks for helping me with the development of the NHC-

catalyzed enantioselective BCA reactions. I also appreciate the enlightening discussions with all the other Hoveyda group members.

The aforementioned work is supported financially by the NIH (GM-57212) and the NSF (CHE-1111074). We thank Boston College and the chemistry department for providing great assistance and facilities. We also acknowledge Frontier Scientific for gifts of $B_2(pin)_2$.

## *1.9. Experimental Section*

### *1.9.1. Preparations and Characterizations of New Compounds*

**General.** Infrared (IR) spectra were recorded on a Bruker FT-IR Alpha (ATR mode) spectrophotometer, $\nu_{max}$ in $cm^{-1}$. Bands are characterized as broad (br), strong (s), medium (m), and weak (w). $^1H$ NMR spectra were recorded on a Varian Unity INOVA 400 (400 MHz) spectrometer. Chemical shifts are reported in ppm from tetramethylsilane with the solvent resonance as the internal standard ($CDCl_3$: 7.26 ppm). Data are reported as follows: chemical shift, integration, multiplicity (s = singlet, d = doublet, t = triplet, q = quartet, m = multiplet), and coupling constants (Hz). $^{13}C$ NMR spectra were recorded on a Varian Unity INOVA 400 (100 MHz) spectrometer with complete proton decoupling. Chemical shifts are reported in ppm from tetramethylsilane with the solvent resonance as the internal standard ($CDCl_3$: 77.16 ppm). $^{11}B$ NMR were recorded on a Varian Unity INOVA 500 (128 MHz) with $BF_3$•$OEt_2$ resonance as the external reference ($d_8$-thf: 0.0 ppm). High-resolution mass spectrometry was performed on a Micromass LCT ESI-MS (positive mode) at the Mass Spectrometry Facility, Boston College. Enantiomeric ratios were determined by GLC analysis (Alltech Associated Chiraldex GTA column (30 m x 0.25 mm), Chiraldex B-DM (30 m x 0.25 mm) and Chiraldex aTA

(30 m x 0.25 mm)) and HPLC analysis (high-performance liquid chromatography) with a Shimadzu chromatograph (Chiral Technologies Chiralcel OJ-H (4.6 x 250 mm), Chiral Technologies Chiralcel OD-H (4.6 x 250 mm), Chiral Technologies Chiralpak AS-H (4.6 x 250 mm) or Chiral Technologies Chiralpak AD-H (4.6 x 250 mm)) in comparison with authentic racemic materials. Specific rotations were measured on a Rudolph Research Analytical Autopol IV Polarimeter.

Unless otherwise noted, reactions were carried out with distilled and degassed solvents under an atmosphere of dry $N_2$ in oven- (135 ºC) or flame-dried glassware with standard dry box or vacuum-line techniques. Tetrahydrofuran (Aldrich Chemical Co.) was purified by distillation from sodium benzophenone ketyl immediately prior to use. Methanol (Acros Organics 99.9% Extra Dry, AcroSeal$^{@}$) was used as received. All work-up and purification procedures were carried out with reagent grade solvents (purchased from Fisher Scientific) under air. **Bis(pinacolato)diboron ($B_2(pin)_2$)**: gifts from Frontier Scientific Inc., recrystallized from pentane and dried under vacuum prior to use. **1,8-Diazabicyclo[5.4.0]undec-7-ene (dbu)**: purchased from Aldrich Chemical Co. and purified by distillation from $CaH_2$ prior to use. **(*E*)-4-Phenylbut-3-en-2-one (1.1a)**: purchased from Aldrich Chemical Co., purified by recrystallization in pentane and dried under vacuum prior to use. **(*E*)-4-(4-Methoxyphenyl)but-3-en-2-one (1.78b):** purchased from Aldrich Chemical Co. and used as received. **(*E*)-4-(Furan-2-yl)but-3-en-2-one (1.78f):** purchased from Aldrich Chemical Co., purified by chromatography and dried under vacuum prior to use. **(*E*)-Non-3-en-2-one (1.78g):** purchased from Aldrich Chemical Co. and purified by distillation from $CaH_2$ prior to use. **(*E*)-5-Methylhex-3-en-2-one (1.78h):** purchased from Aldrich Chemical Co. and purified by distillation from

$CaH_2$ prior to use. **(*E*)-Chalcone (1.78k):** purchased from Aldrich Chemical Co., purified by chromatography and dried under vacuum prior to use. **Methyl cinnamate (1.82a):** purchased from Aldrich Chemical Co., purified by chromatography and dried under vacuum prior to use. **(*E*)-Methyl 3-(4-bromophenyl)acrylate (1.82b):** purchased from Aldrich Chemical Co., purified by chromatography and dried under vacuum prior to use. **(*E*)-Methyl oct-2-enoate (1.82c):** purchased from Aldrich Chemical Co. and purified by distillation from $CaH_2$ prior to use. ***tert*-Butyl cinnamate (1.82d):** purchased from Aldrich Chemical Co., purified by chromatography and dried under vacuum prior to use. **(*E*)-Hex-2-enal (1.87a):** purchased from Aldrich Chemical Co. and purified by distillation from $CaH_2$ prior to use. **(*E*)-4-Methylpent-2-enal (1.87d):** purchased from Acros Organics and purified by distillation from $CaH_2$ prior to use. **Cyclopent-2-enone (1.1q):** purchased from Aldrich Chemical Co. and purified by distillation from $CaH_2$ prior to use. **4,4-Dimethylcyclopent-2-enone:** purchased from Aldrich Chemical Co. and purified by distillation from $CaH_2$ prior to use. **Cyclohex-2-enone (1.1b):** purchased from Aldrich Chemical Co. and purified by distillation from $CaH_2$ prior to use. **Cyclohept-2-enone (1.1r):** purchased from Aldrich Chemical Co. and purified by distillation from $CaH_2$ prior to use. Other α,β-unsaturated carbonyls were prepared according to Wittig olefinations of the corresponding aldehydes, which were purchased from Aldrich Chemical Co. and used as received.

**Representative Experimental Procedure for NHC–Catalyzed Enantioselective (Pinacolato)boron Conjugate Addition:** In a glovebox, an oven-dried vial (8 x 1 cm) equipped with a stir bar was charged with a solution of NHC, which was prepared from **1.61** (11 mg, 0.017 mmol), dbu (10 mg, 0.066 mmol), and thf (0.47 mL, 0.036 M solution

of catalyst) for 30 min at 22 °C under a dry $N_2$ atmosphere. Bis(pinacolato)diboron (93 mg, 0.37 mmol), (*E*)-4-phenylbut-3-en-2-one (**1.1a**) (49 mg, 0.33 mmol) and methanol (0.80 mL) were added to the vial (0.26 M solution of substrate), which was sealed with a cap before removal from the glovebox. The mixture was allowed to stir at 22 °C for 14 h, after which the reaction was quenched by the addition of an aqueous solution of $NH_4Cl$ (1.0 mL, 0.7 M) and the mixture was allowed to stir for an additional 20 min. The aqueous layer was washed with diethyl ether (3 x 5 mL). The combined organic layers were dried over anhydrous $MgSO_4$ and filtered. The volatiles were removed under vacuum and the resulting light yellow oil was purified by silica gel chromatography (hexanes:$Et_2O$ = 10:1) to afford 84 mg (0.31 mmol, 92% yield) of (*R*)-4-phenyl-4-(4,4,5,5-tetramethyl-1,3,2-dioxaborolan-2-yl)butan-2-one (**1.3a**) as a colorless oil. **(*R*)-4-Phenyl-4-(4,4,5,5-tetramethyl-1,3,2-dioxaborolan-2-yl)butan-2-one (1.3a)**: The spectroscopic data match those reported previously.[27] $^1$H NMR (400 MHz, $CDCl_3$): δ 7.26–7.18 (4H, m), 7.14–7.10 (1H, m), 3.02 (1H, dd, *J* = 18.4, 10.8 Hz), 2.82 (1H, dd, *J* = 18.4, 5.6 Hz), 2.62 (1H, dd, *J* = 10.8, 5.6 Hz), 2.12 (3H, s), 1.20 (6H, s), 1.14 (6H, s); Specific Rotation: $[\alpha]_D^{20}$ –34.2 (*c* 1.06, $CHCl_3$) for an enantiomerically enriched sample of 96:4 er. Enantiomeric purity was determined by HPLC analysis in comparison with authentic racemic material (96:4 er shown; Chiralpak AS-H column, 98/2 hexanes/*i*-PrOH, 0.3 mL/min, 220 nm).

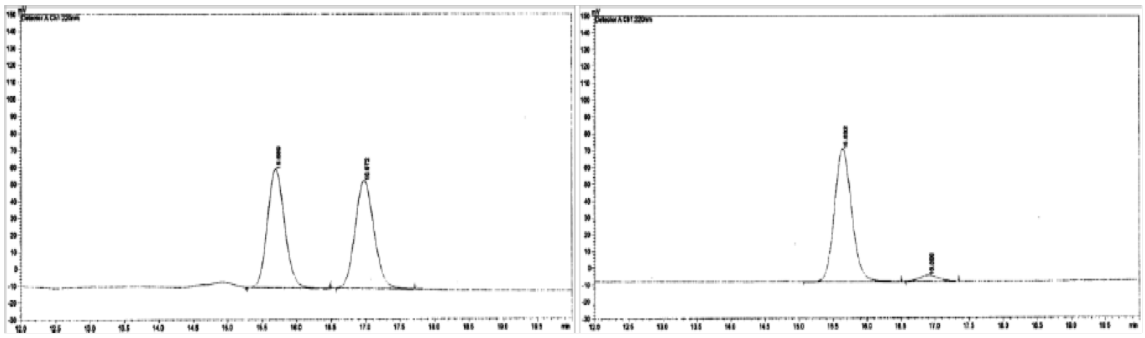

| Peak# | Ret. Time | Area | Height | Area % | Height % |
|---|---|---|---|---|---|
| 1 | 15.689 | 1221221 | 69979 | 50.213 | 52.387 |
| 2 | 16.972 | 1210859 | 63601 | 49.787 | 47.613 |

| Peak# | Ret. Time | Area | Height | Area % | Height % |
|---|---|---|---|---|---|
| 1 | 15.632 | 1389593 | 78739 | 95.776 | 95.950 |
| 2 | 16.899 | 61288 | 3324 | 4.224 | 4.050 |

| Peak # | Time (min) | Area (%) | Peak # | Time (min) | Area (%) |
|---|---|---|---|---|---|
| 1 | 15.689 | 50.213 | 1 | 15.632 | 95.776 |
| 2 | 16.972 | 49.787 | 2 | 16.899 | 4.224 |

**Proof of Stereochemistry:** The corresponding (*R*)-4-hydroxy-4-phenylbutan-2-one was obtained after oxidation of **1.3a**, the spectroscopic data match those reported previously.[27] Specific Rotation of (*R*)-4-hydroxy-4-phenylbutan-2-one: $[\alpha]_D^{20}$ +64.3 (*c* 0.83, $CHCl_3$). Literature value ($[\alpha]_D^{20}$ –49.0 (*c* 0.52, $CHCl_3$), 89.5:10.5 er) is assigned to the (*S*) enantiomer.[27]

**(*E*)-4-(*o*-Tolyl)but-3-en-2-one (1.78a):** The spectroscopic data match those reported previously.[62] $^1$H NMR (400 MHz, $CDCl_3$): δ 7.79 (1H, d, *J* = 16.4 Hz), 7.55–7.53 (1H, m), 7.28–7.17 (3H, m), 6.62 (1H, d, *J* = 16.4 Hz), 2.42 (3H, s), 2.36 (3H, s).

**(*R*)-4-(4,4,5,5-Tetramethyl-1,3,2-dioxaborolan-2-yl)-4-(*o*-tolyl)butan-2-one (1.79a)**: IR (neat): 2976 (m), 1713 (s), 1356 (s), 1318 (s), 1259 (m), 1214 (m), 1165 (m), 1140 (s), 1012 (w), 966 (m), 852 (m), 771 (m), 754 (m) $cm^{-1}$; $^1$H NMR (400 MHz, $CDCl_3$): δ 7.17–7.00 (4H, m), 3.00 (1H, dd, *J* = 17.6, 10.4 Hz), 2.85 (1H, dd, *J* = 10.4, 4.8 Hz), 2.74 (1H, dd, *J* = 17.6, 4.8 Hz), 2.33 (3H, s), 2.12 (3H, s), 1.20 (6H, s), 1.14 (6H, s); $^{13}$C NMR (100 MHz, $CDCl_3$): δ 208.5, 140.1, 136.2, 130.4, 127.6, 126.0, 125.4, 83.3, 46.9, 29.6, 24.5, 24.5, 20.0; HRMS (ESI+): Calcd for $C_{17}H_{26}B_1O_3$ $[M+H]^+$: 289.1975, Found:

(62) Cá, N. D.; Motti, E.; Mega, A.; Catellani, M. *Adv. Synth. Catal.* **2010**, *352*, 1451–1454.

289.1977. Specific Rotation: $[\alpha]_D^{20}$ –18.7 (*c* 1.07, $CHCl_3$) for an enantiomerically enriched sample of 85.5:14.5 er.

Enantiomeric purity was determined by HPLC analysis in comparison with authentic racemic material (85.5:14.5 er shown; Chiralcel OD-H column, 99/1 hexanes/*i*-PrOH, 0.3 mL/min, 220 nm).

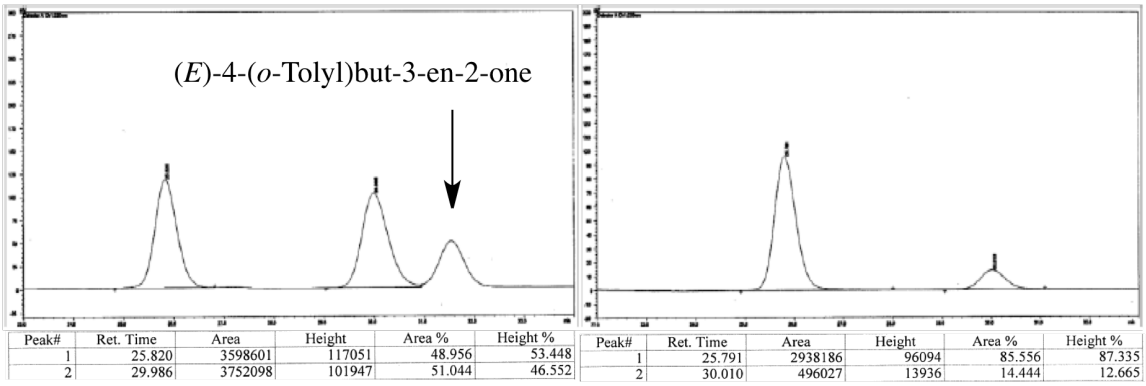


| Peak# | Ret. Time | Area | Height | Area % | Height % |
|---|---|---|---|---|---|
| 1 | 25.820 | 3598601 | 117051 | 48.956 | 53.448 |
| 2 | 29.986 | 3752098 | 101947 | 51.044 | 46.552 |

| Peak# | Ret. Time | Area | Height | Area % | Height % |
|---|---|---|---|---|---|
| 1 | 25.791 | 2938186 | 96094 | 85.556 | 87.335 |
| 2 | 30.010 | 496027 | 13936 | 14.444 | 12.665 |

| Peak # | Time (min) | Area (%) | Peak # | Time (min) | Area (%) |
|---|---|---|---|---|---|
| 1 | 25.820 | 48.956 | 1 | 25.791 | 85.556 |
| 2 | 29.986 | 51.044 | 2 | 30.010 | 14.444 |

**(*R*)-4-(4-Methoxyphenyl)-4-(4,4,5,5-tetramethyl-1,3,2-dioxaborolan-2-yl)butan-2-one (1.79b)**: The spectroscopic data match those reported previously.[63] $^1$H NMR (400 MHz, $CDCl_3$): δ 7.13–7.09 (2H, m), 6.80–6.76 (2H, m), 3.75 (3H, s), 2.96 (1H, dd, *J* = 18.2, 10.6 Hz), 2.78 (1H, dd, *J* = 18.2, 5.6 Hz), 2.56 (1H, dd, *J* = 10.6, 5.6 Hz), 2.11 (3H, s), 1.20 (6H, s), 1.15 (6H, s); Specific Rotation: $[\alpha]_D^{20}$ –29.1 (*c* 1.07, $CHCl_3$) for an enantiomerically enriched sample of 94:6 er.

Enantiomeric purity was determined by HPLC analysis in comparison with authentic racemic material (94:6 er shown; Chiralcel OD-H column, 98/2 hexanes/*i*-PrOH, 0.3 mL/min, 220 nm).

(63) Shiomi, T.; Adachi, T.; Toribatake, K.; Zhou, L.; Nishiyama, H. *Chem. Commun.* **2009**, 5987–5989.

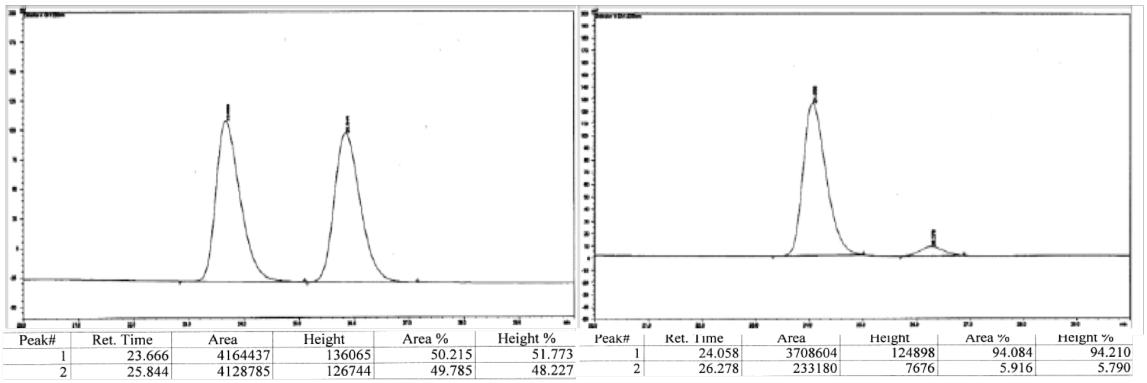

| Peak# | Ret. Time | Area | Height | Area % | Height % |
|---|---|---|---|---|---|
| 1 | 23.666 | 4164437 | 136065 | 50.215 | 51.773 |
| 2 | 25.844 | 4128785 | 126744 | 49.785 | 48.227 |

| Peak# | Ret. Time | Area | Height | Area % | Height % |
|---|---|---|---|---|---|
| 1 | 24.058 | 3708604 | 124898 | 94.084 | 94.210 |
| 2 | 26.278 | 233180 | 7676 | 5.916 | 5.790 |

| Peak # | Time (min) | Area (%) | Peak # | Time (min) | Area (%) |
|---|---|---|---|---|---|
| 1 | 23.666 | 50.215 | 1 | 24.058 | 94.084 |
| 2 | 25.844 | 49.785 | 2 | 26.278 | 5.916 |

**(*E*)-4-(4-Bromophenyl)but-3-en-2-one (1.78d):** The spectroscopic data match those reported previously.[64] $^1$H NMR (400 MHz, $CDCl_3$): δ 7.52 (2H, d, $J$ = 8.4 Hz), 7.43 (1H, d, $J$ = 16.4 Hz), 7.39 (2H, d, $J$ = 8.4 Hz), 6.68 (1H, d, $J$ = 16.4 Hz), 2.36 (3H, s).

**(*R*)-4-(4-Bromophenyl)-4-(4,4,5,5-tetramethyl-1,3,2-dioxaborolan-2-yl)butan-2-one (1.79d)**: IR (neat): 2957 (m), 2922 (s), 2853 (m), 1707 (m), 1362 (m), 1327 (m), 1142 (m) cm$^{-1}$; $^1$H NMR (400 MHz, $CDCl_3$): δ 7.36 (2H, d, $J$ = 8.4 Hz), 7.09 (2H, d, $J$ = 8.4 Hz), 2.99 (1H, dd, $J$ = 18.4, 10.4 Hz), 2.81 (1H, dd, $J$ = 18.4, 5.6 Hz), 2.60 (1H, dd, $J$ = 10.4, 5.6 Hz), 2.14 (3H, s), 1.21 (6H, s), 1.16 (6H, s); $^{13}$C NMR (100 MHz, $CDCl_3$): δ 208.1, 141.0, 131.6, 130.1, 119.5, 83.7, 47.4, 29.8, 24.7; HRMS (ESI+): Calcd for $C_{16}H_{23}B_1Br_1O_3$ $[M+H]^+$: 353.0924, Found: 353.0908. Specific Rotation: $[\alpha]_D^{20}$ –7.2 (*c* 0.33, $CHCl_3$) for an enantiomerically enriched sample of 92:8 er.

Enantiomeric purity was determined by HPLC analysis in comparison with authentic racemic material (92:8 er shown; Chiralpak AS-H column, 99/1 hexanes/*i*-PrOH, 0.3 mL/min, 220 nm).

(64) Stern, T.; Rückbrod, S.; Czekelius, C.; Donner, C.; Brunner, H. *Adv. Synth. Catal.* **2010**, *352*, 1983–1992.

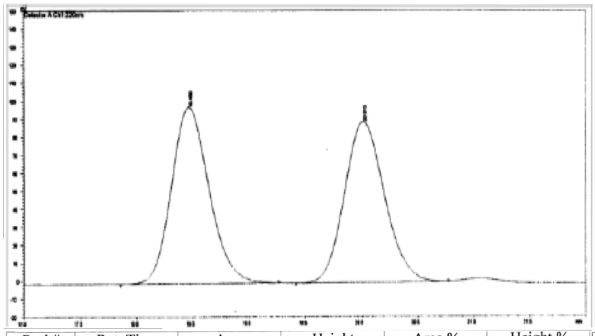

| Peak# | Ret. Time | Area | Height | Area % | Height % |
|---|---|---|---|---|---|
| 1 | 18.460 | 2283801 | 98020 | 50.801 | 52.269 |
| 2 | 20.013 | 2211799 | 89509 | 49.199 | 47.731 |

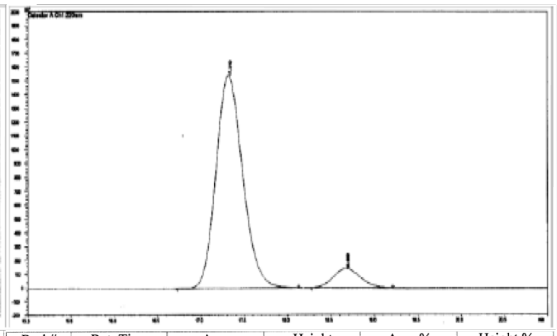

| Peak# | Ret. Time | Area | Height | Area % | Height % |
|---|---|---|---|---|---|
| 1 | 17.310 | 33200851 | 1540116 | 91.628 | 91.682 |
| 2 | 18.669 | 3033602 | 139724 | 8.372 | 8.318 |

| Peak # | Time (min) | Area (%) | Peak # | Time (min) | Area (%) |
|---|---|---|---|---|---|
| 1 | 18.460 | 50.801 | 1 | 17.310 | 91.628 |
| 2 | 20.013 | 49.199 | 2 | 18.669 | 8.372 |

**(*R*)-4-(Furan-2-yl)-4-(4,4,5,5-tetramethyl-1,3,2-dioxaborolan-2-yl)butan-2-one (1.79f)**: IR (neat): 2978 (m), 2928 (m), 1714 (s), 1359 (s), 1324 (s), 1165 (s), 1124 (s), 1008 (m), 850 (m), 727 (m), 799 (m) $cm^{-1}$; $^{1}H$ NMR (400 MHz, $CDCl_3$): δ 7.21–7.19 (1H, m), 6.19–6.18 (1H, m), 5.95–5.94 (1H, m), 2.95–2.81 (2H, m), 2.70–2.66 (1H, m), 2.08 (3H, s), 1.19 (6H, s), 1.16 (6H, s); $^{13}C$ NMR (100 MHz, $CDCl_3$): δ 207.8, 155.1, 140.9, 110.2, 104.9, 83.7, 44.5, 29.5, 24.6, 24.5; HRMS (ESI+): Calcd for $C_{14}H_{22}B_1O_4$ $[M+H]^+$: 265.1611, Found: 265.1616. Specific Rotation: $[\alpha]_D^{20}$ –2.7 (*c* 1.10, $CHCl_3$) for an enantiomerically enriched sample of 92:8 er.

Enantiomeric purity was determined by HPLC analysis in comparison with authentic racemic material (92:8 er shown; Chiralpak AS-H column, 99.5/0.5 hexanes/*i*-PrOH, 0.3 mL/min, 220 nm).

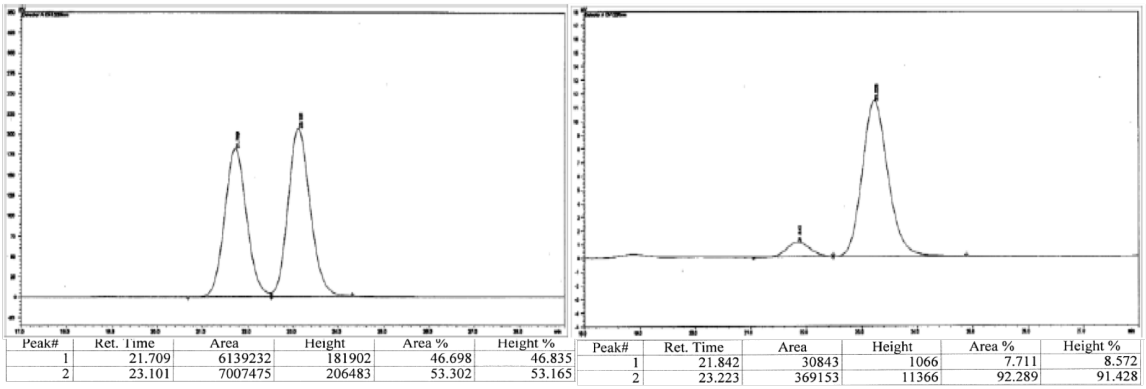

| Peak# | Ret. Time | Area | Height | Area % | Height % |
|---|---|---|---|---|---|
| 1 | 21.709 | 6139232 | 181902 | 46.698 | 46.835 |
| 2 | 23.101 | 7007475 | 206483 | 53.302 | 53.165 |

| Peak# | Ret. Time | Area | Height | Area % | Height % |
|---|---|---|---|---|---|
| 1 | 21.842 | 30843 | 1066 | 7.711 | 8.572 |
| 2 | 23.223 | 369153 | 11366 | 92.289 | 91.428 |

| Peak # | Time (min) | Area (%) | Peak # | Time (min) | Area (%) |
|---|---|---|---|---|---|
| 1 | 21.709 | 46.698 | 1 | 21.842 | 7.711 |
| 2 | 23.101 | 53.302 | 2 | 23.223 | 92.289 |

**(*S*)-4-(4,4,5,5-Tetramethyl-1,3,2-dioxaborolan-2-yl)nonan-2-one (1.79g)**: IR (neat): 2976 (w), 2958 (m), 2925 (m), 1715 (s), 1410 (s), 1379 (s), 1312 (s), 1266 (w), 1244 (w), 1214 (w), 1143 (s), 968 (m), 857 (m), 670 (m) $cm^{-1}$; $^{1}H$ NMR (400 MHz, $CDCl_3$): δ 2.53 (2H, apparent d), 2.08 (3H, s), 1.40–1.34 (1H m), 1.29–1.19 (20H, m), 0.83 (3H, apparent t); $^{13}C$ NMR (100 MHz, $CDCl_3$): δ 209.2, 82.9, 45.8, 31.9, 30.3, 29.6, 28.5, 24.7, 24.6, 22.5, 14.0; HRMS (ESI+): Calcd for $C_{15}H_{30}B_1O_3$ $[M+H]^+$: 269.2288, Found: 269.2279. Specific Rotation: $[\alpha]_D^{20}$ +0.8 (*c* 1.00, $CHCl_3$) for an enantiomerically enriched sample of 94:6 er.

Enantiomeric purity was determined by HPLC analysis in comparison with authentic racemic material (94:6 er shown; Chiralpak AD-H column, 99.8/0.2 hexanes/*i*-PrOH, 0.3 mL/min, 300 nm).

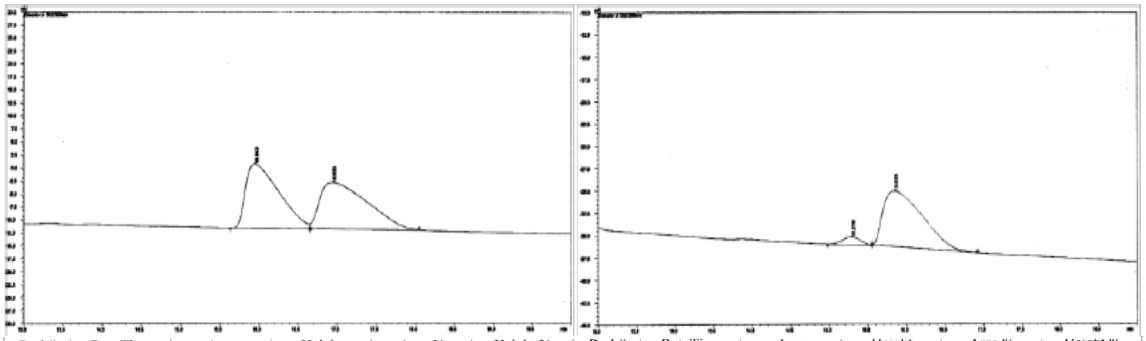

| Peak# | Ret. Time | Area | Height | Area % | Height % |
|---|---|---|---|---|---|
| 1 | 15.943 | 368803 | 12460 | 49.345 | 58.166 |
| 2 | 16.933 | 378598 | 8961 | 50.655 | 41.834 |

| Peak# | Ret. Time | Area | Height | Area % | Height % |
|---|---|---|---|---|---|
| 1 | 15.279 | 13111 | 826 | 5.619 | 11.735 |
| 2 | 15.833 | 220233 | 6211 | 94.381 | 88.265 |

| Peak # | Time (min) | Area (%) | Peak # | Time (min) | Area (%) |
|---|---|---|---|---|---|
| 1 | 15.943 | 49.343 | 1 | 15.279 | 5.619 |
| 2 | 16.933 | 50.635 | 2 | 15.833 | 94.387 |

**(*R*)-5-Methyl-4-(4,4,5,5-tetramethyl-1,3,2-dioxaborolan-2-yl)hexan-2-one (1.79h):** IR (neat): 2976 (m), 2958 (m), 1715 (s), 1412 (w), 1371 (s), 1310 (s), 1279 (s), 1214 (m), 1165 (m), 1142 (s), 1123 (s), 969 (w), 850 (m) $cm^{-1}$; $^{1}H$ NMR (400 MHz, $CDCl_3$): δ 2.59 (1H, dd, *J* = 18.4, 11.2 Hz), 2.48 (1H, dd, *J* = 18.4, 4.8 Hz), 2.09 (3H, s), 1.71–1.63 (1H, m), 1.23–1.13 (13H, m), 0.91–0.88 (6H, m); $^{13}C$ NMR (100 MHz, $CDCl_3$): δ 209.5, 82.9, 43.8, 29.7, 28.9, 25.0, 24.9, 24.7, 22.1, 21.6; HRMS (ESI+): Calcd for $C_{13}H_{26}B_1O_3$ $[M+H]^+$: 241.1975, Found: 241.1984. Specific Rotation: $[\alpha]_D^{20}$ +1.2 (*c* 1.80, $CHCl_3$) for an enantiomerically enriched sample of 94:6 er.

Enantiomeric purity was determined by HPLC analysis in comparison with authentic racemic material (94:6 er shown; Chiralcel OD-H column, 99.9/0.1 hexanes/*i*-PrOH, 0.3 mL/min, 300 nm).

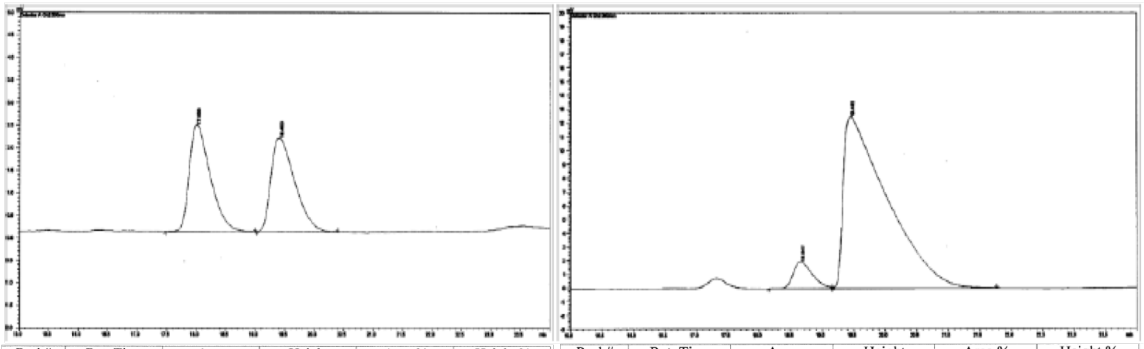

| Peak# | Ret. Time | Area | Height | Area % | Height % |
|---|---|---|---|---|---|
| 1 | 17.999 | 59414 | 2379 | 50.558 | 53.289 |
| 2 | 19.403 | 58102 | 2085 | 49.442 | 46.711 |

| Peak# | Ret. Time | Area | Height | Area % | Height % |
|---|---|---|---|---|---|
| 1 | 18.647 | 41086 | 1953 | 6.344 | 13.555 |
| 2 | 19.442 | 606515 | 12457 | 93.656 | 86.445 |

| Peak # | Time (min) | Area (%) | Peak # | Time (min) | Area (%) |
|---|---|---|---|---|---|
| 1 | 17.999 | 50.558 | 1 | 18.647 | 6.344 |
| 2 | 19.403 | 49.442 | 2 | 19.442 | 93.656 |

**(*E*)-1-Phenylhept-1-en-3-one (1.78i):** The spectroscopic data match those reported previously.[65] $^1$H NMR (400 MHz, $CDCl_3$): δ 7.55–7.51 (3H, m), 7.39–7.37 (3H, m), 6.73 (1H, d, $J$ = 16.4 Hz), 2.65 (2H, t, $J$ = 7.2 Hz), 1.69–1.61 (2H, m), 1.42–1.33 (2H, m), 0.93 (3H, t, $J$ = 7.2 Hz).

**(*R*)-1-Phenyl-1-(4,4,5,5-tetramethyl-1,3,2-dioxaborolan-2-yl)heptan-3-one (1.79i):** IR (neat): 2976 (m), 2931 (m), 1709 (s), 1369 (s), 1319 (s), 1280 (m), 1261 (w), 1214 (w), 1141 (s), 1124 (s), 968 (m), 850 (m), 701 (s) cm$^{-1}$; $^1$H NMR (400 MHz, $CDCl_3$): δ 7.25–7.18 (4H, m), 7.14–7.10 (1H, m), 2.99 (1H, dd, $J$ = 18.2, 10.8 Hz), 2.78 (1H, dd, $J$ = 18.2, 5.2 Hz), 2.63 (1H, dd, $J$ = 10.8, 5.2 Hz), 2.44–2.25 (2H, m), 1.58–1.50 (2H, m), 1.33–1.24 (2H, m), 1.20 (6H, s), 1.14 (6H, s), 0.87 (3H, apparent t); $^{13}$C NMR (100 MHz, $CDCl_3$): δ 210.8, 141.8, 128.4, 128.2, 125.5, 83.3, 46.6, 42.2, 26.2, 24.5, 24.5, 22.3, 13.8; HRMS (ESI+): Calcd for $C_{19}H_{30}B_1O_3$ $[M+H]^+$: 317.2288, Found: 317.2297. Specific Rotation: $[\alpha]_D^{20}$ –21.0 (*c* 1.34, $CHCl_3$) for an enantiomerically enriched sample of 91:9 er.

(65) Badioli, M.; Ballini, R.; Bartolacci, M.; Bosica, G.; Torregiani, E.; Marcantoni, E. *J. Org. Chem.* **2002**, *67*, 8938–8942.

Enantiomeric purity was determined by HPLC analysis in comparison with authentic racemic material (91:9 er shown; Chiralcel OJ-H column, 98/2 hexanes/*i*-PrOH, 0.3 mL/min, 220 nm).

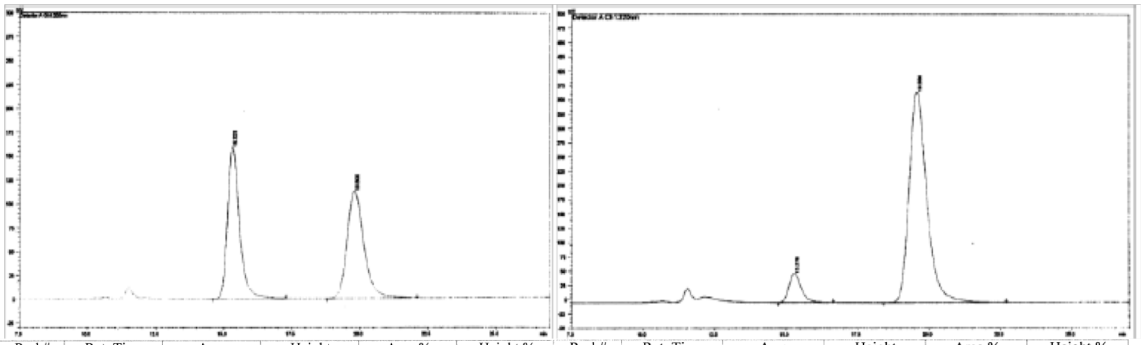

| Peak# | Ret. Time | Area | Height | Area % | Height % |
|---|---|---|---|---|---|
| 1 | 15.323 | 4859526 | 159419 | 49.918 | 58.619 |
| 2 | 19.806 | 4875440 | 112537 | 50.082 | 41.381 |

| Peak# | Ret. Time | Area | Height | Area % | Height % |
|---|---|---|---|---|---|
| 1 | 15.278 | 1492188 | 50800 | 8.601 | 12.089 |
| 2 | 19.556 | 15857595 | 369410 | 91.399 | 87.911 |

| Peak # | Time (min) | Area (%) | Peak # | Time (min) | Area (%) |
|---|---|---|---|---|---|
| 1 | 15.323 | 49.918 | 1 | 15.278 | 8.601 |
| 2 | 19.806 | 50.082 | 2 | 19.556 | 91.399 |

**(*E*)-4-Methyl-1-phenylpent-1-en-3-one (1.78j):** The spectroscopic data match those reported previously.[66] $^1$H NMR (400 MHz, $CDCl_3$): δ 7.60 (1H, d, $J$ = 16.0 Hz), 7.56–7.53 (2H, m), 7.40–7.36 (3H, m), 6.80 (1H, d, $J$ = 16.4 Hz), 2.97–2.87 (1H, m), 1.18 (3H, s), 1.16 (3H, s).

**(*R*)-4-Methyl-1-phenyl-1-(4,4,5,5-tetramethyl-1,3,2-dioxaborolan-2-yl)pentan-3-one (1.79j)**: The spectroscopic data match those reported previously.[27] $^1$H NMR (400 MHz, $CDCl_3$): δ 7.25–7.19 (4H, m), 7.14–7.10 (1H, m), 3.03 (1H, dd, $J$ = 18.2, 11.2 Hz), 2.82 (1H, dd, $J$ = 18.2, 4.8 Hz), 2.63 (1H, dd, $J$ = 11.2, 4.8 Hz), 2.59–2.53 (1H, m), 1.20 (6H, s), 1.13 (6H, s), 1.09–1.04 (6H, m); Specific Rotation: $[\alpha]_D^{20}$ –20.3 (*c* 1.07, $CHCl_3$) for an enantiomerically enriched sample of 90:10 er.

(66) Gillmore, A.; Lauret, C.; Roberts, S. M. *Tetrahedron,* **2003**, *59*, 4363–4375.

Enantiomeric purity was determined by HPLC analysis in comparison with authentic racemic material (90:10 er shown; Chiralpak AS-H column, 98/2 hexanes/*i*-PrOH, 0.3 mL/min, 220 nm).

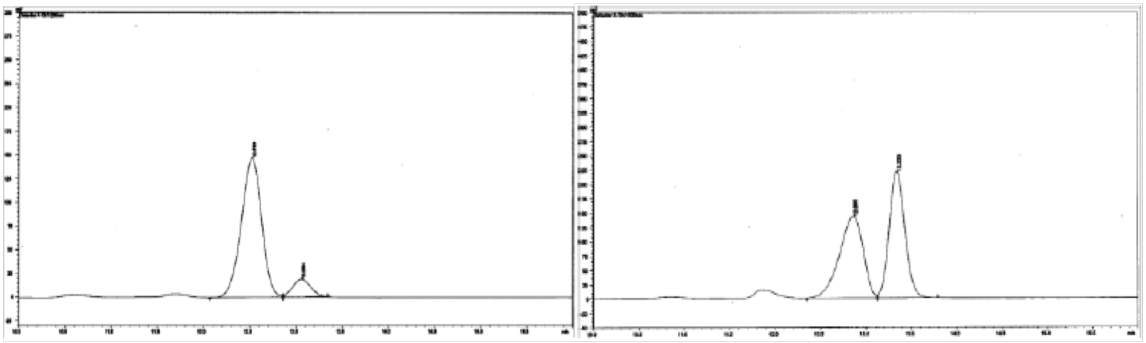

| Peak# | Ret. Time | Area | Height | Area % | Height % |
|---|---|---|---|---|---|
| 1 | 12.855 | 2577826 | 142585 | 49.099 | 39.254 |
| 2 | 13.333 | 2672412 | 220656 | 50.901 | 60.746 |

| Peak# | Ret. Time | Area | Height | Area % | Height % |
|---|---|---|---|---|---|
| 1 | 12.519 | 2250201 | 147162 | 89.879 | 88.721 |
| 2 | 13.054 | 253385 | 18708 | 10.121 | 11.279 |

| Peak # | Time (min) | Area (%) | Peak # | Time (min) | Area (%) |
|---|---|---|---|---|---|
| 1 | 12.855 | 49.099 | 1 | 12.519 | 89.879 |
| 2 | 13.333 | 50.901 | 2 | 13.054 | 10.121 |

**(*R*)-1,3-Diphenyl-3-(4,4,5,5-tetramethyl-1,3,2-dioxaborolan-2-yl)propan-1-one (1.79k)**: The spectroscopic data match those reported previously.[64] $^1$H NMR (400 MHz, $CDCl_3$): δ 7.97–7.94 (2H, m), 7.55–7.50 (1H, m), 7.44–7.40 (2H, m), 7.31–7.24 (4H, m), 7.17–7.13 (1H, m), 3.54 (1H, dd, $J$ = 18.4, 10.8 Hz), 3.41 (1H, dd, $J$ = 18.4, 5.2 Hz), 2.79 (1H, dd, $J$ = 10.8, 5.2 Hz), 1.23 (6H, s), 1.15 (6H, s); Specific Rotation: $[\alpha]_D^{20}$ –18.7 (*c* 1.10, $CHCl_3$) for an enantiomerically enriched sample of 94:6 er.

Enantiomeric purity was determined by HPLC analysis in comparison with authentic racemic material (94:6 er shown; Chiralcel OJ-H column, 98/2 hexanes/*i*-PrOH, 0.3 mL/min, 220 nm).

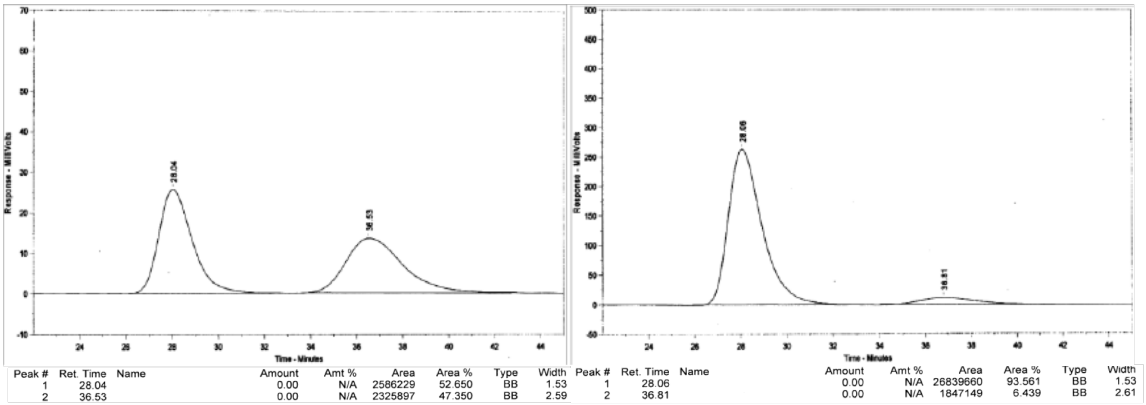


| Peak # | Time (min) | Area (%) | Peak # | Time (min) | Area (%) |
|---|---|---|---|---|---|
| 1 | 28.04 | 52.650 | 1 | 28.06 | 93.561 |
| 2 | 36.53 | 47.350 | 2 | 36.81 | 6.439 |

**(*E*)-4-(4-Fluorophenyl)but-3-en-2-one (1.78l)**: The compound has been previously reported and spectra data match those previously described.[66] $^{1}$H NMR (400 MHz, $CDCl_3$): δ 7.56–7.50 (2H, m), 7.48 (1H, d, $J$ = 16.4 Hz), 7.12–7.06 (2H, m), 6.65 (1H, d, $J$ = 16.4 Hz), 2.37 (3H, s).

**(*R*)-4-(4-Fluorophenyl)-4-(4,4,5,5-tetramethyl-1,3,2-dioxaborolan-2-yl)butan-2-one (1.79l)**: IR (neat): 2977 (m), 2926 (m), 2854 (w), 1714 (m), 1508 (s), 1362 (s), 1322 (s), 1261 (m), 1220 (m), 1166 (m), 1142 (s) cm$^{-1}$; $^{1}$H NMR (400 MHz, $CDCl_3$): δ 7.19–7.14 (2H, m), 7.98–6.91 (2H, m), 2.99 (1H, dd, $J$ = 18.4, 10.4 Hz), 2.81 (1H, dd, $J$ = 18.2, 5.4 Hz), 2.61 (1H, dd, $J$ = 10.4, 5.2 Hz), 2.13 (3H, s), 1.22 (6H, s), 1.16 (6H, s); $^{13}$C NMR (100 MHz, $CDCl_3$): δ 208.3, 161.2 (d, $J$ = 241.8 Hz), 137.4 (d, $J$ = 3 Hz), 129.7 (d, $J$ = 8.2 Hz), 115.3 (d, $J$ = 20.9 Hz), 83.6, 47.7, 29.8, 29.7, 24.7; HRMS (ESI+): Calcd for $C_{16}H_{23}B_1F_1O_3$ $[M+H]^+$: 293.1724, Found: 293.1719. Specific Rotation: $[\alpha]_D^{20}$ –26.5 (*c* 0.25, $CHCl_3$) for an enantiomerically enriched sample of >99:1 er.

Enantiomeric purity was determined by HPLC analysis in comparison with authentic racemic material (>99:1 er shown; Chiralpak AD-H column, 99/1 hexanes/*i*-PrOH, 0.3 mL/min, 220 nm).

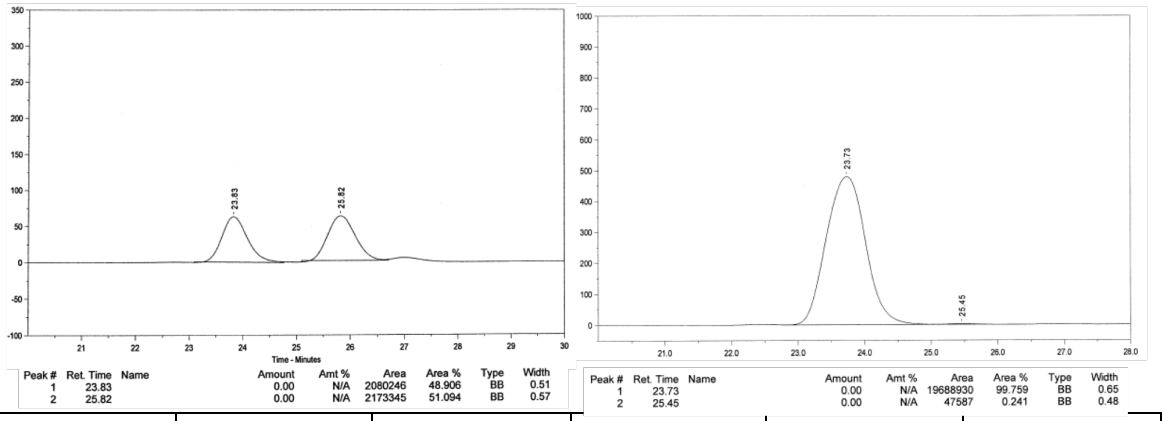


| Peak # | Time (min) | Area (%) | Peak # | Time (min) | Area (%) |
|---|---|---|---|---|---|
| 1 | 23.83 | 48.906 | 1 | 23.73 | 99.759 |
| 2 | 25.82 | 51.094 | 2 | 25.45 | 0.241 |

**(*E*)-4-(4-Chlorophenyl)but-3-en-2-one (1.78m)**: The compound has been previously reported and spectra data match those previously described.[64] $^1$H NMR (400 MHz, $CDCl_3$): δ 7.50–7.44 (3H, m), 7.39–7.36 (2H, m), 6.69 (1H, d, $J$ = 16.4 Hz), 2.38 (3H, s).

**(*R*)-4-(4-Chlorophenyl)-4-(4,4,5,5-tetramethyl-1,3,2-dioxaborolan-2-yl)butan-2-one (1.79m)**: IR (neat): 2975 (m), 2925 (m), 2851 (w), 1707 (s), 1491 (w), 1418 (w), 1359 (s), 1325 (s), 1312 (m), 1141 (s) cm$^{-1}$; $^1$H NMR (400 MHz, $CDCl_3$): δ 7.22 (2H, d, $J$ = 8.4 Hz), 7.14 (2H, d, $J$ = 8.4 Hz), 2.99 (1H, dd, $J$ = 18.4, 10.4 Hz), 2.82 (1H, dd, $J$ = 18.4, 5.6 Hz), 2.61 (1H, dd, $J$ = 10.2, 5.4 Hz), 2.14 (3H, s), 1.21 (6H, s), 1.16 (6H, s); $^{13}$C NMR (100 MHz, $CDCl_3$): δ 208.2, 140.4, 131.4, 129.7, 128.7, 83.7, 47.4, 29.9, 29.7, 24.7; HRMS (ESI+): Calcd for $C_{16}H_{23}B_1Cl_1O_3$ $[M+H]^+$: 309.1429, Found: 309.1429. Specific Rotation: $[\alpha]_D^{20}$ –12.0 (*c* 0.12, $CHCl_3$) for an enantiomerically enriched sample of 95:5 er.

Enantiomeric purity is determined by HPLC analysis in comparison with authentic racemic material (95:5 er shown; Chiralpak AS-H column, 99.5/0.5 hexanes/*i*-PrOH, 0.3 mL/min, 220 nm).

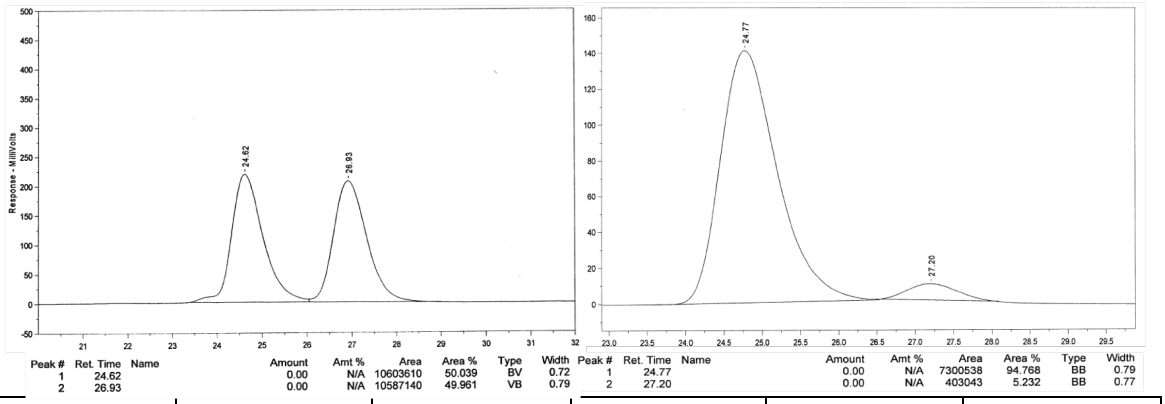


| Peak # | Time (min) | Area (%) | Peak # | Time (min) | Area (%) |
|---|---|---|---|---|---|
| 1 | 24.62 | 50.039 | 1 | 24.77 | 94.768 |
| 2 | 26.93 | 49.961 | 2 | 27.20 | 5.232 |

**(*R*)-Methyl-3-phenyl-3-(4,4,5,5-tetramethyl-1,3,2-dioxaborolan-2-yl)propanoate (1.83a)**: The spectroscopic data match those reported previously.[67] $^1$H NMR (400 MHz, $CDCl_3$): δ 7.26–7.18 (4H, m), 7.15–7.11 (1H, m), 3.63 (3H, s), 2.88 (1H, dd, $J$ = 15.8, 9.6 Hz), 2.74–2.61 (2H, m), 1.24 (6H, s), 1.15 (6H, s); Specific Rotation: $[\alpha]_D^{20}$ –20.3 (*c* 1.05, $CHCl_3$) for an enantiomerically enriched sample of 98:2 er.

Enantiomeric purity was determined by HPLC analysis in comparison with authentic racemic material (98:2 er shown; Chiralcel OJ-H column, 98/2 hexanes/*i*-PrOH, 0.3 mL/min, 220 nm).

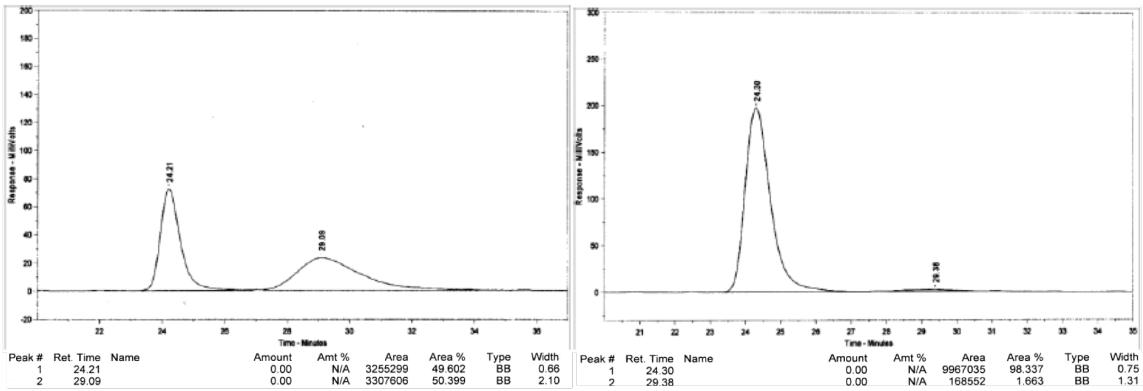


(67) Park, J. K.; Lackey, H. H.; Rexford, M. D.; Kovnir, K.; Shatruk, M.; McQuade, D. T. *Org. Lett.* **2010**, *12*, 5008–5011.

| Peak # | Time (min) | Area (%) | Peak # | Time (min) | Area (%) |
|---|---|---|---|---|---|
| 1 | 24.21 | 49.602 | 1 | 24.30 | 98.337 |
| 2 | 29.09 | 50.399 | 2 | 29.38 | 1.663 |

**(*R*)-Methyl-3-(4-bromophenyl)-3-(4,4,5,5-tetramethyl-1,3,2-dioxaborolan-2-yl)propanoate (1.83b)**: IR (neat): 2976 (m), 2953 (m), 2924 (m), 2853 (w), 1736 (s), 1487 (m), 1437 (m), 1370 (s), 1327 (s), 1169 (m), 1141 (s), 1011 (m), 847 (m) $cm^{-1}$; $^{1}H$ NMR (400 MHz, $CDCl_3$): δ 7.37 (2H, d, $J$ = 8.4 Hz), 7.09 (2H, d, $J$ = 8.4 Hz), 3.64 (3H, s), 2.85 (1H, dd, $J$ = 15.4, 8.6 Hz), 2.71–2.61 (2H, m), 1.21 (6H, s), 1.17 (6H, s); $^{13}C$ NMR (100 MHz, $CDCl_3$): δ 173.9, 140.8, 131.9, 130.3, 119.9, 84.1, 52.0, 37.2, 30.1, 30.5, 24.9, 24.8; HRMS (ESI+): Calcd for $C_{16}H_{23}B_1Br_1O_4$ $[M+H]^+$: 369.0873, Found: 369.0872. Specific Rotation: $[\alpha]_D^{20}$ –10.2 (*c* 0.32, $CHCl_3$) for an enantiomerically enriched sample of 94:6 er.

Enantiomeric purity was determined by HPLC analysis in comparison with authentic racemic material (94:6 er shown; Chiralcel OJ-H column, 99/1 hexanes/*i*-PrOH, 0.3 mL/min, 220 nm).

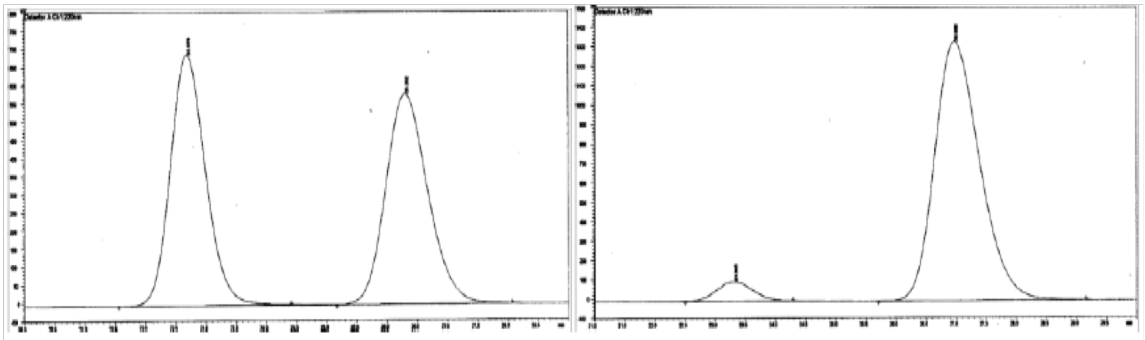

| Peak# | Ret. Time | Area | Height | Area % | Height % |
|---|---|---|---|---|---|
| 1 | 22.676 | 27983858 | 690053 | 49.825 | 54.300 |
| 2 | 26.292 | 28180201 | 580770 | 50.175 | 45.700 |

| Peak# | Ret. Time | Area | Height | Area % | Height % |
|---|---|---|---|---|---|
| 1 | 23.305 | 4266346 | 101913 | 5.785 | 7.093 |
| 2 | 26.966 | 69486710 | 1334807 | 94.215 | 92.907 |

| Peak # | Time (min) | Area (%) | Peak # | Time (min) | Area (%) |
|---|---|---|---|---|---|
| 1 | 22.676 | 49.825 | 1 | 23.305 | 5.785 |
| 2 | 26.292 | 50.175 | 2 | 26.966 | 94.215 |

**(*S*)-Methyl-3-(4,4,5,5-tetramethyl-1,3,2-dioxaborolan-2-yl)octanoate (1.83c):** IR (neat): 2978 (m), 2927 (m), 2857 (w), 1737 (s), 1371 (m), 1318 (m), 1280 (s), 1168 (m), 1143 (s), 1124 (s), 850 (s) $cm^{-1}$; $^1H$ NMR (400 MHz, $CDCl_3$): δ 3.61 (3H, s), 2.44–2.32 (2H, m), 1.44–1.37 (1H, m), 1.32–1.20 (20H, m), 0.84 (3H, apparent t); $^{13}C$ NMR (100 MHz, $CDCl_3$): δ 174.4, 83.1, 51.3, 35.6, 31.9, 30.5, 28.3, 24.7, 24.6, 22.5, 14.0; HRMS (ESI+): Calcd for $C_{15}H_{30}B_1O_4$ $[M+H]^+$: 285.2237, Found: 285.2236. Specific Rotation: $[\alpha]_D^{20}$ +2.5 (*c* 0.85, $CHCl_3$) for an enantiomerically enriched sample of 95:5 er.

Enantiomeric purity was determined by GLC analysis in comparison with authentic racemic material (95:5 er shown; Chiraldex B-DM column, 15 psi, 90 ºC).

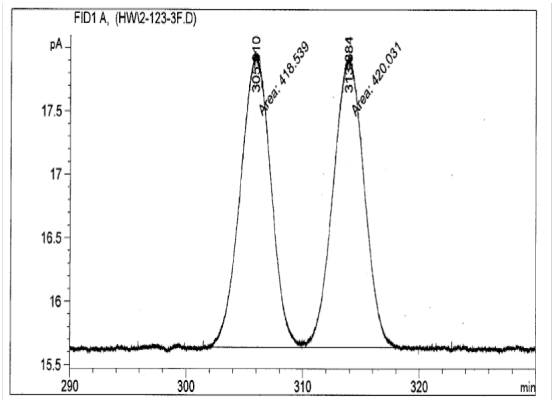


| # | Time | Area | Height | Width | Area% |
|---|---|---|---|---|---|
| 1 | 305.91 | 418.5 | 2.3 | 2.9866 | 49.911 |
| 2 | 313.884 | 420 | 2.3 | 3.0334 | 50.089 |

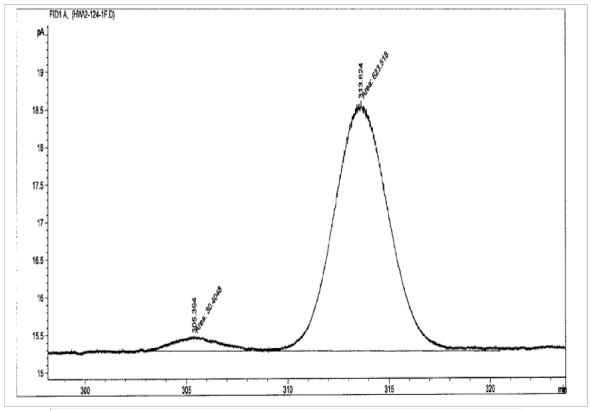


| # | Time | Area | Height | Width | Area% |
|---|---|---|---|---|---|
| 1 | 305.394 | 30.4 | 2E-1 | 2.519 | 4.650 |
| 2 | 313.624 | 623.5 | 3.3 | 3.1168 | 95.350 |

| Peak # | Time (min) | Area (%) | Peak # | Time (min) | Area (%) |
|---|---|---|---|---|---|
| 1 | 305.910 | 49.911 | 1 | 305.394 | 4.650 |
| 2 | 313.884 | 50.089 | 2 | 313.624 | 95.350 |

**(*R*)-*tert*-Butyl-3-phenyl-3-(4,4,5,5-tetramethyl-1,3,2-dioxaborolan-2-yl)propanoate (1.83d)**: The spectroscopic data match those reported previously.[63] $^1H$ NMR (400 MHz, $CDCl_3$): δ 7.25–7.18 (4H, m), 7.14–7.09 (1H, m), 2.78 (1H, dd, *J* = 15.6, 10.0 Hz), 2.68 (1H, dd, *J* = 10.0, 5.6 Hz), 2.56 (1H, dd, *J* = 15.6, 5.6 Hz), 1.39 (9H, s), 1.20 (6H, s), 1.15 (6H, s); Specific Rotation: $[\alpha]_D^{20}$ –19.6 (*c* 1.20, $CHCl_3$) for an enantiomerically enriched sample of 98:2 er.

Enantiomeric purity was determined by HPLC analysis in comparison with authentic racemic material (98:2 er shown; Chiralcel OD-H column, 99.9/0.1 hexanes/*i*-PrOH, 0.3 mL/min, 220 nm).

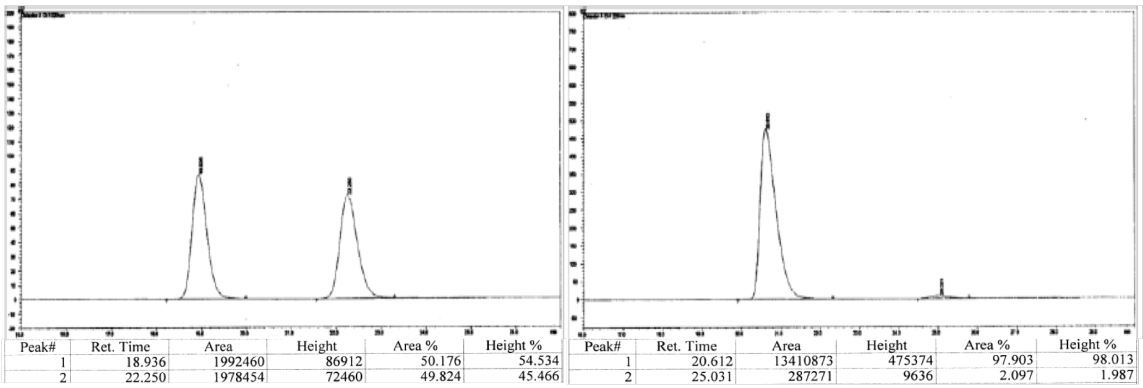

| Peak# | Ret. Time | Area | Height | Area % | Height % |
|---|---|---|---|---|---|
| 1 | 18.936 | 1992460 | 86912 | 50.176 | 54.534 |
| 2 | 22.250 | 1978454 | 72460 | 49.824 | 45.466 |

| Peak# | Ret. Time | Area | Height | Area % | Height % |
|---|---|---|---|---|---|
| 1 | 20.612 | 13410873 | 475374 | 97.903 | 98.013 |
| 2 | 25.031 | 287271 | 9636 | 2.097 | 1.987 |

| Peak # | Time (min) | Area (%) | Peak # | Time (min) | Area (%) |
|---|---|---|---|---|---|
| 1 | 18.936 | 50.176 | 1 | 20.612 | 97.903 |
| 2 | 22.250 | 49.824 | 2 | 25.031 | 2.097 |

***N*-Methoxy-*N*-methylcinnamamide (1.84a):** The spectroscopic data match those reported previously.[68] $^1$H NMR (400 MHz, $CDCl_3$): δ 7.72 (1H, d, $J$ = 15.6 Hz), 7.57–7.54 (2H, m), 7.40–7.24 (3H, m), 7.02 (1H, d, $J$ = 15.6 Hz), 3.75 (3H, s), 3.30 (3H, s).

**(*R*)-*N*-Methoxy-*N*-methyl-3-phenyl-3-(4,4,5,5-tetramethyl-1,3,2-dioxaborolan-2-yl)propanamide (1.85a):** IR (neat): 2975 (w), 2931 (w), 1657 (s), 1359 (s), 1319 (s), 1248 (m), 1140 (s), 1109 (m), 996 (m), 969 (w), 701 (s) cm$^{-1}$; $^1$H NMR (400 MHz, $CDCl_3$): δ 7.27–7.21 (4H, m), 7.16–7.10 (1H, m), 3.61 (3H, s), 3.14 (3H, s), 2.98–2.81 (2H, m), 2.69 (1H, dd, $J$ = 11.2, 5.6 Hz), 1.20 (6H, s), 1.15 (6H, s); $^{13}$C NMR (100 MHz, $CDCl_3$): δ 174.3, 142.1, 128.4, 128.4, 125.5, 83.2, 61.1, 35.9, 32.3, 24.6, 24.5; HRMS (ESI+): Calcd for $C_{16}H_{33}B_1N_1O_4$ $[M+H]^+$: 320.2033, Found: 320.2032. Specific Rotation: $[\alpha]_D^{20}$ –65.3 (*c* 0.73, $CHCl_3$) for an enantiomerically enriched sample of 86.5:13.5 er.

(68) Murphy, J. A.; Commeureuc, A. G. J.; Snaddon, T. N.; McGuire, T. M.; Khan, T. A.; Hisler, K.; Dewis, M. L.; Carling, R. *Org. Lett.* **2005**, *7*, 1427–1429.

Enantiomeric purity was determined by HPLC analysis in comparison with authentic racemic material (86.5:13.5 er shown; Chiralcel OJ-H column, 99/1 hexanes/*i*-PrOH, 0.3 mL/min, 220 nm).

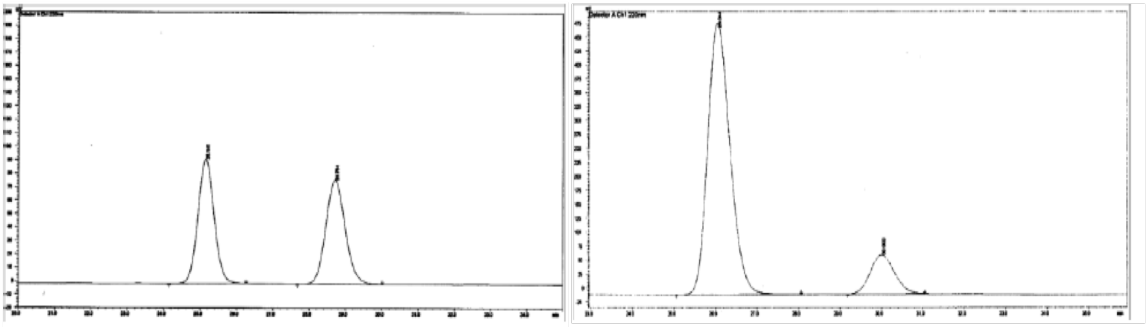

| Peak# | Ret. Time | Area | Height | Area % | Height % |
|---|---|---|---|---|---|
| 1 | 25.141 | 2874969 | 92232 | 49.901 | 54.451 |
| 2 | 28.704 | 2886371 | 77153 | 50.099 | 45.549 |

| Peak# | Ret. Time | Area | Height | Area % | Height % |
|---|---|---|---|---|---|
| 1 | 26.044 | 18287171 | 487358 | 86.472 | 87.461 |
| 2 | 30.000 | 2860809 | 69871 | 13.528 | 12.539 |

| Peak # | Time (mins) | Area (%) | Peak # | Time (mins) | Area (%) |
|---|---|---|---|---|---|
| 1 | 25.141 | 49.901 | 1 | 26.044 | 86.472 |
| 2 | 28.704 | 50.099 | 2 | 30.000 | 13.528 |

**(*E*)-3-(4-Bromophenyl)-*N*-methoxy-*N*-methylacrylamide (1.84b):** IR (neat): 2964 (w), 2935 (w), 1656 (s), 1619 (s), 1488 (s), 1461 (s), 1379 (s), 1199 (m), 1071 (s), 1008 (s), 815 (s), 789 (m), $cm^{-1}$; $^1H$ NMR (400 MHz, $CDCl_3$): δ 7.65 (1H, d, $J$ = 16.0 Hz), 7.50 (2H, d, $J$ = 6.8 Hz), 7.42 (2H, d, $J$ = 6.8 Hz), 7.01 (1H, d, $J$ = 16.0 Hz), 3.76 (3H, s), 3.30 (3H, s); $^{13}C$ NMR (100 MHz, $CDCl_3$): δ 166.7, 142.2, 134.2, 132.1, 129.6, 124.1, 116.6, 62.0, 32.6; HRMS (ESI+): Calcd for $C_{11}H_{13}Br_1N_1O_2$ $[M+H]^+$: 272.0109, Found: 272.0114.

**(*R*)-3-(4-Bromophenyl)-*N*-methoxy-*N*-methyl-3-(4,4,5,5-tetramethyl-1,3,2-dioxaborolan-2-yl)propanamide (1.85b):** IR (neat): 2973 (w), 2922 (m), 2852 (w), 1725 (w), 1659 (s), 1486 (m), 1361 (s), 1324 (s), 1108 (s) $cm^{-1}$; $^1H$ NMR (400 MHz, $CDCl_3$): δ 7.37 (2H, d, $J$ = 8.4 Hz), 7.15 (2H, d, $J$ = 8.4 Hz), 3.64 (3H, s), 3.15 (3H, s), 2.98–2.82 (2H, m), 2.66 (1H, dd, $J$ = 10.0, 6.0 Hz), 1.21 (6H, s), 1.17 (6H, s); $^{13}C$ NMR (100 MHz, $CDCl_3$): δ 174.0, 141.4, 131.5, 130.3, 119.4, 83.5, 61.3, 35.8, 32.5, 29.8, 24.7,

24.7; HRMS (ESI+): Calcd for $C_{17}H_{26}B_1Br_1N_1O_4$ $[M+H]^+$: 398.1138, Found: 398.1139. Specific Rotation: $[\alpha]_D^{20}$ –15.6 (*c* 0.81, $CHCl_3$) for an enantiomerically enriched sample of 94:6 er.

Enantiomeric purity was determined by HPLC analysis in comparison with authentic racemic material (94:6 er shown; Chiralcel OD-H column, 99/1 hexanes/*i*-PrOH, 0.3 mL/min, 220 nm).

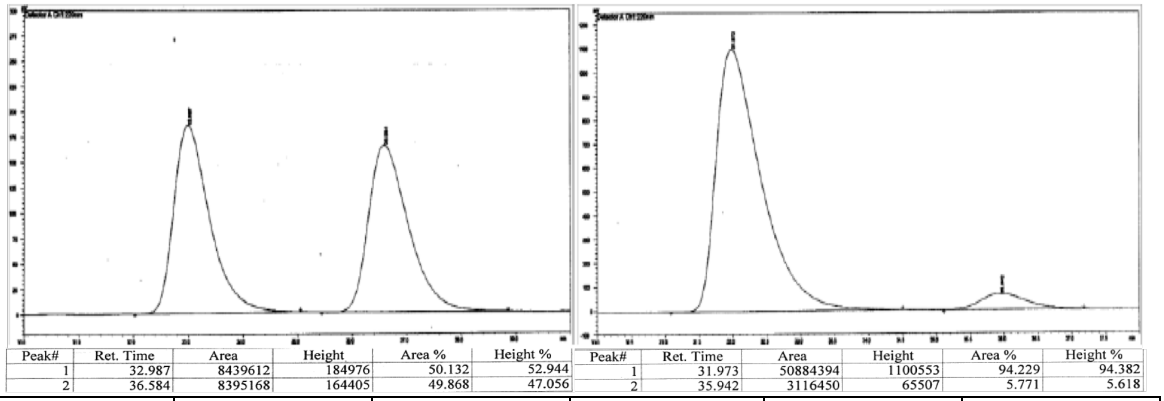

| Peak# | Ret. Time | Area | Height | Area % | Height % |
|---|---|---|---|---|---|
| 1 | 32.987 | 8439612 | 184976 | 50.132 | 52.944 |
| 2 | 36.584 | 8395168 | 164405 | 49.868 | 47.056 |

| Peak# | Ret. Time | Area | Height | Area % | Height % |
|---|---|---|---|---|---|
| 1 | 31.973 | 50884394 | 1100553 | 94.229 | 94.382 |
| 2 | 35.942 | 3116450 | 65507 | 5.771 | 5.618 |

| Peak # | Time (min) | Area (%) | Peak # | Time (min) | Area (%) |
|---|---|---|---|---|---|
| 1 | 32.987 | 50.132 | 1 | 31.973 | 94.229 |
| 2 | 36.584 | 49.868 | 2 | 35.942 | 5.771 |

**(*E*)-*N*-Methoxy-*N*-methyloct-2-enamide (1.84c):** IR (neat): 2957 (m), 2928 (m), 2858 (w), 1665 (s), 1635 (s), 1462 (m), 1442 (m), 1411 (m), 1378 (s), 1177 (w), 993 (m), 967 (w) $cm^{-1}$; $^1H$ NMR (400 MHz, $CDCl_3$): δ 6.96 (1H, dt, *J* = 15.6, 6.8 Hz), 6.37 (1H, dt, *J* = 14.0, 1.2 Hz), 3.68 (3H, s), 3.22 (3H, s), 2.24–2.18 (2H, m), 1.49–1.41 (2H, m), 1.32–1.25 (4H, m), 0.89–0.84 (3H, m); $^{13}C$ NMR (100 MHz, $CDCl_3$): δ 166.9, 147.7, 118.5, 61.5, 32.3, 32.1, 31.2, 27.9, 22.3, 13.8; HRMS (ESI+): Calcd for $C_{10}H_{20}N_1O_2$ $[M+H]^+$:186.1494, Found: 186.1480.

**(*S*)-*N*-Methoxy-*N*-methyl-3-(4,4,5,5-tetramethyl-1,3,2-dioxaborolan-2-yl)octanamide (1.85c):** IR (neat): 2958 (w), 2925 (m), 2856 (w), 1664 (s), 1462 (w), 1414 (m), 1379 (s), 1315 (s), 1242 (w), 1215 (w), 1145 (s), 1003 (m), 968 (w), 867 (w) $cm^{-1}$; $^1H$ NMR (400

MHz, $CDCl_3$): δ 3.64 (3H, s), 3.12 (3H, s), 2.55–2.43 (2H, m), 1.45–1.20 (21H, m), 0.83 (3H, apparent t); $^{13}C$ NMR (100 MHz, $CDCl_3$): δ 174.9, 82.7, 61.1, 33.7, 32.3, 32.0, 30.7, 28.6, 24.8, 24.7, 22.5, 14.0; HRMS (ESI+): Calcd for $C_{16}H_{33}B_1N_1O_4$ $[M+H]^+$: 314.2503, Found: 314.2509. Specific Rotation: $[\alpha]_D^{20}$ –1.1 (*c* 1.08, $CHCl_3$) for an enantiomerically enriched sample of 95:5 er.

Enantiomeric purity was determined by HPLC analysis in comparison with authentic racemic material (95:5 er shown; Chiralcel OD-H column, 99.9/0.1 hexanes/*i*-PrOH, 0.3 mL/min, 220 nm).

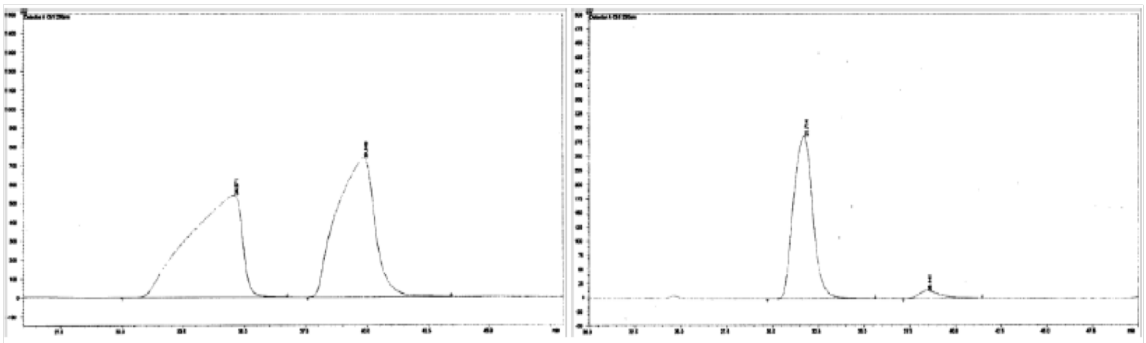

| Peak# | Ret. Time | Area | Height | Area % | Height % |
|---|---|---|---|---|---|
| 1 | 34.571 | 81557786 | 541478 | 50.634 | 42.367 |
| 2 | 39.849 | 79514363 | 736596 | 49.366 | 57.633 |

| Peak# | Ret. Time | Area | Height | Area % | Height % |
|---|---|---|---|---|---|
| 1 | 31.714 | 21296347 | 288660 | 94.796 | 95.481 |
| 2 | 38.441 | 1169098 | 13661 | 5.204 | 4.519 |

| Peak # | Time (min) | Area (%) | Peak # | Time (min) | Area (%) |
|---|---|---|---|---|---|
| 1 | 34.571 | 50.634 | 1 | 31.714 | 94.796 |
| 2 | 39.849 | 49.366 | 2 | 38.441 | 5.204 |

**(*E*)-*N*-Methoxy-*N*,4-dimethylpent-2-enamide (1.84d):** The spectroscopic data match those reported previously.[69] $^1H$ NMR (400 MHz, $CDCl_3$): δ 6.95 (1H, dd, *J* = 15.6, 6.8 Hz), 6.34 (1H, d, *J* = 15.8 Hz), 3.70 (3H, s), 3.24 (3H, s), 2.52–2.47 (1H, m), 1.07 (6H, overlapping d, *J* = 8.0 Hz).

**(*R*)-*N*-Methoxy-*N*,4-dimethyl-3-(4,4,5,5-tetramethyl-1,3,2-dioxaborolan-2-yl)pentanamide (1.85d):** IR (neat): 2957 (m), 2872 (w), 1662 (s), 1464 (w), 1444 (m), 1378 (s), 1317 (s), 1255 (m), 1215 (m), 1165 (m), 1144 (s), 1112 (w), 1099 (w), 1002 (m),

(69) Shintani, R.; Kimura, T.; Hayashi, T. *Chem. Commun.* **2005**, *41*, 3213–3214.

976 (m), 870 (w) $cm^{-1}$; $^1H$ NMR (400 MHz, $CDCl_3$): δ 3.66 (3H, s), 3.12 (3H, s), 2.52–2.50 (2H, m), 1.78–1.66 (1H, m), 1.26–1.23 (7H, m), 1.20 (6H, s), 0.95–0.92 (6H, m); $^{13}C$ NMR (100 MHz, $CDCl_3$): δ 175.3, 82.8, 61.1, 32.2, 31.7, 29.2, 25.0, 24.8, 22.2, 21.7; HRMS (ESI+): Calcd for $C_{14}H_{29}B_1N_1O_4$ $[M+H]^+$: 286.2190, Found: 286.2187. Specific Rotation: $[\alpha]_D^{20}$ –2.0 (*c* 1.30, $CHCl_3$) for an enantiomerically enriched sample of 95:5 er. Enantiomeric purity was determined by HPLC analysis in comparison with authentic racemic material (95:5 er shown; Chiralcel OD-H column, 99.9/0.1 hexanes/*i*-PrOH, 0.3 mL/min, 220 nm).

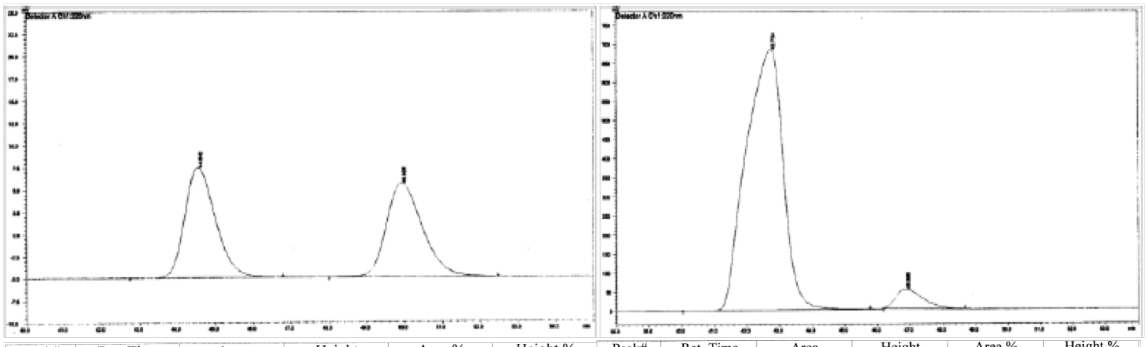

| Peak# | Ret. Time | Area | Height | Area % | Height % |
|---|---|---|---|---|---|
| 1 | 44.542 | 700008 | 12417 | 50.003 | 54.078 |
| 2 | 49.925 | 699936 | 10545 | 49.997 | 45.922 |

| Peak# | Ret. Time | Area | Height | Area % | Height % |
|---|---|---|---|---|---|
| 1 | 42.734 | 54101785 | 684104 | 94.812 | 93.046 |
| 2 | 46.866 | 2960643 | 51129 | 5.188 | 6.954 |

| Peak # | Time (mins) | Area (%) | Peak # | Time (mins) | Area (%) |
|---|---|---|---|---|---|
| 1 | 44.542 | 50.003 | 1 | 42.734 | 94.812 |
| 2 | 49.925 | 49.997 | 2 | 46.866 | 5.188 |

**(*E*)-*N*-Methoxy-*N*,5-dimethylhex-2-enamide (1.84e):** IR (neat): 2956 (m), 2925 (m), 2871 (w), 1664 (s), 1634 (s), 1464 (m), 1411 (m), 1378 (s), 1176 (m), 1152 (w), 1114 (w), 1095 (w), 996 (s), 984 (s) $cm^{-1}$; $^1H$ NMR (400 MHz, $CDCl_3$): δ 6.93 (1H, dt, $J$ = 12.0, 6.0 Hz), 6.36 (1H, d, $J$ = 12.0 Hz), 3.67 (3H, s), 3.21 (3H, s), 2.10 (2H, td, $J$ = 5.2, 1.2 Hz), 1.78–1.70 (1H, m), 0.90 (6H, overlapping d, $J$ = 5.6 Hz); $^{13}C$ NMR (100 MHz, $CDCl_3$): δ 167.3, 147.0, 120.0, 61.9, 42.1, 32.6, 28.2, 22.6; HRMS (ESI+): Calcd for $C_9H_{18}N_1O_2$ $[M+H]^+$: 172.1338, Found: 172.1342.

**(*S*)-*N*-Methoxy-*N*,5-dimethyl-3-(4,4,5,5-tetramethyl-1,3,2-dioxaborolan-2-yl)hexanamide (1.85e):** IR (neat): 2955 (m), 2921 (s), 2852 (m), 1666 (m), 1463 (m), 1378 (s), 1319 (m), 1146 (s) $cm^{-1}$; $^1H$ NMR (400 MHz, $CDCl_3$): δ 3.67 (3H, s), 3.15 (3H, s), 2.57–2.43 (2H, m), 1.67–1.57 (1H, m), 1.41–1.32 (2H, m), 1.24–1.14 (13H, m), 0.89 (3H, d, $J$ = 6.8 Hz), 0.86 (3H, d, $J$ = 6.8 Hz); $^{13}C$ NMR (100 MHz, $CDCl_3$): δ 174.9, 82.7, 61.1, 39.9, 33.8, 30.3, 26.7, 24.8, 24.7, 22.8, 22.6; HRMS (ESI+): Calcd for $C_{15}H_{31}B_1N_1O_4$ $[M+H]^+$: 300.2346, Found: 300.2362. Specific Rotation: $[\alpha]_D^{20}$ +2.8 (*c* 0.67, $CHCl_3$) for an enantiomerically enriched sample of 95:5 er.

Enantiomeric purity was determined by HPLC analysis in comparison with authentic racemic material (95:5 er shown; Chiralpak AS-H column, 99.8/0.2 hexanes/*i*-PrOH, 0.3 mL/min, 220 nm).

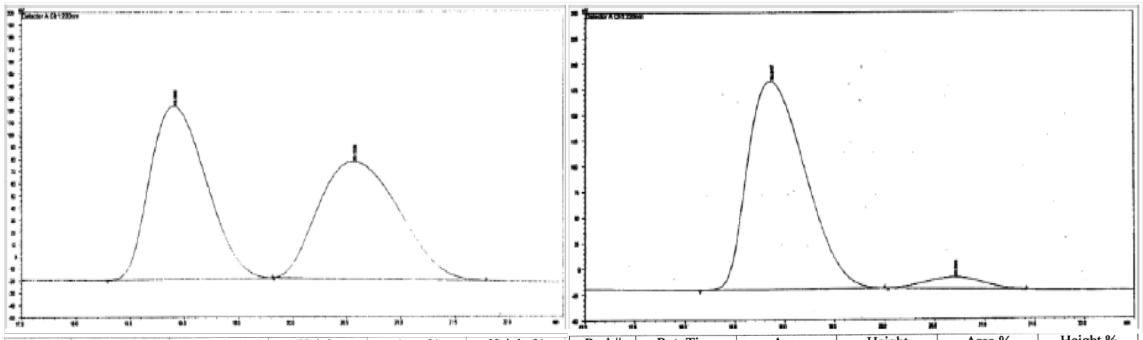

| Peak# | Ret. Time | Area | Height | Area % | Height % |
|---|---|---|---|---|---|
| 1 | 18.899 | 5143401 | 142102 | 50.664 | 59.555 |
| 2 | 20.558 | 5008624 | 96505 | 49.336 | 40.445 |

| Peak# | Ret. Time | Area | Height | Area % | Height % |
|---|---|---|---|---|---|
| 1 | 18.847 | 8185682 | 203240 | 94.706 | 94.675 |
| 2 | 20.688 | 457548 | 11432 | 5.294 | 5.325 |

| Peak # | Time (min) | Area (%) | Peak # | Time (min) | Area (%) |
|---|---|---|---|---|---|
| 1 | 18.899 | 50.664 | 1 | 18.847 | 94.706 |
| 2 | 20.558 | 49.336 | 2 | 20.688 | 5.294 |

**(*E*)-5-[(*tert*-Butyldimethylsilyl)oxy]-*N*-methoxy-*N*-methylpent-2-enamide (1.84f):** IR (neat): 2954 (m), 2930 (m), 2857 (m), 1667 (s), 1637 (s), 1463 (w), 1411 (w), 1379 (s), 1254 (m), 1098 (s), 998 (m), 981 (m), 836 (s), 776 (s) $cm^{-1}$; $^1H$ NMR (400 MHz, $CDCl_3$): δ 6.95 (1H, dt, $J$ = 15.6, 7.2 Hz), 6.46 (1H, dt, $J$ = 15.6, 1.2 Hz), 3.73 (2H, t, $J$ = 6.8 Hz), 3.69 (3H, s), 3.23 (3H, s), 2.48–2.45 (2H, m), 0.88 (9H, s), 0.05 (6H, s); $^{13}C$ NMR (100

MHz, $CDCl_3$): δ 167.1, 144.5, 120.7, 62.0, 61.9, 36.3, 32.6, 26.2, 18.6, –5.0; HRMS (ESI+): Calcd for $C_{13}H_{28}N_1O_3Si_1$ $[M+H]^+$: 274.1838, Found: 274.1848.

**(*S*)-5-[(*tert*-Butyldimethylsilyl)oxy]-*N*-methoxy-*N*-methyl-3-(4,4,5,5-tetramethyl-1,3,2-dioxaborolan-2-yl)pentanamide (1.85f):** IR (neat): 2956 (m), 2926 (s), 2855 (m), 1665 (s), 1463 (w), 1414 (m), 1378 (s), 1316 (m), 1252 (m), 1146 (s), 1097 (s), 1006 (w), 835 (s), 775 (m) $cm^{-1}$; $^1H$ NMR (400 MHz, $CDCl_3$): δ 3.60–3.70 (5H, m), 3.15 (3H, s), 2.67–2.52 (2H, m), 1.79–1.70 (1H, m), 1.58–1.50 (1H, m), 1.38–1.31 (1H, m), 1.24 (6H, s), 1.23 (6H, s), 0.88 (9H, s), 0.04 (6H, s); $^{13}C$ NMR (100 MHz, $CDCl_3$): δ 174.9, 82.8, 62.8, 61.1, 33.7, 30.3, 26.0, 25.0, 24.8, 24.8, 18.3, –5.3; HRMS (ESI+): Calcd for $C_{19}H_{41}B_1N_1O_5Si_1$ $[M+H]^+$: 402.2847, Found: 402.2862. Specific Rotation: $[\alpha]_D^{20}$ –1.8 (*c* 1.28, $CHCl_3$) for an enantiomerically enriched sample of 93:7 er.

Enantiomeric purity was determined by HPLC analysis in comparison with authentic racemic material (93:7 er shown; Chiralpak AS-H column, 99.8/0.2 hexanes/*i*-PrOH, 0.3 mL/min, 220 nm).

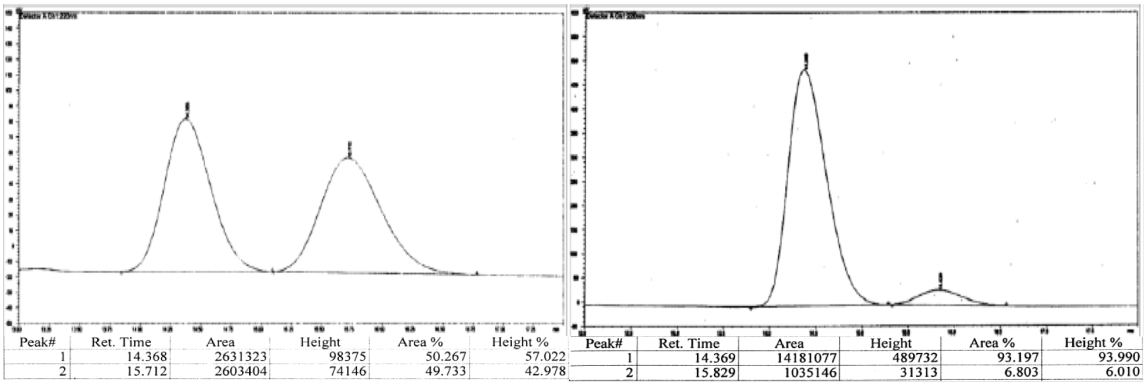

| Peak# | Ret. Time | Area | Height | Area % | Height % |
|---|---|---|---|---|---|
| 1 | 14.368 | 2631323 | 98375 | 50.267 | 57.022 |
| 2 | 15.712 | 2603404 | 74146 | 49.733 | 42.978 |

| Peak# | Ret. Time | Area | Height | Area % | Height % |
|---|---|---|---|---|---|
| 1 | 14.369 | 14181077 | 489732 | 93.197 | 93.990 |
| 2 | 15.829 | 1035146 | 31313 | 6.803 | 6.010 |

| Peak # | Time (min) | Area (%) | Peak # | Time (min) | Area (%) |
|---|---|---|---|---|---|
| 1 | 14.368 | 50.267 | 1 | 14.369 | 93.197 |
| 2 | 15.712 | 49.733 | 2 | 15.829 | 6.803 |

**(*S*)-3-(4,4,5,5-Tetramethyl-1,3,2-dioxaborolan-2-yl)hexanal (1.88a)**: The spectroscopic data match those reported previously.[70] $^1$H NMR (400 MHz, $CDCl_3$): δ 9.74–9.74 (1H, m), 2.59–2.39 (2H, m), 1.47–1.40 (1H, m), 1.36–1.26 (4H, m), 1.22 (6H, s), 1.21 (6H, s), 0.87 (3H, t, $J$ = 7.2 Hz); Specific Rotation: $[\alpha]_D^{20}$ +3.6 (*c* 1.11, $CHCl_3$) for an enantiomerically enriched sample of 95:5 er.

Enantiomeric purity was determined by GLC analysis in comparison with authentic racemic material (95:5 er shown; Chiraldex GTA column, 15 psi, 70 ºC).

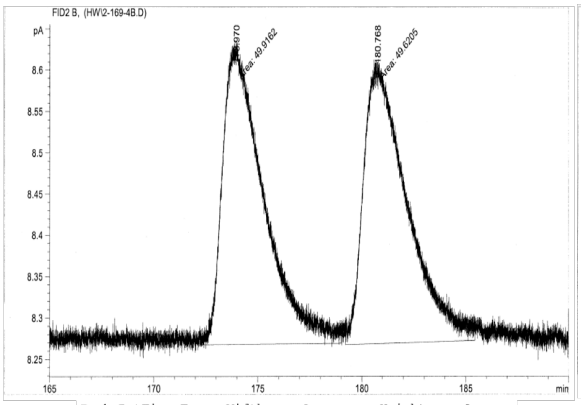


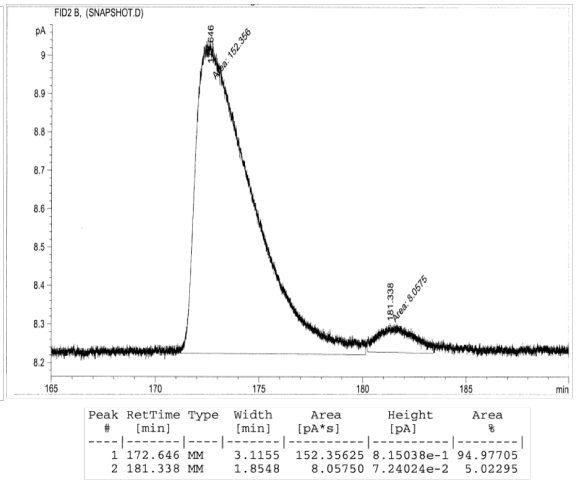


| Peak # | Time (min) | Area (%) | Peak # | Time (min) | Area (%) |
|---|---|---|---|---|---|
| 1 | 173.970 | 50.14852 | 1 | 172.646 | 94.97705 |
| 2 | 180.768 | 49.85148 | 2 | 181.338 | 5.02295 |

**(*E*)-5-Phenylpent-2-enal (1.87b)**: The spectroscopic data match those reported previously.[71] $^1$H NMR (400 MHz, $CDCl_3$): δ 9.50 (1H, d, $J$ = 8.0 Hz), 7.33–7.29 (2H, m), 7.24–7.18 (3H, m), 6.86 (1H, dt, $J$ = 16.0, 6.6 Hz), 6.17–6.11 (1H, m), 2.84 (2H, t, $J$ = 7.6 Hz), 2.70–2.64 (2H, m).

**(*S*)-5-Phenyl-3-(4,4,5,5-tetramethyl-1,3,2-dioxaborolan-2-yl)pentanal (1.88b):** IR (neat): 2976 (m), 2924 (m), 2855 (w), 2713 (w), 1723 (s), 1380 (s), 1318 (s), 1144 (s),

(70) Bonet, A.; Lillo, V.; Ramírez, J.; Mar Díaz-Requejo, M.; Fernández, E. *Org. Biomol. Chem.* **2009**, *7*, 1533–1535.

(71) Palais, L.; Babel, L.; Quintard, A.; Belot, S.; Alexakis, A. *Org. Lett.* **2010**, *12*, 1988–1991.

701 (m) $cm^{-1}$; $^1H$ NMR (400 MHz, $CDCl_3$): δ 9.74 (1H, t, *J* = 1.0 Hz), 7.26–7.23 (2H, m), 7.16–7.14 (3H, m), 2.67–2.53 (4H, m), 1.83–1.75 (1H, m), 1.65–1.58 (1H, m), 1.40–1.35 (1H, m), 1.24 (6H, s), 1.23 (6H, s); $^{13}C$ NMR (100 MHz, $CDCl_3$): δ 202.7, 142.5, 128.5, 128.47, 125.9, 83.5, 46.0, 35.3, 32.7, 30.5, 25.0, 24.9; HRMS (ESI+): Calcd for $C_{17}H_{26}B_1O_3$ $[M+H]^+$: 289.1975, Found: 289.2002. Specific Rotation: $[\alpha]_D^{20}$ –9.6 (*c* 0.37, $CHCl_3$) for an enantiomerically enriched sample of 95:5 er.

Enantiomeric purity was determined by HPLC analysis in comparison with authentic racemic material (95:5 er shown; Chiralcel OJ-H column, 99/1 hexanes/*i*-PrOH, 0.3 mL/min, 220 nm).

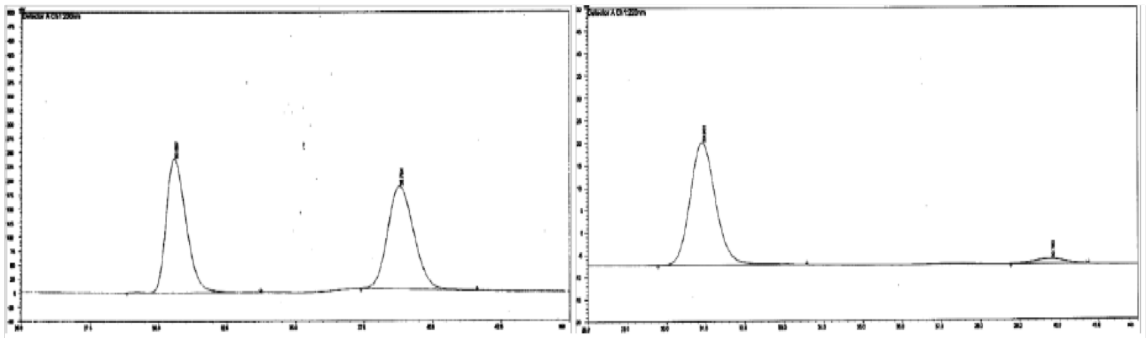

| Peak# | Ret. Time | Area | Height | Area % | Height % | Peak# | Ret. Time | Area | Height | Area % | Height % |
|---|---|---|---|---|---|---|---|---|---|---|---|
| 1 | 30.557 | 12024437 | 237330 | 49.690 | 56.442 | 1 | 30.903 | 1256604 | 27405 | 95.192 | 96.110 |
| 2 | 38.784 | 12174228 | 183157 | 50.310 | 43.558 | 2 | 39.780 | 63468 | 1109 | 4.808 | 3.890 |

| Peak # | Time (min) | Area (%) | Peak # | Time (min) | Area (%) |
|---|---|---|---|---|---|
| 1 | 30.557 | 49.690 | 1 | 30.903 | 95.192 |
| 2 | 38.784 | 50.310 | 2 | 39.780 | 4.808 |

**(*E*)-5-Methylhex-2-enal (1.87c):** IR (neat): 2930 (m), 2871 (w), 2811 (w), 1686 (s), 1638 (m), 1466 (w), 1153 (m), 1112 (m), 1091 (m), 1012 (w), 977 (m), 885 (w) $cm^{-1}$; $^1H$ NMR (400 MHz, $CDCl_3$): δ 9.49 (1H, d, *J* = 8.0 Hz), 6.80 (1H, dt, *J* = 15.6, 7.2 Hz), 6.12–6.05 (1H, m), 2.23–2.18 (2H, m), 1.85–1.75 (1H, m), 0.93 (6H, overlapping d, *J* = 7.2 Hz); $^{13}C$ NMR (100 MHz, $CDCl_3$): δ 194.1, 157.7, 134.1, 41.9, 27.8, 22.3; HRMS (ESI+): Calcd for $C_7H_{13}O_1$ $[M+H]^+$: 113.0966, Found: 113.0961.

**(*S*)-5-Methyl-3-(4,4,5,5-tetramethyl-1,3,2-dioxaborolan-2-yl)hexanal (1.88c):** IR (neat): 2977 (m), 2956 (m), 2926 (m), 2869 (w), 2716 (w), 1725 (s), 1467 (w), 1379 (s), 1372 (s), 1317 (m), 1280 (m), 1168 (w), 1145 (s), 1125 (s), 850 (m) $cm^{-1}$; $^1H$ NMR (400 MHz, $CDCl_3$): δ 9.75 (1H, m), 2.53–2.51 (2H, m), 1.62–1.55 (1H, m), 1.40–1.33 (2H, m), 1.23–1.14 (13H, m), 0.88 (3H, d, *J* = 6.4 Hz), 0.85 (3H, d, *J* = 6.4 Hz); $^{13}C$ NMR (100 MHz, $CDCl_3$): δ 202.9, 83.3, 46.0, 39.6, 26.7, 25.1, 24.8, 22.7, 22.5; HRMS (ESI+): Calcd for $C_{13}H_{26}B_1O_3$ $[M+H]^+$: 241.1975, Found: 241.1964. Specific Rotation: $[\alpha]_D^{20}$ –3.8 (*c* 0.94, $CHCl_3$) for an enantiomerically enriched sample of 94:6 er.

Enantiomeric purity was determined by GLC analysis in comparison with authentic racemic material (94:6 er shown; Chiraldex GTA column, 15 psi, 70 ºC).

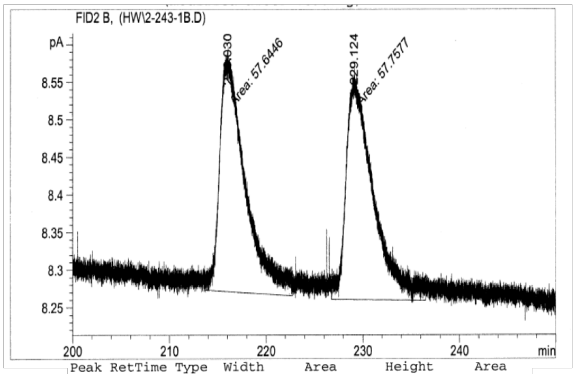


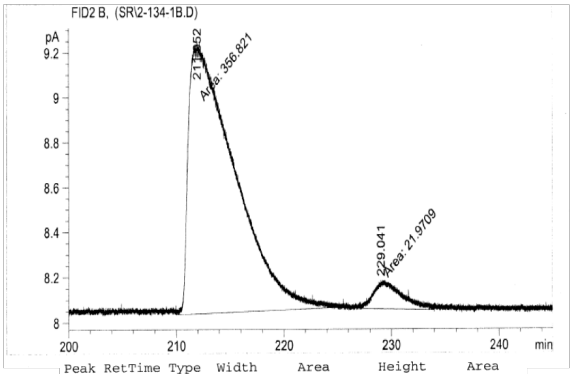


| Peak # | Time (min) | Area (%) | Peak # | Time (min) | Area (%) |
|---|---|---|---|---|---|
| 1 | 216.030 | 49.95908 | 1 | 211.952 | 94.19974 |
| 2 | 229.124 | 50.04902 | 2 | 229.041 | 5.80026 |

**(*S*)-4-Methyl-3-(4,4,5,5-tetramethyl-1,3,2-dioxaborolan-2-yl)pentanal (1.88d):** IR (neat): 2977 (m), 2931 (m), 2873 (w), 2716 (w), 1721 (s), 1372 (s), 1310 (s), 1279 (s), 1214 (w), 1143 (s), 1124 (s), 967 (w), 849 (s) $cm^{-1}$; $^1H$ NMR (400 MHz, $CDCl_3$): δ 9.72 (1H, m), 2.56 (1H, dd, *J* = 18.2, 10.0 Hz), 2.43 (1H, dd, *J* = 18.2, 4.2 Hz), 1.74–1.66 (1H, m), 1.24–1.14 (13H, m), 0.89–0.83 (6H, m); $^{13}C$ NMR (100 MHz, $CDCl_3$): δ 203.1, 83.2,

43.9, 28.9, 24.9, 24.7, 21.9, 21.5; HRMS (ESI+): Calcd for $C_{12}H_{24}B_1O_3$ $[M+H]^+$: 227.1819, Found: 227.1829. Specific Rotation: $[\alpha]_D^{20}$ +2.4 (*c* 1.43, $CHCl_3$) for an enantiomerically enriched sample of 91:9 er.

Enantiomeric purity was determined by GLC analysis in comparison with authentic racemic material (91:9 er shown; Chiraldex GTA column, 15 psi, 70 ºC).

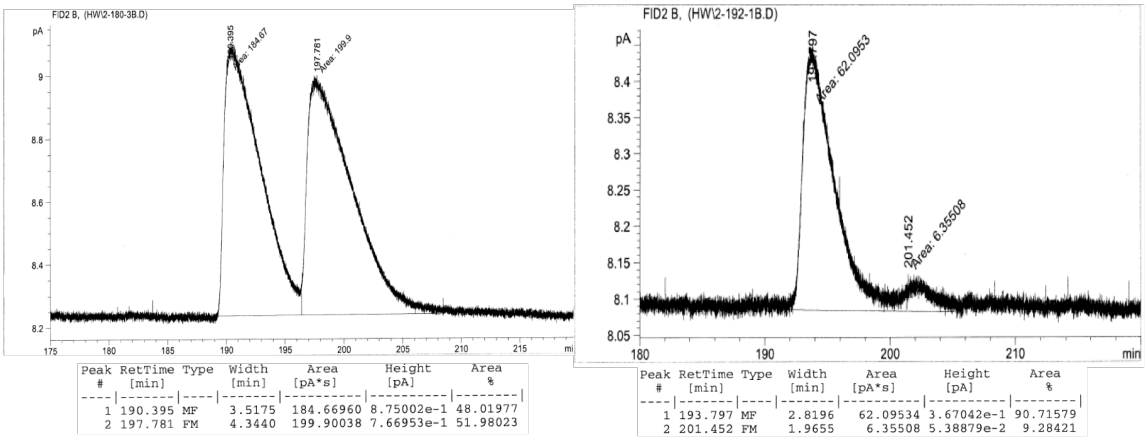


| Peak # | Time (min) | Area (%) | Peak # | Time (min) | Area (%) |
|---|---|---|---|---|---|
| 1 | 190.395 | 48.01977 | 1 | 193.797 | 90.71579 |
| 2 | 197.781 | 51.98023 | 2 | 201.452 | 9.28421 |

**(*R*)-3-(4,4,5,5-Tetramethyl-1,3,2-dioxaborolan-2-yl)cyclopentanone (1.3q)**: The spectroscopic data match those reported previously.[10a] $^1$H NMR (400 MHz, $CDCl_3$): δ 2.31–2.18 (2H, m), 2.15–2.06 (3H, m), 1.88–1.79 (1H, m), 1.67–1.56 (1H, m), 1.24 (12H, overlapping s); Specific Rotation: $[\alpha]_D^{20}$ +24.2 (*c* 1.12, $CHCl_3$) for an enantiomerically enriched sample of 92:8 er.

Enantiomeric purity was determined by GLC analysis in comparison with authentic racemic material (92:8 er shown; Chiraldex GTA column, 15 psi, 100 ºC).

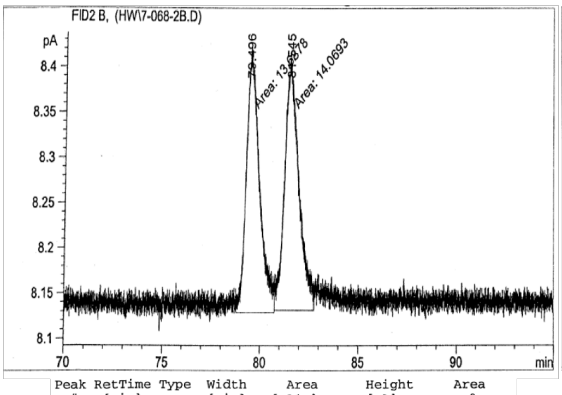


| Peak # | RetTime [min] | Type | Width [min] | Area [pA*s] | Height [pA] | Area % |
|---|---|---|---|---|---|---|
| 1 | 79.496 | MM | 0.7849 | 13.68783 | 2.90639e-1 | 49.31277 |
| 2 | 81.545 | MM | 0.8218 | 14.06934 | 2.85333e-1 | 50.68723 |

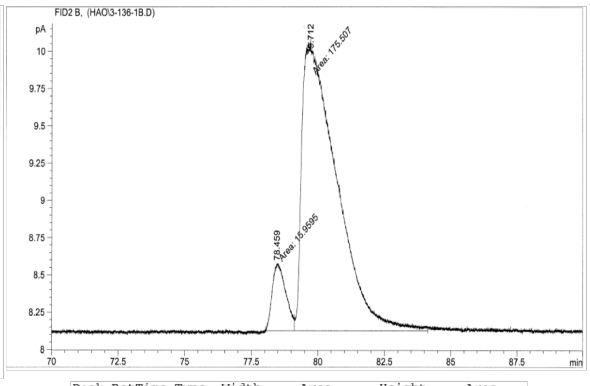


| Peak # | RetTime [min] | Type | Width [min] | Area [pA*s] | Height [pA] | Area % |
|---|---|---|---|---|---|---|
| 1 | 78.459 | MF | 0.5893 | 15.95953 | 4.51385e-1 | 8.33543 |
| 2 | 79.712 | FM | 1.4946 | 175.50662 | 1.95709 | 91.66457 |

| Peak # | Time (min) | Area (%) | Peak # | Time (min) | Area (%) |
|---|---|---|---|---|---|
| 1 | 79.496 | 49.31277 | 1 | 78.459 | 8.35543 |
| 2 | 81.545 | 50.68723 | 2 | 79.712 | 91.66457 |

**(*S*)-3,3-Dimethyl-4-(4,4,5,5-tetramethyl-1,3,2-dioxaborolan-2-yl)cyclopentanone (1.98)**: The spectroscopic data match those reported previously.[10a] $^1$H NMR (400 MHz, $CDCl_3$): δ 2.39–2.25 (2H, m), 2.09–1.99 (2H, m), 1.47–1.42 (1H, m), 1.22 (15H, s), 0.98 (3H, s); Specific Rotation: $[\alpha]_D^{20}$ –6.5 (*c* 1.20, $CHCl_3$) for an enantiomerically enriched sample of 85:15 er.

Enantiomeric purity was determined by GLC analysis in comparison with authentic racemic material (85:15 er shown; Chiraldex B-DM column, 15 psi, 130 ºC).

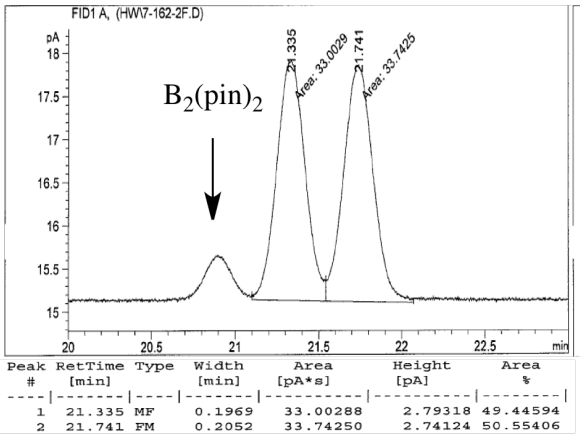


| Peak # | RetTime [min] | Type | Width [min] | Area [pA*s] | Height [pA] | Area % |
|---|---|---|---|---|---|---|
| 1 | 21.335 | MF | 0.1969 | 33.00288 | 2.79318 | 49.44594 |
| 2 | 21.741 | FM | 0.2052 | 33.74250 | 2.74124 | 50.55406 |

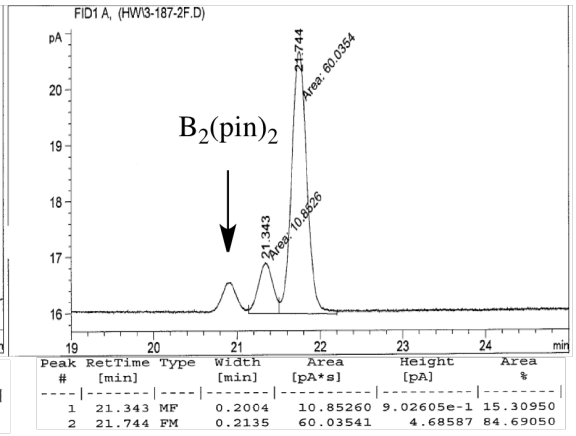


| Peak # | RetTime [min] | Type | Width [min] | Area [pA*s] | Height [pA] | Area % |
|---|---|---|---|---|---|---|
| 1 | 21.343 | MF | 0.2004 | 10.85260 | 9.02605e-1 | 15.30950 |
| 2 | 21.744 | FM | 0.2135 | 60.03541 | 4.68587 | 84.69050 |

| Peak # | Time (min) | Area (%) | Peak # | Time (min) | Area (%) |
|---|---|---|---|---|---|
| 1 | 21.335 | 49.44594 | 1 | 21.343 | 15.30950 |

| | | | | | |
|---|---|---|---|---|---|
| 2 | 21.741 | 50.55406 | 2 | 21.744 | 84.69050 |

**(*R*)-3-(4,4,5,5-Tetramethyl-1,3,2-dioxaborolan-2-yl)cyclohexanone (1.3b)**: The spectroscopic data match those reported previously.[10a] $^1$H NMR (400 MHz, $CDCl_3$): δ 2.39–2.24 (4H, m), 2.09–2.03 (1H, m), 1.89–1.84 (1H, m), 1.79–1.70 (1H, m), 1.66–1.57 (1H, m), 1.45–1.42 (1H, m), 1.23 (12H, overlapping s); Specific Rotation: $[\alpha]_D^{20}$ +6.2 (*c* 1.29, $CHCl_3$) for an enantiomerically enriched sample of 83:17 er.

Enantiomeric purity was determined by GLC analysis in comparison with authentic racemic material (83:17 er shown; Chiraldex B-DM column, 15 psi, 140 ºC).

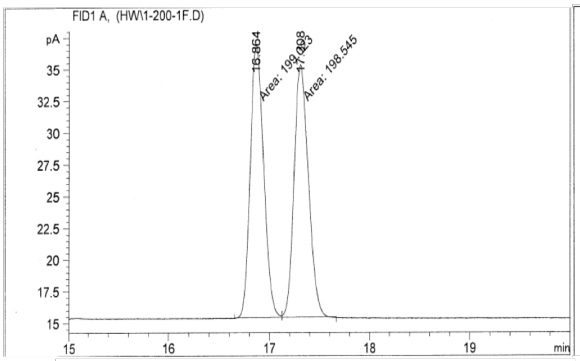


| Peak # | RetTime [min] | Type | Width [min] | Area [pA*s] | Height [pA] | Area % |
|---|---|---|---|---|---|---|
| 1 | 16.864 | MF | 0.1536 | 199.02338 | 21.58923 | 50.06022 |
| 2 | 17.308 | FM | 0.1660 | 198.54451 | 19.93485 | 49.93978 |

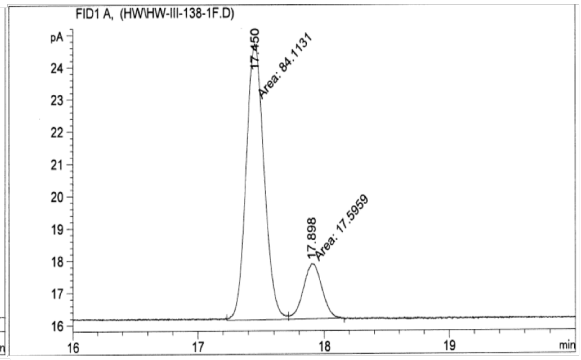


| Peak # | RetTime [min] | Type | Width [min] | Area [pA*s] | Height [pA] | Area % |
|---|---|---|---|---|---|---|
| 1 | 17.450 | MF | 0.1638 | 84.11308 | 8.56030 | 82.69975 |
| 2 | 17.898 | FM | 0.1715 | 17.59591 | 1.70989 | 17.30025 |

| Peak # | Time (min) | Area (%) | Peak # | Time (min) | Area (%) |
|---|---|---|---|---|---|
| 1 | 16.864 | 50.06022 | 1 | 17.450 | 82.69975 |
| 2 | 17.308 | 49.93978 | 2 | 17.898 | 17.30025 |

**Proof of Stereochemistry:** The corresponding (*R*)-3-[(tert-butyldimethylsilyl)oxy]cyclohexanone was obtained after oxidation of **1.3b** and TBS protection of the alcohol, the spectroscopic data match those reported previously.[29] Specific Rotation of (*R*)-3-[(tert-butyldimethylsilyl)oxy]cyclohexanone: $[\alpha]_D^{20}$ +2.2 (*c* 0.48, $CHCl_3$). Literature value ($[a]_D^{20}$ +4.8 (*c* 0.86, $CHCl_3$), 99:1 er) is assigned to the (*R*) enantiomer.

**(*R*)-3-(4,4,5,5-Tetramethyl-1,3,2-dioxaborolan-2-yl)cycloheptanone (1.3r)**: The spectroscopic data match those reported previously.[10a] $^1$H NMR (400 MHz, $CDCl_3$): δ 2.54–2.42 (4H, m), 1.95–1.86 (2H, m), 1.82–1.74 (1H, m), 1.62–1.54 (1H, m), 1.53–1.36 (2H, m), 1.31–1.21 (13H, m); Specific Rotation: $[\alpha]_D^{20}$ +11.3 (*c* 1.10, $CHCl_3$) for an enantiomerically enriched sample of 71:29 er.

Enantiomeric purity was determined by GLC analysis in comparison with authentic racemic material (71:29 er shown; Chiraldex GTA column, 15 psi, 60–90 ºC, 0.1ºC/min).

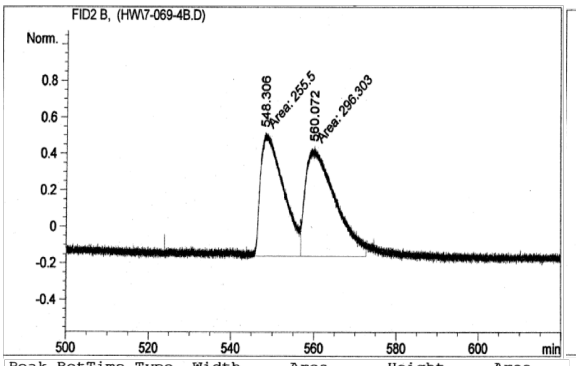


| Peak # | RetTime [min] | Type | Width [min] | Area [pA*s] | Height [pA] | Area % |
|---|---|---|---|---|---|---|
| 1 | 548.306 | MF | 6.2317 | 255.50002 | 6.83331e-1 | 46.30276 |
| 2 | 560.072 | FM | 8.1703 | 296.30295 | 6.04428e-1 | 53.69724 |

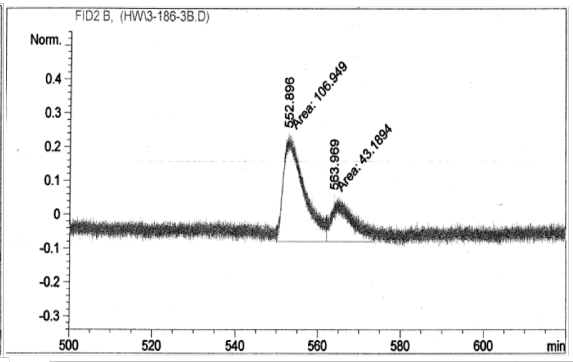


| Peak # | RetTime [min] | Type | Width [min] | Area [pA*s] | Height [pA] | Area % |
|---|---|---|---|---|---|---|
| 1 | 552.896 | MF | 5.5117 | 106.94910 | 3.23398e-1 | 71.23363 |
| 2 | 563.969 | FM | 5.1583 | 43.18940 | 1.39547e-1 | 28.76637 |

| Peak # | Time (min) | Area (%) | Peak # | Time (min) | Area (%) |
|---|---|---|---|---|---|
| 1 | 548.306 | 46.30276 | 1 | 552.896 | 71.23363 |
| 2 | 560.072 | 53.69724 | 2 | 563.969 | 28.76637 |

**(*E*)-Methyl-5-[(*tert*-butyldimethylsilyl)oxy]pent-2-enoate (1.82e):** The spectroscopic data match those reported previously.[72] $^1$H NMR (400 MHz, $CDCl_3$): δ 6.97 (1H, dt, *J* = 15.6, 7.2 Hz), 5.88 (1H, d, *J* = 15.6 Hz), 3.74–3.70 (5H, m), 2.44–2.39 (2H, m), 088 (9H, s), 0.05 (6H, overlapping s).

**(*S*)-4-(4,4,5,5-Tetramethyl-1,3,2-dioxaborolan-2-yl)tetrahydro-2*H*-pyran-2-one (1.3t)**: To a $CH_2Cl_2$ solution of (*S*)-methyl 5-[(*tert*-butyldimethylsilyl)oxy]-3-(4,4,5,5-tetramethyl-1,3,2-dioxaborolan-2-yl)pentanoate (17 mg, 0.044 mmol, 0.09 M),

(72) Caron, P-Y.; Deslongchamps, P. *Org. Lett.* **2010**, *12*, 508–511.

trifluoroacetic acid (34 µL, 10 equivalent) was added dropwise at 0 ºC. The reaction mixture was allowed to stir at 0 ºC for 20 min before quenched by saturated aqueous $NaHCO_3$ solution. The aqueous layer was washed with diethyl ether (3 x 1 mL). The combined organic fractions were dried over $MgSO_4$ and filtered. The volatiles were removed under vacuum and the resulting light yellow oil was purified by silica gel chromatography (pentanes:$Et_2O$ = 1:3) to afford 9.0 mg (0.040 mmol, 90% yield) of (*R*)-4-(4,4,5,5-Tetramethyl-1,3,2-dioxaborolan-2-yl)tetrahydro-2*H*-pyran-2-one (**1.3t**) as a colorless oil. The spectroscopic data match those reported previously.[12] $^1$H NMR (400 MHz, $CDCl_3$): δ 4.39–4.33 (1H, m), 4.30–4.24 (1H, m), 2.61 (1H, dd, *J* = 17.8, 6.8 Hz), 2.49 (1H, dd, *J* = 17.8, 10.4 Hz), 1.99–1.87 (1H, m), 1.84–1.75 (1H, m), 1.65–1.49 (1H, m), 1.25–1.21 (12H, m); Specific Rotation: $[\alpha]_D^{20}$ –9.8 (*c* 0.60, $CHCl_3$) for an enantiomerically enriched sample of 94:6 er.

Enantiomeric purity was determined by GLC analysis in comparison with authentic racemic material (94:6 er shown; Chiraldex B-DM column, 15 psi, 140 ºC).

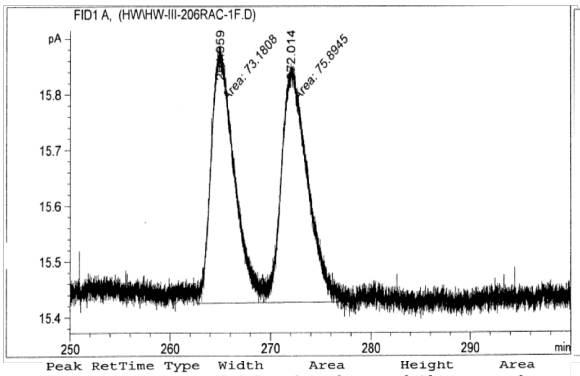


| Peak # | RetTime [min] | Type | Width [min] | Area [pA*s] | Height [pA] | Area % |
|---|---|---|---|---|---|---|
| 1 | 264.959 | MF | 2.6151 | 73.18076 | 4.66390e-1 | 49.08981 |
| 2 | 272.014 | FM | 2.9510 | 75.89449 | 4.28638e-1 | 50.91019 |

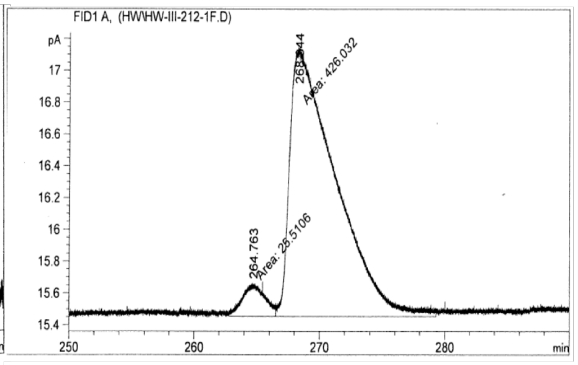


| Peak # | RetTime [min] | Type | Width [min] | Area [pA*s] | Height [pA] | Area % |
|---|---|---|---|---|---|---|
| 1 | 264.763 | MF | 2.0204 | 25.51055 | 2.10441e-1 | 5.64964 |
| 2 | 268.344 | FM | 4.1902 | 426.03223 | 1.69454 | 94.35036 |

| Peak # | Time (min) | Area (%) | Peak # | Time (min) | Area (%) |
|---|---|---|---|---|---|
| 1 | 264.959 | 49.08981 | 1 | 264.763 | 5.64964 |
| 2 | 272.014 | 50.91019 | 2 | 268.344 | 94.35036 |

**(*E*)-Oct-3-en-7-yn-2-one (substrate for 1.118):** IR (neat): 3291 (br), 2962 (m), 2919 (m), 2850 (m), 1697 (m), 1672 (s), 1627 (m), 1432 (m), 1361 (m), 1255 (s), 1018 (m), 972 (m), 798 (m) 638 (br) $cm^{-1}$; $^1H$ NMR (400 MHz, $CDCl_3$): δ 6.82 (1H, dt, $J$ = 16.0, 6.8 Hz), 6.13 (1H, d, $J$ = 16.0 Hz), 2.48–2.43 (2H, m), 2.39–2.35 (2H, m), 2.26 (3H, s), 2.01 (1H, t, $J$ = 2.4 Hz); $^{13}C$ NMR (100 MHz, $CDCl_3$): δ 198.4, 145.3, 132.2, 82.6, 69.6, 31.2, 27.0, 17.5; HRMS (ESI+): Calcd for $C_8H_{11}O_1$ $[M+H]^+$: 123.0810, Found: 123.0790.

**(*S*)-4-(4,4,5,5-Tetramethyl-1,3,2-dioxaborolan-2-yl)oct-7-yn-2-one (1.118):** IR (neat): 3291 (br), 2977 (m), 2922 (m), 2852 (m), 1714 (m), 1380 (s), 1372 (s), 1315 (s), 1166 (s), 1143 (s), 1125 (s), 967 (m), 851 (m), 671 (m), 632 (m) $cm^{-1}$; $^1H$ NMR (400 MHz, $CDCl_3$): δ 2.66–2.54 (2H, m), 2.24–2.19 (2H, m), 2.11 (3H, s), 1.93–1.92 (1H, m), 1.76–1.67 (1H, m), 1.55–1.46 (1H, m), 1.39–1.30 (1H, m), 1.23 (6H, s), 1.22 (6H, s); $^{13}C$ NMR (100 MHz, $CDCl_3$): δ 208.8, 84.6, 83.3, 68.5, 45.3, 29.8, 29.3, 24.9, 24.8, 17.9; HRMS (ESI+): Calcd for $C_{14}H_{24}B_1O_3$ $[M+H]^+$: 251.1819, Found: 251.1813. Specific Rotation: $[\alpha]_D^{20}$ –3.0 (*c* 0.87, $CHCl_3$) for an enantiomerically enriched sample of 94:6 er.

Enantiomeric purity was determined by GLC analysis in comparison with authentic racemic material (94:6 er shown; Chiraldex aTA column, 15 psi, 90 ºC).

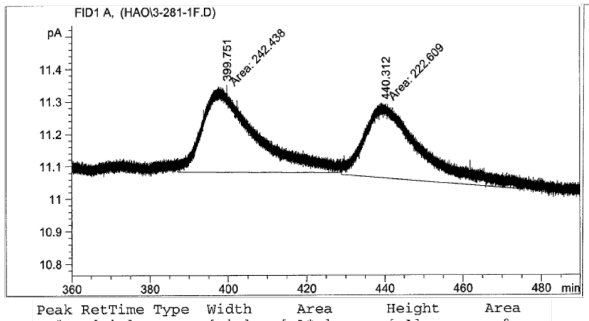


| Peak # | RetTime [min] | Type | Width [min] | Area [pA*s] | Height [pA] | Area % |
|---|---|---|---|---|---|---|
| 1 | 399.751 | MM | 14.9662 | 242.43753 | 2.69983e-1 | 52.13187 |
| 2 | 440.312 | MM | 15.9993 | 222.60918 | 2.31895e-1 | 47.86813 |

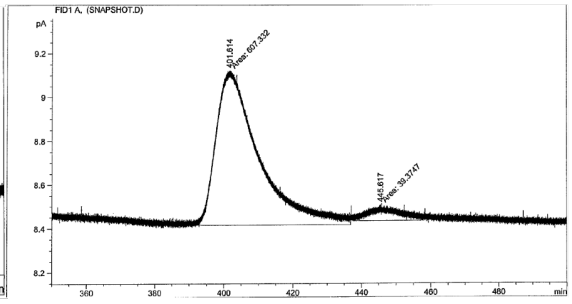


| Peak # | RetTime [min] | Type | Width [min] | Area [pA*s] | Height [pA] | Area % |
|---|---|---|---|---|---|---|
| 1 | 401.614 | MM | 14.2804 | 607.33191 | 7.08815e-1 | 93.91151 |
| 2 | 445.617 | MM | 8.8193 | 39.37469 | 7.44098e-2 | 6.08849 |

| Peak # | Time (min) | Area (%) | Peak # | Time (min) | Area (%) |
|---|---|---|---|---|---|
| 1 | 399.751 | 52.13187 | 1 | 401.614 | 93.91151 |
| 2 | 440.312 | 47.86813 | 2 | 445.617 | 6.08849 |

**(*E*)-Non-2-en-7-ynal (substrate for 1.119):** IR (neat): 2939 (m), 2918 (m), 2712 (m), 1691 (s), 1638 (m), 1434 (m), 1167 (m), 1124 (m), 975 (m) $cm^{-1}$; $^1H$ NMR (400 MHz, $CDCl_3$): δ 9.50 (1H, d, $J$ = 8.0 Hz), 6.84 (1H, dt, $J$ = 15.6, 6.8 Hz), 6.14 (1H, dd, $J$ = 15.6, 8 Hz), 2.47–2.42 (2H, m), 2.22–2.17 (2H, m), 1.78–1.76 (3H, m), 1.76–1.64 (2H, m); $^{13}C$ NMR (100 MHz, $CDCl_3$): δ 194.1, 157.9, 133.4, 78.0, 76.7, 31.8, 27.2, 18.3, 3.5; HRMS (ESI+): Calcd for $C_9H_{13}O_2$ $[M+OH]^+$: 153.0916, Found: 153.0922.

**(*S*)-3-(4,4,5,5-Tetramethyl-1,3,2-dioxaborolan-2-yl)non-7-ynal (1.119):** IR (neat): 2977 (m), 2924 (s), 2857 (m), 2712 (m), 1723 (m), 1458 (m), 1380 (s), 1372 (s), 1318 (s), 1280 (m), 1166 (m), 1144 (s), 1125 (s), 967 (m), 850 (m) $cm^{-1}$; $^1H$ NMR (400 MHz, $CDCl_3$): δ 9.76 (1H, s), 2.64–2.51 (2H, m), 2.13–2.09 (2H, m), 1.77–1.76 (3H, m), 1.56–1.40 (4H, m), 1.36–1.30 (1H, m), 1.24 (6H, s), 1.23 (6H, s); $^{13}C$ NMR (100 MHz, $CDCl_3$): δ 202.8, 83.5, 79.2, 75.7, 46.0, 29.9, 28.5, 24.9, 24.8, 19.0, 3.6; HRMS (ESI+): Calcd for $C_{15}H_{26}B_1O_3$ $[M+H]^+$: 265.1975, Found: 265.1975. Specific Rotation: $[\alpha]_D^{20}$ +11.0 (*c* 0.25, $CHCl_3$) for an enantiomerically enriched sample of 95:5 er.

Enantiomeric purity was determined by GLC analysis in comparison with authentic racemic material (95:5 er shown; Chiraldex GTA column, 15 psi, 90 ºC).

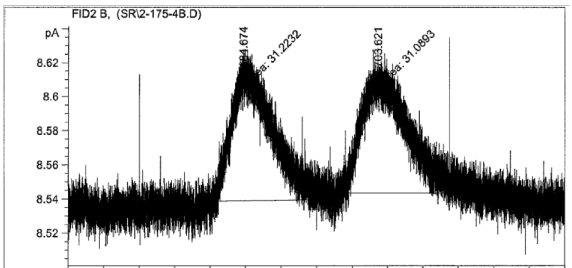


| Peak # | RetTime [min] | Type | Width [min] | Area [pA*s] | Height [pA] | Area % |
|---|---|---|---|---|---|---|
| 1 | 684.674 | MM | 5.9252 | 31.22316 | 8.78263e-2 | 50.10745 |
| 2 | 703.621 | MM | 6.0371 | 31.08926 | 8.58277e-2 | 49.89255 |

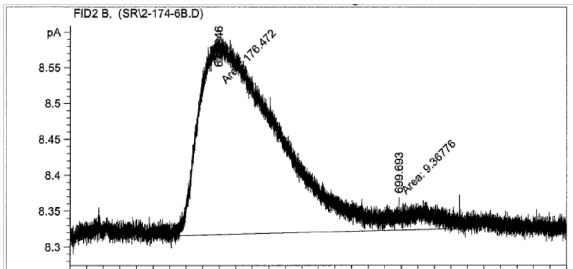


| Peak # | RetTime [min] | Type | Width [min] | Area [pA*s] | Height [pA] | Area % |
|---|---|---|---|---|---|---|
| 1 | 677.946 | MM | 10.6498 | 176.47214 | 2.76173e-1 | 94.95923 |
| 2 | 699.693 | MM | 3.3358 | 9.36776 | 4.68043e-2 | 5.04077 |

| Peak # | Time (min) | Area (%) | Peak # | Time (min) | Area (%) |
|---|---|---|---|---|---|
| 1 | 684.674 | 50.10745 | 1 | 677.946 | 94.95923 |

| | | | | | |
|---|---|---|---|---|---|
| 2 | 703.621 | 49.89255 | 2 | 699.693 | 5.04077 |

**Imidazolinium Tetrafluoroborate Salt (1.61):** The spectroscopic data match those reported previously.[73] $^1$H NMR (400 MHz, $CDCl_3$): δ 8.76 (1H, s), 7.89 (1H, d, *J* = 1.6 Hz), 7.46–7.25 (7H, m), 7.19–7.02 (4H, m), 7.01 (1H, d, *J* = 8.0 Hz), 6.91 (1H, s), 6.59 (1H, s), 6.43–6.41 (2H, m), 5.35 (1H, d, *J* = 7.6 Hz), 5.21 (1H, d, *J* = 7.6 Hz), 3.08–3.01 (1H, m), 2.52 (3H, s), 2.50 (3H, s), 2.17 (3H, s), 2.05 (3H, s), 1.93 (3H, s), 1.58 (3H, s), 1.25 (6H, d, *J* = 8.4 Hz).

**Imidazolinium Tetrafluoroborate Salt (1.94)[74]:** Imidazolinium tetrafluoroborate salt **1.94** was prepared according to a previously reported procedure.[56c] IR (neat): 2961 (m), 2926 (m), 2868 (w), 1615 (s), 1585 (m), 1496 (m), 1271 (m), 1219 (m), 1058 (br), 790 (m), 730 (m) $cm^{-1}$; $^1$H NMR (400 MHz, $CDCl_3$): δ 8.50 (1H, s), 8.14–8.12 (1H, d, *J* = 8.0 Hz), 7.58–7.12 (13H, m), 7.03 (1H, d, *J* = 7.2 Hz), 6.93 (1H, d, *J* = 8.4 Hz), 6.77 (2H, d, *J* = 7.6 Hz), 6.61 (1H, d, *J* = 7.2 Hz), 6.07 (1H, d, *J* = 8.8 Hz), 5.02 (1H, d, *J* = 8.8 Hz), 3.54–3.50 (1H, m), 3.05–2.98 (1H, m), 2.45–2.28 (2H, m), 2.18 (3H, s), 1.36–1.32 (9H, m), 1.24–1.21 (3H, m), 1.17–1.13 (3H, m), 1.05–1.04 (3H, m), 0.99–0.96 (3H, m), 0.92–0.89 (3H, m). $^{13}$C NMR (100 MHz, $CDCl_3$): δ 194.9, 158.0, 150.5, 148.0, 147.7, 147.5, 147.1, 146.7, 146.6, 135.9, 135.6, 135.3, 135.1, 134.9, 134.1, 133.2, 132.8, 132.6, 132.5, 132.3, 132.2, 131.9, 130.9, 130.8, 130.4, 130.1, 129.9, 129.7, 129.5, 129.4, 129.2, 129.1, 128.9, 128.8, 128.7, 128.1, 127.0, 125.0, 122.1, 121.9, 121.7, 72.4, 71.8, 44.9, 34.5, 30.9, 30.8, 30.6, 28.7, 28.5, 26.5, 26.4, 26.2, 26.1, 25.9, 25.7, 24.5, 24.4, 24.2, 24.0, 23.0, 22.4, 22.3, 18.6, 18.5; HRMS (ESI+): Submitted. Specific Rotation: $[\alpha]_D^{20}$ –210.0 (*c* 0.33, $CHCl_3$).

(73) Vieira, E. M.; Snapper, M. L.; Hoveyda, A. H. *J. Am. Chem. Soc.* **2011**, *133*, 3332–3335.
(74) Mixture of two rotamers (2:1), which were generated during the last cyclization reaction.

### *1.9.2. $^{1}$H NMR Spectra of New Compounds*

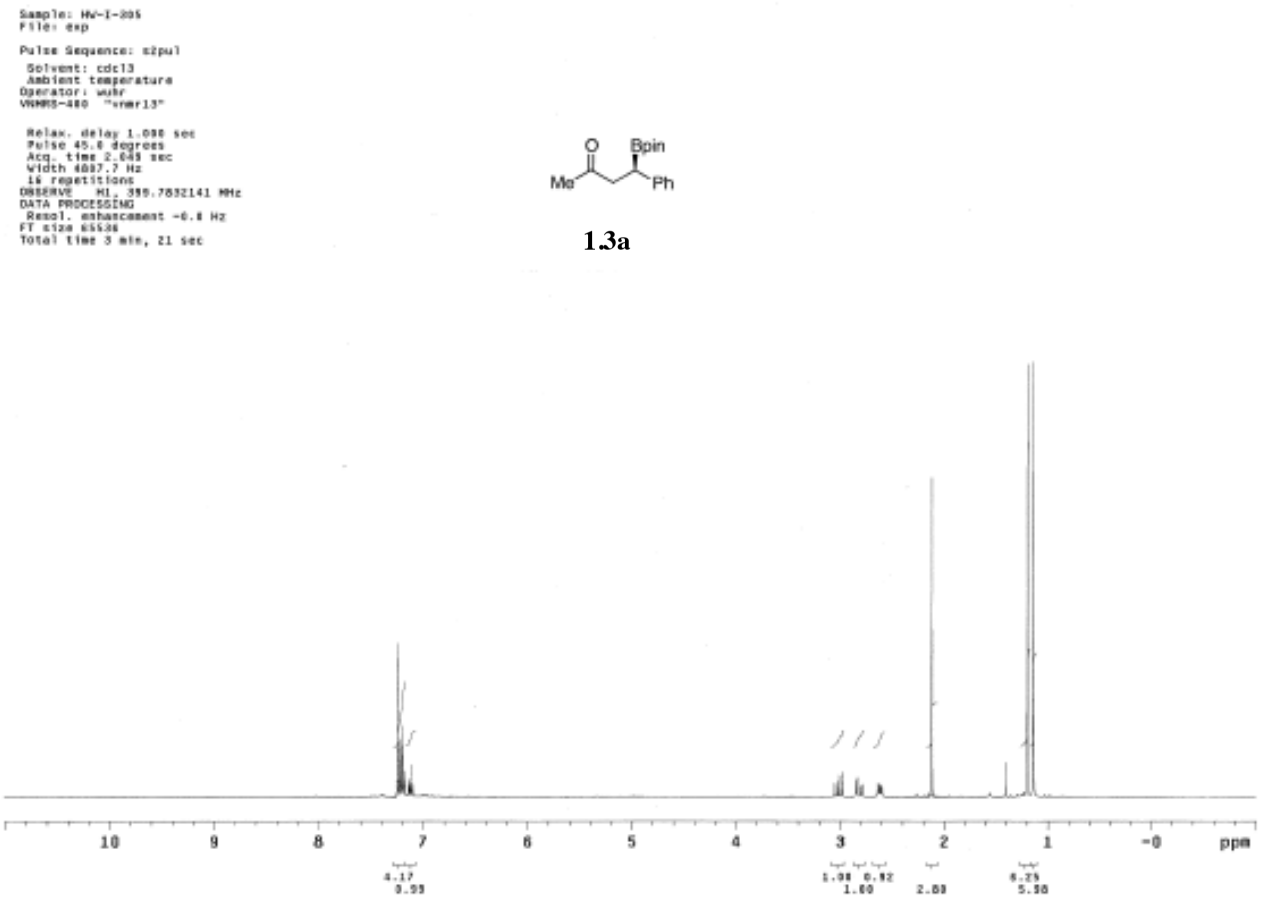
Sample: HW-I-205
File: exp
Pulse Sequence: s2pul
Solvent: cdcl3
Ambient temperature
Operator: wubr
VNMRS-400 "vnmr13"
Relax. delay 1.000 sec
Pulse 45.0 degrees
Acq. time 2.048 sec
Width 4807.7 Hz
16 repetitions
OBSERVE H1, 399.7832141 MHz
DATA PROCESSING
Resol. enhancement -0.8 Hz
FT size 65536
Total time 3 min, 21 sec
O
Bpin
Me
Ph
10
9
8
7
6
5
4
3
2
1
0
ppm
4.17
0.99
1.98
0.92
1.00
2.89
6.25
5.98

**1.3a**

Sample: HW-II-097
File: exp

Pulse Sequence: s2pul
Solvent: cdcl3
Temp. 22.0 C / 295.1 K
Operator: wuhr
VNMRS-400 "vnmr13"

Relax. delay 1.000 sec
Pulse 45.0 degrees
Acq. time 2.049 sec
Width 4807.7 Hz
20 repetitions
OBSERVE H1, 399.7832141 MHz
DATA PROCESSING
Resol. enhancement -0.0 Hz
FT size 65536
Total time 3 min, 21 sec

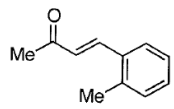


**1.78a**

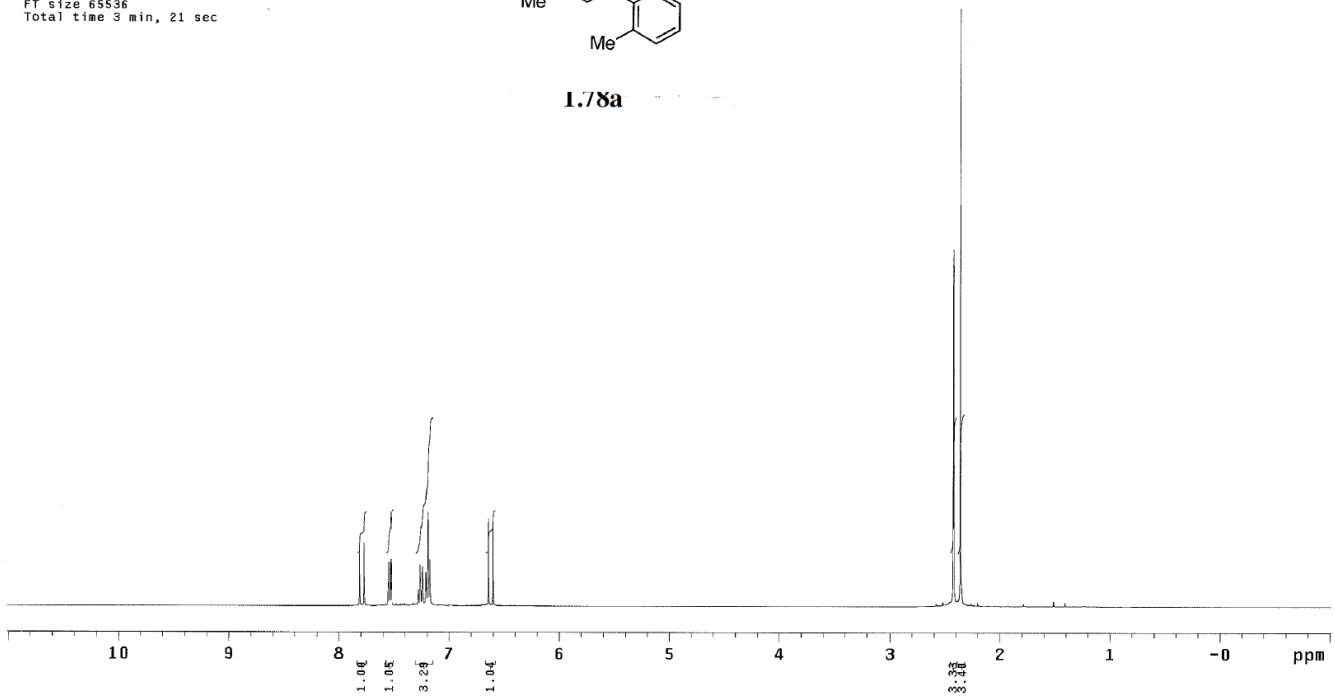

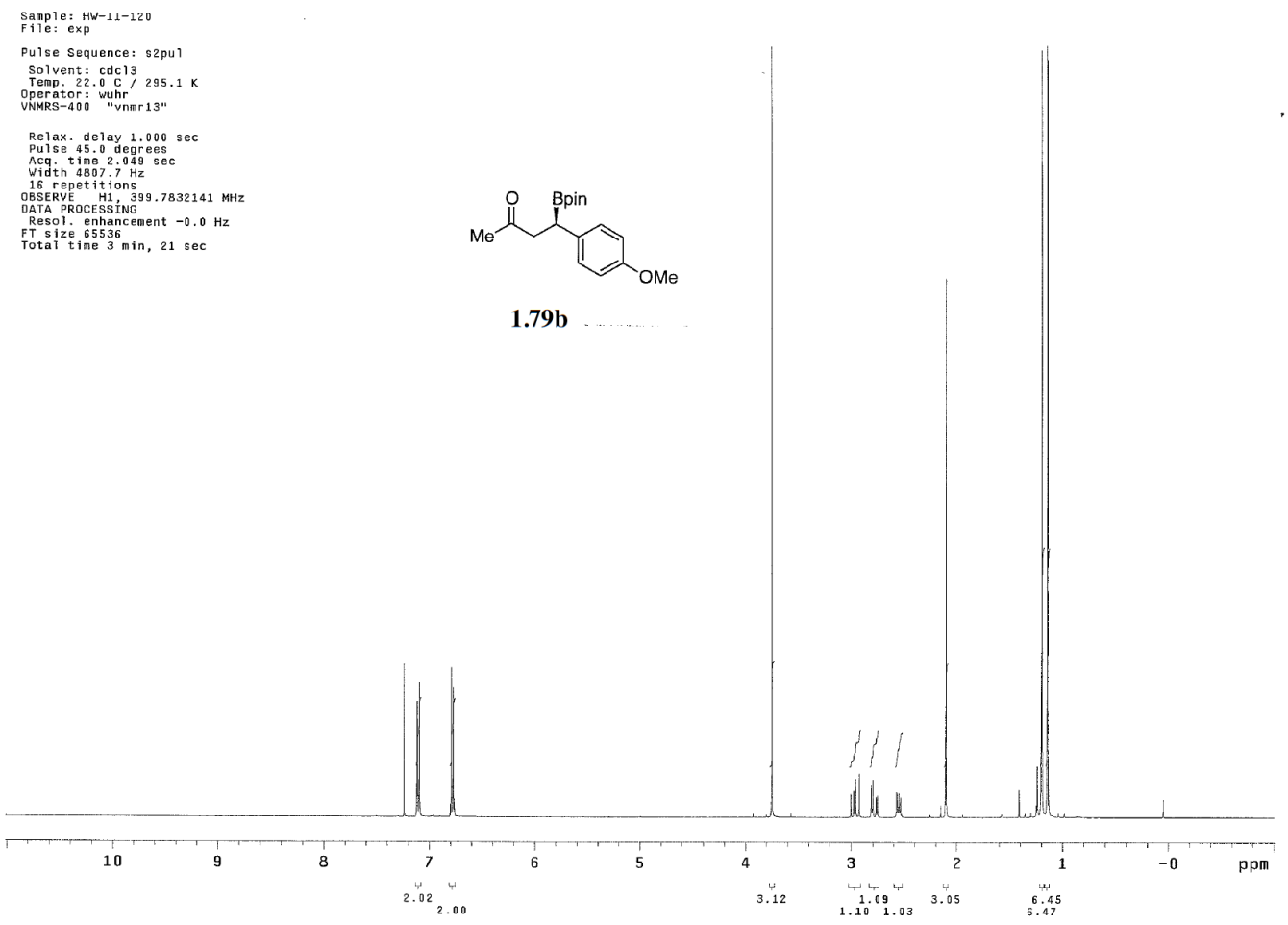
Sample: HW-II-120
File: exp
Pulse Sequence: s2pul
Solvent: cdcl3
Temp. 22.0 C / 295.1 K
Operator: wuhr
VNMRS-400 "vnmr13"
Relax. delay 1.000 sec
Pulse 45.0 degrees
Acq. time 2.049 sec
Width 4807.7 Hz
16 repetitions
OBSERVE H1, 399.7832141 MHz
DATA PROCESSING
Resol. enhancement -0.0 Hz
FT size 65536
Total time 3 min, 21 sec
O
Bpin
Me
OMe
1.79b
10
9
8
7
6
5
4
3
2
1
-0
ppm
2.02
2.00
3.12
1.09
1.10
1.03
3.05
6.45
6.47

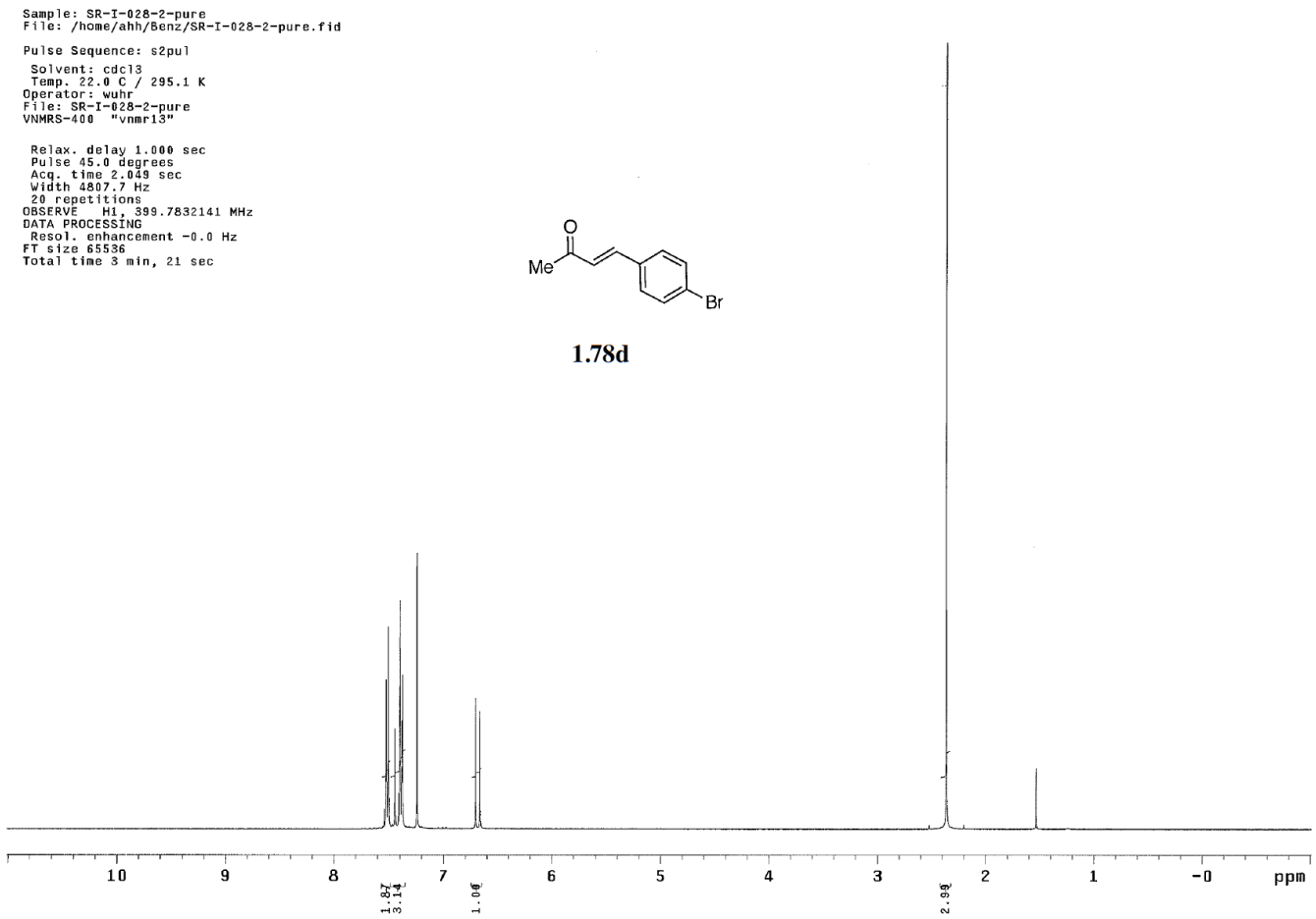
Sample: SR-I-028-2-pure
File: /home/ahh/Benz/SR-I-028-2-pure.fid
Pulse Sequence: s2pul
Solvent: cdcl3
Temp. 22.0 C / 295.1 K
Operator: wuhr
File: SR-I-028-2-pure
VNMRS-400 "vnmr13"
Relax. delay 1.000 sec
Pulse 45.0 degrees
Acq. time 2.049 sec
Width 4807.7 Hz
20 repetitions
OBSERVE H1, 399.7832141 MHz
DATA PROCESSING
Resol. enhancement -0.0 Hz
FT size 65536
Total time 3 min, 21 sec
O
Me
Br
10
9
8
7
6
5
4
3
2
1
-0
ppm
1.87
3.14
1.00
2.99

**1.78d**

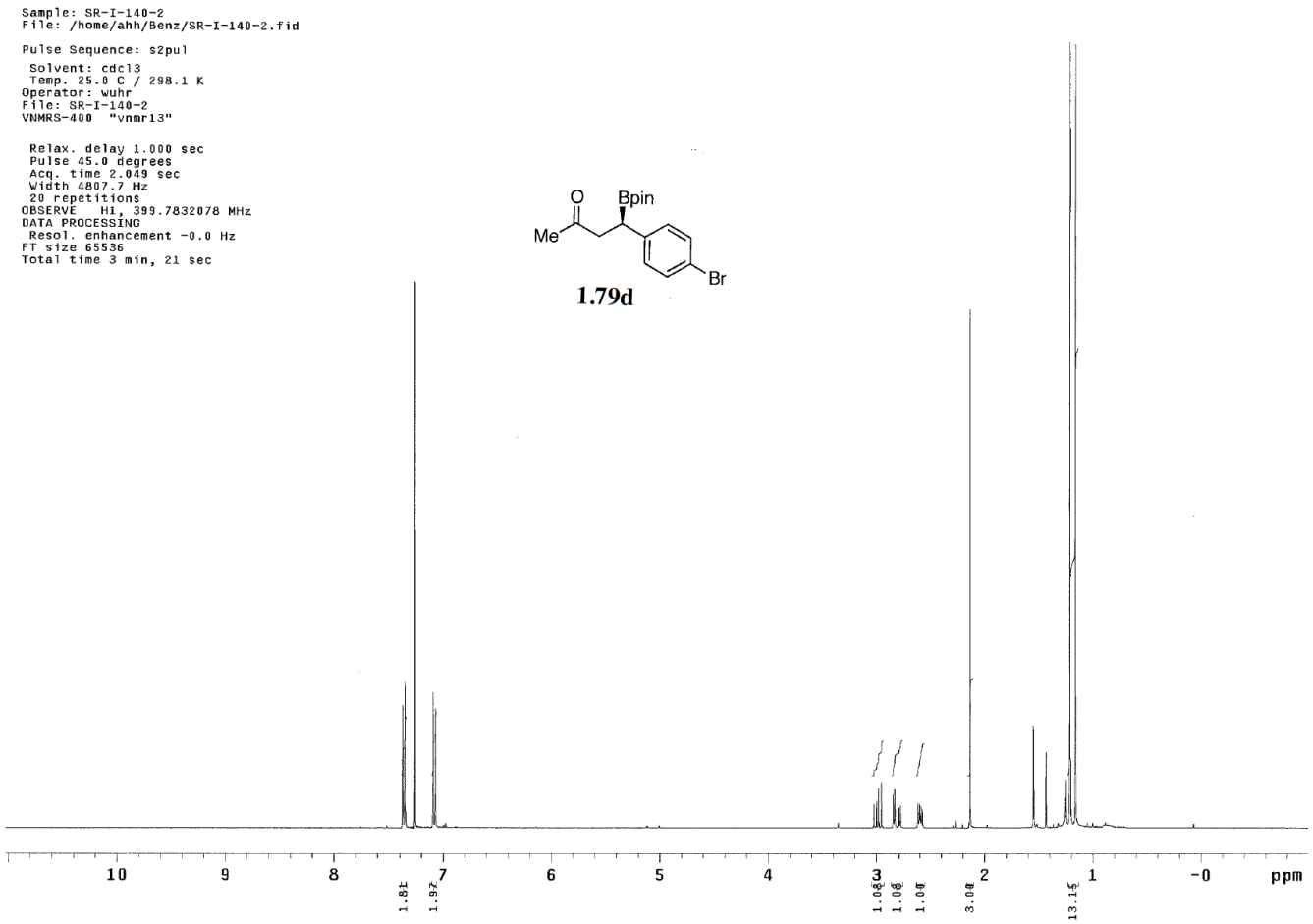
Sample: SR-I-140-2
File: /home/ahh/Benz/SR-I-140-2.fid
Pulse Sequence: s2pul
Solvent: cdcl3
Temp. 25.0 C / 298.1 K
Operator: wuhr
File: SR-I-140-2
VNMRS-400 "vnmr13"
Relax. delay 1.000 sec
Pulse 45.0 degrees
Acq. time 2.049 sec
Width 4807.7 Hz
20 repetitions
OBSERVE H1, 399.7832078 MHz
DATA PROCESSING
Resol. enhancement -0.0 Hz
FT size 65536
Total time 3 min, 21 sec
O
Bpin
Me
Br
1.79d
10
9
8
7
6
5
4
3
2
1
-0
ppm
1.81
1.97
1.06
1.08
1.00
3.04
13.15

Sample: HW-II-116-2
File: /home/ahh/wuhr/HW-II-116-1H.fid

Pulse Sequence: s2pul

Solvent: cdcl3
Temp. 22.0 C / 295.1 K
Operator: wuhr
File: HW-II-116-1H
VNMRS-400 "vnmr13"

Relax. delay 1.000 sec
Pulse 45.0 degrees
Acq. time 2.049 sec
Width 4807.7 Hz
16 repetitions
OBSERVE H1, 399.7832342 MHz
DATA PROCESSING
Resol. enhancement -0.0 Hz
FT size 65536
Total time 3 min, 21 sec

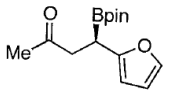


**1.79f**

Sample: HW-II-106
File: exp

Pulse Sequence: s2pul
Solvent: cdcl3
Temp. 22.0 C / 295.1 K
Operator: wuhr
VNMRS-400 "vnmr13"

Relax. delay 1.000 sec
Pulse 45.0 degrees
Acq. time 2.049 sec
Width 4807.7 Hz
20 repetitions
OBSERVE H1, 399.7832141 MHz
DATA PROCESSING
Resol. enhancement -0.0 Hz
FT size 65536
Total time 3 min, 21 sec

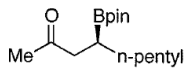


**1.79g**

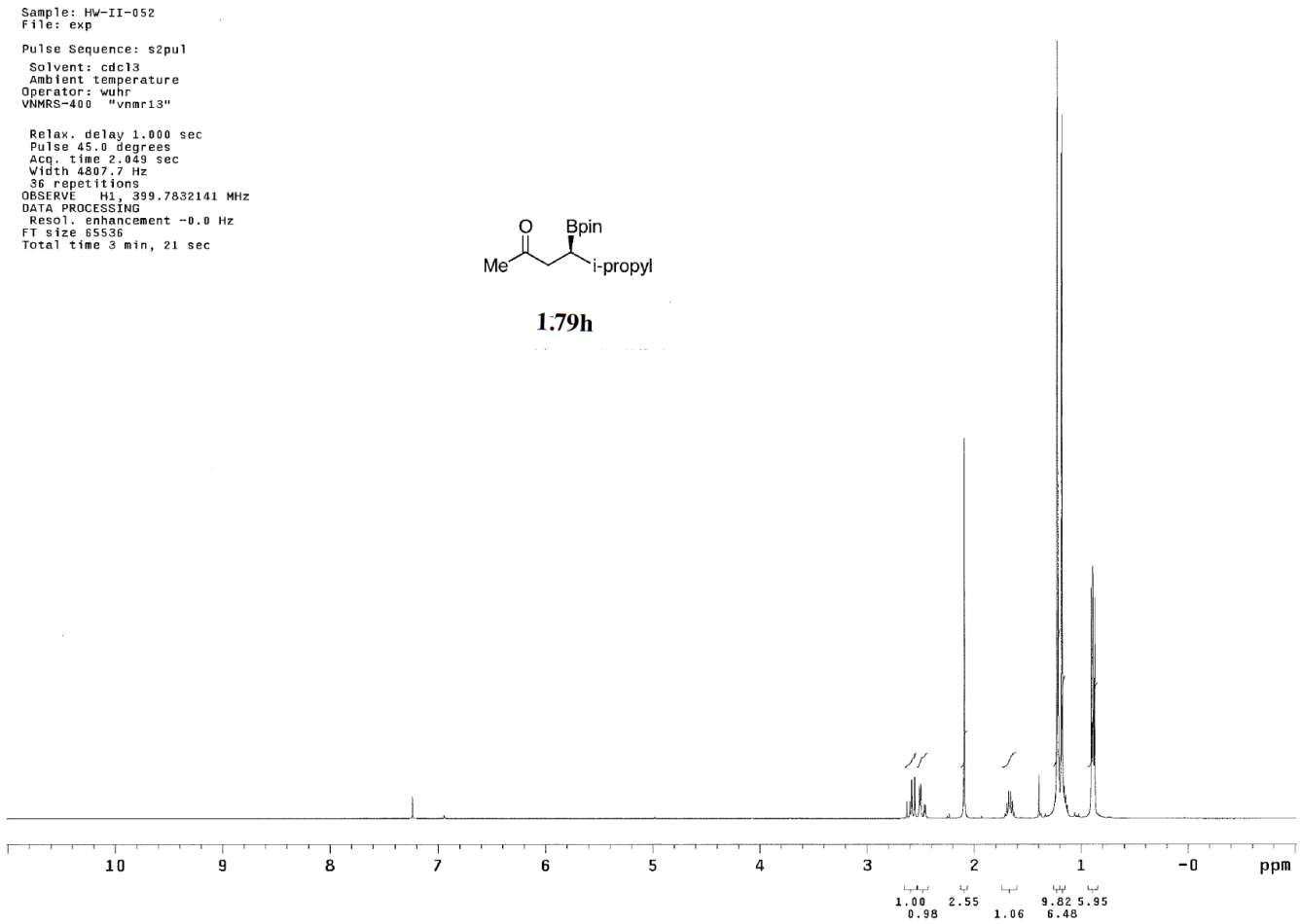
Sample: HW-II-052
File: exp
Pulse Sequence: s2pul
Solvent: cdcl3
Ambient temperature
Operator: wuhr
VNMRS-400 "vnmr13"
Relax. delay 1.000 sec
Pulse 45.0 degrees
Acq. time 2.049 sec
Width 4807.7 Hz
36 repetitions
OBSERVE H1, 399.7832141 MHz
DATA PROCESSING
Resol. enhancement -0.0 Hz
FT size 65536
Total time 3 min, 21 sec
O
Bpin
Me
i-propyl
1.79h
10
9
8
7
6
5
4
3
2
1
-0
ppm
1.00
0.98
2.55
1.06
9.82
6.48
5.95

Sample: HW-II-155
File: exp

Pulse Sequence: s2pul
Solvent: cdcl3
Temp. 25.0 C / 298.1 K
Operator: wuhr
VNMRS-400 "vnmr13"

Relax. delay 1.000 sec
Pulse 45.0 degrees
Acq. time 2.049 sec
Width 4807.7 Hz
12 repetitions
OBSERVE H1, 399.7832141 MHz
DATA PROCESSING
Resol. enhancement -0.0 Hz
FT size 65536
Total time 3 min, 21 sec

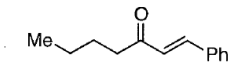


**1.78i**

Sample: HW-II-165
File: exp

Pulse Sequence: s2pul
Solvent: cdcl3
Temp. 25.0 C / 298.1 K
Operator: wuhr
VNMRS-400 "vnmr13"

Relax. delay 1.000 sec
Pulse 45.0 degrees
Acq. time 2.049 sec
Width 4807.7 Hz
16 repetitions
OBSERVE H1, 399.7832141 MHz
DATA PROCESSING
Resol. enhancement -0.0 Hz
FT size 65536
Total time 3 min, 21 sec

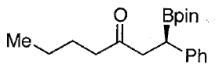


**1.79i**

Sample: HW-II-118
File: exp

Pulse Sequence: s2pul
Solvent: cdcl3
Temp. 22.0 C / 295.1 K
Operator: wuhr
VNMRS-400 "vnmr13"

Relax. delay 1.000 sec
Pulse 45.0 degrees
Acq. time 2.049 sec
Width 4807.7 Hz
16 repetitions
OBSERVE H1, 399.7832141 MHz
DATA PROCESSING
Resol. enhancement -0.0 Hz
FT size 65536
Total time 3 min, 21 sec

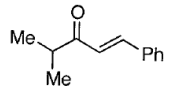


**1.78j**

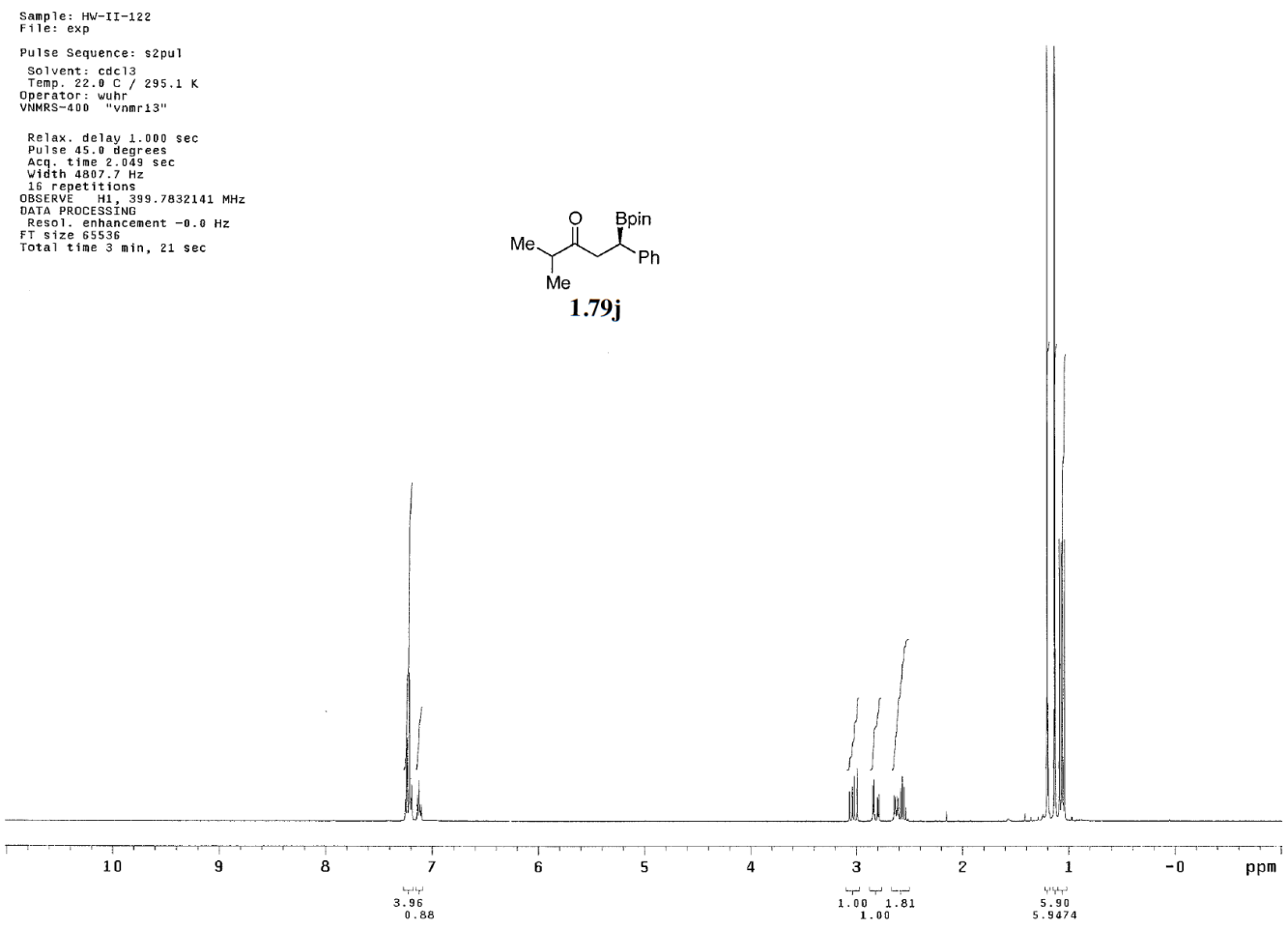
Sample: HW-II-122
File: exp
Pulse Sequence: s2pul
Solvent: cdcl3
Temp. 22.0 C / 295.1 K
Operator: wuhr
VNMRS-400 "vnmr13"
Relax. delay 1.000 sec
Pulse 45.0 degrees
Acq. time 2.049 sec
Width 4807.7 Hz
16 repetitions
OBSERVE H1, 399.7832141 MHz
DATA PROCESSING
Resol. enhancement -0.0 Hz
FT size 65536
Total time 3 min, 21 sec
O
Bpin
Me
Ph
Me
1.79j
10
9
8
7
6
5
4
3
2
1
-0
ppm
3.96
0.88
1.00
1.81
1.00
5.90
5.9474

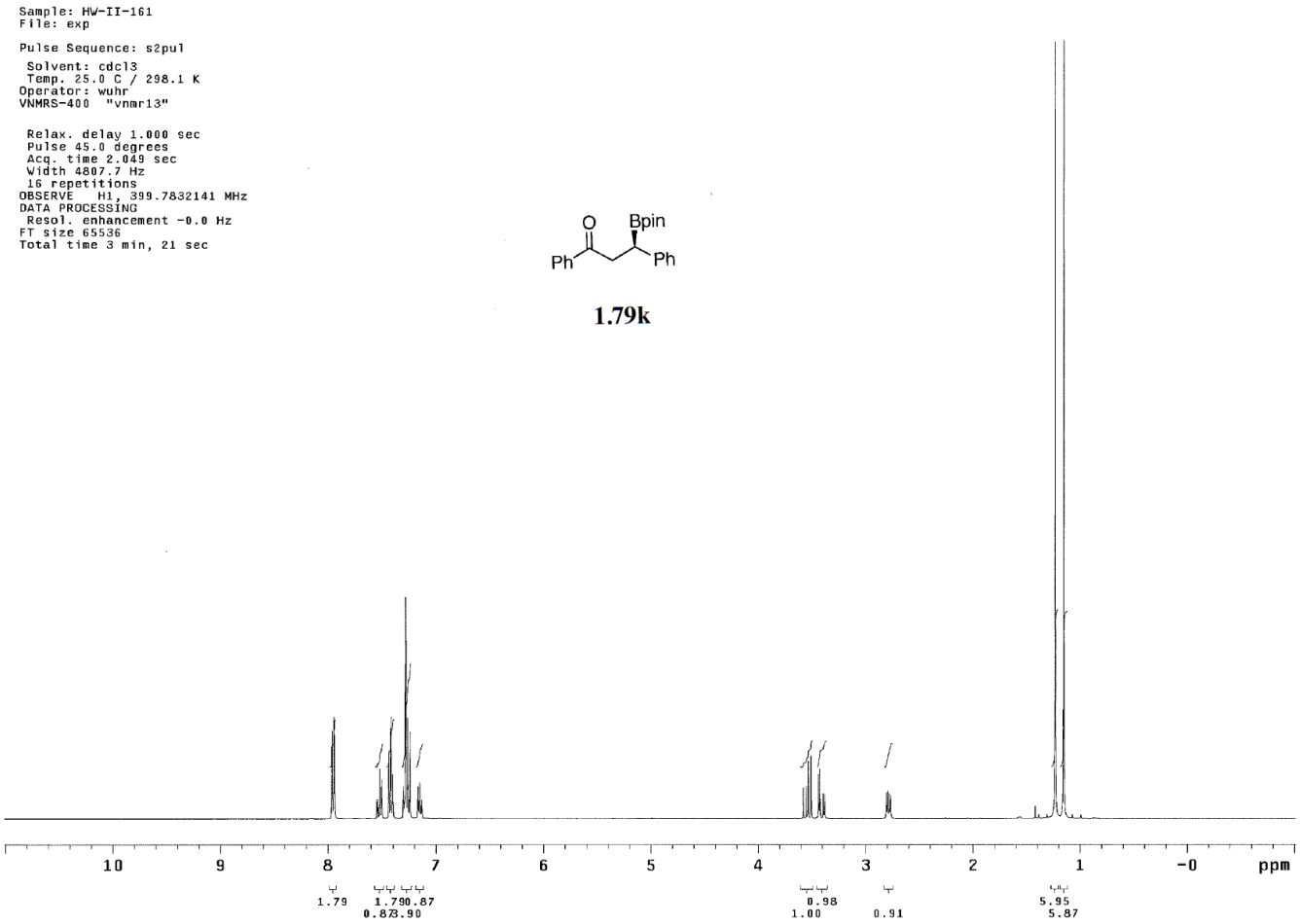
Sample: HW-II-161
File: exp
Pulse Sequence: s2pul
Solvent: cdcl3
Temp. 25.0 C / 298.1 K
Operator: wuhr
VNMRS-400 "vnmr13"
Relax. delay 1.000 sec
Pulse 45.0 degrees
Acq. time 2.049 sec
Width 4807.7 Hz
16 repetitions
OBSERVE H1, 399.7832141 MHz
DATA PROCESSING
Resol. enhancement -0.0 Hz
FT size 65536
Total time 3 min, 21 sec
O
Bpin
Ph
Ph
1.79k
10
9
8
7
6
5
4
3
2
1
-0
ppm
1.79
1.79
0.87
3.90
0.87
0.98
1.00
0.91
5.95
5.87

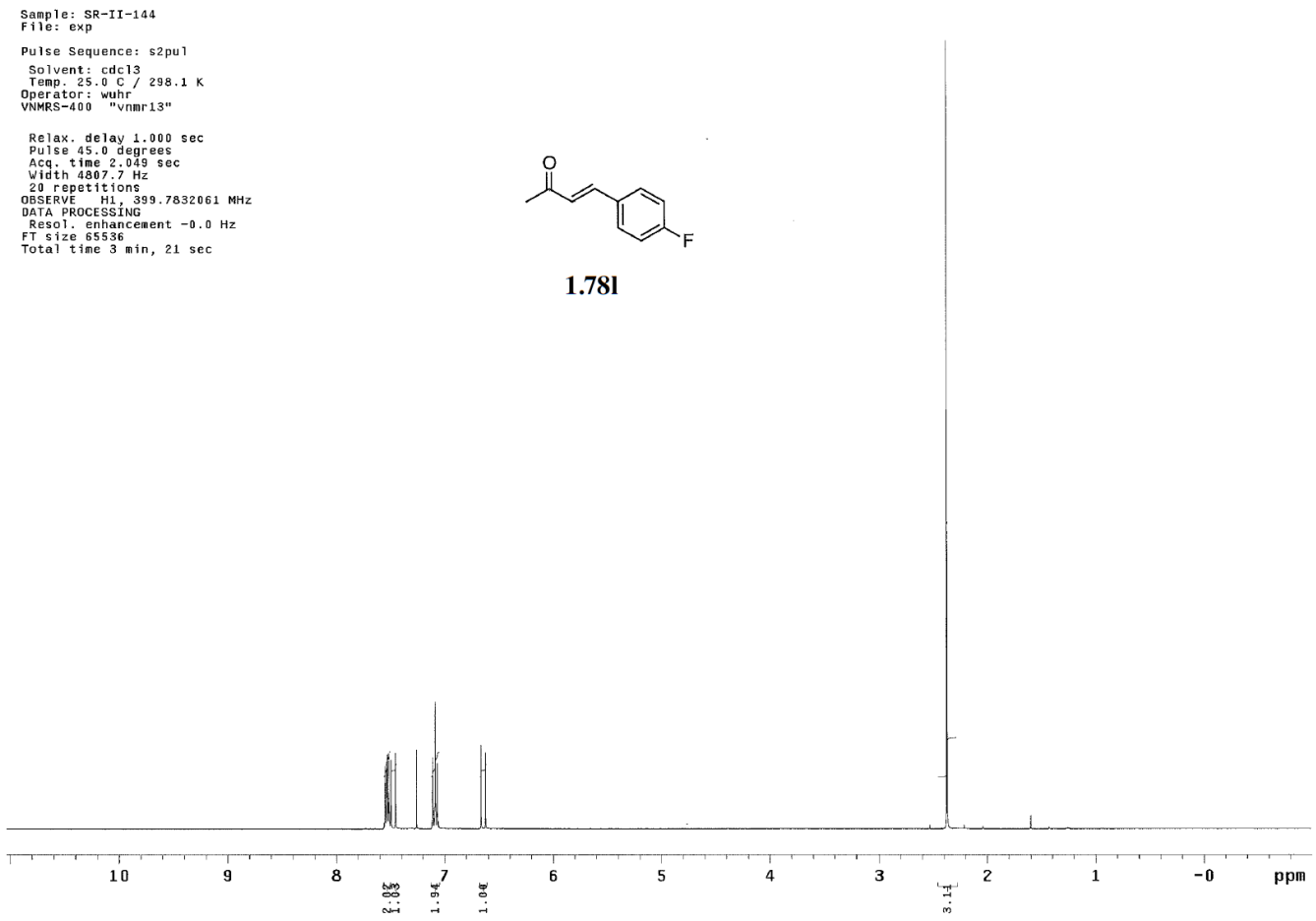
Sample: SR-II-144
File: exp
Pulse Sequence: s2pul
Solvent: cdcl3
Temp. 25.0 C / 298.1 K
Operator: wuhr
VNMRS-400 "vnmr13"
Relax. delay 1.000 sec
Pulse 45.0 degrees
Acq. time 2.049 sec
Width 4807.7 Hz
20 repetitions
OBSERVE H1, 399.7832061 MHz
DATA PROCESSING
Resol. enhancement -0.0 Hz
FT size 65536
Total time 3 min, 21 sec
O
F
1.781
10
9
8
7
6
5
4
3
2
1
-0
ppm
2.03
1.94
1.04
3.14

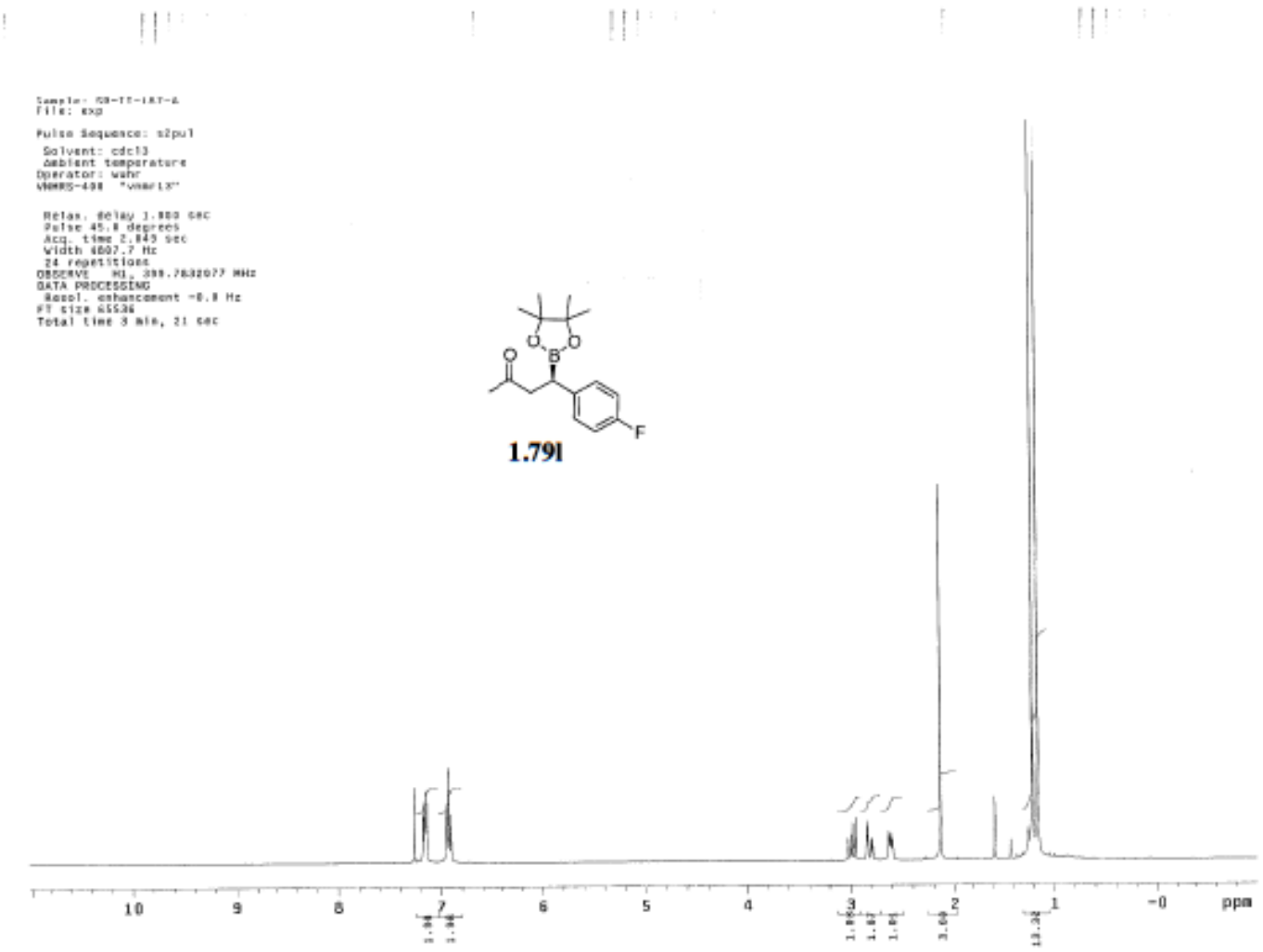
Sample: KB-TT-1A7-A
File: exp
Pulse Sequence: s2pul
Solvent: cdcl3
Ambient temperature
Operator: wahr
VNMRS-400 "vnmr13"
Relax. delay 1.000 sec
Pulse 45.0 degrees
Acq. time 2.849 sec
Width 6807.7 Hz
24 repetitions
OBSERVE H1, 399.7832077 MHz
DATA PROCESSING
Resol. enhancement -0.8 Hz
FT size 65536
Total time 3 min, 21 sec
1.791
10
9
8
7
6
5
4
3
2
1
-0
ppm

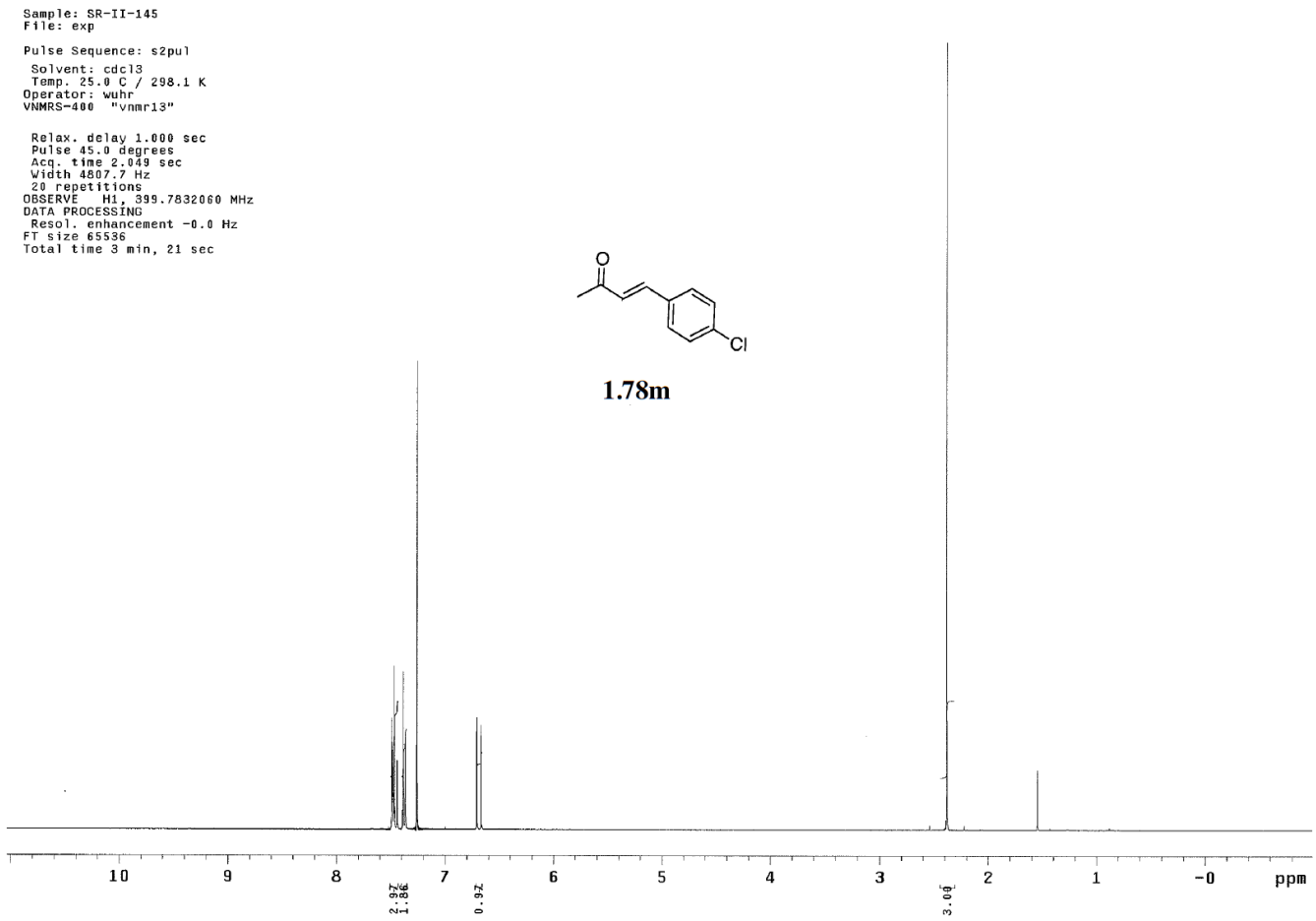
Sample: SR-II-145
File: exp
Pulse Sequence: s2pul
Solvent: cdcl3
Temp. 25.0 C / 298.1 K
Operator: wuhr
VNMRS-400 "vnmr13"
Relax. delay 1.000 sec
Pulse 45.0 degrees
Acq. time 2.049 sec
Width 4807.7 Hz
20 repetitions
OBSERVE H1, 399.7832060 MHz
DATA PROCESSING
Resol. enhancement -0.0 Hz
FT size 65536
Total time 3 min, 21 sec
O
Cl
1.78m
10
9
8
7
6
5
4
3
2
1
-0
ppm
2.07
1.86
0.92
3.00

Sample: SR-II-194-carbon
File: exp

Pulse Sequence: s2pul
Solvent: cdcl3
Temp. 25.0 C / 298.1 K
Operator: wuhr
VNMRS-400 "vnmr13"

Relax. delay 1.000 sec
Pulse 45.0 degrees
Acq. time 2.049 sec
Width 4807.7 Hz
24 repetitions
OBSERVE H1, 399.7832073 MHz
DATA PROCESSING
Resol. enhancement -0.0 Hz
FT size 65536
Total time 3 min, 21 sec

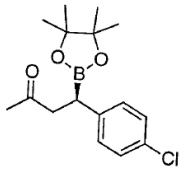


**1.79m**

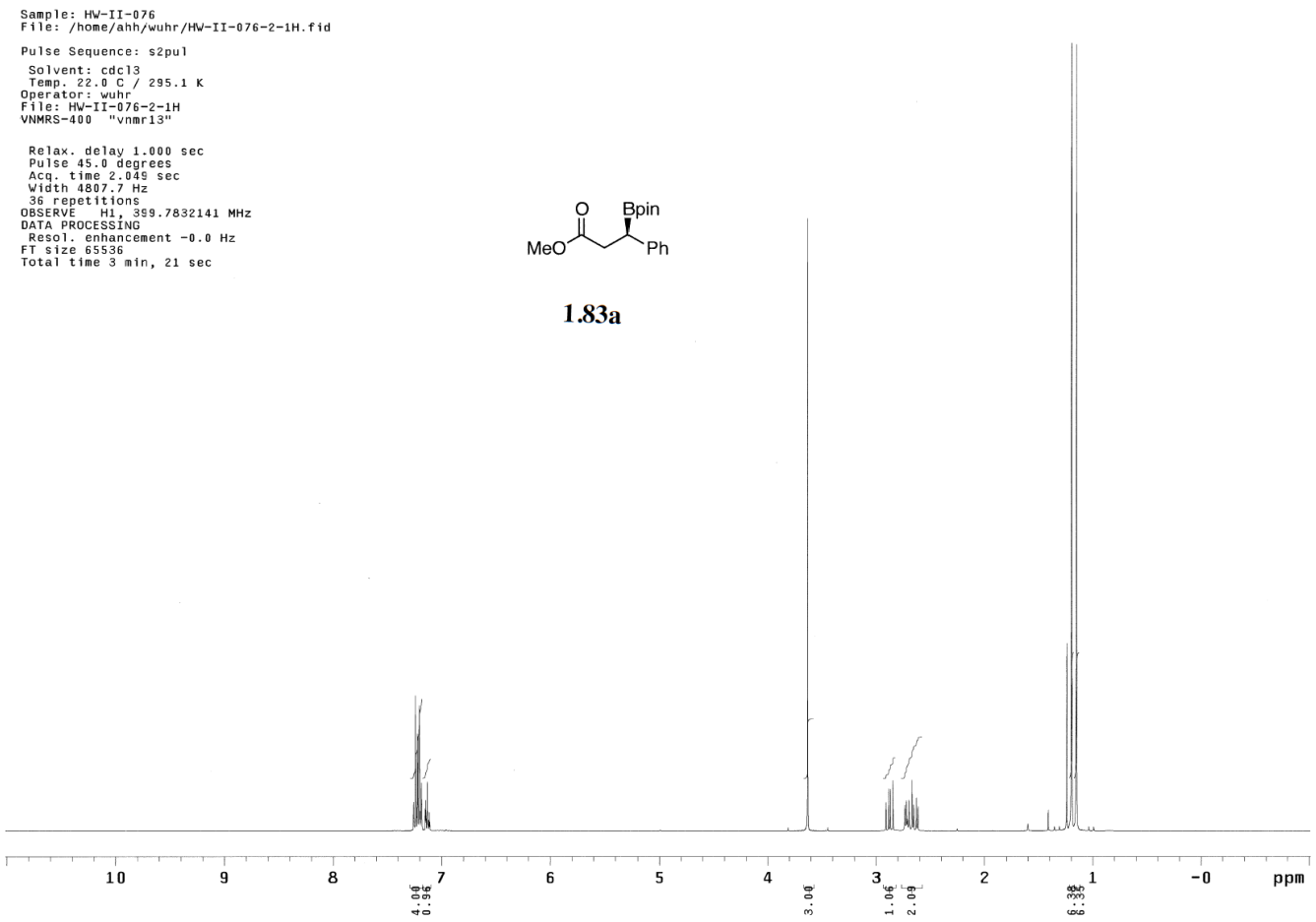
Sample: HW-II-076
File: /home/ahh/wuhr/HW-II-076-2-1H.fid
Pulse Sequence: s2pul
Solvent: cdcl3
Temp. 22.0 C / 295.1 K
Operator: wuhr
File: HW-II-076-2-1H
VNMRS-400 "vnmr13"
Relax. delay 1.000 sec
Pulse 45.0 degrees
Acq. time 2.049 sec
Width 4807.7 Hz
36 repetitions
OBSERVE H1, 399.7832141 MHz
DATA PROCESSING
Resol. enhancement -0.0 Hz
FT size 65536
Total time 3 min, 21 sec
O
Bpin
MeO
Ph
1.83a
10
9
8
7
6
5
4
3
2
1
-0
ppm
4.00
0.96
3.00
1.06
2.09
6.38
6.35

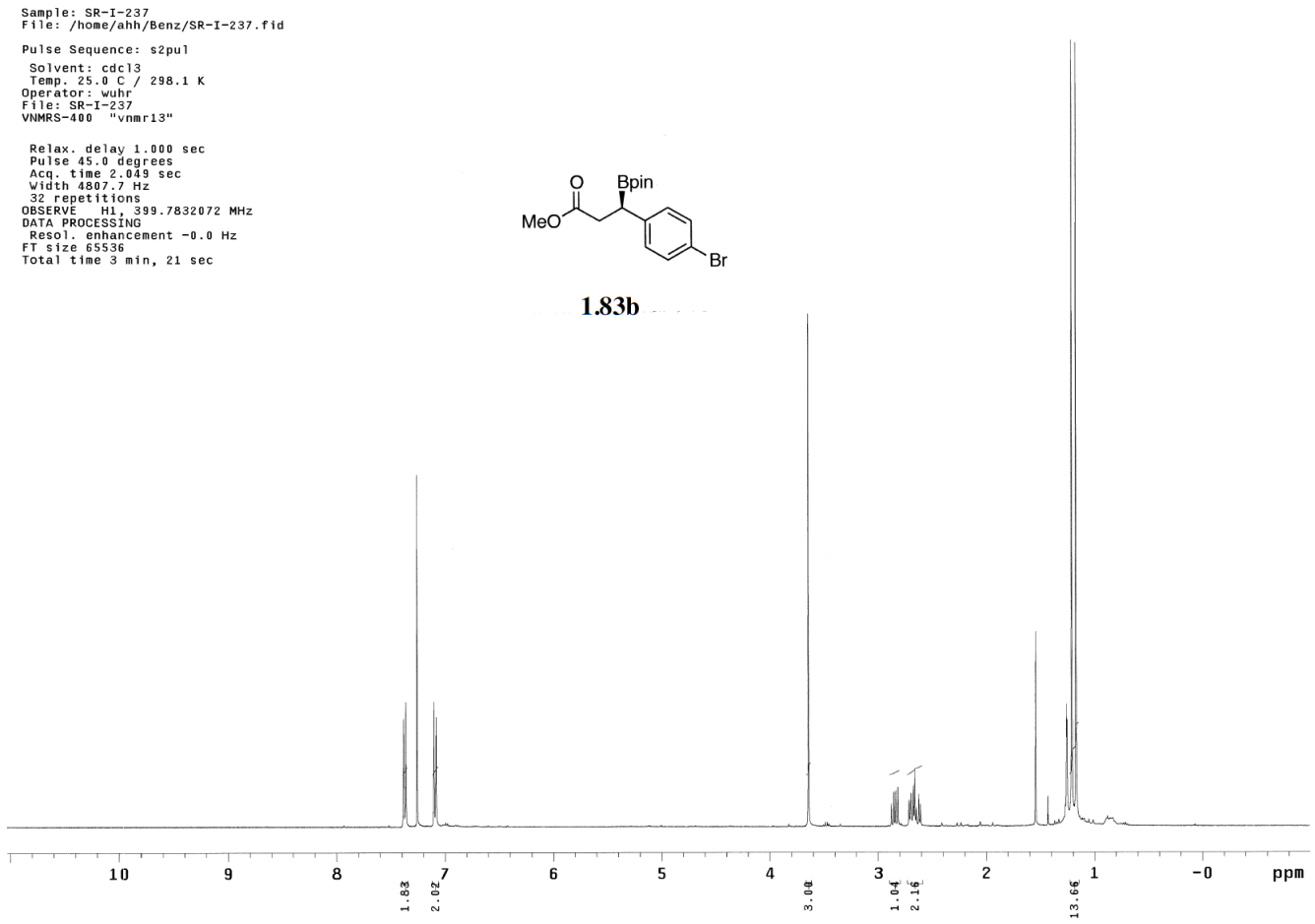
Sample: SR-I-237
File: /home/ahh/Benz/SR-I-237.fid
Pulse Sequence: s2pul
Solvent: cdcl3
Temp. 25.0 C / 298.1 K
Operator: wuhr
File: SR-I-237
VNMRS-400 "vnmr13"
Relax. delay 1.000 sec
Pulse 45.0 degrees
Acq. time 2.049 sec
Width 4807.7 Hz
32 repetitions
OBSERVE H1, 399.7832072 MHz
DATA PROCESSING
Resol. enhancement -0.0 Hz
FT size 65536
Total time 3 min, 21 sec
O
Bpin
MeO
Br
1.83b
10
9
8
7
6
5
4
3
2
1
-0
ppm
1.83
2.02
3.00
1.04
2.16
13.66

Sample: hW-II-123
File: exp

Pulse Sequence: s2pul
Solvent: cdcl3
Temp. 22.0 C / 295.1 K
Operator: wuhr
VNMRS-400 "vnmr13"

Relax. delay 1.000 sec
Pulse 45.0 degrees
Acq. time 2.049 sec
Width 4807.7 Hz
12 repetitions
OBSERVE H1, 399.7832141 MHz
DATA PROCESSING
Resol. enhancement -0.0 Hz
FT size 65536
Total time 3 min, 21 sec

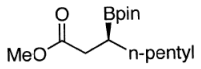


**1.83c**

Sample: HW-II-132
File: exp

Pulse Sequence: s2pul
Solvent: cdcl3
Temp. 22.0 C / 295.1 K
Operator: wuhr
VNMRS-400 "vnmr13"

Relax. delay 1.000 sec
Pulse 45.0 degrees
Acq. time 2.049 sec
Width 4807.7 Hz
16 repetitions
OBSERVE H1, 399.7832141 MHz
DATA PROCESSING
Resol. enhancement -0.0 Hz
FT size 65536
Total time 3 min, 21 sec

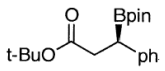


**1.83d**

Sample: HW-II-111-3
File: exp

Pulse Sequence: s2pul

Solvent: cdcl3
Temp. 22.0 C / 295.1 K
Operator: wuhr
VNMRS-400 "vnmr13"

Relax. delay 1.000 sec
Pulse 45.0 degrees
Acq. time 2.049 sec
Width 4807.7 Hz
8 repetitions
OBSERVE H1, 399.7832141 MHz
DATA PROCESSING
Resol. enhancement -0.0 Hz
FT size 65536
Total time 3 min, 21 sec

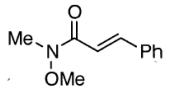


**1.84a**

Sample: HW-II-167
File: exp

Pulse Sequence: s2pul
Solvent: cdcl3
Temp. 25.0 C / 298.1 K
Operator: wuhr
VNMRS-400 "vnmr13"

Relax. delay 1.000 sec
Pulse 45.0 degrees
Acq. time 2.049 sec
Width 4807.7 Hz
12 repetitions
OBSERVE H1, 399.7832141 MHz
DATA PROCESSING
Resol. enhancement -0.0 Hz
FT size 65536
Total time 3 min, 21 sec

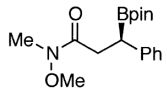


**1.85a**

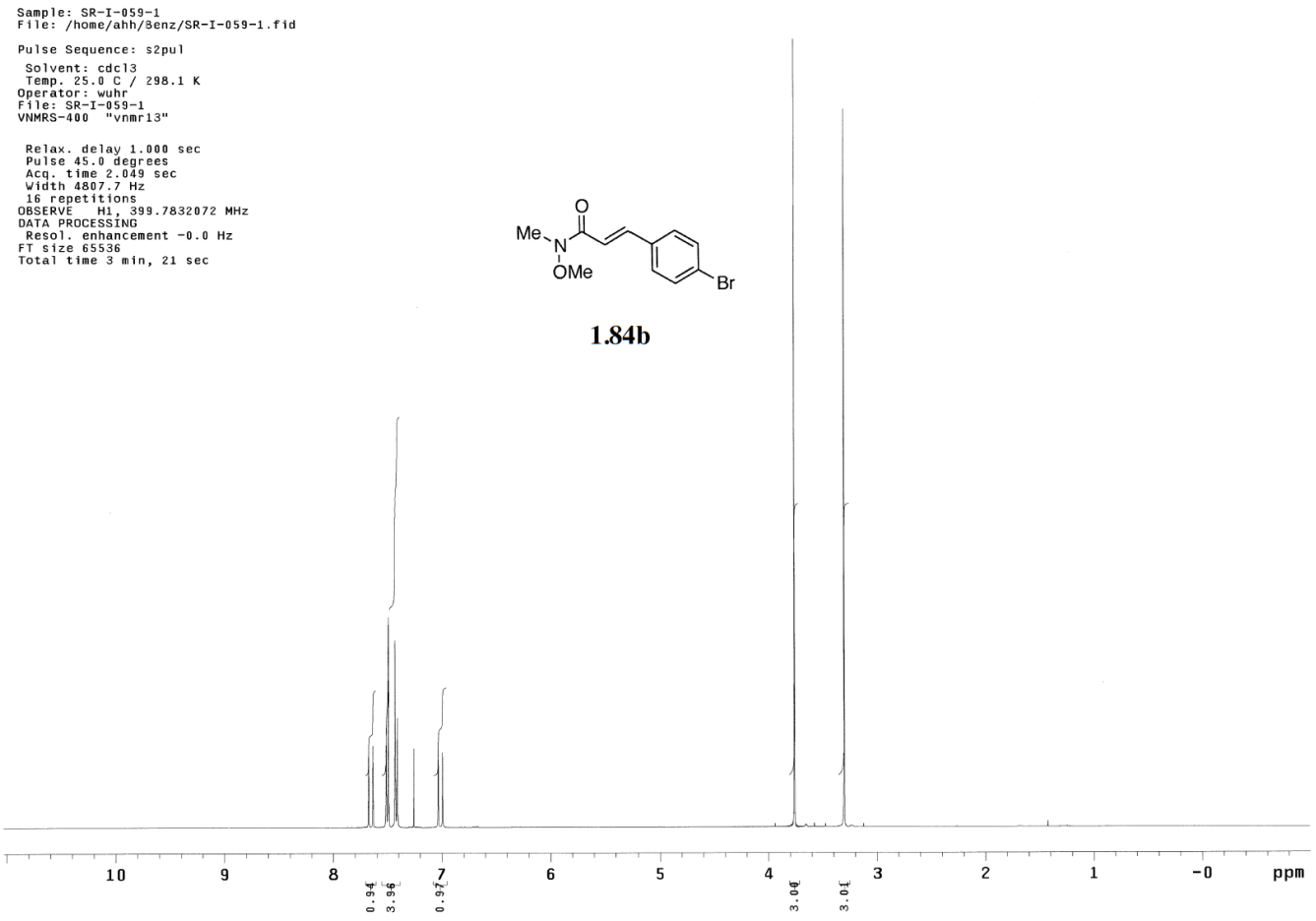
Sample: SR-I-059-1
File: /home/ahh/benz/SR-I-059-1.fid
Pulse Sequence: s2pul
Solvent: cdcl3
Temp. 25.0 C / 298.1 K
Operator: wuhr
File: SR-I-059-1
VNMRS-400 "vnmr13"
Relax. delay 1.000 sec
Pulse 45.0 degrees
Acq. time 2.049 sec
Width 4807.7 Hz
16 repetitions
OBSERVE H1, 399.7832072 MHz
DATA PROCESSING
Resol. enhancement -0.0 Hz
FT size 65536
Total time 3 min, 21 sec
Me
N
OMe
O
Br
1.84b
10
9
8
7
6
5
4
3
2
1
-0
ppm
0.94
3.96
0.97
3.00
3.01

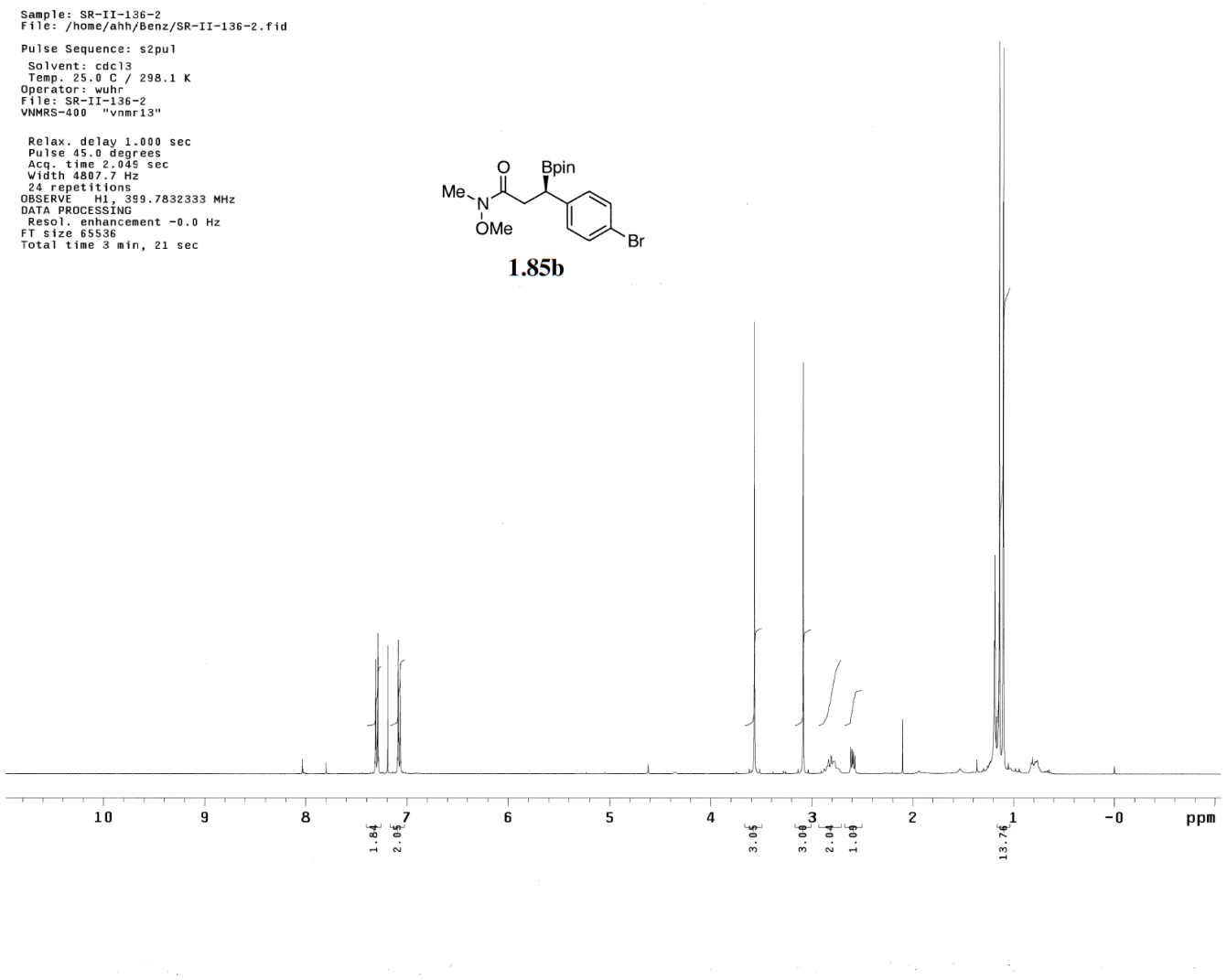
Sample: SR-II-136-2
File: /home/ahh/Benz/SR-II-136-2.fid
Pulse Sequence: s2pul
Solvent: cdcl3
Temp. 25.0 C / 298.1 K
Operator: wuhr
File: SR-II-136-2
VNMRS-400 "vnmr13"
Relax. delay 1.000 sec
Pulse 45.0 degrees
Acq. time 2.049 sec
Width 4807.7 Hz
24 repetitions
OBSERVE H1, 399.7832333 MHz
DATA PROCESSING
Resol. enhancement -0.0 Hz
FT size 65536
Total time 3 min, 21 sec
O
Bpin
Me
N
OMe
Br
1.85b
10
9
8
7
6
5
4
3
2
1
-0
ppm
1.84
2.05
3.05
3.00
2.04
1.09
13.76

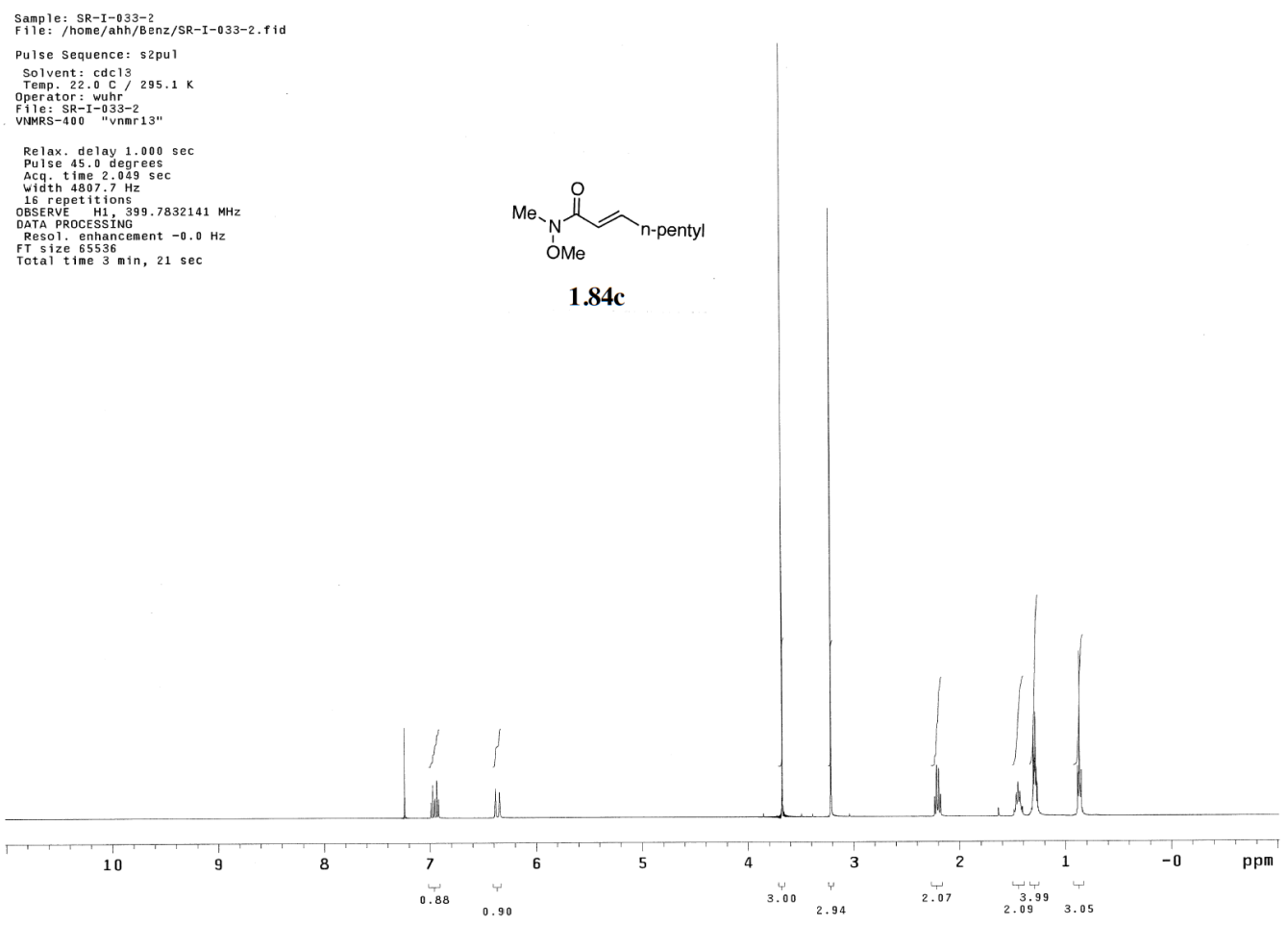
Sample: SR-I-033-2
File: /home/ahh/Benz/SR-I-033-2.fid
Pulse Sequence: s2pul
Solvent: cdcl3
Temp. 22.0 C / 295.1 K
Operator: wuhr
File: SR-I-033-2
VNMRS-400 "vnmr13"
Relax. delay 1.000 sec
Pulse 45.0 degrees
Acq. time 2.049 sec
Width 4807.7 Hz
16 repetitions
OBSERVE H1, 399.7832141 MHz
DATA PROCESSING
Resol. enhancement -0.0 Hz
FT size 65536
Total time 3 min, 21 sec
Me
N
OMe
O
n-pentyl
1.84c
10
9
8
7
6
5
4
3
2
1
-0
ppm
0.88
0.90
3.00
2.94
2.07
3.99
2.09
3.05

Sample: HW-II-137
File: exp

Pulse Sequence: s2pul

Solvent: cdcl3
Temp. 22.0 C / 295.1 K
Operator: wuhr
VNMRS-400 "vnmr13"

Relax. delay 1.000 sec
Pulse 45.0 degrees
Acq. time 2.049 sec
Width 4807.7 Hz
16 repetitions
OBSERVE H1, 399.7832141 MHz
DATA PROCESSING
Resol. enhancement -0.0 Hz
FT size 65536
Total time 3 min, 21 sec

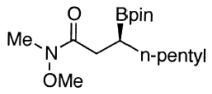


**1.85c**

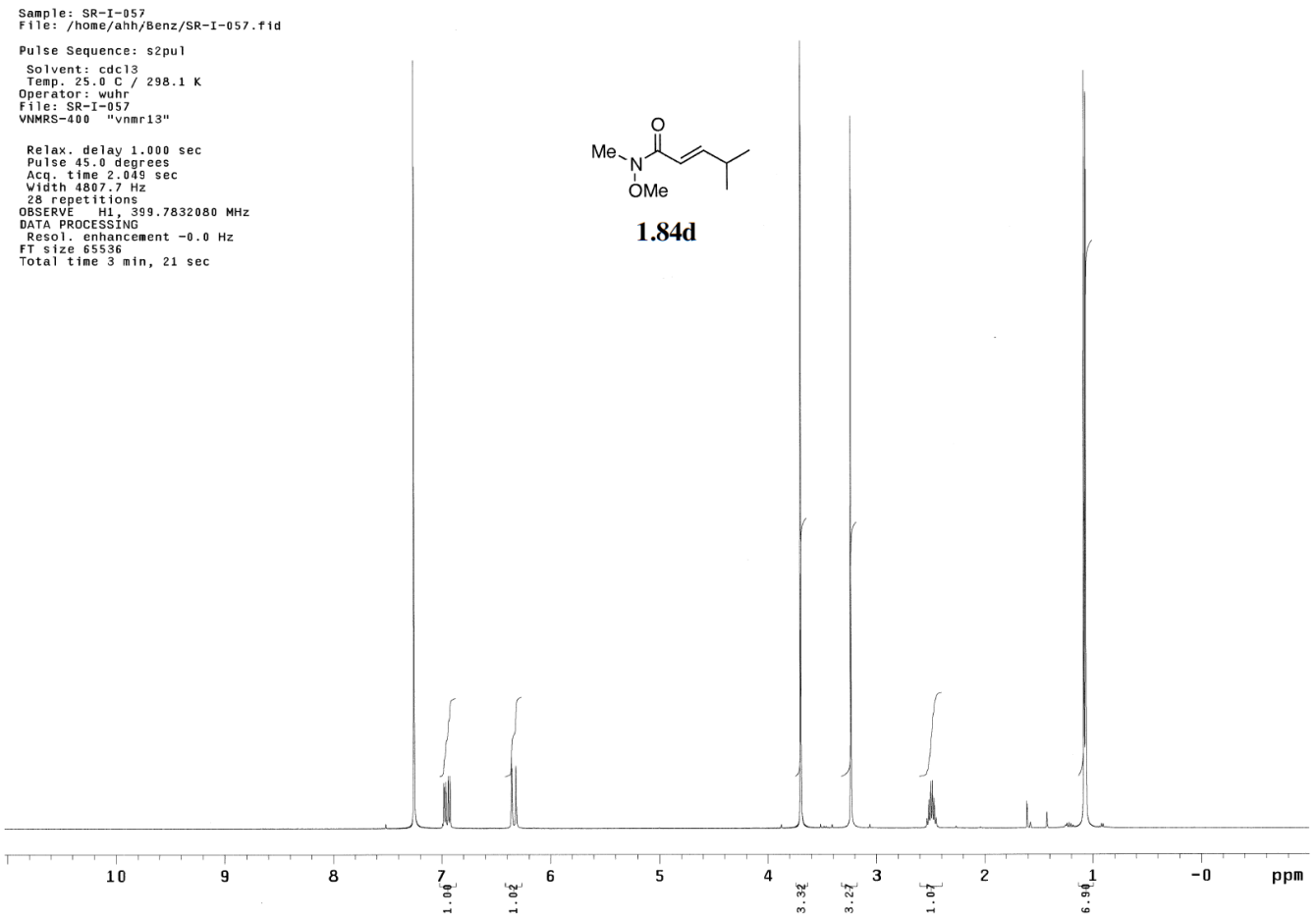
Sample: SR-I-057
File: /home/ahh/Benz/SR-I-057.fid
Pulse Sequence: s2pul
Solvent: cdcl3
Temp. 25.0 C / 298.1 K
Operator: wuhr
File: SR-I-057
VNMRS-400 "vnmr13"
Relax. delay 1.000 sec
Pulse 45.0 degrees
Acq. time 2.049 sec
Width 4807.7 Hz
28 repetitions
OBSERVE H1, 399.7832080 MHz
DATA PROCESSING
Resol. enhancement -0.0 Hz
FT size 65536
Total time 3 min, 21 sec
Me
N
O
OMe
1.84d
10
9
8
7
6
5
4
3
2
1
-0
ppm
1.00
1.02
3.32
3.27
1.07
6.90

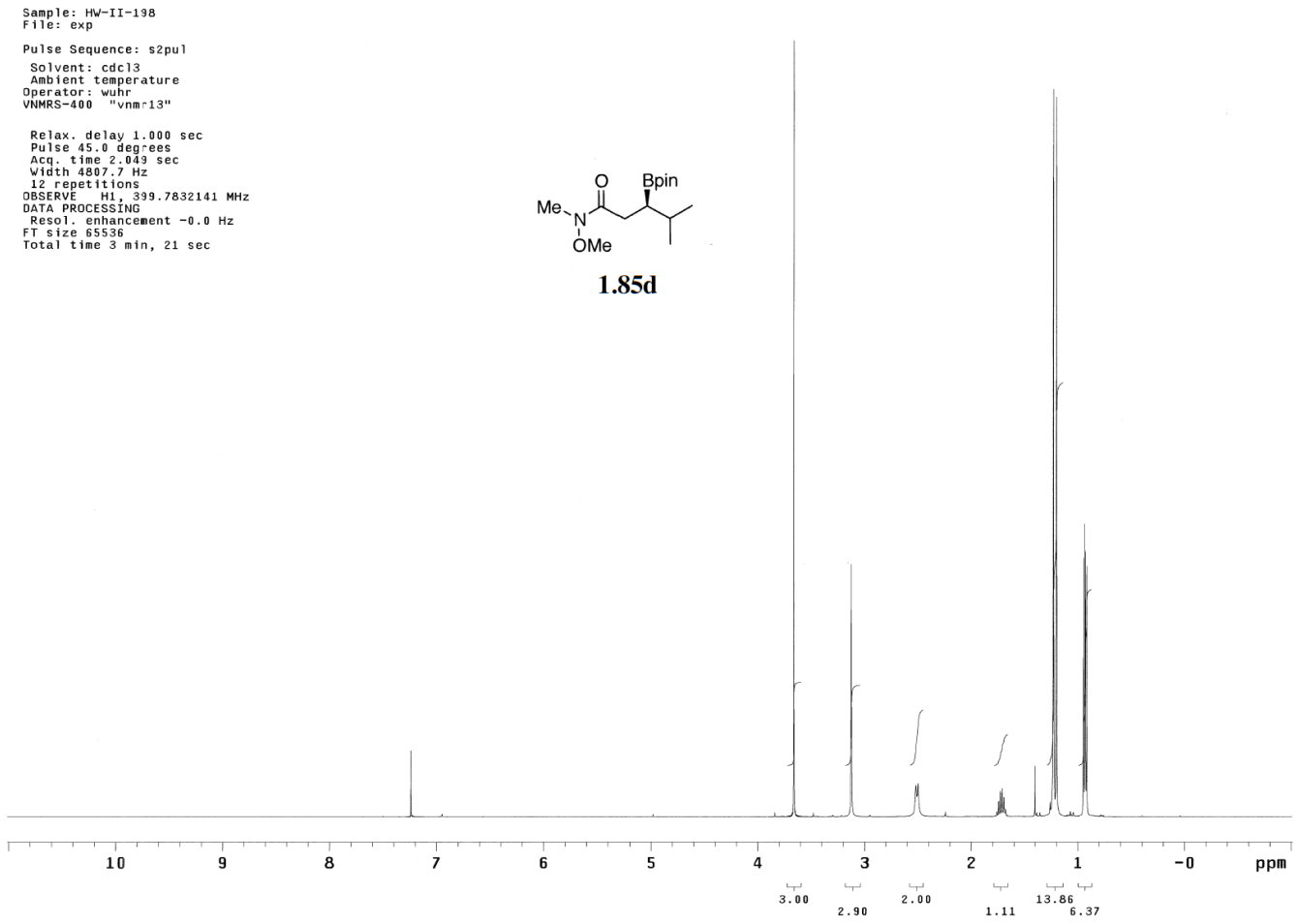
Sample: HW-II-198
File: exp
Pulse Sequence: s2pul
Solvent: cdcl3
Ambient temperature
Operator: wuhr
VNMRS-400 "vnmr13"
Relax. delay 1.000 sec
Pulse 45.0 degrees
Acq. time 2.049 sec
Width 4807.7 Hz
12 repetitions
OBSERVE H1, 399.7832141 MHz
DATA PROCESSING
Resol. enhancement -0.0 Hz
FT size 65536
Total time 3 min, 21 sec
O
Bpin
Me
N
OMe
1.85d
10
9
8
7
6
5
4
3
2
1
-0
ppm
3.00
2.90
2.00
1.11
13.86
6.37

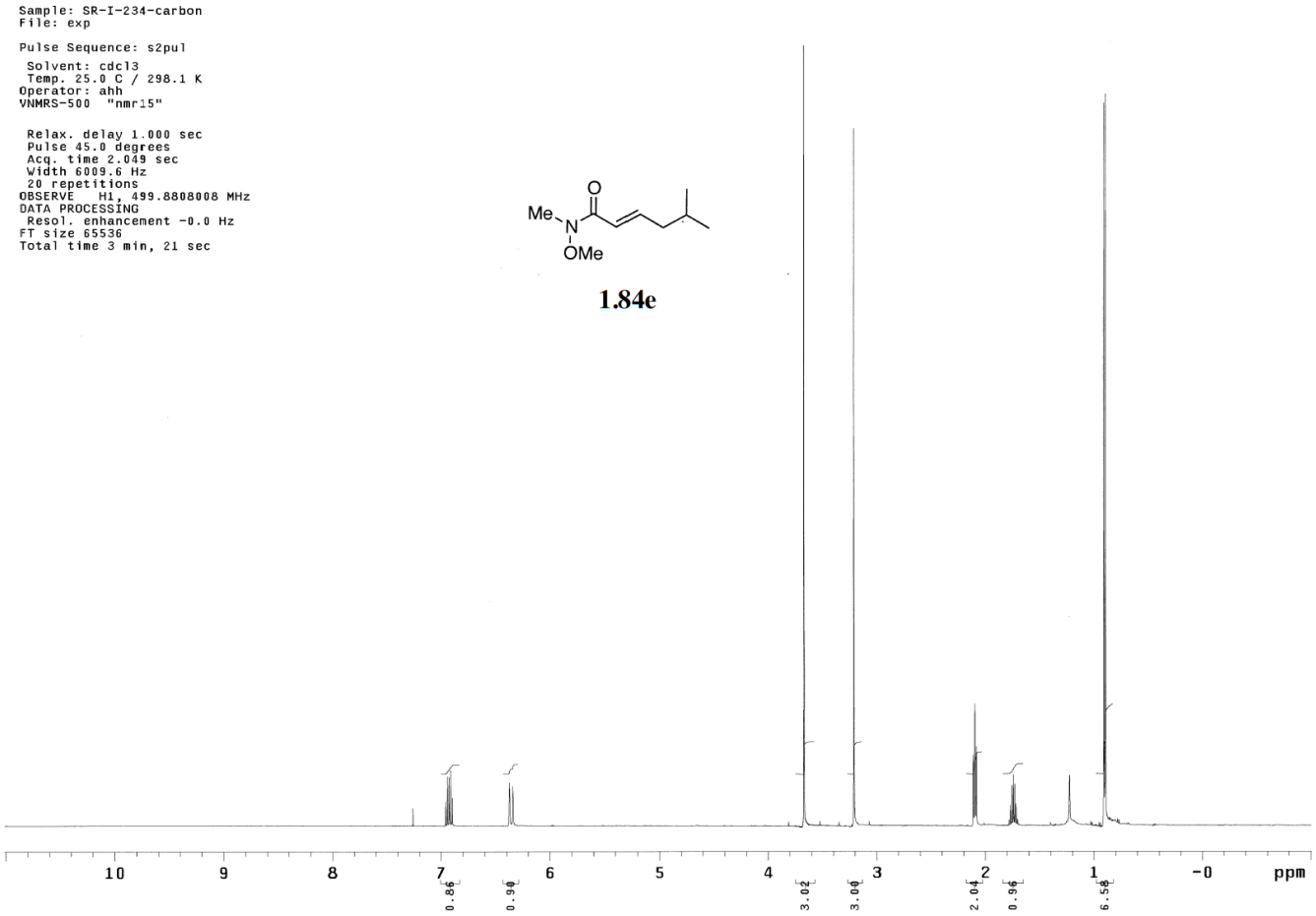
Sample: SR-I-234-carbon
File: exp
Pulse Sequence: s2pul
Solvent: cdcl3
Temp. 25.0 C / 298.1 K
Operator: ahh
VNMRS-500 "nmr15"
Relax. delay 1.000 sec
Pulse 45.0 degrees
Acq. time 2.049 sec
Width 6009.6 Hz
20 repetitions
OBSERVE H1, 499.8808008 MHz
DATA PROCESSING
Resol. enhancement -0.0 Hz
FT size 65536
Total time 3 min, 21 sec
Me
N
OMe
O
1.84e
10
9
8
7
6
5
4
3
2
1
-0
ppm
0.86
0.90
3.02
3.00
2.04
0.96
6.58

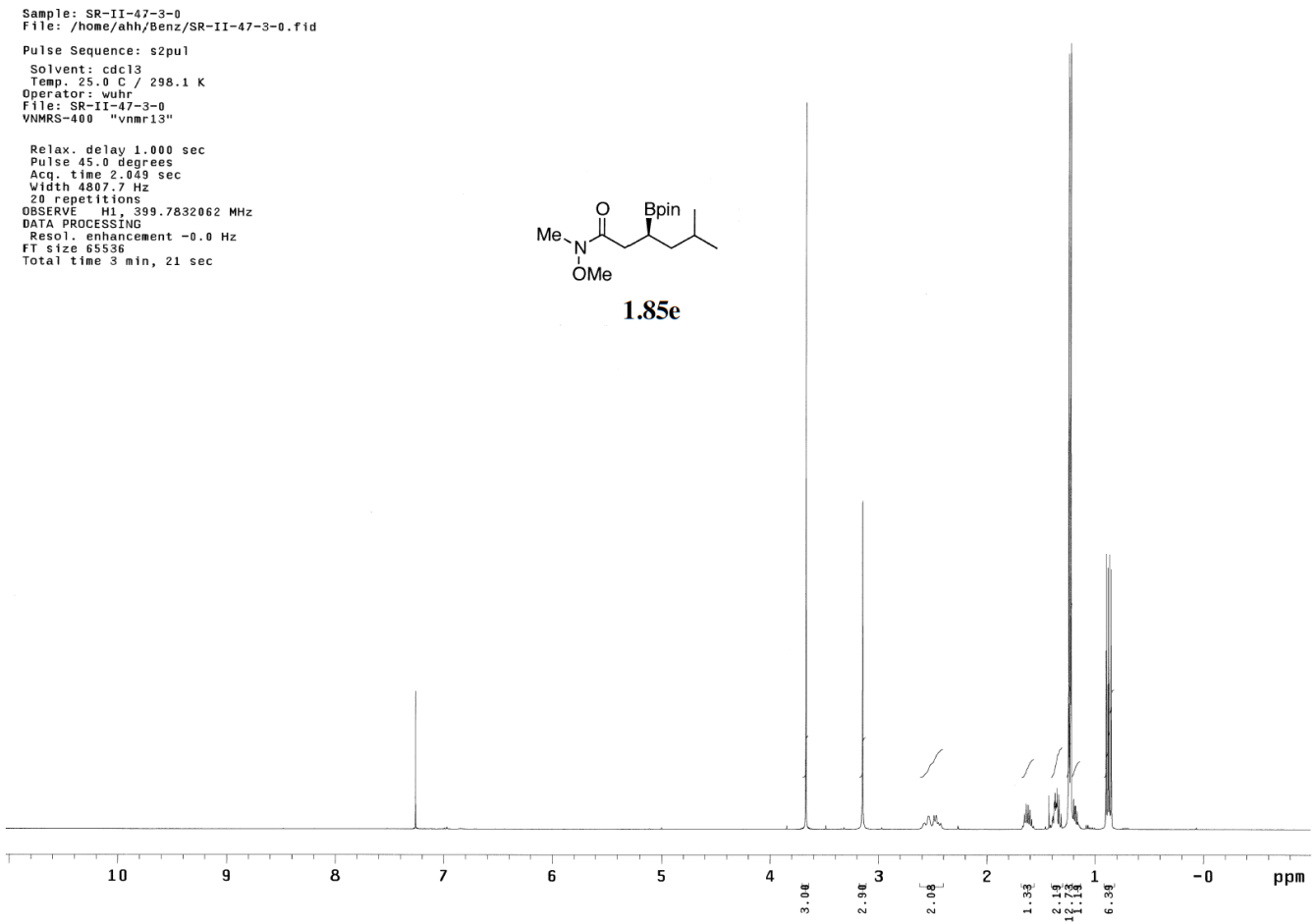
Sample: SR-II-47-3-0
File: /home/ahh/Benz/SR-II-47-3-0.fid
Pulse Sequence: s2pul
Solvent: cdcl3
Temp. 25.0 C / 298.1 K
Operator: wuhr
File: SR-II-47-3-0
VNMRS-400 "vnmr13"
Relax. delay 1.000 sec
Pulse 45.0 degrees
Acq. time 2.049 sec
Width 4807.7 Hz
20 repetitions
OBSERVE H1, 399.7832062 MHz
DATA PROCESSING
Resol. enhancement -0.0 Hz
FT size 65536
Total time 3 min, 21 sec
Me
N
OMe
O
Bpin
1.85e
10
9
8
7
6
5
4
3
2
1
-0
ppm
3.04
2.98
2.08
1.33
2.16
12.13
11.13
6.36

Sample: SR-I-233-2-rerun
File: exp

Pulse Sequence: s2pul
Solvent: cdcl3
Temp. 25.0 C / 298.1 K
Operator: wuhr
VNMRS-400 "vnmr13"

Relax. delay 1.000 sec
Pulse 45.0 degrees
Acq. time 2.049 sec
Width 4807.7 Hz
32 repetitions
OBSERVE H1, 399.7832062 MHz
DATA PROCESSING
Resol. enhancement -0.0 Hz
FT size 65536
Total time 3 min, 21 sec

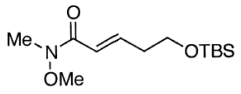


**1.84f**

Sample: SR-I-252
File: /home/ahh/Benz/SR-I-252.fid

Pulse Sequence: s2pul
Solvent: cdcl3
Temp. 25.0 C / 298.1 K
Operator: wuhr
File: SR-I-252
VNMRS-400 "vnmr13"

Relax. delay 1.000 sec
Pulse 45.0 degrees
Acq. time 2.049 sec
Width 4807.7 Hz
28 repetitions
OBSERVE H1, 399.7832077 MHz
DATA PROCESSING
Resol. enhancement -0.0 Hz
FT size 65536
Total time 3 min, 21 sec

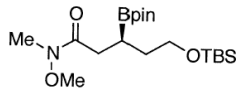


**1.85f**

Sample: HW-II-170-2
File: exp

Pulse Sequence: s2pul
Solvent: cdcl3
Temp. 25.0 C / 298.1 K
Operator: wuhr
VNMRS-400 "vnmr13"

Relax. delay 1.000 sec
Pulse 45.0 degrees
Acq. time 2.049 sec
Width 4807.7 Hz
20 repetitions
OBSERVE H1, 399.7832141 MHz
DATA PROCESSING
Resol. enhancement -0.0 Hz
FT size 65536
Total time 3 min, 21 sec

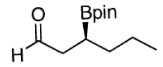


**1.88a**

Sample: SR-I-174
File: /home/ahh/Benz/SR-I-174.fid

Pulse Sequence: s2pul
 Solvent: cdcl3
 Temp. 25.0 C / 298.1 K
Operator: wuhr
File: SR-I-174
VNMRS-400  "vnmr13"

 Relax. delay 1.000 sec
 Pulse 45.0 degrees
 Acq. time 2.049 sec
 Width 4807.7 Hz
 32 repetitions
OBSERVE   H1, 399.7832141 MHz
DATA PROCESSING
 Resol. enhancement -0.0 Hz
FT size 65536
Total time 3 min, 21 sec

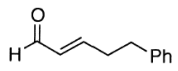


**1.87b**

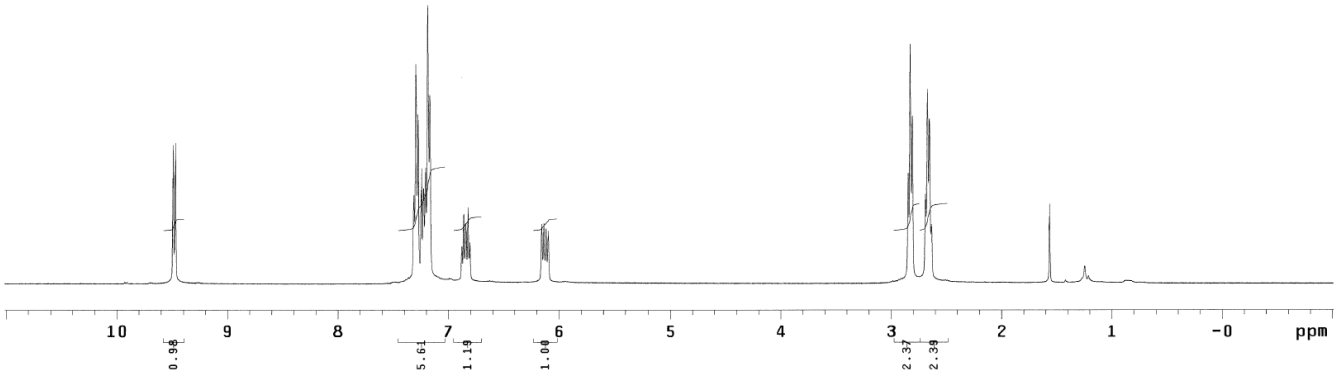

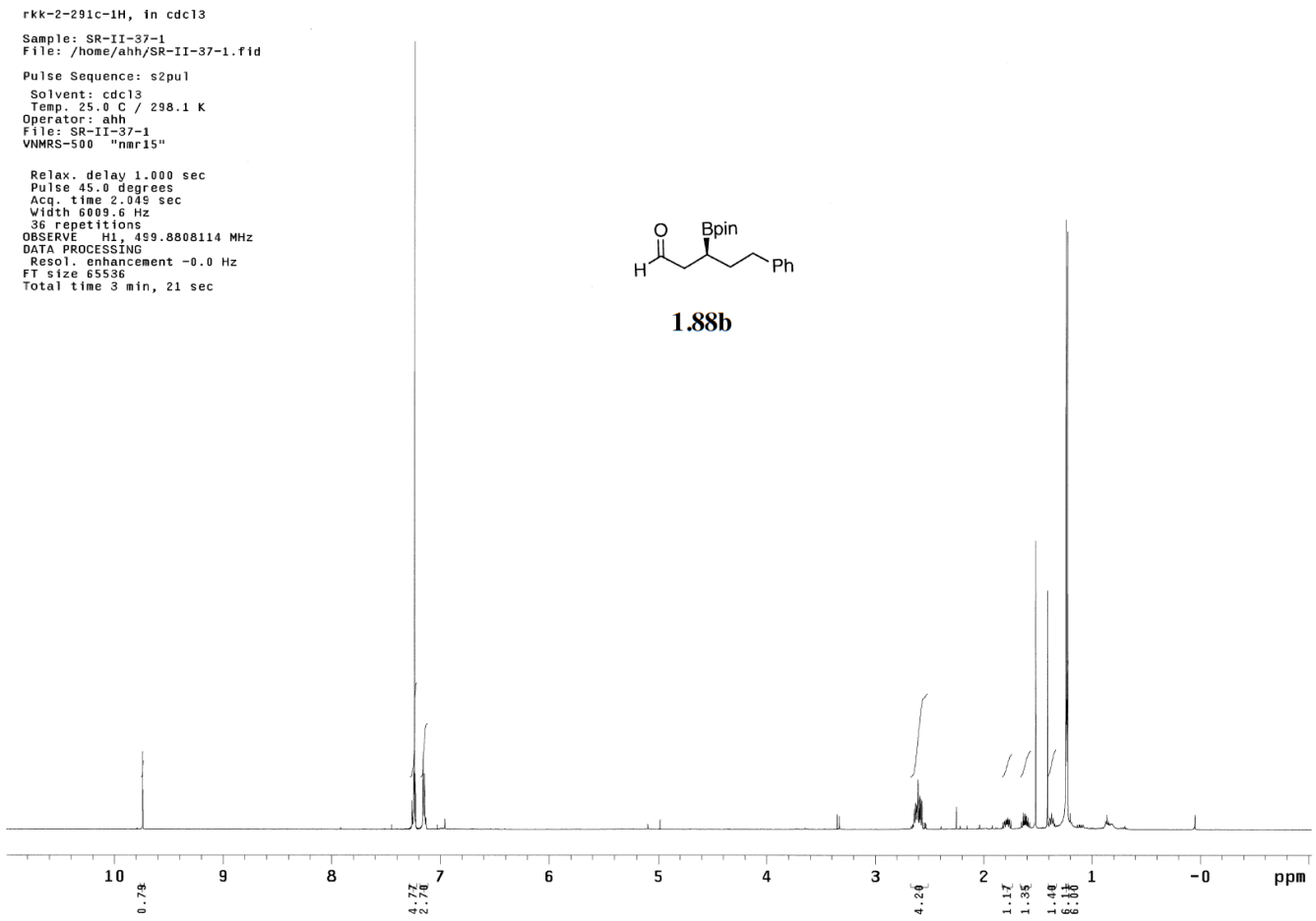
rkk-2-291c-1H, in cdcl3
Sample: SR-II-37-1
File: /home/ahh/SR-II-37-1.fid
Pulse Sequence: s2pul
Solvent: cdcl3
Temp. 25.0 C / 298.1 K
Operator: ahh
File: SR-II-37-1
VNMRS-500 "nmr15"
Relax. delay 1.000 sec
Pulse 45.0 degrees
Acq. time 2.049 sec
Width 6009.6 Hz
36 repetitions
OBSERVE H1, 499.8808114 MHz
DATA PROCESSING
Resol. enhancement -0.0 Hz
FT size 65536
Total time 3 min, 21 sec
O
Bpin
H
Ph
1.88b
10
9
8
7
6
5
4
3
2
1
-0
ppm
0.78
4.77
2.78
4.20
1.17
1.35
1.40
6.11
6.00

Sample: HW-II-244-1-2
File: exp

Pulse Sequence: s2pul
Solvent: cdcl3
Temp. 25.0 C / 298.1 K
Operator: wuhr
VNMRS-400 "vnmr13"

Relax. delay 1.000 sec
Pulse 45.0 degrees
Acq. time 2.049 sec
Width 4807.7 Hz
16 repetitions
OBSERVE H1, 399.7832141 MHz
DATA PROCESSING
Resol. enhancement -0.0 Hz
FT size 65536
Total time 3 min, 21 sec

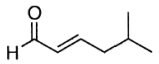


**1.87c**

Sample: HW-II-247
File: /home/ahh/wuhr/HW-II-247.fid

Pulse Sequence: s2pul
Solvent: cdcl3
Temp. 25.0 C / 298.1 K
Operator: wuhr
File: HW-II-247
VNMRS-400 "vnmr13"

Relax. delay 1.000 sec
Pulse 45.0 degrees
Acq. time 2.049 sec
Width 4807.7 Hz
16 repetitions
OBSERVE H1, 399.7832103 MHz
DATA PROCESSING
Resol. enhancement -0.0 Hz
FT size 65536
Total time 3 min, 21 sec

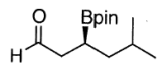


**1.88c**

Sample: HW-II-180
File: /home/ahh/wuhr/HW-II-180-1H.fid

Pulse Sequence: s2pul
Solvent: cdcl3
Temp. 25.0 C / 298.1 K
Operator: wuhr
File: HW-II-180-1H
VNMRS-400 "vnmr13"

Relax. delay 1.000 sec
Pulse 45.0 degrees
Acq. time 2.049 sec
Width 4807.7 Hz
12 repetitions
OBSERVE H1, 399.7832338 MHz
DATA PROCESSING
Resol. enhancement -0.0 Hz
FT size 65536
Total time 3 min, 21 sec

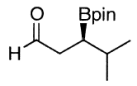


**1.88d**

Sample: HW-II-256
File: exp

Pulse Sequence: s2pul
Solvent: cdcl3
Temp. 25.0 C / 298.1 K
Operator: wuhr
VNMRS-400 "vnmr13"

Relax. delay 1.000 sec
Pulse 45.0 degrees
Acq. time 2.049 sec
Width 4807.7 Hz
8 repetitions
OBSERVE H1, 399.7832141 MHz
DATA PROCESSING
Resol. enhancement -0.0 Hz
FT size 65536
Total time 3 min, 21 sec

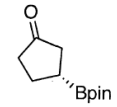


**1.3q**

Sample: HW-III-187
File: exp

Pulse Sequence: s2pul
Solvent: cdcl3
Temp. 25.0 C / 298.1 K
Operator: wuhr
VNMRS-400 "vnmr13"

Relax. delay 1.000 sec
Pulse 45.0 degrees
Acq. time 2.049 sec
Width 4807.7 Hz
8 repetitions
OBSERVE H1, 399.7832141 MHz
DATA PROCESSING
Resol. enhancement -0.0 Hz
FT size 65536
Total time 3 min, 21 sec

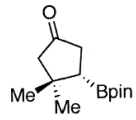


**1.98**

Sample: HW-II-312
File: /home/ahh/wuhr/HW-II-312.fid

Pulse Sequence: s2pul
 Solvent: cdcl3
 Temp. 25.0 C / 298.1 K
Operator: wuhr
File: HW-II-312
VNMRS-400  "vnmr13"

 Relax. delay 1.000 sec
 Pulse 45.0 degrees
 Acq. time 2.049 sec
 Width 4807.7 Hz
 24 repetitions
OBSERVE   H1, 399.7832089 MHz
DATA PROCESSING
 Resol. enhancement -0.0 Hz
FT size 65536
Total time 3 min, 21 sec

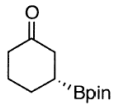


**1.3b**

Sample: HW-III-186
File: /home/ahh/wuhr/HW-III-186.fid

Pulse Sequence: s2pul
Solvent: cdcl3
Temp. 25.0 C / 298.1 K
Operator: wuhr
File: HW-III-186
VNMRS-400 "vnmr13"

Relax. delay 1.000 sec
Pulse 45.0 degrees
Acq. time 2.049 sec
Width 4807.7 Hz
16 repetitions
OBSERVE H1, 399.7832089 MHz
DATA PROCESSING
Resol. enhancement -0.0 Hz
FT size 65536
Total time 3 min, 21 sec

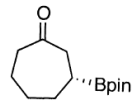


**1.3r**

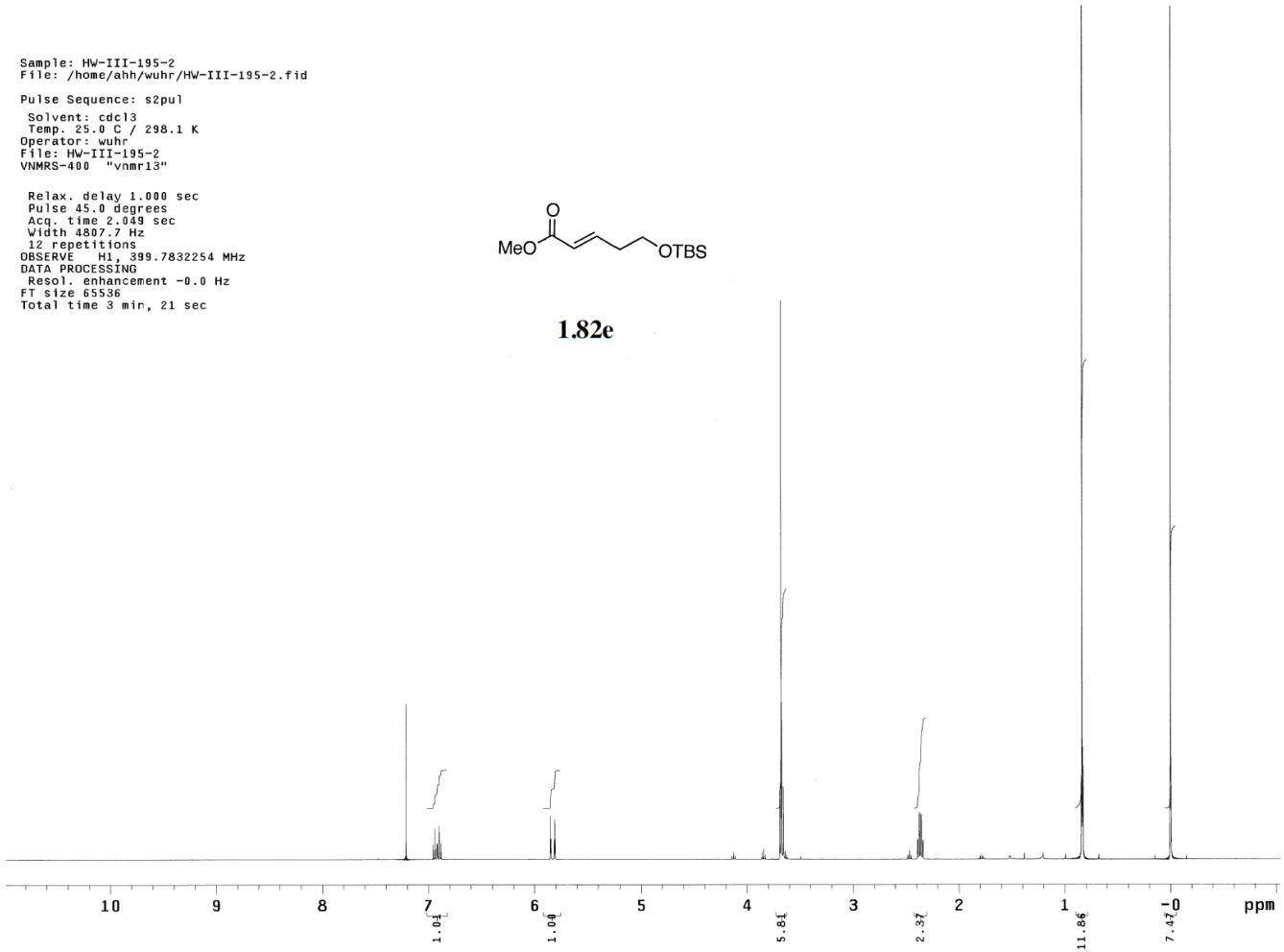
Sample: HW-III-195-2
File: /home/ahh/wuhr/HW-III-195-2.fid
Pulse Sequence: s2pul
Solvent: cdcl3
Temp. 25.0 C / 298.1 K
Operator: wuhr
File: HW-III-195-2
VNMRS-400 "vnmr13"
Relax. delay 1.000 sec
Pulse 45.0 degrees
Acq. time 2.049 sec
Width 4807.7 Hz
12 repetitions
OBSERVE H1, 399.7832254 MHz
DATA PROCESSING
Resol. enhancement -0.0 Hz
FT size 65536
Total time 3 min, 21 sec
MeO
O
OTBS
1.82e
10
9
8
7
6
5
4
3
2
1
0
ppm
1.01
1.00
5.81
2.37
11.86
7.47

Sample: HW-III-212
File: exp

Pulse Sequence: s2pul
Solvent: cdcl3
Temp. 25.0 C / 298.1 K
Operator: wuhr
VNMRS-400 "vnmr13"

Relax. delay 1.000 sec
Pulse 45.0 degrees
Acq. time 2.049 sec
Width 4807.7 Hz
16 repetitions
OBSERVE H1, 399.7832141 MHz
DATA PROCESSING
Resol. enhancement -0.0 Hz
FT size 65536
Total time 3 min, 21 sec

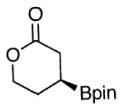


**1.3t**

Sample: HW-III-275
File: exp

Pulse Sequence: s2pul

Solvent: cdcl3
Temp. 25.0 C / 298.1 K
Operator: wuhr
VNMRS-400 "vnmr13"

Relax. delay 1.000 sec
Pulse 45.0 degrees
Acq. time 2.049 sec
Width 4807.7 Hz
12 repetitions
OBSERVE H1, 399.7832062 MHz
DATA PROCESSING
Resol. enhancement -0.0 Hz
FT size 65536
Total time 3 min, 21 sec

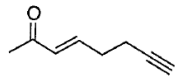

**substrate for 1.118**

Sample: HW-III-281
File: exp

Pulse Sequence: s2pul

Solvent: cdcl3
Temp. 25.0 C / 298.1 K
Operator: wuhr
VNMRS-400 "vnmr13"

Relax. delay 1.000 sec
Pulse 45.0 degrees
Acq. time 2.049 sec
Width 4807.7 Hz
12 repetitions
OBSERVE H1, 399.7832074 MHz
DATA PROCESSING
Resol. enhancement -0.0 Hz
FT size 65536
Total time 3 min, 21 sec

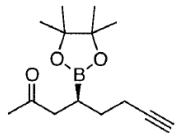

**1.118**

Sample: SR-II-171
File: exp

Pulse Sequence: s2pul
Solvent: cdcl3
Temp. 25.0 C / 298.1 K
Operator: wuhr
VNMRS-400 "vnmr13"

Relax. delay 1.000 sec
Pulse 45.0 degrees
Acq. time 2.049 sec
Width 4807.7 Hz
16 repetitions
OBSERVE H1, 399.7832063 MHz
DATA PROCESSING
Resol. enhancement -0.0 Hz
FT size 65536
Total time 3 min, 21 sec


**substrate for 1.119**

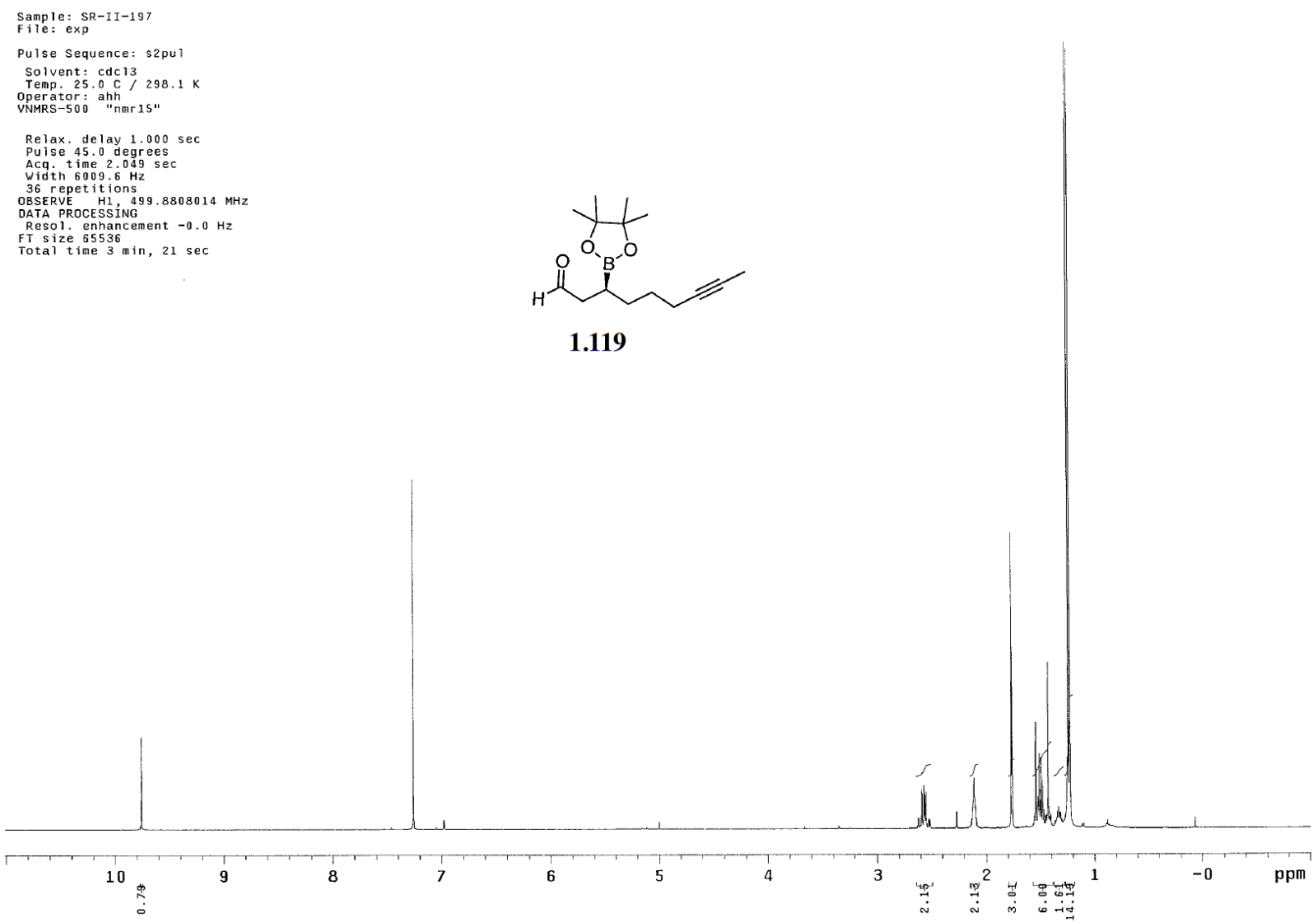
Sample: SR-II-197
File: exp
Pulse Sequence: s2pul
Solvent: cdcl3
Temp. 25.0 C / 298.1 K
Operator: ahh
VNMRS-500 "nmr15"
Relax. delay 1.000 sec
Pulse 45.0 degrees
Acq. time 2.049 sec
Width 6009.6 Hz
36 repetitions
OBSERVE H1, 499.8808014 MHz
DATA PROCESSING
Resol. enhancement -0.0 Hz
FT size 65536
Total time 3 min, 21 sec
O
O
B
O
H
10
9
8
7
6
5
4
3
2
1
-0
ppm
0.79
2.15
2.13
3.01
6.04
1.61
14.14

**1.119**

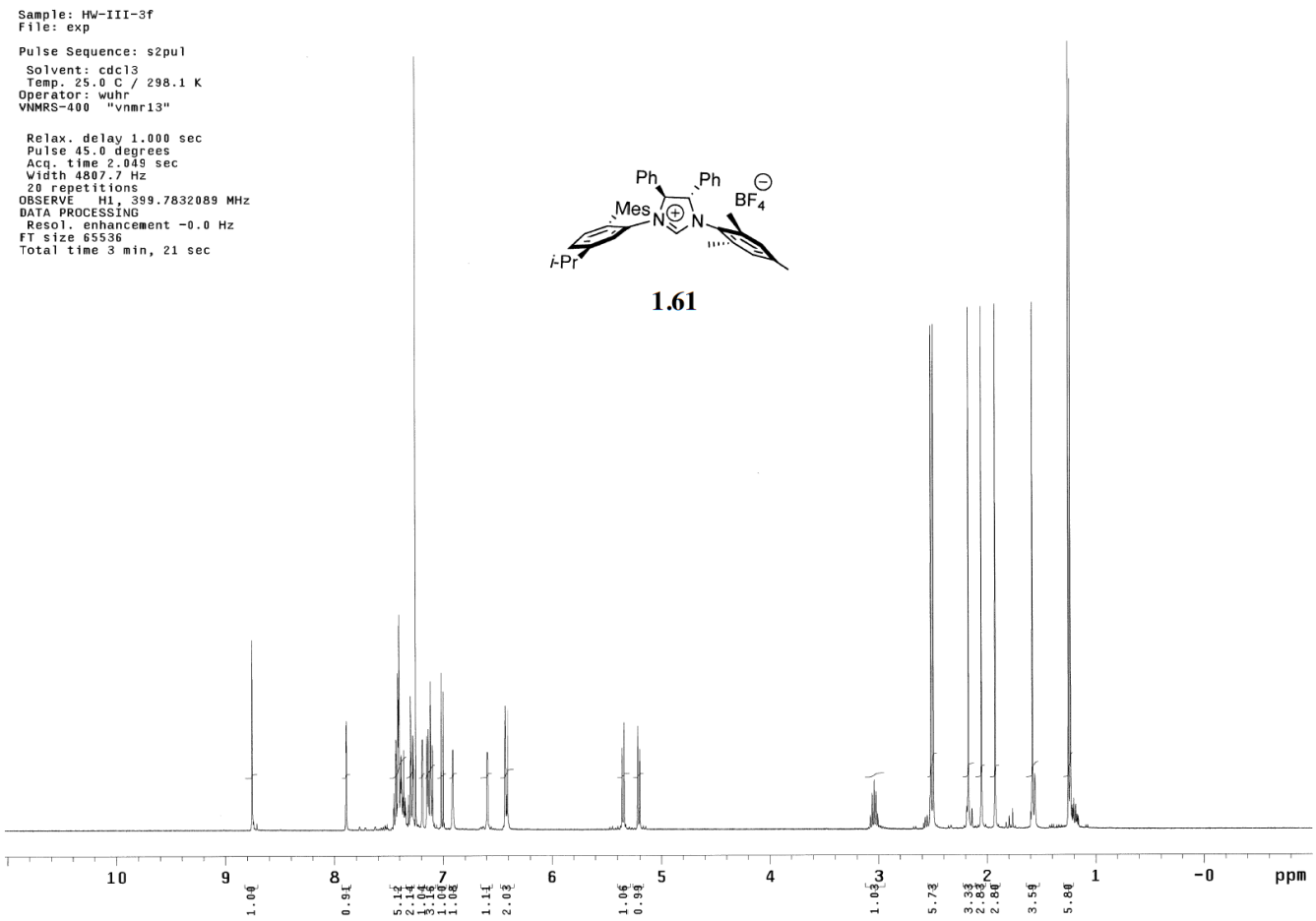
Sample: HW-III-3f
File: exp
Pulse Sequence: s2pul
Solvent: cdcl3
Temp. 25.0 C / 298.1 K
Operator: wuhr
VNMRS-400 "vnmr13"
Relax. delay 1.000 sec
Pulse 45.0 degrees
Acq. time 2.049 sec
Width 4807.7 Hz
20 repetitions
OBSERVE H1, 399.7832089 MHz
DATA PROCESSING
Resol. enhancement -0.0 Hz
FT size 65536
Total time 3 min, 21 sec
Ph
Ph
Mes
N
N
BF4
i-Pr
1.61
10
9
8
7
6
5
4
3
2
1
-0
ppm
1.00
0.91
5.12
2.14
1.04
3.15
1.00
1.08
1.11
2.03
1.06
0.99
1.05
5.73
3.33
2.83
2.80
3.59
5.80

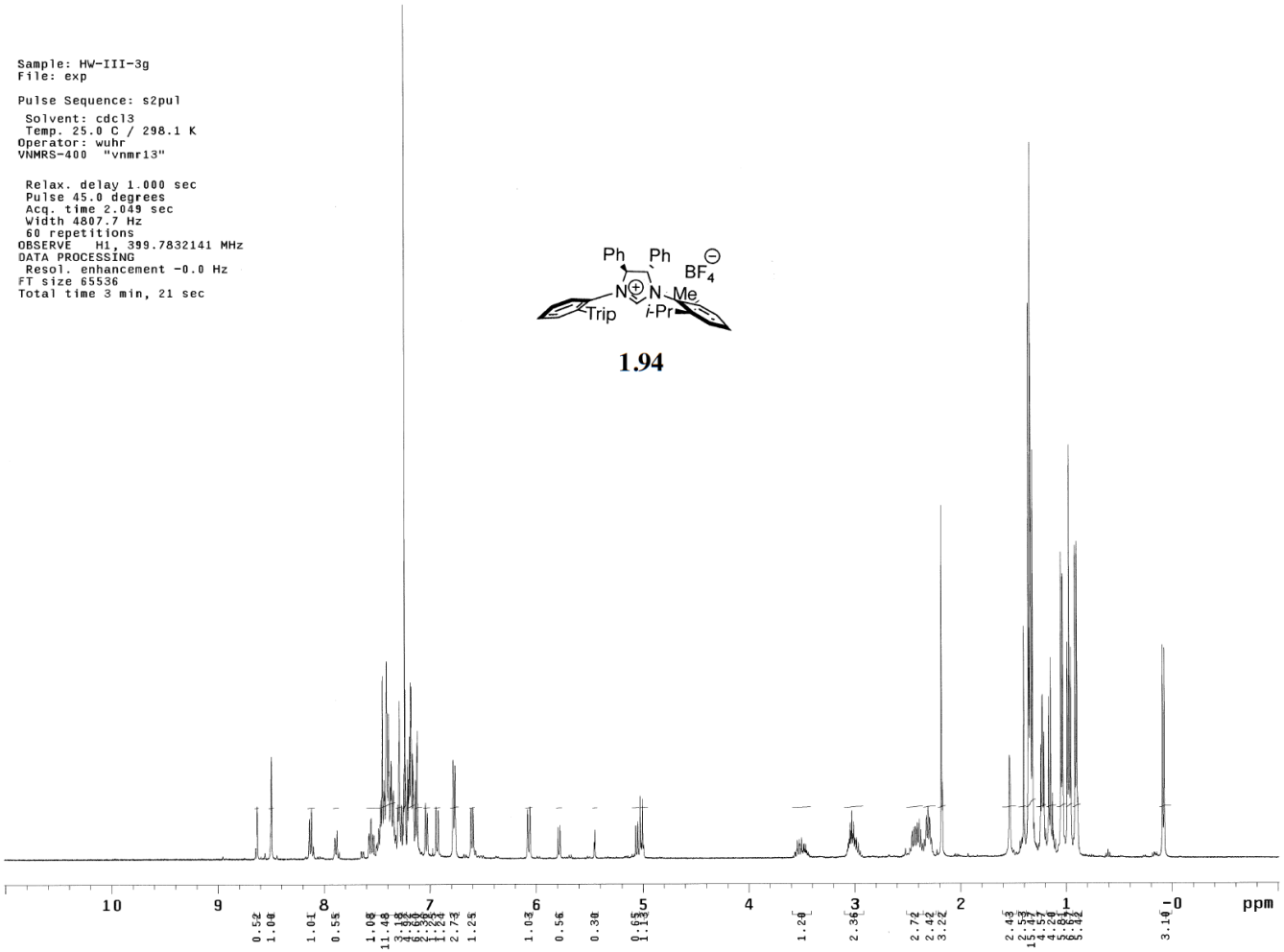
Sample: HW-III-3g
File: exp
Pulse Sequence: s2pul
Solvent: cdcl3
Temp. 25.0 C / 298.1 K
Operator: wuhr
VNMRS-400 "vnmr13"
Relax. delay 1.000 sec
Pulse 45.0 degrees
Acq. time 2.049 sec
Width 4807.7 Hz
60 repetitions
OBSERVE H1, 399.7832141 MHz
DATA PROCESSING
Resol. enhancement -0.0 Hz
FT size 65536
Total time 3 min, 21 sec
Ph
Ph
BF4
N
N
Me
Trip
i-Pr
10
9
8
7
6
5
4
3
2
1
0
ppm

**1.94**

### *1.9.3. $^{11}B$ NMR Spectra of $B_2(pin)_2$ and NHC•$B_2(pin)_2$ Complex 1.62*

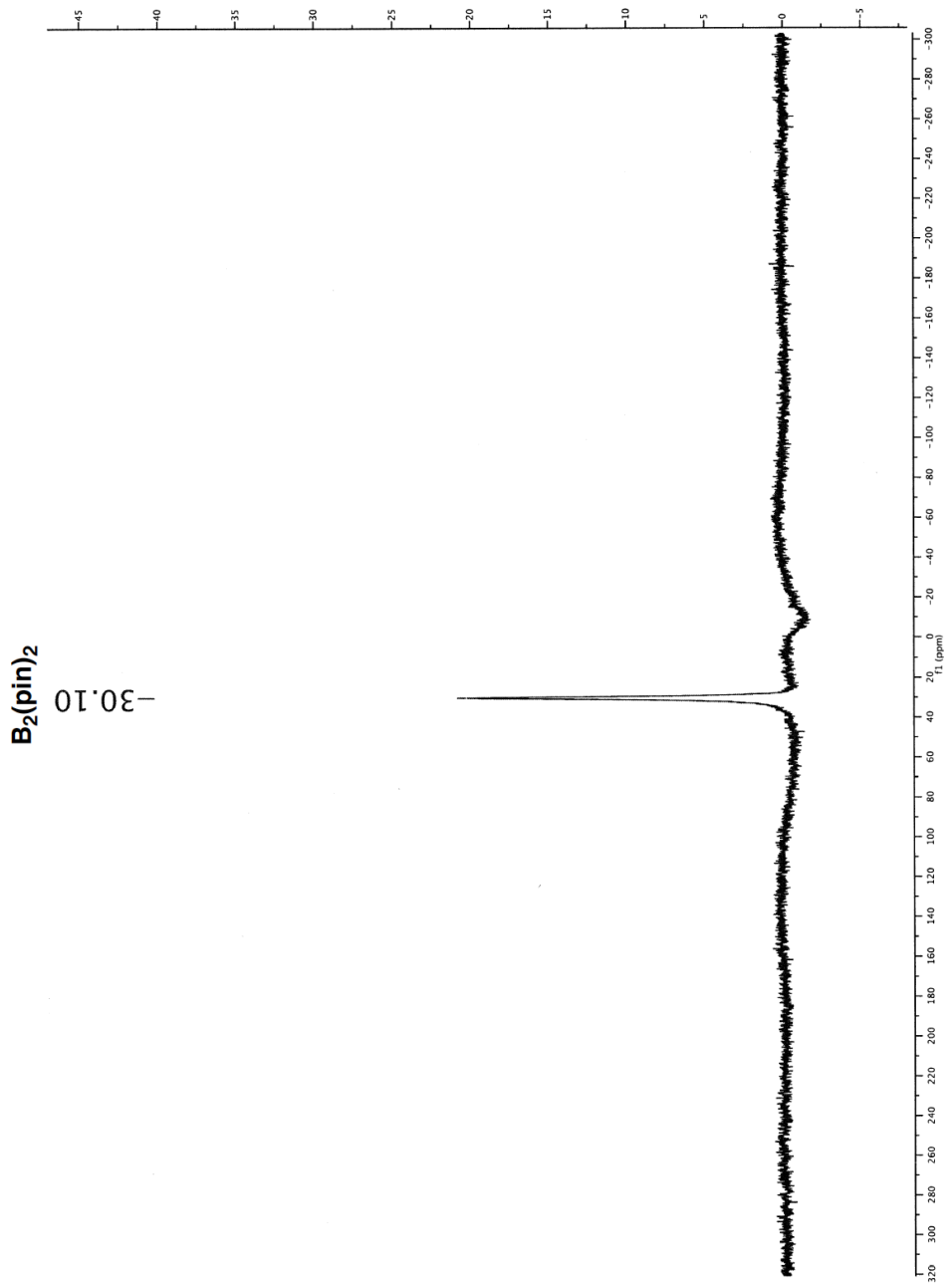

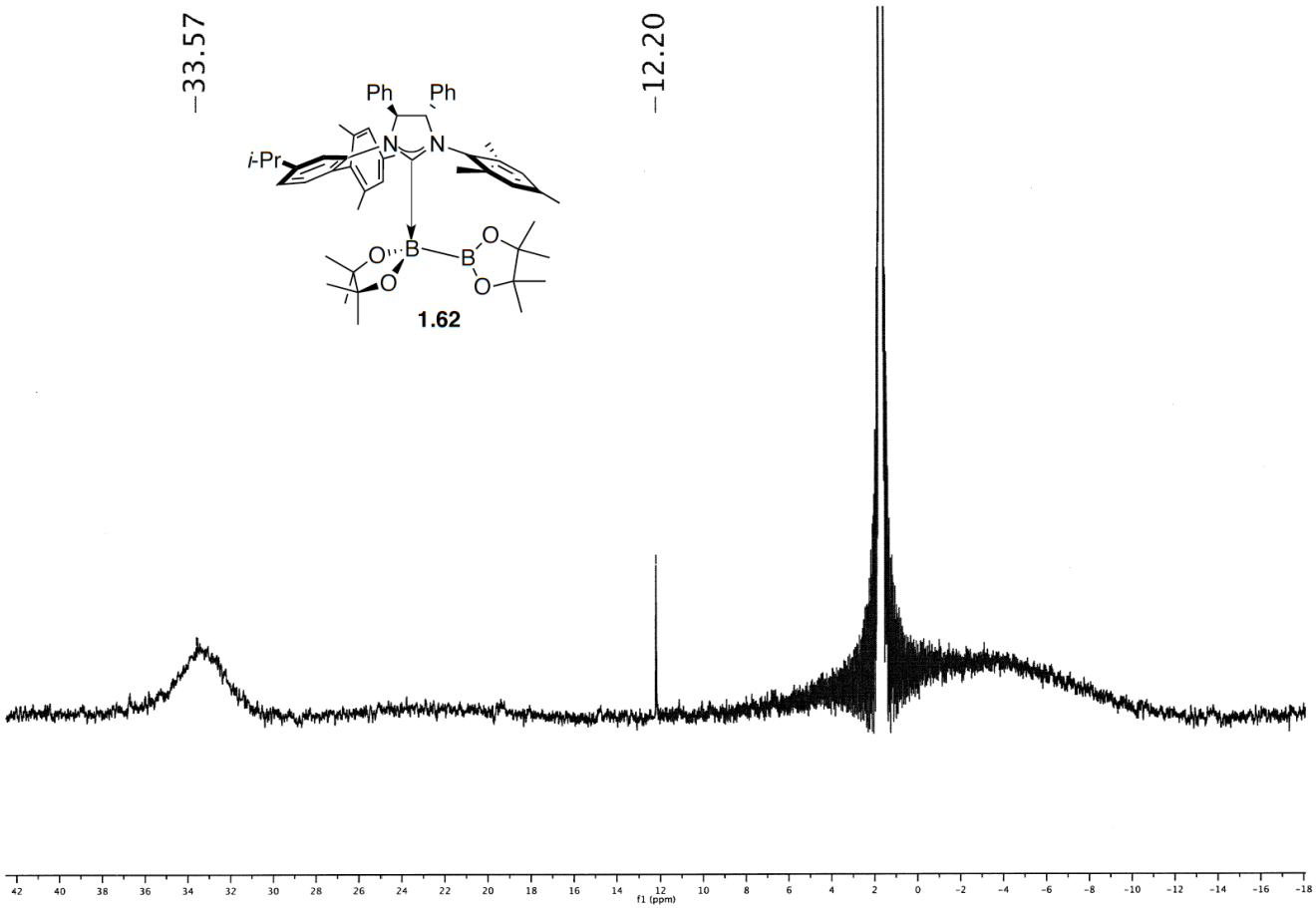
−33.57
−12.20
Ph
Ph
N
N
i-Pr
O
B
B
O
O
O
1.62
42 40 38 36 34 32 30 28 26 24 22 20 18 16 14 12 10 8 6 4 2 0 -2 -4 -6 -8 -10 -12 -14 -16 -18
f1 (ppm)

# Chapter 2

## Mechanistic Studies on *N*-heterocyclic Carbene Catalyzed Boryl and Silyl Conjugate Additions

### *2.1. Introduction*

N-heterocyclic carbenes (NHCs) catalyzed boryl and silyl conjugate additions, useful methodologies illustrated in Chapter 1, have drawn much attention in the region of Lewis base catalysis. However, the mechanisms of these transformations remain to be fully understood. More specifically, there are several fundamental questions that need to be answered:

For the boryl conjugate addition (BCA) reactions:

(1) Why is an excess amount of base (beyond the need for NHC formation) required for efficient transformations when a chiral NHC is employed, while it is not the case for achiral NHC catalyzed reactions?

(2) Why is an alcohol (MeOH) needed in the enantioselective transformations but not in the achiral NHC catalyzed reactions?

(3) How does the chiral NHC influence the stereochemical induction in the C–B bond formation step precisely?

(4) For the absolute stereochemistry, why is the sense of B(pin) addition to acyclic substrates opposite to that of cyclic substrates?

For the silyl conjugate addition (SCA) reactions:

(1) Why is an excess amount of a protic additive and base required for achiral and chiral NHC catalyzed SCA reactions?

(2) Why is $H_2O$ superior than MeOH in the SCA reactions?

(3) For the absolute stereochemistry, why is the sense of silyl addition the same no matter acyclic or cyclic substrates are involved?

In this chapter, mechanistic investigations as well as detailed analysis in order to answer the aforementioned questions will be illustrated. NMR, kinetic and computational studies have been employed aiming at deeply understanding the inner workings of NHC-catalyzed BCA and SCA reactions.

## *2.2. Introduction of N-heterocyclic Carbenes*

Before moving to the central topic of this chapter, it is of great importance to introduce some of the fundamental characteristics of NHC(s) as well as transformations promoted by these heterocyclic carbenes.[75]

Carbenes are defined as neutral compounds containing a divalent carbon atom with a six-electron valence shell. Despite attempted to be synthesized as early as in 1835,[76] the isolation and characterization of a free, uncoordinated carbene were reported by Arduengo and co-workers.[77] 1,3-Di-1-adamantylimidazol-2-ylidene (**2.2**, Scheme 2.2.1a) was synthesized by treatment of the corresponding imidazolinium salt with NaH in tetrahydrofuran with a catalytic amount of DMSO. This N-heterocyclic carbene is

(75) For a recent review on N-heterocyclic carbenes, see: Hopkinson, M. W.; Richter, C.; Schedler, M.; Glorius, F. *Nature*, **2014**, *510*, 485–496.

(76) Dumas, J. B.; Peligot, E. Mémoire sur I'esprit-de-bois et les divers composés éthéres qui en proviennent. *Ann. Chim. Phys.* **1835**. *58,* 5–74.

(77) Arduengo, A. J. III.; Harlow, R. L.; Kline, M. *J. Am. Chem. Soc.* **1991**, *113*, 361–363.

stable in the absence of oxygen and moisture, the crystal structure of which was also obtained (shown in Scheme 2.2.1b). Several features of the crystal structure are worth mentioning: First, the N–$C_{carbene}$–N angle is 102.2º, significantly smaller than the one of imidazolium salt **2.1** (108.5º). This decrease in the carbonic angle is in agreement with theoretical studies on the singlet ($^1$A') carbenes bearing π-donor substituents (nitrogens). Second, The length of the N–$C_{carbene}$ bonds (137 pm) are significantly longer than the ones in the corresponding imidazolium salt **2.1** (132 pm). This suggests a diminished π-delocalization in carbene **2.2** compared to the salt **2.1**. Additionally, in the $^{13}$C NMR spectrum of carbene **2.2**, the carbene carbon appears at 211.4 ppm as a singlet, much more downfield than the one in **2.1**, which indicates its relative electron deficiency.

The overall electronic and steric effects of carbene **2.2** are responsible for its remarkable stability. As demonstrated in Scheme 2.2.1b, the two sterically hindered adamantyl groups protect the carbene center from a variety of reactions including dimerization of carbenes. In addition, the electronic factors are also believed as important ones for the carbene stability. As shown in the Scheme 2.2.1c, the lone pair electrons in the nitrogen *p* orbital are able to partially hyperconjugate into the empty *p* orbital of the carbene carbon. In the meanwhile, the two adjacent nitrogens can withdraw the electron density from the occupied s$p^2$ orbital of the carbene carbon through the two σ bonds, and/or the electrons in the occupied *p* orbital of the carbene carbon can hyperconjugate into the σ∗ orbitals of the C–N bonds. Because of these π-electron donating and σ-electron withdrawing effect. The N-heterocyclic carbene is stabilized as the singlet state ($^1$A'). These unique electronic properties of an NHC reveal itself as a strong σ donor and weak π acceptor.

**Scheme 2.2.1. The first isolated N-heterocyclic carbene**

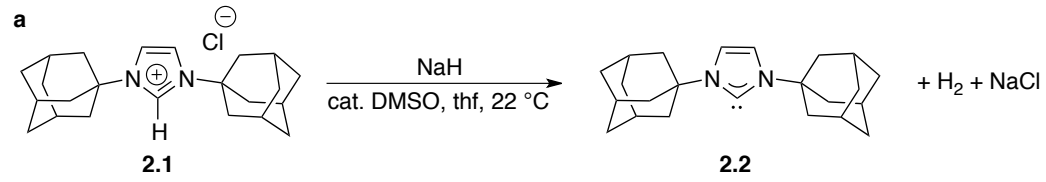


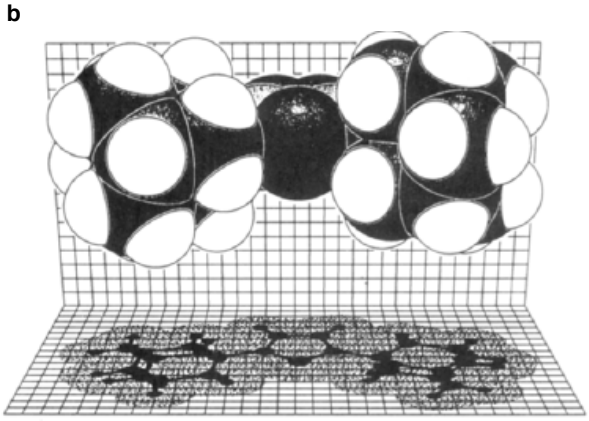


X-ray structure of **2.2**

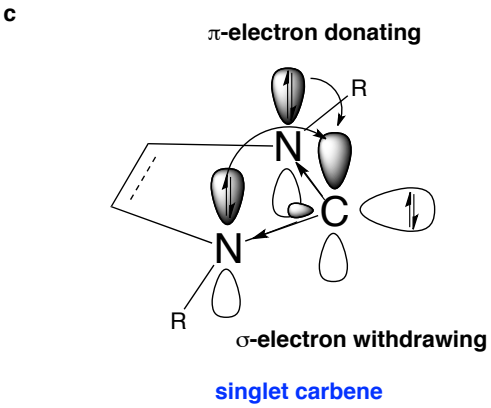


The major applications of NHCs may be divided into four categories: (1) use of an NHC to coordinate into a main-group element. (2) use of an NHC to coordinate into a transition-metal. (3) use of an NHC to interact with a carbonyl compound. (4) use of an NHC as a Brønsted base. The first and second applications will be demonstrated in the next sections of this chapter and chapter 4, respectively. Here, a brief introduction of the third and fourth applications will be demonstrated.

The application of an NHC with carbonyl compounds began with the mechanistic studies of the thiamine action by Ronald Breslow in late 1950s. Thiamine, or vitamin $B_1$, is a naturally occurred NHC bearing a thiazole core. As depicted in Scheme 2.2.2a, it has two forms: the inactive thiazolium form and the active NHC form. Its phosphate derivatives are involved in many cellular processes including transketolation and decarboxylation. Inadequate consumption of thiamine results in neurological diseases

such as *beriberi*. For example, the structure of the thiamine diphosphate residue in *Saccharomyces cerevisiae* transketolase is shown in Scheme 2.2.2b.[78] In organic chemistry, it is known to catalyze benzoin condensation (behave similarly as $CN^-$ anion).

**Scheme 2.2.2. Thiamine and its derivatives**

**a**

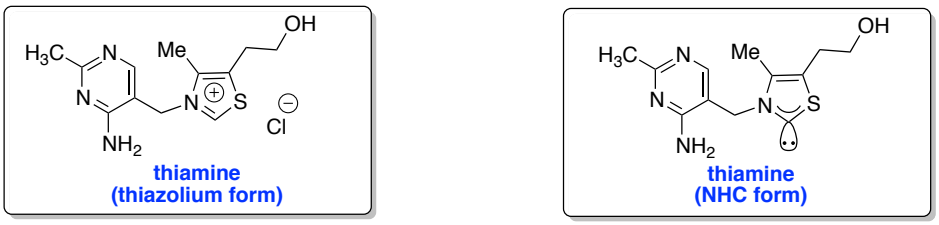


**b**

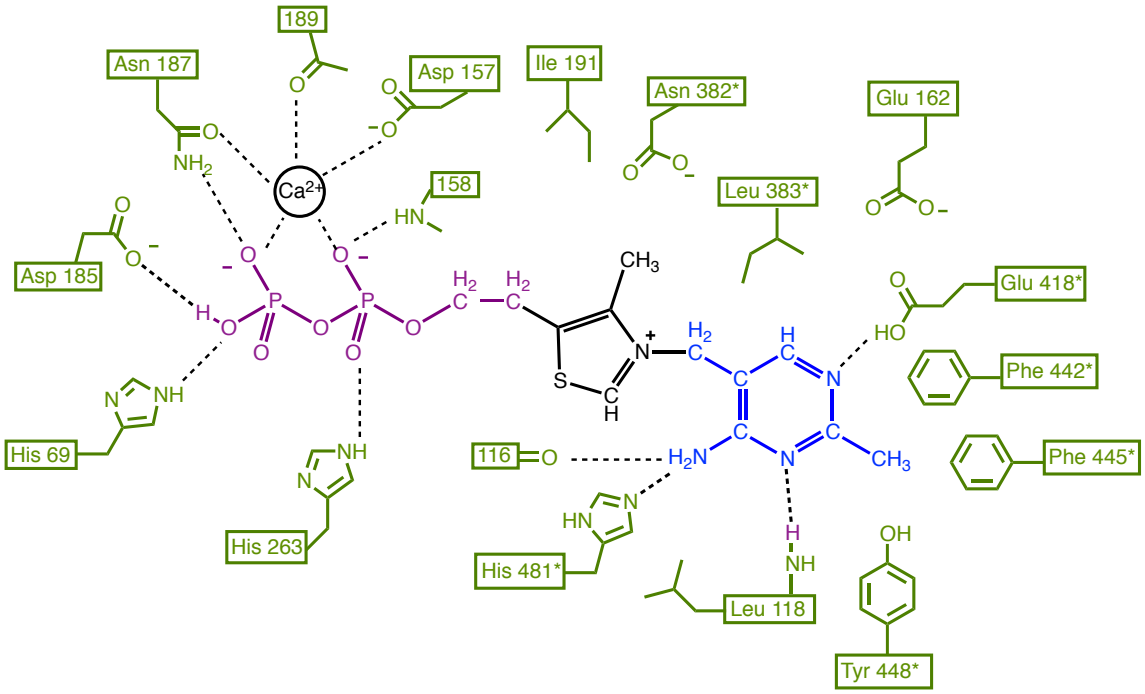


**Thiamine Diphosphate in *Saccharomyces cerevisiae* transketolase**

In 1956–1958, Breslow proposed the mechanism of thiamine catalyzed benzoin condensation based on studies on model systems.[79] Unlike the previous proposals, including the formation of a Schiff base by the amine group by Langenbeck, or an

(78) Lindqvist, Y.; Schneider, G.; Ermler, U.; Sundström, M. *EMBO*, **1992**, *11*, 2373–2379.

(79) (a) Breslow, R. *Chemistry & Industry,* **1956**, 28. (b) Breslow, R. *J. Am. Chem. Soc.* **1957**, *79*, 1762. (c) Breslow, R. *Chemistry & Industry,* **1957**, 893. (d) Breslow, R. *J. Am. Chem. Soc.* **1958**, *80*, 3719–3726.

opening of the thiazole ring during the reaction by Karrer, Breslow believed the thiazole core of thiamine forms a "zwitterion" during the reaction (this zwitterion is later believed to be the carbene form of thiamine). His proposed mechanism was demonstrated in Scheme 2.2.3a.

**Scheme 2.2.3. Breslow-intermediates in Benzoin condensations and Stetter reactions**

**a. Benzoin condensation**

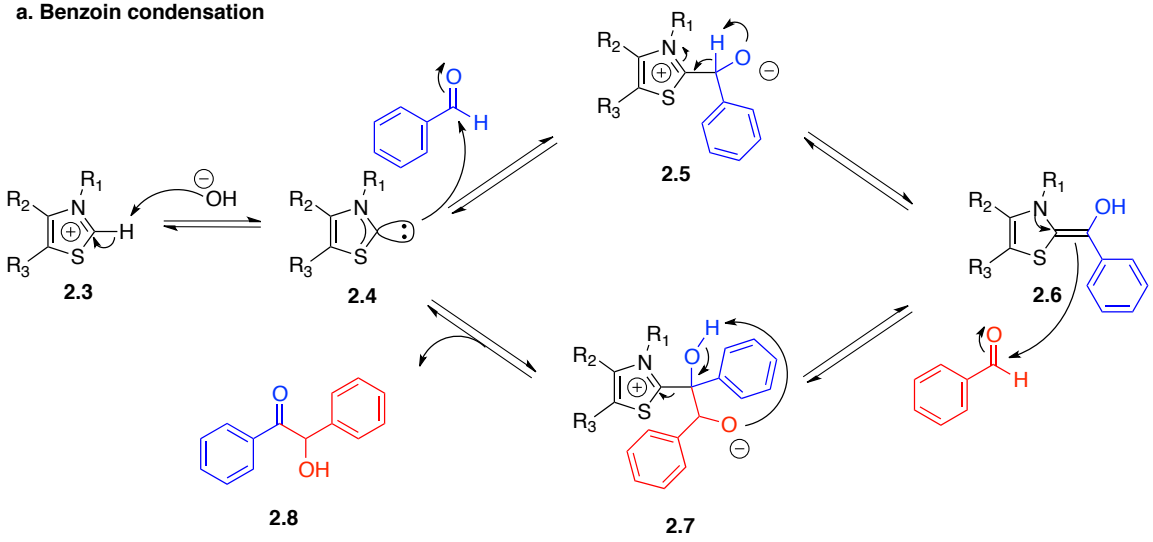


**b. Stetter reaction**

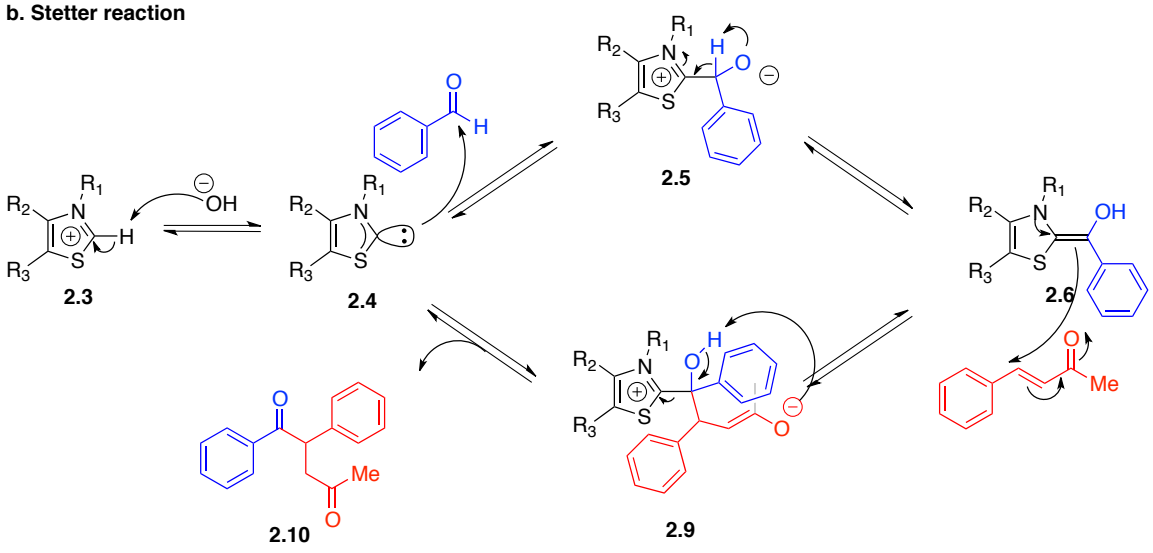


The reaction begins with the deprotonation of the thiazole in thiamine **2.3**, which forms carbene **2.4** (the "zwitterion" original suggested by Breslow). Due to the strong

σ donor ability of the carbene carbon, **2.4** can react with benzaldehyde to form intermediate **2.5**. After proton transfer and electron re-distribution, intermediate **2.6** is generated. This so-called "active aldehyde" by Breslow was later recognized as the "Breslow intermediate". It turns out the enol olefin of **2.6** is highly polarized towards the α carbon, thus it can further react with another molecule of aldehyde to form **2.7**. After proton transfer and release of the NHC, benzoin **2.8** can be generated.

Breslow's studies are of great importance because they suggested an electrophilic carbonyl carbon of an aldehyde could be inverted (that is, "umpolung") as a transient nucleophile after interacting with an NHC. The filed of NHC-catalyzed umpolung chemistry has grown rapidly over the last decades. One of the many important examples is Stetter reaction, as depicted in Scheme 2.2.3b.[80] They have utilized the Breslow intermediate to promote conjugate additions with a variety of α,β-unsaturated carbonyl compounds, forming 1,4-dicarbonyl products (**2.10** as an example).

A summary of other representative reactions involving Breslow intermediates is shown in Scheme 2.2.4.[75] If substituent $R_1$ contains an α leaving group, the Breslow intermediate will be converted into **2.11** through an elimination process, which can further react with another nucleophile to form azolium substitution product **2.13.** Otherwise, deprotonation of **2.11** will give enolate **2.12**, which proves to be a good dienophile for Diels-Alder reactions. When substituent $R_1$ is an alkene, the corresponding Breslow intermediate **2.15** can react with an aldehyde/ketone/imine to generate lactones/lactams. In these reactions, the nucleophilic site is the γ-carbon of **2.15**, which

(80) Stetter, H.; Kuhlmann, H. *Angew. Chem. Int. Ed.* **1974,** *13*, 539.

initiates 1,2-addition/condensation process. Alternatively, if the electrophile is an α,β-unsaturated carbonyl, a cyclopentene will form, releasing one equivalent of $CO_2$.

**Scheme 2.2.4. Other representative reactions with the Breslow intermediates**

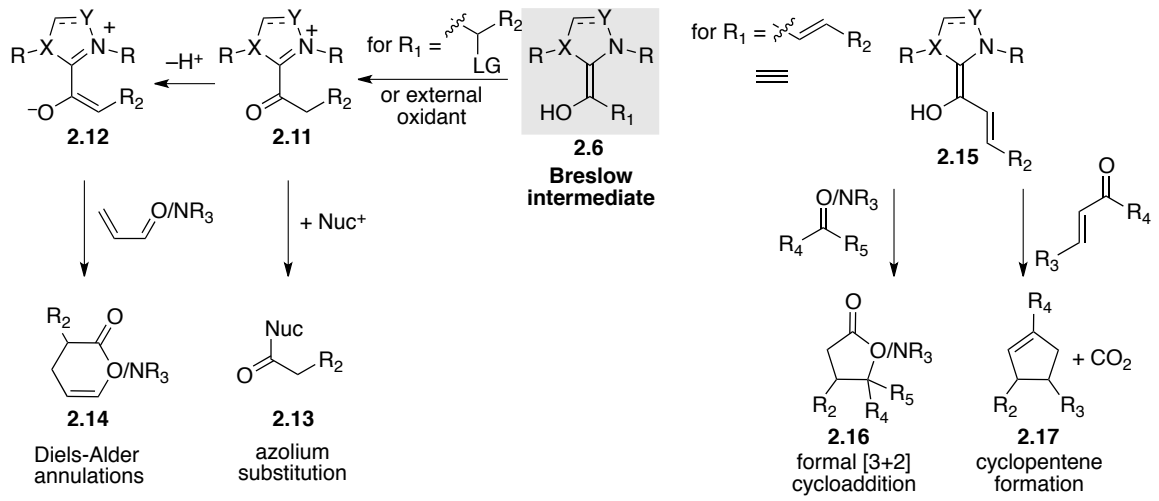


It is noteworthy that Waymouth and co-workers developed a protocol of NHC-catalyzed polymerization of lactones. Interestingly, this method can be used to synthesize gradient copolymers, which exhibit distinct physical properties from random and block copolymers. In these reactions, NHC serves as the initiator to react with the lactone, generating a zwitterionic intermediate which is believed to be the propagating species in polymerizations.[81a]

NHC can also serve as a Brønsted base catalyst. In 2010, Scheidt and co-workers established an NHC-catalyzed alcohol conjugate addition reactions (Scheme 2.2.5).[81b] Specifically, the *in situ* generated NHC is proposed to deprotonate the alcohol and thus promote the alkoxide conjugate addition with the activated enone. The imidazolium salt released can be re-deprotonated by the lithium enolate to re-generate the active NHC. Not surprisingly, the enantioselective version of this reaction is very challenging since the

(81) (a) Jeong, W.; Shin, J.; Culkin, D. A.; Hedrick, J. L.; Waymouth, R. M. *J. Am. Chem. Soc.* **2009**, *131*, 4884–4891. (b) Phillips, E. M.; Riedrich, M.; Scheidt, K. A. *J. Am. Chem. Soc.* **2010**, *132*, 13179–13181.

NHC is not intimately involved in the C–O bond formation step. The highest enantioselectivity achieved is only 55.5:44.5 er if a chiral azolium salt is used as the pre-catalyst.

**Scheme 2.2.5. NHC serves as a Brϕnsted base to catalyze alcohol conjugate additions**

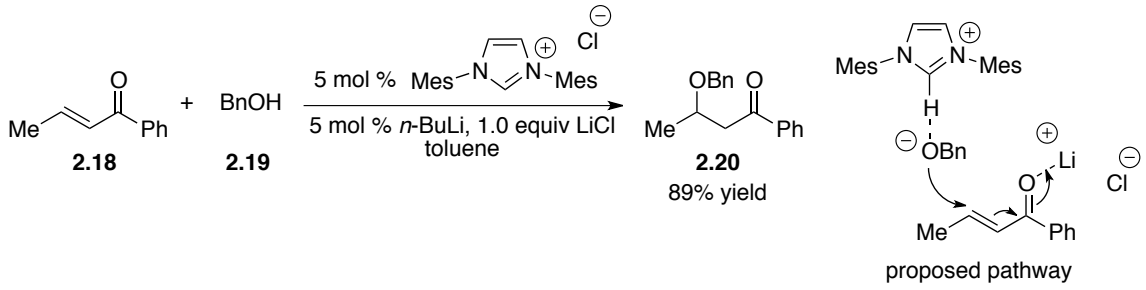


## *2.3. Lewis Base Activations of B–B Reagents and Applications to Catalytic Processes*

### *2.3.1. Early Studies*

From 1970 to 1988, a few Lewis base adducts of diboron species have been characterized as crystal structures: $(B_2H_4)(PPh_3)_2$, $B_2Cl_4(NMe_3)_2$, $B_2$(1-pyrazoly)$_4$(pyrazole)$_2$ and $BCl_2BClN(Me)\text{-}CH_2CH_2NMe_2$. The B–B bond lengths range from 1.698(4) to 1.769(6) Å.[82] In 1995, Marder, Norman and co-workers reported the X-ray crystal structures of Lewis base adducts of $B_2(OR)_4$ compounds (**2.21** and **2.22** shown in Scheme 2.3.1).[83] $B_2(cat)_2$ (B–B bond length is 1.678(3) Å) was first selected as the diboron reagent, which was treated with 1 equiv of 4-picoline in $CHCl_3$ to afford Lewis base adduct **2.21** as a pale yellow-green solid. The B–B bond length of **2.21** is 1.706(3) Å, significantly longer than that of $B_2(cat)_2$. NMR experiments suggest that the

(82) a) van Doorne, W.; Cordes, A. W.; Hunt, G. W. *Inorg. Chem.* **1973**, *12*, 1686–1689. b) Johnson, Q.; Kane, J.; Schaeffer, R. *J. Am. Chem. Soc.* **1970**, *92*, 7614–7615. c) Brock, C. P.; Das, M. K.; Minton, R. P.; Niedenzu, K. *J. Am. Chem. Soc.* **1988**, *110*, 817–822. d) Haubold, W.; Hrebicek, J.; Sawitzki, G. Z. *Naturforsch. B: Chem. Sci.* **1984**, *39*, 1027–1031.

(83) Nguyen, P.; Dai, C.; Taylor, N. J.; Power, W. P.; Marder, T. B. *Inorg. Chem.* **1995**, *34*, 4290–4291.

association of 4-picoline to $B_2(cat)_2$, and exchange of 4-picoline between the two boron atoms in **2.21** are probably fast. Interestingly, if the diboron reagent is treated with 2 equiv of 4-picoline in pentane, analytically pure bis-adduct **2.22** can be generated. The B–B bond length of **2.22** is also notably longer (1.713(4) Å) than that of $B_2(cat)_2$. Later in 1997, more Lewis base adducts of $B_2(OR)_4$ and $B_2(SR)_4$ were reported, among which 4-picoline adduct **2.23** and $PMe_2Ph$ adduct **2.24** are representative examples shown in Scheme 2.3.1.[84] Both Lewis base adducts show longer B–B bond lengths than the one in $B_2(SR)_4$ (1.673 Å), although the difference is smaller in $PMe_2Ph$ adduct **2.24** (1.689(5) Å). The elongation of B–B bond length in **2.21**–**2.24** suggests that the Lewis base activation of the diboron species weakens the B–B bond, which is crucial in the following discussion of catalytic processes.

**Scheme 2.3.1. X-ray structures of Lewis base adducts of diboron compounds**

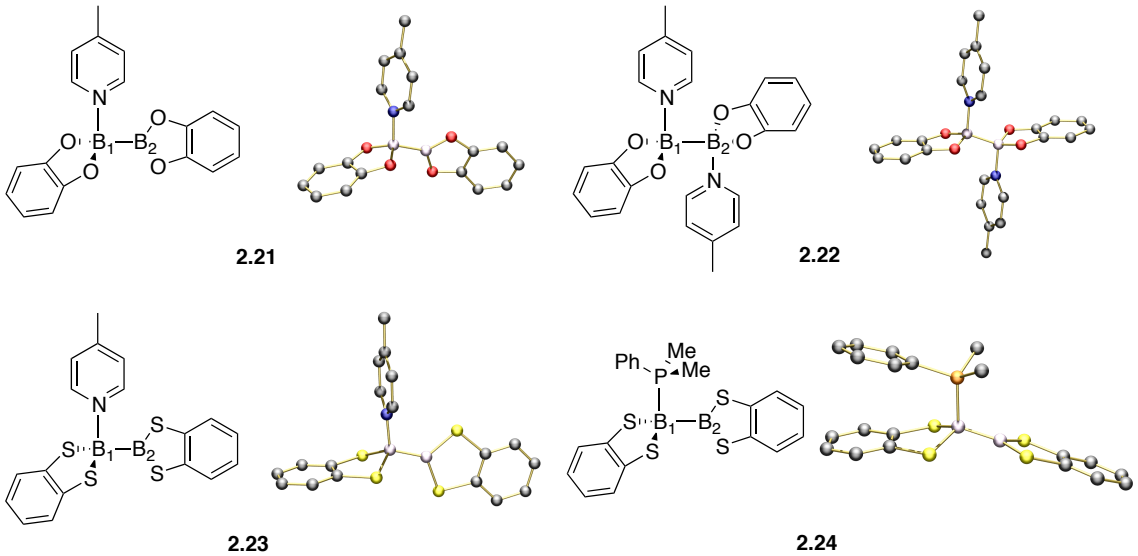


Selected bond lengths (Å): For **2.21**: B1–B2 1.706(3), For **2.22**: B1–B2 1.713(4), For **2.23**: B1–B2 1.701(7), For **2.24**: B1–B2 1.689(5).

(84) Clegg, W.; Dai, C.; Lawlor, F. J.; Marder, T. B.; Nguyen, P.; Norman, N. C.; Pickett, N. L.; Power, W. P.; Scott, A. J. *J. Chem. Soc., Dalton Trans.* **1997**, 839–846.

### *2.3.2. Reactions with Carbene-based Lewis Base Catalysts*

In 2009, our laberatories published the first Lewis base catalyzed boron conjugate additions to α,β-unsaturated ketones and esters.[10] As shown in Scheme 2.3.2, efficient transformations are promoted by 2.5–10 mol % of a simple achiral NHC, which is generated in situ by deprotonation of its commercially available imidazolium salt. Five- to eight-membered cyclic enones serve as good substrates (2.5 mol % imidazolium salt, 1 h, 89–93% yield). Enones bearing steric hindered gem-dimethyl group does not hamper the reaction (such as **2.27e**). *β*-Boryl lactone can also be obtained in high yield through the method, despite of slightly higher catalyst loading and longer reaction time. It merits mention that the achiral NHC catalyzed boron conjugate addition can also be applied in some more difficult substrates, such as steric hindered trisubstituted cyclic enones, di- or tri-substituted acyclic enones and enonates. In most cases, the reaction time is less than 24 hours and the products are obtained in ≥ 70% yield (except for **2.27j**).

In the original proposed mechanistic model (shown in Scheme 2.3.3), a Lewis basic NHC coordinates with one of the Lewis acidic boron atoms in $B_2(pin)_2$ to form NHC•$B_2(pin)_2$ complex. Due to this Lewis base activation, the B–B bond is strongly polarized toward the $sp^2$ hybridized boron center, resulting in the lower partial positive charge on the $sp^2$ hybridized boron than the $sp^3$ hybridized one (+0.777 on $sp^2$ boron vs +0.898 on $sp^3$ boron). The association of NHC to $B_2(pin)_2$ also leads to weakening of B–B bond, as evidenced by an increase in the bond length (1.749 Å in NHC•$B_2(pin)_2$ complex vs 1.703 Å in $B_2(pin)_2$). Thus, NHC•$B_2(pin)_2$ complex would react readily with an appropriate electrophile (such as an enone), release of the NHC generates a precious boron enolate that is difficult to obtain otherwise.

**Scheme 2.3.2. NHC-catalyzed boryl conjugate additions**

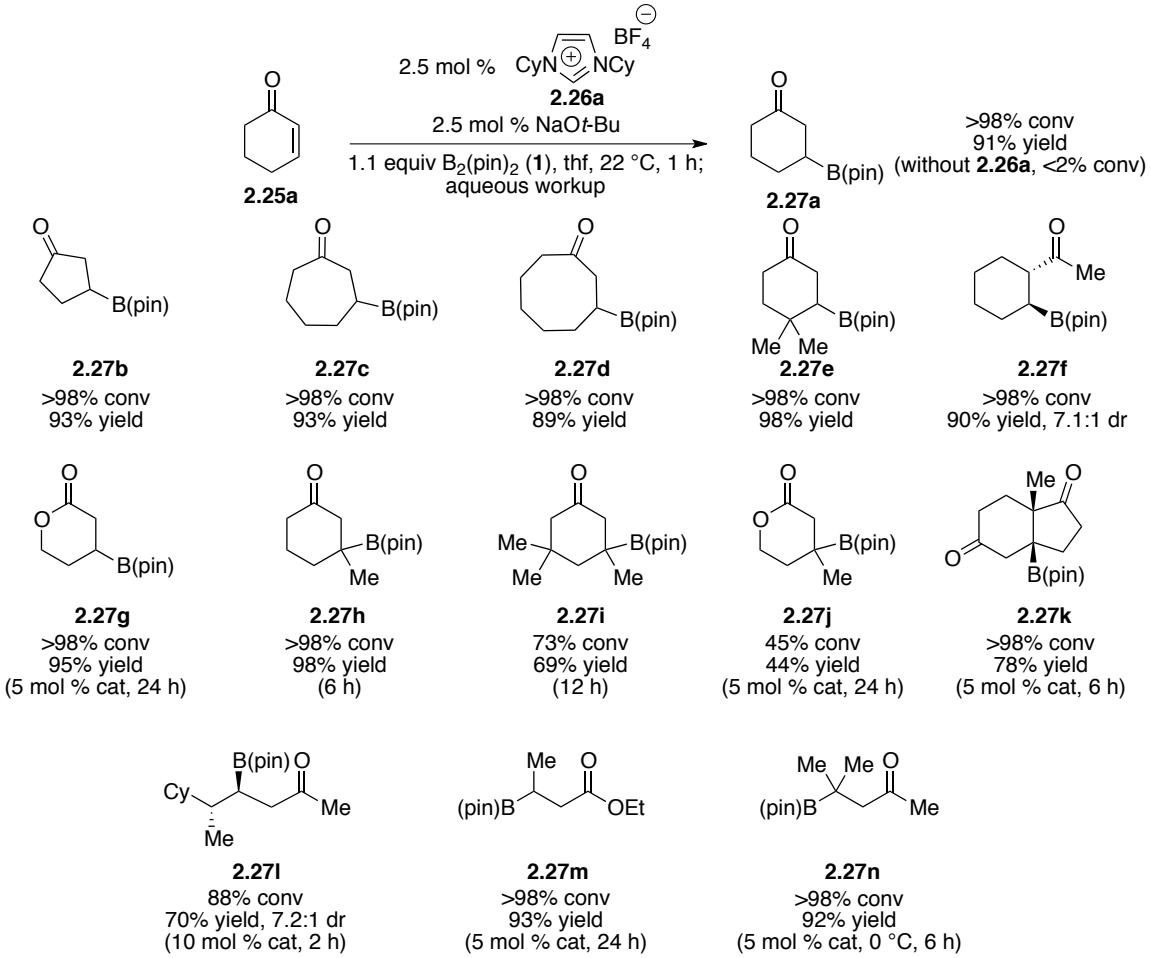


**Scheme 2.3.3. The orignial proposed mechanism**

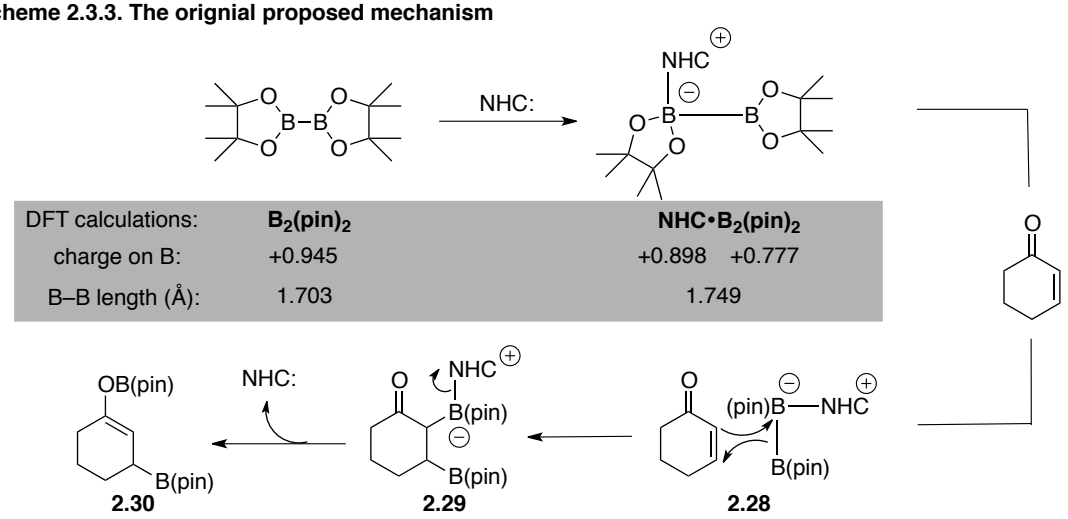

Due to its distinct mechanism, one of the many special attributes of this method is its higher functional group tolerance than the more established Cu-catalyzed variant. The reactions in Scheme 2.3.4 clearly demonstrate this advantage. As shown in Scheme 2.3.4a, although alkyne additive completely shuts down the Cu-catalyzed reaction, likely due to the more facile Cu–B(pin) addition to alkyne vs enone, NHC-catalyzed boron conjugate addition proceed effectively. In Scheme 2.3.4b, when benzaldehyde is present in the NHC-catalyzed protocol, the boron enolate reacts to form alcohol **2.32** efficiently with complete diastereoselectivity. However, in the Cu-catalyzed reaction, benzaldehyde diboration becomes competitive (19%) and only 31% of alcohol **2.32** is detected.

**Scheme 2.3.4. Functional group compatibilities of NHC-catalyzed BCA reactions**

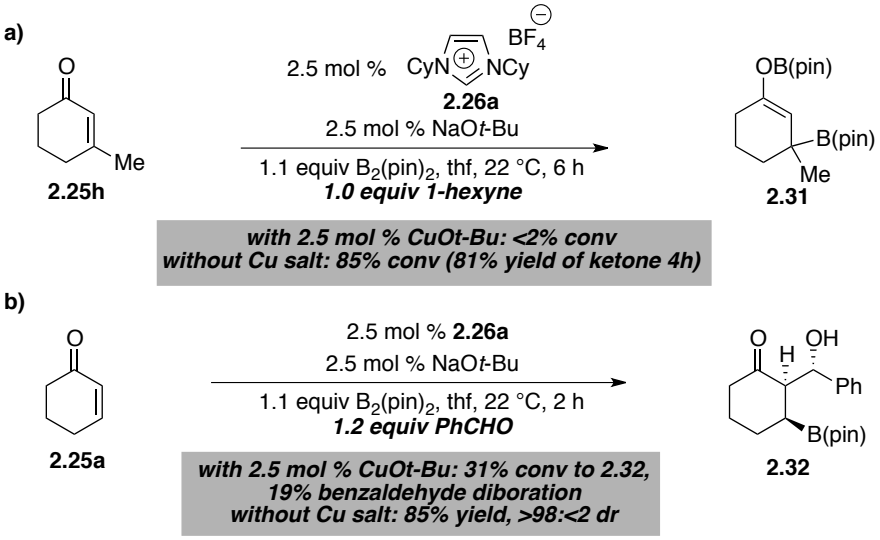


Substantial evidence of the NHC•$B_2(pin)_2$ adduct was reported in 2013. Marder, Lin and co-workers demonstrated the first isolation of the Lewis base adduct of $B_2(pin)_2$ and the NHC (1,3-bis(cyclohexyl)imidazol-2-ylidene, **2.33**), as shown in Scheme 2.3.5.[85] Lewis basic carbene **2.33** reacts with $B_2(pin)_2$ cleanly, forming intermolecular adduct

(85) Kleeberg, C.; Crawford, A. G.; Batsanov, A. S.; Hodgkinson, P.; Apperley, D. C.; Cheung, M. S.; Lin, Z.; Marder, T. B. *J. Org. Chem.* **2012**, *77*, 785–789.

**2.34**, which can be recrystallized in toluene as 1:1 solvate at –20 °C. In the crystal structure of **2.34**, the B–B bond length is 1.743 Å, which is 0.039 Å longer than the one in $B_2(pin)_2$. The $sp^3$ boron (B2) shows a distorted tetrahedral geometry, whereas $sp^2$ (B1) is virtually planar. The distance between the carbene carbon (C13) and $sp^3$ boron (B2) is 1.673 Å. The $^{11}B$ NMR of adduct **2.34** in $d_8$-thf shows two signals: 37.2 ppm (B1) and 2.4 ppm (B2), consistent with the chemical shift observed in the solid-state $^{11}B$ NMR of adduct **2.34** (36 and 2 ppm, respectively). In addition, the variable temperature $^1H$ NMR of adduct **2.34** in $d_8$-thf reveals the binding of NHC to $B_2(pin)_2$ is weak in solution and there is a rapid exchange of the NHC between the two boron centers. The corresponding DFT calculations show that the exchange happens involving dissociation and re-association of NHC rather than an intramolecular pathway.

**Scheme 2.3.5. Formation of NHC•$B_2(pin)_2$ and its X-ray crystal structure**

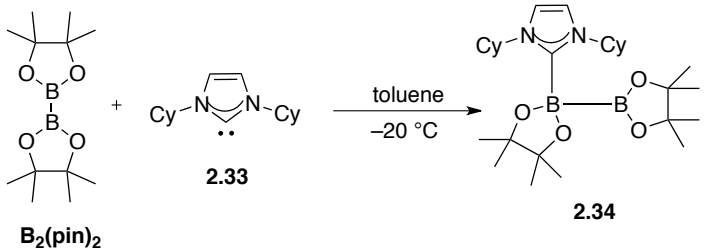


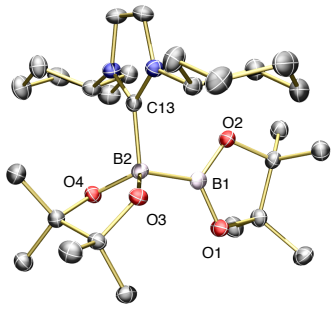


X-ray crystal structure of **2.34**

For the X-ray crystal structure: Thermal ellipsoids are drawn at the 50% probability level; hydrogen atoms and solvent are omitted for clarity. Selected bond lengths (Å) and angles (): B1–B2 1.743(2), O1–B1 1.379(2), O2–B1 1.386(2), O3–B2 1.490(2), O4–B2 1.483(2), C13–B2 1.673(2), O3–B2–O4 104.6(1), O3–B2–C13 107.6(1), O4–B2–C13 111.7(1), O3–B2–B1 116.6(1), O4–B2–B1 111.1(1), C13–B2–B1 105.4(1).

Besides NHC•$B_2(pin)_2$ adduct, Braunschweig and co-workers reported an intriguing NHC adduct of dihalodiborane **2.37** in 2011 by treatment of dichlorodiborane **2.35** with NHC **2.36** in toluene (shown in Scheme 2.3.6).[86] This result is surprising

(86) a) Bissinger, P.; Braunschweig, H. ; Damme, A.; Dewhurst, R. D.; Kupfer, T.; Radacki, K.; Wagner, K. *J. Am. Chem. Soc.* **2011**, *133*, 19044–19047. For a related report on phosphine adducts of 1,2-

because the chlorine and the mesityl substituent exchange with each other. Although the mechanism of this transhalogenation is not fully understood, it has been reported that similar processes are observed by treatment of various 1,2-dichloro-1,2-diaryldiboranes with LiF.[87] In the crystal structure of adduct **2.37**, the B–B bond length is 1.774 Å, significantly longer than the B–B bond in **2.35** (1.681 Å). Reduction of NHC adduct **2.37** with 2 equiv of $KC_8$ generates a new NHC adduct **2.39** (shown in Scheme 2.3.7). It is proposed that the borylene **2.38** forms first, followed by C–H insertion. One of the interesting features about NHC adduct **2.39** is the boron-bound hydrogen, which is strongly distorted toward the second boron atom [$B_1$–$H_1$ 1.25(2) Å, $B_2$–$H_1$ 1.51(2) Å].

**Scheme 2.3.6. Synthesis of NHC adduct of 1,1-dichlorodiborane and its X-ray crystal structure**

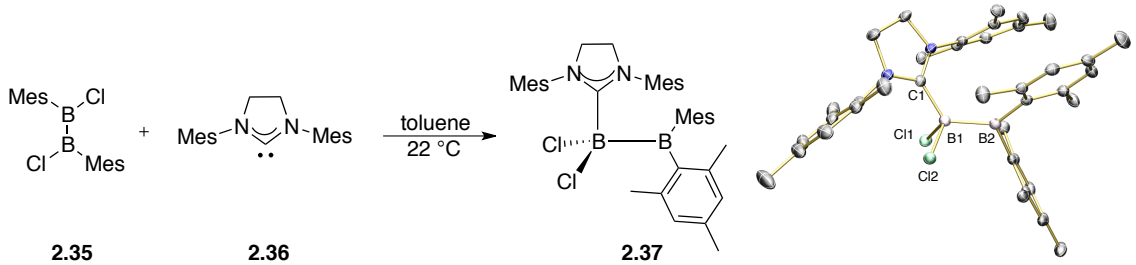


**2.35** **2.36** **2.37**

X-ray crystal structure of **2.37**

Thermal ellipsoids are drawn at the 50% probability level; hydrogen atoms are omitted for clarity. Selected bond lengths (Å) and angles (°): B1–B2 1.774(3), B1–C1 1.653(2), B1–Cl1 1.889(2), B1–Cl2 1.906(2), $\Sigma\angle_{B2}$ 359.4, B2–B1–Cl1 112.5(2), B2–B1–Cl2 101.2(1), B2–B1–C1 124.2(2).

dibromodiborane, see: b) Braunschweig, H.; Damme, A.; Jimenez-Halla, J. O. C.; Kupfer, T.; Radacki, K. *Angew. Chem. Int. Ed.* **2012**, *51*, 6267–6271.

(87) Höfner, A.; Ziegler, B.; Hunold, R.; Willershausen, P.; Massa, W.; Berndt, A. *Angew. Chem. Int. Ed.* **1991**, *30*, 594–596.

**Scheme 2.3.7 Reduction of adduct 2.37 and proposed mechanism for the formation of 2.39**

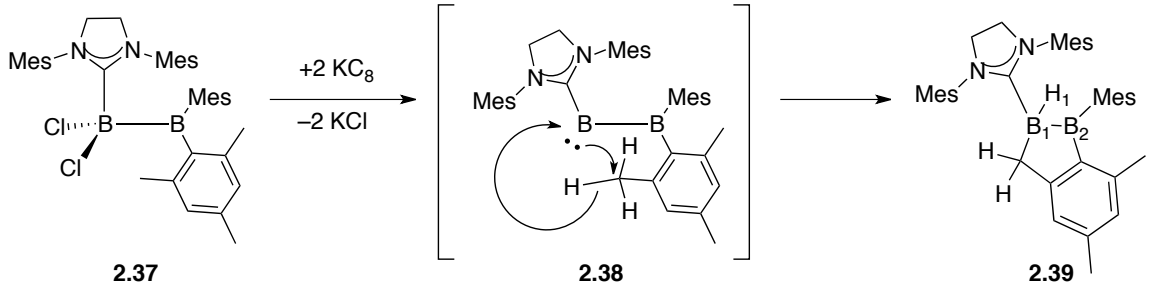


NHC•diboron adduct has also been well characterized by $^{11}B$ DQF-*J*-resolved solid-state NMR experiment (Scheme 2.3.8).[88] According to Bryce and co-workers' report in 2013, the $sp^2$ and $sp^3$ boron centers of NHC adduct **2.42** are well resolved and split by *J* ($^{11}B$,$^{11}B$) coupling of 106.8 ± 0.4 Hz. This *J* coupling is notably smaller than the one in $B_2(cat)_2$ **2.40** [*J*($^{11}B$,$^{11}B$ of **2.40**) = 136 ± 1 Hz], which quantitatively demonstrates the weakening of the B–B bond.

**Scheme 2.3.8. Synthesis and *J* ($^{11}B$,$^{11}B$) coupling of $B_2(cat)_2$ (2.40) and its NHC adduct 2.42**

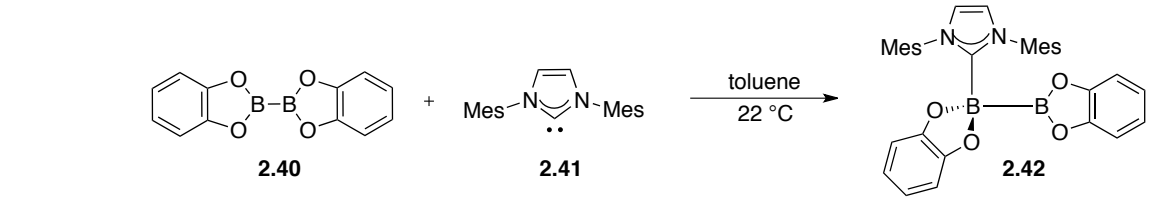


| *J* ($^{11}B$,$^{11}B$) coupling | 136 ± 1 Hz | 106.8 ± 0.4 Hz |
|---|---|---|

In 2013, our laboratories published the first broadly applicable Lewis base-catalyzed enantioselective boron conjugate additions to α,β-unsaturated carbonyls.[55] As illustrated in Scheme 2.3.9, the reactions perform in the presence of 2.5–7.5 mol % $C_1$-symmetric NHC, which is generated in situ from deprotonation of the corresponding chiral imidazolinium salt by 1,8-diazabicyclo[5.4.0]undec-7-ene (dbu). In contrast to the achiral NHC-catalyzed boron conjugate addition previously mentioned (Scheme 2.3.2),

(88) Perras, F. A.; Bryce, D. L. *J. Am. Chem. Soc.* **2013**, *135*, 12596–12599.

methanol is required for efficiency of the reaction (without methanol, <5% conv). Initial mechanistic studies aimed at elucidating the exact nature of the catalytically active species indicate that in the reaction catalyzed by a chiral NHC, less sterically demanding diboron species are likely formed by the exchange of a pinacol group of $B_2(pin)_2$ with methanol. The chiral NHC can interact with these diboron compounds to form the NHC•diboron complexes and facilitate the boron conjugate reaction. Details of studies will be illustrated in the next section.

α,β-Unsaturated ketones (**2.44a**–**h**), esters (**2.44i**, **2.44j**) and Weinreib amides (**2.44k**, **2.44l**) serve as suitable substrates in enantioselective boron conjugate additions, although in certain cases, higher loading of catalyst (7.5 mol % NHC), base (100 mol % dbu) and/or reaction temperature (50 or 66 °C) are necessary for high conversions. Nevertheless, the enantioselectivities are generally high (≥ 93:7 er) except for sterically hindered **2.45b** (85.5:14.5 er). It should be noted that NHC-catalyzed enantioselective boron conjugate additions of α,β-unsaturated alkyl aldehydes are also efficient, chemoselective and enantioselective (**2.45m**, **2.45n**), while the more established Cu-variants generally afford the desired product in lower yield due to competitive Cu–B addition to aldehyde carbonyl. Unfortunately, boron conjugate additions to cyclic enones are less enantioselective and require the use of a more sterically congested imidazolinium salt **2.46**.

**Scheme 2.3.9. NHC-catalyzed enantioselective boron conjugate additions to α,β-unsaturated ketones, esters, amides and aldehydes**

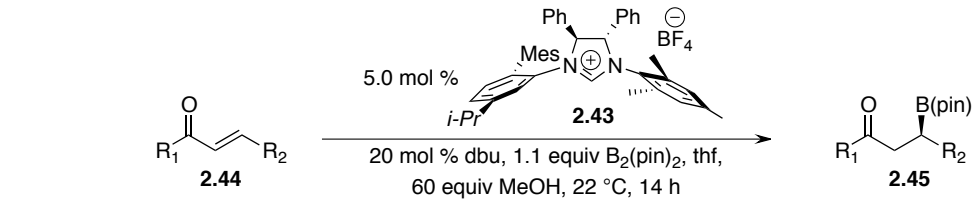


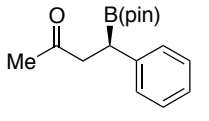

**2.45a**
>98% conv
92% yield
96:4 er

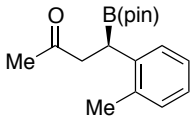

**2.45b**
95% conv
90% yield
85.5:14.5 er
(50 °C)

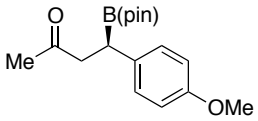

**2.45c**
90% conv
80% yield
94:6 er
(2.5 mol % **2.43**, 10 mol % dbu)

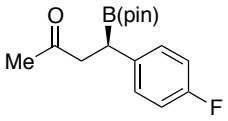

**2.45d**
>98% conv
91% yield
>98:2 er
(100 mol % dbu)

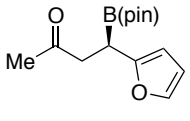

**2.45e**
>98% conv
82% yield
94:6 er
(100 mol % dbu)

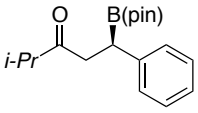

**2.45f**
94% conv
90% yield
90:10 er
(7.5 mol % **2.43**, 30 mol % dbu)

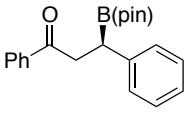

**2.45g**
>98% conv
80% yield
93.5:6.5 er
(100 mol % dbu)

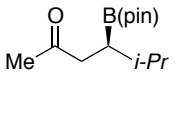

**2.45h**
>98% conv
93% yield
94:6 er

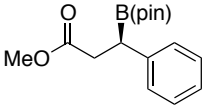

**2.45i**
>98% conv
87% yield
98:2 er

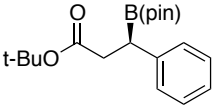

**2.45j**
88% conv
80% yield
98:2 er
(50 °C)

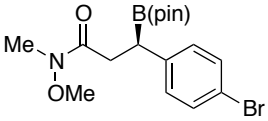

**2.45k**
>98% conv
70% yield
94:6 er
(7.5 mol % **2.43**, 30 mol % dbu, 30 equiv MeOH, 50 °C,10 h)

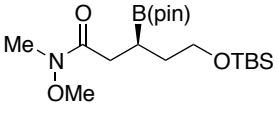

**2.45l**
96% conv
92% yield
93:7 er
(7.5 mol % **2.43**, 30 mol % dbu, 66 °C, 24 h)

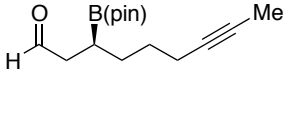

**2.45m**
91% conv
71% yield
95:5 er

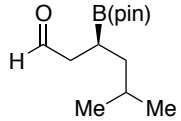

**2.45n**
95% conv
63% yield
94:6 er

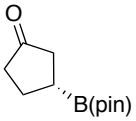

**2.45o**
90% conv
80% yield
92:8 er
(**2.46** used instead)

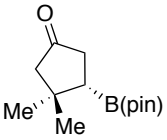

**2.45p**
98% conv
94% yield
85:15 er
(**2.46** used instead)

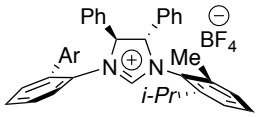


Ar = 2,4,6-(*i*-Pr)$_3$C$_6$H$_2$
**2.46**

The higher functional group tolerance of NHC-catalyzed method (vs Cu-catalyzed variants) was further illustrated in Scheme 2.3.10: while significant side reactions occur (or slower conjugate addition) in the presence of the Cu catalyst, the NHC-catalyzed reactions afford the desired *β*-boryl carbonyls with high efficiency and selectivity.

**Scheme 2.3.10. Functional group tolerance: differences between NHC- and Cu-catalyzed protocols.**

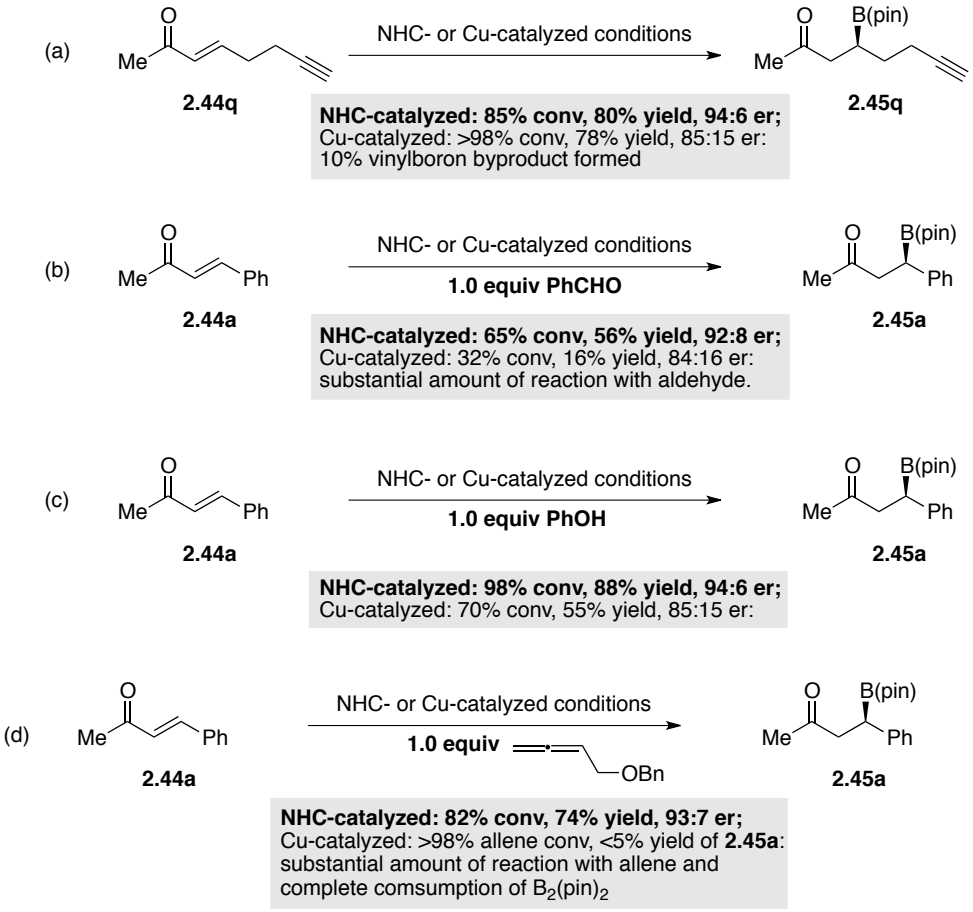


Reactions (a) and (c): 5.0 mol % **2.43**, 20 mol % dbu, 1.1 equiv of $B_2(pin)_2$, thf, 60 equiv of MeOH, 22 °C, 14 h; reactions (b) and (d): 7.5 mol % **2.43**, 30 mol % dbu, 1.1 equiv of $B_2(pin)_2$, thf, 60 equiv of MeOH, 50 °C, 14 h. Cu-catalyzed conditions: Reactions (a) and (c): 5.0 mol % Josiphos, 5.0 mol % CuCl, 5.0 mol % NaO*t*-Bu, 1.1 equiv of $B_2(pin)_2$, thf, 1.0 equiv of MeOH, 22 °C, 14 h; reactions (b) and (d): 7.5 mol % Josiphos, 7.5 mol % CuCl, 7.5 mol % NaO*t*-Bu, 1.1 equiv of $B_2(pin)_2$, thf, 1.0 equiv of MeOH, 50 °C, 14 h.

The related NHC-catalyzed enantioselective boron conjugate additions to $\beta$-substituted cyclic and acyclic enones were disclosed in 2014 by our laboratories.[60] It is also the first Lewis base-catalyzed enantioselective reactions that furnish products with boron-substituted quaternary carbon stereogenic centers. As shown in Scheme 2.3.11, reactions with $\beta$-substituted cyclic enones are efficient and highly enantioselective (generally higher than reactions with disubstituted cyclic enones). Alkyne as well as allene groups do not inhibit this metal-free process (**2.49b** and **2.49c**). In certain cases

(**2.49d** and **2.49e**), the catalyst loading can be lowered to 1.0 mol % while the conversions remain high. Besides substituted cyclohexenones, the enantioselective boron conjugate additions are equally efficient with five-, seven- or eight-membered ring substrates.

**Scheme 2.3.11. NHC-catalyzed enantioselective boron conjugate additions to $\beta$-substituted cyclic enones.**

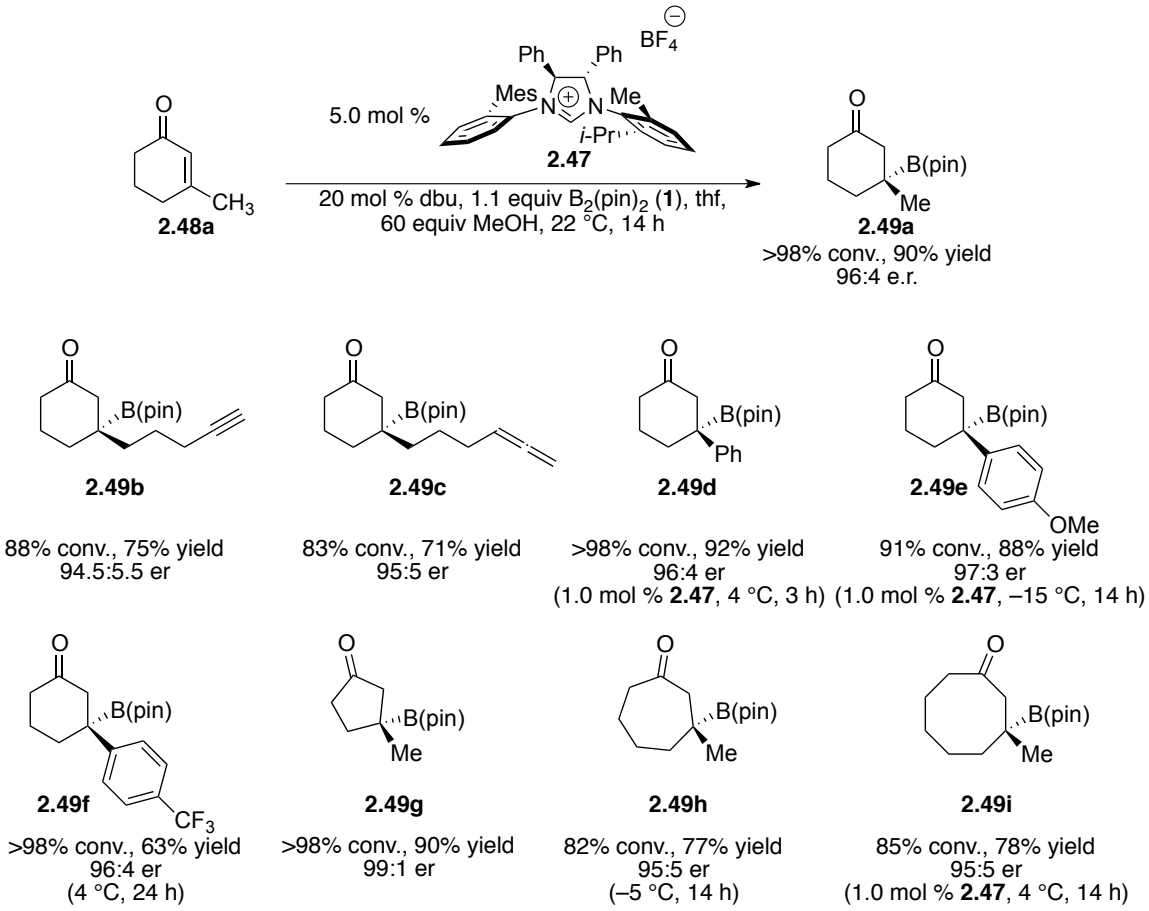


More challenging $\beta$-substituted acyclic enones do not influence high efficiency and enantioselectivity of the NHC catalyzed boron conjugate additions (Scheme 2.3.12). It should be mentioned that in some cases, simple recrystallizations deliver the desired products with exceptional enantioselectivity (**2.52a**, **2.52b** and **2.52c**).

**Scheme 2.3.12. NHC-catalyzed enantioselective boron conjugate additions to $\beta$-substituted acyclic enones.**

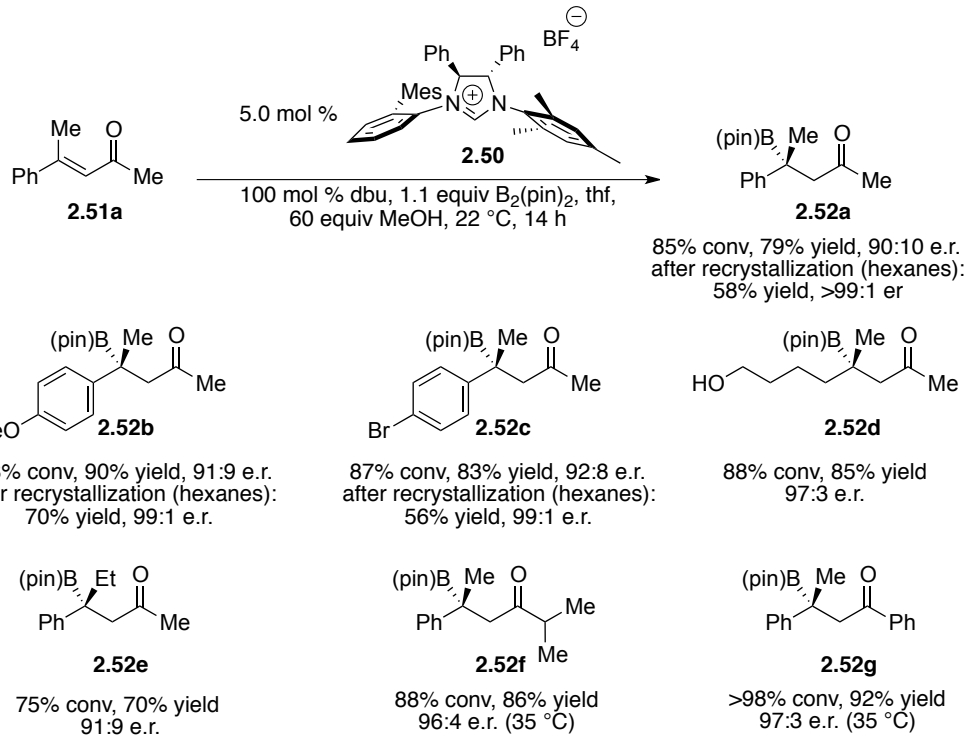


The formal synthesis of antifungal natural product (–)-crassinervic acid clearly demonstrates the advantages of the Lewis base-catalyzed protocol (Scheme 2.3.13). Even though the $\beta$-substituted enone **2.53** bears an aldehyde and phenol substituent. The desired product **2.54** is obtained in 72% yield and 95:5 e.r., in contrast to 19% yield when a previously reported diamine–Cu catalyst is used.

**Scheme 2.3.13. NHC-catalyzed enantioselective boron conjugate additions to polyfunctional enones: application to the formal synthesis of (-)-crassinervic acid.**

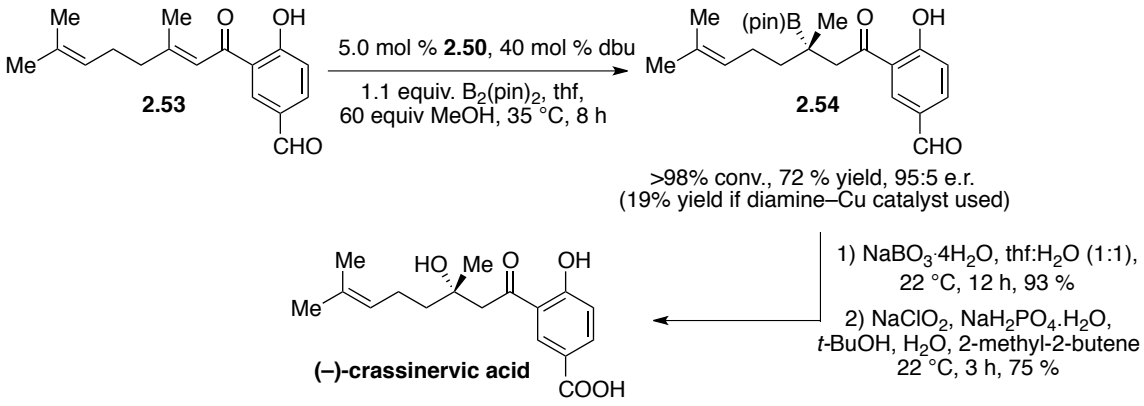


In 2012, Ibrahem, Córdova and co-workers reported an achiral NHC-catalyzed boron conjugate additions to enals and its in-situ functionalization of the corresponding aldehyde by Wittig olefination.[89] As shown in Scheme 2.3.14, the NHC derived from imidazolium salt **2.26a** is crucial for selective 1,4-addition of B(pin) unit (vs 1,2-addition to aldehyde carbonyl group): intermediates **2.56**:**2.57** = 95:5. Unfortunately, β-boryl aldehyde **2.56** cannot be isolated and Wittig olefination is used to obtain homoallylboronate **2.58** in 60% yield. One case of tri-substituted enal was also tested in this reaction and the corresponding homoallylboronate bearing a tertiary B-substituted carbon was isolated in 63% yield (not shown in the scheme). The authors also report an acceleration in reaction rate if a proline-type co-catalyst was used.

(89) Ibrahem, I.; Breistein, P.; Córdova, A. *Chem. Eur. J.* **2012**, *18*, 5175–5179.

**Scheme 2.3.14. NHC catalyzed one-pot three-component reaction for synthesis of homoallylboronates.**

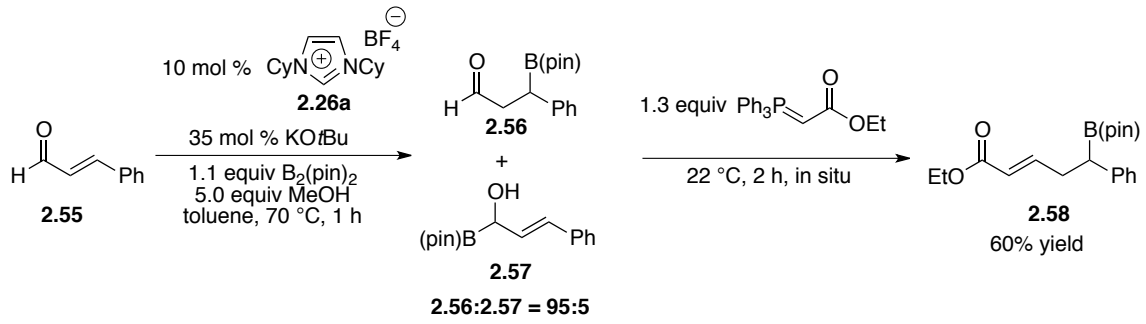


### *2.3.3. Reactions with Phosphines or Alkoxides as Lewis Base Catalysts*

In 2010, Fernández and co-workers reported the first phosphine assisted boron conjugate additions to α,β-unsaturated ketones and esters.[54a] In Scheme 2.3.15, 4–20 mol % achiral phosphine ($PPh_3$ or dppf) is used to promote the reaction at 70 ºC. The base ($Cs_2CO_3$) and alcohol (MeOH) are also essential to afford the desired product. Moderate to good conversions (54–99%) are observed with acyclic enones and enonates. One case of cyclic enones is also reported as a good substrate in the boron conjugate addition although a longer reaction time (16 h) is necessary for high conversion.

**Scheme 2.3.15. Achiral phosphine assisted boron conjugate additions to α,β-unsaturated ketones and esters.**

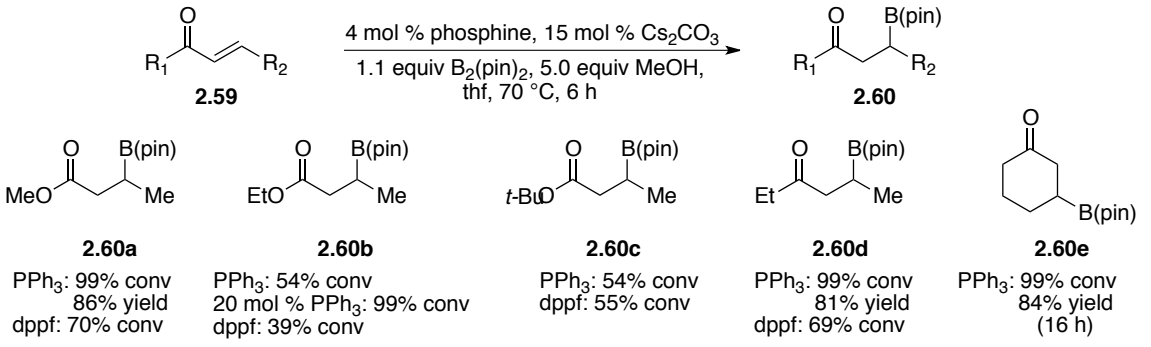


After screening a variety of chiral phosphines, (*R*)-binap or (*R*)-(*S*)-josiphos **2.61** was found to be optimal chiral additives for enantioselective boron conjugate additions. Unfortunately, the method is not general to deliver *β*-boryl carbonyls with high efficiency

and enantioselectivity (Scheme 2.3.16), except a limited number of cases (for example, **2.60a**, 99% conv, 91.5:8.5 er).

**Scheme 2.3.16. Chiral phosphine catalyzed boron conjugate additions to α,β-unsaturated ketones and esters.**

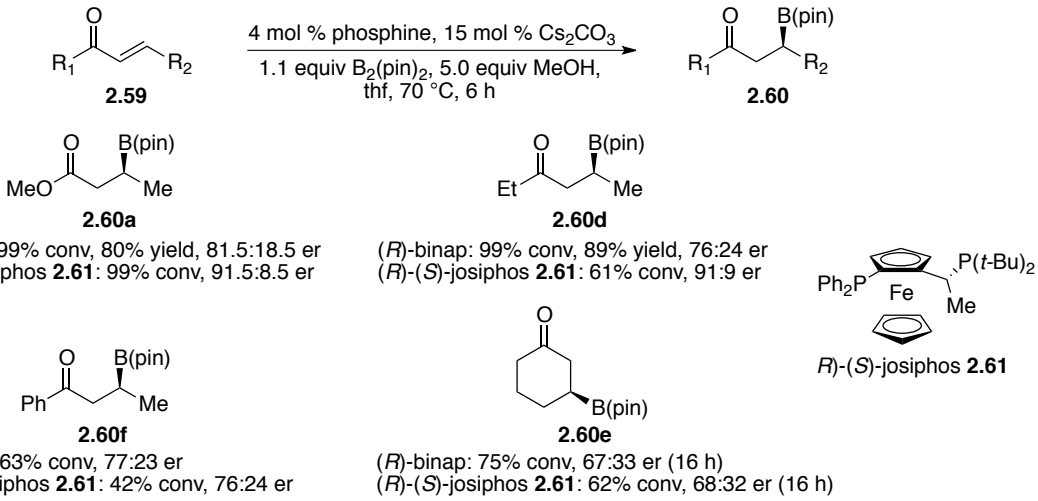


The initially proposed mechanism for this reaction is very similar to the one previously reported in 2009,[10] except a phosphine as the Lewis base catalyst instead of NHC. However, a later mechanistic study published in 2012 by the same group suggests that the original proposed mechanism may not be operative: methoxide (instead of phosphine) was believed to coordinate to $B_2(pin)_2$, while phosphine is essential for interaction with the enone substrate to form a zwitterionic phosphonium enolate.[54b] The resulting ion pair **2.62** was proposed to be the active catalytic species, as shown in Scheme 2.3.17, according to distinct $^{11}B$ NMR and $^{31}P$ NMR signals in the stoichiometric experiment. Further ESI-MS experiments also confirmed the presence of the cation part of the ion pair **2.62**.

**Scheme 2.3.17. Ion pair formation for phosphine assisted boron conjugate additions.**

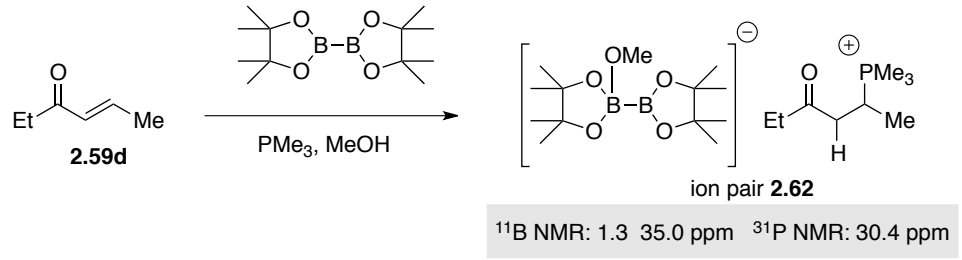


DFT calculations of the catalytic cycle were carried out subsequently. As shown in Scheme 2.3.18, $PMe_3$ reacts with substrate **2.63** in a 1,4-addition manner to form phosphonium enolate **2.64**, which can further bind to diboron•MeOH adduct through a hydrogen bond (**2.66**). Due to the methoxide activation of the diboron species in **2.66**, it reacts with α,β-unsaturated carbonyl **2.63** to deliver the $sp^2$ hybridized boron. The resulting enolate in **2.69** can be protonated to afford the desired product and regenerate the catalyst.

**Scheme 2.3.18. Proposed catalytic cycle for the phosphine assisted base-free boron conjugate addition.**

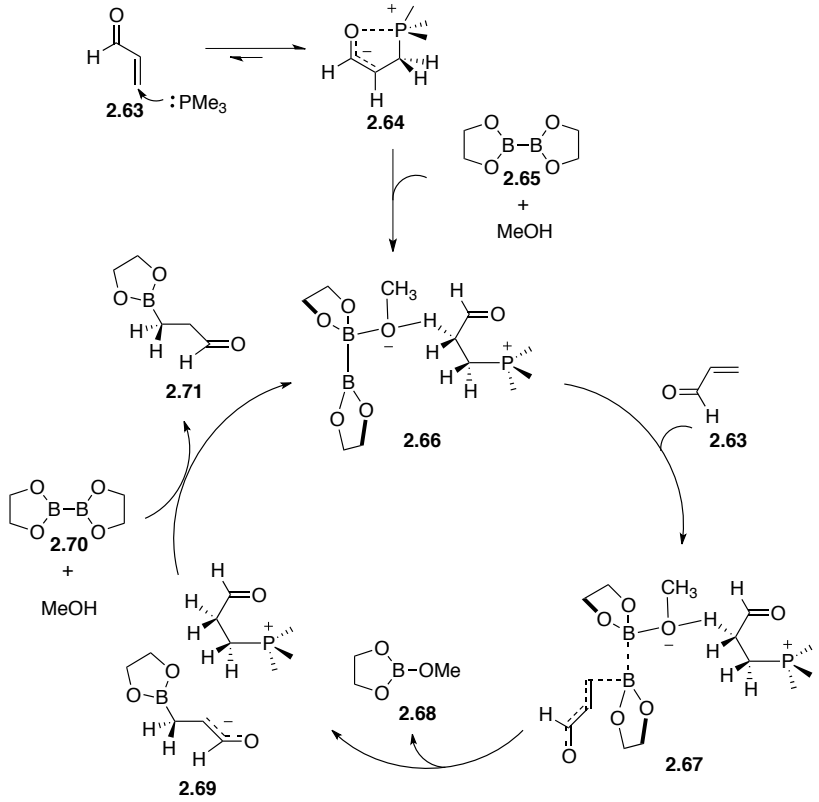


Inspired by this mechanism, Fernández and co-workers developed the phosphine assisted base-free boron conjugate additions to α,β-unsaturated carbonyls (Scheme 2.3.19). Compared to the previous method, use of Brønsted base (such as NaO*t*-Bu) and thf is not necessary and $PCy_3$ is the optimized phosphine additive. The reactions are generally more efficient than the previous reported method delivering racemic β-boryl ketones and esters, except the acyclic ones bearing a quaternary carbon center (**2.60h**).

**Scheme 2.3.19. BrΦnsted base-free phosphine assisted base-free boron conjugate additions**

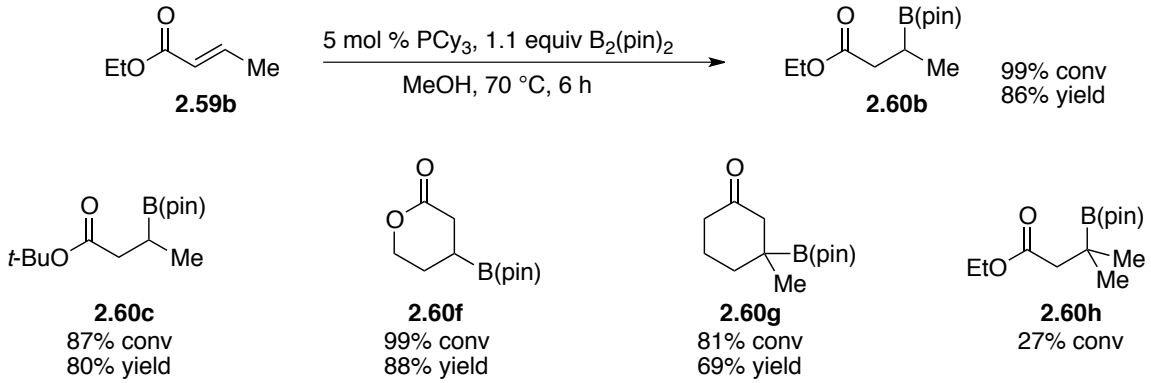


The same group also reported another methoxide catalyzed strategy for the synthesis of racemic $\beta$-boryl ketones and esters promoted by Verkade super base (**2.72**) instead of phosphine, as shown in Scheme 2.3.20.[54c] The reactions generally require a higher catalyst loading (15 mol % **2.72** vs 5 mol % phosphine) and longer reaction time (24 h vs 6 h). Besides $B_2(pin)_2$, other types of diboron reagents [such as $B_2(cat)_2$, cat = catechol] are also suitable for transfering the boron unit. This study further supports that the Lewis base catalyst of the phosphine assisted boron conjugate additions mentioned above is the methoxide anion rather than the phosphine. A detailed DFT calculation of the relative catalytic process has also been reported.

**Scheme 2.3.20. Verkade base promoted boron conjugate additions**

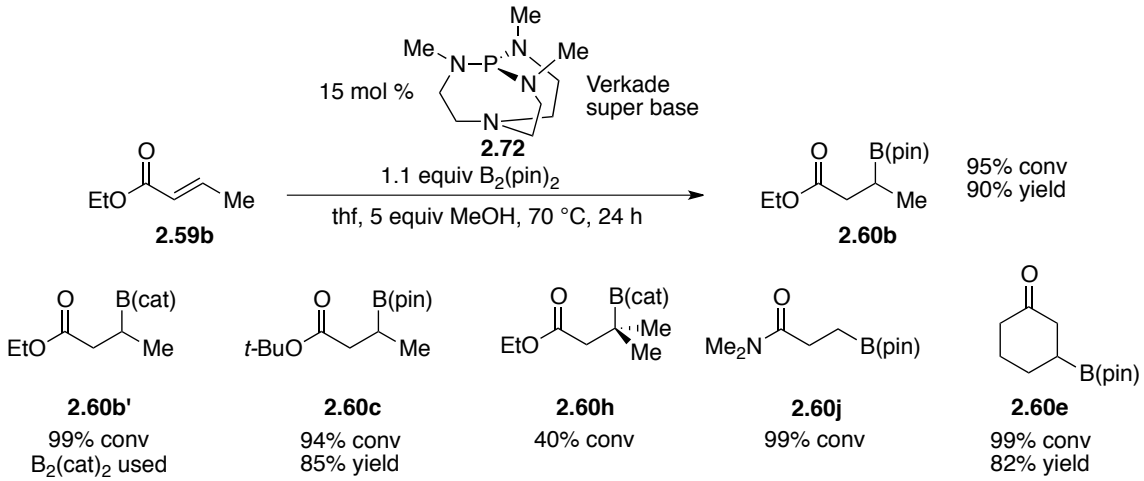


In 2011, Fernández and co-workers reported the first methoxide catalyzed diboration of non-activated alkenes.[90] Although the reaction condition is very similar to the corresponding boron conjugate additions mentioned previously (base, alcohol and diboron reagent), the materials delivered are diboron compounds instead of monoboron ones (<5%). As shown in Scheme 2.3.21, alkyl substituted alkenes as well as one example of allene are reported to be efficient substrates. Besides $B_2(pin)_2$, the authors also demonstrate other diboron reagents [such as $B_2(cat)_2$] are effective. Unfortunately, the competitive "hydroboration" side reaction becomes significant when styrene was used as the substrate.

(90) Bonet, A., Pubill-Ulldemolins, C.; Bo, C.; Gulyás, H.; Fernández, E. *Angew. Chem. Int. Ed.* **2011**, *50*, 7158–7161.

**Scheme 2.3.21. Alkoxide catalyzed diboration reactions with non-activated olefins**

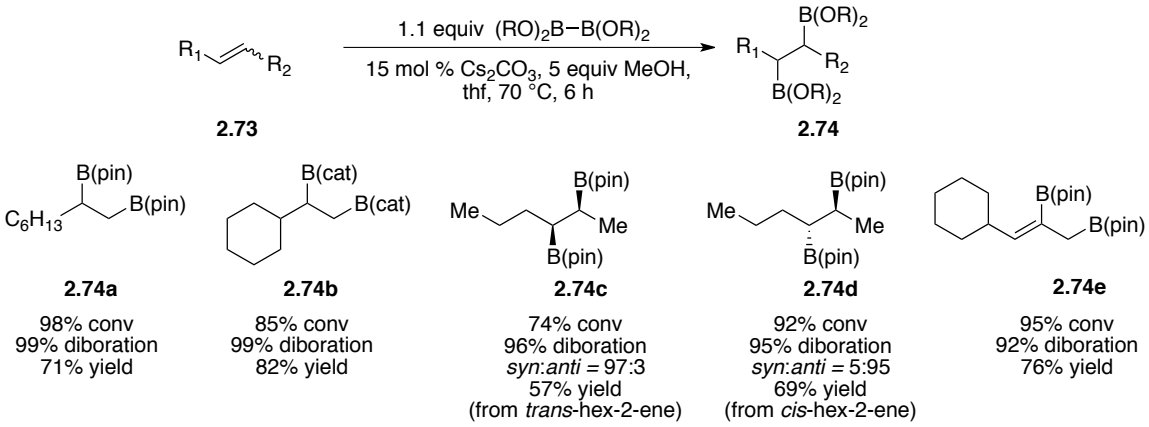


DFT calculations again show that polarization of B–B bond occurs when the methoxide anion coordinates to the diboron species, and the $sp^2$ hybridized boron gains electron density with respect to its partial positive charge in the intact $B_2(pin)_2$. Further mechanistic study, including a proposed catalytic cycle, is shown in Scheme 2.3.22. It is intriguing that the $sp^2$ boron reacts with the terminal olefin carbon initially, followed by a boron migration to form **I1**, which can be protonated to afford the "hydroboration" byproduct. However, if the nucleophilic anion in **I1** reacts with MeO–B(pin), the desired diboration product would be generated, releasing methoxide anion to further catalyze this reaction.

A series of chiral alcohols was investigated to promote enantioselective diborations of alkenes. Unfortunately, the enantiomeric ratios are not satisfying (≤ 70:30 er).[91]

(91) Bonet, A.; Sole, C.; Gulyás, H.; Fernández, E. *Org. Biomol. Chem.* **2012**, *10*, 6621–6623.

**Scheme 2.3.22. Proposed mechanism and the supporting calculations**

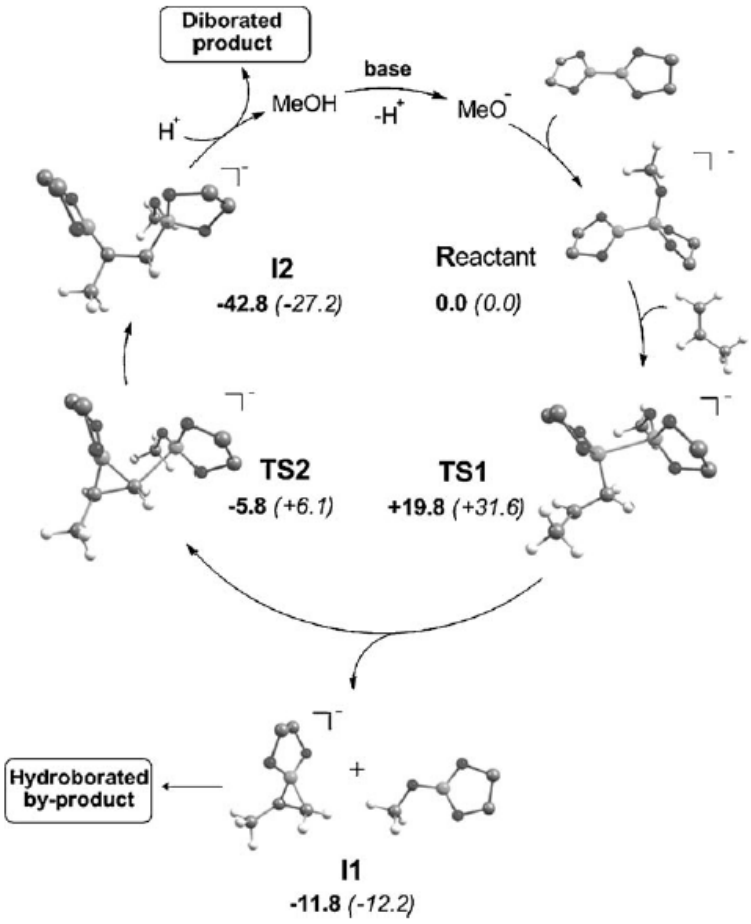


Electronic energy (kcalmol$^{-1}$) and Gibbs free energy (kcalmol$^{-1}$; in parentheses) computed at the M06 level relative to $B_2(pin)_2$·MeO adduct plus propylene. Methyl groups of $B_2(pin)_2$ are omitted for clarity.

To further establish the synthetic strategy utilizing alkoxide activated diboron species, the same group reported the synthesis of α-amino boronic esters via a metal-free boron addition to tosylaldimines, as shown in Scheme 2.3.23.[92] The authors showed that both base and alcohol were necessary for efficient reaction and the phosphine additive improved the conversion (the reaction proceeds to 70% conv without $PPh_3$). A series of chiral phosphines have been tested in the reaction, among which (*R*)-(*R*)-Walphos ($CF_3$)

(92) Solé, C.; Gulyás, H.; Fernández, E. *Chem. Commun.* **2012**, *48*, 3769–3771.

promote the reaction with moderate to good enantioselectivity (62:38 er to 95:5 er).

**Scheme 2.3.23. Alkoxide catalyzed boron additions to tosylimines**

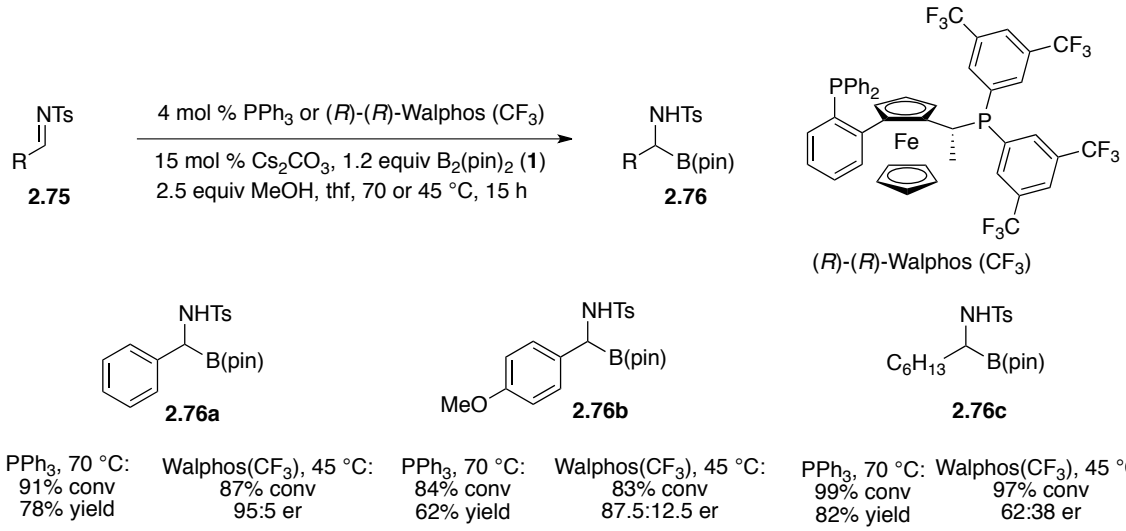


### *2.3.4. Reactions Promoted by Other Lewis Bases*

In 2012, Ohmura, Suginome and co-workers reported an intriguing method for 1,4-diborations of pyrazines, as shown in Scheme 2.3.24.[93] The reactions proceed without any additional base or metal and boron substituted 1,4-dihydropyrazines were isolated in 77–96% yield. The proposed mechanism involves the coordination of pyrazine nitrogen to one of the boron atoms in $B_2(pin)_2$, a subsequent nucleophilic addition of the other B(pin) unit to the C2 carbon of pyrazine and intramolecular rearrangement. The mechanism is consistent with the crystal structure of the 4-picoline•diboron adducts previously discussed.

(93) Oshima, K.; Ohmura, T.; Suginome, M. *Chem. Commun.* **2012**, *48*, 8571–8573.

**Scheme 2.3.24. 1,4-Diboration of pyrazine and a proposed mechanism**

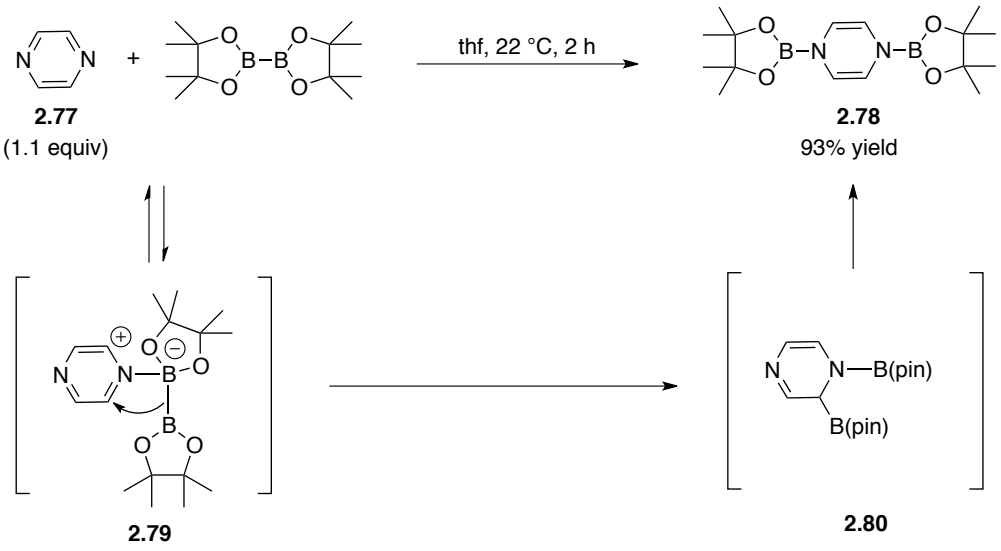


In 2013, Zhang and co-workers reported a metal-free protocol for borylation of aryl iodides.[94] The reactions are promoted by 2.0 equiv. of $Cs_2CO_3$ and methanol under refluxing condition. The desired aryl boronate can be isolated in moderate to good yields, as shown in Scheme 2.3.25. Although the mechanism of this reaction is not clear, preliminary mechanistic study shows that the reaction is neither copper catalyzed nor radical mediated.

**Scheme 2.3.25. Base mediated borylations of aryl iodides**

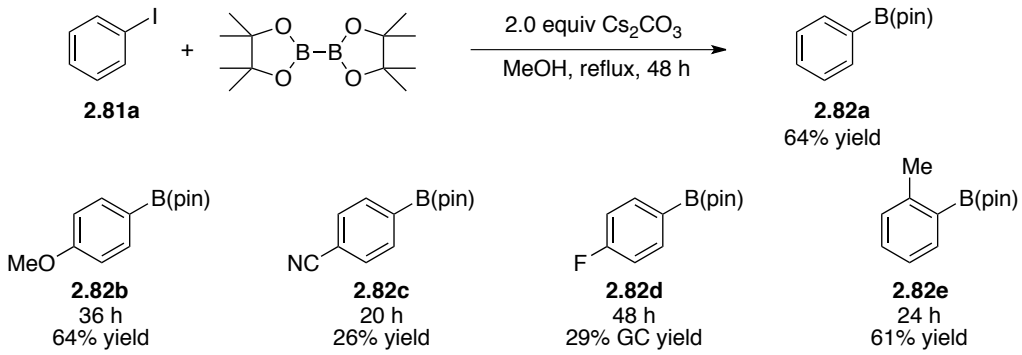


(94) Zhang, J.; Wu, H.-H.; Zhang, J. *Eur. J. Org. Chem.* **2013**, 6263–6266.

## *2.4. Lewis Base Activations of B–Si Reagents and Applications to Catalytic Processes*

### *2.4.1. Early Studies*

In 2001, Kawachi, Tamao and co-worker reported a reaction of (pin)B–$SiPh_3$ with KO*t*-Bu. The mixture of the two compounds at –78 ºC was treated with $Me_3SiCl$, leading to the formation of $Me_3Si$–$SiPh_3$ (Scheme 2.4.1).[95] Although not suggested by the authors, an alkoxide adduct of (pin)B–$SiPh_3$ **2.87** is probably responsible for the cleavage of the B–Si bond, which generates $KSiPh_3$ **2.85** that reacts with the silyl chloride reagent.

**Scheme 2.4.1. Lewis base promoted cleavage of a B–Si bond**

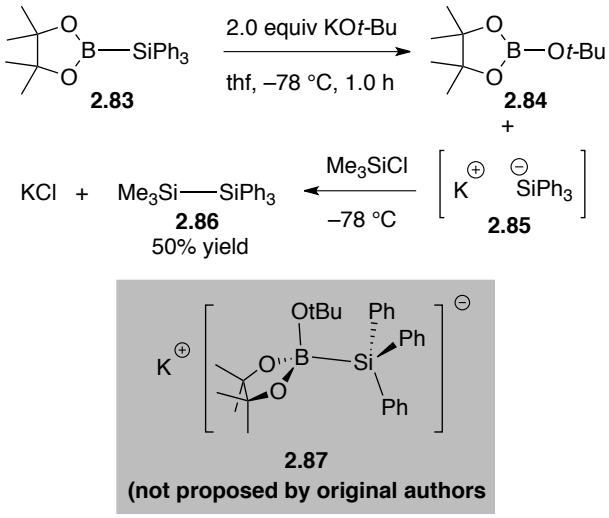


### *2.4.2. Reactions with Carbene-based Lewis Base Catalysts*

Based on the previous studies on the Lewis base activation of Si–B bond, our group explored the possibility of introducing this concept into catalysis. $^{11}B$ NMR studies indicate that the carbene generated from the deprotonation of commercially available **2.26b** is able to bind to (pin)B–$SiMe_2Ph$ (**2.88**). The chemical shift of the boron atom

(95) Kawashi, A.; Minamimoto, T.; Tamao, K. *Chem. Lett.* **2001**, 1216–1217.

shifts significantly upfield from 33.4 ppm to 8.0 ppm (thf-$d_8$; Scheme 2.4.2a). However, 30 minutes is required for the complete complexation, which is in contrast to less than five minutes needed with $B_2(pin)_2$.[10] Additionally, unlike NHC-catalyzed boryl conjugate additions, when cyclohexenone **2.25a** was subjected into the mixture of NHC and (pin)B–$SiMe_2Ph$, there was no conversion to β-silyl ketone product **2.90a** (Scheme 2.4.2b). However, if MeOH serves as co-solvent with thf; there was 34% conversion. Perhaps more strikingly, $H_2O$ serves a better proton additive than MeOH, which promotes the silyl conjugation addition (SCA) to 95% conversion to the desired product. As with the BCA reactions, phosphines are less reactive (only 30% conv with a more Lewis basic $PCy_3$). However, $Ph_3P$ and $Ph_3PO$ cannot promote any silyl conjugate addition, which could be due to their less Lewis basic natures than NHC(s).

**Scheme 2.4.2 Initial studies on NHC catalyzed silyl conjugate additions**

a) Initial spectroscopic observation:

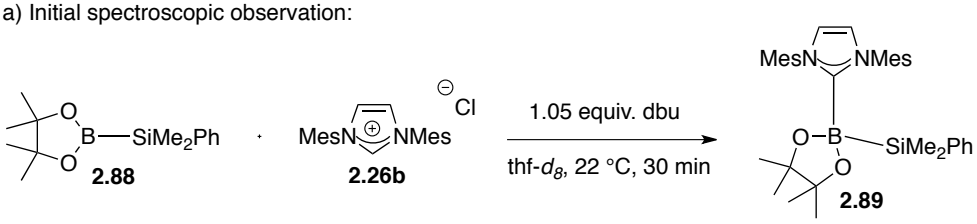


**11B NMR: 33.4 ppm** **8.0 ppm**

Control experiment indicates that the borosilyl reagent does not form a complex with dbu.

b) Examination of different Lewis bases as catalysts:

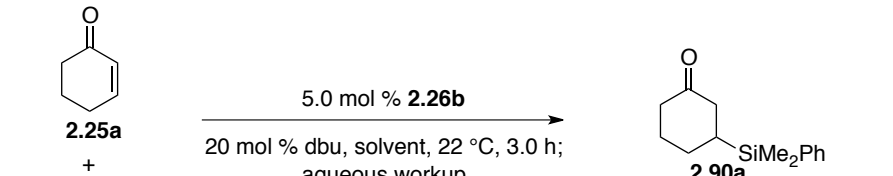


| 10 mol % $PPh_3$ in 1/1 thf/$H_2O$: | 10 mol % $PCy_3$ in 1/1 thf/$H_2O$: | 10 mol % $OPPh_3$ in 1/1 thf/$H_2O$: |
|---|---|---|
| <2% conv | 30% conv | <2% conv |

We then explored a series of NHCs for catalytic enantioselective SCA reactions. It was found that the NHC derived from chiral imidazolinium salt **2.91** gives the best result (for **2.90a**, >98% conv, 97% yield, 98:2 er, Scheme 2.4.3a). Five-, six, seven- and eight-membered cyclic enones are suitable substrates (products obtained with up to 97% yield and >98:2 er with 5.0 mol % **2.91** after 1.0–3.0 hours at 22 ºC). Additions to relatively rigid bicyclic enones and lactones were less efficient and/or enantioselective (**2.90d** and **2.90f**, respectively).

Enantioselective silyl conjugate additions to acyclic enones, enoates and enals require 7.5–12.5 mol% **2.91** and 12 h to proceed to >98% conversion (Scheme 2.4.3b), with good yields (54 to >98%) and er values (91:9–96:4). Notably, NHC-catalyzed SCA reactions to enals are similarly effecient and selective (**2.90j** and **2.90k**). The products are much more difficult to be obtained through alternative metal catalyzed protocols.

**Scheme 2.4.3. NHC catalyzed enantioselective silyl conjugate additions to a variety of unsaturated carbonyls**

**a)** Reactions with cyclic enones and lactones

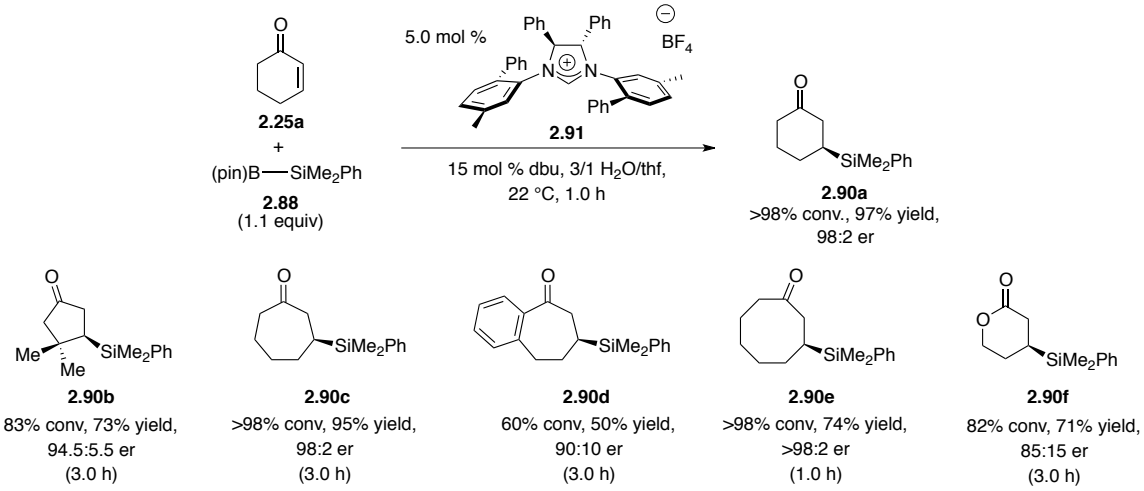

**b)** Reactions with acyclic enones, enoates and enals (3/1 thf/$H_2O$, 12 h)

chemoselectivity issues with Cu-based catalysts

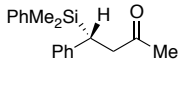

**2.90g**

>98% conv, >98% yield, 94:6 er (7.5 mol % NHC, 22 mol % dbu)

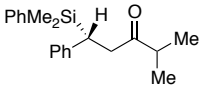

**2.90h**

>98% conv, 95% yield, 96:4 er (7.5 mol % NHC, 22 mol % dbu)

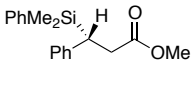

**2.90i**

60% conv, 54% yield, 95:5 er (10 mol % NHC, 30 mol % dbu)

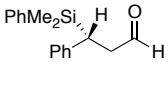

**2.90j**

>98% conv, 66% yield, 95:5 er (12.5 mol % NHC, 37.5 mol % dbu)

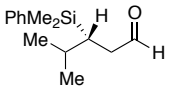

**2.90k**

>98% conv, 85% yield, 91:9 er (12.5 mol % NHC, 37.5 mol % dbu)

### *2.4.3. Reactions with Alkoxide-based Lewis Base Catalysts*

In 2012, Ito and co-workers reported the evidence of alkoxide coordination to (pin)B–$SiMe_2Ph$ (**2.88**). Treatment of **2.88** with 1.0 equivalent of KO*t*-Bu results in a siginificant upfield siginal in $^{11}B$ NMR (3.90 ppm, Scheme 2.4.4a).[96] It was later illustrated that with 10–15 mol % of KO*t*-Bu, aryl-substituted alkenes can be converted into the corresponding borosilyl addition products with exceptional site selectivity (>98% C–B at the benzylic position) and up to 87% yield (Scheme 2.4.4b). Interestingly, electron deficient styrenes (**2.93c**) is inactive even under forcing conditions (e.g., <2% yield with *p*-trifluorostyrene with 1.0 equiv KO*t*-Bu, 50 °C, 42 h), which suggests that the significant loss of electron density at the benzylic carbon is detrimental in the energetically demanding step of the catalytic cycle. Reactions with 1,2-disubstituted alkenes are slightly less efficient but diastereoselective (92:8 dr for β-methylstyrene). Interestingly, the C–B and C–Si bonds generated are exclusively in an anti fashion. In additions, 1,1-disubstituted aryl alkenes are effective in these reactions as well, generating B-substituted benzylic quaternary carbons with complete site selectivity.

(96) Ito, H.; Horita, Y.; Yamamoto, E. *Chem. Commun.* **2012**, *48*, 8006–8008.

**Scheme 2.4.4. Alkoxide catalyzed B–Si additions to olefins**

a) Initial spectroscopic measurements:

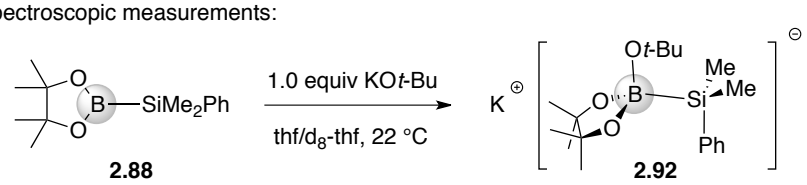


**2.88** **2.92**

**$^{11}$B NMR: 33.60 ppm** **3.90 ppm**

b) Alkoxide-catalyzed reactions with aryl olefins:

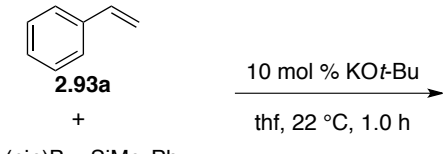

**2.93a**
+
(pin)B—SiMe$_2$Ph
**2.88**
(1.2 equiv)

10 mol % KO*t*-Bu
thf, 22 °C, 1.0 h

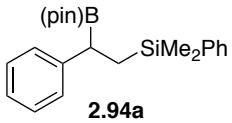

**2.94a**
91% yield

>98% benzylic C–B in all cases

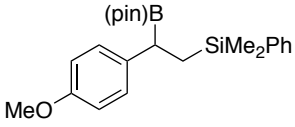

**2.94b**
87% yield
(4.0 h)

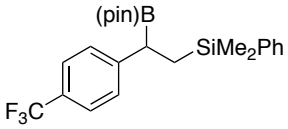

**2.94c**
<2% yield
(1.0 equiv reagent, 50 °C, 42 h)

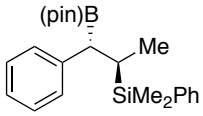

**2.94d**
from E-β-methylstyrene:
85% yield
92:8 dr (17 h)

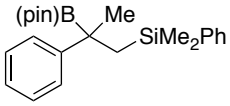

**2.94e**
66% yield (based on NMR analysis),
(1.1 equiv reagent)

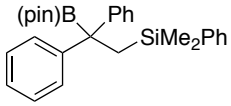

**2.94f**
85% yield

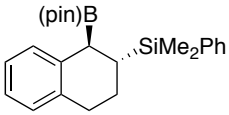

**2.94g**
72% yield,
94:6 dr
(15 mol % KO*t*-Bu, 50 °C)

## *2.4.4. Reactions with Fluoride-based Lewis Base Catalysts*

In 2012 Mita, Sato and co-workers reported a multi-step strategy initiated by CsF activation of (pin)B–SiMe$_2$Ph (**2.88**). The *in situ*-generated Boc-imines from the corresponding sulfones **2.95** were converted to α-amino esters **2.96** through an α-silylamine intermediate (Scheme 2.4.5a).[97] A variety of α-amino esters were thus obtained in 71–85% yield in the presence of five equivalent of the fluoride reagent and

(97) Mita, T.; Chen, J.; Sugawara, M.; Sato, Y. *Org. Lett.* **2012**, *14*, 6202–6205.

(pin)B–$SiMe_2Ph$, 20 mol% *p*-toluenesulfonic acid under 0.5 MPa of $CO_2$ pressure in dmf (22 °C, 3.0–16 h). The mixture was subsequently subjected to diazomethane in $Et_2O$. Both electron-rich as well as electron-deficient aryl imines are suitable substrates.

The proposed mechanism is illustrated in Scheme 2.4.5b. Association of a fluoride with the boron center of (pin)B–$SiMe_2Ph$ results in the formation of fluoride adduct **2.97**. In addition, CsF also facilitates the unmasking of the Boc-imine substrate (protonated by residual HF). Subsequent nucleophilic addition furnishes α-amino silyl intermediate **2.98**, which is activated again by coordination of a fluoride anion (**2.100**). The adduct reacts with $CO_2$ and forms the α-amino acid, which further reacts with $CH_2N_2$ delivering the corresponding ester. It is noteworthy that CsF was utilized to activate the boron atom of (pin)B–$SiMe_2Ph$ as well as the silicon atom of the silyl amide **2.98**. In either process, the Lewis base activation promotes the cleavages of the corresponding B–Si or Si–C bonds, which generate essential nucleophiles for the following reactions.

**Scheme 2.4.5. CsF promoted B–Si additions to aldimines and subsequent reactions with $CO_2$**

a) Synthesis of α-amino acids and esters promoted by CsF:

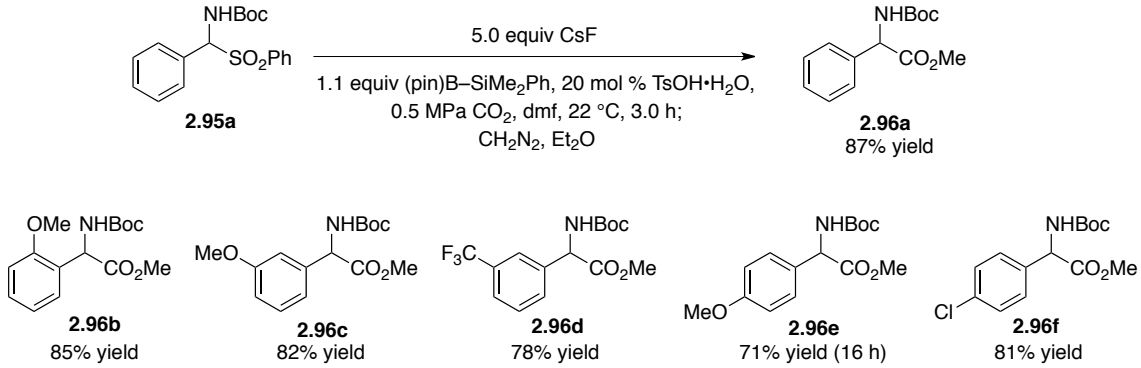

b) The proposed mechanism involving fluoride activation of Si–B and Si–C bonds:

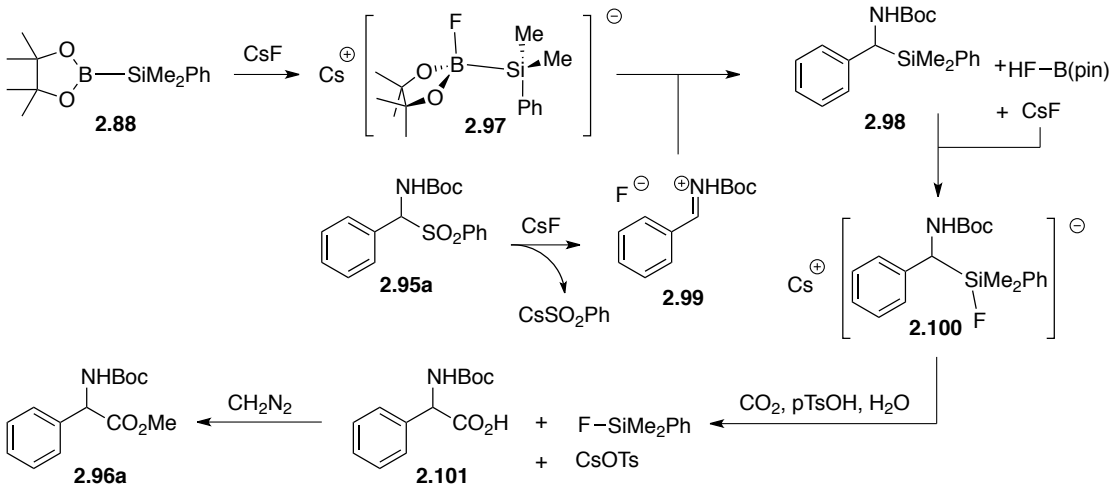


## *2.5. NMR Studies on NHC Activations of B–B/B–Si Bonds*

From this section, detailed mechanistic studies on NHC catalyzed enantioselective boryl or silyl conjugate addition reactions will be provided to help understand the inner workings of those reactions.[98]

As shown in Scheme 2.5.1, a general mechanism has been proposed to explain how the β-boryl carbonyl products form in the NHC catalyzed BCA process. The reaction begins with a partial hydrolysis of $B_2(pin)_2$ into $(MeO)_2B–B(pin)$. This latter diboron species is responsible for the formation of NHC•diboron complex, which serves as the active catalytic species. Because of the Lewis basicity of the NHC, the B–B bond in this complex is elongated, resulting in the subsequent B(pin) unit transfer to the approaching enone **2.44a**. After that, the product is hydrolyzed by MeOH to form **2.45a** and release the chiral NHC. Although this mechanism seems reasonable, several questions remain to be answered:

(98) Wu, H.; Garcia, J. M.; Haeffner, F.; Radomkit, S.; Zhugralin, A. R.; Hoveyda, A. H. *J. Am. Chem. Soc.* **2015**, *137*, 10585–10602.

(1) What are the roles of extra base and MeOH in this transformation?

(2) Can we provide any data to support the formation of a chiral NHC•diboron complex?

(3) What is the rate limiting step of this transformation? Is it the step of hydrolyzing $B_2(pin)_2$, the NHC•diboron formation step or the C–B bond formation step?

(4) Precisely how does the chiral NHC affect the enantioselective formation of the C–B bond? Can we provide any stereochemical model?

**Scheme 2.5.1. Critical questions in the mechanistic studies on NHC catalyzed enantioselective BCA reactions**

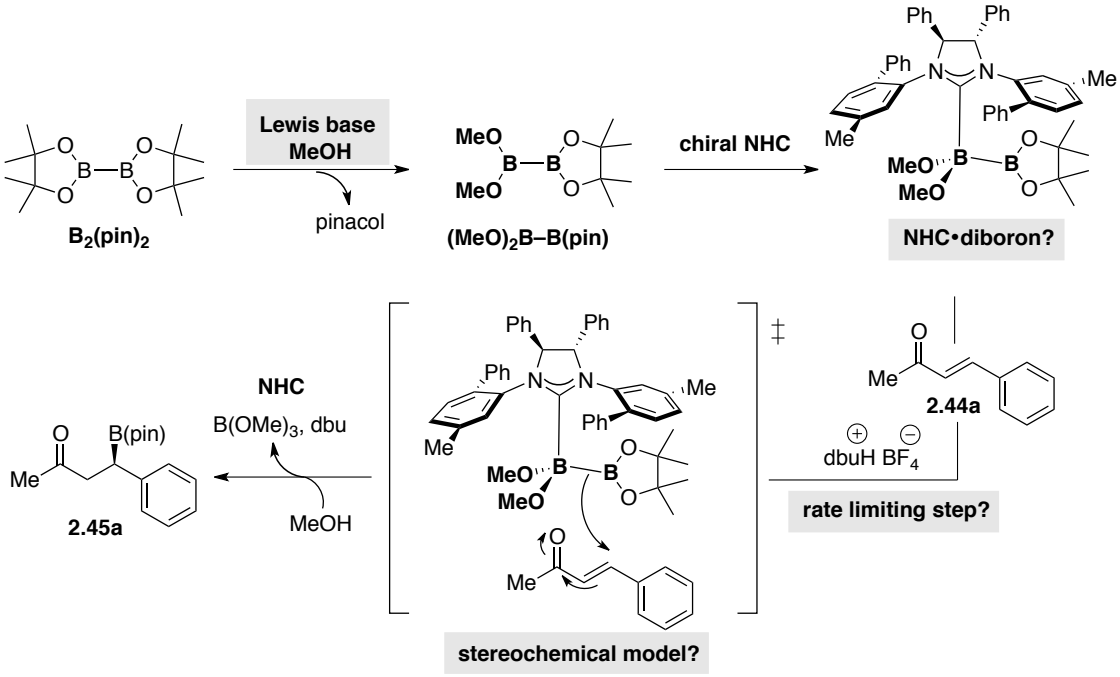


A plausible mechanism has also been proposed for the NHC catalyzed silyl conjugate addition reactions (Scheme 2.5.2). However, besides the similar questions as the BCA reactions that remain to be answered, two additional points are worth mentioning:

(1) Why is $H_2O$ superior than MeOH in the NHC catalyzed SCA reaction?

(2) When cyclic enones serve as substrates, why is the sense of absolute stereochemistry of the SCA product opposite to that of the BCA product (**2.90a** vs **2.45o**, **2.49a**)?

**Scheme 2.5.2. Critical questions in the mechanistic studies on NHC catalyzed enantioselective SCA reactions**

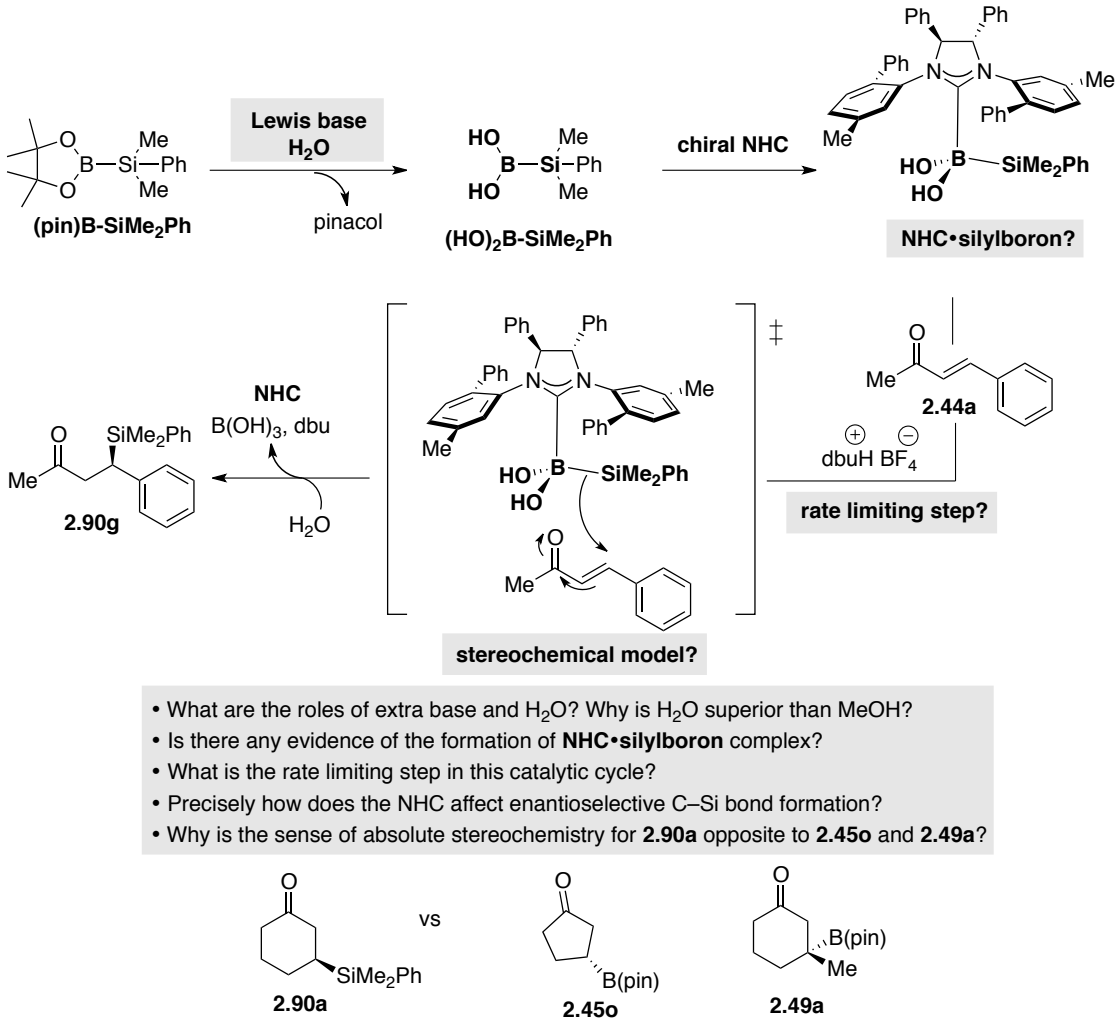


In this section, NMR experiments will be used to demonstrate the important roles of extra base, MeOH (or $H_2O$), as well as the formations of NHC•diboron (NHC•silylboron) complexes.

### *2.5.1. $^{11}B$ NMR Experiments for $B_2(pin)_2$ Hydrolysis and Formation of NHC•diboron*

In the previous studies, we found the chiral NHC cannot promote any BCA reaction without an excess amount of dbu and MeOH. Such observations were further

supported by the $^{11}B$ NMR experiments. In the Scheme 2.5.3, if only 1.0 equivalent of dbu is used to deprotonate **2.91** for the generation of NHC, there is no NHC•$B_2(pin)_2$ complexation observed after 6.0 hours. However, if 6.0 equivalents of dbu and 30 equivalents of MeOH are employed, we observe an upfield signal at 5.1 ppm (accompanied with other signals, spectroscopic details will be shown later), which suggests the coordination of the chiral NHC to diboron species. These observations suggest that one of the roles of extra base and MeOH could be to facilitate partial hydrolysis of $B_2(pin)_2$. The proposed pathway of this hydrolysis is shown in Scheme 2.5.4.

**Scheme 2.5.3. Probing the Effect of Extra Base and MeOH on B–B Bond Activation**

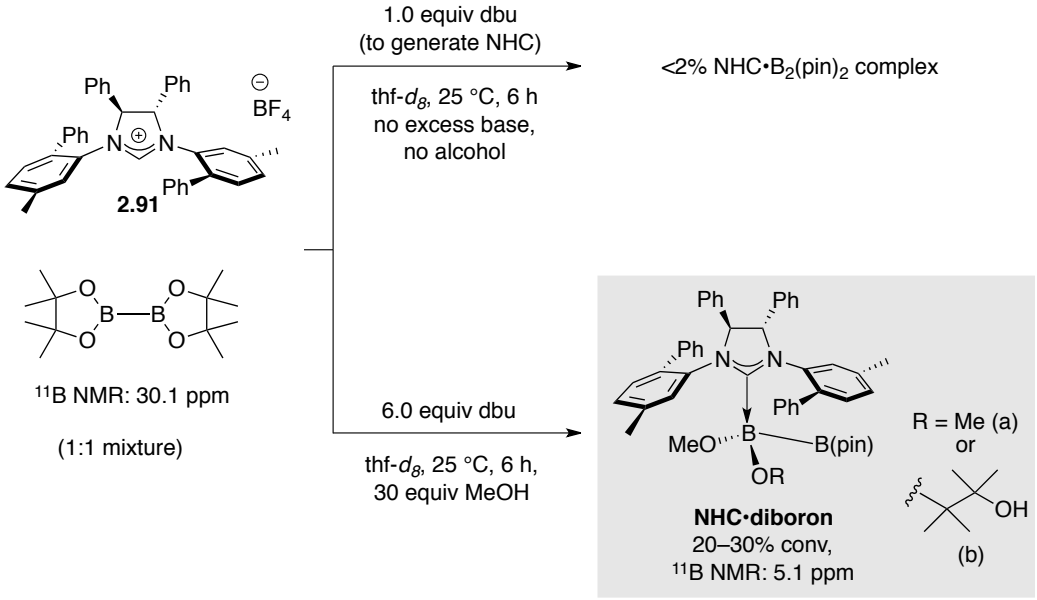


The reaction begins with the deprotonation of MeOH by 1.0 equivalent of dbu to form base-acid adduct **2.102**, which is probably in an equilibrium with **2.103**. The methoxide anion of adduct **2.102** is able to coordinate to 1.0 equivalent of $B_2(pin)_2$, generating borate **2.104.** At this stage, counter ion ($dbuH^+$) may protonate one of the oxygen atoms of borate **2.104**, affording **2.105** and release 1.0 equivalent of dbu.

Apparently, compound **2.105** is not stable and can promote pinacol ring cleavage to form **2.106**. The same pathway starting from **2.106** will fully hydrolyze one of the two borons and afford **2.107**. It should be noted that the two borons in either **2.106** or **2.107** are differentiated. The ones highlighted in gray are sterically more accessible borons. Thus, it is possible the large chiral NHC is able to coordinate to these less hindered borons and form the NHC•diboron complexes.

**Scheme 2.5.4. The mechanism proposed for hydrolysis of $B_2(pin)_2$ by dbu and MeOH**

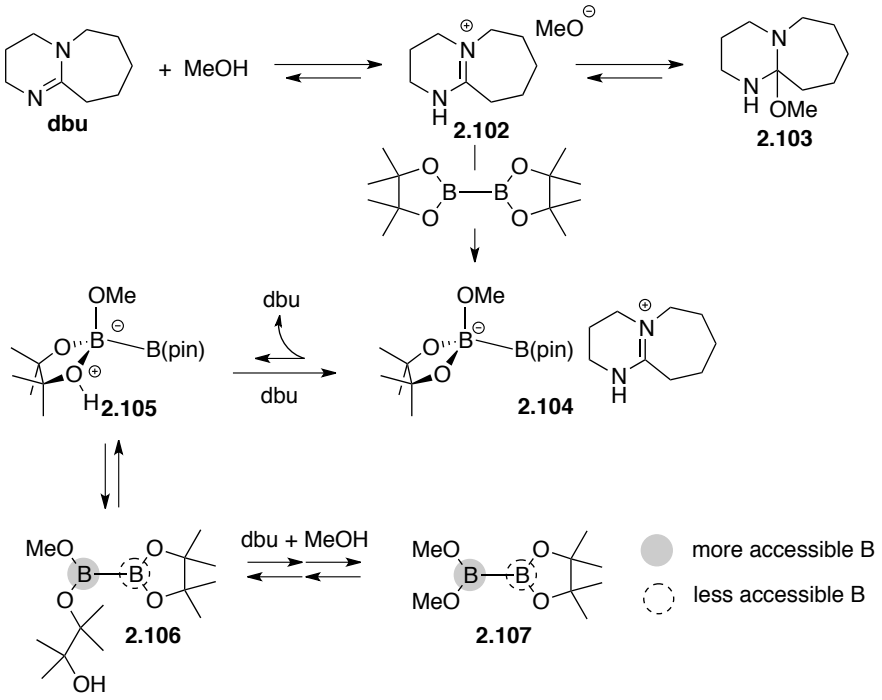


To further probe the formation of the chiral NHC•diboron complexes, a time dependent $^{11}B$ NMR technique was utilized. The reaction condition of this experiment is illustrated in Scheme 2.5.5, where 1.0 equivalent of chiral NHC precursor **2.91** was mixed with $B_2(pin)_2$, dbu and methanol in $d_8$-thf. The temperature was set to be 25 °C.

**Scheme 2.5.5. Coordination of the chiral NHC to diboron species**

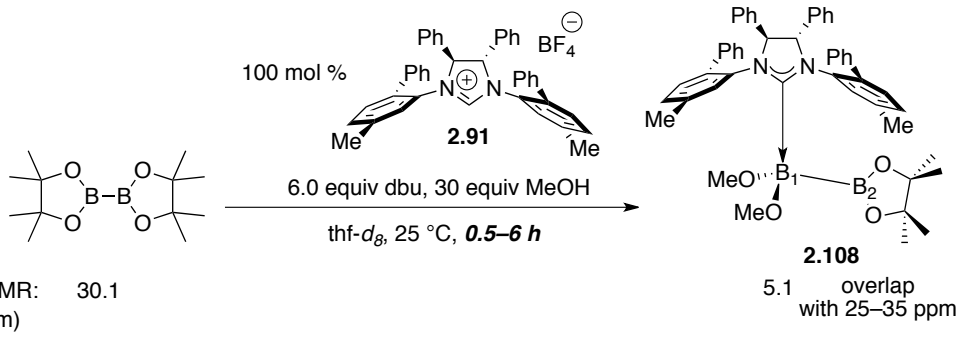


$^{11}$B NMR spectra (shown in Figure 2.5.1) were obtained every 2 h. All the signals have been labeled and the proposed species are shown along with the figure. Signal **a** and **b** (25–35 ppm) correspond to all the species containing a $sp^2$ borons except the borons of $B_2(pin)_2$. We think the borons of $B_2(pin)_2$ may be involved in the average signal **c** (20.4 ppm), and this average signal may account for the fast coordination of MeOH to $B_2(pin)_2$ with dbu. Between 10 and 0 ppm ($sp^3$ boron region), there are three signals (signal **d**, **e** and **f**). The intensities of all three signals increase over time, which implies they may be Lewis base adducts of (RO)(MeO)B–B(pin) (R = pinacol: **2.106**, R = Me: **2.107**), since the hydrolysis of $B_2(pin)_2$ into **2.106** and **2.107** requires time. Signal **d** (7.5 ppm) is probably the $sp^3$ boron of $[(RO)(MeO)_2B–B(pin)]^-dbuH^+$ (**2.109**), and signal **e** (6.5 ppm) may be the $sp^3$ boron of the complex **2.110** (coordination of dbu to **2.106** and/or **2.107**). The reason of these attributions is that the chemical shift of signal **d** barely changes (7.4 to 7.5 ppm) in the variable temperature $^{11}$B NMR experiements (which will be shown later), while the chemical shifts of signal **e** shifts downfield as the temperature increases (5.0 to 7.5 ppm); When we compare complex **2.109** with **2.110**, we think **2.109** is less labile than **2.110**: First, methoxide anion is smaller than dbu; Second, the B–N bond in complex **2.110** is just a dative bond. Noticably, these two signals (signal **d** and **e**) can be

detected in the control experiments (without NHC), suggesting the corresponding species come from background reaction. Signal **f** (5.1 ppm) was observed after 2 h. We believe this signal may account for the coordination of NHC to (RO)(MeO)B–B(pin) (complex **2.108**). The reason why it can only be detected after 2 h is because the generations of its partners [NHC and (RO)(MeO)B–B(pin)] requires longer time. Signal **g** corresponds to $BF_4^-$ anion of imidazolinium **2.91**.

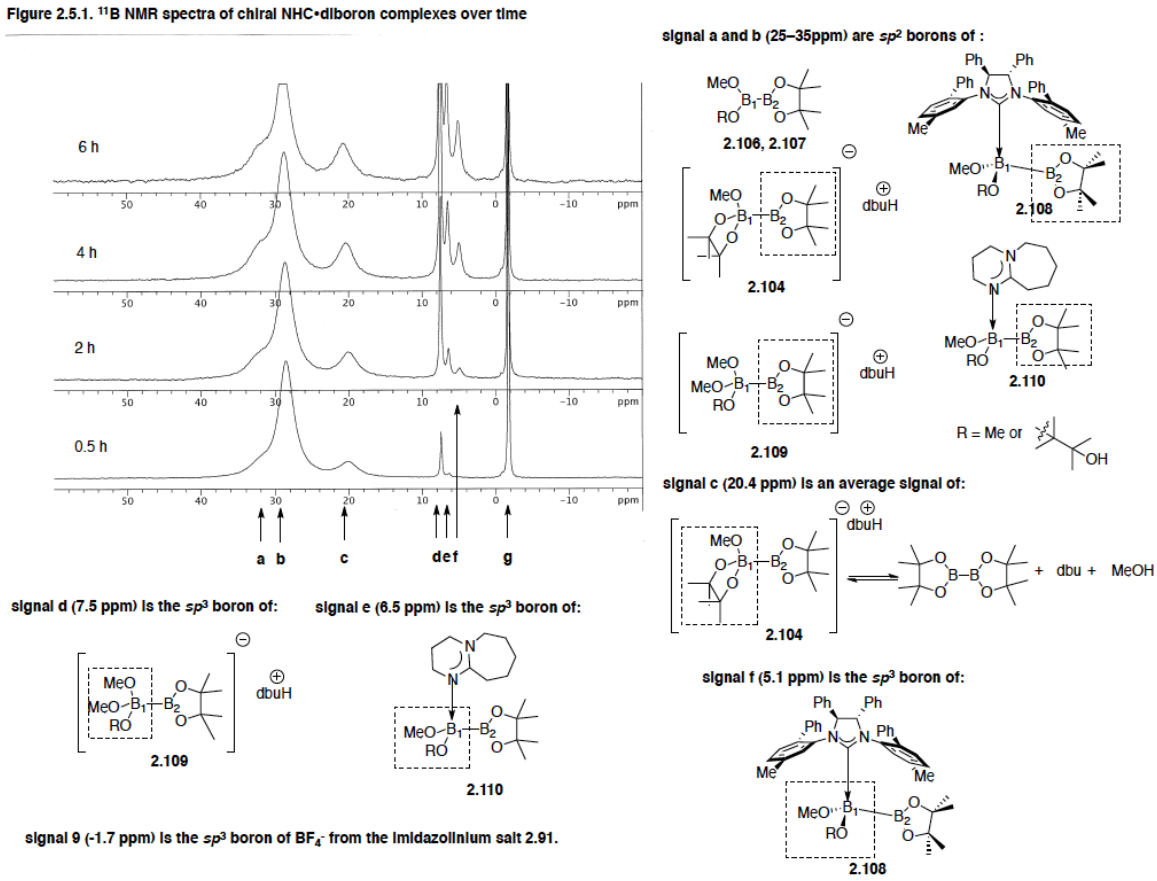


In order to probe how labile the NHC•diboron complex (**2.108**) is, a series of variable temperature (VT) $^{11}$B NMR experiments were designed and performed. The temperature range was selected from –10 to 40 °C. $^{11}$B NMR spectra were obtained every 10 °C. The chemical shifts of the $sp^3$ boron of complex **2.108** in varied temperature is shown in Scheme 2.5.6. The signal which indicates the NHC•diboron complex (**2.108**)

shifts downfield (from 2.6 to 10.2 ppm) as the temperature increases from –10 to 40 °C. The shape of this signal also changes from a sharp one into a broad one. These changes indicate at a lower temperature (–10 °C), NHC•diboron complex (**2.108**) is likely predominant in the solution, while at a higher temperature (40 °C), a significant amount of NHC dissociate from the the complex (**2.108**).

**Scheme 2.5.6. VT $^{11}$B NMR experiments and the changes of chemical shifts of $B_1$**

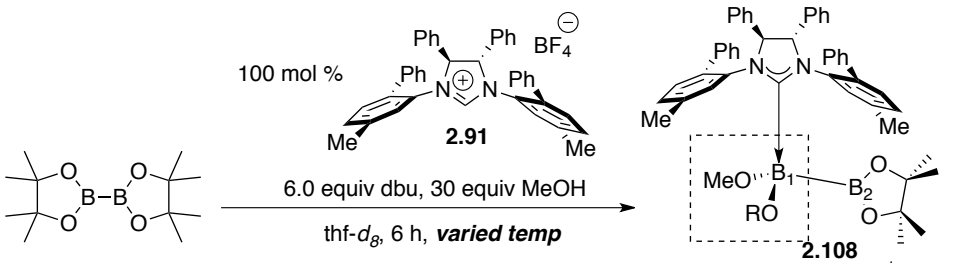


| entry | temp (°C) | chemical shifts of $B_1$ (ppm) | |
|---|---|---|---|
| 1 | –10 | 2.6 | sharp signal |
| 2 | 0 | 2.8 | |
| 3 | 10 | 3.3 | |
| 4 | 20 | 4.5 | |
| 5 | 30 | overlap with 7.5 | |
| 6 | 40 | 10.2 | broad signal |

The VT $^{11}$B NMR spectra are shown in Figure 2.5.2. Signal **a** (35.2 to 29.7 ppm) is broad and shifts upfield as the temperature increases. We attribute this signal to be the $sp^2$ boron of NHC or dbu coordination to (RO)(MeO)B–B(pin) (**2.108** and **2.110**). The reason for the change of their chemical shifts is as follows: at lower temperature, the coordination of the Lewis base (NHC or dbu) to (RO)(MeO)B–B(pin) is stronger than at higher temperature, this will make the $sp^2$ boron of the complex even more electrophilic due to the principle of Lewis base activation of Lewis acid. Thus at lower temperature, the signal of the $sp^2$ boron is more downfield. As the temperature increases, the

coordination of the Lewis base to (RO)(MeO)B–B(pin) is weaker, so the $sp^2$ boron of the complex is less eletrophilic, leading to more upfield chemical shift. Signal **b** (25.2 to 29.7 ppm) is another broad signal which shifts downfield as the temperature increases. We believe it is an average signal of a second coordination of MeOH to complex **2.104** and **2.109**. At lower temperature, such coordination is more pronounced. Thus the chemical shift of signal **b** is more close to $sp^3$ region. As the temperature increases, the equiliburiums shift to left, that is, more complex **2.104** and **2.109** are generated. Thus, the chemical shift of signal **b** is closer to $sp^2$ region. As the temperature increases, the equilibriums shift to the left, that is, more of complex **2.104** and **2.109** are generated. Thus, the chemical shift of signal **b** is closer to $sp^2$ region. We, however, believe that this second coordination of MeOH may not happen on complex **2.108** and **2.110** (complexes involved NHC or dbu), because the steric hinderance of NHC and dbu will prevent another Lewis base coordination. Signal **c** (7.4 to 26.8 ppm) is probably the average signal of the $sp^3$ boron of MeOH coordination to $B_2(pin)_2$. This complex **2.104** is very labile as the temperature increases: the chemical shift changes from 7.4 to 26.8 ppm. This is probably because the steric hinderance of pinacol group in $B_2(pin)_2$ will hamper the coordination of MeOH. As mentioned before, signal **d** (7.364 to 7.510 ppm) is probably the $sp^3$ boron of $[(RO)(MeO)_2B–B(pin)]^-dbuH^+$ (**2.109**), and signal **e** (5.0 to 7.5 ppm) may be the $sp^3$ boron of complex (**2.110**) [coordination of dbu to (RO)(MeO)B–B(pin)]. While signal **e** shifts downfield as the temperature increases (5.0 to 7.5 ppm), the chemical shift of signal **d** almost does not change (7.4 to 7.5 ppm). The reason has been stated before. Again, signal **f** (2.6 to 10.2 ppm) is believed to be the $sp^3$ boron of the NHC–diboron complex (**2.108**). This signal also shifts downfield as the temperature

increases. We believe it is a sign of the dynamic character of this complex (**2.106**): at a lower temperature (–10 °C), most NHC coordinates to (RO)(MeO)B–B(pin), resulting in an $sp^3$ boron signal at 2.6 ppm; At a higher temperature (40 °C), a significant amount of NHC dissociates from the the complex (**2.108**), resulting in an average signal at 10.194 ppm. Signal **g** corresponds to $BF_4^-$ anion of imidazolinium **2.91**.

Additionally, as the temperature increases, the intensity of all signals in the $sp^2$ boron region increases, which implies the amount of species containing $sp^2$ boron increases and the amount of species containing $sp^3$ boron diminishes; in another word, the system becomes more dynamic at higher temperatures.

**Figure 2.5.2. VT $^{11}$B NMR spectra of chiral NHC•diboron complexes**

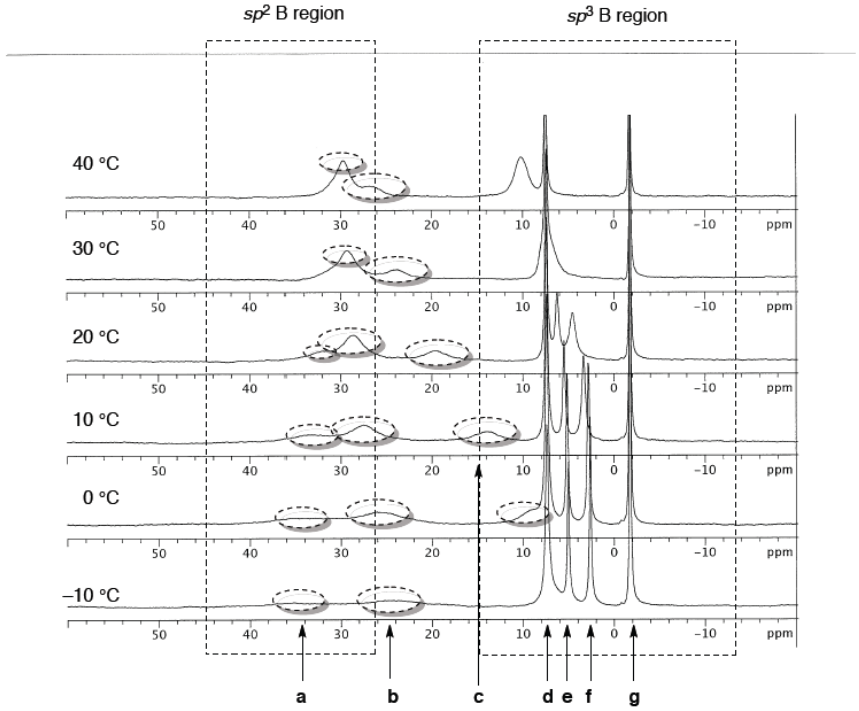


**signal a (35.2 → 29.7 ppm broad) corresponds to *sp*$^2$ borons of :**

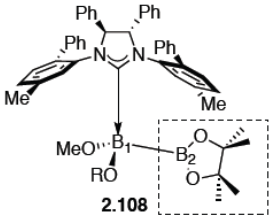


**2.108**

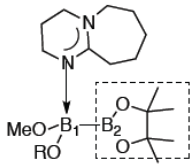


**2.110**

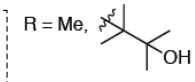


**signal b (25.2 → 29.7 ppm broad) is an average signal of:**

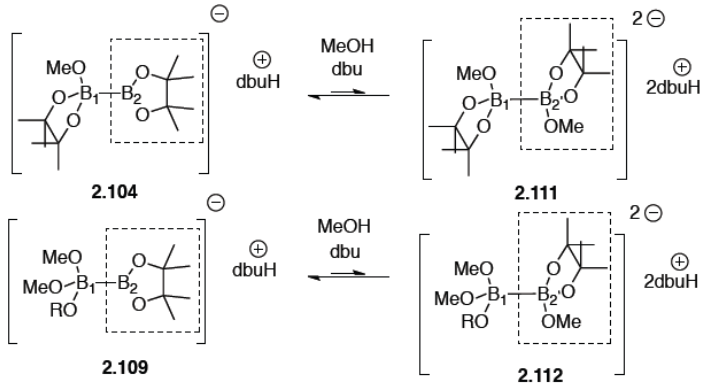


**2.104** **2.111**

**2.109** **2.112**

**signal c (overlap with 7.364 → 26.831 ppm) is an average signal of:**

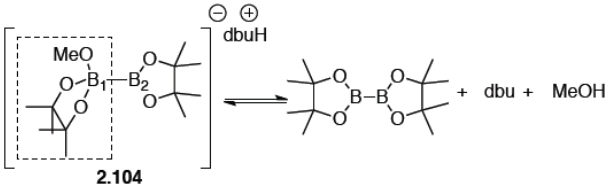


**2.104**

**signal d (7.4 → 7.5 ppm) is the *sp*$^3$ boron of:**

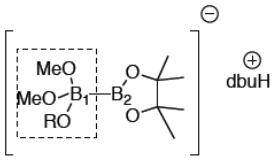


**2.109**

**signal e (5.0 → 7.5 ppm) is the *sp*$^3$ boron of:**

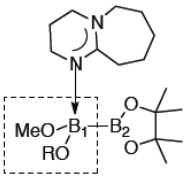


**2.110**

**signal f (2.6 → 10.2 ppm) is the *sp*$^3$ boron of:**

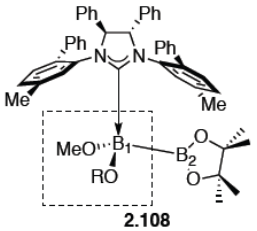


**2.108**

**signal g (-1.8 ppm) is the *sp*$^3$ boron of $BF_4^-$ from the imidazolinium salt 2.91.**

The first control experiment is mixing dbu, MeOH and $B_2(pin)_2$ under the same reaction condition as before but no NHC is involved (Scheme 2.5.7).

**Scheme 2.5.7. Control experiment I: $B_2(pin)_2$, dbu and MeOH**

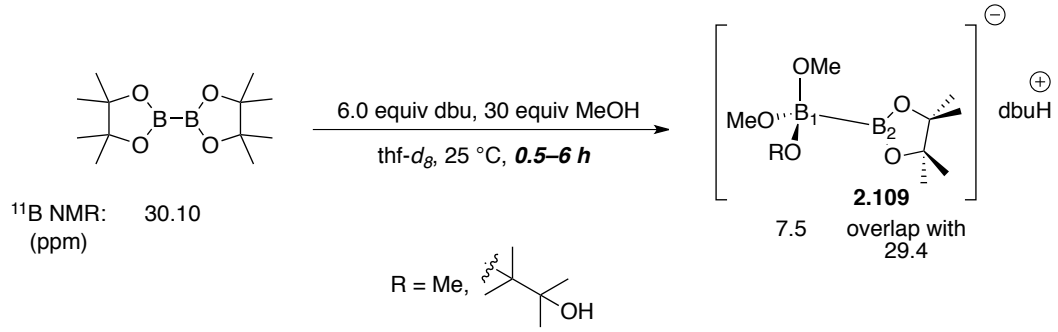


$^{11}$B NMR spectra (shown in Figure 2.5.3 ) were obtained every 2 h at 25 °C. We attribute the broad signal **a** (29.4 ppm) to be the $sp^2$ borons of species **2.104, 2.106, 2.107, 2.109** and **2.110**. This signal is similar as signal **a** and **b** in Figure 2.5.1. Likewise, signal **b** (25.5 ppm) is probably an average signal of MeOH coordination of $B_2(pin)_2$. The signal at 7.5 ppm (signal **c**) corresponds to the $sp^3$ boron of complex **2.109**. All signals mentioned above appear also in the previous experiment involving chiral NHC. However, a major difference compared to the previous experiment is worth to mention:

The signals at 5.1 ppm and 6.5 ppm in Figure 2.5.1 do not appear in Figure 2.5.3. As mentioned before, the signal at 5.1 ppm (see signal **f** in Figure 2.5.1) is believed to be the NHC•diboron complex (**2.108**), while the one at 6.5 ppm (see signal **e** in Figure 2.5.1) is probably the $sp^3$ boron of complex **2.110** [coordination of dbu to (RO)(MeO)B–B(pin)]. The reason why this signal (6.5 ppm) does not appear in the control experiment at 25 °C may be due to its small quantity in this control experiment and partially overlap with the signal at 7.5 ppm. In the VT $^{11}$B NMR which will be described later, this signal appear at lower temperature (<20 °C). The next question is why complex **2.110**

[coordination of dbu to (RO)(MeO)B–B(pin)] is generated in a larger quantity in the experiement involving an NHC than in this control experiment. One possible explanation could be that an NHC as a Lewis base, helps the hydrolysis of $B_2(pin)_2$ into (RO)(MeO)B–B(pin) (**2.106**, **2.107**), just like the role of methoxide in Scheme 2.5.4. Because of this, the amount of dbu coordination to (RO)(MeO)B–B(pin) is enhanced if an NHC is involved.

There is another explanation for the enhancement of hydrolysis by an NHC. The NHC, along with dbu and methanol, can coordinate to (RO)(MeO)B–B(pin) (**2.106, 2.107**). Thus if an NHC is involved, the equilibrium of hydrolysis of $B_2(pin)_2$ will shift forward since some (RO)(MeO)B–B(pin) gets consumed by an NHC. Thus more (RO)(MeO)B–B(pin) (**2.106, 2.107**) is available for dbu binding.

**Figure 2.5.3. $^{11}B$ NMR spectra of dbu, MeOH and $B_2(pin)_2$ over time**

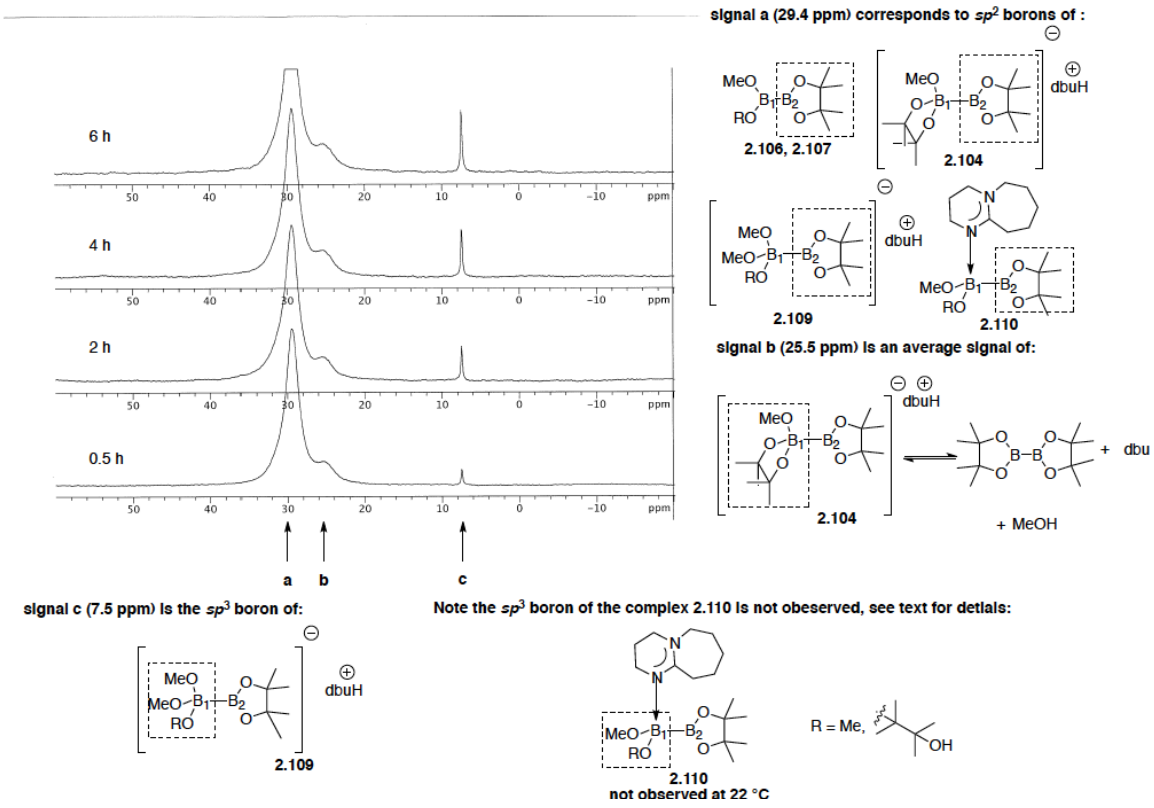

The VT $^{11}$B NMR experiments were also performed in this control study (–10 to 40 °C), where $B_2(pin)_2$, dbu and MeOH were mixed in thf-$d_8$ (Scheme 2.5.8).

**Scheme 2.5.8. VT $^{11}$B NMR experiments: $B_2(pin)_2$, dbu and MeOH**

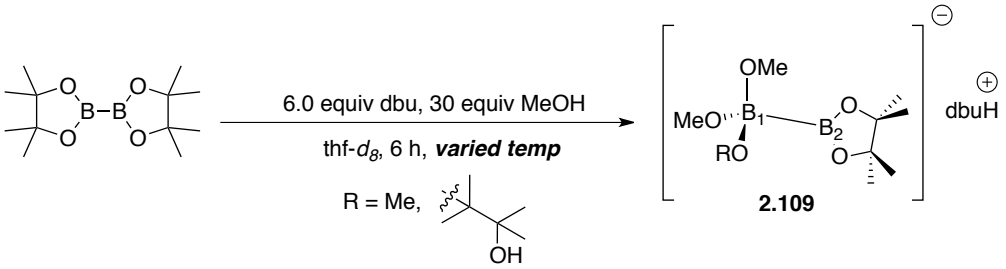


The VT $^{11}$B NMR spectra are depicted in Figure 2.5.4. Signal **a** may be the $sp^2$ boron of complex **2.110**, of which the chemical shift is ~30 to 33 ppm (overlaping with signal **b**). Signal **b** (25.8 to 29.7 ppm) corresponds to the average signals of the aforementioned fast equilibrium of MeOH coordination to complex **2.104** and **2.109**. The downfield shift of this signal indicate the amount of complex **2.111** and **2.112** diminishes as the temperature increases. The dynamic signal **c** (9.3 to 29.7 ppm) is attributed to the average signal of the $sp^3$ boron of MeOH coordination to $B_2(pin)_2$. Like mentioned before, at –10 °C, the formation of complex **2.104** is more pronouced, and thus the chemical shift is closer to $sp^3$ region (9.3 ppm). At 40 °C, more $B_2(pin)_2$ are released, consistent with a chemical shift at 29.7 ppm observed. Signal **d** (7.4 to 7.5 ppm) corresponds to the $sp^3$ boron of complex **2.109** as mentioned before. Interestingly, we can observe signal **2.110** (5.0 to 7.5 ppm) in this VT $^{11}$B NMR. Its chemical shift is very similar to signal **e** in Figure 2.5.2, where an NHC is used. Thus, this signal is likely to be the $sp^3$ boron of complex **2.110** [dbu coordination to (RO)(MeO)B–B(pin)].

**Figure 2.5.4. VT $^{11}B$ NMR spectra: $B_2(pin)_2$, dbu and MeOH**

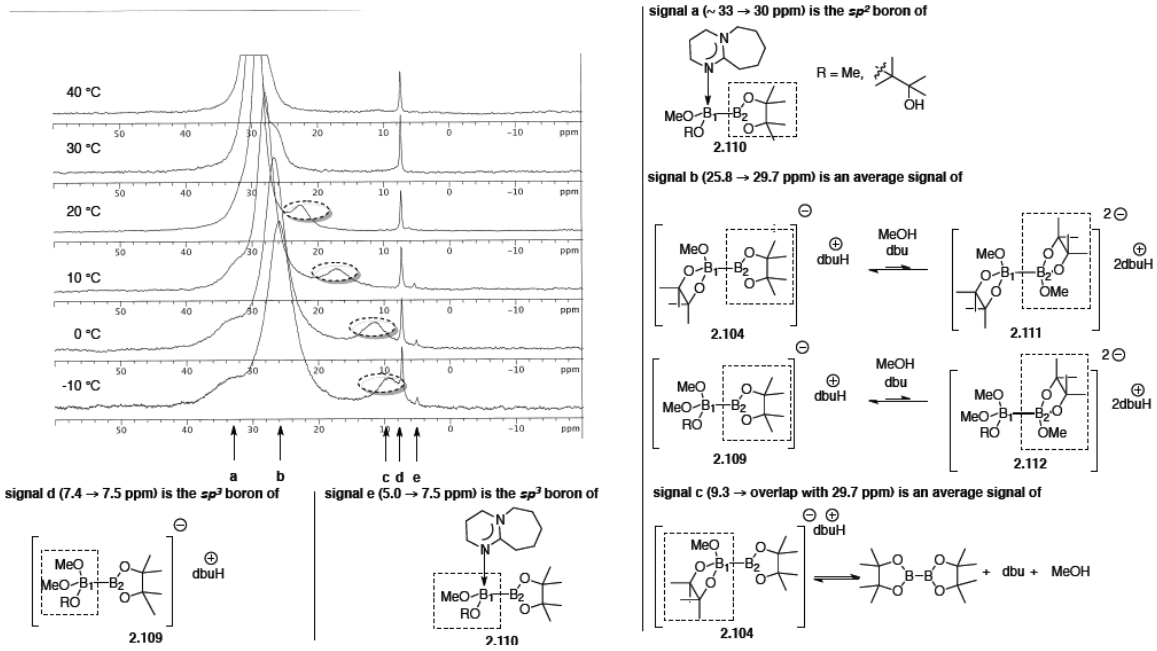


Other control experiments were also conducted (Figure 2.5.5). Experiment I involves the use of chiral imidazolinium salt **2.91** and 1.0 equivalent of dbu in thf-$d_8$ (no MeOH). No NHC•$B_2(pin)_2$ complexation was detected. VT $^{11}B$ NMR spectra of this mixture also only show the signal of pure $B_2(pin)_2$. This means the large chiral NHC is not likely to coordinate to $B_2(pin)_2$, since the pinacols of the boron atoms of $B_2(pin)_2$ will have severe steric interactions with the N-aryl motifs of the NHC.

In the experiment II, only dbu and $B_2(pin)_2$ were involved. Again, the $^{11}B$ NMR spectra did not change within six hours, no matter what reaction temperature was employed. This implies the dbu is also not effective to coordinate to $B_2(pin)_2$.

**Figure 2.5.5. $^{11}$B NMR spectra of other control experiments**

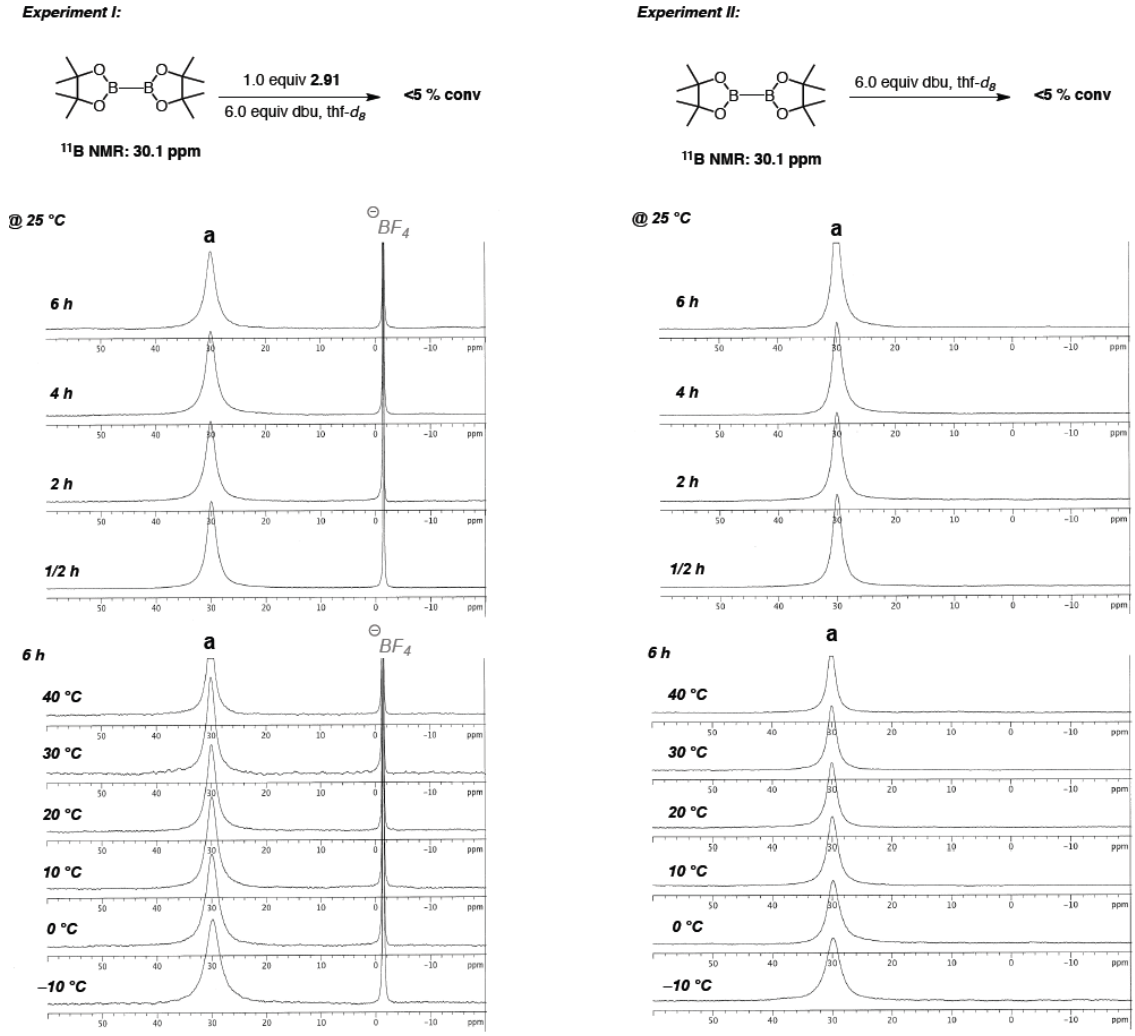


The above findings provide spectroscopic evidences that the chiral NHC•diboron complex is probably formed in the boryl conjugate addition reactions. They also imply the important roles of extra base and MeOH, which are responsible for a partial hydrolysis of $B_2(pin)_2$. The resulting (RO)(MeO)B–B(pin) (R = Me, pinacol) are likely the active diboron species in those reactions.

### *2.5.2. $^{11}$B NMR and $^{13}$C NMR Experiments for (pin)B–SiMe$_2$Ph Hydrolysis and Formation of NHC•silylboron*

A series of $^{11}B$ NMR experiments were also performed to detect the coordination of the chiral NHC derived from **2.91** to $(RO)_2B–SiMe_2Ph$ (R = H or Me). Unfortunately, we cannot find any direct evidence of chiral NHC•borylsilane complexes from the NMR study. Generally, $^{11}B$ NMR spectra are very similar with or without the use of the chiral NHC. In addition, (pin)B–$SiMe_2Ph$ was found to be converted into (pin)B–OH [or (pin)B–OMe] and $HSiMe_2Ph$ has been observed in NMR spectra. The decomposition of the borylsilane reagent in the NMR experiments means that in the reported reaction conditions, the NHC catalyzed enantioselective silyl conjugate addition must overcome the breakdown of (pin)B–$SiMe_2Ph$ and follows the productive pathway with a higher efficiency. It is also possible that the lifetime of (pin)B–$SiMe_2Ph$ in the reported biphasic reaction conditions (thf/$H_2O$ = 3:1 with enone and borylsilane) is much longer than the one in the homogenious NMR experiments, since (pin)B–$SiMe_2Ph$ probably spends much of its time in the organic layer in the catalytic SCA reaction.

The first NMR experiment is illustrated in Scheme 2.5.9, where (pin)B–$SiMe_2Ph$ is mixed with the NHC derived from **2.91**, dbu and 6 equiv of $H_2O$. During the experiment, (pin)B–$SiMe_2Ph$ was found to decompose into $HSiMe_2Ph$ and (pin)B–OH by NMR spectra. $^1H$ NMR and $^{13}C$ NMR of $HSiMe_2Ph$ were recorded, selected signals of which are shown in Scheme 2.5.9.

**Scheme 2.5.9. Coordination of the chiral NHC to $(HO)_2B–SiMe_2Ph$ was not detected**

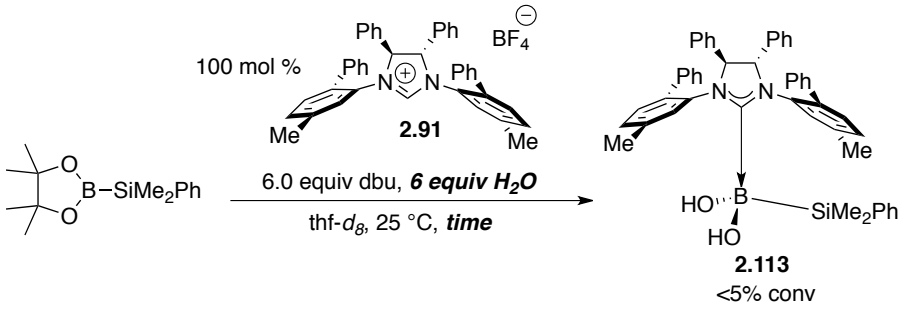


**characteristic NMR signals of the decomposition product: $HSiMe_2Ph$**

| | |
|---|---|
| $^1$H NMR (ppm): | 4.41 |
| $^{13}$C NMR (ppm): | 133.7, 129.0, 127.6 |

The $^{11}$B NMR spectra of this experiment over time has been shown in Figure 2.5.6. Interestingly, the spectra were almost unchanged during the reaction time, which means whatever the reaction is, it finished in 0.5 h. Signal **a** (21.5 ppm) is a broad signal and seems to correspond to more than one species. Compared with the former experiments with $B_2(pin)_2$ (such as Figure 2.5.1), it may include the fast equilibrium between complex **2.114** (methanol adduct of (pin)B–$SiMe_2Ph$) and (pin)B–$SiMe_2Ph$. More importantly, signal **a** is likely evidence of the presence of (pin)B–OH (**2.115**), since the chemical shift of the *sp*$^2$ boron for (pin)B–OMe (20.9 ppm in $CDCl_3$) has been reported before.[99] Signal **b** (7.7 ppm) is very similar as the previously obeserved signal of $[(RO)(MeO)_2B–B(pin)]^-dbuH^+$ (**2.109**) (7.5 ppm). Thus we attribute it as $[(HO)_3B–SiMe_2Ph]^-dbuH^+$ (**2.116**). Signal **c** (4.3 ppm) falls into the region of $B(OH)_4^-$ reported before (4.8 ppm),[100] so we think it may refer to three kinds of borates (**2.117**, **2.118** and/or **2.119**). Signal **d** (–1.7 ppm) is the *sp*$^3$ boron of $BF_4^-$ from imidazolinium salt **2.91**.

(99) Kleeberg, C.; Borner, C. *Eur. J. Inorg. Chem.* **2013**, 2799–2806.

(100) Andrieux, J.; Demirci, U. B.; Hannauer, J.; Gervais, C.; Goutaudier, C.; Miele, P. *International Journal of Hydrogen Energy*, **2011**, *36*, 224–233.

**Figure 2.5.6. Time dependent $^{11}$B NMR spectra**

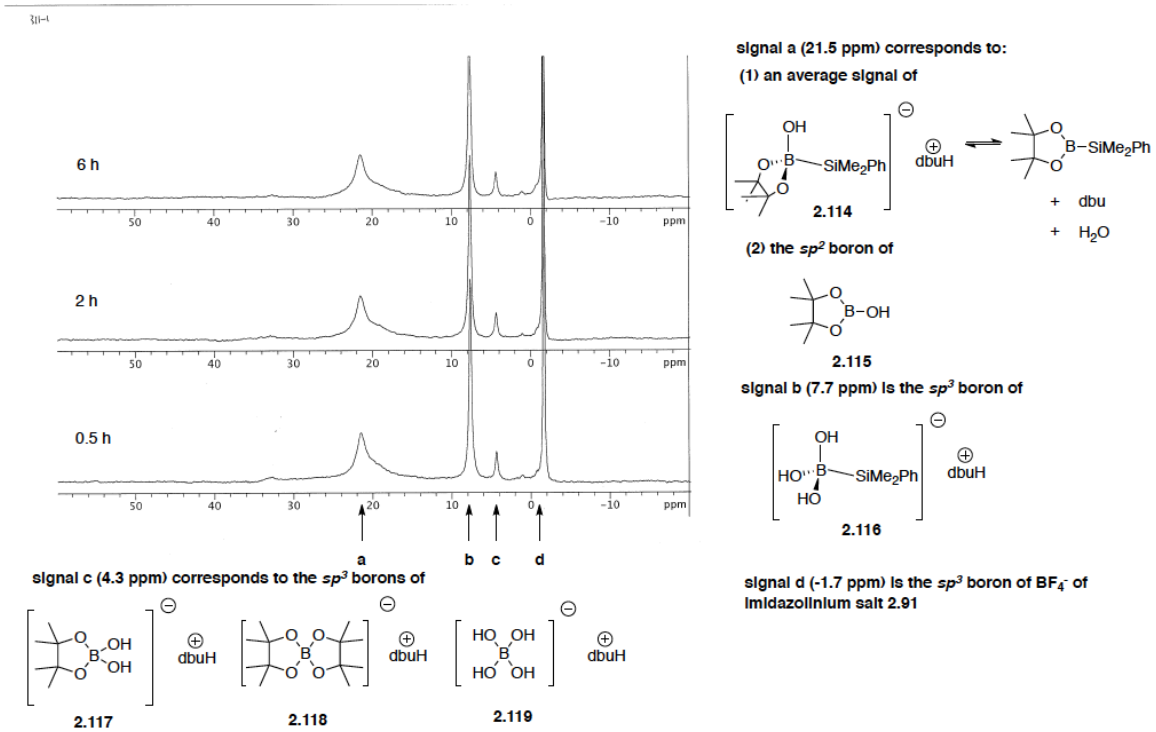


The control experiment in which (pin)B–$SiMe_2Ph$, dbu and $H_2O$ (without NHC) were involved has been depicted in Scheme 2.5.10. Again, the decomposition of (pin)B–$SiMe_2Ph$ into $HSiMe_2Ph$ has been obeserved.

**Scheme 2.5.10. Control experiement: (pin)B–$SiMe_2Ph$, dbu and $H_2O$**

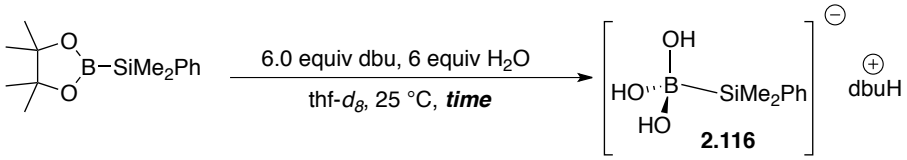


**characteristic NMR signals of the decomposition product: $HSiMe_2Ph$ (~85% conv)**

| | |
|---|---|
| $^1$H NMR (ppm): | 4.35 |
| $^{13}$C NMR (ppm): | 133.5, 128.8, 127.5 |

The $^{11}$B NMR spectra seems very similar as the previous ones with NHC, except the disappearance of the signal of $BF_4^-$. Signal **a** (21.5 ppm) may refer to an average signal of fast association and dissociation of methanol to (pin)B–$SiMe_2Ph$, and the $sp^2$ boron of (pin)B–OH (**2.115**). Signal **b** (7.6 ppm), very similar as 7.7 ppm observed

before, is attributed as the $sp^3$ boron of $[(HO)_3B–SiMe_2Ph]^-dbuH^+$ (**2.116**). Again, signal **c** (4.3 ppm) may be three kinds of borates (**2.117**, **2.118** and **2.119**).

**Figure 2.5.7. Time dependent $^{11}B$ NMR**

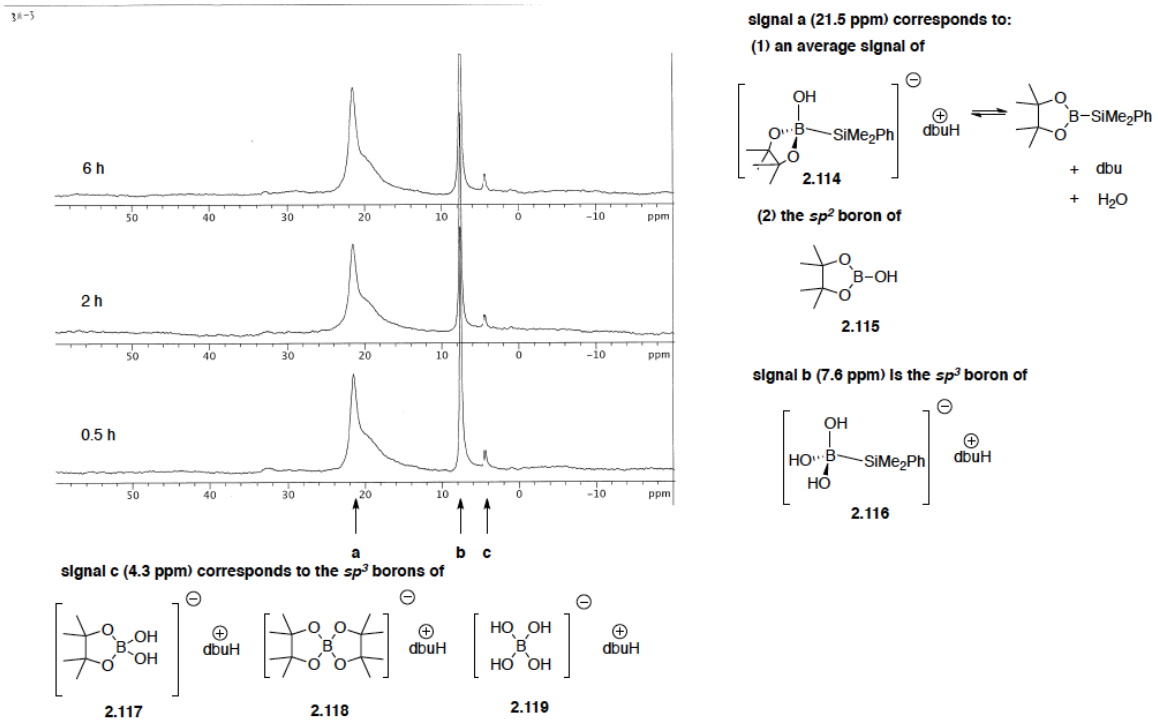


In aware of an efficient decomposition of (pin)B–$SiMe_2Ph$ in $H_2O$, 30 equivalents of MeOH is used instead of $H_2O$. Still we cannot detect any coordination of the chiral NHC to $(MeO)_2B–SiMe_2Ph$ (Scheme 2.5.11).

**Scheme 2.5.11. Coordination of the chiral NHC to $(MeO)_2B–SiMe_2Ph$ with 30 equiv MeOH was not detected.**

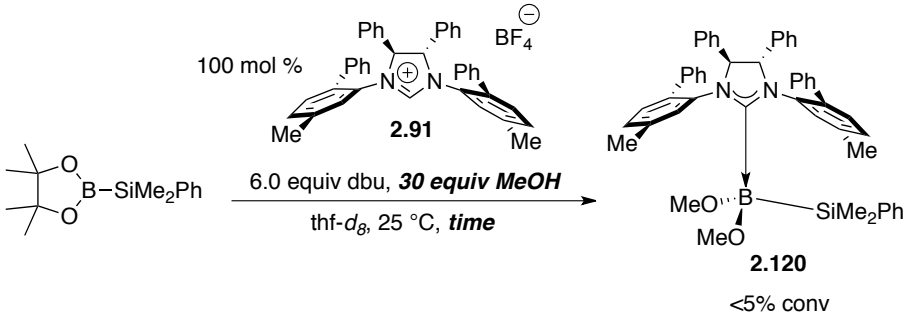


The $^{11}B$ NMR spectra were shown in Figure 2.5.8, where four signals are worth to mention. Signal **a** (33.4 ppm) is a signal which disappeared after 2 h. Its chemical shift is

in the $sp^2$ boron region. Thus we think it could be (pin)B–$SiMe_2Ph$ and/or $(MeO)_2B$–$SiMe_2Ph$ (**2.121**). Interestingly, there is no signal around 21 ppm or a signal at 4.3 ppm in the spectra (see Figure 2.5.6 and 2.5.7), but a broad signal at 10.8 ppm (signal **b**). In my opinion, it could be the average signal of the two (21 and 4.3 ppm). Thus, we attribute this signal as the fast equilibriums between species **2.122** and **2.123**, and/or species **2.124** and **2.125.** There might be two reasons why we did not observe two seperate signals but an average one: (1) 30 equivalents of MeOH used in this experiment is more than 6 equivalents of $H_2O$ used previously, so all of (pin)B–OMe are probably coordinated by MeOH, leading to the disappearance of its signal (21 ppm). (2) $[(pin)B(OMe)_2]^-dbuH^+$ (**2.122**) is likely more labile than $[(pin)B(OH)_2]^-dbuH^+$ (**2.117**), so we can only obeserve an average signal of fast equilibrium between **2.122** and **2.123**, not a sharp signal of **2.117** (4.3 ppm, Figure 2.5.7). Signal **c** (7.5 ppm) is likely to be the $sp^3$ boron of $[(MeO)_3B–SiMe_2Ph]^-dbuH^+$ (**2.120**), like $[(HO)_3B–SiMe_2Ph]^-dbuH^+$ (**2.116**) at 7.7 ppm obeserved before (Figure 2.5.6, 2.5.7). Signal **d** (–1.8 ppm) is the $sp^3$ boron of $BF_4^-$ from imidazolinium salt **2.91**.

**Figure 2.5.8. Time dependent $^{11}$B NMR spectra**

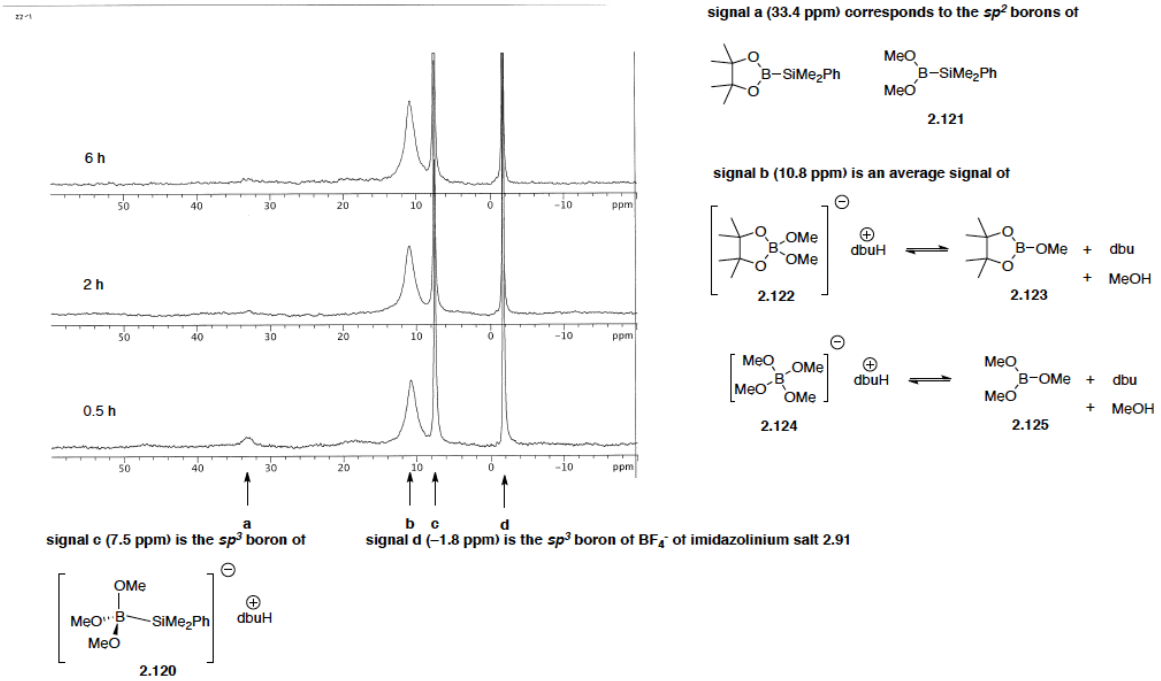


The control experiment in which (pin)B–$SiMe_2Ph$, dbu and 30 equiv MeOH (without NHC) has been depicted in Scheme 2.5.12.

**Scheme 2.5.12. Control experiement: (pin)B–$SiMe_2Ph$, dbu and 30 equiv MeOH**

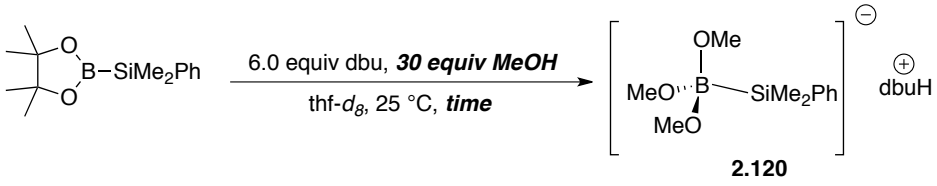


The $^{11}$B NMR spectra over time are summerized in Figure 2.5.9. Like all the experiments using (pin)B–$SiMe_2Ph$, the spectra almost did not change after two hours. Signal **a** (33.4 ppm) is attributed as the $sp^2$ boron of (pin)B–$SiMe_2Ph$ and $(MeO)_2$B–$SiMe_2Ph$ **2.121**. Signal **b** (14.2 ppm) is likely two overlapping signals, which refer to the fast equilibrium of MeOH association and dissociation of **2.122** and **2.124**. The reason why this signal (14.2 ppm) is more downfield than the previous one with NHC (signal **b**:

10.8 ppm, Figure 2.5.8) is not known. Signal **c** (7.5 ppm) may refer to $sp^3$ boron of $[(MeO)_3B–SiMe_2Ph]^-dbuH^+$ (**2.120**).

**Figure 2.5.9. Time dependent $^{11}B$ NMR spectra**

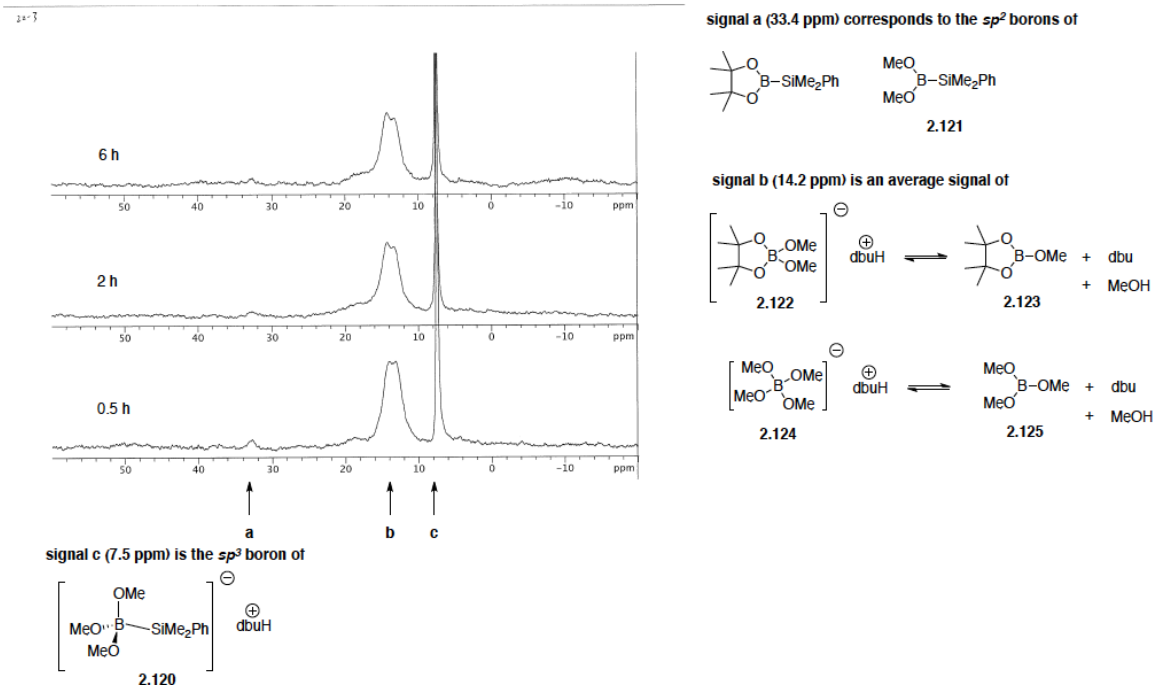


Besides the experiments mentioned above, other NMR experiments (including the use of 2 equivalents of MeOH instead of 30 equivalents) did not provide evidence for chiral NHC•silyboron complexation. The main challenge is still complete decomposition of (pin)B–$SiMe_2Ph$. Thus, instead of trying to generate it *in situ*, we synthesized $(MeO)_2B–SiMe_2Ph$, a species that is probably more easier to be synthesized and handle than $(HO)_2B–SiMe_2Ph$.

As shown in Scheme 2.5.13, $(MeO)_2B–SiMe_2Ph$ (**2.121**) can be prepared in two steps in ~30% conversion as a mixture with other byproducts. Silica gel chromatography or distillation under reduced pressure resulted in a complete decomposition of $(MeO)_2B–SiMe_2Ph$ (**2.121**). Thus, it was isolated by a simple filtration through a plug of celite,

which removed the LiCl and LiOMe generated during the reactions. The presence of desired product **2.121** has been confirmed by the high-resolution mass spectrum.

**Scheme 2.5.13. Synthesis of $(MeO)_2B–SiMe_2Ph$**

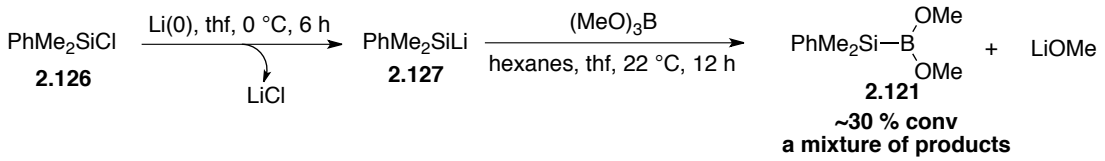


**Chromatography or distillation resulted in product decomposition;**
**Product 2.121 was isolated by filtration through a plug of celite to remove LiCl and LiOMe**

The $^{11}B$ NMR spectrum of unpurified $(MeO)_2B–SiMe_2Ph$ (**2.121**) is shown in Figure 2.5.10. Signal **a** (32.8 ppm) is attributed as the $sp^2$ boron of $(MeO)_2B–SiMe_2Ph$, since it is similar as the one of (pin)B–$SiMe_2Ph$ (33.4 ppm). Signal **b** is partially overlapped with **a**, and thus could be similar species such as $(MeO)_2B–SiMe_2Ph$ or (HO)(MeO)B–$SiMe_2Ph$, ones that were generated during celite filtration or subsequent concentration of the solution. Signal **c, d** and **e** is a mixture of compounds: First, it may contain an equilibrium of LiOMe coordination to $(MeO)_2B–SiMe_2Ph$. Second, it might also include unreacted $B(OMe)_3$. Last, the signals of unknown reaction byproducts or decomposition products of $(MeO)_2B–SiMe_2Ph$ may also be in this region.

**Figure 2.5.10. $^{11}$B NMR Spectrum of Unpurified $PhMe_2Si–B(OMe)_2$**

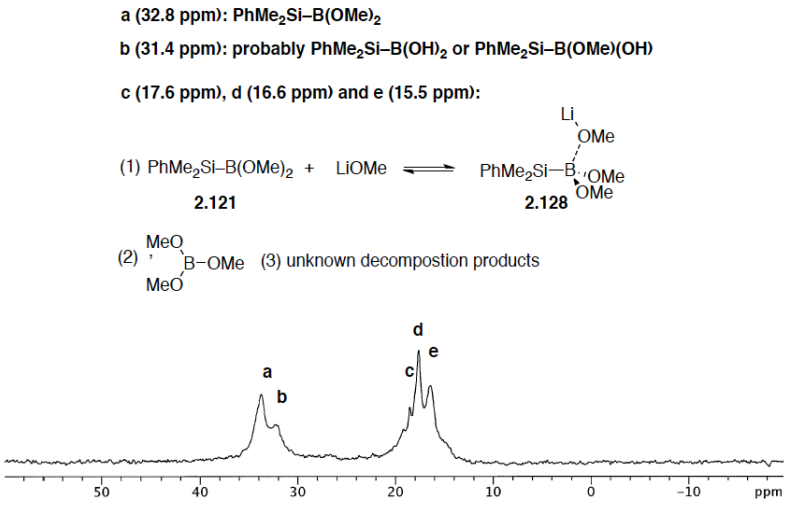


As shown in Scheme 2.5.14, the unpurified $(MeO)_2B–SiMe_2Ph$ (**2.121**) was treated with a chiral NHC solution in $d_8$-thf, which was prepared from deprotonation of the corresponding imidazolinium salt (**2.91**) by KHMDS [potassium bis(trimethylsilyl)amide]. The reason NaO*t*Bu or dbu was not used as base is that their conjugate acids may be able to cleave the Si–B bond of **2.120**, leading to the formation of $PhMe_2SiH$ and the corresponding boronate.

**Scheme 2.5.14. Synthesis of a chiral NHC•borylsilane complex**

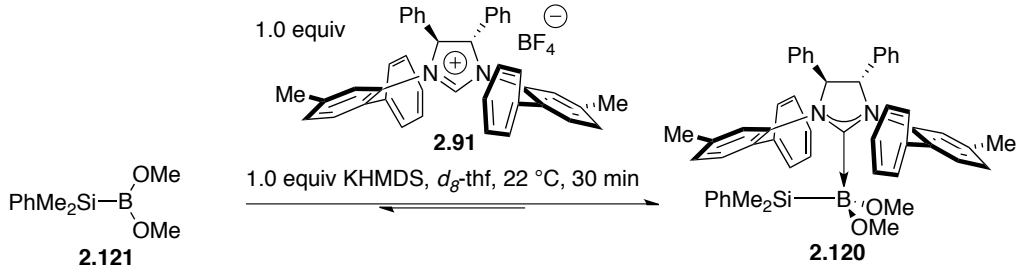


After 30 min, $^{11}$B NMR spectrum (Figure 2.5.11) shows the complete consumption of $(MeO)_2B–SiMe_2Ph$ (**2.121**). Instead, there is a new signal (**f**) at –0.4 ppm,

which is attributed as the chiral NHC•silylboron complexes (**2.120**). In addition, signal **c, d and e** still remain (~15.7 ppm).

**Figure 2.5.11. $^{11}$B NMR spectrum of a chiral NHC•silylboron complex**

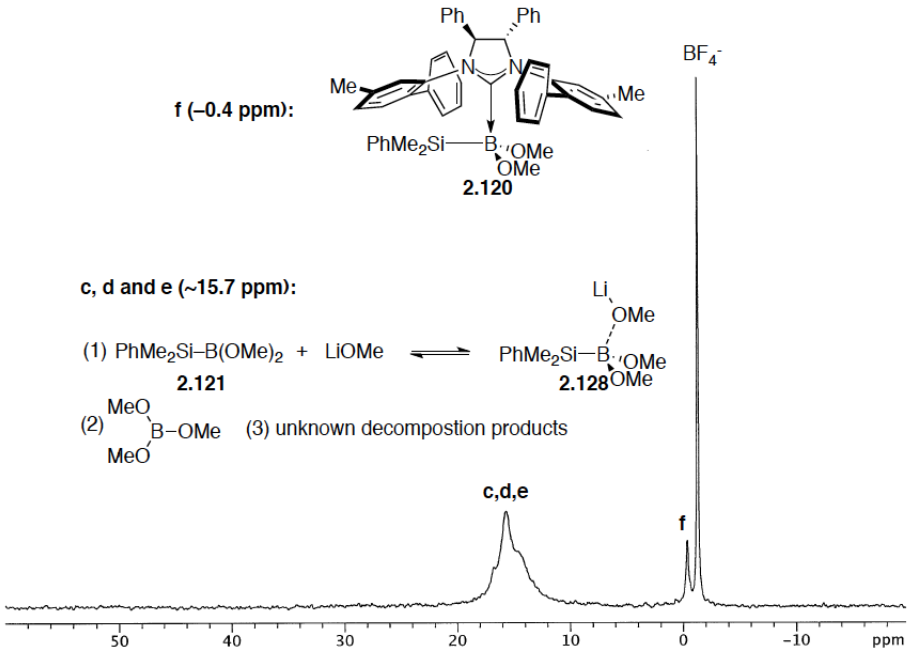


One concern about signal **f** in Figure 2.5.11 is that it could refer to a chiral NHC•$B(OMe)_3$ complex, since $B(OMe)_3$ is one of the starting materials to synthesize $(MeO)_2B–SiMe_2Ph$ (**2.121**). Thus, a control experiment where $B(OMe)_3$ was introduced into a solution of the same chiral NHC was run. As shown in Figure 2.5.12, the newly generated signal **g** likely corresponds to the chiral NHC•$B(OMe)_3$ complex **2.129**. Because the chemical shift of **g** (1.4 ppm) is different from the previously mentioned signal **f** (–0.4 ppm. Figure 2.5.11), we attribute signal **f** in Figure 2.5.11 as the evidence of chiral NHC•silylboron complexes (**2.120**).

**Figure 2.5.12. Control experiment: a chiral NHC•B(OMe)$_3$ complex**

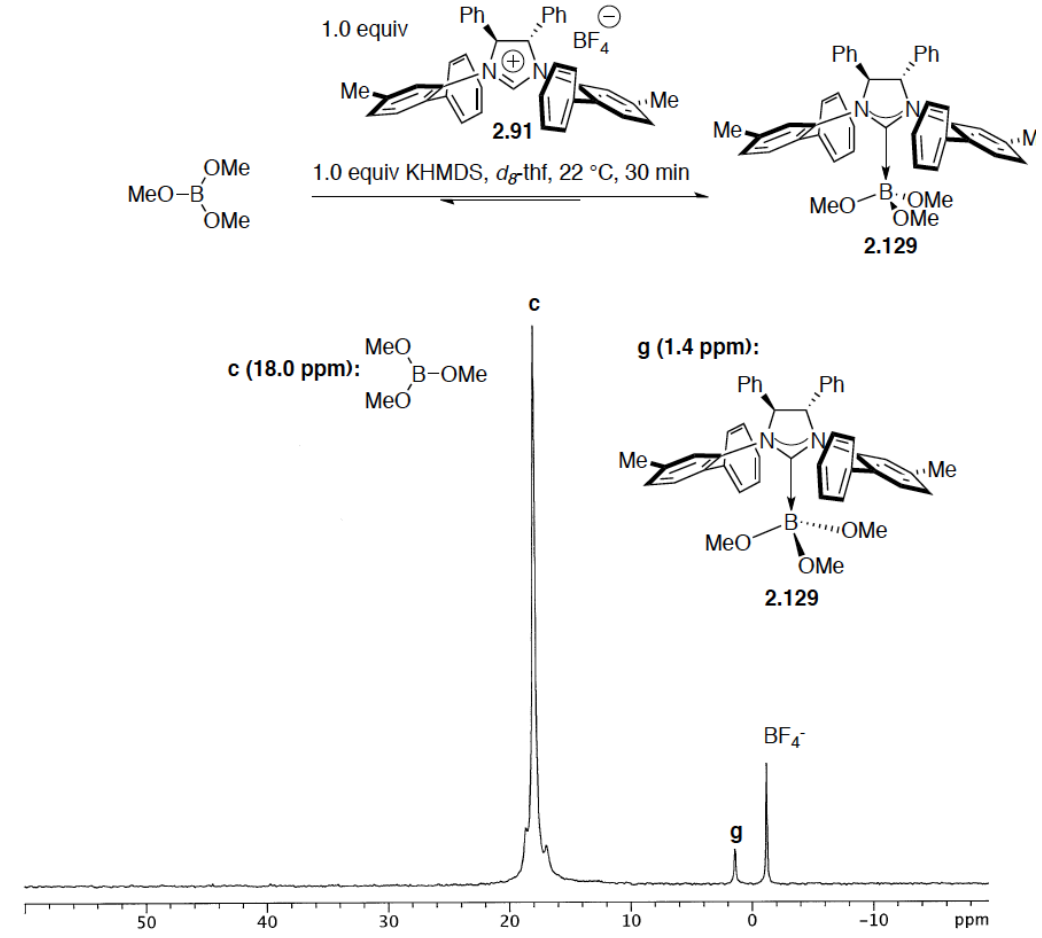


An achiral NHC (derived from **2.26b**) was also used to form the NHC•silylboron complex with $(MeO)_2B–SiMe_2Ph$. The $^{11}B$ NMR spectrum of this complexe is shown in Figure 2.5.13. The resolution of this spectrum is not as high as the previous ones, because **2.26b** is not fully dissolved. Again, complete disappearance of $(MeO)_2B–SiMe_2Ph$ (**2.121**) (32.8 ppm) was observed. Signal **f** corresponds to the $sp^3$ boron of the NHC•silylboron complexes (**2.130**). Its chemical shift (0.1 ppm) is slightly downfield than the one with the chiral NHC•silylboron complexes (–0.4 ppm). However, signal **f** is much more upfield than the one where the same NHC coordinates to (pin)B–$SiMe_2Ph$

(8.0 ppm). This suggests the NHC may form a tighter complex with $(MeO)_2B–SiMe_2Ph$ than with (pin)B–$SiMe_2Ph$.

**Figure 2.5.13. $^{11}B$ NMR spectrum of an achiral NHC•siylboron complex**

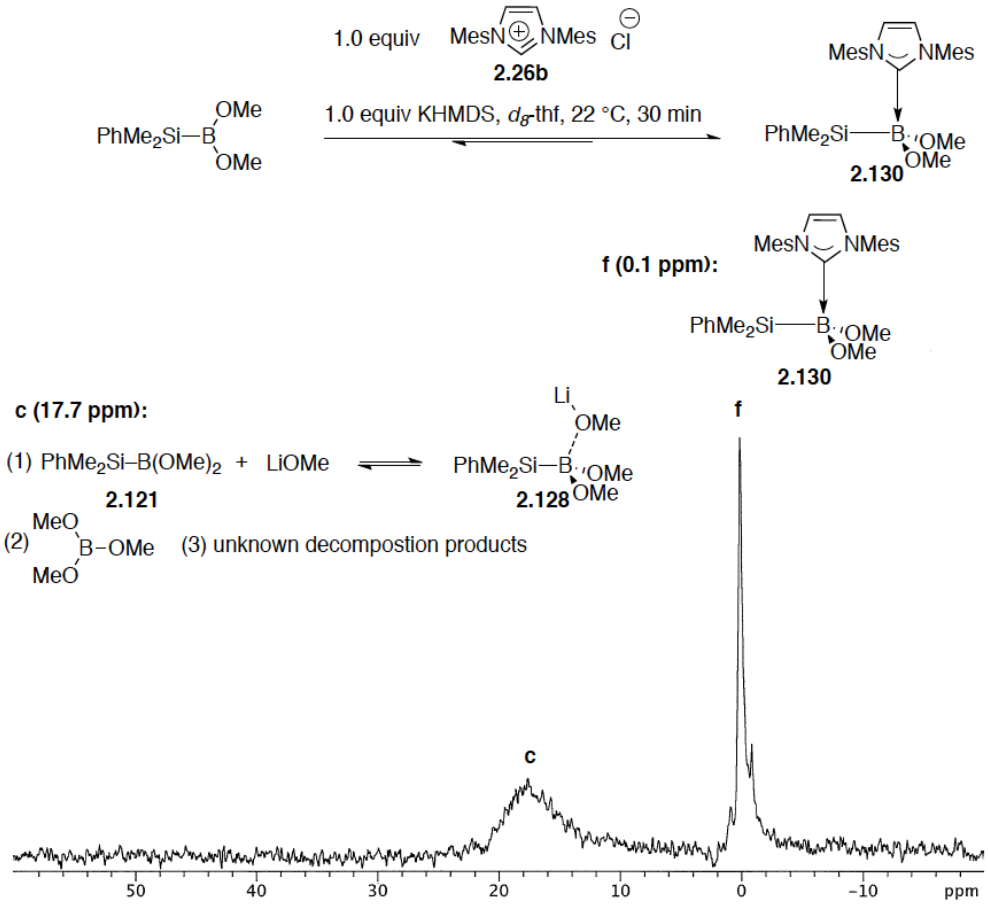


To further probe the chiral NHC•$(MeO)_2B–SiMe_2Ph$ complex, imidazolinium salt **2.91** ($^{13}C$), in which the central carbon is $^{13}C$-labeled, was synthesized. In the $^{13}C$ NMR, the central carbon appears at 160.2 ppm. Noticably, the $^{13}C–H$ coupling constant in the $^1H$ NMR spectrum is 209 Hz. Treatment of **2.91** ($^{13}C$) with 1.0 equivalent of KHMDS generates the NHC•$BF_3$ complex. This complex is very labile as the boron of $BF_3$ in $^{11}B$ NMR spectrum is a very broad signal at –0.9 ppm. In the $^{19}F$ NMR spectrum, the fluorine signal is too broad to be detected. The carbene carbon of this complex is at 164.7 ppm in the $^{13}C$ NMR spectrum, which is similar as the one in **2.91**. Subsequent addition of 1.0

equivalent of $(MeO)_2B–SiMe_2Ph$ results in complex **2.120** ($^{13}C$). In the $^{13}C$ NMR spectrum, the new signal at 181.2 ppm probably corresponds to the carbene carbon of **2.120** ($^{13}C$). In the $^{11}B$ NMR spectrum, the boron signal is still at –0.4 ppm.

**Scheme 2.5.15. Probing the formation of a chiral NHC•silylboron complex by spectroscopic analysis of a $^{13}C$-labeled chiral NHC.**

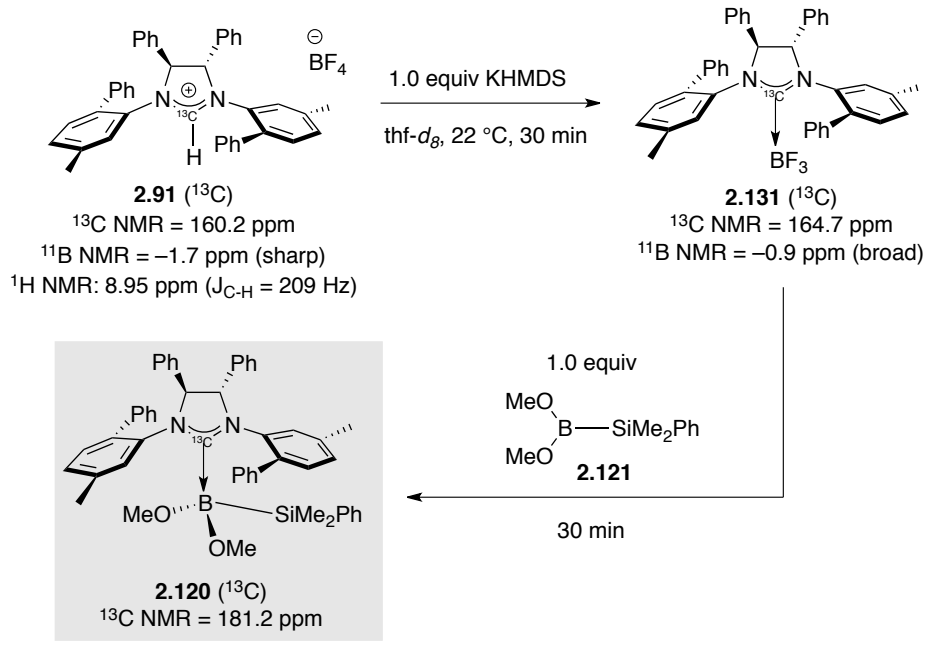


The above NMR experiments suggest the chiral NHC•silylboron complex is probably formed in a very short time in the silyl conjugate addition reactions. Such complex is likely responsible for delivering the $SiMe_2Ph$ unit to α,β-unsaturated carbonyls before its decomposition in the basic aqueous medium.

Then the obvious question would be: if $H_2O$ will decompose the $(pin)B–SiMe_2Ph$, imidazolinium salt and probably the chiral NHC•silylboron complex, why do we need $H_2O$? First, $H_2O$ is responsible for generation of a small amount of $(HO)_2B–SiMe_2Ph$, which is likely the active silylboron species for the chiral NHC binding. Without $H_2O$, we did not detect any formation of a chiral NHC•$(pin)B–SiMe_2Ph$ complex by NMR spectra.

Second, the catalytic enantioselective silyl conjugate addition reactions are much faster if $H_2O$ is used as the proton additive instead of MeOH. This suggests that the corresponding NHC•$(HO)_2$B–$SiMe_2$Ph is probably more reactive towards an α,β-unsaturated carbonyl than NHC•$(MeO)_2$B–$SiMe_2$Ph, which is not surprising since the two methyl groups in the latter complex may interact with the approaching substrate in the C–Si bond formation step. Third, the biphasic property of thf/$H_2O$ in the reaction mixture dramatically decreases the effective hydroxide anion in the organic layer. Thus, the decomposition of (pin)B–$SiMe_2$Ph, imidazolinium salt and the NHC•silylboron complex is much slowed in the actual reaction solutions.

## *2.6. Kinetic Studies on NHC Catalyzed Enantioselective Boryl/Silyl Conjugate Additions*

To better understand which step is the turnover limiting step in the NHC catalyzed boryl or silyl conjugate addition reactions, $^{19}F$ NMR pre-acquisition delay technique was used to study how the concentration of each component among the starting materials influences the rates of those reactions. For the BCA reactions, *p*-fluorophenyl substituted enone (**2.141**) was chosen as the substrate, while *p*-trifluoromethylphenyl substituted enone (**2.143**) as the substrate for the SCA reactions, because a significant amount of the proto-deboration product was detected if **2.143** was used in the kinetic study of BCA reactions. Nevertheless, in either type of reaction, the rate of the reaction was found to be first order in enone, $B_2(pin)_2$ [or $PhMe_2Si$–B(pin)] and imidazolinium salt, while zero order to dbu (Scheme 2.6.1). The $k_{obs}$ of each reaction was also calculated.

**Scheme 2.6.1. The results of kinetic studies on NHC catalyzed BCA reactions (a) and SCA reactions (b)**

**a)**

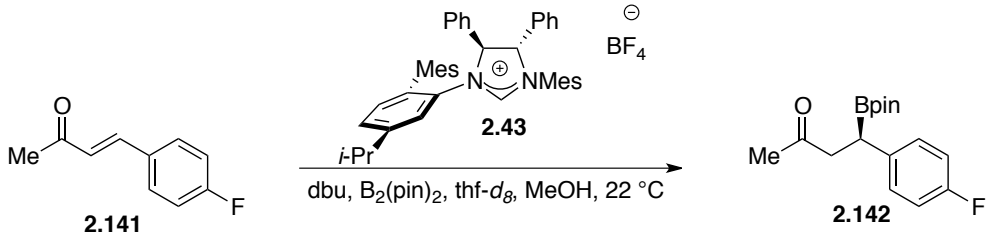


rate = $k_{obs}$[enone][**2.43**][$B_2(pin)_2$], $k_{obs}$ = 0.014 $L^2mol^{-2}s^{-1}$
C–B bond formation is likely the turnover limiting step.

**b)**

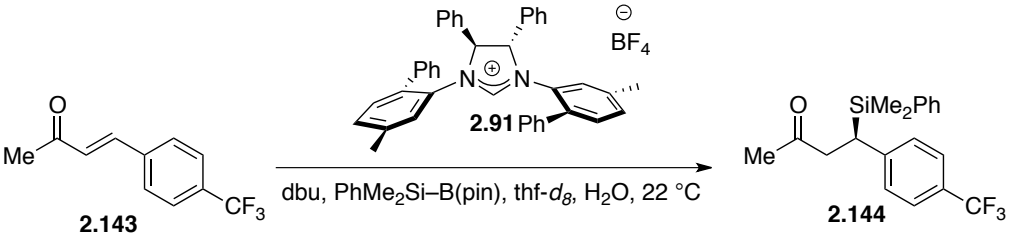


rate = $k_{obs}$[enone][**2.91**][$PhMe_2Si$–B(pin)], $k_{obs}$ = 0.63 $L^2mol^{-2}s^{-1}$
C–Si bond formation is likely the turnover limiting step.

The detailed procedure is as follows: In a $N_2$ filled glovebox, an oven-dried vial (8 x 1 cm) equipped with a stir bar was charged with **2.43** or **2.91**, dbu and thf-$d_8$ (0.60 mL). The mixture was allowed to stir for 30 min at 22 °C. $B_2(pin)_2$ or (pin)B–$SiMe_2Ph$ was added to the vial, followed by the addition of enone **2.141** or **2.143**. The mixture was transferred into an oven-dried NMR tube, sealed with a cap with Teflon tape and brought out of the glovebox. Prior to insertion of the NMR tube into the machine, MeOH (0.16 mL, 4.0 mmol) or $H_2O$ (8.6 mL, 0.048 mmol) was added to the NMR tube by syringe and the tube was inverted twice for mixing. The sample was immediately inserted into the NMR spectrometer and $^{19}F$ NMR spectra were collected every 30 seconds until the reaction reached approximately 15% conversion (initial kinetics). Substrate and product concentrations were determined by $^{19}F$ NMR analysis with the $BF_4^-$ signal serving as the internal reference (–151 ppm). After each experiment, the conversions of the reaction ([enone] vs reaction time) were plotted and the curve was fitted with a $2^{nd}$-order

polynomial function through the use of Microsoft Excel. The initial rate of each reaction was determined as the coefficient of the term $ax^1$ (x = reaction time) of the function. By varying the concentration of one component in the reaction at a time, a series of the initial rates were obtained. Scheme 2.6.2 and 2.6.3 show the relationships between the initial rate of the reaction and the concentration of each component. Based on those results, we drew the conclusions shown in Scheme 2.6.1.

**Scheme 2.6.2. The results of kinetic study on NHC catalyzed BCA reactions**

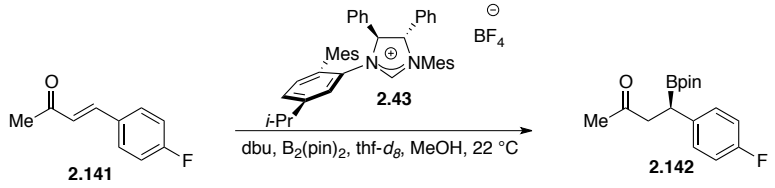


initial rate (mM/min)

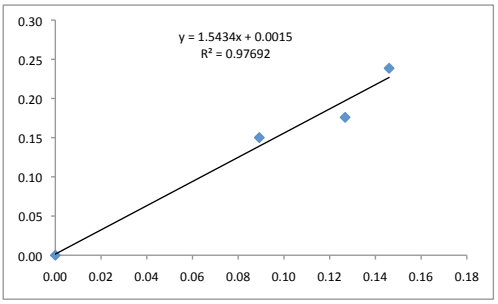


[enone] (M)

| [enone] (M) | initial rate (mM/min) |
|---|---|
| 0 | 0 |
| 0.0892 | 0.150 |
| 0.127 | 0.176 |
| 0.146 | 0.239 |

[**2.43**] = 0.0117 M
$[B_2(pin)_2]$ = 0.146 M
[dbu] = 0.293 M

initial rate (mM/min)

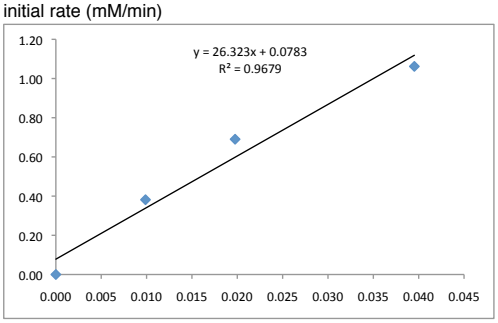


[**2.43**] (M)

| [**2.43**] (M) | initial rate (mM/min) |
|---|---|
| 0 | 0 |
| 0.0099 | 0.382 |
| 0.0198 | 0.690 |
| 0.0395 | 1.06 |

[enone] = 0.258 M
$[B_2(pin)_2]$ = 0.162 M
[dbu] = 0.646 M

initial rate (mM/min)

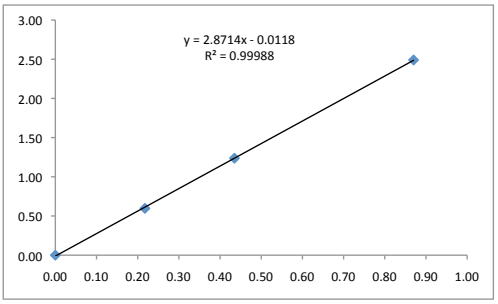


$[B_2(pin)_2]$ (M)

| $[B_2(pin)_2]$ (M) | initial rate (mM/min) |
|---|---|
| 0 | 0 |
| 0.218 | 0.597 |
| 0.435 | 1.24 |
| 0.870 | 2.49 |

[**2.43**] = 0.0129 M
[enone] = 0.258 M
[dbu] = 0.646 M

initial rate (mM/min)

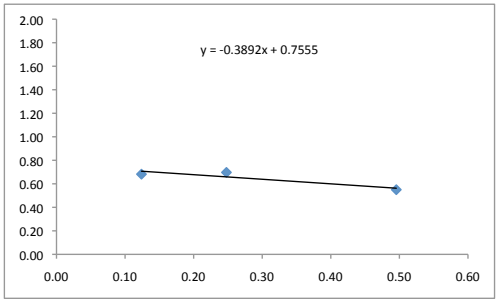


[dbu] (M)

| [dbu] (M) | initial rate (mM/min) |
|---|---|
| 0.124 | 0.682 |
| 0.248 | 0.697 |
| 0.496 | 0.550 |

[enone] = 0.129 M
$[B_2(pin)_2]$ = 0.646 M
[**2.43**] = 0.0129 M

**Scheme 2.6.3. The results of kinetic study on NHC catalyzed SCA reactions**

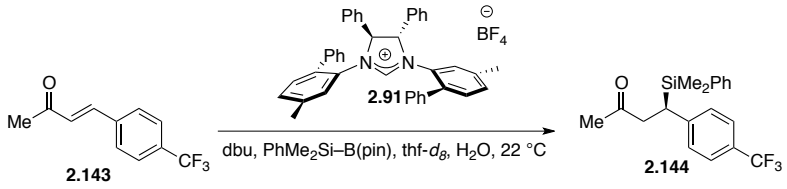


initial rate (mM/min)

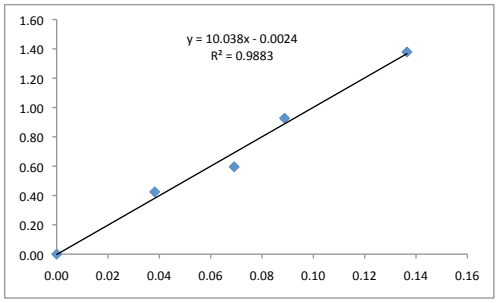


[enone] (M)

| [enone] (M) | initial rate (mM/min) |
|---|---|
| 0 | 0 |
| 0.0382 | 0.425 |
| 0.0692 | 0.596 |
| 0.0888 | 0.927 |
| 0.136 | 1.38 |

[**2.91**] = 0.00286 M
[$PhMe_2Si$–B(pin)] = 0.0956 M
[dbu] = 0.191 M

initial rate (mM/min)

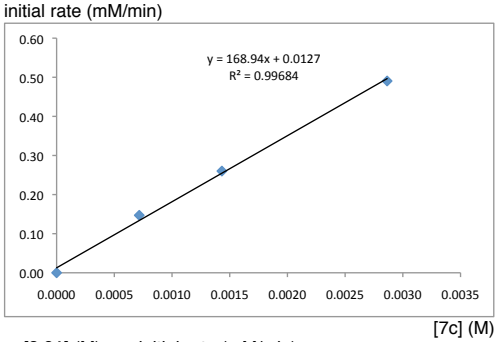


[7c] (M)

| [**2.91**] (M) | initial rate (mM/min) |
|---|---|
| 0 | 0 |
| 0.000716 | 0.147 |
| 0.00143 | 0.260 |
| 0.00286 | 0.491 |

[enone] = 0.0191 M
[$PhMe_2Si$–B(pin)] = 0.191 M
[dbu] = 0.191 M

initial rate (mM/min)

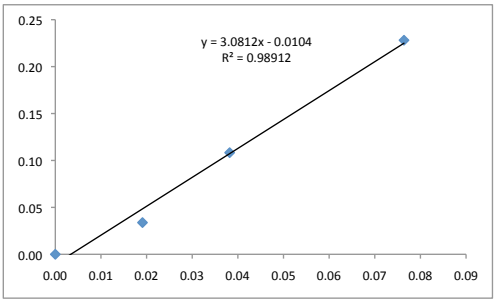


[$PhMe_2Si$–B(pin)] (M)

| [$PhMe_2Si$–B(pin)] (M) | initial rate (mM/min) |
|---|---|
| 0 | 0 |
| 0.0191 | 0.0338 |
| 0.0382 | 0.108 |
| 0.0764 | 0.228 |

[**2.91**] = 0.00286 M
[enone] = 0.0382 M
[dbu] = 0.382 M

initial rate (mM/min)

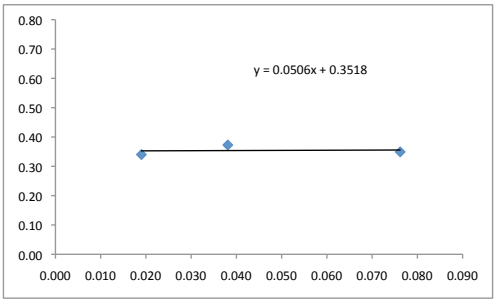


[dbu] (M)

| [dbu] (M) | initial rate (mM/min) |
|---|---|
| 0.0190 | 0.340 |
| 0.0381 | 0.373 |
| 0.0762 | 0.349 |

[enone] = 0.0191 M
[$PhMe_2Si$–B(pin)] = 0.191 M
[**2.91**] = 0.00286 M

In addition to the aforementioned kinetic studies, the rate law derivation was also performed according to our proposed mechanism in a simplified model.[101] Here we used NHC catalyzed boron conjugate additions as an example, and the similar rate law derivation can be performed for the corresponding SCA reactions. Based on the steady

(101) For a review on kinetic analysis of complex catalytic reactions, see: Blackmond, D. G. *Angew. Chem., Int. Ed.* **2005**, *44*, 4302–4320.

state assumption, the concentration of NHC•dibron complex does not change in the reaction mixture. Thus, the rate law can be derived as equation 6. Although further simplifications of the rate law can be performed based on additional assumptions (equations 7–10), we think the rate law of the NHC catalyzed BCA reactions is probably close to equation 11. This is because the fast equilibrium between NHC + diboron and NHC•diboron complex (supported by previously mentioned $^{11}$B NMR studies) probably results in $k_{-1}>>k_2$[enone] and $k_1$[diboron]. Thus, $k_1$[diboron]+$k_{-1}$+$k_2$[enone] ≈ $k_{-1}$, leading to the simplified rate law as equation 11, which is consistent with the previously mentioned $^{19}$F NMR kinetic study.

**Scheme 2.6.4. The rate law derivation of chiral NHC catalyed BCA reactions**

**In a simplified model:**

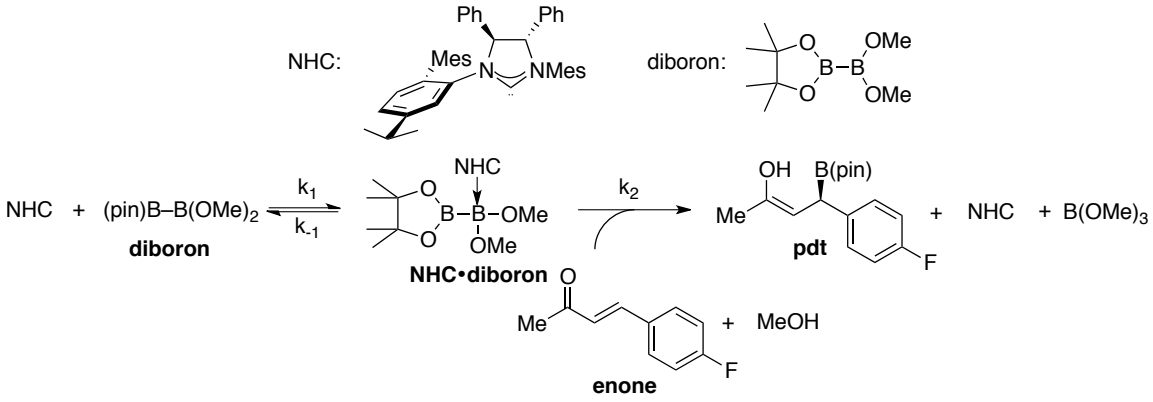

**eq 1** $[NHC] = [NHC]_0 - [NHC\bullet diboron]$ $[NHC]_0$: Initial concentration of NHC

**according to the steady state assumption:**

**eq 2** $d[NHC\bullet diboron]/dt = k_1[NHC][diboron] - k_{-1}[NHC\bullet diboron] - k_2[NHC\bullet diboron][enone] = 0$

**eq 3** $k_1([NHC]_0 - [NHC\bullet diboron])[diboron] - k_{-1}[NHC\bullet diboron] - k_2[NHC\bullet diboron][enone] = 0$

**eq 4**
$$[NHC\bullet diboron] = \frac{k_1[NHC]_0[diboron]}{k_1[diboron] + k_{-1} + k_2[enone]}$$

**eq 5**
$$d[pdt]/dt = k_2[NHC\bullet diboron][enone]$$

**eq 6**
$$d[pdt]/dt = \frac{k_1k_2[NHC]_0[diboron][enone]}{k_1[diboron] + k_{-1} + k_2[enone]}$$

---

When [enone] is low, the rate law can be simplified to:

**eq 7**
$$d[pdt]/dt = \frac{k_1k_2[NHC]_0[diboron][enone]}{k_1[diboron] + k_{-1}}$$
The reaction is first order to enone.

When [enone] is high, the rate law can be simplified to:

**eq 8**
$$d[pdt]/dt = \frac{k_1k_2[NHC]_0[diboron][enone]}{k_2[enone]} = k_1[NHC]_0[diboron]$$
The reaction is zero order to enone (saturation kinetics)

When [diboron] is low:

**eq 9**
$$d[pdt]/dt = \frac{k_1k_2[NHC]_0[diboron][enone]}{k_{-1} + k_2[enone]}$$
The reaction is first order to diboron.

When [diboron] is high:

**eq 10**
$$d[pdt]/dt = \frac{k_1k_2[NHC]_0[diboron][enone]}{k_1[diboron]} = k_2[NHC]_0[enone]$$
The reaction is zero order to diboron (saturation kinetics)

In our case, it is probably $k_1[diboron] + k_{-1} + k_2[enone] \approx k_{-1}$, because of fast and reversible coordination of NHC to diboron. Thus, the rate law can be simplified to:

**eq 11**
$$d[pdt]/dt = \frac{k_1k_2[NHC]_0[diboron][enone]}{k_{-1}}$$

The reaction is first order to NHC, diboron and enone.

In conclusion, since the NHC catalyzed enantioselective boryl or silyl conjugate additions are found to be first order in enone, $B_2(pin)_2$ [or $PhMe_2Si–B(pin)$] and

imidazolinium salt, while zero order in dbu. We believe the C–B or C–Si bond formation is probably the rate limiting step.

## *2.7. Computational Studies on the Stereochemical Models of NHC Catalyzed Enantioselective BCA/SCA Reactions*

Density Functional Theory (DFT) calculations (with Dr. Jan Haeffner) were carried out in an effort to gain more insight into the mechanism of the aforementioned NHC-catalyzed conjugate addition reactions of a B(pin) or $SiPhMe_2$ unit to acyclic and cyclic α,β-unsaturated carbonyl compounds.[102] We have previously demonstrated that the B–B bond (or B–Si bond) upon coordination of a Lewis basic NHC becomes polarized (activated), whereupon the resulting nucleophilic B(pin) (or $SiPhMe_2$) unit of the complex readily attacks the electrophilic enone. The forming of the C–B (or C–Si) bond is, according to our kinetic studies (see the experimental section for details), suggested to be the rate limiting step. Since it involves the enantioselective transfer of the B(pin) or $SiPhMe_2$ unit to the unsaturated carbonyl, we believe this is also the stereochemical determine step. Consequently, we decided to focus our DFT studies on this step with the intention to further understand how these catalytic reactions operate, the differences between the transition states of non-enantioselective and enantioselective reactions, and the origin of enantioselectivity.

Our investigations begin with a non-enantioselective reaction (system **I**), where the boron conjugate addition to cyclohexenone is catalyzed by a small achiral NHC derived from 1,3-dicyclohexylimidazolium salt. As shown in Scheme 2.7.1, the achiral

(102) Ground state and transition state geometries were optimized using DFT methodology. The B97-D functional and 6-31G* basis set were employed. Tetrahydrofuran solvation was modeled using the PCM model. See the supporting information for details.

NHC coordinates to one of the boron atoms in $B_2(pin)_2$ resulting in a tight Lewis acid–base complex **i**. The substrate (cyclohexenone) then approaches to **i**, and the B(pin) group, bearing an $sp^2$ boron, subsequently transfers to the enone. This heterolytic bond cleavage and bond formation step generates a zwitter ion [NHC–B(pin) cation and enolate anion], which rapidly reorganizes to the energetically more stable complex **iv**. This complex then breaks apart and releases the NHC and the boryl enolate species **v**. The transition state of the B(pin) transfer step is depicted in **A**. The calculations show that the B(pin) transfer occurs in a concerted manner, that is, as the B–B bond breaks the C–B bond forms simultaneously. In the transition state, the distance between the two boron atoms is 2.05 Å, and the distance between the β carbon of cyclohexenone and the boron is 1.96 Å. The intrinsic free energy of activation $\Delta G^{\neq}$ is 18.0 kcal/mol.

**Scheme 2.7.1. System I: a small achiral NHC promoted boron conjugate addition to cyclohexenone**

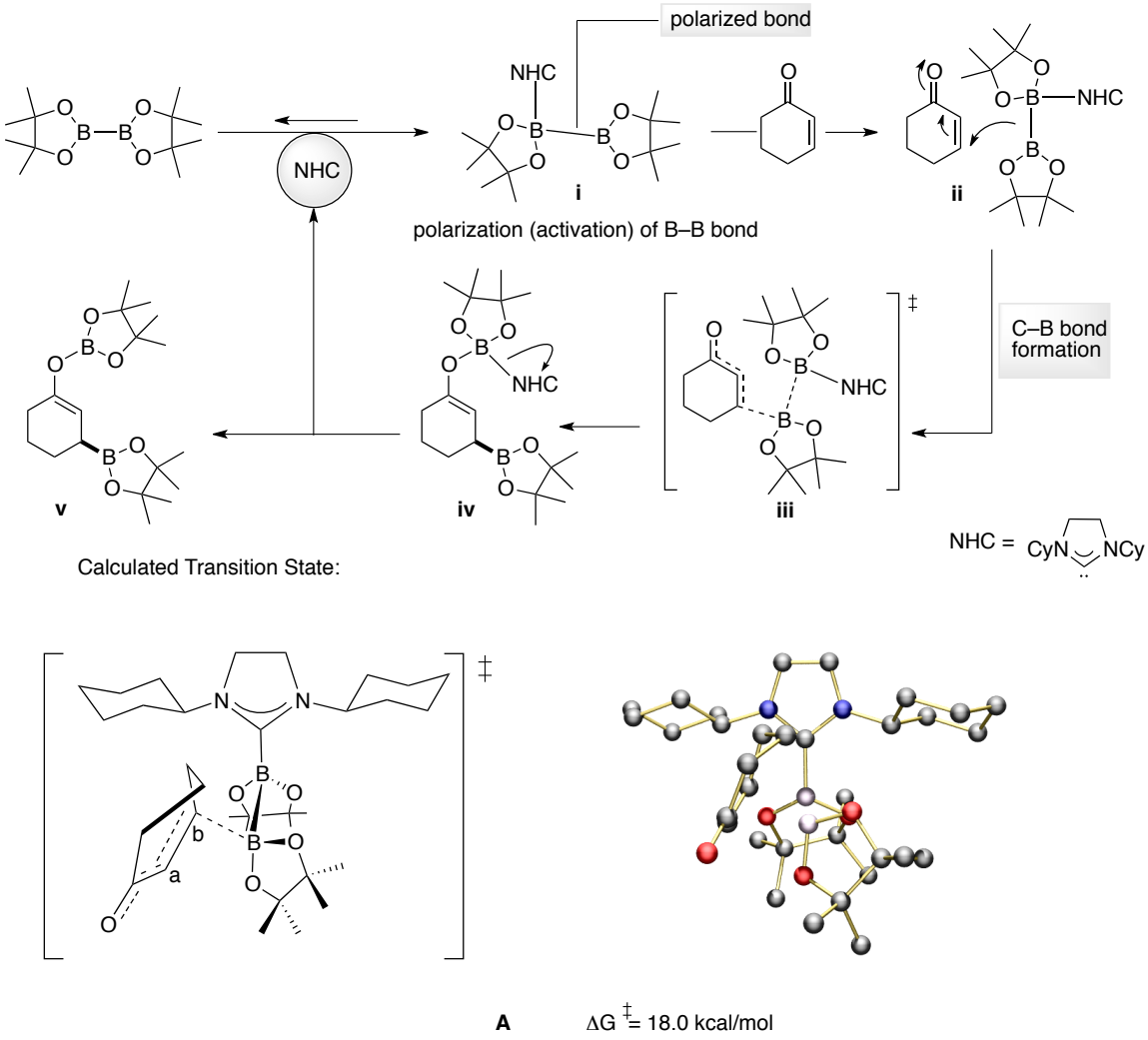


Next, we investigated the enantioselective boron conjugate addition to a cyclic enone catalyzed by a chiral NHC derived from **2.91**. Experimental results obtained from reactions with this and several other chiral NHCs showed poor enantioselectivity when cyclohexenone is used as substrate (for instance, 55:45 er with an NHC derived from **2.91**). However, the boron conjugate addition to a sterically more hindered β-substituted cyclohexenone **2.48a** resulted in good enantioselectivity (er = 84:16) and high yield (85%) (Scheme 2.7.2, system **II**).

Additional noteworthy points merit mention: 1) Boron conjugate additions catalyzed by chiral NHCs only proceed in the presence of MeOH. Experimental results indicate that MeOH may play a dual role in the reaction by acting as a proton source and promoting methanolysis of one of the pinacolato groups of $B_2(pin)_2$. Our computational studies suggest that this hydrolysis eases the coordination of the bulky, chiral NHC to the boron center. 2) Dbu proved to be a more efficient base than the previously used NaO*t*-Bu. Besides deprotonation of the imidazolinium salt (to generate the NHC), we speculate that the protonated form of dbu ($dbuH^+$) serves as a Lewis acid to activate the carbonyl group of the enone. Two transition states (**B1** and **B2**) for the addition of B(pin) unit to the enone that results in the two observed enantiomeric products were optimized. In the transition state **B1** (being lower in energy than that of **B2**), the substrate approaches the NHC•diboron complex from the right side. The distance between the two boron centers is 2.21 Å and the forming C–B bond length is 2.12 Å. The activation barrier $\Delta G^{\neq}$ is 36.8 kcal/mol. The longer bond lengths and the higher activation energy compared to system **I** may be due to the sterically more demanding substrate and NHC. The transition state **B2**, which is higher in energy than **B1** by 4.8 kcal/mol, leads to the minor product. The breaking B–B bond length is 2.09 Å and the forming C–B bond length is 2.08 Å. Unfavorable steric interactions (highlighted in **B2**), which might be responsible for the variation in the N–C–B bond angle (from 123° to 133°), may explain why the reaction follows the pathway involving transition state **B1**.

**Scheme 2.7.2. System II: a chiral NHC promoted boron conjugate addition to β-methyl-cyclohexenone**

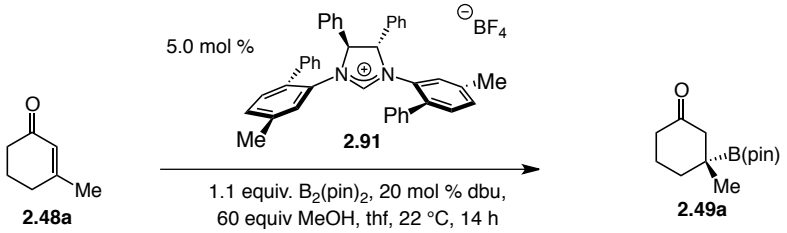


**85% yield, 84:16 er**

**Calculated Transition State:**

**B1 (favored)**

**$\Delta G^{\ddagger}$ = 36.8 kcal/mol**

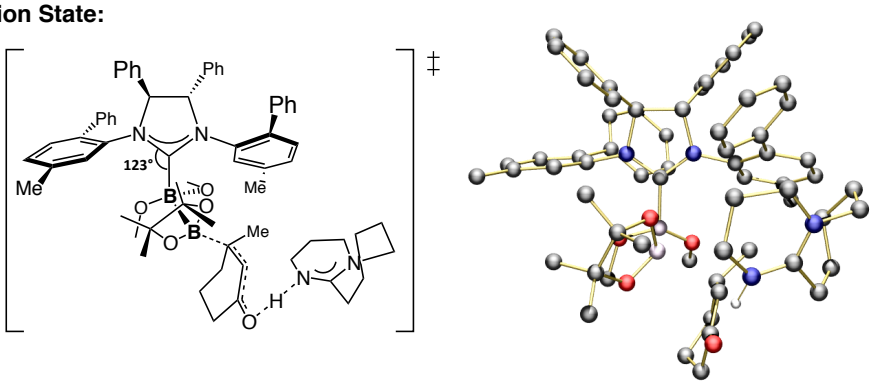


**B2 (unfavored)**

**$\Delta G^{\ddagger}$ = 41.6 kcal/mol**

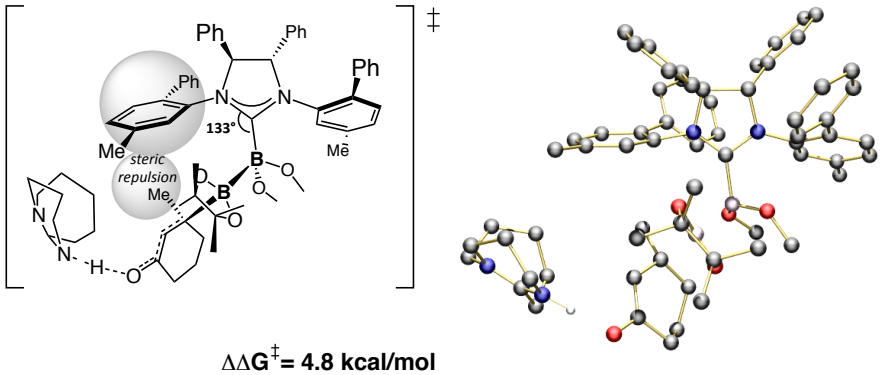


**$\Delta\Delta G^{\ddagger}$ = 4.8 kcal/mol**

The same chiral NHC also catalyzes the boron conjugate addition to acyclic enones with high yield and enantioselectivity. Under the reaction conditions shown in Scheme 3, boron conjugate additions to enone **2.44a** affords the desired β-boryl ketone (**2.45a**) in 82% yield and 92:8 er (system **III**). Similar to the previous reaction, MeOH and 20 mol % dbu are required to facilitate the reaction. The partially methanolyzed diboron species $(MeO)_2B–B(pin)$ is believed to be the active diboron species. In the favored transition state **C1**, the distance between the two borons is 2.22 Å and the one between the β carbon of enone **2.44a** and the boron is 2.12 Å. These values are very

similar to the ones in **B1** (2.21 Å and 2.12 Å, respectively). However, the activation energy of **C1** ($\Delta G^{\neq}$ = 25.8 kcal/mol) is significantly lower than the one of transition state **B1** (36.8 kcal/mol). This is probably due to the less sterically hinderance in acyclic disubstituted enone **2.44a**, compared to cyclic trisubstituted enone **2.48a**. The unfavored transition state **C2** is 1.4 kcal/mol higher in energy than **C1**, probably because of similar steric repulsion interactions between the phenyl substituent of enone **2.44a** and the N-aryl motif of the NHC (highlighted in **C2**). Such interactions may also lead to the variation of the N–C–B angle from 123° to 133° in TS **C1** and **C2**, respectively.

**Scheme 2.7.3. System III: a chiral NHC promoted boron conjugate addition to an acyclic enone**

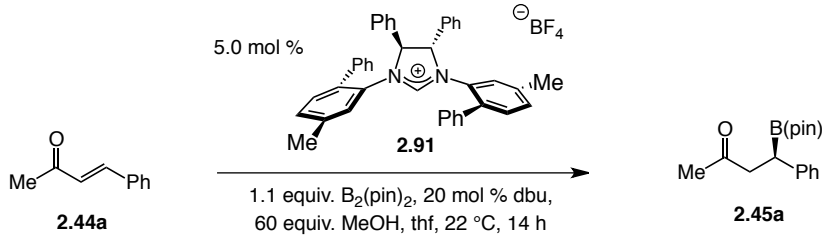


**82% yield, 92:8 er**

**Calculated Transition State:**

**C1 (favored)**

**$\Delta G^{\ddagger}$= 25.8 kcal/mol**

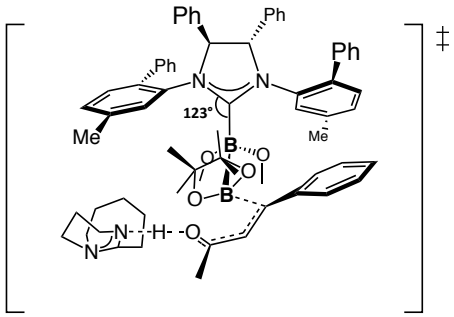


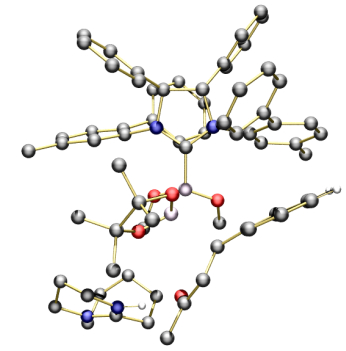

**C2 (unfavored)**

**$\Delta G^{\ddagger}$= 27.2 kcal/mol**

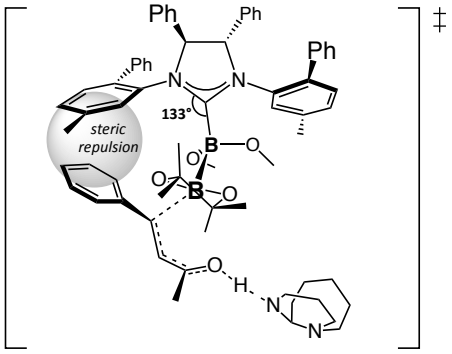


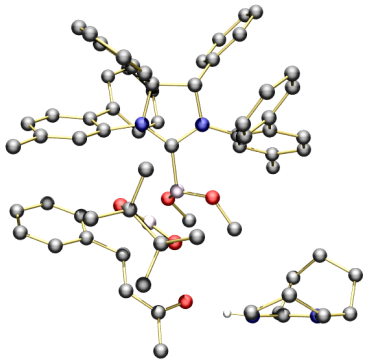

**$\Delta\Delta G^{\ddagger}$= 1.4 kcal/mol**

We also developed NHC-catalyzed silyl conjugate additions to cyclic and acyclic α,β-unsaturated carbonyls. There are several differences compared to the boron conjugate addition variants: 1) The calculated B–Si bond length of (pin)B–$SiPhMe_2$ is 2.05 Å, which is significantly longer than the bond length of B–B in $B_2(pin)_2$ (1.70 Å). 2) The reaction proceeds efficiently when $H_2O$ is used as a co-solvent with thf. As mentioned before, $H_2O$ is probably responsible for the hydrolysis of the B(pin) unit, generating $(HO)_2B$–$SiPhMe_2$, which may facilitate effective coordination of NHC to the boron

center (see the previous discussion on the corresponding $^{11}B$ NMR experiments). In system **IV**, NHC-catalyzed silyl conjugate addition to cyclohexenone **2.25a** proceeds efficiently and affords β-silyl carbonyl **2.90a** in 97% yield and an er value of 98:2 within 3 hours. The geometries optimized for transition states are shown as **D1** (favored) and **D2** (unfavored) in Scheme 2.7.4. In the former one, the cyclohexenone molecule approaches to the NHC•$(HO)_2B–SiPhMe_2$ complex beneath the N-aryl motif of the NHC. The N–C–N angle is 123°, which indicates a low strain energy. However, in transition state **D2**, the methyl groups of $(HO)_2B–SiPhMe_2$ are crowded with the left N-aryl motif of the NHC, since the substrate approaches from the opposite side. The larger N–C–N angle (129°) may be the result of this steric interaction. **D2** is therefore higher in energy (1.6 kcal/mol) than **D1**, which is consistent with the observed enantioselectivity (98:2 er). Another feature of this silyl conjugate addition is that both the B–Si and C–Si bonds in the transition state are significantly longer than the previously described B–B and C–B bonds in the boron conjugate additions. In transition state **D1**, the distance between the silicon and boron centers is 3.37 Å, and the one between the silicon and the β carbon is 2.89 Å. This indicates that the B–Si bond is almost completely broken before the Si–C bond forms.

**Scheme 2.7.4. System IV: a chiral NHC promoted silyl conjugate addition to a cyclic enone**

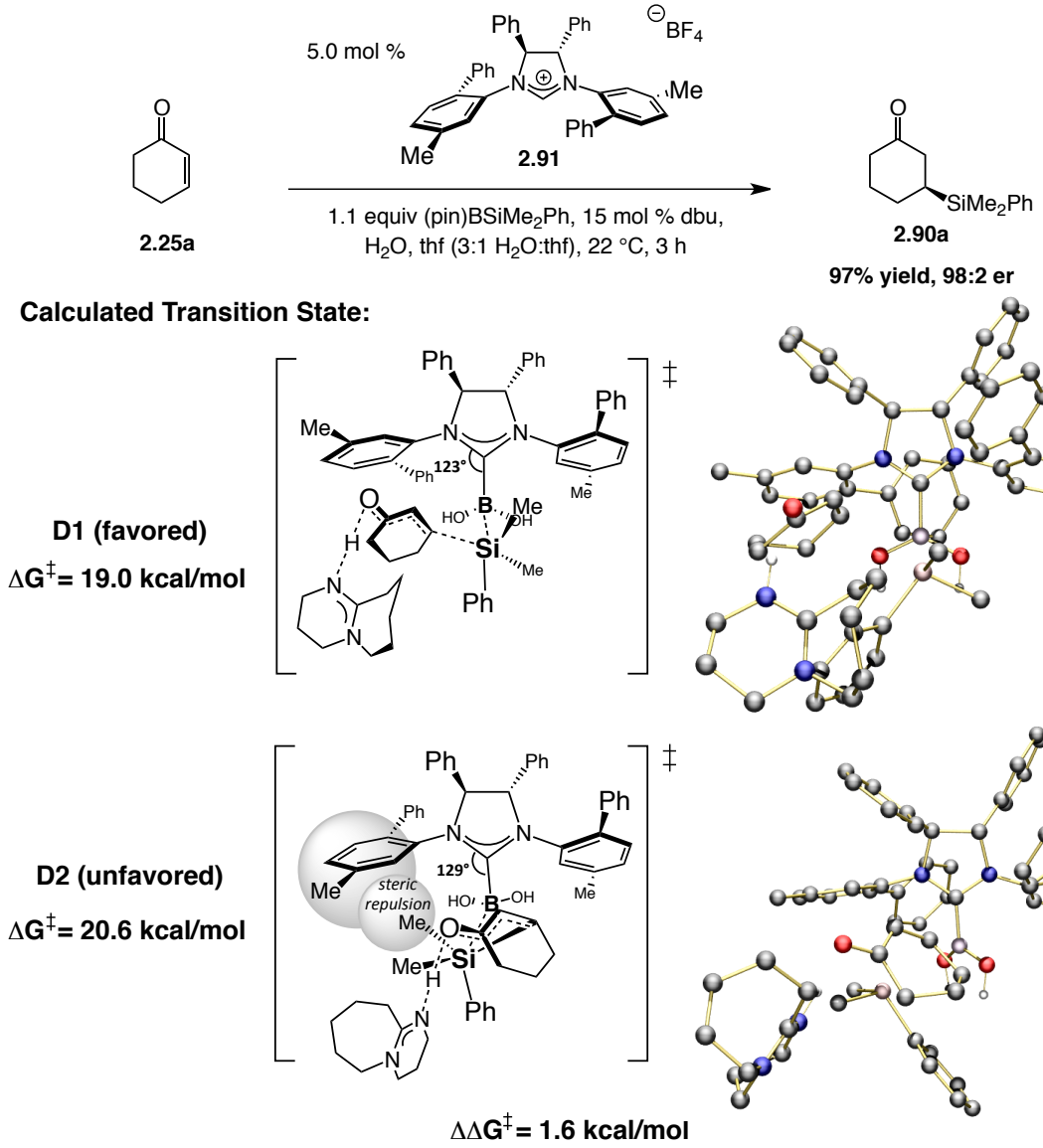


At last, computations were carried out on the NHC catalyzed enantioselective silyl conjugate addition to an acyclic enone (system **V**). The experiment shows that with 7.5 mol % NHC derived from **2.91** in 3:1 thf:$H_2O$, β-silyl carbonyl **2.90g** is isolated in quantitative yield and 94:6 er (Scheme 2.7.5). The computational study suggests an interesting feature of the transformation: instead of Lewis acid activation of the carbonyl group by $dbuH^+$, an intramolecular chelation by the two hydroxyl groups of the $(HO)_2B$–

$SiPhMe_2$ to the carbonyl group of the enone takes place in both transition states **E1** and **E2**. The activation barrier of **E1** is 14.8 kcal/mol. In contrast, the unfavored pathway via transition state **E2** is 2.0 kcal/mol higher in energy than **E1**. This is probably because an unfavored steric repulsion between the phenyl substituent of **2.44a** and the N-aryl motif of the NHC. Such interactions is probably responsible for the larger N–C–N angle (129°) in **E2** compared with 124° in **E1.**

**Scheme 2.7.5. System V: a chiral NHC promoted silyl conjugate addition to an acyclic enone**

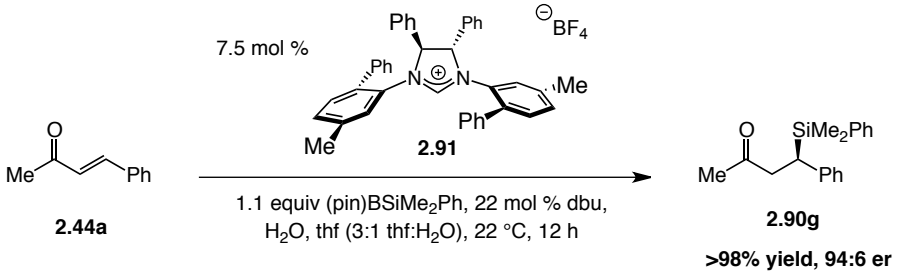


**Calculated Transition State:**

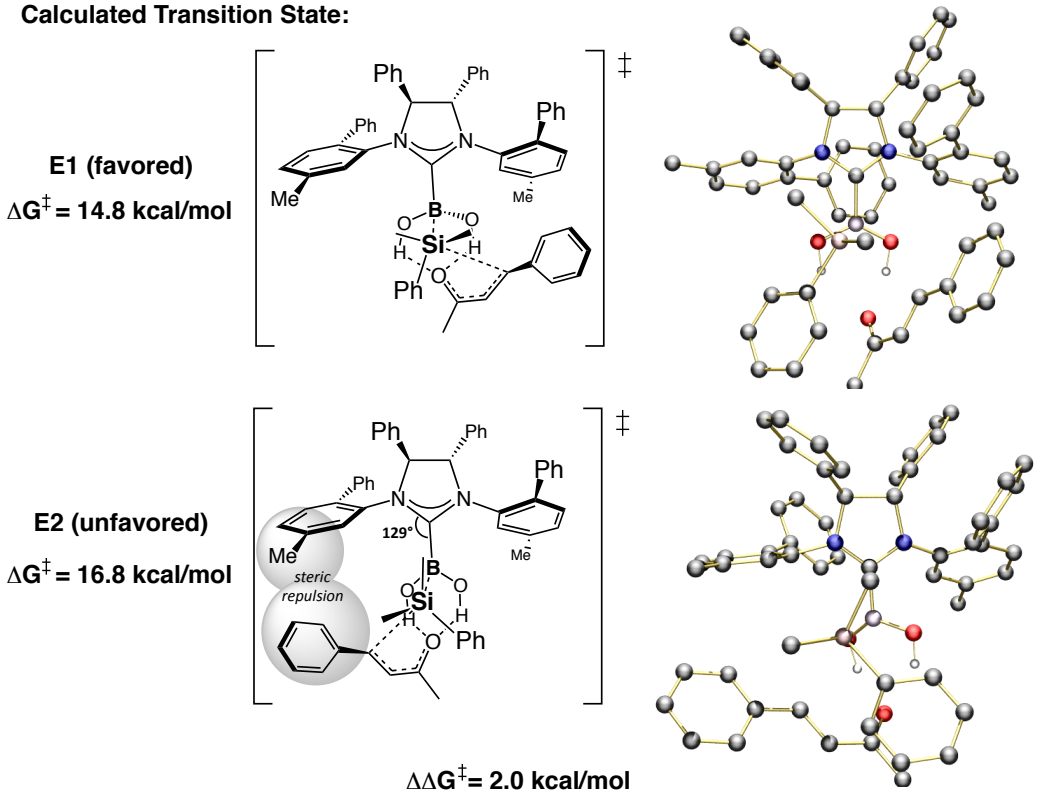


## *2.8. Conclusions*

Mechanistic studies, including NMR, kinetic experiments and computational modelings, have provided useful information for understanding how NHC catalyzed boryl or silyl conjugate additions work. Those reactions are believed to proceed in a way that α,β-unsaturated carbonyls react with NHC•diborons or NHC•silylborons to form C–B or C–Si bonds enantioselectively. MeOH or $H_2O$ are essential for partial hydrolysis of $B_2(pin)_2$ or (pin)B–$SiMe_2Ph$, generating sterically more accessible diboron or silylboron intermediates. The coordination of a chiral NHC to those intermediates is supported directly or indirectly by NMR spectroscopy. Kinetic studies reveal the C–B or C–Si bond formation step is likely the rate limiting step. Through computational investigations we understand how NHC influence the enantioselectivity, and why in certan cases BCA and SCA reactions give products with opposite stereochemistry.

The findings illustrated above offer some of the needed insight for future development of Lewis base catalyzed reactions, which are one of the most fruitful areas in synthetic organic chemistry.

## *2.9. Acknowledgment*

I thank Prof. Amir H. Hoveyda for the guidance in the mechanistic studies. I am also grateful to Dr. Adil R. Zhugralin, Dr. Jeannette M. Garcia, Suttipol Radomkit and Dr. Jan Haeffner for their cooperations in this project. I also appreciate the enlightening discussions with all the other Hoveyda group members.

This work was supported financially by the NIH (GM-57212) and the NSF (CHE-1111074). We thank Boston College and the chemistry department for providing great assistance and facilities.

## *2.10. Experimental Section*

### *2.10.1. Preparations and Characterizations of New Compounds*

**General.** Infrared (IR) spectra were recorded on a Bruker FT-IR Alpha (ATR mode) spectrophotometer, $\nu_{max}$ in $cm^{-1}$. Bands are characterized as broad (br), strong (s), medium (m), and weak (w). $^{1}H$ NMR spectra were recorded on a Varian Unity INOVA 400 (400 MHz), 500 (500 MHz) or 600 (600 MHz) spectrometer. Chemical shifts are reported in ppm from tetramethylsilane with the solvent resonance as the internal standard ($CDCl_3$: δ 7.26 ppm). $^{13}C$ NMR spectra were recorded on a Varian Unity INOVA 400 (100 MHz) spectrometer with complete proton decoupling. Chemical shifts are reported in ppm from tetramethylsilane with the solvent resonance as the internal standard ($CDCl_3$: δ 77.16 ppm). $^{11}B$ NMR were recorded on a Varian Unity INOVA 500 (128 MHz) with $BF_3$•$(OEt)_2$ resonance as the external reference (thf-$d_8$: δ 0.0 ppm). $^{19}F$ NMR were recorded on a Varian Unity INOVA 400 (376 MHz) with $CF_3COOH$ resonance as the external reference (thf-$d_8$: δ –76.55 ppm). Data are reported as follows: chemical shift, integration, multiplicity (s = singlet, d = doublet, t = triplet, q = quartet, m = multiplet, br s = broad singlet), and coupling constants (Hz). High-resolution mass spectrometry was performed on a JEOL AccuTOF-DART (positive mode) or ESI-MS (positive mode) at the Mass Spectrometry Facility, Boston College. Enantiomeric ratios were determined by HPLC analysis (high-performance liquid chromatography) with a Shimadzu chromatograph (Chiral Technologies Chiralpak AD-H (4.6 x 250 mm)) in comparison with authentic racemic materials. Specific rotations were measured on a Rudolph Research Analytical Autopol IV Polarimeter.

Unless otherwise noted, reactions were carried out with distilled and degassed

solvents under an atmosphere of dry $N_2$ in oven- (135 ºC) or flame-dried glassware with standard dry box or vacuum-line techniques. Solvents were purified under a positive pressure of dry Ar by a modified Innovative Technologies purification system: toluene was purified through a copper oxide and alumina column; $CH_2Cl_2$ and $Et_2O$ were purged with Ar and purified by passage through two alumina columns. Tetrahydrofuran (Aldrich) was purified by distillation from sodium benzophenone ketyl prior to use. Methanol and *i*-propanol were distilled over sodium. $CDCl_3$ and $d_8$-thf were purchased from Cambridge Isotope Laboratories and used as received. All work-up and purification procedures were carried out with reagent grade solvents (purchased from Fisher Scientific) under air. **1,3-Bis(2,4,6-trimethylphenyl)imidazolium chloride** was purchased from Aldrich and used as received. **Bis(pinacolato)diboron** [$B_2(pin)_2$] was purchased from Frontier Scientific. It was purified by recrystallization from hot anhydrous pentane and subsequently dried under high vacuum at 50 ºC for 18 h. **Chlorodimethylphenylsilane** ($PhMe_2SiCl$) was purchased from Aldrich and used as received. **2-Cyclohexen-1-one** was purchased from Aldrich and distilled *in vacuo* prior to use. **1,8-Diazabicyclo[5.4.0]undec-7-ene** (dbu) was purchased from Aldrich and distilled *in vacuo* prior to use. **1,3-Dicyclohexylimidazolium tetrafluoroborate** was purchased from Aldrich or TCI America and purified by silica gel chromatography followed by trituration from $CH_2Cl_2$/hexanes prior to use. **Dimethylphenylsilylpinacolatoborane** [$PhMe_2Si–B(pin)$)] was purchased from Aldrich and distilled *in vacuo* prior to use. **Lithium bromide** was purchased from Strem and used as received. **Potassium bis(trimethylsilyl)amide** (KHMDS) was purchased from Aldrich and used as received. **Sodium *tert*-butoxide (NaO*t*-Bu)** was purchased from Strem and used as received.

**Trimethyl borate** was purchased from Aldrich and used as received. Unless otherwise noted, all the other α,β-unsaturated carbonyls, imidazolinium salts and the corresponding β-boryl (or silyl) carbonyls were reported previously.[51,55]

**$^{13}$C-Labeled Imidazolinium Salt 2.91** was prepared according to the reported procedure.[56c] IR (neat): 3061 (m), 3035 (m), 2923 (w), 1618 (m), 1574 (s), 1487 (m), 1457 (m), 1444 (m), 1275 (s), 1216 (s), 1054 (s), 827 (s), 770 (s), 755 (s), 736 (s), 699 (s), 595 (m), 522 (s) cm$^{-1}$; $^{1}$H NMR ($CDCl_3$, 400 MHz): δ 8.95 (d, $J_{C\text{-}H}$ = 208.8 Hz, 1H), 7.56–7.44 (m, 6H), 7.35–7.30 (m, 6H), 7.25–7.16 (m, 6H), 7.10–7.04 (m, 4H), 6.71–6.69 (m, 4H), 4.68 (s, 2H), 2.28 (s, 6H); $^{13}$C NMR ($CDCl_3$, 100 MHz): δ 157.2 ($^{13}$C labeled carbon), 139.8, 138.1, 134.6, 133.7, 131.4, 131.3, 131.0, 130.7, 129.9, 129.4, 129.3, 129.2, 128.4, 128.3, 128.1, 99.1, 75.0, 20.8; $^{11}$B NMR ($d_8$-thf, 160 MHz): $\delta$ –1.7 (s); $^{19}$F NMR ($d_8$-thf, 376 MHz): $\delta$ –152 (s, 4F); HRMS (ESI$^+$): Calcd for $^{12}C_{40}{}^{13}C_1H_{35}N_2$ [M–$BF_4$]$^+$: 556.2828, Found: 556.2837; Specific Rotation: $[\alpha]_D^{22}$ –489.8 (*c* 1.1, $CHCl_3$).

The $^{1}$H NMR spectrum of **2.91** ($^{13}$C-labeled) is shown below. The $^{13}$C and $^{19}$F NMR spectra will be shown in the next section.

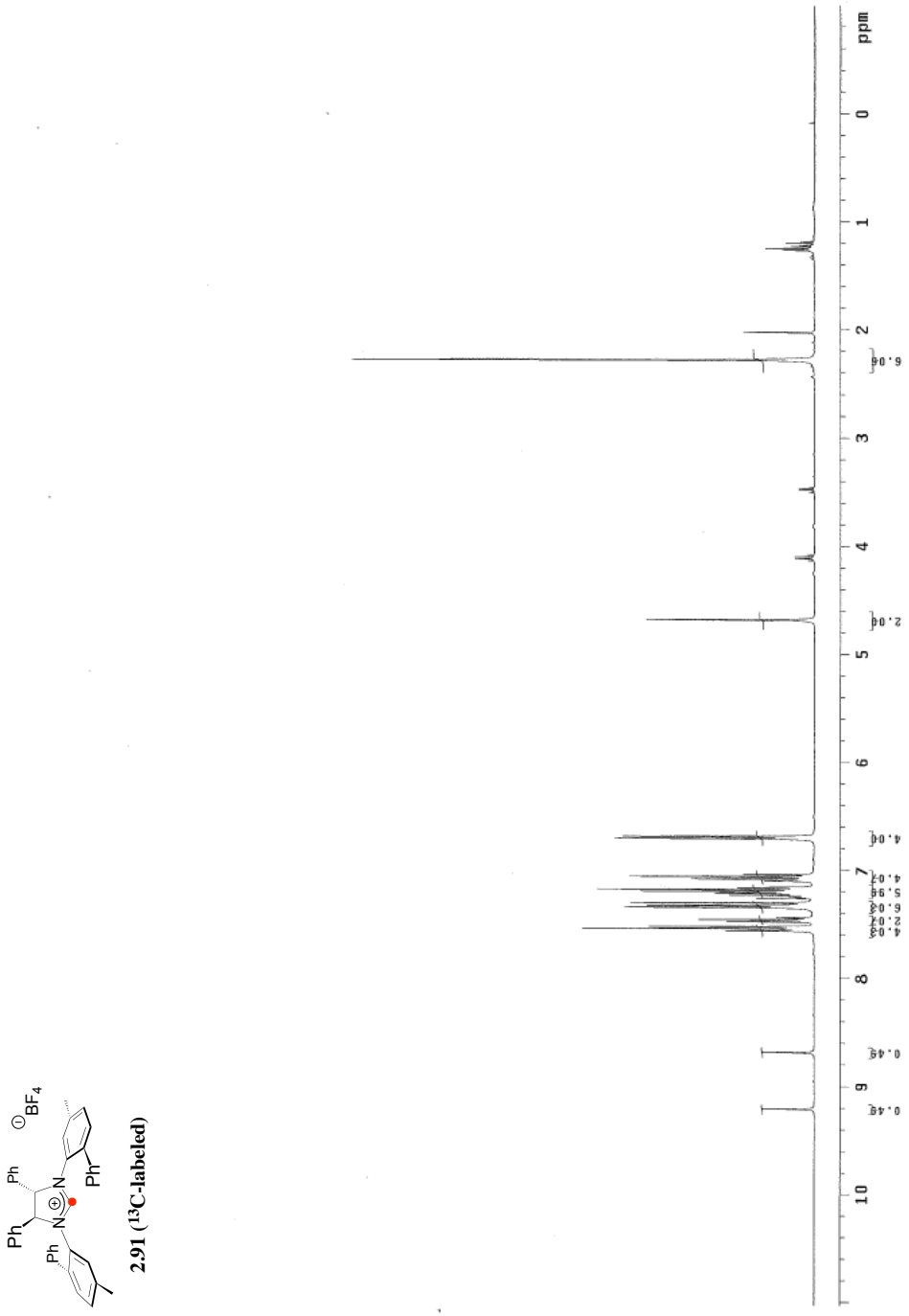


**2.91 ($^{13}$C-labeled)**

**(*R*)-4-(Dimethyl(phenyl)silyl)-4-(4-(trifluoromethyl)phenyl)butan-2-one (2.144):** In dry $N_2$ atomsphere, imidazolinium tetrafluoroborate salt **2.91** (14 mg, 0.023 mmol, 7.5 mol %) was charged into an oven-dried vial (8 x 1 cm) equipped with a stir bar. Dbu was

added into the vial by syringe (10 μL, 10 mg, 0.068 mmol, 23 mol %), followed by addition of $PhMe_2Si$–B(pin) (90 μL, 87 mg, 0.33 mmol, 1.1 equiv). The mixture was allowed to stir for ~ 5 seconds before it was added a solution of (*E*)-4-(4-(trifluoromethyl)phenyl)but-3-en-2-one (64 mg, 0.30 mmol, 1.0 equiv) in 1.0 mL thf by syringe. This was immediately followed by addition of water (18 μL, 18 mg, 3.3 equiv). The mixture was allowed to stir for 1 h at 22 ºC. Pentane (5 mL) was added to the solution (to facilitate imidazolinium salt precipitation), and the resulting solution was dried over anhydrous $MgSO_4$, filtered, and concentrated *in vacuo*. The resulting clear oil was purified by silica gel chromatography (5:1 hexanes:$Et_2O$) to give 90 mg (0.26 mmol, 86% yield) of (*R*)-4-(Dimethyl(phenyl)silyl)-4-(4-(trifluoromethyl)phenyl)butan-2-one (**2.144**). The spectroscopic data match those reported previously.[152] The absolute configuration was assigned by analogy to β-silyl ketones previously reported.[51] IR (neat): 3070 (w), 2960 (w), 1718 (m), 1615 (w), 1580 (w), 1515 (w), 1419 (w), 1357 (w), 1323 (s), 1251(w), 1188 (w), 1161 (s), 1108 (s), 1067 (s), 1015 (w), 998 (w), 952 (w), 910 (w), 850 (w), 831 (w), 807 (s), 773 (s), 734 (s), 670 (m), 646 (s), 611 (s), 599 (w), 569 (w), 537 (w), 513 (w), 467 (w), 420 (w) $cm^{-1}$; $^1H$ NMR (500 MHz, $CDCl_3$): δ 7.43 (overlapping d, $J$ = 8 Hz, 2H), 7.42–7.33 (m, 5H), 7.02 (overlapping d, $J$ = 8 Hz, 2H), 2.99 (dd, $J$ = 11.0, 3.5 Hz, 1H), 2.93 (dd, $J$ = 16.5, 11.0 Hz, 1H), 2.69 (dd, $J$ = 16.5, 3.5 Hz, 1H), 1.97 (s, 3H), 0.25 (s, 3H), 0.23 (s, 3H); $^{13}C$ NMR (100 MHz, $CDCl_3$): δ 207.4, 146.9, 146.9, 154.0, 134.2, 129.7, 128.0, 127.8, 125.2 (q, $J_{C\text{-}F}$ = 29.6, 14.8 Hz), 43.8, 31.7, 30.1, –4.1, –5.2; $^{19}F$ NMR (376 MHz, $d_8$-thf): –60 ppm (s, 3F). Optical rotation: $[\alpha]_D^{22}$ +5.6 (*c* 1.8, $CHCl_3$) for a sample with 87:13 er.

Enantiomeric purity was determined by HPLC analysis in comparison with authentic racemic material (96:4 er shown, Chiralpak AD-H column, 99/1 hexanes/*i*-propanol, 0.3 mL/min, 220 nm).

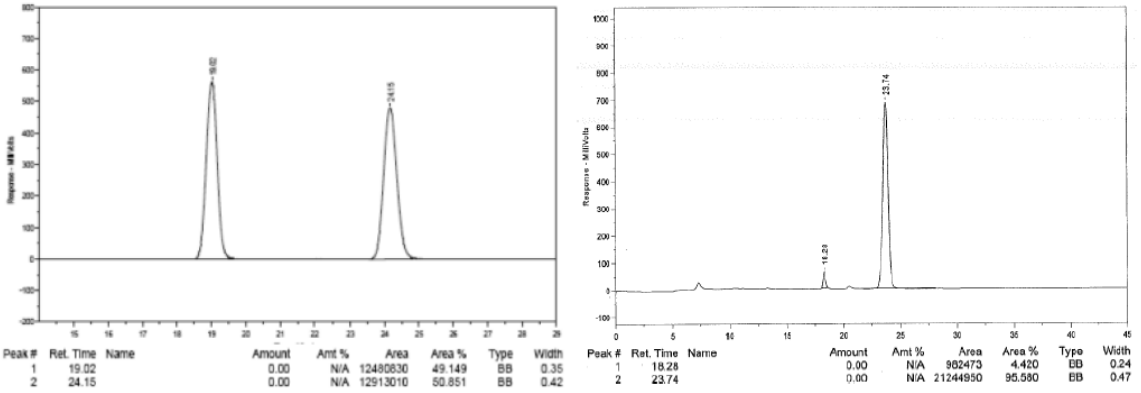


| Peak # | Time (min) | Area (%) | Peak # | Time (min) | Area (%) |
|---|---|---|---|---|---|
| 1 | 19.02 | 49.149 | 1 | 18.28 | 4.420 |
| 2 | 24.15 | 50.851 | 2 | 23.74 | 95.580 |

### *2.10.2. Procedures for NMR Studies on Probing the Formations of Chiral NHC•diboron and NHC•borylsilane Complexes*

**General procedure for probing the formation of a chiral NHC•diboron complex:** In a $N_2$ filled glove box, an oven-dried vial (8 x 1 cm) equipped with a stir bar was charged with **2.91** (39 mg, 0.060 mmol, 1.0 equiv), dbu (55 mg, 0.36 mmol, 6.0 equiv) and thf-$d_8$ (0.60 mL, 0.10 M solution of **2.91**). The mixture was allowed to stir for 30 min at 22 °C. $B_2(pin)_2$(15 mg, 0.060 mmol, 1.0 equiv) was added to the vial, followed by the addition of MeOH (73 mL, 58 mg, 1.8 mmol, 30 equiv). The mixture was transferred into a Wilmad LabGlass 600 MHz Quartz NMR tube, which was sealed with a NMR cap before removal from the glove box. The $^{11}$B NMR spectra were recorded subsequently.

**General procedure for probing the formation of a chiral NHC•borylsilane complex:** In a $N_2$ filled glove box, an oven-dried vial (8 x 1 cm) equipped with a stir bar was charged with **2.91** (39 mg, 0.060 mmol, 1.0 equiv), dbu (55 mg, 0.36 mmol, 6.0 equiv) and thf-$d_8$ (0.60 mL, 0.10 M solution of **7c**). The mixture was allowed to stir for 30 min at 22 °C. $PhMe_2Si$–B(pin)(16 mg, 0.060 mmol, 1.0 equiv) was added to the vial, followed by the addition of $H_2O$ (6.5 mL, 6.5 mg, 0.36 mmol, 6.0 equiv). The mixture was transferred into a Wilmad LabGlass 600 MHz Quartz NMR tube, which was sealed with a NMR cap before removal from the glovebox. The $^{11}B$ NMR spectra were recorded subsequently.

**Preparation of dimethyl(dimethyl(phenyl)silyl)boronate (2.121)** was obtained as a mixture, through the use of a modified procedure reported for the synthesis of $PhMe_2Si$–B(pin).[103] A 100 mL flame–dried Schlenk flask equipped with a stir bar was charged with Li (0.12 g, 18 mmol, 6.0 equiv) and mineral oil (5 mL) under argon. The mixture was allowed to heat to 180 °C and stirred vigorously for 10 min. The suspension was then allowed to cool to 22 °C. The Li particles were washed with thf (3 x 5 mL). Then 3 mL of thf was added into the flask. To the suspension, chlorodimethylphenylsilane (0.5 mL, 3.0 mmol, 1.0 equiv) was added drop-wise at 0 °C. The resulting suspension was allowed to stir at 0 °C for 6 h to generate dimethylphenylsilyllithium completely. To a stirred solution of trimethylborate (0.49 mL, 3.6 mmol, 1.2 equiv) in hexanes (3.0 mL) in another flame–dried Schlenk flask was added the previously prepared dimethylphenylsilyllithium solution drop-wise at 0 °C. The resulting solution was allowed to stir at 22 °C for 12 h. The mixture was filtered through a plug of celite twice,

(103) Meng, F.; Jang, H.; Hoveyda, A. H. *Chem. Eur. J.* **2013**, *19*, 3204–3214.

diluted with hexanes and the filtrate was concentrated *in vacuo*. Purification of the resulting light yellow oil by silica gel chromatography or distillation *in vacuo* resulted in complete decomposition of the desired product. The desired product also decomposed in a day at 22 °C under $N_2$. Thus the material was used immediately after syntesis. The presence of dimethyl(dimethyl(phenyl)silyl)boronate (**2.121**) was confirmed by HRMS (DART): Calcd for $C_{10}H_{18}Si_1O_2B_1$ $[M+H]^+$: 209.11691, Found: 209.11632. Due to the instability of the compound and lack of an effective purification method, other characterization data were not available.

**Preparation of NHC•borosilane Complex (2.120):** In a $N_2$ filled glove box, an oven-dried vial (8 x 1 cm) equipped with a stir bar was charged with imidazolinium salt **2.91** (19 mg, 0.030 mmol, 1.0 equiv), KHMDS (6.0 mg, 0.030 mmol, 1.0 equiv) and thf-$d_8$ (0.60 mL, 0.05 M solution of **2.91**). The resulting mixture was allowed to stir for 30 min at 22 °C. Dimethyl(dimethyl(phenyl)silyl)boronate (**2.121**) (6.2 mg as a mixture, 0.030 mmol, 1.0 equiv) was then added to the vial. The mixture was transferred into a Wilmad LabGlass 600 MHz Quartz NMR tube, which was sealed with a NMR cap before removal from the glovebox. The $^{11}$B NMR spectra were recorded subsequently.

### *2.10.3. NMR Spectra of the $^{13}$C-Labeled Imidazolinium Salt, NHC•$BF_3$ and NHC•borylsilane Complex*

**Figure 2.10.1.** $^{13}C$ NMR spectra for a chiral imidazolinium salt and the derived NHC complex with $BF_3$

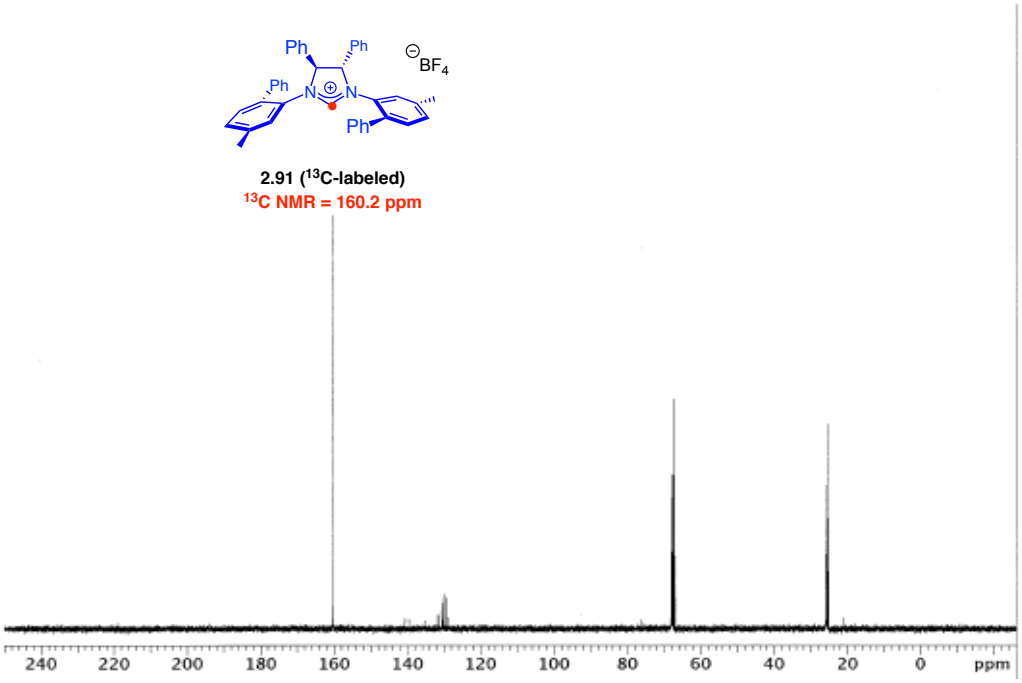


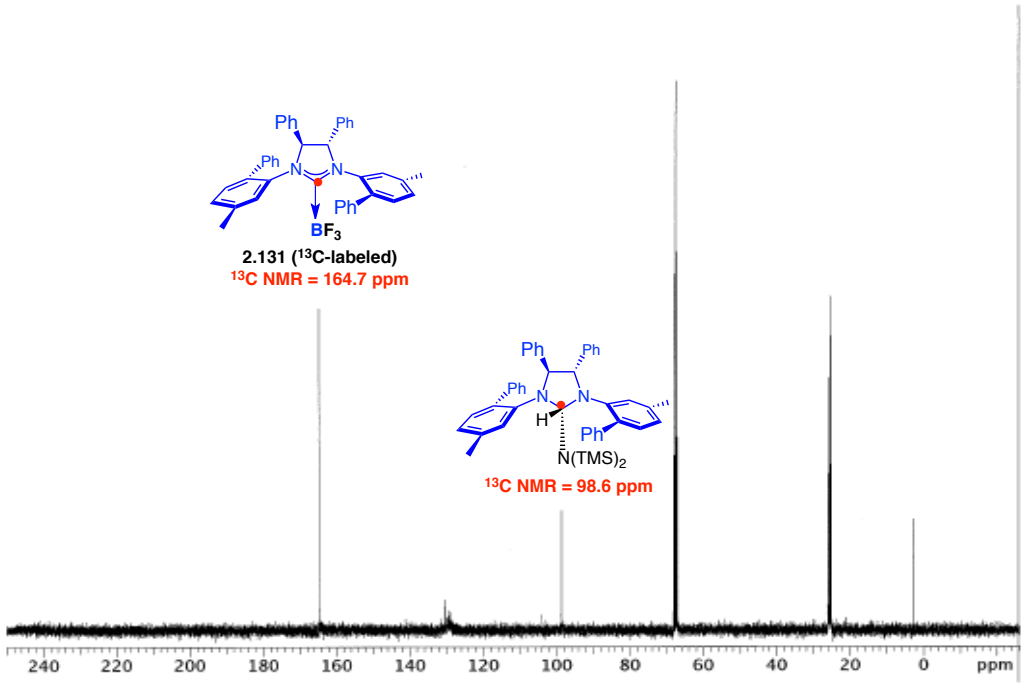

**Figure 2.10.2. $^{13}$C NMR spectrum for a chiral NHC•Borosilane Complex**

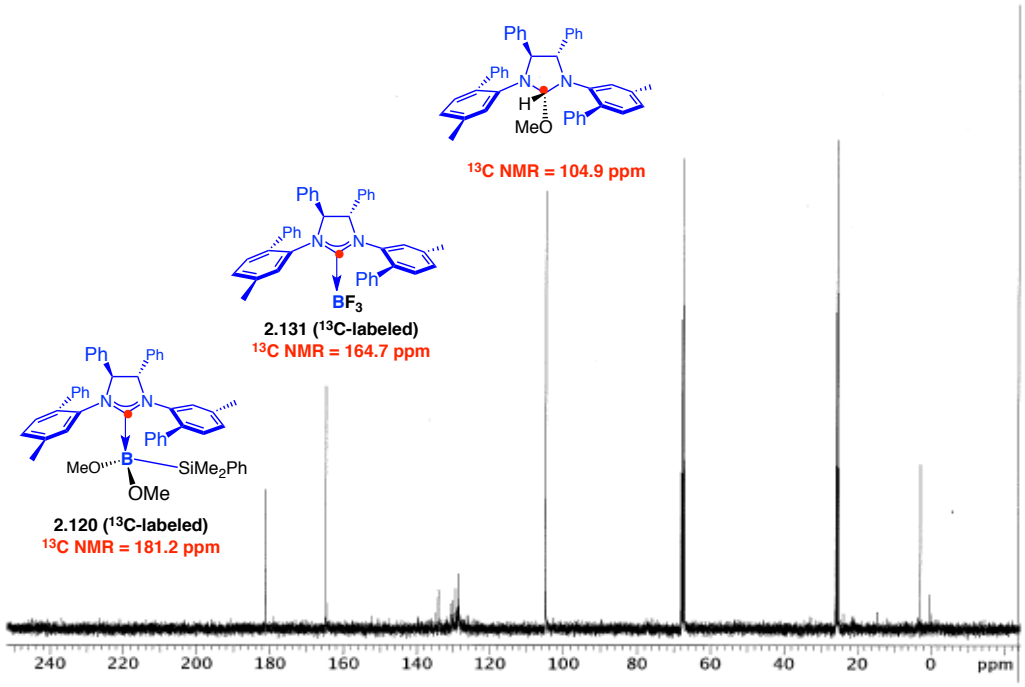

Figure 2.10.3. $^{11}B$ NMR and $^{19}F$ NMR spectra for a chiral NHC and its complex with $BF_3$

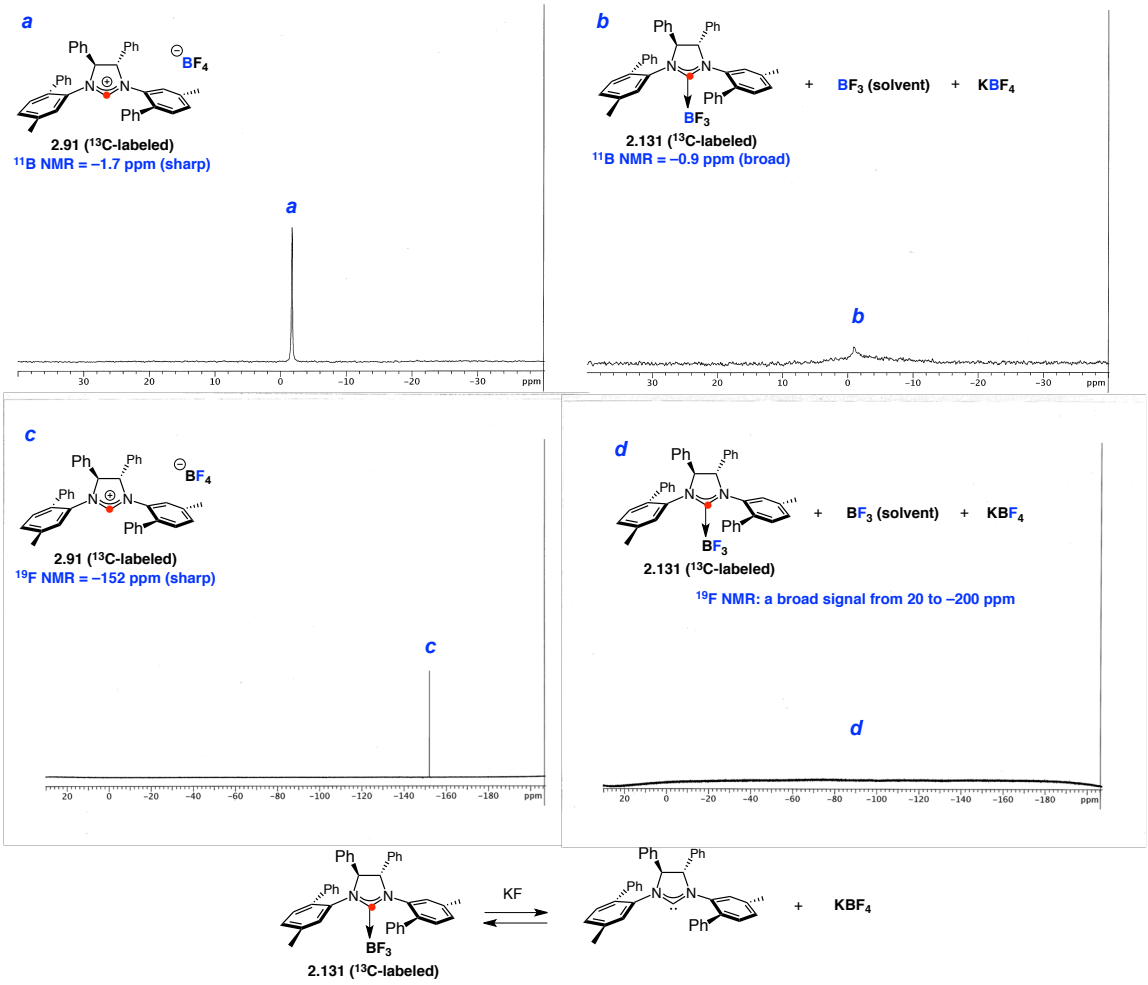


The fast equilibrium between complex 2.131 and NHC + $KBF_4$ results in the broadness of signal *b* and *d*

## *2.10.4. Computational Studies*

Density Functional Theory (DFT) calculations were carried out in an effort to gain more insight into the mechanism of the aforementioned NHC-catalyzed conjugate addition reactions of a B(pin) or $SiPhMe_2$ unit to acyclic and cyclic α,β-unsaturated carbonyl compounds. We have previously demonstrated that the B–B bond (or B–Si bond) upon coordination of a Lewis basic NHC becomes polarized (activated), whereupon the resulting nucleophilic B(pin) (or $SiPhMe_2$) unit of the complex readily attacks the electrophilic enone. The forming of the C–B (or C–Si) bond is, according to

our kinetic studies, likely to be the turnover limiting step. Since it involves the enantioselective transfer of the B(pin) or $SiPhMe_2$ unit to the α,β-unsaturated carbonyl, we believe this is also the stereochemical determining step. Consequently, we decided to focus our DFT studies on this step with the intention to further understand how these catalytic reactions operate and the origin of enantioselectivity. All ground state and transition state geometries were optimized using DFT methodology. The B97-D functional and 6-31G* basis set were employed. Tetrahydrofuran solvation (or tetrahydrofuran/MeOH in boryl conjugate additions catalyzed by a chiral NHC) was modeled using the PCM model. Frequency calculations were carried out on all optimized geometries at the same level of theory to determine the whether these are minima or first-order saddle-points on the potential energy surface.

**Ground State of A**

```
---------------------------------------
 Cartesian coordinates (Angstroms):
---------------------------------------
98

H    -4.036     0.114    -3.129
C    -3.888     0.792    -2.285
H    -2.484    -0.457    -1.317
O    -5.353     2.371    -3.285
C    -3.041     0.481    -1.272
C    -4.616     2.077    -2.337
C    -2.819     1.377    -0.080
H    -1.893     1.960    -0.240
C    -4.361     3.055    -1.182
H    -3.512     3.696    -1.487
C    -4.005     2.336     0.135
H    -5.239     3.710    -1.079
H    -4.877     1.754     0.478
H    -3.768     3.070     0.920
H    -2.628     0.765     0.814
N     0.446     1.293    -1.163
B     0.030    -1.320    -0.336
C     0.926     2.482    -0.624
C     0.509     0.288    -0.237
C     1.276     2.217     0.669
N     1.005     0.875     0.889
H    -4.932    -2.170     0.010
H    -4.269    -0.748     0.859
```

| | | | |
|---|---|---|---|
| H | -4.305 | -4.452 | 0.662 |
| C | -4.553 | -1.803 | 0.975 |
| H | -5.358 | -1.871 | 1.723 |
| O | -2.365 | -2.585 | 0.307 |
| C | -3.344 | -2.656 | 1.393 |
| C | -3.772 | -4.117 | 1.565 |
| H | -4.451 | -4.217 | 2.426 |
| H | -2.903 | -4.771 | 1.721 |
| H | -3.881 | -0.394 | 3.089 |
| H | -4.148 | -1.868 | 4.063 |
| C | -2.546 | -2.054 | 2.610 |
| C | -3.382 | -1.232 | 3.593 |
| H | -2.363 | -3.803 | 3.919 |
| H | -2.731 | -0.830 | 4.384 |
| C | -1.715 | -3.107 | 3.364 |
| H | -1.095 | -3.679 | 2.659 |
| H | -1.053 | -2.594 | 4.077 |
| B | -1.387 | -1.649 | 0.644 |
| O | -1.586 | -1.169 | 1.947 |
| H | 0.971 | 3.399 | -1.196 |
| H | 1.688 | 2.855 | 1.440 |
| H | 0.474 | -2.994 | -4.097 |
| C | 1.295 | -2.959 | -3.363 |
| H | -1.080 | -4.009 | -2.443 |
| H | 1.913 | -2.077 | -3.577 |
| O | -0.033 | -1.704 | -1.773 |
| H | 1.914 | -3.862 | -3.496 |
| C | 0.716 | -2.915 | -1.942 |
| C | -0.233 | -4.118 | -1.748 |
| H | 0.275 | -5.074 | -1.955 |
| H | -0.628 | -4.129 | -0.724 |
| H | 2.632 | -0.933 | -1.494 |
| C | 1.798 | -2.828 | -0.798 |
| C | 2.990 | -1.922 | -1.177 |
| O | 1.076 | -2.216 | 0.277 |
| H | 3.597 | -2.357 | -1.987 |
| C | 2.328 | -4.188 | -0.322 |
| H | 2.814 | -4.728 | -1.152 |
| H | 3.631 | -1.791 | -0.291 |
| H | 1.512 | -4.809 | 0.076 |
| H | 3.072 | -4.038 | 0.476 |
| C | 0.659 | 0.635 | -4.938 |
| C | -0.186 | 1.823 | -5.441 |
| C | 1.173 | 0.879 | -3.505 |
| H | 1.510 | 0.452 | -5.614 |
| H | 0.040 | -0.279 | -4.937 |
| C | -0.015 | 1.153 | -2.566 |
| H | 1.855 | 1.747 | -3.487 |
| H | 1.717 | 0.001 | -3.137 |
| C | -0.807 | 2.385 | -3.041 |
| C | -1.341 | 2.130 | -4.465 |
| H | -0.148 | 3.269 | -3.063 |
| H | -1.634 | 2.596 | -2.349 |
| H | 0.459 | 2.716 | -5.526 |
| H | -0.585 | 1.610 | -6.446 |
| H | -1.917 | 3.005 | -4.806 |
| H | -2.037 | 1.274 | -4.435 |

```
C     0.779     0.147     4.646
C     2.286    -0.022     4.930
C     0.541     0.915     3.330
H     0.284     0.671     5.480
H     0.311    -0.849     4.560
C     1.254     0.190     2.177
H     0.936     1.941     3.430
H    -0.532     0.975     3.101
C     2.765     0.044     2.430
H     0.825    -0.808     2.078
C     2.995    -0.719     3.750
H     3.228     1.045     2.491
H     3.216    -0.493     1.583
H     2.737     0.975     5.084
H     2.436    -0.597     5.858
H     4.075    -0.811     3.947
H     2.594    -1.743     3.640
H    -0.666     0.275    -2.576

                     1                      2                      3
                     A                      A                      A
 Frequencies --    13.1939                20.1958
27.1962
 Red. masses --     5.4714                 6.9319
4.3492
 Zero-point correction=                           0.849032
(Hartree/Particle)
 Thermal correction to Energy=                    0.893423
 Thermal correction to Enthalpy=                  0.894367
 Thermal correction to Gibbs Free Energy=         0.773357
 Sum of electronic and zero-point Energies=          -1824.698238
 Sum of electronic and thermal Energies=             -1824.653847
 Sum of electronic and thermal Enthalpies=           -1824.652903
 Sum of electronic and thermal Free Energies=        -1824.773914

         Item               Value     Threshold  Converged?
 Maximum Force            0.000019     0.000450     YES
 RMS     Force            0.000003     0.000300     YES

----------------------------------------
```

**Transition State of A**

```
----------------------------------------
 Cartesian coordinates (Angstroms):
----------------------------------------
98

N     0.832     1.315    -1.396
B    -0.064    -1.069    -0.525
C     1.472     2.434    -0.885
C     0.622     0.399    -0.406
C     1.652     2.214     0.451
N     1.118     0.966     0.730
C    -2.512     0.470    -0.728
H    -5.004    -3.079     0.342
H    -4.854    -1.494     1.131
H    -3.333    -4.797     0.533
```

| | | | |
|---|---|---|---|
| C | -4.615 | -2.558 | 1.230 |
| H | -5.122 | -2.958 | 2.121 |
| O | -2.497 | -2.284 | 0.099 |
| C | -3.098 | -2.796 | 1.317 |
| C | -2.828 | -4.306 | 1.379 |
| H | -3.225 | -4.732 | 2.315 |
| H | -1.753 | -4.523 | 1.319 |
| H | -4.134 | -0.867 | 3.188 |
| H | -3.730 | -2.336 | 4.125 |
| C | -2.385 | -1.953 | 2.456 |
| C | -3.309 | -1.475 | 3.581 |
| H | -1.461 | -3.575 | 3.594 |
| H | -2.730 | -0.866 | 4.293 |
| C | -1.158 | -2.666 | 3.051 |
| H | -0.448 | -2.929 | 2.258 |
| H | -0.657 | -1.992 | 3.760 |
| B | -1.906 | -1.036 | 0.362 |
| O | -1.899 | -0.774 | 1.744 |
| C | -4.602 | 2.022 | 0.741 |
| O | -6.154 | 0.414 | -0.183 |
| C | -4.952 | 0.773 | -0.087 |
| C | -3.893 | 0.126 | -0.810 |
| C | -2.194 | 1.799 | -0.026 |
| H | -4.186 | -0.724 | -1.428 |
| C | -3.125 | 2.079 | 1.166 |
| H | -2.888 | 3.065 | 1.599 |
| H | -2.936 | 1.321 | 1.939 |
| H | -5.277 | 2.060 | 1.612 |
| H | -4.845 | 2.903 | 0.116 |
| H | -1.942 | 0.306 | -1.648 |
| H | -1.154 | 1.839 | 0.314 |
| H | -2.310 | 2.604 | -0.775 |
| H | 1.742 | 3.275 | -1.509 |
| H | 2.103 | 2.831 | 1.217 |
| H | 0.551 | -2.828 | -4.127 |
| C | 1.221 | -2.947 | -3.262 |
| H | -1.386 | -3.630 | -2.910 |
| H | 1.985 | -2.158 | -3.303 |
| O | -0.167 | -1.536 | -1.880 |
| H | 1.719 | -3.927 | -3.341 |
| C | 0.396 | -2.869 | -1.968 |
| C | -0.754 | -3.885 | -2.045 |
| H | -0.364 | -4.906 | -2.185 |
| H | -1.370 | -3.842 | -1.141 |
| H | 2.690 | -1.450 | -1.244 |
| C | 1.255 | -2.983 | -0.641 |
| C | 2.696 | -2.464 | -0.816 |
| O | 0.591 | -2.077 | 0.274 |
| H | 3.285 | -3.121 | -1.474 |
| C | 1.278 | -4.381 | -0.017 |
| H | 1.744 | -5.102 | -0.707 |
| H | 3.181 | -2.424 | 0.171 |
| H | 0.262 | -4.723 | 0.219 |
| H | 1.868 | -4.358 | 0.913 |
| C | 1.422 | 0.717 | -5.136 |
| C | 0.581 | 1.887 | -5.688 |
| C | 1.786 | 0.947 | -3.655 |

```
H     2.340     0.586    -5.730
H     0.842    -0.219    -5.218
C     0.502     1.159    -2.832
H     2.433     1.836    -3.563
H     2.337     0.085    -3.248
C    -0.319     2.352    -3.352
C    -0.682     2.115    -4.833
H     0.271     3.281    -3.266
H    -1.225     2.470    -2.739
H     1.193     2.807    -5.679
H     0.300     1.692    -6.736
H    -1.258     2.974    -5.215
H    -1.335     1.227    -4.902
C     0.318     0.811     4.483
C     1.710     0.363     4.972
C     0.382     1.393     3.057
H    -0.106     1.565     5.166
H    -0.369    -0.050     4.488
C     1.048     0.390     2.094
H     0.965     2.329     3.081
H    -0.627     1.625     2.686
C     2.445    -0.039     2.569
H     0.407    -0.489     2.017
C     2.351    -0.637     3.988
H     3.116     0.837     2.579
H     2.853    -0.773     1.858
H     2.364     1.249     5.060
H     1.633    -0.087     5.976
H     3.355    -0.930     4.335
H     1.739    -1.555     3.948
H    -0.100     0.250    -2.900
```

```
                     1                      2                      3
                     A                      A                      A
 Frequencies --  -342.3384               16.5905
25.4934
 Red. masses --     9.7213                4.9027
4.2430
 Zero-point correction=                           0.848393
(Hartree/Particle)
 Thermal correction to Energy=                    0.891892
 Thermal correction to Enthalpy=                  0.892836
 Thermal correction to Gibbs Free Energy=         0.775068
 Sum of electronic and zero-point Energies=          -1824.671940
 Sum of electronic and thermal Energies=             -1824.628442
 Sum of electronic and thermal Enthalpies=           -1824.627497
 Sum of electronic and thermal Free Energies=        -1824.745265

         Item               Value     Threshold  Converged?
 Maximum Force            0.000009     0.000450     YES
 RMS     Force            0.000001     0.000300     YES
----------------------------------------
```

**Ground State of B1 and B2**

```
----------------------------------------
 Cartesian coordinates (Angstroms):
----------------------------------------
```

155

| | | | |
|---|---|---|---|
| H | -9.870 | 16.269 | -5.607 |
| H | -10.681 | 24.295 | -6.232 |
| H | -11.169 | 15.183 | -5.097 |
| H | -9.337 | 17.856 | -6.975 |
| C | -10.917 | 16.236 | -5.279 |
| H | -12.892 | 15.083 | -7.150 |
| H | -10.466 | 23.363 | -8.812 |
| H | -11.039 | 22.688 | -3.976 |
| H | -11.510 | 24.339 | 0.610 |
| C | -11.737 | 23.989 | -6.363 |
| H | -11.997 | 25.275 | -0.826 |
| N | -11.770 | 16.697 | -6.395 |
| H | -11.073 | 22.118 | -0.379 |
| C | -10.168 | 18.544 | -6.755 |
| C | -13.071 | 16.008 | -6.579 |
| H | -10.286 | 16.859 | -3.327 |
| C | -12.350 | 24.554 | -0.068 |
| C | -11.562 | 23.209 | -8.773 |
| C | -11.444 | 17.798 | -7.084 |
| H | -11.931 | 25.256 | -8.127 |
| C | -11.919 | 22.257 | -4.486 |
| C | -11.856 | 22.540 | -5.952 |
| C | -11.119 | 17.090 | -4.011 |
| H | -13.189 | 16.816 | -9.271 |
| H | -12.335 | 24.590 | -5.662 |
| C | -12.195 | 24.235 | -7.813 |
| H | -13.435 | 15.735 | -5.579 |
| H | -10.077 | 19.376 | -7.465 |
| H | -9.069 | 18.777 | -4.883 |
| H | -11.970 | 21.184 | -4.267 |
| C | -11.916 | 21.539 | -6.879 |
| C | -12.074 | 22.127 | -0.815 |
| C | -11.784 | 21.773 | -8.311 |
| N | -12.205 | 18.247 | -8.080 |
| C | -10.050 | 19.075 | -5.281 |
| H | -12.885 | 25.317 | -3.212 |
| H | -11.938 | 23.310 | -9.802 |
| C | -13.437 | 17.568 | -8.506 |
| H | -13.149 | 25.051 | 0.504 |
| H | -11.981 | 19.174 | -8.495 |
| H | -12.053 | 16.804 | -3.507 |
| C | -12.860 | 23.293 | -0.731 |
| C | -14.085 | 16.914 | -7.282 |
| O | -11.801 | 20.837 | -9.142 |
| H | -12.805 | 22.764 | -4.066 |
| H | -12.046 | 20.507 | -6.553 |
| C | -11.155 | 18.602 | -4.314 |
| H | -14.960 | 16.321 | -7.579 |
| H | -11.948 | 20.082 | -1.488 |
| C | -12.569 | 20.977 | -1.438 |
| C | -13.942 | 25.454 | -3.500 |
| H | -14.019 | 26.343 | -4.155 |
| H | -13.291 | 24.143 | -7.851 |
| H | -10.064 | 20.172 | -5.319 |
| H | -14.090 | 18.324 | -8.955 |

| | | | |
|---|---|---|---|
| H | -11.059 | 19.160 | -3.371 |
| H | -14.524 | 25.672 | -2.586 |
| C | -14.148 | 23.253 | -1.282 |
| H | -12.145 | 18.864 | -4.724 |
| H | -14.413 | 17.698 | -6.587 |
| O | -14.368 | 24.279 | -4.165 |
| C | -13.847 | 20.943 | -2.038 |
| H | -14.818 | 24.105 | -1.172 |
| C | -14.625 | 22.124 | -1.959 |
| H | -15.597 | 26.275 | -5.890 |
| H | -14.388 | 22.417 | -9.132 |
| H | -14.392 | 21.086 | -7.243 |
| H | -13.550 | 18.433 | -1.091 |
| H | -16.147 | 26.224 | 0.064 |
| C | -14.331 | 19.691 | -2.672 |
| B | -15.819 | 24.063 | -4.356 |
| H | -15.236 | 23.852 | -9.770 |
| C | -14.097 | 18.451 | -2.035 |
| C | -15.373 | 22.835 | -9.373 |
| O | -15.631 | 23.671 | -7.091 |
| C | -16.610 | 26.143 | -5.465 |
| O | -16.603 | 25.315 | -4.320 |
| B | -16.016 | 23.144 | -5.859 |
| C | -15.308 | 20.572 | -7.559 |
| C | -15.060 | 19.699 | -3.883 |
| H | -17.001 | 27.134 | -5.174 |
| C | -17.172 | 25.863 | -0.052 |
| N | -15.981 | 22.146 | -2.406 |
| H | -15.253 | 20.638 | -4.399 |
| H | -15.188 | 20.239 | -8.600 |
| H | -17.024 | 25.666 | -2.215 |
| C | -14.588 | 17.255 | -2.577 |
| C | -16.284 | 22.887 | -8.144 |
| C | -16.547 | 23.095 | -3.184 |
| H | -15.834 | 22.215 | -10.157 |
| H | -15.455 | 19.691 | -6.923 |
| H | -17.255 | 25.729 | -6.264 |
| C | -17.652 | 25.542 | -1.331 |
| C | -16.376 | 21.040 | 2.527 |
| H | -17.620 | 25.962 | 2.070 |
| C | -16.784 | 22.247 | 1.930 |
| H | -14.402 | 16.311 | -2.062 |
| H | -16.210 | 20.991 | 3.605 |
| H | -16.937 | 23.140 | 2.539 |
| C | -17.999 | 25.719 | 1.075 |
| C | -16.180 | 19.898 | 1.732 |
| C | -16.995 | 22.309 | 0.547 |
| C | -16.518 | 21.505 | -7.434 |
| C | -15.576 | 18.505 | -4.405 |
| O | -16.626 | 21.896 | -6.020 |
| C | -15.341 | 17.278 | -3.763 |
| C | -16.390 | 19.964 | 0.345 |
| C | -16.801 | 21.167 | -0.252 |
| H | -15.862 | 18.959 | 2.190 |
| H | -17.301 | 23.248 | 0.086 |
| C | -16.989 | 21.242 | -1.750 |
| H | -17.356 | 24.642 | -8.811 |

```
H   -16.227    19.084    -0.281
C   -17.593    23.618    -8.487
H   -16.181    18.533    -5.312
N   -17.882    22.955    -3.125
H   -16.876    20.240    -2.182
H   -15.750    16.354    -4.175
C   -18.978    25.082    -1.499
C   -19.317    25.259     0.915
C   -17.799    20.773    -7.836
H   -18.245    23.673    -7.605
C   -18.335    21.871    -2.209
H   -18.133    23.106    -9.298
C   -18.894    23.799    -3.686
H   -17.774    20.532    -8.911
C   -19.504    24.768    -2.857
H   -17.882    20.455    -4.495
C   -19.805    24.948    -0.364
H   -17.879    19.832    -7.273
H   -18.854    22.345    -1.362
C   -19.388    23.513    -4.963
H   -18.898    22.733    -5.543
H   -19.965    25.139     1.786
H   -18.692    21.379    -7.632
C   -18.859    20.233    -4.068
C   -20.635    25.435    -3.366
C   -19.268    20.894    -2.894
C   -20.501    24.204    -5.475
H   -21.124    26.188    -2.744
H   -20.470    24.515    -7.622
C   -21.124    25.161    -4.651
H   -20.827    24.586    -0.489
C   -21.012    23.916    -6.871
C   -19.722    19.330    -4.702
H   -19.402    18.825    -5.615
C   -20.546    20.650    -2.367
H   -20.870    22.856    -7.135
H   -22.002    25.696    -5.020
H   -20.862    21.173    -1.461
H   -22.082    24.159    -6.961
C   -20.999    19.080    -4.168
C   -21.411    19.741    -3.000
H   -21.671    18.376    -4.663
H   -22.403    19.555    -2.583

                     1                      2                      3
                     A                      A                      A
 Frequencies --    13.8700                20.4338
24.1635
 Red. masses --     5.1341                 5.5709
4.6885
 Zero-point correction=                           1.299632
(Hartree/Particle)
 Thermal correction to Energy=                    1.374340
 Thermal correction to Enthalpy=                  1.375284
 Thermal correction to Gibbs Free Energy=         1.186880
 Sum of electronic and zero-point Energies=         -3165.919920
 Sum of electronic and thermal Energies=            -3165.845212
```

```
 Sum of electronic and thermal Enthalpies=           -3165.844268
 Sum of electronic and thermal Free Energies=        -3166.032672

         Item               Value     Threshold  Converged?
 Maximum Force            0.000038     0.000450     YES
 RMS     Force            0.000002     0.000300     YES

----------------------------------------
```

**Transition State of B1**

```
----------------------------------------
 Cartesian coordinates (Angstroms):
----------------------------------------
155

B     0.296    -0.717    -0.421
B     0.158    -0.286     1.743
H     2.124    -3.348    -4.301
H     3.935    -3.968    -3.322
H     3.886    -4.179    -1.058
N     1.727    -4.322    -4.381
H    -0.032    -3.560    -5.188
C     3.660    -4.994    -3.048
C     3.729    -5.174    -1.492
H     4.611    -5.785    -1.247
C     0.459    -4.534    -5.089
C     2.317    -5.286    -3.680
H     4.388    -5.659    -3.539
H     0.669    -4.925    -6.098
C     2.478    -5.795    -0.842
H     1.592    -5.207    -1.124
H     2.561    -5.708     0.250
H    -0.675    -5.073    -3.332
C    -0.397    -5.526    -4.293
N     1.769    -6.504    -3.554
H    -1.315    -5.772    -4.842
C     2.239    -7.272    -1.218
C     0.399    -6.808    -4.034
H     3.500    -7.551    -2.982
C     2.432    -7.535    -2.727
H     2.947    -7.924    -0.681
H     0.482    -7.420    -4.945
H     1.223    -7.561    -0.911
H    -0.091    -7.408    -3.255
H     2.011    -8.505    -3.023
C     0.373     2.141     1.232
O    -0.397     1.008     1.629
N    -0.955    -2.623     2.586
C    -2.286    -3.267     2.864
C    -1.064    -1.321     2.236
C     2.009     0.438     3.306
O     1.376    -0.486     2.434
C    -3.253    -2.063     2.780
N    -2.366    -0.962     2.295
H    -3.603    -1.776     3.783
H    -2.488    -3.974     2.051
C    -2.505    -5.390     4.217
```

| | | | |
|---|---|---|---|
| C | -2.088 | -3.979 | 6.609 |
| C | -2.501 | -6.075 | 5.443 |
| C | -2.308 | -4.000 | 4.186 |
| C | -2.098 | -3.297 | 5.386 |
| C | -2.291 | -5.371 | 6.640 |
| H | -1.933 | -2.221 | 5.362 |
| H | -1.922 | -3.423 | 7.534 |
| H | -2.283 | -5.903 | 7.593 |
| H | -2.656 | -7.155 | 5.462 |
| H | -2.648 | -5.932 | 3.280 |
| C | -4.244 | -2.685 | 0.536 |
| C | -6.843 | -2.200 | 1.482 |
| C | -4.440 | -2.276 | 1.868 |
| C | -5.342 | -2.853 | -0.318 |
| C | -6.645 | -2.612 | 0.155 |
| C | -5.741 | -2.030 | 2.336 |
| H | -3.231 | -2.849 | 0.166 |
| H | -5.183 | -3.165 | -1.351 |
| H | -7.500 | -2.743 | -0.511 |
| H | -7.852 | -2.009 | 1.853 |
| H | -5.886 | -1.700 | 3.367 |
| C | -4.451 | 1.949 | 1.233 |
| C | -4.557 | 2.643 | 2.452 |
| C | -3.673 | 0.780 | 1.210 |
| C | -3.908 | 2.173 | 3.602 |
| C | -2.979 | 0.339 | 2.339 |
| C | -3.108 | 1.013 | 3.576 |
| C | 1.599 | -5.327 | 2.925 |
| C | 2.404 | -4.792 | 3.936 |
| C | 0.488 | -4.631 | 2.403 |
| H | 3.261 | -5.360 | 4.303 |
| C | 2.112 | -3.534 | 4.495 |
| C | 0.221 | -3.352 | 2.953 |
| C | 0.994 | -2.843 | 4.005 |
| H | 0.701 | -1.894 | 4.448 |
| H | -4.016 | 2.709 | 4.546 |
| C | -5.147 | 2.427 | -0.023 |
| C | 2.249 | -1.533 | -0.417 |
| H | -1.061 | -2.930 | -3.069 |
| H | 0.348 | -1.874 | -3.352 |
| H | -3.103 | -2.145 | -2.112 |
| C | -0.740 | -1.898 | -3.269 |
| H | -1.169 | -1.583 | -4.233 |
| O | -0.769 | -1.522 | -0.863 |
| C | -1.270 | -0.996 | -2.142 |
| C | -2.797 | -1.091 | -2.167 |
| H | -3.179 | -0.671 | -3.110 |
| H | -3.263 | -0.552 | -1.339 |
| H | 0.744 | 0.216 | -3.801 |
| H | -0.836 | 0.887 | -4.305 |
| C | -0.695 | 0.482 | -2.170 |
| C | -0.071 | 0.891 | -3.512 |
| H | -2.563 | 1.608 | -2.402 |
| H | 0.332 | 1.912 | -3.425 |
| C | -1.702 | 1.552 | -1.718 |
| H | -2.056 | 1.340 | -0.703 |
| H | -1.200 | 2.531 | -1.712 |

| | | | |
|---|---|---|---|
| O | 0.363 | 0.455 | -1.172 |
| H | -3.624 | 0.174 | 0.312 |
| H | -5.166 | 3.548 | 2.506 |
| C | 2.964 | -2.935 | 5.593 |
| H | 1.842 | -6.305 | 2.506 |
| H | -0.099 | 2.595 | 0.350 |
| H | 1.407 | 1.869 | 0.972 |
| H | 0.386 | 2.871 | 2.059 |
| H | 2.148 | -0.043 | 4.290 |
| H | 1.429 | 1.362 | 3.445 |
| H | 3.002 | 0.706 | 2.906 |
| H | -0.857 | -0.705 | 8.180 |
| C | -1.310 | -0.363 | 7.248 |
| H | 0.584 | -0.125 | 6.220 |
| H | -3.341 | -0.484 | 7.998 |
| C | -0.501 | -0.047 | 6.144 |
| C | -2.706 | -0.236 | 7.147 |
| C | -3.289 | 0.206 | 5.949 |
| C | -1.085 | 0.386 | 4.944 |
| H | -4.373 | 0.301 | 5.867 |
| H | -0.471 | 0.663 | 4.093 |
| C | -2.484 | 0.518 | 4.833 |
| H | -2.409 | -6.965 | -1.529 |
| C | -1.821 | -6.493 | -0.740 |
| H | -1.946 | -4.501 | -1.593 |
| H | -1.533 | -8.327 | 0.383 |
| C | -1.559 | -5.113 | -0.777 |
| C | -1.329 | -7.256 | 0.333 |
| C | -0.589 | -6.643 | 1.354 |
| C | -0.805 | -4.503 | 0.233 |
| H | -0.236 | -7.237 | 2.199 |
| H | -0.605 | -3.437 | 0.167 |
| C | -0.314 | -5.257 | 1.320 |
| H | 2.346 | -2.373 | 6.312 |
| H | 3.703 | -2.230 | 5.176 |
| H | 3.516 | -3.714 | 6.139 |
| H | -4.454 | 3.006 | -0.658 |
| H | -6.003 | 3.075 | 0.217 |
| H | -5.505 | 1.576 | -0.624 |
| C | 3.699 | -0.107 | -2.602 |
| O | 2.796 | -1.797 | -4.057 |
| C | 2.833 | -1.340 | -2.862 |
| C | 2.217 | -1.992 | -1.764 |
| C | 3.196 | -0.369 | -0.117 |
| H | 1.700 | -2.931 | -1.966 |
| C | 3.385 | 0.620 | -1.281 |
| H | 4.203 | 1.318 | -1.039 |
| H | 2.467 | 1.207 | -1.401 |
| H | 3.610 | 0.572 | -3.466 |
| H | 4.747 | -0.464 | -2.596 |
| C | 2.302 | -2.646 | 0.613 |
| H | 2.862 | 0.153 | 0.786 |
| H | 4.173 | -0.830 | 0.130 |
| H | 2.091 | -2.285 | 1.618 |
| H | 3.326 | -3.061 | 0.613 |
| H | 1.617 | -3.458 | 0.351 |

```
                     1                      2                      3
                     A                      A                      A
 Frequencies --  -436.7168               13.9287
19.4402
 Red. masses --     9.1130                4.7660
3.7134
 Zero-point correction=                           1.300794
(Hartree/Particle)
 Thermal correction to Energy=                    1.374062
 Thermal correction to Enthalpy=                  1.375006
 Thermal correction to Gibbs Free Energy=         1.192412
 Sum of electronic and zero-point Energies=          -3165.865602
 Sum of electronic and thermal Energies=             -3165.792334
 Sum of electronic and thermal Enthalpies=           -3165.791390
 Sum of electronic and thermal Free Energies=        -3165.973984

         Item               Value     Threshold  Converged?
 Maximum Force            0.000060     0.000450     YES
 RMS     Force            0.000009     0.000300     YES

----------------------------------------
```

**Transition State of B2**

```
----------------------------------------
 Cartesian coordinates (Angstroms):
----------------------------------------
155

H     4.586    -9.825    -2.482
C     4.297    -9.236    -1.597
H     5.216    -8.977    -1.055
H     4.354    -7.302    -2.571
H     2.698    -8.406    -3.967
C     3.619    -7.927    -2.045
C     2.382    -8.128    -2.948
C     3.437   -10.145    -0.652
H     1.861   -10.231    -2.668
H     1.827    -7.179    -3.027
C     1.439    -9.242    -2.444
H     3.327    -7.358    -1.149
H     0.460    -9.188    -2.935
C     2.165    -9.513    -0.127
N     1.202    -9.150    -0.988
N     2.028    -9.358     1.184
C    -0.045    -8.496    -0.526
H    -0.330    -7.759    -1.289
H     0.795    -6.931     0.709
C     0.826    -8.790     1.808
H    -0.837    -9.259    -0.473
C     0.157    -7.815     0.833
H     1.142    -8.284     2.729
H    -0.816    -7.491     1.225
H     0.138    -9.607     2.077
H     2.868    -9.571     1.790
H     4.034   -10.457     0.213
H     3.137   -11.063    -1.180
H     3.402    -4.800    -2.880
```

| | | | |
|---|---|---|---|
| H | 5.715 | -4.023 | -3.334 |
| H | 1.926 | -5.048 | 0.597 |
| C | 4.029 | -4.458 | -2.054 |
| C | 5.333 | -4.020 | -2.312 |
| H | 6.634 | -1.569 | -3.029 |
| H | 8.817 | -0.576 | -3.704 |
| C | 2.067 | -4.793 | -0.464 |
| C | 7.562 | -1.941 | -2.591 |
| C | 3.509 | -4.435 | -0.746 |
| C | 8.792 | -1.383 | -2.969 |
| H | 1.402 | -3.942 | -0.691 |
| H | 1.734 | -5.641 | -1.081 |
| C | 6.174 | -3.555 | -1.280 |
| C | 7.502 | -2.976 | -1.631 |
| H | 6.775 | -7.424 | -0.876 |
| H | 1.882 | -0.010 | -0.164 |
| C | 9.986 | -1.859 | -2.401 |
| H | 5.534 | -6.282 | -0.303 |
| H | 4.306 | -0.424 | -0.609 |
| H | 10.944 | -1.428 | -2.696 |
| C | 6.527 | -6.691 | -0.085 |
| C | 4.345 | -3.998 | 0.292 |
| C | 8.705 | -3.441 | -1.059 |
| C | 5.662 | -3.595 | 0.039 |
| C | 2.525 | -0.389 | 0.633 |
| C | 9.935 | -2.889 | -1.447 |
| H | 4.423 | -7.796 | 1.117 |
| C | 3.888 | -0.614 | 0.382 |
| H | 7.271 | -5.894 | -0.130 |
| C | 5.365 | -8.165 | 1.527 |
| H | 7.478 | -10.146 | 0.890 |
| H | 8.684 | -4.237 | -0.316 |
| O | 4.241 | -9.943 | 2.647 |
| C | 6.553 | -7.426 | 1.246 |
| H | 3.978 | -3.952 | 1.311 |
| H | 6.435 | -1.053 | 0.099 |
| H | 10.858 | -3.266 | -1.002 |
| C | 1.992 | -0.657 | 1.904 |
| C | 5.318 | -9.317 | 2.357 |
| H | 8.605 | -7.936 | 0.754 |
| N | 6.379 | -2.917 | 1.080 |
| C | 4.724 | -1.101 | 1.400 |
| C | 7.747 | -9.630 | 1.828 |
| H | 8.714 | -0.966 | -0.119 |
| C | 6.171 | -1.428 | 1.097 |
| H | 2.541 | -5.940 | 2.821 |
| C | 7.899 | -8.119 | 1.576 |
| H | 10.363 | 0.732 | -0.859 |
| H | 3.445 | -7.463 | 3.066 |
| C | 6.640 | -9.869 | 2.872 |
| C | 8.881 | -0.076 | 0.486 |
| C | 3.119 | -6.535 | 3.546 |
| H | 6.507 | -10.936 | 3.109 |
| C | 9.815 | 0.883 | 0.073 |
| O | 8.843 | -5.333 | 1.433 |
| C | 2.826 | -1.147 | 2.925 |
| H | 8.707 | -10.046 | 2.174 |

| | | | |
|---|---|---|---|
| H | 10.745 | -5.588 | 0.735 |
| O | 5.103 | -5.331 | 2.859 |
| B | 6.271 | -6.096 | 2.816 |
| C | 7.332 | -3.323 | 1.931 |
| C | 4.186 | -1.369 | 2.672 |
| B | 7.901 | -4.864 | 2.391 |
| C | 10.190 | -5.716 | 1.678 |
| H | 2.461 | -6.791 | 4.391 |
| H | 8.340 | -7.678 | 2.475 |
| C | 7.189 | -0.950 | 2.163 |
| C | 8.169 | 0.101 | 1.686 |
| C | 4.316 | -5.700 | 4.032 |
| C | 10.041 | 2.029 | 0.856 |
| H | 10.126 | -2.957 | 1.513 |
| H | 3.131 | -3.892 | 3.957 |
| H | 6.896 | -9.334 | 3.802 |
| H | 2.418 | -1.359 | 3.915 |
| H | 10.769 | 2.776 | 0.534 |
| N | 7.860 | -2.238 | 2.544 |
| H | 10.254 | -6.774 | 1.982 |
| H | 4.426 | -8.495 | 4.739 |
| O | 6.419 | -6.847 | 3.997 |
| H | 4.827 | -1.766 | 3.459 |
| C | 3.799 | -4.405 | 4.664 |
| H | 13.667 | -2.412 | 2.660 |
| H | 6.670 | -0.578 | 3.055 |
| H | 10.659 | -5.092 | 2.451 |
| C | 8.398 | 1.245 | 2.468 |
| C | 10.255 | -2.571 | 2.523 |
| C | 9.330 | 2.209 | 2.053 |
| C | 5.351 | -6.513 | 4.926 |
| C | 4.789 | -7.814 | 5.517 |
| O | 8.227 | -4.683 | 3.765 |
| C | 9.113 | -2.181 | 3.232 |
| H | 12.638 | -2.739 | 1.233 |
| C | 12.755 | -2.921 | 2.312 |
| H | 4.631 | -3.732 | 4.903 |
| H | 3.238 | -4.618 | 5.587 |
| H | 3.961 | -7.588 | 6.209 |
| C | 11.539 | -2.449 | 3.079 |
| H | 9.173 | -6.532 | 4.080 |
| H | 7.851 | 1.373 | 3.404 |
| H | 9.502 | 3.097 | 2.665 |
| C | 9.072 | -5.534 | 4.528 |
| H | 5.583 | -8.322 | 6.086 |
| H | 6.823 | -2.863 | 4.885 |
| C | 5.968 | -5.678 | 6.062 |
| H | 12.906 | -4.006 | 2.446 |
| H | 10.069 | -5.070 | 4.615 |
| H | 6.471 | -4.789 | 5.666 |
| C | 9.212 | -1.596 | 4.515 |
| C | 6.855 | -1.892 | 5.377 |
| C | 8.032 | -1.119 | 5.279 |
| H | 4.850 | -2.025 | 6.181 |
| C | 5.752 | -1.416 | 6.101 |
| C | 11.648 | -1.876 | 4.361 |
| H | 5.200 | -5.369 | 6.787 |

```
H     8.636    -5.644     5.530
H     6.713    -6.294     6.588
C    10.508    -1.453     5.055
C     8.077     0.137     5.925
C     5.803    -0.162     6.732
H    12.634    -1.756     4.815
C     6.971     0.613     6.644
H     8.978     0.746     5.839
H     4.939     0.207     7.289
H    10.612    -1.014     6.049
H     7.019     1.591     7.127
H     0.931    -0.486     2.099

                     1                      2                      3
                     A                      A                      A
 Frequencies --  -428.1144               18.9897
20.5813
 Red. masses --     9.7758                 4.8919
5.0981
 Zero-point correction=                           1.301737
(Hartree/Particle)
 Thermal correction to Energy=                    1.374277
 Thermal correction to Enthalpy=                  1.375221
 Thermal correction to Gibbs Free Energy=         1.195115
 Sum of electronic and zero-point Energies=          -3165.859718
 Sum of electronic and thermal Energies=             -3165.787178
 Sum of electronic and thermal Enthalpies=           -3165.786233
 Sum of electronic and thermal Free Energies=        -3165.966340

         Item               Value     Threshold  Converged?
 Maximum Force            0.000021     0.000450     YES
 RMS     Force            0.000002     0.000300     YES

---------------------------------------
```

**Ground State of C1 and C2**

```
---------------------------------------
 Cartesian coordinates (Angstroms):
---------------------------------------
158

H     7.209     5.333    -5.950
H     8.733     6.239    -7.090
C     7.509     5.588    -4.924
H     6.713     7.538    -5.479
H     6.840     5.032    -4.258
C     9.643     6.515    -6.542
C     7.356     7.132    -4.685
H    10.476     6.473    -7.255
H     9.031     8.567    -6.684
C     8.912     5.059    -4.721
N     9.902     5.482    -5.516
H     8.308     3.877    -3.184
C     9.502     7.923    -5.924
H     6.825     7.277    -3.733
N     9.128     4.186    -3.742
H    11.556     4.264    -5.985
```

| | | | |
|---|---|---|---|
| C | 8.673 | 7.934 | -4.622 |
| H | 10.577 | 2.677 | -3.990 |
| C | 11.311 | 5.077 | -5.284 |
| C | 10.449 | 3.621 | -3.438 |
| H | 8.438 | 8.976 | -4.357 |
| H | 10.501 | 8.338 | -5.716 |
| H | 11.941 | 5.944 | -5.525 |
| H | 9.292 | 7.537 | -3.800 |
| C | 11.525 | 4.639 | -3.831 |
| H | 10.473 | 3.397 | -2.364 |
| H | 12.523 | 4.195 | -3.728 |
| H | 11.460 | 5.514 | -3.167 |
| C | 4.979 | 2.299 | -0.420 |
| B | 6.664 | -0.247 | -3.945 |
| O | 7.395 | 0.010 | -5.107 |
| B | 7.338 | -0.993 | -2.491 |
| C | 7.375 | -2.664 | -2.813 |
| N | 8.238 | -3.309 | -3.637 |
| N | 6.413 | -3.535 | -2.438 |
| H | 10.056 | 0.935 | -1.953 |
| O | 8.734 | -0.604 | -2.219 |
| H | 8.173 | -7.583 | 1.739 |
| H | 8.967 | -5.276 | 1.187 |
| C | 7.498 | -6.869 | 1.264 |
| C | 7.944 | -5.574 | 0.950 |
| H | 5.820 | -8.243 | 1.193 |
| C | 6.177 | -7.238 | 0.959 |
| C | 7.083 | -4.658 | 0.330 |
| H | 7.437 | -3.657 | 0.091 |
| H | 6.216 | -1.851 | 0.309 |
| H | 12.676 | -0.732 | -2.076 |
| H | 3.198 | -4.541 | 0.701 |
| H | 13.819 | -1.987 | -2.611 |
| H | 12.586 | -2.357 | -1.369 |
| C | 5.313 | -6.320 | 0.344 |
| C | 12.777 | -1.807 | -2.304 |
| C | 5.753 | -5.018 | 0.017 |
| H | 7.880 | -1.231 | 0.015 |
| C | 6.804 | -0.987 | -0.057 |
| H | 4.292 | -6.614 | 0.094 |
| H | 6.599 | -0.133 | 0.614 |
| C | 3.497 | -3.941 | -0.160 |
| H | 10.910 | -6.645 | -0.886 |
| C | 4.821 | -4.064 | -0.640 |
| H | 10.157 | -2.547 | -2.027 |
| H | 1.572 | -2.984 | -0.343 |
| O | 6.421 | -0.650 | -1.378 |
| C | 11.804 | -2.220 | -3.388 |
| C | 2.585 | -3.058 | -0.744 |
| H | 9.084 | -5.057 | -1.481 |
| C | 10.480 | -2.549 | -3.065 |
| C | 10.513 | -6.627 | -1.903 |
| H | 13.222 | -2.053 | -5.019 |
| C | 9.487 | -5.734 | -2.234 |
| C | 12.193 | -2.288 | -4.740 |
| C | 5.178 | -3.276 | -1.759 |
| H | 6.728 | -5.618 | -2.235 |

| | | | |
|---|---|---|---|
| H | 8.420 | 1.243 | -1.276 |
| H | 11.830 | -8.195 | -2.623 |
| H | 4.847 | -6.945 | -2.538 |
| C | 2.967 | -2.244 | -1.830 |
| C | 11.028 | -7.499 | -2.879 |
| C | 8.974 | 0.782 | -2.116 |
| C | 9.541 | -2.879 | -4.053 |
| C | 4.263 | -2.390 | -2.341 |
| C | 6.568 | -4.899 | -3.049 |
| H | 1.609 | -0.569 | -1.666 |
| C | 8.964 | -5.705 | -3.540 |
| C | 11.275 | -2.670 | -5.724 |
| C | 2.007 | -1.245 | -2.441 |
| C | 4.546 | -6.373 | -3.418 |
| H | 8.676 | 1.319 | -3.038 |
| H | 2.513 | -0.634 | -3.203 |
| C | 7.856 | -4.740 | -3.899 |
| C | 9.931 | -2.972 | -5.413 |
| C | 10.512 | -7.471 | -4.185 |
| H | 2.768 | -7.551 | -3.793 |
| C | 5.336 | -5.289 | -3.835 |
| H | 4.574 | -1.804 | -3.200 |
| H | 11.590 | -2.727 | -6.767 |
| C | 9.483 | -6.573 | -4.515 |
| C | 3.377 | -6.706 | -4.121 |
| H | 1.146 | -1.749 | -2.911 |
| O | 5.347 | 0.195 | -4.072 |
| H | 10.910 | -8.144 | -4.947 |
| H | 7.619 | -4.842 | -4.964 |
| C | 4.942 | -4.533 | -4.954 |
| H | 9.085 | -6.536 | -5.530 |
| H | 6.820 | 2.579 | -4.669 |
| C | 9.026 | -3.419 | -6.505 |
| H | 7.408 | -2.089 | -5.993 |
| C | 2.989 | -5.950 | -5.239 |
| H | 10.451 | -4.853 | -7.279 |
| H | 8.093 | 2.400 | -5.910 |
| H | 5.550 | -3.686 | -5.272 |
| C | 6.577 | 0.862 | -5.982 |
| H | 5.179 | -1.523 | -6.109 |
| C | 5.120 | 0.560 | -5.473 |
| C | 7.014 | 2.310 | -5.715 |
| C | 7.733 | -2.880 | -6.665 |
| C | 9.458 | -4.420 | -7.404 |
| C | 3.775 | -4.860 | -5.655 |
| H | 2.078 | -6.206 | -5.784 |
| H | 3.565 | -0.940 | -5.620 |
| H | 4.533 | 2.586 | -4.917 |
| C | 4.489 | -0.668 | -6.151 |
| H | 7.900 | 0.705 | -7.684 |
| H | 6.647 | -0.562 | -7.646 |
| C | 6.846 | 0.497 | -7.443 |
| C | 4.157 | 1.748 | -5.520 |
| H | 3.176 | 1.444 | -5.126 |
| H | 6.476 | 3.009 | -6.372 |
| H | 3.478 | -4.265 | -6.521 |
| C | 6.892 | -3.337 | -7.690 |

```
H     4.246    -0.460    -7.204
C     8.615    -4.878    -8.427
H     6.212     1.110    -8.102
H     4.024     2.089    -6.559
H     5.894    -2.907    -7.802
H     8.963    -5.660    -9.105
C     7.325    -4.341    -8.572
H     6.665    -4.700    -9.363
H     1.411     0.039     2.906
H     2.574    -1.322     1.157
C     2.128     0.510     2.231
C     2.779    -0.256     1.249
H     1.896     2.485     3.104
C     2.402     1.887     2.344
C     3.700     0.346     0.383
H     4.207    -0.243    -0.383
C     3.325     2.491     1.486
C     3.994     1.729     0.492
H     3.531     3.557     1.587
C     5.406     3.595    -0.443
C     6.423     4.068    -1.384
O     6.880     3.346    -2.297
H     6.095     6.188    -1.551
C     6.893     5.505    -1.211
H     7.077     5.732    -0.149
H     7.801     5.696    -1.797
H     5.022     4.332     0.265
H     5.429     1.597    -1.130

                     1                      2                      3
                     A                      A                      A
 Frequencies --    11.1958                14.2595
17.3692
 Red. masses --     5.4444                 5.4240
4.8245
 Zero-point correction=                           1.315344
(Hartree/Particle)
 Thermal correction to Energy=                    1.392892
 Thermal correction to Enthalpy=                  1.393836
 Thermal correction to Gibbs Free Energy=         1.195678
 Sum of electronic and zero-point Energies=          -3280.109200
 Sum of electronic and thermal Energies=             -3280.031652
 Sum of electronic and thermal Enthalpies=           -3280.030707
 Sum of electronic and thermal Free Energies=        -3280.228866

         Item               Value     Threshold  Converged?
 Maximum Force            0.000022     0.000450     YES
 RMS     Force            0.000002     0.000300     YES

---------------------------------------
```

**Transition State of C1**

```
---------------------------------------
 Cartesian coordinates (Angstroms):
---------------------------------------
158
```

| | | | |
|---|---|---|---|
| H | 3.890 | 3.060 | 7.855 |
| H | 5.444 | 4.300 | 5.701 |
| H | 4.514 | 1.743 | 8.868 |
| C | 4.396 | 2.082 | 7.827 |
| H | 2.588 | 0.912 | 7.606 |
| H | 4.018 | 3.393 | 3.937 |
| H | 6.263 | 3.204 | 7.549 |
| H | 5.264 | 4.387 | 3.143 |
| H | 3.201 | 1.578 | 6.095 |
| C | 3.511 | 1.096 | 7.036 |
| C | 5.875 | 3.540 | 5.037 |
| C | 5.093 | 3.467 | 3.719 |
| C | 5.816 | 2.253 | 7.235 |
| H | 6.931 | 3.794 | 4.857 |
| N | 5.819 | 2.244 | 5.756 |
| H | 6.481 | 1.454 | 7.587 |
| C | 4.159 | -0.265 | 6.702 |
| H | 4.382 | -0.812 | 7.630 |
| C | 5.545 | 2.248 | 2.906 |
| C | 5.634 | 1.095 | 5.089 |
| H | 3.422 | -0.860 | 6.143 |
| H | 4.852 | 2.032 | 2.084 |
| H | 6.552 | 2.410 | 2.490 |
| N | 5.559 | 1.057 | 3.765 |
| C | 5.475 | -0.201 | 5.851 |
| H | 6.353 | -0.323 | 6.500 |
| H | 5.361 | 0.127 | 3.320 |
| H | 5.494 | -1.024 | 5.126 |
| H | -4.552 | -1.051 | 5.292 |
| H | -2.140 | -1.604 | 4.917 |
| C | -3.897 | -0.338 | 4.786 |
| C | -2.545 | -0.651 | 4.569 |
| H | -5.452 | 1.148 | 4.506 |
| C | -4.401 | 0.897 | 4.348 |
| C | -1.703 | 0.260 | 3.914 |
| H | -0.651 | 0.033 | 3.770 |
| H | 2.638 | 1.862 | 3.258 |
| H | -2.823 | -4.136 | 3.942 |
| H | -1.580 | 3.933 | 4.423 |
| H | -1.245 | -4.934 | 3.804 |
| H | -2.718 | -5.801 | 3.301 |
| C | -3.558 | 1.812 | 3.698 |
| C | -2.226 | -4.817 | 3.313 |
| C | -2.199 | 1.504 | 3.470 |
| H | 0.281 | -5.712 | -0.560 |
| H | 2.133 | 0.530 | 4.345 |
| C | 2.343 | 0.803 | 3.296 |
| H | 1.192 | -3.967 | 0.963 |
| H | -3.950 | 2.772 | 3.356 |
| H | 3.163 | 0.180 | 2.917 |
| C | -1.122 | 3.763 | 3.447 |
| H | -5.874 | -1.479 | 2.671 |
| C | 0.989 | -4.979 | -0.944 |
| C | -1.320 | 2.518 | 2.819 |
| C | 1.507 | -4.004 | -0.080 |
| H | -1.613 | -2.257 | 2.579 |
| H | -0.216 | 5.725 | 3.370 |

| | | | |
|---|---|---|---|
| O | 1.173 | 0.656 | 2.508 |
| C | -2.069 | -4.264 | 1.913 |
| C | -0.355 | 4.774 | 2.851 |
| H | -3.632 | -0.578 | 2.096 |
| O | 4.803 | -1.273 | 2.574 |
| H | 6.914 | -0.036 | 1.254 |
| C | -1.718 | -2.918 | 1.724 |
| C | -5.573 | -1.406 | 1.624 |
| H | 0.943 | -5.747 | -2.972 |
| C | 1.359 | -4.997 | -2.297 |
| H | -2.609 | -6.095 | 0.889 |
| H | 0.875 | -1.419 | 4.329 |
| C | 5.280 | -1.444 | 1.400 |
| C | -4.309 | -0.896 | 1.304 |
| C | 2.443 | -3.055 | -0.543 |
| C | 3.105 | -2.155 | 0.439 |
| C | -2.304 | -5.053 | 0.771 |
| C | -0.709 | 2.324 | 1.558 |
| H | -3.088 | 1.489 | 0.829 |
| B | 0.848 | -0.473 | 1.722 |
| C | 4.497 | -1.914 | 0.314 |
| C | 6.753 | -1.124 | 1.171 |
| H | 2.427 | -1.951 | 3.604 |
| H | -7.430 | -2.218 | 0.850 |
| H | -3.565 | 3.627 | 0.090 |
| C | 0.217 | 4.587 | 1.580 |
| C | -6.445 | -1.819 | 0.601 |
| C | 1.332 | -2.071 | 3.564 |
| N | -1.020 | 1.152 | 0.784 |
| C | -0.566 | -0.115 | 0.928 |
| H | 7.366 | -1.605 | 1.950 |
| C | -1.536 | -2.388 | 0.441 |
| O | 0.825 | -1.781 | 2.263 |
| C | 2.263 | -4.033 | -2.779 |
| C | 0.001 | 3.355 | 0.939 |
| H | 7.105 | -1.446 | 0.179 |
| C | 2.803 | -3.080 | -1.910 |
| C | -2.334 | 1.215 | 0.075 |
| H | 0.794 | 6.661 | 1.313 |
| N | -1.413 | -0.964 | 0.309 |
| C | -3.904 | -0.801 | -0.040 |
| C | -2.151 | -4.515 | -0.512 |
| C | 1.038 | 5.667 | 0.909 |
| C | -3.015 | 3.463 | -0.840 |
| B | 2.365 | -0.196 | 0.127 |
| H | 1.072 | -3.117 | 3.788 |
| H | 2.117 | 5.496 | 1.066 |
| C | -2.541 | -0.246 | -0.385 |
| H | 2.547 | -4.027 | -3.834 |
| C | -1.743 | -3.181 | -0.713 |
| C | -6.046 | -1.719 | -0.742 |
| H | -3.517 | 5.398 | -1.672 |
| C | -2.333 | 2.249 | -1.030 |
| H | 0.356 | 3.198 | -0.075 |
| H | 3.504 | -2.340 | -2.290 |
| H | -2.312 | -5.146 | -1.387 |
| C | -4.775 | -1.213 | -1.061 |

| | | | |
|---|---|---|---|
| C | -2.983 | 4.459 | -1.828 |
| O | 2.013 | -0.099 | -1.217 |
| H | 0.865 | 5.677 | -0.179 |
| O | 3.231 | 0.837 | 0.493 |
| H | -6.720 | -2.037 | -1.540 |
| H | -2.374 | -0.339 | -1.464 |
| C | -1.612 | 2.039 | -2.220 |
| H | -4.451 | -1.146 | -2.101 |
| H | 4.316 | -0.412 | -2.628 |
| C | -1.554 | -2.659 | -2.087 |
| H | 0.320 | -1.664 | -1.646 |
| C | -2.264 | 4.244 | -3.015 |
| H | -3.378 | -3.538 | -2.857 |
| H | 2.902 | -0.197 | -3.693 |
| H | -1.065 | 1.108 | -2.372 |
| C | 2.781 | 0.962 | -1.870 |
| H | 2.409 | 3.285 | -0.205 |
| C | 3.675 | 1.568 | -0.689 |
| C | 3.590 | 0.318 | -3.007 |
| C | -0.434 | -1.862 | -2.401 |
| C | -2.500 | -2.934 | -3.097 |
| C | -1.579 | 3.032 | -3.209 |
| H | -2.237 | 5.017 | -3.786 |
| H | 4.064 | 3.375 | 0.435 |
| H | 5.402 | 0.240 | -0.882 |
| C | 3.456 | 3.064 | -0.428 |
| H | 1.194 | 1.431 | -3.260 |
| H | 1.078 | 2.324 | -1.733 |
| C | 1.779 | 1.946 | -2.484 |
| C | 5.182 | 1.314 | -0.856 |
| H | 5.721 | 1.755 | -0.005 |
| H | 4.135 | 1.089 | -3.572 |
| H | -1.014 | 2.860 | -4.127 |
| C | -0.277 | -1.336 | -3.689 |
| H | 3.768 | 3.660 | -1.300 |
| C | -2.339 | -2.409 | -4.389 |
| H | 2.298 | 2.797 | -2.948 |
| H | 5.555 | 1.780 | -1.780 |
| H | 0.602 | -0.727 | -3.911 |
| H | -3.086 | -2.622 | -5.156 |
| C | -1.229 | -1.601 | -4.688 |
| H | -1.107 | -1.185 | -5.690 |
| H | 2.752 | -2.290 | 1.456 |
| H | 4.990 | -2.048 | -0.650 |

| | 1 | 2 | 3 |
|---|---|---|---|
| | A | A | A |
| Frequencies -- | -412.8472 | 14.9871 | 19.2513 |
| Red. masses -- | 10.7239 | 5.3091 | 4.8421 |

Zero-point correction= 1.316385 (Hartree/Particle)
Thermal correction to Energy= 1.392395
Thermal correction to Enthalpy= 1.393339
Thermal correction to Gibbs Free Energy= 1.202838
Sum of electronic and zero-point Energies= -3280.074135

```
 Sum of electronic and thermal Energies=            -3279.998125
 Sum of electronic and thermal Enthalpies=          -3279.997181
 Sum of electronic and thermal Free Energies=       -3280.187682

         Item               Value     Threshold  Converged?
 Maximum Force            0.000055     0.000450     YES
 RMS     Force            0.000006     0.000300     YES

----------------------------------------
```

**Transition State of C2**

```
----------------------------------------
 Cartesian coordinates (Angstroms):
----------------------------------------
158

H     5.653    19.226     5.250
C     5.926    18.178     5.066
H     4.046    17.855     4.034
H     5.730    18.004     7.204
C     5.104    17.577     3.920
H     5.458    17.968     2.957
N     5.651    17.452     6.314
H     7.004    18.123     4.844
H     2.759    16.347     8.468
H     2.451    16.385     6.026
H     5.070    16.390     8.491
C     5.112    16.241     6.371
C     2.342    15.432     6.564
C     3.149    15.505     7.878
H     1.273    15.344     6.814
C     4.699    15.701     7.721
C     5.230    16.048     3.928
N     4.910    15.505     5.269
H     4.527    15.597     3.216
H     6.250    15.736     3.656
H     2.981    14.592     8.469
C     2.733    14.284     5.611
H     2.212    14.431     4.652
H     5.216    14.743     7.875
C     4.257    14.181     5.365
H     2.402    13.315     6.018
H     4.741    13.615     6.171
H     4.470    13.652     4.428
H    -3.177    21.413    12.061
H    -0.964    20.499    11.331
C    -2.438    22.068    11.597
C    -1.196    21.555    11.183
H    -3.688    23.837    11.712
C    -2.723    23.430    11.404
C    -0.247    22.394    10.579
H     0.712    21.987    10.260
H     2.261    19.592    10.789
H    -1.599    16.366     8.913
H     0.346    26.078    11.431
H    -1.248    17.827     9.885
H     0.082    16.819     9.276
```

| | | | |
|---|---|---|---|
| C | -1.771 | 24.273 | 10.811 |
| C | -0.916 | 17.222 | 9.027 |
| C | -0.521 | 23.765 | 10.390 |
| H | 2.916 | 24.598 | 12.206 |
| H | 1.601 | 18.852 | 9.296 |
| C | 2.356 | 19.549 | 9.694 |
| H | 3.099 | 22.508 | 10.856 |
| H | -1.994 | 25.330 | 10.658 |
| H | 3.361 | 19.189 | 9.425 |
| C | 0.815 | 25.877 | 10.466 |
| H | -4.547 | 21.269 | 9.443 |
| C | 3.680 | 24.516 | 11.432 |
| C | 0.489 | 24.681 | 9.797 |
| C | 3.777 | 23.342 | 10.674 |
| H | -0.397 | 19.914 | 8.772 |
| H | 1.964 | 27.705 | 10.480 |
| O | 2.129 | 20.873 | 9.201 |
| C | -0.858 | 18.049 | 7.761 |
| C | 1.731 | 26.790 | 9.931 |
| H | -2.270 | 22.066 | 8.862 |
| H | 4.282 | 21.122 | 9.396 |
| O | 5.658 | 19.160 | 8.437 |
| H | 8.263 | 18.851 | 8.216 |
| C | -0.548 | 19.417 | 7.815 |
| C | -4.281 | 21.425 | 8.396 |
| H | 4.467 | 26.509 | 11.767 |
| C | 4.547 | 25.591 | 11.183 |
| H | -1.369 | 16.418 | 6.429 |
| H | 2.312 | 18.242 | 7.244 |
| C | 6.501 | 20.112 | 8.288 |
| C | -2.996 | 21.879 | 8.072 |
| C | 4.755 | 23.210 | 9.665 |
| C | 4.914 | 21.898 | 8.981 |
| C | -1.103 | 17.475 | 6.497 |
| C | 1.118 | 24.446 | 8.546 |
| H | -1.450 | 24.053 | 7.948 |
| B | 2.185 | 21.206 | 7.817 |
| C | 6.208 | 21.465 | 8.589 |
| C | 7.884 | 19.769 | 7.740 |
| H | 3.867 | 19.138 | 7.189 |
| H | -6.218 | 20.819 | 7.629 |
| H | -1.494 | 26.362 | 7.759 |
| C | 2.359 | 26.543 | 8.700 |
| C | -5.217 | 21.173 | 7.377 |
| C | 2.877 | 19.034 | 6.727 |
| N | 0.550 | 23.453 | 7.672 |
| C | 0.844 | 22.164 | 7.455 |
| H | 8.605 | 20.587 | 7.888 |
| C | -0.417 | 20.176 | 6.644 |
| H | 7.003 | 22.195 | 8.434 |
| O | 2.161 | 20.249 | 6.774 |
| C | 5.504 | 25.485 | 10.158 |
| C | 2.014 | 25.371 | 8.007 |
| H | 7.817 | 19.574 | 6.656 |
| C | 5.600 | 24.311 | 9.402 |
| C | -0.789 | 23.840 | 7.096 |
| H | 3.299 | 28.495 | 8.578 |

| | | | |
|---|---|---|---|
| N | -0.175 | 21.582 | 6.780 |
| C | -2.636 | 22.084 | 6.728 |
| C | -1.009 | 18.244 | 5.331 |
| C | 3.367 | 27.501 | 8.110 |
| C | -1.065 | 26.319 | 6.756 |
| B | 3.986 | 22.124 | 7.115 |
| H | 2.986 | 18.756 | 5.668 |
| H | 4.390 | 27.119 | 8.270 |
| C | -1.241 | 22.550 | 6.371 |
| H | 6.173 | 26.322 | 9.946 |
| C | -0.648 | 19.607 | 5.374 |
| C | -4.860 | 21.378 | 6.034 |
| H | -1.207 | 28.453 | 6.426 |
| C | -0.669 | 25.076 | 6.231 |
| H | 2.425 | 25.176 | 7.024 |
| H | 6.335 | 24.247 | 8.599 |
| H | -1.187 | 17.783 | 4.358 |
| C | -3.571 | 21.830 | 5.711 |
| C | -0.896 | 27.494 | 6.008 |
| O | 4.547 | 21.371 | 6.070 |
| H | 3.220 | 27.613 | 7.023 |
| O | 3.984 | 23.476 | 6.783 |
| H | -5.583 | 21.184 | 5.239 |
| H | -1.174 | 22.667 | 5.282 |
| C | -0.093 | 25.021 | 4.948 |
| H | -3.282 | 21.979 | 4.669 |
| H | 6.896 | 22.655 | 6.273 |
| C | -0.498 | 20.386 | 4.119 |
| H | 1.458 | 21.138 | 4.633 |
| C | -0.322 | 27.433 | 4.728 |
| H | -2.419 | 19.786 | 3.324 |
| H | 7.031 | 21.269 | 5.164 |
| H | 0.238 | 24.067 | 4.535 |
| C | 5.114 | 22.266 | 5.073 |
| H | 2.443 | 23.083 | 4.677 |
| C | 4.418 | 23.649 | 5.401 |
| C | 6.638 | 22.290 | 5.272 |
| C | 0.665 | 21.152 | 3.885 |
| C | -1.515 | 20.370 | 3.142 |
| C | 0.078 | 26.193 | 4.199 |
| H | -0.187 | 28.345 | 4.144 |
| H | 2.668 | 24.831 | 4.910 |
| H | 6.189 | 24.770 | 6.022 |
| C | 3.155 | 23.909 | 4.566 |
| H | 5.314 | 20.746 | 3.540 |
| H | 3.707 | 21.517 | 3.576 |
| C | 4.784 | 21.700 | 3.686 |
| C | 5.336 | 24.875 | 5.339 |
| H | 4.766 | 25.771 | 5.628 |
| H | 7.120 | 22.934 | 4.521 |
| H | 0.527 | 26.138 | 3.206 |
| C | 0.796 | 21.898 | 2.705 |
| H | 3.402 | 24.027 | 3.501 |
| C | -1.382 | 21.119 | 1.962 |
| H | 5.109 | 22.397 | 2.897 |
| H | 5.715 | 25.018 | 4.315 |
| H | 1.700 | 22.485 | 2.535 |

```
H    -2.183    21.106     1.220
C    -0.229    21.889     1.743
H    -0.127    22.477     0.828

                     1                      2                      3
                     A                      A                      A
 Frequencies --  -404.1519               14.9932
17.9827
 Red. masses --    10.7915                4.6450
4.8961
 Zero-point correction=                           1.316048
(Hartree/Particle)
 Thermal correction to Energy=                    1.391914
 Thermal correction to Enthalpy=                  1.392859
 Thermal correction to Gibbs Free Energy=         1.203083
 Sum of electronic and zero-point Energies=          -3280.072629
 Sum of electronic and thermal Energies=             -3279.996763
 Sum of electronic and thermal Enthalpies=           -3279.995818
 Sum of electronic and thermal Free Energies=        -3280.185594

          Item               Value     Threshold  Converged?
 Maximum Force            0.000004     0.000450     YES
 RMS     Force            0.000000     0.000300     YES

----------------------------------------
```

## Ground State of D1 and D2

```
----------------------------------------
 Cartesian coordinates (Angstroms):
----------------------------------------
145

H    -5.151    -0.058     1.771
O    -3.637     0.697     2.665
H    -4.726     3.018     2.291
C    -3.160     1.592     1.931
C    -4.012     2.778     1.489
H    -4.599     2.430     0.619
C    -1.818     1.481     1.370
C    -3.164     3.996     1.070
H    -2.646     4.393     1.959
H    -3.814     4.793     0.680
C    -1.371     2.348     0.422
C    -2.113     3.587     0.020
H    -2.593     3.393    -0.956
H    -1.383     4.395    -0.155
H    -1.232     0.610     1.656
H    -0.440     2.150    -0.114
C    -1.244    -1.922    -2.127
H    -1.345    -1.987    -1.036
H    -2.240    -2.088    -2.576
H    -0.589    -2.750    -2.434
Si    -0.553    -0.246    -2.764
C    -2.090     0.920    -2.733
C    -3.201     0.673    -1.892
H    -3.177    -0.182    -1.217
C    -4.339     1.493    -1.906
```

| | | | |
|---|---|---|---|
| H | -5.187 | 1.258 | -1.260 |
| C | -4.391 | 2.615 | -2.752 |
| H | -5.274 | 3.257 | -2.762 |
| C | -3.295 | 2.901 | -3.582 |
| H | -3.322 | 3.770 | -4.244 |
| C | -2.169 | 2.058 | -3.574 |
| C | -0.212 | -0.544 | -4.630 |
| H | -1.056 | -1.054 | -5.125 |
| H | -0.023 | 0.404 | -5.161 |
| H | -1.343 | 2.280 | -4.256 |
| H | 0.691 | -1.165 | -4.748 |
| H | -0.076 | 2.478 | -2.357 |
| O | 0.753 | 2.277 | -1.897 |
| B | 1.108 | 0.847 | -2.024 |
| C | 1.772 | 0.400 | -0.519 |
| H | 3.862 | 5.391 | -1.053 |
| C | 3.193 | 4.817 | -0.410 |
| H | 2.356 | 6.579 | 0.521 |
| C | 2.093 | -3.453 | -2.774 |
| C | 2.344 | 5.488 | 0.479 |
| C | 3.233 | 3.409 | -0.490 |
| O | 2.187 | 0.616 | -3.014 |
| H | 2.678 | -1.374 | -2.547 |
| C | 2.205 | -2.238 | -2.079 |
| H | 1.418 | -5.507 | -2.626 |
| C | 1.495 | -4.544 | -2.117 |
| C | 2.352 | 2.688 | 0.353 |
| C | 1.487 | 4.767 | 1.327 |
| N | 2.316 | 1.248 | 0.383 |
| C | 1.510 | 3.365 | 1.246 |
| C | 1.683 | -2.087 | -0.787 |
| H | 2.846 | 1.323 | -2.896 |
| N | 1.941 | -0.868 | -0.075 |
| H | 0.846 | 2.786 | 1.883 |
| C | 0.987 | -4.399 | -0.822 |
| C | 1.047 | -3.171 | -0.131 |
| H | 0.496 | -5.243 | -0.335 |
| C | 2.983 | 0.542 | 1.537 |
| C | 2.713 | -0.952 | 1.206 |
| H | 2.072 | -1.399 | 1.973 |
| H | 4.058 | 0.756 | 1.474 |
| C | 0.551 | 5.453 | 2.300 |
| C | 2.606 | -3.568 | -4.193 |
| H | 5.722 | -4.206 | 2.735 |
| H | 3.620 | -2.865 | 2.909 |
| C | 5.473 | -3.480 | 1.959 |
| C | 4.293 | -2.725 | 2.060 |
| H | 7.239 | -3.898 | 0.773 |
| C | 6.326 | -3.307 | 0.856 |
| C | 3.968 | -1.787 | 1.067 |
| C | 5.994 | -2.377 | -0.146 |
| C | 4.821 | -1.620 | -0.040 |
| H | 6.646 | -2.249 | -1.012 |
| H | 4.551 | -0.910 | -0.821 |
| H | 3.391 | 3.175 | 5.387 |
| H | 4.245 | 2.225 | 3.243 |
| C | 2.781 | 2.467 | 4.825 |

| | | | |
|---|---|---|---|
| C | 3.266 | 1.927 | 3.624 |
| H | 1.128 | 2.525 | 6.226 |
| C | 1.509 | 2.102 | 5.295 |
| C | 2.489 | 1.016 | 2.888 |
| C | 0.731 | 1.185 | 4.567 |
| C | 1.222 | 0.646 | 3.371 |
| H | -0.258 | 0.893 | 4.925 |
| H | 0.612 | -0.053 | 2.805 |
| H | 0.616 | 4.991 | 3.298 |
| H | -0.498 | 5.366 | 1.968 |
| H | 0.788 | 6.524 | 2.393 |
| H | 2.841 | -4.612 | -4.450 |
| H | 3.508 | -2.954 | -4.339 |
| H | 1.848 | -3.209 | -4.910 |
| H | 4.976 | 3.085 | -4.802 |
| H | 3.460 | 4.067 | -3.085 |
| C | 4.152 | 3.269 | -2.811 |
| C | 4.997 | 2.705 | -3.779 |
| C | 4.142 | 2.782 | -1.483 |
| C | 5.852 | 1.645 | -3.436 |
| H | 6.504 | 1.199 | -4.189 |
| C | 5.020 | 1.730 | -1.151 |
| C | 5.863 | 1.164 | -2.117 |
| H | 5.067 | 1.367 | -0.127 |
| H | 6.535 | 0.352 | -1.833 |
| H | 0.218 | -4.803 | 4.169 |
| H | 1.329 | -4.894 | 1.941 |
| C | 0.640 | -4.081 | 2.176 |
| C | 0.018 | -4.024 | 3.431 |
| C | 0.409 | -3.079 | 1.207 |
| C | -0.853 | -2.966 | 3.741 |
| H | -1.336 | -2.920 | 4.719 |
| C | -0.467 | -2.021 | 1.533 |
| C | -1.095 | -1.966 | 2.787 |
| H | -0.649 | -1.240 | 0.796 |
| H | -1.771 | -1.140 | 3.018 |
| H | -5.051 | -5.278 | 1.453 |
| H | -6.016 | -3.805 | 1.350 |
| H | -3.869 | -3.377 | 2.468 |
| H | -8.127 | -1.802 | 0.824 |
| C | -5.109 | -4.296 | 0.960 |
| H | -7.476 | 0.403 | 1.698 |
| C | -3.880 | -3.461 | 1.372 |
| C | -7.907 | -1.015 | 0.087 |
| C | -7.050 | 0.074 | 0.742 |
| N | -5.712 | -0.473 | 1.017 |
| H | -8.856 | -0.587 | -0.260 |
| H | -6.255 | -4.996 | -0.736 |
| C | -5.281 | -4.515 | -0.558 |
| H | -3.398 | -1.319 | 1.500 |
| C | -3.825 | -2.015 | 0.773 |
| H | -2.953 | -3.974 | 1.080 |
| C | -5.168 | -1.485 | 0.338 |
| H | -4.504 | -5.199 | -0.936 |
| C | -7.156 | -1.625 | -1.103 |
| H | -7.679 | -2.515 | -1.475 |
| N | -5.794 | -2.050 | -0.699 |

```
H    -6.959     0.952     0.083
C    -5.187    -3.212    -1.391
H    -3.163    -2.008    -0.101
H    -7.065    -0.905    -1.931
H    -4.143    -2.971    -1.623
H    -5.711    -3.316    -2.349

                     1                      2                      3
                     A                      A                      A
 Frequencies --    14.8637                21.8550
24.4984
 Red. masses --     5.4974                 4.9285
4.2487
 Zero-point correction=                           1.202599
(Hartree/Particle)
 Thermal correction to Energy=                    1.273168
 Thermal correction to Enthalpy=                  1.274112
 Thermal correction to Gibbs Free Energy=         1.094801
 Sum of electronic and zero-point Energies=          -3237.884351
 Sum of electronic and thermal Energies=             -3237.813782
 Sum of electronic and thermal Enthalpies=           -3237.812838
 Sum of electronic and thermal Free Energies=        -3237.992150

          Item               Value     Threshold  Converged?
 Maximum Force            0.000000     0.000450     YES
 RMS     Force            0.000000     0.000300     YES

----------------------------------------
```

**Transition State of D1**

```
----------------------------------------
 Cartesian coordinates (Angstroms):
----------------------------------------
145

H    -5.626     0.232     1.755
O    -4.060     0.103     2.382
H    -4.421     2.605     1.868
C    -3.271     0.808     1.669
C    -3.757     2.151     1.114
H    -4.367     1.956     0.216
C    -1.929     0.409     1.392
C    -2.592     3.089     0.747
H    -2.081     3.408     1.671
H    -2.973     3.995     0.248
C    -1.117     1.070     0.475
C    -1.581     2.363    -0.166
H    -2.068     2.160    -1.133
H    -0.714     3.000    -0.378
H    -1.574    -0.493     1.893
H    -0.058     0.847     0.450
C    -2.192    -2.290    -0.615
H    -2.584    -1.924     0.347
H    -3.043    -2.697    -1.192
H    -1.499    -3.119    -0.405
Si    -1.329    -0.894    -1.640
C    -2.790     0.104    -2.357
```

| | | | |
|---|---|---|---|
| C | -4.048 | 0.122 | -1.704 |
| H | -4.192 | -0.493 | -0.816 |
| C | -5.109 | 0.921 | -2.158 |
| H | -6.067 | 0.901 | -1.634 |
| C | -4.943 | 1.744 | -3.285 |
| H | -5.765 | 2.368 | -3.640 |
| C | -3.705 | 1.750 | -3.953 |
| H | -3.564 | 2.381 | -4.834 |
| C | -2.653 | 0.944 | -3.491 |
| C | -0.629 | -1.840 | -3.195 |
| H | -1.339 | -2.634 | -3.491 |
| H | -0.513 | -1.172 | -4.067 |
| H | -1.703 | 0.962 | -4.037 |
| H | 0.349 | -2.304 | -2.997 |
| H | 0.257 | 1.936 | -2.856 |
| O | 0.852 | 1.906 | -2.088 |
| B | 1.595 | 0.745 | -2.021 |
| C | 2.375 | 0.486 | -0.634 |
| H | 3.294 | 5.511 | -1.464 |
| C | 2.731 | 4.923 | -0.738 |
| H | 1.682 | 6.636 | 0.059 |
| C | 4.739 | -2.466 | -2.990 |
| C | 1.827 | 5.556 | 0.125 |
| C | 2.966 | 3.537 | -0.669 |
| O | 1.879 | -0.099 | -3.066 |
| H | 4.472 | -0.410 | -2.370 |
| C | 4.218 | -1.451 | -2.176 |
| H | 4.840 | -4.613 | -3.267 |
| C | 4.432 | -3.801 | -2.661 |
| C | 2.212 | 2.795 | 0.272 |
| C | 1.108 | 4.817 | 1.084 |
| N | 2.379 | 1.376 | 0.390 |
| C | 1.309 | 3.428 | 1.137 |
| C | 3.377 | -1.747 | -1.093 |
| H | 1.300 | 0.040 | -3.834 |
| N | 2.979 | -0.661 | -0.252 |
| H | 0.734 | 2.823 | 1.834 |
| C | 3.616 | -4.098 | -1.565 |
| C | 3.058 | -3.085 | -0.756 |
| H | 3.381 | -5.137 | -1.329 |
| C | 3.119 | 0.843 | 1.580 |
| C | 3.316 | -0.650 | 1.208 |
| H | 2.564 | -1.253 | 1.728 |
| H | 4.089 | 1.362 | 1.617 |
| C | 0.106 | 5.479 | 2.006 |
| C | 5.605 | -2.123 | -4.184 |
| H | 6.196 | -3.338 | 3.731 |
| H | 3.939 | -2.454 | 3.121 |
| C | 6.093 | -2.623 | 2.913 |
| C | 4.825 | -2.123 | 2.578 |
| H | 8.209 | -2.605 | 2.443 |
| C | 7.224 | -2.211 | 2.189 |
| C | 4.685 | -1.201 | 1.527 |
| C | 7.084 | -1.295 | 1.132 |
| C | 5.819 | -0.789 | 0.805 |
| H | 7.958 | -0.979 | 0.560 |
| H | 5.703 | -0.091 | -0.022 |

| | | | |
|---|---|---|---|
| H | 2.534 | 2.966 | 5.717 |
| H | 3.829 | 2.468 | 3.639 |
| C | 2.139 | 2.260 | 4.985 |
| C | 2.872 | 1.975 | 3.822 |
| H | 0.319 | 1.872 | 6.097 |
| C | 0.895 | 1.644 | 5.199 |
| C | 2.370 | 1.069 | 2.874 |
| C | 0.391 | 0.733 | 4.253 |
| C | 1.130 | 0.443 | 3.099 |
| H | -0.578 | 0.257 | 4.407 |
| H | 0.727 | -0.251 | 2.361 |
| H | 0.015 | 4.926 | 2.953 |
| H | -0.894 | 5.506 | 1.540 |
| H | 0.397 | 6.517 | 2.229 |
| H | 6.331 | -2.924 | -4.394 |
| H | 6.152 | -1.183 | -4.019 |
| H | 4.986 | -1.990 | -5.088 |
| H | 4.603 | 2.407 | -4.903 |
| H | 2.893 | 3.396 | -3.374 |
| C | 3.800 | 2.947 | -2.968 |
| C | 4.759 | 2.383 | -3.823 |
| C | 3.976 | 2.913 | -1.570 |
| C | 5.916 | 1.790 | -3.292 |
| H | 6.666 | 1.358 | -3.956 |
| C | 5.143 | 2.318 | -1.046 |
| C | 6.107 | 1.763 | -1.900 |
| H | 5.306 | 2.315 | 0.033 |
| H | 7.010 | 1.316 | -1.480 |
| H | 2.188 | -5.592 | 3.084 |
| H | 3.568 | -4.980 | 1.103 |
| C | 2.620 | -4.473 | 1.285 |
| C | 1.846 | -4.807 | 2.406 |
| C | 2.206 | -3.450 | 0.403 |
| C | 0.647 | -4.123 | 2.665 |
| H | 0.047 | -4.378 | 3.541 |
| C | 0.992 | -2.781 | 0.664 |
| C | 0.221 | -3.112 | 1.787 |
| H | 0.659 | -1.988 | -0.009 |
| H | -0.720 | -2.591 | 1.965 |
| H | -8.448 | -4.233 | 1.694 |
| H | -8.459 | -2.470 | 1.747 |
| H | -6.247 | -3.379 | 2.315 |
| H | -9.194 | 0.476 | 1.578 |
| C | -8.075 | -3.334 | 1.180 |
| H | -7.259 | 1.943 | 2.037 |
| C | -6.534 | -3.326 | 1.254 |
| C | -8.759 | 1.026 | 0.730 |
| C | -7.319 | 1.427 | 1.070 |
| N | -6.494 | 0.217 | 1.160 |
| H | -9.370 | 1.919 | 0.544 |
| H | -9.754 | -3.126 | -0.171 |
| C | -8.668 | -3.295 | -0.245 |
| H | -4.976 | -1.770 | 1.243 |
| C | -5.827 | -2.076 | 0.623 |
| H | -6.131 | -4.225 | 0.763 |
| C | -6.735 | -0.880 | 0.450 |
| H | -8.522 | -4.263 | -0.750 |

```
C    -8.764     0.137    -0.520
H    -9.748    -0.333    -0.656
N    -7.768    -0.954    -0.404
H    -6.904     2.095     0.297
C    -8.034    -2.207    -1.143
H    -5.420    -2.332    -0.365
H    -8.535     0.722    -1.425
H    -7.091    -2.559    -1.578
H    -8.696    -1.949    -1.979
```

```
                     1                      2                      3
                     A                      A                      A
 Frequencies --   -87.1398               12.7987
16.3093
 Red. masses --     6.0834                5.2748
5.2315
 Zero-point correction=                           1.200175
(Hartree/Particle)
 Thermal correction to Energy=                    1.270579
 Thermal correction to Enthalpy=                  1.271524
 Thermal correction to Gibbs Free Energy=         1.090060
 Sum of electronic and zero-point Energies=          -3237.851811
 Sum of electronic and thermal Energies=             -3237.781407
 Sum of electronic and thermal Enthalpies=           -3237.780463
 Sum of electronic and thermal Free Energies=        -3237.961926

          Item               Value     Threshold  Converged?
 Maximum Force            0.000003     0.000450     YES
 RMS     Force            0.000000     0.000300     YES
```

**Transition State of D2**

```
---------------------------------------
 Cartesian coordinates (Angstroms):
---------------------------------------
145

H     9.613     3.082     6.257
H     9.203     1.864     5.050
H     9.265    -0.495     3.174
C     9.518     2.914     5.174
H    11.564     2.284     4.848
H     7.489     3.635     5.206
C    10.902     3.101     4.518
C     9.402    -0.269     2.106
H     9.766    -1.175     1.603
C     8.404     3.832     4.628
H     7.254    -0.530     1.725
H    11.359     4.047     4.851
H    11.337     0.636     2.539
C     8.064     0.177     1.504
C    10.438     0.852     1.945
N     7.690     1.474     2.080
H     8.675     4.886     4.797
C     8.576     2.365     2.505
N     9.897     2.149     2.419
C     8.062     3.654     3.107
```

| | | | |
|---|---|---|---|
| C | 10.849 | 3.136 | 2.973 |
| H | 6.974 | 3.681 | 2.960 |
| H | 8.142 | 0.273 | 0.408 |
| H | 11.831 | 2.912 | 2.537 |
| H | 10.739 | 0.963 | 0.892 |
| H | 10.560 | 4.134 | 2.618 |
| H | 8.486 | 4.485 | 2.523 |
| H | 4.315 | -0.658 | -6.281 |
| H | 2.753 | -2.479 | -5.555 |
| C | 4.113 | -0.821 | -5.220 |
| C | 3.226 | -1.833 | -4.812 |
| C | 4.755 | -0.040 | -4.244 |
| H | 5.472 | 0.728 | -4.544 |
| C | 2.968 | -2.034 | -3.445 |
| H | 2.350 | -2.888 | -3.153 |
| H | 4.587 | 3.289 | -1.815 |
| H | 5.523 | 1.501 | -0.326 |
| C | 4.481 | -0.244 | -2.882 |
| C | 3.562 | -1.230 | -2.430 |
| H | 3.099 | 1.394 | -1.871 |
| H | 1.256 | 0.035 | -3.034 |
| C | 4.089 | 3.056 | -0.860 |
| C | 5.085 | 2.412 | 0.123 |
| H | 5.920 | 3.093 | 0.347 |
| H | 0.498 | -2.205 | -2.843 |
| C | 2.862 | 2.153 | -1.114 |
| H | 5.006 | 0.371 | -2.146 |
| O | 0.549 | 0.338 | -2.433 |
| H | 2.062 | 2.760 | -1.564 |
| H | 3.748 | 4.012 | -0.428 |
| H | 1.548 | -3.485 | -0.873 |
| O | -0.053 | -2.021 | -2.061 |
| B | 0.039 | -0.705 | -1.685 |
| C | 4.402 | 2.010 | 1.430 |
| H | 6.670 | 1.698 | 2.230 |
| Si | 3.004 | -1.390 | -0.600 |
| C | 2.542 | -3.268 | -0.457 |
| C | 2.348 | 1.500 | 0.153 |
| H | 3.287 | -3.894 | -0.983 |
| O | 5.055 | 2.001 | 2.524 |
| C | 3.034 | 1.606 | 1.355 |
| H | 5.411 | -0.686 | -0.089 |
| H | 1.306 | 1.196 | 0.170 |
| H | 2.525 | -3.570 | 0.600 |
| C | 4.613 | -1.206 | 0.468 |
| H | 4.999 | -2.201 | 0.754 |
| H | 2.576 | 1.273 | 2.287 |
| H | 4.432 | -0.629 | 1.389 |
| C | -0.878 | -0.231 | -0.439 |
| H | -0.298 | -5.101 | 1.807 |
| C | 0.059 | -4.077 | 1.926 |
| H | 1.576 | -4.627 | 3.361 |
| C | -3.505 | 0.567 | -3.875 |
| C | 1.117 | -3.808 | 2.802 |
| C | -0.588 | -3.056 | 1.197 |
| H | -2.758 | -0.839 | -2.404 |
| C | -2.844 | 0.211 | -2.690 |

| | | | |
|---|---|---|---|
| H | -4.207 | 2.243 | -5.055 |
| C | -3.671 | 1.939 | -4.154 |
| C | -0.112 | -1.735 | 1.399 |
| C | 1.612 | -2.501 | 2.956 |
| N | -0.796 | -0.604 | 0.845 |
| C | 0.979 | -1.474 | 2.239 |
| C | -2.323 | 1.194 | -1.833 |
| N | -1.769 | 0.766 | -0.586 |
| H | 1.325 | -0.450 | 2.341 |
| C | -3.153 | 2.916 | -3.296 |
| C | -2.445 | 2.570 | -2.127 |
| H | -3.265 | 3.974 | -3.542 |
| C | -1.721 | 0.202 | 1.720 |
| C | -2.291 | 1.258 | 0.727 |
| H | -1.832 | 2.235 | 0.918 |
| H | -2.517 | -0.472 | 2.065 |
| C | 2.805 | -2.189 | 3.832 |
| C | -4.039 | -0.497 | -4.810 |
| H | -6.144 | 3.576 | 2.004 |
| H | -3.667 | 3.307 | 1.813 |
| C | -5.728 | 2.697 | 1.509 |
| C | -4.336 | 2.545 | 1.408 |
| H | -7.664 | 1.844 | 1.034 |
| C | -6.581 | 1.724 | 0.964 |
| C | -3.792 | 1.415 | 0.776 |
| C | -6.039 | 0.597 | 0.320 |
| C | -4.650 | 0.441 | 0.231 |
| H | -6.698 | -0.156 | -0.116 |
| H | -4.228 | -0.421 | -0.283 |
| H | -0.663 | 0.153 | 6.277 |
| H | -1.906 | -0.663 | 4.273 |
| C | -0.505 | 0.629 | 5.309 |
| C | -1.210 | 0.173 | 4.184 |
| H | 0.957 | 2.046 | 6.054 |
| C | 0.403 | 1.693 | 5.183 |
| C | -1.015 | 0.777 | 2.929 |
| C | 0.598 | 2.301 | 3.931 |
| C | -0.107 | 1.846 | 2.809 |
| H | 1.309 | 3.122 | 3.822 |
| H | 0.075 | 2.310 | 1.840 |
| H | 3.001 | -3.005 | 4.545 |
| H | 2.648 | -1.256 | 4.396 |
| H | 3.709 | -2.051 | 3.214 |
| H | -3.377 | -0.616 | -5.685 |
| H | -5.037 | -0.228 | -5.190 |
| H | -4.105 | -1.473 | -4.304 |
| H | -2.200 | -5.648 | -2.317 |
| H | -0.467 | -4.976 | -0.662 |
| C | -1.434 | -4.473 | -0.674 |
| C | -2.407 | -4.839 | -1.613 |
| C | -1.666 | -3.420 | 0.239 |
| C | -3.637 | -4.163 | -1.657 |
| H | -4.396 | -4.445 | -2.390 |
| C | -2.913 | -2.765 | 0.199 |
| C | -3.890 | -3.130 | -0.740 |
| H | -3.145 | -1.991 | 0.927 |
| H | -4.854 | -2.618 | -0.742 |

```
H    -2.517     6.517     0.398
H    -3.593     4.841    -1.105
C    -2.548     4.725    -0.813
C    -1.942     5.660     0.042
C    -1.823     3.605    -1.266
C    -0.609     5.488     0.452
H    -0.147     6.212     1.126
C    -0.478     3.452    -0.864
C     0.126     4.381    -0.008
H     0.072     2.584    -1.222
H     1.163     4.235     0.300

                     1                      2                      3
                     A                      A                      A
 Frequencies --   -81.1664                8.0797
11.4952
 Red. masses --     5.8588                4.5796
5.3125
 Zero-point correction=                           1.199457
(Hartree/Particle)
 Thermal correction to Energy=                    1.270430
 Thermal correction to Enthalpy=                  1.271374
 Thermal correction to Gibbs Free Energy=         1.085323
 Sum of electronic and zero-point Energies=          -3237.845123
 Sum of electronic and thermal Energies=             -3237.774149
 Sum of electronic and thermal Enthalpies=           -3237.773205
 Sum of electronic and thermal Free Energies=        -3237.959257

         Item               Value     Threshold  Converged?
 Maximum Force            0.000003     0.000450     YES
 RMS     Force            0.000001     0.000300     YES

---------------------------------------
```

**Ground State of E1 and E2**

```
---------------------------------------
 Cartesian coordinates (Angstroms):
---------------------------------------
123

C     0.381    -0.958     3.147
H     2.208     1.536     1.258
H     3.612     0.479     1.138
C     2.688     0.655     1.711
H     2.976     0.916     2.745
H    -0.520    -0.336     3.020
Si    1.567    -0.903     1.625
H     4.595    -1.313     1.923
H     0.883    -0.640     4.078
C     4.126    -2.295     2.002
C     2.719    -2.407     1.906
H     6.029    -3.297     2.279
H     0.036    -1.995     3.293
C     4.945    -3.419     2.202
C     2.169    -3.710     2.012
C     4.374    -4.699     2.300
H     1.087    -3.842     1.933
```

| | | | |
|---|---|---|---|
| C | 2.980 | -4.842 | 2.201 |
| H | 5.008 | -5.576 | 2.450 |
| H | 2.525 | -5.833 | 2.274 |
| H | 6.934 | 4.421 | -0.696 |
| H | 8.395 | 2.395 | -0.703 |
| C | 6.490 | 3.430 | -0.809 |
| C | 7.314 | 2.288 | -0.812 |
| C | 5.099 | 3.292 | -0.950 |
| H | 4.452 | 4.170 | -0.946 |
| H | 7.400 | 0.136 | -0.954 |
| C | 6.754 | 1.014 | -0.953 |
| H | 5.842 | -4.233 | -0.327 |
| H | 6.020 | -4.238 | -2.095 |
| C | 5.282 | -4.205 | -1.275 |
| H | 6.339 | -1.787 | -1.092 |
| C | 4.536 | 2.018 | -1.093 |
| H | 4.614 | -5.073 | -1.337 |
| C | 5.352 | 0.859 | -1.096 |
| H | 1.037 | -3.150 | -0.265 |
| C | 4.480 | -2.914 | -1.359 |
| C | 5.261 | -1.668 | -1.222 |
| H | 3.456 | 1.907 | -1.194 |
| O | 0.203 | -2.648 | -0.266 |
| C | 4.689 | -0.433 | -1.237 |
| H | 3.604 | -0.373 | -1.341 |
| B | 0.576 | -1.214 | -0.221 |
| C | -0.809 | -0.319 | -0.095 |
| H | -3.997 | -4.485 | -1.635 |
| C | -3.575 | -4.027 | -0.738 |
| H | -4.106 | -5.685 | 0.544 |
| C | 1.311 | 2.661 | -2.660 |
| C | -3.632 | -4.703 | 0.489 |
| C | -2.964 | -2.763 | -0.850 |
| O | 1.383 | -0.811 | -1.384 |
| H | 0.131 | 0.852 | -2.540 |
| C | 0.454 | 1.751 | -2.023 |
| H | 2.309 | 4.572 | -2.451 |
| C | 1.656 | 3.839 | -1.973 |
| C | -2.421 | -2.200 | 0.327 |
| C | -3.087 | -4.134 | 1.655 |
| N | -1.986 | -0.833 | 0.320 |
| C | -2.492 | -2.864 | 1.554 |
| C | 0.002 | 1.961 | -0.712 |
| H | 2.026 | -1.539 | -1.521 |
| N | -0.939 | 1.032 | -0.168 |
| H | -2.090 | -2.368 | 2.438 |
| C | 1.173 | 4.076 | -0.682 |
| C | 0.342 | 3.149 | -0.013 |
| H | 1.455 | 4.990 | -0.157 |
| C | -3.078 | 0.183 | 0.408 |
| C | -2.318 | 1.513 | 0.179 |
| O | 3.252 | -2.950 | -1.551 |
| H | -2.263 | 2.091 | 1.108 |
| H | -3.760 | -0.014 | -0.434 |
| C | -3.155 | -4.838 | 2.994 |
| C | 1.859 | 2.357 | -4.036 |
| H | -4.104 | 5.546 | -1.429 |

| | | | |
|---|---|---|---|
| H | -3.140 | 4.103 | 0.374 |
| C | -3.813 | 4.517 | -1.650 |
| C | -3.279 | 3.708 | -0.634 |
| H | -4.379 | 4.634 | -3.739 |
| C | -3.967 | 4.004 | -2.948 |
| C | -2.905 | 2.383 | -0.911 |
| C | -3.587 | 2.679 | -3.228 |
| C | -3.058 | 1.872 | -2.213 |
| H | -3.700 | 2.272 | -4.234 |
| H | -2.755 | 0.849 | -2.431 |
| H | -6.779 | -1.275 | 2.876 |
| H | -5.517 | -0.925 | 0.750 |
| C | -5.808 | -0.776 | 2.895 |
| C | -5.104 | -0.574 | 1.698 |
| H | -5.806 | -0.497 | 5.045 |
| C | -5.261 | -0.340 | 4.112 |
| C | -3.852 | 0.066 | 1.705 |
| C | -4.010 | 0.301 | 4.126 |
| C | -3.310 | 0.500 | 2.929 |
| H | -3.579 | 0.645 | 5.068 |
| H | -2.339 | 0.995 | 2.949 |
| H | -3.617 | -5.832 | 2.898 |
| H | -3.747 | -4.251 | 3.716 |
| H | -2.149 | -4.964 | 3.427 |
| H | 1.129 | 1.798 | -4.642 |
| H | 2.766 | 1.731 | -3.956 |
| H | 2.135 | 3.278 | -4.573 |
| H | -0.744 | -0.775 | -4.468 |
| H | -0.767 | -1.965 | -2.286 |
| C | -1.705 | -1.698 | -2.770 |
| C | -1.699 | -1.038 | -4.008 |
| C | -2.929 | -2.052 | -2.159 |
| C | -2.906 | -0.723 | -4.655 |
| H | -2.896 | -0.206 | -5.617 |
| C | -4.137 | -1.737 | -2.819 |
| C | -4.127 | -1.076 | -4.057 |
| H | -5.086 | -2.005 | -2.348 |
| H | -5.070 | -0.832 | -4.549 |
| H | -1.505 | 6.140 | 3.061 |
| H | -0.688 | 5.511 | 0.796 |
| C | -0.647 | 4.786 | 1.610 |
| C | -1.113 | 5.136 | 2.886 |
| C | -0.148 | 3.490 | 1.350 |
| C | -1.087 | 4.196 | 3.930 |
| H | -1.451 | 4.466 | 4.923 |
| C | -0.128 | 2.557 | 2.408 |
| C | -0.588 | 2.906 | 3.685 |
| H | 0.250 | 1.557 | 2.228 |
| H | -0.554 | 2.166 | 4.487 |

| | 1 | 2 | 3 |
|---|---|---|---|
| | A | A | A |
| Frequencies -- | 11.3593 | 17.9751 | 19.4696 |
| Red. masses -- | 5.6808 | 5.2571 | 5.4842 |

```
 Zero-point correction=                           0.987387
(Hartree/Particle)
 Thermal correction to Energy=                    1.050836
 Thermal correction to Enthalpy=                  1.051780
 Thermal correction to Gibbs Free Energy=         0.884080
 Sum of electronic and zero-point Energies=          -2929.352738
 Sum of electronic and thermal Energies=             -2929.289288
 Sum of electronic and thermal Enthalpies=           -2929.288344
 Sum of electronic and thermal Free Energies=        -2929.456045

         Item               Value     Threshold  Converged?
 Maximum Force            0.000015     0.000450     YES
 RMS     Force            0.000002     0.000300     YES
----------------------------------------
```

**Transition State of E1**

```
----------------------------------------
 Cartesian coordinates (Angstroms):
----------------------------------------
123

C     0.889    -1.344     2.902
H     3.290     1.241     2.679
H     4.613     0.084     2.721
C     3.535     0.194     2.909
H     3.355     0.028     3.988
H     0.178    -0.511     2.809
Si     2.491    -1.057     1.857
H     5.388    -1.873     2.281
H     1.132    -1.471     3.974
C     4.813    -2.797     2.206
C     3.408    -2.728     2.011
H     6.569    -4.031     2.496
H     0.373    -2.248     2.552
C     5.488    -4.021     2.334
C     2.721    -3.967     1.920
C     4.780    -5.231     2.243
H     1.641    -3.967     1.760
C     3.389    -5.196     2.029
H     5.302    -6.186     2.337
H     2.825    -6.130     1.958
H     6.104     4.314     1.606
H     7.617     2.332     1.786
C     5.810     3.360     1.164
C     6.660     2.243     1.267
C     4.581     3.237     0.492
H     3.906     4.092     0.412
H     6.952     0.155     0.813
C     6.286     1.013     0.713
H     5.257    -4.678    -0.318
H     6.694    -3.786    -0.875
C     5.647    -4.024    -1.115
H     6.269    -1.631    -0.153
C     4.209     2.009    -0.062
H     5.596    -4.576    -2.066
C     5.044     0.870     0.043
H     1.778    -3.210    -0.578
```

| | | | |
|---|---|---|---|
| C | 4.772 | -2.782 | -1.195 |
| C | 5.279 | -1.563 | -0.604 |
| H | 3.252 | 1.909 | -0.573 |
| O | 0.945 | -2.770 | -0.326 |
| C | 4.570 | -0.383 | -0.535 |
| H | 3.599 | -0.320 | -1.021 |
| B | 0.986 | -1.441 | -0.761 |
| C | -0.248 | -0.508 | -0.304 |
| H | -2.604 | -4.939 | -1.559 |
| C | -2.433 | -4.366 | -0.646 |
| H | -3.016 | -5.990 | 0.660 |
| C | 0.993 | 2.042 | -3.743 |
| C | -2.672 | -4.955 | 0.606 |
| C | -2.004 | -3.032 | -0.759 |
| O | 1.754 | -1.017 | -1.822 |
| H | -0.083 | 0.304 | -3.037 |
| C | 0.384 | 1.247 | -2.762 |
| H | 1.995 | 3.929 | -4.100 |
| C | 1.528 | 3.284 | -3.353 |
| C | -1.771 | -2.317 | 0.442 |
| C | -2.487 | -4.224 | 1.792 |
| N | -1.314 | -0.960 | 0.412 |
| C | -2.028 | -2.899 | 1.690 |
| C | 0.354 | 1.644 | -1.417 |
| H | 2.505 | -1.672 | -1.938 |
| N | -0.382 | 0.830 | -0.504 |
| H | -1.849 | -2.311 | 2.588 |
| C | 1.469 | 3.699 | -2.018 |
| C | 0.894 | 2.891 | -1.013 |
| H | 1.901 | 4.658 | -1.728 |
| C | -2.333 | 0.119 | 0.613 |
| C | -1.529 | 1.392 | 0.277 |
| O | 3.645 | -2.900 | -1.760 |
| H | -1.126 | 1.836 | 1.194 |
| H | -3.108 | -0.035 | -0.154 |
| C | -2.752 | -4.829 | 3.155 |
| C | 1.061 | 1.561 | -5.177 |
| H | -3.687 | 5.541 | 0.023 |
| H | -2.295 | 3.825 | 1.192 |
| C | -3.435 | 4.606 | -0.482 |
| C | -2.659 | 3.642 | 0.180 |
| H | -4.473 | 5.125 | -2.313 |
| C | -3.877 | 4.372 | -1.795 |
| C | -2.332 | 2.437 | -0.462 |
| C | -3.545 | 3.168 | -2.441 |
| C | -2.780 | 2.202 | -1.775 |
| H | -3.881 | 2.984 | -3.464 |
| H | -2.513 | 1.271 | -2.274 |
| H | -5.890 | -1.037 | 3.415 |
| H | -4.778 | -0.835 | 1.192 |
| C | -4.896 | -0.592 | 3.342 |
| C | -4.274 | -0.474 | 2.091 |
| H | -4.714 | -0.234 | 5.473 |
| C | -4.236 | -0.142 | 4.496 |
| C | -2.991 | 0.093 | 1.976 |
| C | -2.958 | 0.434 | 4.389 |
| C | -2.340 | 0.552 | 3.136 |

```
H    -2.441     0.791     5.282
H    -1.346     0.996     3.075
H    -3.161    -5.847     3.067
H    -3.467    -4.214     3.725
H    -1.824    -4.882     3.750
H     0.120     1.074    -5.475
H     1.864     0.813    -5.297
H     1.266     2.392    -5.869
H     0.131    -2.651    -4.910
H    -0.097    -3.600    -2.613
C    -0.810    -2.859    -2.975
C    -0.678    -2.313    -4.260
C    -1.834    -2.423    -2.111
C    -1.576    -1.329    -4.705
H    -1.476    -0.907    -5.707
C    -2.736    -1.440    -2.570
C    -2.608    -0.895    -3.857
H    -3.560    -1.126    -1.928
H    -3.320    -0.140    -4.198
H     0.190     6.181     2.227
H     0.235     5.365    -0.126
C     0.519     4.697     0.689
C     0.480     5.150     2.016
C     0.879     3.365     0.392
C     0.794     4.275     3.070
H     0.754     4.623     4.103
C     1.219     2.503     1.457
C     1.165     2.950     2.784
H     1.524     1.479     1.236
H     1.429     2.264     3.590
```

```
                     1                      2                      3
                     A                      A                      A
 Frequencies --   -64.2757               14.2858
19.1044
 Red. masses --     6.5243                5.1471
5.2584
 Zero-point correction=                           0.987137
(Hartree/Particle)
 Thermal correction to Energy=                    1.049482
 Thermal correction to Enthalpy=                  1.050426
 Thermal correction to Gibbs Free Energy=         0.886814
 Sum of electronic and zero-point Energies=          -2929.332124
 Sum of electronic and thermal Energies=             -2929.269780
 Sum of electronic and thermal Enthalpies=           -2929.268836
 Sum of electronic and thermal Free Energies=        -2929.432448

         Item               Value     Threshold  Converged?
 Maximum Force            0.000004     0.000450     YES
 RMS     Force            0.000001     0.000300     YES

---------------------------------------
```

**Transition State of E2**

```
---------------------------------------
 Cartesian coordinates (Angstroms):
---------------------------------------
```

123

| | | | |
|---|---|---|---|
| H | 7.578 | 3.886 | -0.549 |
| H | 5.332 | 4.129 | -1.632 |
| C | 6.720 | 3.326 | -0.170 |
| C | 5.458 | 3.459 | -0.777 |
| C | 6.864 | 2.465 | 0.932 |
| H | 7.839 | 2.352 | 1.413 |
| C | 4.357 | 2.742 | -0.284 |
| C | 5.759 | 1.743 | 1.410 |
| C | 4.470 | 1.866 | 0.828 |
| H | 5.894 | 1.083 | 2.269 |
| C | 3.334 | 0.728 | 3.400 |
| H | 3.400 | 1.733 | 3.856 |
| H | 3.388 | 2.865 | -0.769 |
| H | 0.866 | 2.075 | 0.597 |
| C | 1.511 | 2.164 | 1.480 |
| H | 0.870 | 2.027 | 2.367 |
| H | 1.898 | 3.198 | 1.511 |
| Si | 2.980 | 0.876 | 1.498 |
| H | 4.269 | 0.191 | 3.620 |
| H | 2.524 | 0.183 | 3.908 |
| C | -2.049 | -4.479 | -2.520 |
| C | -0.751 | -3.941 | -2.520 |
| C | 0.973 | -1.671 | -5.874 |
| C | -2.776 | -4.533 | -1.319 |
| C | -0.184 | -3.448 | -1.334 |
| C | -2.207 | -4.054 | -0.130 |
| C | 0.573 | -0.440 | -5.088 |
| C | -0.907 | -3.500 | -0.124 |
| C | 0.379 | -0.523 | -3.700 |
| C | 0.348 | 0.799 | -5.715 |
| C | -0.245 | -3.855 | 2.273 |
| C | -4.704 | 1.062 | -3.381 |
| C | -0.344 | -2.993 | 1.160 |
| C | -3.698 | 1.347 | -2.442 |
| C | -4.779 | -0.213 | -3.964 |
| C | 0.010 | 0.603 | -2.953 |
| C | -0.026 | 1.924 | -4.968 |
| C | 0.139 | -3.378 | 3.532 |
| C | 0.441 | -0.297 | -0.697 |
| C | -0.010 | -1.634 | 1.367 |
| N | -0.304 | 0.420 | -1.567 |
| C | -0.183 | 1.860 | -3.570 |
| C | -2.772 | 0.357 | -2.079 |
| N | -0.316 | -0.682 | 0.341 |
| C | -3.852 | -1.206 | -3.600 |
| C | -1.750 | -0.287 | 0.175 |
| C | -1.699 | 0.657 | -1.059 |
| C | 0.437 | -2.017 | 3.736 |
| C | 0.355 | -1.153 | 2.631 |
| C | -2.854 | -0.923 | -2.659 |
| C | -0.512 | 3.072 | -2.783 |
| C | -3.177 | -0.478 | 2.236 |
| C | 0.805 | -1.495 | 5.107 |
| C | -2.320 | 0.307 | 1.444 |
| C | -1.588 | 3.908 | -3.147 |

| | | | |
|---|---|---|---|
| C | 0.257 | 3.400 | -1.646 |
| C | -3.659 | 0.008 | 3.461 |
| C | -1.948 | 1.589 | 1.891 |
| C | -1.906 | 5.034 | -2.372 |
| C | -0.065 | 4.521 | -0.869 |
| C | -3.283 | 1.286 | 3.903 |
| C | -1.151 | 5.338 | -1.226 |
| C | -2.427 | 2.075 | 3.115 |
| O | 2.490 | -1.808 | -0.978 |
| B | 2.032 | -0.501 | -0.933 |
| O | 4.963 | -1.067 | -1.694 |
| O | 2.609 | 0.553 | -1.641 |
| C | 5.926 | -0.843 | -0.899 |
| C | 7.131 | -0.093 | -1.443 |
| C | 4.860 | -1.777 | 1.148 |
| C | 5.940 | -1.224 | 0.493 |
| C | 3.690 | -2.912 | 3.002 |
| C | 4.833 | -2.214 | 2.538 |
| C | 3.615 | -3.379 | 4.318 |
| C | 5.896 | -1.989 | 3.451 |
| C | 4.675 | -3.144 | 5.213 |
| C | 5.813 | -2.444 | 4.772 |
| H | 3.551 | 0.341 | -1.814 |
| H | 3.452 | -1.757 | -1.254 |
| H | -2.489 | -4.854 | -3.446 |
| H | -0.175 | -3.906 | -3.447 |
| H | 1.099 | -1.438 | -6.942 |
| H | 0.209 | -2.462 | -5.784 |
| H | 1.920 | -2.090 | -5.496 |
| H | -3.787 | -4.947 | -1.308 |
| H | 0.830 | -3.049 | -1.333 |
| H | -2.771 | -4.094 | 0.804 |
| H | 0.489 | -1.477 | -3.186 |
| H | 0.474 | 0.885 | -6.797 |
| H | -0.499 | -4.908 | 2.142 |
| H | -5.423 | 1.835 | -3.657 |
| H | -3.623 | 2.339 | -1.995 |
| H | -5.557 | -0.434 | -4.697 |
| H | -0.169 | 2.886 | -5.465 |
| H | 0.181 | -4.068 | 4.378 |
| H | -3.904 | -2.201 | -4.047 |
| H | -2.304 | -1.205 | -0.074 |
| H | -1.763 | 1.710 | -0.753 |
| H | 0.519 | -0.086 | 2.753 |
| H | -2.135 | -1.693 | -2.379 |
| H | -3.456 | -1.476 | 1.892 |
| H | 0.478 | -0.451 | 5.232 |
| H | 1.897 | -1.525 | 5.256 |
| H | 0.343 | -2.106 | 5.898 |
| H | -2.191 | 3.652 | -4.020 |
| H | 1.109 | 2.771 | -1.392 |
| H | -4.323 | -0.610 | 4.068 |
| H | -1.268 | 2.199 | 1.298 |
| H | -2.748 | 5.667 | -2.657 |
| H | 0.536 | 4.753 | 0.013 |
| H | -3.653 | 1.666 | 4.857 |
| H | -1.405 | 6.210 | -0.619 |

```
H    -2.130     3.069     3.455
H     7.307    -0.377    -2.491
H     8.036    -0.272    -0.844
H     6.918     0.990    -1.408
H     3.964    -2.014     0.583
H     6.858    -1.000     1.038
H     2.853    -3.067     2.319
H     2.724    -3.915     4.648
H     6.784    -1.446     3.126
H     4.614    -3.499     6.243
H     6.638    -2.253     5.462

                     1                      2                      3
                     A                      A                      A
 Frequencies --  -104.6940               16.3073
19.7720
 Red. masses --     7.1023                5.4909
5.1635
 Zero-point correction=                           0.987198
(Hartree/Particle)
 Thermal correction to Energy=                    1.049456
 Thermal correction to Enthalpy=                  1.050400
 Thermal correction to Gibbs Free Energy=         0.887837
 Sum of electronic and zero-point Energies=          -2929.329938
 Sum of electronic and thermal Energies=             -2929.267680
 Sum of electronic and thermal Enthalpies=           -2929.266736
 Sum of electronic and thermal Free Energies=        -2929.429299

         Item               Value     Threshold  Converged?
 Maximum Force            0.000273     0.000450     YES
 RMS     Force            0.000045     0.000300     YES

---------------------------------------
```

# Chapter 3

## Enantioselective Allenyl Additions to Boc-Aldimines/Aldehydes Catalyzed by an Aminophenol-Derived Boron-Based Catalyst

### *3.1. Introduction*

Allenes are the simplest class of cumulenes, which contain two contiguous C=C bonds. The fact that allenes bear unique physical and chemical propoperties compared with their alkenyl and alkynyl analogues has drawn much attention by synthetic organic chemists.[104] In the past decades, a variety of strategies have been developed to functionalize allenyl moieties in the context of synthesis of complex organic molecules. Specifically, allenes have been utilized in transition-metal catalyzed cyclizations,[105] cycloaddition reactions,[106] epoxidations,[107] metal catalyzed nucleophilic additions,[108] etc.

(104) For representative reviews on allenes in catalysis and natural product synthesis, see: (a) Ma, S. *Chem. Rev.* **2005**, *105*, 2829–2871. (b) López, F.; Mascareñas, J. L. *Chem. Eur. J.* **2011**, *17*, 418–428. (c) Yu, S.; Ma, S. *Angew. Chem. Int. Ed.* **2012**, *51*, 3074–3112.

(105) For most recent reviews, see: (a) Jeganmohan, M.; Cheng, C. -H. *Chem. Eur. J.* **2008,** *14*, 10876–10886. (b) Jeganmohan, M.; Cheng, C.-H. *Chem. Commun.* **2008,** 3101–3117.

(106) For most recent reviews, see: (a) Pinho e Melo, T. M. V. D. *Curr. Org. Chem.* **2009**, *13*, 1406–1431. (b) Inagaki, F.; Kitagaki, S.; Mukai, C. *Synlett*, **2011**, *17*, 418–428. (c) Alcaide, B.; Almendros, P.; Martínez del Campo, T.; Soriano, E. *Top. Curr. Chem.* **2011**, *302*, 183–224.

(107) For representative examples, see: (a) Camp, R. L.; Greene, F. D. *J. Am. Chem. Soc.* **1968**, *90*, 7349. (b) Crandall, J. K.; Machleder, W. H.; Thomas, M. J. *J. Am. Chem. Soc.* **1968**, *90*, 7346–7347. (c) Katukojvala, S.; Barlett, K. N.; Lotesta, S. D.; Williams, L. J. *J. Am. Chem. Soc.* **2004**, *126*, 15348–15349. (d) Lotesta, S. D.; Kiren, S.; Sauers, R. R.; Williams, L. J. *Angew. Chem. Int. Ed.* **2007**, *46*, 7108–7111. (e) Shangguan, N.; Kiren, S.; Williams, L. J. *Org. Lett.* **2007**, *9*, 1093–1096. (f) Joyasawal, S.; Lotesta, S. D.; Akhmedov, N. G.; Williams, L. J. *Org. Lett.* **2010**, *12*, 988–991.

(108) For representative examples, see: (a) Meng, F.; Jung, B.; Haeffner, F.; Hoveyda, A. H. *Org. Lett.* **2013**, *15*, 1414–1417. (b) Meng, F.; Jang, H.; Jung, B.; Hoveyda, A. H. *Angew. Chem. Int. Ed.* **2013**, *52*, 5046–5051. (c) Meng, F.; Haeffner, F.; Hoveyda, A. H. *J. Am. Chem. Soc.* **2014**, *136*, 11304–11307.

Thus, methods of synthesizing allene moieties or incorporating allenyl groups into organic molecules are of great importance. Among those approaches, direct allenyl additions to aldehydes or imines catalytically and enantioselectively are particularly attractive.

In this chapter, I will first summarize the reported strategies for enantioselective synthesis of homoallenylalcohols or amines, either through direct constructions of the allenyl moieties or allenyl additions to aldehyde or imines. Then I will focus on our development of catalytic enantioselective allenyl additions to Boc-aldimines and some progresses on allenyl additions to aldehydes.

## *3.2. Methods for Enantioseletive Synthesis of Homoallenylalcohols or Homoallenylamines*

### *3.2.1. Direct Synthesis of Allenes From Other Functional Groups*

In 2002, Ma and co-workers reported a useful approach to synthesize homoallenylalcohols enantioselectively.[109] As shown in Scheme 3.2.1, a variety of ynones (**3.1)** are known to be reduced into propargyl alcohols with high enatiomeric ratios.[110] The products (**3.2**) were subjected into Crabbé homologation reactions[111] to efficiently afford homoallenylalcohols with 90:10 to 99:1 er. Although two steps are required in this method, enantiomerically enriched propargyl alcohols are relatively easy to access. Additionally, the homologation reaction is suitable for gram scale preparations

(109) Ma, S.; Hou, H.; Zhao, S.; Wang, G. *Synthesis*, **2002**, *12*, 1643–1645.

(110) For some typical methods, see: (a) Noyori, R.; Tomino, I.; Yamada, M.; Nishizawa, M. *J. Am. Chem. Soc.* **1984**, *106*, 6717. (b) Frantz, D. E.; Fässler, R.; Carreira, E. M. *J. Am. Chem. Soc.* **2000**, *122*, 1806. (c) Corey, E. J.; Cimprich, K. A. *J. Am. Chem. Soc.* **1994**, *116*, 3151. (d) Lütjens, H.; Nowotny, S.; Knochel, P. *Tetrahedron: Asymmetry* **1995**, *6*, 2675. (e) Matsumura, K.; Hashiguchi, S.; Ikariya, T.; Noyori, R. *J. Am. Chem. Soc.* **1997**, *119*, 8738. (f) He, Q.; Ma, S. *Chin. J. Org. chem.* **2002**, *22*, 375.

(111) (a) Crabbé, P.; Fillion, H.; André, D.; Luche, J.-L. *J. Chem. Soc., Chem. Commun.* **1979**, 859. (b) Crabbé, P.; Nassim, B.; Robert-Lopes, M.-T. *Org. Synth.* **1985**, *63*, 203.

of materials. One of the drawbacks of this method is the harsh reaction condition (stoichiometric amount of base, 101 °C) in the homologation step, which may limit its use due to functional group compatibility.

**Scheme 3.2.1. Crabbé homologation of enantiomerically enriched propargyl alcohols**

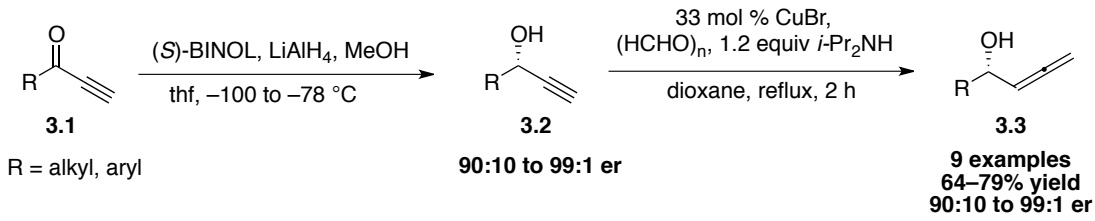


In 2009, Yoshida and co-workers reported a synthetic route to the phenyl-substituted homoallenylalcohol with 63% overall yield and 96:4 er.[112] As shown in Scheme 3.2.2, they synthesized the corresponding ynone **3.4** in two steps, which was converted into propargyl alcohol **3.5** by CBS reduction. At last, $LiAlH_4$ was used to promote the hydride allylic substitution reaction to afford the desired product without erosion of its enantiomeric ratio. The corresponding product was further used in the total synthesis of enokipodins A and B in the same paper, as well as a formal total synthesis of aplysin in 2010.[113] However, the authors did not show any substrate scope of this strategy. Moreover, the use of $LiAlH_4$ may cause some problems in substrates bearing muti-functional groups.

**Scheme 3.2.2. Synthesis of homoallenylalcohols through a hydride allylic substitution**

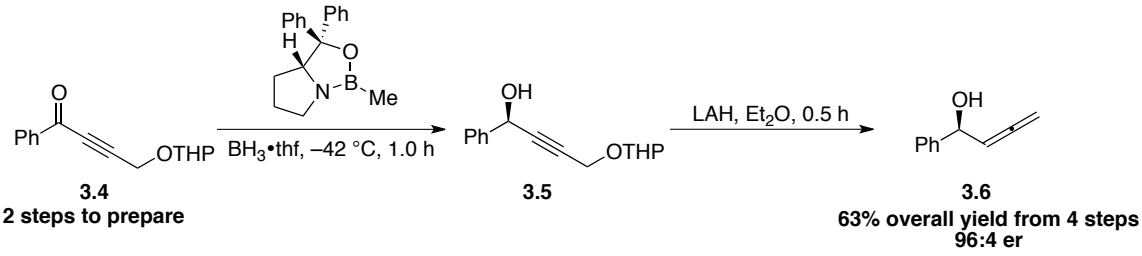


(112) Yoshida, M.; Shoji, Y.; Shishido, K. *Org. Lett.* **2009**, *11*, 1441–1443.
(113) Yoshida, M.; Shoji, Y.; Shishido, K. *Tetrahedron*, **2010**, *66*, 5053–5058.

### *3.2.2. Enantioselective Allenyl Additions to Aldehydes*

The first enantioselective synthesis of homoallenylalcohols was reported by Corey and co-workers.[114] They used the chiral sulfoamide derived from (*R*,*R*)-1,2-diphenyl-1,2-diaminoethane to prepare the corresponding boryl bromide **3.7** (Scheme 3.2.3). It turned out that allenylstannane can react with **3.7** to afford a chiral propargyl boron intermediate **3.8**, which was immediately used after generation for the reaction with aldehydes, affording the desired homoallenylalcohols with good yield (72–82% yield) and extraordinary enantioselectivity (>99:1 er in all cases). Both aryl and alkyl substituted aldehydes are suitable substrates, and homopropargyl products could be generated if a propargylstannane reagent was used. Although these reactions are not catalytic, they shed light on ways for preparation of enantiomerically enriched homoallenylalcohols, rendering this study of great importance.

**Scheme 3.2.3. The first enantioselective synthesis of homoallenylalcohols**

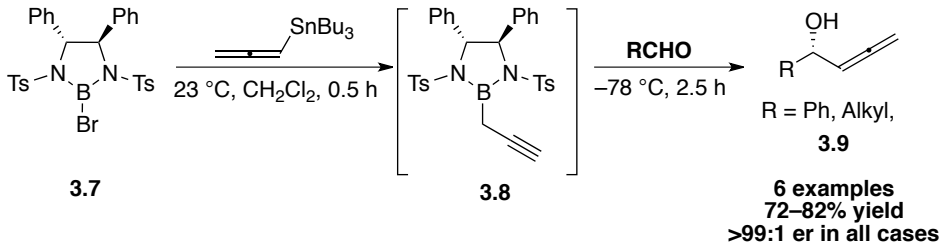


In 1995, Marshall and co-workers published their strategy to synthesize substituted homoallenylacohols with high diastereoselectivities and enantioselectivities.[115] The enantiomerically enriched **3.10**, prepared from $S_N2'$ substitution of the corresponding propargyl ether, was used in the reaction shown in

(114) Corey, E. J.; Yu, C.-M.; Lee, D.-H. *J. Am. Chem. Soc.* **1990**, *112*, 878–879.
(115) Marshall, J. A.; Yu, R. H.; Perkins, J. F. *J. Org. Chem.* **1995**, *60*, 5550–5555.

Scheme 3.2.4. It was found that with the involvemnt of $BuSnCl_3$, the reaction exclusively gave homoallenylalcohols. This is in contrast to without $BuSnCl_3$, in which case the reaction afforded homopropargylalcohols. The significance of this work is the successful synthesis of trisubstiuted homoallenylalcohols, although only three examples were reported.

**Scheme 3.2.4. Marshall's synthesis of homoallenylalcohols**

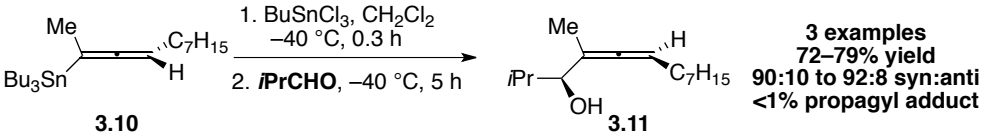


In the same year, Brown and co-workers reported their diastereoselective allenyl additions to aldehydes (Scheme 3.2.5).[116] The installation of trimethylsilyl substituent in the propargyl borane **3.12** is critical since a mixture of allenyl and propargyl boranes would be obtained otherwise. The subsequent allenyl additions to a variety of aldehydes were demonstrated with good efficiency and diastereoselectivity. However, the reations require –100 °C to achieve high selectivity, and the other enantiomer of **3.12** is not easy to access.

**Scheme 3.2.5. Brown's diastereoselective allenyl additions to aldehydes**

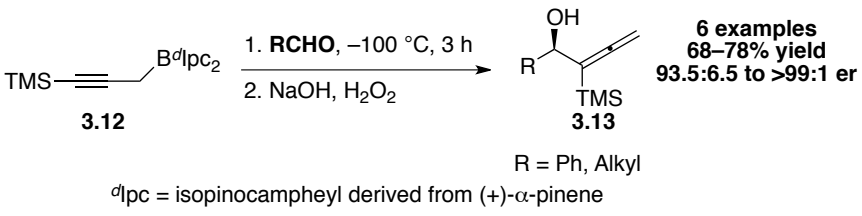


(116) Brown, H. C.; Khire, U. R.; Narla, G. *J. Org. Chem.* **1995**, *60*, 8130–8131.

The first catalytic enantioselective allenyl additions to aldehydes were reported by Yu and co-workers in 1998.[117] The authors use a chiral BINOL-Ti(IV) complex to serve as a Lewis acid catalyst. The allenyl transfer reagents have to be substituted propargyl stannanes **3.15**, since the unsubstituted derivative of **3.15** predominantly gives the homopropargylalcohols upon additions to aldehydes. Twleve examples were provided in this strategy with generally good yields and ers. However, this method involves the use of toxic organostannane reagents, and is not able to prepare unsubstituted homoallenylalcohols.

**Scheme 3.2.6. The first catalytic enantioselective allenyl additions to aldehydes**

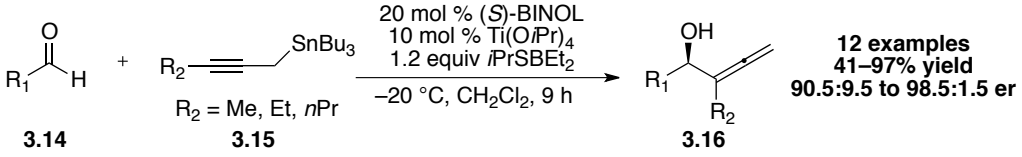


**3.14** **3.15** **3.16**

Besides reactions catalyzed by a chiral Lewis acid, allenyl additions to aldehydes can also be catalyzed by a chiral Lewis base. In 2002, Nakajima and co-workers utilized a chiral Lewis basic N-oxide **3.18** to promote reactions with trichloropropargyl silanes **3.17**.[118] This reactive silane, prepared *in situ* from the corresponding propargyl chloride under a CuCl catalyzed silylation reaction, was treated with various aldehydes to afford the desired homoallenylalcohols with 9:1 to 15:1 allenyl:propargyl selectivities and 44–72% yields. Unfortunately, the enantioselectivities of these transformations are not high (61:39 to 81:19 er).

(117) Yun C.-M.; Yoon, S.-K.; Baek, K.; Lee, J.-Y. *Angew. Chem. Int. Ed.* **1998**, *37*, 2392–2395.
(118) Nakajima, M.; Saito, M.; Hashimoto, S. *Tetrahedron: Asymmetry*, **2002**. *13*, 2449–2452.

**Scheme 3.2.7 Nakajima's catalytic enantioselective allenyl additions to aldehydes**

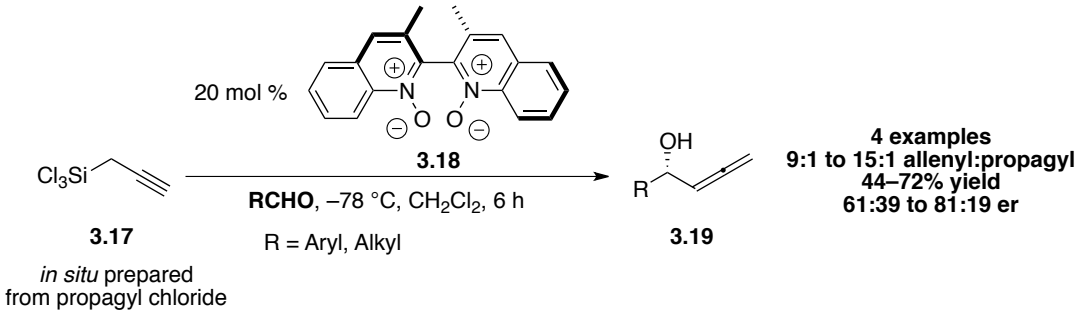


In 2006, Nakada and co-workers reported the first Nozaki-Hiyama type allenylations.[119] As shown in Scheme 3.2.8, the dimethylhydrosilyl (DMS) substituted propargyl bromide **3.20** serves as the effective allenyl reagent. One of the advantages of propargyl bromides is its relative stability (resistant to isomerized to the allenyl bromides), compared to previous utilized propargyl stannanes. The authors found DMS group is superior to other silyl protecting groups (TMS, TES, TIPS, etc) in terms of achieving high enantioselectivity in this allenyl addition. A stereochemical model involving a chiral propargyl chromium complex was proposed to explain the observed selectivity. Despite of all the advantages in this nice piece of work, the use of toxic chromium is still not encouraged in green chemistry.

**Scheme 3.2.8. Nakada's catalytic enantioselective allenyl additions to aldehydes**

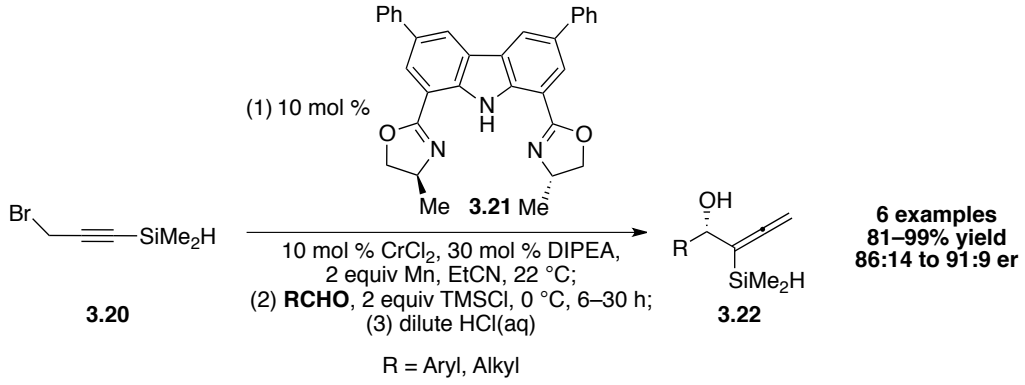


(119) Inoue, M.; Nakada, M. *Angew. Chem. Int. Ed.* **2006**, *45*, 252–255.

In the same year, Yamamoto group reported their discovery of enantioselective allenylations catalyzed by 5 mol % Bis(8-quinolinolato) (TBOx) chromium complex (**3.24**).[120] The reaction condition is similar as the Nakada's system, while a variety of substituted propargyl bromides are suitable reagents. Generally higher enantioselectivities and more examples were shown in this report, although in some cases reaction yields suffer. Like the reactions develop by Nakada and co-workers, these allenylations require the use of a silyl chloride to turn over the catalytic cycle (releasing the chromium complex). Thus, HCl (aq) hydrolysis of the corresponding silyl ether products is necessary to obtain the alcohols **3.25**. In addition, the current reactions need 48–60 hours for completion, which diminishes its usage in organic synthesis.

**Scheme 3.2.9. Yamamoto's catalytic enantioselective allenyl additions to aldehydes**

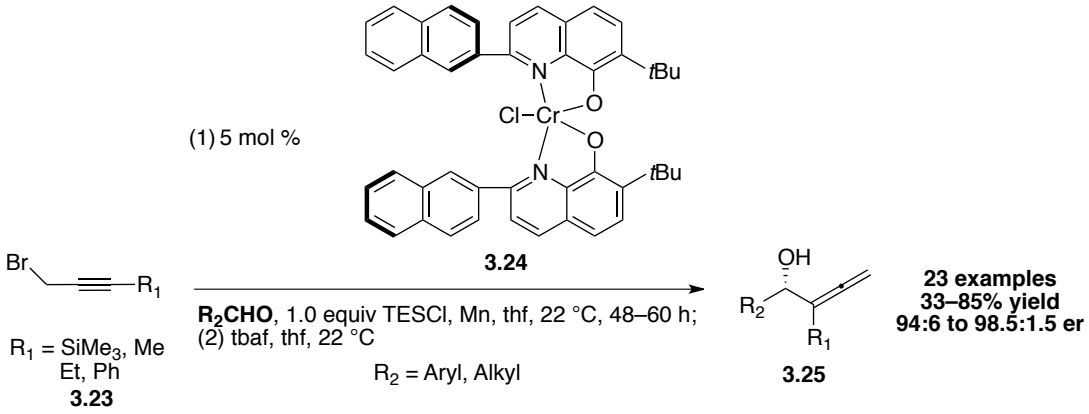


A significant break-through in this realm belongs to the work by Reddy in 2012.[121] The author applied the Antilla's catalytic system[122] into the allenyl additions to aldehydes. The TMS substituted propargyl boronate **3.27** is stable, easy to handle and suitable for gram scale synthesis. A chiral phosphoric acid **3.28** was introduced as the

(120) Xia, G.; Yamamoto, H . *J. Am. Chem. Soc.* **2007**, *129*, 496–497.
(121) Reddy, L. R. *Chem. Commun.* **2012**, *48*, 9189–9191.
(122) Jain, P.; Antilla, J. C. *J. Am. Chem. Soc.* **2010**, *132*, 11884–11886.

chiral Brønsted acid catalyst. In Antilla's catalytic allyl additions to aldehydes, **3.28** was believed as a hydrogen bond donor to direct the six-membered ring transition state of the allenyl addition. Subsequent computational studies, however, provided a different stereochemical model where the P=O double bond was proposed as a hydrogen bond acceptor.[123]

The phosphoric acid catalyzed allenyl additions are as efficient and selective as some of the previous illustrated methods, but do not require the use of toxic stannane or chromium complexes. Thus, it is considered as the state-of-art strategy for synthesis of highly enantiomerically enriched homoallenylalcohols. However, chiral phosphoric acid **3.28**, despite of its commercial availability, is very expensive ($2146/mmol from Sigma-Aldrich®). Moreover, synthesis of unsubstituted homoallenylalcohols **3.29** requires an additional step (tbaf de-silylation). At last, the reaction solvent has to be cyclohexane for achieving high enantioselectivity. However, compounds that bear a heterocycle or other polar functional unit may not be soluble in such a non-polar solvent.

**Scheme 3.2.10. Reddy's catalytic enantioselective allenyl additions to aldehydes**

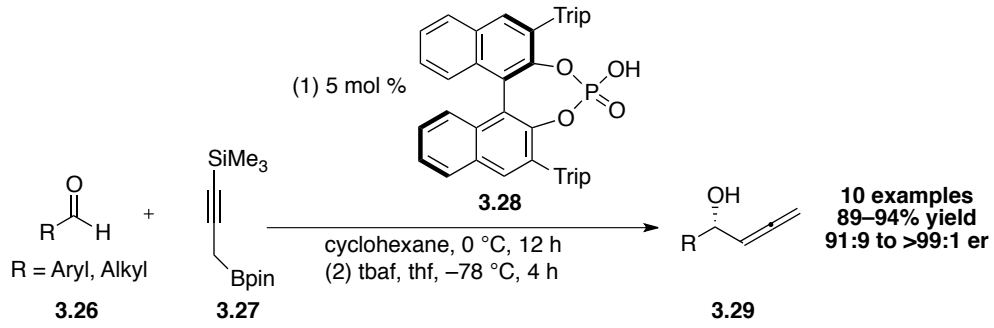


### *3.2.3. Enantioselective Allenyl Additions to Aldimines*

(123) Grayson, M. N.; Pellegrinet, S. C.; Goodman, J. M. *J. Am. Chem. Soc.* **2012**, *134*, 2716–2722.

Unlike previously mentioned reactions to aldehydes, enantioselective allenyl additions to aldimines are limited. The first of notable ones was reported by Miller and co-workers in 2009.[124] The reactions were promoted by a chiral peptide **3.32**, which was believed to interact with the allenoates **3.30** for generation of the corresponding enolates. Such enolates are capable to be added to N-acyl imines **3.31**. After a proton transfer, desired products **3.33** are obtained and the peptide catalyst **3.32** is released. These reactions were efficient and enantioselective for various aryl substituted N-acyl aldimines. However, the only one example of alkyl substituted aldimine afford the product with a diminished yield (42%) and enantioselectivity (80.5:19.5 er). It should be noted that the allenyl moiety has to be an allenoate because of the distinct mechanism of this reaction.

**Scheme 3.2.11. Miller's catalytic enantioselective allenoate additions to *N*-acyl aldimines**

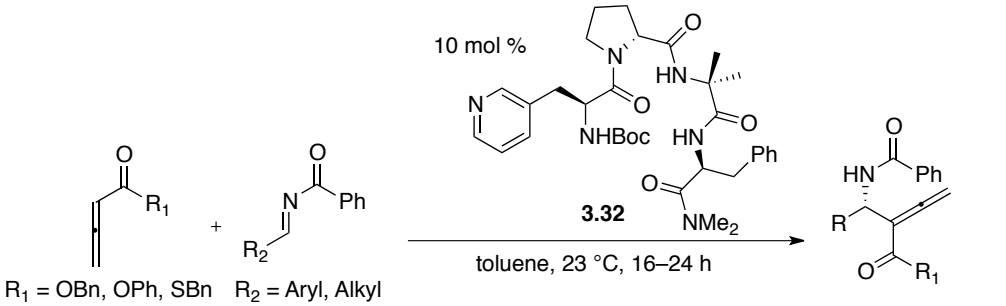


In 2011, Kobayashi and co-workers reported an indium (I) catalyzed allyl additions to Cbz (carboxybenzyl) protected aldimines.[125] In this report, the authors also showed their method were suitable for allenyl additions to aldimines. Despite that a

(124) Cowen, B. J.; Saunders, L. B.; Miller, S. J. *J. Am. Chem. Soc.* **2009**, *131*, 6105–6107.

(125) Huang, Y.-Y.; Chakrabarti, A.; Morita, N.; Schneider, U.; Kobayashi, S. *Angew. chem.. Int. Ed.* **2011**, *50*, 11121–11124.

mixture of homoallenylamides and homopropargylamides were observed, they were able to isolate the major products **3.37** (Scheme 3.2.12). In terms of the mechanism of this reaction, (*rac*)-hemiaminals **3.34** are first converted into the iminium forms, which react with the allenyl indium species once they are generated *in situ*. The high enantioselectivity comes from the chiral phosphate anion of **3.36**, which serves as the counter ion of the iminium substrates. Although only two cases of allenyl additions were reported, alkyl as well as aryl substituted aldimines are equally efficient and selective. The major disadvantage of this method to me is the use of toxic and expensive indium chloride and the chiral silver phosphate salt.

**Scheme 3.2.12. Kobayashi's catalytic enantioselective allenyl additions to aldimines**

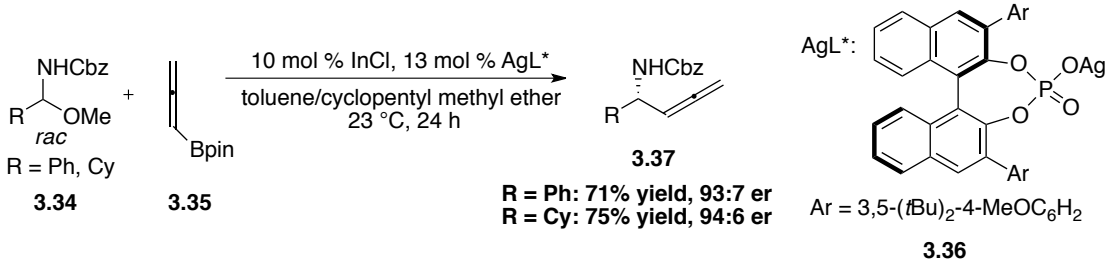


In 2014, our group reported an NHC–Cu-catalyzed enantioselective allenyl additions to phosphinoyl substituted aldimines (Scheme 3.2.13a).[126] The reactions require only 5 mol % NHC–Cu catalyst as well as the user friendly TMS substituted proparygl B(pin) as the allenyl transfer reagent. Noticably, most of the reactions complete in 10 min, affording the desired products **3.40** with high allenyl:propargyl selectivity and enantioselectivity. The valuable TMS substitutent in products **3.40** can be used in a variety of functionalizations, including desilylations and conversions to the

(126) Mszar, N. W.; Haeffner, F.; Hoveyda, A. H. *J. Am. Chem. Soc.* **2014**, *136*, 3362–3365.

corresponding propargyl bromides, the latter of which was further utilized in a eight-step total synthesis of *S*-(–)-cyclooroidin.

Computational studies reveal the critical role of the TMS group of the propargyl B(pin): After transmetallation, the propargyl copper species (**3.42**) is generated. Due to its instability, it can easily isomerize into the corresponding allenyl copper **3.43**. The Gibbs free energy difference between these two organocoppers is 0.9 kcal/mol, slightly favoring allenyl copper **3.43**. In the real reaction, it is probably the more nucleophilic propargyl copper **3.42** ($Cu–C_{sp3}$ vs $Cu–C_{sp2}$) that reacts with the phosphinoyl imine, affording the homoallenylamide product. As a contrast, if there is no TMS substituent, the energy difference between the two organocoppers would be 9.9 kcal/mol, significantly favoring the allenyl copper. Thus, it is the allenyl copper that would react exclusively with the imine substrate, affording the homopropargylamide as the only product.[127] In a word, the TMS substituent shift the equilibrium between the propargyl copper and allenyl copper species, so that the more reactive propargyl one can be generated in a reasonable amount to promote the subsequent allenyl additions to imines.

(127) Vieira, E. M.; Haeffner, F.; Snapper, M. L.; Hoveyda, A. H. *Angew. Chem. Int. Ed.* **2012**, *51*, 6618-6621.

**Scheme 3.2.13 Hoveyda's NHC–Cu-catalyzed allenyl additions to aldimines**

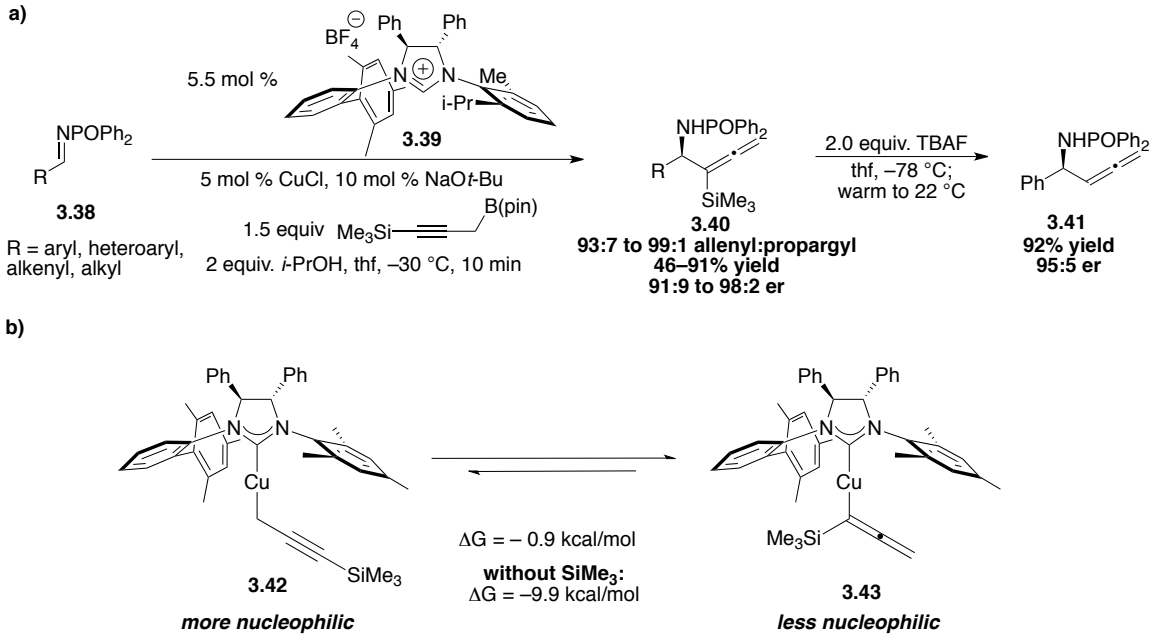


Besides allenyl additions to imines, other protocols were also developed to synthesize homoallenylamides. In 2014, Ma and co-workers reported a Pd-catalyzed enantioselective amination of allenyl phosphates.[128] In the experiments of screening the reaction conditions, the authors found dbu as a critical base (52:48 er with $K_2CO_3$), and chiral bisphosphine **3.47** as the optimal ligand. The reactions were believed to proceed through the initial formation of the chiral Pd-π-allenyl complex, followed by a selective amine substitution. Stereochemical models were proposed to explain the observed enantioselectivity. It should be pointed out that only alkyl-substituted phosphates are suitable substrates. In addition, the current reactions usually require long reaction times (42–120 h) for completions.

(128) Li, Q.; Fu, C.; Ma, S. *Angew. Chem. Int. Ed.* **2014**, *53*, 6511–6514.

**Scheme 3.2.14. Ma's enantioselective synthesis of homoallenylamides**

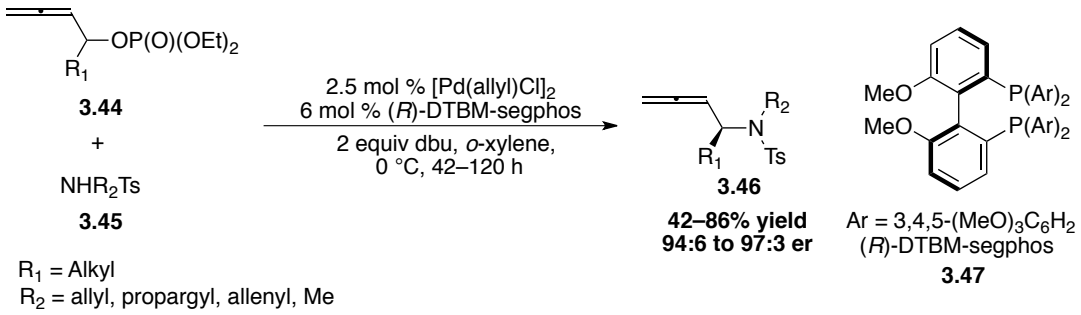


## *3.3. Enantioselective Synthesis of Homoallenylalcohols or amines: Design of the Catalytic System*

The above findings imply the challenges for us to develop catalytic enantioselective allenyl additions to aldehydes or aldimines (Scheme 3.3.1). First, we should use easily accessible substrates and reagents, and avoid toxic and/or environmental unfriendly ones. Allenyl-B(pin) **3.49** is a suitable candidate as the allenyl transfer reagent, since it is stable under air at ambient temperature, can be obtained in a gram-scale preparation[129] or obtained through common commercial vendors. Second, we wonder what catalytic system we can design for efficient synthesis of the homoallenylalcohols or amines. Not only high allenyl to propargyl ratios need to be achieved, high enantioselectivities are also our goal.

Catalysis involving the use of metal may not be a good choice. This is because propargyl metal species **3.52**, generated from reactions of allenylB(pin) **3.49** with metal alkoxide, is prone to isomerize to the more stable allenyl metal species **3.53**. The predominant allenyl metal **3.53** affords the undesired homopropargylalcohols or amines

(129) Tonogaki, K.; Itami, K.; Yoshida, J.-i. *J. Am. Chem. Soc.* **2006**, *128*, 1464–1465.

upon reactions with the aldehydes or imines. In contrast, the minor propargyl metal **3.54** is the species we need for synthesis of homoallenyl products.

**Scheme 3.3.1. Challenges for catalytic enantioselective allenyl additions to aldehydes/aldimines**

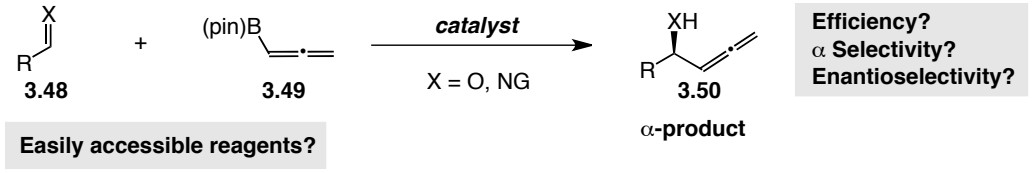


**In the transition metal catalysis:**

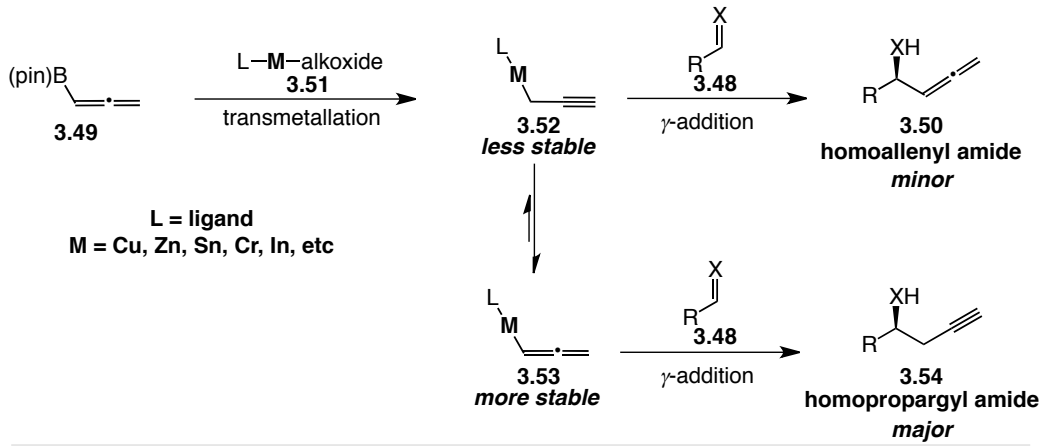


**Propargyl metals tend to isomerize to allenyl metals, which leads to homopropargyl products.**

One solution for this issue of regioselectivity could be the use of a TMS substituted propargyl-B(pin) (shown in Scheme 3.2.13), which shifts the aforementioned equilibrium between the two metal species. Another is to utilize a non-metal element to replace the metal center in **3.52** and **3.53**, since most of the corresponding allenyl or propargyl species are more configurationally stable than allenyl or propargyl metals. Here, we envision that the chiral propargyl boron **3.56**, which can be accessed through allenylB(pin) **3.49** reaction with a chiral methoxy boron **3.55** in a γ-addition fasion, may be stable enough as the active catalytic species for allenyl additions to aldehydes or imines (Scheme 3.3.2). If this hypothesis is true, how can we develop such a chiral boron

catalyst? Are the two γ-additions efficient to turn over the catalytic cycle? How high would the enantioselectivity be in this catalytic system?

**Scheme 3.3.2. Our solution: use of a chiral propargyl boron instead of propargyl metals in the catalysis**

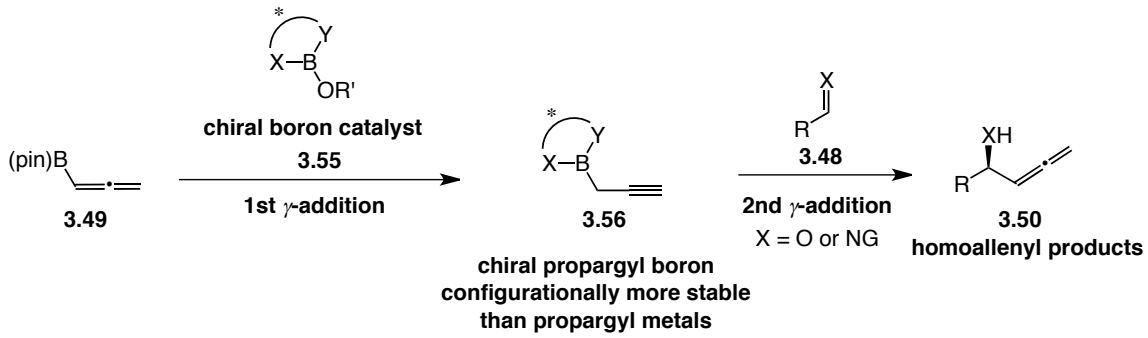


**•Can we develop the chiral boron catalyst?**
**•Is the 1st γ-addition efficient enough to form the chiral propargyl boron intermediate?**
**•Is the 2nd γ-addition efficient to generate the C–C bond?**
**•Is this process enantioselective?**

In 2013, our group reported a new aminophenol-derived boron based catalyst, which was used to promote efficient and enantioselective allyl additions to aldimines and isatins, as well as allenyl additions to isatins.[130] Some of the representative allyl additions to phosphinoyl aldimines are listed in Scheme 3.3.3. This transtion metal-free protocol requires only 3 mol % aminophenol as the pre-catalyst, and the reactions complete in four to six hours. The phosphinoyl aldimines are not only readily accessible (one step preparation) but also easy to handle (usually crystals, purified by recrystallizations). Later studies revealed the critical role of the phosphinoyl group in the control of enantioselectivity in the allyl addition reactions (will be illustrated later). Allyl-B(pin) is a non-toxic commercially available allylation reagent, which has been applied widely in synthetic organic chemistry. The allyl additions are efficient and enantioselective with

(130) Silverio, D. L.; Torker, S.; Pilyugina, T.; Vieira, E. M.; Snapper, M. L.; Haeffner, F.; Hoveyda, A. H. *Nature*, **2013**, *494*, 216–221.

aryl-, heteroaryl-, alkenyl-, alkynyl- as well as alkyl-substitued aldimines. In addition, electron donating or withdrawing substituents barely influence the efficiency and selectivity of the reactions. Sterically hindered substrates give slightly lower enantioselectivity (93:7 er, **3.59b**). Noticably, 2-substituted allyl-B(pin) are suitable reagents, which afford **3.59l** and **3.59m** with high yields and ers. The current process does not require rigorous exclusion of air and moisture, and can be run in a multi-gram scale. The purification of the products is simple filtration and recrystallization, avoiding the use of expensive silica gel chromatography.

**Scheme 3.3.3. Catalytic enantioselective allyl additions to phosphinoyl-aldimines**[a]

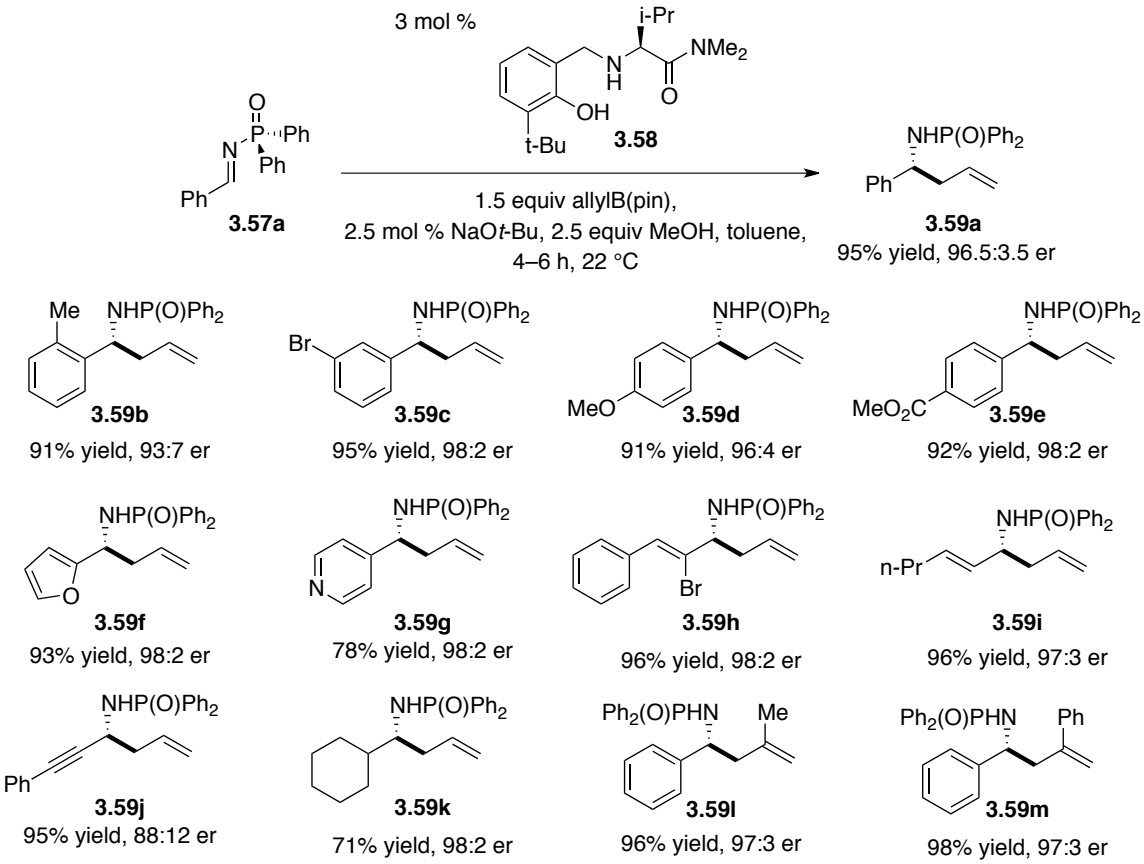


[a] >98% conv for all cases except for **3.59g** (90% conv).

Besides phosphinoyl aldimines, isatins are also suitable substrates (Scheme 3.3.4). The enantioselective allyl addition to isatin **3.60** only requires 0.5 mol % catalyst in 1.5 hours of reaction time, affording the valuable product **3.61** in 94% yield and 98L2 er. This compound was previously used in the synthesis of madindoline A.[131] Interestingly, the catalyst can be applied in the allenyl additions to isatins. The corresponding transformation, which affords **3.62** as the only product, completes in two minute with only 0.25 mol % aminophenol **3.58**. The X-ray structure of **3.62** confirms its absolute stereochemistry.

**Scheme 3.3.4. Catalytic enantioselective allyl or allenyl additions to isatins**

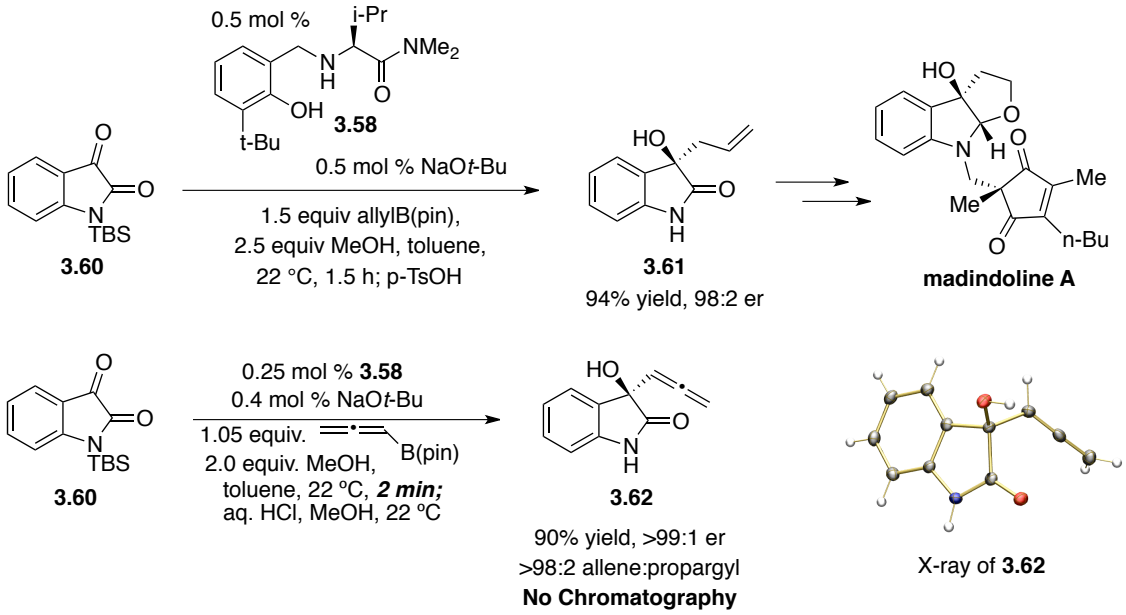


One notable feature of these transformations is their complete α selectivity, that is the breaking C–B bond is directly converted to the forming C–C bond. As illustrated in Scheme 3.3.5a, highly enantiomerically enriched allyl-B(pin) **3.63** affords only the α product **3.64** with high efficiency, diastereoselectivity and enantioselectivity. It should

(131) Itoh, T.; Ishikawa, H.; Hayashi, Y. *Org. Lett.* **2009**, *11*, 3854–3857.

be noted that the tertiary carbon stereogenic center in **3.63** gets inverted during the reaction (opposite absolute stereochemistry in **3.64**). In the case where the enaniomer of the allylboron **3.63** is used in the same reaction condition (**3.65**, Scheme 3.3.5b), the reaction is still exclusively α selective, but diastereomer **3.66** was isolated in 84% yield, 84:16 dr and 95:5 er. Again, the tertiary carbon stereogenic center in **3.65** gets inverted after the allyl addition. This complete α selectivity was further supported by the deuterium-labled experiment (Scheme 3.3.5c). In this case, 95% deuterium was accumulated in the α product **3.59n**.

**Scheme 3.3.5. Complete α selectivity in the catalytic enantioselective allyl addition reactions**

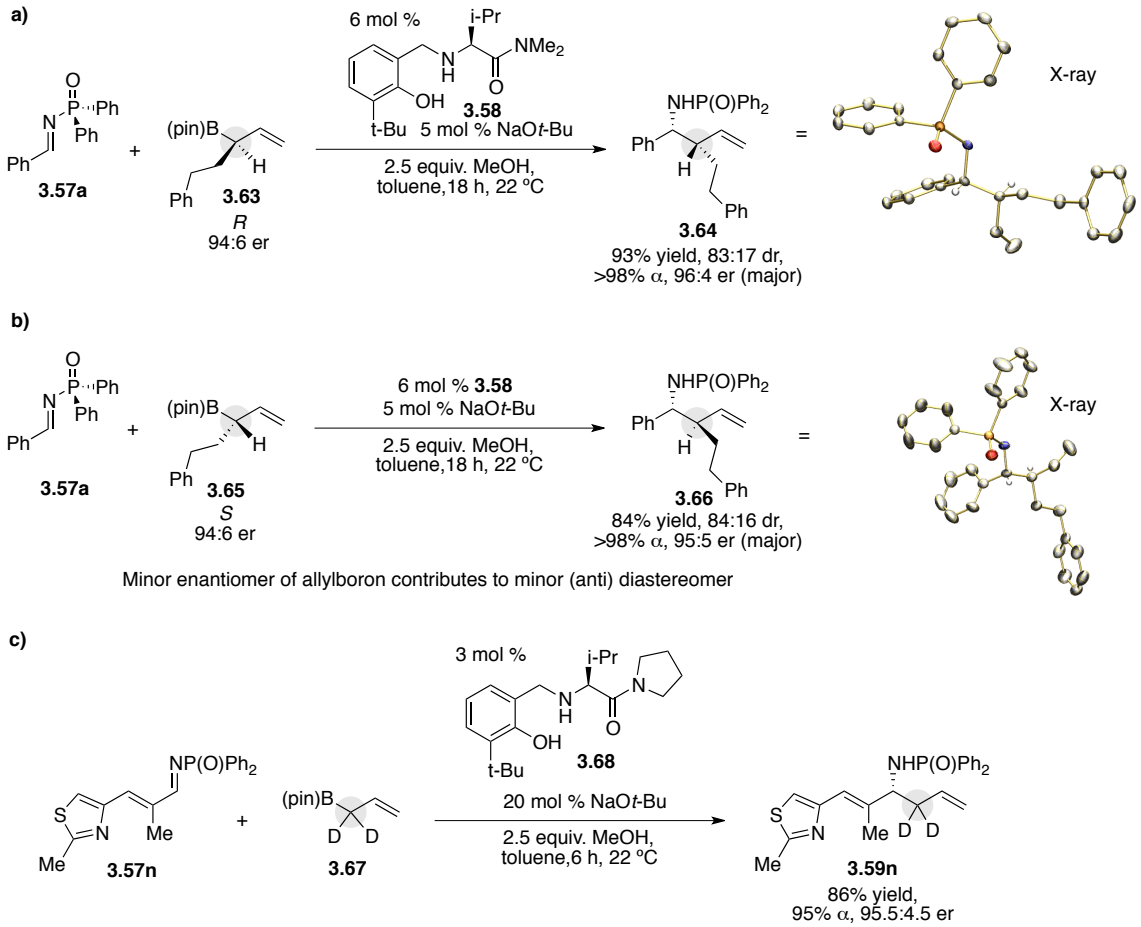

We also proposed a plausible mechanism to explain the observed reaction efficiency, α selectivity, diastereoselectivity and enantioselectivity. As shown in Scheme 3.3.6, the reaction begins with the formation of chiral methoxy boron **3.69**, of which the details are still under investigation. It should be noted that **3.69** bears an intramolecular electrostatic attraction between the ammonium unit and the amide carbonyl group (hydrogen bond-like interaction). This electrostatic attraction not only rigidifies the active catalytic species **3.69**, but also increases the Lewis acidity of the boron center. Thus, **3.69** is able to interact with allyl-boron **3.63**, and promote the first γ-addition (transmetallation) to afford chiral allylboron species **3.71**, through a stereospecific six-membered ring transition state.

**Scheme 3.3.6. Proposed mechanism for catalytic enantioselective allyl addition to aldimines**

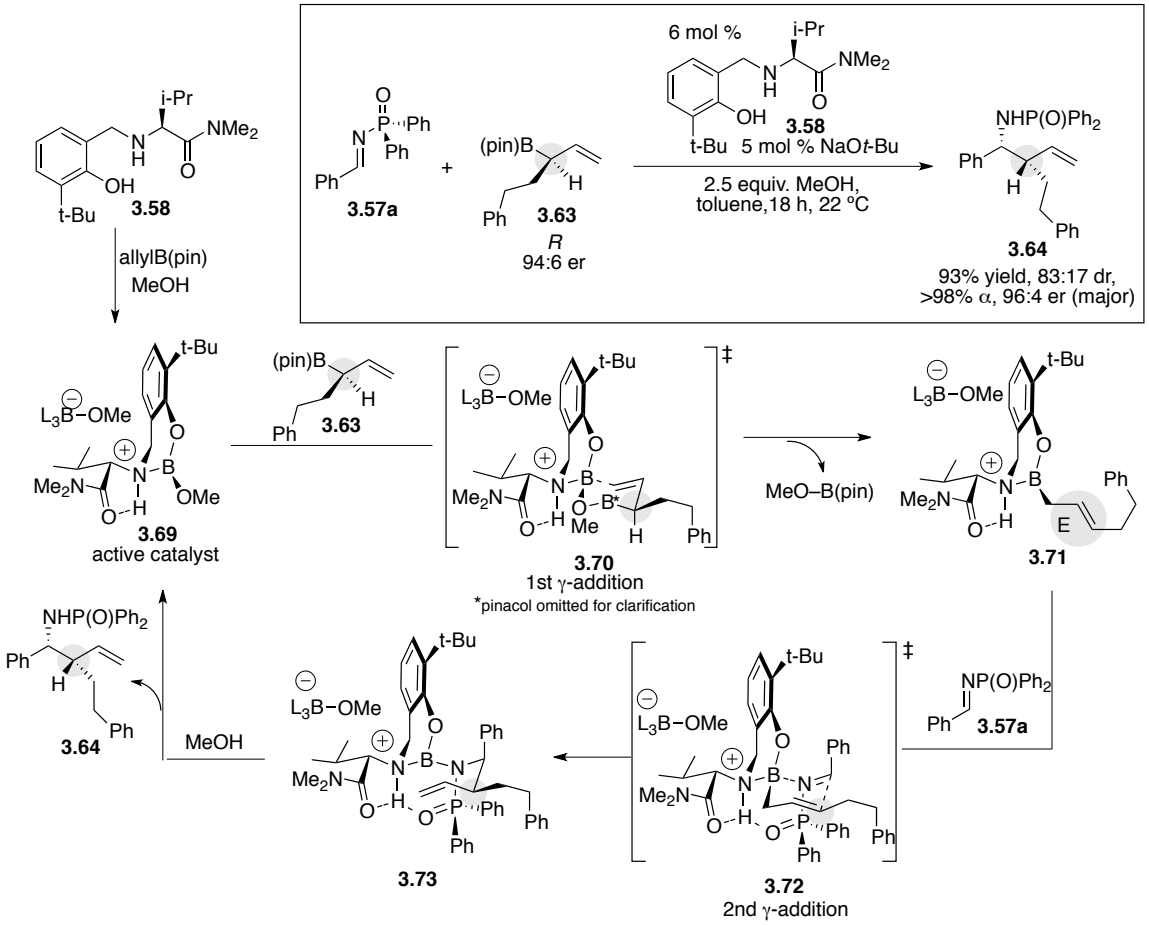


Next, the substrate **3.57a** approaches and coordinates to the allylboron **3.71** in a two-point binding mode (TS **3.72**). It is at this moment the second γ-addition occurs, forming the C–C bond. The P=O double bond of the phosphinoyl group in the aldimine **3.57a** serves as a critical Lewis basic unit to attract the ammonium unit in TS **3.72**. Due to this secondary interaction, the allyl addition step is rigidified and highly selective. After methanol hydrolysis, the product **3.64** is released and the active chiral methoxy boron is re-generated. The whole catalytic cycle contains two γ-additions, and thus results in a net α-addition product **3.64**. The inversion of the tertiary carbon stereogenic center in

**3.63** during the reaction can also be explained: the enantiotopic face of C–B breaking in TS **3.70** is opposite to the enantiotopic face of C–C bond formation in TS **3.72**.

The stereochemical models for explanation of the observed enantioselectivity were also provided. In Scheme 3.3.7, the substrate **3.57a** would bind to the chiral allyboron **3.74** through TS **3.75**, affording the major enantiomer. As a contrast, the enantiomer of the chiral allylboron **3.74** would not be efficiently bond to the substrate, due to the steric repulsion shown in **3.76**. Computational studies reveal that the energy difference between the two transition states is 5.9 kcal/mol, indicating TS **3.75** is strongly favored.

**Scheme 3.3.7. Stereochemical models for allyl additions to aldimines**

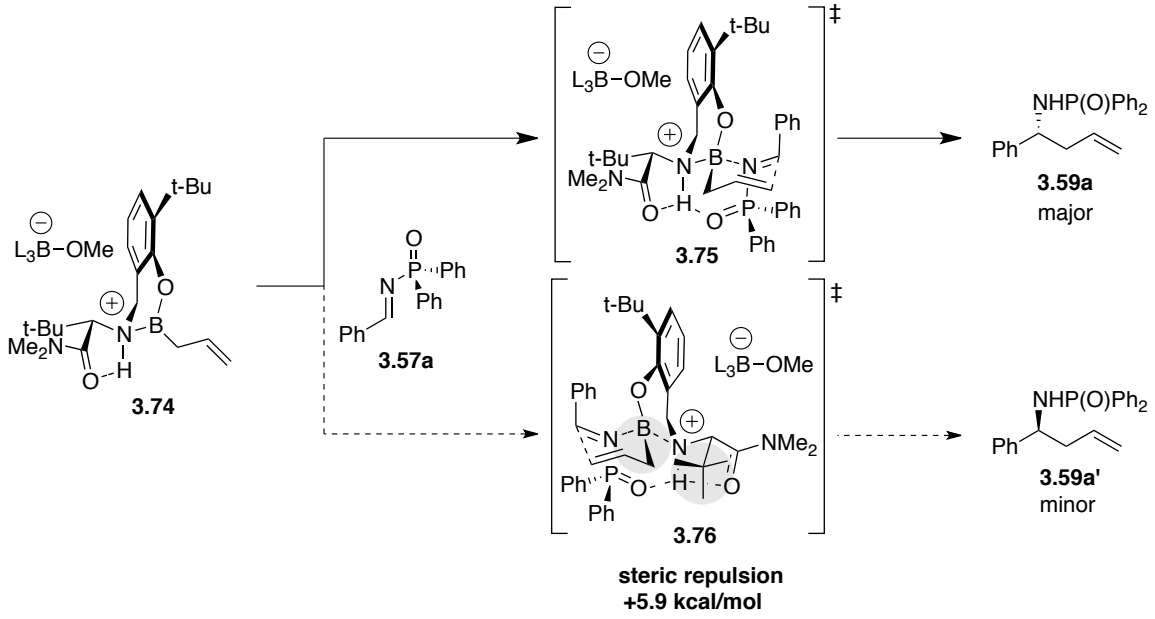


One notable feature of this method is the ease of obtaining the aminophenol pre-catalyst (Scheme 3.3.8). Starting from the commercially available Boc protected valine, Schiff base **3.80** can be accessed through an amide coupling, deprotection and condensation reaction. $NaBH_4$ reduction cleanly affords the desired aminophenol **3.58**,

which is a stable white crystalline solid. The only purification is after the last reduction reaction. Thus after four steps, aminophenol **3.58** can be obtained in 73% yield (~5 g scale). The modification of this aminophenol is also easy, as a variety of amino acid and salicyaldehyde are readily available. As a result, a library of aminophenols has been prepared through similar reactions in our lab.

**Scheme 3.3.8. Synthesis of the aminophenol**

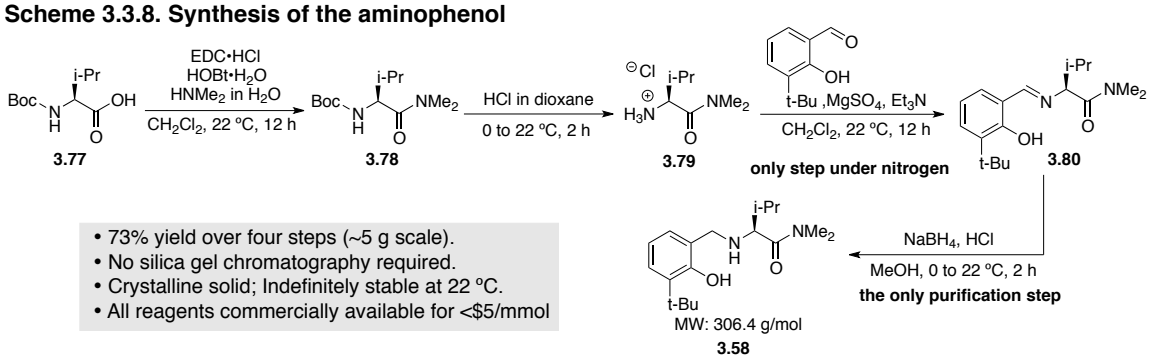


This efficient aminophenol-derived boron-based catalyst implied a new strategy for general allenyl additions (not limited to isatins). It was at this stage that I was involved in this project to explore the enantioselective allenyl additions to aldimines and aldehydes with this novel catalyst.[132]

## *3.4. Catalytic Enantioselective Allenyl Additions to Aldimines*

### *3.4.1. Initial Investigations*

We chose aldimines as the electrophiles to study catalytic enantioselective allenyl additions at the beginning, since similar allyl additions had already been established. Naively, we thought if we used allenylB(pin) instead of allyl-B(pin) in the same reaction condition, homoallenylamides should be obtained selectively. As shown in Scheme 3.4.1a, the allenyl addition to phosphinoyl imine **3.57a** is very sluggish and non-selective.

(132) Wu, H.; Haeffner, F.; Hoveyda, A. H. *J. Am. Chem. Soc.* **2014**, *136*, 3780–3783.

After four hours, only 10–30% conversion is achieved (reaction was not very reproducible), affording a 1:1 mixture of homoallenyl and homopropargyl amides. The enantiomeric ratio of homoallenylamide **3.81a** is only 75:25. Allowing the reaction to proceed longer does not help the reaction, as ~40% conv to 1:3 mixture of allenyl:propargyl addition products was observed after 14 hours of reaction time. A significant amount of those products come from the background process (without aminophenol **3.58**, 20% conv, allenyl:propargyl = 1:3).

**Scheme 3.4.1. Initial investigations of the catalytic allenyl addition to phosphinoyl imine**

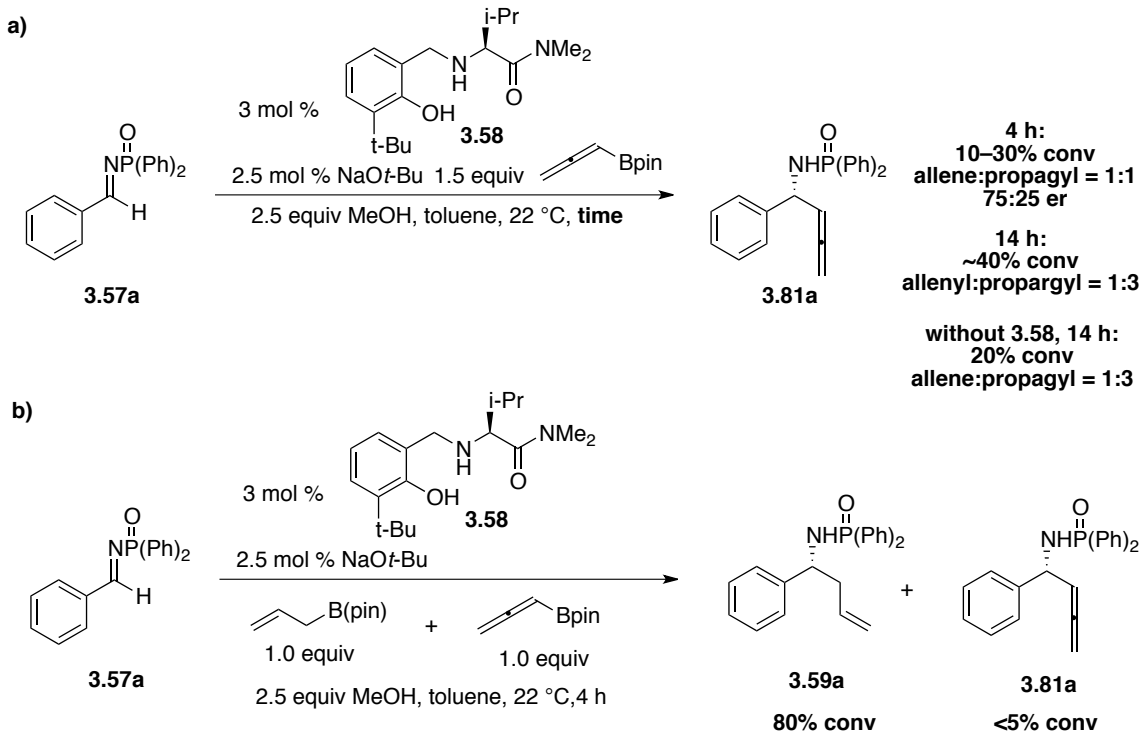


To understand why the catalytic allenyl addition is so slow, a competition experiment was performed (Scheme 3.4.1b): Phosphinoyl imine **3.57a** was subjected into a reaction mixture where one equivalent of allyl-B(pin) and allenylB(pin) were present. As a result, the allyl addition proceeded smoothly (80% conv) while <5%

homoallenylamide was observed. This suggests that the catalytic allenyl addition is inherently much slower than allyl addition.

Interestingly, the aminophenol-derived boron-based catalyst was found to promote an allenyl addition efficiently and selectively to α-ketoester imine **3.82 (**Scheme 3.4.2). With aminophenol **3.58**, the reaction finishes in 1.5 hours with a complete regioselectivity (>98:2 allenyl:propargyl). The product **3.83** was isolated in 93% yield and 91:9 er. With a *tert*-leucine derived aminophenol **3.84**, the reaction is slightly slower but with an enhanced enantioselectivity (97:3 er). These results imply that the active catalytic species (**3.85**) can be formed in the allenyl additions to imines. Then why are the reactions with phosphinoyl imines so sluggish?

**Scheme 3.4.2. The catalytic enantioselective allenyl addition to a α-ketoester imine**

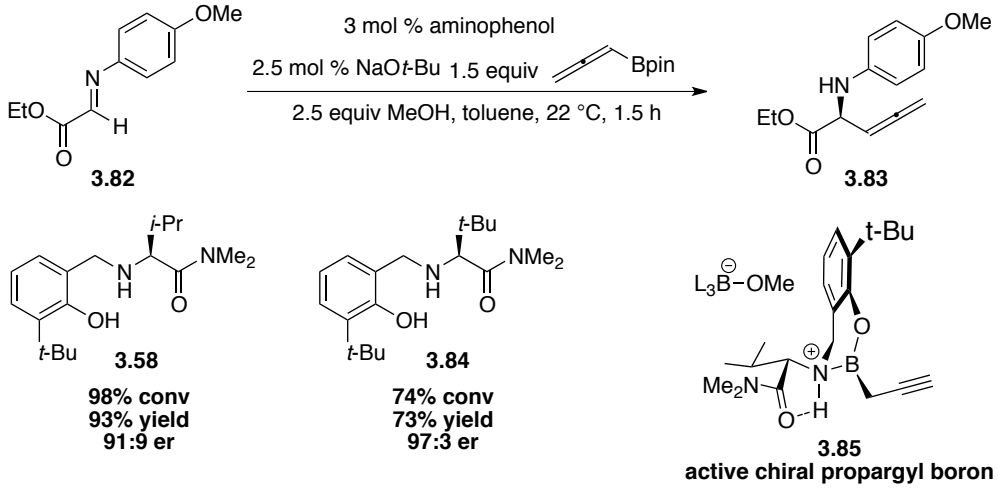


One hypothesis could be that the phosphinoyl imine somehow inhibits the formation of the chiral propargyl boron **3.85**. To test this hypothesis, another competition experiment was performed (Scheme3.4.3): After two hours, α-ketoester imine **3.82** was added into a reaction of allenyl addition to phosphinoyl imine **3.57a**. The reaction was allowed to proceed for an additional half an hour before quenched. Interestingly, there

was still minimal amount of **3.81a** (homoallenylamide from the phosphinoyl imine) generated, while a complete conversion to **3.83** was observed. This experiment indicates that the insufficient allenyl addition reaction with the phosphinoyl imine is because it is inherently not reactive enough, not because it inhibits the formation of the active chiral propargyl boron **3.85**.

**Scheme 3.4.3 Competition experiment with phosphinoyl imine and α-ketoester imine**

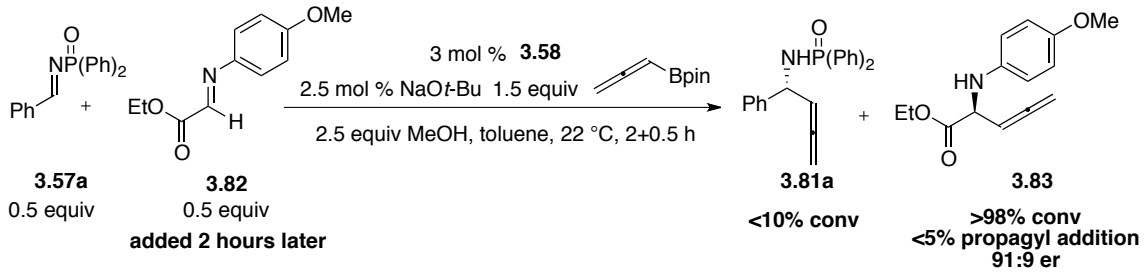


Since phosphinoyl imines are not reactive towards allenyl additions, a series of imines bearing different protecting groups were subjected into the same reaction condition (Scheme 3.4.4). As a result, imines with an electron donating protecting group are not efficient (<5% conv to **3.86**, **3.87** and **3.88**). The same is true with a sterically hindered imine (<5% conv to **3.89**). These data, accompanied with the result of phosphinoyl imine, suggest that the C=N double bond of the imine must be highly activated in order to promote the allenyl addition reaction. Thus, it is pleased to know that a Boc protected imine is very efficient in the allene addition reaction (>98% conv in four hours, 56% conv to homoallenylamide **3.90a**). More importantly, the desired product is highly enantioselective (90:10 er), which undoubtedly indicates the involvement of a chiral catalyst in this reaction.

**Scheme 3.4.4. Screening of the imine protecting groups**

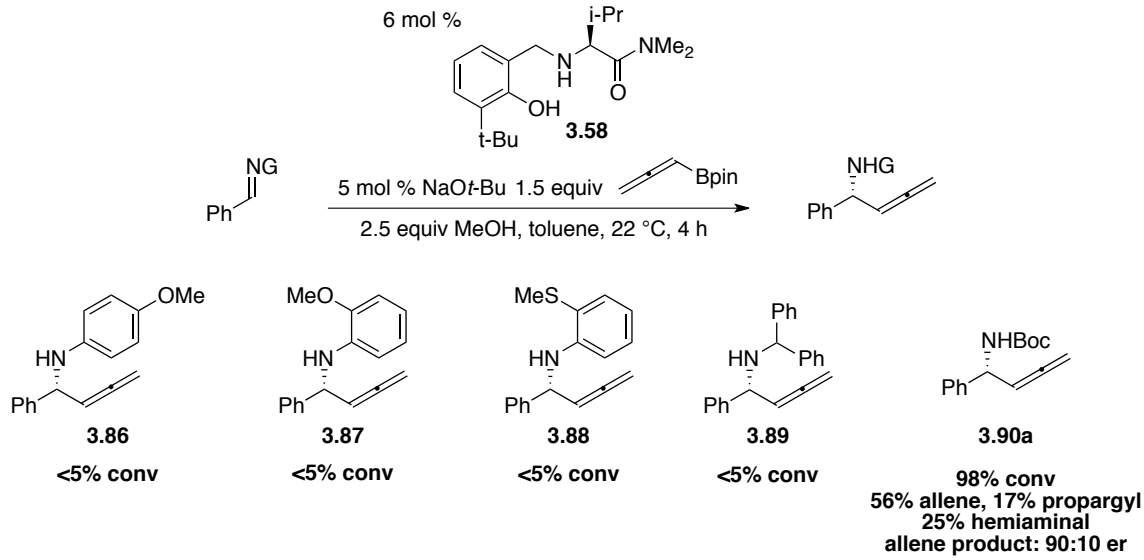


To understand why the allenyl additions to phosphinoyl imines are much more sluggish than the allyl additions, as well as why allenyl additions to Boc imines are facile, DFT calculations (by Dr. Fredrick Haeffner) were carried out. As shown in Scheme 3.4.5, the allyl addition to phosphinoyl imine **3.57a** through transtion state **3.92** requires 6.0 kcal/mol activation energy. This is 2.0 kcal/mol lower than the allenyl addition to **3.57a** through transition state **3.94**. Such a difference in energy probably comes from the poorer orbital overlap between the alkyne π orbital and the imine π* orbital in the allenyl addition, since TS **3.94** is not a perfect six-membered ring transition state. It is also possible that the stericically hindered two phenyl groups in the phosphinoyl imine have repulsion with the alkyne unit in TS **3.94**.

However, the reaction with the Boc imine is much more facile. In the Mayr's studies of electrophilicities of aldehydes and aldimines, Boc imines were found to be more electrophilic than phosphinoyl imines.[133] In addition, the *t*-butyl ester moiety in the

(133) Appel, R.; Mayr, H. *J. Am. Chem. Soc.* **2011**, *133*, 8240–8251.

Boc group is sterically less congested than the phosphinoyl group, and thus diminishes its repulsion with the alkyne unit in TS **3.95**. Last but not least, the Boc imine can also coordinate to the catalyst through a two-point binding mode, which induces the enantioselectivity.

**Scheme 3.4.5. Computational studies and Mayr's electrophilicities for aldimines**

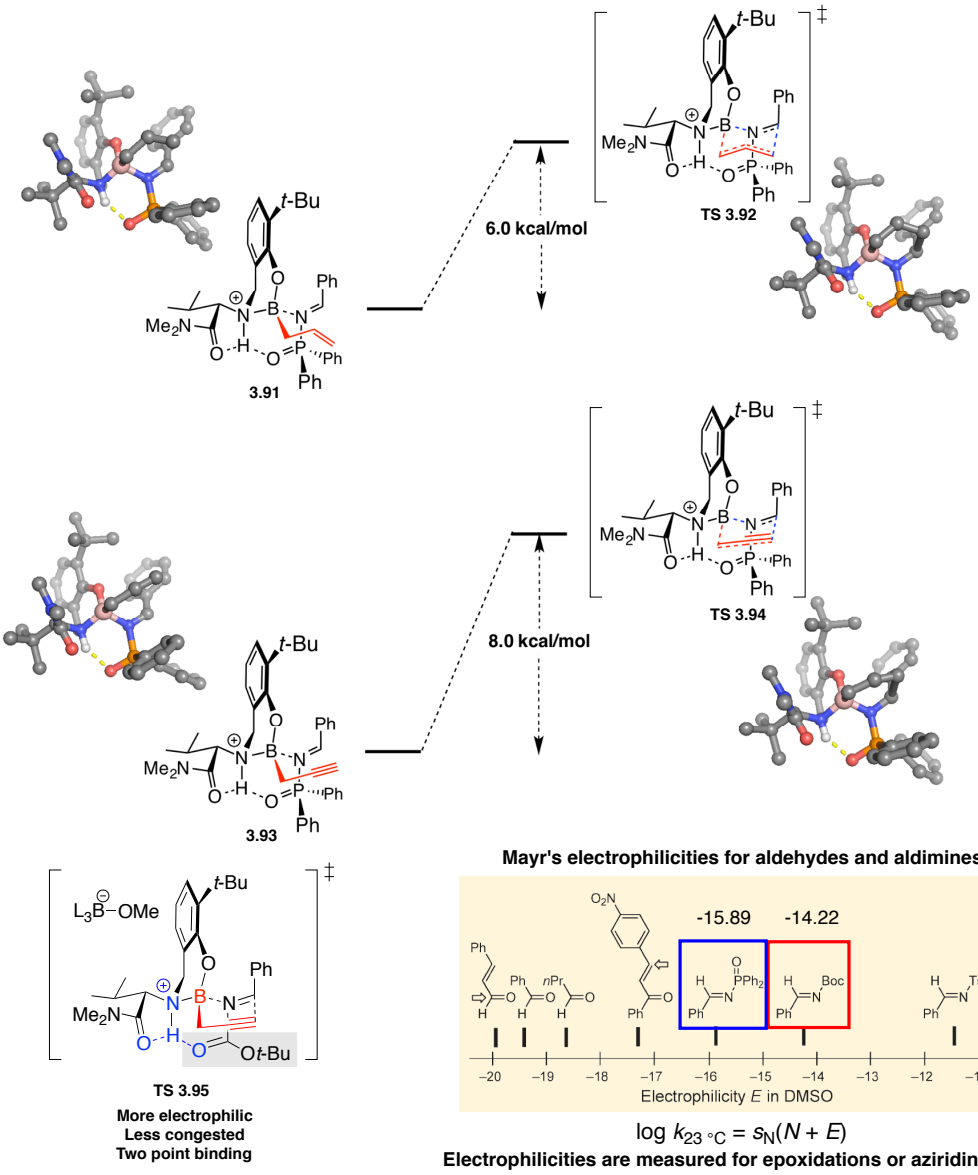

However, there are still challenges for allenyl additions to Boc imines. As shown in Scheme 3.4.6, although 98% conversion can be achieved after four hours, the reaction only affords a mixture: 56% homoallenylamide **3.90a** accompanied with undesired 17% homopropargylamide **3.98a** and 25% hemiaminal **3.97**. Without the catalyst, there is 50% conversion to hemiaminal **3.97** and a 7% of **3.98a**. In the reaction mixture, Boc imine **3.96a** is in equilibrium with its hemiaminal **3.97** due to the presence of MeOH. Notably, such equilibrium is not as significant in reactions with phosphinoyl imines, probably because the latters are less electrophilic. When Boc imine **3.96a** is available, it can be converted to homoallenylamide **3.90a** through the catalytic process, or transformed into **3.98a** mainly through a background reaction. In the TLC analysis, hemiaminal **3.97** is inseparable with our desired product (**3.90a**), rendering the difficulty for purification of the reaction mixture. Luckily, the undesired homopropargylamide **3.98a** can be separated during the silica gel chromatography.

**Scheme 3.4.6. Challenges for catalytic enantioselective allenyl additions to Boc imines**

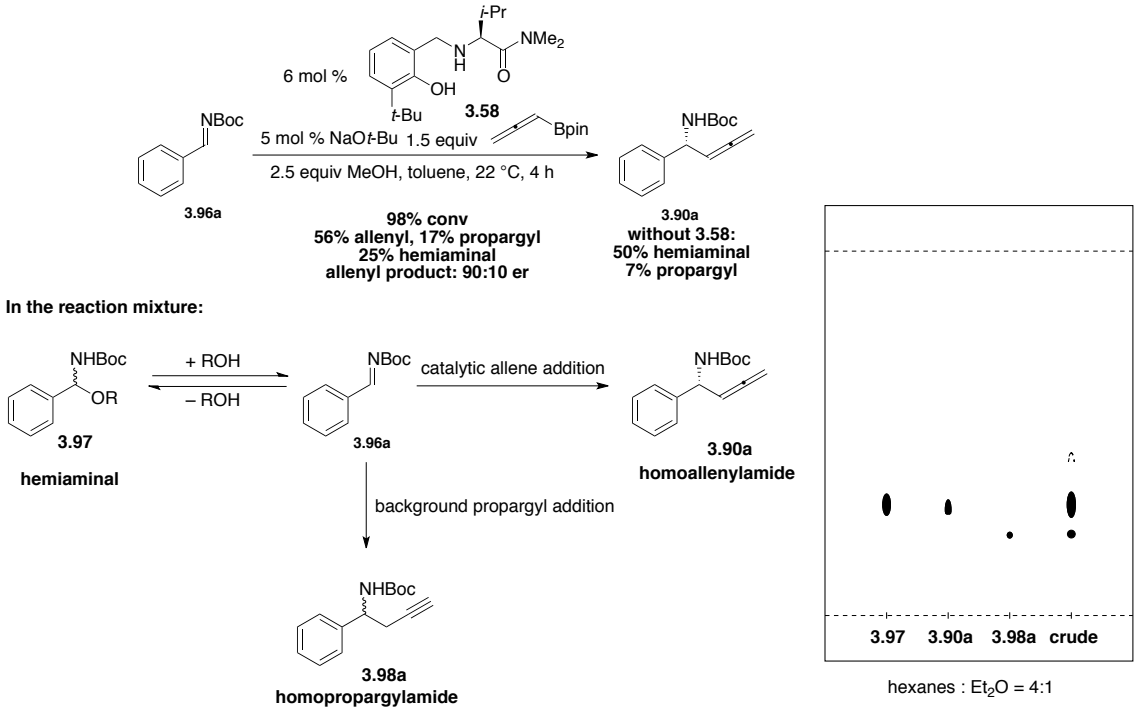


To diminish the formation of the hemiaminal, a sterically more hindered alcohol additive may be applied, since the repulsion between the alcohol substituent and the *t*-butyl unit of Boc group may hamper the formation of the hemiaminal. In fact, it is as we expected. As illustrated in Table 3.4.1, the use of EtOH dramatically diminishes the hemiaminal formation. Pleasingly, the background reaction, affording the homopropargylamide, can also be suppressed (<5% conv, entry 2), likely because of the increasing activation energy for a bulkier alcohol to activate allenylB(pin). The reaction proceeds to 85% conversion after 14 hours, from which **3.90a** can be isolated in 73% yield and 93:7 er. This allenyl addition can be further improved by the use of *i*-PrOH, where >98% conversion and 95% yield of **3.90a** can be obtained with a slightly increased er (95:5).

**Table 3.4.1. Alcohol screening for the catalytic allenyl addition to a Boc imine**

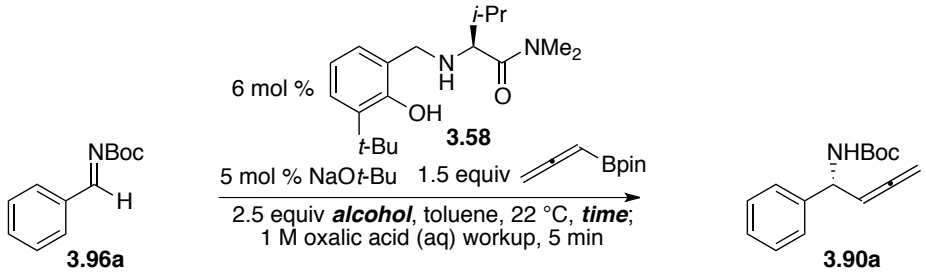


**3.96a** **3.90a**

| entry | alcohol | reaction time (h) | conv (%)[a] | yield (%)[b] | er | propargylation (%) | hemiaminal (%) |
|---|---|---|---|---|---|---|---|
| 1 | MeOH | 4 | 98 | 31 | 90:10 | 17 | 25 |
| 2 | EtOH | 4 | 35 | 21 | 92:8 | <5 | ~5 |
| 3 | EtOH | 14 | 85 | 73 | 93:7 | <5 | <5 |
| 4 | *i*PrOH | 14 | >98 | 95 | 95:5 | <5 | ~5 |
| 5 | *t*BuOH | 14 | ~80 | no allene product | - | no propagyl product | ~80 |

[a] Conversions are disappearance of the starting material. [b] Yields are isolated yields of the allene product.

However, the use of more hindered *t*-BuOH does not promote any productive reaction: only ~80% conversion to hemiaminal was observed after 14 hours. This result is consistent with the previously mentioned mechanism, as if the chiral methoxy boron **3.69** is replaced by chiral *t*-butoxy boron, the allenyl transfer will be greatly disfavored.

A systematic screening of the catalyst loading was also performed. To our surprise, the reaction efficiency merely diminishes even with only 0.1 mol % **3.58** (entry 6, Table 3.4.2). This implies in case where 6 mol % aminophenol **3.58** is used (entry 1), a majority of the aminophenol molecules do not form the active catalytic species. Further investigations aiming at facilitating the active catalyst formation are still in progress. When only 0.1 mol % **3.58** is applied, the reaction does not proceed to a full conversion until 14 hours (70% conv after 8 hours, entry 7). If the catalyst loading is decreased to 0.01 mol %, the allenyl addition is siginificantly hampered, although the product is still highly enantioselective (29% yield of **3.90a**, 91:9 er, entry 8).

**Table 3.4.2. Screening of the catalyst loading**

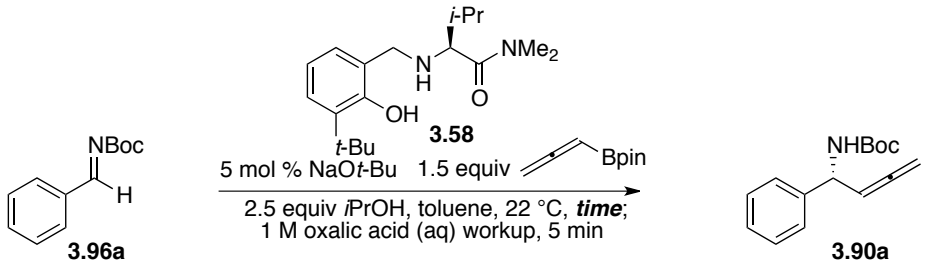


| entry | cat. mol % | reaction time (h) | conv (%)[a] | yield (%)[b] | er | propargylation (%) | hemiaminal (%) |
|---|---|---|---|---|---|---|---|
| 1 | 6 | 14 | >98 | 95 | 95:5 | <5 | 5 |
| 2 | 3 | 14 | >98 | 97 | 95:5 | <5 | <5 |
| 3 | 3 | 8 | 83 | 71 | 95:5 | <5 | 10 |
| 4 | 1 | 14 | >98 | 73 | 95:5 | 5 | 15 |
| 5 | 0.5 | 14 | >98 | 82 | 95:5 | <5 | 10 |
| 6 | 0.1 | 14 | >98 | 81 | 95:5 | 5 | 15 |
| 7 | 0.1 | 8 | 70 | 58 | 95:5 | 5 | 20 |
| 8 | 0.01 | 14 | 81 | 29 | 91:9 | 15 | 24 |

[a] Conversions are disappearance of the starting material. [b] Yields are isolated yields of the allene product.

It should be noted that 1 M oxalic acid (aq) was used to quench the reaction for hydrolysis of the formed hemiaminal (15%, entry 6) without deprotecting the Boc group. In this way, homoallenylamide **3.90a** can be obtained cleanly.

Further optimizations of the reaction resulted in the use of 2.3 equivalents of *i*-PrOH instead of 2.5 equivalents, which diminished the formation of the hemiaminal (<5%) and homopropargylamide (<5%). The catalytic allenyl addition to Boc imine **3.96a** can also be promoted by other aminophenols (Scheme 3.4.7). For example, the aminophenol derived from *t*-leucine gives 81.5% yield (95% conversion) with 96:4 er. Alternation of the amine group into pyrolidine results in aminophenol **3.68**, which promotes the allenyl addition with similar efficiency and regioselectivity as **3.58**, but with

a diminished enantioselectivity (92:8 er). Thus, we chose aminophenol **3.58** in the following studies.

**Scheme 3.4.7. Catalyst screening**

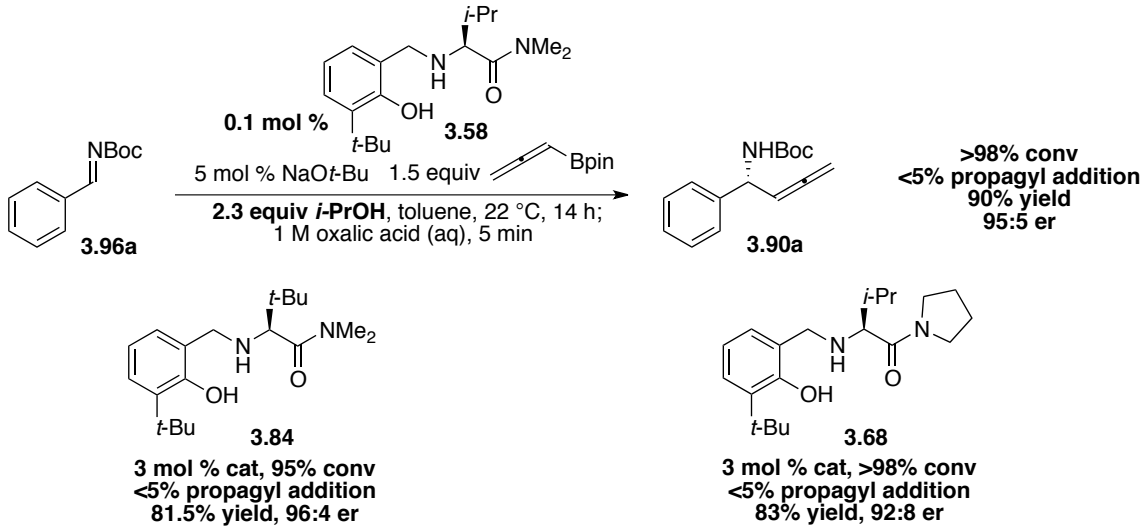


### *3.4.2. Scope of the Catalytic Enantioselective Allenyl Additions*

Various aryl substituted Boc imines were prepared and applied in the catalytic enantioselective allenyl additions (Scheme 3.4.8). In most cases, 0.1 mol % aminophenol is enough to complete reactions in 14 hours. Reactions with *ortho*-chloro or bromo substituted aryl imines are equally efficient and selective (**3.90b** and **3.90c**). The X-ray structure of the former product was obtained and its absolute stereochemistry was confirmed. The allenyl addition to *meta*-bromo substituted phenyl Boc imine **3.96d** gives the desired product with 86% yield and 94:6 er (<2% homopropargylamide).

The electron withdrawing substituents of Boc imines are compatible in our reactions. For example, homoallenylamide **3.90e**, which bears a strongly electron poor *p*-$CF_3$ phenyl moiety, can be isolated in 80% yield (>98% conv), >98:2 regioselectivity as well as 94:6 er. However, the reaction to the aldimine bearing an eletron-rich substituent requires 3 mol % catalyst to promote 85% conversion (74% yield, **3.90f**). In addition,

~5% homopropargylamide was observed in this case. Nevertheless, the enantioselectivity is still high (97:3 er).

**Scheme 3.4.8. Catalytic enantioselective allenyl additions to aryl- or heteroaryl-substituted Boc imines**

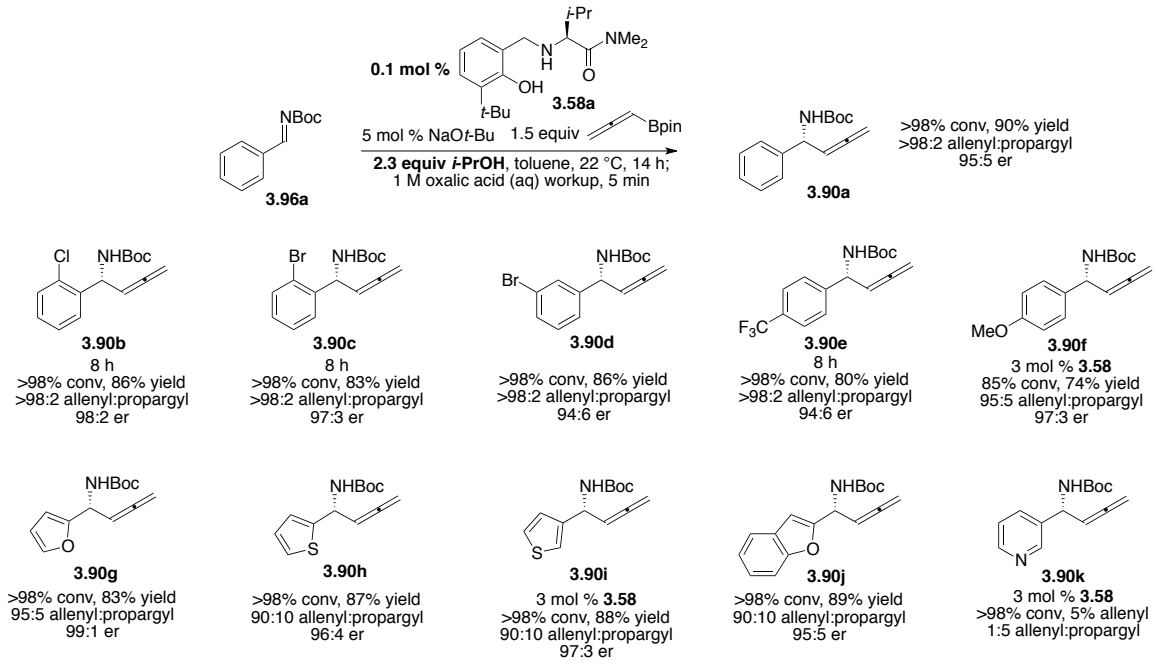


To our delight, our enantioselective allenyl additions promoted by an aminophenol-derived boron-based catalyst are suitable for furyl-, thiophenyl- as well as benzofuryl-substitued aldimines. Reactions are generally efficient with 0.1 mol % catalyst (except for **3.90i**, 3 mol % catayst), but the regioselectivities diminish slightly (90:10 to 95:5 allenyl:propargyl addition). Nevertheless, the homoallenylamides can be isolated as a pure form by chromatography with 83–89% yield and 95:5 to 99:1 er.

To our surprise, the same reaction to a substrate bearing a pyridyl substituent only affords 5% homoallenylamide product (25% propargyl addition, **3.90k**).

Further investigations revealed that the pyridine group did inhibit the catalysis. For example, in Scheme 3.4.9, the reaction with phenyl substituted Boc imine **3.96a** is greatly slowed if 1.0 equivalent of pyridine is involved. Only 38% homoallenylamide

was observed accompanied with 45% propargyl addition product. The enantiomeric ratio of **3.90a** was found to be dramatically diminished (71:29 er). The way that pyridine inhibits the catalytic cycle is still unknown. It could influence the reaction by deprotonating the proton of the intromolecular hydrogen bond of the catalyst, or binding to the Lewis acidic boron of the catalyst.

**Scheme 3.4.9. Catalytic allenyl additions inhibited by the pyridine moiety**

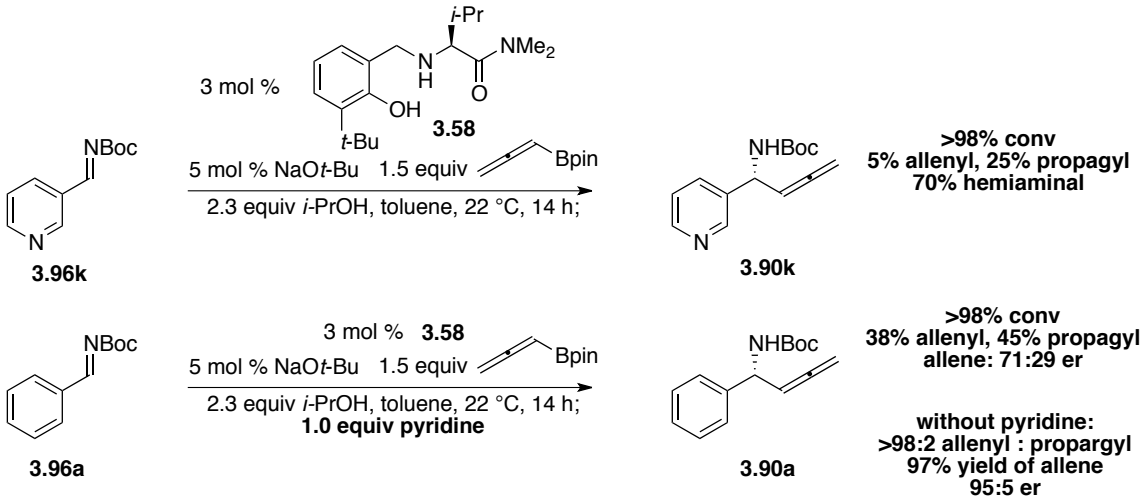


In order to find the optimized condition for the allenyl addition to **3.96k**, a variety of alcohol additives were tested in this reaction (Table 3.4.3). The use of MeOH encourages hemiaminal formation as well as background process. Thus, only 36% of homoallenylamide **3.90k** was observed with a low enantioselectivity (58:42 er). As a contrast, the employment of EtOH gives the best result: 90% allenyl addition and 77% isolated yield of **3.90k** with 84:16 er. The slightly more hindered *n*-PrOH gives similar yield of **3.90k** with 8:1 allenyl:propargyl selectivity. However, the enantioselectivity is significantly decreased (75:25 er).

**Table 3.4.3. Optimizations of the allene addition to a pyridyl substituted Boc Imine.[a]**

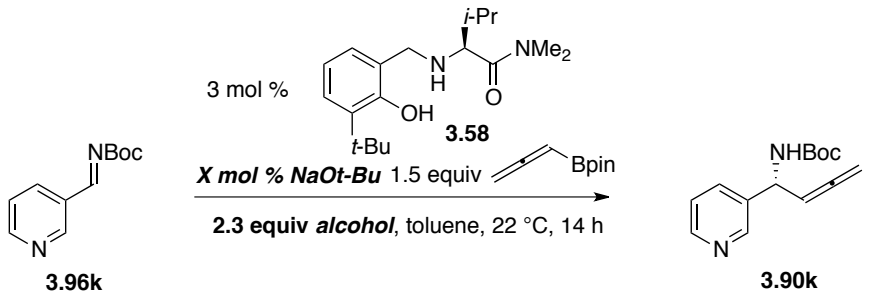


**3.96k** **3.90k**

| entry | alcohol | mol % NaO*t*-Bu | conv (%) | allenyl (%) | propargyl (%) | hemiaminal (%) | yield (%) | er |
|---|---|---|---|---|---|---|---|---|
| 1 | MeOH | 5 | >98 | 36 | 24 | 40 | 16 | 58:42 |
| 2 | EtOH | 5 | >98 | 90 | 10 | <5 | 77 | 84:16 |
| 3 | *n*-PrOH | 5 | >98 | 80 | 10 | 10 | 71 | 75:25 |
| 4 | *i*-PrOH | 5 | >98 | 5 | 25 | 70 | - | - |
| 5 | EtOH | 2.5 | >98 | 80 | 20 | <5 | 73 | 72:28 |
| 6 | EtOH | 0 | 70 | <5 | <5 | 70 | - | - |

[a] Conversions and the ratios of allene to propargyl products determined through analysis of 400 MHz 1H NMR spectra of unpurified mixtures (±5%). [b] Yields of isolated the homoallenylamide product. [c] Enantiomeric ratios (ers) determined by chiral GC or HPLC.

Considering the pyridyl group is Brønsted basic, we tested to use less NaO*t*-Bu in the catalytic allenyl addition to **3.96k**. However, the reaction does not improve at all (entry 5 and 6). This suggest the role of pyridyl for catalyst inhibition is not merely changing the pH value of the reaction solution, or else the use of less base should give a better result.

**Scheme 3.4.10. Catalytic enantioseletive allenyl additions to akyl substituted aldimines**

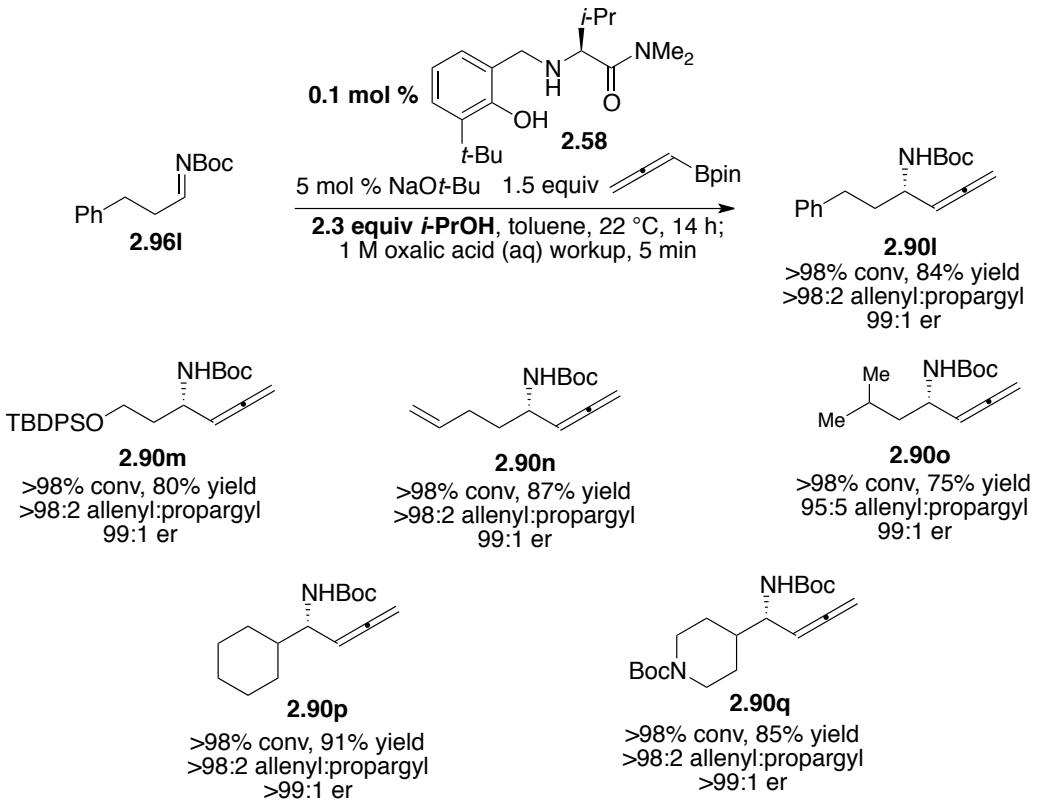


The catalytic enantioselective allenyl additions to Boc imines were further proved to be efficient for alkyl substituted aldimines (shown in Scheme 3.4.10). It is noteworthy that those substrates have been found to be more difficult for nucleophilic additions due to their stability (prone to isomerize to enamines). In some reports, the reactions with alkyl imines are also less selective.[123] Nevertheless, in all cases of our catalytic reactions, the use of 0.1 mol % aminoalcohol **3** is effective enough to generate the desired homoallenylamides with >98% conv after 14 hours. The reactions are compatible with substrates bearing a phenyl (**2.90l**), silyl ether (**2.90m**) or alkene (**2.90n**) group. In addition, α- or β-branched alkyl substituents do not influence the reaction significantly (**2.90o** and **2.90p**, 75–91% yield, ≥99:1 er). The reactions are also efficient and highly selective with substrates bearing a N-Boc unit (**2.90q**, 85% yield, >99:1 er). The fact that

all the alkyl amides can be isolated in high yields, regio- and enantiomeric ratios (≥95:5 allenyl:propargyl, ≥99:1 er) highlights this methodology.

Another advantage of using Boc as the protecting group relies on the ease to synthesize the corresponding imine. For example, benzofuryl substituted imine **3.96j** can be obtained in two steps: (1) The corresponding aldehyde **3.99** (commercially available) reacts with Boc-$NH_2$ and phenylsulfinic acid sodium salt to afford sulfone **3.100** in 64% yield. This sulfone (same as all other sulfones) is a white solid, which is isolated by a simply filtration and aqueous wash. No further purification is needed. (2) Sulfone **3.100** can be converted into the aldimine by deprotonation. $Cs_2CO_3$ (or $K_2CO_3$ under reflux) is sufficient enough in this reaction, which gives the corresponding aldimine **3.96j** in a quantitative yield without any purification (simply filtration to remove the inorganic salts). It should be noted all other Boc-imines were prepared through similar procedure. In cases where Boc imines are less stable (for example, alkyl substituted ones), the corresponding sulfones were synthesized in a gram scale, stored under air at ambient temperature and converted into the imines prior to the allenyl addition reactions.

**Scheme 3.4.11. Facile synthesis of Boc imines**

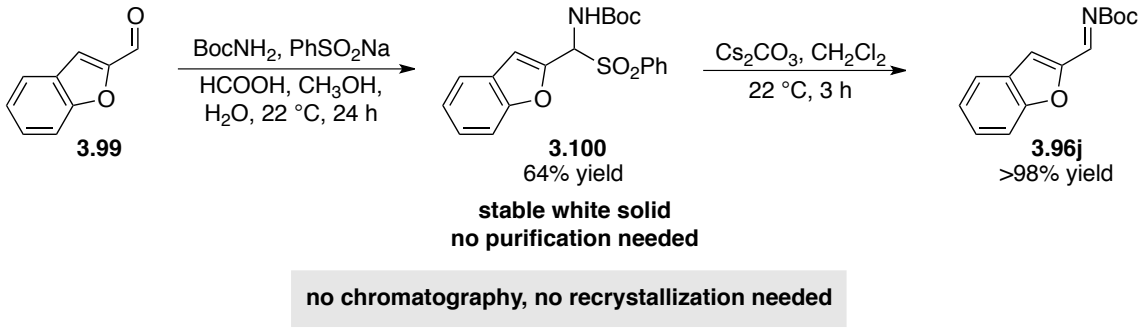


Our catalytic enantioselective allenyl additions to Boc aldimines are suitable for gram-scale preparations of materials (Scheme 3.4.12). For example, the allenyl addition

to *p*-MeO-phenyl substituted aldimine **3.96f** is more difficult as mentioned previously (with 3 mol % catalyst: 85% conv, 74% yield, 95:5 allenyl:propargyl and 97:3 er). However, if the same reaction is performed in a 1.90-gram scale, the catalyst loading can be diminished into 0.5 mol %. In addition, the reaction is even more efficient (>98% conv, 90% yield) and regio-selective (>98:2 allenyl:propargyl) in a larger scale, where no rigorous exclusion of air and moisture are provided. Thus, this method is a synthetically useful one which has its potentials to be applied in industry.

**Scheme 3.4.12. Reaction performed in a gram scale**

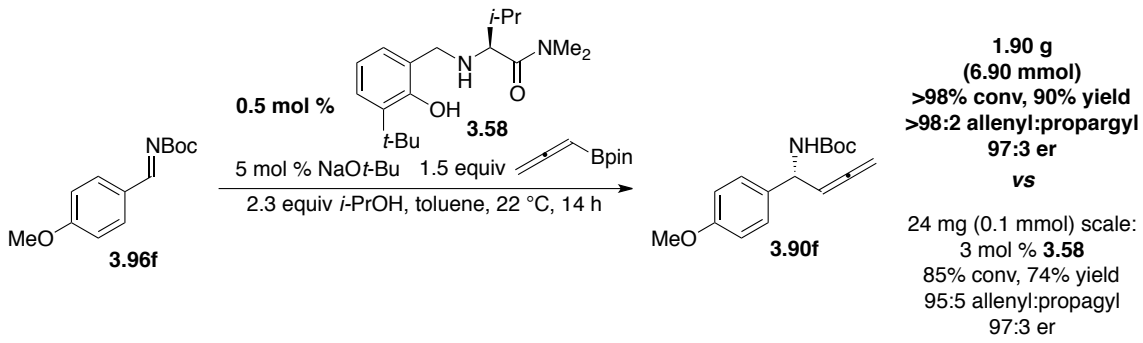


### *3.4.3. Kinetic Studies*

One of the key mechanistic questions about our catalytic enantioselective allenyl additions relies on the understanding of the turnover-limiting step. It could be the step of generating the active chiral alkoxy boron catalyst, or forming the chiral propargyl boron intermediate through transmetallation, or allenyl addition to an imine forming the C-C bond. To answer this question, we utilized the React-IR technique to perform kinetic studies of the allenyl addition reactions. Our goal was to investigate the Hammett correlation of this reaction, so that the electronic effect of the aryl substituent on the

reaction rate of allene addition reactions could be determined.[134] Thus, four different aryl substituted Boc imines, of which the Hammett constants range from –0.27 to 0.54, were selected as the substrates in this study (Scheme 3.4.13). React-IR was used to monitor the conversions of those reactions in real time, so that we could determine the initial rate of each reaction. After that, the Hammett plot of our catalytic enantioselective allenyl additions could be generated, from which the Hammett reaction constant ρ value was calculated.

**Scheme 3.4.13. Reaction conditions for kinetic studies**

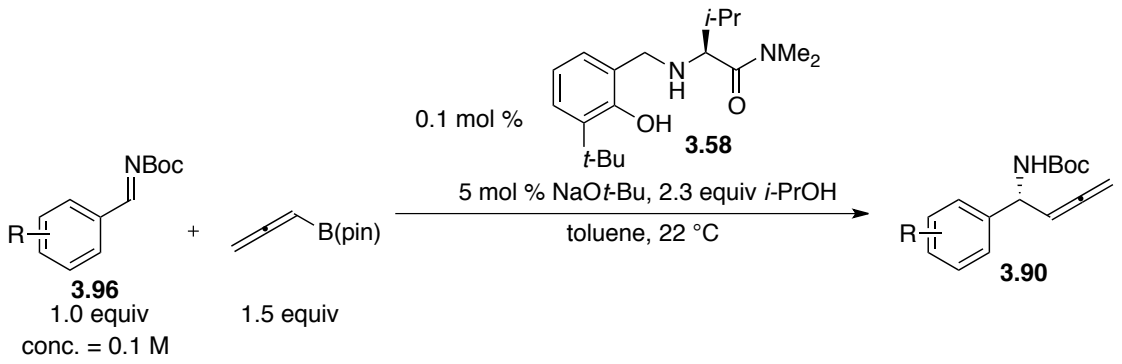


| substrate | Hammett substituent constant (σ) |
|---|---|
| **3.96e** R = *p*-$CF_3$ | 0.54 |
| **3.96d** R = *m*-Br | 0.39 |
| **3.96a** R = H | 0.00 |
| **3.96f** R = *p*-MeO | –0.27 |

**Increasing rate of reaction**

The kinetic experiments showed that the reaction with the substrate bearing an electron withdrawing group (such as *p*-$CF_3$-phenyl) is generally faster than the one with the substrate bearing an electron donating group (such as *p*-MeO-phenyl). This rate difference is huge as we can directly see in Figure 3.4.1: After 30 min of the reaction time, allenyl addition to *p*-$CF_3$-phenyl substituted aldimine proceeds to ~80% conv, while

(134) Hammett, L. P. *J. Am. Chem. Soc.* **1937**, *59*, 96–103.

the one to *m*-Br-phenyl or phenyl substituted aldimines proceed to ~40% and 30% conv, respectively. In contrast, the conversion of the allenyl addition to *p*-MeO-phenyl aldimine is only ~5%.

**Figure 3.4.1. Conversions of allenyl additions to Boc–imines vs time (min)**

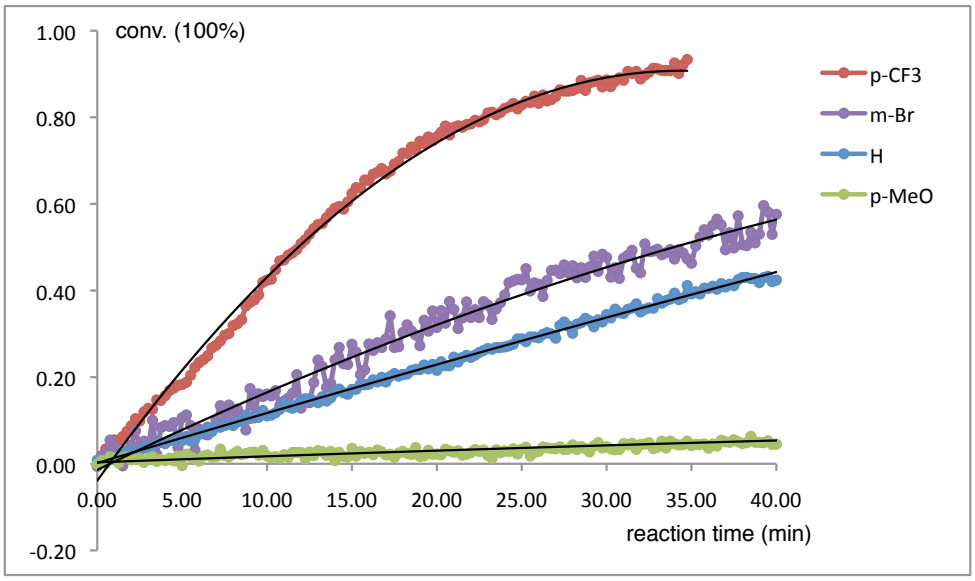


This observation is quantified in the Hammett plot shown in Scheme 3.4.14. The Hammett reaction constant ρ value is +1.70, indicating there is a significant electronic substituent effect on the reaction rate. More specifically, a partial negative charge is likely built or a partial positive charge is lost during the rate determining step.

Because of this, we believe that the C–C bond forming step is likely the turnover-limiting step. After binding to the catalyst, the carbon of C=N double bond in the substrate develops a partial positive charge (activated by Lewis acidic boron of the catalyst). This partial positive charge gets diminished during the C–C bond formation (nucleophilic addition). Thus, substrates with an electron withdrawing group accelerate this process in TS **3.95** and bear a higher reaction rate than ones with an electron donating group.

**Scheme 3.4.14. Hammett plot for catalytic enantioselective allenyl additions to aldimines**

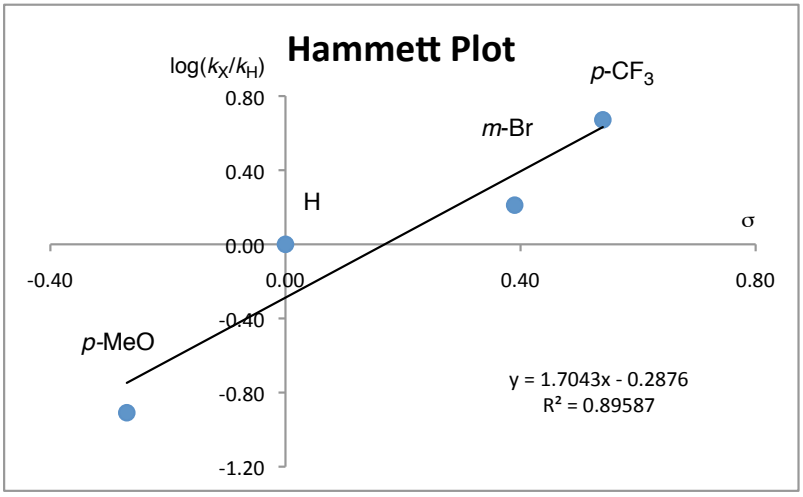


**Hammett Equation:** $\log(k_X/k_0) = \rho\sigma$ $\rho = 1.70$

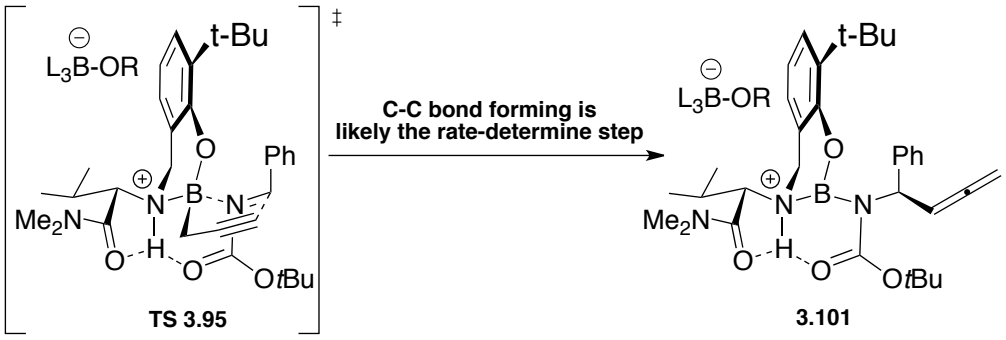


### *3.4.4. Functionalizations of Homoallenylamides*

The Boc protected enantiomerically enriched homoallenylamides are valuable compounds that are not easily to be accessed through other methods. Thus, we would like to demonstrate their synthetic utilities in our studies.

The first example relies on the use of selective protoborations of allenes.[135] In 2013, my colleagues Fanke Meng and Byunghyuck Jung discovered that NHC–Cu complexes can selective catalyze protoborations of monosubstituted allenes. With a sterically hindered NHC–Cu complex, terminal alkenyl boron can be generated in a high

(135) Meng, F.; Jung, B.; Haeffner, F.; Hoveyda, A. H. *Org. Lett.* **2013**, *15*, 1414–1417.

efficiency and regioselectivity. As we tested this reaction to our homoallenylamide **3.90a**, we found terminal alkenyl boronate **3.102** was exclusively formed (>98% conv, 90% yield). No internal alkenyl boronate **3.103** was detected by NMR spectra. We believe this is a good strategy for generations of β-amine-substituted terminal alkenyl boronates.

**Scheme 3.4.15. NHC–Cu-catalyzed protoborations of homoallenylamides**

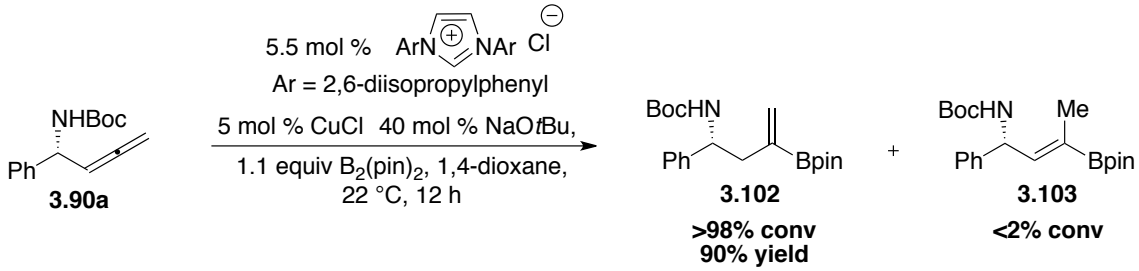


Another application of the current method is the formal synthesis of (+)-anisomycin.[136] The route begins with an efficient Johnson-Corey-Chaykovsky reaction[137], affording the epoxide **3.105** in a quantitative yield. Then a Lewis acid promoted 1,2-hydride shift gives the benzyl aldehyde **3.106**. Due to its instability, this compound was converted into the corresponding Boc aldimine **3.107** through the aforementioned protocol in 41% yield over three steps. The aldimine **3.107** was not stable (prone to isomerize into enamine) and was subjected into the catalytic enantioselective allenyl addition. The product **3.108** was found to be accompanied with 20% enamine byproduct. After silica gel chromatography, the desired homoallenylamide can be isolated in 66% yield and 96:4 er. Thus, we were pleased to see for this challenging substrate (**3.107**), the allenyl addition catalyzed by our boron catalyst could still compete with the

(136) (a) Sobin, B. A.; Tanner, F. W. Jr. *J. Am. Chem. Soc.* **1954**, *76*, 4053. (b) Schumacher, D. P.; Hall, S. S. *J. Am. Chem. Soc.* **1982**, *104*, 6076–6080. (c) Meyers, A. I.; Dupre, B. *Heterocycles* **1987**, *25*, 113–116. (d) Detz, R. J.; Abiri, Z.; le Griel, R.; Hiemstra, H.; van Maarseveen, J. H. *Chem.- Eur. J.* **2011**, 17, 5921–5930.

(137) (a) Johnson, A. W.; LaCount, R. B. *J. Am. Chem. Soc.* **1961**, *83*, 417–423. (b) Corey, E. J.; Chaykovsky, M. *J. Am. Chem. Soc.* **1965**, *87*, 1353–1364.

isomerization of the starting material. It is noteworthy that our approach to **3.108** is more efficient (27% overall yield in five steps) than a previously reported procedure[135d], where six steps were required to give the same compound in 9% overall yield.

Following the previous reported synthesis, dihydro pyrrolidine derivative **3.109** can be efficiently synthesized through a Au(I) catalyzed cyclization, which had already been demonstrated in the synthesis of (+)-anisomycin.[135b,d]

**Scheme 3.4.16 Formal synthesis of (+)-anisomycin**

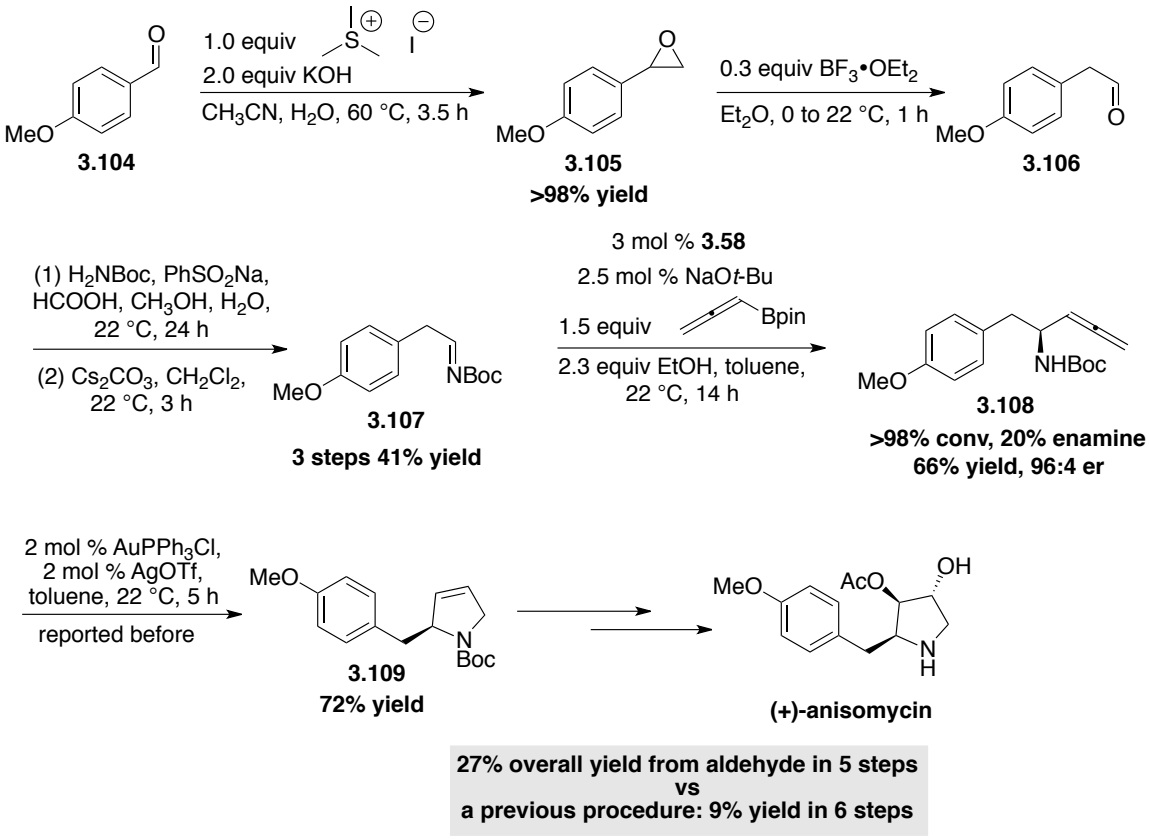


The current protocol for efficient synthesis of homoallenylamides in a high regio- and enantioselective fashion was further utilized in a total synthesis of (*epi*)-cytoxazone.[138] As mentioned above, highly enantiomerically enriched **3.90f** can be

(138) For previous studies in connection to enantioselective synthesis of *epi*-cytoxazone, see: (a)

prepared in a gram scale. Thus, with a reasonable amount of **3.90f** in hand, we initiated the synthesis with an iodination of the allene unit, generating diiodide **3.110** as a 1:1 *E* : *Z* mixture. This unstable intermediate (**3.110**) was used directly in an Ag-promoted cyclization (76% overall yield, >20:1 dr).[139] This reaction is noteworthy because the Boc group, commonly used as the protecting group of an amine, was used to construct the oxazolidinone core of the product. Then *t*-BuLi/MeOH sequence for replacement of the iodine with hydrogen and ozonolysis/reduction to convert the alkene into the primary alcohol afford *epi*-cytoxazone in 75% overall yield (0.52 g). Notably, only five steps were used from the homoallenylamide **3.90f** to prepare the ultimate product. The entire sequence completes in eight hours (including two chromatographic purifications) with 57% overall yield.

**Scheme 3.4.17. Total synthesis of *epi*-cytoxazone**

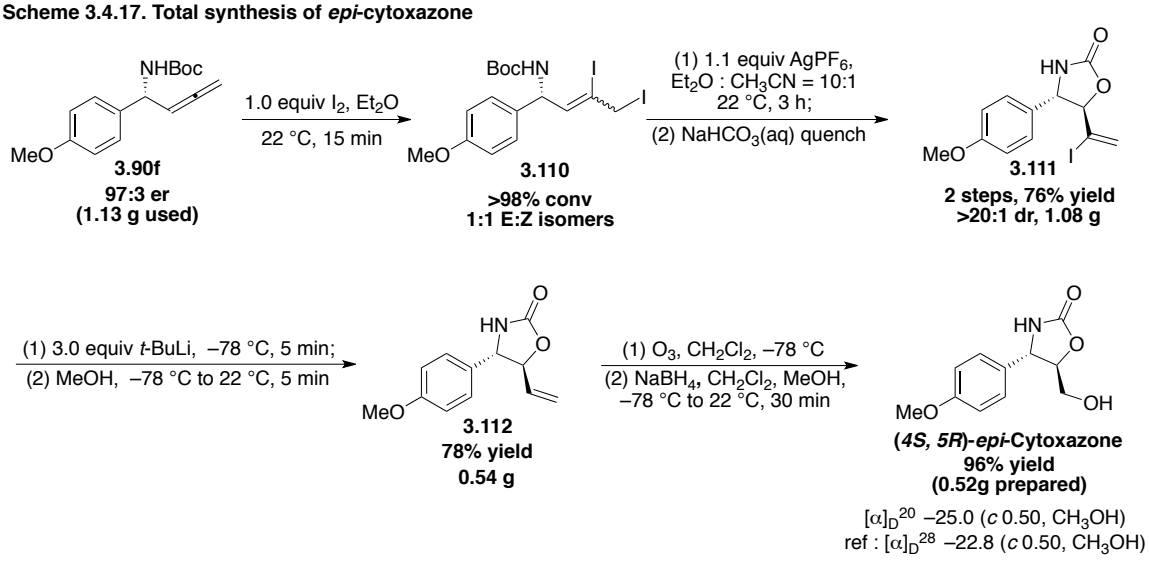


Matsunaga, S.; Yoshida, T.; Morimoto, H.; Kumagai, N.; Shibasaki, M. *J. Am. Chem. Soc.* **2004**, *126*, 8777–8785. (b) Sohtome, Y.; Hashimoto, Y.; Nagasawa, K. *Eur. J. Org. Chem.* **2006**, *13*, 2894–2897. (c) Kim, I. S.; Kim, J. D.; Ryn, C. B.; Zee, O. P.; Jung, Y. H. *Tetrahedron* **2006**, *62*, 9349–9358. (d) Mishra, R. K.; Coates, C. M.; Revell, K. D.; Turos, E. *Org. Lett.* **2007**, *9*, 575–578. (e) Reddy, R. S.; Chouthaiwale, P. V.; Suryavanshi, G.; Chavan, V. B.; Sudalai, A. *Chem. Commun.* **2010**, *46*, 5012–5014. (f) Qian, Y.; Xu, X.; Jiang, L.; Prajapati, D.; Hu, W. *J. Org. Chem.* **2010**, *75*, 7483–7486.

(139) Friesen, R. W.; Giroux, A. *Can. J. Chem.* **1994**, *72*, 1857.

### *3.4.5. Conclusions*

We have developed the first general catalytic enantioselective synthesis of homoallenylamides, through highly selective allenyl additions to Boc aldimines. The reactions are promoted by only 0.1–3 mol % an easily accessible aminophenol catalyst precursor in 14 hours at room temperature, affording valuable products in 66–91% yield, ≥90:10 allenyl:propargyl selectivity and 84:16 to >99:1 enantioselectivity. Aryl, heteroaryl- as well as more challenging alkyl-substituted aldimines are suitable substrates. The allenyl addition reaction can be performed in a gram scale, the product of which was utilized in a total synthesis of (*epi*)-cytoxazone within five steps. Computational as well as kinetic studies were achieved to understand the mechanism of this reaction. Future studies will focus on catalytic enantioselective allenyl additions to other types of electrophiles (including aldehydes), and development of new chiral boron-based catalysts.

## *3.5. Progesses in Catalytic Enantioselective Allenyl Additions to Aldehydes*

After success in developing allenyl additions to aldimines, we wondered if the aminophenol-derived boron based catalyst could promote allenyl additions to aldehydes. There are two major challenges for this type of transformations:

(1) Aldehydes are generally more reactive than imines, which means a more facile background process may occur. Can we develop a catalysis that is able to compete with the background reaction?

(2) Aldehydes cannot bind to our chiral boron catalyst through a two-point binding mode, like phosphinoyl- or Boc-aldimines. Then how can we control the enantioselectivities of allenyl additions to aldehydes?

**Scheme 3.5.1. Catalyst screening: aminophenol-derived catalysts**

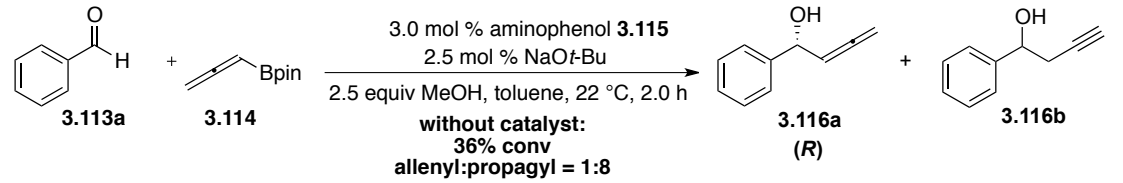


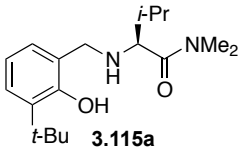

**3.115a**

>98% conv, >95% yield
allenyl:propagyl > 98:2
65:35 er

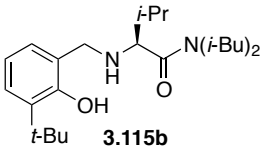

**3.115b**

58% conv, 50% yield
allenyl:propagyl = 1.5:1
58:42 er

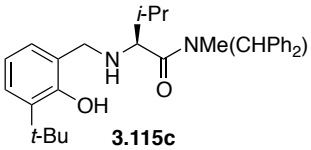

**3.115c**

63% conv, 57% yield
allenyl:propagyl = 5:1
64:36 er

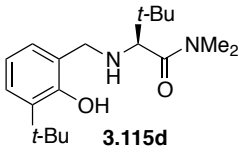

**3.115d**

86% conv, 79% yield
allenyl:propagyl = 11:1
65:35 er

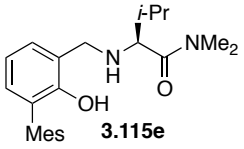

**3.115e**

68% conv, 58% yield
allenyl:propagyl = 7.5:1
40:60 er

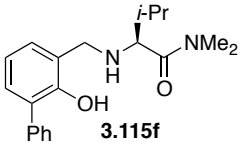

**3.115f**

46% conv, 41% yield
allenyl:propagyl = 5:1
45:55 er

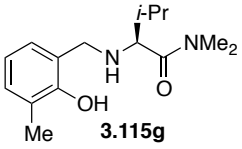

**3.115g**

51% conv, 49% yield
allenyl:propagyl = 4.5:1
43:57 er

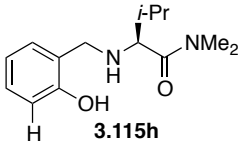

**3.115h**

48% conv, 41% yield
allenyl:propagyl = 4:1
53:47 er

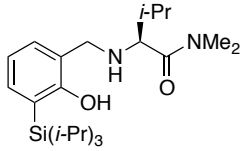

**3.115i**

>98% conv, 83% yield
allenyl:propagyl = 15:1
79:21 er

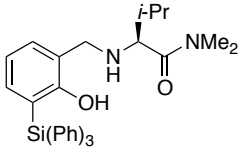

**3.115j**

>98% conv
allenyl:propagyl = 15:1
76:24 er

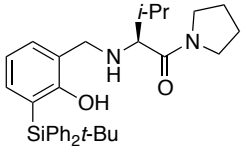

**3.115k**

>98% conv, 83% yield
allenyl:propagyl = 16:1
76:24 er

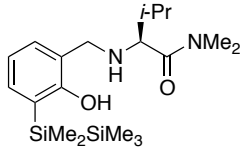

**3.115l**

96% conv, 85% yield
allenyl:propagyl = 12:1
65:35 er

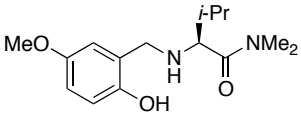

**3.115m**

95% conv
allenyl:propagyl = 9.5:1
52:48 er

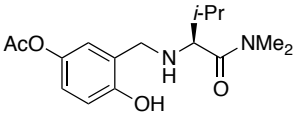

**3.115n**

40% conv
allenyl:propagyl = 1.2:1
51:49 er

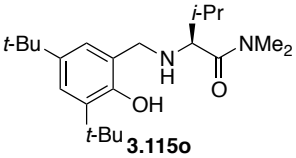

**3.115o**

65% conv
allenyl:propagyl = 3.6:1
56:44 er

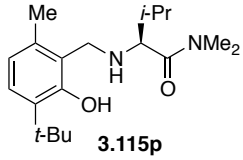

**3.115p**

91% conv, 86% yield
allenyl:propagyl = 5:1
61:39 er

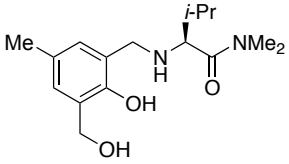

**3.115q**

>98% conv
allenyl:propagyl = 12:1
40:60 er

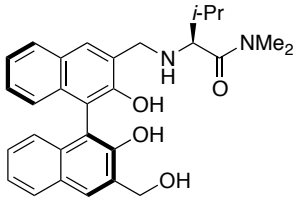

**3.115r**

17% conv
allenyl:propagyl = 1:3
er nd

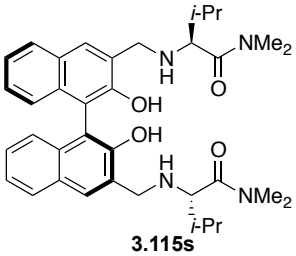

**3.115s**

25% conv
allenyl:propagyl = 1:1
39:61 er

Benzaldehyde was first chosen as the model substrate to study the catalytic

enantioselective allenyl additions. As illustrated in Scheme 3.5.1, aminophenol **3.115a** was tested as the initial catalyst precursor for enantioselective allenyl additions. The reaction completes in 2.0 hours and the desired homoallenyl alcohol is isolated in a quantitative yield (>95% yield, allenyl:propargyl >98:2). However, the enantioselectivity is poor (65:35 er). The poor enantioselectivity is not due to the competitive background reaction since the reaction proceeds to 36% conversion, favoring homopropargyl products (allenyl:propargyl = 1:8) without aminophenol **3.115a**. Instead, the low er probably comes from the lack of two point binding between benzaldehyde and the active catalyst, resulting a series of binding modes that are similar in energy.

A systematic screening of aminophenols was carried out to study the substituent effect of the catalyst. Changing the substituents of the amide nitrogen from two methyl groups to sterically more hindered groups (**3.115b** and **3.115c**) does not help to improve the enantioselectivity (58:42 and 64:36 er, respectively). The aminophenol derived from *t*-Leucine (**3.115d**) promotes the reaction efficiently (86% conv) but with the same enantioselectivity (65:35 er) compared to **3.115a**. To test the influence of the *ortho*-substituent on the phenyl ring, aminophenols **3.115e** to **3.115h** were synthesized and examined in the allenyl addition of benzaldehyde. Unfortunately, all the reactions are neither as efficient (~50% conv), nor as selective (allenyl:propargyl < 8:1, homoallenyl alcohols: < 60:40 er), probably because the active chiral boron species do not form effectively for those amino phenols. Interestingly, when the *ortho*-substituent is a silyl group (**3.115i** to **3.115l**), the enantioselectivity increases (65:35–79:21 er), and the reactions are still very efficient (96% to >98% conv, 83–85% yield) and regioselective (allenyl:propargyl ≥ 12:1). It is plausible that since a C–Si bond (~1.8 Å) is significantly

longer than a C–C bond (~1.54 Å), the silyl groups in **3.115i–3.115l** are much more hindered than the *t*-butyl group in **3.115a**, which influences the substrate binding modes to the catalyst. An exploration of the *para*-substituent effect on the phenyl ring indicates that the electron donating *p*-MeO group enhances the reaction efficiency and regioselectivity (95% conv, allenyl:propargyl = 9.5:1 for **3.115m**, compare 48% conv, allenyl:propargyl = 4:1 for **3.115h**), while the electron withdrawing *p*-OAc group has the opposite effect (40% conv, allenyl:propargyl = 1.2:1 for **3.115n**). Nevertheless, the enantioselectivity is poor in both cases (~50:50 er). The more hindered *p*-*t*-butyl substituent slows the catalytic process (65% conv for **3.115o** compared to >98% conv for **3.115a**). The *meta*-methyl group in **3.115p** does not affect the reaction significantly. Aminophenol **3.115q**, which contains a hydroxymethyl substituent promotes the allenylation effectively (>98% conv) but with a reverse enantioselectivity (40:60 er favored the *S* enantiomer). The binol derived aminophenols **3.115r** and **3.115s** do not catalyze the reaction efficiently.

**Scheme 3.5.2. Proposed two modes of allenyl additions to aldehydes**

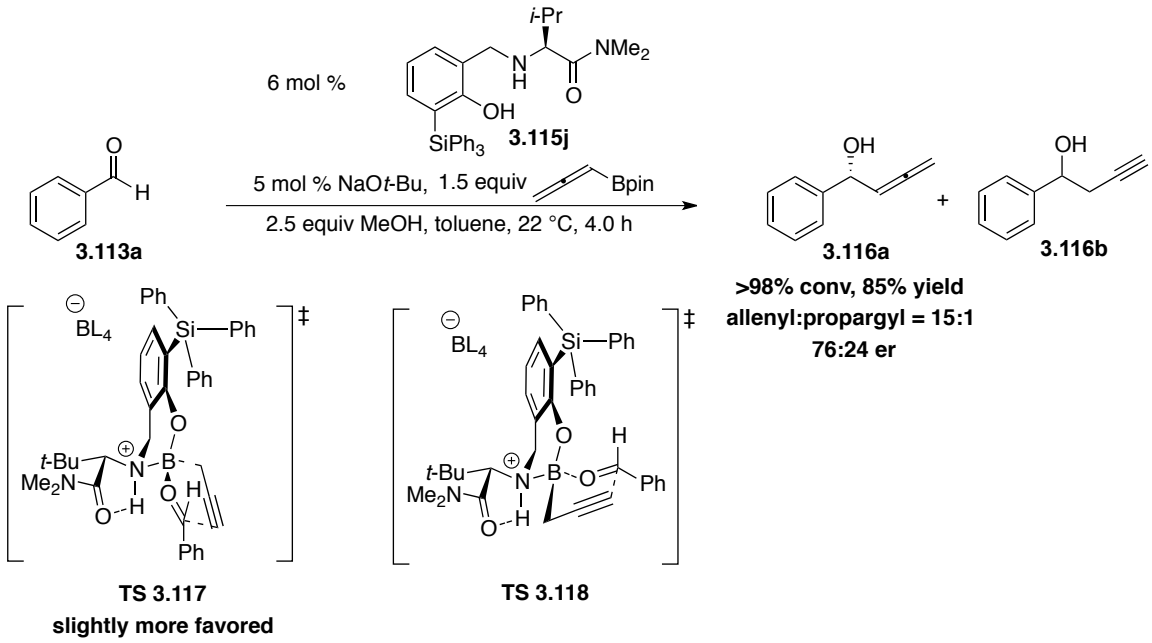


To understand why the enantioselectivity for allenyl addition to benzaldehydes are so low, computational studies on the stereochemical models of reactions promoted by **3.115j** have been done with Farid and Fredrik. As shown in Scheme 3.5.2, there are two modes of allenyl additions that are competitive. **TS 3.117**, which affords the major enantiomer of the products, is slightly lower in energy than **TS 3.118**. It should be noted that **TS 3.117** is not operational in previous explored reactions with other electrophiles (phosphinoyl-imines, Boc-imines, ketones etc). This is because the substituents of those electrophiles (compared to the hydrogen of aldehyde) would have severe steric interactions with the $SiPh_3$ group of the aminophenol, if they replace the aldehyde in **TS 3.117**.

**Scheme 3.5.3. Allenyl additions to aldehydes promoted by benzylic substituted aminophenols**[a]

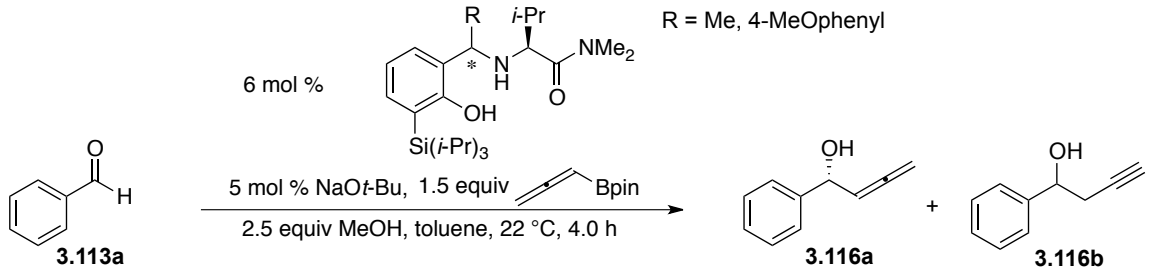


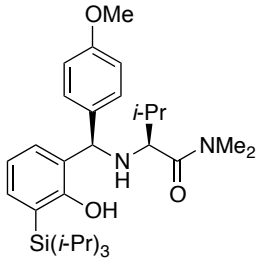

**3.115t**

**71% conv, 49% yield**
**allenyl:propargyl = 7:1**
**allenyl: 62:38 er**
**propargyl: 56:44 er**

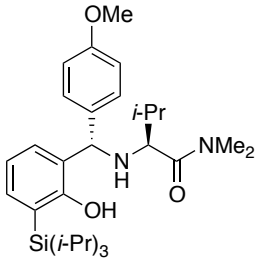

**3.115u**

**22% conv**
**allenyl:propargyl = 1:1**
**allenyl: 54:46 er**
**propargyl: 50:50 er**

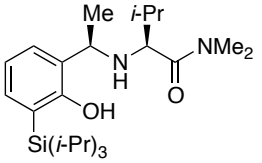

**3.115v**

**>98% conv, 96% yield**
**allenyl:propargyl = 10:1**
**allenyl: 83:17 er**

[a] Under $N_2$ atm.

We then hypothesized that an installation of a substituent on the benzylic position of the aminophenol might differentiate the two modes of additions by steric effects. Thus, three different aminophenols **3.115t, 3.115u** and **3.115v** were synthesized and tested in the catalytic enantioselective allenyl additions to benzaldehyde (Scheme 3.5.3). Although the reaction with **3.115t** (*syn p*-MeO-phenyl substituted aminophenol) is slightly less efficient (71% conv, 49% yield) and regioselective (allenyl:propargyl = 7:1), the enantioselectivity drops significantly (**3.116a**: 62:38 er vs 79:21 er with **3.115i**). It is likely that the sterically demanding *p*-MeO-phenyl group in **3.115t** will hamper both modes of additions by steric interactions. The diastereomer **3.115u** almost shuts down the catalytic process: only 22% conversion is achieved after 4.0 h, and the products are 1:1 mixture of homoallenyl and homopropargyl alcohols. The facts that the reaction are non-

enantioselective, regioselective and low in efficiency imply the active catalytic species may not form. Interestingly, the *syn* methyl substituted aminophenol (**3.115v**) promotes the allenyl additions with >98% conversion (96% yield), high regioselectivity (10:1) and enhanced enantioselectivity (83:17 er vs 79:21 er with **3.115i**). This promising result shows how sensitive the reaction is to the steric hinderance of the benzylic substituents of aminophenols.

**Scheme 3.5.4. Synthesis of 3.115v**

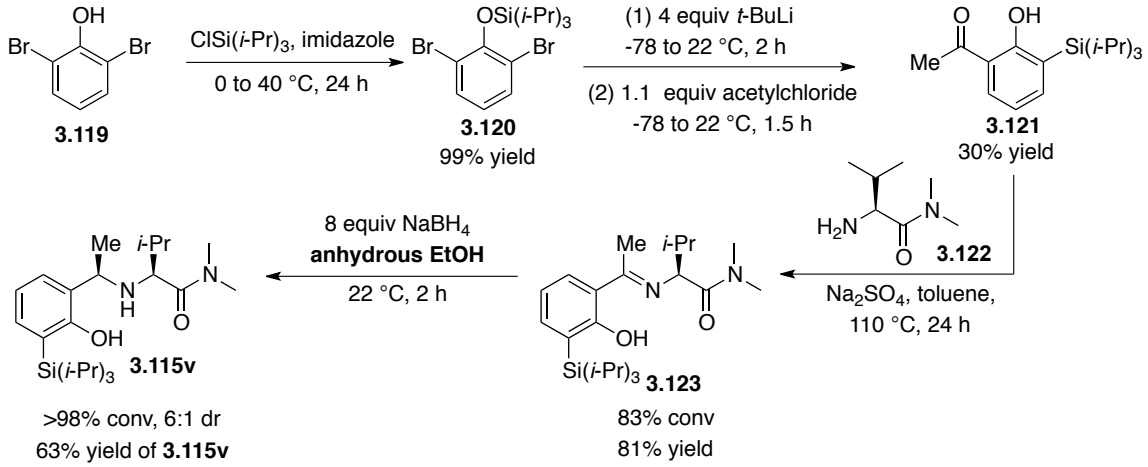


The synthesis of **3.115v** is shown in Scheme 3.5.4. First, 2,6-dibromophenol **3.119** is protected with TIPSCl to afford **3.120** in quantitative yield. Double lithium-halogen exchanges accompanied with silyl group migration and subsequent trap of acetyl chloride give **3.121** in 30% yield. This step is problematic since a significant amount of the O-acylation product was observed (~40%). The following Schiff base formation is efficient (81% yield of **3.123**), while amide **3.122** needs to be handled with caution due to its volatility. The $NaBH_4$ reduction of **3.123** affords **3.115v** as the major product (6:1 dr) with 63% yield.

**Table 3.5.1. Alcohol and temperature effects of catalytic enantioselective allenyl additions to aldehydes[a]**

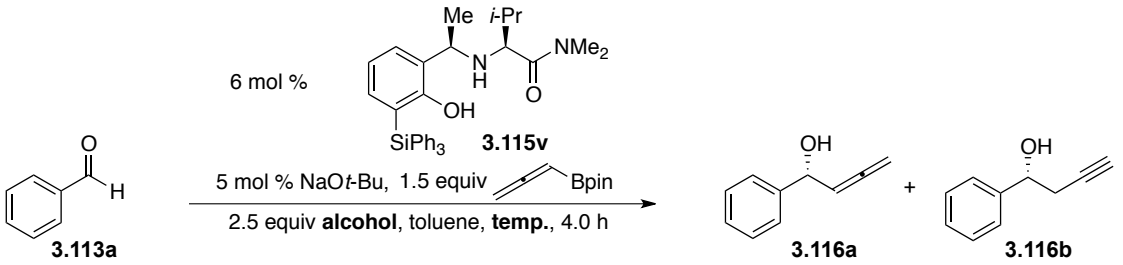


| entry | alcohol | temperature (°C) | conv of **3.113a** (%) | er of **3.116a** | conv of **3.116b** (%) | er of **3.116b** |
|---|---|---|---|---|---|---|
| 1 | MeOH | 22 | 90 | 83:17 | 10 | - |
| 2 | EtOH | 22 (14 h) | 64 | 81:19 | 32 | 61:39 |
| 3 | *i*PrOH | 22 (14 h) | ~5 | 74:26 | 29 | 51:49 |
| 4 | MeOH | 50 | 91 | 78:22 | 9 | 69:31 |
| 5 | MeOH | –15 (14 h) | 13 | 83:17 | 6 | 55:45 |

[a] Under $N_2$ atm.

The effect of alcohol additive in the allenyl additions catalyzed by **3.115v** was investigated (Table 3.5.1). Surprisingly, from MeOH, EtOH to *i*-PrOH, the conversions to the desired homoallenyl product **3.116a** is diminished dramatically (90%, 64%, to ~5%, respectively). The enantioselectivity of **3.116a** also drops as a sterically more hindered alcohol is used. These results suggest that a larger alcohol will inhibit the formation of the active catalytic species, probably in the trans-borylation step, as the benzylic methyl group of **3.115v** may prohibit the coordination of allenyl B(pin) to the larger chiral boryl alkoxide. Since the catalytic process is hampered, the background reaction may be competitive (more propargyl addition product **3.116b**). Next, we studied the temperature effect of this reaction. As shown in entry 4, increasing the reaction temperature to 50 ºC will probably bring more background reaction (9% of **3.116b**), and the enantioselectivity of **3.115a** slightly diminishes. On the other hand, lowering the

reaction temperature will greatly inhibit the catalytic reaction (~19% conv after 14 h, –15 ºC).

**Scheme 3.5.5. The effect of $Zn(OMe)_2$**

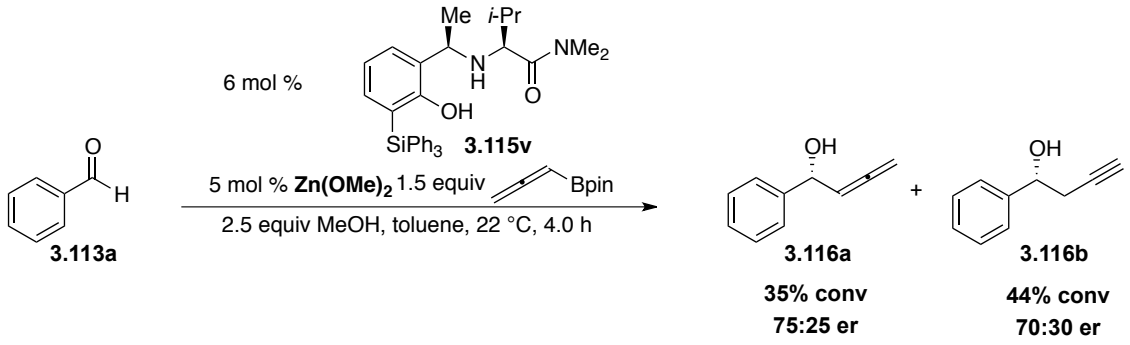


The use of $Zn(OMe)_2$ instead of NaO*t*-Bu alters the regioselectivity (Scheme 3.5.5): the homopropargyl alcohol **3.116b** is slightly more favored than **3.116a**. Interestingly, both products are moderate enantioselective (70:30 to 75:25 er), implying the passway forming **3.116b** also involves the catalyst. It is likely that the $Zn(OMe)_2$ facilitates the boryl shift from the chiral propargyl boron to the chiral allenyl boron, the latter of which affords homopropargyl alcohol **3.116b** with benzaldehyde.

## *3.6. Cu-Catalyzed Chemoselective Preparation of 2-(Pinacolato)boron-Substituted Allylcopper Complexes and their in Situ Site-, Diastereo-, and Enantioselective Additions to Aldimines*

In addition to catalytic enantioselective allenyl additions to aldimines, we would also like to develop a catalytic method for enantioselective allyl additions with 2-boryl substituted allyl reagent. In 2013, our laboratories discovered a Cu-catalyzed protocol for site-selective generation of 2-B(pin) substituted allyl coppers and utilized them in allyl

additions to aldehydes and ketones.[140] Thus, we wondered if it could be applied into reactions with aldimines. The hypothesis is illustrated in Scheme 3.6.1.

**Scheme 3.6.1. Hypothesis of selective allyl additions to aldimines with boryl substitued allyl copper**

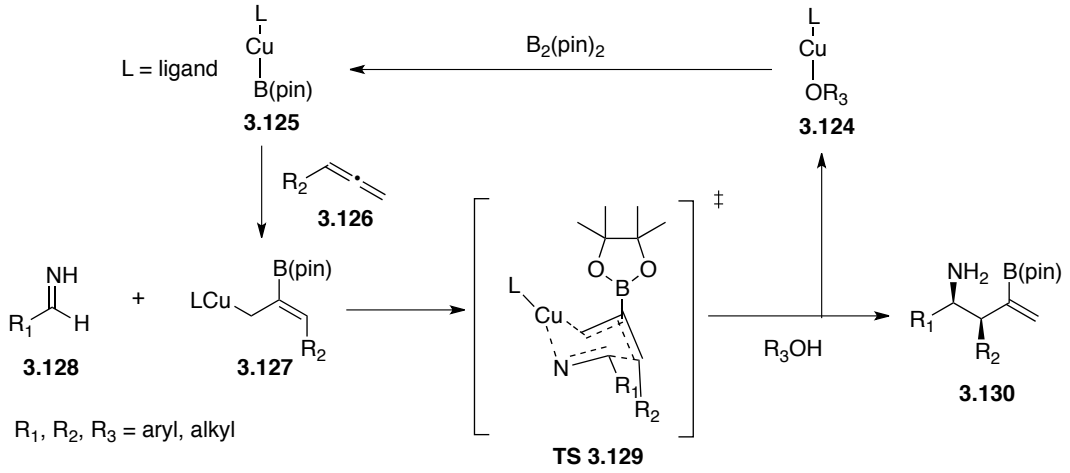


The catalysis begins with the reaction of L–Cu-$OR_3$ **3.124** with $B_2(pin)_2$, generating L–Cu-B(pin) **3.125**. This nucleophilic B(pin) species is able to react wih an allene **3.126** affording 2-B(pin) substituted allyl copper **3.127**. Upon coordination with one molecule of aldimine **3.128**, allyl copper **3.127** promotes the allyl addition through transition state **3.129**. After protonation, the desired product **3.130** is generated and L–Cu-$OR_3$ **3.124** is released to re-enter the catalytic cycle.

Our studies revealed the principle of the aforementioned catalysis was correct, that is, the desired vinylB(pin) **3.130** product could be generated efficiently. More specifically, hydrobenzamide **3.131** (trimer of phenylmethanimine) was found as a suitable substrate in this transformation (Scheme 3.6.2). Since two equivalents of **3.131** can provide three equivalents of active imine **3.133**, only 0.66 equivalent of **3.131** was needed for complete transformation in the allyl addition. Unfortunately, the

(140) Meng, F.; Jang, H.; Jung, B.; Hoveyda, A. H. *Angew. Chem. Int. Ed.* **2013**, *52*, 5046–5051.

corresponding vinylB(pin) product cannot be isolated due to its instability, and thus has to be oxidized into ketone **3.132**.

**Scheme 3.6.2. Ligand screening for Cu-catalyzed chemoselective preparation of 2-boryl substituted allyl copper and its enantioselective additions to an aldmine**

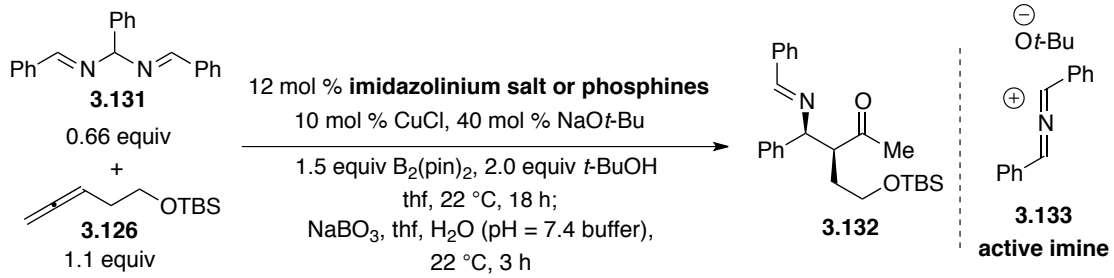


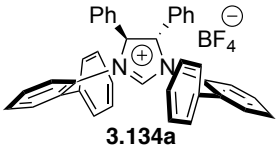


**3.134a**
98% conv, 75:25 dr
61% yield (78:22 dr)
65:35 er

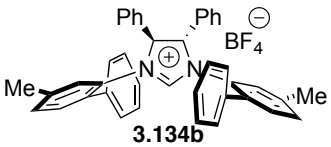


**3.134b**
>98% conv, 75:25 dr
81% yield (77:23 dr)
67:33 er

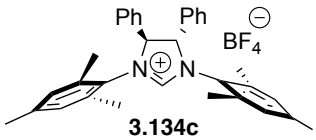


**3.134c**
61% conv, 84:16 dr
46% yield (89:11 dr)
67:33 er

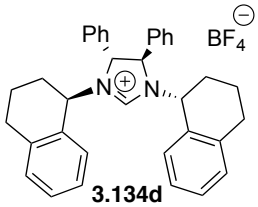


**3.134d**
21% conv, 46:54 dr
15% yield (50:50 dr)
major: 50:50 er
minor: 63:37 er

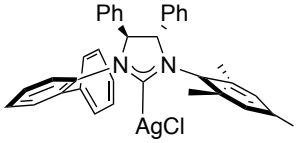


**3.134e**
96% conv, 80:20 dr
81% yield (83:17 dr)
54:46 er

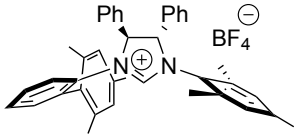


**3.134f**
63% conv, 81:19 dr
56% yield (83:17 dr)
57:43 er

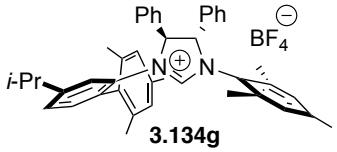


**3.134g**
18% conv, 63:37 dr
62:38 er

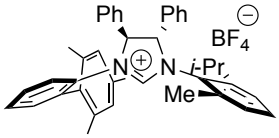


**3.134h**
86% conv, 56:44 dr
66% yield (65:35 dr)
major 39:61 er
minor 53:47 er

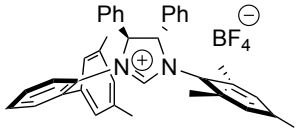


**3.134i**
92% conv, 82:18 dr
85% yield (85:15 dr)
68:32 er

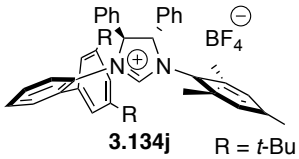

**3.134j** R = *t*-Bu

87% conv, 85:15 dr
61% yield (83:17 dr)
55:45 er

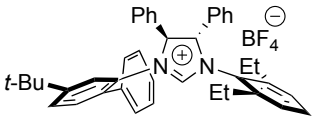

**3.134k**

94% conv, 80:20 dr
76% yield (80:20 dr)
69:31 er

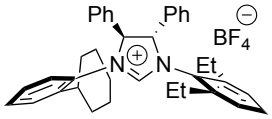

**3.134l**

72% conv, 69:31 dr
tbd% yield (71:29 dr)
major: 35:65 er
minor: 53:47 er

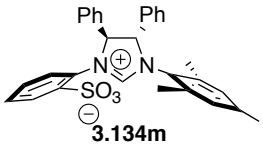

**3.134m**

88% conv, 70:30 dr
59% yield (78:22 dr)
63:37 er

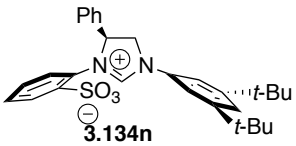

**3.134n**

91% conv, 53:47 dr
66% yield (64:36 dr)
major: 48:52 er
minor: 53:47 er

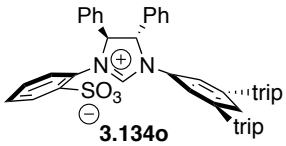

**3.134o**

18% conv, 56:44 dr
(63:37 dr)
major: 57:43 er
minor: 48:52 er

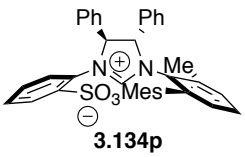

**3.134p**

75% conv, 58:42 dr
49% yield (71:29 dr)
major: 54:46 er
minor: 62:38 er

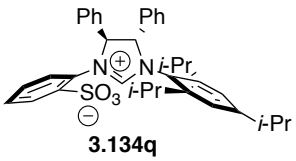

**3.134q**

96% conv, 58:42 dr
44% yield (61:39 dr)
major: 50:50 er
minor: 53:47 er

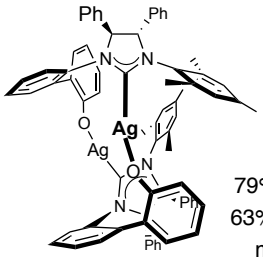

**3.134r**

79% conv, 76:24 dr
63% yield (79:21 dr)
major: 60:40 er
minor: 63:37 er

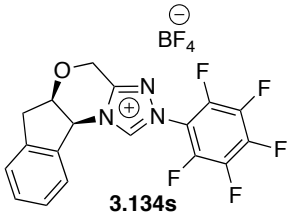

**3.134s**

>98% conv, 64:36 dr
71% yield (75:25 dr)
major: 60:40 er
minor: 46:54 er

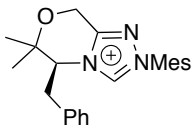

**3.134t**

93% conv, 48:52 dr
46% yield (53:47 dr)
major: 51:49 er
minor: 49:51 er

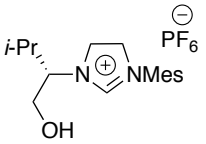

**3.134u**

83% conv, 74:26 dr
55% yield (80:20 dr)
50:50 er

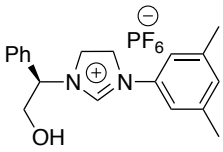

**3.134v**

74% conv, 65:35 dr
60% yield (71:29 dr)
51:49 er

A systematic NHC screening (ones with a biphenyl backbone or not), however, did not give a promising result: moderate diastereoselectivity and low enantioselectivity were observed, despite of good isolation yield and exclusive site-selectivity. Among them, NHC derived from **3.134i** is the best one in terms of reaction efficiency (85% yield) and diastereoselectivity (85:15 dr). Unfortunately, the enantiomeric ratio of **3.132**

is low (68:32 er).

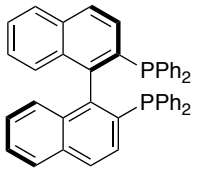


**3.135a**
94% conv, 45:55 dr
61% yield (57:43 dr)
major: 35:65 er
minor: 53:47 er

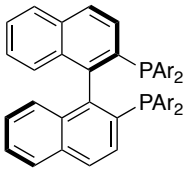


Ar = 3,5-dimethylphenyl
**3.135b**
41% conv, 45:55 dr
20% yield (57:43 dr)
major: 22:78 er
minor: 48:52 er

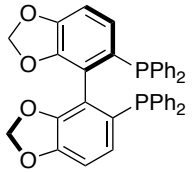


**3.135c**
83% conv, 39:61 dr
37% yield (45:55 dr)
major: 30:70 er
minor: 52:48 er

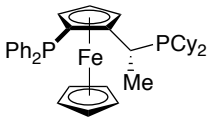


**3.135d**
40% conv, 50:50 dr
33% yield (64:36 dr)
major: 63:37 er
minor: 54:46 er

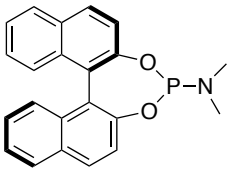


**3.135e**
17% conv, 48:52 dr
(50:50 dr)
43:57 er

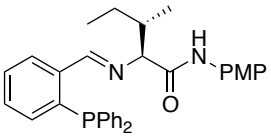


**3.135f**
71% conv, 30:70 dr
37% yield (45:55 dr)
major: 49:51 er
minor: 50:50 er

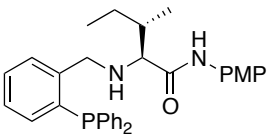


**3.135g**
84% conv, 28:72 dr
66% yield (38:62 dr)
major: 55:45 er
minor: 42:58 er

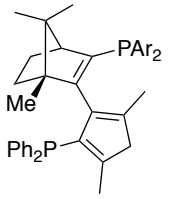


Ar = 3,5-dimethylphenyl
**3.135h**
97% conv, 29:71 dr
56% yield (41:59 dr)
major: 40:60 er
minor: 52:48 er

A variety of phosphines were also investigated in this reaction. However, none of reactions promoted by these phosphine–Cu complexes were selective (low diastereoselectivity and enantioselectivity). It is possible that this transformation does not proceed throught the proposed six-membered transition state **3.129**. Because the active imine **3.133** cannot bind to the Cu complex (lack of a lone pair of electrons in the nitrogen), the allyl addition likely undergo through an open transition state. If this is true, it will be difficult to control the diastereoselectivity as well as enantioselectivity since imine **3.133** is $C_2$-symmetric.

## *3.7. Acknowledgment*

I thank Prof. Amir H. Hoveyda for providing me this great project to study. I am also grateful to Dr. Dan L. Silverio, Dr. Sebastian Torker and Dr. Jan Haeffner for their

cooperations in this project. Farid W. van der Mei, Kyung A Lee and Nick W. Mszar deserve my thanks for helpful discussions and computational studies. I also appreciate the enlightening discussions with all the other Hoveyda group members.

This work was supported financially by the NIH (GM-57212). We thank Boston College and the chemistry department for providing great assistance and facilities.

## *3.8. Experimental Section*

### *3.8.1. Preparations and Characterizations of New Compounds*

**General.** Infrared (IR) spectra were recorded on a Bruker FT-IR Alpha (ATR mode) spectrophotometer, $\nu_{max}$ in $cm^{-1}$. Bands are characterized as broad (br), strong (s), medium (m), and weak (w). $^{1}H$ NMR spectra were recorded on a Varian Unity INOVA 400 (400 MHz) spectrometer. Chemical shifts are reported in ppm from tetramethylsilane with the solvent resonance as the internal standard ($CDCl_3$: δ 7.26 ppm). Data are reported as follows: chemical shift, integration, multiplicity (s = singlet, d = doublet, t = triplet, q = quartet, m = multiplet, br s = broad singlet), and coupling constants (Hz). $^{13}C$ NMR spectra were recorded on a Varian Unity INOVA 400 (100 MHz) spectrometer with complete proton decoupling. Chemical shifts are reported in ppm from tetramethylsilane with the solvent resonance as the internal standard ($CDCl_3$: δ 77.16 ppm). High-resolution mass spectrometry was performed on a JEOL AccuTOF-DART (positive mode) at the Mass Spectrometry Facility, Boston College. Enantiomeric ratios were determined by GC analysis (Alltech Associated Chiraldex GTA column (30 m x 0.25 mm), Chiraldex B-DM (30 m x 0.25 mm) or Chiraldex B-DA (30 m x 0.25 mm)) and HPLC analysis (high-performance liquid chromatography) with a Shimadzu chromatograph (Chiral Technologies Chiralcel OJ-H (4.6 x 250 mm), Chiral

Technologies Chiralcel OD-H (4.6 x 250 mm), Chiral Technologies Chiralpak AS-H (4.6 x 250 mm) or Chiral Technologies Chiralpak AZ-H (4.6 x 250 mm)) in comparison with authentic racemic materials. Specific rotations were measured on a Rudolph Research Analytical Autopol IV Polarimeter. Kinetic study was performed on a React-IR iC 10 instrument equipped with a 6.3 mm AgX DiComp Fiber probe (2000–650 $cm^{-1}$). X-ray structures for compound **3.90b** and dehalogenation product **3.112** were obtained, as described in the cif files, with a Microfocus sealed Cu tube from Incote. It is well established that the aforementioned detector allows for the determination of absolute configuration of molecules that do not have a heavy atom. The absolute configuration was verified by the flack parameter of 0.0 with a standard deviation of 2 and corroborated by Bijvoet parameter test. Melting points were determined using a Thomas Hoover Uni-melt capillary melting point apparatus.

Unless otherwise noted, reactions were carried out with distilled and degassed solvents under an atmosphere of dry $N_2$ in oven- (135 ºC) or flame-dried glassware with standard dry box or vacuum-line techniques. Solvents were purified under a positive pressure of dry Ar by a modified Innovative Technologies purification system: toluene was purified through a copper oxide and alumina column; $CH_2Cl_2$ and $Et_2O$ were purged with Ar and purified by passage through two alumina columns. Methanol, ethanol and *i*-propanol were distilled over sodium. All work-up and purification procedures were carried out with reagent grade solvents (purchased from Fisher Scientific) under air. **Aminophenol (3.58):** prepared according to previously reported procedures.[130] **4,4,5,5-Tetramethyl-2-(propa-1,2-dien-1-yl)-1,3,2-dioxaborolane (allenylB(pin)):** purchased from Frontier Scientific Inc. and distilled over $CaH_2$ prior to use. **Boc-imines (unless**

**otherwise noticed):** prepared according to previously reported procedures.[141] The aldehydes used in the synthesis were purchased from Aldrich Chemical Co. and used as received. **Sodium *tert*-butoxide:** purchased from Strem Chemicals Inc. and used as received. **Acetonitrile:** purchased from Acros Organics and used as received. ***tert*-Butyl carbamate:** purchased from Aldrich Chemical Co. and used as received. **Sodium benzenesulfinate:** purchased from Aldrich Chemical Co. and used as received. **Formic acid:** purchased from Fisher Scientific and used as received. **Cesium carbonate:** purchased from Aldrich Chemical Co. and used as received. **Iodine:** purchased from Aldrich Chemical Co. and used as received. **Silver hexafluorophosphate:** purchased from Strem Chemicals Inc. and used as received. ***tert*-Butyllithium solution (1.7 M in pentane):** purchased from Aldrich Chemical Co. and used as received. **Sodium borohydride:** purchased from Aldrich Chemical Co. and used as received. **Oxalic acid:** purchased from Aldrich Chemical Co. and used as received.

**Representative Experimental Procedure for Enantioselective Allene Additions to Boc–imines (Smaller Scale):** Under $N_2$ atmosphere, 20 μL aminoalcohol (**3.58**) solution (0.010 M in toluene, $2.0 \times 10^{-4}$ mmol, 0.10 mol %) was transferred into an oven-dried vial, followed by addition of 0.80 mL NaO*t*-Bu solution (0.013 M in toluene, 0.010 mmol, 5.0 mol %). The resulting solution was diluted to 2.0 mL with toluene. To the same vial allenylB(pin) (50 mg, 0.30 mmol, 1.5 equiv) and *i*-propanol (35 μL, 0.46 mmol, 2.3

(141) (a) Uraguchi, D.; Sorimachi, K.; Terada, M. *J. Am. Chem. Soc.* **2004**, *126*, 11804–11805. (b) Song, J.; Wang, Y.; Deng, L. *J. Am. Chem. Soc.* **2006**, *128*, 6048–6049. (c) Robak, M. T.; Trincado, M.; Ellman, J. A. *J. Am. Chem. Soc.* **2007**, *129*, 15110–15111. (d) Uraguchi, D.; Koshimoto, K.; Ooi, T. *J. Am. Chem. Soc.* **2008**, *130*, 10878–10879. (e) Rampalakos, C.; Wulff, W. D. *Adv. Synth. Catal.* **2008**, *350*, 1785–1790. (f) Chen, Z.; Yakura, K.; Matsunaga, S.; Shibasaki, M. *Org. Lett.* **2008**, *10*, 3239–3242. (g) Huang, L.; Wulff, W. D. *J. Am. Chem. Soc.* **2011**, *133*, 8892–8895. (h) Bandar, J. S.; Lambert, T. H. *J. Am. Chem. Soc.* **2013**, *135*, 11799–11802.

equiv) were introduced subsequently, followed by addition of *tert*-butyl benzylidenecarbamate (**3.96a**) (41 mg, 0.2 mmol, 1.0 equiv). The vial was sealed with a cap and the solution was allowed to stir at 22 °C for 14 h. 1 mL Oxalic acid aqueous solution (1.0 M) was then added to hydrolyze the corresponding hemiaminal formed as a minor byproduct (~7%). The resulting mixture was allowed to stir at 22 ºC for 5 min before neutralized by addition of 3 mL saturated $NaHCO_3$ aqueous solution. The aqueous layer was washed with $Et_2O$ (3x5 mL). The combined organic layers were dried over anhydrous $MgSO_4$. After filtration, the volatiles were removed under vacuum and the resulting colorless oil was purified by silica gel chromatography (hexanes:$Et_2O$ = 10:1) to afford (*R*)-*tert*-butyl (1-phenylbuta-2,3-dien-1-yl)carbamate (**3.90a**) (44 mg, 0.18 mmol, 90% yield) as a white solid.

**Representative Experimental Procedure for Enantioselective Allene Additions to Boc–imines (Large Scale):** Under $N_2$ atmosphere, aminoalcohol (**3.58**) (12 mg, 0.038 mmol, 0.50 mol %), NaO*t*-Bu (37 mg, 0.38 mmol, 5.0 mol %) and *tert*-butyl 4-methoxybenzylidenecarbamate (**3.96f**) (1.8 g, 7.7 mmol, 1.0 equiv) were introduced into a flame-dried flask (100 mL). The mixture was dissolved in 77 mL toluene. AllenylB(pin) (2.1 mL, 11 mmol, 1.5 equiv) and *i*-propanol (1.4 mL, 18 mmol, 2.3 equiv) were transferred into the same flask subsequently. The resulting solution was allowed to stir at 22 ºC for 14 h. Since there was <5% hemiaminal formation, oxalic acid was not used. The volatiles were removed under vacuum and the resulting colorless oil was purified by silica gel chromatography (hexanes:$Et_2O$ = 3:1) to afford **(***R***)**-*tert*-butyl (1-(4-methoxyphenyl)buta-2,3-dien-1-yl)carbamate (**3.90f**) (1.9 g, 6.9 mmol, 90% yield) as a white solid.

**(*R*)-*tert*-Butyl (1-phenylbuta-2,3-dien-1-yl)carbamate (3.90a):** m.p. = 53–54 ºC. IR (neat): 3334 (br), 2977 (m), 2926 (m), 2853 (w), 1958 (m), 1699 (s), 1494 (s), 1455 (m), 1391 (m), 1366 (s), 1248 (s), 1166 (s), 1048 (m), 1025 (m), 855 (m), 699 (s) $cm^{-1}$; $^1H$ NMR (400 MHz, $CDCl_3$): δ 7.36–7.32 (4H, m), 7.29–7.25 (1H, m), 5.39 (1H, dd, *J* = 12.0, 6.0 Hz), 5.29 (1H, br s), 5.01–4.92 (3H, m), 1.43 (9H, s); $^{13}C$ NMR (100 MHz, $CDCl_3$): δ 207.0, 155.1, 141.7, 128.7, 127.7, 127.0, 93.4, 79.8, 79.1, 52.8, 28.5; HRMS (ESI+): Calcd for $C_{15}H_{20}N_1O_2$ $[M+H]^+$: 246.14940, Found: 246.14981. Specific Rotation: $[\alpha]_D^{20}$ +92.0 (*c* 1.09, $CHCl_3$) for an enantiomerically enriched sample of 95:5 er.

Enantiomeric purity was determined by GC analysis in comparison with authentic racemic material (95:5 er shown, Chiraldex GTA column, 100 ºC, 15 psi).

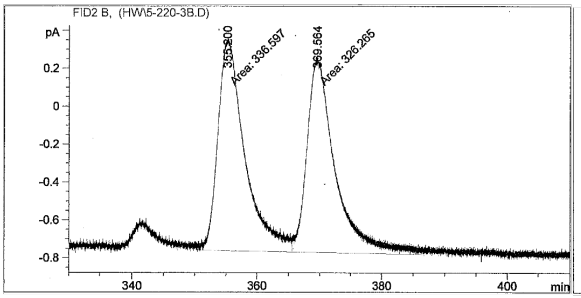


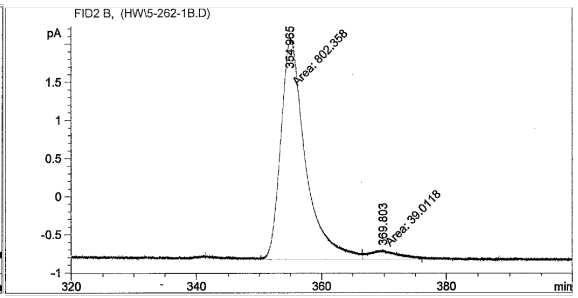


| Peak # | RetTime [min] | Type | Width [min] | Area [pA*s] | Height [pA] | Area % |
|---|---|---|---|---|---|---|
| 1 | 355.200 | MF | 4.9706 | 336.59708 | 1.12862 | 50.77937 |
| 2 | 369.564 | FM | 5.2258 | 326.26483 | 1.04055 | 49.22063 |

| Peak # | RetTime [min] | Type | Width [min] | Area [pA*s] | Height [pA] | Area % |
|---|---|---|---|---|---|---|
| 1 | 354.965 | MF | 4.5933 | 802.35846 | 2.91132 | 95.36330 |
| 2 | 369.803 | FM | 4.6692 | 39.01181 | 1.39252e-1 | 4.63670 |

| Peak # | Time (min) | Area (%) | Peak # | Time (min) | Area (%) |
|---|---|---|---|---|---|
| 1 | 355.200 | 50.77937 | 1 | 354.965 | 95.36330 |
| 2 | 369.564 | 49.22063 | 2 | 369.803 | 4.63670 |

**(*R*)-*tert*-Butyl (1-(2-chlorophenyl)buta-2,3-dien-1-yl)carbamate (3.90b):** X-ray crystal structure was obtained. m.p. = 68–69 ºC. IR (neat): 3431 (br), 2977 (m), 2928 (m), 2954 (w), 1958 (m), 1701 (s), 1492 (s), 1475 (s), 1445 (m), 1391 (m), 1366 (s), 1281 (m), 1249 (m), 1164 (s), 1051 (m), 1038 (m), 855 (m), 755 (s) $cm^{-1}$; $^1H$ NMR (400 MHz, $CDCl_3$): δ 7.36–7.33 (2H, m), 7.27–7.18 (2H, m), 5.65 (1H, br s), 5.43 (1H, br s), 5.15 (1H, br s), 4.95–4.90 (2H, m), 1.43 (9H, s); $^{13}C$ NMR (100 MHz, $CDCl_3$): δ 207.1, 154.9, 130.0,

129.1, 128.8, 127.9, 127.2, 127.1, 92.3, 80.0, 79.6, 50.6, 28.5; HRMS (ESI+): Calcd for $C_{15}H_{18}Cl_1N_1O_2Na$ $[M+Na]^+$: 302.09183, Found: 302.09110. Specific Rotation: $[\alpha]_D^{20}$ +44.4 (*c* 0.90, $CHCl_3$) for an enantiomerically enriched sample of 98:2 er.

Enantiomeric purity was determined by GC analysis in comparison with authentic racemic material (98:2 er shown, Chiraldex GTA column, 120 ºC, 15 psi).

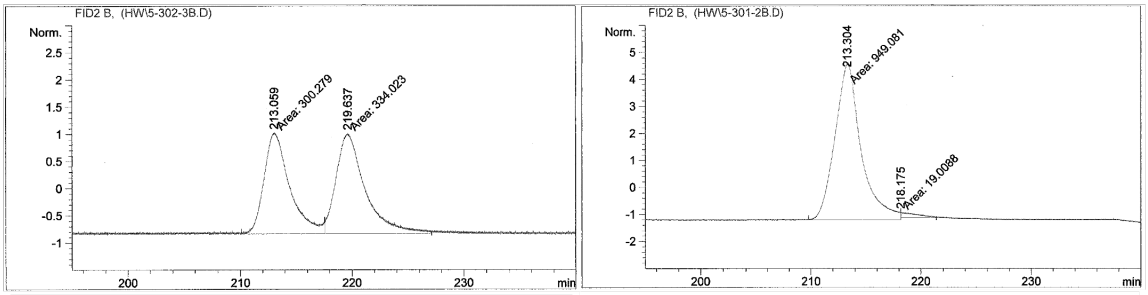


| Peak # | RetTime [min] | Type | Width [min] | Area [pA*s] | Height [pA] | Area % |
|---|---|---|---|---|---|---|
| 1 | 213.059 | MF | 2.6846 | 300.27863 | 1.86422 | 47.34001 |
| 2 | 219.637 | FM | 3.0108 | 334.02335 | 1.84904 | 52.65999 |

| Peak # | RetTime [min] | Type | Width [min] | Area [pA*s] | Height [pA] | Area % |
|---|---|---|---|---|---|---|
| 1 | 213.304 | MM | 2.7378 | 949.08118 | 5.77769 | 98.03647 |
| 2 | 218.175 | MM | 1.6180 | 19.00877 | 1.95805e-1 | 1.96353 |

**(*R*)-*tert*-Butyl (1-(2-bromophenyl)buta-2,3-dien-1-yl)carbamate (3.90c):** IR (neat): 3430 (br), 3310 (br), 2976 (m), 2928 (m), 2853 (w), 1960 (m), 1701 (s), 1491 (m), 1468 (m), 1439 (m), 1390 (m), 1366 (m), 1278 (m), 1249 (m), 1163 (s), 1047 (m), 1024 (m), 853 (m), 754 (m), 735 (m) $cm^{-1}$; $^1H$ NMR (400 MHz, $CDCl_3$): δ 7.54 (1H, d, *J* = 8.0 Hz), 7.35–7.29 (2H, m), 7.14–7.10 (1H, m), 5.61 (1H, br s), 5.43 (1H, br s), 5.13 (1H, br s), 4.93–4.90 (2H, m), 1.43 (9H, s); $^{13}C$ NMR (100 MHz, $CDCl_3$): δ 154.8, 141.4, 133.3, 129.4, 129.0, 128.0, 127.8, 94.1, 92.4, 80.0, 79.6, 52.6, 28.5; HRMS (ESI+): Calcd for $C_{15}H_{19}Br_1N_1O_2$ $[M+H]^+$: 324.05992, Found: 324.06047. Specific Rotation: $[\alpha]_D^{20}$ +77.6 (*c* 0.90, $CHCl_3$) for an enantiomerically enriched sample of 97:3 er.

Enantiomeric purity was determined by GC analysis in comparison with authentic racemic material (97:3 er shown, Chiraldex GTA column, 120 ºC, 15 psi).

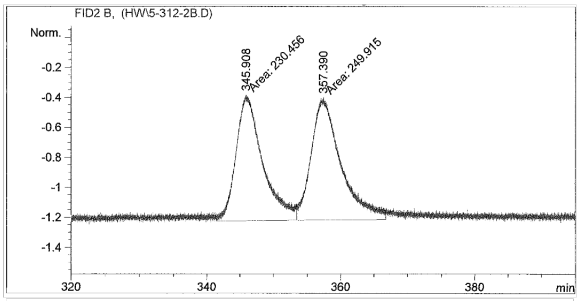


| Peak # | RetTime [min] | Type | Width [min] | Area [pA*s] | Height [pA] | Area % |
|---|---|---|---|---|---|---|
| 1 | 345.908 | MF | 4.5683 | 230.45561 | 8.40786e-1 | 47.97451 |
| 2 | 357.390 | FM | 5.0785 | 249.91536 | 8.20175e-1 | 52.02549 |

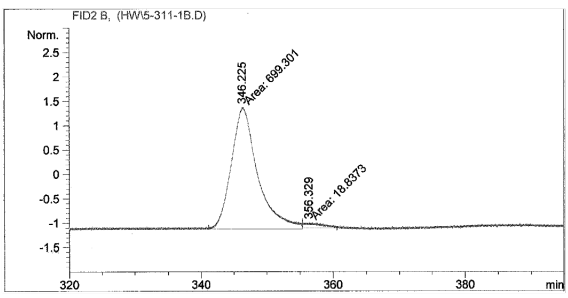


| Peak # | RetTime [min] | Type | Width [min] | Area [pA*s] | Height [pA] | Area % |
|---|---|---|---|---|---|---|
| 1 | 346.225 | MM | 4.6567 | 699.30127 | 2.50285 | 97.37692 |
| 2 | 356.329 | MM | 2.8019 | 18.83732 | 1.12050e-1 | 2.62308 |

| Peak # | Time (min) | Area (%) | Peak # | Time (min) | Area (%) |
|---|---|---|---|---|---|
| 1 | 346.908 | 47.97451 | 1 | 346.225 | 97.37692 |
| 2 | 357.390 | 52.02549 | 2 | 356.329 | 2.62308 |

**(*R*)-*tert*-Butyl (1-(3-bromophenyl)buta-2,3-dien-1-yl)carbamate (3.90d):** IR (neat): 3331 (br), 2975 (m), 2926 (m), 2853 (m), 1958 (m), 1703 (s), 1493 (s), 1475 (m), 1367 (m), 1247 (m), 1165 (s), 1046 (m), 1023 (m), 849 (m), 783 (m), 697 (m) $cm^{-1}$; $^{1}H$ NMR (400 MHz, $CDCl_3$): δ 7.47–7.46 (1H, m), 7.41–7.38 (1H, m), 7.27–7.25 (1H, m), 7.22–7.18 (1H, m), 5.35 (1H, dd, $J$ = 12.0, 6.8 Hz), 5.24 (1H, br s), 4.97–4.92 (3H, m), 1.43 (9H, s); $^{13}C$ NMR (100 MHz, $CDCl_3$): δ 207.0, 155.0, 130.8, 130.3, 130.0, 129.4, 125.7, 122.8, 92.9, 80.1, 79.6, 52.4, 28.5; HRMS (ESI+): Calcd for $C_{15}H_{19}Br_1N_1O_2$ $[M+H]^+$: 324.05992, Found: 324.06013. Specific Rotation: $[\alpha]_D^{20}$ +40.0 (*c* 0.50, $CHCl_3$) for an enantiomerically enriched sample of 94:6 er.

Enantiomeric purity was determined by GC analysis in comparison with authentic racemic material (94:6 er shown, Chiraldex GTA column, 120 ºC, 15 psi).

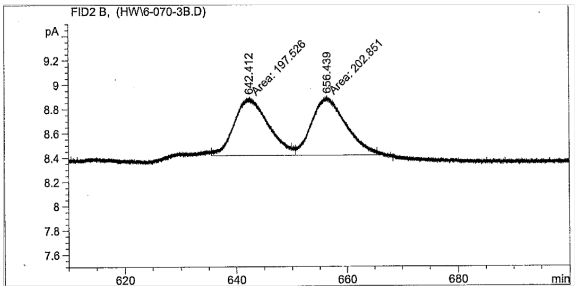


| Peak # | RetTime [min] | Type | Width [min] | Area [pA*s] | Height [pA] | Area % |
|---|---|---|---|---|---|---|
| 1 | 642.412 | MF | 6.9444 | 197.52608 | 4.74064e-1 | 49.33504 |
| 2 | 656.439 | FM | 7.0312 | 202.85080 | 4.80836e-1 | 50.66496 |

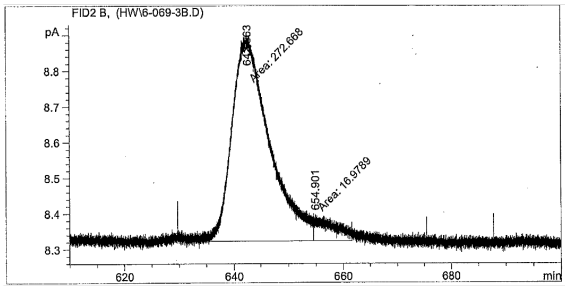


| Peak # | RetTime [min] | Type | Width [min] | Area [pA*s] | Height [pA] | Area % |
|---|---|---|---|---|---|---|
| 1 | 642.563 | MF | 7.8902 | 272.66809 | 5.75966e-1 | 94.13807 |
| 2 | 654.901 | FM | 3.7058 | 16.97889 | 7.63615e-2 | 5.86193 |

| Peak # | Time (min) | Area (%) | Peak # | Time (min) | Area (%) |
|---|---|---|---|---|---|
| 1 | 642.412 | 49.33504 | 1 | 642.563 | 94.13807 |
| 2 | 656.439 | 50.66496 | 2 | 654.901 | 5.86193 |

**(*R*)-*tert*-Butyl (1-(4-(trifluoromethyl)phenyl)buta-2,3-dien-1-yl)carbamate (3.90e):** m.p. = 75–76 ºC. IR (neat): 3312 (br), 2926 (s), 2855 (m), 1959 (m), 1703 (s), 1620 (w), 1495 (m), 1367 (m), 1325 (s), 1250 (m), 1165 (s), 1127 (s), 1068 (s), 1018 (m), 847 (m) $cm^{-1}$; $^{1}H$ NMR (400 MHz, $CDCl_3$): δ 7.59 (2H, d, $J$ = 8.0 Hz), 7.44 (2H, d, $J$ = 8.0 Hz), 5.38–5.32 (2H, m), 5.03–4.95 (3H, m), 1.43 (9H, s); $^{13}C$ NMR (100 MHz, $CDCl_3$): δ 207.0, 155.0, 145.8, 129.9 (q, $J_{C–F}$ = 32 Hz), 127.2, 125.7, 124.3 (q, $J_{C–F}$ = 273 Hz), 92.8, 80.2, 79.7, 52.5, 28.5; HRMS (ESI+): Calcd for $C_{16}H_{19}F_3N_1O_3$ $[M+H]^+$: 314.13679, Found: 314.13721. Specific Rotation: $[\alpha]_D^{20}$ +36.3 (*c* 1.10, $CHCl_3$) for an enantiomerically enriched sample of 94:6 er.

Enantiomeric purity was determined by GC analysis in comparison with authentic racemic material (94:6 er shown, Chiraldex GTA column, 110 ºC, 15 psi).

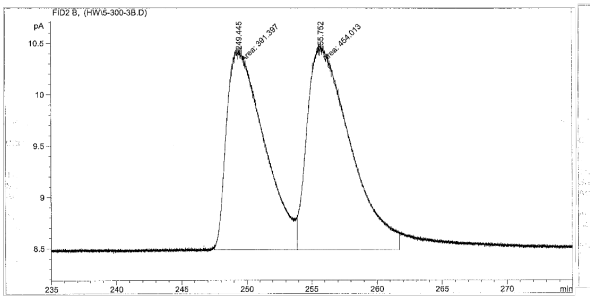


| Peak # | RetTime [min] | Type | Width [min] | Area [pA*s] | Height [pA] | Area % |
|---|---|---|---|---|---|---|
| 1 | 249.445 | MF | 3.2981 | 391.39731 | 1.97790 | 46.29670 |
| 2 | 255.752 | FM | 3.7485 | 454.01349 | 2.01864 | 53.70330 |

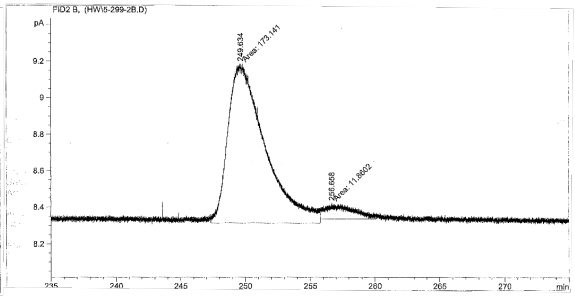


| Peak # | RetTime [min] | Type | Width [min] | Area [pA*s] | Height [pA] | Area % |
|---|---|---|---|---|---|---|
| 1 | 249.634 | MM | 3.2994 | 173.14069 | 8.74613e-1 | 93.58913 |
| 2 | 256.658 | MM | 2.2157 | 11.86016 | 8.92112e-2 | 6.41087 |

| Peak # | Time (min) | Area (%) | Peak # | Time (min) | Area (%) |
|---|---|---|---|---|---|
| 1 | 249.445 | 46.29670 | 1 | 249.634 | 93.58913 |
| 2 | 255.752 | 53.70330 | 2 | 256.658 | 6.41087 |

**(*R*)-*tert*-Butyl (1-(4-methoxyphenyl)buta-2,3-dien-1-yl)carbamate (3.90f):** m.p. = 57–60 ºC. IR (neat): 3345 (br), 2976 (m), 2933 (w), 2836 (w), 1958 (m), 1701 (s), 1612 (m), 1511 (s), 1366 (m), 1302 (m), 1247 (s), 1168 (s), 1035 (m), 831 (m) $cm^{-1}$; $^1H$ NMR (400 MHz, $CDCl_3$): δ 7.26 (2H, d, $J$ = 8.4 Hz), 6.89–6.85 (2H, m), 5.37 (1H, dd, $J$ = 12.0, 6.0 Hz), 5.23 (1H, br s), 4.94–4.92 (3H, m), 3.80 (3H, s), 1.42 (9H, s); $^{13}C$ NMR (100 MHz, $CDCl_3$): δ 207.0, 159.2, 155.1, 128.3, 114.1, 113.9, 93.7, 79.7, 79.2, 55.5, 52.2, 28.6; HRMS (ESI+): Calcd for $C_{16}H_{22}N_1O_3$ $[M+H]^+$: 276.15997, Found: 276.16074. Specific Rotation: $[\alpha]_D^{20}$ +99.9 (*c* 1.00, $CHCl_3$) for an enantiomerically enriched sample of 97:3 er. Enantiomeric purity was determined by HPLC analysis in comparison with authentic racemic material (97:3 er shown, Chiralcel OJ-H column, 98/2 hexanes/*i*-propanol, 1.0 mL/min, 220 nm).

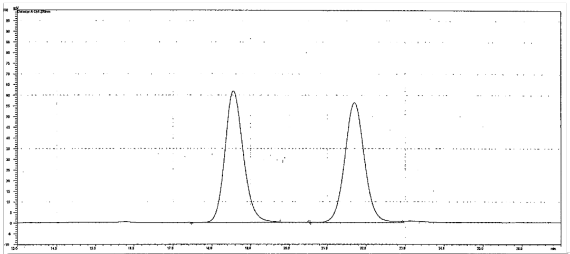

| Peak# | Ret. Time | Area | Height | Area % | Height % |
|---|---|---|---|---|---|
| 1 | 18.552 | 2040100 | 61773 | 50.451 | 52.300 |
| 2 | 21.694 | 2003594 | 56340 | 49.549 | 47.700 |
| Total | | 4043694 | 118113 | 100.000 | 100.000 |

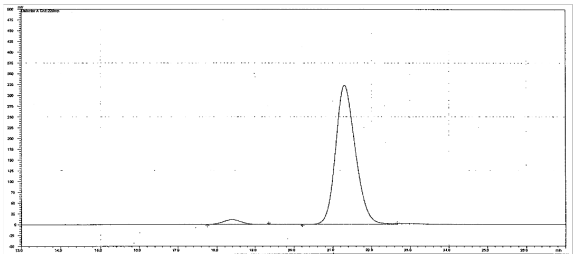

| Peak# | Ret. Time | Area | Height | Area % | Height % |
|---|---|---|---|---|---|
| 1 | 18.389 | 357866 | 11016 | 3.024 | 3.296 |
| 2 | 21.298 | 11476762 | 323198 | 96.976 | 96.704 |
| Total | | 11834628 | 334214 | 100.000 | 100.000 |

| Peak # | Time (min) | Area (%) | Peak # | Time (min) | Area (%) |
|---|---|---|---|---|---|
| 1 | 18.552 | 50.451 | 1 | 18.389 | 3.024 |
| 2 | 21.694 | 49.549 | 2 | 21.298 | 96.976 |

**(*R*)-*tert*-Butyl (1-(furan-2-yl)buta-2,3-dien-1-yl)carbamate (3.90g):** Isolated as a mixture of allenyl and propargyl amides (5% propargyl amide). IR (neat): 3340 (br), 2977 (m), 2928 (m), 2852 (w), 1959 (m), 1702 (s), 1500 (s), 1367 (m), 1247 (m), 1166 (s), 1048 (m), 1010 (m), 857 (m), 736 (m) $cm^{-1}$; $^1H$ NMR (400 MHz, $CDCl_3$): δ 7.36 (1H, dd, *J* = 1.6, 0.8 Hz), 6.31 (1H, dd, *J* = 3.2, 1.6 Hz), 6.22 (1H, d, *J* = 3.2 Hz), 5.43–5.39 (2H, m), 5.01–4.92 (3H, m), 1.45 (9H, s); $^{13}C$ NMR (100 MHz, $CDCl_3$): δ 207.5, 155.0, 153.7, 142.3, 110.3, 106.6, 91.2, 80.0, 79.2, 47.3, 28.5; HRMS (ESI+): Calcd for $C_{13}H_{18}N_1O_3$ $[M+H]^+$: 236.12867, Found: 236.12899. Specific Rotation: $[\alpha]_D^{20}$ +70.5 (*c* 0.85, $CHCl_3$) for an enantiomerically enriched sample of 99:1 er.

Enantiomeric purity was determined by HPLC analysis in comparison with authentic racemic material (99:1 er shown, Chiralpak AZ-H column, 98/2 hexanes/*i*-propanol, 1.0 mL/min, 220 nm).

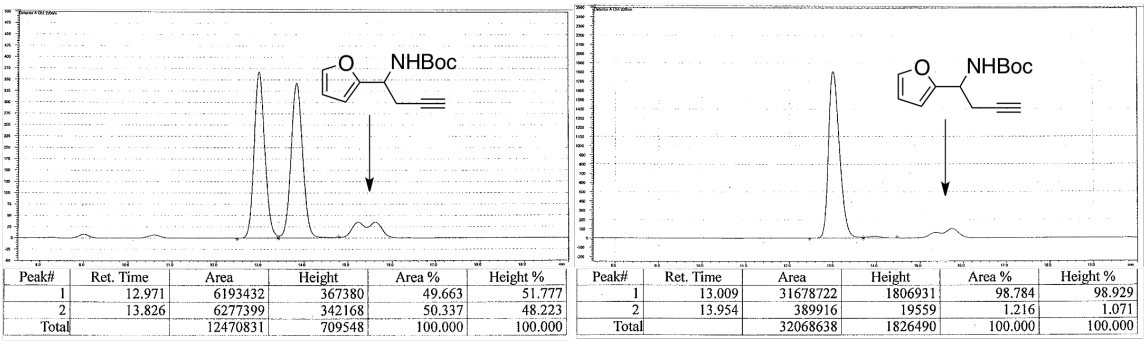


| Peak# | Ret. Time | Area | Height | Area % | Height % |
|---|---|---|---|---|---|
| 1 | 12.971 | 6193432 | 367380 | 49.663 | 51.777 |
| 2 | 13.826 | 6277399 | 342168 | 50.337 | 48.223 |
| Total | | 12470831 | 709548 | 100.000 | 100.000 |

| Peak# | Ret. Time | Area | Height | Area % | Height % |
|---|---|---|---|---|---|
| 1 | 13.009 | 31678722 | 1806931 | 98.784 | 98.929 |
| 2 | 13.954 | 389916 | 19559 | 1.216 | 1.071 |
| Total | | 32068638 | 1826490 | 100.000 | 100.000 |

| Peak # | Time (min) | Area (%) | Peak # | Time (min) | Area (%) |
|---|---|---|---|---|---|
| 1 | 12.971 | 49.663 | 1 | 13.009 | 98.784 |
| 2 | 13.826 | 50.337 | 2 | 13.954 | 1.216 |

**(*R*)-*tert*-Butyl (1-(thiophen-2-yl)buta-2,3-dien-1-yl)carbamate (3.90h):** IR (neat): 3322 (br), 2977 (m), 2929 (m), 1958 (m), 1700 (s), 1494 (s), 1366 (s), 1246 (s), 1164 (s), 1049

(m), 851 (m), 699 (m) $cm^{-1}$; $^1H$ NMR (400 MHz, $CDCl_3$): δ 7.22 (1H, dd, *J* = 5.0, 1.2 Hz), 7.01 (1H, d, *J* = 3.6 Hz), 6.95 (1H, dd, *J* = 5.0, 3.6 Hz), 5.55 (1H, br s), 5.48 (1H, dd, *J* = 12.2, 6 Hz), 4.99–4.97 (3H, m), 1.45 (9H, s); $^{13}C$ NMR (100 MHz, $CDCl_3$): δ 207.1, 154.9, 145.7, 126.9, 125.0, 124.6, 93.1, 80.0, 79.6, 48.6, 28.5; HRMS (ESI+): Calcd for $C_{13}H_{18}S_1N_1O_2$ $[M+H]^+$: 252.10582, Found: 252.10644. Specific Rotation: $[\alpha]_D^{20}$ +76.8 (*c* 1.30, $CHCl_3$) for an enantiomerically enriched sample of 96:4 er.

Enantiomeric purity was determined by GC analysis in comparison with authentic racemic material (96:4 er shown, Chiraldex B-DM column, 105 ºC, 15 psi).

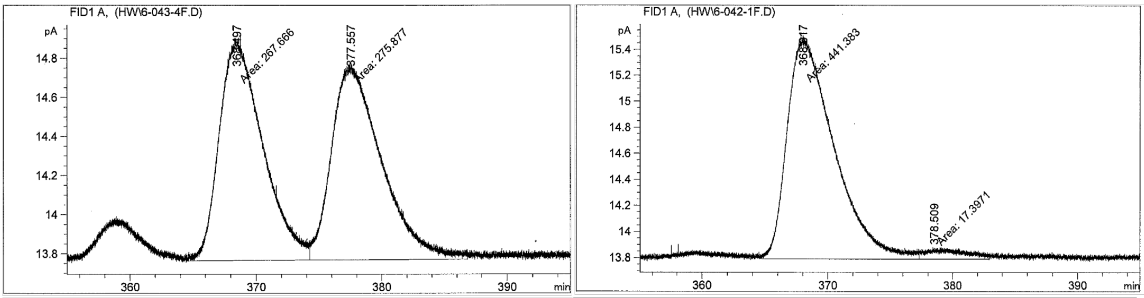


| Peak # | RetTime [min] | Type | Width [min] | Area [pA*s] | Height [pA] | Area % |
|---|---|---|---|---|---|---|
| 1 | 368.497 | MF | 3.9303 | 267.66595 | 1.13504 | 49.24469 |
| 2 | 377.557 | FM | 4.5565 | 275.87680 | 1.00909 | 50.75531 |

| Peak # | RetTime [min] | Type | Width [min] | Area [pA*s] | Height [pA] | Area % |
|---|---|---|---|---|---|---|
| 1 | 368.017 | MF | 4.2842 | 441.38297 | 1.71711 | 96.20797 |
| 2 | 378.509 | FM | 3.3275 | 17.39707 | 8.71375e-2 | 3.79203 |

**(*R*)-*tert*-Butyl (1-(thiophen-3-yl)buta-2,3-dien-1-yl)carbamate (3.90i):** IR (neat): 3314 (br), 2976 (m), 2926 (m), 2853 (w), 1957 (m), 1699 (s), 1497 (s), 1391 (m), 1366 (m), 1246 (m), 1164 (s), 1049 (m), 1023 (m), 854 (m), 785 (m) $cm^{-1}$; $^1H$ NMR (400 MHz, $CDCl_3$): δ 7.29 (1H, dd, *J* = 5.0, 3.2 Hz), 7.18 (1H, m), 7.05 (1H, dd, *J* = 5.0, 1.6 Hz), 5.46–5.38 (2H, m), 4.94–4.89 (3H, m), 1.45 (9H, s); $^{13}C$ NMR (100 MHz, $CDCl_3$): δ 207.2, 155.1, 126.8, 126.3, 126.2, 121.8, 93.0, 80.2, 79.1, 48.8, 28.5; HRMS (ESI+):

Calcd for $C_{13}H_{18}S_1N_1O_2$ $[M+H]^+$: 252.10582, Found: 252.10552. Specific Rotation: $[\alpha]_D^{20}$ +57.1 (*c* 0.70, $CHCl_3$) for an enantiomerically enriched sample of 97:3 er.

Enantiomeric purity was determined by GC analysis in comparison with authentic racemic material (97:3 er shown, Chiraldex B-DM column, 120 ºC, 15 psi).

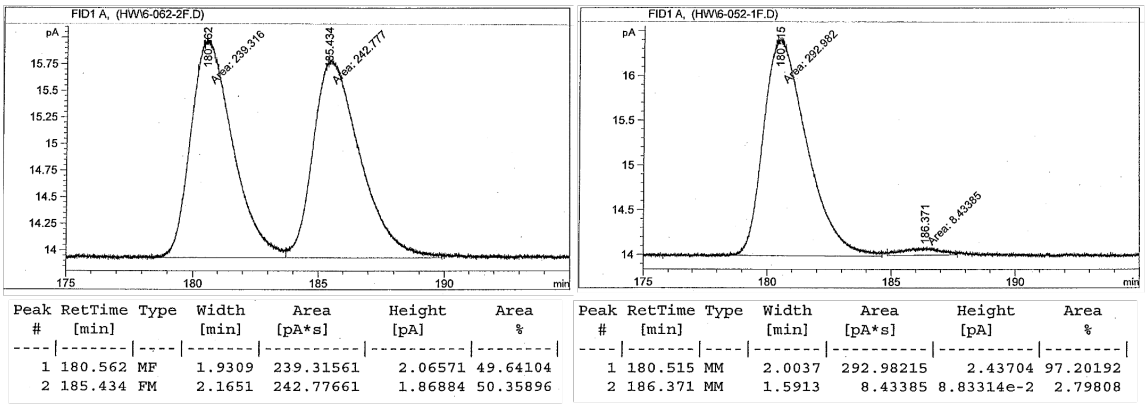


| Peak # | RetTime [min] | Type | Width [min] | Area [pA*s] | Height [pA] | Area % |
|---|---|---|---|---|---|---|
| 1 | 180.562 | MF | 1.9309 | 239.31561 | 2.06571 | 49.64104 |
| 2 | 185.434 | FM | 2.1651 | 242.77661 | 1.86884 | 50.35896 |

| Peak # | RetTime [min] | Type | Width [min] | Area [pA*s] | Height [pA] | Area % |
|---|---|---|---|---|---|---|
| 1 | 180.515 | MM | 2.0037 | 292.98215 | 2.43704 | 97.20192 |
| 2 | 186.371 | MM | 1.5913 | 8.43385 | 8.83314e-2 | 2.79808 |

| Peak # | Time (min) | Area (%) | Peak # | Time (min) | Area (%) |
|---|---|---|---|---|---|
| 1 | 180.562 | 49.64104 | 1 | 180.515 | 97.20192 |
| 2 | 185.434 | 50.35896 | 2 | 186.371 | 2.79808 |

***tert*-Butyl (benzofuran-2-yl(phenylsulfonyl)methyl)carbamate (3.100):** IR (neat): 3292 (s), 2982 (m), 2956 (m), 2931 (m), 1700 (s), 1520 (s), 1454 (m), 1310 (s), 1298 (s), 1248 (m), 1170 (m), 1146 (s), 762 (m), 601 (m) $cm^{-1}$; $^1H$ NMR (400 MHz, $CDCl_3$): δ 7.95–7.93 (2H, m), 7.68–7.64 (1H, m), 7.60–7.52 (3H, m), 7.49–7.47 (1H, m), 7.35–7.24 (2H, m), 6.96 (1H, s), 6.17 (1H, d, *J* = 10.0 Hz), 5.97 (1H, d, *J* = 10.0 Hz), 1.30 (9H, s); $^{13}C$ NMR (100 MHz, $CDCl_3$): δ 155.4, 153.4, 145.4, 136.6, 134.4, 129.8, 129.3, 127.6, 125.6, 123.6, 121.8, 111.7, 109.2, 81.7, 69.6, 28.2; This compound decomposes completely under HRMS conditions.

***tert*-Butyl (benzofuran-2-ylmethylene)carbamate (3.96j):** IR (neat): 2978 (m), 2931 (m), 1710 (s), 1619 (s), 1566 (w), 1476 (w), 1451 (m), 1393 (m), 1368 (m), 1247 (s), 1154 (s), 1127 (s), 956 (m), 871 (m), 752 (m) $cm^{-1}$; $^1H$ NMR (400 MHz, $CDCl_3$): δ 8.87 (1H, s), 7.70–7.68 (1H, m), 7.59–7.57 (1H, m), 7.49–7.44 (2H, m), 7.36–7.28 (1H, m),

1.59 (9H, s); $^{13}$C NMR (100 MHz, $CDCl_3$): δ 162.0, 158.2, 156.7, 151.5, 128.7, 127.5, 124.1, 123.0, 118.3, 112.6, 82.6, 28.0; HRMS (ESI+): Calcd for $C_{14}H_{16}N_1O_3$ $[M+H]^+$: 246.11302, Found: 246.11194.

**(*R*)-*tert*-Butyl (1-(benzofuran-2-yl)buta-2,3-dien-1-yl)carbamate (3.90j):** Isolated as a mixture of allenyl and propargyl amides (10% propargyl amide). IR (neat): 3315 (br), 2977 (m), 2929 (m), 1959 (m), 1701 (s), 1497 (s), 1454 (s), 1392 (s), 1248 (s), 1161 (s), 1049 (m), 1023 (m), 856 (m), 807 (m), 750 (s) $cm^{-1}$; $^1$H NMR (400 MHz, $CDCl_3$): δ 7.54–7.51 (1H, m), 7.46–7.43 (1H, m), 7.28–7.18 (2H, m), 6.61 (1H, s), 5.52–5.47 (2H, m), 5.09 (1H, br s), 4.98–4.96 (2H, m), 1.46 (9H, s); $^{13}$C NMR (100 MHz, $CDCl_3$): δ 207.5, 156.4, 155.1, 155.0, 128.2, 124.3, 122.9, 121.2, 111.3, 103.3, 90.9, 80.2, 79.5, 47.6, 28.5; HRMS (ESI+): Calcd for $C_{17}H_{20}N_1O_3$ $[M+H]^+$: 286.14432, Found: 286.14535. Specific Rotation: $[\alpha]_D^{20}$ +99.8 (*c* 1.00, $CHCl_3$) for an enantiomerically enriched sample of 95:5 er.

Enantiomeric purity was determined by HPLC analysis in comparison with authentic racemic material (95:5 er shown, Chiralcel OD-H column, 98/2 hexanes/*i*-propanol, 0.3 mL/min, 220 nm).

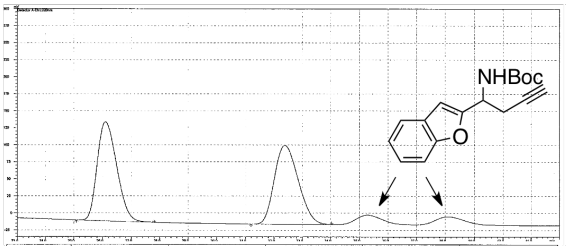


| Peak# | Ret. Time | Area | Height | Area % | Height % |
|---|---|---|---|---|---|
| 1 | 26.094 | 6836478 | 145027 | 50.024 | 55.631 |
| 2 | 32.374 | 6829841 | 115665 | 49.976 | 44.369 |
| Total | | 13666318 | 260692 | 100.000 | 100.000 |

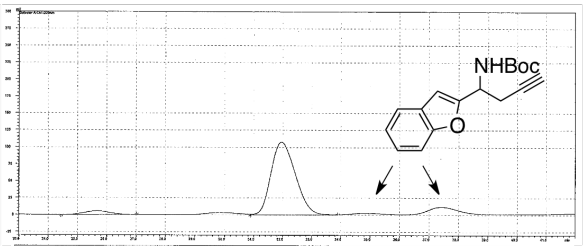


| Peak# | Ret. Time | Area | Height | Area % | Height % |
|---|---|---|---|---|---|
| 1 | 25.673 | 329935 | 5495 | 4.946 | 4.863 |
| 2 | 31.950 | 6340941 | 107502 | 95.054 | 95.137 |
| Total | | 6670876 | 112997 | 100.000 | 100.000 |

| Peak # | Time (min) | Area (%) | Peak # | Time (min) | Area (%) |
|---|---|---|---|---|---|
| 1 | 26.094 | 50.024 | 1 | 25.673 | 4.946 |
| 2 | 32.374 | 49.976 | 2 | 31.950 | 95.054 |

**(*R*)-*tert*-Butyl (1-(pyridin-3-yl)buta-2,3-dien-1-yl)carbamate (3.90k):** Isolated as a mixture of the product and aminoalcohol. IR (neat): 3310 (br), 2956 (m), 2921 (m), 2851 (m), 1958 (m), 1706 (s), 1510 (m), 1480 (m), 1366 (s), 1248 (s), 1165 (s), 1049 (m), 1024 (m), 851(m), 713 (s) $cm^{-1}$; $^1H$ NMR (400 MHz, $CDCl_3$): δ 8.58 (1H, s), 8.50 (1H, d, *J* = 4.0 Hz), 7.62 (1H, d, *J* = 8.0 Hz), 7.27–7.24 (1H, m), 5.39 (1H, dd, *J* = 12.0, 6.0 Hz), 5.31 (1H, br s), 5.02 (1H, br s), 4.97–4.94 (2H, m), 1.40 (9H, s); $^{13}C$ NMR (100 MHz, $CDCl_3$): δ 207.2, 154.9, 149.1, 148.9, 148.7, 134.8, 123.6, 92.6, 80.3, 79.8, 50.9, 28.5; HRMS (ESI+): Calcd for $C_{14}H_{19}N_2O_2$ $[M+H]^+$: 247.14465, Found: 247.14458. Specific Rotation: $[\alpha]_D^{20}$ –12.5 (*c* 0.80, $CHCl_3$) for an enantiomerically enriched sample of 84:16 er.

Enantiomeric purity was determined by HPLC analysis in comparison with authentic racemic material (84:16 er shown, Chiralcel OD-H column, 95/5 hexanes/*i*-propanol, 0.5 mL/min, 220 nm).

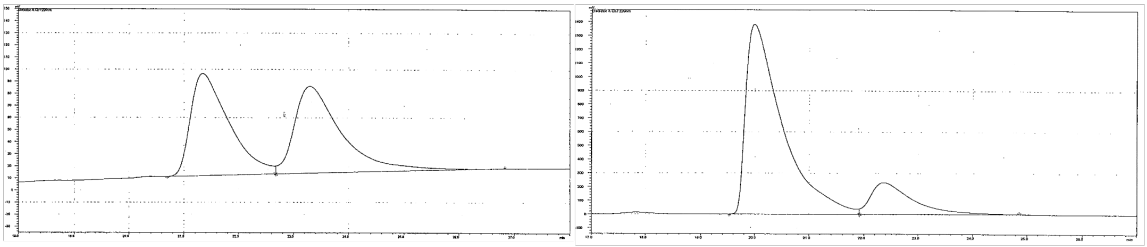

| Peak# | Ret. Time | Area | Height | Area % | Height % |
|---|---|---|---|---|---|
| 1 | 21.336 | 4164757 | 84682 | 49.331 | 54.087 |
| 2 | 23.287 | 4277734 | 71885 | 50.669 | 45.913 |
| Total | | 8442492 | 156567 | 100.000 | 100.000 |

| Peak# | Ret. Time | Area | Height | Area % | Height % |
|---|---|---|---|---|---|
| 1 | 19.984 | 65372690 | 1380957 | 84.132 | 85.722 |
| 2 | 22.359 | 12329746 | 230010 | 15.868 | 14.278 |
| Total | | 77702436 | 1610967 | 100.000 | 100.000 |

| Peak # | Time (min) | Area (%) | Peak # | Time (min) | Area (%) |
|---|---|---|---|---|---|
| 1 | 21.336 | 49.331 | 1 | 19.984 | 84.132 |
| 2 | 23.287 | 50.669 | 2 | 22.359 | 15.868 |

**(*S*)-*tert*-Butyl (1-phenylhexa-4,5-dien-3-yl)carbamate (3.90l):** Isolated as a mixture of the product and hemiaminal (10%). IR (neat): 3340 (br), 2975 (m), 2928 (m), 2858 (w), 1956 (m), 1698 (s), 1497 (s), 1455 (m), 1391 (m), 1366 (s), 1245 (m), 1167 (s), 1044 (m),

1027 (m), 854 (m), 747 (m), 699 (m) $cm^{-1}$; $^1H$ NMR (400 MHz, $CDCl_3$): δ 7.30–7.26 (2H, m), 7.20–7.17 (3H, m), 5.25–5.23 (1H, m), 4.89–4.86 (2H, m), 4.54 (1H, br s), 4.21 (1H, br s), 2.75–2.63 (2H, m), 1.95–1.79 (2H, m), 1.46 (9H, s); $^{13}C$ NMR (100 MHz, $CDCl_3$): δ 207.2, 155.5, 141.8, 128.6, 128.5, 126.0, 93.1, 79.3, 78.3, 48.7, 37.3, 32.3, 28.5; HRMS (ESI+): Calcd for $C_{17}H_{24}N_1O_2$ $[M+H]^+$: 274.18070, Found: 274.18070. Specific Rotation: $[\alpha]_D^{20}$ –20.0 (*c* 1.00, $CHCl_3$) for an enantiomerically enriched sample of 99:1 er. Enantiomeric purity was determined by HPLC analysis in comparison with authentic racemic material (99:1 er shown, Chiralcel OD-H column, 98/2 hexanes/*i*-propanol, 0.2 mL/min, 220 nm).

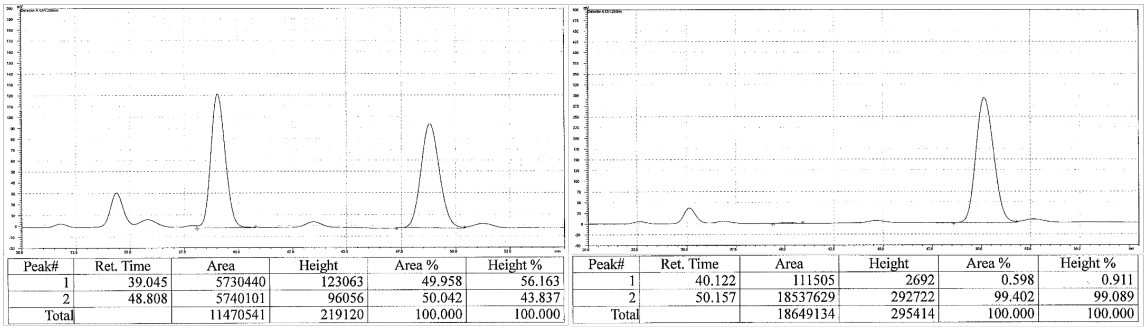

| Peak# | Ret. Time | Area | Height | Area % | Height % |
|---|---|---|---|---|---|
| 1 | 39.045 | 5730440 | 123063 | 49.958 | 56.163 |
| 2 | 48.808 | 5740101 | 96056 | 50.042 | 43.837 |
| Total | | 11470541 | 219120 | 100.000 | 100.000 |

| Peak# | Ret. Time | Area | Height | Area % | Height % |
|---|---|---|---|---|---|
| 1 | 40.122 | 111505 | 2692 | 0.598 | 0.911 |
| 2 | 50.157 | 18537629 | 292722 | 99.402 | 99.089 |
| Total | | 18649134 | 295414 | 100.000 | 100.000 |

| Peak # | Time (min) | Area (%) | Peak # | Time (min) | Area (%) |
|---|---|---|---|---|---|
| 1 | 39.045 | 49.958 | 1 | 40.122 | 0.598 |
| 2 | 48.808 | 50.042 | 2 | 50.157 | 99.402 |

**(*S*)-*tert*-Butyl (1-((*tert*-butyldiphenylsilyl)oxy)hexa-4,5-dien-3-yl)carbamate (3.90m):** IR (neat): 3420 (br), 3071 (w), 2958 (m), 2929 (s), 2857 (m), 1958 (m), 1702 (s), 1499 (s), 1473 (m), 1428 (m), 1390 (m), 1365 (m), 1245 (m), 1169 (s), 1109 (s), 1062 (s), 846 (m), 822 (m), 738 (s), 702 (s), 614 (m), 504 (s) $cm^{-1}$; $^1H$ NMR (400 MHz, $CDCl_3$): δ 7.69–7.66 (4H, m), 7.46–7.37 (6H, m), 5.45 (1H, br s), 5.22 (1H, dd, *J* = 12.0, 6.4 Hz), 4.83–4.81 (2H, m), 4.38 (1H, br s), 3.89 (1H, br s), 3.74–3.69 (1H, m), 1.95 (1H, br s), 1.75–1.68 (1H, m), 1.44 (9H, s), 1.06 (9H, s); $^{13}C$ NMR (100 MHz, $CDCl_3$): δ 207.3, 155.5,

135.7, 133.4, 129.9, 127.9, 93.1, 79.1, 78.0, 61.4, 47.7, 36.4, 28.6, 26.9, 19.2; HRMS (ESI+): Calcd for $C_{27}H_{38}N_1O_3Si_1$ $[M+H]^+$: 452.26209, Found: 452.26258. Specific Rotation: $[\alpha]_D^{20}$ –18.7 (*c* 1.60, $CHCl_3$) for an enantiomerically enriched sample of 99:1 er. Enantiomeric purity was determined by HPLC analysis in comparison with authentic racemic material (99:1 er shown, Chiralcel OD-H column, 98/2 hexanes/*i*-propanol, 0.2 mL/min, 220 nm).

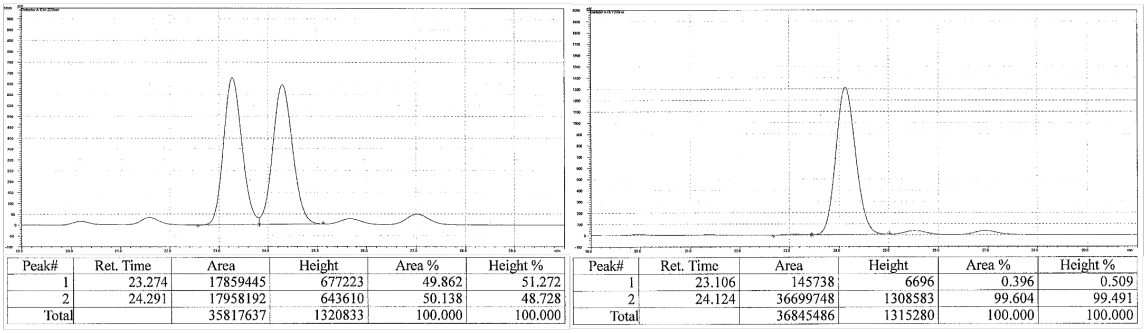

| Peak# | Ret. Time | Area | Height | Area % | Height % |
|---|---|---|---|---|---|
| 1 | 23.274 | 17859445 | 677223 | 49.862 | 51.272 |
| 2 | 24.291 | 17958192 | 643610 | 50.138 | 48.728 |
| Total | | 35817637 | 1320833 | 100.000 | 100.000 |

| Peak# | Ret. Time | Area | Height | Area % | Height % |
|---|---|---|---|---|---|
| 1 | 23.106 | 145738 | 6696 | 0.396 | 0.509 |
| 2 | 24.124 | 36699748 | 1308583 | 99.604 | 99.491 |
| Total | | 36845486 | 1315280 | 100.000 | 100.000 |

| Peak # | Time (min) | Area (%) | Peak # | Time (min) | Area (%) |
|---|---|---|---|---|---|
| 1 | 23.274 | 49.862 | 1 | 23.106 | 0.396 |
| 2 | 24.291 | 50.138 | 2 | 24.124 | 99.604 |

**(*S*)-*tert*-Butyl octa-1,2,7-trien-4-ylcarbamate (3.90n):** IR (neat): 3339 (br), 2977 (m), 2927 (m), 2854 (w), 1958 (m), 1696 (s), 1501 (s), 1453 (m), 1391 (m), 1366 (s), 1246 (m), 1170 (s), 1050 (m), 1021 (m), 911 (m), 848 (m) $cm^{-1}$; $^1H$ NMR (400 MHz, $CDCl_3$): δ 5.86–5.76 (1H, m), 5.21–5.20 (1H, m), 5.05–4.86 (2H, m), 4.86–4.84 (2H, m), 4.50 (1H, br s), 4.15 (1H, br s), 2.17–2.10 (2H, m), 1.70–1.62 (2H, m), 1.44 (9H, s); $^{13}C$ NMR (100 MHz, $CDCl_3$): δ 207.2, 155.4, 138.0, 115.2, 93.1, 79.5, 78.2, 48.5, 34.8, 30.2, 28.5; HRMS (ESI+): Calcd for $C_{13}H_{22}N_1O_2$ $[M+H]^+$: 224.16505, Found: 224.16582. Specific Rotation: $[\alpha]_D^{20}$ –40.9 (*c* 0.73, $CHCl_3$) for an enantiomerically enriched sample of 99:1 er.

Enantiomeric purity was determined by HPLC analysis in comparison with authentic racemic material (99:1 er shown, Chiralpak AS-H column, 98/2 hexanes/*i*-propanol, 0.2 mL/min, 220 nm).

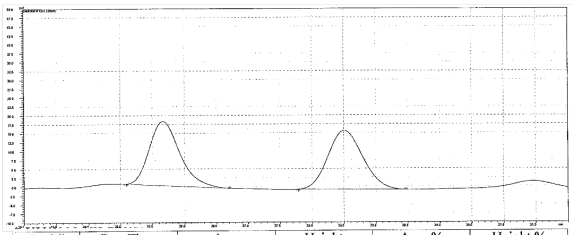

| Peak# | Ret. Time | Area | Height | Area % | Height % |
|---|---|---|---|---|---|
| 1 | 25.661 | 595348 | 18021 | 48.568 | 52.167 |
| 2 | 28.505 | 630449 | 16524 | 51.432 | 47.833 |
| Total | | 1225797 | 34545 | 100.000 | 100.000 |

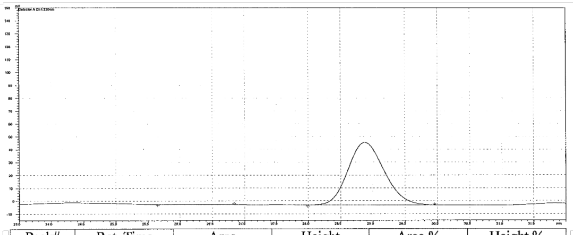

| Peak# | Ret. Time | Area | Height | Area % | Height % |
|---|---|---|---|---|---|
| 1 | 26.548 | 8755 | 218 | 0.461 | 0.447 |
| 2 | 28.870 | 1892132 | 48626 | 99.539 | 99.553 |
| Total | | 1900887 | 48844 | 100.000 | 100.000 |

| Peak # | Time (min) | Area (%) | Peak # | Time (min) | Area (%) |
|---|---|---|---|---|---|
| 1 | 25.661 | 48.568 | 1 | 26.548 | 0.461 |
| 2 | 28.505 | 51.432 | 2 | 28.870 | 99.539 |

**(*S*)-*tert*-Butyl (6-methylhepta-1,2-dien-4-yl)carbamate (3.90o):** IR (neat): 3344 (br), 2957 (m), 2930 (m), 2870 (m), 1957 (m), 1694 (s), 1499 (s), 1470 (m), 1455 (m), 1390 (m), 1366 (s), 1247 (s), 1167 (s), 1048 (m), 1013 (m), 845 (m) $cm^{-1}$; $^1H$ NMR (400 MHz, $CDCl_3$): δ 5.21–5.19 (1H, m), 4.84–4.82 (2H, m), 4.43 (1H, br s), 4.19 (1H, br s), 1.75–1.65 (1H, m), 1.47-1.37 (2H, m), 1.44 (9H, s), 0.93 (3H, s), 0.91 (3H, s); $^{13}C$ NMR (100 MHz, $CDCl_3$): δ 207.2, 155.5, 93.6, 79.4, 78.0, 47.3, 44.8, 28.5, 25.0, 22.8, 22.6; HRMS (ESI+): Calcd for $C_{13}H_{24}N_1O_2$ $[M+H]^+$: 226.18070, Found: 226.18167. Specific Rotation: $[\alpha]_D^{20}$ –41.6 (*c* 0.80, $CHCl_3$) for an enantiomerically enriched sample of 99:1 er.

Enantiomeric purity was determined by GC analysis in comparison with authentic racemic material (99:1 er shown, Chiraldex B-DM column, 140 ºC, 15 psi).

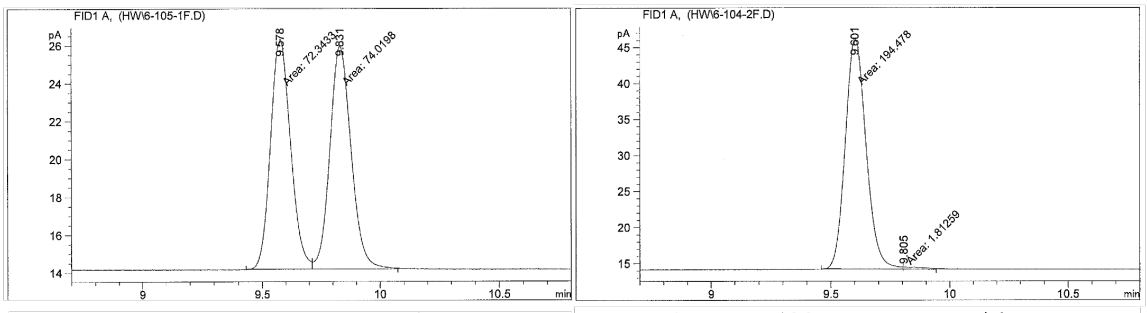


| Peak # | RetTime [min] | Type | Width [min] | Area [pA*s] | Height [pA] | Area % |
|---|---|---|---|---|---|---|
| 1 | 9.578 | MF | 0.0993 | 72.34332 | 12.13855 | 49.42727 |
| 2 | 9.831 | FM | 0.1047 | 74.01984 | 11.77741 | 50.57273 |

| Peak # | RetTime [min] | Type | Width [min] | Area [pA*s] | Height [pA] | Area % |
|---|---|---|---|---|---|---|
| 1 | 9.601 | MF | 0.1011 | 194.47842 | 32.05725 | 99.07658 |
| 2 | 9.805 | FM | 0.1024 | 1.81259 | 2.95138e-1 | 0.92342 |

| Peak # | Time (min) | Area (%) | Peak # | Time (min) | Area (%) |
|---|---|---|---|---|---|
| 1 | 9.578 | 49.42727 | 1 | 9.601 | 99.07658 |
| 2 | 9.831 | 50.57273 | 2 | 9.805 | 0.92342 |

**(*S*)-*tert*-Butyl (1-cyclohexylbuta-2,3-dien-1-yl)carbamate (3.90p):** IR (neat): 3341 (br), 2976 (m), 2924 (s), 2853 (m), 1958 (m), 1699 (s), 1499 (m), 1451 (m), 1390 (m), 1365 (m), 1243 (m), 1170 (s), 1055 (m), 1014 (m), 842 (m) $cm^{-1}$; $^{1}H$ NMR (400 MHz, $CDCl_3$): δ 5.17–5.13 (1H, m), 4.84–4.81 (2H, m), 4.56 (1H, br s), 4.02 (1H, br s), 1.77–1.64 (5H, m), 1.44 (9H, s), 1.28–0.95 (6H, m); $^{13}C$ NMR (100 MHz, $CDCl_3$): δ 207.3, 155.7, 91.7, 79.3, 77.8, 53.6, 42.9, 29.3, 28.8, 28.6, 26.5, 26.3, 26.3; HRMS (ESI+): Calcd for $C_{15}H_{26}N_1O_2$ $[M+H]^+$: 252.19635, Found: 252.19531. Specific Rotation: $[\alpha]_D^{20}$ +20.0 (*c* 1.00, $CHCl_3$) for an enantiomerically enriched sample of >99:1 er.

Enantiomeric purity was determined by GC analysis in comparison with authentic racemic material (>99:1 er shown, Chiraldex B-DA column, 140 ºC, 15 psi).

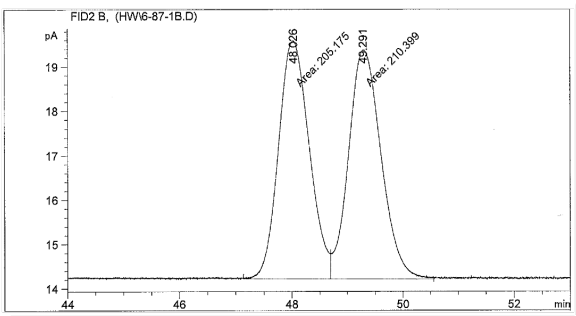


| Peak # | RetTime [min] | Type | Width [min] | Area [pA*s] | Height [pA] | Area % |
|---|---|---|---|---|---|---|
| 1 | 48.026 | MF | 0.6366 | 205.17532 | 5.37152 | 49.37156 |
| 2 | 49.291 | FM | 0.6791 | 210.39856 | 5.16376 | 50.62844 |

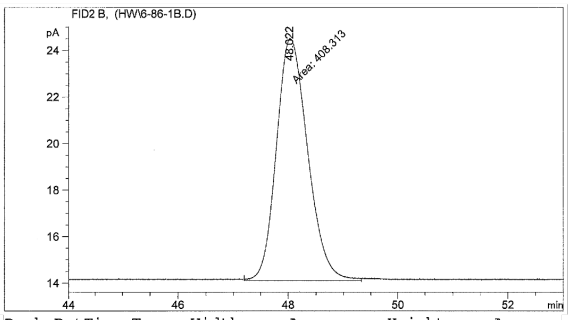


| Peak # | RetTime [min] | Type | Width [min] | Area [pA*s] | Height [pA] | Area % |
|---|---|---|---|---|---|---|
| 1 | 48.022 | MM | 0.6537 | 408.31265 | 10.41043 | 1.000e2 |

| Peak # | Time (min) | Area (%) | Peak # | Time (min) | Area (%) |
|---|---|---|---|---|---|
| 1 | 48.026 | 49.37156 | 1 | 48.022 | 100.00000 |
| 2 | 49.291 | 50.62844 | 2 | - | - |

**(*S*)-*tert*-Butyl 4-(1-((*tert*-butoxycarbonyl)amino)buta-2,3-dien-1-yl)piperidine-1-carboxylate (3.90q):** IR (neat): 3325 (br), 2975 (m), 2930 (m), 2853 (m), 1957 (m), 1692 (s), 1516 (m), 1423 (m), 1365 (m), 1246 (m), 1165 (s), 1064 (m), 1042 (m), 1012 (m), 967 (m), 864 (m), 769 (m) $cm^{-1}$; $^{1}H$ NMR (400 MHz, $CDCl_3$): δ 5.15–5.12 (1H, m), 4.86–4.84 (2H, m), 4.58–4.56 (1H, m), 4.12–4.07 (3H, m), 2.66–2.63 (2H, m), 1.70–1.59 (3H, m), 1.45–1.43 (18H, m), 1.28–1.16 (2H, m); $^{13}C$ NMR (100 MHz, $CDCl_3$): δ 207.4, 155.5, 154.9, 90.9, 83.9, 79.5, 78.2, 52.8, 44.1, 41.3, 28.6, 28.5, 28.0; HRMS (ESI+): Calcd for $C_{19}H_{33}N_2O_4$ $[M+H]^+$: 353.24403, Found: 353.24538. Specific Rotation: $[\alpha]_D^{20}$ +22.2 (*c* 0.90, $CHCl_3$) for an enantiomerically enriched sample of >99:1 er.

Enantiomeric purity was determined by HPLC analysis in comparison with authentic racemic material (>99:1 er shown, Chiralcel OD-H column, 98/2 hexanes/*i*-propanol, 0.2 mL/min, 220 nm).

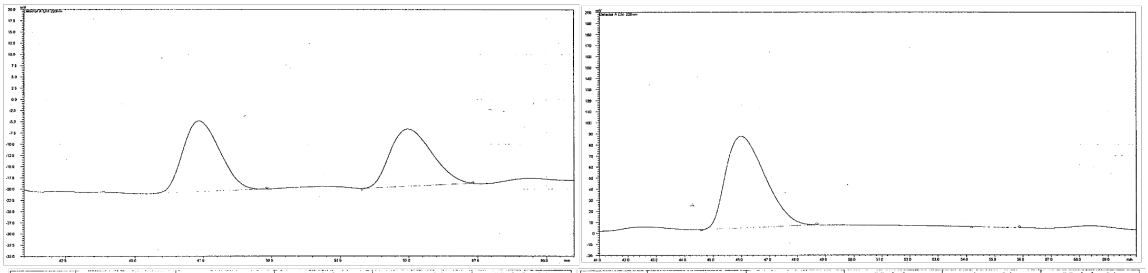

| Peak# | Ret. Time | Area | Height | Area % | Height % |
|---|---|---|---|---|---|
| 1 | 47.350 | 1462786 | 15768 | 51.850 | 55.158 |
| 2 | 54.952 | 1358395 | 12819 | 48.150 | 44.842 |
| Total | | 2821181 | 28587 | 100.000 | 100.000 |

| Peak# | Ret. Time | Area | Height | Area % | Height % |
|---|---|---|---|---|---|
| 1 | 45.987 | 7990938 | 83044 | 100.005 | 100.000 |
| 2 | 54.200 | -432 | 0 | -0.005 | 0.000 |
| Total | | 7990506 | 83044 | 100.000 | 100.000 |

| Peak # | Time (min) | Area (%) | Peak # | Time (min) | Area (%) |
|---|---|---|---|---|---|
| 1 | 47.350 | 51.850 | 1 | 45.987 | 100.005 |
| 2 | 54.952 | 48.150 | 2 | 54.200 | -0.005 |

**(*R*)-*tert*-Butyl (1-phenyl-3-(4,4,5,5-tetramethyl-1,3,2-dioxaborolan-2-yl)but-3-en-1-yl)carbamate (3.102):** IR (neat): 2977 (s), 2929 (m), 1704 (s), 1497 (m), 1453 (m), 1390 (m), 1368 (s), 1310 (s), 1249 (m), 1197 (s), 1168 (s), 1076 (m), 1046 (m), 973 (m), 952 (m), 755 (m), 700 (m), 579 (s) $cm^{-1}$; $^1H$ NMR (400 MHz, $CDCl_3$): δ 7.32–7.26 (4H, m), 7.22–7.18 (1H, m), 5.91 (1H, d, *J* = 3.2 Hz), 5.68 (1H, d, *J* = 3.2 Hz), 5.58 (1H, br s), 4.67 (1H, br s), 2.55–2.42 (2H, m), 1.38 (9H, s), 1.29 (6H, s), 1.28 (6H, s); $^{13}C$ NMR (100 MHz, $CDCl_3$): δ 155.4, 133.4, 128.4, 126.9, 126.2, 84.0, 79.1, 56.3, 42.9, 29.8, 28.5, 25.0, 24.8; HRMS (ESI+): Calcd for $C_{21}H_{33}B_1N_1O_4$ $[M+H]^+$: 374.25026, Found: 374.24997.

***tert*-Butyl (2-(4-methoxyphenyl)-1-(phenylsulfonyl)ethyl)carbamate:** m.p. = 127–130 ºC. IR (neat): 3337 (br), 2977 (m), 2932 (m), 2837 (w), 1729 (s), 1612 (m), 1585 (w), 1513 (s), 1446 (m), 1393 (w), 1368 (m), 1305 (s), 1248 (s), 1139 (s), 1084 (m), 1034 (m), 822 (m), 759 (m), 741 (m), 687 (m), 596 (s), 562 (w), 544 (m), 526 (m) $cm^{-1}$; $^1H$ NMR (400 MHz, $CDCl_3$): δ 7.92–7.90 (2H, m), 7.63–7.59 (1H, m), 7.53–7.50 (2H, m), 7.14–7.10 (2H, m), 6.83–6.79 (2H, m), 5.07 (1H, dt, *J* = 10.8, 4.0 Hz), 4.95 (1H, d, *J* = 10.8 Hz), 3.75 (3H, s), 3.54 (1H, dd, *J* = 14.8, 4.0 Hz), 2.97 (1H, dd, *J* = 14.8, 10.8 Hz), 1.10

(9H, s); $^{13}C$ NMR (100 MHz, $CDCl_3$): δ 158.7, 153.5, 136.9, 133.9, 130.2, 129.3, 129.0, 126.5, 114.1, 80.7, 71.2, 55.2, 31.7, 27.8; HRMS (ESI+): Calcd for $C_{20}H_{25}N_1O_5Na_1S_1$ $[M+Na]^+$: 414.13456, Found: 414.13380.

***tert*-Butyl (2-(4-methoxyphenyl)ethylidene)carbamate (3.107):** Boc–imine **3.107** is not stable under room temperature, since the isomerization into the corresponding enamine is significant. Thus, as soon as synthesized, it was used directly in the catalytic enantioselective allene addition reaction.

**(*S*)-*tert*-Butyl (1-(4-methoxyphenyl)penta-3,4-dien-2-yl)carbamate (3.108):** The spectroscopic data match those reported previously.[136d] $^1H$ NMR (400 MHz, $CDCl_3$): δ 7.12 (2H, d, $J$ = 8.8 Hz), 6.83 (2H, d, $J$ = 8.8 Hz), 5.22–5.17 (1H, m), 4.84–4.81 (2H, m), 4.54 (1H, br s), 4.37 (1H, br s), 3.79 (3H, s), 2.87–2.75 (2H, m), 1.42 (9H, s). Specific Rotation: $[\alpha]_D^{20}$ +27.9 (*c* 0.70, $CHCl_3$) for an enantiomerically enriched sample of 96:4 er. Enantiomeric purity was determined by HPLC analysis in comparison with authentic racemic material (96:4 er shown, Chiralpak AS-H column, 98/2 hexanes/*i*-propanol, 0.3 mL/min, 220 nm).

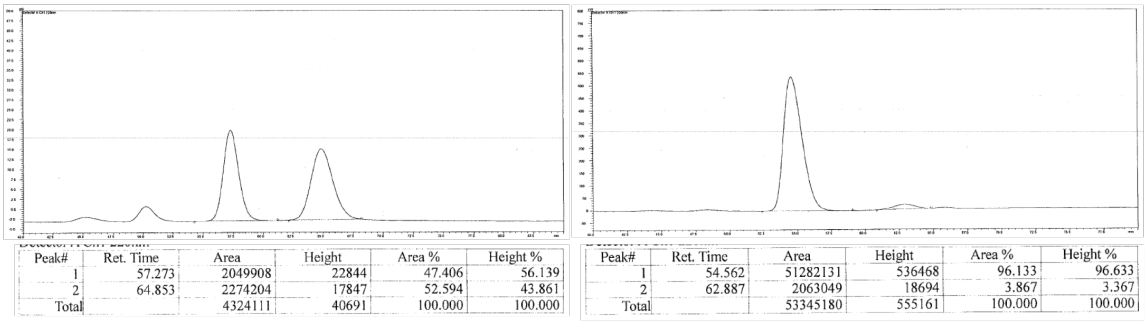

| Peak# | Ret. Time | Area | Height | Area % | Height % |
|---|---|---|---|---|---|
| 1 | 57.273 | 2049908 | 22844 | 47.406 | 56.139 |
| 2 | 64.853 | 2274204 | 17847 | 52.594 | 43.861 |
| Total | | 4324111 | 40691 | 100.000 | 100.000 |

| Peak# | Ret. Time | Area | Height | Area % | Height % |
|---|---|---|---|---|---|
| 1 | 54.562 | 51282131 | 536468 | 96.133 | 96.633 |
| 2 | 62.887 | 2063049 | 18694 | 3.867 | 3.367 |
| Total | | 53345180 | 555161 | 100.000 | 100.000 |

| Peak # | Time (min) | Area (%) | Peak # | Time (min) | Area (%) |
|---|---|---|---|---|---|
| 1 | 57.273 | 47.406 | 1 | 54.562 | 96.133 |
| 2 | 64.853 | 52.594 | 2 | 62.887 | 3.867 |

**(*4S*,*5R*)-5-(1-Iodovinyl)-4-(4-methoxyphenyl)oxazolidin-2-one (3.111):** Under $N_2$ atmosphere, homoallenylamide **3.90f** (1.1 g, 4.1 mmol, 1.0 equiv) was dissolved in $Et_2O$ (12 mL) in a flame dried flask (50 mL). To another flame-dried flask (25 mL), iodine (1.0 g, 4.1 mmol, 1.0 equiv) was introduced and dissolved in $Et_2O$ (13 mL). The resulting iodine solution was transferred into the homoallenylamide solution through a cannula. The mixture was allowed to stir at 22 ºC for 15 min. The $^1$H NMR spectrum of the resulting brown solution showed >98% formation of diiodide **3.110** as 1:1 *E*:*Z* isomers. Then $CH_3CN$ (2.5 mL) was charged into the solution, followed by addition of $AgPF_6$ (1.1 g, 4.5 mmol, 1.1 equiv). The resulting mixture was allowed to stir at 22 ºC for 3.0 h before the reaction was quenched by the addition of a saturated solution of aqueous $NaHCO_3$ (10 mL). The aqueous layer was washed with $Et_2O$ (3x10 mL), and the combined organic layers were combined and dried over $MgSO_4$ and concentrated under vacuum. The resulting brown oil was purified by silica gel chromatography (hexanes:$Et_2O$ = 1:2, 2% $Et_3N$) to afford (4*S*,5*R*)-5-(1-iodovinyl)-4-(4-methoxyphenyl)oxazolidin-2-one (**3.111**) (1.1 g, 3.1 mmol, 76% yield) as yellow oil.

IR (neat): 3285 (br), 2956 (m), 2924 (m), 2853 (w), 1754 (s), 1613 (m), 1513 (s), 1375 (m), 1278 (w), 1249 (s), 1176 (m), 1030 (s), 831 (m) $cm^{-1}$; $^1$H NMR (400 MHz, $CDCl_3$): δ 7.29 (2H, d, *J* = 8.8 Hz), 6.93 (2H, d, *J* = 8.8 Hz), 6.47 (1H, m), 6.02 (1H, d, *J* = 2.4 Hz), 5.36 (1H, br s), 4.66 (1H, d, *J* = 6.0 Hz), 4.47 (1H, d, *J* = 6.0 Hz), 3.82 (3H, s); $^{13}$C NMR (100 MHz, $CDCl_3$): δ 172.5, 160.3, 130.7, 129.0, 127.8, 114.7, 107.0, 88.3, 61.6, 55.5; HRMS (ESI+): Calcd for $C_{12}H_{13}N_1O_3I_1$ $[M+H]^+$: 345.99401, Found: 345.99330. Specific Rotation: $[\alpha]_D^{20}$ –52.5 (*c* 0.95, $CHCl_3$).

**(*4S*,*5S*)-4-(4-Methoxyphenyl)-5-vinyloxazolidin-2-one (3.112):** Under $N_2$ atmosphere, oxazolidinone (**3.111**) (1.1 g, 3.1 mmol, 1.0 equiv) was dissolved in 120 mL thf in a flame-dried flask (250 mL). The light yellow solution was allowed to cool to –78 ºC in a dry ice/acetone bath. Then *t*-BuLi solution (5.5 mL, 1.7 M in pentane, 3.0 equiv) was added dropwise into the solution through a syringe. The resulting red solution was allowed to stir at the same temperature for 5 min, before the reaction was quenched by addition of 5 mL methanol. The colorless solution was allowed to warm to 22 ºC and stir for an additional 5 min. The mixture was passed through a plug of silica gel and then concentrated under vacuum. The resulting colorless oil was purified by silica gel chromatography (hexanes:$Et_2O$ = 1:2, 2% $Et_3N$) to afford (4*S*,5*S*)-4-(4-methoxyphenyl)-5-vinyloxazolidin-2-one (**3.112**) (0.537 g, 2.4 mmol, 78% yield) as white solid. The spectroscopic data match those reported previously.[142] X-ray crystal structure was obtained. $^1$H NMR (400 MHz, $CDCl_3$): δ 7.26 (2H, d, *J* = 8.8 Hz), 6.92 (2H, d, *J* = 8.8 Hz), 6.01–5.92 (1H, m), 5.42 (1H, br s), 5.36–5.32 (2H, m), 4.70 (1H, dd, *J* = 7.6, 7.2 Hz), 4.55 (1H, d, *J* = 7.2 Hz), 3.82 (3H, s); Specific Rotation: $[\alpha]_D^{20}$ –50.0 (*c* 0.40, $CHCl_3$).

**(*4S*,*5R*)-5-(Hydroxymethyl)-4-(4-methoxyphenyl)oxazolidin-2-one ((*4S,5R*)-*epi*-cytoxazone):** (*4S,5R*)-epi-Cytoxazone was synthesized according to the previous report.[141] m.p. = 121–122 ºC. IR (neat): 3330 (br), 2925 (s), 2854 (m), 1742 (s), 1613 (w), 1552 (w), 1514 (s), 1457 (m), 1389 (m), 1304 (m), 1287 (m), 1249 (s), 1177 (m), 1097 (m), 1033 (s), 832 (w), 701 (w) $cm^{-1}$; $^1$H NMR (400 MHz, $CDCl_3$): δ 7.29 (2H, d, *J* = 8.8 Hz), 6.93 (2H, d, *J* = 8.8 Hz), 5.27 (1H, br s), 4.82 (1H, d, *J* = 7.2 Hz), 4.41–4.38 (1H, m),

(142) Miyata, O.; Koizumi, T.; Asai, H.; Iba, R.; Naito, T. *Tetrahedron*, **2004**, *60*, 3893–3914.

3.96 (1H, dd, $J$ = 13.0, 3.6 Hz), 3.82 (3H, s), 3.72 (1H, dd, $J$ = 13.0, 3.6 Hz), 2.06 (1H, br s); $^{13}$C NMR (100 MHz, $CDCl_3$): δ 160.3, 158.3, 130.9, 127.8, 114.8, 85.2, 61.7, 57.1, 55.5; HRMS (ESI+): Calcd for $C_{11}H_{14}N_1O_4$ $[M+H]^+$: 224.09228, Found: 224.09142. Specific Rotation: $[\alpha]_D^{25}$ –25.0 (*c* 0.50, MeOH). The previous reported specific rotation of the same compound: $[\alpha]_D^{28}$ –22.8 (*c* 0.50, MeOH).[143]

**(*R*)-1-Phenylbuta-2,3-dien-1-ol (3.116a):** The spectroscopic data match those reported previously.[121] $^1$H NMR (400 MHz, $CDCl_3$): δ 7.36–7.20 (m, 5H), 5.42 (ap q, 1H), 5.23–5.22 (m, 1H), 4.90–4.85 (m, 2H), 2.20 (br s, 1H). Specific Rotation: $[\alpha]_D^{20}$ –14.8 (*c* 1.35, $CHCl_3$) for an enantiomerically enriched sample of 76:24 er. Enantiomeric purity was determined by HPLC analysis in comparison with authentic racemic material (83:17 er shown, Chiralcel OD-H column, 95/5 hexanes/*i*-propanol, 1.0 mL/min, 220 nm).

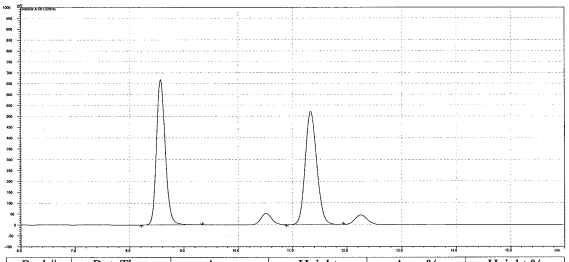

| Peak# | Ret. Time | Area | Height | Area % | Height % |
|---|---|---|---|---|---|
| 1 | 8.564 | 7638533 | 668614 | 49.705 | 56.237 |
| 2 | 11.329 | 7729252 | 520302 | 50.295 | 43.763 |
| Total | | 15367785 | 1188916 | 100.000 | 100.000 |

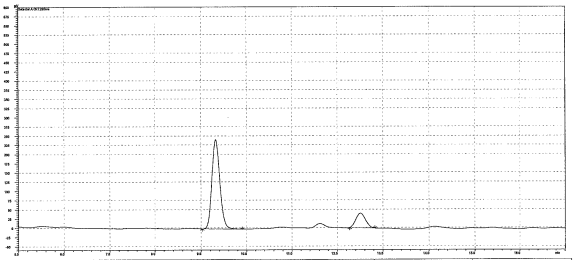

| Peak# | Ret. Time | Area | Height | Area % | Height % |
|---|---|---|---|---|---|
| 1 | 9.316 | 2920738 | 242297 | 83.252 | 85.953 |
| 2 | 12.503 | 587564 | 39599 | 16.748 | 14.047 |
| Total | | 3508302 | 281896 | 100.000 | 100.000 |

| Peak # | Time (min) | Area (%) | Peak # | Time (min) | Area (%) |
|---|---|---|---|---|---|
| 1 | 8.564 | 49.705 | 1 | 9.316 | 83.252 |
| 2 | 11.329 | 50.295 | 2 | 12.503 | 16.748 |

**(*S*)-2-(((*R*)-1-(2-Hydroxy-3-(triisopropylsilyl)phenyl)ethyl)amino)-*N*,*N*,3-trimethylbutanamide (3.115v):** IR (neat): 2960 (s), 2941 (s), 2862 (s), 1641(s), 1594 (m), 1578 (m), 1463 (s), 1421 (s), 1397 (s), 1264 (m), 1238 (m), 1124 (m), 1085 (m), 1019 (m), 920 (s), 810 (m), 755 (s), 673 (s), 652 (s), 560 (m), 510 (m), 502 (m), 402 (m)

(143) Kim, I. S.; Kim, J. D.; Ryu, C. B.; Zee, O. P.; Jung, Y. H. *Tetrahedron*, **2006**, *62*, 9349–9358.

$cm^{-1}$; $^{1}H$ NMR (400 MHz, $CDCl_3$): δ 10.77 (1H, br s), 7.28–7.26 (1H, m), 6.98–6.92 (1H, m), 6.76–6.71 (1H, m), 3.93 (1H, t, *J* = 6.8 Hz), 3.53 (1H, d, *J* = 5.6 Hz), 3.00 (3H, s), 2.98 (3H, s), 1.99–1.91 (1H, m), 1.55–1.44 (3H, m), 1.33 (3H, d, *J* = 6.8 Hz), 1.10–1.07 (18H, m), 1.00 (3H, d, *J* = 6.8 Hz), 0.94 (3H, d, *J* = 6.8 Hz); $^{13}C$ NMR (100 MHz, $CDCl_3$): δ 173.2, 162.8, 136.0, 128.9, 127.1, 122.4, 118.6, 100.7, 57.8, 55.6, 37.4, 35.9, 31.1, 19.6, 19.3, 18.3, 12.0; HRMS (ESI+): Calcd for $C_{24}H_{45}N_2O_2Si_1$ $[M+H]^+$: 421.324484, Found: 421.324585. Specific Rotation: $[\alpha]_D^{25}$ +13.3 (*c* 1.50, MeOH).

### *3.8.2. DFT Calculations*

Molecular modeling studies were conducted on the allyl as well as allenyl additions to a representative phosphinoylimine substrate (see Scheme 3.4.5). Ground states and transition states for the C–C bond forming step were located and the geometry optimized. The computed intrinsic Gibbs free energy barriers of the C–C bond forming step are ΔG = 6.0 kcal/mol (for allyl addition) and ΔG = 8.0 kcal/mol (for allenyl addition).

The reported Gibbs free energies were calculated as follows: All geometries were optimized with the B97-D functional and the 6-31G** basis set. Frequency calculations were carried out at the same level of theory. The ground state geometries have real-valued normal mode frequencies. The two optimized transition state geometries all have real-valued frequencies except one (for each structure), which has an imaginary value. Energy calculations were then carried out on these geometries using the larger 6-311++G** basis set. The Gibbs free energy (298.15 K and 1 atm) of each structure was computed as the sum of the energy (determined with the larger basis set) and the enthalpic and entropic contributions (through the use of the un-scaled frequencies). In

order to simulate solvent effects all calculations were performed with the polarizing continuum model (PCM) by the use of the parameters for toluene. The calculations were carried out with the Gaussian 09 computer program.[144]

**1. Allyl-containing complex 3.91:**

```
---------------------------------------
Cartesian coordinates (Angstroms):
---------------------------------------
C     1.764    -4.545    -2.370
O     0.267    -3.691    -0.210
N     2.230    -3.563    -1.382
C     1.402    -3.209    -0.355
C     3.222    -4.241     1.496
C     3.375    -2.178     2.849
C     3.555    -3.021    -1.687
C     2.400    -3.013     1.982
C     1.905    -2.204     0.710
C     1.214    -3.548     2.814
B     0.361    -0.331    -0.364
N     0.734    -1.253     0.939
C     0.908    -0.264     2.074
O     1.396     0.647    -0.534
C     2.023     0.708     1.779
C     2.256     1.080     0.440
C     2.834     1.227     2.799
C     2.613     2.931    -2.137
C     3.368     1.882     0.067
C     3.729     2.136    -1.412
C     3.882     2.092     2.473
C     3.953     0.774    -2.125
C     4.149     2.386     1.126
C     5.036     2.947    -1.555
C     0.121    -1.035    -1.839
C    -0.225     0.021    -2.832
```

(144) Gaussian 09, Revision D.01, Frisch, M. J.; Trucks, G. W.; Schlegel, H. B.; Scuseria, G. E.; Robb, M. A.; Cheeseman, J. R.; Scalmani, G.; Barone, V.; Mennucci, B.; Petersson, G. A.; Nakatsuji, H.; Caricato, M.; Li, X.; Hratchian, H. P.; Izmaylov, A. F.; Bloino, J.; Zheng, G.; Sonnenberg, J. L.; Hada, M.; Ehara, M.; Toyota, K.; Fukuda, R.; Hasegawa, J.; Ishida, M.; Nakajima, T.; Honda, Y.; Kitao, O.; Nakai, H.; Vreven, T.; Montgomery, J. A., Jr.; Peralta, J. E.; Ogliaro, F.; Bearpark, M.; Heyd, J. J.; Brothers, E.; Kudin, K. N.; Staroverov, V. N.; Kobayashi, R.; Normand, J.; Raghavachari, K.; Rendell, A.; Burant, J. C.; Iyengar, S. S.; Tomasi, J.; Cossi, M.; Rega, N.; Millam, N. J.; Klene, M.; Knox, J. E.; Cross, J. B.; Bakken, V.; Adamo, C.; Jaramillo, J.; Gomperts, R.; Stratmann, R. E.; Yazyev, O.; Austin, A. J.; Cammi, R.; Pomelli, C.; Ochterski, J. W.; Martin, R. L.; Morokuma, K.; Zakrzewski, V. G.; Voth, G. A.; Salvador, P.; Dannenberg, J. J.; Dapprich, S.; Daniels, A. D.; Farkas, Ö.; Foresman, J. B.; Ortiz, J. V.; Cioslowski, J.; Fox, D. J. Gaussian, Inc., Wallingford CT, 2009.

| | | | |
|---|---|---|---|
| C | -1.444 | 0.190 | -3.393 |
| H | 1.633 | -4.054 | -3.347 |
| H | 0.813 | -4.972 | -2.041 |
| H | 2.517 | -5.341 | -2.472 |
| H | 3.630 | -4.751 | 2.380 |
| H | 4.066 | -3.939 | 0.861 |
| H | 2.604 | -4.963 | 0.948 |
| H | 2.906 | -1.357 | 3.396 |
| H | 4.178 | -1.751 | 2.229 |
| H | 3.837 | -2.842 | 3.594 |
| H | 3.532 | -2.516 | -2.666 |
| H | 4.282 | -3.846 | -1.737 |
| H | 3.897 | -2.307 | -0.937 |
| H | 2.722 | -1.569 | 0.360 |
| H | 0.592 | -2.751 | 3.242 |
| H | 1.608 | -4.146 | 3.648 |
| H | 0.567 | -4.182 | 2.196 |
| H | -0.067 | 0.230 | 2.170 |
| H | 1.081 | -0.803 | 3.005 |
| H | 2.643 | 0.943 | 3.835 |
| H | 2.516 | 3.935 | -1.704 |
| H | 1.641 | 2.433 | -2.062 |
| H | 2.878 | 3.038 | -3.200 |
| H | 4.514 | 2.510 | 3.256 |
| H | 4.759 | 0.211 | -1.630 |
| H | 4.251 | 0.954 | -3.169 |
| H | 3.042 | 0.165 | -2.123 |
| H | 5.002 | 3.021 | 0.898 |
| H | 5.888 | 2.428 | -1.091 |
| H | 4.944 | 3.945 | -1.101 |
| H | 5.257 | 3.080 | -2.624 |
| H | -0.628 | -1.833 | -1.820 |
| H | 1.089 | -1.475 | -2.120 |
| H | 0.566 | 0.739 | -3.064 |
| H | -1.632 | 1.004 | -4.095 |
| H | -2.258 | -0.509 | -3.203 |
| H | -0.102 | -1.828 | 1.178 |
| H | -5.666 | -0.729 | -3.229 |
| H | -4.652 | 0.245 | -1.179 |
| C | -4.902 | -1.285 | -2.685 |
| C | -4.326 | -0.732 | -1.532 |
| H | -4.943 | -2.978 | -4.032 |
| C | -4.495 | -2.552 | -3.134 |
| C | -3.342 | -1.456 | -0.827 |
| C | -3.521 | -3.276 | -2.426 |
| C | -2.944 | -2.736 | -1.269 |
| H | -3.214 | -4.263 | -2.772 |
| H | -2.182 | -3.287 | -0.717 |

```
H    -1.855     3.178    -2.674
C    -1.206     3.518    -1.867
C     0.467     4.365     0.232
C    -0.652     4.799    -1.891
C    -0.899     2.633    -0.805
C    -0.066     3.074     0.249
C     0.181     5.226    -0.840
H    -0.873     5.471    -2.720
C    -1.598     1.363    -0.693
H     0.127     2.414     1.090
H     0.600     6.233    -0.855
H     1.106     4.695     1.051
N    -1.165     0.298    -0.028
P    -2.478    -0.769     0.606
O    -1.853    -1.811     1.507
C    -3.583     0.416     1.431
C    -5.298     2.089     2.897
C    -4.950     0.087     1.562
C    -3.077     1.577     2.055
C    -3.936     2.411     2.782
C    -5.803     0.927     2.291
H    -5.344    -0.814     1.093
H    -2.023     1.835     1.970
H    -3.543     3.310     3.257
H    -6.859     0.675     2.383
H    -5.965     2.741     3.461
H    -2.636     1.367    -1.045

                     1                      2                      3
                     A                      A                      A
 Frequencies --    22.9047                30.0720
34.5794
 Red. masses --     5.3414                 4.9097
4.6970
 Zero-point correction=                           0.841898
(Hartree/Particle)
 Thermal correction to Energy=                    0.890741
 Thermal correction to Enthalpy=                  0.891685
 Thermal correction to Gibbs Free Energy=         0.762716
 Sum of electronic and zero-point Energies=          -2347.595031
 Sum of electronic and thermal Energies=             -2347.546188
 Sum of electronic and thermal Enthalpies=           -2347.545244
 Sum of electronic and thermal Free Energies=        -2347.674213

         Item               Value     Threshold  Converged?
 Maximum Force            0.000041     0.000450     YES
 RMS     Force            0.000006     0.000300     YES
E(RB97D/6-31G**) =               -2348.43692942 Hartree
E(RB97D/6-311++G**//6-31G**) =   -2348.90463337 Hartree
```

**Transition state 3.92 for allyl addition**

```
---------------------------------------
 Cartesian coordinates (Angstroms):
---------------------------------------
C     1.974    -4.424    -2.364
O     0.350    -3.572    -0.293
N     2.368    -3.421    -1.366
C     1.492    -3.091    -0.369
C     3.153    -4.213     1.546
C     3.358    -2.162     2.907
C     3.733    -2.923    -1.556
C     2.371    -2.952     2.013
C     1.942    -2.111     0.735
C     1.141    -3.444     2.807
B     0.380    -0.212    -0.339
N     0.771    -1.159     0.940
C     0.958    -0.165     2.075
O     1.448     0.730    -0.534
C     2.085     0.791     1.776
C     2.311     1.168     0.438
C     2.908     1.297     2.792
C     2.607     3.061    -2.105
C     3.413     1.979     0.061
C     3.746     2.266    -1.419
C     3.957     2.160     2.463
C     3.977     0.921    -2.162
C     4.208     2.470     1.116
C     5.040     3.097    -1.568
C     0.222    -0.958    -1.910
C    -0.092     0.176    -2.741
C    -1.386     0.676    -2.852
H     2.025    -3.976    -3.368
H     0.956    -4.764    -2.157
H     2.669    -5.277    -2.323
H     3.511    -4.742     2.439
H     4.029    -3.948     0.938
H     2.518    -4.905     0.977
H     2.920    -1.303     3.422
H     4.208    -1.795     2.313
H     3.751    -2.839     3.680
H     3.834    -2.536    -2.581
H     4.452    -3.746    -1.420
H     3.985    -2.120    -0.861
H     2.778    -1.475     0.437
H     0.555    -2.630     3.254
H     1.484    -4.092     3.626
H     0.473    -4.021     2.156
```

| | | | |
|---|---|---|---|
| H | -0.009 | 0.342 | 2.174 |
| H | 1.127 | -0.708 | 3.004 |
| H | 2.724 | 1.008 | 3.828 |
| H | 2.485 | 4.045 | -1.631 |
| H | 1.647 | 2.540 | -2.041 |
| H | 2.861 | 3.216 | -3.165 |
| H | 4.599 | 2.569 | 3.243 |
| H | 4.808 | 0.367 | -1.700 |
| H | 4.241 | 1.124 | -3.211 |
| H | 3.080 | 0.291 | -2.142 |
| H | 5.056 | 3.110 | 0.886 |
| H | 5.907 | 2.582 | -1.128 |
| H | 4.941 | 4.085 | -1.094 |
| H | 5.241 | 3.253 | -2.638 |
| H | -0.551 | -1.731 | -1.868 |
| H | 1.211 | -1.371 | -2.127 |
| H | 0.736 | 0.800 | -3.081 |
| H | -1.565 | 1.550 | -3.476 |
| H | -2.225 | -0.010 | -2.740 |
| H | -0.073 | -1.721 | 1.192 |
| H | -5.712 | -0.779 | -3.104 |
| H | -4.653 | 0.290 | -1.124 |
| C | -4.913 | -1.295 | -2.572 |
| C | -4.315 | -0.691 | -1.457 |
| H | -4.955 | -3.032 | -3.863 |
| C | -4.488 | -2.565 | -2.996 |
| C | -3.286 | -1.363 | -0.763 |
| C | -3.470 | -3.239 | -2.299 |
| C | -2.868 | -2.646 | -1.181 |
| H | -3.149 | -4.229 | -2.623 |
| H | -2.080 | -3.162 | -0.635 |
| H | -1.814 | 3.478 | -2.669 |
| C | -1.173 | 3.726 | -1.824 |
| C | 0.433 | 4.411 | 0.370 |
| C | -0.660 | 5.022 | -1.709 |
| C | -0.869 | 2.745 | -0.855 |
| C | -0.079 | 3.114 | 0.252 |
| C | 0.151 | 5.369 | -0.615 |
| H | -0.897 | 5.764 | -2.472 |
| C | -1.512 | 1.400 | -0.908 |
| H | 0.126 | 2.386 | 1.030 |
| H | 0.551 | 6.380 | -0.529 |
| H | 1.052 | 4.666 | 1.230 |
| N | -1.079 | 0.377 | -0.083 |
| P | -2.381 | -0.609 | 0.619 |
| O | -1.784 | -1.639 | 1.558 |
| C | -3.480 | 0.606 | 1.405 |
| C | -5.177 | 2.343 | 2.818 |

```
C    -4.831     0.255     1.620
C    -2.981     1.822     1.916
C    -3.831     2.688     2.616
C    -5.674     1.126     2.323
H    -5.221    -0.688     1.238
H    -1.942     2.098     1.757
H    -3.443     3.631     3.001
H    -6.718     0.854     2.482
H    -5.837     3.019     3.361
H    -2.600     1.471    -1.014
```

```
                     1                      2                      3
                     A                      A                      A
 Frequencies --  -272.1889               20.0622
28.6402
 Red. masses --     8.3490                5.3268
3.4945
 Zero-point correction=                           0.843482
(Hartree/Particle)
 Thermal correction to Energy=                    0.890816
 Thermal correction to Enthalpy=                  0.891760
 Thermal correction to Gibbs Free Energy=         0.766165
 Sum of electronic and zero-point Energies=          -2347.588268
 Sum of electronic and thermal Energies=             -2347.540935
 Sum of electronic and thermal Enthalpies=           -2347.539990
 Sum of electronic and thermal Free Energies=        -2347.665586

          Item               Value     Threshold  Converged?
 Maximum Force            0.000001     0.000450     YES
 RMS     Force            0.000000     0.000300     YES


E(RB97D/6-31G**) =               -2348.43175047 Hartree
E(RB97D/6-311++G**//6-31G**) =   -2348.89858645 Hartree
```

**2. Propargyl-containing complex 3.93:**

```
---------------------------------------
Cartesian coordinates (Angstroms):
---------------------------------------
H    -0.821     5.794    -2.101
C    -0.589     5.056    -1.333
H    -1.953     3.573    -2.118
H     0.828     6.337    -0.307
C    -1.225     3.815    -1.344
C     0.343     5.360    -0.321
C    -0.901     2.842    -0.366
C     0.637     4.418     0.678
C     0.020     3.165     0.657
H     1.343     4.657     1.471
```

| | | | |
|---|---|---|---|
| H | 0.211 | 2.451 | 1.452 |
| C | -1.669 | 1.611 | -0.312 |
| H | -2.721 | 1.719 | -0.595 |
| N | -1.278 | 0.445 | 0.178 |
| H | -4.211 | -3.855 | -3.681 |
| H | -3.298 | -4.929 | -1.621 |
| C | -3.912 | -3.239 | -2.832 |
| C | -3.400 | -3.846 | -1.674 |
| C | -4.041 | -1.842 | -2.906 |
| H | -4.433 | -1.374 | -3.808 |
| C | -3.011 | -3.059 | -0.581 |
| H | -2.582 | -3.511 | 0.309 |
| C | -3.657 | -1.046 | -1.821 |
| C | -3.142 | -1.657 | -0.658 |
| H | -5.463 | -0.501 | 0.080 |
| O | -1.969 | -1.496 | 1.876 |
| P | -2.584 | -0.683 | 0.758 |
| C | -5.228 | 0.287 | 0.792 |
| C | -3.909 | 0.452 | 1.261 |
| H | -7.259 | 1.018 | 0.886 |
| C | -6.240 | 1.145 | 1.250 |
| C | -3.612 | 1.468 | 2.199 |
| H | -2.597 | 1.590 | 2.576 |
| C | -5.941 | 2.159 | 2.172 |
| C | -4.628 | 2.319 | 2.649 |
| H | -6.730 | 2.824 | 2.524 |
| H | -4.398 | 3.103 | 3.370 |
| H | -3.745 | 0.037 | -1.886 |
| C | 1.262 | -4.429 | -2.342 |
| O | 0.017 | -3.604 | -0.014 |
| N | 1.854 | -3.493 | -1.377 |
| C | 1.142 | -3.141 | -0.268 |
| C | 3.046 | -4.231 | 1.448 |
| C | 3.379 | -2.171 | 2.773 |
| C | 3.166 | -2.987 | -1.787 |
| C | 2.311 | -2.970 | 1.986 |
| C | 1.757 | -2.149 | 0.746 |
| C | 1.172 | -3.450 | 2.911 |
| B | 0.199 | -0.222 | -0.238 |
| N | 0.641 | -1.151 | 1.047 |
| C | 0.952 | -0.154 | 2.147 |
| O | 1.235 | 0.730 | -0.488 |
| C | 2.092 | 0.748 | 1.749 |
| C | 2.208 | 1.117 | 0.393 |
| C | 3.027 | 1.220 | 2.681 |
| C | 2.337 | 2.952 | -2.195 |
| C | 3.306 | 1.874 | -0.090 |
| C | 3.512 | 2.135 | -1.598 |

```
C     4.077     2.035     2.251
C     3.630     0.774    -2.338
C     4.216     2.331     0.884
C     4.812     2.926    -1.871
C    -0.125    -0.959    -1.690
C    -0.672     0.010    -2.624
C    -1.169     0.880    -3.323
H     1.207    -3.944    -3.330
H     0.259    -4.708    -2.010
H     1.894    -5.326    -2.423
H     3.497    -4.756     2.301
H     3.853    -3.963     0.751
H     2.361    -4.928     0.948
H     2.976    -1.346     3.364
H     4.139    -1.756     2.094
H     3.881    -2.854     3.473
H     3.065    -2.360    -2.688
H     3.819    -3.840    -2.026
H     3.649    -2.401    -1.004
H     2.569    -1.547     0.332
H     0.613    -2.623     3.370
H     1.606    -4.048     3.725
H     0.460    -4.070     2.355
H     0.011     0.392     2.301
H     1.161    -0.687     3.075
H     2.929     0.942     3.731
H     2.259     3.928    -1.698
H     1.382     2.429    -2.093
H     2.531     3.124    -3.266
H     4.806     2.417     2.965
H     4.468     0.187    -1.932
H     3.820     0.955    -3.407
H     2.706     0.192    -2.244
H     5.067     2.932     0.573
H     5.700     2.389    -1.506
H     4.784     3.920    -1.401
H     4.919     3.065    -2.956
H    -0.787    -1.829    -1.608
H     0.842    -1.316    -2.077
H    -0.189    -1.689     1.369
H    -1.563     1.595    -4.014

                     1                     2                     3
                     A                     A                     A
 Frequencies --    22.1792               30.1749
34.3999
 Red. masses --     5.3325                4.5870
4.4346
```

```
 Zero-point correction=                           0.818524
(Hartree/Particle)
 Thermal correction to Energy=                    0.867197
 Thermal correction to Enthalpy=                  0.868142
 Thermal correction to Gibbs Free Energy=         0.739559
 Sum of electronic and zero-point Energies=          -2346.359938
 Sum of electronic and thermal Energies=             -2346.311264
 Sum of electronic and thermal Enthalpies=           -2346.310320
 Sum of electronic and thermal Free Energies=        -2346.438902

         Item               Value     Threshold  Converged?
 Maximum Force            0.000024     0.000450     YES
 RMS     Force            0.000003     0.000300     YES

E(RB97D/6-31G**) =               -2347.17846109 Hartree
E(RB97D/6-311++G**//6-31G**) =   -2347.65007469 Hartree
```

**Transition state 3.94 for allenyl addition**

```
---------------------------------------
Cartesian coordinates (Angstroms):
---------------------------------------
H    -0.790     5.859    -2.155
C    -0.604     5.097    -1.398
H    -1.748     3.599    -2.437
H     0.605     6.395    -0.151
C    -1.145     3.818    -1.557
C     0.180     5.399    -0.270
C    -0.905     2.814    -0.594
C     0.402     4.416     0.706
C    -0.145     3.137     0.548
H     0.997     4.638     1.591
H    -0.002     2.390     1.322
C    -1.588     1.496    -0.684
H    -2.668     1.589    -0.837
N    -1.207     0.442     0.118
H    -4.688    -3.220    -3.844
H    -3.175    -4.427    -2.267
C    -4.298    -2.708    -2.964
C    -3.446    -3.388    -2.079
C    -4.660    -1.374    -2.714
H    -5.332    -0.852    -3.395
C    -2.945    -2.736    -0.943
H    -2.277    -3.253    -0.255
C    -4.161    -0.713    -1.584
C    -3.297    -1.392    -0.699
H    -5.443    -0.607     0.934
O    -1.964    -1.548     1.740
P    -2.534    -0.572     0.730
```

| | | | |
|---|---|---|---|
| C | -5.094 | 0.317 | 1.394 |
| C | -3.720 | 0.638 | 1.383 |
| H | -7.072 | 0.945 | 1.993 |
| C | -6.010 | 1.194 | 1.990 |
| C | -3.272 | 1.834 | 1.986 |
| H | -2.214 | 2.090 | 1.979 |
| C | -5.563 | 2.387 | 2.579 |
| C | -4.195 | 2.706 | 2.578 |
| H | -6.279 | 3.068 | 3.039 |
| H | -3.846 | 3.632 | 3.035 |
| H | -4.460 | 0.315 | -1.382 |
| C | 1.661 | -4.428 | -2.211 |
| O | 0.189 | -3.627 | -0.012 |
| N | 2.113 | -3.425 | -1.237 |
| C | 1.309 | -3.115 | -0.177 |
| C | 3.110 | -4.142 | 1.663 |
| C | 3.317 | -2.063 | 2.983 |
| C | 3.465 | -2.928 | -1.509 |
| C | 2.312 | -2.897 | 2.149 |
| C | 1.803 | -2.099 | 0.874 |
| C | 1.136 | -3.407 | 3.010 |
| B | 0.209 | -0.219 | -0.172 |
| N | 0.630 | -1.151 | 1.109 |
| C | 0.857 | -0.138 | 2.217 |
| O | 1.280 | 0.688 | -0.441 |
| C | 1.970 | 0.814 | 1.856 |
| C | 2.162 | 1.158 | 0.502 |
| C | 2.806 | 1.362 | 2.839 |
| C | 2.354 | 2.963 | -2.098 |
| C | 3.244 | 1.973 | 0.080 |
| C | 3.536 | 2.230 | -1.414 |
| C | 3.837 | 2.228 | 2.463 |
| C | 3.794 | 0.873 | -2.125 |
| C | 4.054 | 2.503 | 1.104 |
| C | 4.798 | 3.100 | -1.612 |
| C | -0.009 | -1.057 | -1.706 |
| C | -0.655 | -0.086 | -2.492 |
| C | -1.366 | 0.927 | -2.674 |
| H | 1.702 | -3.993 | -3.221 |
| H | 0.637 | -4.732 | -1.975 |
| H | 2.326 | -5.305 | -2.177 |
| H | 3.527 | -4.647 | 2.545 |
| H | 3.947 | -3.858 | 1.010 |
| H | 2.473 | -4.863 | 1.135 |
| H | 2.870 | -1.228 | 3.529 |
| H | 4.111 | -1.655 | 2.341 |
| H | 3.785 | -2.723 | 3.727 |
| H | 3.495 | -2.491 | -2.518 |

```
H     4.179    -3.766    -1.471
H     3.785    -2.170    -0.792
H     2.613    -1.463     0.514
H     0.536    -2.597     3.446
H     1.539    -4.005     3.840
H     0.468    -4.037     2.410
H    -0.109     0.364     2.344
H     1.065    -0.665     3.148
H     2.647     1.102     3.886
H     2.166     3.929    -1.609
H     1.433     2.374    -2.060
H     2.611     3.151    -3.152
H     4.489     2.668     3.218
H     4.643     0.350    -1.659
H     4.039     1.055    -3.182
H     2.910     0.226    -2.080
H     4.887     3.149     0.837
H     5.691     2.626    -1.179
H     4.676     4.096    -1.160
H     4.970     3.235    -2.689
H    -0.597    -1.977    -1.607
H     1.018    -1.277    -2.023
H    -0.205    -1.709     1.390
H    -1.919     1.568    -3.334

                     1                      2                      3
                     A                      A                      A
 Frequencies --  -291.3849               19.4144
29.9674
 Red. masses --     9.2688                5.3488
3.9122
 Zero-point correction=                           0.818970
(Hartree/Particle)
 Thermal correction to Energy=                    0.866322
 Thermal correction to Enthalpy=                  0.867266
 Thermal correction to Gibbs Free Energy=         0.741623
 Sum of electronic and zero-point Energies=          -2346.351049
 Sum of electronic and thermal Energies=             -2346.303697
 Sum of electronic and thermal Enthalpies=           -2346.302753
 Sum of electronic and thermal Free Energies=        -2346.428397

         Item               Value     Threshold  Converged?
 Maximum Force            0.000003     0.000450     YES
 RMS     Force            0.000001     0.000300     YES

E(RB97D/6-31G**) =              -2347.17001905 Hartree
E(RB97D/6-311++G**//6-31G**) =  -2347.63938652 Hartree
```

### *3.8.3. Kinetic Studies*

**General Procedure for The Enantioselective Allene Additions to Boc–imines Applied in React-IR Measurements**: **Preparation of solution A:** In a $N_2$-filled glove box, 20 μL aminoalcohol (**3.58**) solution (0.010 M in toluene, $2.0x10^{-4}$ mmol, 0.10 mol %) was charged into an oven-dried vial, followed by addition of 0.80 mL NaO*t*-Bu solution (0.013 M in toluene, 0.010 mmol, 5.0 mol %) and *tert*-butyl benzylidenecarbamate (**3.96a**) (41 mg, 0.2 mmol, 1.0 equiv). The solution was diluted by addition of 0.18 mL toluene and the vial was sealed with a cap (phenolic open top cap with a white silicon septum) and taken out of the glove box.

**Preparation of solution B:** In a $N_2$-filled glove box, allenylB(pin) (50 mg, 0.30 mmol, 1.5 equiv) and toluene (1.0 mL) were introduced into an oven-dried vial, followed by addition of *i*-propanol (35 μL, 0.46 mmol, 2.3 equiv). The vial was sealed with a cap (phenolic open top cap with a white silicon septum) and taken out of the glove box.

**React-IR measurements:** Measurements were performed on a React-IR iC10 instrument equipped with a 6.3 mm AgX DiComp Fiber probe. Spectra were recorded from 2000 $cm^{-1}$ to 650 $cm^{-1}$ at standard resolution (8 $cm^{-1}$) in 15 s intervals. The probe, which had been dried with a heat gun (Tmax = 200 °C), was inserted into a flame-dried vial through a 14/20 rubber septum with a 4 mm diameter hole. The rubber septum was further sealed with electrical tape. The vial was allowed to purge with $N_2$ for 15 min. Then solution A was transferred into the empty vial through a syringe. After 3 min, the reaction was initiated through addition of solution B through a syringe. All the reactions were stopped after 40 min except those for **3.96e (**R = *p*-$CF_3$) (the reaction time was 35 min) and **3.96f** (R = *p*-MeO) (the reaction time was 120 min). 400 MHz $^1$H NMR was used to measure the conversions of the reactions.

**Analysis:** The increase in the concentration of *i*-PrO–B(pin) or the decrease in the concentration of imines were monitored as a function of time [min]. For reactions with Boc–imines **3.96a** ( R = H) or **3.96d** (R = *m*-Br ), the IR absorption frequencies of *i*-PrO–B(pin) at 1457–1437 $cm^{-1}$ were used. For reactions with Boc–imine **3.96e** (R = *p*-$CF_3$), frequencies of the imine at 1280–1248 $cm^{-1}$ was used. For reactions with Boc–imine **3.96f** (R = *p*-MeO), frequencies of the imine at 1050–1020 $cm^{-1}$ was used. The intensities were calibrated as following: the difference between the intensities of the selected frequencies at the start of the reaction and the intensities at the end of the reaction was set to the conversion [%] determined by 400 MHz $^1$H NMR. The conversions of the reactions (vs time [min]) were plotted in Figure 3.4.1. Each curve was the average result of three experiments. Curves were fitted with a 2$^{nd}$-order polynomial function through the use of Microsoft Excel (Table 3.7.1). The relative rates $k_X$ (for time → 0 min) can be read directly from the polynomial equations (values in red), which are used for the generation of the Hammett plot in Scheme 3.4.14 (plot of $\log(k_X/k_H)$ vs σ constant). Linear regression results in a ρ value of +1.7 (slope), indicating there is a significant electronic substituent effect on the rate of the reactions and thus the C–C bond forming step is likely the rate-limiting step.

**Table 3.8.1. The Polynomial Equation and $k_X$ of Each Reaction**

| substrate | polynomial equation | $k_X$ |
|---|---|---|
| R = *p*-$CF_3$ | y = -7.9854E-04$x^2$ + 5.4983E-02x - 3.8919E-02 | 0.0550 |
| R = *m*-Br | y = -1.1499E-04$x^2$ + 1.9045E-02x - 1.4105E-02 | 0.0190 |
| R = H | y = -1.7042E-05$x^2$ + 1.1706E-02x + 1.8154E-03 | 0.0117 |
| R = *p*-MeO | y = -4.5273E-06$x^2$ + 1.4440E-03x + 3.2346E-03 | 0.00144 |

### *3.8.4. Data of X-ray Structures*

**(*R*)-*tert*-Butyl (1-(2-chlorophenyl)buta-2,3-dien-1-yl)carbamate (3.90b):**

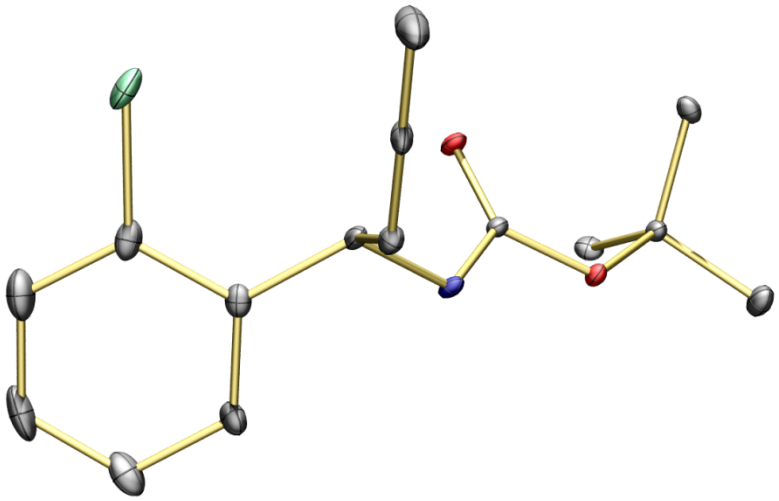

***Table 1.*** Crystal data and structure refinement for $C_{15}H_{18}ClNO_2$

| | | |
|---|---|---|
| Identification code | $C_{15}H_{18}ClNO_2$ | |
| Empirical formula | $C_{15}H_{18}ClNO_2$ | |
| Formula weight | 279.75 | |
| Temperature | 100(2) K | |
| Wavelength | 1.54178 Å | |
| Crystal system | Monoclinic | |
| Space group | P 21 | |
| Unit cell dimensions | a = 10.1012(4) Å | α= 90°. |
| | b = 9.8645(4) Å | β= 92.917(3)°. |
| | c = 14.7218(6) Å | γ = 90°. |
| Volume | 1465.03(10) $Å^3$ | |
| Z | 4 | |
| Density (calculated) | 1.268 $Mg/m^3$ | |
| Absorption coefficient | 2.288 $mm^{-1}$ | |
| F(000) | 592 | |
| Crystal size | 0.560 x 0.050 x 0.020 $mm^3$ | |
| Theta range for data collection | 5.400 to 66.297°. | |
| Index ranges | -11<=h<=8, -11<=k<=11, -17<=l<=17 | |
| Reflections collected | 13797 | |
| Independent reflections | 4861 [R(int) = 0.0861] | |
| Completeness to theta = 66.000° | 98.3% | |

| | |
|---|---|
| Absorption correction | Semi-empirical from equivalents |
| Max. and min. transmission | 0.7452 and 0.6101 |
| Refinement method | Full-matrix least-squares on $F^2$ |
| Data / restraints / parameters | 4861 / 99 / 367 |
| Goodness-of-fit on $F^2$ | 1.030 |
| Final R indices [I>2sigma(I)] | R1 = 0.0597, wR2 = 0.1402 |
| R indices (all data) | R1 = 0.0787, wR2 = 0.1505 |
| Absolute structure parameter | 0.066(17) |
| Extinction coefficient | na |
| Largest diff. peak and hole | 0.331 and -0.415 e. $Å^{-3}$ |

***Table 2.*** Atomic coordinates ($x10^4$) and equivalent isotropic displacement parameters ($Å^2 x\ 10^3$) for $C_{15}H_{18}ClNO_2$. U(eq) is defined as one third of the trace of the orthogonalized $U^{ij}$ tensor

| | x | y | z | U(eq) |
|---|---|---|---|---|
| Cl(1) | 10084(1) | 5057(2) | 739(1) | 26(1) |
| O(1) | 10734(3) | 5098(5) | 3865(3) | 22(1) |
| O(2) | 9256(3) | 4423(5) | 4895(3) | 20(1) |
| N(1) | 8545(4) | 4821(5) | 3480(3) | 19(1) |
| C(1) | 8914(5) | 3878(6) | 1065(4) | 19(1) |
| C(2) | 8598(6) | 2837(7) | 456(4) | 25(2) |
| C(3) | 7670(6) | 1873(7) | 675(5) | 29(2) |
| C(4) | 7092(6) | 1961(7) | 1500(4) | 26(2) |
| C(5) | 7420(6) | 3005(7) | 2108(4) | 23(1) |
| C(6) | 8340(5) | 3994(6) | 1903(4) | 19(1) |
| C(7) | 8633(5) | 5177(7) | 2528(4) | 18(1) |
| C(8) | 7693(6) | 6338(7) | 2270(4) | 22(1) |
| C(9) | 8031(6) | 7431(7) | 1839(4) | 25(1) |
| C(10) | 8374(7) | 8495(8) | 1400(5) | 35(2) |
| C(11) | 9615(5) | 4812(6) | 4072(4) | 18(1) |
| C(12) | 10232(5) | 4324(7) | 5678(4) | 18(1) |
| C(13) | 9393(5) | 3739(7) | 6408(4) | 23(2) |
| C(14) | 10740(6) | 5723(7) | 5944(4) | 26(2) |
| C(15) | 11344(5) | 3355(7) | 5479(4) | 23(1) |
| Cl(2) | 4812(2) | 4568(2) | 717(1) | 40(1) |
| O(3) | 5729(3) | 4647(5) | 3847(3) | 24(1) |
| O(4) | 4289(3) | 5127(5) | 4951(3) | 18(1) |
| N(2) | 3528(4) | 4943(6) | 3521(3) | 18(1) |
| C(16) | 3671(7) | 3490(7) | 1193(5) | 32(2) |
| C(17) | 3278(9) | 2347(8) | 713(6) | 47(2) |
| C(18) | 2318(9) | 1504(8) | 1060(6) | 52(2) |
| C(19) | 1787(8) | 1803(8) | 1879(6) | 45(2) |
| C(20) | 2214(7) | 2946(7) | 2361(5) | 31(2) |
| C(21) | 3169(6) | 3802(7) | 2039(4) | 24(1) |

| | | | | |
|---|---|---|---|---|
| C(22) | 3628(5) | 5057(7) | 2544(4) | 21(1) |
| C(23) | 2849(6) | 6299(7) | 2201(4) | 22(2) |
| C(24) | 3397(6) | 7304(7) | 1811(4) | 26(2) |
| C(25) | 3977(9) | 8306(9) | 1417(6) | 50(2) |
| C(26) | 4618(5) | 4885(6) | 4089(4) | 16(1) |
| C(27) | 5286(5) | 5079(7) | 5719(4) | 19(1) |
| C(28) | 5781(6) | 3652(7) | 5852(4) | 24(1) |
| C(29) | 4488(6) | 5549(8) | 6502(4) | 33(2) |
| C(30) | 6390(6) | 6102(7) | 5573(4) | 24(2) |

***Table 3.*** Bond lengths [Å] and angles [°] for $C_{15}H_{18}ClNO_2$

| | |
|---|---|
| Cl(1)-C(1) | 1.743(6) |
| O(1)-C(11) | 1.218(6) |
| O(2)-C(11) | 1.338(7) |
| O(2)-C(12) | 1.482(7) |
| N(1)-C(11) | 1.353(7) |
| N(1)-C(7) | 1.451(7) |
| N(1)-H(1N) | 0.88(3) |
| C(1)-C(2) | 1.389(9) |
| C(1)-C(6) | 1.395(8) |
| C(2)-C(3) | 1.385(9) |
| C(2)-H(2) | 0.9500 |
| C(3)-C(4) | 1.377(8) |
| C(3)-H(3) | 0.9500 |
| C(4)-C(5) | 1.393(9) |
| C(4)-H(4) | 0.9500 |
| C(5)-C(6) | 1.392(8) |
| C(5)-H(5) | 0.9500 |
| C(6)-C(7) | 1.507(8) |
| C(7)-C(8) | 1.523(9) |
| C(7)-H(7) | 0.99(3) |
| C(8)-C(9) | 1.306(9) |
| C(8)-H(8) | 0.9500 |

| | |
|---|---|
| C(9)-C(10) | 1.289(10) |
| C(10)-H(10A) | 0.96(3) |
| C(10)-H(10B) | 0.96(3) |
| C(12)-C(13) | 1.515(8) |
| C(12)-C(15) | 1.516(8) |
| C(12)-C(14) | 1.517(9) |
| C(13)-H(13A) | 0.9800 |
| C(13)-H(13B) | 0.9800 |
| C(13)-H(13C) | 0.9800 |
| C(14)-H(14A) | 0.9800 |
| C(14)-H(14B) | 0.9800 |
| C(14)-H(14C) | 0.9800 |
| C(15)-H(15A) | 0.9800 |
| C(15)-H(15B) | 0.9800 |
| C(15)-H(15C) | 0.9800 |
| Cl(2)-C(16) | 1.742(7) |
| O(3)-C(26) | 1.217(6) |
| O(4)-C(26) | 1.349(6) |
| O(4)-C(27) | 1.475(6) |
| N(2)-C(26) | 1.350(7) |
| N(2)-C(22) | 1.451(7) |
| N(2)-H(2N) | 0.87(3) |
| C(16)-C(17) | 1.377(10) |
| C(16)-C(21) | 1.404(9) |
| C(17)-C(18) | 1.394(11) |
| C(17)-H(17) | 0.9500 |
| C(18)-C(19) | 1.377(11) |
| C(18)-H(18) | 0.9500 |
| C(19)-C(20) | 1.389(10) |
| C(19)-H(19) | 0.9500 |
| C(20)-C(21) | 1.384(9) |
| C(20)-H(20) | 0.9500 |
| C(21)-C(22) | 1.505(9) |
| C(22)-C(23) | 1.527(9) |
| C(22)-H(22) | 1.00(3) |

| | |
|---|---|
| C(23)-C(24) | 1.286(9) |
| C(23)-H(23) | 0.9500 |
| C(24)-C(25) | 1.300(10) |
| C(25)-H(25A) | 0.97(3) |
| C(25)-H(25B) | 0.95(3) |
| C(27)-C(28) | 1.504(9) |
| C(27)-C(29) | 1.512(7) |
| C(27)-C(30) | 1.527(8) |
| C(28)-H(28A) | 0.9800 |
| C(28)-H(28B) | 0.9800 |
| C(28)-H(28C) | 0.9800 |
| C(29)-H(29A) | 0.9800 |
| C(29)-H(29B) | 0.9800 |
| C(29)-H(29C) | 0.9800 |
| C(30)-H(30A) | 0.9800 |
| C(30)-H(30B) | 0.9800 |
| C(30)-H(30C) | 0.9800 |

| | |
|---|---|
| C(11)-O(2)-C(12) | 121.6(4) |
| C(11)-N(1)-C(7) | 122.5(4) |
| C(11)-N(1)-H(1N) | 115(4) |
| C(7)-N(1)-H(1N) | 122(4) |
| C(2)-C(1)-C(6) | 122.6(5) |
| C(2)-C(1)-Cl(1) | 116.9(4) |
| C(6)-C(1)-Cl(1) | 120.5(5) |
| C(3)-C(2)-C(1) | 119.6(5) |
| C(3)-C(2)-H(2) | 120.2 |
| C(1)-C(2)-H(2) | 120.2 |
| C(4)-C(3)-C(2) | 119.0(6) |
| C(4)-C(3)-H(3) | 120.5 |
| C(2)-C(3)-H(3) | 120.5 |
| C(3)-C(4)-C(5) | 121.1(6) |
| C(3)-C(4)-H(4) | 119.5 |
| C(5)-C(4)-H(4) | 119.5 |
| C(6)-C(5)-C(4) | 121.2(6) |

| | |
|---|---|
| C(6)-C(5)-H(5) | 119.4 |
| C(4)-C(5)-H(5) | 119.4 |
| C(5)-C(6)-C(1) | 116.6(6) |
| C(5)-C(6)-C(7) | 121.5(5) |
| C(1)-C(6)-C(7) | 121.8(5) |
| N(1)-C(7)-C(6) | 112.5(5) |
| N(1)-C(7)-C(8) | 110.8(5) |
| C(6)-C(7)-C(8) | 109.2(5) |
| N(1)-C(7)-H(7) | 105(3) |
| C(6)-C(7)-H(7) | 113(3) |
| C(8)-C(7)-H(7) | 107(4) |
| C(9)-C(8)-C(7) | 124.5(6) |
| C(9)-C(8)-H(8) | 117.7 |
| C(7)-C(8)-H(8) | 117.7 |
| C(10)-C(9)-C(8) | 178.9(7) |
| C(9)-C(10)-H(10A) | 124(5) |
| C(9)-C(10)-H(10B) | 123(4) |
| H(10A)-C(10)-H(10B) | 113(6) |
| O(1)-C(11)-O(2) | 126.2(5) |
| O(1)-C(11)-N(1) | 123.9(5) |
| O(2)-C(11)-N(1) | 109.9(4) |
| O(2)-C(12)-C(13) | 101.7(4) |
| O(2)-C(12)-C(15) | 111.1(5) |
| C(13)-C(12)-C(15) | 110.1(5) |
| O(2)-C(12)-C(14) | 110.1(5) |
| C(13)-C(12)-C(14) | 111.0(5) |
| C(15)-C(12)-C(14) | 112.3(5) |
| C(12)-C(13)-H(13A) | 109.5 |
| C(12)-C(13)-H(13B) | 109.5 |
| H(13A)-C(13)-H(13B) | 109.5 |
| C(12)-C(13)-H(13C) | 109.5 |
| H(13A)-C(13)-H(13C) | 109.5 |
| H(13B)-C(13)-H(13C) | 109.5 |
| C(12)-C(14)-H(14A) | 109.5 |
| C(12)-C(14)-H(14B) | 109.5 |

| | |
|---|---|
| H(14A)-C(14)-H(14B) | 109.5 |
| C(12)-C(14)-H(14C) | 109.5 |
| H(14A)-C(14)-H(14C) | 109.5 |
| H(14B)-C(14)-H(14C) | 109.5 |
| C(12)-C(15)-H(15A) | 109.5 |
| C(12)-C(15)-H(15B) | 109.5 |
| H(15A)-C(15)-H(15B) | 109.5 |
| C(12)-C(15)-H(15C) | 109.5 |
| H(15A)-C(15)-H(15C) | 109.5 |
| H(15B)-C(15)-H(15C) | 109.5 |
| C(26)-O(4)-C(27) | 121.6(4) |
| C(26)-N(2)-C(22) | 121.5(4) |
| C(26)-N(2)-H(2N) | 117(4) |
| C(22)-N(2)-H(2N) | 121(4) |
| C(17)-C(16)-C(21) | 121.8(7) |
| C(17)-C(16)-Cl(2) | 118.3(6) |
| C(21)-C(16)-Cl(2) | 119.9(6) |
| C(16)-C(17)-C(18) | 119.2(7) |
| C(16)-C(17)-H(17) | 120.4 |
| C(18)-C(17)-H(17) | 120.4 |
| C(19)-C(18)-C(17) | 120.2(8) |
| C(19)-C(18)-H(18) | 119.9 |
| C(17)-C(18)-H(18) | 119.9 |
| C(18)-C(19)-C(20) | 119.8(8) |
| C(18)-C(19)-H(19) | 120.1 |
| C(20)-C(19)-H(19) | 120.1 |
| C(21)-C(20)-C(19) | 121.6(7) |
| C(21)-C(20)-H(20) | 119.2 |
| C(19)-C(20)-H(20) | 119.2 |
| C(20)-C(21)-C(16) | 117.4(6) |
| C(20)-C(21)-C(22) | 122.4(6) |
| C(16)-C(21)-C(22) | 120.2(6) |
| N(2)-C(22)-C(21) | 113.0(5) |
| N(2)-C(22)-C(23) | 109.2(5) |
| C(21)-C(22)-C(23) | 110.9(5) |

| | |
|---|---|
| N(2)-C(22)-H(22) | 106(4) |
| C(21)-C(22)-H(22) | 107(4) |
| C(23)-C(22)-H(22) | 111(4) |
| C(24)-C(23)-C(22) | 122.7(6) |
| C(24)-C(23)-H(23) | 118.7 |
| C(22)-C(23)-H(23) | 118.7 |
| C(23)-C(24)-C(25) | 178.7(8) |
| C(24)-C(25)-H(25A) | 112(5) |
| C(24)-C(25)-H(25B) | 120(5) |
| H(25A)-C(25)-H(25B) | 127(7) |
| O(3)-C(26)-O(4) | 125.7(5) |
| O(3)-C(26)-N(2) | 124.2(5) |
| O(4)-C(26)-N(2) | 110.1(4) |
| O(4)-C(27)-C(28) | 109.9(5) |
| O(4)-C(27)-C(29) | 101.8(4) |
| C(28)-C(27)-C(29) | 112.0(6) |
| O(4)-C(27)-C(30) | 110.3(5) |
| C(28)-C(27)-C(30) | 113.3(5) |
| C(29)-C(27)-C(30) | 109.0(6) |
| C(27)-C(28)-H(28A) | 109.5 |
| C(27)-C(28)-H(28B) | 109.5 |
| H(28A)-C(28)-H(28B) | 109.5 |
| C(27)-C(28)-H(28C) | 109.5 |
| H(28A)-C(28)-H(28C) | 109.5 |
| H(28B)-C(28)-H(28C) | 109.5 |
| C(27)-C(29)-H(29A) | 109.5 |
| C(27)-C(29)-H(29B) | 109.5 |
| H(29A)-C(29)-H(29B) | 109.5 |
| C(27)-C(29)-H(29C) | 109.5 |
| H(29A)-C(29)-H(29C) | 109.5 |
| H(29B)-C(29)-H(29C) | 109.5 |
| C(27)-C(30)-H(30A) | 109.5 |
| C(27)-C(30)-H(30B) | 109.5 |
| H(30A)-C(30)-H(30B) | 109.5 |
| C(27)-C(30)-H(30C) | 109.5 |

| | |
|---|---|
| H(30A)-C(30)-H(30C) | 109.5 |
| H(30B)-C(30)-H(30C) | 109.5 |

Symmetry transformations used to generate equivalent atoms:

***Table 4.*** Anisotropic displacement parameters ($Å^2 x\ 10^3$) for $C_{15}H_{18}ClNO_2$. The anisotropic displacement factor exponent takes the form: $-2\pi^2[h^2a^{*2}U^{11} + ... + 2hka^*b^*U^{12}]$

| | $U^{11}$ | $U^{22}$ | $U^{33}$ | $U^{23}$ | $U^{13}$ | $U^{12}$ |
|---|---|---|---|---|---|---|
| Cl(1) | 27(1) | 29(1) | 23(1) | 1(1) | 9(1) | -5(1) |
| O(1) | 11(2) | 30(3) | 27(2) | 2(2) | 3(2) | -2(2) |
| O(2) | 14(2) | 34(3) | 14(2) | 1(2) | 2(2) | 2(2) |
| N(1) | 10(2) | 32(4) | 15(3) | 2(2) | 1(2) | -1(2) |
| C(1) | 20(3) | 14(3) | 24(3) | 5(3) | 4(2) | 1(2) |
| C(2) | 29(3) | 26(4) | 20(4) | -6(3) | 11(3) | 0(3) |
| C(3) | 34(4) | 22(4) | 30(4) | -5(3) | 0(3) | -2(3) |
| C(4) | 28(3) | 23(3) | 28(4) | 1(3) | 7(3) | -5(3) |
| C(5) | 23(3) | 25(4) | 20(4) | 1(3) | 7(3) | 0(3) |
| C(6) | 19(3) | 17(3) | 22(3) | 4(3) | 3(2) | 2(2) |
| C(7) | 16(3) | 23(3) | 15(3) | 2(3) | 4(2) | 0(3) |
| C(8) | 21(3) | 22(3) | 23(4) | -3(3) | 3(3) | 2(3) |
| C(9) | 30(3) | 26(4) | 18(3) | -5(3) | -4(3) | 5(3) |
| C(10) | 50(4) | 22(4) | 33(4) | 8(4) | -7(3) | 1(3) |
| C(11) | 18(3) | 16(4) | 19(3) | -2(3) | 5(2) | 5(2) |
| C(12) | 15(3) | 25(4) | 16(3) | 1(3) | -1(2) | 0(3) |
| C(13) | 22(3) | 35(4) | 13(3) | 5(3) | 2(2) | 7(3) |
| C(14) | 25(3) | 28(4) | 27(4) | -2(3) | -2(3) | -2(3) |
| C(15) | 16(3) | 26(4) | 26(4) | 5(3) | -1(2) | 5(3) |
| Cl(2) | 42(1) | 58(1) | 21(1) | -1(1) | 10(1) | 16(1) |
| O(3) | 11(2) | 41(3) | 19(2) | -4(2) | 3(2) | 1(2) |
| O(4) | 13(2) | 27(2) | 13(2) | -2(2) | 0(1) | 3(2) |
| N(2) | 10(2) | 31(3) | 14(2) | 1(2) | 1(2) | 3(2) |
| C(16) | 41(4) | 29(4) | 25(4) | -2(3) | 0(3) | 15(3) |

| | | | | | | |
|---|---|---|---|---|---|---|
| C(17) | 68(5) | 36(5) | 36(5) | -11(4) | -10(4) | 17(4) |
| C(18) | 80(6) | 27(4) | 44(5) | -13(4) | -29(4) | 10(4) |
| C(19) | 62(5) | 25(4) | 46(5) | 3(4) | -18(4) | -3(4) |
| C(20) | 37(4) | 31(4) | 24(4) | -4(3) | -5(3) | -4(3) |
| C(21) | 26(3) | 24(3) | 20(3) | 0(3) | -6(3) | 9(3) |
| C(22) | 16(3) | 33(4) | 15(3) | -4(3) | 3(2) | -1(3) |
| C(23) | 24(3) | 25(4) | 17(3) | 0(3) | 1(3) | 1(3) |
| C(24) | 41(4) | 23(4) | 16(3) | -5(3) | 4(3) | -3(3) |
| C(25) | 83(6) | 39(5) | 29(5) | -3(4) | 7(4) | -22(4) |
| C(26) | 14(3) | 20(4) | 15(3) | 0(3) | 2(2) | 0(2) |
| C(27) | 16(3) | 26(3) | 15(3) | -3(3) | 0(2) | -2(3) |
| C(28) | 26(3) | 24(4) | 23(4) | 9(3) | -2(3) | -2(3) |
| C(29) | 26(3) | 50(5) | 22(4) | -8(3) | 0(3) | 4(3) |
| C(30) | 20(3) | 24(4) | 26(4) | -4(3) | -7(3) | 0(3) |

***Table 5.*** Hydrogen coordinates (x $10^4$) and isotropic displacement parameters (Å$^2$x $10^3$) for $C_{15}H_{18}ClNO_2$

| | x | y | z | U(eq) |
|---|---|---|---|---|
| H(1N) | 7790(40) | 4580(60) | 3710(40) | 23 |
| H(2) | 9016 | 2786 | -107 | 30 |
| H(3) | 7436 | 1162 | 262 | 34 |
| H(4) | 6459 | 1300 | 1656 | 32 |
| H(5) | 7007 | 3042 | 2673 | 27 |
| H(7) | 9550(30) | 5530(60) | 2480(40) | 22 |
| H(8) | 6798 | 6261 | 2434 | 26 |
| H(10A) | 8330(70) | 8570(80) | 750(20) | 42 |
| H(10B) | 8660(60) | 9320(50) | 1700(40) | 42 |
| H(13A) | 9073 | 2839 | 6220 | 35 |
| H(13B) | 8636 | 4337 | 6496 | 35 |
| H(13C) | 9929 | 3663 | 6979 | 35 |
| H(14A) | 11275 | 6081 | 5462 | 40 |

| | | | | |
|---|---|---|---|---|
| H(14B) | 11287 | 5662 | 6512 | 40 |
| H(14C) | 9988 | 6328 | 6031 | 40 |
| H(15A) | 11878 | 3740 | 5005 | 34 |
| H(15B) | 10969 | 2486 | 5269 | 34 |
| H(15C) | 11906 | 3211 | 6033 | 34 |
| H(2N) | 2780(40) | 5080(70) | 3770(40) | 22 |
| H(17) | 3657 | 2137 | 153 | 57 |
| H(18) | 2030 | 721 | 730 | 62 |
| H(19) | 1131 | 1229 | 2114 | 54 |
| H(20) | 1840 | 3145 | 2925 | 37 |
| H(22) | 4590(30) | 5170(60) | 2440(40) | 25 |
| H(23) | 1922 | 6329 | 2280 | 26 |
| H(25A) | 3850(70) | 8260(90) | 760(20) | 60 |
| H(25B) | 4290(70) | 9060(60) | 1760(50) | 60 |
| H(28A) | 6283 | 3383 | 5329 | 37 |
| H(28B) | 5027 | 3039 | 5907 | 37 |
| H(28C) | 6358 | 3605 | 6407 | 37 |
| H(29A) | 4175 | 6477 | 6386 | 49 |
| H(29B) | 5046 | 5528 | 7066 | 49 |
| H(29C) | 3725 | 4947 | 6560 | 49 |
| H(30A) | 6006 | 7008 | 5487 | 35 |
| H(30B) | 6861 | 5848 | 5033 | 35 |
| H(30C) | 7012 | 6106 | 6107 | 35 |

***Table 6.*** Torsion angles [°] for $C_{15}H_{18}ClNO_2$

| | |
|---|---|
| C(6)-C(1)-C(2)-C(3) | 0.6(10) |
| Cl(1)-C(1)-C(2)-C(3) | -179.7(5) |
| C(1)-C(2)-C(3)-C(4) | -0.8(10) |
| C(2)-C(3)-C(4)-C(5) | 0.5(10) |
| C(3)-C(4)-C(5)-C(6) | 0.1(10) |
| C(4)-C(5)-C(6)-C(1) | -0.3(9) |
| C(4)-C(5)-C(6)-C(7) | 175.8(6) |
| C(2)-C(1)-C(6)-C(5) | 0.0(9) |

| | |
|---|---|
| Cl(1)-C(1)-C(6)-C(5) | -179.8(5) |
| C(2)-C(1)-C(6)-C(7) | -176.1(6) |
| Cl(1)-C(1)-C(6)-C(7) | 4.1(8) |
| C(11)-N(1)-C(7)-C(6) | 113.3(6) |
| C(11)-N(1)-C(7)-C(8) | -124.1(6) |
| C(5)-C(6)-C(7)-N(1) | 33.9(8) |
| C(1)-C(6)-C(7)-N(1) | -150.2(5) |
| C(5)-C(6)-C(7)-C(8) | -89.5(7) |
| C(1)-C(6)-C(7)-C(8) | 86.4(6) |
| N(1)-C(7)-C(8)-C(9) | 130.3(7) |
| C(6)-C(7)-C(8)-C(9) | -105.2(7) |
| C(12)-O(2)-C(11)-O(1) | 1.3(10) |
| C(12)-O(2)-C(11)-N(1) | -179.9(5) |
| C(7)-N(1)-C(11)-O(1) | 0.1(10) |
| C(7)-N(1)-C(11)-O(2) | -178.8(5) |
| C(11)-O(2)-C(12)-C(13) | -175.2(5) |
| C(11)-O(2)-C(12)-C(15) | -58.0(8) |
| C(11)-O(2)-C(12)-C(14) | 67.1(7) |
| C(21)-C(16)-C(17)-C(18) | 2.5(11) |
| Cl(2)-C(16)-C(17)-C(18) | -176.9(6) |
| C(16)-C(17)-C(18)-C(19) | -1.0(12) |
| C(17)-C(18)-C(19)-C(20) | -0.2(12) |
| C(18)-C(19)-C(20)-C(21) | -0.1(12) |
| C(19)-C(20)-C(21)-C(16) | 1.5(10) |
| C(19)-C(20)-C(21)-C(22) | 179.0(6) |
| C(17)-C(16)-C(21)-C(20) | -2.7(10) |
| Cl(2)-C(16)-C(21)-C(20) | 176.7(5) |
| C(17)-C(16)-C(21)-C(22) | 179.7(6) |
| Cl(2)-C(16)-C(21)-C(22) | -0.8(8) |
| C(26)-N(2)-C(22)-C(21) | 111.6(6) |
| C(26)-N(2)-C(22)-C(23) | -124.6(6) |
| C(20)-C(21)-C(22)-N(2) | 28.9(8) |
| C(16)-C(21)-C(22)-N(2) | -153.6(5) |
| C(20)-C(21)-C(22)-C(23) | -94.0(7) |
| C(16)-C(21)-C(22)-C(23) | 83.4(7) |

| | |
|---|---|
| N(2)-C(22)-C(23)-C(24) | 118.5(7) |
| C(21)-C(22)-C(23)-C(24) | -116.4(7) |
| C(27)-O(4)-C(26)-O(3) | -2.1(10) |
| C(27)-O(4)-C(26)-N(2) | 177.9(5) |
| C(22)-N(2)-C(26)-O(3) | -15.6(10) |
| C(22)-N(2)-C(26)-O(4) | 164.5(6) |
| C(26)-O(4)-C(27)-C(28) | -66.7(7) |
| C(26)-O(4)-C(27)-C(29) | 174.5(6) |
| C(26)-O(4)-C(27)-C(30) | 58.9(8) |

Symmetry transformations used to generate equivalent atoms:

***Table 7.*** Hydrogen bonds for $C_{15}H_{18}ClNO_2$ [Å and °]

| D-H...A | d(D-H) | d(H...A) | d(D...A) | <(DHA) |
|---|---|---|---|---|
| N(1)-H(1N)...O(3) | 0.88(3) | 2.11(4) | 2.928(5) | 155(6) |
| N(2)-H(2N)...O(1)#1 | 0.87(3) | 2.08(3) | 2.897(5) | 157(6) |

Symmetry transformations used to generate equivalent atoms:
#1 x-1,y,z

**(*4S*,*5S*)-4-(4-Methoxyphenyl)-5-vinyloxazolidin-2-one (3.112)**

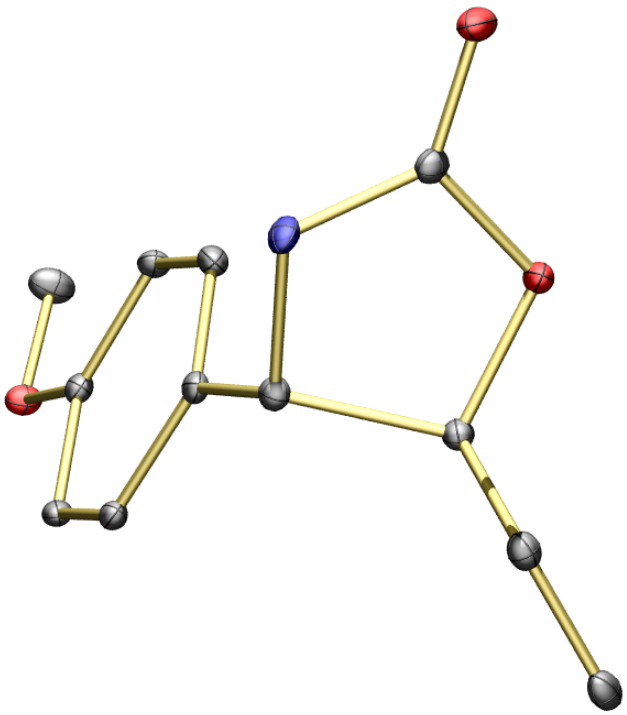

***Table 1.*** Crystal data and structure refinement for $C_{12}H_{13}NO_3$

| | | |
|---|---|---|
| Identification code | $C_{12}H_{13}NO_3$ | |
| Empirical formula | $C_{12}H_{13}NO_3$ | |
| Formula weight | 219.23 | |
| Temperature | 100(2) K | |
| Wavelength | 1.54178 Å | |
| Crystal system | Orthorhombic | |
| Space group | P 21 21 21 | |
| Unit cell dimensions | a = 5.6723(5) Å | α= 90º. |
| | b = 12.2790(10) Å | β= 90º. |
| | c = 16.0430(13) Å | γ = 90º. |
| Volume | 1117.40(16) $Å^3$ | |
| Z | 4 | |
| Density (calculated) | 1.303 $Mg/m^3$ | |
| Absorption coefficient | 0.778 $mm^{-1}$ | |
| F(000) | 464 | |
| Crystal size | 0.480 x 0.120 x 0.040 $mm^3$ | |
| Theta range for data collection | 4.535 to 67.882º. | |
| Index ranges | -6<=h<=6, -14<=k<=11, -19<=l<=19 | |

| | |
|---|---|
| Reflections collected | 14797 |
| Independent reflections | 1962 [R(int) = 0.0400] |
| Completeness to theta = 67.679° | 98.5% |
| Absorption correction | Semi-empirical from equivalents |
| Max. and min. transmission | 0.7530 and 0.6250 |
| Refinement method | Full-matrix least-squares on $F^2$ |
| Data / restraints / parameters | 1962 / 2 / 149 |
| Goodness-of-fit on $F^2$ | 1.070 |
| Final R indices [I>2sigma(I)] | R1 = 0.0284, wR2 = 0.0690 |
| R indices (all data) | R1 = 0.0297, wR2 = 0.0699 |
| Absolute structure parameter | -0.01(9) |
| Extinction coefficient | na |
| Largest diff. peak and hole | 0.325 and -0.185 e. $Å^{-3}$ |

***Table 2.*** Atomic coordinates ($x10^4$) and equivalent isotropic displacement parameters ($Å^2 x\ 10^3$) for $C_{12}H_{13}NO_3$. U(eq) is defined as one third of the trace of the orthogonalized $U^{ij}$ tensor

| | x | y | z | U(eq) |
|---|---|---|---|---|
| O(1) | 1996(2) | 7359(1) | 6692(1) | 23(1) |
| O(2) | -2712(2) | 10666(1) | 3581(1) | 22(1) |
| O(3) | -3810(3) | 12166(1) | 4274(1) | 29(1) |
| N(1) | 15(3) | 11514(1) | 4326(1) | 21(1) |
| C(1) | 473(3) | 9481(2) | 1979(1) | 24(1) |
| C(2) | 281(4) | 10277(2) | 2558(1) | 21(1) |
| C(3) | -530(3) | 10067(2) | 3427(1) | 18(1) |
| C(4) | 1182(3) | 10498(2) | 4113(1) | 19(1) |
| C(5) | 1410(3) | 9716(2) | 4837(1) | 18(1) |
| C(6) | 3315(3) | 8999(2) | 4878(1) | 18(1) |
| C(7) | 3468(3) | 8224(2) | 5501(1) | 19(1) |
| C(8) | 1697(3) | 8158(2) | 6102(1) | 18(1) |
| C(9) | 138(4) | 7219(2) | 7285(1) | 33(1) |
| C(10) | -2251(4) | 11522(2) | 4096(1) | 21(1) |
| C(11) | -328(3) | 9642(2) | 5449(1) | 20(1) |
| C(12) | -193(3) | 8871(2) | 6081(1) | 20(1) |

***Table 3.*** Bond lengths [Å] and angles [º] for $C_{12}H_{13}NO_3$

| | |
|---|---|
| O(1)-C(8) | 1.374(2) |
| O(1)-C(9) | 1.430(3) |
| O(2)-C(10) | 1.361(2) |
| O(2)-C(3) | 1.461(2) |
| O(3)-C(10) | 1.221(3) |
| N(1)-C(10) | 1.337(3) |
| N(1)-C(4) | 1.453(3) |
| N(1)-H(1N) | 0.897(18) |
| C(1)-C(2) | 1.352(3) |
| C(1)-H(1A) | 0.9500 |
| C(1)-H(1B) | 0.9500 |
| C(2)-C(3) | 1.491(3) |
| C(2)-H(2) | 0.9500 |
| C(3)-C(4) | 1.560(3) |
| C(3)-H(3) | 1.0000 |
| C(4)-C(5) | 1.512(3) |
| C(4)-H(4) | 1.0000 |
| C(5)-C(11) | 1.395(3) |
| C(5)-C(6) | 1.396(3) |
| C(6)-C(7) | 1.382(3) |
| C(6)-H(6) | 0.9500 |
| C(7)-C(8) | 1.395(3) |
| C(7)-H(7) | 0.9500 |
| C(8)-C(12) | 1.385(3) |
| C(9)-H(9A) | 0.9800 |
| C(9)-H(9B) | 0.9800 |
| C(9)-H(9C) | 0.9800 |
| C(11)-C(12) | 1.388(3) |
| C(11)-H(11) | 0.9500 |
| C(12)-H(12) | 0.9500 |
| | |
| C(8)-O(1)-C(9) | 116.97(16) |
| C(10)-O(2)-C(3) | 109.17(14) |

| | |
|---|---|
| C(10)-N(1)-C(4) | 112.27(17) |
| C(10)-N(1)-H(1N) | 119.1(15) |
| C(4)-N(1)-H(1N) | 123.4(15) |
| C(2)-C(1)-H(1A) | 120.0 |
| C(2)-C(1)-H(1B) | 120.0 |
| H(1A)-C(1)-H(1B) | 120.0 |
| C(1)-C(2)-C(3) | 122.82(18) |
| C(1)-C(2)-H(2) | 118.6 |
| C(3)-C(2)-H(2) | 118.6 |
| O(2)-C(3)-C(2) | 109.47(15) |
| O(2)-C(3)-C(4) | 103.72(14) |
| C(2)-C(3)-C(4) | 114.16(16) |
| O(2)-C(3)-H(3) | 109.8 |
| C(2)-C(3)-H(3) | 109.8 |
| C(4)-C(3)-H(3) | 109.8 |
| N(1)-C(4)-C(5) | 113.75(15) |
| N(1)-C(4)-C(3) | 99.99(15) |
| C(5)-C(4)-C(3) | 112.34(15) |
| N(1)-C(4)-H(4) | 110.1 |
| C(5)-C(4)-H(4) | 110.1 |
| C(3)-C(4)-H(4) | 110.1 |
| C(11)-C(5)-C(6) | 118.20(17) |
| C(11)-C(5)-C(4) | 121.47(17) |
| C(6)-C(5)-C(4) | 120.21(16) |
| C(7)-C(6)-C(5) | 121.16(17) |
| C(7)-C(6)-H(6) | 119.4 |
| C(5)-C(6)-H(6) | 119.4 |
| C(6)-C(7)-C(8) | 119.63(18) |
| C(6)-C(7)-H(7) | 120.2 |
| C(8)-C(7)-H(7) | 120.2 |
| O(1)-C(8)-C(12) | 124.34(17) |
| O(1)-C(8)-C(7) | 115.41(17) |
| C(12)-C(8)-C(7) | 120.24(18) |
| O(1)-C(9)-H(9A) | 109.5 |
| O(1)-C(9)-H(9B) | 109.5 |

| | |
|---|---|
| H(9A)-C(9)-H(9B) | 109.5 |
| O(1)-C(9)-H(9C) | 109.5 |
| H(9A)-C(9)-H(9C) | 109.5 |
| H(9B)-C(9)-H(9C) | 109.5 |
| O(3)-C(10)-N(1) | 129.54(19) |
| O(3)-C(10)-O(2) | 120.18(18) |
| N(1)-C(10)-O(2) | 110.27(17) |
| C(12)-C(11)-C(5) | 121.30(18) |
| C(12)-C(11)-H(11) | 119.3 |
| C(5)-C(11)-H(11) | 119.3 |
| C(8)-C(12)-C(11) | 119.45(17) |
| C(8)-C(12)-H(12) | 120.3 |
| C(11)-C(12)-H(12) | 120.3 |

Symmetry transformations used to generate equivalent atoms:

***Table 4.*** Anisotropic displacement parameters ($Å^2 x\ 10^3$) for $C_{12}H_{13}NO_3$. The anisotropic displacement factor exponent takes the form: $-2\pi^2[h^2a^{*2}U^{11} + ... + 2hka^*b^*U^{12}]$

| | $U^{11}$ | $U^{22}$ | $U^{33}$ | $U^{23}$ | $U^{13}$ | $U^{12}$ |
|---|---|---|---|---|---|---|
| O(1) | 26(1) | 22(1) | 20(1) | 3(1) | 4(1) | 3(1) |
| O(2) | 17(1) | 27(1) | 21(1) | -7(1) | -1(1) | 1(1) |
| O(3) | 32(1) | 33(1) | 23(1) | -7(1) | -2(1) | 11(1) |
| N(1) | 26(1) | 16(1) | 22(1) | -4(1) | -6(1) | -2(1) |
| C(1) | 19(1) | 35(1) | 18(1) | 7(1) | 0(1) | 2(1) |
| C(2) | 19(1) | 24(1) | 21(1) | 5(1) | -1(1) | -1(1) |
| C(3) | 18(1) | 18(1) | 18(1) | -1(1) | -1(1) | 1(1) |
| C(4) | 18(1) | 19(1) | 19(1) | 0(1) | 0(1) | -2(1) |
| C(5) | 17(1) | 20(1) | 18(1) | -3(1) | -3(1) | -2(1) |
| C(6) | 16(1) | 22(1) | 17(1) | -4(1) | 0(1) | -2(1) |
| C(7) | 17(1) | 19(1) | 20(1) | -5(1) | 0(1) | 2(1) |
| C(8) | 21(1) | 18(1) | 16(1) | -2(1) | -2(1) | -1(1) |
| C(9) | 34(1) | 37(1) | 28(1) | 11(1) | 11(1) | 6(1) |
| C(10) | 24(1) | 23(1) | 15(1) | 0(1) | -1(1) | 1(1) |

| | | | | | | |
|---|---|---|---|---|---|---|
| C(11) | 16(1) | 22(1) | 22(1) | -2(1) | -1(1) | 2(1) |
| C(12) | 18(1) | 25(1) | 18(1) | -2(1) | 4(1) | 0(1) |

***Table 5.*** Hydrogen coordinates (x $10^4$) and isotropic displacement parameters (Å$^2$x $10^3$) for $C_{12}H_{13}NO_3$

| | x | y | z | U(eq) |
|---|---|---|---|---|
| H(1N) | 480(40) | 11946(18) | 4745(13) | 26 |
| H(1A) | 83 | 8751 | 2120 | 29 |
| H(1B) | 998 | 9651 | 1432 | 29 |
| H(2) | 680 | 11001 | 2403 | 25 |
| H(3) | -806 | 9270 | 3507 | 22 |
| H(4) | 2768 | 10648 | 3866 | 23 |
| H(6) | 4529 | 9045 | 4472 | 22 |
| H(7) | 4772 | 7739 | 5519 | 22 |
| H(9A) | -1353 | 7099 | 6991 | 50 |
| H(9B) | 12 | 7874 | 7632 | 50 |
| H(9C) | 485 | 6589 | 7639 | 50 |
| H(11) | -1630 | 10128 | 5434 | 24 |
| H(12) | -1387 | 8834 | 6495 | 24 |

***Table 6.*** Torsion angles [º] for $C_{12}H_{13}NO_3$

| | |
|---|---|
| C(10)-O(2)-C(3)-C(2) | -107.32(17) |
| C(10)-O(2)-C(3)-C(4) | 14.90(19) |
| C(1)-C(2)-C(3)-O(2) | -117.7(2) |
| C(1)-C(2)-C(3)-C(4) | 126.6(2) |
| C(10)-N(1)-C(4)-C(5) | -99.95(19) |
| C(10)-N(1)-C(4)-C(3) | 20.01(19) |
| O(2)-C(3)-C(4)-N(1) | -19.98(17) |
| C(2)-C(3)-C(4)-N(1) | 99.07(18) |
| O(2)-C(3)-C(4)-C(5) | 100.99(17) |
| C(2)-C(3)-C(4)-C(5) | -139.96(17) |
| N(1)-C(4)-C(5)-C(11) | 34.7(2) |
| C(3)-C(4)-C(5)-C(11) | -78.0(2) |
| N(1)-C(4)-C(5)-C(6) | -149.34(17) |

| | |
|---|---|
| C(3)-C(4)-C(5)-C(6) | 98.0(2) |
| C(11)-C(5)-C(6)-C(7) | 1.0(3) |
| C(4)-C(5)-C(6)-C(7) | -175.16(17) |
| C(5)-C(6)-C(7)-C(8) | -0.3(3) |
| C(9)-O(1)-C(8)-C(12) | 4.3(3) |
| C(9)-O(1)-C(8)-C(7) | -175.98(18) |
| C(6)-C(7)-C(8)-O(1) | 179.65(17) |
| C(6)-C(7)-C(8)-C(12) | -0.7(3) |
| C(4)-N(1)-C(10)-O(3) | 168.9(2) |
| C(4)-N(1)-C(10)-O(2) | -12.0(2) |
| C(3)-O(2)-C(10)-O(3) | 176.32(17) |
| C(3)-O(2)-C(10)-N(1) | -2.8(2) |
| C(6)-C(5)-C(11)-C(12) | -0.6(3) |
| C(4)-C(5)-C(11)-C(12) | 175.46(17) |
| O(1)-C(8)-C(12)-C(11) | -179.35(17) |
| C(7)-C(8)-C(12)-C(11) | 1.0(3) |
| C(5)-C(11)-C(12)-C(8) | -0.3(3) |

Symmetry transformations used to generate equivalent atoms:

***Table 7.*** Hydrogen bonds for $C_{12}H_{13}NO_3$ [Å and º]

| D-H...A | d(D-H) | d(H...A) | d(D...A) | <(DHA) |
|---|---|---|---|---|
| N(1)-H(1N)...O(3)#1 | 0.897(18) | 1.956(19) | 2.849(2) | 174(2) |

Symmetry transformations used to generate equivalent atoms:
#1 x+1/2,-y+5/2,-z+1

### *3.8.5. NMR Spectra of New Compounds*

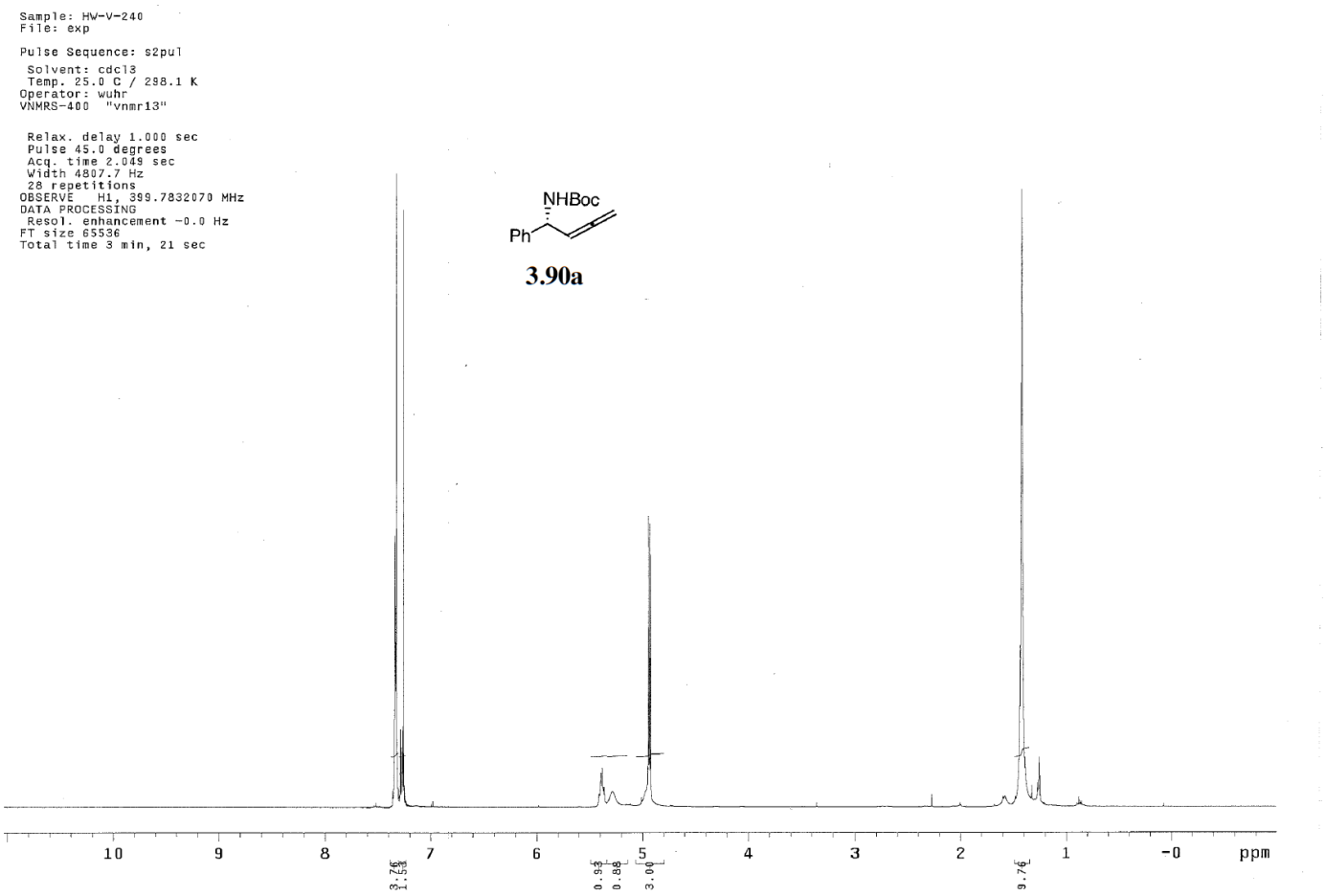
Sample: HW-V-240
File: exp
Pulse Sequence: s2pul
Solvent: cdcl3
Temp. 25.0 C / 298.1 K
Operator: wuhr
VNMRS-400 "vnmr13"
Relax. delay 1.000 sec
Pulse 45.0 degrees
Acq. time 2.049 sec
Width 4807.7 Hz
28 repetitions
OBSERVE H1, 399.7832070 MHz
DATA PROCESSING
Resol. enhancement -0.0 Hz
FT size 65536
Total time 3 min, 21 sec
NHBoc
Ph
3.90a
10
9
8
7
6
5
4
3
2
1
-0
ppm
3.76
1.53
0.94
0.88
3.00
9.76

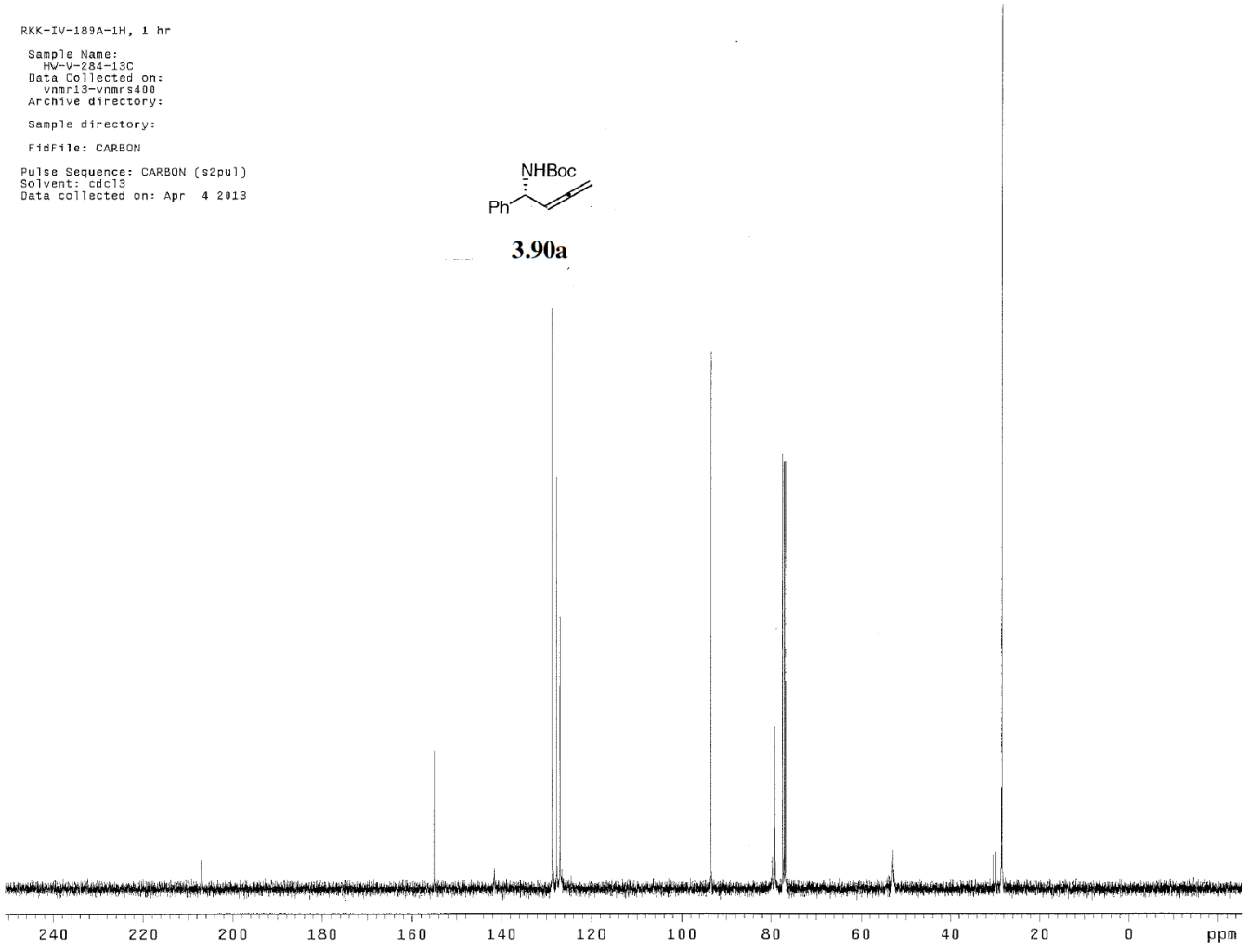
RKK-IV-189A-1H, 1 hr
Sample Name:
HV-V-284-13C
Data Collected on:
vnmr13-vnmrs400
Archive directory:
Sample directory:
FidFile: CARBON
Pulse Sequence: CARBON (s2pul)
Solvent: cdcl3
Data collected on: Apr 4 2013
NHBoc
Ph
3.90a
240
220
200
180
160
140
120
100
80
60
40
20
0
ppm

Sample Name:
HW-VI-036-1H-2
Data Collected on:
vnmr13-vnmrs400
Archive directory:

Sample directory:

FidFile: PROTON

Pulse Sequence: PROTON (s2pul)
Solvent: cdcl3
Data collected on: Feb 22 2014

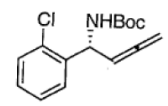


**3.90b**

HJ-VII-150-13C
Oct.21.13

Sample Name:
HW-V-301-13C
Data Collected on:
vnmr13-vnmrs400
Archive directory:

Sample directory:

FidFile: CARBON

Pulse Sequence: CARBON (s2pul)
Solvent: cdcl3
Data collected on: Oct 21 2013

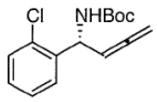


**3.90b**

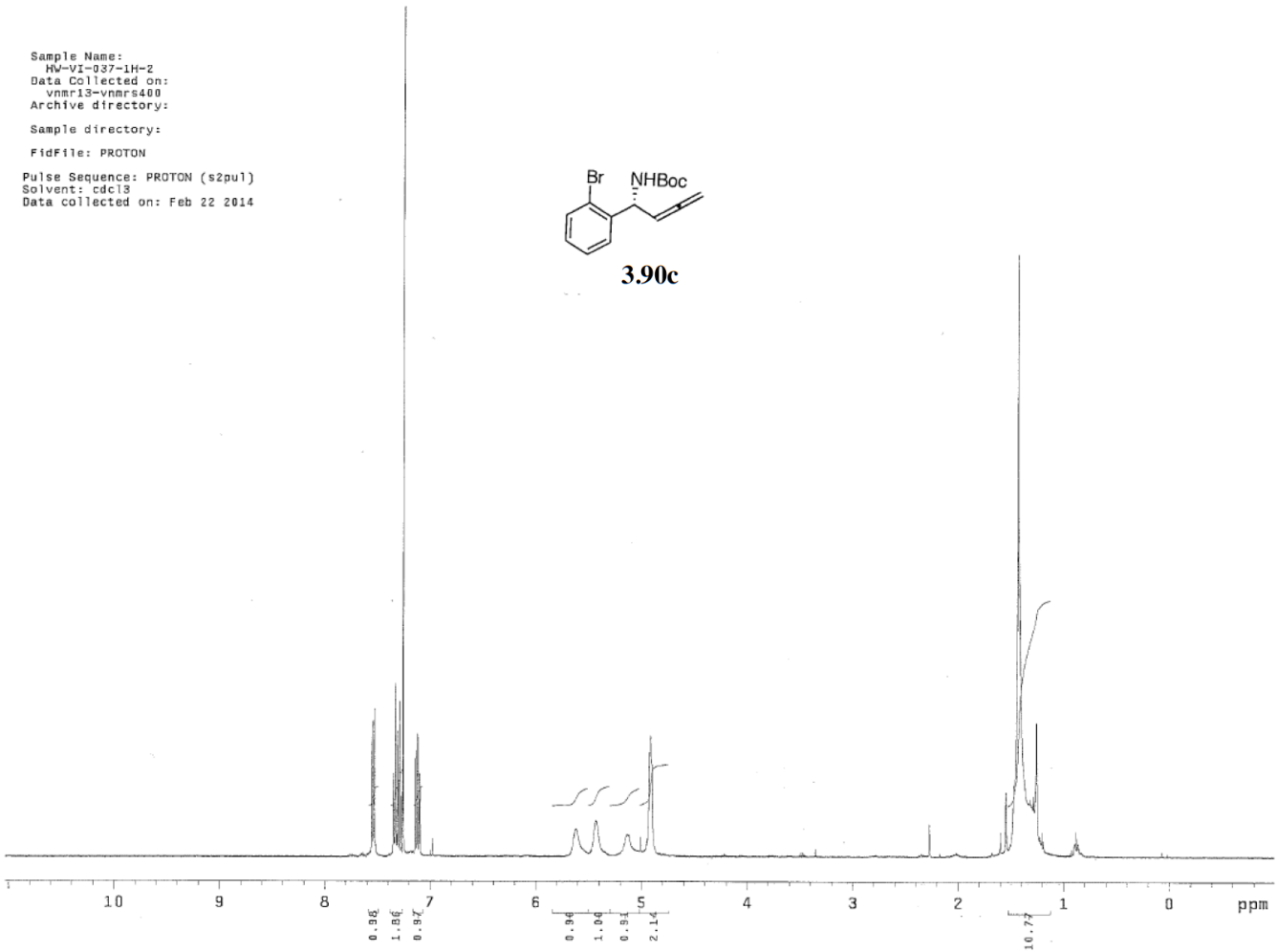
Sample Name:
HW-VI-037-1H-2
Data Collected on:
vnmr13-vnmrs400
Archive directory:
Sample directory:
FidFile: PROTON
Pulse Sequence: PROTON (s2pul)
Solvent: cdcl3
Data collected on: Feb 22 2014
Br
NHBoc
3.90c
10
9
8
7
6
5
4
3
2
1
0
ppm
0.96
1.86
0.97
0.96
1.04
0.91
2.14
10.77

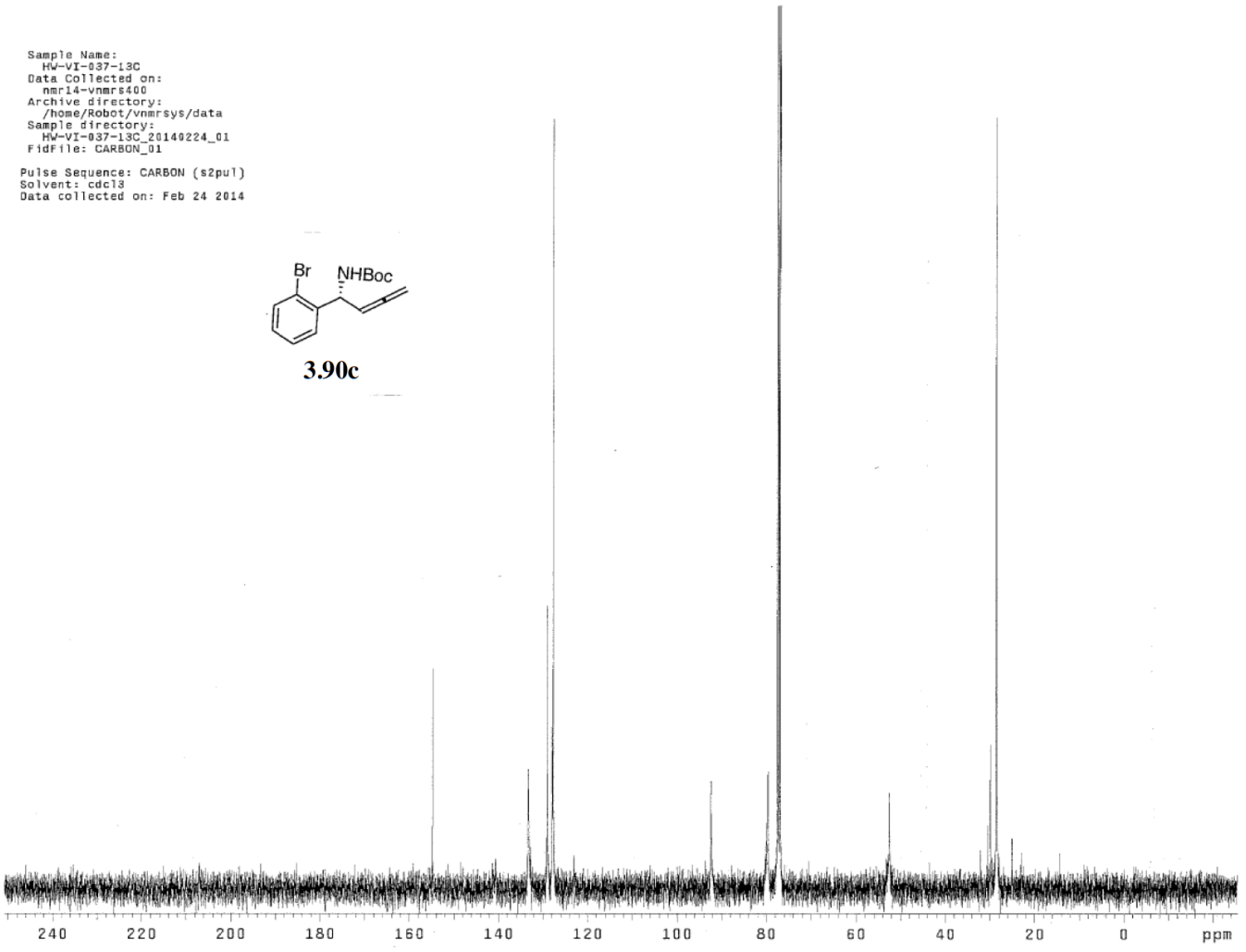
Sample Name:
HW-VI-037-13C
Data Collected on:
nmr14-vnmrs400
Archive directory:
/home/Robot/vnmrsys/data
Sample directory:
HW-VI-037-13C_20140224_01
FidFile: CARBON_01
Pulse Sequence: CARBON (s2pul)
Solvent: cdcl3
Data collected on: Feb 24 2014
Br
NHBoc
240
220
200
180
160
140
120
100
80
60
40
20
0
ppm

**3.90c**

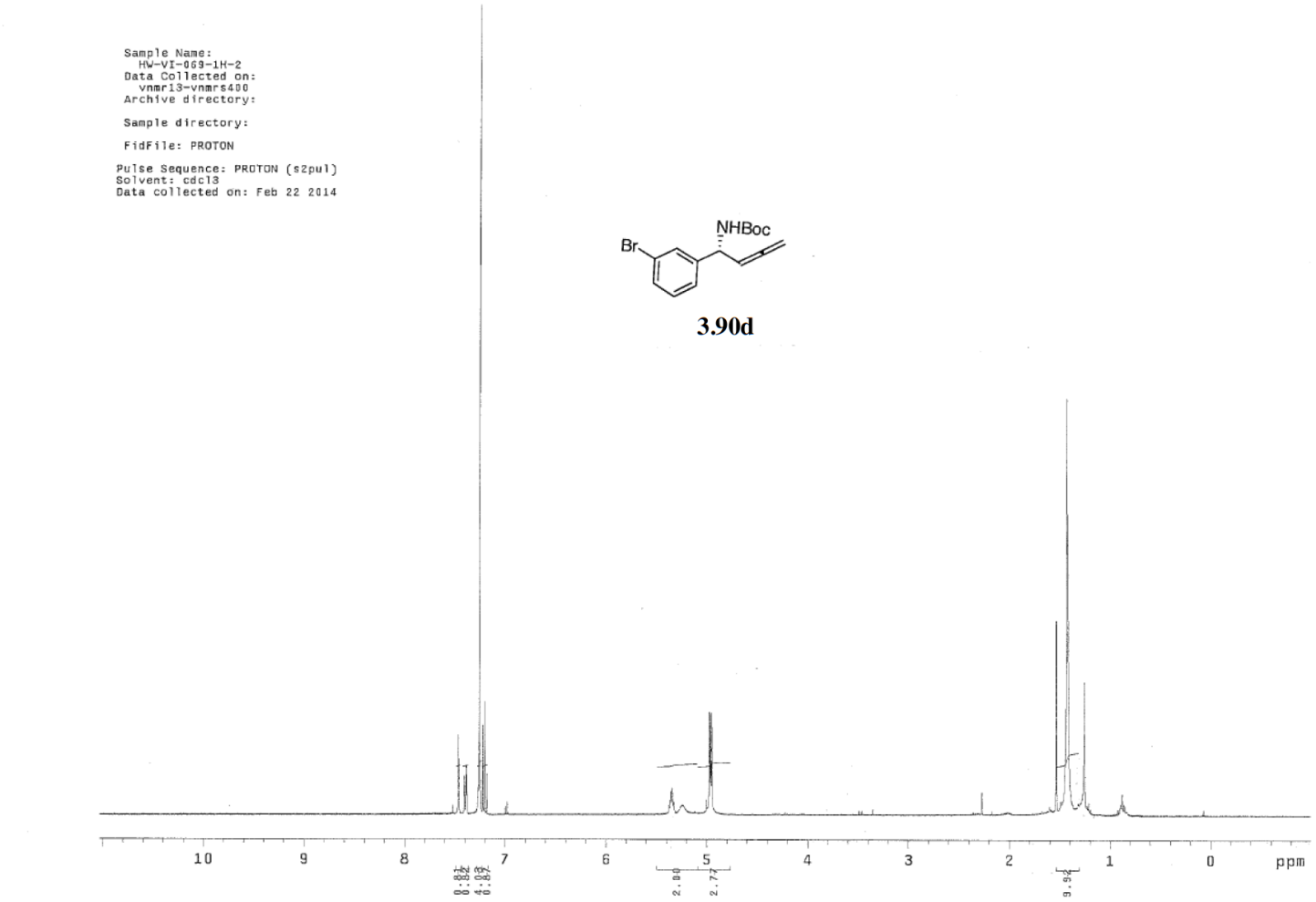
Sample Name:
HW-VI-069-1H-2
Data Collected on:
vnmr13-vnmrs400
Archive directory:
Sample directory:
FidFile: PROTON
Pulse Sequence: PROTON (s2pul)
Solvent: cdcl3
Data collected on: Feb 22 2014
NHBoc
Br
3.90d
10
9
8
7
6
5
4
3
2
1
0
ppm
0.81
0.82
4.03
6.87
2.00
2.77
9.94

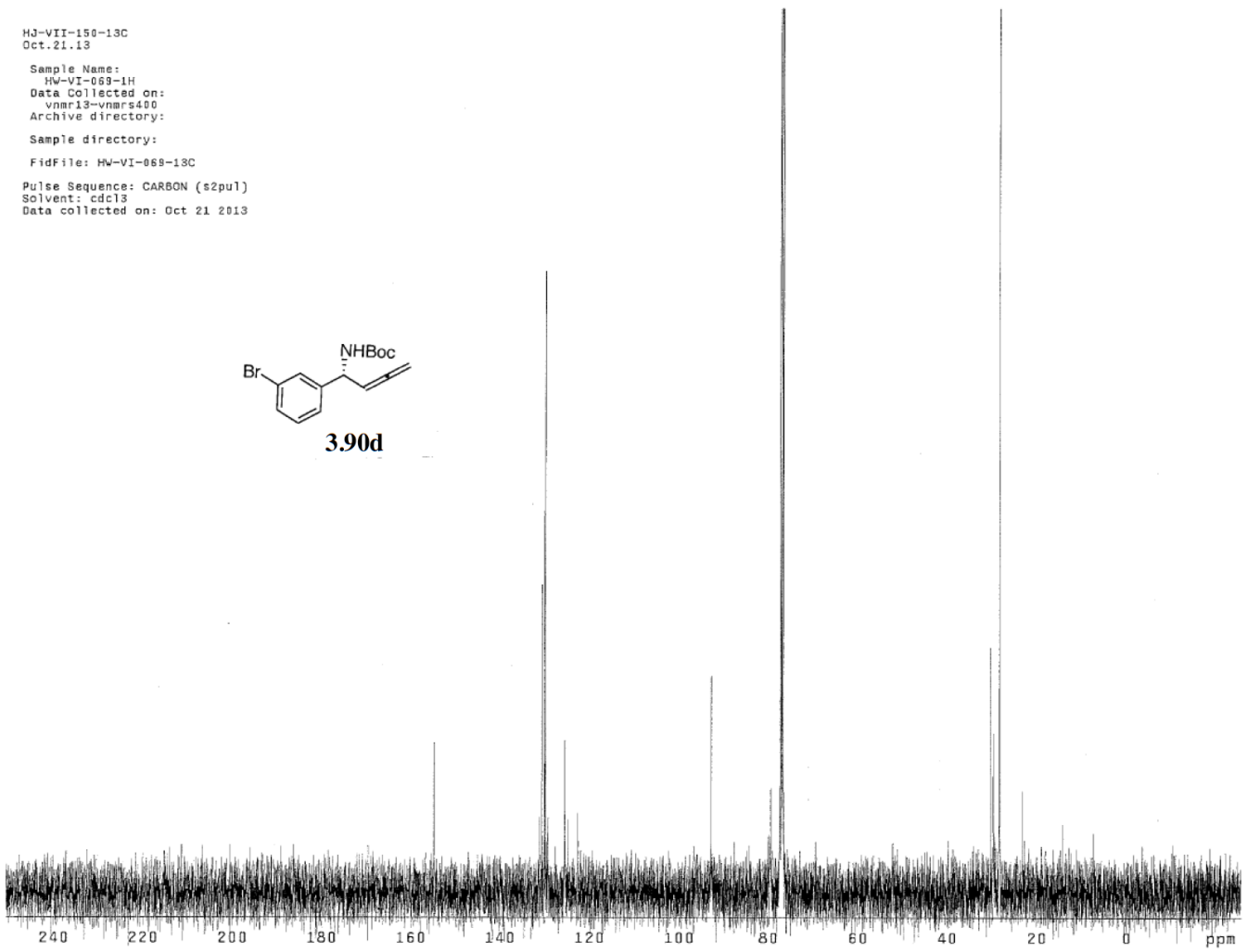
HJ-VII-150-13C
Oct.21.13
Sample Name:
HW-VI-069-1H
Data Collected on:
vnmr13-vnmrs400
Archive directory:
Sample directory:
FidFile: HW-VI-069-13C
Pulse Sequence: CARBON (s2pul)
Solvent: cdcl3
Data collected on: Oct 21 2013
NHBoc
Br
240
220
200
180
160
140
120
100
80
60
40
20
0
ppm

**3.90d**

LKA-I-122-C1-F

Sample Name:
HW-V-299
Data Collected on:
vnmr13-vnmrs400
Archive directory:

Sample directory:

FidFile: PROTON

Pulse Sequence: PROTON (s2pul)
Solvent: cdcl3
Data collected on: Apr 15 2013

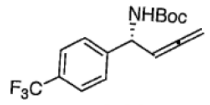


**3.90e**

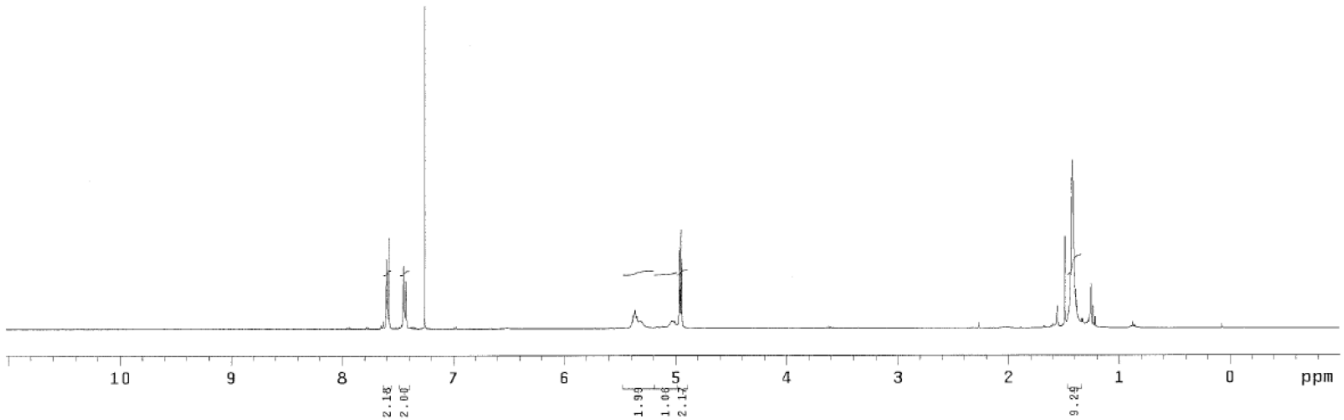

NM-3-266Dcrude

Sample Name:
HW-V-299-13C
Data Collected on:
vnmr13-vnmrs400
Archive directory:

Sample directory:

FidFile: HW-V-299-13C

Pulse Sequence: CARBON (s2pul)
Solvent: cdcl3
Data collected on: Apr 17 2013

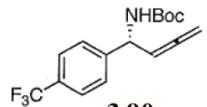


**3.90e**

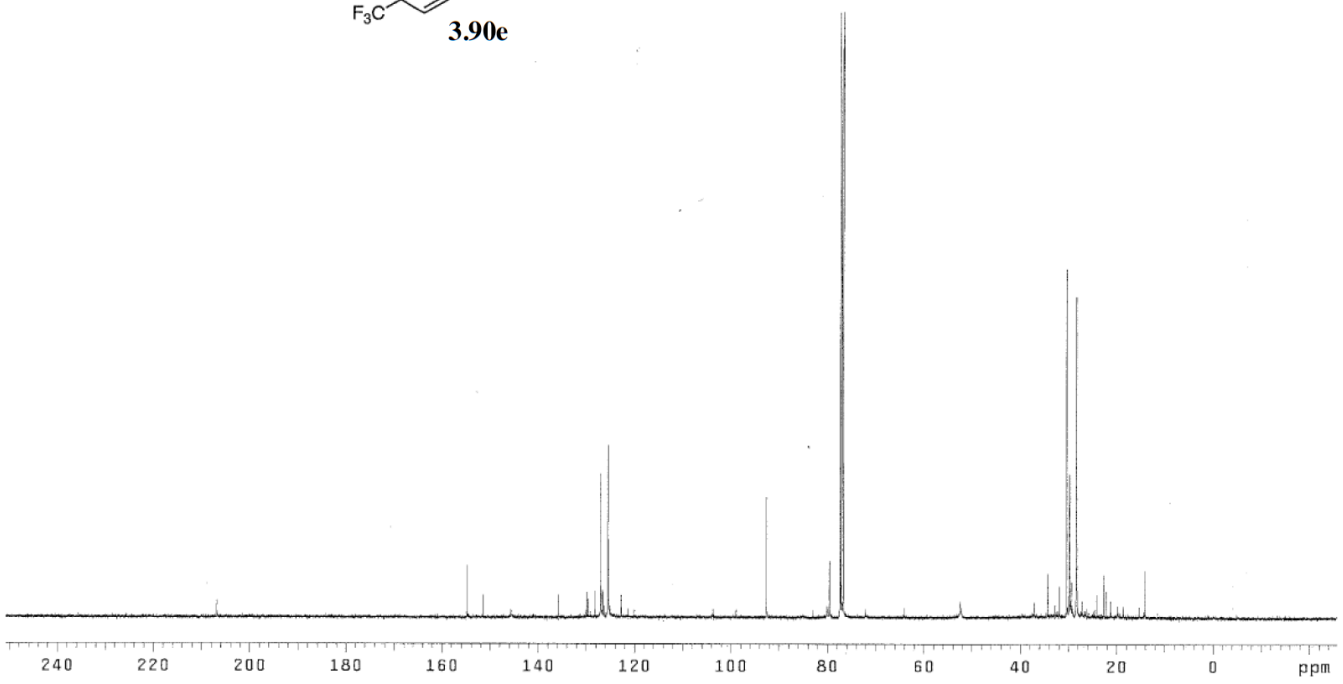

Sample Name:
HW-VI-234
Data Collected on:
vnmri3-vnmrs400
Archive directory:

Sample directory:

FidFile: PROTON

Pulse Sequence: PROTON (s2pul)
Solvent: cdcl3
Data collected on: Oct 11 2013

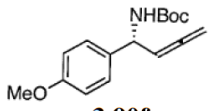


**3.90f**

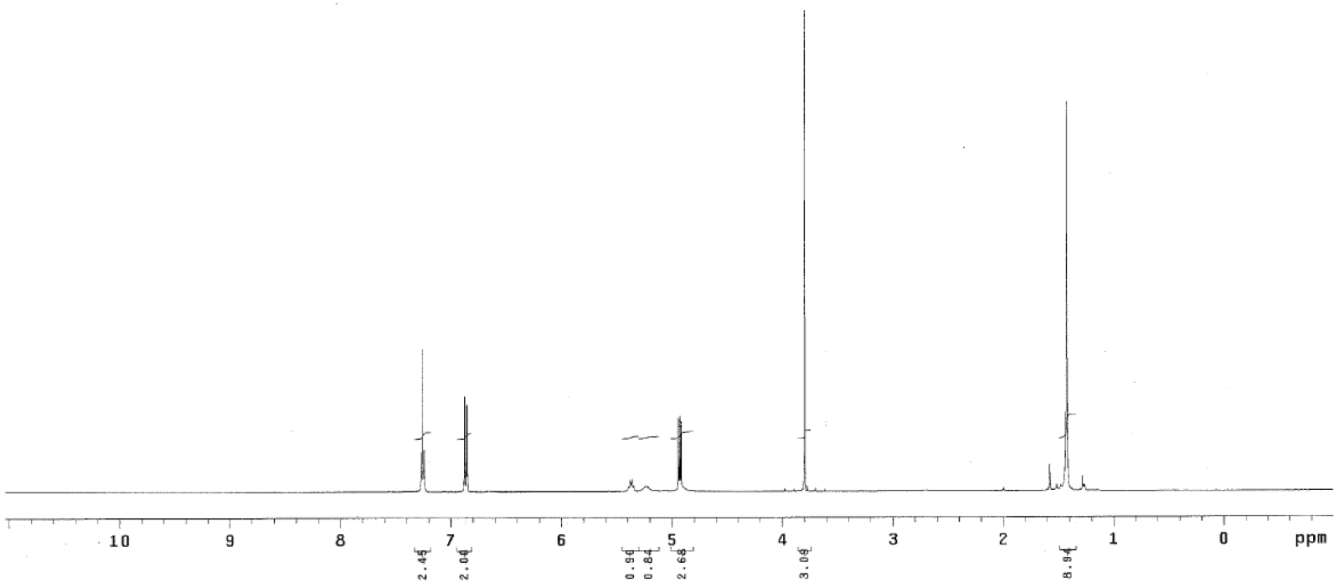

NM-3-264crude2
2.8equiv NBS

Sample Name:
HW-V-294-13C
Data Collected on:
vnmr13-vnmrs400
Archive directory:

Sample directory:

FidFile: HW-V-294-13C

Pulse Sequence: CARBON (s2pul)
Solvent: cdcl3
Data collected on: Apr 16 2013

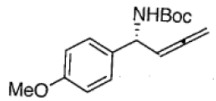


**3.90f**

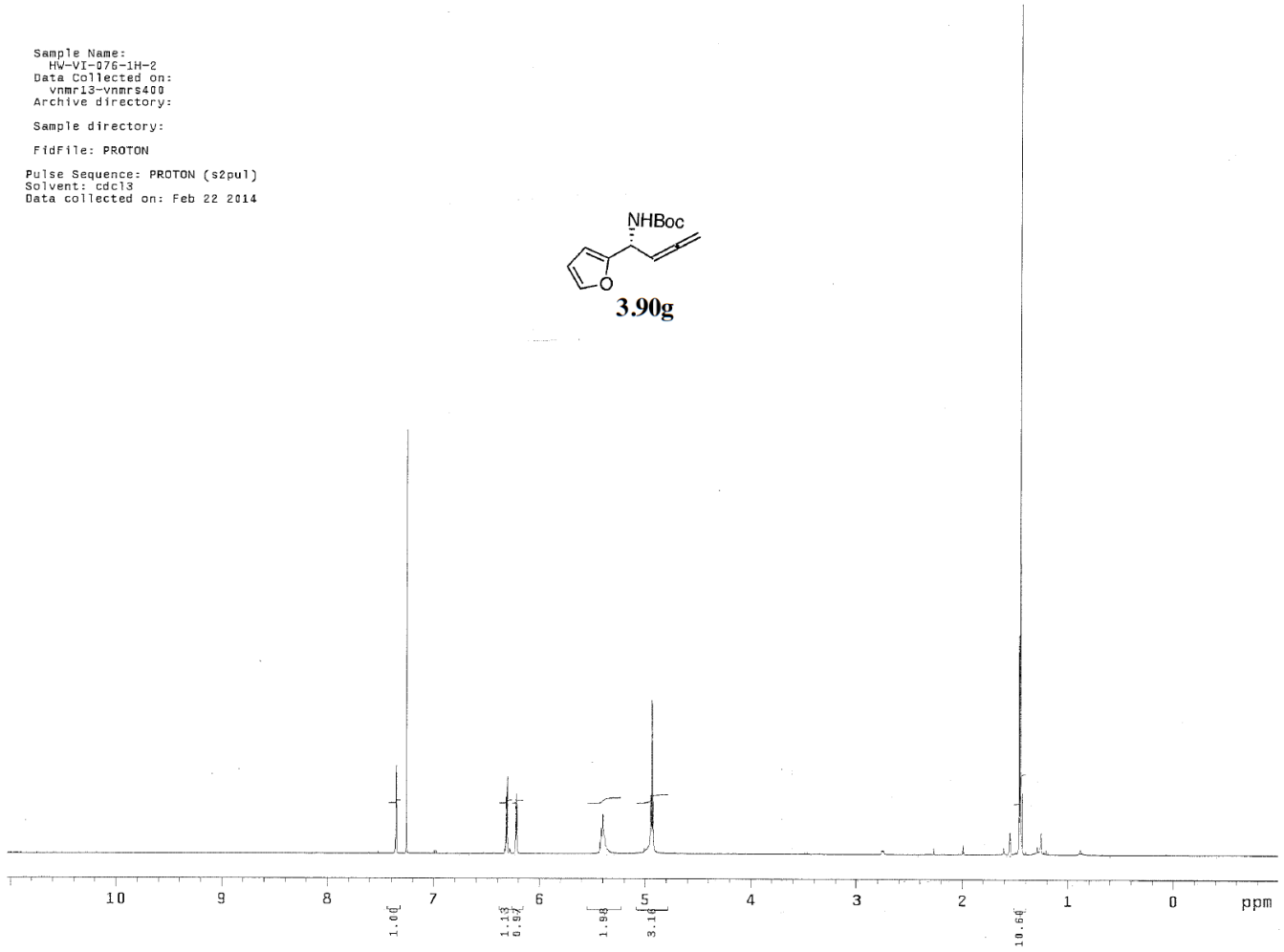
Sample Name:
HW-VI-076-1H-2
Data Collected on:
vnmr13-vnmrs400
Archive directory:
Sample directory:
FidFile: PROTON
Pulse Sequence: PROTON (s2pul)
Solvent: cdcl3
Data collected on: Feb 22 2014
NHBoc
3.90g
10
9
8
7
6
5
4
3
2
1
0
ppm
1.00
1.13
0.97
1.98
3.18
10.66

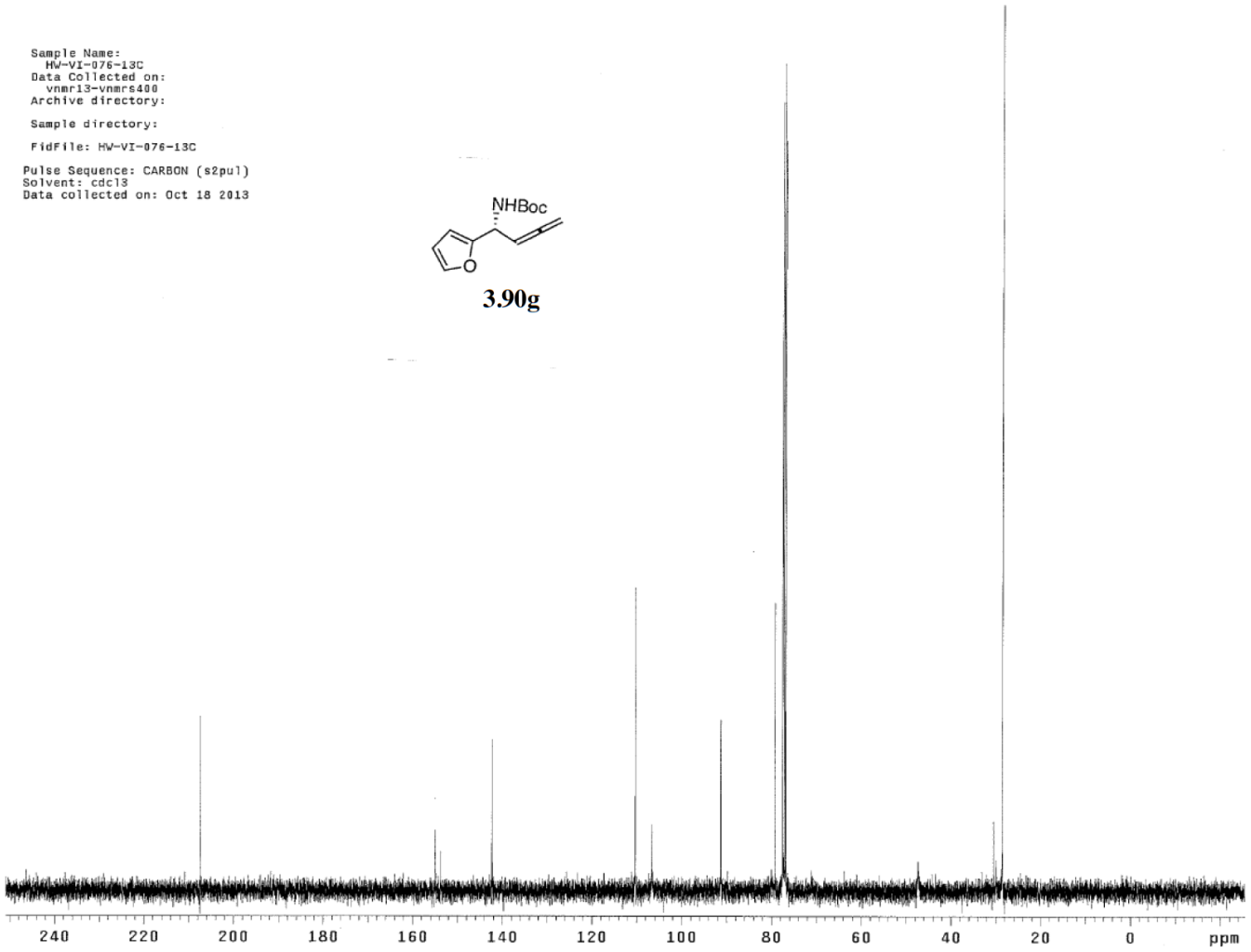
Sample Name:
HW-VI-076-13C
Data Collected on:
vnmr13-vnmrs400
Archive directory:
Sample directory:
FidFile: HW-VI-076-13C
Pulse Sequence: CARBON (s2pul)
Solvent: cdcl3
Data collected on: Oct 18 2013
NHBoc
O
3.90g
240
220
200
180
160
140
120
100
80
60
40
20
0
ppm

TMS-acetylene_chiral_sec_alcohol_1

Sample Name:
HW-VI-042-1
Data Collected on:
vnmr13-vnmrs400
Archive directory:

Sample directory:

FidFile: PROTON

Pulse Sequence: PROTON (s2pul)
Solvent: cdcl3
Data collected on: Apr 30 2013

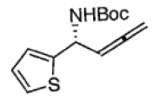


**3.90h**

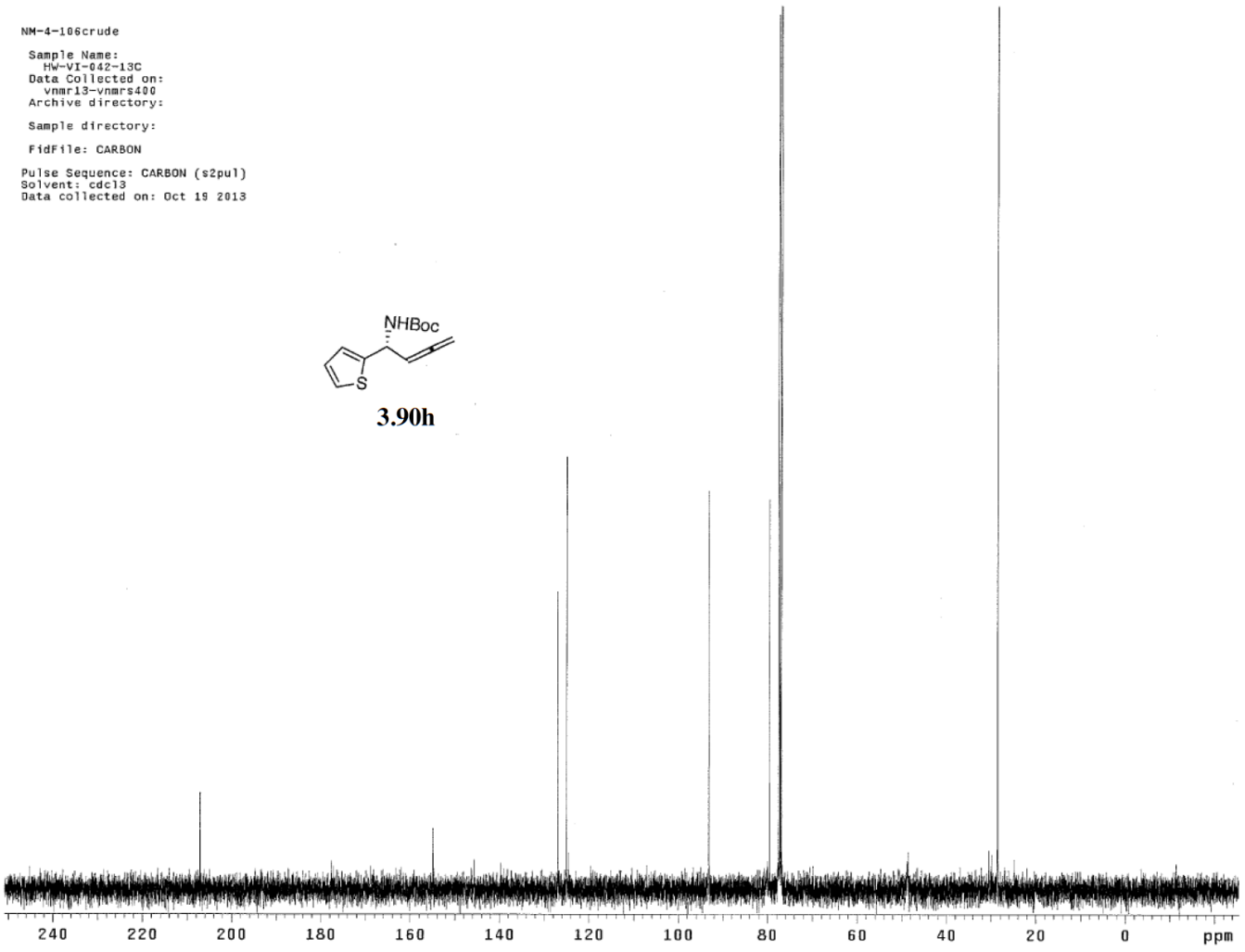
NM-4-106crude
Sample Name:
HW-VI-042-13C
Data Collected on:
vnmr13-vnmrs400
Archive directory:
Sample directory:
FidFile: CARBON
Pulse Sequence: CARBON (s2pul)
Solvent: cdcl3
Data collected on: Oct 19 2013
NHBoc
S
3.90h
240
220
200
180
160
140
120
100
80
60
40
20
0
ppm

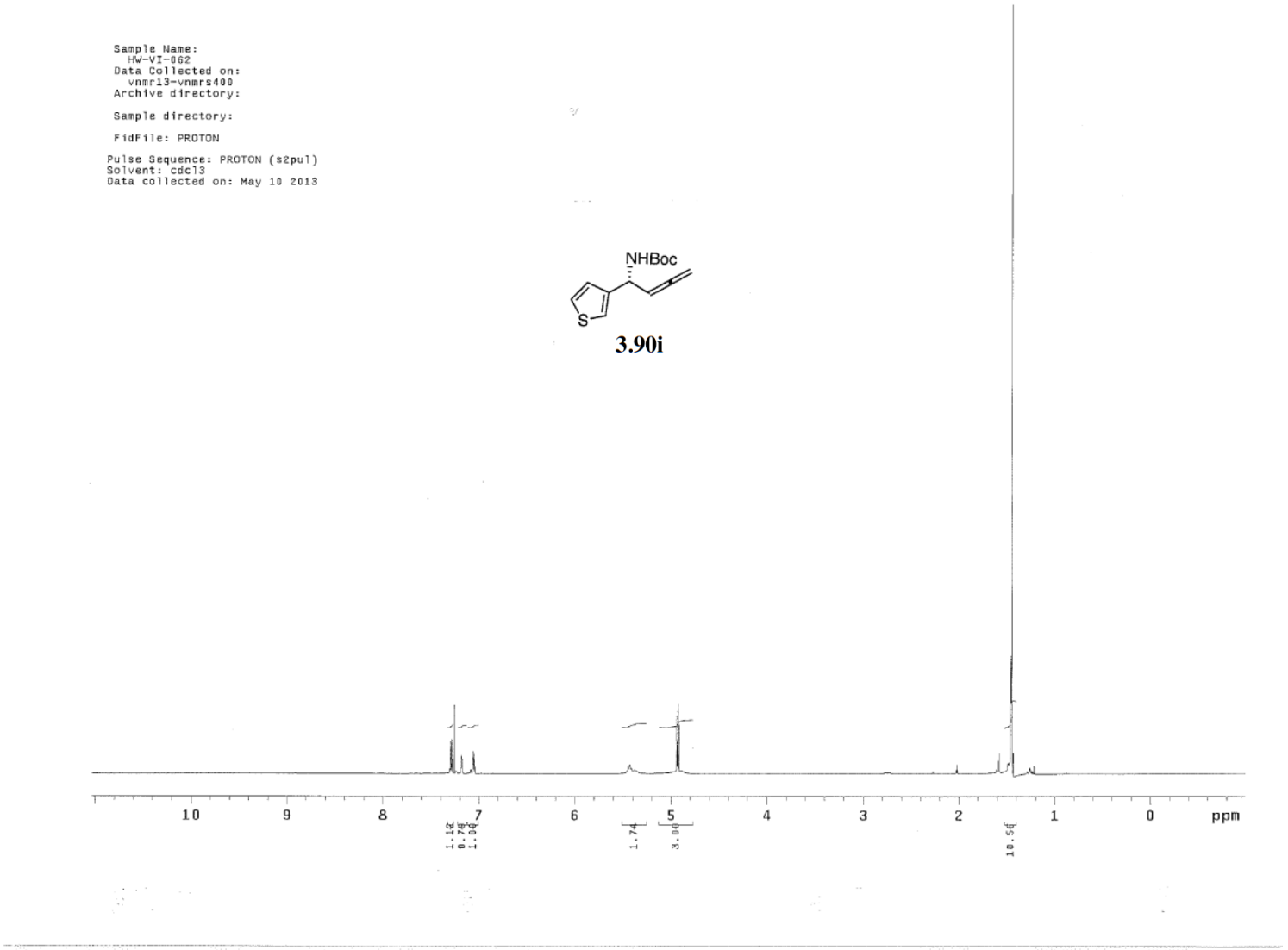
Sample Name:
HW-VI-062
Data Collected on:
vnmr13-vnmrs400
Archive directory:
Sample directory:
FidFile: PROTON
Pulse Sequence: PROTON (s2pul)
Solvent: cdcl3
Data collected on: May 10 2013
NHBoc
S
3.90i
10
9
8
7
6
5
4
3
2
1
0
ppm
1.12
0.75
1.00
1.74
3.00
10.56

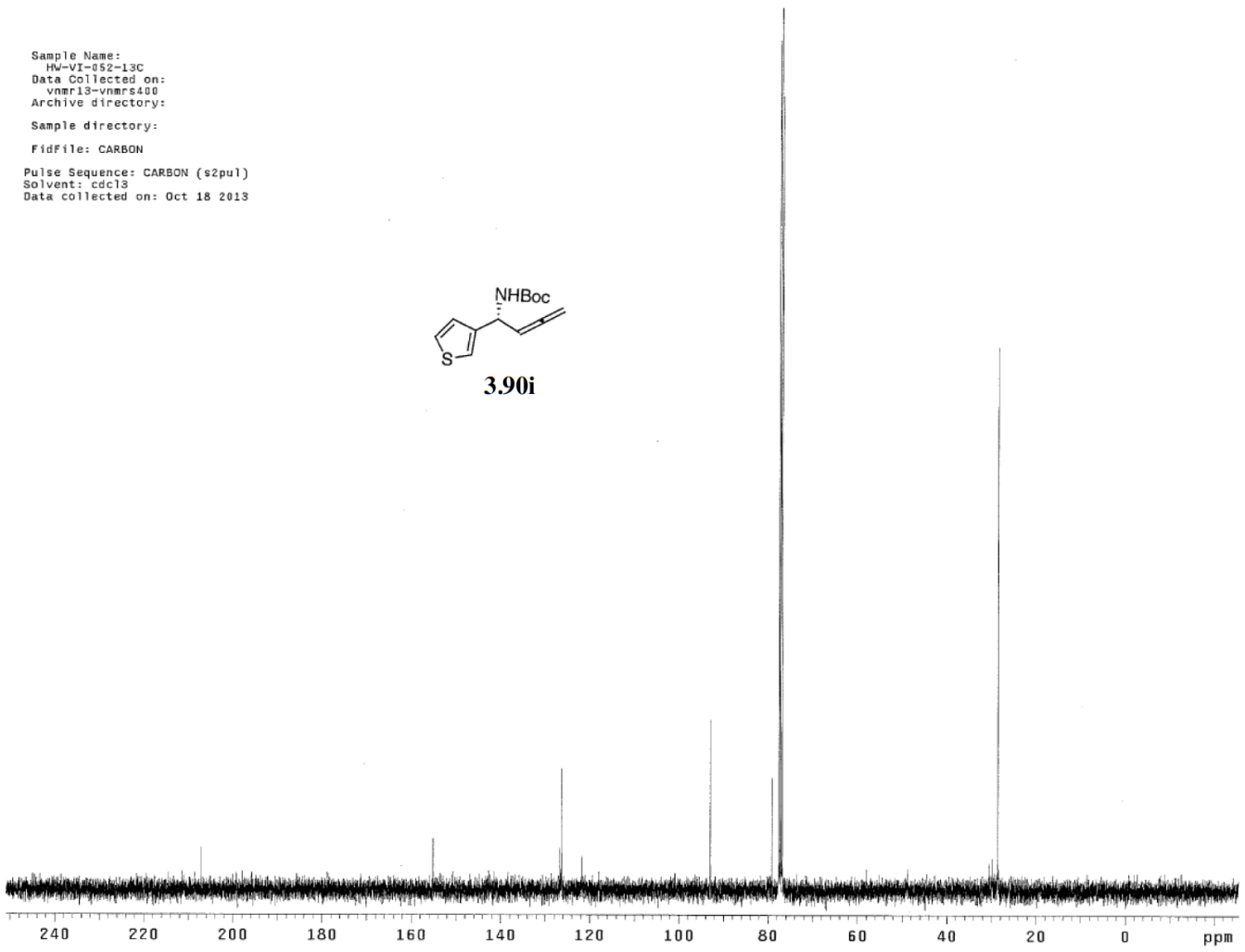
Sample Name:
HW-VI-052-13C
Data Collected on:
vnmr13-vnmrs400
Archive directory:
Sample directory:
FidFile: CARBON
Pulse Sequence: CARBON (s2pul)
Solvent: cdcl3
Data collected on: Oct 18 2013
NHBoc
S
240
220
200
180
160
140
120
100
80
60
40
20
0
ppm

**3.90i**

MJK-II-184A-1H, 24h

Sample Name:
HW-VI-246-1H
Data Collected on:
vnmr13-vnmrs400
Archive directory:

Sample directory:

FidFile: PROTON

Pulse Sequence: PROTON (s2pul)
Solvent: cdcl3
Data collected on: Nov 13 2013

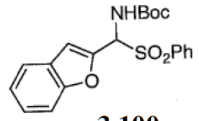


**3.100**

MJK-II-184A-1H, 24h

Sample Name:
HW-VI-246-13C
Data Collected on:
vnmr13-vnmrs400
Archive directory:

Sample directory:

FidFile: CARBON

Pulse Sequence: CARBON (s2pul)
Solvent: cdcl3
Data collected on: Nov 13 2013

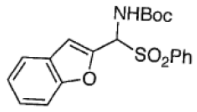


**3.100**

LKA-I-286-CP

Sample Name:
HW-VI-250-1H
Data Collected on:
vnmr13-vnmrs400
Archive directory:

Sample directory:

FidFile: PROTON

Pulse Sequence: PROTON (s2pul)
Solvent: cdcl3
Data collected on: Nov 14 2013

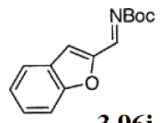


**3.96j**

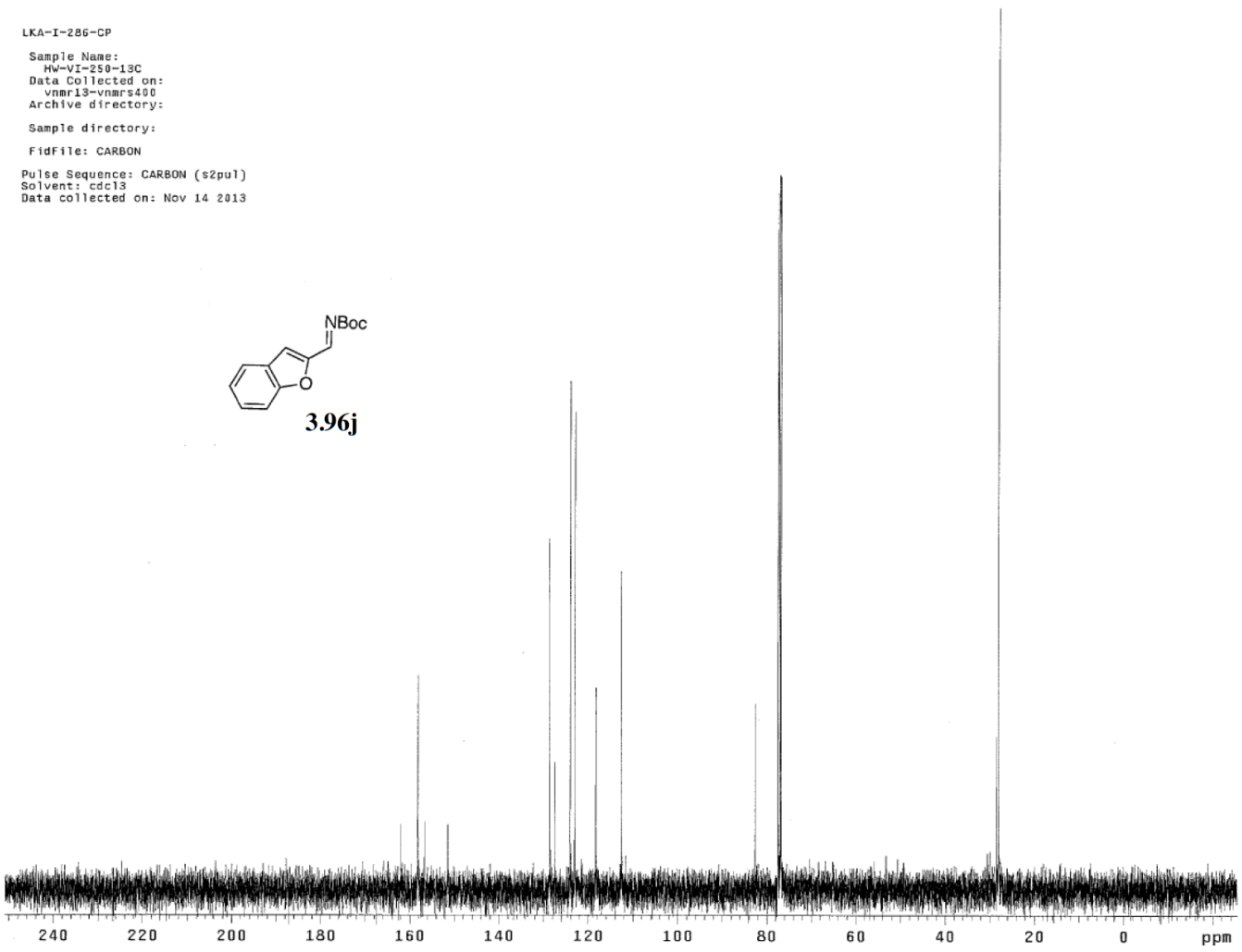
LKA-I-286-CP
Sample Name:
HW-VI-250-13C
Data Collected on:
vnmr13-vnmrs400
Archive directory:
Sample directory:
FidFile: CARBON
Pulse Sequence: CARBON (s2pul)
Solvent: cdcl3
Data collected on: Nov 14 2013
NBoc
O
3.96j
240
220
200
180
160
140
120
100
80
60
40
20
0
ppm

Sample Name:
HW-VI-252
Data Collected on:
vnmr13-vnmrs400
Archive directory:

Sample directory:

FidFile: PROTON

Pulse Sequence: PROTON (s2pul)
Solvent: cdcl3
Data collected on: Nov 7 2013

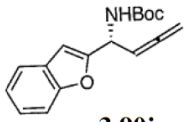


**3.90j**

NM-2-242dist2remain

Sample Name:
Hw-VI-252-13C
Data Collected on:
vnmr13-vnmrs400
Archive directory:

Sample directory:

FidFile: CARBON

Pulse Sequence: CARBON (s2pul)
Solvent: cdcl3
Data collected on: Nov 7 2013

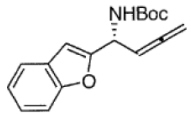


**3.90j**

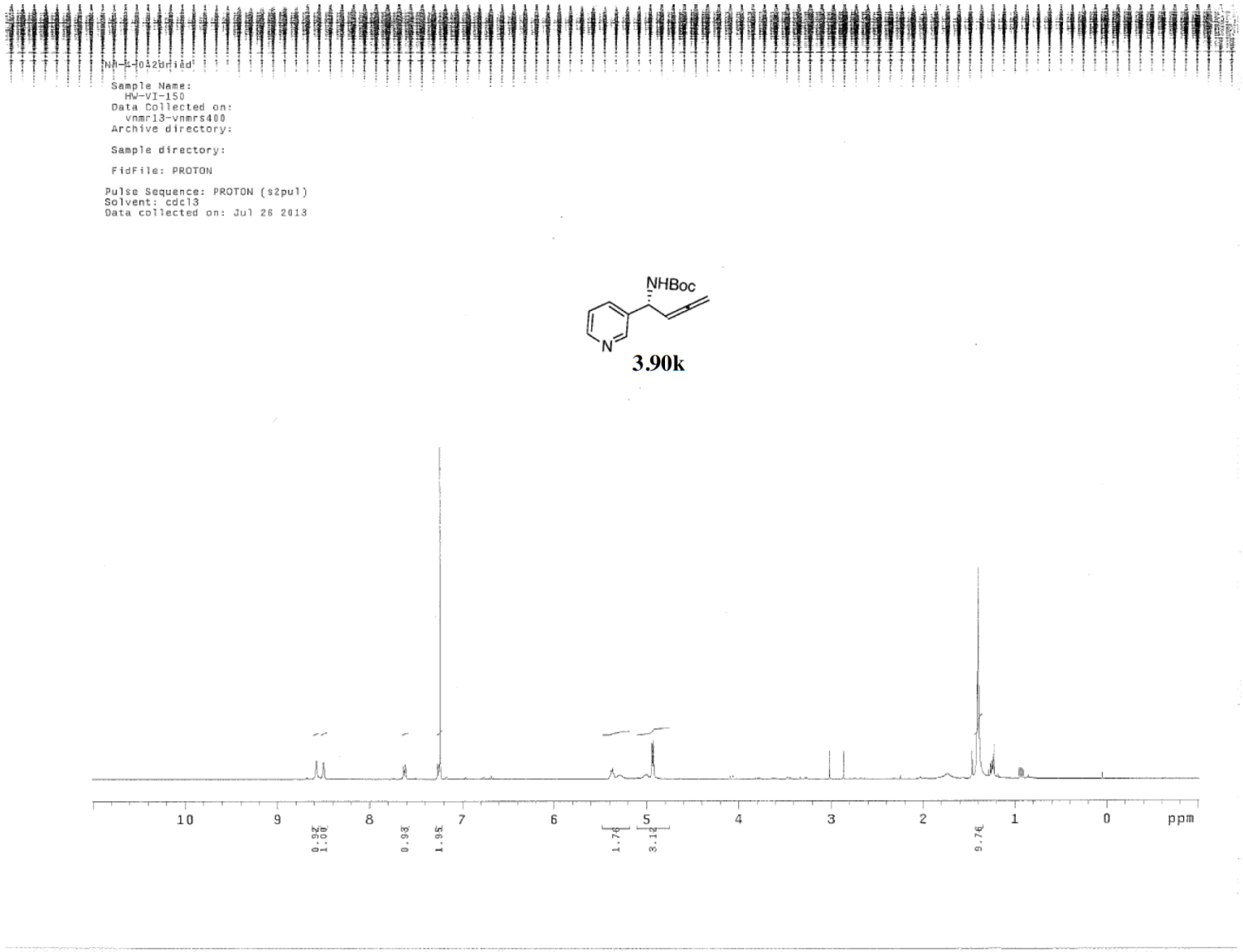
NA-4-1012dried
Sample Name:
HW-VI-150
Data Collected on:
vnmr13-vnmrs400
Archive directory:
Sample directory:
FidFile: PROTON
Pulse Sequence: PROTON (s2pul)
Solvent: cdcl3
Data collected on: Jul 26 2013
NHBoc
N
3.90k
10
9
8
7
6
5
4
3
2
1
0
ppm
0.92
1.00
0.93
1.95
1.76
3.14
9.76

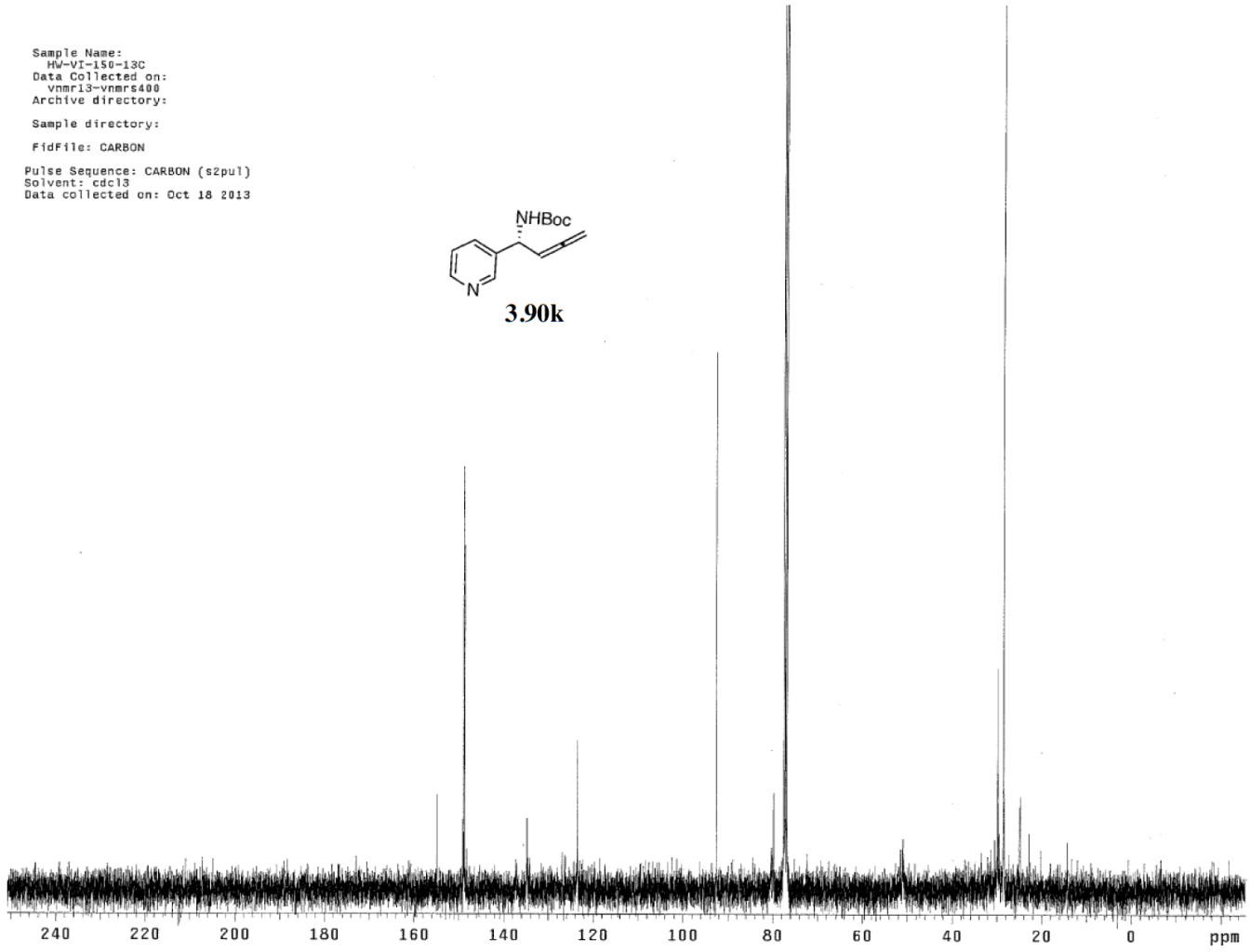
Sample Name:
HW-VI-150-13C
Data Collected on:
vnmr13-vnmrs400
Archive directory:
Sample directory:
FidFile: CARBON
Pulse Sequence: CARBON (s2pul)
Solvent: cdcl3
Data collected on: Oct 18 2013
NHBoc
N
3.90k
240
220
200
180
160
140
120
100
80
60
40
20
0
ppm

Sample Name:
HW-VI-211-2
Data Collected on:
vnmr13-vnmrs400
Archive directory:

Sample directory:

FidFile: PROTON

Pulse Sequence: PROTON (s2pul)
Solvent: cdcl3
Data collected on: Sep 24 2013

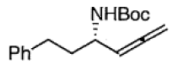


**3.901**

Sample Name:
HW-VI-211-13C-2
Data Collected on:
vnmr13-vnmrs400
Archive directory:

Sample directory:

FidFile: HW-VI-211-13C-2

Pulse Sequence: CARBON (s2pul)
Solvent: cdcl3
Data collected on: Sep 24 2013

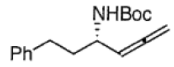


**3.901**

NM-4-0908crude

Sample Name:
HW-VI-217
Data Collected on:
vnmr13-vnmrs400
Archive directory:

Sample directory:

FidFile: PROTON

Pulse Sequence: PROTON (s2pul)
Solvent: cdcl3
Data collected on: Sep 23 2013

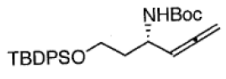


**3.90m**

NM-4-090Bcrude

Sample Name:
HW-VI-217-13C
Data Collected on:
vnmr13-vnmrs400
Archive directory:

Sample directory:

FidFile: HW-VI-217-13C

Pulse Sequence: CARBON (s2pul)
Solvent: cdcl3
Data collected on: Sep 23 2013

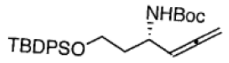


**3.90m**

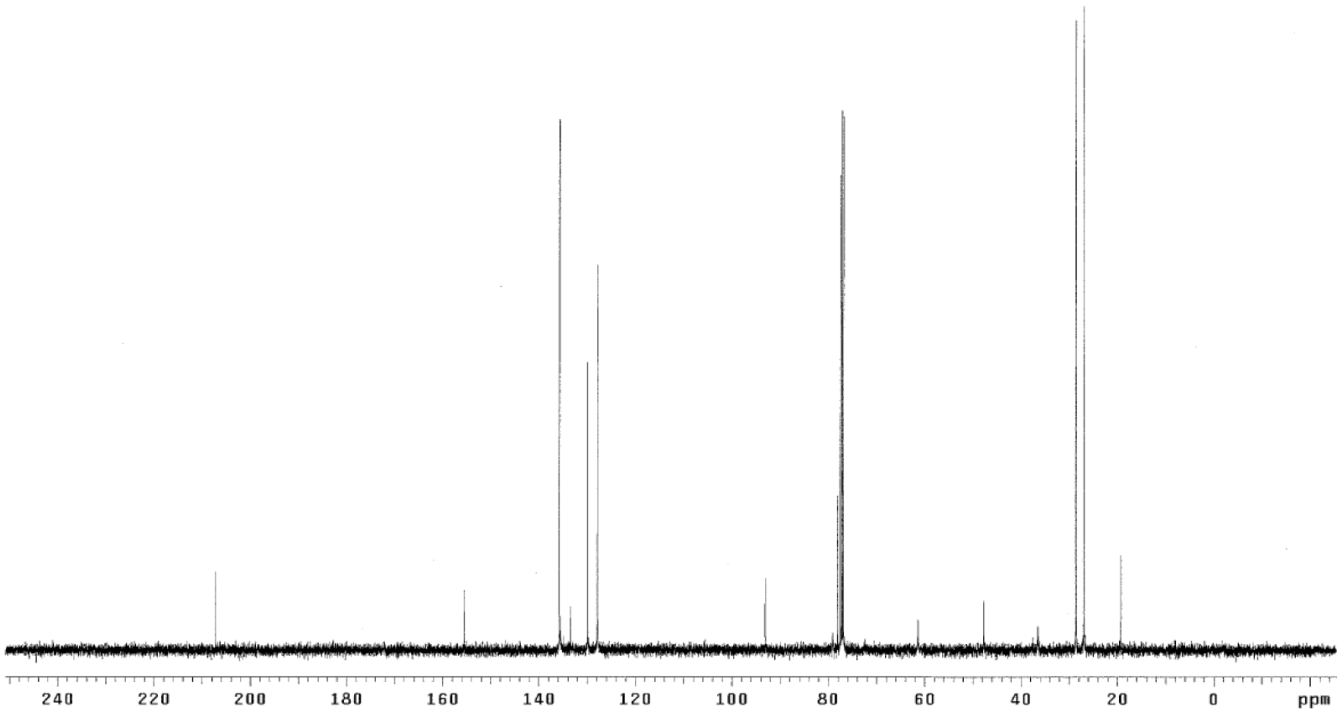

NM-4-092Bcrude

Sample Name:
HW-VI-227
Data Collected on:
vnmr13-vnmrs400
Archive directory:

Sample directory:

FidFile: PROTON

Pulse Sequence: PROTON (s2pul)
Solvent: cdcl3
Data collected on: Oct 2 2013

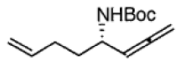


**3.90n**

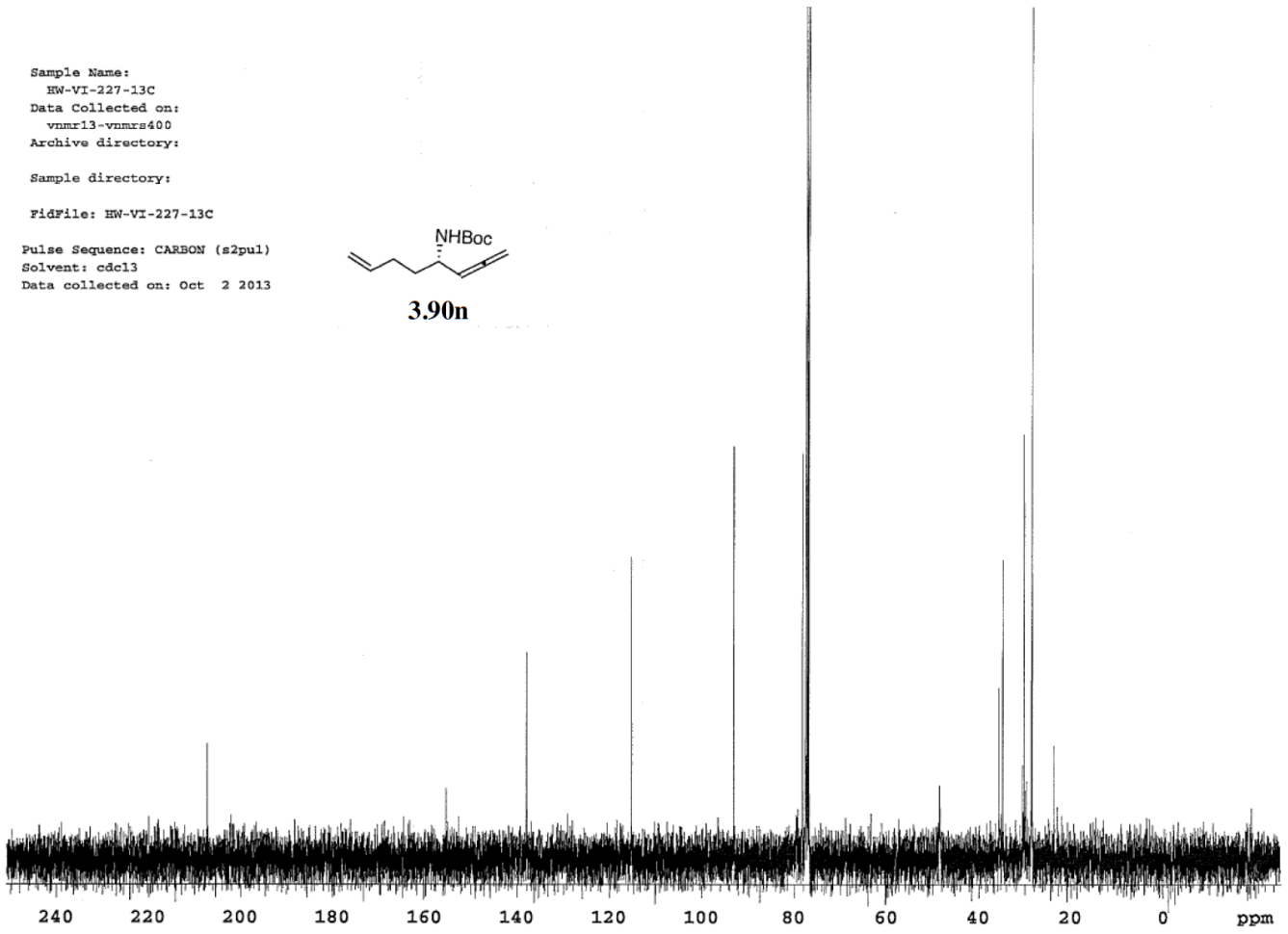
Sample Name:
HW-VI-227-13C
Data Collected on:
vnmr13-vnmrs400
Archive directory:
Sample directory:
FidFile: HW-VI-227-13C
Pulse Sequence: CARBON (s2pul)
Solvent: cdcl3
Data collected on: Oct 2 2013
NHBoc
3.90n
240
220
200
180
160
140
120
100
80
60
40
20
0
ppm

Sample Name:
HW-VI-104
Data Collected on:
vnmr13-vnmrs400
Archive directory:

Sample directory:

FidFile: PROTON

Pulse Sequence: PROTON (s2pul)
Solvent: cdcl3
Data collected on: Jun 5 2013

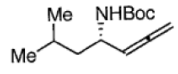


**3.90o**

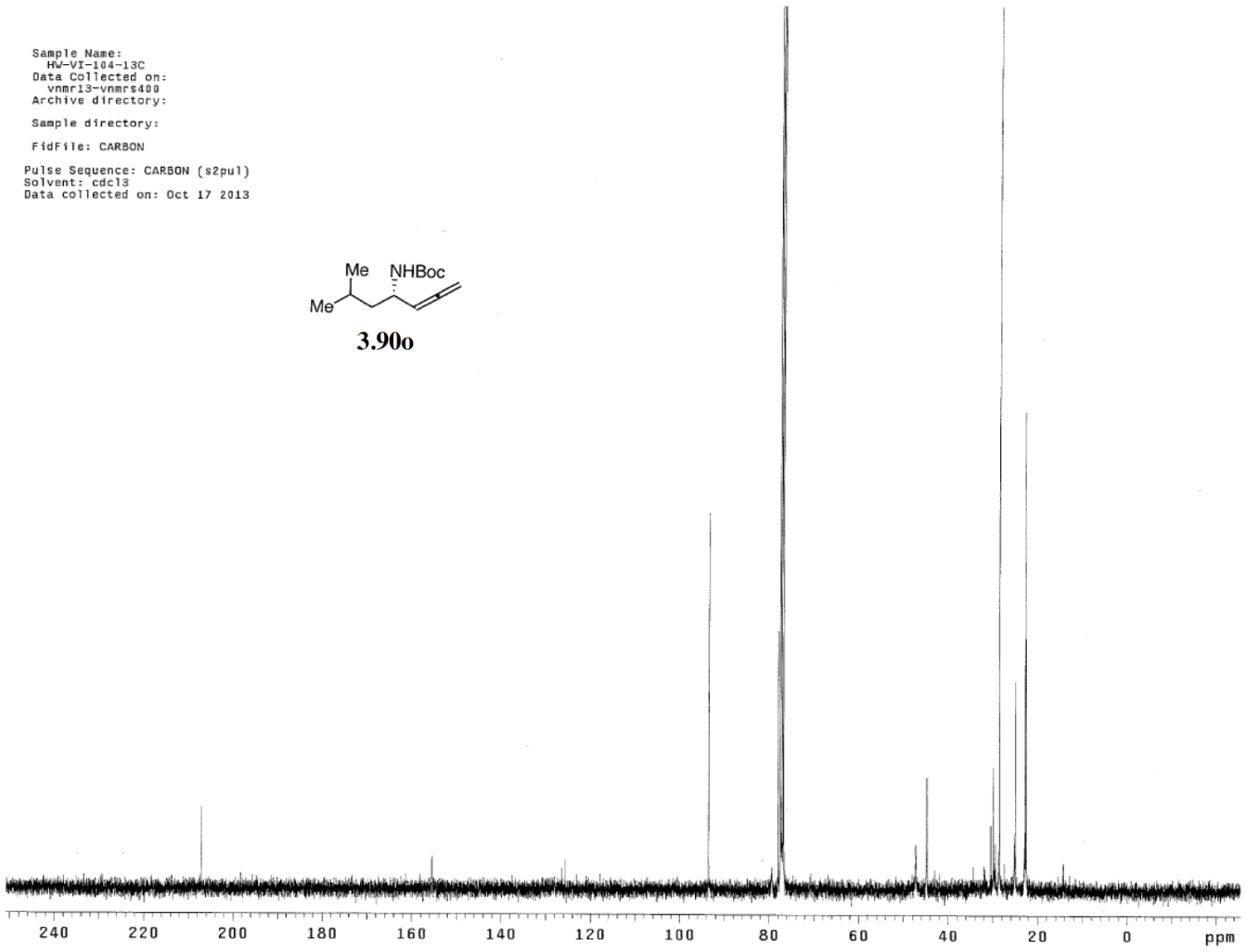
Sample Name:
HW-VI-104-13C
Data Collected on:
vnmr13-vnmrs400
Archive directory:
Sample directory:
FidFile: CARBON
Pulse Sequence: CARBON (s2pul)
Solvent: cdcl3
Data collected on: Oct 17 2013
Me
NHBoc
Me
240
220
200
180
160
140
120
100
80
60
40
20
0
ppm

**3.90o**

MJK-I-245B-1H, 6h

Sample Name:
HW-VI-086
Data Collected on:
vnmr13-vnmrs400
Archive directory:

Sample directory:

FidFile: PROTON

Pulse Sequence: PROTON (s2pul)
Solvent: cdcl3
Data collected on: May 24 2013

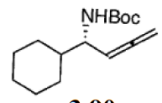


**3.90p**

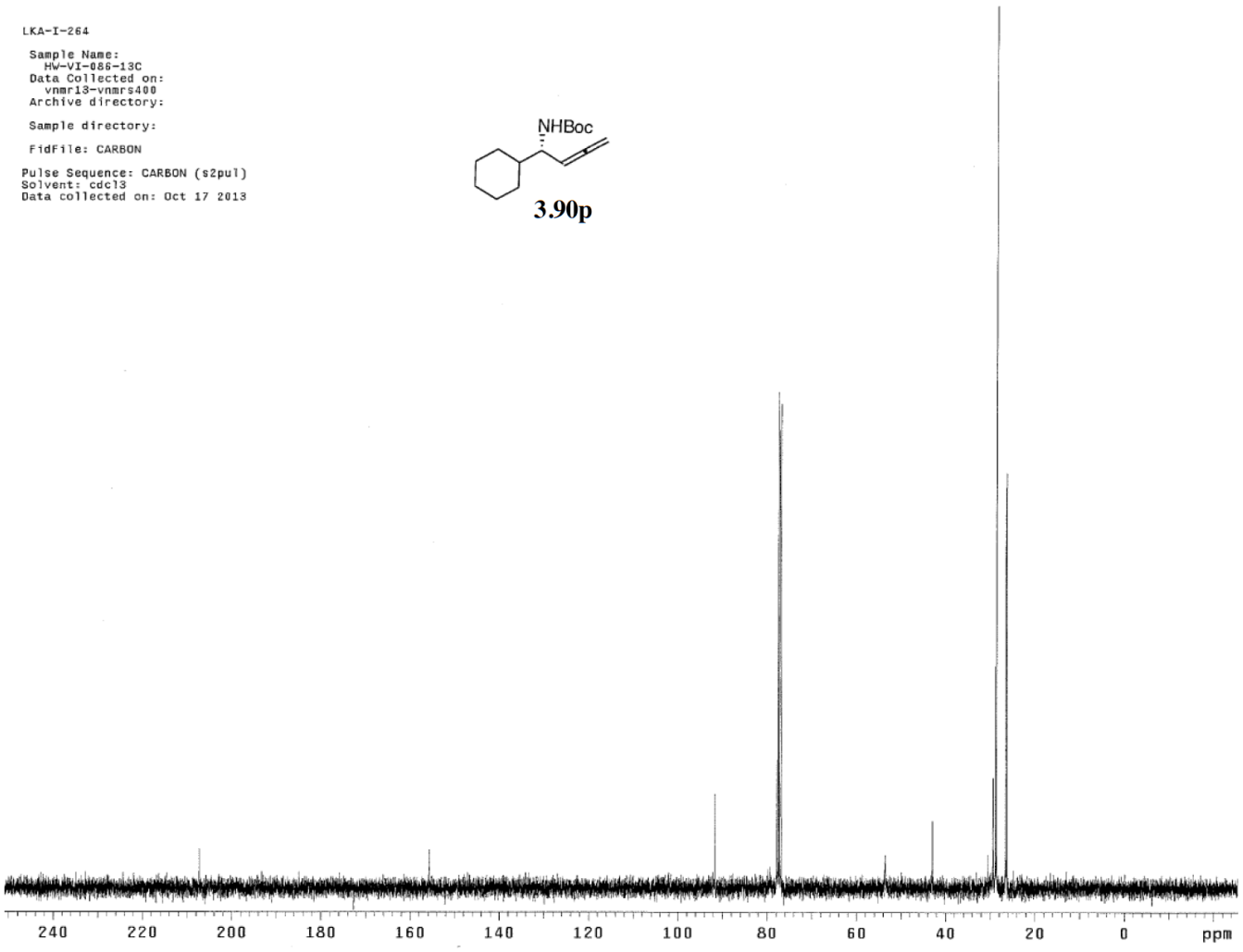
LKA-I-264
Sample Name:
HW-VI-086-13C
Data Collected on:
vnmr13-vnmrs400
Archive directory:
Sample directory:
FidFile: CARBON
Pulse Sequence: CARBON (s2pul)
Solvent: cdcl3
Data collected on: Oct 17 2013
NHBoc
3.90p
240
220
200
180
160
140
120
100
80
60
40
20
0
ppm

HJ-VII-119-A-13C
Sep.26.13

Sample Name:
HW-VI-222
Data Collected on:
vnmr13-vnmrs400
Archive directory:

Sample directory:

FidFile: HW-VI-222

Pulse Sequence: PROTON (s2pul)
Solvent: cdcl3
Data collected on: Sep 26 2013

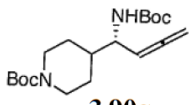


**3.90q**

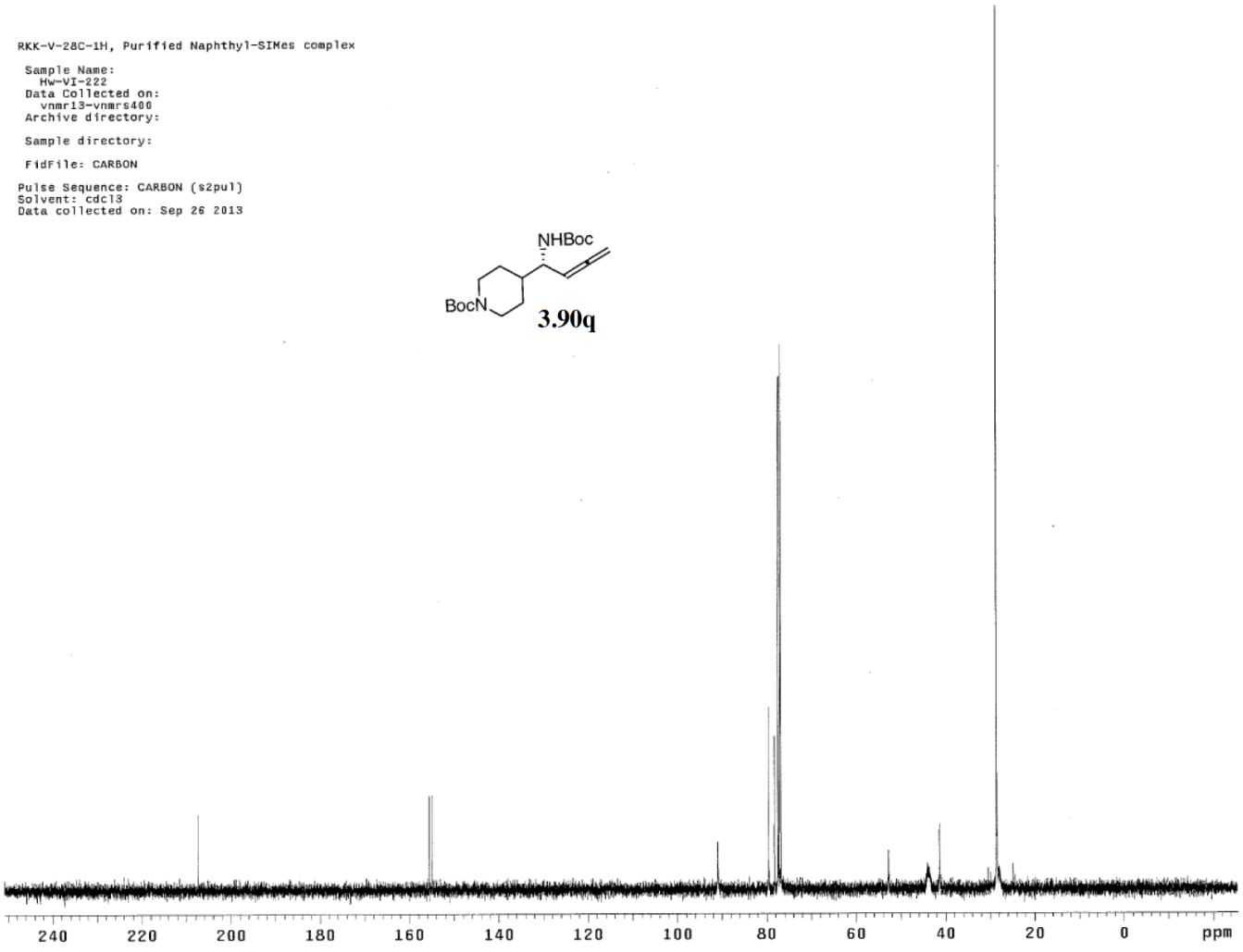
RKK-V-28C-1H, Purified Naphthyl-SIMes complex
Sample Name:
Hw-VI-222
Data Collected on:
vnmr13-vnmrs400
Archive directory:
Sample directory:
FidFile: CARBON
Pulse Sequence: CARBON (s2pul)
Solvent: cdcl3
Data collected on: Sep 26 2013
NHBoc
BocN
3.90q
240
220
200
180
160
140
120
100
80
60
40
20
0
ppm

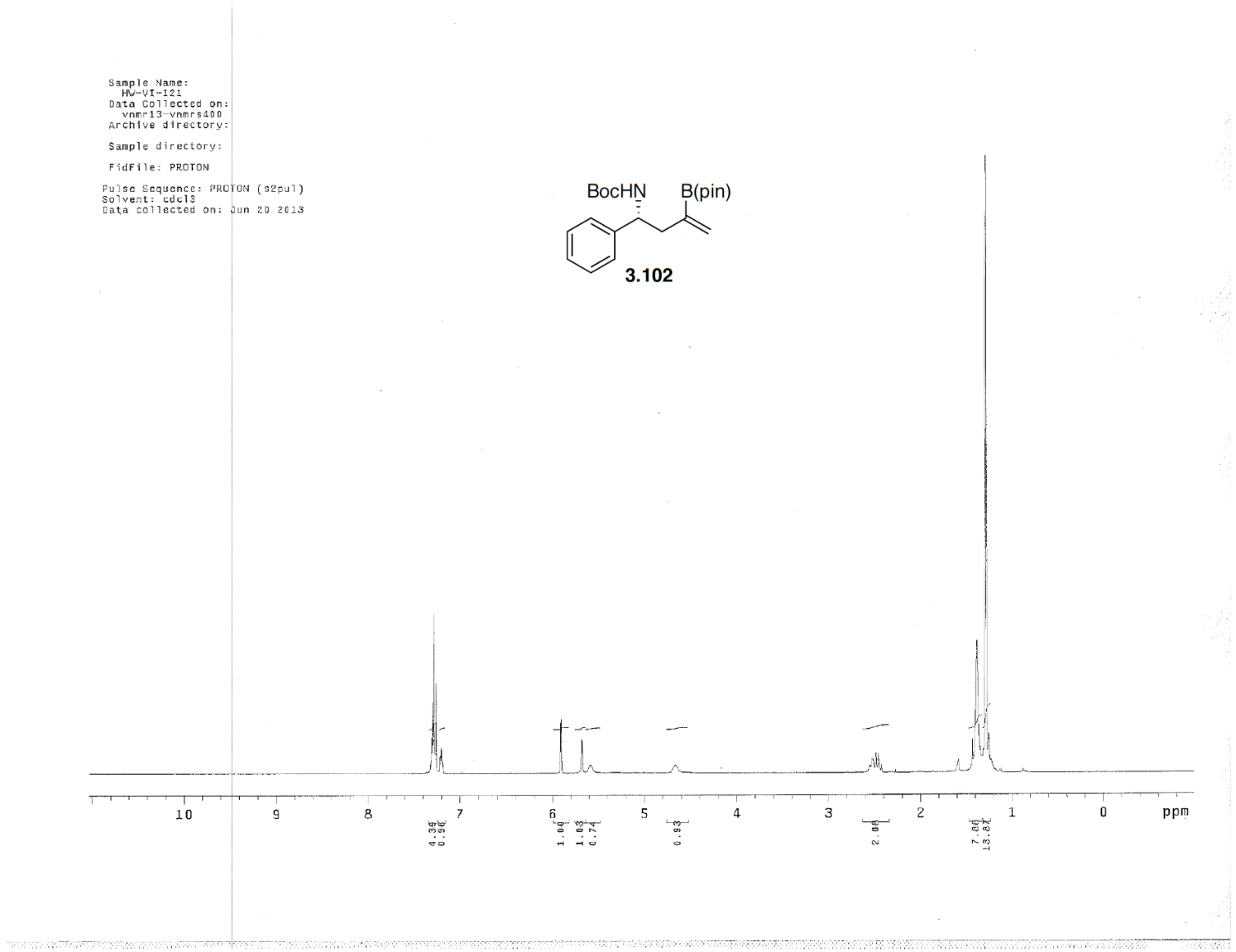
Sample Name:
HW-VI-121
Data Collected on:
vnmr13-vnmrs400
Archive directory:
Sample directory:
FidFile: PROTON
Pulse Sequence: PROTON (s2pul)
Solvent: cdcl3
Data collected on: Jun 20 2013
BocHN
B(pin)
3.102
10
9
8
7
6
5
4
3
2
1
0
ppm
4.38
0.96
1.00
1.03
0.74
0.93
2.00
7.00
13.87

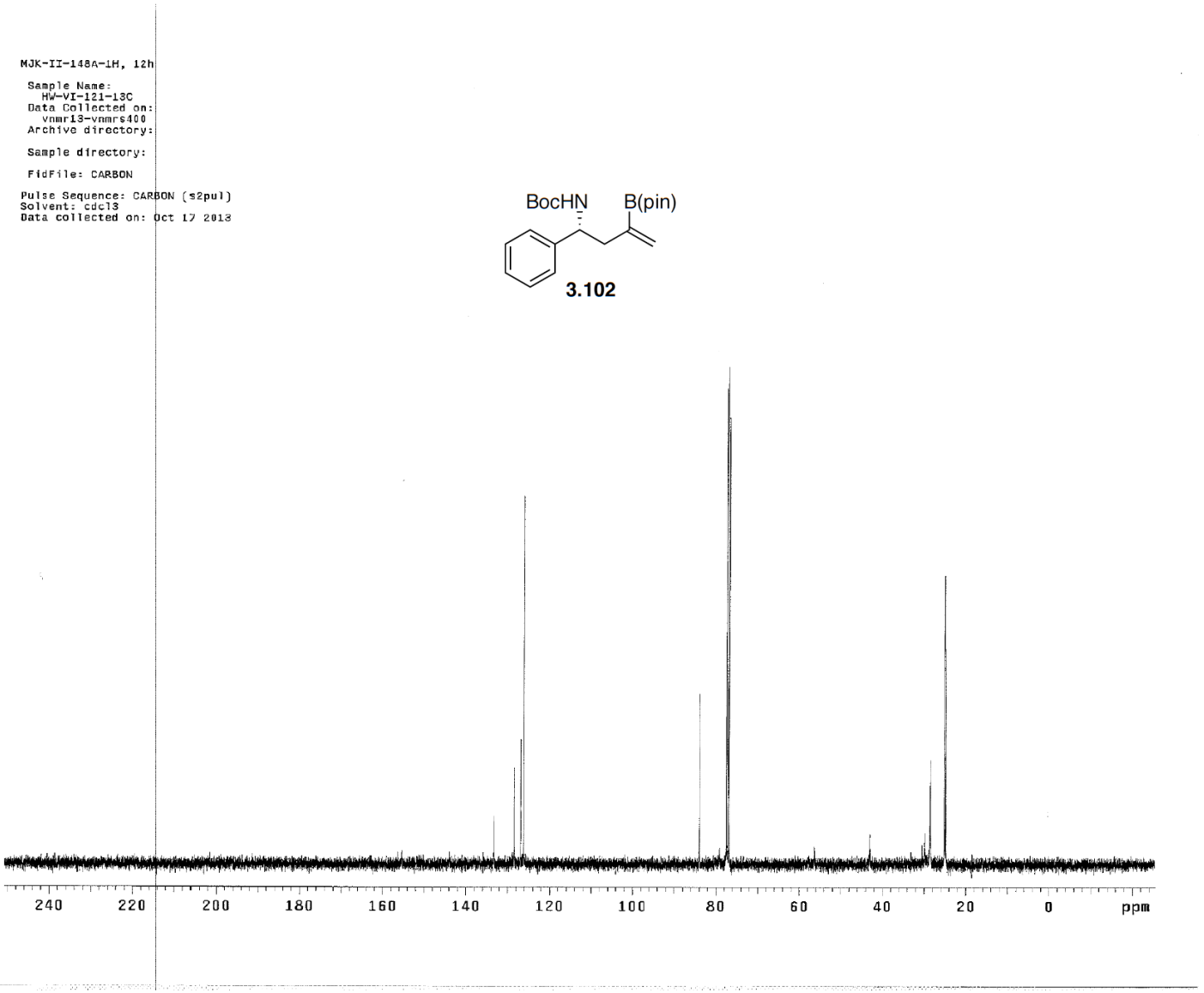
MJK-II-148A-1H, 12h
Sample Name:
HW-VI-121-13C
Data Collected on:
vnmr13-vnmrs400
Archive directory:
Sample directory:
FidFile: CARBON
Pulse Sequence: CARBON (s2pul)
Solvent: cdcl3
Data collected on: Oct 17 2018
BocHN
B(pin)
3.102
240
220
200
180
160
140
120
100
80
60
40
20
0
ppm

Sample Name:
HW-VI-147-1H
Data Collected on:
vnmr13-vnmrs400
Archive directory:

Sample directory:

FidFile: PROTON

Pulse Sequence: PROTON (s2pul)
Solvent: cdcl3
Data collected on: Oct 21 2013

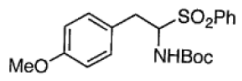


**precursor of 3.107**

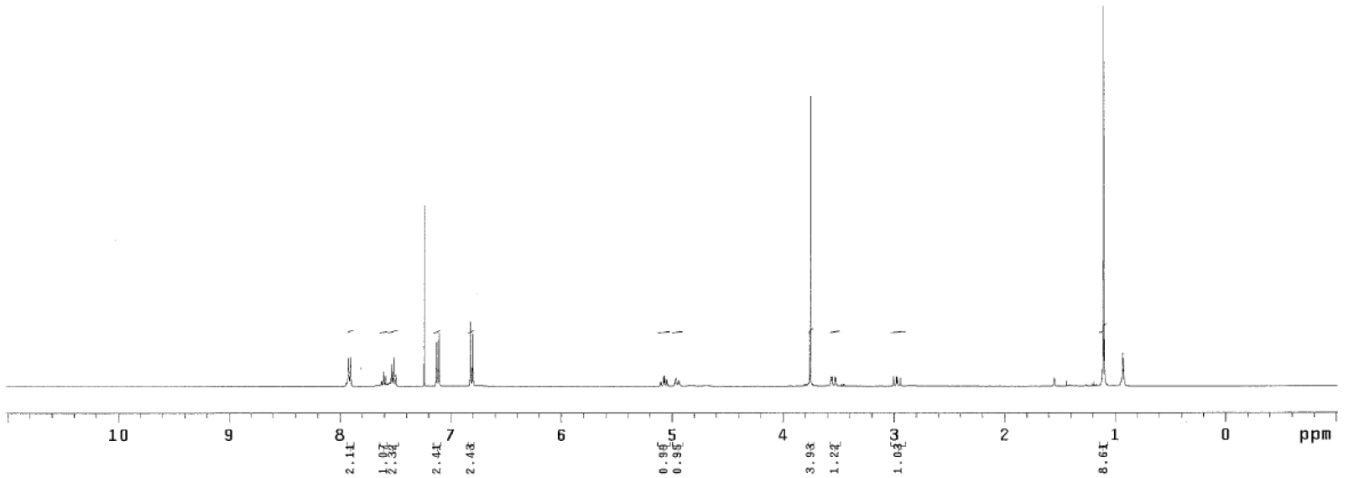

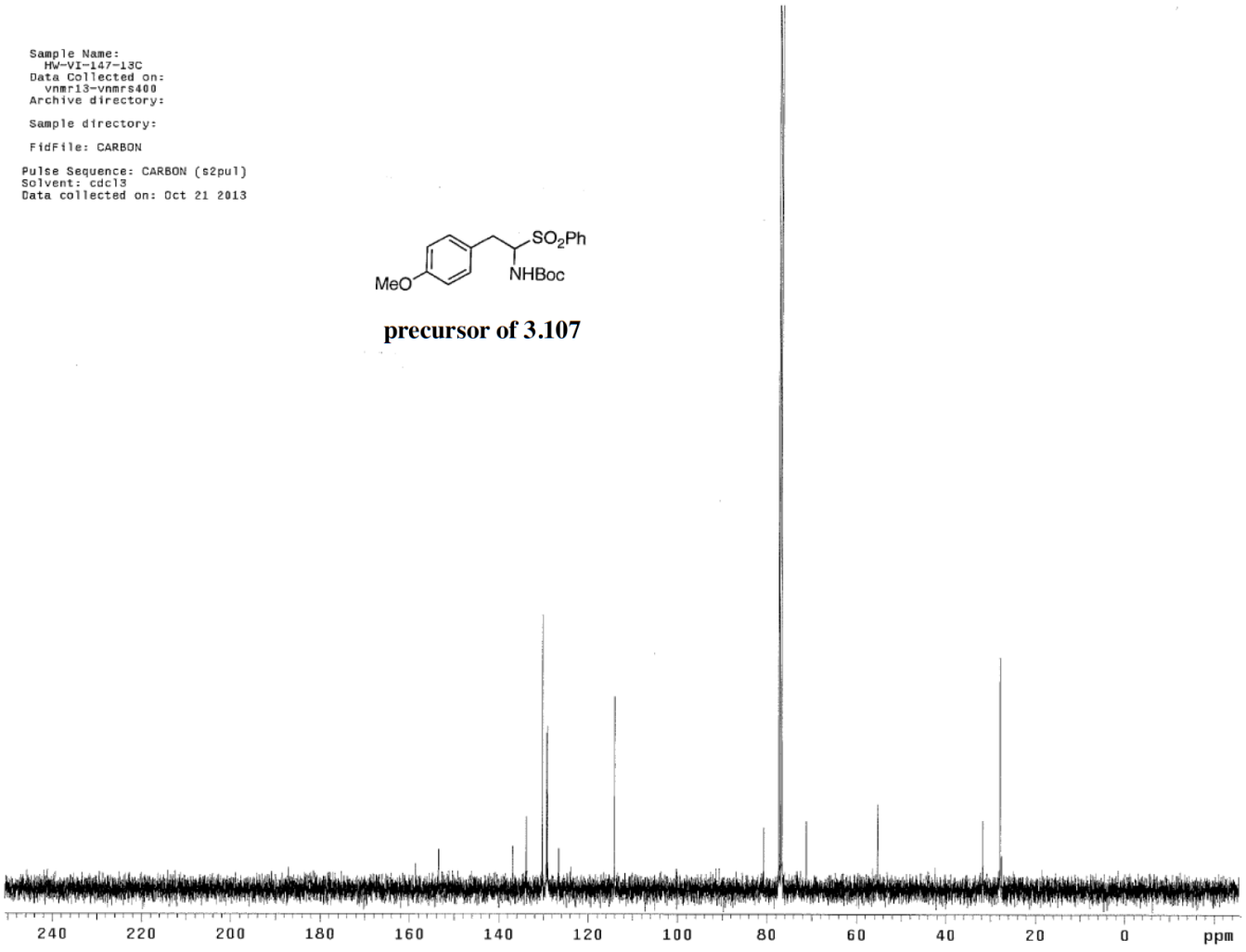


**precursor of 3.107**

TJM-V-011-c

Sample Name:
HW-VI-214
Data Collected on:
vnmr13-vnmrs400
Archive directory:

Sample directory:

FidFile: PROTON

Pulse Sequence: PROTON (s2pul)
Solvent: cdcl3
Data collected on: Sep 19 2013

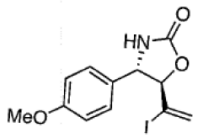


**3.111**

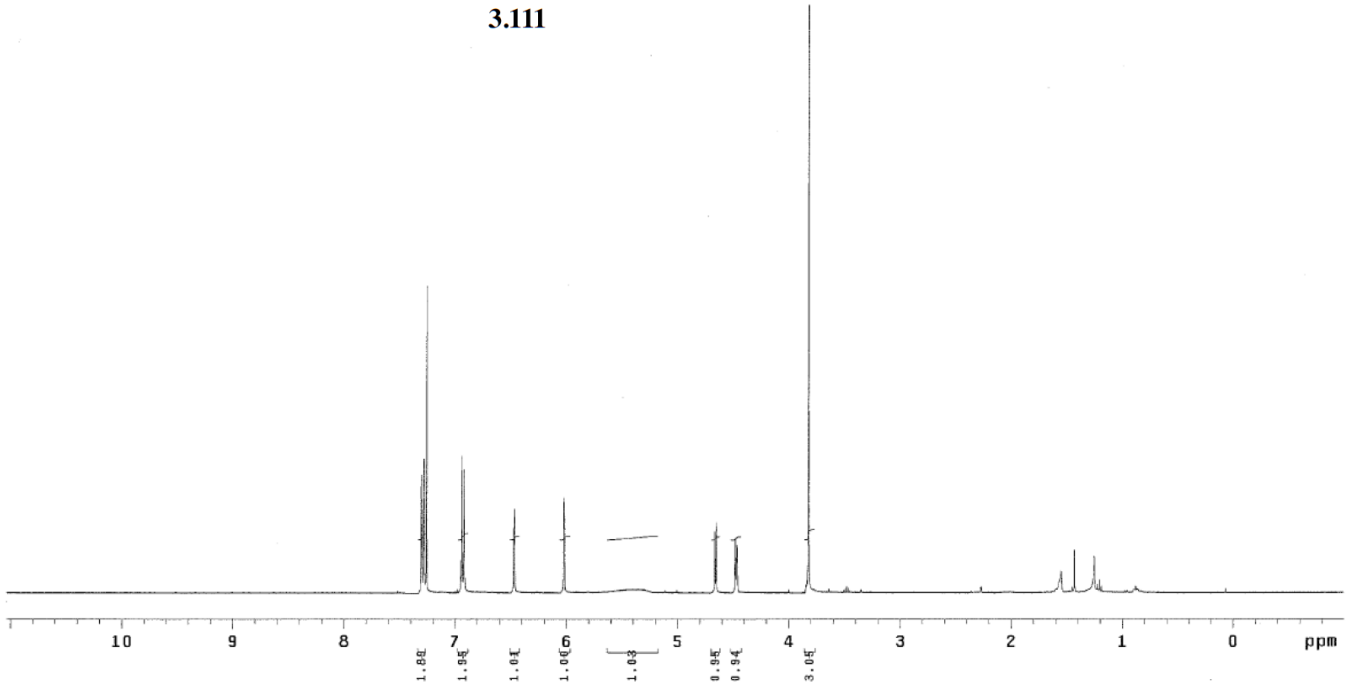

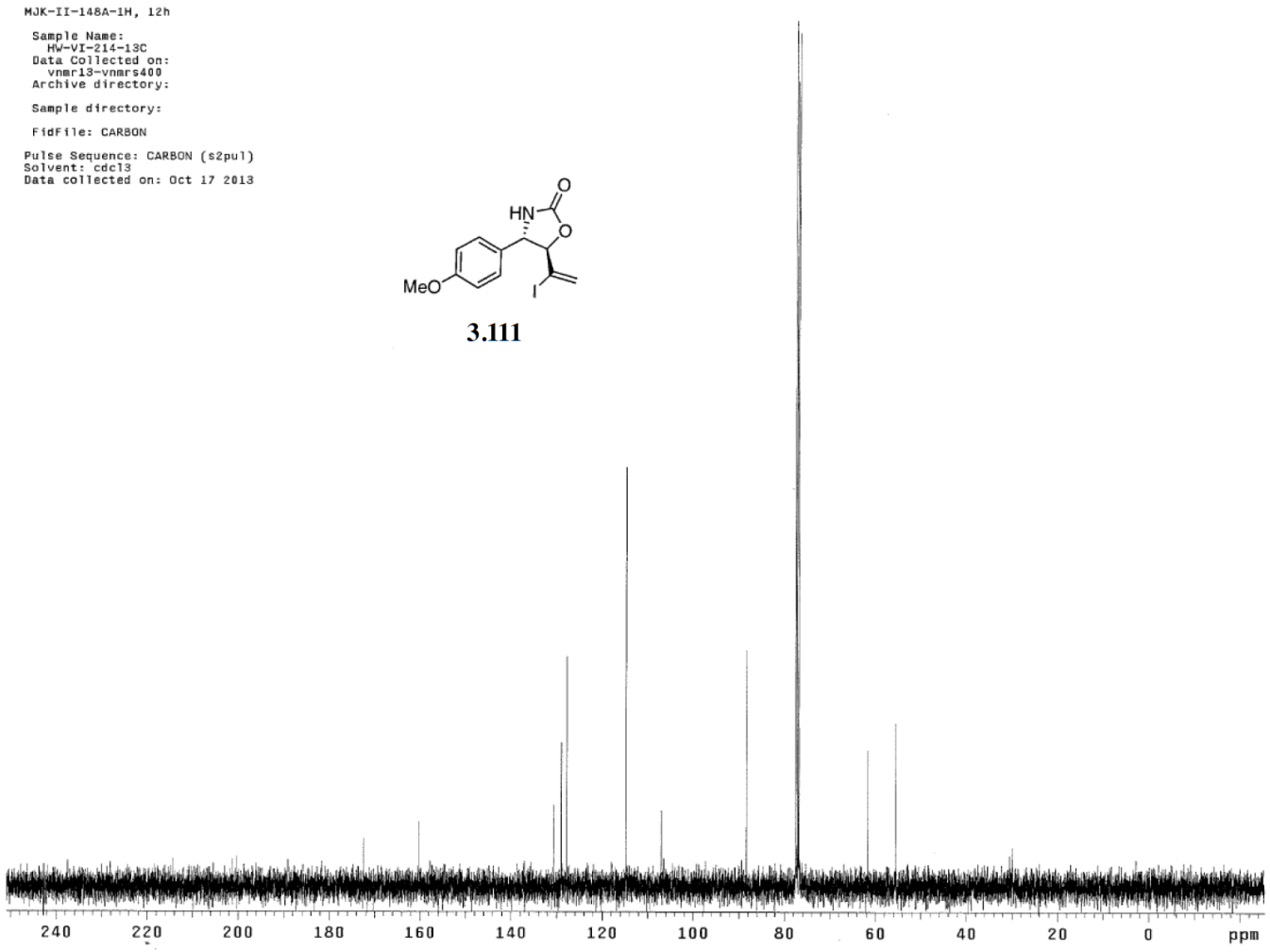
MJK-II-148A-1H, 12h
Sample Name:
HW-VI-214-13C
Data Collected on:
vnmr13-vnmrs400
Archive directory:
Sample directory:
FidFile: CARBON
Pulse Sequence: CARBON (s2pul)
Solvent: cdcl3
Data collected on: Oct 17 2013
HN
O
O
MeO
I
240
220
200
180
160
140
120
100
80
60
40
20
0
ppm

**3.111**

Sample Name:
HW-VI-224-c
Data Collected on:
vnmr13-vnmrs400
Archive directory:

Sample directory:

FidFile: PROTON

Pulse Sequence: PROTON (s2pul)
Solvent: cdcl3
Data collected on: Sep 30 2013

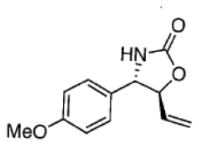


**3.112**

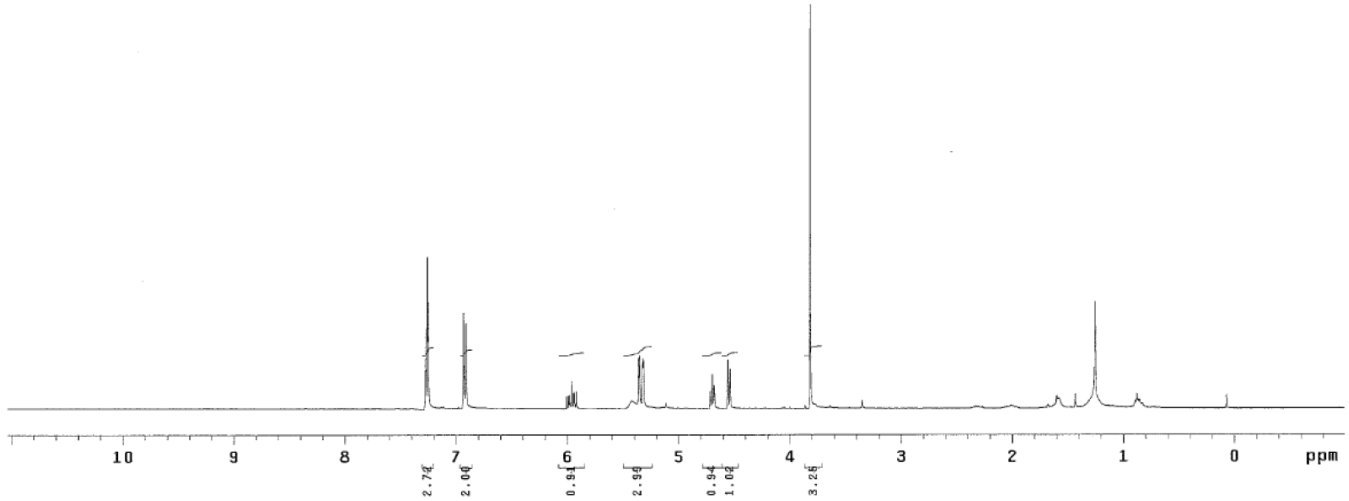

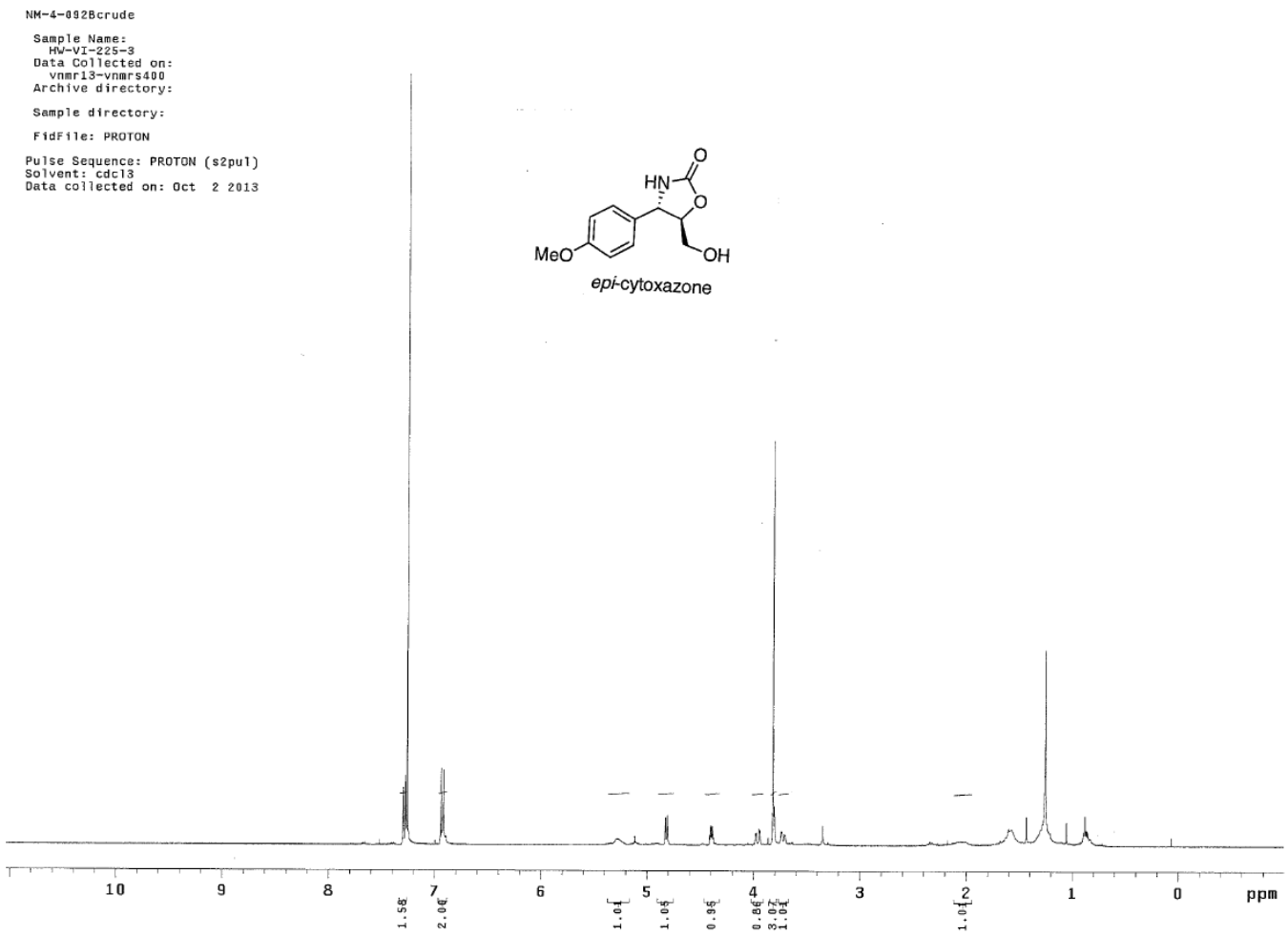
NM-4-092Bcrude
Sample Name:
HW-VI-225-3
Data Collected on:
vnmr13-vnmrs400
Archive directory:
Sample directory:
FidFile: PROTON
Pulse Sequence: PROTON (s2pul)
Solvent: cdcl3
Data collected on: Oct 2 2013
HN
O
O
MeO
OH
epi-cytoxazone
10
9
8
7
6
5
4
3
2
1
0
ppm
1.58
2.00
1.01
1.05
0.95
0.86
3.07
1.04
1.01

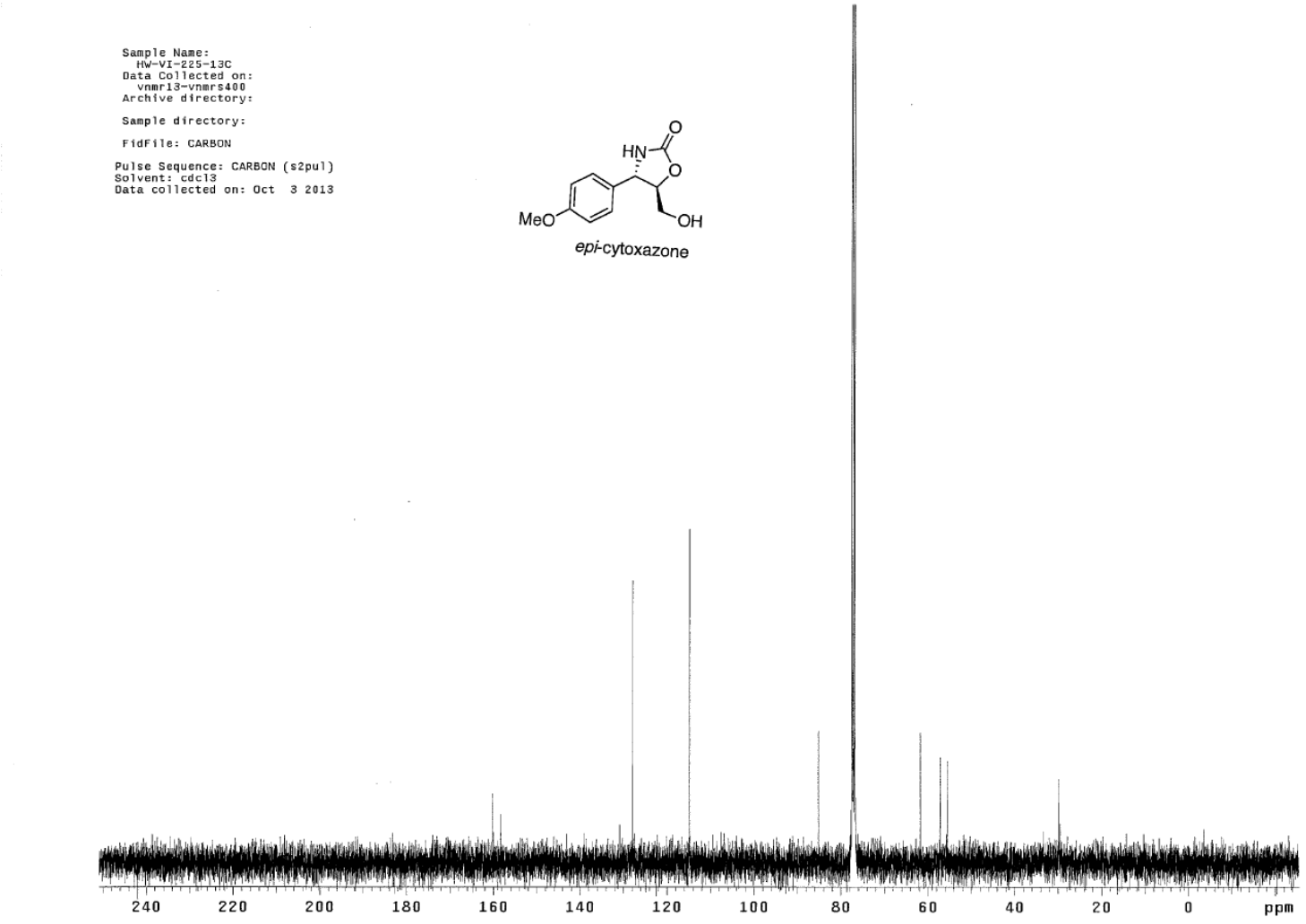
Sample Name:
HW-VI-225-13C
Data Collected on:
vnmr13-vnmrs400
Archive directory:
Sample directory:
FidFile: CARBON
Pulse Sequence: CARBON (s2pul)
Solvent: cdcl3
Data collected on: Oct 3 2013
HN
O
O
MeO
OH
epi-cytoxazone
240
220
200
180
160
140
120
100
80
60
40
20
0
ppm

Sample Name:
HW-VIII-220
Data Collected on:
vnmr13-vnmrs400
Archive directory:

Sample directory:

FidFile: PROTON

Pulse Sequence: PROTON (s2pul)
Solvent: cdcl3
Data collected on: Oct 13 2015

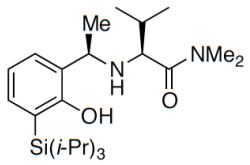


**3.115v**

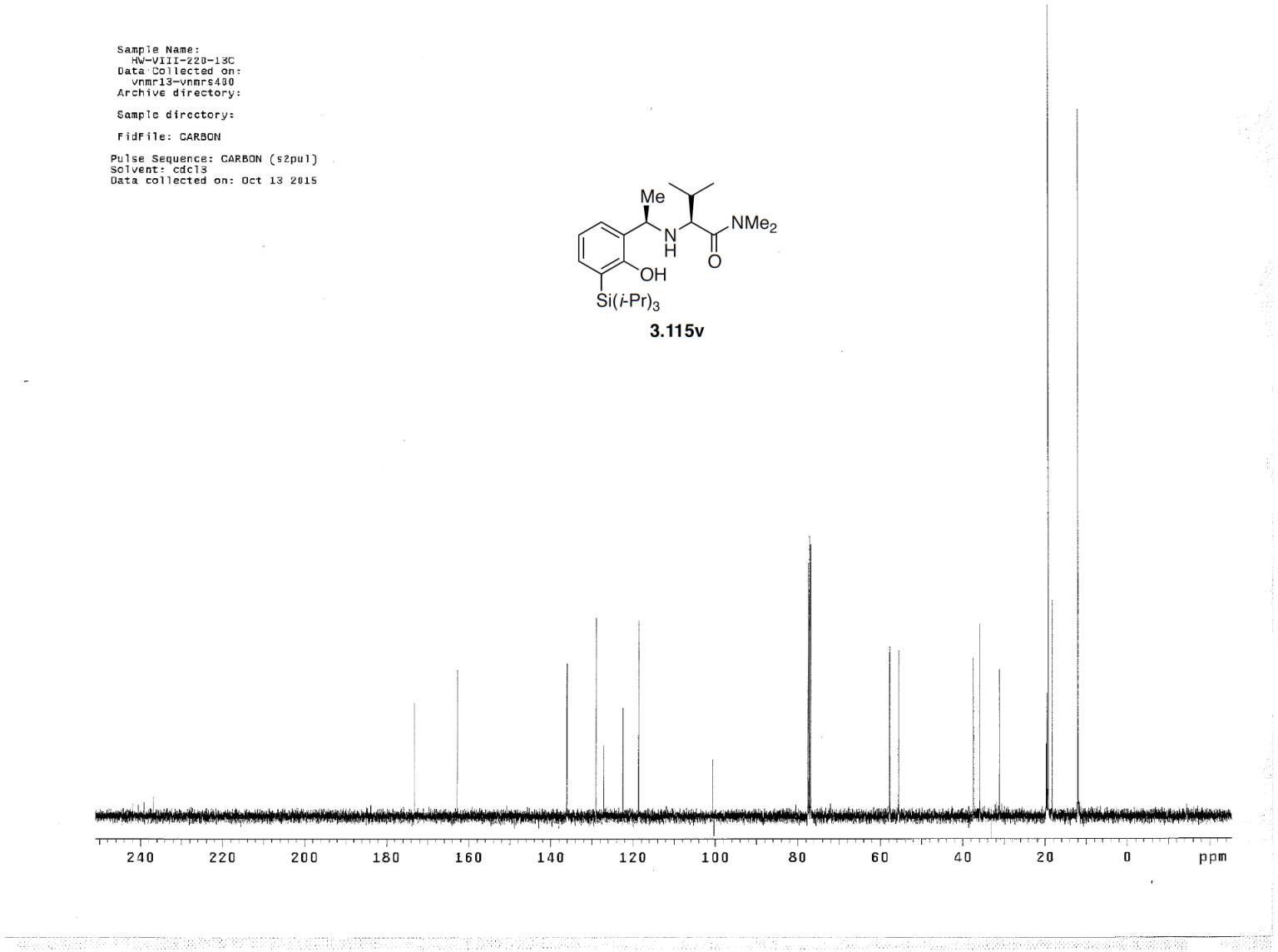
Sample Name:
HW-VIII-220-13C
Data Collected on:
vnmr13-vnmrs400
Archive directory:
Sample directory:
FidFile: CARBON
Pulse Sequence: CARBON (s2pul)
Solvent: cdcl3
Data collected on: Oct 13 2015
Me
N
H
NMe2
O
OH
Si(i-Pr)3
3.115v
240
220
200
180
160
140
120
100
80
60
40
20
0
ppm

# Chapter 4

## NHC–Cu-Catalyzed Enantioselective Silyl Conjugate Additions to Acyclic and Cyclic α,β,γ,δ-Unsaturated Ketones and Esters

### *4.1. Introduction*

Silicon, the second most abundant element in Earth's crust (about 28% by mass)[145], was first prepared and characterized in pure form in 1823 by Swedish chemist Jons Jakob Berzelius. Introducing silicon to the realm of organic chemistry led to a variety of fruitful discoveries of transformations that organosilanes can undergo.[146] One of the direct functionalizations of a C–Si bond is oxidation, resulting in a C–O bond. This method is considered a powerful tool in organic synthesis since a silicon group can be used as a masked hydroxy group. The pioneering work of C–Si oxidations were done by Tamao, Kumada and Fleming.[147]

As a consequence, enantiomerically enriched β-silyl carbonyl compounds are believed as valuable intermediates in organic synthesis, since oxidation of the C–Si bonds

(145) Nave, R. *Abundances of the Elements in the Earth's Crust*, Georgia State University.

(146) For representative reviews regarding the use of organosilicon species in organic synthesis, see: (a) Fleming, I. In *Comprehensive Organic Synthesis*; Trost, B. M., Fleming, I., Eds; Pergamon: Oxford, U.K., **1991**; Vol. 2, p 563–593. (b) Chan, T. H.; Wang, D. *Chem. Rev.* **1992**, *92*, 995–1006. (c) Davies, A. G. In *Comprehensive Organometallic Chemistry II*; Pergamon: New York, **1995**; Vol. 2, p 217. (d) Fleming, I.; Barbero, A.; Walter, D. *Chem. Rev.* **1997**, *97*, 2063–2192. (e) Suginome, M.; Ito, Y. *Chem. Rev*. **2000**, *100*, 3221–3256.

(147) For a review on the oxidation of a C–Si bond, see: Jones, G. R.; Landais, Y. *Tetrahedron*, **1996**, *52*, 7599–7662.

lead to enantioselective Aldol-type products (β-hydroxy carbonyls). Compared with β-boryl carbonyls, compounds that can also be converted into β-hydroxy carbonyls after C–B bond oxidations, β-silyl carbonyls are sufficiently robust to allow for a range of functionalizations of the the carbonyl unit without causing decomposition or side reactions (e.g. retro-aldol reactions, nucleophilic additions to the boron of β-boryl carbonyls). Thus, several protocols have been developed for transition metal-catalyzed enantioselective synthesis of β-silyl carbonyls: enantioselective conjugate reductions,[148] alkylations of *β*-silyl enones [149] and silyl conjugate additions to *α,β*-unsaturated carbonyls.[150]

In this chapter, I will first introduce the reported processes of transition metal-catalyzed enantioselective silyl conjugate additions. Then I will focus on our studies of NHC–Cu-catalyzed enantioselective silyl additions to α,β,γ,δ-unsaturated ketones and esters.[151] The products belong to chiral allyl silanes, a class of important intermediates for various organic transformations.

## *4.2. Catalytic Enantioselective Silyl Conjugate Additions to α,β-Unsaturated Carbonyls*

(148) Lipshutz, B. H.; Tanaka, N.; Taft, B. R.; Lee, C.-t. *Org. Lett*. **2006**, *8*, 1963–1966.

(149) (a) Shintani, R.; Okamoto, K.; Hayashi, T. *Org. Lett*. **2005**, *7*, 4757–4759. (b) Balskus, E. P.; Jacobsen, E. N. *J. Am. Chem. Soc.* **2006**, *128*, 6810–6812. (c) Kacprzynski, M. A.; Kazane, S. A.; May, T. L.; Hoveyda, A. H. *Org. Lett*. **2007**, *9*, 3187–3190.

(150) For reviews on catalytic enantioselective silyl conjugate additions, see: (a) Fleming, I., *Science of Synthesis*; Thieme: Stuttgart, Germany, **2002**; Vol. 4; p 927. (b) Hartmann, E.; Vyas, D. J.; Oestreich, M. *Chem. Commun.* **2011**, *47*, 7917–7932.

(151) Lee, K.-s.; Wu, H.; Haeffner, F.; Hoveyda, A. H. *Organometallics* **2012**, *31*, 7823–7826.

The first catalytic enantioselective silyl conjugate additions to α,β-unsaturated ketones were developed by Hayashi and co-workers.[152] The authors utilized the *in situ* generated chiral BINAP–Pd(0) complex to promote an oxidative insertion between the Si–Si bond of $PhCl_2Si–SiMe_3$. The subsequent enone coordination, migratory insertion and reductive elimination resulted in β-silyl enol ether **4.3**. It is interesting that the electron poorer dichlorophenylsilyl unit gets transferred onto the β-carbon of enone **4.1**, and not the trimethylsilyl group. Products **4.3** are not stable and have to be further functionalized by addition of MeLi. Notably, the corresponding lithium enolates can be quenched by HCl (aq) or alkyl halides, the latters of which give α-substituted organosilanes with >20:1 dr. The enantioselectivities of these reactions are generally high (87:13 to 96:4 er), which must come from the BINAP control of the two enantiotopic faces of an approaching substrate. In conclusions, the discovery of the BINAP–Pd-catalyzed silyl conjugate additions is ground-breaking, especially considering such a low catalyst loading (0.5 mol %) and mild reaction conditions afford valuable β-silyl carbonyls in a high enantiomeric ratios in 1988. Despite the cumbersome and instability preparation of $PhCl_2Si–SiMe_3$, as well as necessary methyl alkylations for product isolations, this method remained the only enantioselective conjugate additions for almost two decades.

(152) Hayashi, T.; Matsumoto, Y.; Ito, Y. *J. Am. Chem. Soc.* **1988**, *110*, 5579–5581.

**Scheme 4.2.1. The first catalytic enantioselective silyl conjugate additions**

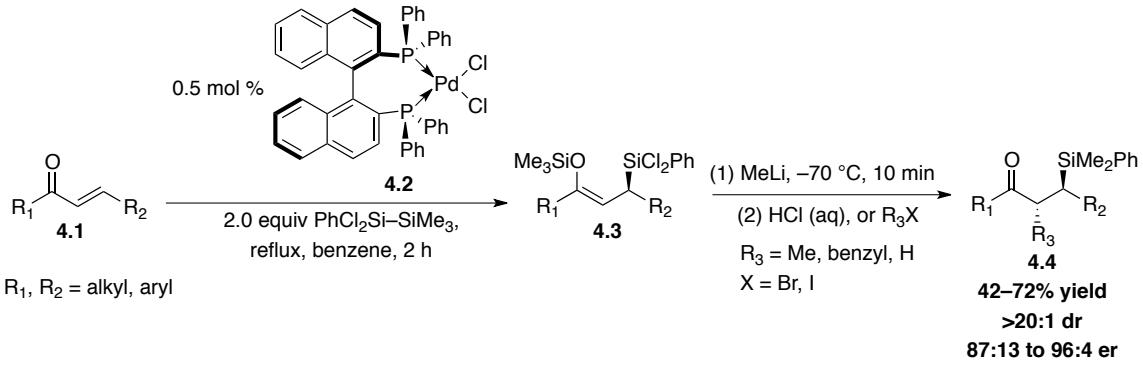


In 1994, the same group published a full article of this protocol in Tetrahedron,[153] where they demonstrated the whole journey of discovery of this method, including none-enantioselective disilylations as well as enantioselective ones. They also showed intermediates **4.3** can be quenched with EtOH/$Et_3N$ instead of MeLi to obtain the the corresponding $Ph(EtO)_2Si$ substituted products.

In 2006, Oestreich and co-workers reported a protocol of BINAP–Rh-catalyzed enantioselective silyl conjugate additions to cyclic enones.[154] Interestingly, instead of a disilane reagent, they employed $PhMe_2Si$–B(pin) in the silyl additions. It should be noted that $PhMe_2Si$–B(pin) is an user-friendly compound that is commercially available, can be prepared in a muti-gram quantity and can be widely used in a variety of chemical transformations.[155] The reactions are generally efficient and highly enantioselective towards five-, six- and seven-membered cyclic enones (**4.6**) and an enoate (**4.7**), although cycloheptenone gives only 22% yield. Unfortunately, the reaction to chalcone was inert under the BINAP–Rh catalytic system. The screening of reaction conditions reveal that a

(153) Matsumoto, Y.; Hayashi, T. *Tetrahedron*, **1994**, *50*, 335–346.

(154) Walter, C.; Auer, G.; Oestreich, M. *Angew. Chem. Int. Ed.* **2006**, *45*, 5675–5677.

(155) For reviews involving the use of borosilanes in various transformations, see: (a) Suginome, M.; Ito, Y. *Chem. Rev.* **2000**, *100*, 3221–3256. (b) Beletskaya, I.; Moberg, C. *Chem. Rev.* **2006**, *106*, 2320–2354.

proper base ($Et_3N$), dioxane/$H_2O$ and the absence of strongly coordinating counterions on the Rh(I) catalyst are critical for product formation. The authors also reported that the use of [(dppp)Rh(cod)]$ClO_4$ could afford the racemic products (cyclic and acyclic enones and enoates) efficiently.

**Scheme 4.2.2. Rh-catalyzed enantioselective silyl conjugate additions to cyclic enones and enoates**

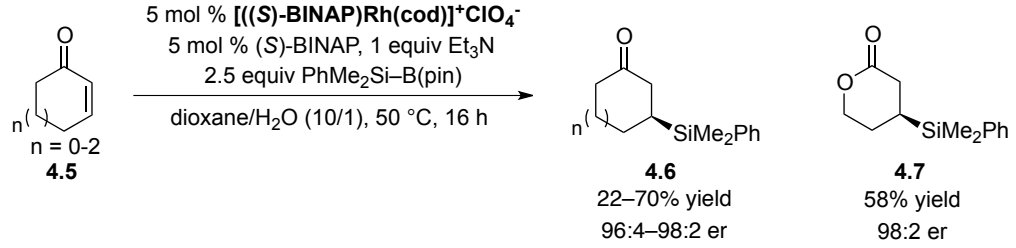


In 2008, the same group reported the enantioselective silyl additions to (*Z*)-α,β-unsaturated carbonyls (not ketones) with a similar catalytic system.[156] The reactions are suitable with alkyl- or aryl-substituted unsaturated esters (**4.9**, **4.10** and **4.11**) and oxazolidinones (**4.12**), while inefficient with thioesters (**4.13**), nitriles (**4.14**) and amides (not shown, reported in a subsequent full article[157]). Notably, the enantiomeric ratios of the desired products are all very high (≥99:1 er). However, if (*E*)-α,β-unsaturated carbonyls are involved in this reaction, conjugate hydride reductions will be the competitive pathway (~50%) and the enantioselectivities drop significantly (for example, the er of **4.11** from (*E*)-enoate is 58.5:41.5). If (*Z*)-α,β-unsaturated ketones are used, they will first isomerize into the (*E*) isomers and promote the conjugate reduction reactions.

(156) Walter, C.; Oestreich, M. *Angwe. Chem. Int. Ed.* **2008**, *47*, 3818–3820.
(157) Walter, C.; Oestreich, M. *Tetrahedron* **2009**, *65*, 5513–5520.

**Scheme 4.2.3. Rh-catalyzed enantioselective silyl conjugate additions to acyclic enoates**

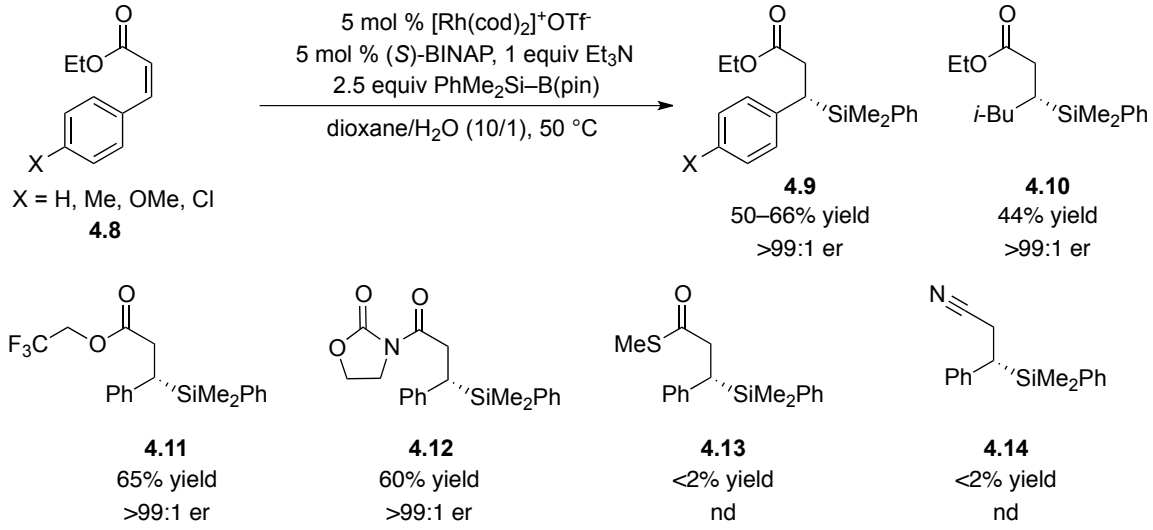


The mechanism of these transformations was also proposed (Scheme 4.2.4). The reaction starts with the generation of a Rh(I)–OH species, which binds the boron atom of the borylsilane reagent **4.16** and activates the B–Si bond. It is noteworthy that this selective coordination is because the B–O bond (120 kcal/mol) is stronger than the Si–O bond (115 kcal/mol), resulting in the preferred transfer of the silyl group onto the catalyst. The generated [Rh(I)]–Si species **4.19** promotes the silyl conjugate additions to an unsaturated carbonyl **4.20**, affording the β-silyl substituted enolate **4.21**. Upon hydrolysis, **4.21** is converted into product **4.22** and regenerates the active [Rh(I)]–OH **4.15**.

**Scheme 4.2.4. The proposed mechanism**

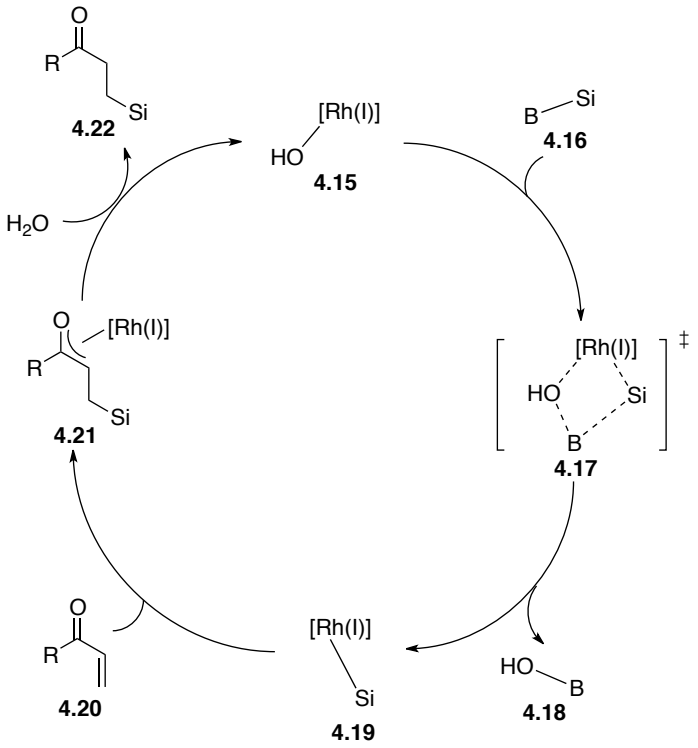


In 2010, our group reported the first NHC–Cu-catalyzed enantioselective silyl conjugate additions (Scheme 4.2.5).[158] The transformations are promoted by 1.0–2.0 mol % of an *in situ*-generated chiral NHC–Cu-O*t*-Bu and complete within one hour at –78 °C in most cases, affording the desired β-silyl carbonyls in 85–97% yields and 90:10 to 99:1 er. It was found that the enantioselectivity of the reaction catalyzed by a chiral monodentate NHC (derived from **4.24a**) is slightly higher than the ones by chiral bidentate NHC(s). Increasing the reaction temperature will also erode the enantiomeric ratios of products. Five- to eight-membered cyclic enones (**4.23a-d**) are suitable substrates, although the er of **4.26b** is lower (90:10 er), probably because the control of the silyl additions to the enantiotopic faces of this small substrate is more difficult. Notably, enones bearing sterically bulky gem-dimethyl substituents are well tolerated in

(158) Lee, K.-s.; Hoveyda, A. H. *J. Am. Chem. Soc.* **2010**, *132*, 2898–2900.

the silyl conjugate additions (**4.26e** and **4.26f**). The reaction with lactone **4.23g** is significantly slower and thus requires 2 mol % NHC–Cu-O*t*-Bu as well as 12 hours of reaction time. In contrast to the previously discussed Rh(I) catalyzed method, (*E*)-α,β-unsaturated carbonyls (enones and esters) are equally efficient in the NHC–Cu-catalyzed silyl conjugate additions. The aryl- (eletron rich or poor) or alkyl- (linear or branched) substituent of an enone or enoate does not affect the efficiency as well as enantioselectivity of this reaction.

**Scheme 4.2.5. NHC–Cu-catalyzed enantioselective silyl conjugate additions to enones and enoates**

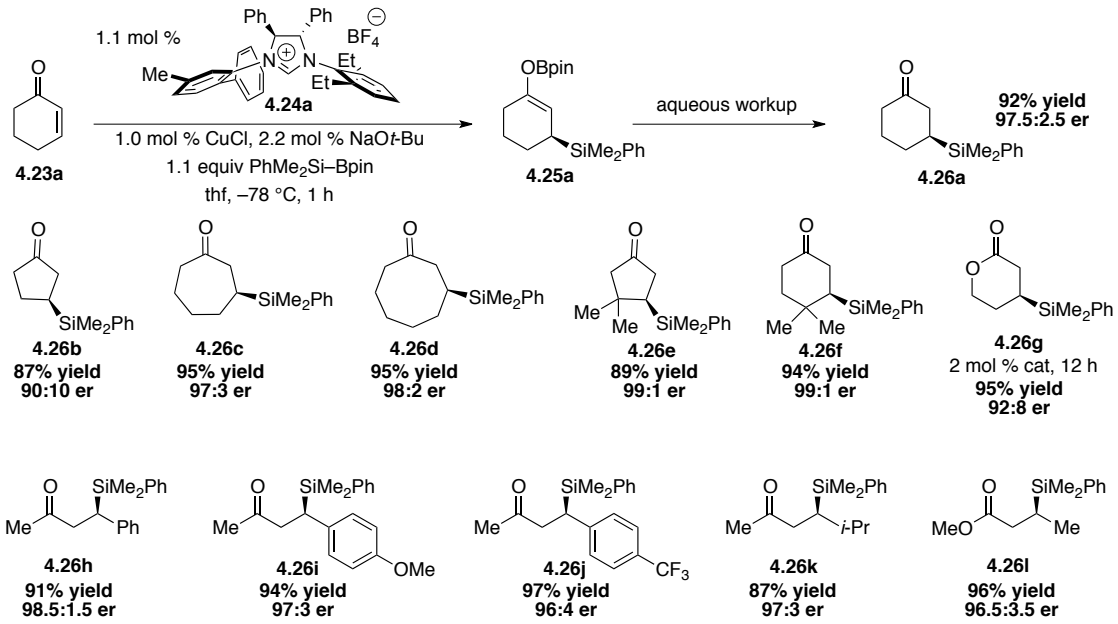


The enantiomerically enriched β-silyl carbonyls were shown to be versatile in organic synthesis (Scheme 4.2.6). First, if the reaction is quenched by addition of 1.5 equivalents of benzaldehyde instead of $H_2O$, aldol product **4.27** is generated with 91% yield, 6:1 dr and 90:10 er. It is noteworthy that the corresponding enolate derived from boryl conjugate additions is unreactive with benzaldeyhde.[10,35] Thus, the silyl conjugate addition/aldol reactions are complementary with the known boryl conjugate additions.

Moreover, nucleophilic additions to the β-silyl carbonyls with common organometallic reagents (aryl- or alkyl-lithium reagents, etc) are chemo- and diastereoselective. For example, PhLi selectively adds to the C=O double bond of **4.26e** without interacting with the silyl group. The product (**4.28**) is obtained as a single diastereomer and can be further converted to *syn*-1,3-diol **4.29** after oxidation of the C–Si bond. However, the same reaction sequence cannot be applied to β-boryl carbonyls since boronates are sensitive to the organolithium reagent.

At last, the NHC–Cu-catalyzed protocol was shown to be effective in complex molecule synthesis. Substituted β-silyl ketone **4.30** can be isolated in 92% yield, >98:2 dr and 97.5:2.5 er through a one-pot silyl conjugate addition/alkylation reaction. The stability of the silyl group towards *n*-BuLi allows the boryl enolate generated after the silyl conjugate addition be converted to its more mucleophilic Li enolate for the following alkylation. **4.30** was previously showed in the total synthesis of (+)-erysotramidine.[159]

(159) Tietze, L. F.; Tölle, N.; Kratzert, D.; Stalke, D. *Org. Lett.* **2009**, *11*, 5230–5233.

**Scheme 4.2.6. Functionalizations of β-silyl carbonyls**

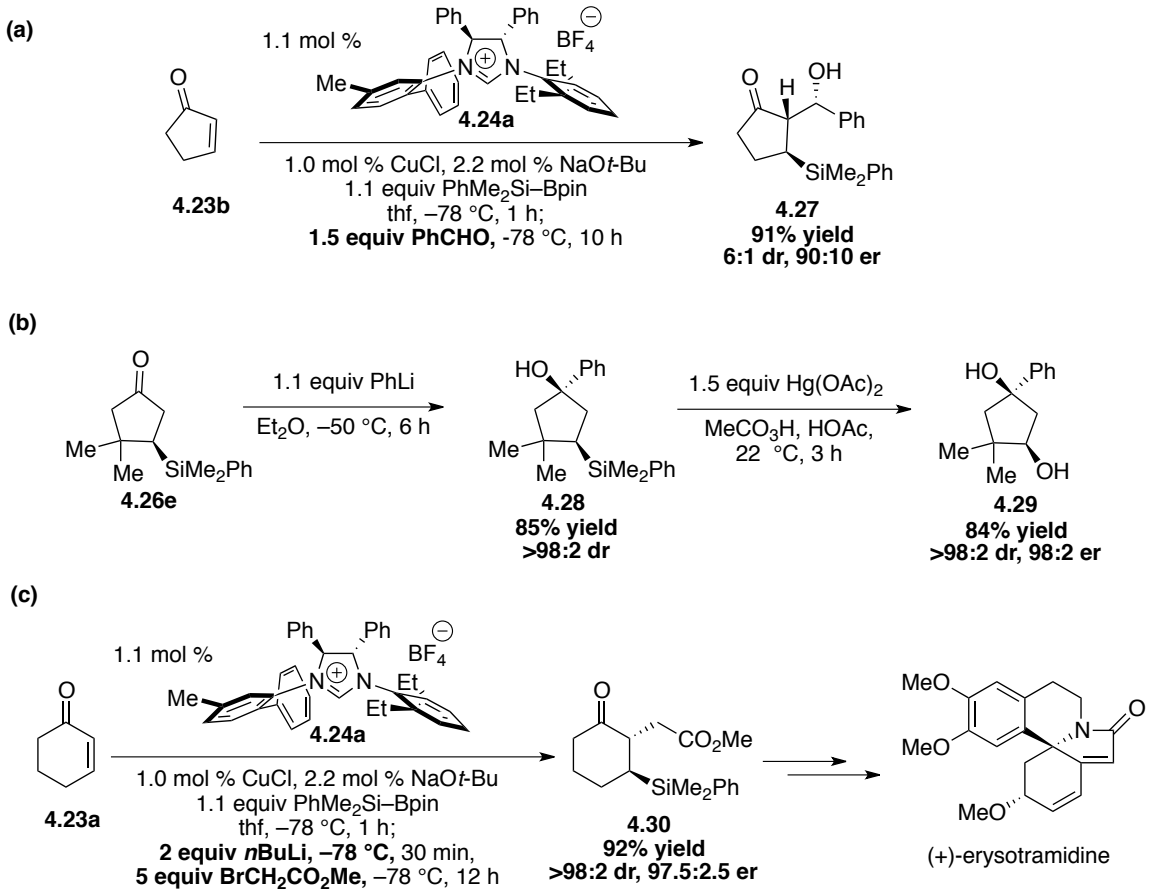


The proposed mechanism is illustrated in Scheme 4.2.7. The *in situ* generated NHC–Cu-OR is proposed to react with $PhMe_2Si$–B(pin) through a similar fashion as it reacts with $B_2(pin)_2$, as previously reported.[17] Because the B–O bond is stronger than the Si–O bond, the NHC–Cu-$SiMe_2Ph$ (**4.33**) is preferentially generated, releasing one molecule of RO–B(pin). The NHC–Cu-$SiMe_2Ph$ (**4.33**) is able to react with an enone after its coordination to generate β-silyl copper enolate **4.35**. Since this C-Si bond formation step is irreversible, we believe it is also the stereochemical determining step. Copper enolate **4.35** can further react with another molecule of $PhMe_2Si$–B(pin) to regenerate the catalyst. In the meantime, the resulting boryl enolate **4.36** is afforded and can be further functionalized (for example through hydrolysis to β-silyl ketone **4.37**.

**Scheme 4.2.7. Proposed mechanism**

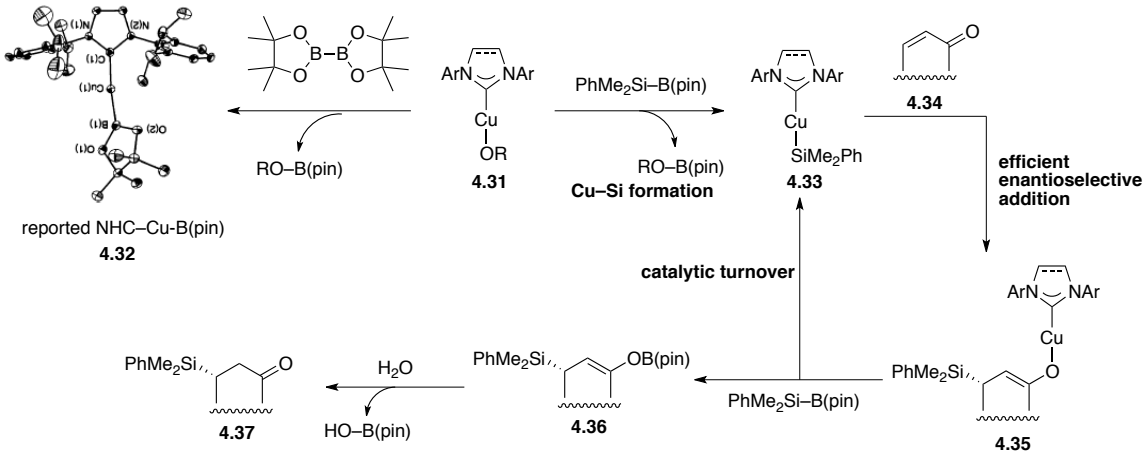


In 2011, our group reported an NHC-catalyzed enantioselective silyl conjugate addition strategy. Here, an NHC (chiral or achiral) serves as an effective Lewis base to activate the Si–B bond, in contrast to the metal-alkoxide as the Lewis base in the previously discussed protocols. The distinct mechanism of this transition-metal free approach reveals its complementary reactivity and selectivity profiles. The details of this study have already been illustrated in chapter 1 and 2.

## *4.3. NHC–Cu-Catalytic Enantioselective Silyl Conjugate Additions to α,β,γ,δ-Unsaturated Carbonyls*

### *4.3.1. Project Design and Challenges*

After finding success in the development of NHC–Cu-catalyzed enantioselective silyl conjugate additions to α,β-unsaturated carbonyl compounds, we wondered what if we employed this protocol to α,β,γ,δ-unsaturated carbonyls **4.38**. As shown in Scheme 4.3.1, there are several major challenges accompanied with this simple alteration of substrates: First, will the NHC–Cu-$SiMe_2Ph$ still be reactive enough for silyl conjugate additions to α,β,γ,δ-unsaturated carbonyls?

Secondly, if the conjugate addition occurs, will it be regioselective? If so, which one will predominate, 1,4-addition or 1,6-addition? Thirdly, regardless the regioselectivity of the reaction, will the allylsilanes generated be diastereoselective (*E* or *Z* olefin geometry)? Fourthly, will the chiral NHC still promote highly enantioselective reactions? Lastly, can copper enolate **4.39** or **4.40** still react with $PhMe_2Si$–B(pin) efficiently to regenerate the catalyst?

**Scheme 4.3.1. Challenges for catalytic enantioselective silyl conjugate additions to dienones and dienoates**

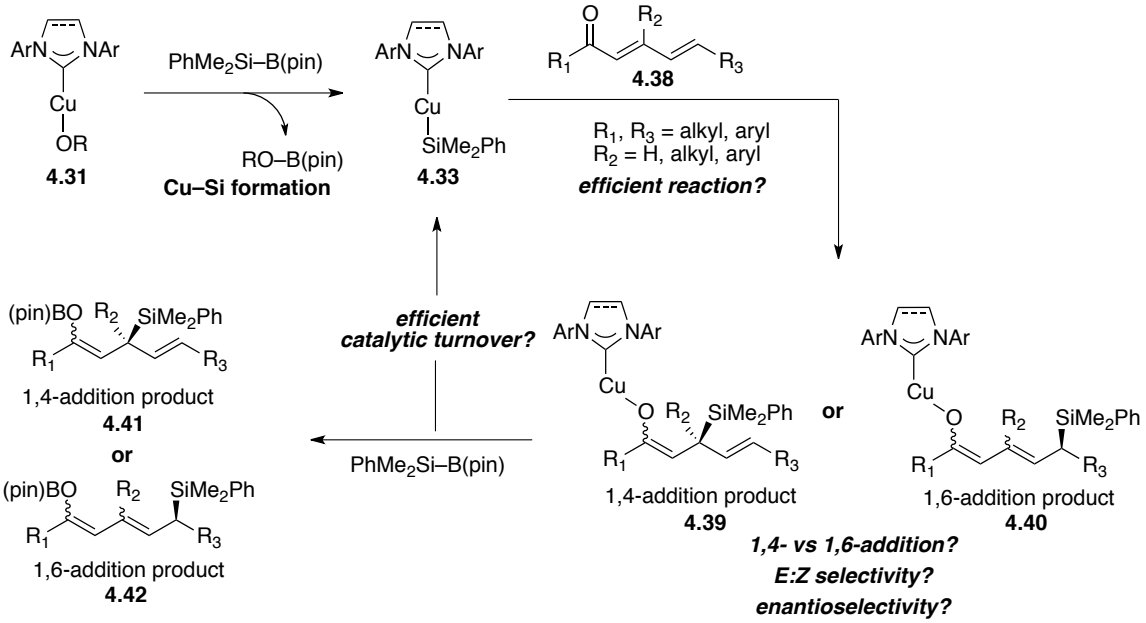


Beyond those questions, there is another major issue that needs to be seriously considered: Are these allylsilanes (**4.41** or **4.42**) worth being synthesized?

In this section, I will first briefly introduce the versatile utilities of chiral allylsilanes in organic synthesis and some representative approaches to synthesize those enantiomerically enriched allysilanes. Then, I will focus on our studies on catalytic enantioselective silyl conjugate additions to α,β,γ,δ-unsaturated carbonyls.

### *4.3.2. Enantiomerically Enriched Allylsilanes in Organic Synthesis*

Allylsilanes have been widely used in a variety of transformations in the context of complex molecule synthesis, especially ones that contain a silyl substituted carbon stereogenic center.[160] Among those functionalizations, Hosomi-Sakurai reaction is the mostly widely used. It is the reaction of carbonyl or α,β-unsaturated carbonyl electrophiles with allylsilanes catalyzed by a Lewis acid, which has been shown to be a powerful tool to construct C–C bonds.[161] In the past four decades, related allylations using a chiral allylsilane for efficient and diastereoselective synthesis of homoallyic ethers, alcohols and amines, as well as substituted tetrahydrofurans, pyrrolidines and cyclopetanes have been developed (a general scheme is shown in Scheme 4.3.2).[154a]

(160) For reviews on the utility of allylsilanes in organic synthesis, see: (a) Masse, C. E.; Panek, J. S. *Chem. Rev.* **1995**, *95*, 1293–1316. (b) Barbero, A.; Pulido, F. J. *Acc. Chem. Res.* **2004**, *37*, 817–825. (c) Chabaud, L.; James, P.; Landais, Y. *Eur. J. Org. Chem.* **2004**, 3173–3199.

(161) Hosomi, A.; Sakurai, H. *Tetrahedron Lett.* **1976**, *17*, 1295–1298.

**Scheme 4.3.2. Selective transformations of chiral allylsilanes**

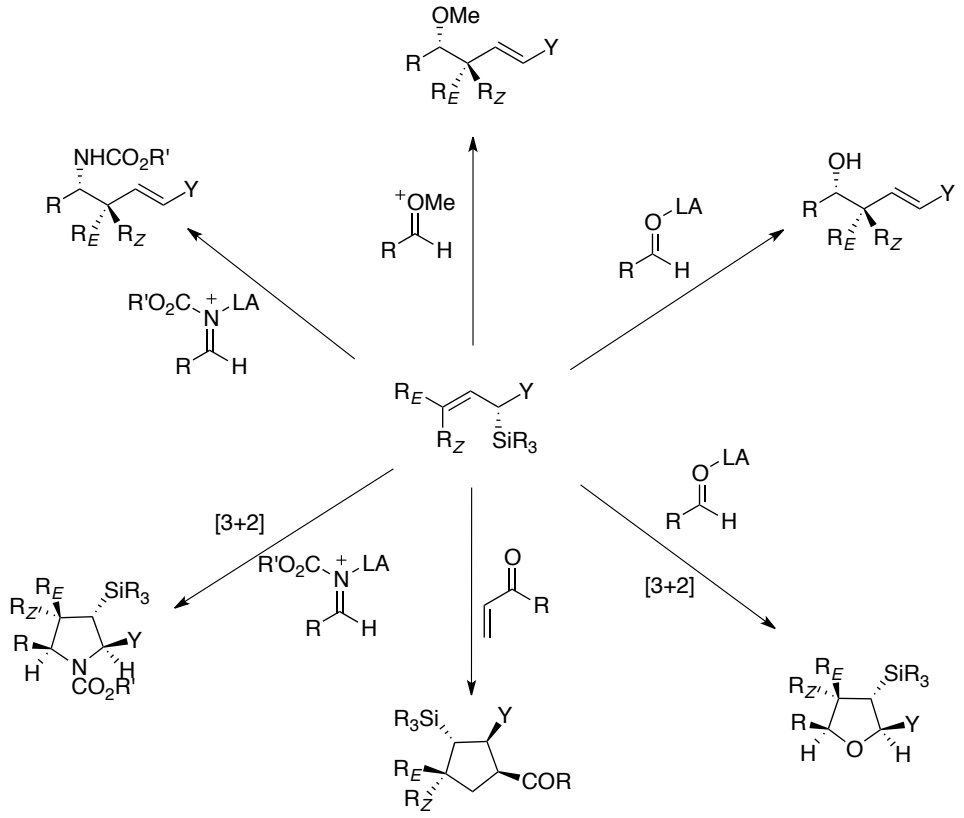


There are several beautiful total syntheses of complex molecules that have been reported using chiral allylsilanes for C–C bond formations. For example, Panek and co-workers applied an enantiomerically enriched allylsilane **4.43** in their synthesis of (+)-macbecin I, an antitumor antibiotic compound.[162] **4.43** underwent a highly diastereoselective allyl addition reaction with a chiral aldehyde, affording homoallylic ether **4.44** in 80% yield and >12:1 dr. Similar transformations were utilized another two times to construct the core structure of (+)-macbecin I (the C–C bonds formed by allylations of **4.43** are highlighted in the final product). Notably, as a relatively early step of a total synthesis, the allylations of **4.43** are quite reliable and can be set up on a ten-

(162) Panek, J. S.; Xu, F. *J. Am. Chem. Soc.* **1995**, *117*, 10587–10588.

gram scale. The stereochemical model of allylation is proposed to be **4.45**, where the reaction probably proceeds through a linear transition state.

**Scheme 4.3.3. Total synthesis of (+)-macbecin I and other molecules using enantiomerically enriched allylsilanes in allylations**

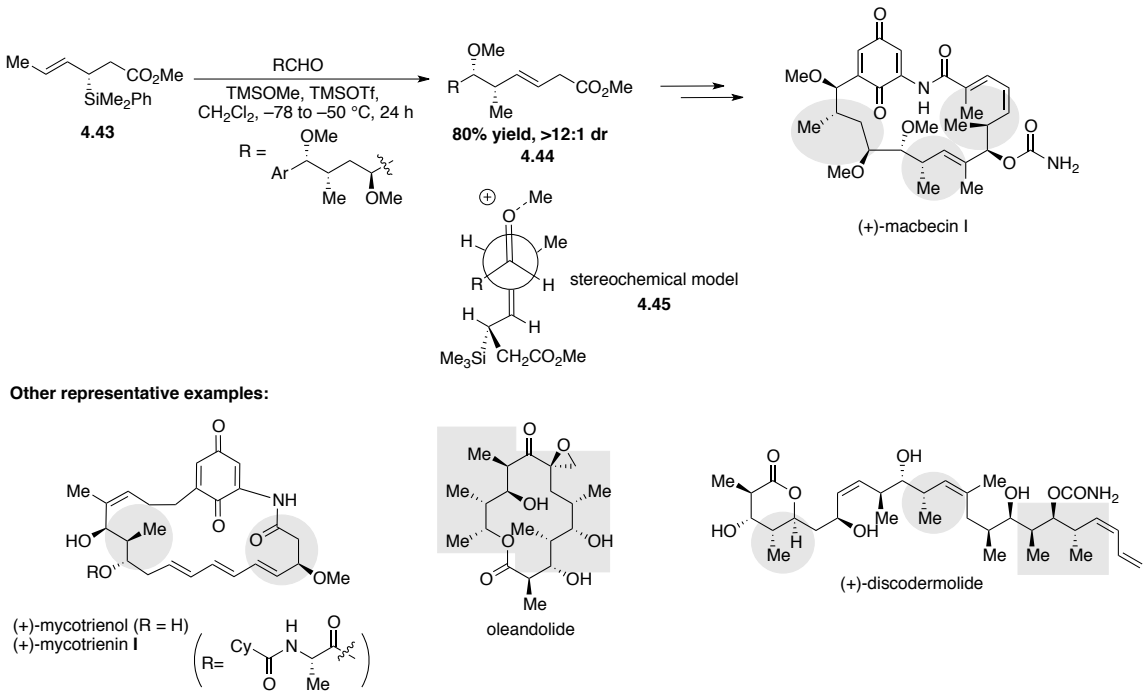


The same group has reported a number of total syntheses of complex molecules based on the aforementioned strategy. In general, chiral allylsilanes bearing a β-carbonyl group (like **4.43**) are prepared enantioselectively and applied in the diastereoselective allylations of aldehydes. Several representative examples are illustrated in Scheme 4.3.3. (+)-Mycotrienol and (+)-mycotrienin I were prepared in 32 and 35 steps with 3% and 1.5% yield, respectively, where two diastereoselective allylation of allylsilanes were employed (highlighted in gray).[163] The synthesis of oleandolide is noteworthy since nine out of twelve C–C bonds were introduced by the aforementioned allylation. Specifically, the authors used the allylation/$O_3$ oxidation/allylation sequence to introduce 1,3-*syn*-

(163) Masse, C. E.; Yang, M.; Solomon, J.; Panek, J. S. *J. Am. Chem. Soc.* **1998**, *120*, 4123–4134.

dimethyl or 1,3-*anti*-dimethyl moieties.[164] Another example is their total synthesis of (+)-discodermolide, a potent immunosuppressive agent.[165] The synthetic route includes the same strategy four times, again to construct some of the 1,3-dimethyl motieves. This convergent and enantioselective synthesis (27 steps longest linear sequence) was achieved to afford the final product in 2.1% overall yield.

Moreover, Wender and co-workers have applied a diastereoselective allylation and subsequent etherification to form tetrahydropyran **4.47** in 93% yield and >95:5 dr.[166] A similar intermediate was prepared and utilized in the total synthesis of bryostatin.[167]

**Scheme 4.3.4. Diastereoselective allylation/cyclization**

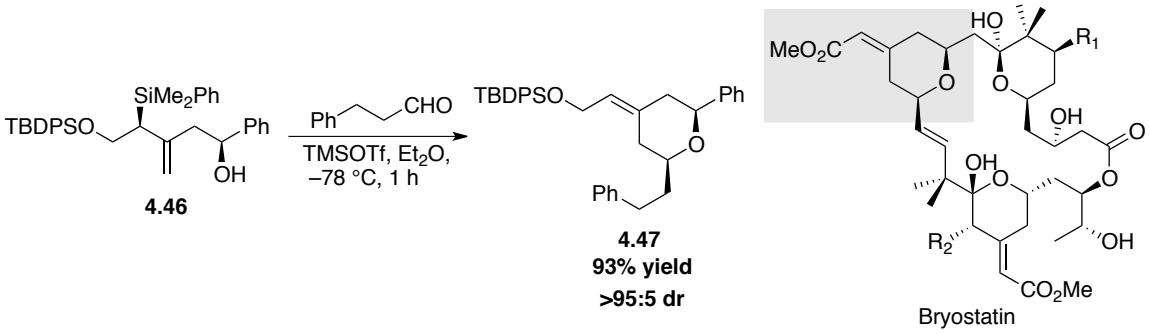


Besides allylations, a variety of functionalizations of enantiomerically enriched allylsilanes have been developed (Scheme 4.3.5). For example, Hayashi and co-workers discovered the first catalytic enantioselective silyl allylic substitutions in 1982.[168] The products were used to promote $S_N2$ reactions with a complete stereoselectivity, generating an alkene with an all-carbon tertiary stereogenic center in 96.5:3.5 er (Scheme 4.3.5a). Panek and co-workers found the *m*-CPBA (*meta*-chloroperoxybenzoic

(164) Hu, T.; Takenaka, N.; Panek, J. S. *J. Am Chem. Soc.* **1999**, *121*, 9229–9230.
(165) Arefolov, A.; Panek, J. S. *J. Am. Chem. Soc.* **2005**, *127*, 5596–5603.
(166) Ogawa, Y.; Painter, P. P.; Tantillo, D. J.; Wender, P. A. *J. Org. Chem.* **2013**, *78*, 104–105.
(167) Wender, P. A.; DeChristopher, B. A.; Schrier, A. J. *J. Am. Chem. Soc.* **2008**, *130*, 6658–6659.
(168) Hayashi, T.; Konishi, M.; Ito, H.; Kumada, M. *J. Am. Chem. Soc.* **1982**, *104*, 4962–4963.

acid) epoxidation/ring opening of the chiral allylsilane **4.50** was diastereoselective (6:1 *anti*:*syn*) probably due to the difference in sterics between the bulky silyl group and the alkyl one. Thus, substituted tetrahydrofuran **4.51** can be obtained in 81% yield (Scheme 4.3.5b).[169]

**Scheme 4.3.5. Other functionalizations of chiral allylsilanes**

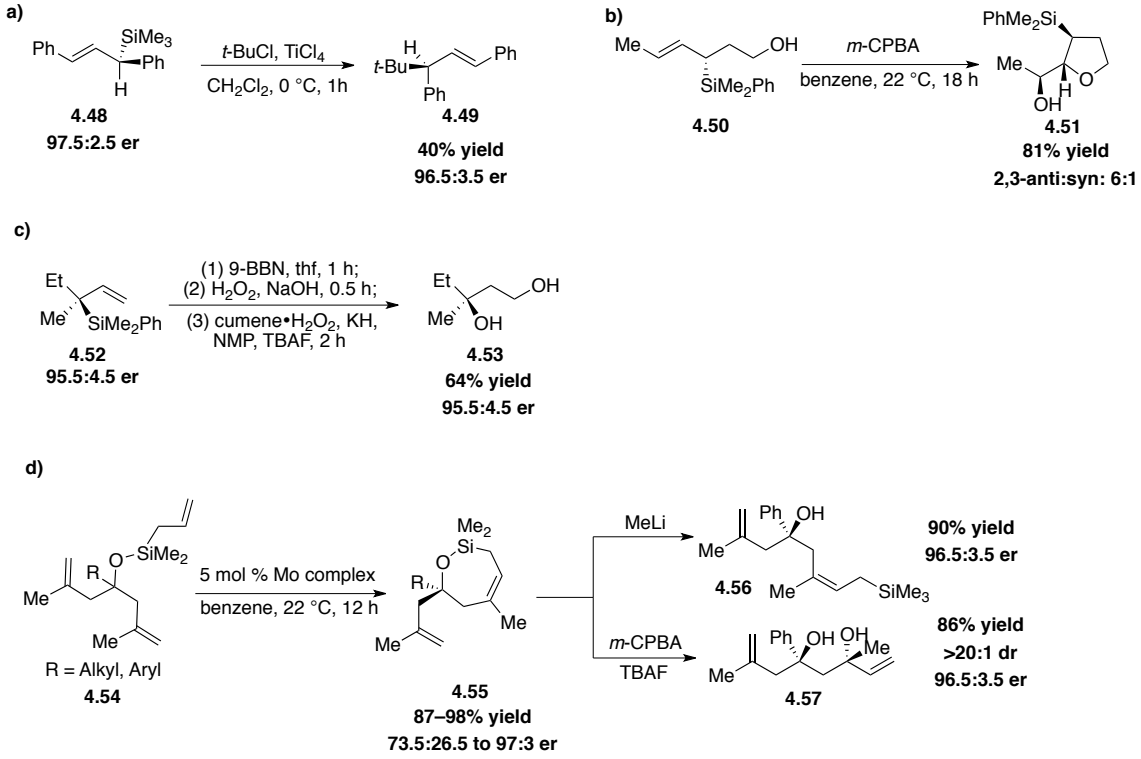


It should be noted that direct oxidation of a C–Si bond of allylsilanes would result in a complex mixture because the enhanced HOMO of the olefin is easier to be oxidized. Instead, functionalization of the olefin first followed by C–Si oxidation is normally a better solution. One example is illustrated in Scheme 4.3.5c, where the alkene is first converted into a primary alcohol after hydroboration/oxidation, followed by the C–Si bond oxidation affording the diol **4.53** in 64% overall yield with a complete stereo-

(169) Panek, J. S.; Garbaccio, R. M.; Jain, N. F. *Tetrahedron. Lett.* **1994**, *35*, 6453–6456.

retention.[170] At last, allylsilanes have also been employed in ring-closing metathesis (RCM)(Scheme 4.3.5d).[171] Chiral medium-ring siloxanes **4.55** obtained from Mo-catalyzed RCM reactions were used to prepare two different tertiary alcohols (**4.56** and **4.57**) in high yields, diastereoselectivity and enantioselectivity. The former one (**4.56**) was obtained after MeLi alkylation of the O–Si bond, whiles the latter one was formed from the epoxidation/desilylation reaction sequence.

Several catalytic protocols have been developed to synthesize those synthetically useful chiral allylsilanes with high enantioselectivitiy (Scheme 4.3.6). The first one was published by Hayashi and co-workers in 1982.[162] (*E*)- or (*Z*)-disubstituted allylsilanes **4.59** were obtained by a chiral phosphine–Pd-catalyzed cross coupling reactions. The reactions only require 0.5 mol % Pd complex as catalyst for full consumptions of vinylbromides **4.58**, although the reaction time is very long (2–5 days). The products were functionalized by stereoselective $S_N2$ reactions as illustrated before (Scheme 4.3.5a).

In 1986, the same group reported a catalytic enantioselective hydrosilylation of cyclic dienes (Scheme 4.3.6b).[172a] The reaction was promoted by 0.25 mol % of a similar phosphine–Pd catalyst in three days at –10 ºC. $HSiMeCl_2$ was found to be the proper silane reagent probably due to its enhanced reactivity. 1,4-Hydrosilation products (such as **4.61**) were obtained exclusively with 95% yield and 94.5:5.5 er. In 2001, the same

(170) Kacprzynski, M.; May, T. L.; Kazane, S. A.; Hoveyda, A. H. *Angew. Chem. Int. Ed.* **2007**, *46*, 4554–4558.

(171) Kiely, A. F.; Jernelius, J. A.; Schrock, R. R.; Hoveyda, A. H. *J. Am. Chem. Soc.* **2002**, *124*, 2868–2869.

(172) (a) Hayashi, T.; Kabeta, K.; Yamamoto, T.; Tamao, K.; Kumada, M. *Tetrahedron Lett.* **1983**, *24*, 5661–5664. (b) Hayashi, T.; Han, J. W.; Takeda, A.; Tang, J.; Nohmi, K.; Mukaide, K.; Tsuji, H.; Uozumi, Y. *Adv. Synth. Catal.* **2001**, *343*, 279–285.

group reported a modification of the current method, where $HSiCl_3$ was used for hydrosilylations. The reaction generally completes in 24 hours with 74–95% yield and 73.5:26.5 to 95:5 er.[166b]

**Scheme 4.3.6. Catalytic enantioselective synthesis of allylsilanes**

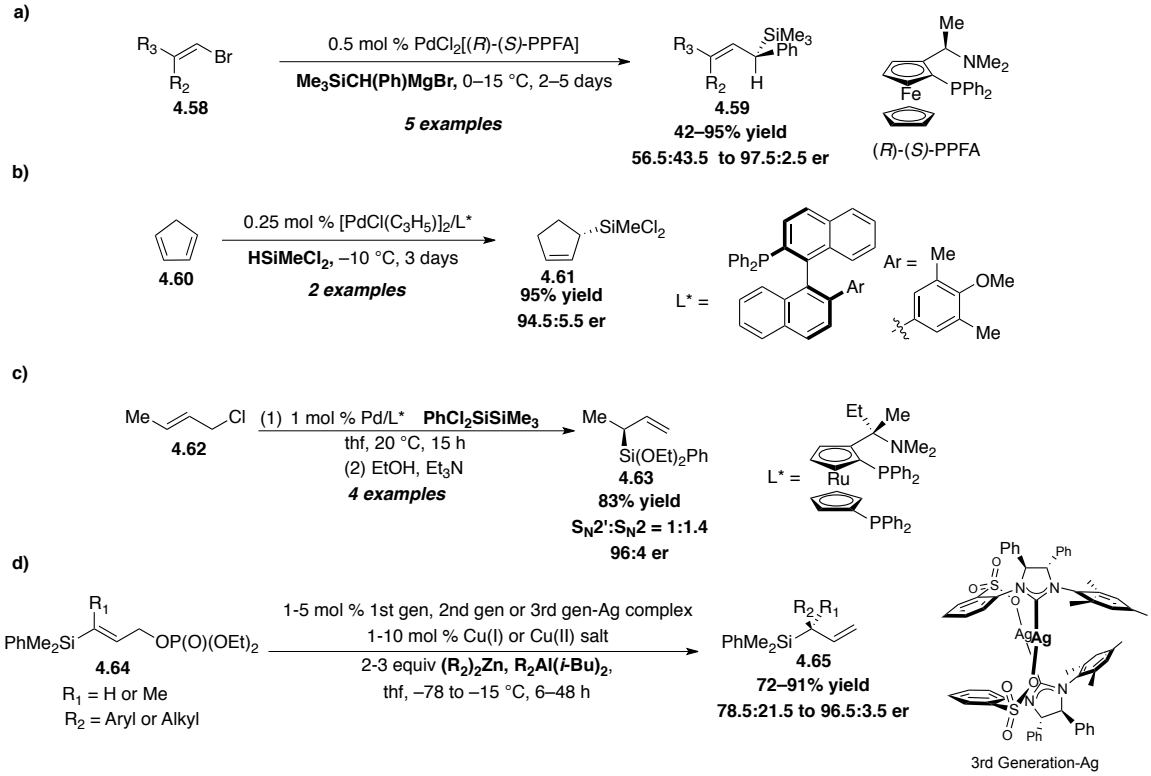


In addition, Pd-catalytic enantioselective silyl allylic substitutions have also been developed by the same group.[173] In Scheme 4.3.6c, the author prepared a chiral bisphosphine–Pd complex, which was able to promote the Si–Si bond cleavage and subsequent allylic substitution with allyl chlorides. However, the enantioselectivities of products in the four reported examples (including cyclic and acyclic allyl chlorides) vary significantly (55:45 to 96:4 er). The $S_N2'$ : $S_N2$ selectivity is also low (1:1.4).

Our laboratories have reported the enantioselective synthesis of chiral allylsilanes

(173) Hayashi, T.; Ohno, A.; Lu, S.-j.; Matsumoto, Y.; Fukuyo, E.; Yanagi, K. *J. Am. Chem. Soc.* **1994**, *116*, 4221–4226.

with NHC-Cu complexes as catalysts (Scheme 4.3.6d). However, instead of transfer of a silyl group to the eletrophile, we generated a catalytically active chiral organocuprate and promoted allylic substitutions with those carbon-based nucleophiles to vinyl silanes **4.64**. Bidentate NHCs (phenoxy containing (2nd gen) or sulfonate containing (3rd gen) NHCs) were proven to be extraordinarily effective and selective. Alkyl zinc,[164] alkenyl aluminum,[174] and alkynyl aluminum[175] were used to generate proper organocuprates. Through allylic substitutions, allylsilanes that bear a tertiary or quaternary carbon stereogenic center are efficiently produced with high $S_N2'$ : $S_N2$ selectivity and enantioselectivity.

Despite of the protocols disucssed above, there is still no general method for the catalytic enantioselective synthesis of chiral β-carbonyl-allylsilanes, compounds that are of high values in complex molecule synthesis (Scheme 4.3.3). There are only two examples for obtaining these allylsilanes in high enantiomeric ratios (Scheme 4.3.7). The first one was developed by Panek and co-workers in 1993: the racemic silyl substituted allyl alcohols were resolved by amino A. K. lipase with vinyl acetate. The enantiomerically enriched **4.67** was allowed to react with $CH_3CH(OMe)_3$ affording the corresponding ester, which was converted into allylsilane **4.68** through a Claisen rearrangment catalyzed by propanoic acid.[176] The latter reaction is highly stereoselective so that **4.68** can be obtained in 96.5:3.5 er.

The other case was demonstrated by Hayashi and co-workers in their studies of

(174) Lee, Y.; Akiyama, K.; Gillingham, D. G.; Brown, M. K. Hoveyda, A. H. *J. Am. Chem. Soc.* **2008**, *130*, 446–447.

(175) Dabrowski, J. A.; Gao, F.; Hoveyda, A. H. *J. Am. Chem. Soc.* **2011**, *133*, 4778–4781.

(176) Johnson, W. S.; Werthemann, L.; Barlett, W. R.; Brocksom, T. J.; Lu, T.-t.; Faulkner, D. J.; Petersen, M. R. *J. Am. Chem. Soc.* **1970**, *92*, 741–743.

Rh-catalyzed alkenyl conjugate additions.[177] In Scheme 4.3.7b, chiral allylsilane **4.71** was isolated in 91% yield and 98.5:1.5 er after the enantioselective conjugate addition. Unfortunately, it is the only case that was reported in this study.

Thus, if we succeed in developing the catalytic enantioselective silyl conjugate additions to α,β,γ,δ-unsaturated carbonyls, it would be the first general method to synthesize those useful allylsilanes.

**Scheme 4.3.7. Enantioselective synthesis of chiral β-carbonyl-allylsilanes**

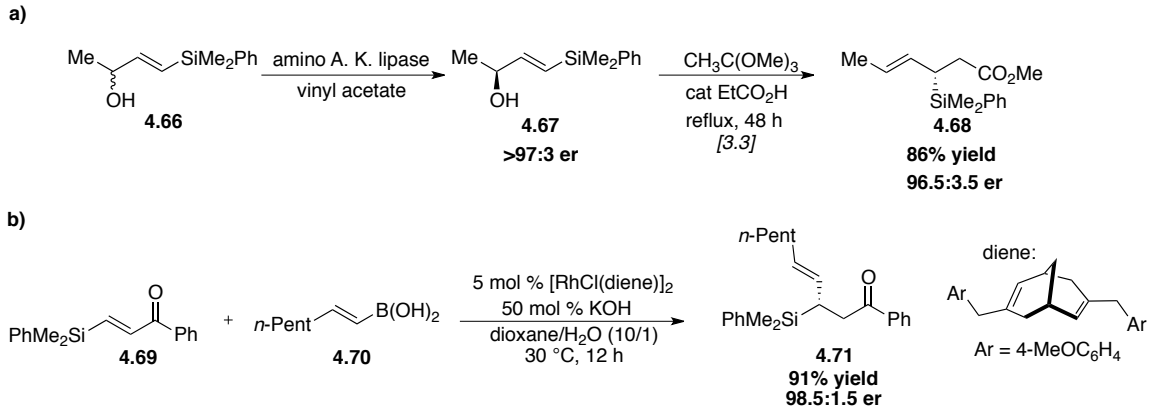


### *4.3.3. Our Studies on Catalytic Enantioselective Silyl Conjugate Additions to β-Unsubstituted α,β,γ,δ-Unsaturated Carbonyls*

Being aware of the potential values in this study, we first explored the catalytic enantioselective silyl conjugate additions to β-unsubstituted α,β,γ,δ-unsaturated carbonyls. In the beginning, we investigated similar reaction conditions that were previously employed in our NHC–Cu-catalyzed silyl conjugate adition to α,β-unsaturated carbonyls,[152] but with a variety of different chiral NHCs. This systematic ligand screening is illustrated in Scheme 4.3.8. A slight excess of imidazolinium salt (NHC precursor) than CuCl was used to make sure all the Cu(I) was coordinated with the NHC.

(177) Shintani, R.; Ichikawa, Y.; Takatsu, K.; Chen, F.-X.; Hayashi, T. *J. Org. Chem.* **2009**, *74*, 869–873.

NaO*t*-Bu was used to deprotonate the imidazolinium salt as well as generate the NHC-Cu-O*t*-Bu complex.

**Scheme 4.3.8. Ligand screening for catalytic enantioselective silyl conjugate additions to a β-unsubstituted dienone**

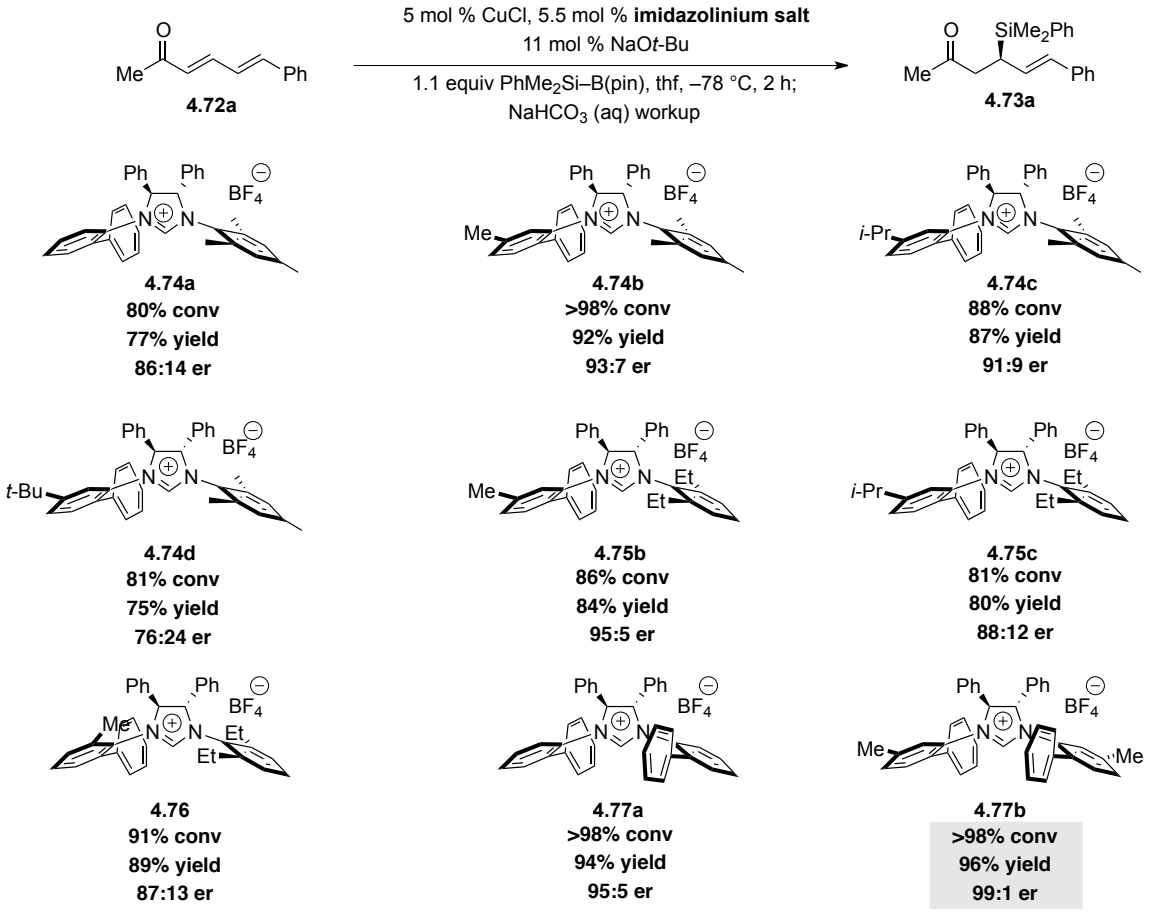


Generally, 1,4-additions were observed in all cases when various chiral NHC-Cu complexes were utilized. Since the higer coefficient of the LUMO of the unsubstituted acyclic dienone **4.72a** is on the β carbon, and there is no substituent at this site in the case of this particular substrate, the exclusive 1,4-silyl conjugate addition products **4.73a** are obtained as expected. The silyl addition proceeds to 80% conversion with the monodentate $C_1$-symmetric NHC derived from **4.74a**. The enantioselectivity is moderate (86:14 er). The installation of a methyl group onto the *meta* position of the aryl group of

the NHC results in a significant enhancement of the product er (**4.74b**, 93:7 er). Unfortunately, further increasing the steric bulk of this *meta* substituent (from Me, *i*-Pr to *t*-Bu) lowers reactivity and enantioselectivity (**4.74b** to **4.74d**). Alterations of the symmetric N-aryl motif of **4.74b** from mesity to 2,6-diethylphenyl results in imidazolinium salt **4.75b**, which gives the desired product with a slightly diminished efficiency (86% conv, 84% yield) but a higher er (95:5). Further increasing the steric bulk of the *meta* substituent of the dissymmetric N-aryl motif of **4.75b** does not improve the enantioselectivity (88:12 er, **4.75c**). The NHC derived from **4.76** bears an ortho methyl group on the dissymmetric N-aryl motif. However, this substitution pattern does not increase the enantioselectivity of this reaction either (87:13 er). Finally, the reaction with the $C_2$-symmetric NHC derived from **4.77a** affords the desired product with 94% yield and 95:5 er, which was further improved to 96% yield and 99:1 er in the reaction with **4.77b**.

**Scheme 4.3.9. Substrate scope of catalytic enantioselective silyl conjugate additions to β-unsubstituted dienones and dienoates**

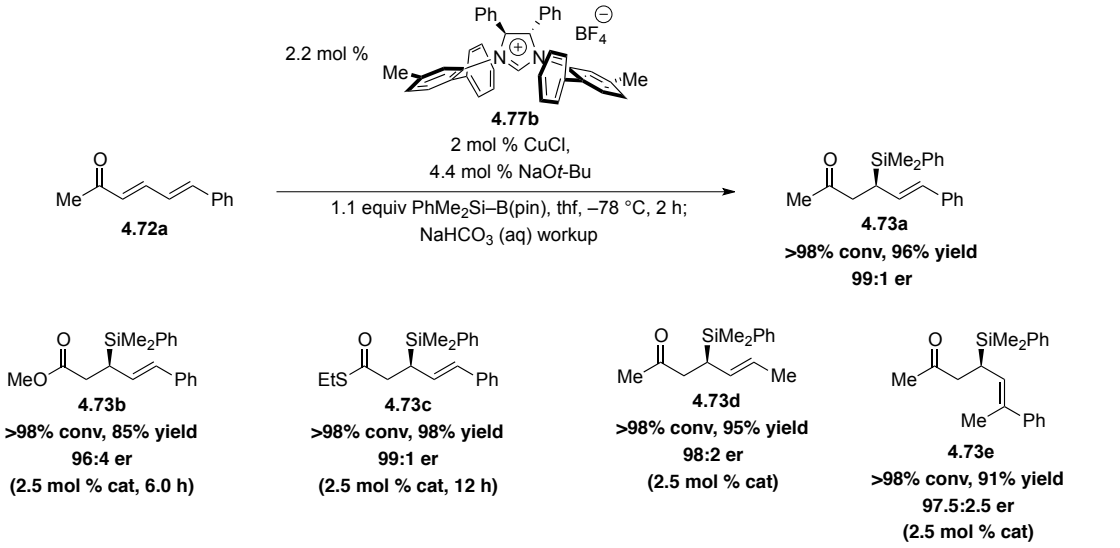


The reaction with dienone **4.72a** was found out to be equally efficient (96% yield) and enantioselective (99:1 er) with 2.0 mol % catalyst (2.2 mol % **4.77b**, 2.0 mol % CuCl

and 4.4 mol % NaO*t*-Bu, Scheme 4.3.9). β-unsubstituted α,β,γ,δ-unsaturated esters as well as thioesters are suitable substrates (**4.72b** and **4.72c**), affording the desired products with 85% and 98% yield, 96:4 and 99:1 er, respectively, despite a higher catalyst loading and longer reaction time need to be employed.

The reaction efficiency, regioselectivity and enantioselectivity do not drop if an alkyl substituted dienone was used as the substrate. For instance, allylsilane **4.73d** was isolated in 95% yield and 98:2 er. Similarly, dienone that bears a δ-substituent merely affect the silyl conjugate addition. In this case, allylsilane with a trisubstituted alkene unit (**4.73e**) can be obtained in 91% yield and 97.5:2.5 er.

The high efficiency of this reaction must account for the readily generated NHC–Cu-$SiMe_2Ph$ complex, effective substrate coordination and subsequent silyl migration, as well as efficient catalytic turnover. The high regioselectivity is probably because of the intrinsic molecular orbital of the β-unsubstituted α,β,γ,δ-unsaturated carbonyl, whose LUMO mostly resides on the β-carbon.

To understand the observed enantioselectivity of this transformation, computational analysis of two different modes of substrate coordination were performed.[178] This is based on the hypothesis that the enantioselectivity determining step of this reaction is the substrate coordination step, as one could imagine the following silyl migration step would not change the conformations of the complexes significantly. As a result, complex **4.78**, which affords the major product, was found to be 3.3 kcal/mol lower in energy than complex **4.79**. This difference in energy is probably due to the steric

(178) Calculations were performed by Dr. Fredrik Haeffner. B97D functional including dispersion together with the split-valence 6-31G* basis set were employed in the calculations. For detailed information, see the experimental section.

repulsion between the methyl substitutent of the substrate and the N-aryl motif of the NHC in complex **4.79**.

**Scheme 4.3.10. Computational studies on coordination of an unsubstituted dienone to the NHC-Cu complex**

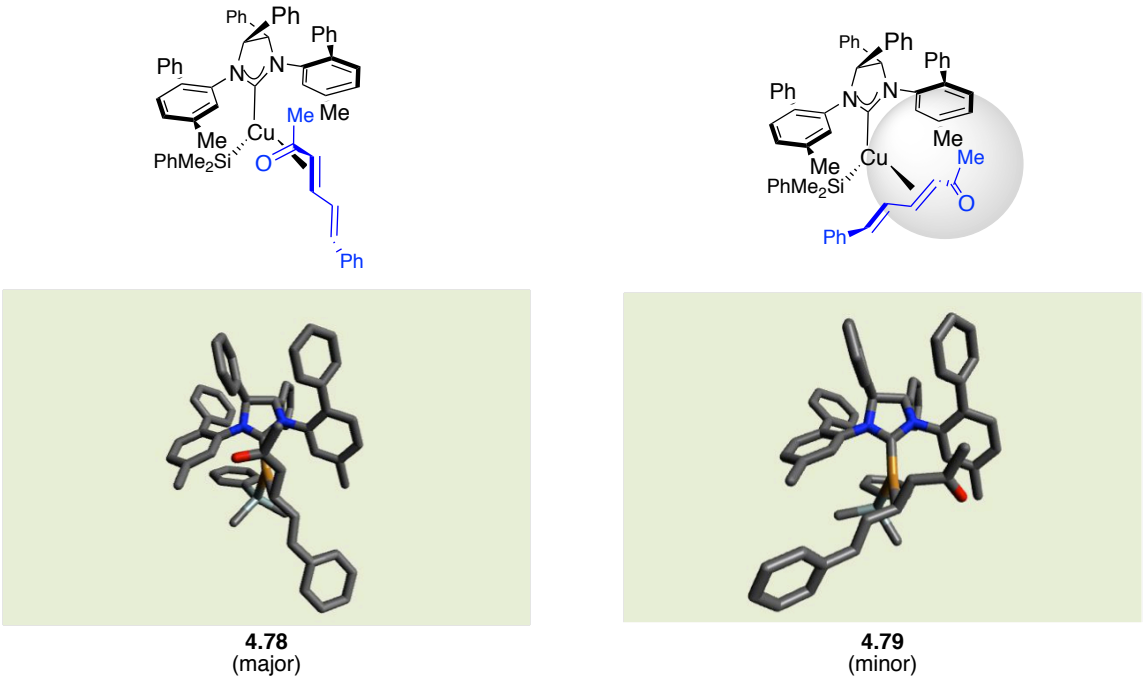


**4.78**
(major)

**4.79**
(minor)

ΔG(**4.79**) – ΔG(**4.78**) = +3.3 kcal/mol

### *4.3.4. Our Studies on Catalytic Enantioselective Silyl Conjugate Additions to β-Substituted α,β,γ,δ-Unsaturated Carbonyls*

Next, we would like to investigate the more challenging β-substituted α,β,γ,δ-unsaturated carbonyls in the NHC–Cu-catalyzed enantioselective silyl conjugate additions. As shown in Scheme 4.3.11, dienone **4.80a** was selected as the model substrate for a systematic ligand screening. To our surprise, 1,6-addition occurred exclusively (<2% 1,4-addition) no matter what NHC was employed. This is probably because the 1,4-addition is sterically less favored than the 1,6-addition since the α-olefin is a trisubstituted one. Perhaps more intriguingly, the trisubstituted olefin of the product **4.81a** is *Z* selective. This was confirmed by NOE experiment of selected hydrogens.

In contrast to the β-unsubstituted dienone **4.72a**, increasing the steric bulk of the *meta* substitutent of the dissymmetric N-aryl motif of the NHC does not improve the selectivity. For example, comparing reactions with **4.74b** and **4.74a**, the regio- and enantioselectivity of the product drops slightly (>20:1 *Z*:*E* vs 13:1 *Z*:*E*, 92:8 vs 91:1 er, respectively). Installation of an *ortho* cyclohexyl group (**4.83a)** gives similar results to **4.74a**, although a slight decrease in enantioselectivity (89:11 er) was observed.

**Scheme 4.3.11. Ligand screening for catalytic enantioselective silyl conjugate additions to a β-substituted dienone**

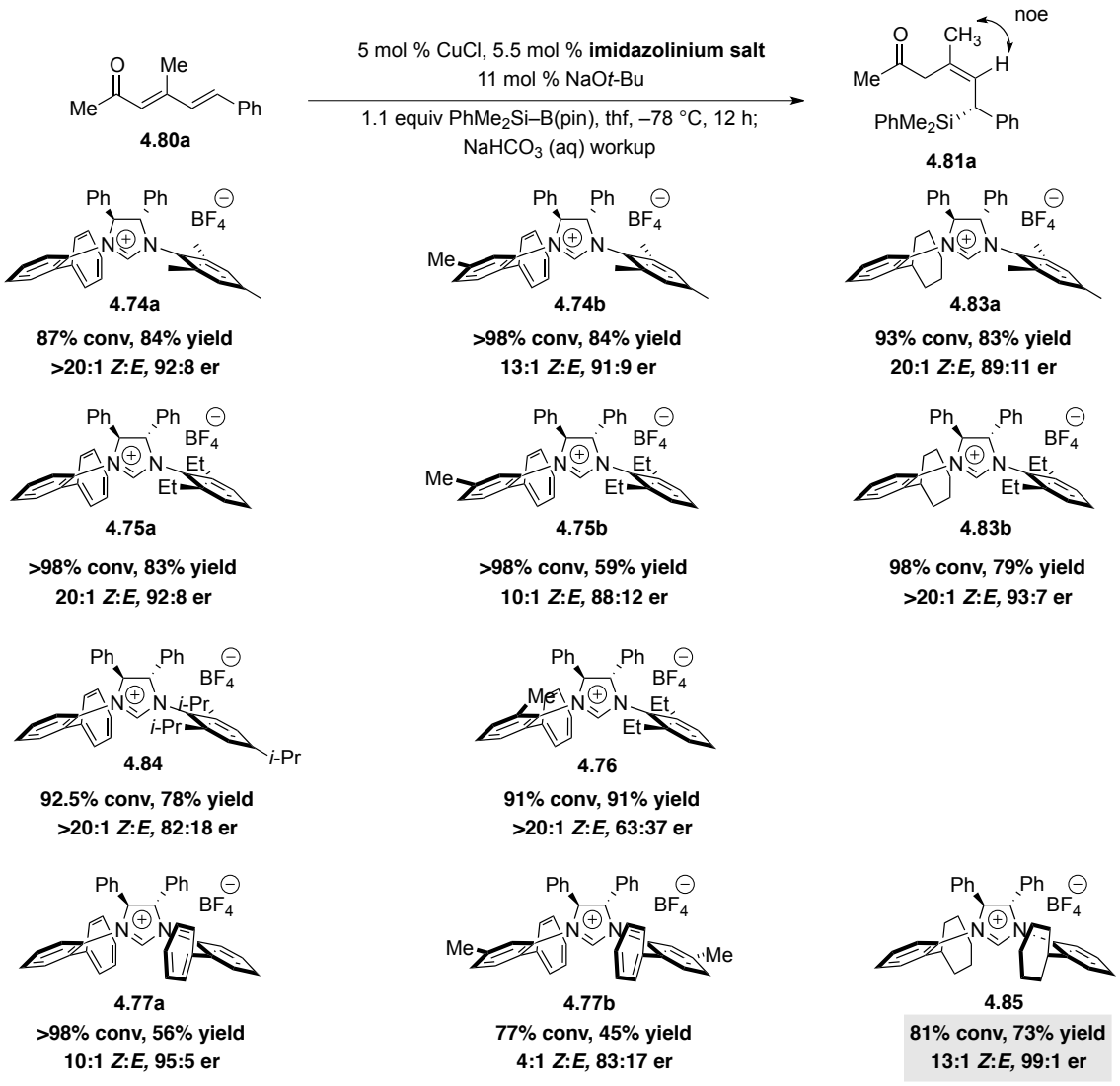


Similarly, the silyl conjugate addition is less regio- and enantioselective with

**4.75b** compared with the one with **4.75a**. Again, the *ortho* cyclohexyl group in **4.83b** does not seem to affect the reaction significantly.

Alternation of the symmetric N-aryl motif of the NHC with a trip (2,4,6-triisopropoylphenyl) group significantly diminishes the enantioselectivity of this reaction (82:18 er, **4.84**). Again, NHC derived from **4.76** is not an effective one in the silyl conjugate addition to **4.80a**.

Three different $C_2$-symmetric NHC(s) were also tested in the reactions. In general, the *Z*:*E* selectivities are slightly lower than with $C_1$-symmetric NHC(s). The same is true of the reaction efficiency (45–73% yield for reactions with $C_2$-symmetric NHC(s)). Surprisingly, the enantioselectivity of the reaction with **4.85** is much higher than others, the reason of which is unknown. In our opinion, it could be that the less sterically hindered cyclohexyl groups of **4.85** are able to accommondate the large dienone substrate better than the more hindered NHC(s) (such as **4.76** and **4.77**).

**Scheme 4.3.12. Computational studies on coordinations of a β-substituted dienone to the NHC-Cu complex**

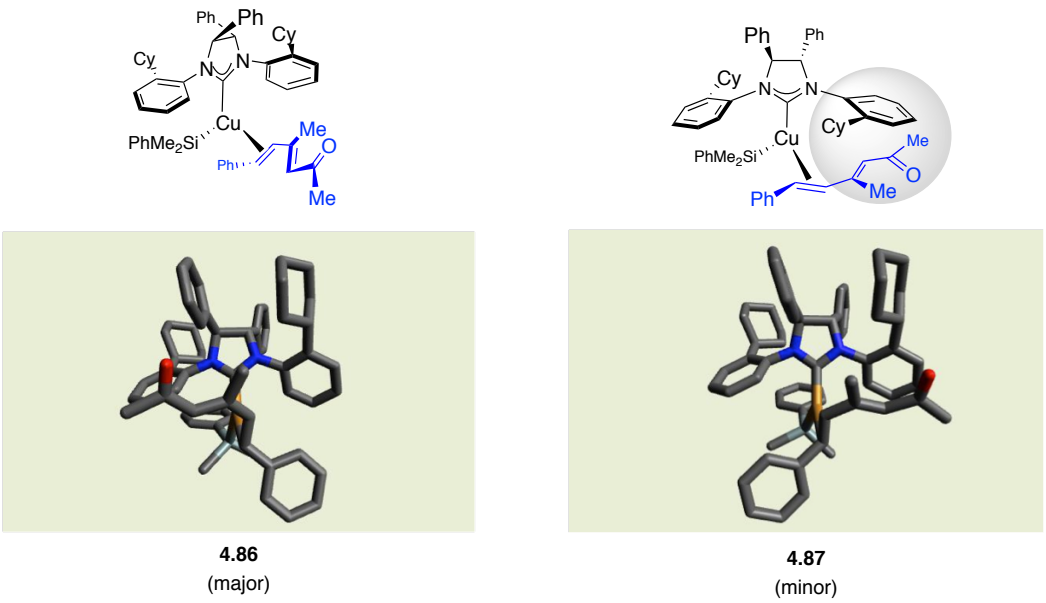


**4.86**
(major)

**4.87**
(minor)

ΔG(**4.87**) – ΔG(**4.86**) = +4.4 kcal/mol

To get more insights about why the silyl conjugate addition is regio-, *Z*:*E* and enantioselective. A series of computational studies were performed.[172] First, the two binding modes of the substrate **4.80a**, with its two enantiotopic faces, to the NHC–Cu-$SiR_3$ complex were calculated. As shown in Scheme 4.3.12, complex **4.86**, which gives the major enantiomer of the product **4.81a**, is 4.4 kcal/mol lower in energy than complex **4.87**. The steric repulsion between the substrate **4.80a** and one of the N-aryl motives of the NHC probably results in this energy difference. Here, we made the same assumption that the enantioselectivity determining step is the substrate coordination as the reactions with β-unsubstituted substrates. In addition, the NHC–Cu-$SiR_3$ complex prefers to coordinate to the less hindered γ-olefin (not the α-olefin), leading to the 1,6-addition products.

**Scheme 4.3.13. The energy difference between *s-cis* and *s-trans* conformations of 4.80a**

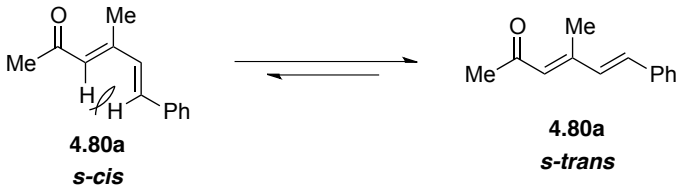


ΔG(***s-cis***) – ΔG(***s-trans***) = +3.3 kcal/mol

Apparently, the *Z* selectivity of the silyl conjugate addition must come from the *s-cis* comformation of the substrate as it binds to the NHC–Cu-$SiR_3$ complex. However, computational analysis reveals that the *s-cis* conformation of **4.80a** is 2.8 kcal/mol higher in energy than the *s-trans* conformation (Scheme 4.3.13), probably because of the $A_{1,4}$ interaction in the former conformer.

To better understand why the substrate choose the energetically less favored conformation to bind the NHC–Cu-$SiR_3$ complex, DFT calculations on model systems comprising of smaller achiral NHC–Cu-$SiMe_3$ (**4.88**) and a trienone (**4.89**) were used to

explore the *Z*,*E*-selectivity of the silyl addition.[179]

**Scheme 4.3.14. Computational studies on model systems**

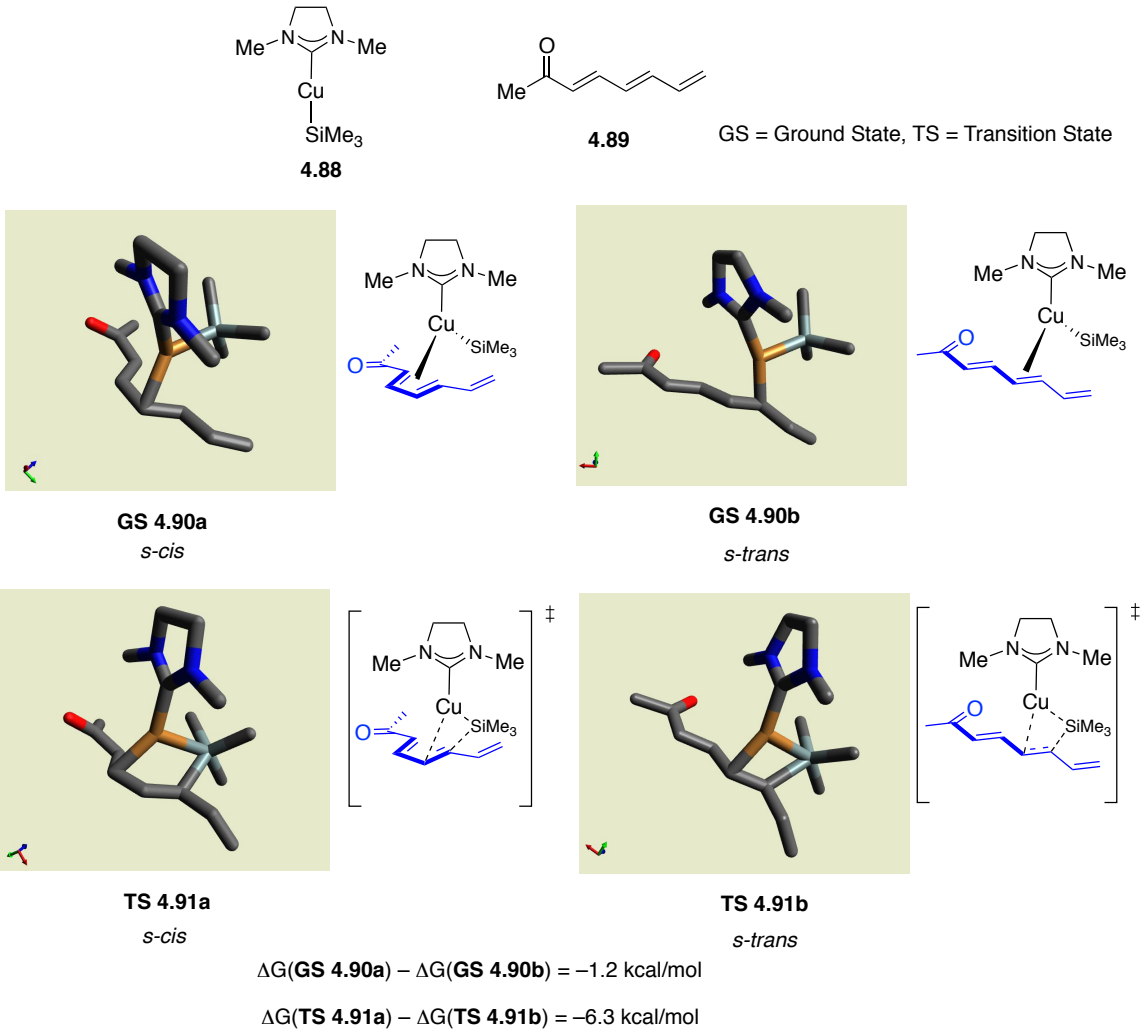


ΔG(**GS 4.90a**) – ΔG(**GS 4.90b**) = –1.2 kcal/mol

ΔG(**TS 4.91a**) – ΔG(**TS 4.91b**) = –6.3 kcal/mol

Ground states and transition states of the complexes of NHC–Cu-$SiMe_3$ with the substrate were computed in both its *s-cis*- and *s-trans*- conformations (Scheme 4.3.14). The results show that the ground state of the complex (**GS 4.90a**) with a *s-cis* substrate is 1.6 kcal/mol lower in energy than the corresponding complex with a *s-trans* substrate

(179) Calculations were performed by Dr. Fredrik Haeffner. The geometries were optimized and checked by means of frequency calculations using the B97D/LANL2DZ method. Free energies were computed at 298.15 K and 1.00 atm. using the unscaled frequencies. For detailed information, see the experimental section.

(**GS 4.90b**). Interestingly, this energy difference is increased in the transition states of C–Si bond formations (6.3 kcal/mol between **TS 4.91a** and **TS 4.91b**). Although the exact reason why the substrate adopts the *s-cis* conformation when it coordinates to the Cu complex is unkown, it could be due to the partial $\eta^4$ character of the olefin coordination in **GS 4.90a** and **TS 4.91a**. In another word, there is probably partial overlapping between the π* obital of the α-olefin and the filled d orbital of the Cu in **GS 4.90a (**and **TS 4.91a**), which lowers the Gibbs free energy of the two complexes. In conclusion, the computational analysis is in agreement with the observed *Z* selectivity in this NHC–Cu-catalyzed silyl conjugate additions.

The substrate scope was explored for the current method on β-substituted dienones and dienoates. As shown in Scheme 4.3.15, 1,6-additions of the $SiMe_2Ph$ motif occur exclusively in all cases. The trisubstitued olefins formed in all the products are all *Z* selective. In addition, the catalyst loading can be diminished to 2.5 mol % without affecting the reaction efficiency or selectivity (>98% conv in all cases, 69–85% yield, ≥8:1 *Z*:*E*, ≥99:1 er). Reactions with substrates bearing a *p*-OMe or *p*-$CF_3$ phenyl on the δ-position afford desired products in 81% and 75% yield, 20:1 and 10:1 of *Z*:*E* ratio, and 98.6:1.4 er and >99:1 er, respectively (**4.81b** and **4.81c**). Slightly diminished *Z*:*E* selectivity (8:1) is observed when dienones bearing linear (*n*-Pr) or branched (cyclohexyl) alkyl substituents are used (**4.81d** and **4.81e**). β-Substituted α,β,γ,δ-unsaturated esters and thioesters were subsequently investigated in NHC–Cu-catalyzed conjugate silyl additions (**4.81f** and **4.81g**). Although with relatively lower yields (73% and 69%, respectively) and longer reaction time for the thioester, the reactions proceed with equally high enantioselectivity (>99:1 er) and with enhanced *Z*:*E* selectivity (>20:1).

**Scheme 4.3.15. Catalytic enantioselective silyl conjugate additions to β-substituted dienones and dienoates**

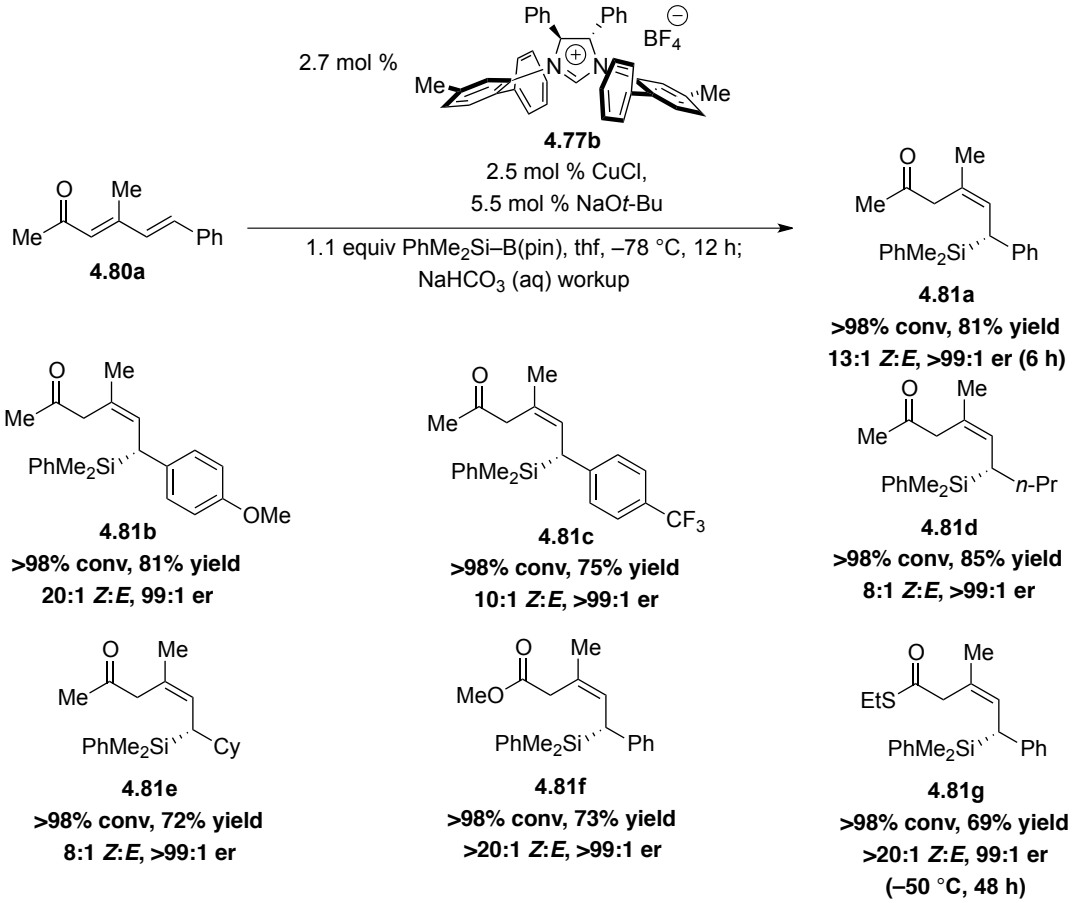


**Scheme 4.3.16. Reactions with (*Z,E*)-dienoates**

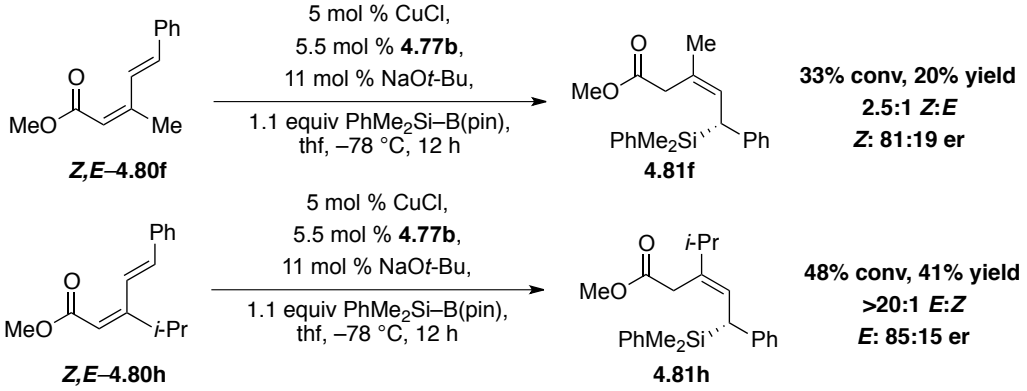


When we turned to (*Z*,*E*)-β-substituted dienoates **4.80f** and **4.80h**, significantly diminished reactivity towards the 1,6-conjugate silyl additions promoted by NHC–Cu complex derived from **4.77b** is observed (33% and 48% conv, respectively). While the

reaction with β-isopropyl substituted substrate **4.80h** affords high *Z*:*E* selectivity (>20:1), dienoate **4.80f**, bearing a smaller substituent (methyl vs isopropyl) is delivered as a 1,6-adduct with a lower *Z*:*E* ratio (2.5:1). In both cases, moderate enantioselectivities (81:19 er and 85:15 er) are observed. The diminished reactivity as well as selectivity may come from the enhanced allylic strain when the (*Z*,*E*)-dienoates adopt *s-cis* conformations. As a result, alternative conformations (such as *s-trans*) would be more competitive, affording a mixture of products.

The final segment of our investigations is catalytic enantioselective silyl conjugate additions to cyclic α,β,γ,δ-unsaturated carbonyls. As shown in Scheme 4.3.17, an extensive NHC screening was performed for the reaction with dienone **4.92b**. Similar as the acyclic substrates, the cyclic one only affords 1,6-addition product **4.93b** with a high *Z*:*E* selectivity. In addition, *Z*:*E* selectivity and enantioselectivity decrease when increasing the size of *meta* substituents of the dissymmetric *N*-aryl motives of NHCs. For example, alternating the imidazolinium salts from **4.74a** to **4.74c** (from H to *i*-Pr group), *Z*:*E* ratio decreases from 20:1 to 2.5:1, and enantioselectivity decreases from 91:9 to 70:30 er. Similarly, from **4.75a** to **4.75c**, *Z*:*E* ratio, as well as enantioselectivity, diminishes. Nevertheless, the efficiencies of these silyl additions are still high (>98% conv, 2 h). The increasing steric bulk of the symmetric *N*-aryl moiety from mesityl group to 2,6-diethylphenyl group and to 2,4,6-triisopropylphenyl group results in a diminished *Z*:*E* selectivity as well. For example, the use of **4.74a** vs **4.75a**, vs **4.84** affords better *Z*:*E* selectivity [20:1 vs 17:1, vs 10:1] without a significant decrease of enantioselectivity [91:9 vs 92:8, vs 90:10 er].

Notably, the NHC–Cu-$SiMe_2Ph$ complex derived from the $C_2$-symmetric NHC from **4.77a** promotes reaction with >98% conv, >20:1 of *Z*:*E* selectivity and 96:4 er. Modifications of **4.77a** do not improve the reaction efficiency nor selectivity (**4.77b** and **4.77c**).

**Scheme 4.3.17. Ligand screening for catalytic enantioselective silyl conjugate additions to a cyclic dienone**

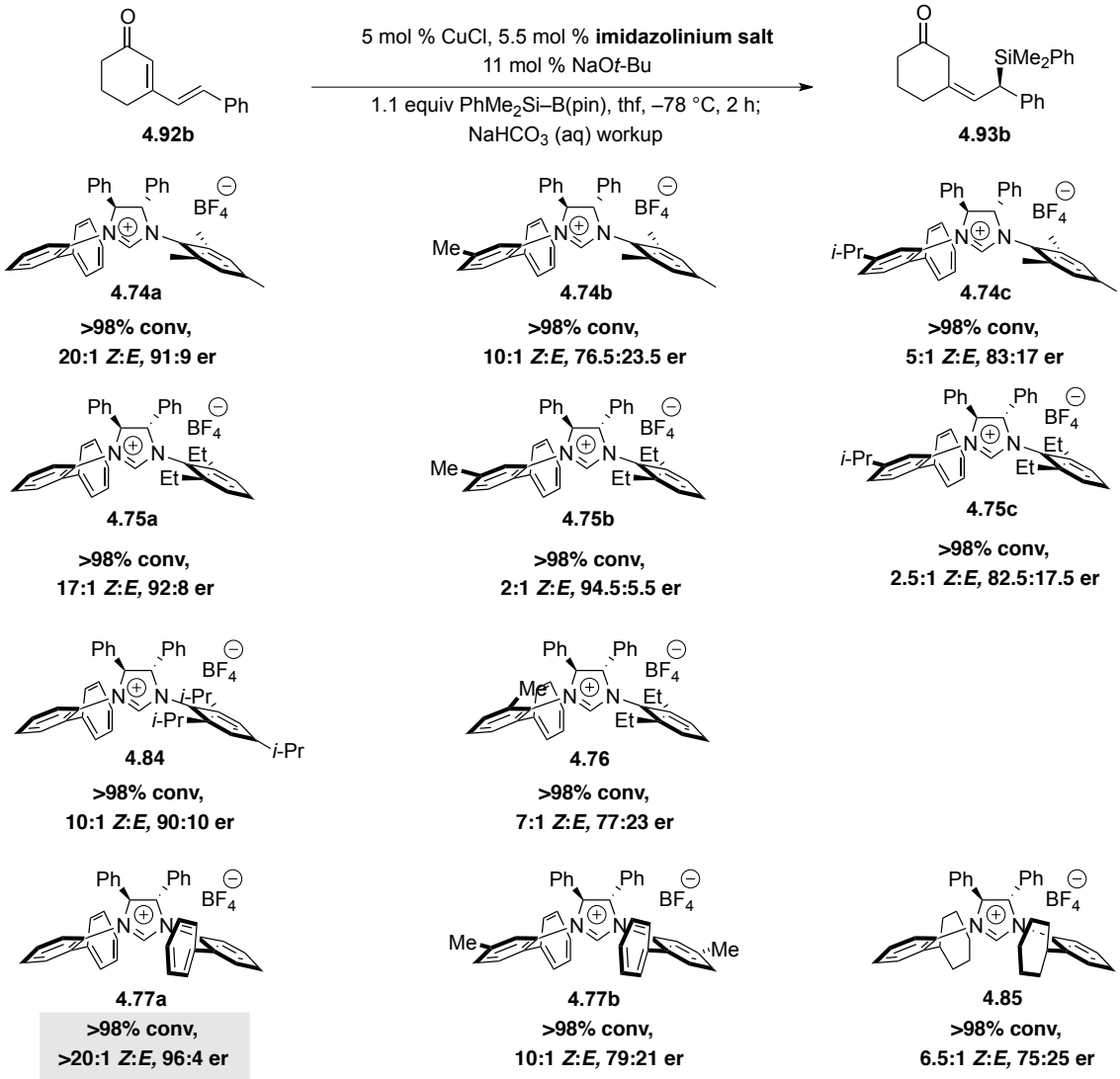


A variety of cyclic dienones were investigated in the NHC–Cu-catalyzed enantioselective silyl conjugate additions. Only 2 mol % of the NHC–Cu-O*t*-Bu complex is sufficient to promote complete transformations in two hours for all cases. Dienone

**4.92a** bearing a cyclopentenone affords the product with a diminished *Z*:*E* selectivity (3.6:1 *Z*:*E*). It is possible that the $\eta^4$ characteristics in the coordination of the *s-cis* conformer of the substrate to the Cu complex is less pronounced in this case (maybe due to the five membered ring), so that the *s-trans* conformer is more competitive, affording more *E* product.

Reactions with dienones bearing a cyclohexenone with different aryl substituents (**4.92b** to **4.92e**) are all highly efficient, regio-, *Z*:*E* and enantioselective. This is also true with the dienone with a cyclohexyl substituent (**4.92f**). The desired product can be obtained in 92% yield, 20:1 *Z*:*E* and 98:2 er. Notably, dienone **4.92g** which contains a gem-dimethyl group is also a suitable substrate. The steric bulk of the dimethyl substituents does not seem to interact with the NHC–Cu complex. At last, the silyl conjugate addition is also equally efficient and selective with a seven-membered ring dienone **4.92h**.

**Table 4.3.1. Substrate scope for cyclic dienones in silyl conjugate additions**

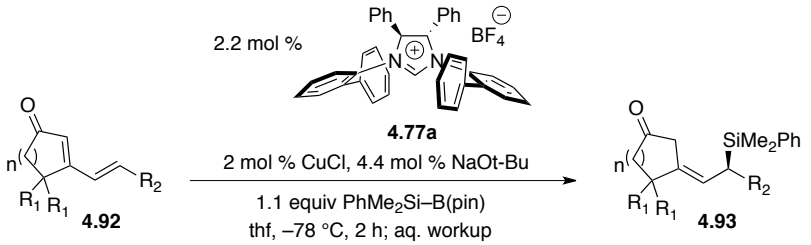


**>98% conv in all cases**

| entry | n | $R_1$ | $R_2$ | substrate | yield (%) | *Z:E* | er |
|---|---|---|---|---|---|---|---|
| 1 | 1 | H | Ph | **4.92a** | 85 | 3.6:1 | 95:5 |
| 2 | 2 | H | Ph | **4.92b** | 91 | 20:1 | 98:2 |
| 3 | 2 | H | *p*-$MeC_6H_4$ | **4.92c** | 95 | >20:1 | 95:5 |
| 4 | 2 | H | *p*-$MeOC_6H_4$ | **4.92d** | 91 | >20:1 | 97:3 |
| 5 | 2 | H | *p*-$CF_3C_6H_4$ | **4.92e** | 88 | >20:1 | 94.5:5.5 |
| 6 | 2 | H | Cy | **4.92f** | 92 | 20:1 | 98:2 |
| 7 | 2 | Me | Ph | **4.92g** | 95 | <1:20 | 96:4 |
| 8 | 3 | H | Ph | **4.92h** | 98 | 20:1 | 96:4 |

Computational studies explain the observed selectivity of the silyl additions to cyclic dienones.[172] The NHC–Cu-$SiMe_2Ph$ complex prefers to coordinate to the γ-olefin of the substrate (not the α-olefin), probably because of the steric bulk of the trisubstituted olefin. In addition, the dienone (**4.92g** in Scheme 4.3.18) adopts the *s-cis* conformation in this coordination like the acyclic ones. It is likely there is a secondary interaction between the Cu and the α-olefin of the *s-cis* conformer. At last, the substrate probably has to bind to the NHC–Cu complex in a way like **4.94**, to avoid the steric repulsion between the cyclohexenone and one of the N-aryl motives of the NHC when its opposite enantiotopic face coordinate to the NHC–Cu complex (highlighted in **4.95**). The energy difference between **4.94** and **4.95** is 1.8 kcal/mol, smaller than the 4.4 kcal/mol in the reactions with acyclic dienones.

**Scheme 4.3.18. Computational studies on the silyl conjugate addition to a cyclic dienone**

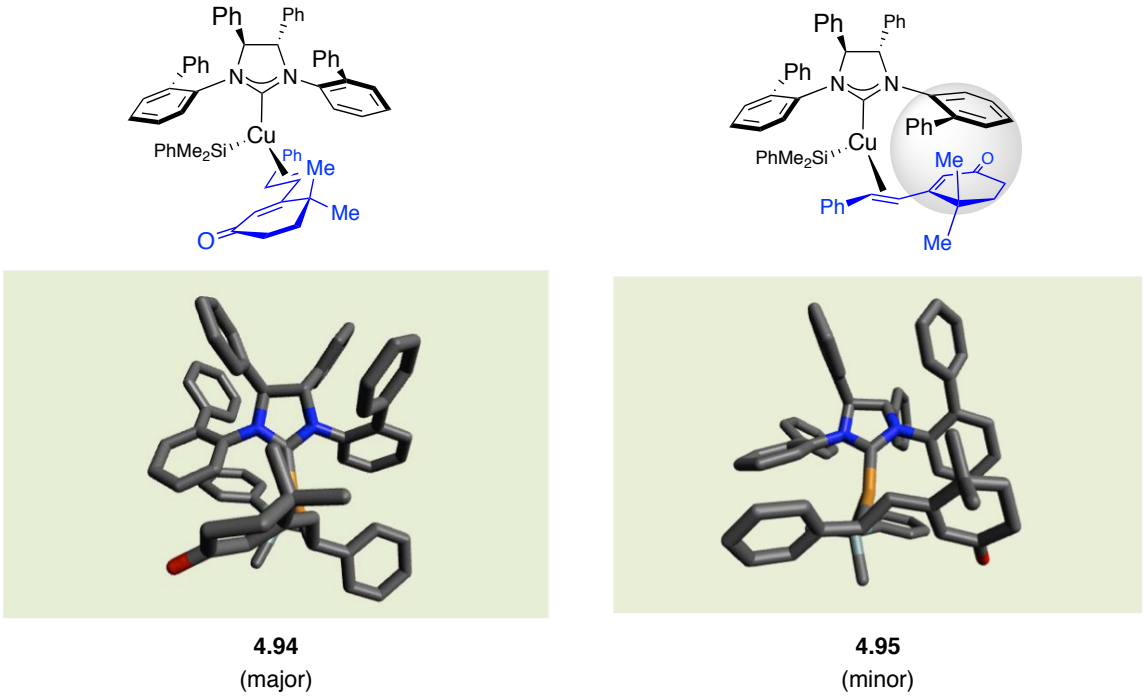


**4.94**
(major)

**4.95**
(minor)

ΔG(**4.95**) – ΔG(**4.94**) = +1.8 kcal/mol

### *4.3.5. Functionalization of the Enantiomerically Enriched Allylsilanes*

The enantiomerically enriched allylsilanes are of great values in synthetic organic chemistry. Strategies that convert the C–Si bonds of such allylsilanes into C–C bonds through allylation and alkylations, as well as oxidations of the C–Si bonds have been illustrated previously (Scheme 4.3.5). In addition, we have employed an epoxidation/desilylation sequence to transform one of the allylsilanes into an enantiomerically enriched allylalcohol. As shown in Scheme 4.3.19, the diastereoselective epoxidation by *m*-CPBA of allylsilane **4.81a** affords the epoxide **4.96** in 80% yield and 83:17 dr. The epoxidation occurs from the front side of the olefin probably because the hindered $SiMe_2Ph$ group blocks the other side. TBAF desilylation

quantitatively gives the tertiary alcohol **4.97** in 93.5:6.5 er. The erosion of the enantiomeric ratio of **4.97** comes from the other diastereomer of **4.96**. It is noteworthy that alcohol **4.97** is difficult to obtain through a catalytic enantioselective aldol reaction to the corresponding ketone.[180]

**Scheme 4.3.19. Epoxidation/desilylation of an enantiomerically enriched allylsilane product**

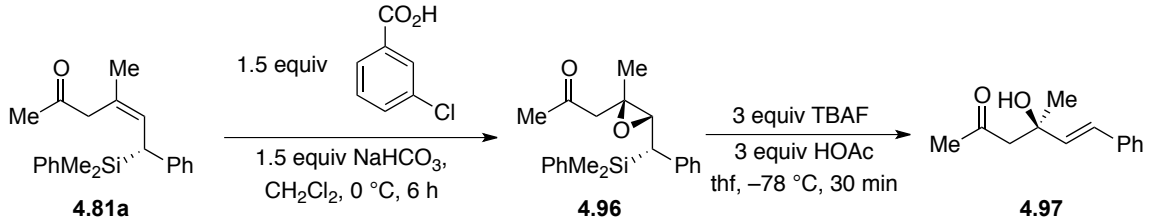


### *4.3.6. Conclusions*

We have developed the first catalytic enantioselective silyl conjugate additions to α,β,γ,δ-unsaturated carbonyl compounds. In general, 2–2.5 mol % of a chiral NHC–Cu-O*t*-Bu is sufficient to promote complete transformations at –78 to –50 °C in 2–48 hours, affording highly valuable chiral allylsilanes with high efficiency, regio-, *Z*:*E* selectivity and enantioselectivity. The regioselectivity is controlled by substrates: with β-unsubstituted dienone and dienoates, 1,4-additions occur exclusively; with β-substituted dienone and dienoates (acyclic and cyclic), only 1,6-addition products are observed. The *Z*:*E* selectivity and enantioselectivity are dominated by the chiral NHC–Cu catalyst. Computational studies reveal some of the insights about the origins of those selectivities.

(180) Broadly applicable, efficient, and highly enantioselective catalytic protocols for aldol additions to ketones remain lacking. For key reports, see: (a) List, B.; Shabat, D.; Zhong, G.; Turner, J. M.; Li, A.; Bui, T.; Anderson, J.; Lerner, L. A.; Barbas, C. F. *J. Am. Chem. Soc.* **1999**, *121*, 7283–7291. (b) Denmark, S. E.; Fan, Y.; Eastgate, M. D. *J. Org. Chem*. **2005**, *70*, 5235–5248. For a recent review on Cu-catalyzed ketone aldol processes, see: (c) Shibasaki, M.; Kanai, M. *Chem. Rev.* **2008**, *108*, 2853–2873. For Ag-catalyzed aldol adition to α-keto esters, see: (d) Akullian, L. C.; Snapper, M. L.; Hoveyda, A. H. *J. Am. Chem. Soc.* **2006**, *128*, 6532–6533.

The allylsilane product can be converted into a teritiary alcohol with high yield and enantiomeric ratio, which is otherwise difficult to obtain through alternative methods.

## *4.4. Catalytic Enantioselective Silyl Allylic Substitutions*

Next, we would like to investigate whether our NHC–Cu catalyst can be applied in catalytic enantioselective silyl allylic substitutions. The $S_N2'$ product, a general allylsilane with a terminal olefin, is of great values (see Scheme 4.3.2 to 4.3.5). The general concept of designing enantioselective silyl allylic substitutions with the NHC–Cu catalyst is shown in Scheme 4.4.1. We hoped that if a proper NHC was discovered, the reaction would be highly efficient, regioselective ($S_N2'$ selective) and enantioselective.

**Scheme 4.4.1. General concept for catalytic enantioselective silyl allylic substitutions**

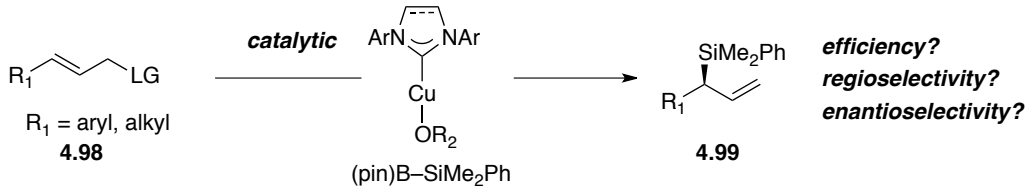


Allylic phosphate **4.100a** was chosen as the model substrate (Scheme 4.4.2). After a screening of different types of NHC precursors, we were pleased to find sulfonate-containing NHC derived from **4.102** is particularly effective (1 mol %) to promote the allylic substitution of a silyl group. The allylsilane product (**4.101a**) was obtained in 84% yield, 96:4 $S_N2'$:$S_N2$ selectivity and 98:2 er. It is noteworthy that this NHC–Cu catalyst has been utilized in the enantioselective boryl allylic substitutions of allylic carbonates, with similar reaction conditions.[181] There are several additional attributes of the silyl allylic substitution that need to be pointed out: First, without NHC or CuCl, there is minimal conversion. It is the NHC–Cu complex that serves as the active catalyst.

(181) Guzman-Martinez, A.; Hoveyda, A. H. *J. Am. Chem. Soc.* **2010**, *132*, 10634–10637

Secondly, 80 mol % NaOMe is required for a high conversion of this reaction, because the NHC–Cu-phosphate (generated after the C–Si bond formation) is not Lewis basic enough for activation of the Si–B bond in $PhMe_2Si$–B(pin). Thus, additional sodium alkoxide is needed to regenerate active NHC–Cu-alkoxide. Lastly, other allylic eletrophiles are inferior to allylic phosphates in this reaction. For example, if a phenyl-substituted allyl bromide is employed under the same reaction condition, more $S_N2$ product is obtained (77:23 $S_N2$':$S_N2$). If an allyl carbonate is used instead, only 15% conversion was obtained (6% $S_N2$' product).

**Scheme 4.4.2. Screening of different types of NHC precursors**

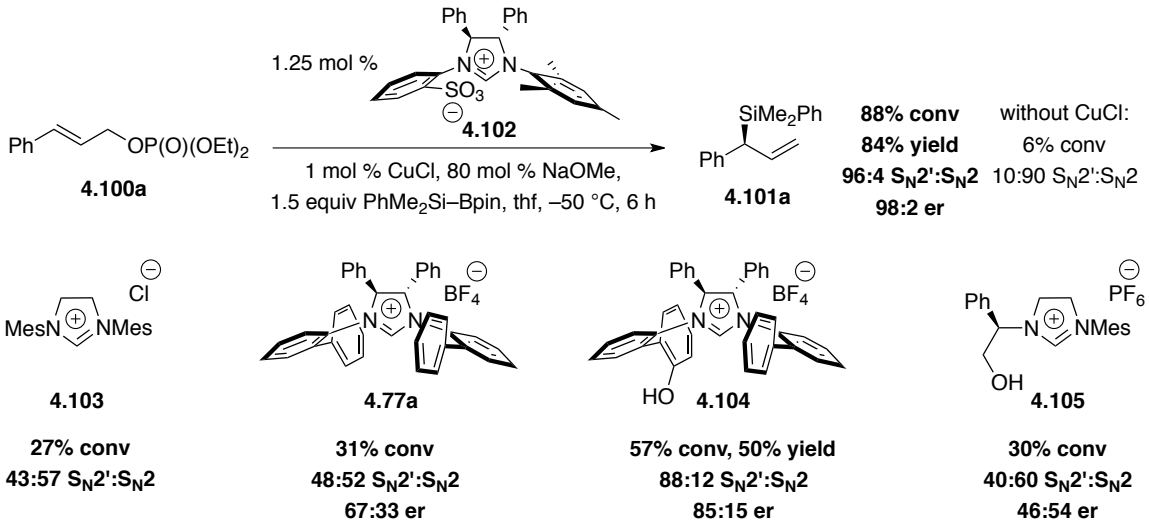


It turned out that other NHCs, including achiral or chiral monodentate ones (**4.103** and **4.77a**), or ones that contain a phenol/alcohol (**4.104** and **4.105**), are much less efficient and regioselective. Only 27–57% conversions of a mixture of $S_N2$' and $S_N2$ products were delivered. The enantiomeric ratios of the $S_N2$' product (**4.101a**) are also significantly lower (46:54 to 85:15 er).

**Scheme 4.4.3. Substrate scope of the catalytic enantioselective silyl allylic substitutions**

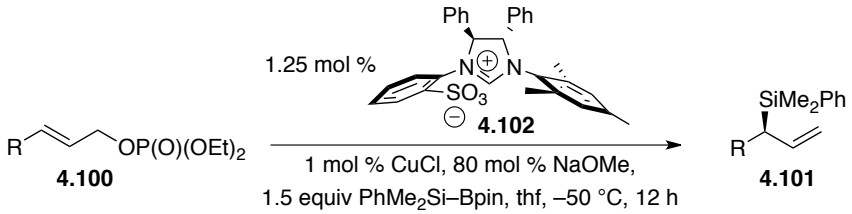


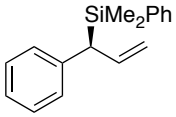


**4.101a**
**84% yield, 96:4 $S_N2'$:$S_N2$**
**98:2 er, (6 h)**

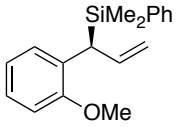


**4.101b**
**83% yield, 96:4 $S_N2'$:$S_N2$**
**96:4 er**

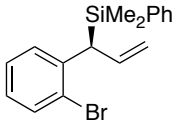


**4.101c**
**79% yield, 94:6 $S_N2'$:$S_N2$**
**96:4 er**

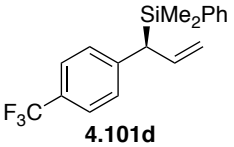


**4.101d**
**80% yield, 96:4 $S_N2'$:$S_N2$**
**94:6 er**

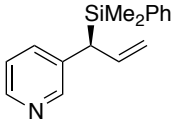


**4.101e**
**74% yield, 90:10 $S_N2'$:$S_N2$**
**96:4 er**
**(3 mol % cat, 4 h)**

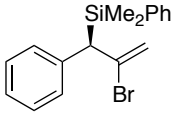


**4.101f**
**43% conv, 92:8 $S_N2'$:$S_N2$**
**66:34 er**
**(5 mol % cat, 12 h)**

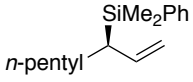


**4.101g**
**71% yield, 94:6 $S_N2'$:$S_N2$**
**94:6 er**
**(2 mol % cat, 6 h)**

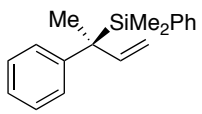


**4.101h**
**72% yield, 96:4 $S_N2'$:$S_N2$**
**97:3 er**
**(3 mol % cat, –30 °C)**

To explore the substrate scope of this transformation, a variety of allylic phosphates were investigated. The electron rich (**4.100b**) or poor (**4.100d**) aryl substitituent of the alkene does not affect the reaction efficiency and selectivity. Sterically more encumbered **4.100c**, which bears an *ortho* bromo group, proved to be an equally effective substrate. To our delight, the silyl allylic substitution with the allylic phosphate bearing a pyridyl substituent is still efficient (74% yield) and enantioselective (96:4 er), despite of a higher catalyst loading (3 mol % cat) and a slightly diminished regioselectivity (90:10 $S_N2'$:$S_N2$).

The reaction is greatly hampered with a 2-bromo-substituted allylic phosphate. Only 43% conversion was observed, and the product was much less enantioselective (66:34 er).

Alkyl allylic phosphates are suitable substrates in the silyl allylic substitution reaction, as allylsilane **4.101g** was isolated in 71% yield, 94:6 $S_N2'$:$S_N2$ and 94:6 er. The reaction can also be applied in the enantioselective synthesis of allylsilanes containing a quaternary carbon stereogenic center (**4.101h**, 72% yield, 96:4 $S_N2'$:$S_N2$ and 97:3 er).

Unfortunately, other groups have discovered similar protocols during the course of this study. In 2013, Oestreich and co-workers reported the first catalytic enantioselective silyl allylic substitutions with a chiral NHC–Cu complex.[182] In the same year, Hayashi group developed a similar NHC-Cu catalyzed protocol for silyl allylic substitutions.[183] The latter report involves reactions with trisubstituted allyl phosphates.

## *4.5. Conclusions*

We have successfully developed the first general enantioselective silyl conjugate additions to α,β,γ,δ-unsaturated carbonyl compounds using a chiral NHC–Cu complex as catalyst. 1,4- or 1,6-Additions were achieved exclusively depending on the type of substrate utilized. In case of the 1,6-additions, high *Z* selectivities for the trisubstitued allylsilanes were observed. The highly enantiomerically enriched allylsilanes can be utilized in a variety of transformations, including converting into a ketone-aldol product. Computational studies were performed to help understand the distinct selectivity profiles of these reactions.

---

(182) Delvos, L. B.; Vyas, D. J.; Oestreich, M. *Angew. Chem. Int. Ed.* **2013**, *52*, 4650–4653.
(183) Takeda, M.; Shintani, R.; Hayashi, T. *J. Org. Chem.* **2013**, 78, 5007–5017

A general catalytic enantioselective silyl allylic substitution protocol has been developed. The chiral NHC bearing a sulfonate moiety was found to be the optimal ligand. Aryl-, alkyl- as well as heteroaryl-substituted allylsilanes, including one bearing a quarternary carbon center, can be synthesized in high yields and enantiomeric ratios.

Those aforementioned studies reveal the great potential of the NHC–Cu complex in catalytic enantioselective transformations. Future studies will focus on the use of these Cu complexes for discoveries of new transformations, as well as development of new catalysts in organometallic chemistry.

## *4.6. Acknowledgment*

I thank Prof. Amir H. Hoveyda for providing me this great project to study, especially as my first project. Dr. Kangsang Lee deserves my thanks because of his mentorship and cooperation on this project. I am also grateful of Dr. Fredrik Haeffner for his computational analysis. I appreciate the enlightening discussions with all the other Hoveyda group members.

This work was supported financially by the NIH (GM-57212) and the NSF (CHE-1111074). We thank Boston College and the chemistry department for providing great assistance and facilities.

## *4.7. Experimental Section*

### *4.7.1. Preparations and Characterizations of New Compounds*

**General.** Infrared (IR) spectra were recorded on a Bruker FT-IR Alpha (ATR mode) spectrophotometer, $\nu_{max}$ in $cm^{-1}$. Bands are characterized as broad (br), strong (s), medium (m), and weak (w). $^1H$ NMR spectra were recorded on a Varian Unity INOVA 400 (400 MHz) spectrometer. Chemical shifts are reported in ppm from tetramethylsilane

with the solvent resonance as the internal standard ($CDCl_3$: δ 7.26 ppm). Data are reported as follows: chemical shift, integration, multiplicity (s = singlet, d = doublet, t = triplet, q = quartet, sep = septet, bs = broad singlet, m = multiplet), and coupling constants (Hz). $^{13}C$ NMR spectra were recorded on a Varian Unity INOVA 400 (100 MHz) spectrometer with complete proton decoupling. Chemical shifts are reported in ppm from tetramethylsilane with the solvent resonance as the internal standard ($CDCl_3$: δ 77.16 ppm). High-resolution mass spectrometry was performed on a Micromass LCT ESI-MS (positive mode) at the Mass Spectrometry Facility at Boston College. Enantiomer ratios were determined by HPLC analysis (Chiral Technologies Chiralpak AD-H, 4.6 x 250 mm, Chiral Technologies Chiralcel OD, 4.6 x 250 mm, Chiral Technologies Chiralcel AS, 4.6 x 250 mm, and Chiral Technologies Chiralcel OB-H, 4.6 x 250 mm) in comparison with authentic racemic materials. Unless otherwise noted, all reactions were carried out with distilled and degassed solvents under an atmosphere of dry $N_2$ in oven- (135 °C) and flame-dried glassware with standard dry box or vacuum-line techniques. Tetrahydrofuran (thf) was purified by distillation from sodium benzophenone ketyl immediately prior to use. All work-up and purification procedures were carried out in air. All solvents were purchased from Doe and Ingalls. (Dimethylphenylsilyl)boronic acid pinacol ester [$PhMe_2Si$–B(pin)] was purchased from Aldrich and distilled prior to use. All substrates were purchased from Aldrich and distilled prior to use. 2-Cyclic dienones were prepared based on a previously reported procedure.[184] Sodium *t*-butoxide and copper(I) chloride were purchased from Strem and

(184) (a) Hayashi, T.; Yamamoto, S.; Tokunaga, N. *Angew. Chem., Int. Ed.* **2005**, *44*, 4224–4227. (b) Henon, H.; Mauduit, M.; Alexakis, A. *Angew. Chem., Int. Ed.* **2008**, *47*, 9122–9124.

used as received.

**NOTE:** It is imperative that dry and pure reagents, Cu salt and imidazolinium salt are utilized in order to achieve optimal efficiency and enantioselectivity.

**Representative Procedure for Chiral NHC–Cu-Catalyzed Enantioselective Silyl Conjugate Additions:** Preparation of the desired NHC–CuO*t*-Bu: In an oven-dried vial (6 x 1 cm) equipped with a stir bar, imidazolinium tetrafluoroborate salt **4.77b** (24 mg, 0.036 mmol), NaO*t*-Bu (6.9 mg, 0.072 mmol), and CuCl (3.3 mg, 0.033 mmol) were placed and 2.5 mL of thf was added. The solution was allowed to stir for 2 hours at 22 °C under a dry $N_2$ atmosphere in a glovebox.

An appropriate portion of the solution of NHC–CuO*t*-Bu (0.0066 mmol in 0.50 mL thf) was placed in a separate oven-dried vial (6 x 1 cm), and the resulting solution was charged with $PhMe_2Si$–B(pin) (96 mg, 0.36 mmol). The vessel was removed from the glovebox, placed in a fume hood and cooled to –78 °C. A solution of (3*E*,5*E*)-6-phenylhexa-3,5-dien-2-one (**4.72a**) (57 mg, 0.33 mmol, in 0.50 mL thf) was added and the mixture was allowed to stir for 2 hours at –78 °C, after which the reaction was quenched by the addition of $H_2O$ (3 mL) and the mixture was allowed to warm to 22 °C and stir for an additional 15 minutes. The layers were separated, and the aqueous layer was washed with $Et_2O$ (10 mL x 3). The combined organic layers were dried over $MgSO_4$ and filtered. The volatiles were removed *in vacuo* and the resulting light yellow oil was purified by silica gel chromatography (hexanes/$Et_2O$:5/1) to afford 98 mg (0.32 mmol, 96% yield) of (*R*,*E*)-4-(dimethyl(phenyl)silyl)-6-phenylhex-5-en-2-one (**4.73a**), as colorless oil.

**(*R*,*E*)-4-(Dimethylphenylsilyl)-6-phenylhex-5-en-2-one (4.73a).** IR (neat): 3023 (w),

2973 (w), 2867 (w), 1711 (s), 1427 (m), 1381 (m), 1249 (m), 1113 (s) $cm^{-1}$; $^1H$ NMR (400 MHz, $CDCl_3$): δ 7.54–7.50 (2H, m), 7.44–7.36 (3H, m), 7.31–7.27 (4H, m), 7.22–7.16 (1H, m), 6.23 (1H, d, *J* = 16.0 Hz), 6.14–6.06 (1H, m), 2.65–2.47 (3H, m), 2.07 (3H, s), 0.37 (3H, s), 0.37 (3H, s); $^{13}C$ NMR (100 MHz, $CDCl_3$): δ 208.4, 137.9, 136.6, 134.1, 130.5, 129.5, 128.5, 128.4, 128.0, 126.7, 125.8, 43.4, 29.9, 29.2, –4.3, –5.0; HRMS ($ESI^+$) Calcd for $C_{20}H_{25}OSi$ [M+H]: 309.1675, Found: 309.1684. Optical rotation: $[a]_D^{20}$ +12.9 (*c* 2.14, $CHCl_3$) for a sample with >98:2 er. The absolute configuration was assigned by analogy to a previous report.[185] Enantiomeric purity was determined by HPLC analysis in comparison with authentic racemic material (>98:2 er shown below; chiralpak AS-H column (25 cm x 0.46 cm), 97/3 hexanes/*i*-PrOH, 0.3 mL/min, 220 nm).

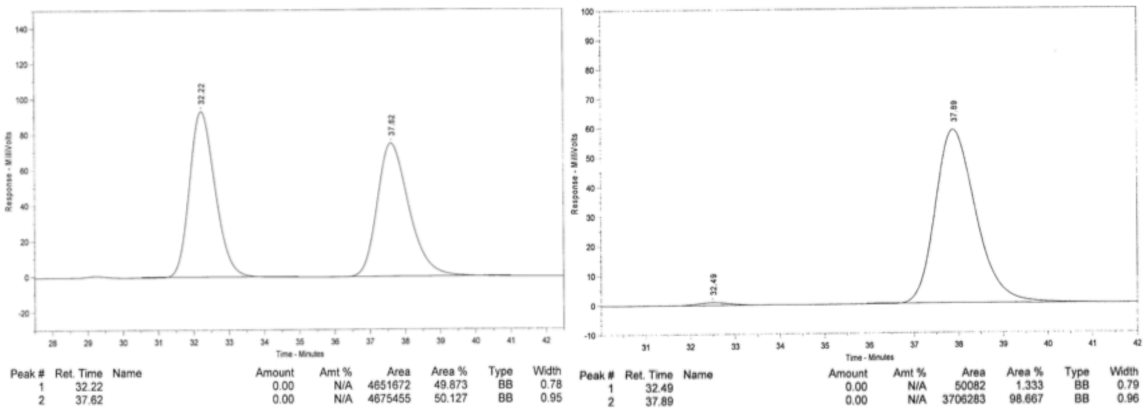


| Time (min) | Area | Area % | Time (min) | Area | Area % |
|---|---|---|---|---|---|
| 32.22 | 4651672 | 49.873 | 32.49 | 50082 | 1.333 |
| 37.62 | 4675455 | 50.127 | 37.89 | 3706283 | 98.667 |

**(*R*,*E*)-Methyl 3-(dimethylphenylsilyl)-5-phenylpent-4-enoate (4.73b).** IR (neat): 2952 (w), 1737 (s), 1428 (m), 1249 (s), 1161 (m), 1114 (m) $cm^{-1}$; $^1H$ NMR (400 MHz, $CDCl_3$): δ 7.52–7.49 (2H, m), 7.41–7.34 (3H, m), 7.30–7.23 (4H, m), 7.20–7.15 (1H, m), 6.23 (1H, d, *J* = 16.0 Hz), 6.12–6.06 (1H, m), 3.56 (3H, s), 2.50–2.42 (3H, m), 0.34 (6H, s);

(185) Lee, K-s.; Hoveyda, A. H. *J. Am. Chem. Soc.* **2010**, 132, 2898–2900.

$^{13}$C NMR (100 MHz, $CDCl_3$): δ 173.6, 138.0, 136.4, 134.0, 130.2, 129.4, 128.4, 128.3, 127.9, 126.6, 125.8, 51.5, 34.2, 29.9, –4.5, –5.3; HRMS ($ESI^+$) Calcd for $C_{20}H_{25}O_2Si$ [M+H]: 325.1624, Found: 325.1619. Optical rotation: $[a]_D^{20}$ +2.24 (*c* 1.51, $CHCl_3$) for a sample with 96:4 er. Enantiomeric purity was determined by HPLC analysis in comparison with authentic racemic material (96:4 er shown below; chiralcel OJ-H column (25 cm x 0.46 cm), 97/3 hexanes/*i*-PrOH, 0.2 mL/min, 220 nm).

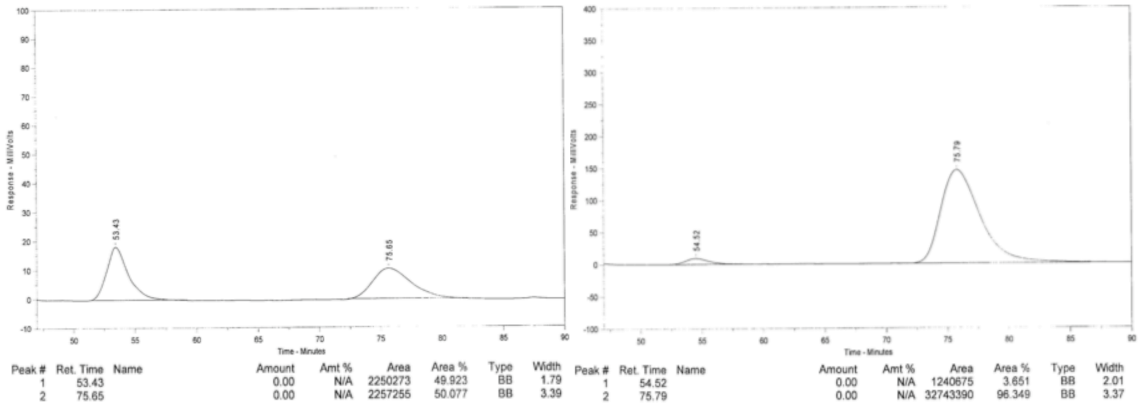


| Time (min) | Area | Area % | Time (min) | Area | Area % |
|---|---|---|---|---|---|
| 53.43 | 2250273 | 49.923 | 54.52 | 1240675 | 3.651 |
| 75.65 | 2257255 | 50.077 | 75.79 | 32743390 | 96.349 |

**(*R*,*E*)-*S*-Ethyl 3-(dimethyl(phenyl)silyl)-5-phenylpent-4-enethioate (4.73c).** IR (neat): 2958 (w), 2929 (w), 1686 (s), 1427 (w), 1413 (m), 1249 (m), 1113 (m) $cm^{-1}$; $^1$H NMR (400 MHz, $CDCl_3$): δ 7.51–7.48 (2H, m), 7.41–7.33 (3H, m), 7.29–7.24 (4H, m), 7.18–7.14 (1H, m), 6.21 (1H, dd, *J* = 15.6, 0.4 Hz), 6.04 (1H, dd, *J* = 15.6, 9.2 Hz), 2.84–2.75 (2H, m), 2.71–2.51 (3H, m), 1.15 (3H, t, *J* = 7.6 Hz), 0.34 (6H, s); $^{13}$C NMR (100 MHz, $CDCl_3$): δ 199.1, 138.0, 136.3, 134.0, 129.7, 129.4, 128.7, 128.4, 127.9, 126.6, 125.8, 43.6, 30.6, 23.4, 14.7, –4.4, –5.2; HRMS ($ESI^+$) Calcd for $C_{21}H_{27}OSSi$ [M+H]: 355.1552, Found: 355.1565. Optical rotation: $[a]_D^{20}$ –68.1 (*c* 1.54, $CHCl_3$) for a sample with >98:2 er. Enantiomeric purity was determined by HPLC analysis in comparison with authentic

racemic material (>98:2 er shown below; chiralcel OJ-H column (25 cm x 0.46 cm), 97/3 hexanes/*i*-PrOH, 0.2 mL/min, 220 nm).

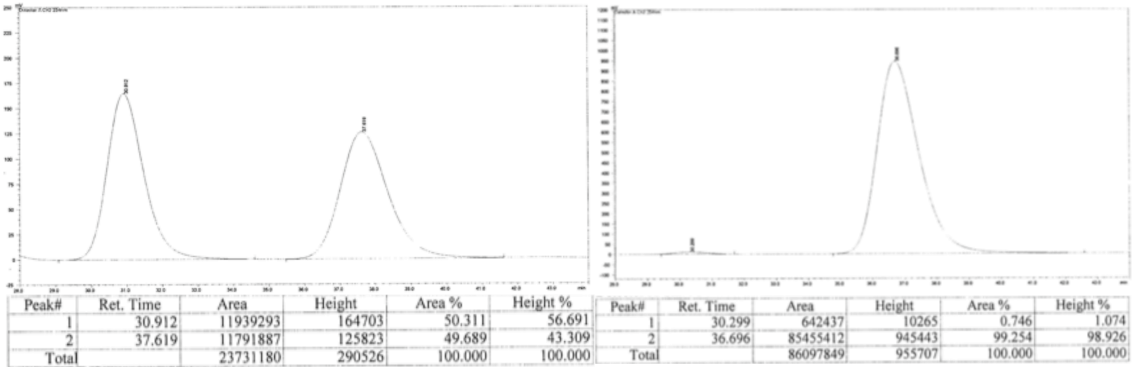

| Peak# | Ret. Time | Area | Height | Area % | Height % |
|---|---|---|---|---|---|
| 1 | 30.912 | 11939293 | 164703 | 50.311 | 56.691 |
| 2 | 37.619 | 11791887 | 125823 | 49.689 | 43.309 |
| Total | | 23731180 | 290526 | 100.000 | 100.000 |

| Peak# | Ret. Time | Area | Height | Area % | Height % |
|---|---|---|---|---|---|
| 1 | 30.299 | 642437 | 10265 | 0.746 | 1.074 |
| 2 | 36.696 | 85455412 | 945443 | 99.254 | 98.926 |
| Total | | 86097849 | 955707 | 100.000 | 100.000 |

| Time (min) | Area | Area % | Time (min) | Area | Area % |
|---|---|---|---|---|---|
| 30.912 | 11939293 | 50.311 | 30.299 | 642437 | 0.746 |
| 37.619 | 11791887 | 49.689 | 36.696 | 85455412 | 99.254 |

**(*R*,*E*)-4-(Dimethylphenylsilyl)hept-5-en-2-one (4.73d).** IR (neat): 3014 (w), 2957 (w), 2917 (w), 1709 (s), 1427 (m), 1355 (m), 1248 (s), 1167 (m), 1112 (s) $cm^{-1}$; $^{1}H$ NMR (400 MHz, $CDCl_3$): δ 7.47–7.44 (2H, m), 7.36–7.32 (3H, m), 5.28–5.21 (2H, m), 2.43–2.17 (3H, m), 2.01 (3H, s), 1.61 (3H, d, $J$ = 4.0 Hz), 0.26 (6H, s); $^{13}C$ NMR (100 MHz, $CDCl_3$): δ 209.2, 137.2, 134.1, 130.2, 129.3, 127.9, 123.9, 43.6, 29.9, 28.2, 18.2, –4.3, –5.2; HRMS ($ESI^+$) Calcd for $C_{15}H_{23}OSi$ [M+H]: 247.1518, Found: 247.1521. Optical rotation: $[a]_D^{20}$ +28.5 (*c* 1.74, $CHCl_3$) for a sample with 98:2 er. Enantiomeric purity was determined by HPLC analysis in comparison with authentic racemic material (98:2 er shown below; chiralpak AS-H column (25 cm x 0.46 cm), 97/3 hexanes/*i*-PrOH, 0.3 mL/min, 220 nm).

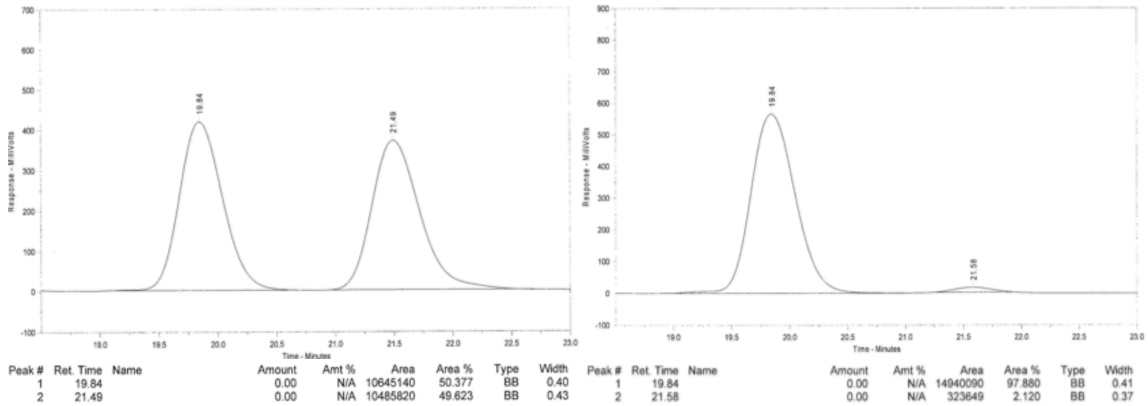


| Time (min) | Area | Area % | Time (min) | Area | Area % |
|---|---|---|---|---|---|
| 19.84 | 10645140 | 50.377 | 19.84 | 14940090 | 97.880 |
| 21.49 | 10485820 | 49.623 | 21.58 | 323649 | 2.120 |

**(*R*,*E*)-4-(Dimethylphenylsilyl)-6-phenylhept-5-en-2-one (4.73e).** IR (neat): 2955 (w), 2918 (w), 1710 (s), 1493 (m), 1444 (m), 1427 (m), 1355 (m), 1249 (s), 1165 (m), 1114 (m), 1111(s) $cm^{-1}$; $^{1}H$ NMR (400 MHz, $CDCl_3$): δ 7.54–7.51 (2H, m), 7.41–7.34 (3H, m), 7.31–7.26 (4H, m), 7.23–7.18 (1H, m), 5.49 (1H, dq, *J* = 11.2, 1.2 Hz), 2.75–2.66 (1H, m), 2.52–2.43 (2H, m), 2.04 (3H, s), 1.92 (3H, d, *J* = 1.6 Hz), 0.36 (3H, s), 0.34 (3H, s); $^{13}C$ NMR (100 MHz, $CDCl_3$): δ 208.8, 144.0, 136.8, 134.0, 133.9, 129.3, 128.3, 128.1, 127.8, 126.4, 125.6, 44.4, 29.7, 26.2, 16.3, –4.4, –5.1; HRMS ($ESI^+$) Calcd for $C_{21}H_{27}OSi$ [M+H]: 323.1831, Found: 323.1829. Optical rotation: $[a]_D^{20}$ +57.0 (*c* 1.94, $CHCl_3$) for a sample with 97.5:2.5 er. Enantiomeric purity was determined by HPLC analysis in comparison with authentic racemic material (97.5:2.5 er shown below; chiralpak AS-H column (25 cm x 0.46 cm), 97/3 hexanes/*i*-PrOH, 0.3 mL/min, 220 nm).

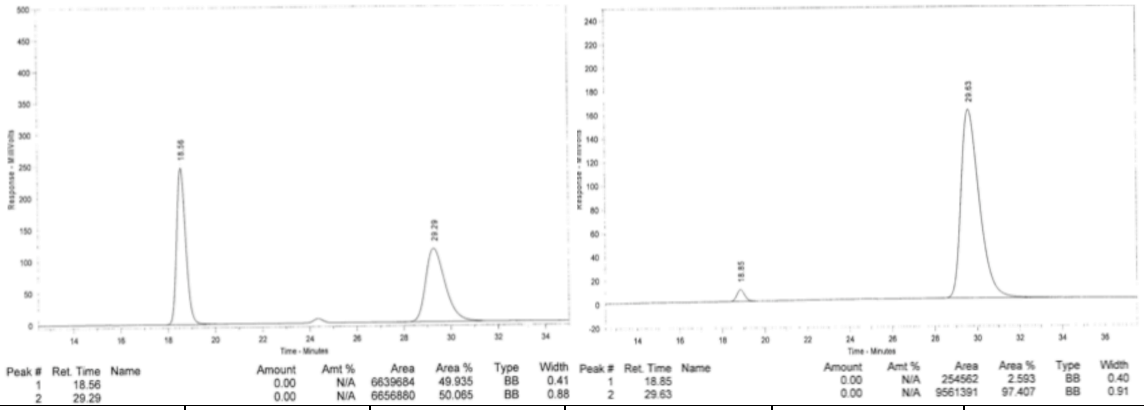


| Time (min) | Area | Area % | Time (min) | Area | Area % |
|---|---|---|---|---|---|
| 18.56 | 6639684 | 49.935 | 18.85 | 254562 | 2.593 |
| 29.29 | 6656880 | 50.065 | 29.63 | 9561391 | 97.407 |

**(*R*,*Z*)-6-(Dimethylphenylsilyl)-4-methyl-6-phenylhex-4-en-2-one (4.81a).** IR (neat): 2960 (m), 2915 (m), 1708 (s), 1248 (m), 1113 (m) $cm^{-1}$; $^1H$ NMR (400 MHz, $CDCl_3$): δ 7.36–7.27 (5H, m), 7.17 (2H, dd, *J* = 6.8, 6.4 Hz), 7.06 (1H, dd, *J* = 7.6, 7.2 Hz), 6.94–6.92 (2H, m), 5.77 (1H, d, *J* = 10.8 Hz), 3.22 (1H, d, *J* = 11.2 Hz), 3.04 (1H, d, *J* = 14.8 Hz), 2.71 (1H, d, *J* = 14.8 Hz), 1.87 (3H, s), 1.74 (3H, s), 0.25 (3H, s), 0.20 (3H, s); $^{13}C$ NMR (100 MHz, $CDCl_3$): δ 206.9, 142.0, 136.7, 134.2, 129.2, 128.2, 127.7, 127.6, 127.5, 127.3, 124.7, 47.4, 38.1, 28.8, 24.3, –4.4, –5.0; HRMS ($ESI^+$) Calcd for $C_{21}H_{27}OSi$ [M+H]: 323.1831, Found: 323.1830. Optical rotation: $[a]_D^{20}$ +90.0 (*c* 1.50, $CHCl_3$) for a sample with >98:2 er. Enantiomeric purity was determined by HPLC analysis in comparison with authentic racemic material (>98:2 er shown below; chiralpak AS-H column (25 cm x 0.46 cm), 99/1 hexanes/*i*-PrOH, 0.3 mL/min, 220 nm).

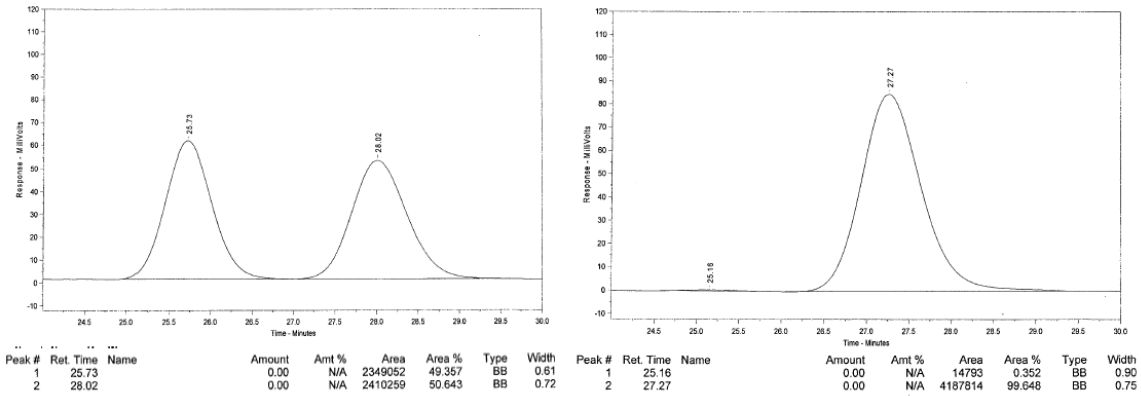


| Time (min) | Area | Area % | Time (min) | Area | Area % |
|---|---|---|---|---|---|
| 25.73 | 2349052 | 49.357 | 25.16 | 14793 | 0.352 |
| 28.02 | 2410259 | 50.643 | 27.27 | 4187814 | 99.648 |

**(*R*,*Z*)-6-(Dimethylphenylsilyl)-6-(4-methoxyphenyl)-4-methylhex-4-en-2-one (4.81b).** IR (neat): 2956 (m), 1708 (s), 1508 (s), 1244 (s) 1178 (m), 1112 (m), 1035 (m) $cm^{-1}$; $^1H$ NMR (400 MHz, $CDCl_3$): δ 7.34–7.27 (5H, m), 6.83 (2H, d, $J$ = 8.4 Hz), 6.72 (2H, d, $J$ = 8.4), 5.71 (1H, d, $J$ = 11.2 Hz), 3.74 (3H, s), 3.16 (1H, d, $J$ = 11.6), 3.03 (1H, d, $J$ = 14.8 Hz), 2.70 (1H, d, $J$ = 15.2 Hz), 1.88 (3H, s), 1.72 (3H, s), 0.23 (3H, s), 0.19 (3H, s); $^{13}C$ NMR (100 MHz, $CDCl_3$): δ 207.0, 156.9, 136.9, 134.3, 134.0, 129.2, 128.1, 128.0, 127.9, 127.5, 113.7, 55.2, 47.4, 36.9, 28.8, 24.3, –4.4, –5.0; HRMS ($ESI^+$) Calcd for $C_{22}H_{29}SiO_2$ [M+H]: 353.1937, Found: 353.1934. Optical rotation: $[a]_D^{20}$ +63.4 (*c* 1.76, $CHCl_3$) for a sample with >98:2 er. Enantiomeric purity was determined by HPLC analysis in comparison with authentic racemic material (>98:2 er shown below; chiralcel OD-H column (25 cm x 0.46 cm), 99.5/0.5 hexanes/*i*-PrOH, 0.3 mL/min, 220 nm).

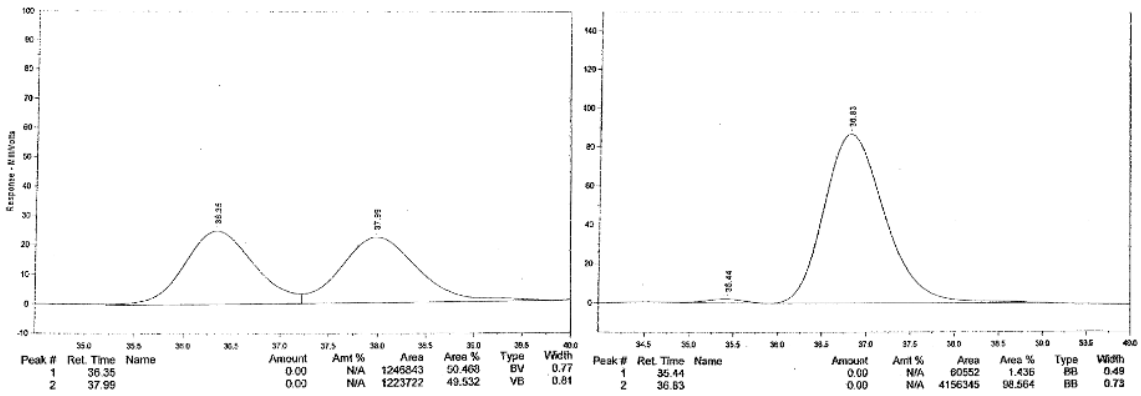


| Time (min) | Area | Area % | Time (min) | Area | Area % |
|---|---|---|---|---|---|
| 36.35 | 1246843 | 50.468 | 35.44 | 60552 | 1.436 |
| 37.99 | 1223722 | 49.532 | 36.83 | 4156345 | 98.564 |

**(*R*,*Z*)-6-(Dimethylphenylsilyl)-4-methyl-6-[4-(trifluoromethyl)phenyl]hex-4-en-2-one (4.81c).** IR (neat): 2960 (m), 2920 (m), 1710 (s), 1615 (m), 1356 (s), 1185 (m), 1110 (s), 1066 (s) $cm^{-1}$; $^1H$ NMR (400 MHz, $CDCl_3$): δ 7.40 (2H, d, *J* = 8.4 Hz), 7.37–7.33 (1H, m), 7.32–7.29 (4H, m), 6.99 (2H, d, *J* = 8.4 Hz), 5.74 (1H, dt, *J* = 11.6, 0.8 Hz), 3.292 (1H, d, *J* = 11.2 Hz), 3.03 (1H, d, *J* = 14.8 Hz), 2.76 (1H, d, *J* = 15.2 Hz), 1.90 (3H, s), 1.76 (3H, s), 0.25 (3H, s), 0.22 (3H, s); $^{13}C$ NMR (100 MHz, $CDCl_3$): δ 206.3, 146.6, 135.9, 134.2, 129.5, 128.8, 127.7, 127.4, 126.5, 125.0, 47.3, 38.4, 29.0, 24.5, –4.7, –5.0; HRMS ($ESI^+$) Calcd for $C_{22}H_{26}F_3SiO$ [M+H]: 391.1705, Found: 391.1705. Optical rotation: $[a]_D^{20}$ +53.0 (*c* 1.35, $CHCl_3$) for a sample with >98:2 er. Enantiomeric purity was determined by HPLC analysis in comparison with authentic racemic material (>98:2 er shown below; chiralcel OD-H column (25 cm x 0.46 cm), 99.5/0.5 hexanes/*i*-PrOH, 0.3 mL/min, 220 nm).

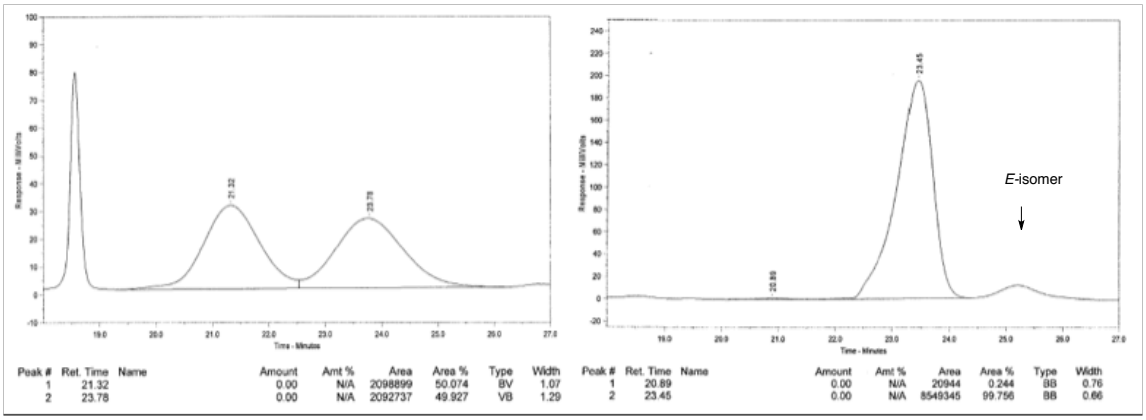


| Time (min) | Area | Area % | Time (min) | Area | Area % |
|---|---|---|---|---|---|
| 21.32 | 2098899 | 50.074 | 20.89 | 20944 | 0.244 |
| 23.78 | 2092737 | 49.927 | 23.45 | 8549345 | 99.756 |

**(*S*,*Z*)-6-(Dimethylphenylsilyl)-4-methylnon-4-en-2-one (4.81d).** IR (neat): 2956 (m), 2925 (m), 1712 (s), 1427 (m), 1355 (m), 1247 (s), 1157 (m), 1112 (s) $cm^{-1}$; $^1H$ NMR (400 MHz, $CDCl_3$): δ 7.48–7.43 (2H, m), 7.36–7.29 (3H, m), 5.10 (1H, dd, *J* = 11.2, 1.2 Hz), 3.01 (1H, d, *J* = 15.2 Hz), 2.62 (1H, d, *J* = 15.2 Hz), 2.00 (3H, s), 1.85–1.79 (1H, m), 1.69 (3H, s), 1.46–1.33 (2H, m), 1.28–1.22 (1H, m), 1.09–1.05 (1H, m), 0.82–0.78 (3H, m), 0.26 (3H, s), 0.22 (3H, s); $^{13}C$ NMR (100 MHz, $CDCl_3$): δ 207.3, 137.8, 134.0, 130.8, 128.9, 127.6, 126.5, 55.4, 47.6, 32.3, 29.1, 24.0, 22.9, 14.0, –4.6, –5.0; HRMS ($ESI^+$) Calcd for $C_{18}H_{29}SiO$ [M+H]: 289.1988, Found: 289.1986. Optical rotation: $[a]_D^{20}$ +119.8 (*c* 1.47, $CHCl_3$) for a sample with >98:2 er. Enantiomeric purity was determined by HPLC analysis in comparison with authentic racemic material (>98:2 er shown below; chiralcel OD-H column (25 cm x 0.46 cm), 99.9/0.1 hexanes/*i*-PrOH, 0.3 mL/min, 220 nm).

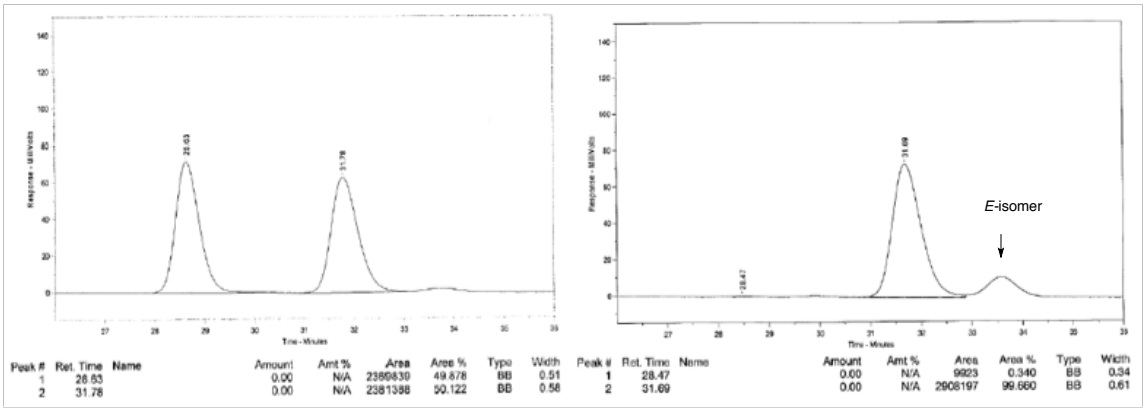


| Time (min) | Area | Area % | Time (min) | Area | Area % |
|---|---|---|---|---|---|
| 28.63 | 2369839 | 49.878 | 28.47 | 9923 | 0.340 |
| 31.78 | 2381388 | 50.122 | 31.69 | 2908197 | 99.660 |

**(*S*,*Z*)-6-Cyclohexyl-6-(dimethylphenylsilyl)-4-methylhex-4-en-2-one (4.81e).** IR (neat): 2921 (s), 2850 (m), 1713 (s), 1448 (m), 1427 (m), 1354 (m), 1247 (s), 1156 (m), 1110 (s) $cm^{-1}$; $^1H$ NMR (400 MHz, $CDCl_3$): δ 7.47–7.42 (2H, m), 7.34–7.27 (3H, m), 5.30 (1H, dd, $J$ = 12.0, 1.2 Hz), 2.96 (1H, d, $J$ = 15.2 Hz), 2.56 (1H, d, $J$ = 15.2 Hz), 1.98 (3H, s), 1.82–1.77 (1H, m), 1.69 (3H, s), 1.65–1.43 (7H, m), 1.20–0.91 (4H, m), 0.30 (3H, s), 0.24 (3H, s); $^{13}C$ NMR (100 MHz, $CDCl_3$): δ 207.4, 139.0, 133.9, 128.8, 128.3, 127.5, 126.9, 47.3, 39.6, 36.1, 34.4, 31.6, 29.1, 26.8, 26.7, 26.2, 24.1, –3.0, –3.3; HRMS ($ESI^+$) Calcd for $C_{21}H_{33}SiO$ [M+H]: 329.2301, Found: 329.2305. Optical rotation: $[a]_D^{20}$ +72.6 (*c* 1.54, $CHCl_3$) for a sample with >98:2 er. Enantiomeric purity was determined by HPLC analysis in comparison with authentic racemic material (>98:2 er shown below; chiralcel OD-H column (25 cm x 0.46 cm), 99.9/0.1 hexanes/*i*-PrOH, 0.3 mL/min, 220 nm).

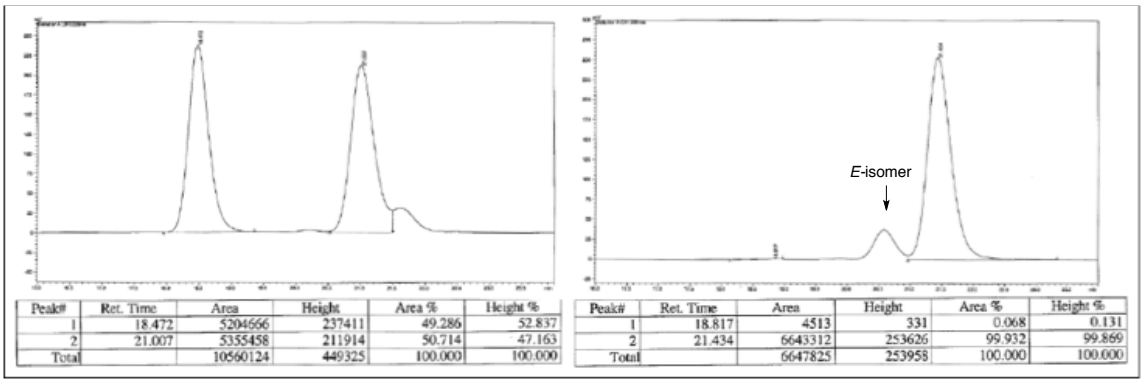


| Peak# | Ret. Time | Area | Height | Area % | Height % |
|---|---|---|---|---|---|
| 1 | 18.472 | 5204666 | 237411 | 49.286 | 52.837 |
| 2 | 21.007 | 5355458 | 211914 | 50.714 | 47.163 |
| Total | | 10560124 | 449325 | 100.000 | 100.000 |

| Peak# | Ret. Time | Area | Height | Area % | Height % |
|---|---|---|---|---|---|
| 1 | 18.817 | 4513 | 331 | 0.068 | 0.131 |
| 2 | 21.434 | 6643312 | 253626 | 99.932 | 99.869 |
| Total | | 6647825 | 253958 | 100.000 | 100.000 |

| Time (min) | Area | Area % | Time (min) | Area | Area % |
|---|---|---|---|---|---|
| 18.47 | 5204666 | 49.286 | 18.82 | 4513 | 0.068 |
| 21.01 | 5355458 | 50.714 | 21.43 | 6643312 | 99.932 |

**(*R*,*Z*)-Methyl-5-(dimethylphenylsilyl)-3-methyl-5-phenylpent-3-enoate (4.81f).** IR (neat): 2953 (m), 2919 (m), 1736 (s), 1428 (m), 1248 (s), 1152 (s), 1114 (s), 1017 (m) $cm^{-1}$; $^1H$ NMR (400 MHz, $CDCl_3$): δ 7.36–7.26 (5H, m), 7.17–7.13 (2H, m), 7.07–7.03 (1H, m), 6.91 (2H, d, $J$ = 8.0 Hz), 5.71 (1H, d, $J$ = 11.2 Hz), 3.56 (3H, s), 3.30 (1H, d, $J$ = 11.2 Hz), 2.88 (1H, d, $J$ = 14.8 Hz), 2.82 (1H, d, $J$ = 14.8 Hz), 1.81 (3H, s), 0.23 (3H, s), 0.21 (3H, s); $^{13}C$ NMR (100 MHz, $CDCl_3$): δ 171.7, 142.1, 136.8, 134.3, 129.1, 128.1, 127.4, 127.4, 126.9, 124.6, 51.6, 37.9, 37.4, 24.3, –4.5, –4.8; HRMS ($ESI^+$) Calcd for $C_{21}H_{27}SiO_2$ [M+H]: 339.1780, Found: 339.1777. Optical rotation: $[a]_D^{20}$ -3.7 (*c* 1.35, $CHCl_3$) for a sample with >98:2 er. Enantiomeric purity was determined by HPLC analysis in comparison with authentic racemic material (>98:2 er shown below; chiralcel OJ-H column (25 cm x 0.46 cm), 98.5/1.5 hexanes/*i*-PrOH, 0.3 mL/min, 220 nm).

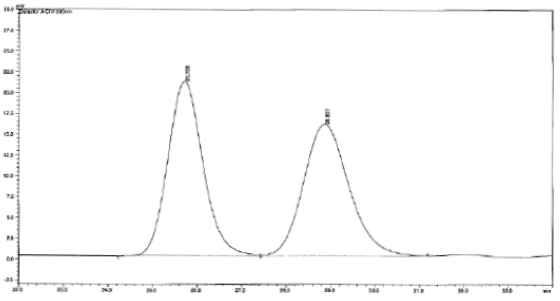

Detector A Ch1 220nm

| Peak# | Ret. Time | Area | Height | Area % | Height % |
|---|---|---|---|---|---|
| 1 | 25.709 | 1149186 | 20951 | 50.588 | 57.028 |
| 2 | 28.857 | 1122471 | 15787 | 49.412 | 42.972 |
| Total | | 2271657 | 36737 | 100.000 | 100.000 |

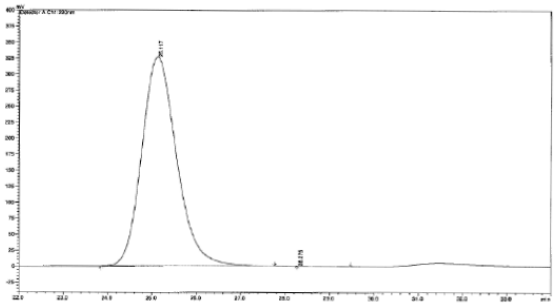

Detector A Ch1 220nm

| Peak# | Ret. Time | Area | Height | Area % | Height % |
|---|---|---|---|---|---|
| 1 | 25.117 | 17794235 | 326667 | 100.021 | 100.000 |
| 2 | 28.275 | -3785 | -0 | -0.021 | -0.000 |
| Total | | 17790450 | 326667 | 100.000 | 100.000 |

| Time (min) | Area | Area % | Time (min) | Area | Area % |
|---|---|---|---|---|---|
| 25.709 | 1149186 | 50.588 | 25.117 | 17794235 | 100.021 |
| 28.857 | 1122471 | 49.412 | 28.275 | –3785 | –0.021 |

**(*R*,*Z*)-*S*-Ethyl-5-(dimethylphenylsilyl)-3-methyl-5-phenylpent-3-enethioate (4.81g).** IR (neat): 2962 (m), 2928 (m), 1687 (s), 1596 (m), 1492 (m), 1459 (m), 1427 (m), 1377 (m), 1249 (s), 1113 (s), 1069 (s) $cm^{-1}$; $^{1}H$ NMR (400 MHz, $CDCl_3$): δ 7.40–7.31 (5H, m), 7.21–7.18 (2H, m), 7.11–7.08 (1H, m), 6.98–6.96 (2H, m), 5.79 (1H, d, *J* = 8.8 Hz), 3.37 (1H, d, *J* = 8.8 Hz), 3.13 (1H, d, *J* = 11.6 Hz), 2.97 (1H, d, *J* = 12.0 Hz), 2.83 (2H, q, *J* = 6.0 Hz), 1.84 (3H, s), 1.22 (3H, t, *J* = 6.0 Hz), 0.29 (3H, s), 0.26 (3H, s); $^{13}C$ NMR (100 MHz, $CDCl_3$): δ 197.1, 142.0, 136.8, 134.3, 129.2, 128.5, 128.1, 127.5, 127.0, 124.6, 46.9, 38.2, 24.3, 23.4, 14.7, –4.4; HRMS ($ESI^+$) Calcd for $C_{22}H_{29}SiOS$ [M+H]: 369.1708, Found: 369.1697. Optical rotation: $[a]_D^{20}$ +43.0 (*c* 1.01, $CHCl_3$) for a sample with >98:2 er. Enantiomeric purity was determined by HPLC analysis in comparison with authentic racemic material (>98:2 er shown below; chiralcel OJ-H column (25 cm x 0.46 cm), 99.5/0.5 hexanes/*i*-PrOH, 0.3 mL/min, 220 nm).

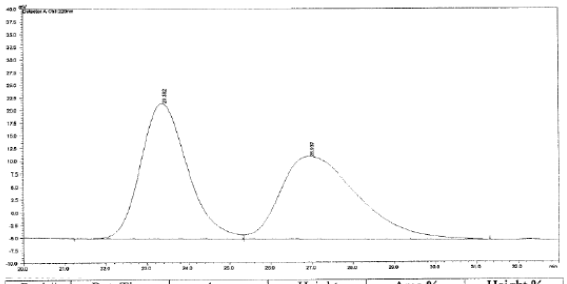

| Peak# | Ret. Time | Area | Height | Area % | Height % |
|---|---|---|---|---|---|
| 1 | 23.362 | 2086533 | 26530 | 49.841 | 62.309 |
| 2 | 26.937 | 2099827 | 16048 | 50.159 | 37.691 |
| Total | | 4186360 | 42578 | 100.000 | 100.000 |

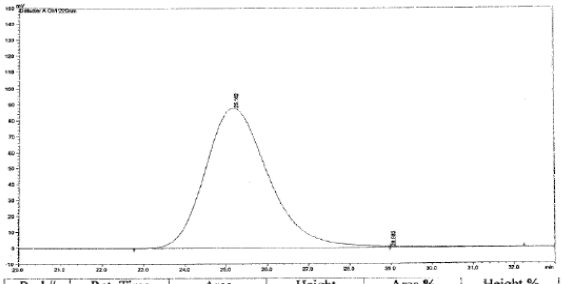

| Peak# | Ret. Time | Area | Height | Area % | Height % |
|---|---|---|---|---|---|
| 1 | 25.162 | 9431650 | 88068 | 99.343 | 99.144 |
| 2 | 28.983 | 62368 | 760 | 0.657 | 0.856 |
| Total | | 9494018 | 88828 | 100.000 | 100.000 |

| Time (min) | Area | Area % | Time (min) | Area | Area % |
|---|---|---|---|---|---|
| 23.362 | 2086533 | 49.841 | 25.16 | 9431650 | 99.343 |
| 26.937 | 2099827 | 50.159 | 28.98 | 62368 | 0.657 |

**(*R*,*Z*)-3-{2-[Dimethyl(phenyl)silyl]-2-phenylethylidene}cyclopentanone (4.93a).** IR (neat): 2956 (m), 2919 (m), 2850 (m), 1746 (s), 1249 (m), 1113 (m) $cm^{-1}$; $^1H$ NMR (400 MHz, $CDCl_3$): δ 7.39–7.19 (7H, m), 7.09 (1H, dd, *J* = 7.2, 7.2 Hz), 6.99–6.98 (2H, m), 5.86 (1H, dt, *J* = 11.2, 2.0 Hz), 3.06 (1H, d, *J* = 11.2 Hz), 2.67–2.61 (2H, m), 2.32–2.04 (4H, m), 0.27 (3H, s), 0.21 (3H, s); $^{13}C$ NMR (100 MHz, $CDCl_3$): δ 217.9, 142.3, 137.5, 134.8, 133.8, 130.0, 129.0, 128.3, 127.8, 125.5, 123.9, 41.7, 40.7, 39.8, 31.4, –3.7, –4.8; HRMS ($ESI^+$) Calcd for $C_{21}H_{25}OSi$ [M+H]: 321.1675, Found: 321.1663. Optical rotation: $[a]_D^{20}$ –20.5 (*c* 2.03, $CHCl_3$) for a sample with 95:5 er. Enantiomeric purity was determined by HPLC analysis in comparison with authentic racemic material (95:5 er shown below; chiralcel OJ-H column (25 cm x 0.46 cm), 97/3 hexanes/*i*-PrOH, 0.3 mL/min, 220 nm).

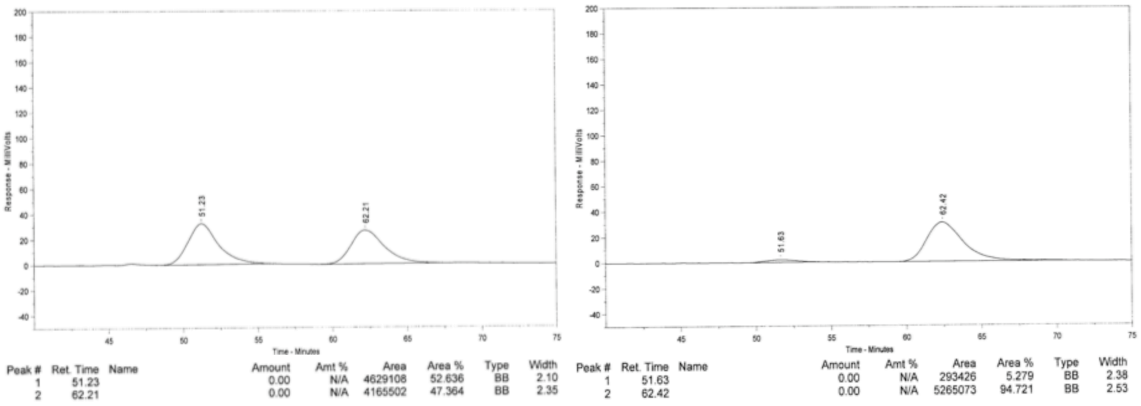


| Time (min) | Area | Area % | Time (min) | Area | Area % |
|---|---|---|---|---|---|
| 51.23 | 4629108 | 52.636 | 51.63 | 293426 | 5.279 |
| 62.21 | 4165502 | 47.364 | 62.42 | 5265073 | 94.721 |

**(*R*,*Z*)-3-[2-(Dimethylphenylsilyl)-2-phenylethylidene]cyclohexanone (4.93b).** IR (neat): 3023 (m), 2956 (m), 1714 (s), 1248 (m) $cm^{-1}$; $^1H$ NMR (400 MHz, $CDCl_3$): δ 7.36–7.26 (5H, m), 7.18 (2H, t, *J* = 8.0 Hz), 7.07 (1H, t, *J* = 7.4 Hz), 6.97–6.93 (2H, m), 5.67 (1H, d, *J* = 11.6 Hz), 3.25 (1H, d, *J* = 11.6 Hz), 2.94 (1H, d, *J* = 16.4 Hz), 2.69 (1H, dd, *J* = 16.4, 1.6 Hz), 2.38–2.26 (4H, m), 1.80–1.65 (2H, m), 0.22 (3H, s), 0.19 (3H, s); $^{13}C$ NMR (100 MHz, $CDCl_3$): δ 209.3, 142.4, 137.3, 134.9, 132.2, 129.9, 128.9, 128.2, 127.9, 125.4, 124.7, 46.0, 42.0, 38.0, 35.8, 25.6, –3.7, –4.5; HRMS ($ES^+$) Calcd for $C_{22}H_{26}SiONa$ [M+Na]: 357.1651, Found: 357.1645. Optical rotation: $[a]_D^{20}$ –5.90 (*c* 1.81, $CHCl_3$) for a sample with 98:2 er. Enantiomeric purity was determined by HPLC analysis in comparison with authentic racemic material (98:2 er shown below; chiralpak AD-H column (25 cm x 0.46 cm), 95/5 hexanes/*i*-PrOH, 0.3 mL/min, 220 nm).

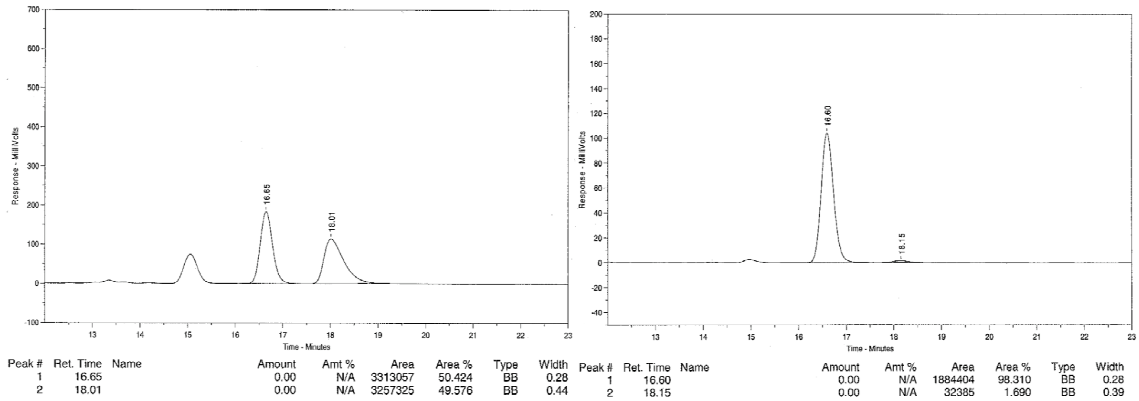


Peak # Ret. Time Name Amount Amt % Area Area % Type Width
1 16.65 0.00 N/A 3313057 50.424 BB 0.28
2 18.01 0.00 N/A 3257325 49.576 BB 0.44

Peak # Ret. Time Name Amount Amt % Area Area % Type Width
1 16.60 0.00 N/A 1884404 98.310 BB 0.28
2 18.15 0.00 N/A 32385 1.690 BB 0.39

| Time (min) | Area | Area % | Time (min) | Area | Area % |
|---|---|---|---|---|---|
| 16.65 | 3313057 | 50.424 | 16.60 | 1884404 | 98.310 |
| 18.01 | 3257325 | 49.576 | 18.15 | 32385 | 1.690 |

**(*R*,*Z*)-3-[2-(Dimethylphenylsilyl)-2-*p*-tolylethylidene]cyclohexanone (4.93c).** IR (neat): 2955 (m), 2865 (w), 1713 (s), 1510 (s), 1427 (m), 1248 (s), 1113 (s), 1066 (m) $cm^{-1}$; $^1H$ NMR (400 MHz, $CDCl_3$): δ 7.36–7.24 (5H, m), 7.00 (2H, d, *J* = 8.0 Hz), 6.84 (2H, d, *J* = 8.0 Hz), 5.64 (1H, d, *J* = 11.6 Hz), 3.22 (1H, d, *J* = 11.6 Hz), 2.93 (1H, d, *J* = 16.0 Hz), 2.67 (1H, dd, *J* = 16.4, 1.2 Hz), 2.37–2.29 (4H, m), 2.27 (3H, s), 1.79–1.66 (2H, m), 0.22 (3H, s), 0.19 (3H, s); $^{13}C$ NMR (100 MHz, $CDCl_3$): δ 208.8, 138.8, 137.0, 134.4, 134.3, 131.4, 129.3, 129.1, 127.7, 127.3, 124.5, 45.5, 41.5, 36.9, 35.2, 25.0, 21.0, –4.2, –5.1; HRMS ($ESI^+$) Calcd for $C_{23}H_{29}OSi$ [M+H]: 349.1988, Found: 349.2001. Optical rotation: $[a]_D^{20}$ –14.6 (*c* 2.35, $CHCl_3$) for a sample with 95:5 er. Enantiomeric purity was determined by HPLC analysis in comparison with authentic racemic material (95.1:4.9 er shown below; chiralcel OD-H column (25 cm x 0.46 cm), 95/5 hexanes/*i*-PrOH, 0.2 mL/min, 220 nm).

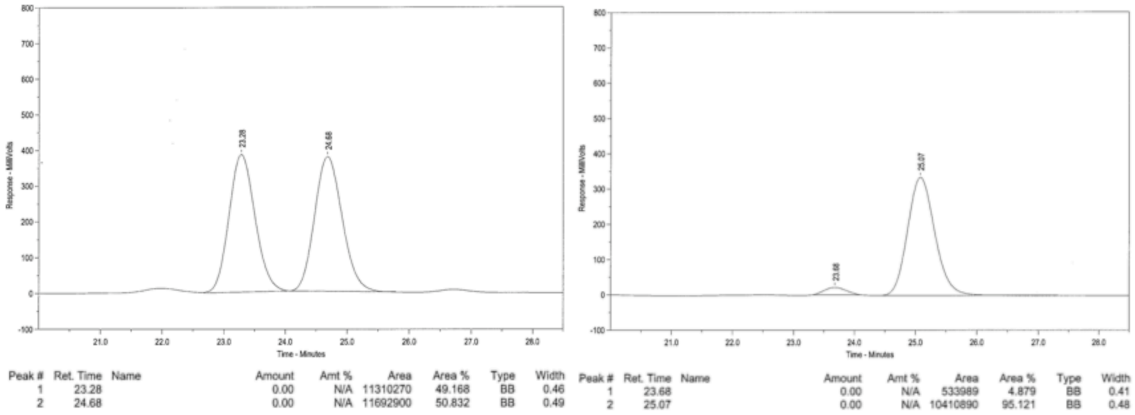


| Time (min) | Area | Area % | Time (min) | Area | Area % |
|---|---|---|---|---|---|
| 23.28 | 11310270 | 49.168 | 23.68 | 533989 | 4.879 |
| 24.68 | 11692900 | 50.832 | 25.07 | 10410890 | 95.121 |

**(*R*,*Z*)-3-[2-(Dimethylphenylsilyl)-2-(4-methoxyphenyl)ethylidene]cyclohexanone (4.93d).** IR (neat): 2954 (m), 2834 (w), 1713 (s), 1508 (s), 1427 (m), 1244 (s), 1180 (s) $cm^{-1}$; $^1H$ NMR (400 MHz, $CDCl_3$): δ 7.39–7.24 (5H, m), 6.85 (2H, d, *J* = 8.8 Hz), 6.74 (2H, d, *J* = 8.8 Hz), 5.61 (1H, d, *J* = 11.6 Hz), 3.75 (3H, s), 3.19 (1H, d, *J* = 12.0 Hz), 2.94 (1H, d, *J* = 16.4 Hz), 2.69 (1H, d, *J* = 16.0 Hz), 2.35–2.30 (4H, m), 1.78–1.66 (2H, m), 0.21 (3H, s), 0.18 (3H, s); $^{13}C$ NMR (100 MHz, $CDCl_3$): δ 208.8, 157.2, 137.0, 134.4, 133.9, 131.4, 129.3, 128.2, 127.7, 124.6, 113.9, 55.4, 45.5, 41.5, 36.2, 35.2, 25.1, –4.2, –5.0; HRMS ($ESI^+$) Calcd for $C_{23}H_{28}O_2Si$: 364.1859, Found: 364.1853. Optical rotation: $[a]_D^{20}$ –23.0 (*c* 3.00, $CHCl_3$) for a sample with 97:3 er. Enantiomeric purity was determined by HPLC analysis in comparison with authentic racemic material (97:3 er shown below; chiralcel OD-H column (25 cm x 0.46 cm), 97/3 hexanes/*i*-PrOH, 0.3 mL/min, 220 nm).

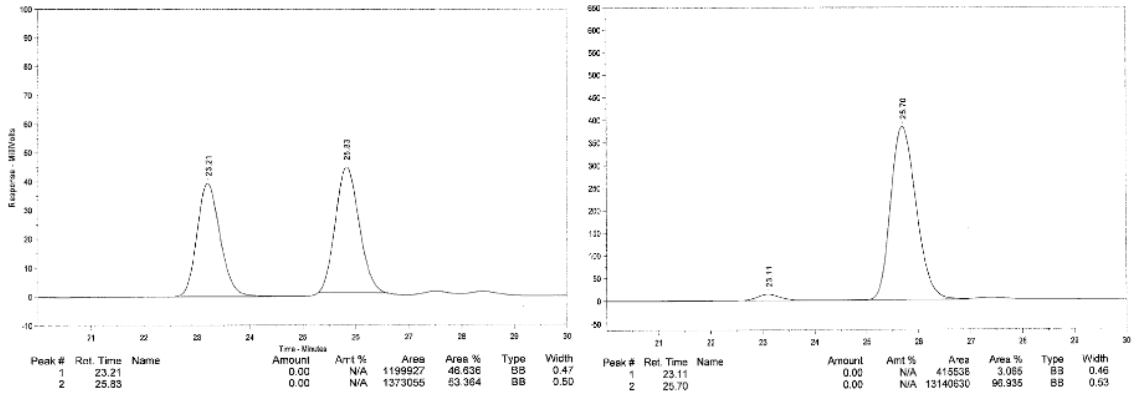


| Time (min) | Area | Area % | Time (min) | Area | Area % |
|---|---|---|---|---|---|
| 23.21 | 1199927 | 46.636 | 23.11 | 415538 | 3.065 |
| 25.83 | 1373055 | 53.364 | 25.70 | 13140630 | 96.935 |

**(*R*,*Z*)-3-[2-(Dimethylphenylsilyl)-2-(4-trifluoromethylphenyl)ethylidene]-cyclohexanone (4.93e).** IR (neat): 2957 (w), 1715 (s), 1615 (m), 1324 (s), 1251 (m), 1161 (s), 1112 (s), 1067 (s) $cm^{-1}$; $^1H$ NMR (400 MHz, $CDCl_3$): δ 7.42 (2H, d, *J* = 8.4 Hz), 7.38–7.24 (5H, m), 7.01 (2H, d, *J* = 8.4 Hz), 5.65 (1H, d, *J* = 11.6 Hz), 3.34 (1H, d, *J* = 11.6 Hz), 2.95 (1H, d, *J* = 16.0 Hz), 2.74 (1H, dd, *J* = 16.0, 1.2 Hz), 2.42–2.32 (4H, m), 1.80–1.70 (2H, m), 0.23 (3H, s), 0.22 (3H, s); $^{13}C$ NMR (100 MHz, $CDCl_3$): δ 208.5, 146.5, 136.1, 134.4, 133.3, 132.9, 129.8, 129.7, 128.1, 127.9, 127.6, 125.3 (1C, q, *J* = 4.0 Hz), 45.7, 41.6, 37.8, 35.3, 25.1, –4.4, –5.0; HRMS ($ESI^+$) Calcd for $C_{23}H_{25}F_3OSi$: 402.1627, Found: 402.1632. Optical rotation: $[a]_D^{20}$ –16.7 (*c* 2.67, $CHCl_3$) for a sample with 94.5:5.5 er. Enantiomeric purity was determined by HPLC analysis in comparison with authentic racemic material (94.5:5.5 er shown below; chiralcel OD-H column (25 cm x 0.46 cm), 97/3 hexanes/*i*-PrOH, 0.3 mL/min, 220 nm).

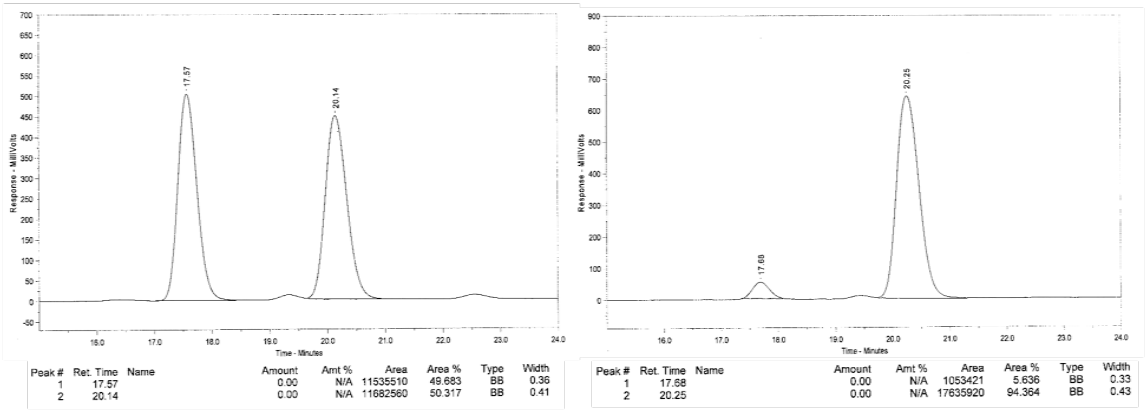


| Time (min) | Area | Area % | Time (min) | Area | Area % |
|---|---|---|---|---|---|
| 17.57 | 11535510 | 49.683 | 17.68 | 1053421 | 5.636 |
| 20.14 | 11682560 | 50.317 | 20.25 | 17635920 | 94.364 |

**(*S*,*Z*)-3-[2-Cyclohexyl-2-(dimethylphenylsilyl)ethylidene]cyclohexanone (4.93f).** IR (neat): 2922 (s), 2850 (m), 1716 (s), 1447 (m), 1427 (m), 1247 (m), 1110 (s), 1065 (m) $cm^{-1}$; $^1H$ NMR (400 MHz, $CDCl_3$): δ 7.44–7.40 (2H, m), 7.32–7.24 (3H, m), 5.17 (1H, d, *J* = 12.4 Hz), 2.93 (1H, d, *J* = 15.6 Hz), 2.66 (1H, d, *J* = 16.0 Hz), 2.38–2.19 (4H, m), 1.93–1.37 (9H, m), 1.24–0.86 (5H, m), 0.27 (3H, s), 0.23 (3H, s); $^{13}C$ NMR (100 MHz, $CDCl_3$): δ 209.7, 139.7, 134.5, 132.6, 129.4, 128.2, 125.6, 46.3, 42.2, 39.9, 35.9, 35.5, 34.8, 32.4, 27.3, 27.3, 26.9, 26.1, –2.4, –2.5; HRMS ($ESI^+$) Calcd for $C_{22}H_{32}OSi$: 340.2222, Found: 340.2213. Optical rotation: $[a]_D^{20}$ –0.857 (*c* 2.10, $CHCl_3$) for a sample with 98:2 er. Enantiomeric purity was determined by HPLC analysis in comparison with authentic racemic material (98:2 er shown below; chiralpak AD-H column (25 cm x 0.46 cm), 99.3/0.7 hexanes/*i*-PrOH, 0.2 mL/min, 220 nm).

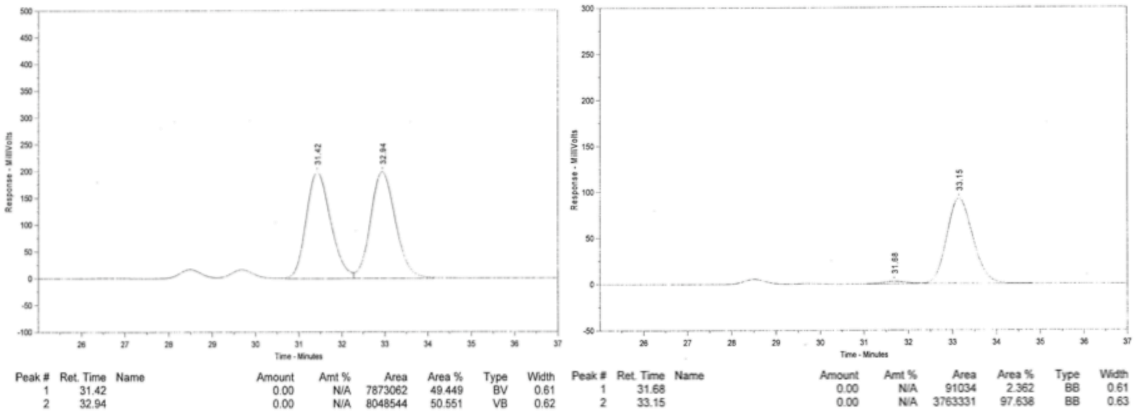


| Time (min) | Area | Area % | Time (min) | Area | Area % |
|---|---|---|---|---|---|
| 31.42 | 7873062 | 49.449 | 31.68 | 91034 | 2.362 |
| 32.94 | 8048544 | 50.551 | 33.15 | 3763331 | 97.638 |

**(*R*,*E*)-3-[2-(Dimethylphenylsilyl)-2-phenylethylidene]-4,4-dimethylcyclohexanone (4.93g).** IR (neat): 2959 (m), 1686 (s), 1253 (s) $cm^{-1}$; $^1H$ NMR (400 MHz, $CDCl_3$): δ 7.37–7.27 (5H, m), 7.19 (2H, t, *J* = 7.6 Hz), 7.08 (1H, t, *J* = 7.4 Hz), 6.95 (2H, d, *J* = 7.2 Hz), 5.69 (1H, d, *J* = 11.6 Hz), 3.16 (1H, d, *J* = 11.6 Hz), 3.04 (1H, d, *J* = 17.2 Hz), 2.73 (1H, dd, *J* = 17.2, 1.6 Hz), 2.33–2.27 (2H, m), 1.59 (2H, t, *J* = 6.8 Hz) 1.18 (3H, s), 1.15 (3H, s), 0.22 (3H, s), 0.19 (3H, s); $^{13}C$ NMR (100 MHz, $CDCl_3$): δ 210.5, 142.6, 138.0, 137.3, 134.9, 129.9, 128.9, 128.2, 127.9, 125.4, 122.7, 43.0, 38.2, 38.0, 38.0, 36.7, 28.5, 28.3, –3.7, –4.5; HRMS ($ES^+$) Calcd for $C_{24}H_{30}SiONa$ [M+Na]: 385.1964, Found: 385.1955. Optical rotation: $[a]_D^{20}$ +16.0 (*c* 1.30, $CHCl_3$) for a sample with 96:4 er. Enantiomeric purity was determined by HPLC analysis in comparison with authentic racemic material (96:4 er shown below; chiralpak AD-H column (25 cm x 0.46 cm), 99.3/0.7 hexanes/*i*-PrOH, 0.3 mL/min, 220 nm).

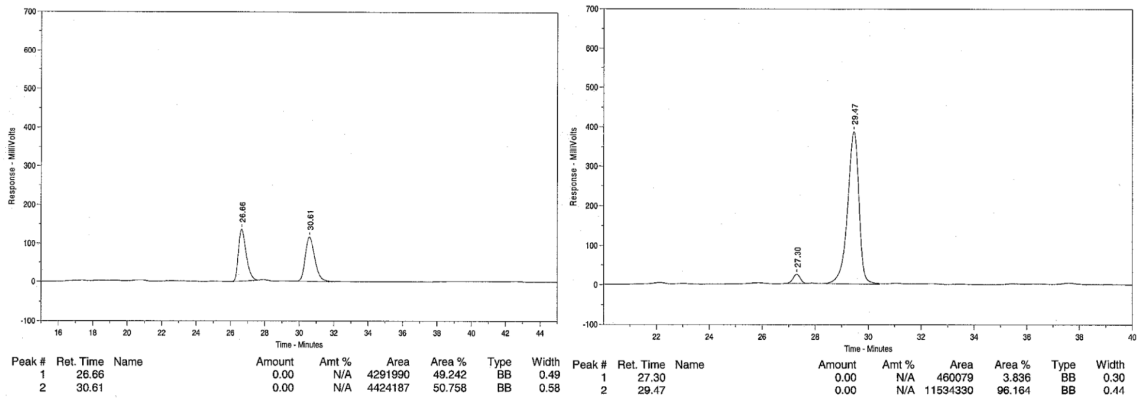


| Time (min) | Area | Area % | Time (min) | Area | Area % |
|---|---|---|---|---|---|
| 26.66 | 4291990 | 49.242 | 27.30 | 460079 | 3.836 |
| 30.61 | 4424187 | 50.758 | 29.47 | 11534330 | 96.164 |

**(*R*,*Z*)-3-[2-(Dimethylphenylsilyl)-2-phenylethylidene]cycloheptanone (4.93h).** IR (neat): 3023 (m), 2927 (m), 2856 (w), 1699 (s), 1248 (m), 1114 (m) $cm^{-1}$; $^1H$ NMR (400 MHz, $CDCl_3$): d 7.37–7.28 (5H, m), 7.20–7.16 (2H, m), 7.08–7.05 (1H, m), 6.96–6.93 (2H, m), 5.80 (1H, d, *J* = 11.6 Hz), 3.31 (1H, d, *J* = 11.6 Hz), 3.09–3.00 (2H, m), 2.33–2.17 (3H, m), 2.06–1.99 (1H, m), 1.78–1.53 (4H, m), 0.25 (3H, s), 0.21 (3H, s); $^{13}C$ NMR (100 MHz, $CDCl_3$): d 211.9, 142.7, 137.4, 135.0, 131.9, 129.9, 129.1, 128.8, 128.3, 128.0, 125.4, 47.6, 43.9, 40.9, 38.2, 32.1, 25.0, –3.6, –4.5; HRMS ($ESI^+$) Calcd for $C_{23}H_{28}OSi$: 348.1909, Found: 348.1895. Optical rotation: $[a]_D^{20}$ –8.01 (*c* 2.80, $CHCl_3$) for a sample with 96:4 er. Enantiomeric purity was determined by HPLC analysis in comparison with authentic racemic material (96:4 er shown below; chiralpak AD-H column (25 cm x 0.46 cm), 97/3 hexanes/*i*-PrOH, 0.3 mL/min, 220 nm).

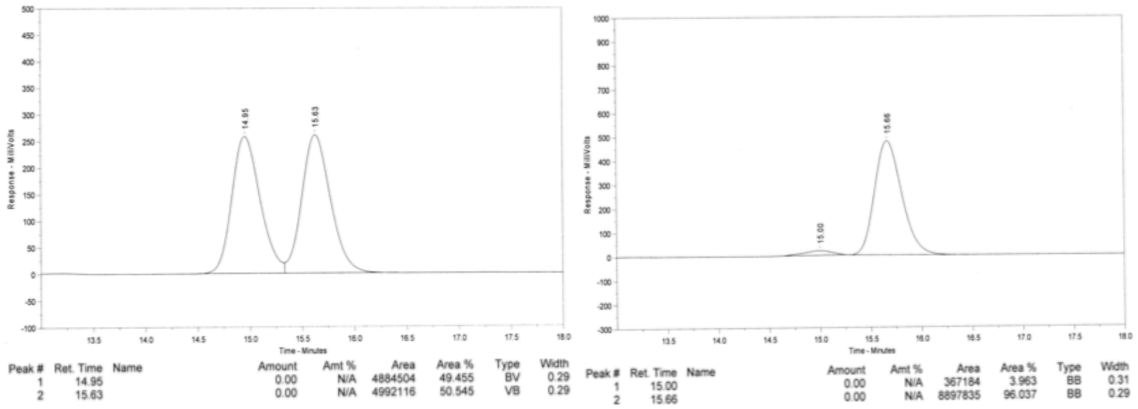


| Time (min) | Area | Area % | Time (min) | Area | Area % |
|---|---|---|---|---|---|
| 14.95 | 4884504 | 49.455 | 15.00 | 367184 | 3.963 |
| 15.63 | 4992116 | 50.545 | 15.66 | 8897835 | 96.037 |

**1-(2*R*,3*R*)-3-(*S*)-[(Dimethylphenylsilyl)(phenyl)methyl-2-methyloxiran-2-yl]-propan-2-one (4.96).** IR (neat): 2959 (m), 2925 (m), 1712 (s), 1428 (m), 1360 (m), 1251 (s), 1115 (s) $cm^{-1}$; $^1H$ NMR (400 MHz, $CDCl_3$): δ 7.45–7.37 (5H, m), 7.28–7.25 (2H, m), 7.17–7.14 (1H, m), 7.07–7.05 (2H, m), 3.28 (1H, d, *J* = 8.4 Hz), 2.30 (1H, d, *J* = 12.0 Hz), 2.25 (1H, d, *J* = 8.4 Hz), 2.09 (3H, s), 1.94 (1H, d, *J* = 12.0 Hz), 1.24 (3H, s), 0.34 (3H, s), 0.29 (3H, s); $^{13}C$ NMR (100 MHz, $CDCl_3$): δ 206.7, 139.5, 136.2, 134.0, 129.7, 128.3, 127.9, 127.7, 125.3, 64.2, 59.7, 47.3, 36.7, 30.5, 22.7, –4.2, –5.4; HRMS ($ESI^+$) Calcd for $C_{21}H_{25}OSi$ [M–OH]: 321.1675, Found: 321.1672. Optical rotation: $[a]_D^{20}$ +34.0 (*c* 0.43, $CHCl_3$)

**(*R*,*E*)-4-Hydroxy-4-methyl-6-phenylhex-5-en-2-one (4.97).** IR (neat): 3467 (w), 2924 (s), 2853 (m), 1723 (s), 1709 (s), 1448 (m), 1366 (m), 1287 (m), 1173 (m), 1122 (m), 1073 (m) $cm^{-1}$; $^1H$ NMR (400 MHz, $CDCl_3$): δ 7.36–7.33 (2H, m), 7.30–7.26 (2H, m), 7.22–7.18 (1H, m), 6.58 (1H, d, *J* = 16.0 Hz), 6.24 (1H, d, *J* = 16.0 Hz), 4.14 (1H, s), 2.85 (1H, d, *J* = 17.2 Hz), 2.70 (1H, d, *J* = 17.2 Hz), 2.16 (3H, s), 1.38 (3H, s); $^{13}C$ NMR (100 MHz, $CDCl_3$): δ 210.4, 136.9, 135.2, 128.7, 127.9, 127.7, 126.6, 71.9, 53.2, 32.0,

28.6; HRMS (ESI$^+$) Calcd for $C_{13}H_{15}O$ [M–H]: 187.1123, Found: 187.1127. Optical rotation: $[a]_D^{20}$ +17.3 (*c* 0.533, $CHCl_3$) for a sample with 93.5:6.5 er. Enantiomeric purity was determined by HPLC analysis in comparison with authentic racemic material (93.5:6.5 er shown below; chiralcel OD-H column (25 cm x 0.46 cm), 95/5 hexanes/*i*-PrOH, 0.3 mL/min, 220 nm).

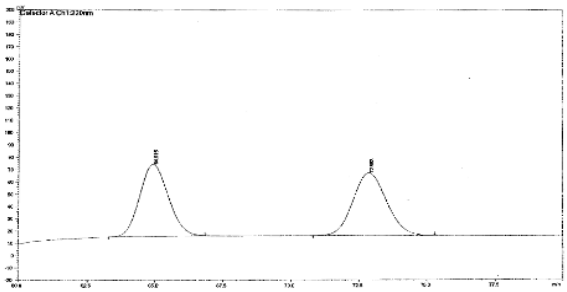

Detector A Ch1 220nm

| Peak# | Ret. Time | Area | Height | Area % | Height % |
|---|---|---|---|---|---|
| 1 | 64.916 | 4306509 | 58557 | 49.727 | 53.588 |
| 2 | 72.853 | 4353774 | 50716 | 50.273 | 46.412 |
| Total | | 8660283 | 109273 | 100.000 | 100.000 |

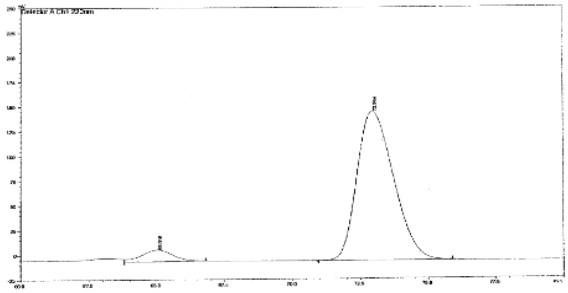

Detector A Ch1 220nm

| Peak# | Ret. Time | Area | Height | Area % | Height % |
|---|---|---|---|---|---|
| 1 | 65.018 | 970701 | 11793 | 6.396 | 7.252 |
| 2 | 72.944 | 14207023 | 150815 | 93.604 | 92.748 |
| Total | | 15177724 | 162607 | 100.000 | 100.000 |

| Time (min) | Area | Area % | Time (min) | Area | Area % |
|---|---|---|---|---|---|
| 64.916 | 4306509 | 49.727 | 65.018 | 970701 | 6.396 |
| 72.853 | 4353774 | 50.273 | 72.944 | 14207023 | 93.604 |

**(3*E*,5*E*)-6-Phenylhexa-3,5-dien-2-one (4.72a).**[186] $^1$H NMR (400 MHz, $CDCl_3$): δ 7.47–7.44 (2H, m), 7.37–7.27 (4H, m), 6.95 (1H, d, *J* = 15.6 Hz), 6.87 (1H, ddd, *J* = 15.6, 10.4, 0.8 Hz), 6.25 (1H, d, *J* = 15.6 Hz), 2.30 (3H, s).

**(2*E*,4*E*)-Methyl 5-phenylpenta-2,4-dienoate (4.72b).**[187] $^1$H NMR (400 MHz, $CDCl_3$): δ 7.47–7.41 (3H, m), 7.36–7.27 (3H, m), 6.92–6.82 (2H, m), 5.98 (1H, d, *J* = 15.2 Hz), 3.76 (3H, s).

**(2*E*,4*E*)-*S*-Ethyl 5-phenylpenta-2,4-dienethioate (4.72c).**[188] $^1$H NMR (400 MHz, $CDCl_3$): δ 7.46–7.43 (2H, m), 7.39–7.28 (4H, m), 6.95 (1H, d, *J* = 15.6 Hz), 6.82 (1H,

(186) Nongkhlaw, R. L.; Nongrum, R.; Myrboh, B. *J. Chem. Soc. Perkin Trans. 1,* **2001**, 1300–1303.

(187) El-Batta, A.; Jiang, C.; Zhao, W.; Anness, R.; Cooksy, A. L.; Bergdahl, M. *J. Org. Chem.* **2007**, *72*, 5244–5259.

(188) Liu, H.-J.; Rose, P. A.; Sasaki, D. J. *Can. J. Chem.* **1991**, *69*, 934–936.

ddd, $J$ = 15.6, 10.8, 0.8 Hz), 6.26 (1H, d, $J$ = 15.2 Hz), 2.97 (2H, q, $J$ = 7.2 Hz), 1.29 (3H, t, $J$ = 7.2 Hz).

**(3*E*,5*E*)-Hepta-3,5-dien-2-one (4.72d).**[189] $^1$H NMR (400 MHz, $CDCl_3$): δ 7.10–6.96 (1H, m), 6.19–6.09 (2H, m), 5.99 (1H, d, $J$ = 15.2 Hz), 2.21 (3H, s), 1.82–1.81 (3H, m).

**(3*E*,5*E*)-6-Phenylhepta-3,5-dien-2-one (4.72e).** IR (neat): 3051 (w), 2919 (w), 1681 (m), 1664 (s), 1611 (s), 1581 (s), 1358 (m), 1288 (m), 1250 (s), 1148 (m) $cm^{-1}$; $^1$H NMR (400 MHz, $CDCl_3$): δ 7.59 (1H, dd, $J$ = 15.2, 11.6 Hz), 7.49–7.47 (2H, m), 7.38–7.29 (3H, m), 6.57 (1H, d, $J$ = 11.6 Hz), 6.26 (1H, d, $J$ = 15.2 Hz), 2.31 (6H, s); $^{13}$C NMR (100 MHz, $CDCl_3$): δ 198.7, 146.7, 142.0, 139.3, 130.5, 128.7, 128.6, 126.1, 125.3, 27.9, 16.9; HRMS ($ESI^+$) Calcd for $C_{13}H_{15}O$ [M+H]: 187.1123, Found: 187.1129.

**(3*E*,5*E*)-4-Methyl-6-phenylhexa-3,5-dien-2-one (4.80a).** IR (neat): 3032 (w), 2918 (w), 1672 (s), 1572 (s), 1494 (m), 1448 (m), 1443 (m), 1393 (m), 1172 (s) $cm^{-1}$; $^1$H NMR (400 MHz, $CDCl_3$): δ 7.47–7.44 (2H, m), 7.36–7.24 (3H, m), 6.98 (1H, d, $J$ = 16.0 Hz), 6.76 (1H, d, $J$ = 16.0 Hz), 6.26 (1H, s), 2.36 (3H, d, $J$ = 1.2 Hz), 2.24 (3H, s); $^{13}$C NMR (100 MHz, $CDCl_3$): δ 199.0, 150.3, 136.4, 135.3, 132.2, 128.8, 128.7, 127.2, 127.0, 32.1, 14.0; HRMS ($ESI^+$) Calcd for $C_{13}H_{15}O$ [M+H]: 187.1123, Found: 187.1131.

**(3*E*,5*E*)-6-(4-Methoxyphenyl)-4-methylhexa-3,5-dien-2-one (4.80b).** IR (neat): 2961 (w), 2920 (w), 1672 (s), 1576 (s), 1510 (m), 1355 (m), 1255 (s), 1174 (s), 1025 (m) $cm^{-1}$; $^1$H NMR (400 MHz, $CDCl_3$): δ 7.42–7.38 (2H, m), 6.94 (1H, d, $J$ = 16.0 Hz), 6.89–6.85 (2H, m), 6.64 (1H, dd, $J$ = 16.0, 0.4 Hz), 6.22 (1H, s), 3.81 (3H, s), 2.35 (3H, d, $J$ = 1.2 Hz), 2.23 (3H, s); $^{13}$C NMR (100 MHz, $CDCl_3$): δ 199.0, 160.1, 150.9, 135.1, 130.1, 129.1, 128.4, 126.3, 114.2, 55.3, 32.1, 14.0; HRMS ($ESI^+$) Calcd for $C_{14}H_{17}O_2$ [M+H]:

(189) Nishimura, T.; Yasuhara, Y.; Hayashi, T. *Agnew. Chem. Int. Ed.* **2006**, *45*, 5164–5166.

217.1229, Found: 217.1238.

**(3*E*,5*E*)-4-Methyl-6-[4-(trifluoromethyl)phenyl]hexa-3,5-dien-2-one (4.80c).** IR (neat): 3006 (w), 2926 (w), 1673 (s), 1612 (w), 1579 (s), 1319 (s), 1233 (w), 1166 (s), 1128 (s), 1108 (s), 1018 (s) $cm^{-1}$; $^{1}H$ NMR (400 MHz, $CDCl_3$): δ 7.54 (2H, d, *J* = 8.4 Hz), 7.49 (2H, d, *J* = 8.8 Hz), 6.93 (1H, d, *J* = 16.0 Hz), 6.77 (1H, d, *J* = 16.0 Hz), 6.25 (1H, s), 2.30 (3H, d, *J* = 1.2 Hz), 2.20 (3H, s); $^{13}C$ NMR (100 MHz, $CDCl_3$): δ 199.2, 149.5, 140.0, 140.0, 134.8, 133.7, 130.4 (1C, q, *J* = 32.3 Hz), 128.5, 127.2, 125.9 (1C, q, *J* = 3.6 Hz), 32.3, 14.1; HRMS ($ESI^+$) Calcd for $C_{14}H_{14}OF_3$ [M+H]: 255.0997, Found: 255.1004.

**(3*E*,5*E*)-4-Methylnona-3,5-dien-2-one (4.80d).** IR (neat): 2959 (w), 2929 (w), 1679 (s), 1633 (w), 1583 (s), 1435 (w), 1359 (m), 1232 (m), 1173 (s) $cm^{-1}$; $^{1}H$ NMR (400 MHz, $CDCl_3$): δ 7.18 (1H, dt, *J* = 15.6, 6.8 Hz), 6.04 (2H, d, *J* = 13.6 Hz), 2.22–2.11 (8H, m), 1.49–1.40 (2H, m), 0.91 (3H, m); $^{13}C$ NMR (100 MHz, $CDCl_3$): δ 199.2, 150.8, 138.7, 134.1, 125.1, 35.2, 32.0, 22.1, 14.1, 13.6; HRMS ($ESI^+$) Calcd for $C_{10}H_{17}O$ [M+H]: 153.1279, Found: 153.1286.

**(3*E*,5*E*)-6-Cyclohexyl-4-methylhexa-3,5-dien-2-one (4.80e).** IR (neat): 2922 (m), 2851 (m), 1679 (s), 1630 (m), 1581 (s), 1447 (m), 1354 (m), 1230 (m), 1171 (s) $cm^{-1}$; $^{1}H$ NMR (400 MHz, $CDCl_3$): δ 6.13–5.98 (3H, m), 2.20 (3H, s), 2.18 (3H, s), 2.11–2.04 (1H, m), 1.74–1.58 (5H, m), 1.33–1.05 (5H, m); $^{13}C$ NMR (100 MHz, $CDCl_3$): δ 199.2, 151.2, 144.4, 131.5, 125.3, 41.3, 32.6, 32.1, 26.0, 25.9, 14.1; HRMS ($ESI^+$) Calcd for $C_{13}H_{21}O$ [M+H]: 193.1592, Found: 193.1595.

**(2*E*,4*E*)-Methyl 3-methyl-5-phenylpenta-2,4-dienoate (4.80f).** IR (neat): 2948 (w), 1708 (s), 1608 (s), 1434 (m), 1381 (m), 1273 (m), 1237 (s), 1151 (s) $cm^{-1}$; $^{1}H$ NMR (400

MHz, $CDCl_3$): δ 7.46–7.44 (2H, m), 7.36–7.31 (2H, m), 7.29–7.25 (1H, m), 6.93 (1H, d, *J* = 16.0 Hz), 6.80 (1H, d, *J* = 16.0 Hz), 5.89 (1H, s), 3.72 (3H, s), 2.40 (3H, d, *J* = 1.2 Hz); $^{13}C$ NMR (100 MHz, $CDCl_3$): δ 167.4, 152.3, 136.3, 134.2, 131.8, 128.8, 128.6, 127.0, 119.3, 51.0, 13.7; HRMS ($ESI^+$) Calcd for $C_{13}H_{15}O_2$ [M+H]: 203.1072, Found: 203.1077.

**(2*E*,4*E*)-*S*-Ethyl 3-methyl-5-phenylpenta-2,4-dienethioate (4.80g).** IR (neat): 2967 (w), 2928 (w), 1658 (s), 1615 (m), 1582 (s), 1449 (m), 1065 (s), 1006 (m) $cm^{-1}$; $^1H$ NMR (400 MHz, $CDCl_3$): δ 7.47–7.44 (2H, m), 7.37–7.26 (3H, m), 6.98 (1H, d, *J* = 16.0 Hz), 6.74 (1H, d, *J* = 16.4 Hz), 6.15 (1H, s), 2.94 (2H, q, *J* = 7.6 Hz), 2.38 (3H, d, *J* = 1.2 Hz), 1.29 (3H, t, *J* = 7.6 Hz); $^{13}C$ NMR (100 MHz, $CDCl_3$): δ 189.7, 148.6, 136.3, 135.7, 131.5, 128.8, 128.8, 127.1, 126.5, 23.5, 14.9, 14.5; HRMS ($ESI^+$) Calcd for $C_{14}H_{17}OS$ [M+H]: 233.1000, Found: 233.1009.

**(*E*)-3-Styrylcyclopent-2-enone (4.92a).**[190] $^1H$ NMR (400 MHz, $CDCl_3$): δ 7.53–7.50 (2H, m), 7.40–7.31 (3H, m), 7.21 (1H, d, *J* = 16.4 Hz), 7.06 (1H, d, *J* = 16.4 Hz), 6.15 (1H, s), 2.89–2.86 (2H, m), 2.52–2.49 (2H, m).

**(*E*)-3-(4-Methylstyryl)cyclohex-2-enone (4.92c).** IR (neat): 2940 (m), 2877 (w), 1652 (s), 1615 (s), 1578 (s), 1414 (m), 1383 (m), 1347 (s), 1241 (s) $cm^{-1}$; $^1H$ NMR (400 MHz, $CDCl_3$): δ 7.34 (2H, d, *J* = 8.4 Hz), 7.13 (2H, d, *J* = 8.0 Hz), 6.93 (1H, d, *J* = 16.4 Hz), 6.78 (1H, d, *J* = 16.4 Hz), 6.01 (1H, s), 2.54 (2H, dd, *J* = 6.0, 6.0 Hz), 2.40 (2H, dd, *J* = 6.4, 6.4 Hz), 2.32 (3H, s), 2.08–2.00 (2H, m); $^{13}C$ NMR (100 MHz, $CDCl_3$): δ 200.6, 157.7, 139.8, 135.7, 133.8, 130.1, 128.8, 128.3, 127.8, 38.3, 25.5, 22.9, 21.9; HRMS ($ESI^+$) Calcd for $C_{15}H_{17}O$ [M+H]: 213.1279, Found: 213.1279.

(190) Wenkert, E.; Schorp, M. K. *J. Org. Chem.* **1994**, *59*, 1943–1944.

**(*E*)-3-(4-Methoxystyryl)cyclohex-2-enone (4.92d).** IR (neat): 2936 (w), 2834 (w), 1644 (s), 1600 (s), 1579 (s), 1510 (s), 1273 (s), 1244 (s) $cm^{-1}$; $^1H$ NMR (400 MHz, $CDCl_3$): δ 7.41–7.38 (2H, m), 6.91 (1H, d, *J* = 16.4 Hz), 6.87–6.84 (2H, m), 6.70 (1H, d, *J* = 16.0 Hz), 5.99 (1H, s), 3.78 (3H, s), 2.55 (2H, dd, *J* = 6.0, 6.0 Hz), 2.40 (2H, dd, *J* = 6.4, 6.4 Hz), 2.06–2.00 (2H, m); $^{13}C$ NMR (100 MHz, $CDCl_3$): δ 200.1, 160.5, 157.5, 134.9, 128.8, 128.8, 127.4, 127.1, 114.4, 55.4, 37.8, 25.0, 22.4; HRMS ($ESI^+$) Calcd for $C_{15}H_{17}O_2$ [M+H]: 229.1228, Found: 229.1225.

**(*E*)-3-[4-(Trifluoromethyl)styryl]cyclohex-2-enone (4.92e).** IR (neat): 2952 (w), 1656 (s), 1622 (m), 1584 (m), 1322 (s), 1271 (m), 1248 (m), 1192 (m), 1156 (m), 1140 (m), 1109 (s) $cm^{-1}$; $^1H$ NMR (400 MHz, $CDCl_3$): δ 7.56 (2H, d, *J* = 8.8 Hz), 7.53 (2H, d, *J* = 8.4 Hz), 6.96 (1H, d, *J* = 16.0 Hz), 6.89 (1H, d, *J* = 16.0 Hz), 6.06 (1H, s), 2.57 (2H, dd, *J* = 6.0, 6.0 Hz), 2.42 (2H, dd, *J* = 6.4, 6.4 Hz), 2.26 (2H, dddd, *J* = 6.4, 6.4, 6.4, 6.4 Hz); $^{13}C$ NMR (100 MHz, $CDCl_3$): δ 200.0, 156.2, 139.5, 139.5, 133.4, 131.8, 130.5 (1C, q, *J* = 32.3 Hz), 129.3, 127.4, 125.8 (1C, q, *J* = 4.0 Hz), 37.7, 25.0, 22.3; HRMS ($ESI^+$) Calcd for $C_{15}H_{14}F_3O$ [M+H]: 267.0997, Found: 267.1003.

**(*E*)-3-Styrylcyclohept-2-enone (4.92h).** IR (neat): 2934 (m), 2864 (w), 1644 (s), 1613 (s), 1579 (s), 1448 (m), 1255 (s), 1201 (m), 1187 (m) $cm^{-1}$; $^1H$ NMR (400 MHz, $CDCl_3$): δ 7.45 (2H, d, *J* = 8.0 Hz), 7.36–7.24 (3H, m), 6.94 (1H, d, *J* = 16.0 Hz), 6.81 (1H, d, *J* = 16.4 Hz), 6.12 (1H, s), 2.71 (2H, dd, *J* = 6.0, 6.0 Hz), 2.63 (2H, dd, *J* = 6.0, 6.0 Hz), 1.91–1.79 (4H, m); $^{13}C$ NMR (100 MHz, $CDCl_3$): δ 204.9, 154.3, 136.9, 134.3, 133.2, 132.2, 129.5, 129.4, 127.7, 42.7, 27.8, 25.5, 21.8; HRMS ($ESI^+$) Calcd for $C_{15}H_{17}O$ [M+H]: 213.1279, Found: 213.1276.

**(2*Z*,4*E*)-Methyl 3-methyl-5-phenylpenta-2,4-dienoate (*Z*,*E*-4.80f).** IR (neat): 2948 (w),

1708 (s), 1621 (s), 1595 (m), 1448 (m), 1432 (m), 1278 (m), 1231 (s), 1205 (s), 1151 (s), 1050 (m) $cm^{-1}$; $^1H$ NMR (400 MHz, $CDCl_3$): δ 8.39 (1H, d, *J* = 16.4 Hz), 7.53 (2H, d, *J* = 7.6 Hz), 7.35–7.24 (3H, m), 6.91 (1H, d, *J* = 16.4 Hz), 5.74 (1H, s), 3.72 (3H, s), 2.12 (3H, s); $^{13}C$ NMR (100 MHz, $CDCl_3$): δ 167.0, 151.1, 136.7, 135.4, 128.7, 128.6, 127.4, 125.9, 117.2, 51.0, 20.9.

**Stereochemical Comparison of 4.93b and 4.93g:** To confirm that the stereogenic carbon centers of **4.93b** and **4.93g** have the same absolute stereochemistry, ozonolysis followed by reductive workup of **4.93b** and **4.93g** were performed (Scheme 4.7.1). Alcohols **4.106** and **4.107** were isolated and the spectroscopic data were found to match those reported.[191] $^1H$ NMR (400 MHz, $CDCl_3$): δ 7.42–7.29 (5H, m), 7.25–7.12 (3H, m), 7.03–7.00 (2H, m), 4.09 (1H, dd, *J* = 11.2, 11.2 Hz), 3.94 (1H, dd, *J* = 11.2, 4.4 Hz), 3.63 (1H, s), 2.67 (1H, dd, *J* = 11.2, 4.4 Hz), 0.27 (3H, s), 0.23 (3H, s). Enantiomeric purity was determined by HPLC analysis in comparison with authentic racemic material (**4.106:** 96:4 er and **4.107**: 94:6 er shown below; chiralcel OD-H column (25 cm x 0.46 cm), 98/2 hexanes/*i*-PrOH, 0.3 mL/min, 220 nm).

**Scheme 4.7.1. Ozonolysis of 4.93b and 4.93g**

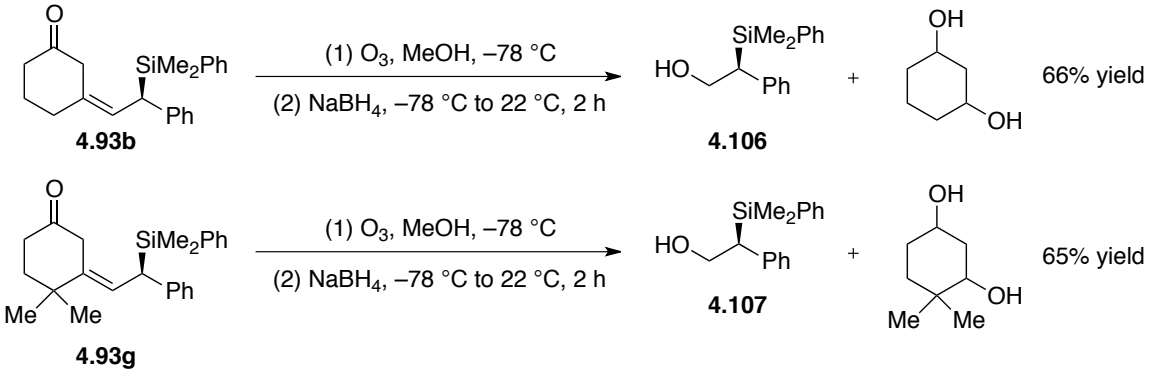


(191) Buck, R. T.; Coe, D. M.; Drysdale, M. J.; Ferris, L.; Haigh, D.; Moody, C. J.; Pearson, N. D.; Sanghera, J. B. *Tetrahedron: Asymmetry*, **2003**, *14*, 791–816.

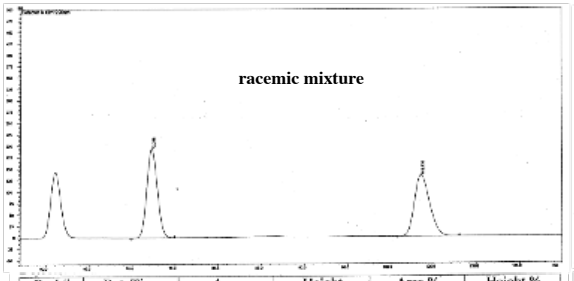


| Peak# | Ret. Time | Area | Height | Area % | Height % |
|---|---|---|---|---|---|
| 1 | 72.248 | 16498975 | 194540 | 49.966 | 59.064 |
| 2 | 103.530 | 16521205 | 134834 | 50.034 | 40.936 |
| Total | | 33020180 | 329374 | 100.000 | 100.000 |

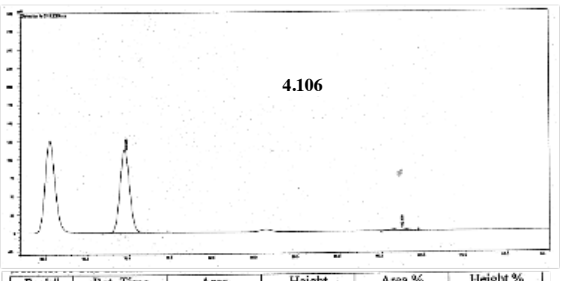


| Peak# | Ret. Time | Area | Height | Area % | Height % |
|---|---|---|---|---|---|
| 1 | 69.366 | 9117616 | 113650 | 95.787 | 96.968 |
| 2 | 102.109 | 401064 | 3553 | 4.213 | 3.032 |
| Total | | 9518680 | 117204 | 100.000 | 100.000 |

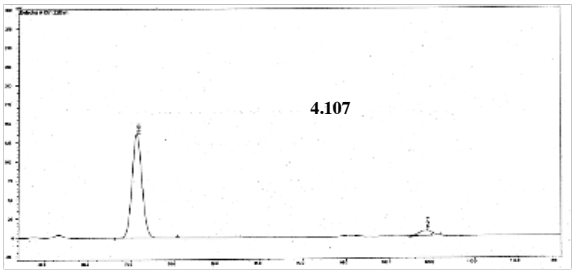


| Peak# | Ret. Time | Area | Height | Area % | Height % |
|---|---|---|---|---|---|
| 1 | 70.651 | 10961549 | 136158 | 93.971 | 95.306 |
| 2 | 104.213 | 703251 | 6706 | 6.029 | 4.694 |
| Total | | 11664800 | 142863 | 100.000 | 100.000 |

| Retention time | Area | Area % | Retention time | Area | Area % |
|---|---|---|---|---|---|
| 72.248 | 16498975 | 49.966 | 69.366 | 9117616 | 95.787 |
| 103.530 | 16521205 | 50.034 | 102.109 | 401064 | 4.213 |
| Retention time | Area | Area % | | | |
| 70.651 | 10961549 | 93.971 | | | |
| 104.213 | 703251 | 6.029 | | | |

**(*S*)-Dimethyl(phenyl)(1-phenylallyl)silane (4.101a).**[182] $^1$H NMR (400 MHz, $CDCl_3$): δ 7.36–7.24 (5H, m), 7.19–7.15 (2H, m), 7.09–7.05 (2H, m), 6.92–6.89 (1H, m), 6.10 (1H, ddd, $J$ = 16.8, 10.0, 10.0 Hz), 4.95–4.87 (2H, m), 3.13 (1H, d, $J$ = 10.0 Hz), 0.26 (3H, s), 0.23 (3H, s); Optical rotation: $[a]_D^{20}$ +11.5 (*c* 0.87, $CHCl_3$) for a sample with 98:2 er. Enantiomeric purity was determined by GC analysis in comparison with authentic racemic material (98:2 er shown, Chiraldex GTA column, 90 ºC, 20 psi).

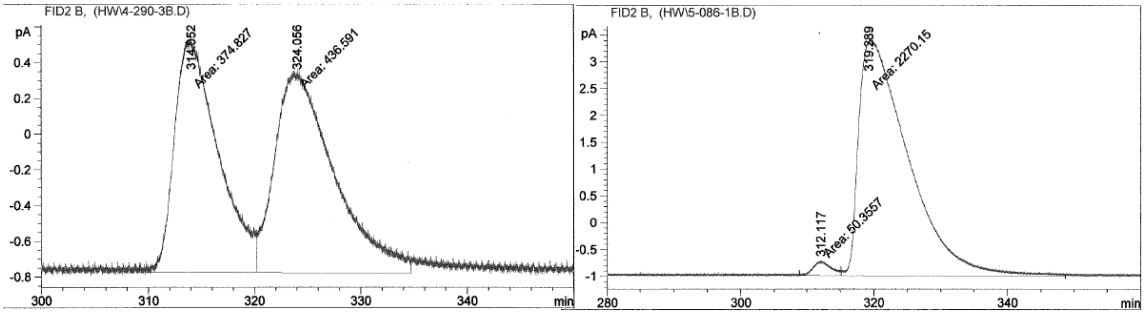


Peak RetTime Type Width Area Height Area
# [min] [min] [pA*s] [pA] %

1 314.052 MF 4.7378 374.82727 1.31858 46.19407
2 324.056 FM 6.4235 436.59125 1.13280 53.80593

1 312.117 MF 2.9409 50.35573 2.85377e-1 2.17003
2 319.289 FM 8.5346 2270.15088 4.43321 97.82997

| Time (min) | Area | Area % | Time (min) | Area | Area % |
|---|---|---|---|---|---|
| 314.052 | 374.82727 | 46.19407 | 312.117 | 50.35573 | 2.17003 |
| 324.056 | 436.59125 | 53.80593 | 319.289 | 2270.15088 | 97.82997 |

**(*S*)-(1-(2-Methoxyphenyl)allyl)dimethyl(phenyl)silane (4.101b).**[192] $^1$H NMR (400 MHz, $CDCl_3$): δ 7.39–7.27 (5H, m), 7.10–7.05 (1H, m), 6.99–6.96 (1H, m), 6.87–6.83 (1H, m), 6.76–6.74 (1H, m), 6.14 (1H, ddd, *J* = 16.8, 10.6, 9.6 Hz), 4.95–4.90 (2H, m), 3.74 (1H, d, *J* = 9.6 Hz), 3.62 (3H, s), 0.27 (3H, s), 0.23 (3H, s); Optical rotation: $[a]_D^{20}$ +18.2 (*c* 1.10, $CHCl_3$) for a sample with 96:4 er. Enantiomeric purity was determined by GC analysis in comparison with authentic racemic material (96:4 er shown, Chiraldex GTA column, 100 ºC, 20 psi).

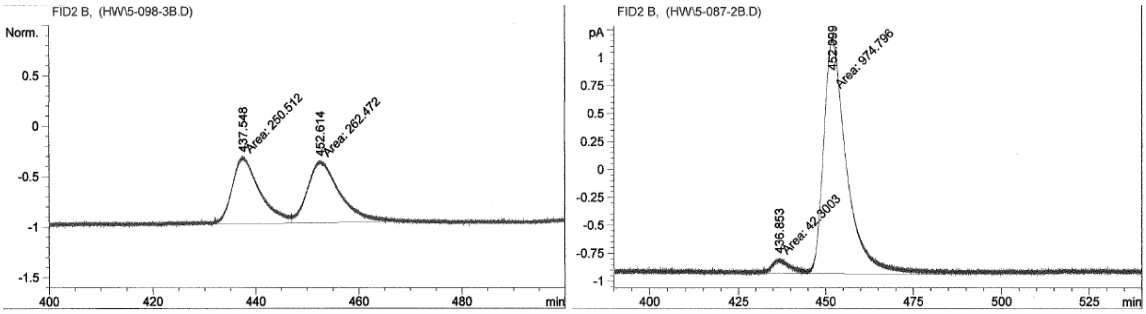


Peak RetTime Type Width Area Height Area
# [min] [min] [pA*s] [pA] %

1 437.548 MF 6.1890 250.51210 6.74616e-1 48.83429
2 452.614 FM 7.0300 262.47195 6.22267e-1 51.16571

1 436.853 MF 4.8178 42.30031 1.46335e-1 4.15893
2 452.099 FM 7.6677 974.79626 2.11884 95.84107

| Time (min) | Area | Area % | Time (min) | Area | Area % |
|---|---|---|---|---|---|
| 437.548 | 250.51210 | 48.83429 | 436.853 | 42.30031 | 4.15893 |

(192) Vyas, D. J.; Oestreich, M. *Chem. Commun.*, **2010**, *46*, 568–570.

| | | | | | |
|---|---|---|---|---|---|
| 452.614 | 262.47195 | 51.16571 | 452.099 | 974.79626 | 95.84107 |

**(*S*)-(1-(2-Bromophenyl)allyl)dimethyl(phenyl)silane (4.101c).**[183] $^1$H NMR (400 MHz, $CDCl_3$): δ 7.53–7.50 (1H, m), 7.44–7.30 (5H, m), 7.18–7.14 (1H, m), 6.98–6.93 (2H, m), 6.00 (1H, ddd, *J* = 16.8, 10.0, 9.2 Hz), 4.98–4.88 (2H, m), 3.88 (1H, d, *J* = 9.2 Hz), 0.31 (3H, s), 0.29 (3H, s); Optical rotation: $[a]_D^{20}$ +33.3 (*c* 0.60, $CHCl_3$) for a sample with 96:4 er. Enantiomeric purity was determined by HPLC analysis of the hydroboration (9-BBN)/oxidation product in comparison with authentic racemic material (96:4 er shown, chiralcel OD-H column (25 cm x 0.46 cm), 98/2 hexanes/*i*-PrOH, 0.3 mL/min, 220 nm).

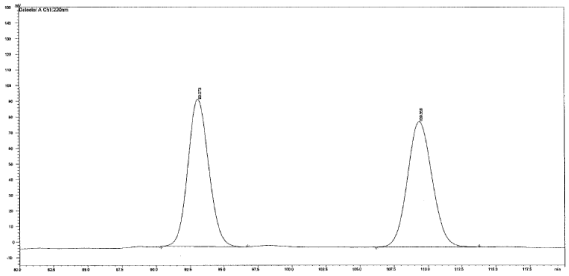

| Peak# | Ret. Time | Area | Height | Area % | Height % |
|---|---|---|---|---|---|
| 1 | 93.073 | 10168769 | 94153 | 50.143 | 53.988 |
| 2 | 109.359 | 10110945 | 80242 | 49.857 | 46.012 |
| Total | | 20279714 | 174396 | 100.000 | 100.000 |

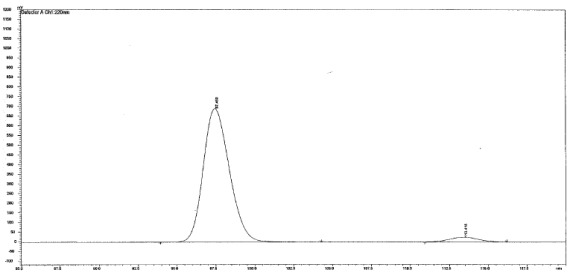

| Peak# | Ret. Time | Area | Height | Area % | Height % |
|---|---|---|---|---|---|
| 1 | 97.450 | 80743856 | 690283 | 96.101 | 96.436 |
| 2 | 113.418 | 3275903 | 25515 | 3.899 | 3.564 |
| Total | | 84019759 | 715798 | 100.000 | 100.000 |

| Time (min) | Area | Area % | Time (min) | Area | Area % |
|---|---|---|---|---|---|
| 93.073 | 10168769 | 50.143 | 97.450 | 80743856 | 96.436 |
| 109.359 | 10110945 | 49.857 | 113.418 | 3275903 | 3.564 |

**(*S*)-Dimethyl(phenyl)(1-(4-(trifluoromethyl)phenyl)allyl)silane (4.101d).**[182] $^1$H NMR (400 MHz, $CDCl_3$): δ 7.42 (2H, d, *J* = 8.0 Hz), 7.40–7.30 (5H, m), 6.99 (2H, d, *J* = 8.0 Hz), 6.09 (1H, ddd, *J* = 17.0, 10.0, 10.0 Hz), 5.02–4.93 (2H, m), 3.22 (1H, d, *J* = 10.0 Hz), 0.28 (3H, s), 0.27 (3H, s); Optical rotation: $[a]_D^{20}$ +14.8 (*c* 1.35, $CHCl_3$) for a sample with 94:6 er. Enantiomeric purity was determined by GC analysis in comparison with authentic racemic material (94:6 er shown, Chiraldex GTA column, 90 ºC, 15 psi).

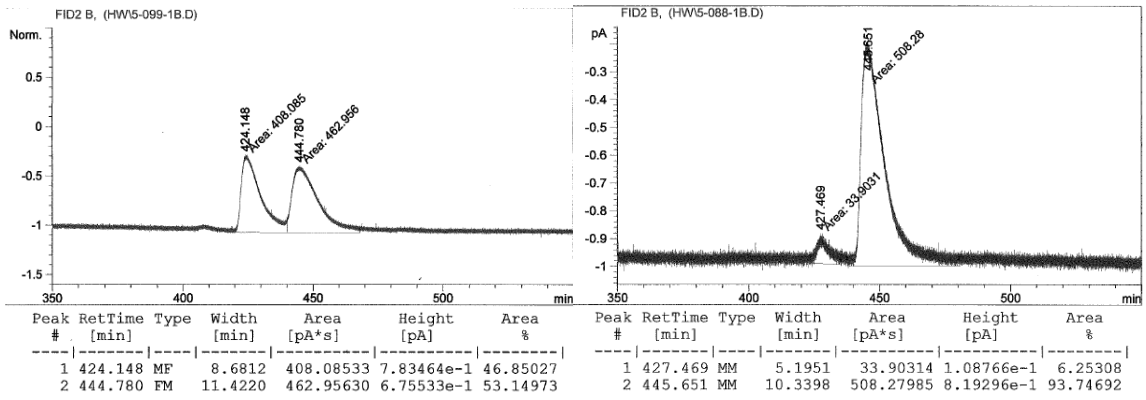


| Peak # | RetTime [min] | Type | Width [min] | Area [pA*s] | Height [pA] | Area % |
|---|---|---|---|---|---|---|
| 1 | 424.148 | MF | 8.6812 | 408.08533 | 7.83464e-1 | 46.85027 |
| 2 | 444.780 | FM | 11.4220 | 462.95630 | 6.75533e-1 | 53.14973 |

| Peak # | RetTime [min] | Type | Width [min] | Area [pA*s] | Height [pA] | Area % |
|---|---|---|---|---|---|---|
| 1 | 427.469 | MM | 5.1951 | 33.90314 | 1.08766e-1 | 6.25308 |
| 2 | 445.651 | MM | 10.3398 | 508.27985 | 8.19296e-1 | 93.74692 |

| Time (min) | Area | Area % | Time (min) | Area | Area % |
|---|---|---|---|---|---|
| 424.148 | 408.08533 | 46.85027 | 427.469 | 33.90314 | 6.25308 |
| 444.780 | 462.95630 | 53.14973 | 445.651 | 508.27985 | 93.74692 |

**(*S*)-3-(1-(Dimethyl(phenyl)silyl)allyl)pyridine (4.101e) (mixture with $S_N2$ product).** IR (neat): 3070 (m), 3049 (m), 2957 (s), 2925 (s), 2853 (m), 1626 (m), 1588 (m), 1571 (m), 1477 (s), 1426 (s), 1410 (m), 1249 (s), 1182 (m), 1114 (s), 1078 (m), 1024 (m), 900 (s), 825 (s), 776 (s), 736 (s), 714 (s), 699 (s), 655 (m), 573 (m), 470 (m) $cm^{-1}$; $^1H$ NMR (400 MHz, $CDCl_3$): δ 8.36-8.24 (2H, ap d), 7.40–7.29 (5H, m), 7.17–7.11 (2H, m), 6.06 (1H, ddd, *J* = 16.8, 10.0, 10.0 Hz), 5.03–4.93 (2H, m), 3.14 (1H, d, *J* = 10.0 Hz), 0.29 (6H, s); $^{13}C$ NMR (100 MHz, $CDCl_3$): δ 149.1, 147.7, 147.5, 146.4, 138.2, 137.6, 136.6, 135.9, 134.6, 134.4, 133.7, 133.2, 132.1, 130.1, 129.7, 129.6, 129.4, 128.0, 127.8, 125.7, 125.4, 123.2, 114.2, 41.6, -4.5, -4.7; HRMS ($ESI^+$) Calcd for $C_{16}H_{20}N_1Si_1$ [M+H]: 254.13650, Found: 254.13549. Optical rotation: $[a]_D^{20}$ +7.68 (*c* 1.30, $CHCl_3$) for a sample with 96:4 er. Enantiomeric purity was determined by HPLC analysis of product in comparison with authentic racemic material (96:4 er shown, chiralcel OD-H column (25 cm x 0.46 cm), 95/5 hexanes/*i*-PrOH, 0.1 mL/min, 220 nm).

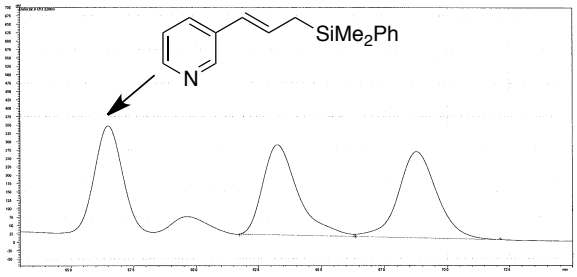


| Peak# | Ret. Time | Area | Height | Area % | Height % |
|---|---|---|---|---|---|
| 1 | 63.259 | 26168918 | 268910 | 48.874 | 51.063 |
| 2 | 68.776 | 27374405 | 257710 | 51.126 | 48.937 |
| Total | | 53543323 | 526620 | 100.000 | 100.000 |

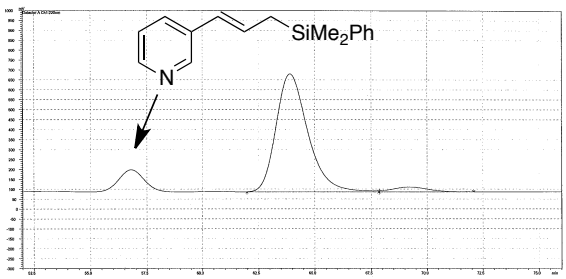


| Peak# | Ret. Time | Area | Height | Area % | Height % |
|---|---|---|---|---|---|
| 1 | 63.903 | 58469676 | 593971 | 95.667 | 96.025 |
| 2 | 69.221 | 2648418 | 24589 | 4.333 | 3.975 |
| Total | | 61118094 | 618560 | 100.000 | 100.000 |

| Time (min) | Area | Area % | Time (min) | Area | Area % |
|---|---|---|---|---|---|
| 63.259 | 26168918 | 48.874 | 63.903 | 58469676 | 95.667 |
| 68.776 | 27374405 | 51.126 | 69.221 | 2648418 | 4.333 |

**(*R*)-Dimethyl(oct-1-en-3-yl)(phenyl)silane (4.101g).**[193] $^1$H NMR (400 MHz, $CDCl_3$): δ 7.51–7.49 (2H, m), 7.36–7.34 (3H, m), 5.59 (1H, ddd, *J* = 17.0, 10.0, 10.0 Hz), 4.90–4.79 (2H, m), 1.76–1.72 (1H, m), 1.44–1.13 (8H, m), 0.85 (3H, t, *J* = 7.0 Hz), 0.27 (3H, s), 0.26 (3H, s); Optical rotation: $[a]_D^{20}$ –74.9 (*c* 0.80, $CHCl_3$) for a sample with 94:6 er. Enantiomeric purity was determined by HPLC analysis of the hydroboration (9-BBN)/oxidation product in comparison with authentic racemic material (94:6 er shown, chiralcel OD-H column (25 cm x 0.46 cm), 98/2 hexanes/*i*-PrOH, 0.3 mL/min, 220 nm).

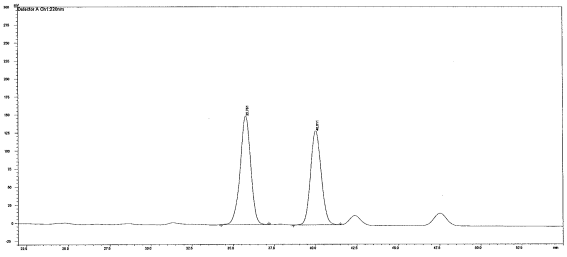

| Peak# | Ret. Time | Area | Height | Area % | Height % |
|---|---|---|---|---|---|
| 1 | 35.761 | 6731132 | 150566 | 53.184 | 53.540 |
| 2 | 40.011 | 5925289 | 130657 | 46.816 | 46.460 |
| Total | | 12656421 | 281223 | 100.000 | 100.000 |

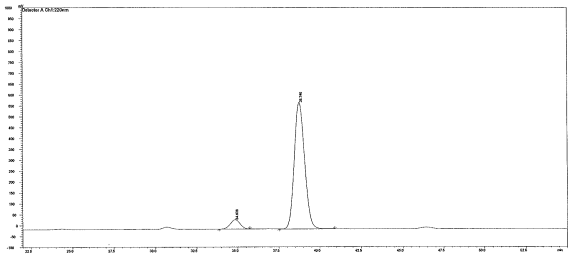

| Peak# | Ret. Time | Area | Height | Area % | Height % |
|---|---|---|---|---|---|
| 1 | 34.838 | 1742379 | 42401 | 6.385 | 6.792 |
| 2 | 38.746 | 25544831 | 581895 | 93.615 | 93.208 |
| Total | | 27287210 | 624296 | 100.000 | 100.000 |

| Time (min) | Area | Area % | Time (min) | Area | Area % |
|---|---|---|---|---|---|
| 35.761 | 6731132 | 53.184 | 34.838 | 1742379 | 6.385 |
| 40.011 | 5925289 | 46.816 | 38.746 | 25544831 | 93.615 |

**(*S*)-Dimethyl(phenyl)(2-phenylbut-3-en-2-yl)silane (4.101h).**[183] $^1$H NMR (400 MHz,

(193) Zhao, K.; Loh, T.-P. *Chem. Eur. J.* **2014**, *20*, 16764–16772.

$CDCl_3$): δ 7.37–7.19 (7H, m), 7.12–7.07 (3H, m), 6.47 (1H, dd, *J* = 17.2, 11.2 Hz), 5.11–4.93 (2H, m), 1.47 (3H, s), 0.25 (3H, s), 0.24 (3H, s); Optical rotation: $[a]_D^{20}$ +18.8 (*c* 1.30, $CHCl_3$) for a sample with 97:3 er. Enantiomeric purity was determined by HPLC analysis of the hydroboration (9-BBN)/oxidation product in comparison with authentic racemic material (97:3 er shown, chiralcel OD-H column (25 cm x 0.46 cm), 98/2 hexanes/*i*-PrOH, 0.3 mL/min, 220 nm).

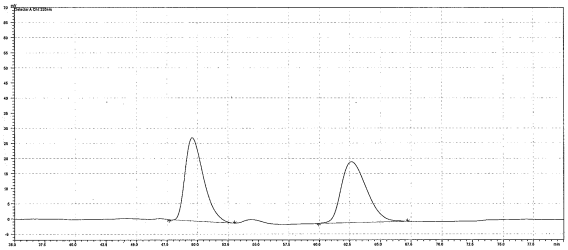

| Peak# | Ret. Time | Area | Height | Area % | Height % |
|---|---|---|---|---|---|
| 1 | 49.555 | 2904909 | 27520 | 50.016 | 57.713 |
| 2 | 62.648 | 2903096 | 20165 | 49.984 | 42.287 |
| Total | | 5808004 | 47685 | 100.000 | 100.000 |

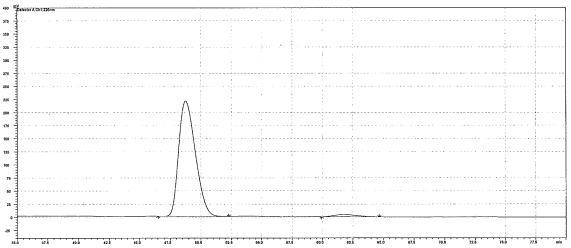

| Peak# | Ret. Time | Area | Height | Area % | Height % |
|---|---|---|---|---|---|
| 1 | 48.758 | 20743910 | 220367 | 97.396 | 98.073 |
| 2 | 61.716 | 554519 | 4329 | 2.604 | 1.927 |
| Total | | 21298430 | 224696 | 100.000 | 100.000 |

| Time (min) | Area | Area % | Time (min) | Area | Area % |
|---|---|---|---|---|---|
| 49.555 | 2904909 | 50.016 | 48.758 | 20743910 | 97.396 |
| 62.648 | 2903096 | 49.984 | 61.716 | 554519 | 2.604 |

### *4.7.2. Stereochemical Identity of 4.81a*

**Experimental Circular Dichroism Spectrum of 4.81a:** A 0.158 M solution was prepared by dissolving 51.0 mg **4.81a** (*Z*:*E* = 13:1, >98:2 er) in 1 mL of *n*-pentane (from solvent purification system). The ambient-temperature (25 ºC) electronic circular dischroism (CD) spectrum was recorded in 200–500 nm spectral region, on a AVIV MODEL 420 Circular Dichroism Spectrometer, together with a blank spectrum of the solvent. The cell path length is 1.0 cm. The spectrum of **4.81a** (shown in Figure 4.7.1) was corrected by subtraction of the solvent spectrum.

**Calculated Circular Dichroism Spectrum of 4.81a:** Stereochemical identity of **4.81a** was determined by comparing the experimental electronic circular dischroism (CD)

spectrum to the calculated spectrum (by Adil R. Zhugralin). Geometries of eight *cis*-**4.81a** conformers and eight *trans*-**4.81a** conformed were optimized at B3LYP/6-311G(d) level of theory, employing ultrafine grids and tight convergence criteria in Gaussian 09, Revision A.02.[194] The minimum nature of stationary points was ascertained by frequency calculations, in which no imaginary vibrational frequencies were observed. The energies of all conformers are listed in Table 4.7.1, and geometries (Cartesian coordinates) are listed in Table 4.7.2. One *cis*-**4.81a** conformer and two *trans*-**4.81a** conformers were identified as being too high in energy to have measurable impact on the overall CD spectrum. For each geometry that was deemed as energetically accessible 50 lowest excitations were calculated with TD-DFT at B3LYP/6-311+G(2df,2p) level of theory with ultrafine grids and tight SCF convergence criteria. Solvation was approximated by means of a polarizable continuum model (IEFPCM with *n*-pentane as a solvent). The excitation energies (in units of nm) and corresponding R(length) were utilized to model a CD spectrum for each conformer according to the following procedure. Each excitation was modeled as a normal distribution (Gaussian curve) centered on the wavelength corresponding to each excitation with standard deviation set to 8. Each Gaussian curve was multiplied by corresponding R(length) values. The sum of Gaussians, thus, afforded a CD spectrum for each conformer. Weighted sums of CD spectra for *cis*-**4.81a** and

(194) Gaussian 09, Revision A.02, Frisch, M. J.; Trucks, G. W.; Schlegel, H. B.; Scuseria, G. E.; Robb, M. A.; Cheeseman, J. R.; Scalmani, G.; Barone, V.; Mennucci, B.; Petersson, G. A.; Nakatsuji, H.; Caricato, M.; Li, X.; Hratchian, H. P.; Izmaylov, A. F.; Bloino, J.; Zheng, G.; Sonnenberg, J. L.; Hada, M.; Ehara, M.; Toyota, K.; Fukuda, R.; Hasegawa, J.; Ishida, M.; Nakajima, T.; Honda, Y.; Kitao, O.; Nakai, H.; Vreven, T.; Montgomery, J. A. Jr.; Peralta, J. E.; Ogliaro, F.; Bearpark, M.; Heyd, J. J.; Brothers, E.; Kudin, K. N.; Staroverov, V. N.; Kobayashi, R.; Normand, J.; Raghavachari, K.; Rendell, A.; Burant, J. C.; Iyengar, S. S.; Tomasi, J.; Cossi, M.; Rega, N.; Millam, N. J.; Klene, M.; Knox, J. E.; Cross, J. B.; Bakken, V.; Adamo, C.; Jaramillo, J.; Gomperts, R.; Stratmann, R. E.; Yazyev, O.; Austin, A. J.; Cammi, R.; Pomelli, C.; Ochterski, J. W.; Martin, R. L.; Morokuma, K.; Zakrzewski, V. G.; Voth, G. A.; Salvador, P.; Dannenberg, J. J.; Dapprich, S.; Daniels, A. D.; Farkas, Ö.; Foresman, J. B.; Ortiz, J. V.; Cioslowski, J.; Fox, D. J. *Gaussian 09* (Gaussian, Inc., Wallingford CT, 2009).

*trans*-**4.81a** conformers gave average CD spectra for *cis*-**4.81a** and *trans*-**4.81a**. Weighting coefficients were determined from the relative enthalpies for each conformer employed in the TD-DFT calculations. The average CD spectra for *cis*-**481a** and *trans*-**4.81a** were weighted by their experimental ratio (*cis*-**4.81a**:*trans*-**4.81a** = 0.93:0.07) and summed to give the CD spectrum in Figure 4.7.1. In Figure 4.7.1, the calculated CD spectrum (blue) is shown along with the experimental CD spectrum (red).

**Figure 4.7.1. Calculated and Experimental Circular Dichroism Spectra for Compound 4.81a**

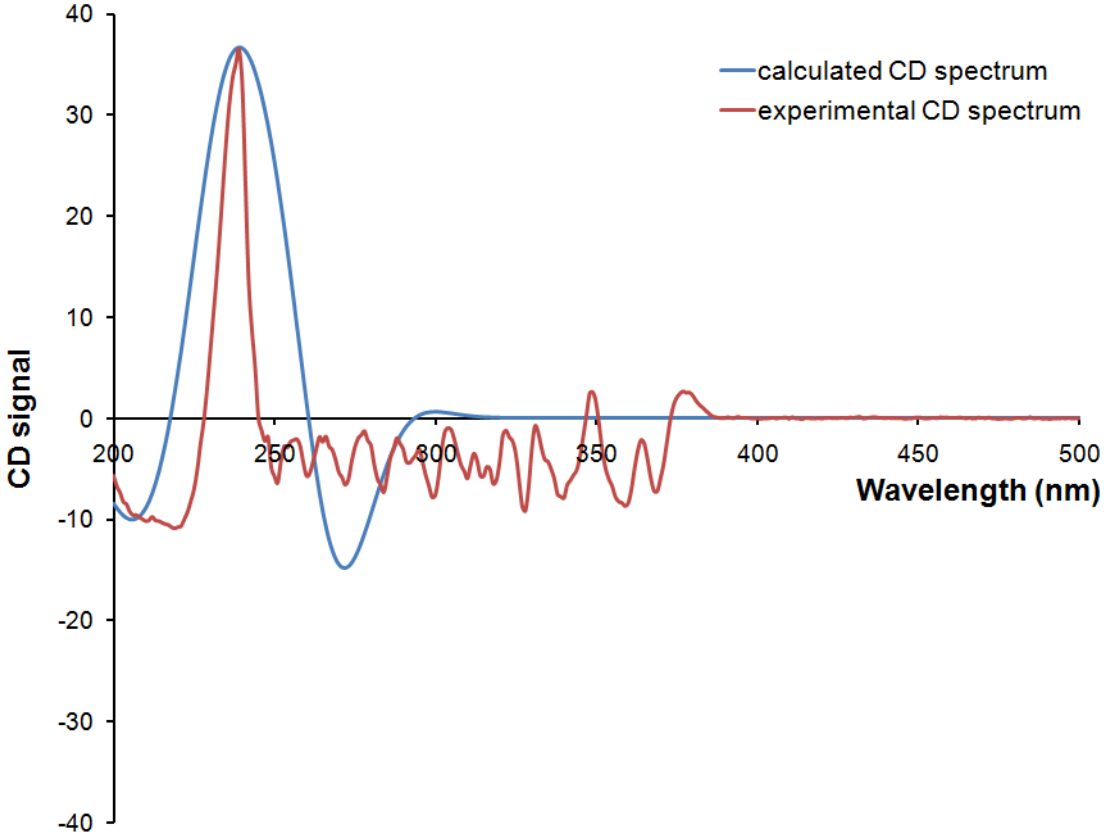

**Table 4.7.1. Energies and Relative Populations of Conformers of Compound 4.81a**

| Conformer | E+ZPE[a] | H[a] | Δ(E+ZPE)[b] | ΔH[b] | Weighting Coefficient[c] |
|---|---|---|---|---|---|
| *cis*-**4.81aa** | -1180.438182 | -1180.411878 | 1.70 | 1.84 | 0.025 |
| *cis*-**4.81ab** | -1180.439596 | -1180.413429 | 0.81 | 0.87 | 0.130 |
| *cis*-**4.81ac** | -1180.438933 | -1180.412698 | 1.23 | 1.33 | 0.060 |
| *cis*-**4.81ad** | -1180.440887 | -1180.414815 | 0.00 | 0.00 | 0.565 |
| *cis*-**4.81ae** | -1180.437970 | -1180.411770 | 1.83 | 1.91 | 0.022 |
| *cis*-**4.81af** | -1180.430641 | -1180.404465 | 6.43 | 6.49 | 0.000 |
| *cis*-**4.81ag** | -1180.439255 | -1180.412971 | 1.02 | 1.16 | 0.080 |
| *cis*-**4.81ah** | -1180.439357 | -1180.413328 | 0.96 | 0.93 | 0.117 |
| *trans*-**4.81aa** | -1180.440939 | -1180.414788 | 1.30 | 1.23 | 0.092 |
| *trans*-**4.81ab** | -1180.438946 | -1180.412574 | 2.55 | 2.62 | 0.009 |
| *trans*-**4.81ac** | -1180.443015 | -1180.416755 | 0.00 | 0.00 | 0.736 |
| *trans*-**4.81ad** | -1180.439921 | -1180.413573 | 1.94 | 2.00 | 0.025 |
| *trans*-**4.81ae** | -1180.431520 | -1180.405373 | 7.21 | 7.14 | 0.000 |
| *trans*-**4.81af** | -1180.431363 | -1180.405377 | 7.31 | 7.14 | 0.000 |
| *trans*-**4.81ag** | -1180.441338 | -1180.415098 | 1.05 | 1.04 | 0.127 |
| *trans*-**4.81ah** | -1180.439246 | -1180.412851 | 2.37 | 2.45 | 0.012 |

[a] Values in units of hartree. [b] Relative energies in units of kcal/mol. [c] Weighting coefficients were determined from relative populations, which were calculated from the relative enthalpies.

**Table 4.7.2. Calculated Geometries of Conformers of 4.81a**

| | *cis*-**4.81aa** | | | | *cis*-**4.81ab** | | |
|---|---|---|---|---|---|---|---|
| C | 3.52188070 | -0.02520607 | 3.79391842 | C | -5.01654195 | -0.24814251 | -2.18193790 |
| H | 2.48175920 | 0.19545617 | 4.05774410 | H | -5.44437514 | -1.03720592 | -2.80979903 |
| H | 3.69825790 | -1.07562826 | 4.04331852 | H | -5.11676046 | -0.57980348 | -1.14429727 |
| H | 4.17543863 | 0.61313569 | 4.38728713 | H | -5.58410957 | 0.66904936 | -2.33426034 |
| C | 3.74121707 | 0.24532572 | 2.31492140 | C | -3.56253153 | -0.02248219 | -2.55910951 |
| O | 4.36901390 | 1.20353143 | 1.93272080 | O | -3.20597243 | 0.98198071 | -3.13023123 |
| C | 3.11277004 | -0.78034620 | 1.36049285 | C | -2.59412952 | -1.14501363 | -2.17180634 |
| H | 3.69522060 | -1.70591650 | 1.48556766 | H | -2.59306195 | -1.20085022 | -1.07794695 |
| H | 2.11788771 | -1.02729057 | 1.74024967 | H | -3.04595749 | -2.09322312 | -2.49789375 |
| C | 3.09341588 | -0.38163503 | -0.09544582 | C | -1.20029984 | -1.02103752 | -2.73303296 |
| C | 4.43549337 | -0.40858917 | -0.78392891 | C | -1.10208605 | -1.21504381 | -4.22627479 |
| H | 5.12842077 | 0.28301014 | -0.29837634 | H | -1.51701736 | -2.18466570 | -4.52862886 |
| H | 4.88738740 | -1.40757596 | -0.73564039 | H | -1.66693116 | -0.44338276 | -4.75766501 |
| H | 4.35531071 | -0.12875325 | -1.83655722 | H | -0.06728633 | -1.17300005 | -4.57221865 |
| C | 1.98493395 | -0.02175825 | -0.75719765 | C | -0.10677071 | -0.78293408 | -1.99618607 |
| H | 2.11853216 | 0.23759168 | -1.80569504 | H | 0.83505610 | -0.74980680 | -2.54052586 |
| C | 0.56519923 | 0.06131659 | -0.25743199 | C | 0.01406895 | -0.54254070 | -0.51344492 |
| H | 0.54125236 | -0.13263049 | 0.81948692 | H | -0.96558788 | -0.65758115 | -0.03693133 |
| C | -0.08692740 | 1.41866891 | -0.47642205 | C | 0.96344632 | -1.51035644 | 0.17682322 |
| C | 0.04913939 | 2.13606772 | -1.67315526 | C | 2.22872517 | -1.82187508 | -0.34093892 |
| C | -0.87799895 | 1.98281524 | 0.53291020 | C | 0.59143168 | -2.11095294 | 1.38639444 |
| C | -0.57799088 | 3.36746475 | -1.85032227 | C | 3.08361965 | -2.69908444 | 0.32320184 |
| H | 0.65797605 | 1.73985963 | -2.47832989 | H | 2.55631411 | -1.38205418 | -1.27674791 |
| C | -1.50736471 | 3.21264577 | 0.35925550 | C | 1.44280200 | -2.98791031 | 2.05347733 |
| H | -1.00583156 | 1.44793868 | 1.46950167 | H | -0.38002879 | -1.88349840 | 1.81580662 |
| C | -1.36042475 | 3.91334013 | -0.83546290 | C | 2.69585776 | -3.28793456 | 1.52467779 |
| H | -0.44863372 | 3.90390795 | -2.78545417 | H | 4.05600878 | -2.92477431 | -0.10411009 |
| H | -2.11066048 | 3.62449752 | 1.16243450 | H | 1.12365911 | -3.43826711 | 2.98842513 |
| H | -1.84503279 | 4.87468165 | -0.97240473 | H | 3.36045671 | -3.97373099 | 2.04023653 |
| Si | -0.48817149 | -1.38138481 | -1.01678281 | Si | 0.46794898 | 1.31766238 | -0.17277696 |
| C | -0.59673499 | -1.20066602 | -2.89243997 | C | 2.06914165 | 1.76955158 | -1.06666724 |
| H | 0.39409254 | -1.22489840 | -3.35596675 | H | 1.98050315 | 1.62202759 | -2.14705749 |
| H | -1.17724235 | -2.02335924 | -3.32051191 | H | 2.30741145 | 2.82442202 | -0.90058112 |
| H | -1.07995917 | -0.26864682 | -3.19573973 | H | 2.92634418 | 1.18662419 | -0.72020593 |
| C | 0.36231358 | -3.01337836 | -0.59022746 | C | -0.94250884 | 2.39053786 | -0.81186575 |
| H | 1.35227973 | -3.06161626 | -1.05083063 | H | -1.13894772 | 2.19852344 | -1.86898099 |
| H | 0.50246233 | -3.14587372 | 0.48673228 | H | -1.88173138 | 2.20615977 | -0.28168544 |
| H | -0.21477598 | -3.86902753 | -0.95326202 | H | -0.70937370 | 3.45397686 | -0.70069817 |
| C | -2.22892116 | -1.36652271 | -0.27220784 | C | 0.68712907 | 1.59258745 | 1.68904621 |
| C | -3.20117433 | -0.44921850 | -0.70781733 | C | 1.82272860 | 1.11847801 | 2.36967883 |
| C | -2.60137301 | -2.27124795 | 0.73627329 | C | -0.27235608 | 2.28798377 | 2.44360517 |
| C | -4.48329876 | -0.43651906 | -0.16385696 | C | 1.99234117 | 1.33018637 | 3.73556844 |
| H | -2.95791377 | 0.27302092 | -1.48102788 | H | 2.58810870 | 0.56769166 | 1.83142563 |
| C | -3.88252746 | -2.26294629 | 1.28587926 | C | -0.10902177 | 2.50278498 | 3.81157106 |
| H | -1.88644663 | -3.00443691 | 1.09869144 | H | -1.16246101 | 2.67940304 | 1.96014329 |
| C | -4.82770074 | -1.34465983 | 0.83552699 | C | 1.02580228 | 2.02434766 | 4.46119205 |
| H | -5.21387426 | 0.28344174 | -0.51995017 | H | 2.87938908 | 0.95151429 | 4.23432321 |
| H | -4.14328948 | -2.97619729 | 2.06214680 | H | -0.86631257 | 3.04714470 | 4.36795994 |
| H | -5.82708458 | -1.33713916 | 1.25967629 | H | 1.15746964 | 2.19170200 | 5.52586002 |

**Table 4.7.2. (continued)**

| | *cis*-**4.81ac** | | | | *cis*-**4.81ad** | | |
|---|---|---|---|---|---|---|---|
| C | 1.60298791 | 4.95665642 | -1.90054942 | C | -4.21617069 | 0.36191470 | 3.60857839 |
| H | 1.70985791 | 5.00450842 | -0.81124842 | H | -5.07585036 | -0.31599385 | 3.56796318 |
| H | 2.60434591 | 4.79995742 | -2.31216142 | H | -3.56020052 | -0.00557520 | 4.40318649 |
| H | 1.20001291 | 5.90526342 | -2.25339942 | H | -4.57023986 | 1.36309889 | 3.85127262 |
| C | 0.65870591 | 3.82505642 | -2.27222942 | C | -3.51414837 | 0.37338658 | 2.26266112 |
| O | -0.46143409 | 4.04025342 | -2.66897042 | O | -3.59234086 | 1.32216071 | 1.51583777 |
| C | 1.23213591 | 2.41111942 | -2.10595842 | C | -2.70546141 | -0.88211399 | 1.92072019 |
| H | 2.01427391 | 2.31011742 | -2.87383042 | H | -1.84058656 | -0.88601851 | 2.59408179 |
| H | 1.77558491 | 2.37701442 | -1.15789742 | H | -3.30076054 | -1.75512954 | 2.22400434 |
| C | 0.23467691 | 1.28540742 | -2.24151942 | C | -2.29941988 | -1.00935011 | 0.47457855 |
| C | -0.24989509 | 1.02676642 | -3.64664142 | C | -3.44149860 | -1.27666749 | -0.47529619 |
| H | -0.75350109 | 1.91120442 | -4.04521342 | H | -3.98643697 | -2.18686992 | -0.19500485 |
| H | 0.58498091 | 0.79796442 | -4.32139842 | H | -4.16342088 | -0.45388296 | -0.46339119 |
| H | -0.95026809 | 0.18987542 | -3.68492042 | H | -3.09219234 | -1.39985025 | -1.50217228 |
| C | -0.21158909 | 0.55503242 | -1.21030742 | C | -1.04088641 | -0.91612774 | 0.02540773 |
| H | -0.92549409 | -0.23160958 | -1.44480642 | H | -0.90192332 | -1.04709517 | -1.04529841 |
| C | 0.13727791 | 0.66865142 | 0.25313558 | C | 0.23244831 | -0.64300945 | 0.78215021 |
| H | 0.68496391 | 1.60173342 | 0.42559758 | H | 0.03633127 | -0.65946438 | 1.86059194 |
| C | -1.08587409 | 0.70169942 | 1.15735858 | C | 1.31159301 | -1.67824966 | 0.50339703 |
| C | -2.07084409 | -0.29502058 | 1.11462658 | C | 1.74196351 | -1.96975632 | -0.79903985 |
| C | -1.24637809 | 1.73884442 | 2.08470158 | C | 1.92547503 | -2.35987292 | 1.56125517 |
| C | -3.17358609 | -0.25110358 | 1.96444158 | C | 2.74421560 | -2.90862418 | -1.03090856 |
| H | -1.97666209 | -1.11995758 | 0.41709258 | H | 1.29793142 | -1.45259317 | -1.64311129 |
| C | -2.34616809 | 1.78395642 | 2.93847458 | C | 2.93042529 | -3.29764644 | 1.33312942 |
| H | -0.50185509 | 2.52892842 | 2.13409658 | H | 1.60854401 | -2.15685672 | 2.58084861 |
| C | -3.31749909 | 0.78769942 | 2.88159358 | C | 3.34482702 | -3.57789654 | 0.03365566 |
| H | -3.92306209 | -1.03466958 | 1.90847658 | H | 3.05768160 | -3.11610073 | -2.04956519 |
| H | -2.44627109 | 2.60355542 | 3.64354758 | H | 3.38600011 | -3.81268835 | 2.17351534 |
| H | -4.17821509 | 0.82181542 | 3.54178658 | H | 4.12528409 | -4.30983046 | -0.14799913 |
| Si | 1.39511991 | -0.70326258 | 0.79409758 | Si | 0.86381672 | 1.16972075 | 0.46280353 |
| C | 3.01613091 | -0.40828058 | -0.13236042 | C | -0.21203833 | 2.35392769 | 1.46031665 |
| H | 3.46775391 | 0.54767742 | 0.15189558 | H | -0.09570867 | 2.17811458 | 2.53520002 |
| H | 3.74354091 | -1.19237358 | 0.09740158 | H | 0.08005636 | 3.39102280 | 1.26916744 |
| H | 2.87847891 | -0.39507758 | -1.21651542 | H | -1.27467635 | 2.26075871 | 1.22615949 |
| C | 1.70257891 | -0.54471058 | 2.64883358 | C | 2.65389430 | 1.30410608 | 1.04394097 |
| H | 2.12957291 | 0.43486342 | 2.88605058 | H | 2.73329419 | 1.08346832 | 2.11298758 |
| H | 0.78596891 | -0.64306558 | 3.23530458 | H | 3.31608939 | 0.60703644 | 0.52538688 |
| H | 2.41013491 | -1.30156658 | 3.00056758 | H | 3.04161390 | 2.31580029 | 0.89009769 |
| C | 0.74809791 | -2.43359958 | 0.38353758 | C | 0.74370582 | 1.60527304 | -1.37611098 |
| C | 0.78511791 | -2.92883158 | -0.93211342 | C | -0.49240652 | 1.95296998 | -1.95015803 |
| C | 0.21319791 | -3.27320258 | 1.37466358 | C | 1.87026315 | 1.60318716 | -2.21515366 |
| C | 0.30598991 | -4.19923058 | -1.24434042 | C | -0.59797587 | 2.27806019 | -3.30076864 |
| H | 1.19297091 | -2.31615258 | -1.73095342 | H | -1.38824121 | 1.97024661 | -1.33656302 |
| C | -0.26550509 | -4.54624858 | 1.06917758 | C | 1.77036979 | 1.92853212 | -3.56730805 |
| H | 0.16546091 | -2.93308158 | 2.40463858 | H | 2.84528602 | 1.34691537 | -1.81154055 |
| C | -0.22133309 | -5.01208358 | -0.24261042 | C | 0.53432830 | 2.26605941 | -4.11340106 |
| H | 0.34681391 | -4.55621958 | -2.26904942 | H | -1.56428330 | 2.54450522 | -3.71834424 |
| H | -0.67245809 | -5.17410558 | 1.85609558 | H | 2.65804621 | 1.92137461 | -4.19282377 |
| H | -0.59343209 | -6.00313458 | -0.48336942 | H | 0.45374611 | 2.52166910 | -5.16554024 |

**Table 4.7.2. (continued)**

| | *cis*-**4.81ae** | | | | *cis*-**4.81af** | | |
|---|---|---|---|---|---|---|---|
| C | 3.72397114 | -1.73692819 | 2.57206490 | C | -3.28480453 | -0.69543491 | 2.71551334 |
| H | 3.46221512 | -2.38466169 | 1.72848425 | H | -4.32370100 | -0.85468783 | 2.40610642 |
| H | 4.59559580 | -1.14891186 | 2.26921911 | H | -2.79714993 | -1.67455704 | 2.69878022 |
| H | 3.97226817 | -2.35914654 | 3.43126673 | H | -3.27689284 | -0.29020801 | 3.72669362 |
| C | 2.53716111 | -0.85170439 | 2.89966359 | C | -2.61557563 | 0.27608967 | 1.76081875 |
| O | 1.85078054 | -1.04220189 | 3.87612781 | O | -2.36044985 | 1.41264430 | 2.08937723 |
| C | 2.28013163 | 0.29584475 | 1.91049873 | C | -2.26964032 | -0.28338015 | 0.37873440 |
| H | 3.02503100 | 1.06931082 | 2.15349906 | H | -1.40334427 | -0.93440298 | 0.51469947 |
| H | 2.53663476 | -0.05214725 | 0.90711837 | H | -3.07279135 | -0.96747351 | 0.07522733 |
| C | 0.89216621 | 0.88495533 | 1.96339236 | C | -2.04664060 | 0.75329609 | -0.69115294 |
| C | 0.59257699 | 1.75173627 | 3.15826076 | C | -3.32803091 | 1.37356573 | -1.20008929 |
| H | 0.70751030 | 1.17897712 | 4.08171007 | H | -4.00112664 | 0.61362451 | -1.61547652 |
| H | 1.28929105 | 2.59746052 | 3.21340151 | H | -3.87002940 | 1.86861176 | -0.38658454 |
| H | -0.42167312 | 2.15502362 | 3.12178310 | H | -3.14259292 | 2.11884495 | -1.97535178 |
| C | -0.02471208 | 0.65447509 | 1.01509090 | C | -0.87028873 | 1.15515289 | -1.18697229 |
| H | -0.99378590 | 1.12952455 | 1.15886650 | H | -0.93997052 | 1.93290250 | -1.94930846 |
| C | 0.15726413 | -0.17629332 | -0.24734850 | C | 0.58598351 | 0.84169076 | -0.88752130 |
| H | 1.02634862 | 0.21287573 | -0.79729649 | H | 1.05159482 | 0.72109130 | -1.87781719 |
| C | 0.40359509 | -1.66031665 | -0.01877175 | C | 1.25930162 | 2.07395419 | -0.27657285 |
| C | 1.24952019 | -2.37946699 | -0.87607947 | C | 0.68797340 | 2.73790670 | 0.81785142 |
| C | -0.21679915 | -2.36121413 | 1.02429123 | C | 2.46268349 | 2.56787745 | -0.79580447 |
| C | 1.46277644 | -3.74556573 | -0.70544104 | C | 1.31083673 | 3.85075896 | 1.37807098 |
| H | 1.75238831 | -1.85942472 | -1.68716172 | H | -0.25925364 | 2.39414232 | 1.21993711 |
| C | -0.00583688 | -3.72744587 | 1.19749327 | C | 3.08682992 | 3.68041978 | -0.23448070 |
| H | -0.84862388 | -1.82528868 | 1.72394730 | H | 2.91520656 | 2.08013850 | -1.65478264 |
| C | 0.83228562 | -4.42858508 | 0.33296619 | C | 2.51374409 | 4.32602386 | 0.85821300 |
| H | 2.12604733 | -4.27512506 | -1.38281034 | H | 0.84796227 | 4.35112302 | 2.22317056 |
| H | -0.49231549 | -4.24275909 | 2.01979606 | H | 4.01716685 | 4.04625622 | -0.65843129 |
| H | 0.99873719 | -5.49197691 | 0.47154406 | H | 2.99507140 | 5.19529215 | 1.29515629 |
| Si | -1.32316769 | 0.09395858 | -1.45878004 | Si | 1.24194117 | -0.74253416 | 0.00359138 |
| C | -0.98262076 | -0.78615384 | -3.09315624 | C | 3.07579686 | -0.87338663 | -0.44085181 |
| H | -0.86275978 | -1.86368134 | -2.95432082 | H | 3.64729598 | -0.01917593 | -0.06915403 |
| H | -1.81217979 | -0.63010375 | -3.78935560 | H | 3.50698885 | -1.77807541 | -0.00113238 |
| H | -0.07780470 | -0.41483327 | -3.58373174 | H | 3.23140456 | -0.93710944 | -1.52198082 |
| C | -2.91284482 | -0.57634268 | -0.69619645 | C | 1.13174268 | -0.66352719 | 1.88809721 |
| H | -2.83306877 | -1.65415131 | -0.53138749 | H | 1.63537525 | 0.23690125 | 2.24952106 |
| H | -3.14836895 | -0.11875487 | 0.26869296 | H | 0.11467389 | -0.64037792 | 2.28379550 |
| H | -3.76899227 | -0.41028365 | -1.35702974 | H | 1.64249278 | -1.51907181 | 2.34103251 |
| C | -1.48671892 | 1.95485542 | -1.77954052 | C | 0.38584221 | -2.30191383 | -0.66304858 |
| C | -0.46757328 | 2.65586290 | -2.44733908 | C | -0.12699213 | -2.35637348 | -1.97011347 |
| C | -2.61138809 | 2.68811035 | -1.36940641 | C | 0.30248849 | -3.47145222 | 0.11184159 |
| C | -0.56389009 | 4.02281721 | -2.69351503 | C | -0.69511244 | -3.52179191 | -2.48044370 |
| H | 0.42139137 | 2.12941380 | -2.78691422 | H | -0.09747403 | -1.47305937 | -2.60120740 |
| C | -2.71544911 | 4.05736517 | -1.61240198 | C | -0.26561804 | -4.64055657 | -0.39200947 |
| H | -3.42572432 | 2.18779647 | -0.85346175 | H | 0.68433070 | -3.47715044 | 1.12929371 |
| C | -1.69115507 | 4.72813436 | -2.27517141 | C | -0.76616539 | -4.66825079 | -1.69155063 |
| H | 0.23882444 | 4.53850000 | -3.21203802 | H | -1.08520138 | -3.53435120 | -3.49377284 |
| H | -3.59727211 | 4.59960877 | -1.28452134 | H | -0.31649103 | -5.52942648 | 0.22975773 |
| H | -1.76990386 | 5.79396786 | -2.46573270 | H | -1.20900879 | -5.57705821 | -2.08716341 |

**Table 4.7.2. (continued).**

| | *cis*-**4.81ag** | | | | *cis*-**4.81ah** | | |
|---|---|---|---|---|---|---|---|
| C | 0.86797365 | 4.16512714 | -1.60043703 | C | -3.31790320 | 2.13203886 | -2.21325328 |
| H | 0.97074665 | 4.17521514 | -0.50976403 | H | -3.85531987 | 1.43096525 | -2.85723512 |
| H | 1.86644765 | 3.99042814 | -2.01141203 | H | -3.60309318 | 1.90877163 | -1.17927133 |
| H | 0.49509065 | 5.13586114 | -1.92535003 | H | -3.61888326 | 3.15475713 | -2.43837812 |
| C | -0.10709935 | 3.07369314 | -2.01141703 | C | -1.81201661 | 1.99526992 | -2.34574207 |
| O | -1.21838735 | 3.33523514 | -2.40747603 | O | -1.08697775 | 2.96370526 | -2.32953783 |
| C | 0.42346165 | 1.64117414 | -1.88571703 | C | -1.29204319 | 0.56005889 | -2.47806562 |
| H | 1.20468165 | 1.53658814 | -2.65329003 | H | -1.79376032 | -0.04326484 | -1.71551574 |
| H | 0.96750565 | 1.55632514 | -0.94179103 | H | -1.68497695 | 0.18286850 | -3.43513267 |
| C | -0.60685735 | 0.55160814 | -2.05865703 | C | 0.20646117 | 0.39039323 | -2.44910988 |
| C | -1.08254435 | 0.33681614 | -3.47361303 | C | 0.93824880 | 0.96591382 | -3.63744878 |
| H | -1.55286035 | 1.24521314 | -3.85925903 | H | 0.56665881 | 0.53007715 | -4.57353484 |
| H | -0.24672635 | 0.09554714 | -4.14247603 | H | 0.78797543 | 2.04593601 | -3.70457173 |
| H | -1.80944035 | -0.47585286 | -3.53766103 | H | 2.01123509 | 0.77051088 | -3.58245361 |
| C | -1.08698935 | -0.18656386 | -1.04896803 | C | 0.87273777 | -0.25802612 | -1.48310101 |
| H | -1.81832035 | -0.94863486 | -1.31067103 | H | 1.95100598 | -0.32834134 | -1.61459836 |
| C | -0.75279035 | -0.10863786 | 0.41995597 | C | 0.35077335 | -0.94289191 | -0.24403740 |
| H | -0.22295835 | 0.82710514 | 0.62439597 | H | -0.73890828 | -0.85316342 | -0.20059442 |
| C | -1.97616335 | -0.13143886 | 1.32337297 | C | 0.68137022 | -2.42942486 | -0.22623011 |
| C | -2.98580935 | -1.09599486 | 1.19624597 | C | 1.98198869 | -2.91004398 | -0.43479987 |
| C | -2.11094435 | 0.81832714 | 2.34429997 | C | -0.32550931 | -3.36922101 | 0.02734303 |
| C | -4.08358935 | -1.10792386 | 2.05352097 | C | 2.26193875 | -4.27372876 | -0.39234260 |
| H | -2.92366135 | -1.84739886 | 0.41615197 | H | 2.79073255 | -2.21552345 | -0.63781001 |
| C | -3.20529035 | 0.80825614 | 3.20565697 | C | -0.04956353 | -4.73395086 | 0.07294957 |
| H | -1.34972235 | 1.58489414 | 2.46105697 | H | -1.34428729 | -3.02673354 | 0.18785631 |
| C | -4.19927035 | -0.15689986 | 3.06468097 | C | 1.24773351 | -5.19429984 | -0.13713785 |
| H | -4.85281835 | -1.86380986 | 1.92782597 | H | 3.27817828 | -4.61731318 | -0.56014090 |
| H | -3.28381435 | 1.56174614 | 3.98341597 | H | -0.85251756 | -5.43826989 | 0.26831452 |
| H | -5.05580835 | -0.16510986 | 3.73092197 | H | 1.46596600 | -6.25683436 | -0.10512948 |
| Si | 0.51866165 | -1.48474186 | 0.91939597 | Si | 0.95511440 | -0.06665830 | 1.38591474 |
| C | 0.76259065 | -1.45710686 | 2.79055997 | C | 0.86218011 | -1.28406059 | 2.82455628 |
| H | -0.15969235 | -1.73765686 | 3.30560097 | H | 1.53412670 | -2.12974873 | 2.65940485 |
| H | 1.54278565 | -2.16097586 | 3.09567897 | H | 1.15791270 | -0.80670430 | 3.76390652 |
| H | 1.04609265 | -0.46901086 | 3.16442197 | H | -0.14095996 | -1.69720492 | 2.96298150 |
| C | -0.08875035 | -3.19017386 | 0.38347997 | C | 2.73570581 | 0.53138398 | 1.18751552 |
| H | -0.99236735 | -3.47862786 | 0.92720497 | H | 3.42013806 | -0.28998605 | 0.95496872 |
| H | -0.31724735 | -3.23958886 | -0.68453003 | H | 2.83369653 | 1.28056273 | 0.39762704 |
| H | 0.67197465 | -3.94891186 | 0.59012697 | H | 3.08443104 | 0.99206039 | 2.11667673 |
| C | 2.16568265 | -1.10213786 | 0.06233497 | C | -0.17796478 | 1.40886658 | 1.73950111 |
| C | 3.14957065 | -0.31985786 | 0.69083197 | C | -0.98538029 | 1.45053120 | 2.88921000 |
| C | 2.44461565 | -1.56929886 | -1.23333903 | C | -0.24479231 | 2.50461887 | 0.86093163 |
| C | 4.35252165 | -0.01267186 | 0.05683897 | C | -1.81832898 | 2.53663927 | 3.15398549 |
| H | 2.98476565 | 0.05282014 | 1.69816597 | H | -0.96548218 | 0.62633334 | 3.59601481 |
| C | 3.64537065 | -1.26763586 | -1.87299103 | C | -1.08113909 | 3.58972542 | 1.11647094 |
| H | 1.71591665 | -2.18125186 | -1.75604503 | H | 0.34801274 | 2.51471068 | -0.04762825 |
| C | 4.60301165 | -0.48625286 | -1.22918503 | C | -1.86774113 | 3.60968783 | 2.26698489 |
| H | 5.09654665 | 0.58981514 | 0.56936197 | H | -2.42776876 | 2.54463525 | 4.05289873 |
| H | 3.83593865 | -1.64649686 | -2.87269303 | H | -1.11892801 | 4.41285892 | 0.41042519 |
| H | 5.54062765 | -0.25312386 | -1.72430803 | H | -2.51599203 | 4.45667680 | 2.47056866 |

**Table 4.7.2. (continued).**

| | *trans*-**4.81aa** | | | | *trans*-**4.81ab** | | |
|---|---|---|---|---|---|---|---|
| C | 5.86513508 | 2.64728534 | -0.43665147 | C | -0.24417530 | 5.92351532 | 2.65051204 |
| H | 6.39162597 | 1.81783818 | -0.91766059 | H | 0.11948670 | 5.84106932 | 3.67888304 |
| H | 5.94117403 | 3.50617898 | -1.11250825 | H | 0.62785870 | 6.12576332 | 2.01888904 |
| H | 6.34964640 | 2.89942382 | 0.50590229 | H | -0.93740530 | 6.75965632 | 2.56619904 |
| C | 4.40253286 | 2.31842115 | -0.19562870 | C | -0.92018930 | 4.64372632 | 2.18727804 |
| O | 3.86479634 | 2.56184499 | 0.86011495 | O | -1.96566630 | 4.66510832 | 1.58186204 |
| C | 3.66513213 | 1.65732678 | -1.36625828 | C | -0.17933630 | 3.34756332 | 2.53935004 |
| H | 3.94505709 | 2.18910173 | -2.28656084 | H | 0.88747170 | 3.50722332 | 2.34668604 |
| H | 4.09351790 | 0.65262729 | -1.47461931 | H | -0.25779530 | 3.24057132 | 3.63294704 |
| C | 2.16577965 | 1.58753502 | -1.21026290 | C | -0.67106430 | 2.09557132 | 1.84880804 |
| C | 1.45241002 | 2.90589755 | -1.36134921 | C | -2.02585130 | 1.60857232 | 2.29212204 |
| H | 1.70097210 | 3.58013836 | -0.53550243 | H | -2.01896930 | 1.36343132 | 3.36160604 |
| H | 1.75929124 | 3.40754180 | -2.28672171 | H | -2.77183330 | 2.39260732 | 2.14516504 |
| H | 0.36745375 | 2.80487190 | -1.38942371 | H | -2.35966230 | 0.72025332 | 1.75617704 |
| C | 1.57918179 | 0.41491934 | -0.93512850 | C | 0.10299070 | 1.50859432 | 0.92487704 |
| H | 2.23478139 | -0.45045170 | -0.85673293 | H | 1.06178870 | 1.98181032 | 0.72042204 |
| C | 0.12447916 | 0.13275540 | -0.67337100 | C | -0.17002530 | 0.26129832 | 0.12511704 |
| H | -0.47392664 | 1.00076174 | -0.96745492 | H | -1.22048330 | -0.02212468 | 0.24093104 |
| C | -0.41216505 | -1.06747776 | -1.43504187 | C | 0.08534270 | 0.42530032 | -1.36528996 |
| C | 0.25482152 | -2.30086147 | -1.46383218 | C | 1.25483170 | 1.01107632 | -1.87053096 |
| C | -1.62720289 | -0.97109731 | -2.12564838 | C | -0.85947230 | -0.03977368 | -2.28905096 |
| C | -0.27109478 | -3.38966544 | -2.15589715 | C | 1.46709170 | 1.13010632 | -3.24241596 |
| H | 1.19748403 | -2.42107391 | -0.94031198 | H | 2.01318870 | 1.38535732 | -1.19088396 |
| C | -2.15748461 | -2.05738393 | -2.81694915 | C | -0.65011230 | 0.07490832 | -3.66078496 |
| H | -2.16865509 | -0.02968118 | -2.11846532 | H | -1.77406830 | -0.49958768 | -1.92664296 |
| C | -1.48119889 | -3.27475130 | -2.83654738 | C | 0.51583570 | 0.66222032 | -4.14608896 |
| H | 0.26938420 | -4.33147887 | -2.16266440 | H | 2.37985270 | 1.59332832 | -3.60492296 |
| H | -3.10086385 | -1.94941978 | -3.34339490 | H | -1.40350930 | -0.29246568 | -4.35076796 |
| H | -1.88985668 | -4.12248573 | -3.37710680 | H | 0.67976270 | 0.75769032 | -5.21465996 |
| Si | -0.17947154 | 0.00947024 | 1.24454517 | Si | 0.79384270 | -1.24861068 | 0.87135304 |
| C | 0.81493698 | -1.41869153 | 1.97820767 | C | 2.65844070 | -0.96959168 | 0.75999204 |
| H | 1.88603594 | -1.29912646 | 1.78974932 | H | 2.95695870 | -0.05419368 | 1.28015904 |
| H | 0.67792280 | -1.45232582 | 3.06324262 | H | 3.19526670 | -1.80030668 | 1.22787404 |
| H | 0.51123343 | -2.39112568 | 1.58305434 | H | 3.01171470 | -0.89419168 | -0.27112596 |
| C | 0.37405672 | 1.63263379 | 2.02543867 | C | 0.30361770 | -1.42275368 | 2.68669604 |
| H | 1.43368604 | 1.81704893 | 1.83158758 | H | 0.62272570 | -0.54478068 | 3.25415004 |
| H | -0.17830495 | 2.49301391 | 1.63590431 | H | -0.77679030 | -1.52017368 | 2.82515804 |
| H | 0.23040217 | 1.61573505 | 3.11028450 | H | 0.77521970 | -2.29949768 | 3.14061204 |
| C | -2.02463008 | -0.26608501 | 1.57688614 | C | 0.32284570 | -2.82468568 | -0.06548696 |
| C | -2.64508501 | -1.49988913 | 1.31220762 | C | 0.84734370 | -3.10284868 | -1.33990396 |
| C | -2.82709524 | 0.75887206 | 2.10549682 | C | -0.57328230 | -3.75815468 | 0.48181604 |
| C | -4.00041288 | -1.69979609 | 1.56316351 | C | 0.49390970 | -4.25739268 | -2.03407996 |
| H | -2.06807281 | -2.32035972 | 0.89659919 | H | 1.53828870 | -2.40728868 | -1.80648796 |
| C | -4.18435473 | 0.56514868 | 2.35899849 | C | -0.93168930 | -4.91520168 | -0.20821296 |
| H | -2.38934218 | 1.72652484 | 2.33216407 | H | -0.99881230 | -3.58873768 | 1.46674304 |
| C | -4.77459392 | -0.66650232 | 2.08797415 | C | -0.39773330 | -5.16744968 | -1.46937396 |
| H | -4.45279702 | -2.66319817 | 1.34797076 | H | 0.91357170 | -4.44594168 | -3.01759196 |
| H | -4.77896298 | 1.37521576 | 2.77085802 | H | -1.62499730 | -5.62027168 | 0.24062604 |
| H | -5.83093332 | -0.82154985 | 2.28548630 | H | -0.67348530 | -6.06833168 | -2.00894296 |

**Table 4.7.2. (continued).**

| | *trans*-**4.81ac** | | | | *trans*-**4.81ad** | | |
|---|---|---|---|---|---|---|---|
| C | 2.99695389 | 4.68864780 | 0.48008111 | C | -0.69024487 | 5.51359688 | 1.56348610 |
| H | 3.11545889 | 4.62445280 | 1.56565711 | H | -0.55913587 | 5.49291488 | 2.64930210 |
| H | 4.00221589 | 4.79324580 | 0.05721111 | H | 0.31193413 | 5.51447888 | 1.12092610 |
| H | 2.41342689 | 5.57109480 | 0.22014811 | H | -1.20331087 | 6.42785888 | 1.26721210 |
| C | 2.33630089 | 3.44403280 | -0.08322389 | C | -1.46267187 | 4.30340788 | 1.06557710 |
| O | 1.43867189 | 3.51530680 | -0.89238989 | O | -2.34667587 | 4.41116288 | 0.24867610 |
| C | 2.86496689 | 2.10615280 | 0.44861711 | C | -1.03547787 | 2.95932088 | 1.66874610 |
| H | 3.95948589 | 2.17235380 | 0.51735211 | H | 0.05921813 | 2.94014088 | 1.71053410 |
| H | 2.51504689 | 2.03236580 | 1.48661111 | H | -1.36100687 | 2.98297088 | 2.72097110 |
| C | 2.43305989 | 0.89988680 | -0.34843489 | C | -1.56872687 | 1.72561988 | 0.97554310 |
| C | 3.15932489 | 0.71329280 | -1.65513689 | C | -3.04837387 | 1.48880988 | 1.13118810 |
| H | 2.94826689 | 1.53832880 | -2.34385189 | H | -3.31519187 | 1.37604388 | 2.18950210 |
| H | 4.24426289 | 0.70197180 | -1.49615789 | H | -3.60652187 | 2.34566988 | 0.74779110 |
| H | 2.89313889 | -0.21290620 | -2.16409789 | H | -3.39672187 | 0.59657088 | 0.61139210 |
| C | 1.44699489 | 0.11933780 | 0.11267211 | C | -0.72149887 | 0.94237488 | 0.29270510 |
| H | 1.02026189 | 0.38757180 | 1.07709611 | H | 0.32385913 | 1.24407788 | 0.27686710 |
| C | 0.79322989 | -1.06126520 | -0.55099789 | C | -1.01573087 | -0.32479812 | -0.46727390 |
| H | 1.41231089 | -1.39979720 | -1.38885989 | H | -2.09918987 | -0.43431512 | -0.58354290 |
| C | 0.59179289 | -2.24653220 | 0.37721611 | C | -0.41279487 | -0.33995412 | -1.86313790 |
| C | -0.07890211 | -2.12856420 | 1.60314811 | C | 0.94981713 | -0.10029312 | -2.09073490 |
| C | 1.06518989 | -3.51339020 | 0.01268211 | C | -1.22032787 | -0.61864912 | -2.97316490 |
| C | -0.26309711 | -3.23385520 | 2.43061211 | C | 1.48003913 | -0.13538012 | -3.37843190 |
| H | -0.47356311 | -1.16699020 | 1.91327411 | H | 1.60975913 | 0.10899688 | -1.25578890 |
| C | 0.87926289 | -4.62166320 | 0.83598311 | C | -0.69260887 | -0.65820312 | -4.26171290 |
| H | 1.59407889 | -3.63297020 | -0.92904789 | H | -2.28166487 | -0.79976312 | -2.82688690 |
| C | 0.21419789 | -4.48700220 | 2.05207311 | C | 0.66255813 | -0.41550912 | -4.47124490 |
| H | -0.78576211 | -3.11363120 | 3.37476011 | H | 2.53852313 | 0.05630988 | -3.52621390 |
| H | 1.26042689 | -5.59048020 | 0.52747911 | H | -1.34482887 | -0.87186712 | -5.10305590 |
| H | 0.07033889 | -5.34741120 | 2.69777911 | H | 1.07630313 | -0.44097012 | -5.47425690 |
| Si | -0.85516111 | -0.49701820 | -1.41323889 | Si | -0.51398387 | -1.89094612 | 0.55912510 |
| C | -0.38820811 | 0.64541180 | -2.83902589 | C | -1.60309587 | -1.95057812 | 2.10141910 |
| H | 0.22569389 | 0.12305280 | -3.57976289 | H | -2.65991087 | -2.04968912 | 1.83489610 |
| H | -1.28254211 | 1.00926680 | -3.35379889 | H | -1.34181087 | -2.80706012 | 2.72990910 |
| H | 0.17429289 | 1.51727580 | -2.49677789 | H | -1.50652787 | -1.05031212 | 2.71357110 |
| C | -1.74214711 | -2.02632020 | -2.07527689 | C | -0.82307887 | -3.42847512 | -0.49009790 |
| H | -1.12130611 | -2.54502420 | -2.81257089 | H | -1.88378387 | -3.51345112 | -0.74642590 |
| H | -1.97633311 | -2.74899120 | -1.28974289 | H | -0.26872687 | -3.40885912 | -1.43128390 |
| H | -2.67877111 | -1.75450820 | -2.57142689 | H | -0.54340587 | -4.34015912 | 0.04640210 |
| C | -1.97433711 | 0.43244080 | -0.20166289 | C | 1.30437813 | -1.81441712 | 1.08335010 |
| C | -1.75747411 | 1.79406780 | 0.07883211 | C | 1.70354013 | -1.04975512 | 2.19382010 |
| C | -3.05386211 | -0.19879920 | 0.43878211 | C | 2.30558413 | -2.51095212 | 0.38596510 |
| C | -2.58128211 | 2.48930980 | 0.96228011 | C | 3.03828313 | -0.97908912 | 2.58722010 |
| H | -0.93761711 | 2.32436680 | -0.39610989 | H | 0.96179113 | -0.50041612 | 2.76630810 |
| C | -3.88021811 | 0.49319180 | 1.32281111 | C | 3.64254613 | -2.44600312 | 0.77532110 |
| H | -3.25900011 | -1.24773520 | 0.24700911 | H | 2.04352113 | -3.11565612 | -0.47692490 |
| C | -3.64485211 | 1.84055280 | 1.58691111 | C | 4.01242613 | -1.67803212 | 1.87706010 |
| H | -2.39481511 | 3.54102680 | 1.15846411 | H | 3.31800913 | -0.38254012 | 3.45048710 |
| H | -4.70953111 | -0.01870120 | 1.80200011 | H | 4.39514913 | -2.99648312 | 0.21886510 |
| H | -4.28914411 | 2.38286180 | 2.27235011 | H | 5.05293713 | -1.62712812 | 2.18269410 |

**Table 4.7.2. (continued).**

| | *trans*-**4.81ae** | | | | *trans*-**4.81af** | | |
|---|---|---|---|---|---|---|---|
| C | 1.78092281 | 5.59850593 | 2.63467017 | C | 1.23107310 | 5.63027275 | 2.73532789 |
| H | 1.51118281 | 5.36811293 | 3.66955017 | H | 0.80001710 | 5.69894675 | 3.74011189 |
| H | 2.87314481 | 5.67407693 | 2.60070517 | H | 2.31554510 | 5.56047475 | 2.85939689 |
| H | 1.35159481 | 6.55712193 | 2.34606917 | H | 0.97796110 | 6.53428475 | 2.18273289 |
| C | 1.30812781 | 4.51480593 | 1.68194417 | C | 0.66912810 | 4.41413675 | 2.02030189 |
| O | 0.69769881 | 4.78137693 | 0.67248817 | O | -0.12413690 | 4.52457875 | 1.11381289 |
| C | 1.65344981 | 3.07524093 | 2.08233817 | C | 1.17213310 | 3.05570275 | 2.52193289 |
| H | 2.72599381 | 3.04517193 | 2.32422517 | H | 2.24861210 | 3.02084975 | 2.31415489 |
| H | 1.13986581 | 2.87501593 | 3.03067217 | H | 1.09302110 | 3.05686775 | 3.61879989 |
| C | 1.30049181 | 2.03458193 | 1.04754017 | C | 0.47161610 | 1.85622075 | 1.92831989 |
| C | 2.17526681 | 2.03976293 | -0.17810383 | C | -0.96229490 | 1.68728975 | 2.35762589 |
| H | 2.22222881 | 3.04282793 | -0.61114683 | H | -1.04236590 | 1.69566575 | 3.45164089 |
| H | 3.20405481 | 1.75285693 | 0.07547017 | H | -1.57233090 | 2.51811675 | 1.99038289 |
| H | 1.81654381 | 1.37019093 | -0.95644783 | H | -1.40249890 | 0.75635875 | 2.00852789 |
| C | 0.26487381 | 1.21188993 | 1.25818317 | C | 1.13450410 | 1.05437575 | 1.08363789 |
| H | -0.26002519 | 1.33909193 | 2.20473117 | H | 2.16744210 | 1.33519075 | 0.87927389 |
| C | -0.31290019 | 0.11897993 | 0.38078817 | C | 0.68242710 | -0.17415925 | 0.31669489 |
| H | -1.10223619 | -0.34604007 | 0.98530417 | H | 1.52414610 | -0.42181325 | -0.34261011 |
| C | -1.01812619 | 0.57830593 | -0.90024383 | C | 0.43439410 | -1.44610725 | 1.12879089 |
| C | -0.96625819 | 1.89545693 | -1.36988383 | C | 0.27295510 | -1.45186525 | 2.51851989 |
| C | -1.79128719 | -0.34348807 | -1.62566383 | C | 0.39588910 | -2.68525325 | 0.46747989 |
| C | -1.64034019 | 2.26934093 | -2.53348983 | C | 0.05708510 | -2.64029825 | 3.21700989 |
| H | -0.42315919 | 2.64974693 | -0.81419583 | H | 0.34373810 | -0.52331025 | 3.06964389 |
| C | -2.46243719 | 0.02918893 | -2.78595083 | C | 0.17881210 | -3.87113725 | 1.16152689 |
| H | -1.88129919 | -1.36523207 | -1.27092883 | H | 0.54585210 | -2.72190625 | -0.60597411 |
| C | -2.38550519 | 1.34072093 | -3.25228183 | C | 0.00168310 | -3.85624525 | 2.54420889 |
| H | -1.58403519 | 3.30042493 | -2.86922383 | H | -0.06034190 | -2.61002525 | 4.29627289 |
| H | -3.05345719 | -0.70728707 | -3.32229883 | H | 0.15658710 | -4.81135025 | 0.61873689 |
| H | -2.90875019 | 1.63459293 | -4.15677883 | H | -0.16601590 | -4.78036525 | 3.08816089 |
| Si | 0.87897381 | -1.40699707 | 0.13280317 | Si | -0.69386690 | 0.20421475 | -1.02027511 |
| C | 1.81392981 | -1.39475007 | -1.50754683 | C | -2.45697390 | -0.07812625 | -0.40489311 |
| H | 2.61411981 | -0.65175307 | -1.50912283 | H | -2.79590090 | 0.73643975 | 0.23786389 |
| H | 2.28412181 | -2.36681707 | -1.68583883 | H | -3.14801290 | -0.12176925 | -1.25237811 |
| H | 1.16167481 | -1.17841007 | -2.35719683 | H | -2.56136290 | -1.01073525 | 0.15606589 |
| C | 2.11120681 | -1.47767807 | 1.56406017 | C | -0.48574990 | 1.97780175 | -1.62437011 |
| H | 2.79240381 | -0.62335407 | 1.55521517 | H | -0.60773490 | 2.70602675 | -0.81940411 |
| H | 1.61276781 | -1.48279907 | 2.53761917 | H | 0.50328610 | 2.14790175 | -2.06085411 |
| H | 2.71285581 | -2.38962607 | 1.50119017 | H | -1.22274590 | 2.20052975 | -2.40246011 |
| C | -0.18384719 | -2.98143807 | 0.21900517 | C | -0.38509590 | -0.95715525 | -2.49513611 |
| C | -0.30513219 | -3.86813107 | -0.86270683 | C | -1.27004990 | -1.99366825 | -2.83324311 |
| C | -0.87750319 | -3.30632407 | 1.39780017 | C | 0.75328310 | -0.79501125 | -3.30379611 |
| C | -1.08252319 | -5.02273307 | -0.77516083 | C | -1.03124890 | -2.83009025 | -3.92318011 |
| H | 0.20892581 | -3.65711407 | -1.79552983 | H | -2.16158290 | -2.16020325 | -2.23637711 |
| C | -1.65578319 | -4.45713507 | 1.49372117 | C | 0.99965910 | -1.62621325 | -4.39404711 |
| H | -0.81159519 | -2.65296807 | 2.26479117 | H | 1.46473110 | -0.00153825 | -3.08718211 |
| C | -1.76054319 | -5.32008407 | 0.40413617 | C | 0.10540510 | -2.64858625 | -4.70690311 |
| H | -1.15859219 | -5.68932107 | -1.62901183 | H | -1.73409590 | -3.62329825 | -4.16011511 |
| H | -2.17990519 | -4.68178407 | 2.41783317 | H | 1.88682110 | -1.47464025 | -5.00167411 |
| H | -2.36668119 | -6.21788007 | 0.47498417 | H | 0.29325810 | -3.29753825 | -5.55669511 |

**Table 4.7.2. (continued).**

| | *trans*-**4.81ag** | | | | *trans*-**4.81ah** | | |
|---|---|---|---|---|---|---|---|
| C | 2.69193107 | 4.58779471 | 1.85263784 | C | 0.36178150 | 5.58167067 | 1.24339844 |
| H | 2.77478507 | 4.43741971 | 2.93299984 | H | 0.46994650 | 5.54224067 | 2.33120144 |
| H | 3.71354307 | 4.62918571 | 1.45903584 | H | 1.37286250 | 5.61129667 | 0.82270644 |
| H | 2.19756207 | 5.53616971 | 1.64529984 | H | -0.16304550 | 6.49150767 | 0.95421244 |
| C | 1.93755007 | 3.45196471 | 1.18544284 | C | -0.37733350 | 4.36701467 | 0.70563544 |
| O | 1.07871907 | 3.66372871 | 0.35978484 | O | -1.24944750 | 4.47537467 | -0.12360556 |
| C | 2.32312107 | 2.03931971 | 1.63733484 | C | 0.07071350 | 3.01914067 | 1.28349044 |
| H | 3.41474907 | 2.00754771 | 1.75904284 | H | 1.16663350 | 3.01004767 | 1.29912844 |
| H | 1.92001707 | 1.92553771 | 2.65222584 | H | -0.22865850 | 3.02520667 | 2.34333244 |
| C | 1.84849607 | 0.91700071 | 0.74460984 | C | -0.46999250 | 1.78911467 | 0.59075144 |
| C | 2.59812607 | 0.78409371 | -0.55494816 | C | -1.94278350 | 1.54068367 | 0.78227344 |
| H | 2.47613707 | 1.68195571 | -1.16865316 | H | -2.17419050 | 1.39569467 | 1.84417744 |
| H | 3.67278107 | 0.66330071 | -0.37074216 | H | -2.51642250 | 2.40327667 | 0.43561344 |
| H | 2.26547607 | -0.06081229 | -1.15640516 | H | -2.30104850 | 0.65825467 | 0.25353244 |
| C | 0.83743507 | 0.13390171 | 1.14377184 | C | 0.36547150 | 1.01261667 | -0.11334056 |
| H | 0.39957507 | 0.36349571 | 2.11364984 | H | 1.40880050 | 1.32111467 | -0.15059956 |
| C | 0.20187307 | -1.03207029 | 0.43311384 | C | 0.05564950 | -0.25728733 | -0.86292856 |
| H | 0.83314107 | -1.33508929 | -0.40777916 | H | -1.02884450 | -0.36001233 | -0.96576556 |
| C | 0.02728507 | -2.24760029 | 1.33028184 | C | 0.64667550 | -0.30190033 | -2.26353756 |
| C | -0.59496893 | -2.17212229 | 2.58473284 | C | 1.99160650 | -0.00217833 | -2.52328856 |
| C | 0.47188307 | -3.50499229 | 0.90169784 | C | -0.15515450 | -0.67908833 | -3.34885956 |
| C | -0.76422793 | -3.30594629 | 3.37592884 | C | 2.51116950 | -0.07662433 | -3.81362756 |
| H | -0.95507993 | -1.21769029 | 2.95500484 | H | 2.64758250 | 0.29672567 | -1.71242056 |
| C | 0.30198107 | -4.64203129 | 1.68817584 | C | 0.36091750 | -0.75772433 | -4.64000656 |
| H | 0.96476507 | -3.59346529 | -0.06257716 | H | -1.20406050 | -0.90658633 | -3.18016556 |
| C | -0.31789093 | -4.54861129 | 2.93174184 | C | 1.69936150 | -0.45657933 | -4.87987156 |
| H | -1.24832093 | -3.21644229 | 4.34376984 | H | 3.55576750 | 0.16512667 | -3.98514156 |
| H | 0.66052507 | -5.60193829 | 1.32905584 | H | -0.28788350 | -1.04772433 | -5.46084956 |
| H | -0.44940493 | -5.43194029 | 3.54828884 | H | 2.10380150 | -0.51262533 | -5.88533056 |
| Si | -1.47624393 | -0.51830829 | -0.40903516 | Si | 0.57357450 | -1.81454233 | 0.16957044 |
| C | -2.44207293 | -2.07890229 | -0.85118116 | C | 0.27165250 | -3.36583833 | -0.86288756 |
| H | -2.72972593 | -2.62506729 | 0.05063484 | H | 0.93430350 | -3.38840333 | -1.73182756 |
| H | -3.35850393 | -1.83221229 | -1.39605716 | H | 0.45859450 | -4.27083933 | -0.27709656 |
| H | -1.86468293 | -2.77117729 | -1.47072016 | H | -0.75239650 | -3.42548033 | -1.24263756 |
| C | -2.50143393 | 0.54605771 | 0.76660084 | C | 2.39769050 | -1.72132733 | 0.65017444 |
| H | -2.76001593 | 0.00807071 | 1.68343684 | H | 3.04164350 | -1.78346333 | -0.23119956 |
| H | -1.98034993 | 1.46365271 | 1.05164684 | H | 2.64821350 | -0.79618833 | 1.17650444 |
| H | -3.43939593 | 0.84145571 | 0.28693484 | H | 2.66411850 | -2.55357933 | 1.30852144 |
| C | -1.09636893 | 0.45806871 | -1.98503616 | C | -0.48865750 | -1.88110133 | 1.73670144 |
| C | -1.27113093 | -0.11326929 | -3.25694516 | C | -1.71669450 | -2.56335233 | 1.75451844 |
| C | -0.62583193 | 1.78211371 | -1.92618416 | C | -0.09122650 | -1.23916333 | 2.92168644 |
| C | -0.99098293 | 0.60174271 | -4.42048216 | C | -2.51380950 | -2.60069633 | 2.89718644 |
| H | -1.63604993 | -1.13213829 | -3.34922816 | H | -2.06142450 | -3.08344333 | 0.86498844 |
| C | -0.34382793 | 2.49976871 | -3.08689716 | C | -0.88221450 | -1.27262733 | 4.06841744 |
| H | -0.45104593 | 2.26436871 | -0.97075216 | H | 0.85328750 | -0.70440933 | 2.95712744 |
| C | -0.52704593 | 1.91249371 | -4.33748316 | C | -2.09794050 | -1.95352933 | 4.05847744 |
| H | -1.13810493 | 0.13609971 | -5.39059216 | H | -3.45721650 | -3.13816533 | 2.88203044 |
| H | 0.02022207 | 3.51968571 | -3.00887916 | H | -0.54790350 | -0.77090733 | 4.97171844 |
| H | -0.30979593 | 2.47265771 | -5.24204216 | H | -2.71511950 | -1.98297533 | 4.95112744 |

### *4.7.3. Enantioselectivity Models Based on DFT Calculations*

In order to find a structural basis for the enantioselectivity of the NHC–Cu-catalyzed silyl conjugate additions, three representative substrates: **4.72a**, **4.80a**, and **4.92g**, in complex with three NHC–Cu-$SiMe_2Ph$, were studied using Density Functional Theory (DFT). Each substrate was manually docked with its both enantiotopic faces to a certain NHC–Cu complex (**4.72a** in complex with $NHC_{4.77b}$–Cu-$SiMe_2Ph$, **4.80a** in complex with $NHC_{4.85}$–Cu-$SiMe_2Ph$, and **4.92g** in complex with $NHC_{4.77a}$–Cu-$SiMe_2Ph$, shown in Scheme 4.3.10, 4.3.12 and 4.3.18**)** and subjected to geometry optimizations. Grimme's[195] B97D functional including dispersion together with the split-valence 6-31G* basis set were employed in the calculations. Frequency calculations were carried out on the optimized geometries at the same level of theory. All normal modes frequencies were found to be real demonstrating that the geometry optimized substrate–NHC–Cu complexes are true minima. Free energies were calculated at 195.15 K and 1.0 atm. using the unscaled normal modes frequencies. All calculations were carried out using the Gaussian 09 program[196].

The herein suggested stereochemical model assumes that the enantioselectivity is

---

(195) S. Grimme, "Semiempirical GGA-type density functional constructed with a long-range dispersion correction," *J. Comp. Chem.*, **2006**, *27*, 1787–1799.

(196) Gaussian 09, Revision A.1, M. J. Frisch, G. W. Trucks, H. B. Schlegel, G. E. Scuseria, M. A. Robb, J. R. Cheeseman, G. Scalmani, V. Barone, B. Mennucci, G. A. Petersson, H. Nakatsuji, M. Caricato, X. Li, H. P. Hratchian, A. F. Izmaylov, J. Bloino, G. Zheng, J. L. Sonnenberg, M. Hada, M. Ehara, K. Toyota, R. Fukuda, J. Hasegawa, M. Ishida, T. Nakajima, Y. Honda, O. Kitao, H. Nakai, T. Vreven, J. A. Montgomery, Jr., J. E. Peralta, F. Ogliaro, M. Bearpark, J. J. Heyd, E. Brothers, K. N. Kudin, V. N. Staroverov, R. Kobayashi, J. Normand, K. Raghavachari, A. Rendell, J. C. Burant, S. S. Iyengar, J. Tomasi, M. Cossi, N. Rega, J. M. Millam, M. Klene, J. E. Knox, J. B. Cross, V. Bakken, C. Adamo, J. Jaramillo, R. Gomperts, R. E. Stratmann, O. Yazyev, A. J. Austin, R. Cammi, C. Pomelli, J. W. Ochterski, R. L. Martin, K. Morokuma, V. G. Zakrzewski, G. A. Voth, P. Salvador, J. J. Dannenberg, S. Dapprich, A. D. Daniels, Ö. Farkas, J. B. Foresman, J. V. Ortiz, J. Cioslowski, and D. J. Fox, Gaussian, Inc., Wallingford CT, 2009.

determined as the energy difference between the two substrate–NHC–Cu complexes, in which the substrate is oriented towards the NHC–Cu complex either via its *Re*- or *Si*-face. Addition of the copper bound $SiMe_2Ph$ group affords the major and minor enantiomeric product. The computed energy differences between the complexes are shown in Scheme 4.3.10, 4.3.12 and 4.3.18. The calculated data are in agreement with the experimental results.

**Complex 4.78**

---

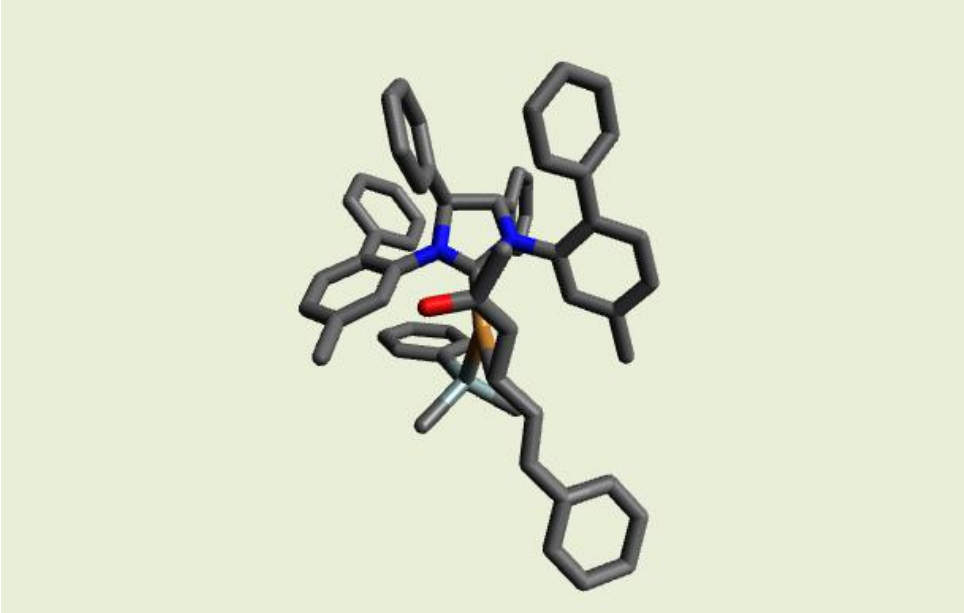

```
 #p b97d/6-31G* freq geom=check guess=check

-----------------------------------
 Cartesian coordinates (Angstroms):
-----------------------------------
C  -0.439   3.251  -3.198
O  -0.880   1.006  -3.929
C  -1.085   1.867  -3.052
C  -1.939   1.664  -1.884
C  -2.959   0.643  -1.845
C  -4.169   0.842  -1.060
C  -5.344   0.191  -1.266
C  -6.555   0.294  -0.452
H  -5.400  -0.507  -2.108
C  -6.647   1.105   0.709
C  -7.693  -0.466  -0.815
```

| | | | |
|---|---|---|---|
| C | -8.871 | -0.421 | -0.059 |
| C | -7.823 | 1.150 | 1.463 |
| C | -8.944 | 0.388 | 1.086 |
| H | -4.078 | 1.551 | -0.230 |
| H | -3.048 | 0.006 | -2.732 |
| H | -2.062 | 2.521 | -1.215 |
| H | -0.953 | 3.786 | -4.015 |
| H | 0.617 | 3.147 | -3.487 |
| H | -0.513 | 3.858 | -2.284 |
| H | -7.639 | -1.101 | -1.703 |
| H | -5.791 | 1.704 | 1.021 |
| H | -7.868 | 1.781 | 2.354 |
| H | -9.732 | -1.020 | -0.362 |
| H | -9.859 | 0.424 | 1.680 |
| H | -3.893 | 1.242 | 2.345 |
| H | 0.888 | -1.609 | 4.562 |
| H | 2.870 | -0.952 | 5.948 |
| H | -3.164 | 1.357 | 3.953 |
| C | -3.391 | 1.933 | 3.039 |
| H | -4.097 | 2.732 | 3.313 |
| C | 1.628 | -0.909 | 4.170 |
| C | 2.744 | -0.547 | 4.942 |
| H | 0.605 | -0.692 | 2.282 |
| H | -1.369 | 0.585 | 1.801 |
| C | 1.464 | -0.388 | 2.880 |
| C | -2.129 | 2.505 | 2.430 |
| C | -1.194 | 1.661 | 1.809 |
| H | -2.541 | 4.560 | 2.973 |
| C | 3.695 | 0.341 | 4.416 |
| C | -1.834 | 3.878 | 2.495 |
| H | 4.564 | 0.631 | 5.011 |
| H | -0.954 | -1.493 | -4.718 |
| H | 1.753 | -2.644 | 1.382 |
| H | -0.086 | -0.686 | -2.680 |
| C | 2.410 | 0.507 | 2.351 |
| C | -0.020 | 2.160 | 1.218 |
| C | 3.523 | 0.869 | 3.128 |
| C | 0.400 | 0.220 | -0.207 |
| H | 3.399 | -2.836 | 3.227 |
| C | 0.470 | -1.604 | -2.498 |
| H | -1.642 | -3.057 | -4.226 |
| C | -0.644 | 4.376 | 1.954 |
| N | 0.855 | 1.245 | 0.560 |
| C | -0.708 | -2.546 | -4.520 |
| C | 0.325 | -2.652 | -3.418 |
| C | 2.798 | -2.843 | 1.159 |
| N | 1.458 | -0.573 | -0.519 |
| C | 1.383 | -1.671 | -1.431 |
| C | 0.285 | 3.544 | 1.293 |
| C | 2.279 | 1.065 | 0.945 |
| C | 3.731 | -2.962 | 2.196 |
| H | -0.433 | 5.445 | 2.000 |
| H | 4.255 | 1.572 | 2.719 |
| H | 3.462 | -0.623 | 0.230 |
| C | 1.170 | -3.769 | -3.289 |
| C | 2.229 | -2.800 | -1.293 |
| H | -0.352 | -3.018 | -5.449 |

```
C   2.745   0.092  -0.179
H   1.967   5.288   2.496
C   2.113  -3.822  -2.257
C   3.204  -2.969  -0.185
H   2.824   2.011   0.869
H   1.097  -4.592  -4.004
C   1.507   4.157   0.709
C   5.081  -3.219   1.907
C   2.274   5.064   1.472
H   2.761  -4.695  -2.154
H   5.809  -3.304   2.717
C   3.350   0.781  -1.393
C   4.559  -3.238  -0.468
H   1.353   3.148  -1.196
C   1.926   3.856  -0.604
C   5.492  -3.364   0.572
H   1.519   0.918  -2.551
H   5.328   0.771  -0.518
C   3.430   5.649   0.937
C   2.582   1.146  -2.514
H   4.016   6.342   1.545
C   4.726   1.069  -1.381
H   4.878  -3.320  -1.509
H   6.541  -3.562   0.338
C   3.085   4.433  -1.137
C   3.841   5.333  -0.368
C   3.185   1.785  -3.606
C   5.327   1.723  -2.466
H   3.400   4.163  -2.144
H   4.748   5.780  -0.781
H   2.574   2.041  -4.475
C   4.558   2.080  -3.586
H   6.397   1.941  -2.444
H   5.027   2.573  -4.439
Cu  -1.396   0.026  -0.781
Si  -2.311  -1.880   0.081
C  -3.148  -2.908  -1.303
C  -3.596  -1.499   1.457
H  -2.402  -3.216  -2.054
H  -3.918  -2.312  -1.818
H  -3.628  -3.821  -0.907
H  -3.136  -0.972   2.310
H  -4.033  -2.435   1.848
H  -4.417  -0.873   1.077
H   0.080  -4.004   4.031
H  -1.373  -2.322   2.934
C  -0.054  -4.027   2.946
C  -0.869  -3.071   2.318
H   1.216  -5.764   2.665
C   0.579  -5.020   2.183
C  -1.081  -3.079   0.918
C   0.403  -5.036   0.790
C  -0.411  -4.076   0.171
H   0.911  -5.789   0.183
H  -0.528  -4.105  -0.914
---------------------------------
```

```
 SCF Done:  E(RB97D) =  -4472.28845279     A.U. after    1 cycles

                     1                      2                      3
                     A                      A                      A
Frequencies --    12.7831                18.0262                22.5034
Red. masses --     5.7001                 5.6017                 5.0868

 Zero-point correction=                           0.988317
(Hartree/Particle)
 Thermal correction to Energy=                    1.050779
 Thermal correction to Enthalpy=                  1.051724
 Thermal correction to Gibbs Free Energy=         0.888488
 Thermal correction to Gibbs Free Energy at 195.15 K = 0.937813
 Sum of electronic and zero-point Energies=          -4471.300136
 Sum of electronic and thermal Energies=             -4471.237673
 Sum of electronic and thermal Enthalpies=           -4471.236729
 Sum of electronic and thermal Free Energies=        -4471.399965

         Item               Value     Threshold  Converged?
 Maximum Force            0.000011     0.000450     YES
 RMS     Force            0.000002     0.000300     YES
```

**Complex 4.79**

---

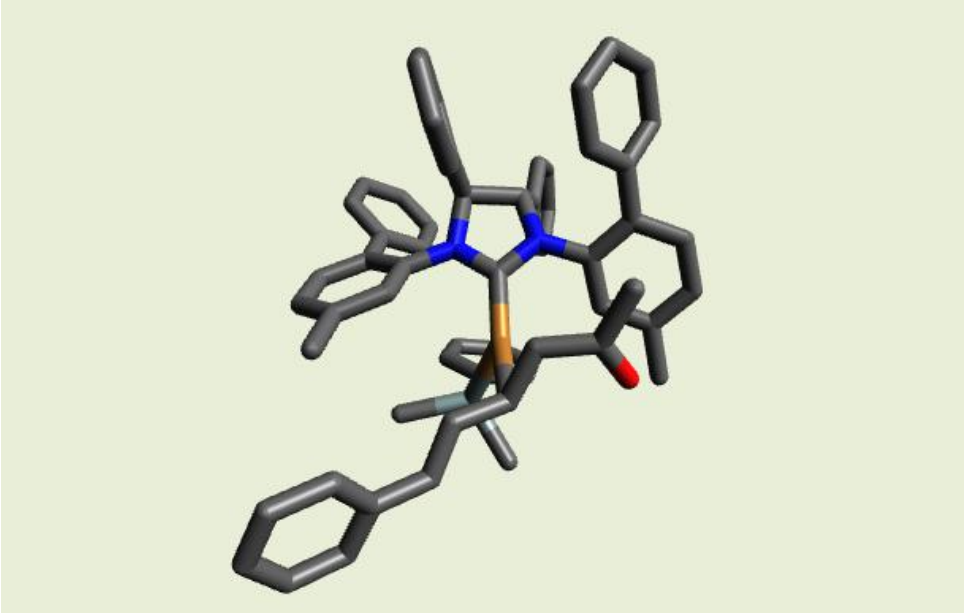

```
 #p b97d/6-31G* freq

------------------------------------
 Cartesian coordinates (Angstroms):
------------------------------------
H  -0.298  -3.356  -4.179
H   3.230   2.042  -3.700
H   5.604   2.679  -3.208
H   0.619  -1.990  -4.865
```

| | | | |
|---|---|---|---|
| C | 0.715 | -2.988 | -4.408 |
| H | 1.174 | -3.666 | -5.143 |
| C | 3.684 | 1.785 | -2.744 |
| C | 5.012 | 2.145 | -2.462 |
| H | 1.887 | 0.831 | -2.017 |
| H | 0.590 | -1.113 | -2.435 |
| C | 2.918 | 1.099 | -1.790 |
| C | 1.518 | -2.934 | -3.130 |
| C | 1.283 | -1.919 | -2.192 |
| H | 2.704 | -4.694 | -3.545 |
| C | 5.579 | 1.808 | -1.223 |
| C | 2.490 | -3.902 | -2.825 |
| H | 6.614 | 2.077 | -0.999 |
| H | -3.875 | -0.014 | 3.087 |
| H | 1.030 | 2.834 | -0.894 |
| H | -1.743 | -0.111 | 1.769 |
| C | 3.485 | 0.753 | -0.551 |
| C | 1.925 | -1.903 | -0.945 |
| C | 4.819 | 1.105 | -0.278 |
| C | 0.396 | -0.285 | 0.094 |
| H | 3.031 | 4.143 | -1.520 |
| C | -1.724 | 0.979 | 1.759 |
| H | -4.726 | 0.761 | 1.740 |
| C | 3.169 | -3.866 | -1.604 |
| N | 1.629 | -0.841 | -0.037 |
| C | -4.101 | 0.960 | 2.625 |
| C | -2.838 | 1.687 | 2.232 |
| C | 1.401 | 3.602 | -0.222 |
| N | 0.536 | 0.842 | 0.849 |
| C | -0.556 | 1.628 | 1.323 |
| C | 2.889 | -2.892 | -0.623 |
| C | 2.707 | 0.017 | 0.524 |
| C | 2.531 | 4.350 | -0.573 |
| H | 3.906 | -4.636 | -1.366 |
| H | 5.262 | 0.817 | 0.679 |
| H | 2.264 | 1.947 | 1.452 |
| C | -2.746 | 3.087 | 2.305 |
| C | -0.458 | 3.043 | 1.402 |
| H | -4.703 | 1.550 | 3.332 |
| C | 1.879 | 0.924 | 1.479 |
| H | 5.551 | -3.128 | -0.219 |
| C | -1.576 | 3.741 | 1.909 |
| C | 0.742 | 3.827 | 1.004 |
| H | 3.403 | -0.585 | 1.114 |
| H | -3.596 | 3.666 | 2.672 |
| C | 3.592 | -2.969 | 0.683 |
| C | 3.021 | 5.340 | 0.293 |
| C | 4.997 | -3.097 | 0.722 |
| H | -1.519 | 4.830 | 1.960 |
| H | 3.907 | 5.918 | 0.021 |
| C | 1.857 | 0.424 | 2.914 |
| C | 1.242 | 4.826 | 1.868 |
| H | 1.804 | -2.782 | 1.881 |
| C | 2.886 | -2.901 | 1.903 |
| C | 2.372 | 5.577 | 1.516 |
| H | 0.202 | -0.940 | 2.651 |
| H | 3.516 | 1.686 | 3.486 |

```
C    5.678  -3.147   1.946
C    0.945  -0.553   3.348
H    6.767  -3.236   1.958
C    2.812   0.919   3.819
H    0.750   4.992   2.829
H    2.751   6.339   2.200
C    3.566  -2.940   3.126
C    4.964  -3.064   3.153
C    0.983  -1.025   4.667
C    2.863   0.439   5.136
H    3.003  -2.852   4.056
H    5.495  -3.089   4.107
H    0.262  -1.778   4.994
C    1.945  -0.533   5.565
H    3.609   0.832   5.829
H    1.974  -0.898   6.593
Cu  -1.255  -0.962  -0.583
Si  -2.230   0.481  -2.066
C   -3.470   1.692  -1.262
C   -3.104  -0.478  -3.487
H   -2.968   2.366  -0.549
H   -4.237   1.132  -0.704
H   -3.982   2.312  -2.020
H   -2.422  -1.218  -3.940
H   -3.441   0.204  -4.287
H   -3.981  -1.035  -3.123
H    1.289   1.302  -5.606
H   -0.325  -0.060  -4.308
C    0.721   1.761  -4.793
C   -0.186   0.993  -4.050
H    1.595   3.730  -5.073
C    0.893   3.124  -4.495
C   -0.953   1.552  -2.998
C    0.155   3.702  -3.450
C   -0.756   2.923  -2.717
H    0.288   4.757  -3.203
H   -1.326   3.393  -1.913
H   -7.266  -0.126  -1.461
H   -3.010  -2.565  -1.566
H   -5.277  -1.481  -1.463
H   -9.308   0.727  -0.322
C   -7.399  -0.284  -0.387
C   -2.826  -2.206  -0.550
C   -5.189  -1.418  -0.374
C   -8.546   0.199   0.255
C   -6.386  -0.962   0.333
C   -3.989  -1.722   0.187
C   -1.725  -2.823   0.142
C   -8.715   0.006   1.636
H   -3.860  -1.599   1.267
H   -1.734  -2.843   1.237
C   -6.584  -1.166   1.722
H   -9.610   0.378   2.139
C   -7.728  -0.683   2.364
H   -5.836  -1.721   2.290
H   -7.860  -0.854   3.435
O   -1.040  -4.087  -1.760
```

```
C  -0.939  -3.860  -0.543
H   0.195  -4.260   1.302
H   0.957  -4.840  -0.220
C   0.006  -4.705   0.313
H  -0.443  -5.702   0.461
-------------------------------------

 SCF Done:  E(RB97D) =  -4472.28271069     A.U. after   18 cycles

                     1                      2                      3
                     A                      A                      A
Frequencies --    11.3265                17.7798                19.4924
Red. masses --     5.4715                 4.8861                 5.4193

 Zero-point correction=                           0.988022
(Hartree/Particle)
 Thermal correction to Energy=                    1.050460
 Thermal correction to Enthalpy=                  1.051404
 Thermal correction to Gibbs Free Energy=         0.887952
 Thermal correction to Gibbs Free Energy at 195.15 K = 0.937349
 Sum of electronic and zero-point Energies=          -4471.294689
 Sum of electronic and thermal Energies=             -4471.232251
 Sum of electronic and thermal Enthalpies=           -4471.231307
 Sum of electronic and thermal Free Energies=        -4471.394759

         Item               Value     Threshold  Converged?
 Maximum Force            0.000024     0.000450     YES
 RMS     Force            0.000004     0.000300     YES
```

**Complex 4.86**

```
-----------------------------------------
```

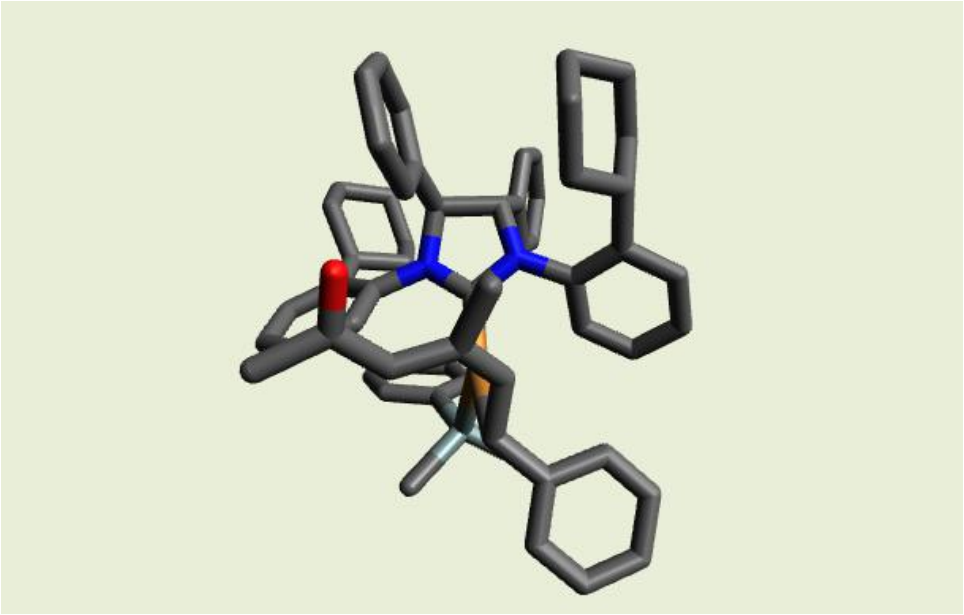

```
 #p b97d/6-31G* freq geom=check guess=check
```

```
---------------------------------
 Cartesian coordinates (Angstroms):
---------------------------------
H    2.567    3.866    0.929
H    2.602    4.043    2.718
C    2.204    3.454    1.883
H    1.112    3.578    1.917
C    2.343    1.029    5.754
O    1.615    3.033    4.659
C    2.165    1.925    4.516
C    2.625    1.368    3.250
C    2.605    1.996    2.014
C    2.986    1.333    0.781
C    3.737    0.105    0.678
C    4.741   -0.086   -0.396
H    4.019   -0.376    1.620
C    4.601    0.495   -1.676
C    5.865   -0.906   -0.159
C    6.812   -1.146   -1.164
C    5.545    0.258   -2.680
C    6.656   -0.567   -2.433
H    3.038    1.999   -0.085
H    2.989    0.338    3.295
H    1.375    0.554    5.992
H    2.623    1.653    6.615
H    3.093    0.234    5.610
H    5.988   -1.361    0.827
H    3.731    1.112   -1.900
H    5.405    0.711   -3.664
H    7.672   -1.787   -0.955
H    7.389   -0.757   -3.220
H   -2.456   -2.349   -4.095
H   -4.662   -1.441   -4.854
C   -2.849   -1.427   -3.664
C   -4.089   -0.920   -4.084
H   -1.173   -1.179   -2.323
H    0.981   -0.777   -2.343
C   -2.113   -0.760   -2.676
C    1.962    0.424   -3.834
C    1.109    0.225   -2.747
H    2.761    1.899   -5.213
C   -4.591    0.259   -3.511
C    2.103    1.713   -4.363
H   -5.554    0.661   -3.834
H    0.823    0.041    2.507
C   -2.609    0.421   -2.098
C    0.404    1.292   -2.149
C   -3.850    0.928   -2.525
C    0.034    0.102   -0.048
C    0.192   -0.814    2.728
C    1.388    2.768   -3.785
N   -0.410    0.958   -1.012
C    0.451   -1.571    3.872
N   -1.031   -0.277    0.708
C   -0.902   -1.091    1.883
C    0.529    2.607   -2.675
C   -1.883    1.134   -0.973
```

```
H   1.499   3.774  -4.197
H  -4.234   1.849  -2.079
H  -3.126   0.016   0.442
C  -0.427  -2.609   4.213
C  -1.790  -2.152   2.196
C  -2.202   0.597   0.461
C  -1.523  -2.869   3.386
H  -2.137   2.197  -1.001
H  -0.261  -3.211   5.108
C  -0.200   3.858  -2.194
C  -1.593   3.978  -2.884
H  -2.198  -3.690   3.641
C  -2.341   1.704   1.493
C  -0.209   4.059  -0.659
H  -0.254   1.785   2.059
H  -4.472   1.870   1.146
C  -2.402   5.183  -2.364
C  -1.243   2.214   2.205
C  -3.613   2.272   1.691
C  -1.051   5.275  -0.233
C  -1.408   3.274   3.109
C  -3.780   3.346   2.577
H  -0.543   3.627   3.672
C  -2.678   3.846   3.290
H  -4.771   3.781   2.722
H  -2.810   4.670   3.993
Cu   1.870  -0.335   0.219
Si   2.303  -2.533  -0.251
C   3.296  -3.346   1.174
C   3.255  -2.746  -1.905
H   2.765  -3.229   2.134
H   4.284  -2.870   1.278
H   3.452  -4.425   1.004
H   2.714  -2.285  -2.748
H   3.375  -3.819  -2.137
H   4.251  -2.284  -1.865
H  -1.172  -5.118  -2.908
H   0.656  -3.467  -2.623
C  -0.790  -4.897  -1.907
C   0.236  -3.953  -1.738
H  -2.108  -6.311  -0.919
C  -1.316  -5.569  -0.792
C   0.768  -3.653  -0.460
C  -0.824  -5.270   0.489
C   0.197  -4.321   0.648
H  -1.234  -5.778   1.366
H   0.566  -4.105   1.653
H   1.311  -1.326   4.494
H   2.509  -0.422  -4.253
H   0.832   4.184  -0.335
H  -0.580   3.177  -0.129
H  -1.423   4.072  -3.970
H  -2.177   3.056  -2.761
H   0.376   4.716  -2.585
C  -2.471   5.201  -0.825
H  -0.567   6.205  -0.585
H  -1.093   5.319   0.866
```

```
H  -3.413   5.166  -2.806
H  -1.918   6.117  -2.703
H  -3.075   6.057  -0.481
H  -2.969   4.287  -0.455
H  -3.990  -3.316  -1.867
H  -1.939  -3.032  -0.456
H  -4.071  -4.403  -0.462
C  -4.084  -3.342  -0.770
C  -2.894  -2.606  -0.135
H  -2.925  -1.582  -0.505
H  -6.272  -3.201  -0.782
C  -5.408  -2.687  -0.327
H  -3.073  -3.720   1.648
H  -5.423  -1.643  -0.691
C  -2.997  -2.646   1.400
H  -5.595  -3.746   1.553
C  -5.538  -2.696   1.211
C  -4.331  -2.022   1.897
H  -6.474  -2.203   1.525
H  -4.350  -0.937   1.699
H  -4.401  -2.137   2.992
-----------------------------------

 SCF Done:  E(RB97D) =  -4440.24390324     A.U. after    1 cycles

                     1                      2                      3
                     A                      A                      A
Frequencies --     8.6691                15.4163                23.5061
Red. masses --     4.9571                 5.0290                 4.5974

 Zero-point correction=                           1.101717
(Hartree/Particle)
 Thermal correction to Energy=                    1.164102
 Thermal correction to Enthalpy=                  1.165046
 Thermal correction to Gibbs Free Energy=         1.003947
 Thermal correction to Gibbs Free Energy at 195.15 K = 1.052454
 Sum of electronic and zero-point Energies=          -4439.142186
 Sum of electronic and thermal Energies=             -4439.079801
 Sum of electronic and thermal Enthalpies=           -4439.078857
 Sum of electronic and thermal Free Energies=        -4439.239956

          Item               Value     Threshold  Converged?
 Maximum Force            0.000011     0.000450     YES
 RMS     Force            0.000001     0.000300     YES
```

**Complex 4.87**

```
-----------------------------------------
```

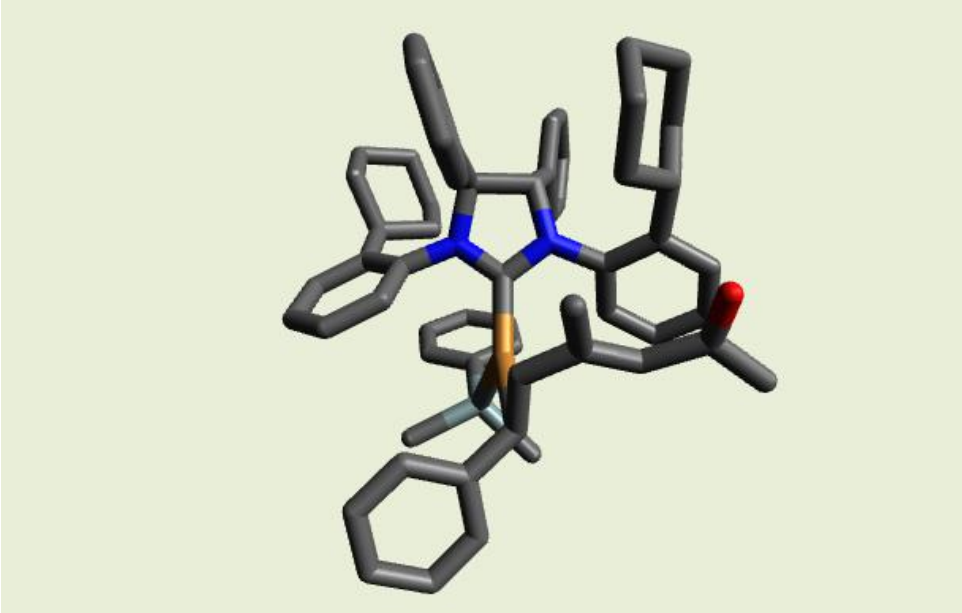

#p b97d/6-31G* freq

---
Cartesian coordinates (Angstroms):
---

| | | | |
|---|---|---|---|
| H | -1.125 | -4.408 | 2.586 |
| H | 0.334 | -3.441 | 2.295 |
| C | -0.339 | -4.188 | 1.842 |
| H | 0.245 | -5.089 | 1.630 |
| C | -0.157 | -5.825 | -2.451 |
| O | 1.012 | -5.747 | -0.356 |
| C | 0.123 | -5.235 | -1.059 |
| C | -0.742 | -4.118 | -0.674 |
| C | -0.978 | -3.621 | 0.587 |
| C | -1.927 | -2.542 | 0.848 |
| C | -3.060 | -2.215 | 0.017 |
| C | -4.391 | -1.899 | 0.585 |
| H | -3.124 | -2.751 | -0.936 |
| C | -4.568 | -1.351 | 1.875 |
| C | -5.545 | -2.125 | -0.197 |
| C | -6.822 | -1.801 | 0.280 |
| C | -5.840 | -1.027 | 2.355 |
| C | -6.978 | -1.244 | 1.559 |
| H | -2.051 | -2.329 | 1.915 |
| H | -1.286 | -3.660 | -1.504 |
| H | -0.954 | -6.584 | -2.361 |
| H | 0.747 | -6.322 | -2.830 |
| H | -0.496 | -5.061 | -3.166 |
| H | -5.429 | -2.555 | -1.195 |
| H | -5.946 | -0.593 | 3.352 |
| H | -7.696 | -1.982 | -0.350 |
| H | -7.970 | -0.984 | 1.932 |
| H | 2.161 | 2.922 | -3.824 |
| H | 4.552 | 3.627 | -3.572 |
| C | 2.767 | 2.534 | -3.003 |

```
C   4.104   2.936  -2.855
H   1.140   1.380  -2.180
H  -0.406  -0.221  -2.415
C   2.188   1.650  -2.084
C   0.144  -1.825  -3.740
C   0.245  -1.078  -2.566
H   0.985  -3.488  -4.857
C   4.864   2.446  -1.780
C   1.030  -2.889  -3.946
H   5.906   2.751  -1.659
H  -1.423  -0.275   2.445
C   2.944   1.153  -1.009
C   1.189  -1.387  -1.563
C   4.286   1.554  -0.866
C   0.009  -0.047   0.117
C  -1.575   0.801   2.482
C   1.974  -3.187  -2.958
N   1.172  -0.533  -0.401
C  -2.623   1.338   3.232
N   0.315   0.966   0.968
C  -0.684   1.625   1.762
C   2.084  -2.475  -1.743
C   2.355   0.244   0.053
H   2.647  -4.034  -3.108
H   4.875   1.162  -0.033
H   2.136   2.014   1.343
C  -2.781   2.729   3.283
C  -0.821   3.035   1.804
C   1.759   0.989   1.296
C  -1.886   3.543   2.584
H   3.134  -0.437   0.404
H  -3.595   3.176   3.857
C   3.166  -2.961  -0.784
C   4.507  -2.209  -1.033
H  -2.014   4.628   2.621
C   2.067   0.287   2.607
C   2.725  -3.059   0.694
H   0.544  -1.229   2.392
H   3.679   1.647   3.088
C   5.602  -2.621  -0.030
C   1.363  -0.861   3.009
C   3.134   0.750   3.396
C   3.887  -3.448   1.625
C   1.725  -1.543   4.177
C   3.502   0.067   4.565
H   1.173  -2.438   4.473
C   2.799  -1.082   4.958
H   4.333   0.435   5.171
H   3.082  -1.614   5.868
Cu  -1.731  -0.767  -0.177
Si  -3.089   0.664  -1.360
C  -4.508   1.352  -0.273
C  -3.804  -0.208  -2.918
H  -4.110   1.775   0.664
H  -5.233   0.573  -0.003
H  -5.047   2.155  -0.807
H  -2.989  -0.574  -3.566
```

```
H  -4.434   0.469  -3.520
H  -4.415  -1.080  -2.632
H  -0.229   3.305  -4.651
H  -1.213   1.248  -3.704
C  -0.862   3.370  -3.762
C  -1.415   2.203  -3.211
H  -0.724   5.532  -3.621
C  -1.147   4.621  -3.192
C  -2.252   2.239  -2.068
C  -1.983   4.689  -2.067
C  -2.514   3.514  -1.511
H  -2.211   5.657  -1.614
H  -3.150   3.591  -0.627
H  -3.303   0.678   3.771
H  -0.604  -1.557  -4.490
H   1.941  -3.822   0.736
H   2.283  -2.127   1.056
H   4.832  -2.427  -2.064
H   4.368  -1.120  -0.996
H   3.368  -4.007  -1.071
C   5.103  -2.525   1.425
H   4.191  -4.489   1.415
H   3.541  -3.412   2.671
H   6.498  -1.996  -0.183
H   5.900  -3.667  -0.227
H   5.913  -2.795   2.124
H   4.813  -1.483   1.656
H   1.806   4.815  -1.772
H  -0.049   3.391  -0.913
H   0.623   5.838  -0.929
C   1.378   5.044  -0.784
C   0.700   3.784  -0.220
H   1.477   3.026  -0.125
H   2.967   6.443  -0.219
C   2.477   5.537   0.177
H  -0.603   4.957   0.973
H   3.255   4.756   0.254
C   0.065   4.093   1.149
H   1.186   6.665   1.503
C   1.896   5.821   1.578
C   1.144   4.600   2.148
H   2.693   6.131   2.275
H   1.860   3.789   2.365
H   0.665   4.859   3.107
H  -3.696  -1.152   2.497
-----------------------------------

 SCF Done:  E(RB97D) =  -4440.23841622     A.U. after   18 cycles

                     1                      2                      3
                     A                      A                      A
Frequencies --    14.1885                20.2149                26.7918
Red. masses --     4.8268                 5.2786                 4.8117

 Zero-point correction=                           1.102511
(Hartree/Particle)
 Thermal correction to Energy=                    1.164693
```

```
 Thermal correction to Enthalpy=                  1.165637
 Thermal correction to Gibbs Free Energy=         1.005869
 Thermal correction to Gibbs Free Energy at 195.15 K = 1.053926
 Sum of electronic and zero-point Energies=          -4439.135906
 Sum of electronic and thermal Energies=             -4439.073723
 Sum of electronic and thermal Enthalpies=           -4439.072779
 Sum of electronic and thermal Free Energies=        -4439.232547

         Item               Value     Threshold  Converged?
 Maximum Force            0.000010     0.000450     YES
 RMS     Force            0.000003     0.000300     YES
```

**Complex 4.94**

---

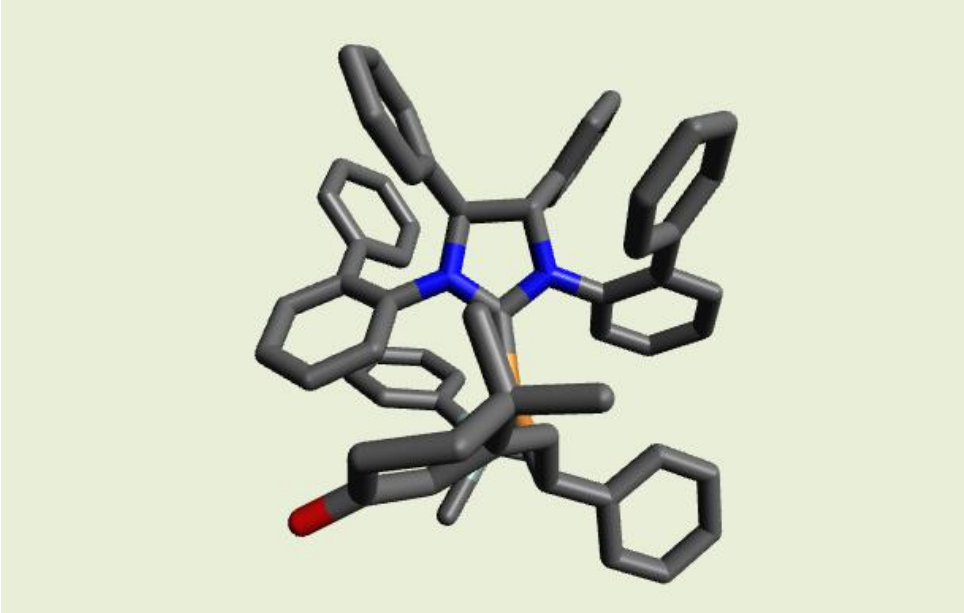

```
 #p b97d/6-31G* freq geom=check guess=check

------------------------------------
 Cartesian coordinates (Angstroms):
------------------------------------
C    3.020  -2.117   2.463
C    2.883  -2.852   3.710
C    2.785  -2.031   5.001
C    3.352  -0.616   4.833
C    2.784   0.128   3.595
C    2.984  -0.739   2.334
C    3.049  -0.082   1.040
C    3.588  -0.737  -0.131
C    4.344   0.020  -1.155
H    3.969  -1.750   0.016
C    4.048   1.361  -1.488
C    5.394  -0.622  -1.847
C    6.129   0.050  -2.833
```

| | | | |
|---|---|---|---|
| C | 4.784 | 2.034 | -2.470 |
| C | 5.827 | 1.384 | -3.150 |
| H | 3.119 | 1.006 | 1.048 |
| H | 5.629 | -1.660 | -1.603 |
| H | 3.223 | 1.875 | -0.993 |
| H | 4.528 | 3.067 | -2.712 |
| H | 6.936 | -0.469 | -3.354 |
| H | 6.396 | 1.910 | -3.919 |
| H | -3.825 | 2.469 | -3.983 |
| H | -4.641 | 4.741 | -3.330 |
| C | -3.588 | 2.874 | -2.997 |
| C | -4.046 | 4.151 | -2.629 |
| H | -2.468 | 1.125 | -2.377 |
| H | 0.333 | 0.560 | -2.789 |
| C | -2.826 | 2.118 | -2.099 |
| C | 1.376 | 2.313 | -3.527 |
| C | 0.677 | 1.570 | -2.571 |
| H | 2.284 | 4.229 | -3.984 |
| C | -3.738 | 4.666 | -1.361 |
| C | 1.751 | 3.635 | -3.240 |
| H | -4.093 | 5.658 | -1.071 |
| H | -2.313 | -1.766 | -1.904 |
| H | 0.645 | -1.710 | 1.832 |
| C | -2.512 | 2.633 | -0.827 |
| C | 0.389 | 2.120 | -1.310 |
| C | -2.970 | 3.909 | -0.463 |
| C | -0.112 | 0.050 | -0.109 |
| H | -4.202 | -1.049 | -3.352 |
| C | -0.198 | -2.362 | 1.619 |
| C | 1.456 | 4.186 | -1.987 |
| N | -0.397 | 1.343 | -0.413 |
| C | -0.200 | -3.682 | 2.087 |
| C | -3.333 | -1.788 | -1.522 |
| N | -1.218 | -0.494 | 0.452 |
| C | -1.291 | -1.845 | 0.903 |
| C | 0.789 | 3.440 | -0.992 |
| C | -1.698 | 1.813 | 0.146 |
| C | -4.401 | -1.382 | -2.332 |
| H | 1.773 | 5.202 | -1.746 |
| H | -2.712 | 4.308 | 0.519 |
| H | -3.101 | 0.200 | -0.241 |
| C | -1.339 | -4.478 | 1.889 |
| C | -2.428 | -2.653 | 0.656 |
| C | -2.369 | 0.460 | 0.530 |
| H | -0.243 | 5.892 | -0.418 |
| C | -2.437 | -3.957 | 1.193 |
| C | -3.565 | -2.232 | -0.203 |
| H | -1.496 | 2.403 | 1.051 |
| H | -1.367 | -5.502 | 2.265 |
| C | 0.554 | 4.034 | 0.347 |
| C | -5.717 | -1.422 | -1.841 |
| C | 0.021 | 5.332 | 0.481 |
| H | -3.312 | -4.581 | 1.001 |
| H | -6.549 | -1.102 | -2.473 |
| C | -3.055 | 0.485 | 1.873 |
| C | -4.889 | -2.287 | 0.276 |
| H | 1.289 | 2.305 | 1.404 |

```
C    0.869    3.304    1.512
C   -5.959   -1.883   -0.537
H   -1.241    0.261    3.019
H   -5.019    0.689    0.998
C   -0.206    5.880    1.751
C   -2.318    0.405    3.067
H   -0.630    6.883    1.840
C   -4.450    0.647    1.928
H   -5.069   -2.619    1.300
H   -6.979   -1.919   -0.148
C    0.639    3.849    2.781
C    0.096    5.139    2.905
C   -2.969    0.483    4.305
C   -5.102    0.734    3.167
H    0.887    3.266    3.668
H   -0.089    5.563    3.894
H   -2.389    0.408    5.228
C   -4.363    0.652    4.358
H   -6.186    0.858    3.203
H   -4.871    0.711    5.323
Cu   1.632   -0.681   -0.375
Si   1.746   -2.082   -2.182
C    2.844   -3.601   -1.769
C    2.407   -1.266   -3.785
H    2.530   -4.071   -0.822
H    3.901   -3.308   -1.660
H    2.785   -4.369   -2.560
H    1.699   -0.528   -4.194
H    2.573   -2.031   -4.564
H    3.359   -0.745   -3.603
H   -2.290   -2.921   -5.165
H   -0.207   -1.752   -4.502
C   -1.792   -3.189   -4.230
C   -0.618   -2.521   -3.843
H   -3.236   -4.723   -3.713
C   -2.320   -4.205   -3.419
C    0.063   -2.852   -2.646
C   -1.674   -4.537   -2.217
C   -0.504   -3.866   -1.837
H   -2.088   -5.312   -1.569
H   -0.024   -4.137   -0.894
O    2.803   -4.092    3.745
H    3.150   -0.007    5.731
H    4.448   -0.678    4.720
H    1.718   -1.989    5.285
H    3.298   -2.584    5.802
C    1.266    0.372    3.776
C    3.510    1.491    3.511
H    3.088   -2.750    1.575
H    4.574    1.353    3.262
H    3.446    1.993    4.491
H    3.065    2.167    2.768
H    0.724   -0.576    3.901
H    0.852    0.882    2.896
H    1.082    1.001    4.665
H    0.672   -4.067    2.615
H    1.616    1.864   -4.491
```

```
-----------------------------------

 SCF Done:  E(RB97D) =  -4549.64582916     A.U. after    1 cycles

                     1                      2                      3
                     A                      A                      A
Frequencies --     7.0907                18.1028                21.5352
Red. masses --     5.4707                 5.3711                 5.4076

 Zero-point correction=                           1.025997
(Hartree/Particle)
 Thermal correction to Energy=                    1.088381
 Thermal correction to Enthalpy=                  1.089325
 Thermal correction to Gibbs Free Energy=         0.926485
 Thermal correction to Gibbs Free Energy at 195.15 K = 0.975585
 Sum of electronic and zero-point Energies=          -4548.619832
 Sum of electronic and thermal Energies=             -4548.557448
 Sum of electronic and thermal Enthalpies=           -4548.556504
 Sum of electronic and thermal Free Energies=        -4548.719344

         Item               Value     Threshold  Converged?
 Maximum Force            0.000018     0.000450     YES
 RMS     Force            0.000002     0.000300     YES
```

**Complex 4.95**

```
----------------------------------------
```

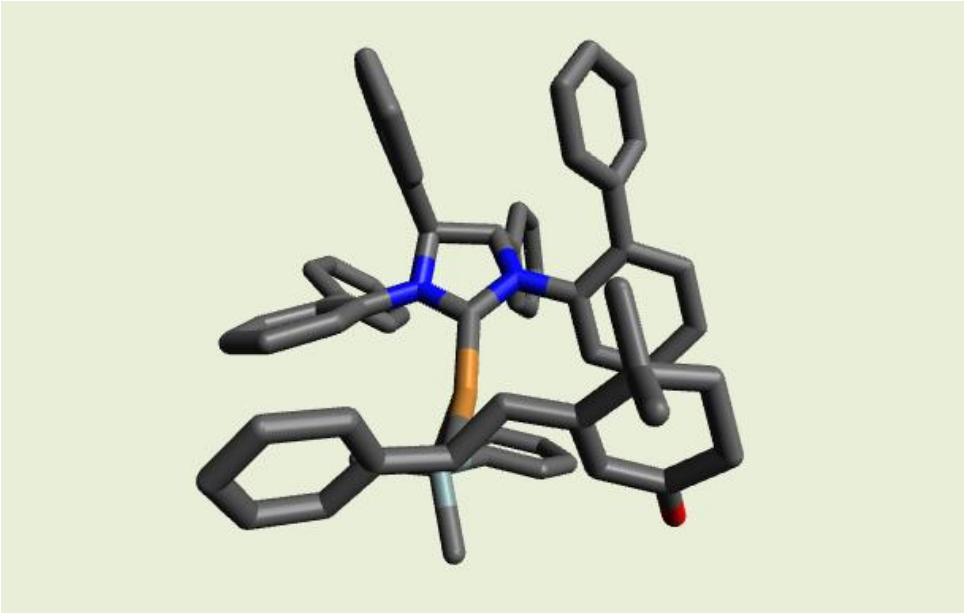

```
 #p b97d/6-31G* freq geom=check guess=check

-----------------------------------
 Cartesian coordinates (Angstroms):
-----------------------------------
H    3.663    1.263   -3.283
H    4.132    3.385   -4.461
```

| | | | |
|---|---|---|---|
| C | 3.798 | 2.175 | -2.701 |
| C | 4.082 | 3.376 | -3.370 |
| C | 3.748 | 2.121 | -1.290 |
| C | 4.319 | 4.554 | -2.644 |
| C | 3.971 | 3.321 | -0.577 |
| C | 4.256 | 4.520 | -1.241 |
| H | 4.547 | 5.487 | -3.165 |
| H | 4.426 | 5.429 | -0.661 |
| H | 3.905 | 3.306 | 0.509 |
| C | 3.639 | -1.804 | 0.730 |
| C | 3.937 | -3.060 | 1.396 |
| C | 4.157 | -4.268 | 0.483 |
| C | 3.240 | -4.199 | -0.750 |
| C | 3.366 | -2.879 | -1.553 |
| C | 3.351 | -1.663 | -0.614 |
| C | 3.097 | -0.350 | -1.185 |
| C | 3.546 | 0.847 | -0.545 |
| C | -3.172 | -1.096 | 3.338 |
| C | -4.515 | -1.499 | 3.285 |
| C | -2.461 | -0.848 | 2.155 |
| C | 0.787 | -3.536 | 1.889 |
| C | 0.412 | -2.327 | 1.299 |
| C | -5.146 | -1.668 | 2.042 |
| C | 0.310 | -4.742 | 1.356 |
| C | -3.084 | -1.029 | 0.909 |
| C | -0.421 | -2.297 | 0.170 |
| C | -4.426 | -1.446 | 0.860 |
| C | -0.175 | 0.127 | -0.272 |
| C | 0.431 | 2.740 | -1.641 |
| C | -0.511 | -4.719 | 0.223 |
| N | -0.890 | -1.032 | -0.305 |
| C | 0.823 | 4.048 | -1.940 |
| C | -2.416 | 2.494 | 1.797 |
| N | -1.045 | 1.141 | -0.535 |
| C | -0.658 | 2.491 | -0.791 |
| C | -0.888 | -3.510 | -0.404 |
| C | -2.363 | -0.794 | -0.405 |
| C | -3.471 | 2.342 | 2.703 |
| C | 0.089 | 5.124 | -1.421 |
| C | -1.401 | 3.568 | -0.245 |
| C | -2.393 | 0.666 | -0.933 |
| C | -1.013 | 4.878 | -0.594 |
| C | -2.527 | 3.381 | 0.705 |
| C | -1.771 | -3.579 | -1.599 |
| C | -4.661 | 3.066 | 2.530 |
| C | -2.931 | -4.385 | -1.559 |
| C | -2.594 | 0.753 | -2.436 |
| C | -3.727 | 4.106 | 0.540 |
| C | -1.508 | -2.837 | -2.771 |
| C | -4.786 | 3.949 | 1.445 |
| C | -3.803 | -4.444 | -2.654 |
| C | -1.534 | 0.514 | -3.329 |
| C | -3.874 | 1.027 | -2.946 |
| C | -2.383 | -2.891 | -3.863 |
| C | -3.534 | -3.694 | -3.810 |
| C | -1.751 | 0.550 | -4.713 |
| C | -4.097 | 1.051 | -4.331 |

```
C  -3.035   0.814  -5.218
Cu   1.675   0.510   0.091
Si   1.931   1.616   2.087
C   1.326   3.432   2.037
C   3.733   1.603   2.773
C   0.802  -1.187   5.030
C   1.442  -0.529   3.970
C  -0.297  -0.589   5.671
C   0.999   0.736   3.508
C  -0.745   0.670   5.242
C  -0.105   1.318   4.173
O   4.021  -3.145   2.633
C   4.706  -2.840  -2.332
C   2.195  -2.857  -2.562
H   4.242   0.728   0.289
H   2.800  -0.307  -2.230
H   2.253  -2.012  -3.265
H   1.240  -2.815  -2.024
H   2.214  -3.785  -3.157
H   3.608  -0.935   1.388
H   3.445  -5.043  -1.431
H   2.197  -4.297  -0.414
H   4.797  -1.898  -2.896
H   4.751  -3.683  -3.042
H   5.565  -2.910  -1.646
H   5.217  -4.269   0.169
H   3.987  -5.187   1.063
H  -2.665  -0.969   4.294
H  -5.066  -1.692   4.209
H  -1.422  -0.526   2.209
H   0.730  -1.385   1.737
H  -6.189  -1.989   1.993
H   0.588  -5.695   1.809
H  -4.901  -1.605  -0.112
H   0.958   1.900  -2.089
H  -0.861  -5.654  -0.217
H  -1.500   1.923   1.927
H  -2.799  -1.451  -1.162
H  -3.364   1.642   3.532
H   0.380   6.151  -1.651
H  -3.167   1.244  -0.416
H  -1.568   5.711  -0.159
H  -5.487   2.939   3.232
H  -3.157  -4.938  -0.646
H  -3.827   4.780  -0.314
H  -0.633  -2.192  -2.811
H  -5.711   4.511   1.298
H  -4.700  -5.064  -2.599
H  -0.540   0.307  -2.934
H  -4.694   1.225  -2.252
H  -2.176  -2.285  -4.746
H  -4.219  -3.727  -4.659
H  -0.918   0.373  -5.397
H  -5.096   1.266  -4.717
H  -3.204   0.844  -6.296
H   1.633   3.982   2.945
H   0.230   3.489   1.962
```

```
H    1.730    3.960    1.159
H    3.771    2.126    3.745
H    4.474    2.076    2.108
H    4.073    0.570    2.953
H    1.167   -2.161    5.363
H    2.303   -1.017    3.502
H   -0.792   -1.097    6.503
H   -1.587    1.153    5.746
H   -0.459    2.305    3.867
H    1.689    4.213   -2.578
H    1.446   -3.526    2.756
-----------------------------------

 SCF Done:  E(RB97D) =  -4549.64494024     A.U. after    2 cycles

                     1                      2                      3
                     A                      A                      A
Frequencies --    12.1277                16.1590                22.6139
Red. masses --     5.4817                 5.1275                 4.8442

 Zero-point correction=                           1.026997
(Hartree/Particle)
 Thermal correction to Energy=                    1.088960
 Thermal correction to Enthalpy=                  1.089904
 Thermal correction to Gibbs Free Energy=         0.929158
 Thermal correction to Gibbs Free Energy at 195.15 K = 0.977549
 Sum of electronic and zero-point Energies=          -4548.617944
 Sum of electronic and thermal Energies=             -4548.555981
 Sum of electronic and thermal Enthalpies=           -4548.555037
 Sum of electronic and thermal Free Energies=        -4548.715782

          Item               Value     Threshold  Converged?
 Maximum Force            0.000004     0.000450     YES
 RMS     Force            0.000001     0.000300     YES
```

### *4.7.4. Z,E-Selectivity Models Based on DFT Calculations*

Furthermore, we were interested in finding an explanation for the observed *Z*-selectivity of the transformations of β-substituted substrates. Calculations of the *s-cis* and *s-trans* conformers of **4.80a**, as well as **4.92b** (Scheme 4.7.2), demonstrated that the *s-trans* conformers are lower in energy than the corresponding *s-cis* conformers (shown Table 4.7.3).

**Scheme 4.7.2. Conformations of 4.80a and 4.92b**

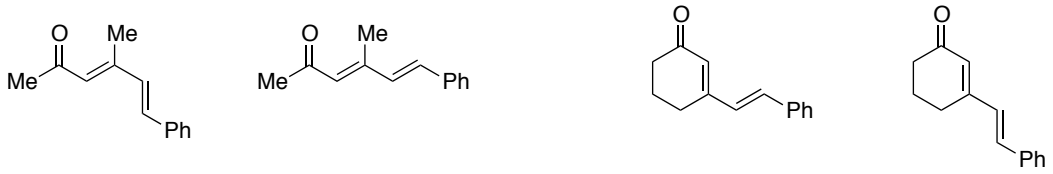


*s-cis* **4.80a** *s-trans* **4.80a** *s-cis* **4.92b** *s-trans* **4.92b**

**Table 4.7.3. Calculations on different conformers of 4.80a and 4.92b**

| | *s-cis* **4.80a** | *s-trans* **4.80a** | *s-cis* **4.92b** | *s-trans* **4.92b** |
|---|---|---|---|---|
| ΔG (298 K)(Hartree) | -578.408047 | -578.412441 | -616.480355 | -616.483572 |
| $\Delta G_{s\text{-}cis}$–$\Delta G_{s\text{-}trans}$ (kcal/mol) | 2.8 | | 2.0 | |

Model systems comprising the smaller achiral NHC–Cu-TMS (**4.88**) (shown Figure 4.3.14) and a trienone (**4.89**) were used to explore the *Z*,*E*-selectivity. Ground states and transition states of the NHC–Cu-**4.89** complexes were computed with the substrate in both its *s-cis*- and *s-trans*- conformations (shown in Figure 4.3.14). The results showed that both the ground state and transition state of the *s-cis* complexes were lower in energy than the corresponding *s-trans* complexes, which could be due to the partial $\eta^4$ character of the *s-cis* complexes.

The geometries were optimized and checked by means of frequency calculations using the B97D/LANL2DZ method. Free energies were computed at 298.15 K and 1.00 atm. using the unscaled frequencies.

***s-cis* 4.80a**

---

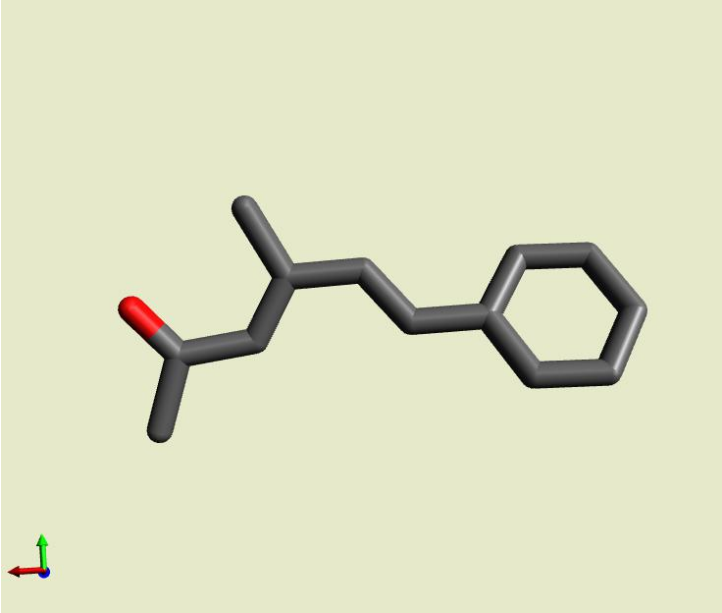

```
 #p b97d/6-31G* freq geom=check guess=check

---------------------------------
 Cartesian coordinates (Angstroms):
---------------------------------
H  -5.992  -0.234   0.109
H  -4.723  -2.267  -0.612
C  -4.901  -0.214   0.065
C  -4.189  -1.355  -0.338
C  -4.201   0.954   0.419
C  -2.791  -1.324  -0.390
H  -4.749   1.842   0.740
H  -2.237  -2.212  -0.706
C  -2.805   0.984   0.368
C  -2.068  -0.156  -0.044
H  -2.277   1.894   0.658
H  -0.180  -1.161  -0.369
C  -0.609  -0.184  -0.124
H  -0.183   1.866   0.184
C   0.241   0.869   0.034
H   1.680   2.958  -0.412
H   2.934   2.054  -1.320
C   1.702   0.818  -0.044
C   2.401   2.127  -0.360
H   1.820  -1.238   0.461
H   3.878  -2.679  -0.304
C   2.390  -0.350   0.172
H   5.439  -1.993   0.272
C   3.850  -0.532   0.076
C   4.348  -1.951   0.380
O   4.644   0.368  -0.222
H   3.176   2.352   0.387
H   4.065  -2.245   1.406
---------------------------------
```

```
 SCF Done:  E(RB97D) =  -578.592964228     A.U. after    1 cycles

                     1                      2                      3
                     A                      A                      A
Frequencies --    27.1911                52.0613                59.9884
Red. masses --     3.3937                 4.9117                 3.9427

 Zero-point correction=                           0.227481
(Hartree/Particle)
 Thermal correction to Energy=                    0.241639
 Thermal correction to Enthalpy=                  0.242583
 Thermal correction to Gibbs Free Energy=         0.184918
 Sum of electronic and zero-point Energies=          -578.365483
 Sum of electronic and thermal Energies=             -578.351325
 Sum of electronic and thermal Enthalpies=           -578.350381
 Sum of electronic and thermal Free Energies=        -578.408047

         Item               Value     Threshold  Converged?
 Maximum Force            0.000012     0.000450     YES
 RMS     Force            0.000003     0.000300     YES
```

***s-trans* 4.80a**

---

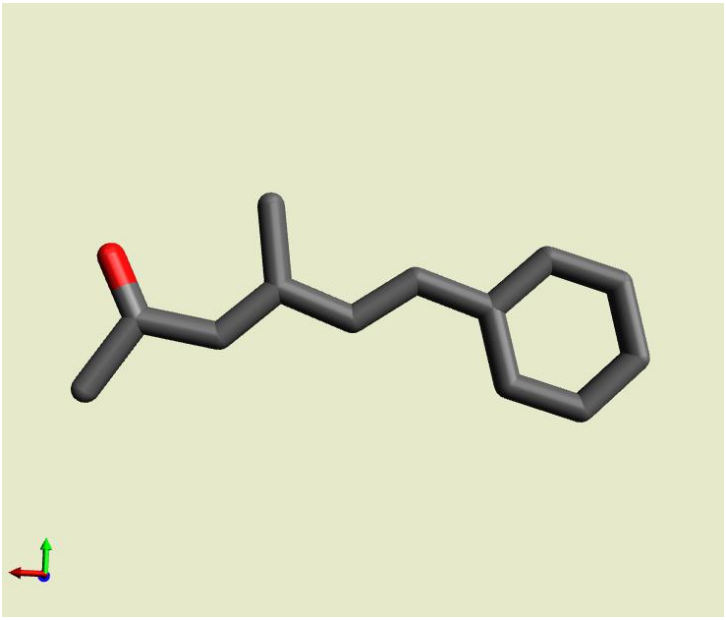

```
 #p b97d/6-31G* freq geom=check guess=check

---------------------------------
 Cartesian coordinates (Angstroms):
---------------------------------
H    1.387    2.334   -0.886
H    2.934    2.136   -0.000
C    1.870    1.888   -0.000
H    1.386    2.334    0.885
C    4.991   -1.569    0.001
```

```
O   4.690   0.820  -0.000
C   4.145  -0.289   0.000
C   2.683  -0.528  -0.000
C   1.658   0.388  -0.000
C   0.294  -0.122  -0.000
C  -0.830   0.648  -0.000
C  -2.217   0.185  -0.000
H  -0.710   1.735  -0.000
C  -2.585  -1.185  -0.000
C  -3.253   1.151   0.000
C  -4.601   0.771   0.001
C  -3.930  -1.564  -0.000
C  -4.945  -0.590   0.000
H   0.195  -1.212   0.000
H   2.398  -1.586   0.000
H   4.757  -2.184   0.887
H   6.057  -1.309   0.001
H   4.758  -2.184  -0.886
H  -2.986   2.211   0.001
H  -1.812  -1.954  -0.001
H  -4.192  -2.624  -0.001
H  -5.381   1.535   0.001
H  -5.995  -0.892   0.000
-----------------------------------

 SCF Done:  E(RB97D) =  -578.597802887     A.U. after    1 cycles

                     1                      2                      3
                     A                      A                      A
Frequencies --    29.3991                50.4822                72.5618
Red. masses --     3.5108                 5.8477                 2.9427

 Zero-point correction=                           0.227754
(Hartree/Particle)
 Thermal correction to Energy=                    0.241897
 Thermal correction to Enthalpy=                  0.242842
 Thermal correction to Gibbs Free Energy=         0.185362
 Sum of electronic and zero-point Energies=           -578.370049
 Sum of electronic and thermal Energies=              -578.355905
 Sum of electronic and thermal Enthalpies=            -578.354961
 Sum of electronic and thermal Free Energies=         -578.412441

          Item               Value     Threshold  Converged?
 Maximum Force            0.000011     0.000450     YES
 RMS     Force            0.000003     0.000300     YES
```

***s-cis* 4.92b**

```
---------------------------------------
```

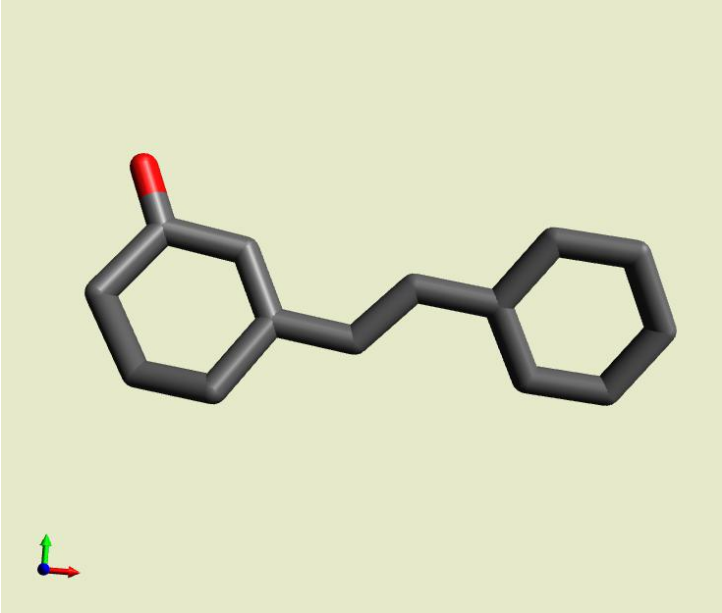

#p b97d/6-31G* freq geom=check guess=check

---
Cartesian coordinates (Angstroms):
---

| | | | |
|---|---|---|---|
| C | -2.098 | 0.795 | -0.238 |
| C | -3.546 | 1.036 | -0.115 |
| C | -4.408 | -0.159 | 0.323 |
| C | -3.804 | -1.499 | -0.137 |
| C | -2.353 | -1.630 | 0.360 |
| C | -1.503 | -0.414 | 0.015 |
| C | -0.059 | -0.623 | -0.020 |
| C | 0.888 | 0.354 | 0.066 |
| C | 2.338 | 0.180 | 0.022 |
| H | 0.550 | 1.385 | 0.206 |
| C | 2.967 | -1.060 | -0.261 |
| C | 3.164 | 1.304 | 0.270 |
| C | 4.560 | 1.196 | 0.248 |
| C | 4.360 | -1.167 | -0.282 |
| C | 5.164 | -0.041 | -0.027 |
| H | 0.263 | -1.667 | -0.082 |
| H | 2.694 | 2.266 | 0.484 |
| H | 2.358 | -1.940 | -0.474 |
| H | 4.824 | -2.130 | -0.504 |
| H | 5.175 | 2.076 | 0.444 |
| H | 6.252 | -0.129 | -0.047 |
| O | -4.037 | 2.148 | -0.324 |
| H | -4.409 | -2.345 | 0.227 |
| H | -3.809 | -1.539 | -1.240 |
| H | -4.463 | -0.141 | 1.428 |
| H | -5.429 | -0.005 | -0.056 |
| H | -2.348 | -1.762 | 1.459 |
| H | -1.879 | -2.535 | -0.057 |
| H | -1.504 | 1.659 | -0.543 |

---

```
 SCF Done:  E(RB97D) =  -616.675143981     A.U. after    7 cycles

                     1                      2                      3
                     A                      A                      A
Frequencies --    22.4190                47.5324                62.0648
Red. masses --     3.7943                 4.2061                 4.4826

 Zero-point correction=                           0.236282
(Hartree/Particle)
 Thermal correction to Energy=                    0.249520
 Thermal correction to Enthalpy=                  0.250464
 Thermal correction to Gibbs Free Energy=         0.194789
 Sum of electronic and zero-point Energies=          -616.438862
 Sum of electronic and thermal Energies=             -616.425624
 Sum of electronic and thermal Enthalpies=           -616.424680
 Sum of electronic and thermal Free Energies=        -616.480355

         Item               Value     Threshold  Converged?
 Maximum Force            0.000023     0.000450     YES
 RMS     Force            0.000005     0.000300     YES
```

***s-trans* 4.92b**

```
----------------------------------------
```

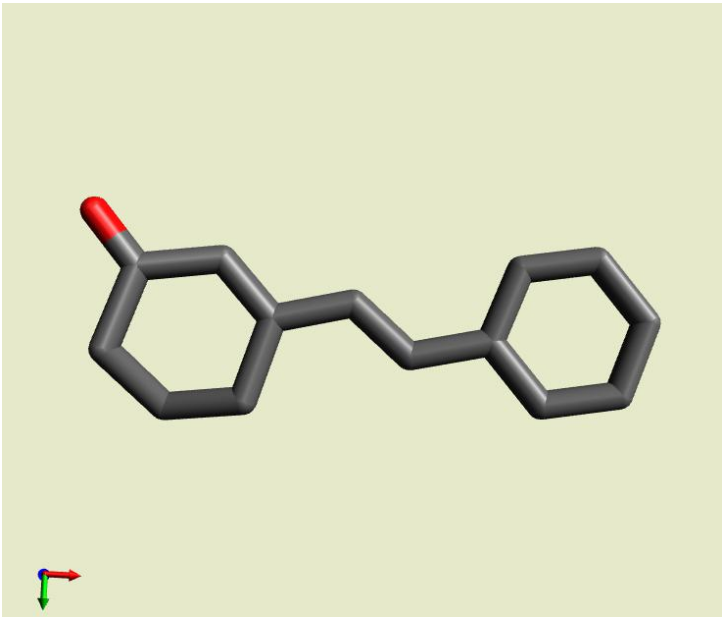

```
 #p b97d/6-31G* freq geom=check guess=check

---------------------------------
 Cartesian coordinates (Angstroms):
---------------------------------
C  -2.430  -1.049   0.043
C  -3.881  -0.822  -0.073
C  -4.329   0.635  -0.263
C  -3.367   1.620   0.427
C  -1.921   1.408  -0.062
```

```
C  -1.489  -0.049   0.024
C  -0.080  -0.398   0.059
C   0.960   0.480  -0.025
C   2.385   0.157  -0.016
H   0.735   1.546  -0.116
C   2.887  -1.166   0.068
C   3.321   1.219  -0.096
C   4.699   0.974  -0.089
C   4.263  -1.410   0.075
C   5.177  -0.343  -0.003
H   0.130  -1.469   0.140
H   2.949   2.245  -0.162
H   2.194  -2.007   0.127
H   4.629  -2.437   0.140
H   5.399   1.809  -0.151
H   6.251  -0.539   0.002
O  -4.687  -1.756  -0.055
H  -3.677   2.661   0.242
H  -3.401   1.455   1.517
H  -4.346   0.836  -1.351
H  -5.362   0.731   0.103
H  -1.827   1.743  -1.112
H  -1.234   2.037   0.527
H  -2.118  -2.095   0.118
-------------------------------------

 SCF Done:  E(RB97D) =  -616.679326860     A.U. after    1 cycles

                     1                      2                      3
                     A                      A                      A
Frequencies --    26.7630                47.6618                78.3551
Red. masses --     3.9292                 4.2610                 4.8122

 Zero-point correction=                           0.236740
(Hartree/Particle)
 Thermal correction to Energy=                    0.249847
 Thermal correction to Enthalpy=                  0.250791
 Thermal correction to Gibbs Free Energy=         0.195755
 Sum of electronic and zero-point Energies=           -616.442587
 Sum of electronic and thermal Energies=              -616.429480
 Sum of electronic and thermal Enthalpies=            -616.428535
 Sum of electronic and thermal Free Energies=         -616.483572

         Item               Value     Threshold  Converged?
 Maximum Force            0.000016     0.000450     YES
 RMS     Force            0.000003     0.000300     YES
```

**GS 4.90a**

```
-----------------------------------------
```

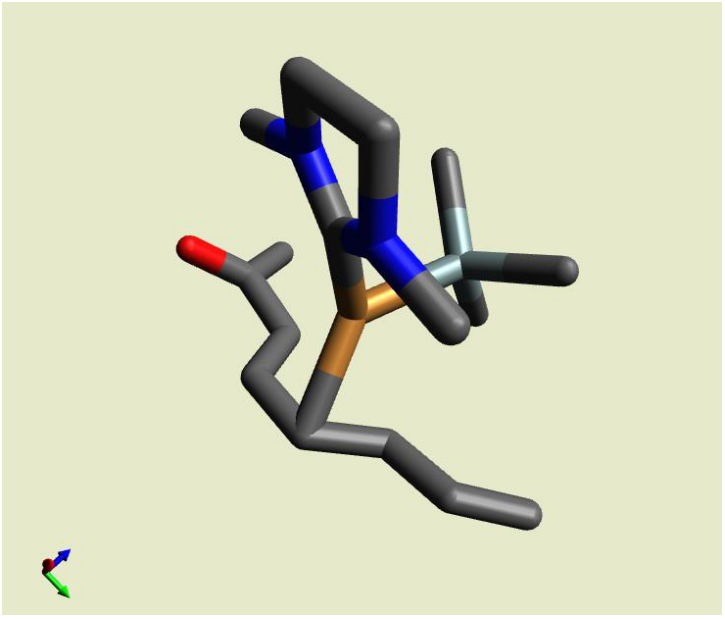

#p b97d/6-31G* freq geom=check guess=check

---
Cartesian coordinates (Angstroms):
---

| | | | |
|---|---|---|---|
| C | -2.125 | -0.654 | -1.013 |
| C | -2.456 | -2.053 | -0.711 |
| C | -3.483 | -2.258 | 0.409 |
| C | -1.292 | -0.322 | -2.117 |
| C | -0.755 | 0.994 | -2.261 |
| C | -1.006 | 2.019 | -1.313 |
| C | -0.284 | 3.279 | -1.344 |
| H | -1.937 | 2.020 | -0.745 |
| C | -0.547 | 4.353 | -0.562 |
| H | -0.009 | 1.168 | -3.042 |
| C | 2.861 | 1.497 | -0.603 |
| C | 1.601 | -0.621 | -0.312 |
| N | 2.771 | 0.053 | -0.477 |
| N | 1.913 | -1.866 | 0.116 |
| C | 0.969 | -2.969 | 0.193 |
| C | 3.933 | -0.700 | 0.031 |
| C | 3.363 | -2.129 | 0.110 |
| Cu | -0.171 | 0.123 | -0.423 |
| Si | -0.574 | 0.686 | 1.724 |
| C | -2.320 | 1.422 | 2.037 |
| C | 0.701 | 1.993 | 2.311 |
| H | -3.118 | 0.743 | 1.691 |
| H | -2.450 | 2.383 | 1.510 |
| H | -2.487 | 1.610 | 3.113 |
| H | 1.723 | 1.575 | 2.302 |
| H | 0.491 | 2.346 | 3.338 |
| H | 0.688 | 2.870 | 1.641 |
| C | -0.411 | -0.858 | 2.855 |
| O | -1.931 | -3.021 | -1.280 |
| H | -3.170 | -1.713 | 1.316 |

```
H  -3.586  -3.329   0.631
H  -4.464  -1.850   0.109
H  -0.958  -1.122  -2.778
H  -2.778   0.100  -0.568
H   0.038   5.271  -0.634
H  -1.360   4.333   0.170
H   0.545   3.342  -2.061
H   0.585  -1.322   2.750
H  -1.160  -1.625   2.593
H  -0.554  -0.600   3.920
H   1.884   1.883  -0.912
H   3.624   1.764  -1.353
H   3.131   1.958   0.364
H  -0.038  -2.562   0.316
H   1.221  -3.600   1.060
H   0.988  -3.582  -0.724
H   3.668  -2.673   1.016
H   3.634  -2.734  -0.775
H   4.223  -0.312   1.026
H   4.794  -0.607  -0.647
-----------------------------------

 SCF Done:  E(RB97D) =  -2741.83980138     A.U. after    1 cycles

                     1                      2                      3
                     A                      A                      A
Frequencies --    28.2277                34.7205                43.3939
Red. masses --     3.6108                 3.7699                 3.1803

 Zero-point correction=                           0.413930
(Hartree/Particle)
 Thermal correction to Energy=                    0.442643
 Thermal correction to Enthalpy=                  0.443587
 Thermal correction to Gibbs Free Energy=         0.355287
 Sum of electronic and zero-point Energies=         -2741.425871
 Sum of electronic and thermal Energies=            -2741.397158
 Sum of electronic and thermal Enthalpies=          -2741.396214
 Sum of electronic and thermal Free Energies=       -2741.484514

         Item               Value     Threshold  Converged?
 Maximum Force            0.000028     0.000450     YES
 RMS     Force            0.000005     0.000300     YES
```

**GS 4.90b**

```
-----------------------------------------
```

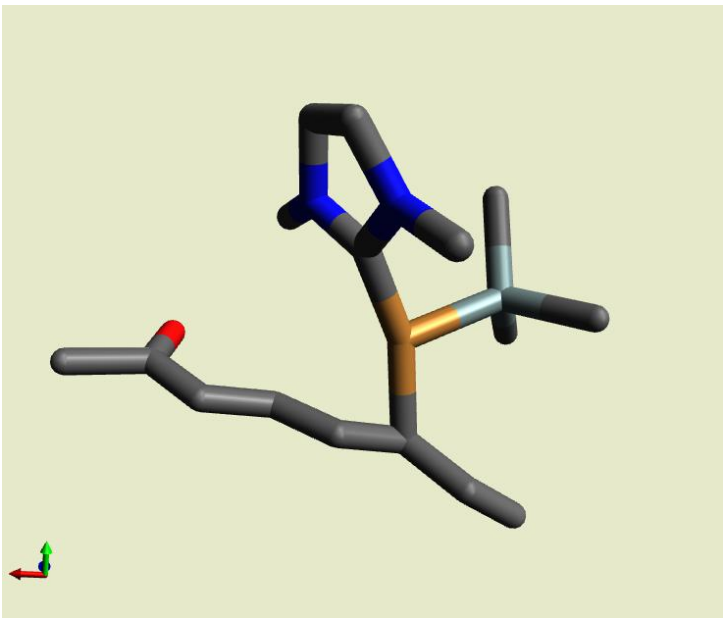

#p b97d/6-31G* freq geom=check guess=check

---
Cartesian coordinates (Angstroms):
---

| | | | |
|---|---|---|---|
| C | 3.033 | -1.483 | -0.600 |
| C | 4.108 | -1.223 | 0.357 |
| C | 5.510 | -1.034 | -0.239 |
| C | 1.761 | -1.775 | -0.171 |
| C | 0.572 | -1.910 | -0.957 |
| C | -0.682 | -2.320 | -0.370 |
| C | -1.782 | -2.805 | -1.212 |
| H | -0.642 | -2.757 | 0.635 |
| C | -2.795 | -3.593 | -0.794 |
| H | 0.658 | -1.860 | -2.048 |
| C | -1.004 | 2.069 | -2.416 |
| C | 0.243 | 1.380 | -0.390 |
| N | -0.208 | 2.344 | -1.234 |
| N | 1.165 | 1.944 | 0.421 |
| C | 1.640 | 1.331 | 1.655 |
| C | 0.555 | 3.597 | -1.112 |
| C | 1.211 | 3.411 | 0.269 |
| Cu | -0.502 | -0.349 | -0.197 |
| Si | -2.451 | 0.139 | 0.879 |
| C | -2.941 | -1.122 | 2.239 |
| C | -3.900 | 0.261 | -0.376 |
| H | -2.166 | -1.176 | 3.023 |
| H | -3.065 | -2.132 | 1.817 |
| H | -3.893 | -0.843 | 2.728 |
| H | -3.736 | 1.079 | -1.100 |
| H | -4.858 | 0.461 | 0.137 |
| H | -4.008 | -0.679 | -0.941 |
| C | -2.314 | 1.856 | 1.743 |
| O | 3.929 | -1.141 | 1.585 |
| H | 5.500 | -0.260 | -1.027 |

```
H    5.853  -1.970  -0.714
H    6.217  -0.748   0.552
H    1.641  -1.894   0.913
H    3.253  -1.406  -1.669
H   -3.586  -3.915  -1.473
H   -2.854  -3.936   0.242
H   -1.758  -2.482  -2.260
H   -2.001   2.628   1.019
H   -1.558   1.832   2.548
H   -3.270   2.178   2.196
H   -1.591   1.158  -2.236
H   -0.370   1.926  -3.312
H   -1.694   2.908  -2.599
H    1.800   0.259   1.500
H    0.920   1.494   2.478
H    2.609   1.775   1.926
H    0.620   3.889   1.072
H    2.245   3.779   0.319
H   -0.111   4.471  -1.166
H    1.306   3.668  -1.921
-----------------------------------

 SCF Done:  E(RB97D) =  -2741.83323992     A.U. after    1 cycles

                     1                      2                      3
                     A                      A                      A
Frequencies --    21.1317                29.2999                34.8332
Red. masses --     3.9786                 4.0516                 3.5886

 Zero-point correction=                           0.412317
(Hartree/Particle)
 Thermal correction to Energy=                    0.441871
 Thermal correction to Enthalpy=                  0.442815
 Thermal correction to Gibbs Free Energy=         0.350679
 Sum of electronic and zero-point Energies=         -2741.420923
 Sum of electronic and thermal Energies=            -2741.391369
 Sum of electronic and thermal Enthalpies=          -2741.390425
 Sum of electronic and thermal Free Energies=       -2741.482561

         Item               Value     Threshold  Converged?
 Maximum Force            0.000013     0.000450     YES
 RMS     Force            0.000003     0.000300     YES
```

**TS 4.91a**

```
-----------------------------------------
```

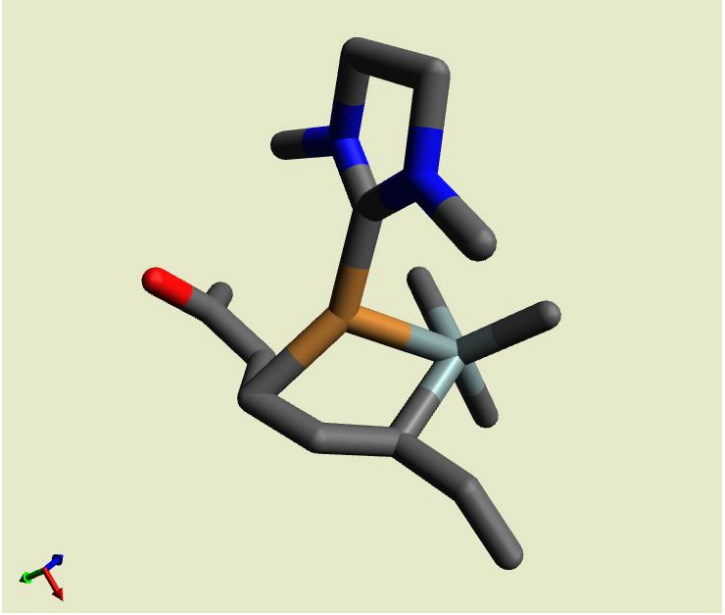

#p b97d/6-31G* freq geom=check guess=check

---
Cartesian coordinates (Angstroms):
---

| | | | |
|---|---|---|---|
| C | 0.049 | 2.362 | -0.537 |
| C | -1.182 | 3.100 | -0.361 |
| C | -1.288 | 3.984 | 0.896 |
| C | 0.329 | 1.710 | -1.791 |
| C | 1.291 | 0.702 | -1.925 |
| C | 2.207 | 0.337 | -0.772 |
| C | 3.126 | -0.778 | -1.164 |
| H | 2.788 | 1.226 | -0.469 |
| C | 4.465 | -0.782 | -1.062 |
| H | 1.472 | 0.230 | -2.891 |
| C | -0.385 | -3.143 | -1.138 |
| C | -1.438 | -1.118 | -0.137 |
| N | -1.476 | -2.422 | -0.514 |
| N | -2.595 | -0.859 | 0.527 |
| C | -3.064 | 0.493 | 0.816 |
| C | -2.655 | -3.137 | 0.000 |
| C | -3.566 | -1.963 | 0.414 |
| Cu | -0.124 | 0.155 | -0.537 |
| Si | 1.712 | -0.198 | 1.227 |
| C | 3.327 | 0.467 | 2.000 |
| C | 1.649 | -2.092 | 1.429 |
| H | 3.348 | 1.570 | 1.962 |
| H | 4.230 | 0.089 | 1.499 |
| H | 3.374 | 0.173 | 3.062 |
| H | 0.614 | -2.455 | 1.338 |
| H | 2.018 | -2.365 | 2.433 |
| H | 2.273 | -2.617 | 0.690 |
| C | 0.373 | 0.529 | 2.406 |
| O | -2.158 | 3.035 | -1.139 |
| H | -0.470 | 3.814 | 1.614 |

```
H  -2.256   3.804   1.392
H  -1.273   5.046   0.596
H  -0.347   1.920  -2.625
H   0.873   2.558   0.151
H   5.060  -1.639  -1.386
H   5.007   0.079  -0.662
H   2.621  -1.655  -1.586
H  -0.589   0.005   2.309
H   0.196   1.598   2.223
H   0.734   0.411   3.446
H   0.363  -2.407  -1.462
H  -0.756  -3.703  -2.013
H   0.085  -3.850  -0.433
H  -2.200   1.111   1.081
H  -3.767   0.450   1.662
H  -3.552   0.953  -0.059
H  -4.087  -2.129   1.368
H  -4.315  -1.727  -0.363
H  -2.370  -3.769   0.862
H  -3.097  -3.779  -0.776
-----------------------------------

 SCF Done:  E(RB97D) =  -2741.81096787     A.U. after    1 cycles

                     1                      2                      3
                     A                      A                      A
Frequencies --  -100.7459               39.9034                42.4891
Red. masses --     8.1231                2.4746                 2.8392

 Zero-point correction=                           0.414000
(Hartree/Particle)
 Thermal correction to Energy=                    0.441627
 Thermal correction to Enthalpy=                  0.442571
 Thermal correction to Gibbs Free Energy=         0.356909
 Sum of electronic and zero-point Energies=         -2741.396968
 Sum of electronic and thermal Energies=            -2741.369341
 Sum of electronic and thermal Enthalpies=          -2741.368397
 Sum of electronic and thermal Free Energies=       -2741.454059

         Item               Value     Threshold  Converged?
 Maximum Force            0.000002     0.000450     YES
 RMS     Force            0.000000     0.000300     YES
```

**TS 4.91b**

```
-----------------------------------------
```

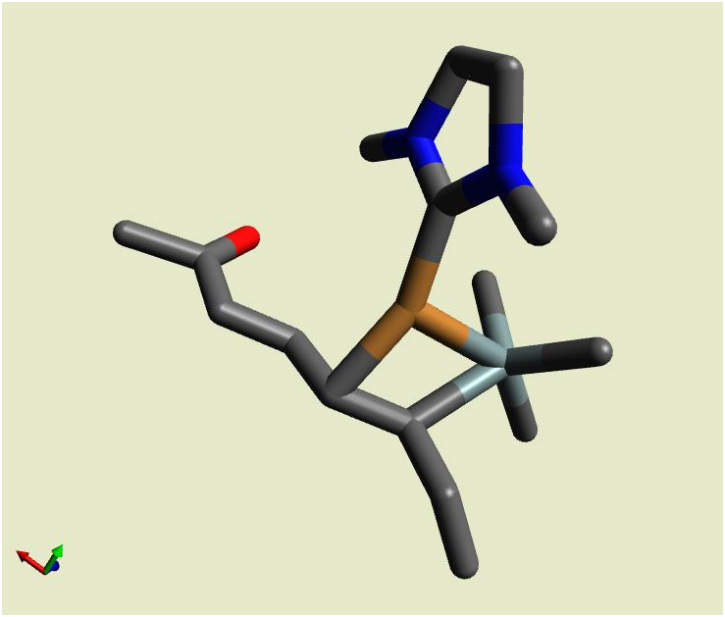

#p b97d/6-31G* freq geom=check guess=check

---
Cartesian coordinates (Angstroms):
---

| | | | |
|---|---|---|---|
| C | 2.523 | -2.040 | -0.881 |
| C | 3.617 | -1.927 | 0.053 |
| C | 5.033 | -2.194 | -0.484 |
| C | 1.209 | -1.905 | -0.440 |
| C | -0.002 | -1.818 | -1.176 |
| C | -1.337 | -1.842 | -0.434 |
| C | -2.502 | -1.928 | -1.367 |
| H | -1.353 | -2.659 | 0.305 |
| C | -3.493 | -2.834 | -1.311 |
| H | -0.014 | -1.987 | -2.255 |
| C | -1.232 | 2.771 | -1.918 |
| C | 0.292 | 1.765 | -0.249 |
| N | -0.317 | 2.864 | -0.792 |
| N | 1.367 | 2.198 | 0.447 |
| C | 2.197 | 1.379 | 1.321 |
| C | 0.521 | 4.070 | -0.658 |
| C | 1.456 | 3.666 | 0.497 |
| Cu | -0.204 | -0.012 | -0.463 |
| Si | -2.067 | -0.438 | 1.075 |
| C | -3.213 | -1.700 | 1.935 |
| C | -3.176 | 0.996 | 0.476 |
| H | -2.640 | -2.546 | 2.350 |
| H | -3.977 | -2.103 | 1.254 |
| H | -3.728 | -1.202 | 2.775 |
| H | -2.598 | 1.923 | 0.345 |
| H | -3.983 | 1.185 | 1.207 |
| H | -3.657 | 0.745 | -0.483 |
| C | -0.856 | 0.118 | 2.459 |
| O | 3.485 | -1.621 | 1.263 |
| H | 5.057 | -2.374 | -1.571 |

```
H    5.455  -3.074   0.030
H    5.686  -1.338  -0.242
H    1.125  -1.889   0.659
H    2.739  -2.189  -1.943
H   -4.307  -2.837  -2.040
H   -3.509  -3.606  -0.538
H   -2.507  -1.178  -2.168
H   -0.505   1.147   2.292
H    0.036  -0.528   2.508
H   -1.353   0.067   3.444
H   -1.792   1.831  -1.842
H   -0.687   2.793  -2.881
H   -1.941   3.613  -1.889
H    2.128   0.321   1.039
H    1.891   1.494   2.376
H    3.247   1.691   1.217
H    1.092   4.034   1.475
H    2.495   4.001   0.360
H   -0.092   4.956  -0.439
H    1.081   4.247  -1.596
---------------------------------

 SCF Done:  E(RB97D) =  -2741.79856156     A.U. after    1 cycles

                     1                      2                      3
                     A                      A                      A
Frequencies --  -148.5264               26.2556                34.8240
Red. masses --     7.5128                4.0732                 3.6744

 Zero-point correction=                           0.412804
(Hartree/Particle)
 Thermal correction to Energy=                    0.440819
 Thermal correction to Enthalpy=                  0.441764
 Thermal correction to Gibbs Free Energy=         0.354487
 Sum of electronic and zero-point Energies=         -2741.385758
 Sum of electronic and thermal Energies=            -2741.357742
 Sum of electronic and thermal Enthalpies=          -2741.356798
 Sum of electronic and thermal Free Energies=       -2741.444074

         Item               Value     Threshold  Converged?
 Maximum Force            0.000001     0.000450     YES
 RMS     Force            0.000000     0.000300     YES
```

### *4.7.5. NMR Spectra of New Compounds*

Sample: CL-IX-295-1H
File: exp

Pulse Sequence: s2pul
 Solvent: cdcl3
 Temp. 25.0 C / 298.1 K
Operator: loawz
VNMRS-400 "vnmr13"

 Relax. delay 1.000 sec
 Pulse 45.0 degrees
 Acq. time 2.048 sec
 Width 4395.4 Hz
 16 repetitions
OBSERVE H1, 399.7832141 MHz
DATA PROCESSING
 Resol. enhancement -0.6 Hz
FT size 65536
Total time 3 min, 21 sec

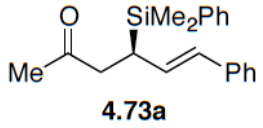


**4.73a**

Sample: KL-IX-304
File: exp

Pulse Sequence: s2pul

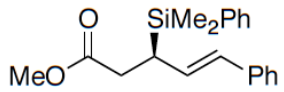


**4.73b**

Sample: HW-I-157-2
File: exp

Pulse Sequence: s2pul
 Solvent: cdcl3
 Temp. 25.0 C / 298.1 K
Operator: wuhr
VNMRS-400  "vnmr13"

 Relax. delay 1.000 sec
 Pulse 45.0 degrees
 Acq. time 2.049 sec
 Width 4807.7 Hz
 24 repetitions
OBSERVE   H1, 399.7832141 MHz
DATA PROCESSING
 Resol. enhancement -0.0 Hz
FT size 65536
Total time 3 min, 21 sec

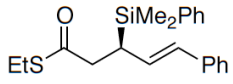


**4.73c**

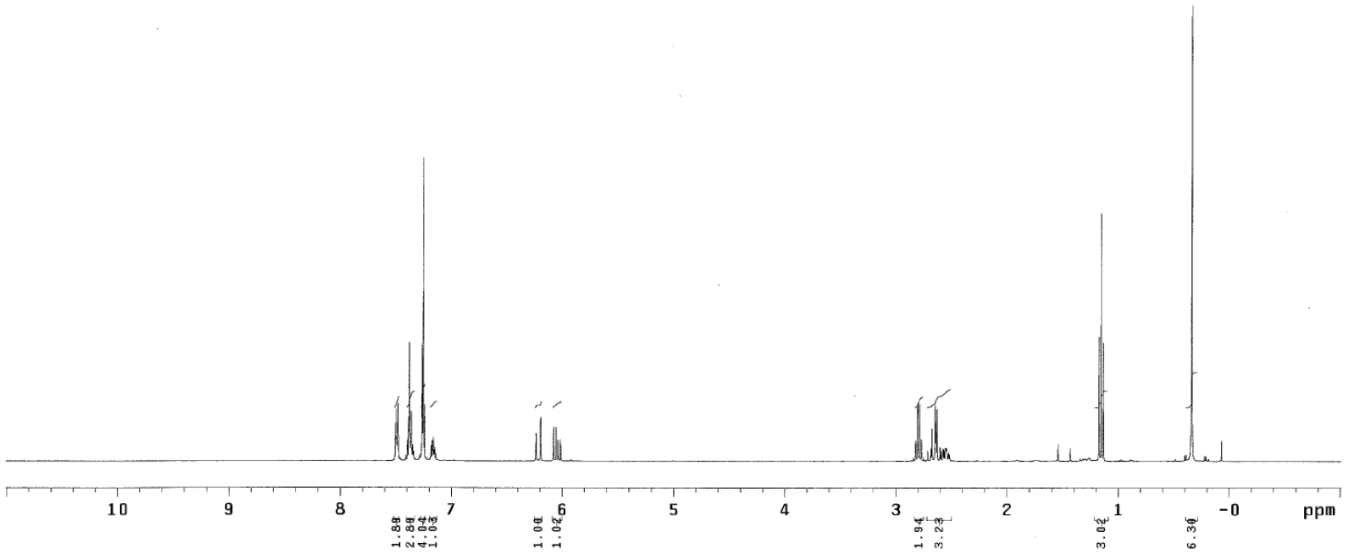

Sample: KL-TX-263-1H
File: exp

Pulse Sequence: s2pul
 Solvent: cdcl3
 Temp. 25.0 C / 298.1 K
Operator: leewz
VNMR3-400 "vnmr13"

 Relax. delay 1.000 sec
 Pulse 45.0 degrees
 Acq. time 2.048 sec
 Width 4006.4 Hz
 16 repetitions
OBSERVE H1, 399.7832141 MHz
DATA PROCESSING
 Resol. enhancement -0.0 Hz
FT size 65536
Total time 3 min, 21 sec

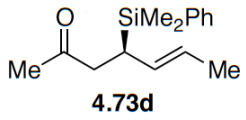


**4.73d**

Sample: HW-I-091
File: exp

Pulse Sequence: s2pul
 Solvent: cdcl3
 Temp. 25.0 C / 298.1 K
Operator: wuhr
VNMRS-400 "vnmr13"

 Relax. delay 1.000 sec
 Pulse 45.0 degrees
 Acq. time 2.049 sec
 Width 4807.7 Hz
 36 repetitions
OBSERVE H1, 399.7832141 MHz
DATA PROCESSING
 Resol. enhancement -0.0 Hz
FT size 65536
Total time 3 min, 21 sec

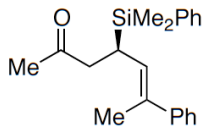


**4.73e**

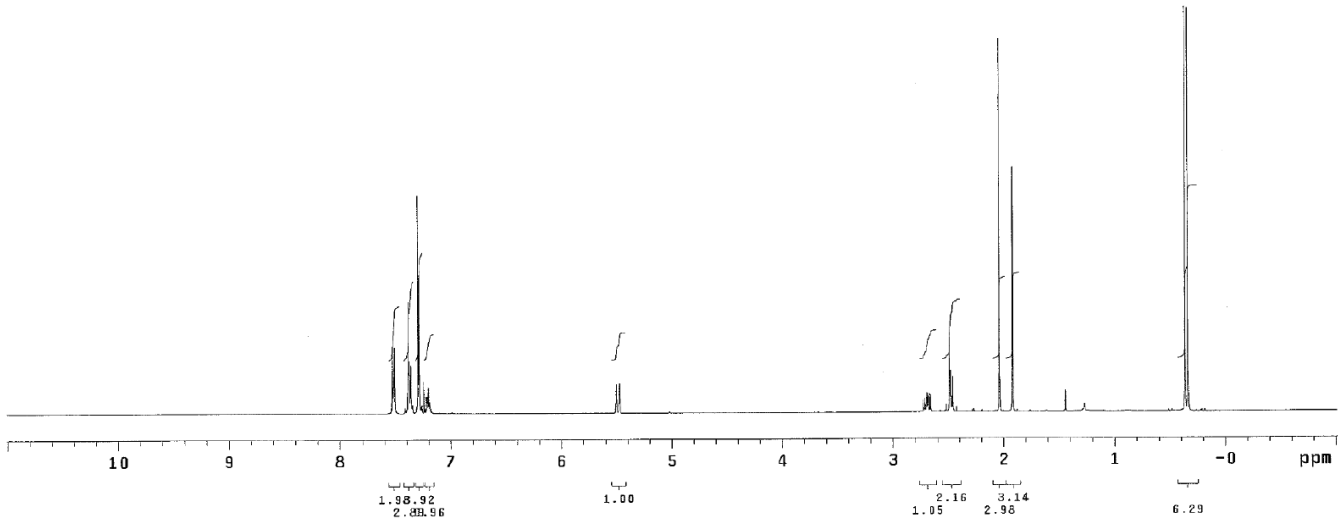

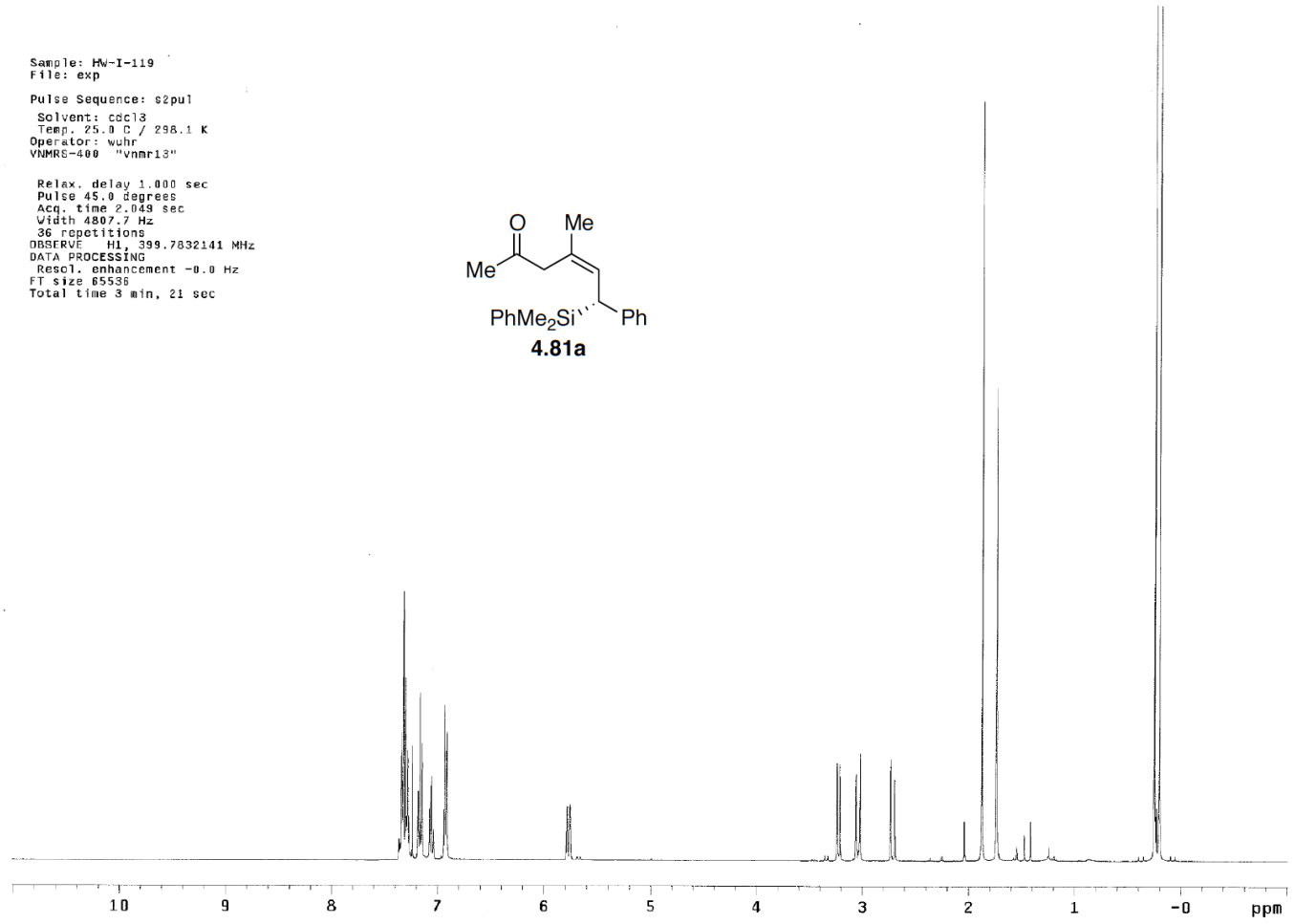
Sample: HW-I-119
File: exp
Pulse Sequence: s2pul
Solvent: cdcl3
Temp. 25.0 C / 298.1 K
Operator: wuhr
VNMRS-400 "vnmr13"
Relax. delay 1.000 sec
Pulse 45.0 degrees
Acq. time 2.049 sec
Width 4807.7 Hz
36 repetitions
OBSERVE H1, 399.7832141 MHz
DATA PROCESSING
Resol. enhancement -0.0 Hz
FT size 65536
Total time 3 min, 21 sec
O
Me
Me
PhMe2Si
Ph
4.81a
10
9
8
7
6
5
4
3
2
1
-0
ppm

Sample: HW-I-132
File: exp

Pulse Sequence: s2pul
 Solvent: cdcl3
 Temp. 25.0 C / 298.1 K
Operator: wuhr
VNMRS-400  "vnmr13"

 Relax. delay 1.000 sec
 Pulse 45.0 degrees
 Acq. time 2.049 sec
 Width 4807.7 Hz
 28 repetitions
OBSERVE   H1, 399.7832141 MHz
DATA PROCESSING
 Resol. enhancement -0.0 Hz
FT size 65536
Total time 3 min, 21 sec

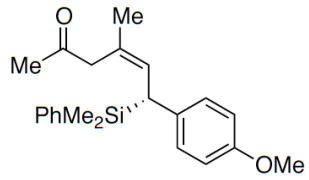


**4.81b**

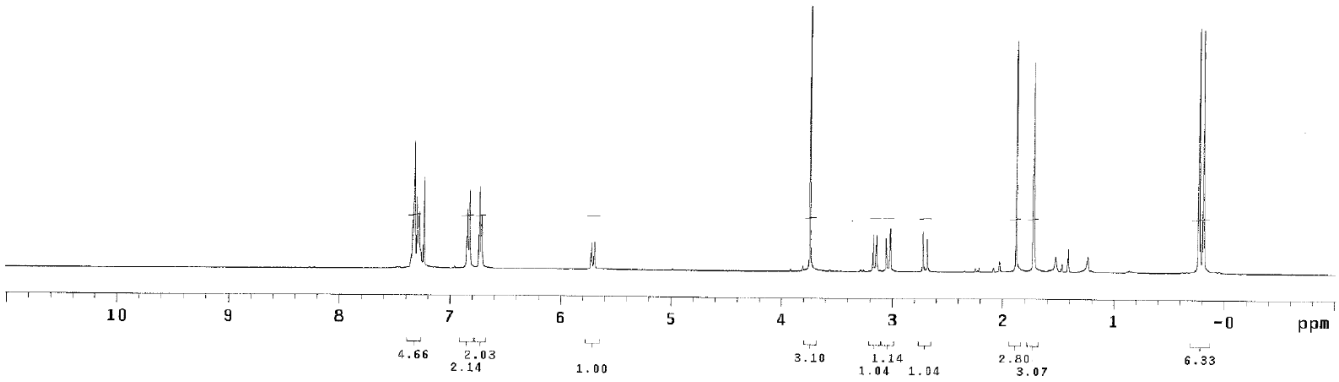

Sample: HW-I-132
File: exp

Pulse Sequence: s2pul
 Solvent: cdcl3
 Temp. 25.0 C / 298.1 K
Operator: wuhr
VNMRS-400 "vnmr13"

 Relax. delay 1.000 sec
 Pulse 45.0 degrees
 Acq. time 2.049 sec
 Width 4807.7 Hz
 36 repetitions
OBSERVE H1, 399.7832141 MHz
DATA PROCESSING
 Resol. enhancement -0.0 Hz
FT size 65536
Total time 3 min, 21 sec

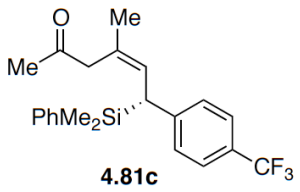


**4.81c**

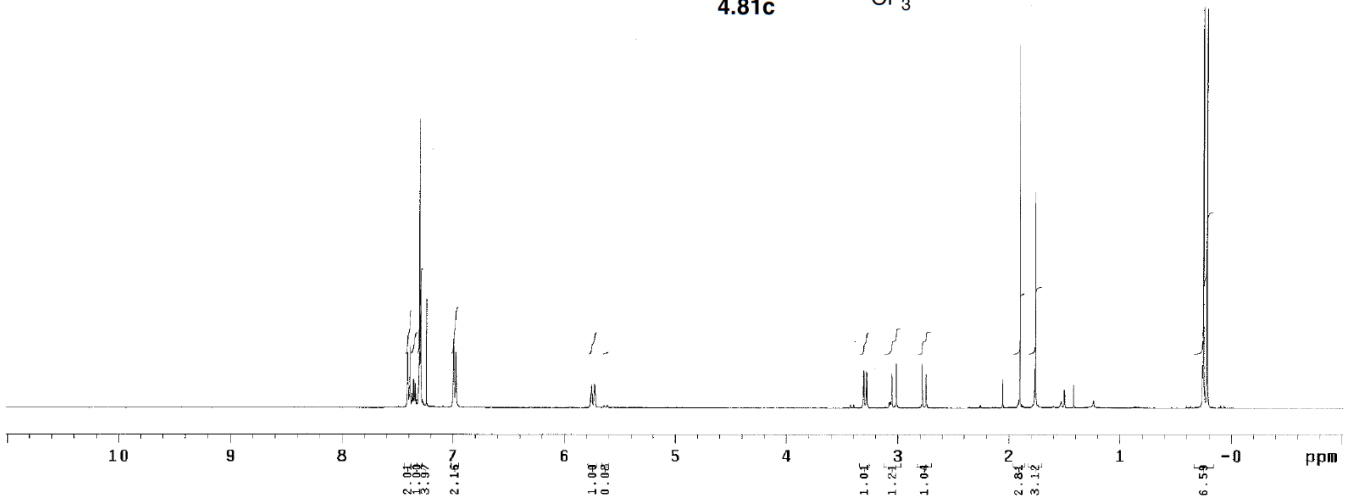

Sample: HW-I-142
File: exp

Pulse Sequence: s2pul
Solvent: cdcl3
Temp. 25.0 C / 298.1 K
Operator: wuhr
VNMRS-400 "vnmr13"

Relax. delay 1.000 sec
Pulse 45.0 degrees
Acq. time 2.049 sec
Width 4807.7 Hz
40 repetitions
OBSERVE H1, 399.7832141 MHz
DATA PROCESSING
Resol. enhancement -0.0 Hz
FT size 65536
Total time 3 min, 21 sec

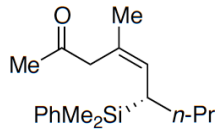


**4.81d**

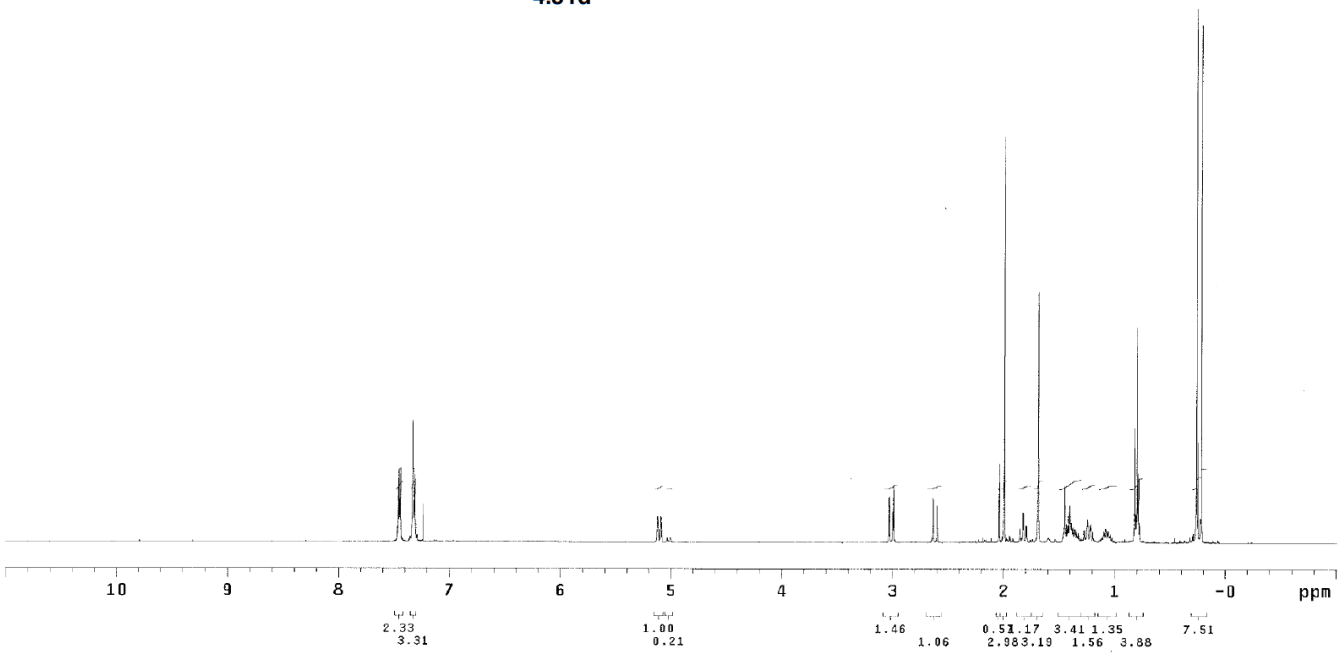

Sample: MW-I-138
File: exp
Pulse Sequence: s2pul
Solvent: cdcl3
Temp. 25.0 C/ 298.1 K
Operator: wuhr
VNMRS-400 "vnmr13"
Relax. delay 1.000 sec
Pulse 45.0 degrees
Acq. time 2.049 sec
Width 4807.7 Hz
52 repetitions
OBSERVE H1, 399.7832141 MHz
DATA PROCESSING
Resol. enhancement -0.0 Hz
FT size 65536
Total time 3 min, 21 sec
Me
O
Me
PhMe2Si
Cy
4.81e
ppm

Sample: HW-I-145-3
File: exp

Pulse Sequence: s2pul
 Solvent: cdcl3
 Temp. 25.0 C / 298.1 K
Operator: wuhr
VNMRS-400  "vnmr13"

 Relax. delay 1.000 sec
 Pulse 45.0 degrees
 Acq. time 2.049 sec
 Width 4807.7 Hz
 32 repetitions
OBSERVE    H1, 399.7832141 MHz
DATA PROCESSING
 Resol. enhancement -0.0 Hz
FT size 65536
Total time 3 min, 21 sec

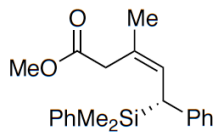


**4.81f**

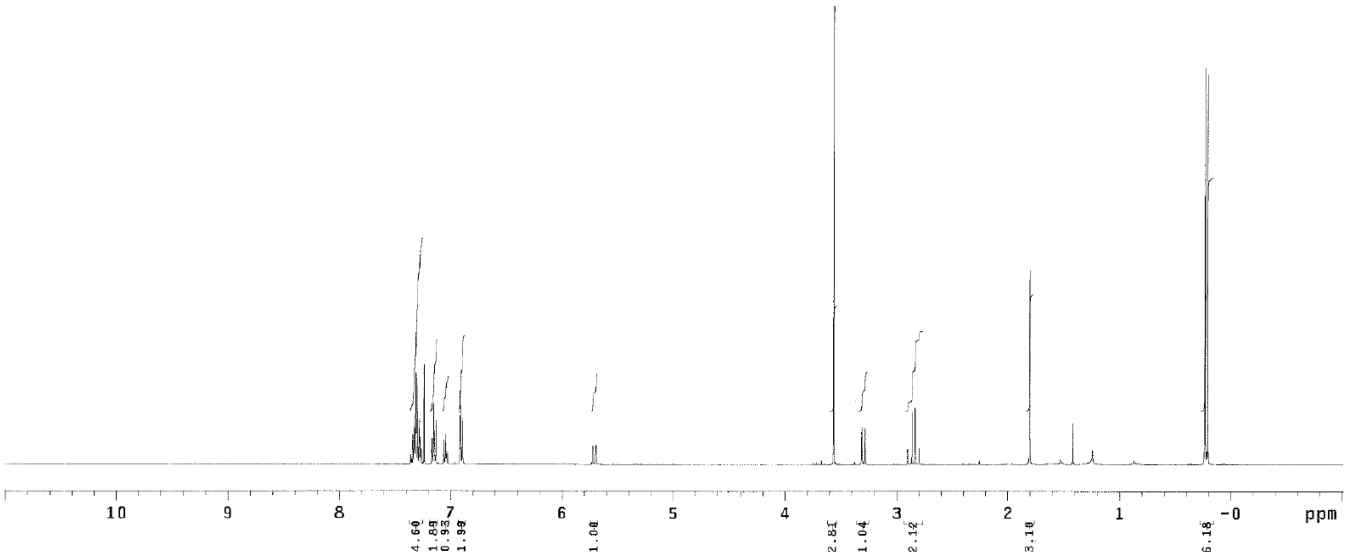

Sample: HW-I-191
File: exp
Pulse Sequence: s2pul
Solvent: cdcl3
Temp. 25.0 C / 298.1 K
Operator: ahh
INOVA-500 "nmr11"
Relax. delay 1.000 sec
Pulse 45.0 degrees
Acq. time 3.000 sec
Width 5997.5 Hz
24 repetitions
OBSERVE H1, 499.7720124 MHz
DATA PROCESSING
Resol. enhancement -0.0 Hz
FT size 65536
Total time 4 min, 25 sec
O
Me
EtS
PhMe2Si
Ph
4.81g
ppm

Sample: KL-IX-267-1-1H
File: exp

Pulse Sequence: s2pul
 Solvent: cdcl3
 Temp. 25.0 C / 298.1 K
Operator: leewz
VNMRS-400 "vnmr13"

 Relax. delay 1.000 sec
 Pulse 45.0 degrees
 Acq. time 2.048 sec
 Width 4006.4 Hz
 24 repetitions
OBSERVE H1, 399.7832141 MHz
DATA PROCESSING
 Resol. enhancement -0.0 Hz
FT size 65536
Total time 3 min, 21 sec

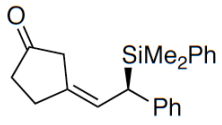


**4.93a**

Sample: KL-IX-136-1H
File: exp

Pulse Sequence: s2pul
 Solvent: cdcl3
 Temp. 25.0 C / 298.1 K
Operator: leewz
VNMRS-400 "vnmr13"

 Relax. delay 1.000 sec
 Pulse 45.0 degrees
 Acq. time 2.048 sec
 Width 4006.4 Hz
 28 repetitions
OBSERVE H1, 399.7832141 MHz
DATA PROCESSING
 Resol. enhancement -0.0 Hz
FT size 65536
Total time 3 min, 21 sec

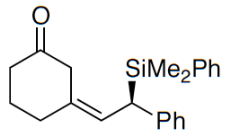


**4.93b**

Sample: KL-IX-272-1H
File: exp

Pulse Sequence: s2pul
Solvent: cdcl3
Temp. 25.0 C / 298.1 K
Operator: leewz
VNMRS-400 "vnmr13"

Relax. delay 1.000 sec
Pulse 45.0 degrees
Acq. time 2.048 sec
Width 4006.4 Hz
16 repetitions
OBSERVE H1, 399.7832141 MHz
DATA PROCESSING
Resol. enhancement -0.0 Hz
FT size 65536
Total time 3 min, 21 sec

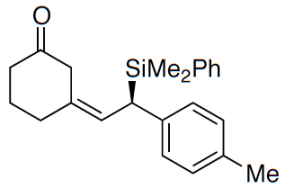


**4.93c**

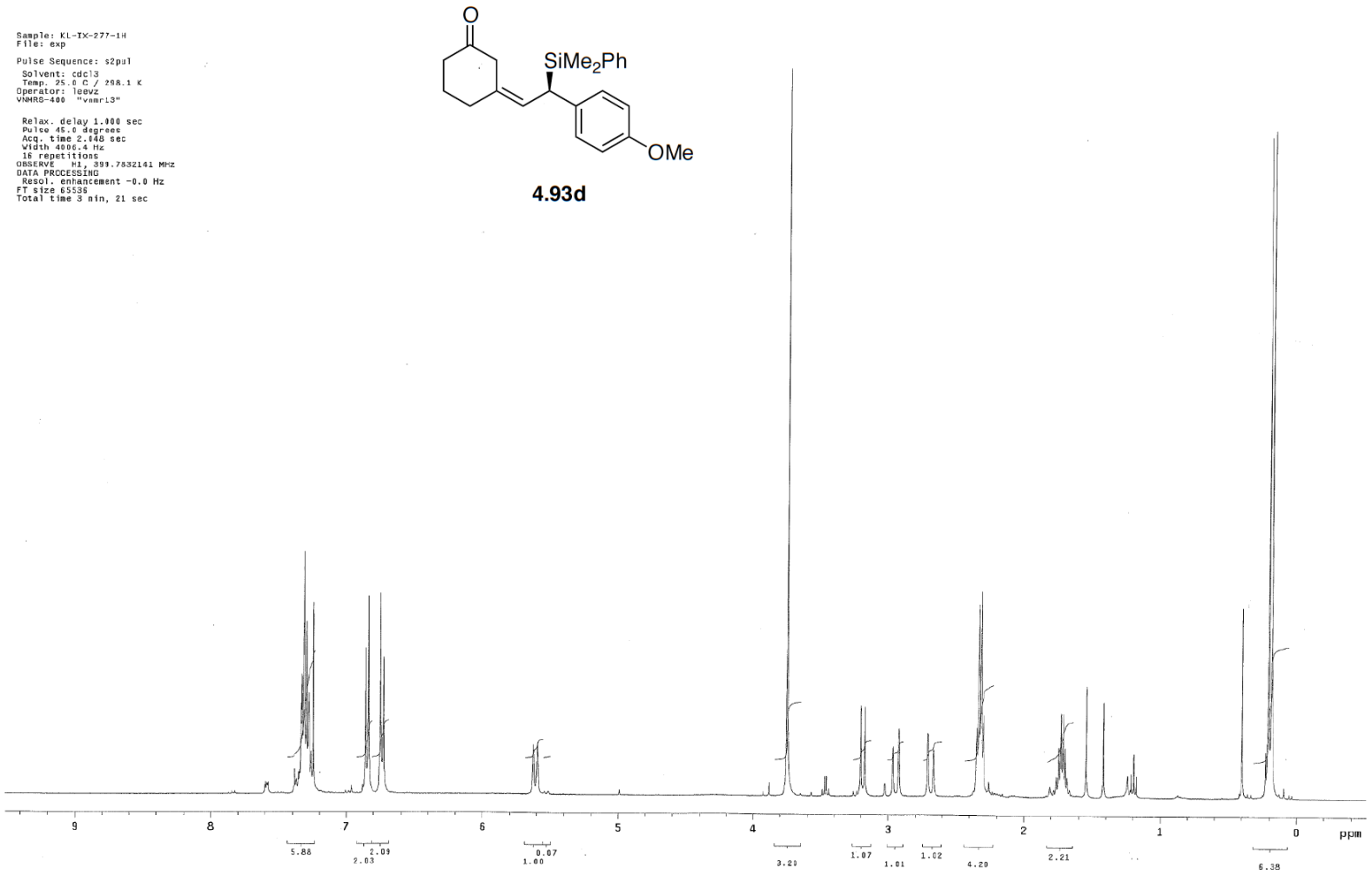
Sample: KL-IX-277-1H
File: exp
Pulse Sequence: s2pul
Solvent: cdcl3
Temp. 25.0 C / 298.1 K
Operator: leewz
VNMRS-400 "vnmrl3"
Relax. delay 1.000 sec
Pulse 45.0 degrees
Acq. time 2.648 sec
Width 4006.4 Hz
16 repetitions
OBSERVE H1, 399.7832141 MHz
DATA PROCESSING
Resol. enhancement -0.0 Hz
FT size 65536
Total time 3 min, 21 sec
O
SiMe2Ph
OMe
4.93d
9
8
7
6
5
4
3
2
1
0
ppm
5.88
2.09
2.03
0.07
1.00
3.29
1.07
1.01
1.02
4.20
2.21
6.38

Sample: KL-IX-275-1H
File: exp

Pulse Sequence: s2pul

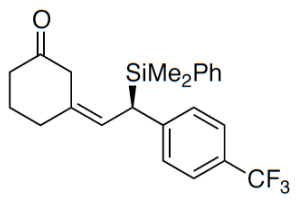


**4.93e**

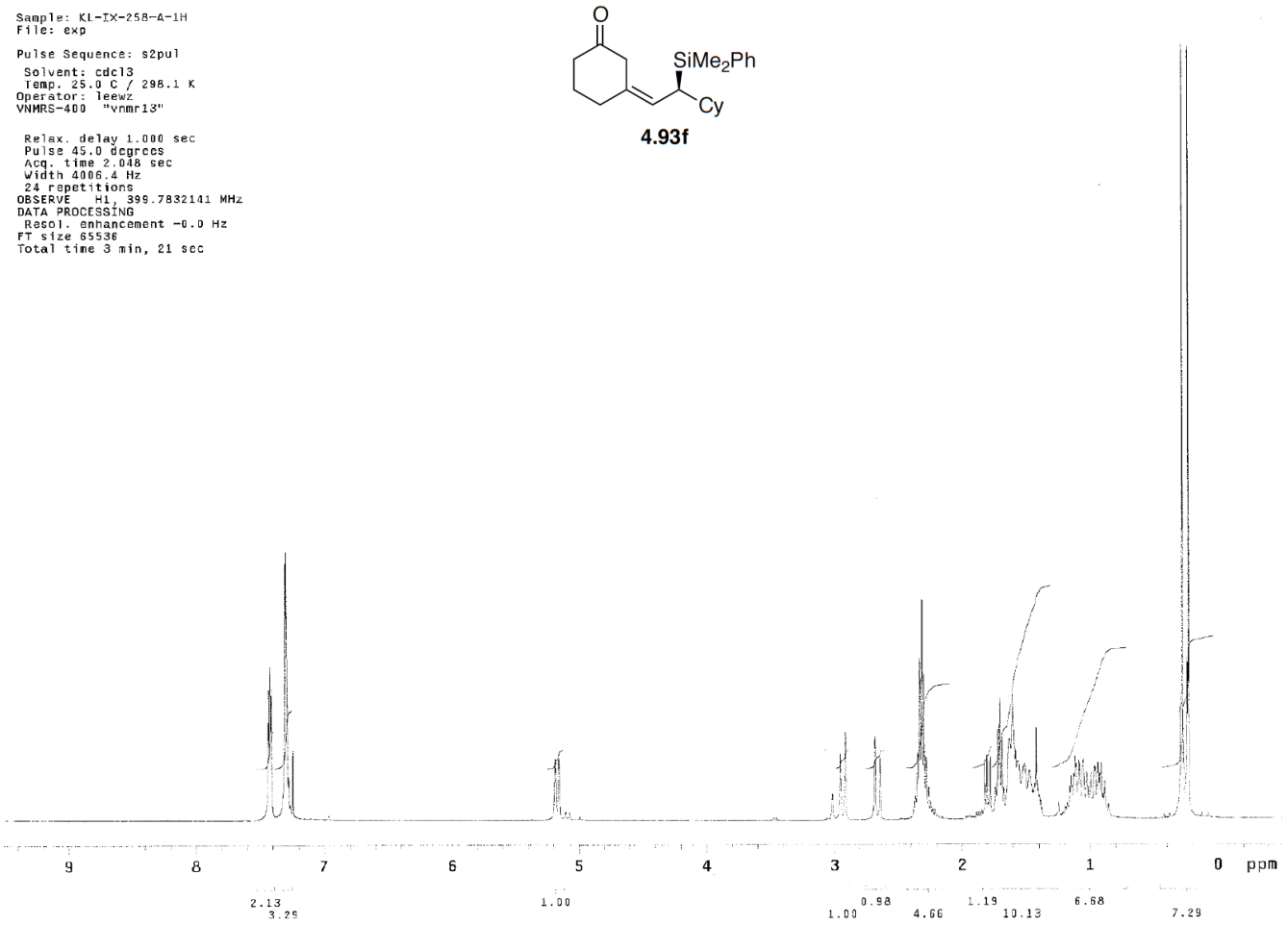
Sample: KL-IX-258-A-1H
File: exp
Pulse Sequence: s2pul
Solvent: cdcl3
Temp. 25.0 C / 298.1 K
Operator: leewz
VNMRS-400 "vnmr13"
Relax. delay 1.000 sec
Pulse 45.0 degrees
Acq. time 2.048 sec
Width 4006.4 Hz
24 repetitions
OBSERVE H1, 399.7832141 MHz
DATA PROCESSING
Resol. enhancement -0.0 Hz
FT size 65536
Total time 3 min, 21 sec
O
SiMe2Ph
Cy
4.93f
9
8
7
6
5
4
3
2
1
0
ppm
2.13
3.29
1.00
1.00
0.98
4.66
1.19
10.13
6.68
7.29

Sample: KL-IX-139-1H
File: exp

Pulse Sequence: s2pul
Solvent: cdcl3
Temp. 25.0 C / 298.1 K
Operator: lgewz
VNMRS-400 "vnmrs"

Relax. delay 1.000 sec
Pulse 45.0 degrees
Acq. time 2.048 sec
Width 4006.4 Hz
24 repetitions
OBSERVE H1, 399.7832141 MHz
DATA PROCESSING
Resol. enhancement -0.0 Hz
FT size 65536
Total time 3 min, 21 sec

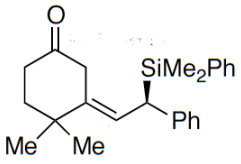


**4.93g**

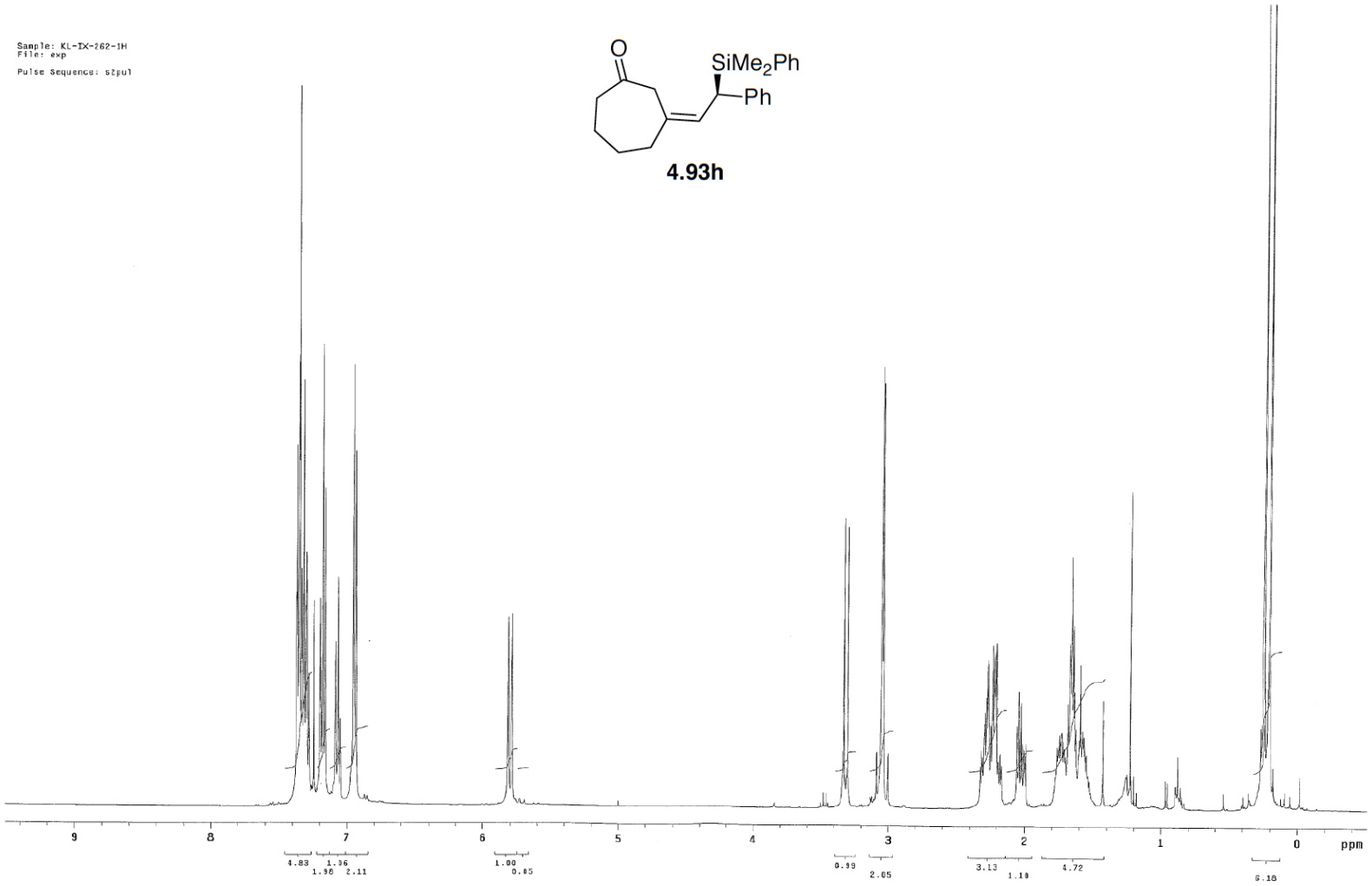
Sample: KL-IX-262-1H
File: exp
Pulse Sequence: s2pul
O
SiMe2Ph
Ph
4.93h
9
8
7
6
5
4
3
2
1
0
ppm
4.83
1.96
1.36
2.11
1.00
0.85
0.99
2.05
3.13
1.18
4.72
6.18

NM-3-195crude

Sample Name:
HW-V-252
Data Collected on:
vnmr13-vnmrs400
Archive directory:

Sample directory:

FidFile: PROTON

Pulse Sequence: PROTON (s2pul)
Solvent: cdcl3
Data collected on: Mar 18 2013

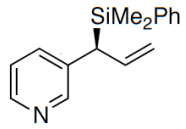


**4.101e**

glycosylation of phthalimide substrate, flash
mixed fractions

Sample: HV-I-193
File: exp

Pulse Sequence: s2pul
 Solvent: cdcl3
 Temp. 25.0 C / 298.1 K
Operator: ahh
VNMRS-500  "nmr15"

 Relax. delay 1.000 sec
 Pulse 45.0 degrees
 Acq. time 2.049 sec
 Width 6009.6 Hz
 24 repetitions
OBSERVE  H1, 499.8853621 MHz
DATA PROCESSING
 Resol. enhancement -0.0 Hz
FT size 65536
Total time 3 min, 21 sec

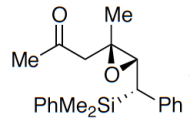


**4.96**

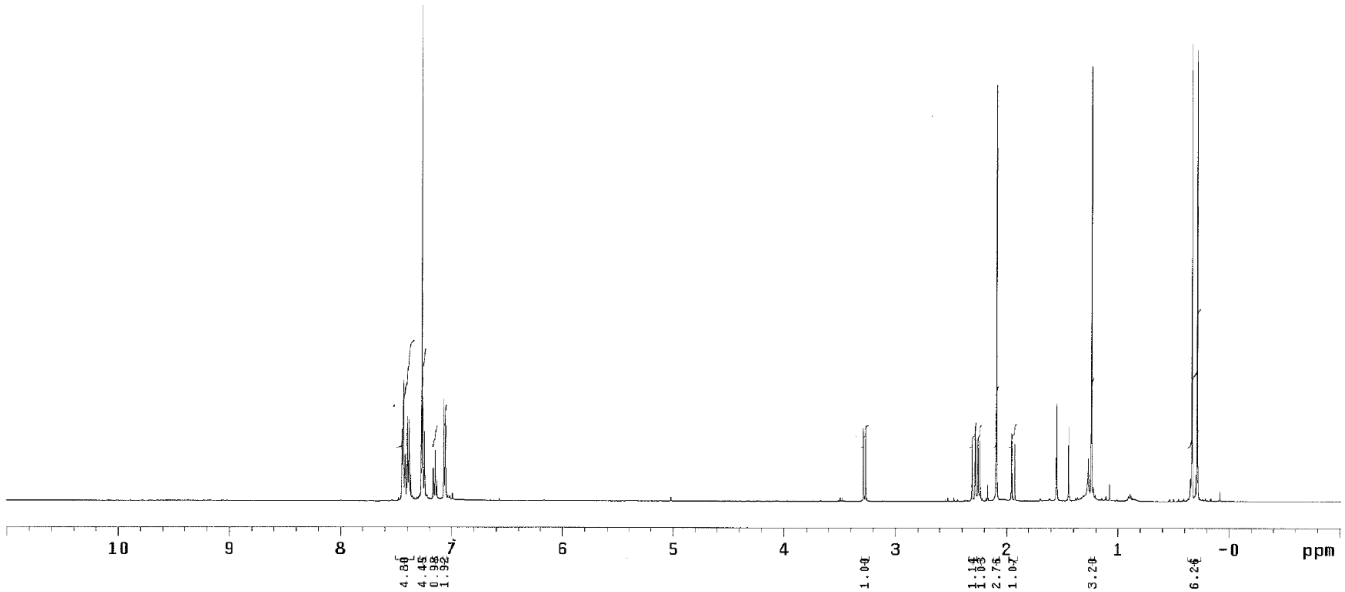

Sample: HV-I-254-4
File: exp

Pulse Sequence: s2pul
Solvent: cdcl3
Temp. 25.0 C / 298.1 K
Operator: wuhr
VNMRS-400 "vnmr13"

Relax. delay 1.000 sec
Pulse 45.0 degrees
Acq. time 2.049 sec
Width 4807.7 Hz
8 repetitions
OBSERVE H1, 399.7832141 MHz
DATA PROCESSING
Resol. enhancement -0.0 Hz
FT size 65536
Total time 3 min, 21 sec

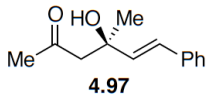


**4.97**

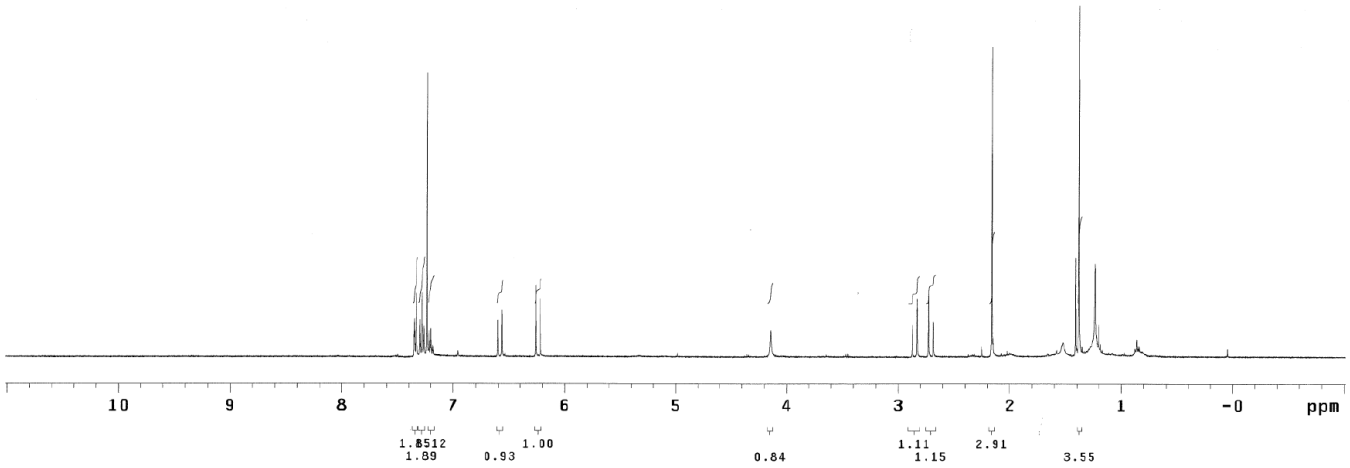

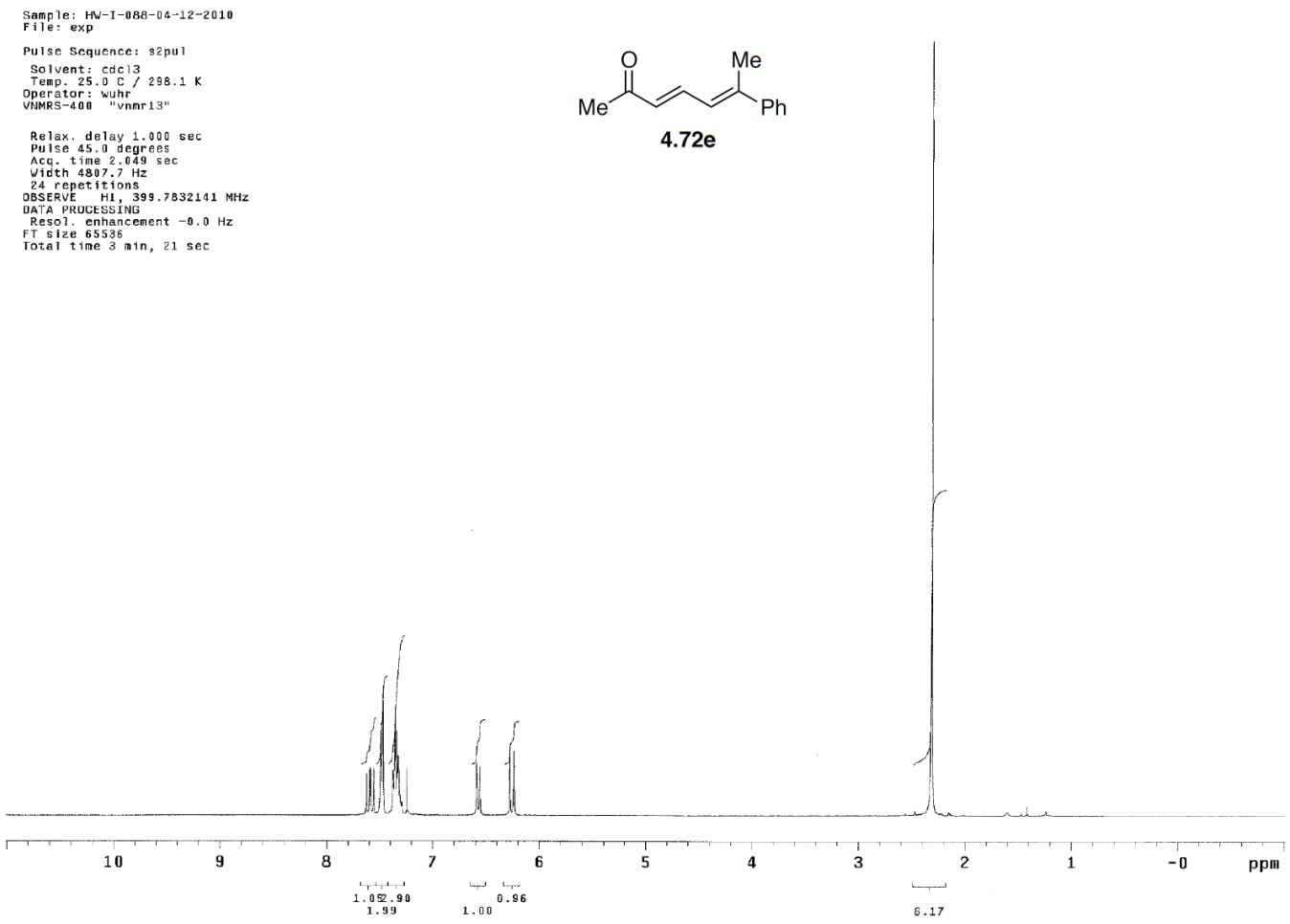
Sample: HW-I-088-04-12-2010
File: exp
Pulse Sequence: s2pul
Solvent: cdcl3
Temp. 25.0 C / 298.1 K
Operator: wuhr
VNMRS-400 "vnmr13"
Relax. delay 1.000 sec
Pulse 45.0 degrees
Acq. time 2.049 sec
Width 4807.7 Hz
24 repetitions
OBSERVE H1, 399.7832141 MHz
DATA PROCESSING
Resol. enhancement -0.0 Hz
FT size 65536
Total time 3 min, 21 sec
O
Me
Me
Ph
4.72e
10
9
8
7
6
5
4
3
2
1
-0
ppm
1.05
2.90
0.96
1.99
1.00
6.17

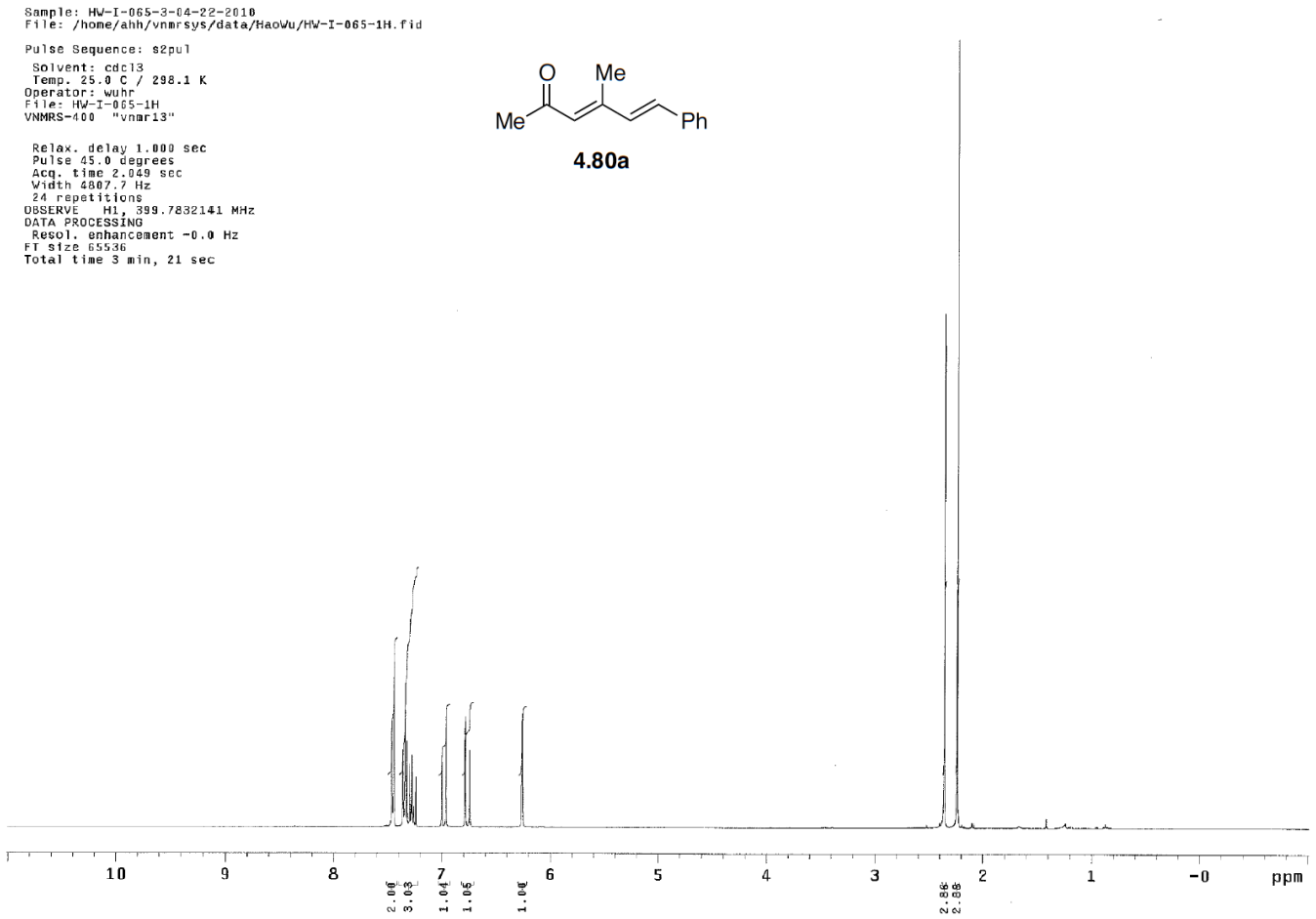
Sample: HW-I-065-3-04-22-2010
File: /home/ahh/vnmrsys/data/HaoWu/HW-I-065-1H.fid
Pulse Sequence: s2pul
Solvent: cdcl3
Temp. 25.0 C / 298.1 K
Operator: wuhr
File: HW-I-065-1H
VNMRS-400 "vnmr13"
Relax. delay 1.000 sec
Pulse 45.0 degrees
Acq. time 2.049 sec
Width 4807.7 Hz
24 repetitions
OBSERVE H1, 399.7832141 MHz
DATA PROCESSING
Resol. enhancement -0.0 Hz
FT size 65536
Total time 3 min, 21 sec
O
Me
Me
Ph
4.80a
10
9
8
7
6
5
4
3
2
1
-0
ppm
2.00
3.03
1.04
1.05
1.00
2.86
2.88

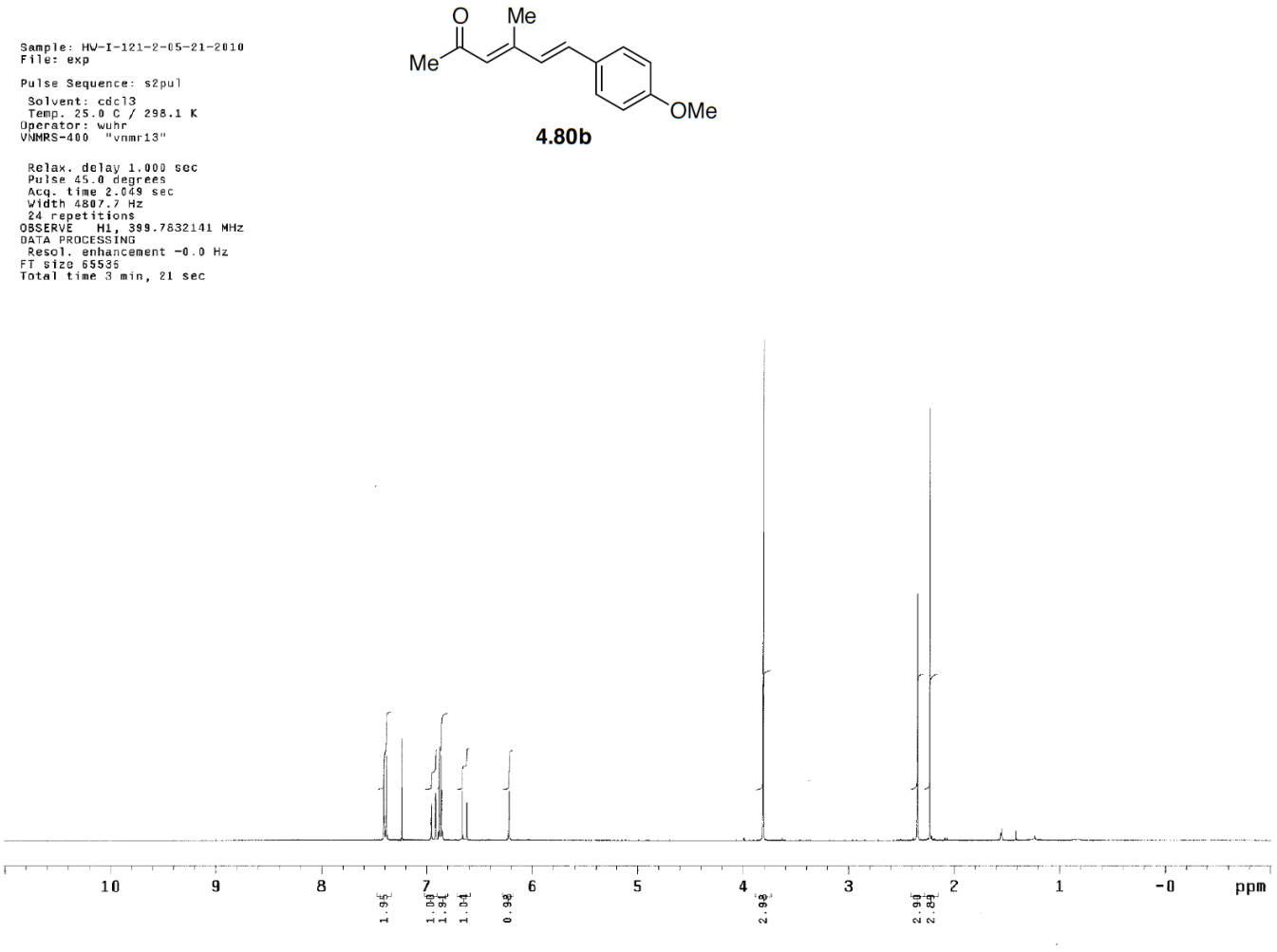
Sample: HW-I-121-2-05-21-2010
File: exp
Pulse Sequence: s2pul
Solvent: cdcl3
Temp. 25.0 C / 298.1 K
Operator: wuhr
VNMRS-400 "vnmr13"
Relax. delay 1.000 sec
Pulse 45.0 degrees
Acq. time 2.049 sec
Width 4807.7 Hz
24 repetitions
OBSERVE H1, 399.7832141 MHz
DATA PROCESSING
Resol. enhancement -0.0 Hz
FT size 65536
Total time 3 min, 21 sec
O
Me
Me
OMe
4.80b
10
9
8
7
6
5
4
3
2
1
-0
ppm
1.95
1.00
1.94
1.04
0.98
2.98
2.90
2.84

Sample: HW-I-112-2
File: /home/ahh/vnmrsys/data/HaoWu/HW-I-112-1H.fid

Pulse Sequence: s2pul

Solvent: cdcl3
Temp. 25.0 C / 298.1 K
Operator: wuhr
File: HW-I-112-1H
VNMRS-400 "vnmr13"

Relax. delay 1.000 sec
Pulse 45.0 degrees
Acq. time 2.049 sec
Width 4807.7 Hz
24 repetitions
OBSERVE H1, 399.7832335 MHz
DATA PROCESSING
Resol. enhancement -0.0 Hz
FT size 65536
Total time 3 min, 21 sec

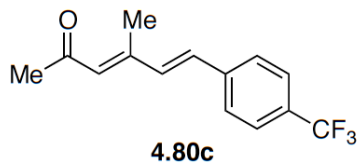


**4.80c**

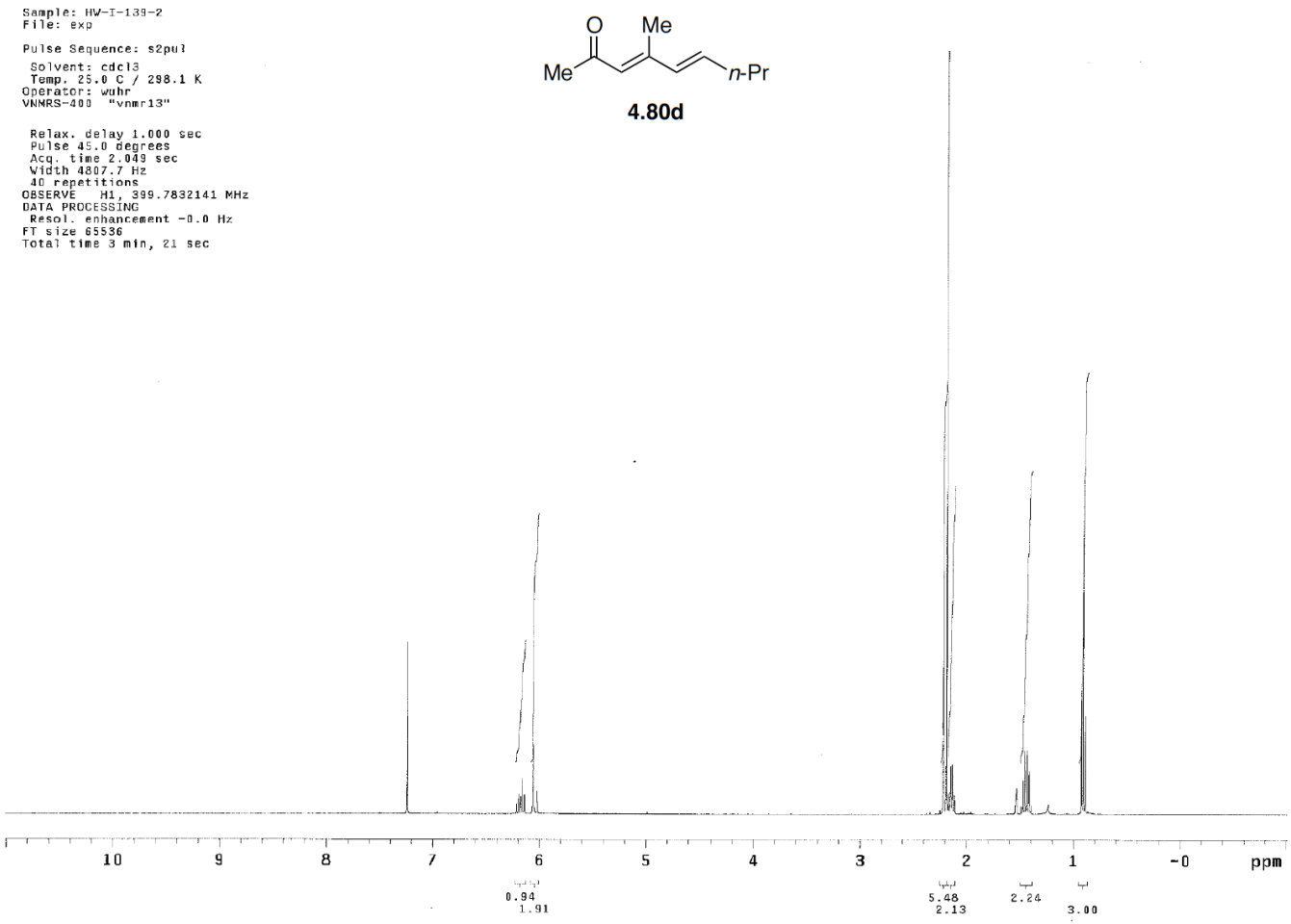
Sample: HW-I-139-2
File: exp
Pulse Sequence: s2pul
Solvent: cdcl3
Temp. 25.0 C / 298.1 K
Operator: wuhr
VNMRS-400 "vnmr13"
Relax. delay 1.000 sec
Pulse 45.0 degrees
Acq. time 2.049 sec
Width 4807.7 Hz
40 repetitions
OBSERVE H1, 399.7832141 MHz
DATA PROCESSING
Resol. enhancement -0.0 Hz
FT size 65536
Total time 3 min, 21 sec
O
Me
Me
n-Pr
4.80d
10
9
8
7
6
5
4
3
2
1
-0
ppm
0.94
1.91
5.48
2.13
2.24
3.00

Sample: HW-I-134-6-06-14-2010
File: exp

Pulse Sequence: s2pul

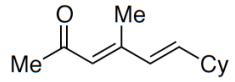


**4.80e**

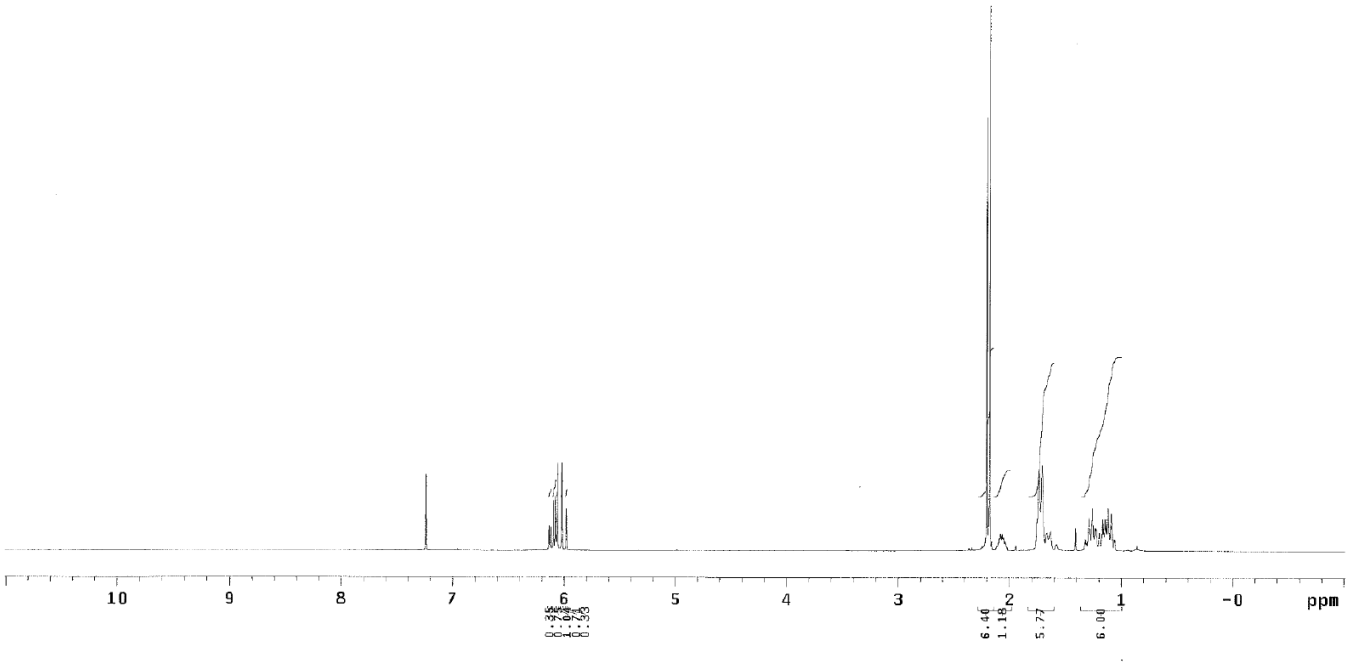

Sample: HW-I-143-1-06-23-2010
File: exp

Pulse Sequence: s2pul

Solvent: cdcl3
Temp. 25.0 C / 298.1 K
Operator: wuhr
VNMRS-400 "vnmr13"

Relax. delay 1.000 sec
Pulse 45.0 degrees
Acq. time 2.049 sec
Width 4807.7 Hz
20 repetitions
OBSERVE H1, 399.7832141 MHz
DATA PROCESSING
Resol. enhancement -0.0 Hz
FT size 65536
Total time 3 min, 21 sec

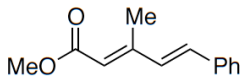


**4.80f**

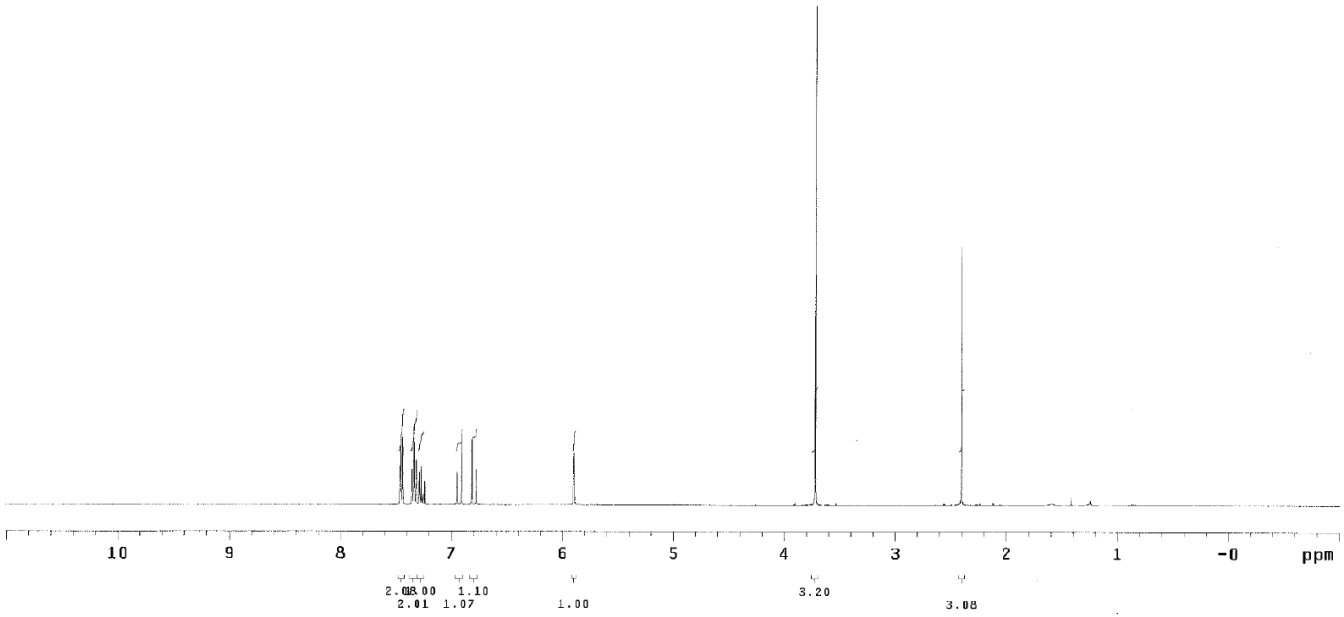

Sample: HW-I-160-2
File: exp

Pulse Sequence: s2pul
 Solvent: cdcl3
 Temp. 25.0 C / 298.1 K
Operator: wuhr
VNMRS-400  "vnmr13"

 Relax. delay 1.000 sec
 Pulse 45.0 degrees
 Acq. time 2.049 sec
 Width 4807.7 Hz
 10 repetitions
OBSERVE   H1, 399.7832141 MHz
DATA PROCESSING
 Resol. enhancement -0.0 Hz
FT size 65536
Total time 3 min, 21 sec

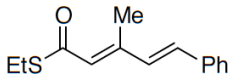


**4.80g**

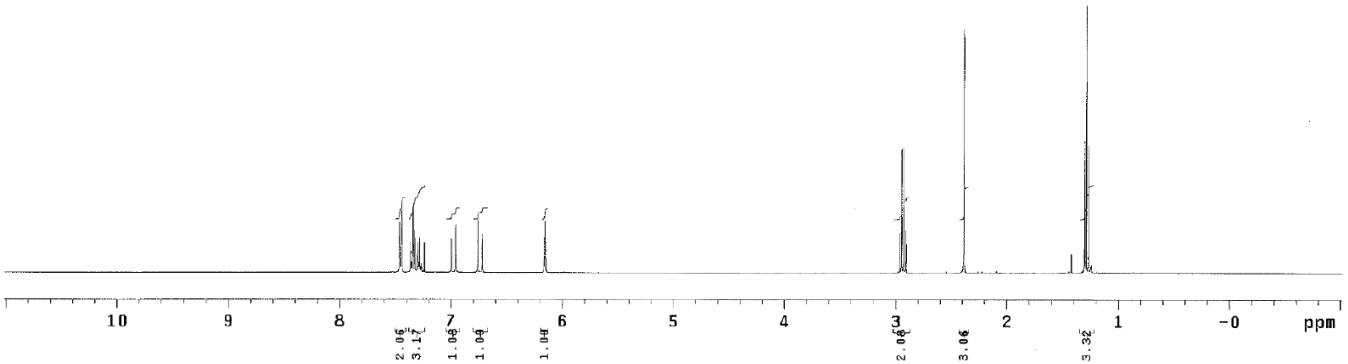

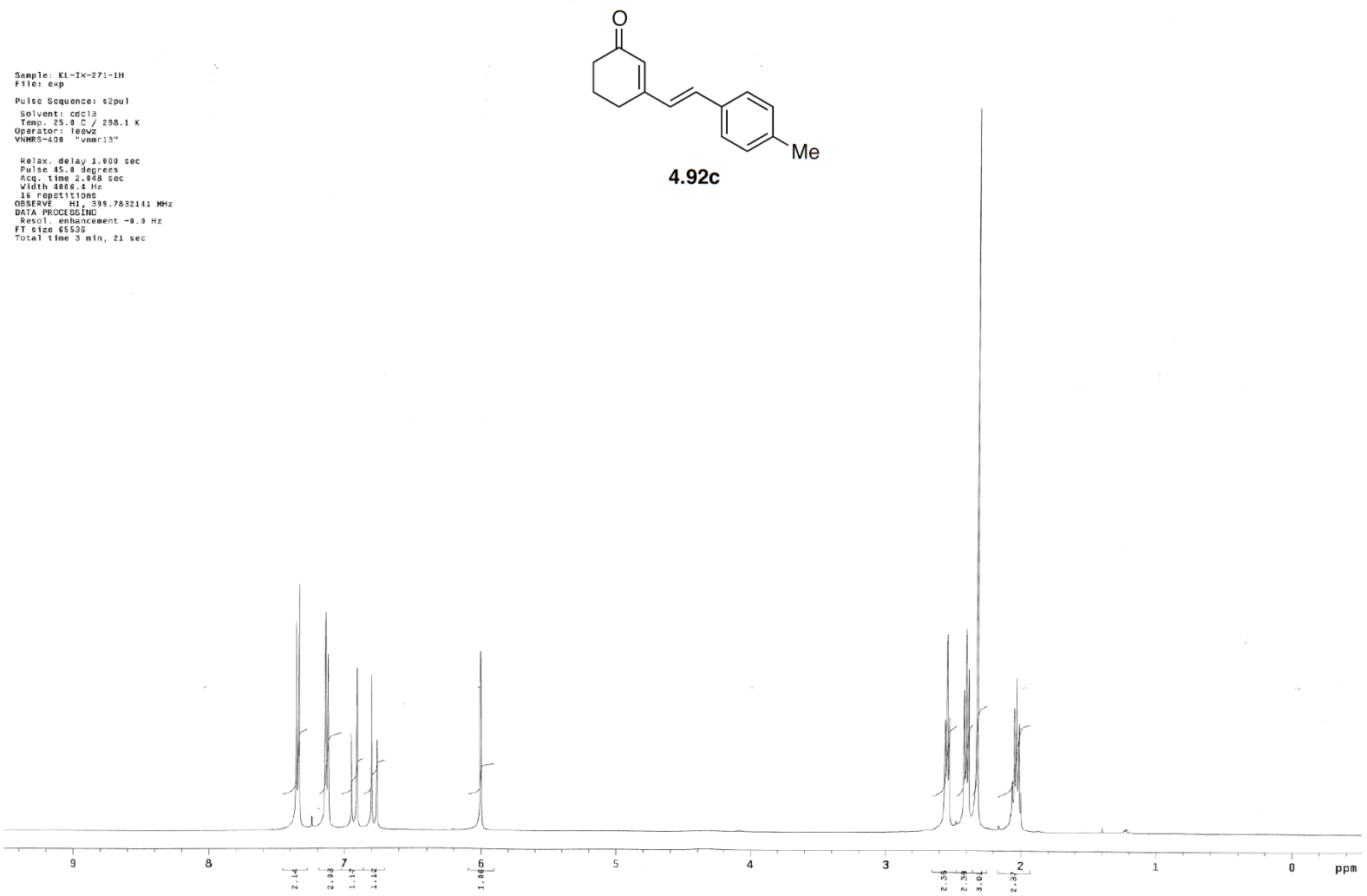
Sample: KL-IK-271-1H
File: exp
Pulse Sequence: s2pul
Solvent: cdcl3
Temp. 25.0 C / 298.1 K
Operator: leawz
VNMRS-400 "vnmr13"
Relax. delay 1.000 sec
Pulse 45.0 degrees
Acq. time 2.048 sec
Width 4008.4 Hz
16 repetitions
OBSERVE H1, 399.7832141 MHz
DATA PROCESSING
Resol. enhancement -0.9 Hz
FT size 65536
Total time 3 min, 21 sec
O
Me
4.92c
9
8
7
6
5
4
3
2
1
0
ppm
2.14
2.03
1.17
1.12
1.00
2.35
2.39
3.01
2.37

Sample: KL-IX-268-1H
File: exp

Pulse Sequence: s2pul

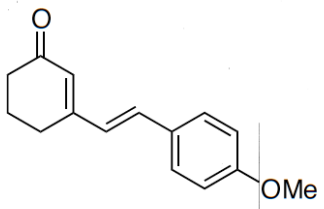


**4.92d**

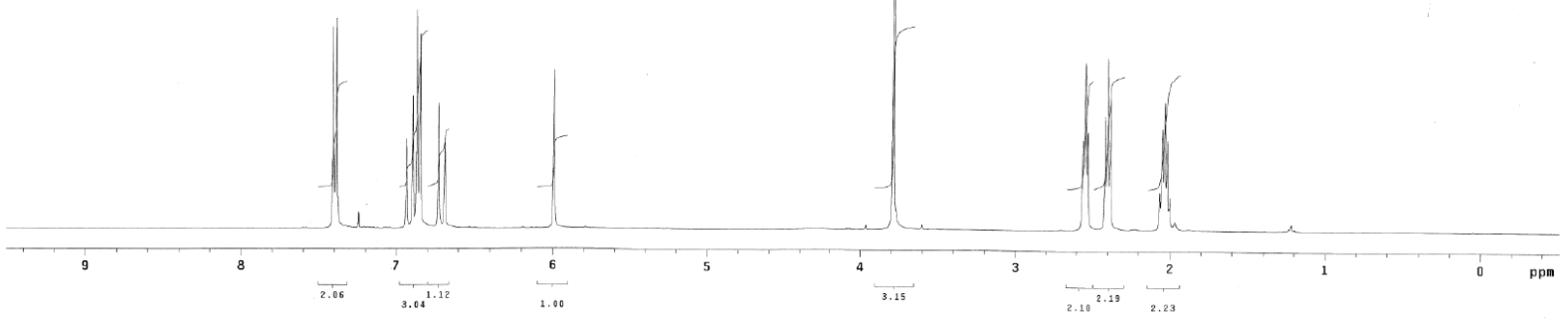

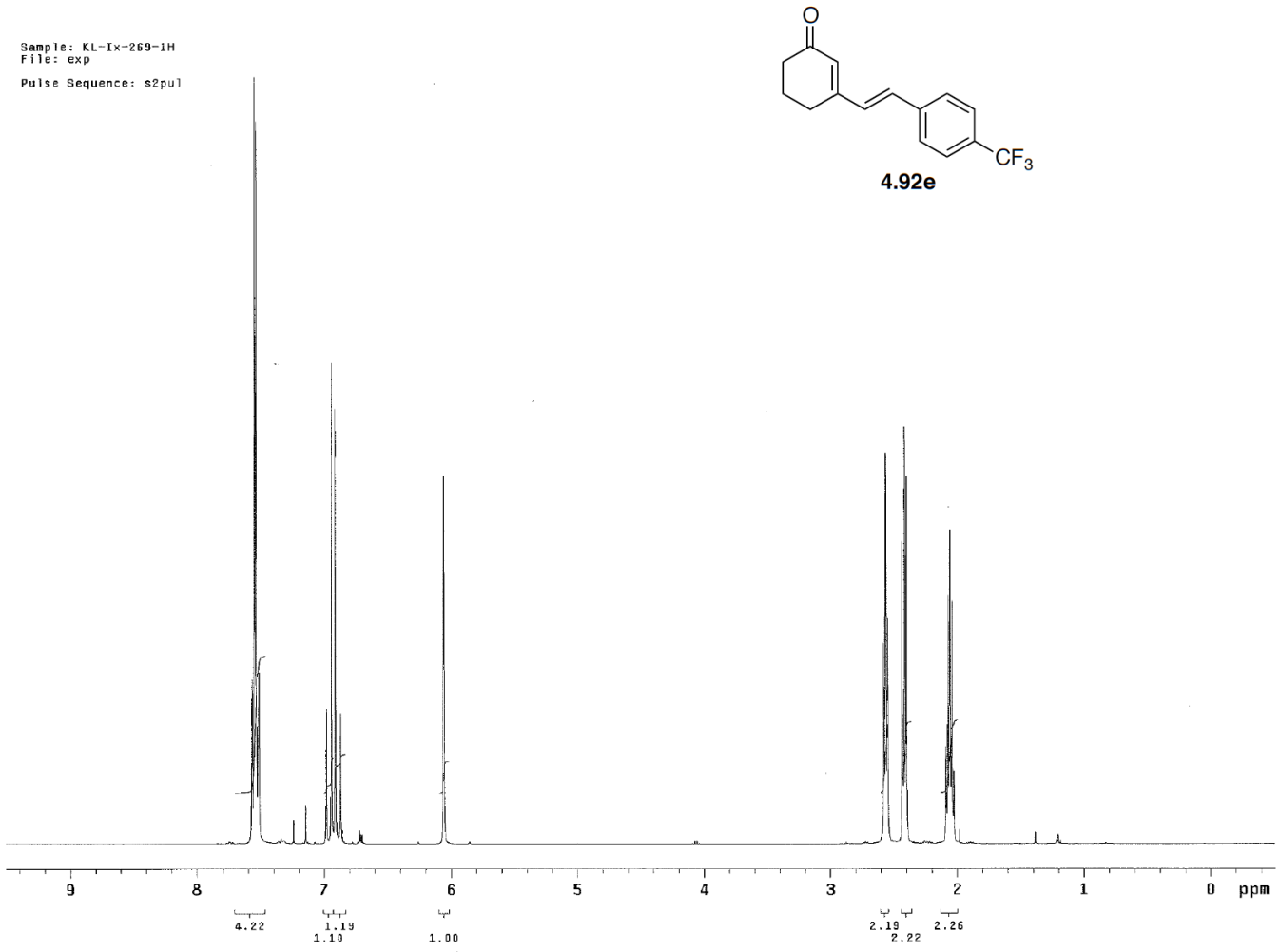
Sample: KL-Ix-269-1H
File: exp
Pulse Sequence: s2pul
O
CF3
4.92e
9
8
7
6
5
4
3
2
1
0 ppm
4.22
1.19
1.10
1.00
2.19
2.22
2.26

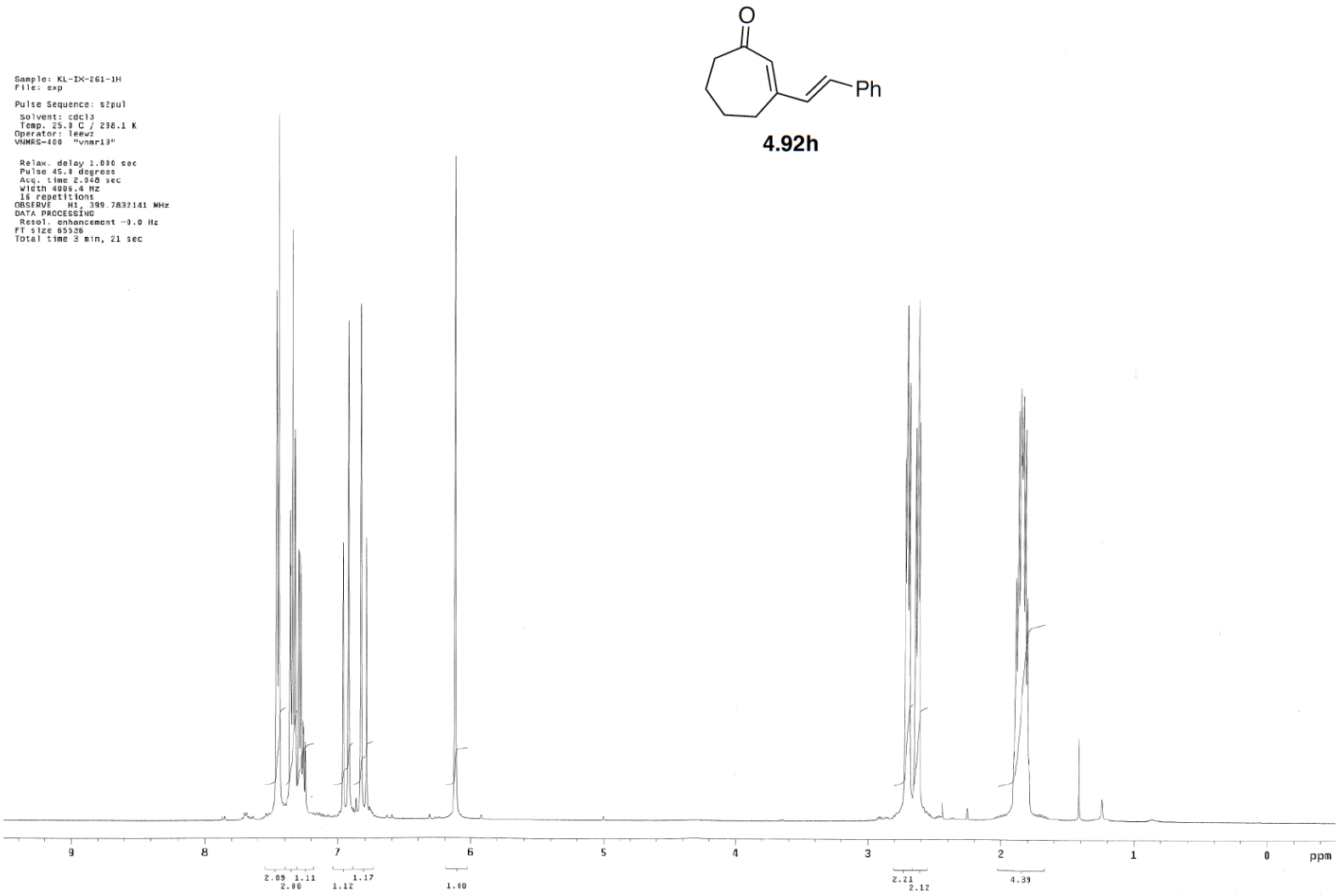
Sample: KL-IX-261-1H
File: exp
Pulse Sequence: s2pul
Solvent: cdcl3
Temp. 25.0 C / 298.1 K
Operator: leewz
VNMRS-400 "vnmr13"
Relax. delay 1.000 sec
Pulse 45.0 degrees
Acq. time 2.048 sec
Width 4006.4 Hz
16 repetitions
OBSERVE H1, 399.7832141 MHz
DATA PROCESSING
Resol. enhancement -0.0 Hz
FT size 65536
Total time 3 min, 21 sec
O
Ph
4.92h
9
8
7
6
5
4
3
2
1
0
ppm
2.09
2.00
1.11
1.17
1.12
1.00
2.21
2.12
4.39

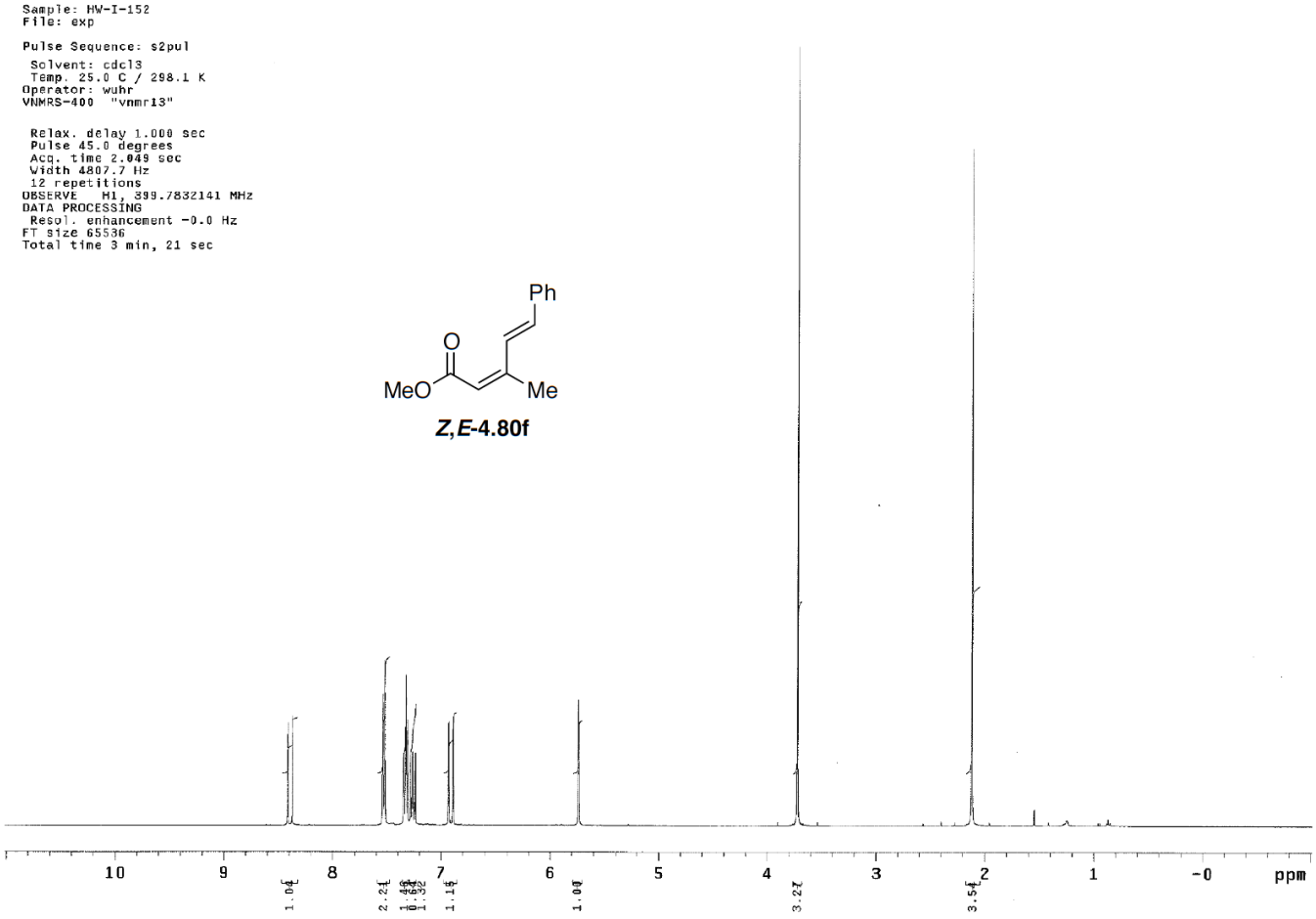
Sample: HW-I-152
File: exp
Pulse Sequence: s2pul
Solvent: cdcl3
Temp. 25.0 C / 298.1 K
Operator: wuhr
VNMRS-400 "vnmr13"
Relax. delay 1.000 sec
Pulse 45.0 degrees
Acq. time 2.049 sec
Width 4807.7 Hz
12 repetitions
OBSERVE H1, 399.7832141 MHz
DATA PROCESSING
Resol. enhancement -0.0 Hz
FT size 65536
Total time 3 min, 21 sec
Ph
O
MeO
Me
Z,E-4.80f
10
9
8
7
6
5
4
3
2
1
-0
ppm
1.04
2.21
1.46
1.52
1.14
1.00
3.27
3.54